UNIVERSITY OF TECHNOLOGY SYDNEY

Machine Learning Techniques for Pricing, Hedging and Statistical Arbitrage in Finance

by Prateek Samuel Daniels

Thesis submitted in fulfilment of the requirements for the degree of

PhD in Finance

under the supervision of Assoc. Prof Christina Sklibosios Nikitopoulos
Dr Otto Konstandatos
Prof. Xue-Zhong (Tony) He
Dr Mesias Alfeus

University of Technology Sydney
Faculty of Business

December 2022

Certificate of original authorship

I, Prateek Samuel Daniels, declare that this thesis is submitted in fulfilment of the requirements for the award of Doctor of Philosophy in the UTS Business School at the University of Technology Sydney.

This thesis is wholly my own work unless otherwise referenced or acknowledged. In addition, I certify that all information sources and literature used are indicated in the thesis.

This document has not been submitted for qualifications at any other academic institution.

This research is supported by the Australian Government Research Training Program.

Signature:

Production Note:
Signature removed prior to publication.

Date: 28 December, 2022

Acknowledgement

"I will be glad and rejoice in you; I will sing the praises of your name, O Most High."

- Psalm, *9:1-2*

I am forever grateful to God Almighty for helping me sail through the most challenging phase of my life. During this journey, there have been many setbacks physically and mentally, and without Him, I would not have progressed this far. I want to wholeheartedly thank and express my sincere gratitude to my current and former supervisors: Assoc. Prof Christina Nikitopoulos, Dr Otto Konstandatos, and Prof. Anthony David Hall for being a mentor and offering guidance, support and technical advice throughout this journey. I highly appreciate Assoc. Prof Christina Nikitopoulos, for her patience and constant perseverance, which has enabled me to get through this journey. Additionally, I am also thankful to Dr Otto Konstandatos for providing valuable technical advice that has been critical in my thesis. I also express my most profound appreciation to Prof. Xue-Zhong (Tony) He and Dr Mesias Alfeus for their continuous advice, support, and invaluable suggestions.

I gratefully acknowledge the funding and scholarship provided by the University of Technology Sydney (UTS). I am also thankful to the UTS Graduate Research School staff, UTS Business HDR staff, Reka Sadagopal, Ashleigh Hall, UTS Finance Discipline Group staff, Andrea Greer and Duncan Ford, and the UTS iHPC (Interactive High-Performance Computing) staff for all their administrative support.

I am also grateful to OptionMetrics, MathWorks, JetBrains, MySQL, dbForge Studio, MongoDB, Studio 3T, Thomson Reuters, Overleaf, Tableau and PairTrade Finder for providing access to their software, which was essential to the technical development and research of this thesis.

I want to express my gratitude to my wife, Anna, for her love and support and for standing beside me through thick and thin. I am incredibly appreciative of my parents' unwavering love, prayers, support, encouragement and patience throughout this journey. I would also like to thank my brother, Pranav, for his love, guidance and support. I am also very thankful to my in-laws, who have constantly supported me through this journey. I am also very grateful to my family members, Susanna, Sarah, Allen, Linda, and Lesley, for their constant love and support.

Last but not least, I would like to also thank my friends and family in Sydney: Chacko, Soji, Sibi, Christine, Sanju, Deepa, Tijo, Jinju, Aylwin, Rinu, Andrew, Bozena, Christo, Supriya and parishioners of the St. Thomas Indian Orthodox Church Cathedral, Sydney, for their hospitality and support. I sincerely appreciate Dr Mahesh and Dr Rajya Gantasala for their love and financial support. A special thanks goes out to Anirudh, Mai, Man, Chung, and Linh, my fellow UTS PhD friends.

To my beloved Anna, Grace and Noah

Contents

Abstract

This thesis aims to evaluate the performance of deep learning artificial neural network (ANN) (multi-layer perceptron (MLP) and long short-term memory (LSTM)) models and parametric (Black–Scholes–Merton, Heston, Heston jump diffusion and finite moment log stable) models in the daily prediction of Standard and Poor's (S&P) 500 call option prices and delta and optimally trading ETF pairs. We use multiple specifications of hidden layers and neurons for ANN models that reflect a more granular level of deep learning, aiming to provide insight into the efficacy of increasing granularity in improving performance. For comparison, we employ classical option parametric pricing models widely used in academia and practice to comprehensively assess the models' performance based on their practical relevance.

In the first study, an extensive empirical assessment of the forecasting performance of daily S&P 500 call option prices/moneyness is performed, and we experiment with single, double, and triple hidden layers specifications of ANN and parametric models. Deep learning ANN models are trained on lagged and one-trading-day-ahead input variables. The numerical investigations reveal that the best-performing models for daily forecasts of call option prices and moneyness are LSTM models (with lagged input variables) and MLP models (with one-trading-day-ahead input variables) compared to parametric models. Moreover, most triple hidden layer ANN models outperform single and double hidden layer ANN models. These results have practical implications for pricing options without look-ahead bias and for network architectures that empirically demonstrate performance improvement from single to triple hidden layers ANN models.

In the second study, the empirical performance of triple hidden layer deep learning ANN and parametric models (with lagged and one-trading-day-ahead input variables) is assessed by predicting daily S&P500 call option delta and the corresponding replicating portfolio value. The delta is computed directly and may also be analytically inferred from option prices. We find that the Black–Scholes–Merton model and the LSTM models typically outperform the other parametric and ANN models. In particular, the LSTM models outperform when the delta is analytically inferred from option prices. The results of this chapter have practical relevance for short-term dynamic hedging applications of options portfolios.

The third study amalgamates the models discussed in the first and second studies by comparing model averaging predictions of prices, deltas and replicating portfolios from deep learning ANN and parametric models. It is shown that the average triple hidden layer MLP models tend to

perform the best in forecasting option prices, with the parametric models performing better in forecasting delta. For the replicating portfolio, the pricing forecasts seem to dominate the delta forecasts, revealing the superiority of the average triple hidden layer MLP models. These findings provide empirical evidence of the effectiveness of model averaging techniques for forecasting options prices and delta risks, which would be helpful in short-term risk management and derivatives evaluation.

The fourth study introduces a new methodology for pair trading equity ETFs, which is formulated by effectively applying commonly used technical indicators and machine learning algorithms (decision tree and deep learning MLP models) to the spreads generated by traditional approaches, thereby generating unique ways to enhance returns. We perform a comparative analysis based on actual PnL(Profit and Loss), returns, Sharpe ratios, and other performance indicators. Eight ETF pairs across three rolling windows (30 days, 50 days and 100 days) yield 3,084 pair trading strategies, which are back-tested. We find that there are alternate and profitable ways to trade pairs that provide a practitioner with many profitable opportunities, unlike traditional approaches in which one is confined to a limited number of opportunities. A pair of ETFs can be traded irrespective they are cointegrated or correlated, thereby enabling hedge funds, institutional investors and retail traders to deploy this strategy as a long/short equity investment tool.

Chapter 1

Introduction

1.1 Motivation and Literature Review

"The most valuable commodity I know of is information."

- Gordon Gekko, *Wall Street (1987)*

In this era of big data, surplus computing power, and the recent advanced developments in GPU(graphics processing unit) computations, deep learning techniques for forecasting asset prices have been extensively used by practitioners and academicians. Also, it is now economically possible to address large-scale optimisation problems because of the falling cost of computing power. In recent years, researchers have developed several machine learning algorithms to predict asset prices and trading strategies around them for short- and long-term investing. The research presented in this thesis was motivated by a desire to address some of the problems that practitioners, derivative and retail traders face, particularly issues with pricing and hedging S&P 500 Index options and optimally trading statistical arbitrage strategies on Exchange Traded Funds (ETFs).

The landmark Black–Scholes (BS) option pricing model was introduced by the celebrated authors in Black and Scholes (1973). Their so-called BS option pricing formula is still a prominent conventional model for pricing options and is considered the most crucial achievement in financial theory in the last five decades. Empirical research has shown that the formula suffers from systematic biases compared to options market prices, particularly failing to account for the so-called volatility smile in observed option price data (see Black and Scholes (1975), Rubinstein

(1985), Bakshi et al. (1997a) and Andersen et al. (2002)). Several parametric option pricing models have attempted to generalise the BS assumptions. The Stochastic Volatility (SV) model introduced by Heston (1993) incorporates a second parametric process to model the underlying volatility. This model seems to provide results more consistent with the volatility smile of observed market data. The SV model was further extended by Bakshi et al. (1997a), who concluded that incorporating stochastic volatility and jumps is essential for pricing and internal consistency and can improve on BS prices. Despite its limitations, the BS model is still frequently used in many practical contexts to price European options despite the many alternative parametric models that have been proposed, whether they incorporate parametric modelling of stochastic volatility as in Heston (1993) or a jump-diffusion component, as proposed in Merton (1976). More complicated models, such as that of Bates (1996), include parametric modelling of stochastic volatility and add a jump-diffusion component to the underlying asset process, and modelling stochastic interest rates, as in Bakshi et al. (1997b). However, one criticism of such approaches is that using the aforementioned parametric models involves complex empirical modelling. These models often prove challenging to implement for use in "real-world" pricing, hedging and trading applications.

Various non-parametric models have been introduced in the literature to remedy the perceived defects of the parametric models and to provide alternative approaches for pricing and hedging applications. The most important non-parametric models in recent years employ artificial neural networks (ANN). Such models propose a purely data-driven modelling approach and have been extensively used in forecasting, pricing and hedging options, bankruptcy prediction, and stock market prediction. ANNs do not make any distributional assumptions about the stock process, thereby avoiding imposing a rigid model structure, unlike parametric models. This makes the ANNs universal function approximators (Hornik et al. (1990)).

The single-layer perceptron neural network, which has an input layer, a hidden layer and an output layer, is by far the most common and, in many ways, the most basic. The multi-layer perceptron (MLP) neural network is an extension of the single-layer perceptron neural network with multiple hidden layers, where nodes in each hidden layer are connected to nodes in the next hidden layer. Similarly, recurrent neural networks (RNNs) are neural networks that generalise and extend the MLP model. In the case where we have a Deep ANN model with several network layers, the RNN variant of an ANN model allows previous outputs in network layers to be used as inputs to subsequent layers while also allowing hidden states. In contrast to a conventional MLP deep network where every layer is independent, in an RNN, the previous layer's output is vital in predicting the output from the next layer. In this regard, RNNs introduce memory into the network model. The architectures employed in the early generations of RNNs displayed practical implementation issues mainly related to their limited memory capacity, which is less of an issue with current hardware. However, more serious problems would arise due to pathological features caused by the vanishing or exploding gradient problem(Hihi and Bengio (1995)).

The long short-term memory (LSTM) Network is a specific form of RNN proposed by Sepp and Jurgen (1997). The architecture of the LSTM network tries to solve the latter problem by not imposing any bias towards recent observations but instead keeping the constant error flowing back through time. The LSTM network avoids long-term dependence problems and is likely suitable for processing and predicting time-dependent data encountered in financial time series. The LSTM network can handle long sequences of inputs compared to other RNNs, which can only deal with short sequences. Outstanding results have been achieved using LSTM and RNNs as documented in Alex and Jurgen (2008) for unsegmented connected handwriting, for automatic speech recognition in Alex (2014), for music composition by Douglas E. (2002), and in the context of grammar learning by Gers and Schmidhuber (2001). Similarly, exceptional results were achieved in Meire et al. (2017) when LSTM networks were paired with convolutional neural networks (CNN) to automatically provide annotations for images. In the area of financial time series prediction, very few studies have applied LSTM networks, and even where they have been applied, most of the studies have been in the area of stock price prediction. Chen et al. (2015) proposed an LSTM-based system to predict stock returns on the Chinese stock market using historical price data of stock and market indexes and found that, as the number of inputs increased, the LSTMs showed improvements in forecasting accuracy. A stock trading simulation based on a method using LSTM was demonstrated by Nelson et al. (2017), where the forecast performance of the LSTM was compared to baseline models, such as the MLP, random forest (RF), pseudo-random model and results showed that the LSTM-based model was comparatively more accurate than other machine learning models. Moreover, it also had a lower risk-adjusted return. Similarly, Bao et al. (2017) used a three-stage process to predict six market index futures. They initially used a wavelet transformation to reduce high-dimensionality stock data to low-dimensionality signal data, which was reproduced using a stacked auto-encoder and then finally used the LSTM network to predict stock prices. They concluded that the forecasting performance of the LSTM was better than the RNN, LSTM, and Wavelet-LSTM models. In addition to using time series data with the LSTM network, Jiahong et al. (2017) extracted investor sentiment from forum posts and fed it to the LSTM network along with historical market data to predict the next day's China Securities Index (CSI) 300 open price. They concluded that LSTM networks outperformed Support Vector Machines (SVM), and adding the sentiment as a feature to the LSTM network led to a remarkable improvement in accuracy (from 78.57% to 87.86%). Along similar lines, Akita et al. (2016) used textual data from the Nikkei newspaper as input for the LSTM network together with time-series data to predict the open prices of 10 companies. They concluded that the LSTM model trained with numerical and textual representations made higher profits (1.67 times higher) than the LSTM model otherwise trained with only numerical data. Motivated by these findings, this thesis uses MLP and LSTM networks and compare performance relative to parametric models in a variety of applications involving S&P 500 Index options, including forecasting option prices and deltas and identifying optimal trading strategies.

1.1.1 European Options Pricing Using Machine Learning:

The architectures of ANN models applied to forecast S&P 500 Index options prices have typically been a single hidden layer ANN (Ghaziri et al. (2000) is an exception), as shown in the list of papers in Table 1.1.

In one strand of literature, the target forecasting variable is the call price or the call price scaled by the strike price, which reflects the option's 'moneyness' (employing the 'homogeneity hint' of Merton (1976)). By using the 'homogeneity hint', Hutchinson et al. (1994) showed that the rate of convergence of non-parametric estimators is accelerated as fewer inputs to the model are used. Furthermore, Hutchinson et al. (1994) applied three non-parametric models on S&P 500 futures options for both option pricing and hedging. They used the Radial-Basis Function (RBF) network, the MLP and the Projection Pursuit (PP) networks and showed that all three networks exhibited superior performance to the BS model. However, these networks were trained on artificially generated BS option prices rather than traded prices.

Hutchinson et al. (1994), Lajbcygier et al. (1997), Anders et al. (1998), Garcia and Gençay (1998), and Garcia and Gençay (2000) show that the 'homogeneity hint' helps to reduce overfitting. The study by Hutchinson et al. (1994) was extended by Garcia and Gençay (1998, 2000), who found that an ANN using S_t/K_t was superior to an ANN using S_t and K_t separately and that the 'homogeneity hint' consistently reduced the out-of-sample mean squared prediction error compared with a feed-forward neural network with no hint. Bennell and Sutcliffe (2004) concluded that for out-the-money (OTM) options, an ANN is superior to BS, whereas, for in-the-money (ITM) options, the performance of BS is better than that of the ANN. The effectiveness of ANN models was further enhanced in Gençay and Qi (2001), who introduced cross-validation, Bayesian regularisation, early stopping and bagging to mitigate overfitting. They concluded that bagging is computationally intensive but provides the most accurate pricing and delta-hedging. As the BS model is known to under-price (over-price) in-the-money (out-of-the-money) options and this error increases with the extent to which the option is in-the-money (out-of-the-money) and decreases as time-to-maturity decreases, Gençay and Salih (2003) concluded that for the deeper out-of-the-money call and put options, an ANN provides more accurate pricing estimates and performs better during high volatility periods. The homogeneity hint was also applied in an inverted manner by Carverhill and Cheuk (2003) as K/S on options based on the S&P 500 Index futures using a single hidden layer neural network with two outputs, the delta and the volatility. They concluded that by inverting the homogeneity hint, an ANN still outperforms the Cox–Ross–Rubinstein (CRR) model in terms of forecasting performance.

Though most literature is supportive of the use of ANNs and the application of the homogeneity hint to their inputs, Gradojevic and Kukolj (2011) found contradictory effects. They introduced a fuzzy rule-based parametric model, known as the Takagi–Sugeno–Kang (TSK) model, that accounts for the non-normality in S&P 500 Index returns. The TSK model exhibits an option pricing performance similar to that of non-parametric ANN models, and this holds true despite providing the ANNs with inputs possessing the homogeneity hint. Furthermore, Hamid and Habib (2005) studied the pricing of call S&P 500 Index futures options finding that ANNs display a similar lack of performance when the single hidden layer ANN model is compared to the Black (1976) model. They also found that, in shorter horizons, the ANNs fail to generate output close to the market call price. Accordingly, in this thesis, the forecasting performance of both prices and moneyness is considered while we extend this strand of literature to multiple layers in order to assess the relative performance of increased granularity in ANN networks.

In another literature strand, ANNs are employed to provide estimates of the parameters of parametric option pricing models required to implement these models–for example, estimating volatility as an input to the BS model. Qi and Maddala (1996) extended Hutchinson et al. (1994)'s study on pricing S&P 500 Index options by training single hidden layer feed-forward neural networks using input variables from the BS model but excluding volatility and including open interest instead. They reported a minor improvement of ANNs in pricing S&P 500 call options compared to the BS model. The usage of open interest was referred to as a crucial factor in the improvement in pricing, as the usage of open interest is not affected by the variance of the target variable. Andreou et al. (2002) extended the Lajbcygier and Flitman (1996) model for option pricing by training ANNs on the difference between the actual market price and the BS option price. They concluded that while ANNs are superior to BS models, no input variable combinations rendered either a specific BS or ANN model superior. As the SV, stochastic volatility with Jumps (SVJ) and stochastic interest rates (SI) models could not manage to provide results consistent with the observed market data, and as they were too complex to implement, Andreou et al. (2004) extended their study to SVJ models with one jump and two jump components. They also considered the model of Corrado and Su (1997) (CS), which allows for excess skewness and kurtosis. They found that these advanced parametric option pricing models (POPMs) perform better in pricing and trading than ANNs, which use parametric models' implied parameters.

Andreou et al. (2008) compared the BS, the semi-parametric CS models, with several ANN configurations in which the target function of the ANNs was the residual between the actual call market price and the parametric option price estimate. They concluded that, in the presence of transaction costs, the BS-based hybrid ANN models with contract-specific volatility are the best-performing ANN models. Dumas et al. (1996) formulated a quadratic form for estimating per-contract volatility called deterministic volatility regression functions (DVF) to predict option prices, finding that an interpolative regression approach produces more accurate option prices than the Crank-Nicholson finite-difference method. This method of pricing was extended by Andreou et al. (2010), who designed a nonparametric method of enhancing the parameter values used in parametric option pricing models, thereby creating a semi-parametric method to price options. They propose a method (that outperforms Dumas et al. (1996)'s DVF method) for estimating parameters such as volatility, skewness, and kurtosis using the Generalised Parameter Functions (GPF). The semi-parametric/enhanced-parametric option pricing models (i.e. ePOPMs) are simpler and three times faster to compute than SVJ models. The parameter enhancement (in ePOPMs) provides volatility to the BS model and skewness or kurtosis to the CS model. To estimate the GPFs nonparametrically, they used a single hidden layer feed-forward ANN. Among parametric models (i.e. non-DVF versions of the BS, CS, SVJ and SV models), the SVJ model, followed by the SV model, exhibited superior performance in pricing. During in-sample and out-of-sample performance, the DVF-based CS models provided better pricing performance than other corresponding DVF-based models, but the parametric SVJ model outperformed all of them. The ePOPMs have an excellent out-of-sample pricing performance, where the root mean square error (RMSE) for all the models ranged between 1.50 to 1.75.

ANN techniques can estimate option prices inductively using historical or implied input variables and option market data. These nonparametric methods do not make any theoretical assumptions about the underlying process or directly involve any financial theory in their approaches. Kim et al. (2004) observed that the impact of the stationarity on the forecasting power of ANNs was minuscule and that it was feasible to relax the stationarity condition to non-stationary time series when using ANNs for forecasting. Since option pricing functions are necessarily multivariate and highly nonlinear, ANNs may be desirable approximators of the empirical option pricing function. In addition, approaches based on parametric models necessarily describe a stationary nonlinear relationship between a theoretical option price and the various input variables. It is well known that market participants may change their option pricing attitudes over time, so any stationary model may fail to adjust to such changing market behaviour (Rubinstein (1985)). Frequently re-trained ANNs may also be able to adapt to changing market conditions and correct for parametric model biases, particularly for the BS model (see Lajbcygier and Flitman (1996), Garcia and Gençay (2000), andYao et al. (2000)). Since non-parametric pricing methods do not rely on specific assumptions about the underlying asset price dynamics, they are therefore robust to specification errors that might adversely affect any parametric pricing model.[1]

1.1.2 Forecasting volatility using Machine Learning

Regarding applications related to forecasting volatility, initially, Donaldson and Kamstra (1997) studied the application of ANN to capture the volatility effects overlooked by GARCH, EGARCH and GJR models for the S&P 500, Toronto Stock Exchange Composite Index, the Nikkei Index, and the FTSE Index. In-sample comparisons concluded that the GARCH model often fails to capture the empirical regularity, and the EGARCH model may not be appropriate since it sometimes produces erratic volatility estimates; the GJR model seems more able to fit the

[1]The use of ANNs has been extensively extended in several related directions, including pricing and/or hedging of American and exotic style of options, warrants, etc. For example, recent contributions include Pires and Marwala (2004, 2005) used an SVM to price American options; Kohler et al. (2010) employed a modified version of the ANN to price American put options on several instruments and used the least-squares Monte Carlo algorithm instead of regressions; Ferguson and Green (2018) applied the Monte Carlo algorithm to price American call options on a basket of stocks; Ye and Zhang (2019) presented techniques for using a stochastic process and ANNs to price American options, Jang and Lee (2019) applied generative Bayesian Neural Networks (BNN) for pricing away out-of-the-money S&P 100 American put options; Becker et al. (2019) use ANNs to price American and Bermudan max-call, callable multi-barrier reverse convertibles and estimate optimal values for stopping time problems, a study that was extended by Fécamp et al. (2019).

asymmetric heteroskedasticity in the data than either GARCH or EGARCH and thus, the best-performing model appeared to be the ANN model. Mantri et al. (2014) builds on Donaldson and Kamstra (1997)'s work by using a similar set of models, which includes an ANN, GARCH, EGARCH, IGARCH, and GJR-GARCH model, to forecast volatility for the BSE Sensex and NSE Nifty. But, they found that the volatility forecasts from ANNs are no different than those from GARCH, EGARCH, IGARCH, and GJR-GARCH models, which was confirmed by an ANOVA test. A similar set of econometric models was also used by Kumar and Patil (2015) to forecast volatility for the S&P 500 index for ten years using five types of historical implied volatility estimating techniques, namely the Close, Garman Klass, Parkinson, Roger, and Yang methods, as well as the MLP and econometric models, namely the ARIMA, ARFIMA. The Garman Klass estimation technique and the ARIMA forecasting technique were found to have the highest forecasting accuracy. Similar performance of the ANNs was also reported by Hamid and Iqbal (2004), where they forecast volatility for the S&P 500 Index futures options using ANNs and Barone-Adesi and Whaley options pricing model. They conclude that, while forecasts from ANNs outperform implied volatility forecasts, but do not differ significantly from realised volatility. However, a recent study by Cao et al. (2020) has shown to differ in the forecasting performance of ANNs, where they examined the S&P 500 index option volatility surface using MLPs, and on a daily basis, and derived a relationship between the expected change in implied volatility, the return on the index, the option's moneyness, and the option's time to expiry. They conclude that the MLP model outperforms the Hull and White (2017) model by 10.72%, and a further improvement of 62.12% was possible if the MLP model was given the level of the VIX index as an additional input. Some of these studies have considered Support Vector Regression (SVR) to estimate the dynamics of parametric volatility models. For instance, for modelling the E-mini S&P 500 options implied volatility surface, Zeng and Klabjan (2019) used a variety of support vector regression models (EKPSVR, BKPSVR, KPSVR, NORMA, and BSGD) and concluded that the EKPSVR algorithm not only outperforms other algorithms in terms of speed but also in terms of pricing. Much of the literature also suggests that Support Vector Machines (SVM) are one of the alternate best regression algorithms for forecasting volatility. Liu (2019) puts this claim to the test by applying three modelling techniques, the v-SVR, LSTM and the GARCH model, for forecasting the volatility of the S&P 500 and AAPL. For the S&P 500 and AAPL, they found that LSTMs were just as good as v-SVR at forecasting volatility and that both were much better than the GARCH model. A similar set of models was also used by Ramos-Pérez et al. (2019), where they created hybrid models for forecasting S&P 500 volatilities using a set of machine learning models (Gradient Descent Boosting, Random Forest, Support Vector Machine, ANN) based on a combination of GARCH and EGARCH. They conclude that, in a highly volatile regime period, the Stacked-ANN model generated more accurate volatility forecasts than other hybrid models (ANN-GARCH or ANN-EGARCH), owing to model flexibility, and that under and overvalued derivatives could be identified using the Stacked-ANNs volatility forecasts.

Recently, many studies have also considered LSTM models for forecasting the volatility surface. Given the LSTMs ability to characterise the long memory of financial volatility, Chen et al. (2019) applies an LSTM model with an attention mechanism to the S&P 500 options implied volatility surface, which enhances the ability of LSTM networks to select input features. They conclude that the LSTM forecasted implied volatility surface is more accurate than other predicting systems. Using this surface, they price options and back-test two trading strategies: time spread and butterfly spread. These two strategies constructed using the predicted implied volatility surfaces had higher returns and Sharpe ratios. A similar study based on LSTMs was done to forecast the realised volatility surface for the S&P 500, 10-year Treasury note future and 1-month Treasury bond future by Bucci (2020), who employs an Elman, Jordan, Nonlinear Autoregressive Exogenous Neural Network models, LSTM model, and Cholesky decomposition. They point out that as the number of hidden layers, hidden nodes, and inputs in these ANN models grew, the risk of missing the local minimum grew as well. The out-of-sample tests reveal that the Elman and Jordan Neural Network models could not strongly outperform the traditional econometric methods, like GARCH, and the Nonlinear Autoregressive Exogenous Neural Network and the LSTM were the best forecasting models. Similarly, to forecast volatility for the S&P 500, NASDAQ, German DAX, Korean KOSPI200, and Mexico IPC Index, Kyoung-Sook and Hongjoong (2019) use technical indicators like Moving Average, Exponential Moving Average, Momentum, and hybrid Momentum as inputs to an LSTM model. They conclude that combining hybrid Momentums with traditional Momentums improves forecasting.

1.1.3 Hedging Options using Machine Learning

MLP ANN techniques have been used extensively to study empirical hedge ratios (specifically delta). These ANN techniques involve inferring delta from ANN option prices or training an ANN directly on the empirically observed hedge ratios or delta. Some studies inferring the delta from call prices involve taking the partial derivative of the ANN call prices with respect to the underlying index/futures price. For a representative list of such works, see Table 1.2. All of these studies except Carverhill and Cheuk (2003) and Chen and Sutcliffe (2012) derived the hedge ratios analytically from an ANN fitted to option prices. In Hutchinson et al. (1994), the hedging performance of three ANN models (RBF network, the MLP network, and PP network) on the S&P 500 futures options is shown to be superior to the BS model. Herrmann and Narr (1997) followed Hutchinson et al. (1994) approach to training an ANN model on German stock index (DAX) options and found that the delta derived from ANN call option prices performs slightly better (approximately 1%) than the BS delta. As systematic biases in BS implied volatilities (BS implied volatilities tend to vary across moneyness and times to maturity) are documented by Bates (1996) and Dumas et al. (1996), Lajbcygier and Flitman (1996) stated that these biases could be reduced using a novel combination of bootstrap and bagging methods. This approach was applied to a hybrid ANN option pricing model, which predicts the residuals between the conventional parametric model option price (the modified-Black model) and the actual transaction price. Through a delta trading strategy, the hybrid delta captures most of the trading opportunities. Hutchinson et al. (1994)'s study was extended by Ormoneit (1999) to implement an ANN regularised network weights using an Iterative Extended Kalman Filter (IKEF) as the learning rule on DAX options. They find that training the ANN using IEKF leads to more accurate option price predictions and superior hedging performance than that of the BS model.

The Mixture Density Network (MDN) method is an alternative hybrid approach using both parametric and non-parametric estimation. MDNs were first proposed by Schittenkopf and Dorffner (2001) as an alternative method to estimate the risk-neutral density of assets using a mixture of Gaussian distributions and thus overcome the shortcomings of the systematic errors of the term structure of volatility or volatility smile in the BS model. The idea is to use MLPs to determine the parameters of the mixtures as a non-linear function of the information set. These authors found that the MDN model displayed higher pricing accuracy than the basic and adjusted BS models. However, it did not necessarily display better hedging performance.

Using the 'homogeneity hint', Hutchinson et al. (1994) non-parametric models had fewer inputs, leading to a faster convergence rate of the non-parametric estimators and superior outperformance. This method was later extended by Garcia and Gençay (2000), who found that using an ANN model with the homogeneity hint (call prices scaled by the strike price) provides more stable average delta hedging errors than ANN networks without it. Both have smaller delta-hedging errors relative to the BS model. Similarly, Gençay and Qi (2001) concluded that an ANN with Bayesian regularisation could effectively reduce overfitting and generate significantly smaller pricing and delta-hedging errors than the BS model or an ANN model without Bayesian regularisation. Amilon (2003) also extended Hutchinson et al. (1994)'s study by using additional inputs on two sets of MLP models (one set of MLP models using lagged historical variables and the other using lagged implied parameters). With the help of bootstrap techniques, they showed that hedging using both (BS and MLP) models result in losses, with loss in the MLP models being considerably less than that in the BS model. At the bootstrapped 95% confidence intervals, the MLP model (using lagged historical variables) performed significantly better than the BS model (with implied volatility estimates). Carverhill and Cheuk (2003)'s study is an extension of Hutchinson et al. (1994), which investigates if an MLP model could produce better hedging parameters than the standard Cox-Ross-Rubinstein option pricing model. They found that training MLP models on observed option prices and subsequently deriving the hedge ratios from the resulting pricing equation is not the best strategy. It is better to train an MLP model directly on delta and vega (inferred from observed option price changes). Moreover, they mentioned that the hedging performance of the MLP model trained on option prices is always inferior to that of the MLP model trained on delta/vega and performs worse than the Cox-Ross-Rubinstein model. Similarly, Chen and Sutcliffe (2012) extended both Hutchinson et al. (1994) and Carverhill and Cheuk (2003), as they derived hedge ratios (delta) for hedging short sterling options positions using short sterling futures analytically from ANN option prices and also by training ANNs directly on the empirical hedge ratios. They concluded that the performance of hedge ratios from ANNs directly trained on empirical hedge ratios is significantly superior to those based on a pricing model or the parametric modified Black model. A similar exercise of comparing the delta-hedging error of MLP models to that of the BS model was carried out by Ko (2009). It was concluded that the derived average absolute delta-hedging error of the ANN model is tenfold times smaller than that of the BS model, and the ANN model achieved a 66.94% winning rate over the BS model, compared to Hutchinson et al. (1994)'s winning rate of 38% over the BS model.

To improve on the ANNs ability to hedge out-of-sample options by learning the BS implied volatility, Mostafa and Dillon (2008) compared the Generalised Autoregressive Conditional Heteroskedasticity Option Pricing Model (GOPM) to two types of MLP models. The first type of MLP model followed the standard approach of using the option price as the target output of the network, and in the second method, the MLP was directly trained on the BS implied volatility. It then used the BS formula to derive the theoretical option price and subsequently derive the delta analytically from the option price. They concluded that GOPM performs the worst, with the BS model, on average, outperforming the others, except for the ITM options.

Reinforcement Learning (RL) involves the procedure of training machine learning models to make a series of decisions, which are to be made in a dynamic environment. The use of RL for hedging options has been gaining prominence, and recently, Buehler et al. (2019) used the Heston and modern deep RL methods to hedge a portfolio of derivatives in the presence of market frictions such as transaction costs, liquidity constraints and risk limits. According to them, parametric models are only a rough approximation of machine learning models, which could produce more precise results using convex risk measures. They hedged a portfolio of over-the-counter (OTC) derivatives by training the machine learning models with simulated data. Based on synthetic data, the simulations used to train these RL models took into account transaction costs and other market frictions to produce optimal hedge ratios. This study was further expanded by Carbonneau and Godin (2021), where the authors applied deep reinforcement learning models to hedge exotic options to implement an equal risk pricing and hedging framework that relies on convex risk measures. Developed using the methodology introduced by Buehler et al. (2019), this framework tries to optimally hedge the residual risk exposure associated with the long and short positions in a contingent claim. Hence, this method could price and hedge various types of contingent claims and underlying assets with different dynamics, such as regime-switching, stochastic volatility, and stochastic volatility with jumps. Similarly, Cao et al. (2021) also applied RL to optimally hedge a short position in an S&P 500 Index call option while accounting for transaction costs. The RL uses an objective function based on the first and second non-central moments of the probability distribution of the cost of hedging and produces an optimal hedge when a stochastic process is used. The authors concluded that by combining a simple pricing model with more complex asset-pricing processes, effective hedging strategies could be developed. This method may also be useful for pricing exotic options, which are difficult to hedge using Greeks. The use of an ANN to hedge options by replicating the entire volatility surface of the rough Bergomi volatility model was also demonstrated recently by Horvath et al. (2021). The ANN model used by the authors can calibrate an entire implied volatility surface in a matter of milliseconds. This method could be used with a variety of second-generation stochastic and rough volatility models, and it eliminates the bottleneck caused by slow derivative contract pricing and hedging.

Zhang and Huang (2021) extended Buehler et al. (2019)'s study by introducing a hedging strategy using the LSTM-RNN networks, which incorporates market frictions such as transaction costs, liquidity constraints, trading limits and costs of funds for the 50 ETF options, Hang Seng Index (HSI), Nikkei, S&P 500 and Financial Times stock exchange (FTSE) 100 Index Options. The LSTM-RNN networks were benchmarked with the Leland (1985), Boyle and Vorst (1992), and Wilmott et al. (1994) using simulated market data generated by geometric Brownian motion (GBM) and real market data. They found that the LSTM-RNN model outperformed other models for OTM moneyness when volatility is low or medium, and there is less than 80% risk level in the models that use the simulated market data. Using real market data, for the 50 ETF options, the LSTM-RNN model outperforms the benchmark for ATM options with low-risk levels. For the HSI Index options, the LSTM-RNN model outperforms benchmark models when transaction costs are smaller than 1.5%. For Nikkei and S&P 500 Index options, the LSTM-RNN model always outperforms benchmark models, and finally, for the FTSE Index options, the LSTM-RNN model outperforms benchmark models when moneyness is not too deeply ITM. Accordingly, we also employ LSTM models in this thesis.

Although ANNs have been widely used for hedging options, the use of linear regressions has not been investigated, and Ruf and Wang (2021) compared linear regressions with their newly designed neural network, known as ‘HedgeNet’, which incorporates the homogeneity hint by training in two parts. They initially controlled for moneyness and then for time to maturity, a procedure partially inspired by Garcia and Gençay (1998). The HedgeNet was designed for the hedging of options and trained to minimise the hedging error instead of the pricing error. The performance of HedgeNet was tested on several different datasets: (a) data simulated from the standard BS stochastic integral equation, (b) data simulated from Heston’s model, and (c) daily end-of-day mid-prices obtained from OptionMetrics (applied to end-of-day and tick prices of S&P 500 and Euro Stoxx 50 options, respectively). The goal is to determine the hedging ratio by minimising the variance over one period of the hedged portfolio. In doing so, they reduced the mean squared hedging error of the BS benchmark significantly; however, similar results were also obtained using simple linear regressions. They concluded that ANNs could not find additional non-linear features, and option greeks–in particular, delta, vega, and vanna–combined with a simple linear regression model are superior in hedging performance. The linear regression models improvement over the hedging performance (without considering transaction costs) of the BS model is about 15-20% for a daily re-balancing, but for the two-day re-balancing, all regressions outperform the BS–Delta, where relative to the BS-Delta, the regressions are about 2% to 3% better.

1.1.4 Model Averaging Approach to ANN

Researchers have attempted to make predictive models robust, reduce model uncertainty and increase the predictive power of parametric and non-parametric models. One such method, called bagging, was introduced by Breiman (1996), where it involved taking an aggregate value of the predictions from multiple versions of a model through bootstrapping. The process of bagging is computationally intensive, and Gençay and Qi (2001) noted that it provides the most accurate pricing and delta hedging. To improve generalisation as per Gençay and Qi (2001), multiple versions of the ANN were generated using a random seed, and the outputs of these networks are aggregated to get an average predicted call price. As shown in Figure 2.4, in the bagging process, iteration 1 would be performed multiple times to arrive at an average call price or the average delta. The division of training, validation and test set data across the multiple neural networks would randomly vary. Gençay and Qi (2001) also showed that using this bagging approach, the standard deviation of the mean squared prediction errors (MSPEs) is significantly smaller than that of forecasts of individual baseline models, while such regularisation methods are effective on models implementing the homogeneity hint. Another drawback of large neural networks is overfitting, especially when applied to small datasets, which can be managed by employing bagging or boosting to combine several different models. Considering that this is a computationally expensive exercise, Opitz et al. (2017) proposed a maximisation of individual networks via the DivLoss loss function that avoids the training of expensive ANN models. With a particular focus on financial series applications, such as stock indices and interest rate yields, Ravazzolo et al. (2007b,a) used model averaging techniques and found that the benefits of model averaging benefits in terms of parameter and model uncertainty improve the power to forecast financial time series. Guo et al. (2021) demonstrated the capacity for model averaging to significantly improve the performance of Apache Spark, a well-known slow engine for executing data engineering. Motivated by this literature, we use the model averaging approach to assess performance in pricing and hedging predictability of S&P 500 options.

1.1.5 Pairs Trading using Machine Learning

Since 1980, professional traders, institutional investors and hedge fund managers have been using pairs trading (PT) as one of the most popular statistical arbitrage techniques (Vidyamurthy (2004), Dunis et al. (2010), Gatev et al. (2006), Hogan et al. (2004)).

PT is a statistical arbitrage method that invests in the spread between two equities whose prices have historically moved in unison (Gatev et al. (2006)). A long position is taken in one stock, and a short position is taken in the other simultaneously. Trading signals are based on deviations from the long-term equilibrium spread, and the spread between the two stocks creates a stationary process. We act and profit from the momentary inconsistency if the spread deviates from its historical equilibrium, believing it will revert shortly. PT is a market-neutral strategy (a crucial principle of PT) because it generates returns regardless of whether the market rises or falls (see (Vidyamurthy (2004)) and (Krauss (2017)) for a comprehensive review). According to Huck (2015), these strategies mitigate specific market risks by taking offsetting long and short positions on instruments that are actually related.

Machine learning approaches are somewhat uncharted in the subject of PT, as most relevant publications only apply them to a few select securities, but they offer a promising avenue for future research (Krauss (2017)). The MLP and the LSTM-based neural networks are two methodologies that are pertinent to this study. Both methods are widely utilised and have been demonstrated to be reliable when it comes to forecasting stationary time series. These methods have also been applied to PT by Dunis et al. (2006, 2015) and Sarmento and Horta (2020).

The distance measure can be used to quantify the similarity of price series and was first introduced by Gatev et al. (1999) for pairs selection. In this approach, each price series is paired with the price series that has the minimum sum of the squared differences between the two normalised stock price series. This approach could have a disadvantage, as minimising the sum of the squared difference between two normalised prices series will also minimise the variance of the spread (Van der Have et al. (2017)).[2] This distance method may also not be statistically sound since the spread between two price series can theoretically have a small sum of squared differences but still be non-mean reverting (Krauss (2017)). By back-testing the distance-based PT strategy on US equities from 1967 to 1997, Gatev et al. (1999) generated an 11% excess return, which was unaffected by transaction costs. The same study was repeated in 2006, but this time with a five-year data period, and the results were still positive. Broussard and Vaihekoski (2012) looked into the practicalities of putting Gatev et al. (1999)'s self-financing pairs portfolio trading approach into practice, and their annualised returns were as high as 12.5% on average.

The distance approach, proposed by Gatev et al. (2006), is the most well-known and widely used method and dominates empirical work on PT (Krauss (2017)). This method entails starting the price series at one and then normalising it. The purpose is to locate pairs with the lowest possible sum of squared deviations or pairs with a small gap between the normalised price series by subtracting one series from the other. In contrast to the distance approach, Alexander and Dimitriu (2002), Vidyamurthy (2004), Lin et al. (2006), and Miao (2014) have emphasised that only the cointegration-based approach can reliably estimate the size of a pricing differential that deviates from the long-run equilibrium.

[2] The spread must have some variance to have more trade entry opportunities to profit.

Nath (2003) used another distance measure to find potential pairs in the US Treasury securities market. Instead of constructing a cumulative total return index (as proposed by Gatev et al. (1999)), Nath (2003) normalised the prices by subtracting the sample mean and then dividing by the sample standard deviation over a 40-day period. For each pair in the trading universe, an empirical distribution of price differences (distance) is recorded, and trading signals are triggered by the observed distance exceeding the 15th percentile (rather than in units of standard deviations) during the subsequent 40-day trading period. The positions are unwound if the distance narrows and crosses the empirical distribution's median, the spread widens even more to reach a stop loss trigger (to the 5th percentile) or if the trading period is complete.

Do et al. (2006) pointed out that Gatev et al. (1999)'s approach is model-free and is immune to model misspecifications and misestimations. Moreover, it is simple to set up, resistant to data snooping and generates statistically significant risk-adjusted excess returns. However, the use of the Euclidean squared distance as a selection metric is analytically sub-optimal. According to Krauss (2017), the distance method is one of the most studied PT frameworks because of its simplicity, transparency and non-parametric nature, which make it relatively easy to implement in practice. However, the distance method has a few major flaws (Krauss (2017)). Gatev et al. (1999) may not have paired stocks from the proper asset universe, and thus it is likely that trading with this pair will result in a loss. Second, minimising the variance of the spread results in fewer deviations from the mean and, thus, fewer potential opportunities to trade and profit. Finally, the methodology of pairing stocks was not based on any statistical criteria; hence, the chosen pairs might not have a long-run mean-reverting relationship. The mean-reverting behaviours of pairs were also assessed by Huck and Afawubo (2015), who showed that pairs chosen based on the cointegration method are more likely than pairs chosen using the distance method to exhibit mean-reverting behaviour, even though the pairs do not converge until the end of the trading period. This increases the risk of divergence leading to less profitable trades with pairs whose spreads do not converge back to the mean. Krauss (2017) also used Gatev et al. (1999)'s methodology and found that 32% of pairs chosen by distance diverged. Due to these flaws, using the distance method to select pairs may be a poor choice, and a statistical relationship-based pair selection method should be used. On a similar note, Huck (2013) also highlighted that the returns of the distance-based PT method are very sensitive to key parameters such as the length of the formation period and the trigger used to open trades. In our study, the distance method serves as a benchmark for our proposed strategies because it is still the most commonly used trading strategy.

Papadakis and Wysocki (2007) used Gatev et al. (1999)'s rules for pair selection and trading on a subset of stocks from the US equity market to investigate the impact of accounting events on PT profitability. They discovered that trades opened during periods of accounting events are significantly less profitable than trades opened during periods of non-accounting events. Gatev et al. (1999)'s methodology was replicated by Do and Faff (2010, 2012) on the same stock universe with a longer sample period up to 2009. They found a decline in profitability owing to an increase in the number of non-converging pairs. Moreover, using Gatev et al. (1999)'s methodology is unprofitable when trading costs are factored in. Gatev et al. (1999)'s selection criteria were further refined in Do and Faff (2010, 2012) by limiting the matching of securities within the 48 Fama–French industries and pairs with a high number of zero-crossings. The additional criterion of zero-crossings was used as a proxy to account for mean reversions. Although these restrictions resulted in fewer spurious correlations and more meaningful pairs, the result was only slightly more profitable than that of Gatev et al. (1999) after including transaction costs. In addition, with 29 different combinations of selection algorithms, Do and Faff (2012)'s methodology is more vulnerable to data snooping. Nonetheless, Do and Faff (2010), in agreement with Gatev et al. (2006), claimed that PT performs particularly well during times of financial crisis. Using the distance-based pairs trading methodology, Muslumov et al. (2009) evaluated pairs on the Istanbul Stock Exchange (ISE) using the distance approach and found that the top 20 best PT portfolios generated an average excess return of 5.4%. The distance-based approach was also applied to a 60-minute-interval-based FTSE 100 stocks from January 2007 to December 2009 by Bowen et al. (2010), who discovered that the strategy's returns were affected by both transaction costs and execution speed. Chen et al. (2019) also extended Gatev et al. (1999)'s study by using the same dataset and time frame, but for pair selection, they used the Pearson correlation coefficient based on pair returns. They opted for the correlation-based framework because return divergences could successfully be captured. The monthly pairwise return correlations for all stocks were calculated over a five-year formation period. They reported a 1.70% average monthly raw return, which was almost twice that of Gatev et al. (1999).

The concept of cointegration was introduced by Engle and Granger (1987) and applied in the practical context of pairs selection by Vidyamurthy (2011). Cointegration is a statistical relationship in which two time series of the same order, i.e. $I(1)$, are combined to produce stationary time series. The Engle and Granger (1987) or Johansen (1991) tests are the most commonly used cointegration tests. The two-step approach to TP using cointegration involves first performing a linear regression on the two-time series to determine the hedge ratio and estimate the residual time series and then using the Augmented Dicker-Fuller test to determine the estimated residual's stationarity. Although Vidyamurthy (2011) formulates an explanation of why it might work, the author did not provide empirical results for the cointegration method but a framework that can be used as a foundation for cointegration-based PT research. Caldeira and Moura (2013) used the cointegration-based method to select pairs on the Brazilian stock index and found excess returns of more than 16% per year. The cointegration method outperforms the distance method in terms of pair selection, according to Huck and Afawubo (2015).

Cointegration tests were also used by Schmidt (2009) to identify pairs of stocks in the Australian Stock Market. Schmidt (2009) used the Vector Error Correction Model (VECM) to model residuals, but he did not intend to backtest the trading strategy with the VECM, instead opting for Johansen's cointegration method. He found that PT is profitable if the residuals have a high rate of zero-crossing and large deviations around the mean. Using the cointegration technique, Puspaningrum et al. (2010) identified the optimal preset boundaries for the PT strategy. The goal was to estimate the average trade duration, average inter-trade interval, and the average number of trades and then find the best-preset boundaries for maximising the minimum total profit for cointegration error in an $AR(1)$ process. Bogomolov (2011) used three estimation techniques–the distance, cointegration, and stochastic spread methods–to compare the profitability of these PT strategies on the Australian stock market (ASX). Before transaction costs, all approaches showed statistically significant monthly excess returns. Transaction costs, however, have a negative impact on all three strategies, particularly the stochastic spread method.

The performance of the distance and cointegration methods was also compared to Liu et al. (2017)'s method, which provides a unique way of modelling spreads to search for temporary market mispricing inefficiencies in a more dynamic way. They mainly focused on pairs of oil companies listed on the New York Stock Exchange. Data were collected at 5-minute intervals in 2008 and then at 10-minute intervals from June 2013 to April 2015, with the back-testing in 2008 yielding overwhelmingly positive results. Their findings backed up previous research (Gatev et al. (2006), Kim (2011), Do and Faff (2010) and Rad et al. (2016)) that found PT to be profitable in bear markets. Similarly, Mikkelsen and Kjærland (2018) used a small sample of Oslo Børs All Share Index (OSE)-listed seafood companies to test the performance of both the distance and cointegration approaches. The study compared the use of high-frequency data to that of daily data and discovered that neither the distance nor the cointegration methods produced significant profits. Relevant studies have found ambiguous results when it comes to the profitability of PT. Gatev et al. (2006), Do and Faff (2010, 2012), Jacobs and Weber (2015), Engelberg et al. (2009), and Krauss (2017) have all claimed that profits have fallen in recent years and that the profitability of PT is negatively correlated with market liquidity. Using 1-minute-interval data for the constituents of the S&P 500 from January 1998 to December 2015, Stübinger and Bredthauer (2017) performed a pair selection using the distance and correlation and Liu et al. (2017)'s approach. They tested these methods on three different thresholds: a static and two dynamic threshold approaches, one of which used a running mean and standard deviation and the other of which used Bollinger (1992)'s reverting thresholds approach. They discovered that combining the distance approach with a dynamic threshold yielded a 50% annual return, while the static method yielded only 21.5%. They also found that the returns for PT have declined over time. This research was extended in Stübinger and Endres (2018), who modelled the spreads using a mean-reverting jump-diffusion model on 1-minute-interval data for oil and gas companies listed on the S&P 500 from January to December of 1998, reporting an annual return of 60% and a Sharpe ratio of 5.3 after accounting for transaction costs.

Dunis et al. (2010) also examined daily and high-frequency data, i.e. 10-, 20-, 30-, and 60-min data on the constituents of the EuroStoxx 50 Index using the cointegration method. They limited the formation of pairs to 10 industry groups, resulting in 176 possible pairs that may or may not have been cointegrated. Time-varying parameters were estimated using the Kalman filter, and the spreads of all pairs were later standardised and traded according to a simple standard deviation logic similar to that of Gatev et al. (1999). They discovered that the cointegration method is profitable by using the top five pairs with the most appealing in-sample indicators. Kim et al. (2006) also used the cointegration approach with the Kalman filter to estimate the time-varying coefficients for equities listed on the Korea composite stock price index (KOSPI) 100 Index and fund positive excess returns after transaction costs were factored in. The authors also affirmed that during a financial crisis, such a strategy performs better. In a similar way, Dunis et al. (2010) and Kim (2011) also used the Kalman filter to estimate the adaptive hedge ratio. The change in the hedge ratio was modelled as a random walk, and the spread is modelled as Gaussian white noise in the state space equations from the Kalman filter model. Vidyamurthy (2011) also used the Kalman filter in PT but did not go into detail on how to use it for parameter estimation (i.e. estimating the hedge ratio). Rad et al. (2016) applied the cointegration approach to the US centre for research in security prices (CRSP) data from 1962 to 2014. Initially, stock pairs with the lowest sum of square differences (SSD) are identified over a 12-month formation period, and by using the Engle–Granger cointegration approach, they chose the top 20 cointegrated stocks from the SSD rankings. Later, they used Gatev et al. (1999)'s threshold rule to generate trading signals, where one USD was invested in the long leg of each pair and the dollar amount in the short leg. Prior to transaction costs, the cointegration approach had a monthly excess return of 0.83%, whereas a similar trading approach using the distance method had a return of 0.88%. According to Rad et al. (2016), the underperformance of the cointegration approach may be due to the selection bias introduced by limiting cointegration to the subset of pairs with the lowest SSDs.

According to Baur (2003), the correlation or cointegration technique can be used to measure the co-movement of two assets, and the correlation technique has been suggested as an alternative to the cointegration and distance methods. The methodology for trading pairs using the correlation technique is fairly straightforward and is inherently a short-run measure, which means that a correlation strategy would perform better with a lower-frequency trading strategy. Cointegration and correlation are related but distinct concepts that refer to price changes rather than returns. Cointegrated pairs can either be correlated or not. The correlation method, along with fuzzy genetic algorithms, was proposed by Cao et al. (2006) as a method for mining stock pairs on the Australian Stock Exchange. They used the correlation coefficient to find highly correlated stocks, which led to the discovery of unexpected pairs of stocks from different sectors. Miao (2014) used 15-minute interval data for 177 oil and gas stocks from the US market in a study from May 2012 onwards to choose pairs using a two-stage approach based on the correlation and cointegration methods. According to Miao (2014), the strategy generated a cumulative return of 56.58% over a 12-month period.

The most cited article on principal component analysis (PCA) in PT was written by Avellaneda and Lee (2010), who devised a statistical arbitrage strategy based on PCA and ETFs for US stocks exceeding USD 1 billion in market capitalisation between 1997 and 2007. The results of back-testing revealed that, after transaction costs were taken into account, the PCA-based strategies had an average annual Sharpe ratio of 1.44, whereas the ratio was 1.1 for ETF-based strategies. PCA filters out idiosyncratic noise by decomposing and extracting risk components. On the other hand, the performance of PCA-based strategies declined after 2002. From 2003 to 2007, the average annualised Sharpe ratio of PCA-based strategies was only 0.9, and it was 1.1 for ETF-based strategies. They also found that from 2003 to 2007, the Sharpe ratio of ETF strategies that use volume information increased to 1.51.

Neural networks have been shown to be a very good approximation to almost all nonlinear functions, according to Franses et al. (2000). Given the nonlinear nature of time series data and without specifying any nonlinear relationship beforehand, neural networks can detect nonlinearities in data. Hence, Franses et al. (2000) suggested that neural networks may be a better choice for predicting and modelling stock prices than a traditional linear framework. Furthermore, according to Lam (2004), a neural network can incorporate new data without having to reprocess old data, which is a significant benefit over more traditional methods, where the old data need to be processed again.

In the past, classification techniques using neural networks, random forests, and gradient-boosted trees have been widely used to predict whether a stock will rise or fall the next trading day. They have also been widely used to identify stocks with the potential to outperform the market. Sarmento and Horta (2020) used clustering to find the number of possible pair combinations using density-based spatial clustering of applications with noise (DBSCAN) and ordering points to identify the clustering structure (OPTICS). The classification algorithms were used to find pairs that could generate the highest average portfolio Sharpe ratio of 3.79, compared to 3.58 when no clustering was done and 2.59 when grouping by category. Applying classification algorithms to clustering pairs showed more consistency in terms of the percentage of profitable pairs in the portfolio, with an average of 86% profitable pairs in the portfolio, compared to 80% when grouping by category and 79% when doing no clustering at all. Finally, more consistent portfolio drawdowns were achieved, thereby keeping the maximum drawdown (MDD) values within an acceptable range. Our study also looks into using these algorithms but to determine whether to buy or sell a pair instead of clustering them.

ANNs consisting of the feedforward neural networks (FNN) and RNNs were used by Dunis et al. (2006) to model the spreads of gasoline and corn/ethanol. They showed that ANNs could be a relatively simple and profitable trading strategy. Their RNNs could generate returns of up to 19%, while their FNNs could generate returns of up to 41% (excluding transaction costs). Only Dunis et al. (2006, 2015) applied neural networks directly to PT, and their motivation stemmed from the neural network's superior abilities to detect nonlinearities in time series data. Due to the profitability of these methods in specific applications, it would be interesting to see how these neural networks would perform in the ETF equity markets. As a result, based on Dunis et al. (2006, 2015) approach, we use the advanced versions of the FNNs, such as the MLP, and LSTM models, instead of RNNs in this study. Fallahpour et al. (2016) also conducted a study on high-frequency PT for stocks based on the S&P 500 from June 2015 to January 2016, and they concluded that reinforcement learning outperformed other methods in obtaining the best parameters for carrying out cointegration-based high-frequency PT strategies.

1.2 Thesis Contributions

This thesis consists of four studies investigating the applications of machine learning techniques in pricing and hedging options and optimally trading ETF pairs. A summary of the contributions of the thesis per chapter is provided below.

- **Daily Forecasting of S&P 500 Index Option Prices using Deep Learning Models (Chapter 2)**
  - This chapter uses two Deep Learning ANN models, MLP and LSTM networks, along with four popular parametric models used in the industry, namely Black–Scholes–Merton, Heston, Heston Jump Diffusion, and the Finite Moment Log Stable.
  - The ANN networks are trained on lagged and one-trading-day-ahead input variables.
  - The impact of the granularity of the networks is assessed. The effects of the single, double and triple hidden layers are investigated.
  - The empirical forecasting performance of S&P 500 call option prices and moneyness is assessed from September 2012 to December 2017.
  - LSTM models (with lagged input variables) have the best forecasting performance of daily call option prices and moneyness, while MLP models (with one-trading-day-ahead input variables) outperformed the forecasting for the daily option prices.
  - Typically, three hidden layer ANN models outperform single and double hidden layer ANN models in terms of pricing performance.
- **Daily Forecasting of Delta for S&P 500 Index Options using Deep Learning Models (Chapter 3)**
  - Two deep learning ANN models are used, the triple hidden layer MLP and LSTM networks, along with four popular parametric models used in the industry, namely the Black–Scholes–Merton, Heston, Heston Jump Diffusion, and the Finite Moment Log Stable.
  - The ANN networks are trained on lagged and one-trading-day-ahead input variables.
  - The empirical forecasting performance of S&P 500 call option delta is assessed from September 2012 to December 2017.
  - The delta is predicted in two ways: directly from the network and analytically from forecasted option prices.

- The economic significance of the forecasts is evaluated by assessing the forecasting performance of corresponding replicating portfolios.
- When predicting delta directly, the Black–Scholes–Merton model outperforms the other parametric and deep learning ANN models. When the delta is computed analytically from option prices, the LSTM models outperform all other models.

- **Can Model Averaging Improve Forecasting Performance? (Chapter 4)**
  - The model averaging techniques of deep learning ANN models, namely the triple hidden layer MLP and LSTM networks with four popular parametric models used in the industry, namely the Black–Scholes–Merton, Heston, Heston Jump Diffusion, and the Finite Moment Log Stable. The ANN networks are trained on lagged and one-trading-day-ahead input variables.
  - The empirical forecasting performance of S&P 500 call option prices, moneyness and delta is assessed from September 2012 to December 2017. The delta is predicted directly from the network and analytically from forecasted option prices.
  - The economic significance of the forecasts is evaluated by assessing the forecasting performance of corresponding replicating portfolios.
  - Model averaging tends to provide improved forecasts for prices and deltas.

- **Optimal pairs trading - An Alternate Way of Trading Equity ETF Pairs Using Deep Learning Models (Chapter 5)**
  - Nine different methods are used to obtain the spread, including five different versions of the distance method, the cointegration method (using the Johansen and Engle-Granger tests), the Kalman Filter, and the ratio methods.
  - Several technical indicators, such as the Exponential Moving Averages (EMA), Relative Strength Index (RSI), Moving Average Convergence Divergence (MACD), and Bollinger Bands (BB), are used to find an alternate way to trade the spread.
  - Use Decision Trees (DT) and deep learning ANN models based on the MLP network architecture to find alternate ways to trade the spread.
  - A total of 3,084 trading strategies using the nine different methods for obtaining the spread across the 30-, 50- and 100-day rolling windows (i.e. 381 strategies across all three rolling windows for each ETF pair) are deployed and back-tested from 01 January 2019 to 31 January 2022.

– The empirical forecasting performance of eight ETF pairs is assessed, of which four ETF pairs, ITOT.N/IXUS.N, IWF.N/XLE.N, SCHB.N/SCHF.N, and SCHF.N/VO.N, that are cointegrated/correlated, and four ETF pairs, QQQ.N/XLE.N, USMV.N/XLE.N, VO.N/VXUS.N, and VWO.N/XLE.N that are not cointegrated/uncorrelated as of 01 January 2019.

– Forecasting performance is assessed using a comparative analysis based on actual PnL ($ value), returns, Sharpe ratios, max drawdown and other performance indicators.

– The impact of the profitability of these tradings strategies is gauged across the 30-, 50- and 100-day rolling windows.

– The back-test/forecasting performance of the 3,084 trading strategies across the 30-, 50-, and 100-day rolling windows demonstrates that the modified strategies can provide significant returns compared to traditional strategies.

– Machine learning-based trading strategies tend to have more predictive power than traditional strategies.

– The modified set of strategies can be applied regardless of whether the pairs are cointegrated or correlated. These strategies are designed to have a dynamic stop-loss barrier rather than the fixed stop-loss barriers that traditional strategies have. Thus, traders can hold the trade for a long duration.

1.3 Thesis Structure

This thesis consists of four studies investigating the applications of machine learning techniques in pricing and hedging options and optimally trading ETF pairs. The list of the chapters in this thesis is as follows:

- Chapter 2: Daily Forecasting of S&P 500 Index Option Prices using Deep Learning Models
- Chapter 3: Daily Forecasting of Delta for S&P 500 Index Options using Deep Learning Models
- Chapter 4: Model Averaging–Can Averaging Forecasts from Pricing and Hedging models Improve Pricing/Hedging performance?
- Chapter 5: Optimal Pairs Trading–An Alternate Way of Trading Equity ETF Pairs Using Deep Learning Models

Chapter 6 concludes the thesis and suggests avenues for future research.

Table 1.1: Non-parametric models used for pricing S&P 500 Index options

(I) No.	(II) Author(s)	(III) Data period	(IV) Data frequency	(V) Input variables	(VI) Target variable	(VII) Algorithm	(VIII) Forecasting horizon	(IX) Evaluation measure
1	Garcia and Gençay (2000)	January 1987– October 1994	Daily	S/K, T	C/K	Single Hidden Layer ANN	6 months training, 3 months validation, 3 months test	MSPE
2	Ghaziri et al. (2000)	January 1997– February 1997	Daily	S, K , r_f, TTM, σ_{60}, open interest	C	Multilayered ANN (2 hidden Layers)	Indexed observations are split into varying sizes of training, validation and test set	RMSE
3	Gençay and Qi (2001)	January 1988– December 1993	Daily	S/K, T	C/K	Modular ANN	6 months training, 3 months validation, 3 months test	MSPE, DM test
4	Dugas et al. (2001)	January 1988– December 1993	Daily	S/K, T	C/K	Single Hidden Layer ANN	6 months training, 3 months validation, 64 months test	MSE
5	Ghosn and Bengio (2002)	January 1987– December 1993	Daily	S/K, T	C/K	Single Hidden Layer ANN	3, 6, 12 and 24 months of training, 3 months of validation, followed by 12 of test	Genearlised MSE
6	Andreou et al. (2002)	May 1998– December 2000	Daily	$S^{e-\delta T}/K$, r_f, T_{365}, σ_{60}, σ_{30}, and σ_{VIX}	C/K and $(C/K - C^{BS}/K)$	Single Hidden Layer ANN	6 months training, 6 months test	MSE, MAE
7	Gençay and Salih (2003)	January 1988– December 1993	Daily	S/K, 1, σ_{20}, r_f, T	C/K	Single Hidden Layer ANN	Indexed observations are split into varying sizes of training, validation and test set	MSPE, DM test
8	Andreou et al. (2004)	January 1998– August 2001	Daily	$S^{e-\delta T}/K$, r_f, T_{365}, $\sigma^{BS}_{imp}\sqrt{T}$	$(C/K - C^{BS}/K)$, $(C/K - C^{CS}/K)$, $(C/K - C^{IJ})$, $(C/K - C^{2J}$, $(C/K - C^{SV})$, $(C/K - C^{SVJ})$	Single Hidden Layer ANN	10 different overlapping training and validation sets, separate and non-overlapping testing set	RMSE, MAE, RMeSE
9	Gençay and Gibson (2007)	January 1989– December 1991	Daily	S, K, T, $\sigma_{\text{GARCH}(1,1)}$, r_f	C	Single Hidden Layer ANN	Indexed observations are split into varying sizes of training, validation and test set	Average absolute (AAE), Average squared errors (ASE)
10	Andreou et al. (2006)	April 1998– August 2001	Daily	$S^{e-\delta T}/K$, r_f, T_{365}, $\sigma^{BS}_{imp}\sqrt{T}$	C/K and $(C/K - C^{BS}/K)$	Single Hidden Layer ANN	9 different overlapping training and validation sets, separate and non-overlapping testing set	RMSE, MAE
11	Thomaidis et al. (2006b)	08/05/2002 and 19/07/2002	Daily	S, K, δ , r_f, σ_{45}, T	C	Single Hidden Layer ANN	08/05/2002 : train and and 19/07/2002: test	MAE
12	Andreou et al. (2008)	January 1998– August 2001	Daily	$S^{e-\delta T}/K$, r_f, T_{365}, $\sigma^{BS}_{imp}\sqrt{T}$	$(C/K - C^{BS}/K)$	Single Hidden Layer ANN	10 different overlapping training and validation sets, separate and non-overlapping testing set	RMSE, MAE, MeAE
13	Gradojevic et al. (2009)	January 1987– December 1994	Daily	S/K, T	C/K	Modular ANN	Indexed observations are split into varying sizes of training, validation and test set	MAPE, DM test
14	Andreou et al. (2010)	January 2002– August 2004	Daily	$S^{e-\delta T}/K$, T, σ^{BS}_{av}, σ^{CS}_{av}	$(C/K - C^{BS}/K)$, $(C/K - C^{CS}/K)$, $(C/K - C^{SVJ}/K)$	Single Hidden Layer ANN	12 months training, 2 months validation, 1 month test	RMSE, MAE, MeAE

Table 1.2: Non-parametric models used for hedging European Index options

(I) No.	(II) Author(s)	(III) Asset Class	(IV) Data period	(V) Data frequency	(VI) Input variables	(VII) Target variable	(VIII) Algorithm	(IX) Forecasting horizon	(X) Method of inferring Delta
1	Hutchinson et al. (1994)	S&P Future 500 Options	January 1987 – December 1991	Daily	S/K, $T-t$	C/K	Single Hidden Layer ANN	10 different non-overlapping train and test set	Derived from the ANN option price
2	Herrmann and Narr (1997)	DAX Index	January 1995 – December 1995	Daily	S, K, r_f, T, σ	C	Single Hidden Layer ANN	Unknow	Derived from the ANN option price
3	Lajbcygier and Connor (1997)	SPI Futures Option	January 1993 – December 1993	Daily	F/K, $T-t$, σ	C/K	Single Hidden Layer ANN	6 months train, 6 months test set	Derived from the ANN option price
4	Ormoneit (1999)	DAX Index	March 1997	Daily	S/K	C/K	Single Hidden Layer ANN	Unknown	Derived from the ANN option price
5	Garcia and Gençay (2000)	S&P 500 Index	January 1987 – October 1994	Daily	S/K, T	C/K	Single Hidden Layer ANN	6 months train, 3 months validation, 3 months test	Derived from the ANN option price
6	Gençay and Qi (2001)	S&P 500 Index	January 1988 – October 1994	Daily	S/K, T	C/K	Single Hidden Layer ANN	6 months train, 3 months validation, 3 months test set	Derived from the ANN option price
7	Schittenkopf and Dorffner (2001)	FTSE 100 Index	January 1993 – October 1997	Daily	T	α, μ and σ	Three Single Hidden Layer ANN's	10 days training, 10 days test set	The three target variables α, μ and σ are later used in the risk-neutral density to infer the call price
8	Amilon (2003)	Swedish OMX Index	June 1997 -– March 1999	Daily	$Lagged S_t/K$, r_f, T_{365}, T, σ_{30}^{hist}, σ_{10}^{hist}, Lagged C_t^{bid}/K, Lagged C_t^{ask}/K	C/K	Single Hidden Layer ANN	4 months train (which in later iterations transforms into an expanding set), 2 months validation set, 1 month test set	Derived from the ANN option price
9	Carverhill and Cheuk (2003)	S&P Futures Option	January 1990 – December 2000	Daily	S/K, r_f, T, σ	C, δ, ν	Single Hidden Layer ANN		Derived from the ANN option price and also from ANN models trained on deltas
10	Andreou et al. (2008)	S&P 500 Index	January 1998 – August 2001	Daily	$S^{e-\delta T}/K$, r_f, T_{365}, $\sigma_{imp}^{BS}\sqrt{T}$	$(C/K - C^{BS}/K)$	Single Hidden Layer ANN	10 different overlapping training and validation sets, separate and nonoverlapping testing set	Derived from the ANN option price
11	Mostafa and Dillon (2008)	FTSE 100 Index	January 2000 – December 2001	Daily	S/K, T and σ_{hist}	C and σ_{imp}^{BS}	Single Hidden Layer ANN	1. For ANN model having C/K as target - ATM/ITM Options: 168 days train, 84 days validation, 1 day test set and OTM Options: 64 days train, 20 days validation, 1 day test. 2. For ANN model having σ_{imp}^{BS} as target - 168 days training, 84 days validation, 1 day test	1. Derived from the ANN option price. 2. Derived from the C price after plugging in the ANN predicted σ_{imp}^{BS} into the BS formula.
12	Ko (2009)	Taiwan Stock Exchange Capitalization Weighted Stock Index	January 2005 – December 2006	Daily	S, K, T, r_f, σ^{hist}	C	Two Hidden Layer ANN	80% train, 20% test	Derived from the ANN option price
13	Martel et al. (2009)	IBEX 35 Index	January 2006 – February 2008	Daily	S/K, T_{252}, T_{365}, σ_{30}, r_f	C/K	Single Hidden Layer ANN	Expanding test set of 10 months, 6 months validation and 2 months test set	Derived from the ANN option price
14	Andreou et al. (2010)	S&P 500 Index	January 2002 – August 2004	Daily	$S^{e-\delta T}/K$, T, σ_{av}^{BS}, σ_{av}^{CS}	$(C/K - C^{BS}/K)$, $(C/K - C^{CS}/K)$, $(C/K - C^{SVJ}/K)$	Single Hidden Layer ANN	12 months training, 2 months validation, 1 month test	Derived from the ANN option price
15	Chen and Sutcliffe (2012)	Short sterling futures(NYSE LIFFE)	January 2005 – December 2006	Daily	S, T, S/K	C/K	Single Hidden Layer	Expanding window where indexed obs. are split into varying sizes of training and test set	Derived from the ANN option price, the bias between the parametric model and the ANN model, and from ANN models trained on deltas.

Table 1.3: Machine Learning based models used in Pairs Trading/Selection

No.	Author(s)	Asset Class	Data period	Data frequency	Input variables	Target variables	Algorithm	Forecasting horizon
1	Dunis et al. (2006)	Gasoline crack spread	1995–2005	Daily	Percentage returns of WTI, and NYMEX Unleaded Gasoline	Percentage change in spread	RNN, MLP	One-day
2	Thomaidis et al. (2006a)	10 semiconductor stocks listed on Taiwan Stock Exchange	2003-2012	Daily	Unknown	Unknown	GA, Bollinger Bands	Quarterly
3	Dunis et al. (2009)	Soybean/oil crush spread	1995–2005	Daily	Percentage change in spread	Percentage change in spread	GARCH, ARMA, RNN, MLP	One-day
4	Dunis et al. (2015)	Corn/eth. crush spread	2005-2010	Daily	Percentage change in spread	Percentage change in spread	Naive, ARMA, MLP, HONN, GPA	One-day
5	Huck (2009)	U.S S&P 100	1992–2006	Weekly	Direction, Excess Returns	Pair selection	ELECTRE III	Weekly
6	Huck (2010)	U.S S&P 100	1993–2006	Weekly	Lagged returns	Pair selection	ELECTRE III	Weekly
7	Sarmento and Horta (2020)	Commodity linked ETF's	2009-2018	Daily	Lagged percentage change in spread	Percentage change in spread	DBSCAN, Optics, MLP, LSTM	Daily

Chapter 2

Daily Forecasting of S&P 500 Index Option Prices Using Deep Learning Models

2.1 Introduction

The Black–Scholes(BS) option pricing model introduced by Black and Scholes (1973) is a prominent conventional model for pricing options, but it assumes constant volatility, thereby failing to account for the volatility smile in observed option price data. This drawback was rectified by the Stochastic Volatility (SV) model of Heston (1993), which incorporated a second parametric process to model the underlying volatility. Doing so provided results consistent with the volatility smile of observed market data. Bakshi et al. (1997a) extended the models of Heston (1993) and Black and Scholes (1973) by incorporating stochastic volatility and jumps. These models capture more realistic features of the price dynamics, and there is empirical evidence that incorporating jumps improves pricing performance (Eberlein and Raible (1999)). Despite many alternative parametric models and the limitations in Black and Scholes (1973), the BS model is still frequently used in price European options because of its simplicity in implementing and achieving a closed-form pricing solution. However, these approaches involve complex empirical modelling, which often proves challenging to implement in real trading situations. Artificial Neural Networks (ANNs) are considered an alternative to the standard parametric option models, where the forecast of S&P 500 index option prices has typically performed using a single hidden layer ANN (see Andreou et al. (2002, 2004, 2006, 2008, 2010), Dugas et al. (2001), Garcia and

Gençay (2000), Gençay and Salih (2003), Ghosn and Bengio (2002), Thomaidis et al. (2006a)).

This chapter offers a comprehensive assessment of daily forecasting of European-style index options using parametric models, which practitioners commonly use compared to non-parametric models. The non-parametric models used in this study are Deep Learning ANN models, including the Multilayer Perceptron (MLP) and the Long Short-Term Memory (LSTM) networks [1]. MLPs are likely to perform best for high-frequency financial data for optimal results in pricing and hedging of options (Hutchinson et al. (1994), Gençay and Qi (2001), Garcia and Gençay (2000), Andreou et al. (2008), Thomaidis et al. (2006a)). Furthermore, LSTM addresses the issue of the vanishing or exploding gradient with the first RNNs and has provided improved time series forecasting (Masini et al. (2021), Lim and Zohren (2021), Figueiredo and Saporito (2022)). Thus, this study aims to empirically investigate the relative performance of deep learning models compared to parametric models. To this end, an extensive data set of daily data on S&P 500 index option prices from September 2012 to December 2017 is used to forecast one-trading-day-ahead call option prices and moneyness. We investigate the forecasting performance of single, double and triple hidden layer Deep Learning ANN models using MLP and LSTM networks along with four parametric models (Black–Scholes–Merton, Heston, Heston Jump Diffusion, and the Finite Moment Log Stable(FMLS)). These MLP and LSTM networks with single, double, and triple hidden layers are trained on various lagged and one-trading-day-ahead input variables. More specifically, we forecast one-trading-day-ahead call option prices and corresponding moneyness by comparing 72 MLP and 72 LSTM models, with 8 parametric models having lagged input variables, 18 triple hidden layer MLP, and 18 triple hidden layer

[1] ANNs, technically speaking, can be called parametric since it has a fixed number of parameters, i.e. one for each weight that is tuned during training; as the number of weights generally stays constant, they technically have fixed degrees of freedom. However, most ANNs have so many parameters that they could be interpreted as non-parametric; it has been proven that in the limit of infinite width, a deep neural network can be seen as a Gaussian process, which is a non-parametric model(Lee et al. (2017)) (the Gaussian processes here uses each observation as a new weight and as the number of points goes to infinity so do the number of weights). Nevertheless, ANNs would not be considered parametric as parametric models are defined as models which are based on an a priori assumption about the distributions that generate the data, which tends to be a hallmark of non-parametric models. ANNs do not make assumptions about the data-generating process; rather, they use large amounts of data to learn a function that maps inputs to outputs. Alternatively, parametric models force the data to fit into the assumed distribution, whether correct or not. In past literature the following studies have considered MLPs: Lee et al. (2017), Umeorah et al. (2023), Hutchinson et al. (1994), Ince (2006), Ivașcu (2021), Hajizadeh (2020), Bloch (2019), and Khaldi et al. (2019), and LSTMs: Lee et al. (2017), Gupta et al. (2020), Ouyang et al. (2018), Gautam and Singh (2020), and Gu et al. (2021) to be non-parametric because they can represent such a wide range of input-output mappings that they effectively do not share the distributional assumptions. Hence, ANN models can be termed as non-parametric by reasonable definition.

LSTM models with 8 parametric models having one-trading-day-ahead input variables.

These different input variable specifications would allow comparing forecasting performance based on the selection of input variables. Furthermore, we perform robustness tests based on bounds assessments and DM tests to assess the significance of pairwise comparisons between the corresponding ANN and parametric models. This study focus on (only) one-trading-day-ahead forecasts aiming to provide an assessment suitable for short-term trading and risk-management applications. These methodologies can be extended to longer forecast windows, but it is beyond the purpose of this thesis. The purpose of only using one-trading-day-ahead forecast is to tackle look-ahead bias, and more importantly, forecasting on a short-term window enables traders to quickly adjust their positions to changing market conditions.

We find that forecasting one-trading-day-ahead call option prices and moneyness with various inputs provide considerable improvement in the out-of-sample forecasting performance of these networks. Even though the comparison between a large number of models was not conclusive, regarding the forecasting performance of (one-trading-day-ahead) call option prices or moneyness, the overall best-performing models are the LSTM models using lagged input variables and the MLP models using one-trading-day-ahead input variables. When the comparison is confined only to parametric models, the Heston Jump Diffusion model has the lowest RMSEs than other parametric models (when using lagged or one-trading-day-ahead input variables). We also demonstrate that when we re-scaled the moneyness of models that use lagged input variables to forecast the call option price, these re-scaled models perform poorly to the models that directly forecast the call option price using lagged input variables, with again the LSTM models outperforming the other models. The results remain the same based on a bound assessment of performance, while the DM tests showed that out of the 3768 model pairs, only 1.69% of the pairs had insignificant forecasting power.

Compared to previous literature,[2] this study makes the following key contributions: a) It provides daily forecasts of S&P 500 option prices, while most of the literature is based on longer forecasting windows; thus, this study has relevance to short-term trading and investment applications. b) It considers a wider range of explanatory variables and network sizes,[3] e.g. employing triple hidden layers networks. c) It introduces lagged input variables to tackle look-ahead bias while using a test set for the parametric, MLP and LSTM models. We benchmarked our model performance against the performance achieved by Andreou et al. (2010) (Andreou et al. (2010)

[2]Refer to the list of papers in Table 1.1

[3]Refer to Tables A.1.1, A.1.2, A.1.3, A.1.4

extended the models of Andreou et al. (2004), Andreou et al. (2006) and Andreou et al. (2008)), as they studied pricing S&P 500 index options from January 2002–August 2004 and compared an SV and SVJ with an ANN. They partitioned their data set into 18 different training/estimation validation sets, each followed by a separate and non-overlapping test set. Although Andreou et al. (2010) had a test set, which was non-overlapping and distinct from other data sets (train and validation) and termed as an out-of-sample set, this method did not use lagged variables in the test set, resulting in a look-ahead bias. Consequently, their SV model displayed an out-performance compared to the best-performing ANN models used in their study. Andreou et al. (2010) (and much of the associated literature) used input variables, for example, the end-of-day index close prices belonging to the test set to forecast the end-of-day call option prices or moneyness, where the index price was only available at the close of that trading day, thus inducing look-ahead bias. Similarly, Ghaziri et al. (2000) used the BSM model and the MLP model for pricing S&P 500 index call options (excluding deep ITM options) and found that the ANN models outperformed the BSM model. Most other similar studies[2] have presented their results in an evaluation measure other than RMSE. However, as our study assessed the daily forecast of call option prices and moneyness, and we used RMSE as a measure. The RMSEs were reported on a daily basis for 1,328 days, unlike, for example, Andreou et al. (2010), who had eighteen tests set forecasts. Thus, if we calculate the overall RMSE (from the respective models' daily RMSEs for a window spanning from September 2012 to December 2017) of all that use one-trading-day-ahead input variables for forecasting call option prices and moneyness, we can see at par forecasting performance.

This chapter is organised into six sections. Section 2.2 provides the theoretical aspects of the parametric and non-parametric ANN pricing models used in the study, namely, MLP and LSTM models. Section 2.3 describes the data and methodology, including the calibration procedures used in the parametric models and the network parameters, the division of the data set, and the optimisation and generalisation procedures to improve the accuracy of ANN models. Section 2.4 presents the findings of comparing the forecasting performance of the parametric models with the MLP and LSTM models and the robustness tests performed on these models. The chapter concludes with Section 2.5.

2.2 Pricing Models

In this section, we discuss the theoretical aspects of the parametric (Black–Scholes–Merton (BSM), Heston, Bates Model (Heston Jump Diffusion (HJD)), and Finite Moment Log Stable (FMLS)) and non-parametric models (Multilayer Perceptron and Long Short Term Memory Network) used for forecasting call option prices.

2.2.1 Black–Scholes–Merton Model

The simplest parametric model we consider is the so-called Black–Scholes–Merton model of option pricing, proposed in the seminal papers of Black and Scholes (1973) and Merton (1973). This model proposes that the underlying (index spot price) S_t is a random process modelled by the stochastic dynamics of geometric Brownian motion, given by the stochastic differential equation:

$$\frac{dS_t}{S_t} = \mu dt + \sigma dW_t, \tag{2.1}$$

where W_t is a standard Wiener process. The parameter μ is referred to as the instantaneous expected total return of the index, and the parameter σ is referred to as the instantaneous standard deviation of index price returns. The choice $\mu = r - q$ is required under so-called risk-neutral dynamics for risk-free rate r and continuous dividend yield rate q. The prices of European call options on a continuous dividend-paying stock/index are well known and are given by:

$$C_t = S_t e^{-q(T-t)} N(d_1) - K e^{-r(T-t)} N(d_2), \tag{2.2}$$

where, K is the strike price, T is the time to expiration and $N(\cdot)$ is the cumulative normal distribution, and d_1 and d_2 are given by

$$d_1 = \frac{\ln(S_t/K) + (r - q + \sigma^2/2)(T-t)}{\sigma\sqrt{(T-t)}}, \tag{2.3}$$

$$d_2 = \frac{\ln(S_t/K) + (r - q - \sigma^2/2)(T-t)}{\sigma\sqrt{(T-t)}}. \tag{2.4}$$

We used the approach of using characteristic functions for contingent claims pricing to have a consistent approach across all the parametric models discussed in this chapter. The use of characteristic functions was proposed by Martin (2006), and Bakshi and Madan (2000). They showed how Fourier transformed state price densities or Arrow–Debreu securities could be used to reduce the valuation problem of Black and Scholes (1973) by using appropriately modified equivalent probability measures. Thus, the call option formula reduces to

$$C_t = \frac{1}{2}\left(S_t - e^{-rT}K\right) + \frac{1}{\pi}\int_0^\infty S_0\Re\left[\frac{e^{iuk}\phi_T(u-i)}{iu}\right] - e^{-rT}K\Re\left[\frac{e^{iuk}\phi_T(u)}{iu}\right]\mathrm{d}u \tag{2.5}$$

where, $\Re$ is the real part of the complex-valued integrand, $k = \ln(K)$, and the characteristic function has the form,

$$\phi_T(u) = \mathbb{E}\left[e^{\mathrm{i}uX_T}\right] = \exp\left[\mathrm{i}\omega uT - \frac{\sigma^2u^2}{2}T\right] \tag{2.6}$$

where, u is an arbitrary real number, $\omega = -\frac{1}{2}\sigma^2$, $X_T = \ln(S_T)$, $\mathrm{i} = \sqrt{-1}$ is the imaginary unit.

2.2.2 Heston Model

Heston (1993) proposed a model that extended the model of Black and Scholes (1973) and considered the non-lognormality of asset returns, the leverage effect, and the mean-reverting property of volatility. The model is defined by a coupled set of stochastic differential equations:

$$\frac{dS_t}{S_t} = \mu dt + \sqrt{V_t}dW_{1,t} \tag{2.7}$$

$$dV_t = \kappa(\theta - V_t)dt + \sigma\sqrt{V_t}dW_{2,t} \tag{2.8}$$

where the Wiener processes $(W_{1,t}, W_{2,t})$ are correlated with a quadratic variation given by

$$dW_{1,t}dW_{2,t} = \rho dt \tag{2.9}$$

where V_t is the variance, $\kappa > 0$ is the mean reversion speed for the variance, $\theta > 0$ is the mean reversion level for the variance, $\sigma > 0$ is the volatility of the variance, $V_0 > is0$ the initial (time zero) level of the variance, $\rho \in [-1, 1]$ is the correlation between the two Brownian motions $W_{1,t}$ and $W_{2,t}$ (see Rouah (2013)). According to Rouah (2013), at time t, the price C_t, of a European call on a dividend-paying index with spot price S_t, when the strike price is K and the time to maturity is T is

$$C_t\left(S_t, K, V_t, T\right) \quad = \quad \mathbb{E}[e^x]P_1 - Ke^{-r\tau}P_2 \ , \tag{2.10}$$

where the time maturity $\tau = T-t$, $x = x_t = \ln S_t$, and P_1 and P_2 are the conditional risk-neutral probability/in-the-money probabilities that can be derived from the characteristic function using the Gil-Pelaez (1951) inversion theorem, when the characteristic functions $f(\phi; x, v)$ are known as below,

$$P_1 = \mathbb{E}\left[\mathrm{e}^x \mathbb{I}_{\{\mathrm{e}^x > K\}}\right] / \mathbb{E}\left[\mathrm{e}^x\right] = \frac{1}{2} + \frac{1}{\pi}\int_0^\infty \Re\left[\frac{\mathrm{e}^{-\mathrm{i}\phi \ln K} f(\phi - i; x, v)}{i\phi f(-i; x, v)}\right] d\phi, \tag{2.11}$$

$$P_2 = \Pr\left(\ln S_T > \ln K\right) = \frac{1}{2} + \frac{1}{\pi}\int_0^\infty \Re\left[\frac{e^{-\mathrm{i}\phi \ln K} f(\phi; x, v)}{i\phi}\right] d\phi, \tag{2.12}$$

where the characteristic functions, $f\left(\phi; x_t, v_t\right)$ for the logarithm of the terminal stock price $x_T = \ln S_T$ have the form,

$$f\left(\phi; x_t, v_t\right) = E\left[e^{i\phi x_T}\right] = \exp\left(C(\tau, \phi) + D(\tau, \phi)v_t + i\phi x_t\right), \tag{2.13}$$

where, $C(\tau, \phi)$ and $D(\tau, \phi)$ are defined as:

$$C(\tau, \phi) \quad = \quad ri\phi\tau + \frac{a}{\sigma^2}\left[\left(b_i - \rho\sigma i\phi + d\right)\tau - 2\ln\left(\frac{1 - ge^{d\tau}}{1 - g}\right)\right] \ , \tag{2.14}$$

$$D(\tau, \phi) \quad = \quad \frac{b - \rho\sigma i\phi + d}{\sigma^2}\left(\frac{1 - e^{d\tau}}{1 - ge^{d\tau}}\right) \ , \tag{2.15}$$

where, $a = \kappa\theta$, and

$$g \quad = \quad \frac{b - \rho\sigma i\phi + d}{b - \rho\sigma i\phi - d} \ , \tag{2.16}$$

$$d \quad = \quad \sqrt{\left(\rho\sigma i\phi - b\right)^2 - \sigma^2\left(2ui\phi - \phi^2\right)} \ , \tag{2.17}$$

$$b \quad = \quad \kappa + \lambda - \rho\sigma \ , \tag{2.18}$$

$$\phi \quad = \quad -0.5 \ . \tag{2.19}$$

2.2.3 Bates Model (Heston Jump Diffusion (HJD))

The Bates (1996) option pricing model was designed to capture the conditional volatility, which evolves in a stochastic but mean-reverting fashion, and the presence of occasional substantial outliers in asset returns. The Stochastic Differential Equations (SDEs) for the asset follow a geometric jump diffusion with the instantaneous conditional variance (V_t) following a mean reverting square root process, which are given by,

$$\frac{dS_t}{S_t} = (\mu - \lambda\bar{k})dt + \sqrt{V_t}dW_{1,t} + kdq \tag{2.20}$$

$$dV_t = (\alpha - \beta V_t)dt + \sigma\sqrt{V_t}dW_{2,t} \tag{2.21}$$

where, λ is the annual frequency of jumps and k is the random percentage jump conditional on a jump occurring, with the Brownian motions correlated as in Eq.2.9 and the Poisson process (dq) given by,

$$dq = \begin{cases} 0 & \text{with probability } 1 - \lambda dt \\ 1 & \text{with probability } \lambda dt \end{cases}$$

According to Martin (2006), the value of a European call option evaluated using Bates (2006)'s approach of using a characteristic function is,

$$C\left(S_0, T, K\right) = S_0 - e^{-rT} K \left(\frac{1}{2} + \frac{1}{\pi} \int_0^\infty \Re \left[\frac{e^{-\mathrm{i}u \ln \frac{K}{S_0}} \phi_T(u)}{\mathrm{i}u(1-\mathrm{i}u)} \right] \mathrm{d}u \right) \quad , \tag{2.22}$$

where the characteristic function ϕ_T is the expected value of the complex exponential of the logarithmic price $x = \ln S_T$ and is defined as

$$\phi_T(u) = \mathbb{E}\left[e^{\mathrm{i}ux}\right] = \int_{-\infty}^{\infty} e^{\mathrm{i}ux} q_T(x) \mathrm{d}x \quad , \tag{2.23}$$

and q_T is the risk-neutral density of x relative to the martingale measure $\mathbb{Q}$,

$$q\left(S_T\right) = \frac{1}{S_T \sigma \sqrt{2\pi T}} e^{-\frac{\left\{\ln S_T - \left(\ln S_0 + \left(r - \frac{1}{2}\sigma^2\right)T\right)\right\}^2}{2\sigma^2 T}} \quad . \tag{2.24}$$

2.2.4 Finite Moment Log Stable (FMLS) Model

Carr and Wu (2003) addresses the volatility skew for S&P 500 index options, which does not flatten as the time to maturity increases. According to Martin (2006), Carr and Wu (2003) defines the characteristic function as follows:

$$\phi_T(u) = \mathbb{E}\left[e^{\mathrm{i}uX_T}\right] = \exp\left[\mathrm{i}u\omega T - (\mathrm{i}u\sigma)^\alpha T \sec\frac{\pi\alpha}{2}\right] \quad , \tag{2.25}$$

where the convexity adjustment term is introduced to maintain the martingale property as,

$$\omega = \sigma^{\alpha} \sec \frac{\pi \alpha}{2} \quad , \tag{2.26}$$

and the tail index $\alpha \in (1, 2]$ controls the tail behaviour and σ controls the width of the risk neutral density. When $\alpha = 2$, the FMLS model coincides with the Black–Scholes–Merton model, and the Black–Scholes–Merton volatility (σ_{BSM}) relates to risk-neutral on measure (σ_{FMLS}) where $\sigma_{BS} = \sigma_{FMLS}\sqrt{2}$.

2.2.5 Deep Learning Neural Networks

Ruf and Wang (2021) cite that ANNs have been used as a non-parametric method for partial differential equations, option pricing and hedging, and model calibration since they do not assume an underlying stochastic model, and they eliminate unrealistic assumptions present in pricing methods based on modelling the movement of underlying assets. They are also capable of learning the pricing function directly from data, and this method of pricing European options is known as the nonparametric pricing approach. Even though training ANNs takes time, they have a significant computational advantage over more conventional numerical pricing techniques like Monte Carlo and partial differential equations.

2.2.5.1 Multilayer Perceptron (MLP)

The multilayer perceptron network model belongs to the class of feedforward artificial neural networks (ANN). The MLP network has multiple inputs, which are connected to hidden layers having multiple neurons and to the output layer. An ANN consists of a set of input variables $(X_i), i = 1, ..., N$, to an output variable y, and uses functions to transform the X_i using one or more hidden layers. This hidden layer approach is an efficient way to model non-linear statistical processes. The architecture of an ANN consisting of a single hidden layer and j number of neurons can be represented as:

$$y = \gamma_0 + \sum_{j=1}^{J} \gamma_j f_j \left(\beta_{j,0} + \sum_{k=1}^{K} \beta_{j,k} X_k \right) \tag{2.27}$$

The linear regression model can also be stated as a variant of the feedforward ANN, in which the hidden layer consists of a single neuron using a linear function (having a weight of one) that connects to the output layer or target variable. In Eq.(2.27), the parameters γ_0 and $\beta_{j,0}$, for $j = 1, .., J$, are called biases, while the parameters γ_j and $\beta_{j,k}$, for $j = 1, .., J$ and $k = 1, .., K$, are known as the weights. These parameters are generally estimated by specialised non-linear optimisation methods known as back-propagation algorithms, which are implemented in many software packages.

Many of the networks used in past literature in modelling S&P 500 Index options were single-layer artificial neural networks. Table 1.1 provides a summary of a representative selection of these studies, with details of the data period, the data frequency, the input and target variables, the prediction or forecasting horizon, and as the architecture of the study's network.

According to Heaton (2008), an ANN with a single hidden layer can approximate any function that contains a continuous mapping from one finite space to another, whereas a network with two hidden layers can represent functions of any shape. The recommended rule-of-thumb method of Heaton (2008) for determining the number of neurons to use in the hidden layers is to have the total number of neurons in the hidden layers between the size or dimension of the input layer and the size or dimension of the output layer. As a result, Heaton (2008) preferred having the total number of hidden neurons to be two-thirds the size of the inputs used in the input layer plus the size of the output layer, thereby ensuring that the total number of neurons in the hidden layer be less than twice the size of the input layer. Though these rules for selecting the number of hidden neurons are based on modelling experience, ultimately, in any application, selecting an architecture of the ANN will come down to trial and error. Thus, in this study, we follow Heaton (2008) and also try to simplify the process of selecting the total number of neurons by comparing three network architectures: a single, double and triple hidden layer network having the total number of neurons in each hidden layer equal to the number of inputs. For the purpose of pictorially illustrating an ANN having the total number of neurons in each hidden layer equal to the number of inputs, we depict the network architecture of the three hidden layer MLP model in Figure 2.1, which has an input layer with 10 input variables, three hidden layers, each having 10 neurons, and a single neuron output layer. Each neuron is connected with all neurons in the previous layer and in the forward layer. Each layer has one or more neurons, and the output of each layer passes through a transfer function. In the MLP models used in this study, the transfer function employed is the hyperbolic tangent sigmoid (tansig) function, as Hahn (2013) used the tansig function in their MLP models and also because, after comparing a number of transfer functions, we concluded the tansig function to be the best at forecasting. The number of neurons across each hidden layer uses the same type of activation function, whereas we employ a simple linear activation function for the output neuron.

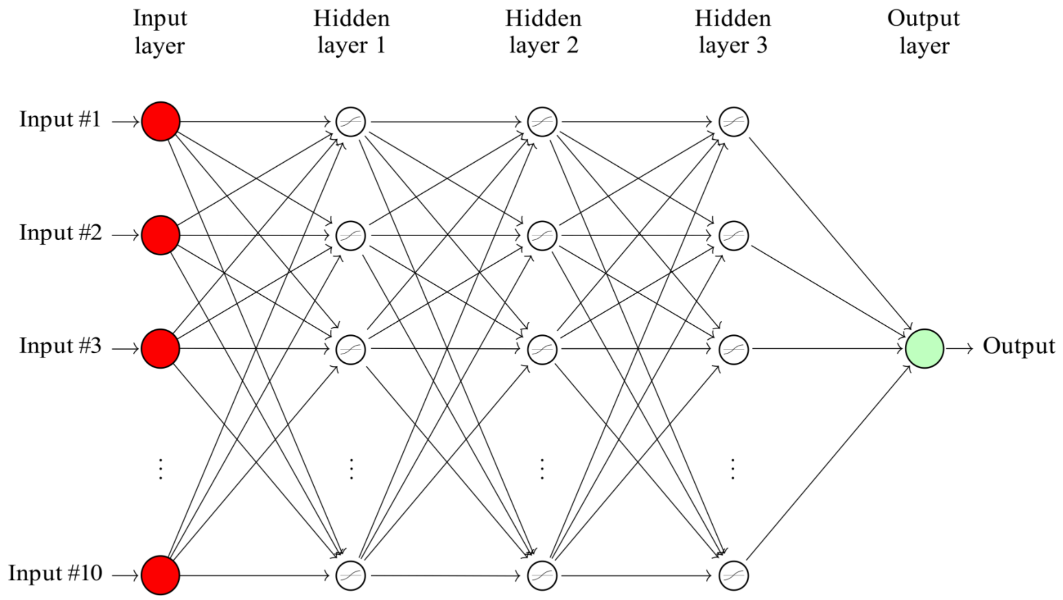

Figure 2.1: Deep Learning Network: A three hidden layer network and a single neuron output layer. The hidden layers use the tansig activation function and the output layer a simple linear activation function.

2.2.5.2 Long Short-Term Memory (LSTM) Network

The fundamental characteristic of a Recurrent Neural Network (RNN) is that it has at least one feedback connection, which means that the hidden layer (layer A in Figure 2.2) forms a loop and this looping makes the RNNs memorise the previous state. A simple unfolded RNN with multiple loops is shown in Figure 2.2, which illustrates unrolling at times 0 to t.

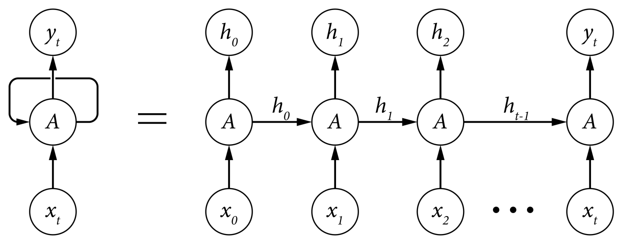

Figure 2.2: The structural diagram of a folded /unfolded Recurrent Neural Network.

The RNN can be described using the following equations:

$$\begin{aligned} h_t &= f_t\left(w_i x_t + w_t h_{t-1}\right) \\ y_t &= f_o\left(w_o h_t\right) \end{aligned}$$

where x_t is the input, h_t is the memory of the RNN, w_i is the weight matrix between the input and the hidden layer, w_t is the weight matrix between the delayed hidden layer and current hidden layer, f_t is the hidden layer activation function, y_t is the final output from the RNN (as shown in the unfolded RNN, Figure 2.2), f_o is the output hidden unit activation function, and w_o is the weight matrix between the output hidden layer and final output.

LSTMs are a variation of RNN, which are composed of long short-term memory blocks. The LSTMs help the error to be back-propagated through time and layers, which allows the network to learn over multiple time steps. Although the LSTM model has been explained in the past literature, we use the notations and explanations provided by Hou and Edara (2018), and Zhang et al. (2019). The LSTM network has two states: cell state and hidden state, as well as three gates: input gate, forget gate, and output gate. The forget and input gates are based on sigmoid functions. The procedures during a single pass are as follows:

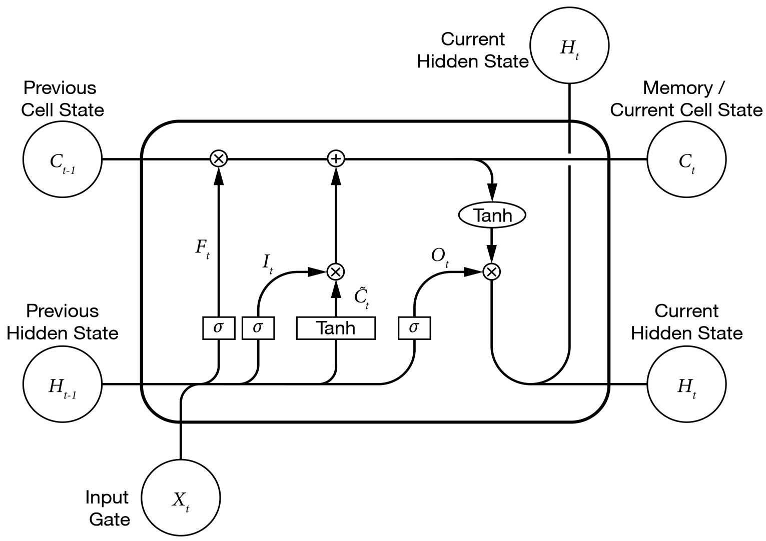

Figure 2.3: The structural diagram of a single LSTM node.

1. The forget gate (F_t) selectively adds or removes information to the memory cell state. The network initially commences by deciding the amount of information that needs to be discarded, for which the information is initially funnelled through the forget gate (sigmoid function) and along with that it also uses the output from the previous LSTM cell (H_{t-1}), also known as the hidden state. The output from the forget gate is as below (w_F is the weight and b_F is the bias matrix associated with the forget gate layer):

$$F_t = \sigma \left(w_F \cdot [H_{t-1}, X_t] + b_F \right)$$

2. Later, the new information that needs to be added and stored to the previous cell state (C_{t-1}) happens in two steps. The input gate (I_t) (which is a sigmoid function) first determines which values ought to be updated, and the output is as follows (w_I is the

weight and b_I is the bias matrix associated with the information gate layer):

$$I_t = \sigma\left(w_I \cdot [H_{t-1}, X_t] + b_I\right)$$

3. The output from the tanh function creates a set of candidate values ($\tilde{C}_t$), which updates the previous cell state (C_{t-1}), as follows ($w_{\tilde{C}}$ is the weight and $b_{\tilde{C}}$ is the bias matrix associated with the candidate gate layer):

$$\tilde{C}_t = \tanh\left(w_{\tilde{C}} \cdot [H_{t-1}, X_t] + b_{\tilde{C}}\right)$$

4. This creates the new memory cell state (C_t), which is passed onto the next LSTM cell as follows:

$$C_t = F_t * C_{t-1} + I_t * \tilde{C}_t$$

5. Finally, using the new memory cell state and the information from O_t, we get the outcome from the output gate as (w_O is the weight and b_O is the bias matrix associated with the output gate layer),

$$\begin{aligned} O_t &= \sigma\left(w_O\left[H_{t-1}, X_t\right] + b_O\right) \\ H_t &= O_t * \tanh\left(C_t\right) \end{aligned}$$

where the activation function tanh is the hyperbolic tangent function, which squeezes the value between -1 and 1.

$$\begin{aligned} \sigma(x) &= \frac{1}{1+e^{-x}} \\ \tanh(x) &= \frac{e^x - e^{-x}}{e^x + e^{-x}} \end{aligned}$$

2.3 Data and Methodology

2.3.1 Optionmetrics

The S&P 500 Index is widely regarded as the best gauge of the US large capitalisation equity market. The Chicago Board Options Exchange offers a suite of highly liquid S&P option products on this index. This chapter focuses on the traditional SPX options that are AM-settled on the third Friday of every month. These are European-style options with a large contract size and with a cash settlement. It is a highly liquid market, with the average daily volume exceeding a million contracts since 2016. The data source is end-of-day data from OptionMetrics, which compiles option data and the corresponding spot S&P 500 index level at 3:59 pm each day (which avoids any non-synchronicity issues). The options data period is from September 2012 to December 2017. [4] The call prices used for this study are defined as the mid-point price calculated from the best bid and best offer prices. Another advantage of this data source is that data and methodology to obtain daily interest rate curves are provided as well as the daily S&P 500 Index dividend yield. The variables and their field descriptions from the OptionMetrics database are listed in Appendix A.1.1.

2.3.2 Data Filtering

The study focuses on SPX call options. The data period is from September 9, 2012, through December 31, 2017, and the database has a total of 1,669,494 observations on SPX call options. The following filters have been applied:

- All trades having a bid price equal to zero are deleted (75,746 observations).
- The maturity of the options is limited to the range of 7 days to 365 days inclusive. This is a common restriction in the literature and is usually justified by the illiquidity of the options excluded (53,739 observations).
- As the trading volume tends to concentrate on options close to being at-the-money, we delete 55,647 options with a moneyness (i.e. S_t/K_t) less than 0.8 (55,647 observations) and greater than 1.2 (832,892 observations).
- As the previous trading day's call price is used as an input to the neural networks, we remove those observations having no previous day option price (16,393 observations).

[4] The options data were obtained from OptionMetrics via Wharton Research Data Services (WRDS), which is the most clean and reliable historical data provider. OptionMetrics provides the best bid and ask quotes for each strike and expiration, underlying prices, implied volatility and greeks for each option, CUSIP and ticker information for each option, and the daily index dividend yield for S&P 500 Index options. Also, OptionMetrics provides the daily zero curves which are crucial for interpolating interest rates. Users of WRDS could access S&P 500 Index options data through OptionMetrics only as of September 2012. This is a representative period for the study to investigate the performance of such models. Under more volatile market conditions, such as the 2008 global financial crisis (GFC), more advanced models may be more suitable (e.g. incorporating stochastic volatility features). We also do not expect results to change significantly, as the thesis considers a wide range of model specifications.

Thus, the total number of observations on call options used in this study is 560,526. For each option on each trading day, N, we have available the call price C_N, the call price on the previous trading day C_{N-1}, the index price S_N, the exercise price K_N, the time to maturity T_N, the risk-free rate of interest matching that time to maturity R_N, and, the S&P 500 Index dividend yield Q_N.

2.3.3 Summary Statistics

Table A.1.17 provides the summary statistics for the call option prices used in this chapter. The monthly summary statistics show that the total number of daily option prices each month varies from $2,005$ to $10,956$, with the number of transactions growing from about $6,500$ in 2012 to about $10,000$ in 2017. The monthly average call price varies from \$67.11 to \$156.71, so we see that these average prices have more than doubled from 2012 to 2017. In contrast, the average bid-ask spread, which varies from \$0.81 (in December 2012) to \$1.84 (in November 2017), has increased by a smaller percentage. The CBOE reports that the annual average daily volume has increased from $698,000$ SPX contracts in 2012 to $1,163,000$ SPX contracts in 2017.

2.3.4 Forecasting Errors

Consider the situation of modelling or forecasting call prices (C_{N+1}) on day $N+1$ based on information sets F_{N+1}, X_{N+1}, or X_N, where F represents all available information and X is a subset of F. If there is a true model relating the call prices to the information set, then we represent this functional form as:

$$C_{N+1} = g\left(F_{N+1}; \theta_{N+1}\right) + u^r_{N+1} \tag{2.28}$$

for some function $g(.)$, and parameter vector θ_{N+1}, where u^r_{N+1} is a random error caused by market frictions such as the bid-ask spread. Let any model be represented as:

$$\hat{C}_{N+1} = h\left(X_{N+1}; \phi_{N+1}\right) \tag{2.29}$$

for some function $h(.)$, where X_{N+1} is the con-current information set and ϕ_{N+1} a parameter vector. All of the parametric and non-parametric models could be represented in this manner.

By considering various decompositions of Eq. (2.28) we can carefully describe a number of types of forecast errors. First, consider:

$$C_{N+1} = h\left(X_{N+1};\phi_{N+1}\right) + \left[g\left(F_{N+1};\theta_{N+1}\right) - h\left(X_{N+1};\phi_{N+1}\right)\right] + u^{r}_{N+1} \quad (2.30)$$

$$C_{N+1} = h\left(X_{N+1};\phi_{N+1}\right) + u^{g}_{N+1} + u^{r}_{N+1} \quad (2.31)$$

where u^{g}_{N+1} can be considered an error in not using the unknown true model. Second, consider:

$$C_{N+1} = h\left(X_{N+1};\hat{\phi}_{N+1}\right) + \left[h\left(X_{N+1};\phi_{N+1}\right) - h\left(X_{N+1};\hat{\phi}_{N+1}\right)\right] + u^{g}_{N+1} + u^{r}_{N+1} \quad (2.32)$$

$$C_{N+1} = h\left(X_{N+1};\hat{\phi}_{N+1}\right) + u^{\phi}_{N+1} + u^{g}_{N+1} + u^{r}_{N+1} \quad (2.33)$$

where u^{ϕ}_{N+1} can be considered the error made in using the estimated or calibrated parameters rather than the true parameter values. Third, consider:

$$C_{N+1} = h\left(X_{N};\hat{\phi}_{N+1}\right) + \left[h\left(X_{N+1};\hat{\phi}_{N+1}\right) - h\left(X_{N};\hat{\phi}_{N+1}\right)\right] + u^{\phi}_{N+1} + u^{g}_{N+1} + u^{r}_{N+1} \quad (2.34)$$

$$C_{N+1} = h\left(X_{N};\hat{\phi}_{N+1}\right) + u^{X}_{N+1} + u^{\phi}_{N+1} + u^{g}_{N+1} + u^{r}_{N+1} \quad (2.35)$$

$$C_{N+1} = h\left(X_{N};\hat{\phi}_{N+1}\right) + \epsilon_{N+1} \quad (2.36)$$

where u^{X}_{N+1} is the error caused by using X_N rather than X_{N+1}, which is interpreted as forecasting using observations from the previous trading day rather than the trading day that the call option is observed. The decomposition of the out-of-sample forecast errors demonstrates that there are four components (see Eq. (2.35)). It may be that the error caused by having to forecast the inputs (that is, using X_N as the input variables rather than X_{N+1}) is the dominant source of error. If the forecast errors are computed using (the unobserved) actual values of the input variables (that is, using X_{N+1} as the input variables), then these errors have only three components (see equation (2.33)). In the analysis presented in Sections 2.4.1, and 2.4.2, we consider the forecast errors as defined by ϵ_{N+1} so that the forecasts are made for the trading day $N + 1$ based on information available at the end of the trading day N. Similarly, in the above-mentioned sections, we also consider the forecast errors as defined by ϵ_{N+1}, so that the forecasts are made for the trading day $N + 1$ based on information available at the end of the trading day $N + 1$. The definition of this forecasting error shows that there are a number of potential sources of forecasting errors, only one of which is due to the choice of model type —

that is parametric or non-parametric. By applying these techniques, we can get some insight into whether the global approximation property of Deep Learning ANN models is able to produce some advantage over parametric models in forecasting, along with considering the performance of other parametric models. This question is the focus of current research.

2.3.5 Information Sets for Models

The focus of this chapter is the forecasting performance of parametric option pricing models relative to Deep Learning ANN (MLP and LSTM) models. The calibration of parametric models is performed under two different specifications: use option prices as input variables, called the *C-Models*, and use option prices scaled by the strike price as input variables called the *CK-Models*. Thus we have parametric and non-parametric models that fall under two categories, *C-Models* and *CK-Models*. In this section, we discuss the information sets employed for calibration and parameter estimation of each type of these models and for subsequently forecasting the one-trading-day-ahead option price C_{N+1} or C_{N+1}/K_{N+1}.

2.3.5.1 Information Sets for *C-Models*

We define the information sets required for each model for calibration or estimation of parameters and for forecasting the call option price (C_{N+1}). We implement a single forecasting horizon, that is one-trading-day-ahead forecasts, so we use the information available on day $t = N$ to forecast option prices for day $t = N + 1$. The parametric models are calibrated daily, based only on the data available for day N. In contrast, the MLP models use an expanding window, the LSTM models use a fixed window, and both the MLP and LSTM use data for $t = 1, ..., N$ for estimation and forecast for day $t = N + 1$. Thus the parametric models follow the usual convention of daily calibrations, whereas the expanding (for the MLP) and fixed-sliding (for the LSTM) window allows the ANNs to cover a wide range of values for its input variables. We use ϕ to represent a generic parameter scalar or vector for each model.

2.3.5.1.1 *C-Models*: Parametric Models (Black–Scholes–Merton, Heston, Heston Jump Diffusion, and Finite Moment Log Stable Model)

For the parametric models that fall under the *C-Models* category, on day N the information used to calibrate the model parameters for each option ($C_N, S_N, K_N, T_N,$

$R_N, Q_N; \phi_N^{Model}$), and we define the in-sample pricing error, $\epsilon_N^{Model_N}$ for each option under each model as:

$$\epsilon_N^{Model_N} = C_N - f^{Model}\left(S_N, K_N, T_N, R_N, Q_N; \phi_N^{Model}\right) \tag{2.37}$$

where ϕ_N^{Model} and f^{Model} for each model are as follows:

- Black–Scholes–Merton model: $\phi_N^{Model} = \phi_N^{BSM^C} = (\sigma_N^{CALIB^C})$, and $f^{Model}(.)$ is the Black–Scholes–Merton with the characteristic function (see Eq. (2.6)).
- Heston model: $\phi_N^{Model} = (\sigma_N^{CALIB^{C^2}}; \phi_N^{H^C})$, where $\sigma_N^{CALIB^{C^2}}$ is the square of $\sigma_N^{CALIB^C}$ which is used as the initial value for the long-term variance parameter and $\phi_N^{H^C} = HParams_N^C = (\kappa_N^{H^C}, \sigma_N^{H^C}, \theta_N^{H^C}, \rho_N^{H^C}, V_{0,N}^{H^C})$, and $f^{Model}(.)$ is the Heston with the characteristic function (see Eq. (2.13)).
- Heston Jump Diffusion model: $\phi_N^{Model} = (\sigma_N^{CALIB^{C^2}}; \phi_N^{HJD^C})$, where $\phi_N^{HJD^C} = HJDParams_N^C$ $= (\kappa_N^{HJD^C}, \sigma_N^{HJD^C}, \theta_N^{HJD^C}, \rho_N^{HJD^C}, V_{0,N}^{HJD^C}, \sigma_N^{HJD^C}, \mu_N^{HJD^C},$ $\lambda_N^{HJD^C})$, and $f^{Model}(.)$ is the Heston Jump Diffusion with the characteristic function (see Eq. (2.22)).
- Finite Moment Log Stable model: $\phi_N^{Model} = \phi_N^{FMLS^C} = (\alpha_N^{FMLS^C}, \sigma_N^{FMLS^C})$, and $f^{Model}(.)$ is the Finite Moment Log Stable with the characteristic function (see Eq. (2.25)).

We calibrate each model for each day (over historical empirical call option prices) by choosing ϕ_N^{Model} to minimise the mean square error. In this case, we retain the fitted option prices and the calibrated parameters for each respective model are as follows:

- $\sigma_N^{CALIB^C}$ for the Black–Scholes–Merton model,
- $HParams_N^C$ for the Heston model,
- $HJDParams_N^C$ for the Heston Jump Diffusion model,
- $\alpha_N^{FMLS^C}$, and $\sigma_N^{FMLS^C}$ for the Finite Moment Log Stable model,

We compute the one-trading-day-ahead forecast errors, $\epsilon_{N+1}^{Model_N}$, for each of the respective model as:

$$\epsilon_{N+1}^{Model_N} = C_{N+1} - f^{Model}\left(S_N, K_N, T_N, R_N, Q_N; \phi_N^{Model}\right) \tag{2.38}$$

where f^{Model} is a pricing function under a generic model. We evaluate the option price at the index value on the previous trading day and use the known exercise price and time to maturity, as well as the previous day's interest rate, dividend yield and respective calibrated parameters for each of the respective models. Finally, for the parametric models that fall under the *C-Models* category that use one-trading-day-ahead input variables for forecasting the one-trading-day C_{N+1}, we compute the one-trading-day-ahead forecast errors as:

$$\epsilon_{N+1}^{Model_{N+1}} = C_{N+1} - f^{Model}\left(S_{N+1}, K_{N+1}, T_{N+1}, R_{N+1}, Q_{N+1}; \phi_N^{Model}\right). \tag{2.39}$$

We report the root mean square error of these forecast errors.

2.3.5.1.2 *C-Models*: Deep Learning Neural Network Models

A total of 72 MLPs and LSTMs are estimated and reported under the *C-Models* category. In this section, we list the 72 ANN models (36 MLPs and 36 LSTMs), which were trained on empirical call option prices of the S&P 500 Index (C_N). These models forecast the call option prices of the S&P 500 Index for the next trading day. Amongst the 36 MLPs and 36 LSTMs, we analysed the performance of:

- Using the information available on day $t = N$ to forecast one-day-ahead option prices C_{N+1} with nine single hidden layer MLP $M1C_N$-Models ($M1C1_N$ to $M1C9_N$), nine single hidden layer LSTM $L1C_N$-Models ($L1C1_N$ to $L1C9_N$), nine double hidden layer MLP $M2C_N$-Models ($M2C1_N$ to $M2C9_N$), nine double hidden layer LSTM $L2C_N$-Models ($L2C1_N$ to $L2C9_N$), nine triple hidden layer MLP $M3C_N$-Models ($M3C1_N$ to $M3C9_N$), and nine triple hidden layer LSTM $L3C_N$-Models ($L3C1_N$ to $L3C9_N$). ($3 \times 9 = 27$ MLPs and $3 \times 9 = 27$ LSTMs)

- Use the information available (except for calibrated model parameters) on day $t = N+1$ to forecast one-day-ahead option prices C_{N+1} with nine triple hidden layer MLP $M3C_{N+1}$-Models ($M3C1_{N+1}$ to $M3C9_{N+1}$) and nine triple hidden layer LSTM $L3C_{N+1}$-Models ($L3C1_{N+1}$ to $L3C9_{N+1}$). (9 MLPs and 9 LSTMs)

The nine MLP and nine LSTM models under each of the categories above are differentiated by choice of input variables and the network architecture. As in the parametric models, each model here has a set of input variables and a set of parameters, ϕ, called biases and weights. The input variables for the MLP models ($M1C_N$-Models, $M2C_N$-Models, and $M3C_N$-Models) and the LSTM models ($L1C_N$-Models, $L2C_N$-Models, and $L3C_N$-Models) that use the information available on day $t = N$ to forecast the call option price for day $t = N + 1$ are mentioned in Table A.1.1. Similarly, the input variables for the MLP models ($M3C_{N+1}$-Models) and the LSTM models ($L3C_{N+1}$-Models) that use the information available (except for calibrated model parameters) on day $t = N+1$ to forecast the call option price for day $t = N+1$ are mentioned in Table A.1.2. We compute the one-trading-day-ahead forecast errors under the respective models as follows:

1. **MLP MnC_N-Models ($MnC1_N$ to $MnC9_N$):**

$$\epsilon_{N+1}^{MnC_N\text{-}Models} = C_{N+1} - f\left(X_N; \phi^{MnC_N\text{-}Models}\right), \quad \textit{where } n = 1,2,3 \tag{2.40}$$

2. **LSTM LnC_N-Models ($LnC1_N$ to $LnC9_N$):**

$$\epsilon_{N+1}^{LnC_N\text{-}Models} = C_{N+1} - f\left(X_N; \phi^{LnC_N\text{-}Models}\right), \quad \textit{where } n = 1,2,3 \tag{2.41}$$

3. **MLP $M3C_{N+1}$-Models ($M3C1_{N+1}$ to $M3C9_{N+1}$):**

$$\epsilon_{N+1}^{M3C_{N+1}\text{-}Models} = C_{N+1} - f\left(X_{N+1}; \phi^{M3C_{N+1}\text{-}Models}\right), \tag{2.42}$$

4. **LSTM $L3C_{N+1}$-Models ($L3C1_{N+1}$ to $L3C9_{N+1}$):**

$$\epsilon_{N+1}^{L3C_{N+1}\text{-}Models} = C_{N+1} - f\left(X_{N+1}; \phi^{L3C_{N+1}\text{-}Models}\right), \tag{2.43}$$

where $f(.)$ represents a Deep Learning MLP model in Eqs. (2.40) and (2.42), and $f(.)$ represents a Deep Learning LSTM model in Eqs. (2.41) and (2.43). We estimate these models each day (over historical empirical call option prices) by choosing their respective ϕ to minimise the mean square error. We report the root mean square error of these forecast errors. Thus, the above models are defined by identifying the inputs of each model (X_N) for the MLP ($M1C_N$-Models, $M2C_N$-Models, and $M3C_N$-Models) and LSTM ($L1C_N$-Models, $L2C_N$-Models, and $L3C_N$-Models) models. Similarly, models that have defined by having X_{N+1} as their inputs are the MLP ($M3C_{N+1}$-Models) and LSTM ($L3C_{N+1}$-Models) models.

Unlike the parametric models, the MLP models ($M1C_N$-Models, $M2C_N$-Models, $M3C_N$-Models, and $M3C_{N+1}$-Models) are estimated with an expanding window of observations, whereas, the

LSTM models ($L1C_N$-Models, $L2C_N$-Models, $L3C_N$-Models, and $L3C_{N+1}$-Models) are estimated with a fixed-sliding window of observations. However, the forecast horizon remains one trading day for all the models, so we compute the one-trading-day-ahead forecasts and report the root mean square error of the forecast errors. We have hierarchically classified the non-parametric MLP models ($M1C_N$-Models, $M2C_N$-Models, $M3C_N$-Models, and $M3C_{N+1}$-Models) and LSTM models ($L1C_N$-Models, $L2C_N$-Models, $L3C_N$-Models, and $L3C_{N+1}$-Models) into the following nine series:

1. **Series 1:** $MnC1_N$, $M3C1_{N+1}$, $LnC1_N$, and $L3C1_{N+1}$ models, where $n = 1, 2, 3$.
2. **Series 2:** $MnC2_N$, $M3C2_{N+1}$, $LnC2_N$, and $L3C2_{N+1}$ models, where n = 1, 2, 3.
3. **Series 3:** $MnC3_N$, $M3C3_{N+1}$, $LnC3_N$, and $L3C3_{N+1}$ models, where $n = 1, 2, 3$.
4. **Series 4:** $MnC4_N$, $M3C4_{N+1}$, $LnC4_N$, and $L3C4_{N+1}$ models, where $n = 1, 2, 3$.
5. **Series 5:** $MnC5_N$, $M3C5_{N+1}$, $LnC5_N$, and $L3C5_{N+1}$ models, where $n = 1, 2, 3$.
6. **Series 6:** $MnC6_N$, $M3C6_{N+1}$, $LnC6_N$, and $L3C6_{N+1}$ models, where $n = 1, 2, 3$.
7. **Series 7:** $MnC7_N$, $M3C7_{N+1}$, $LnC7_N$, and $L3C7_{N+1}$ models, where $n = 1, 2, 3$.
8. **Series 8:** $MnC8_N$, $M3C8_{N+1}$, $LnC8_N$, and $L3C8_{N+1}$ models, where $n = 1, 2, 3$.
9. **Series 9:** $MnC9_N$, $M3C9_{N+1}$, $LnC9_N$, and $L3C9_{N+1}$ models, where $n = 1, 2, 3$.

The **Series 1** set of models uses the inputs required to calibrate the Black–Scholes–Merton model. The input variables are extended further by the **Series 2** set of models by adding the lagged call option price of the S&P 500 Index. The **Series 3** set of models extends the input variables of Series 2 models by adding the lagged Black–Scholes–Merton greeks. The **Series 4** set of models extends the input variables of Series 3 models by adding the lagged calibrated Heston model parameters. The **Series 5** set of models extends the input variables of Series 4 models by adding the lagged in-sample Heston model call option price. From **Series 6** onwards, apart from the standard information/input vector $(S_N, K_{N+1}, T_{N+1}, R_N, Q_N)$, we provide input parameters to the ANN models that are specific to a particular parametric model. Thus, in addition to the standard input vector, **Series 6** would be provided with the lagged calibrated Heston model parameters and the lagged in-sample Heston model call option price. **Series 7** models replicate the Black–Scholes–Merton model, and hence along with the standard input vector, they would be provided with the lagged Black–Scholes–Merton greeks and the lagged in-sample Black–Scholes–Merton model call option price. Similarly, **Series 8** models would replicate the information set available to the Heston Jump Diffusion model, whereby, along with the standard input vector, they would be provided the lagged calibrated Heston Jump Diffusion model parameters and the lagged in-sample Heston Jump Diffusion model call option price. Finally, the **Series 9** models would replicate the information set available to the Finite Moment Log Stable model, whereby, along with the standard input vector, they would be provided the lagged calibrated Finite Moment Log Stable model parameters, and the lagged in-sample Finite Moment Log Stable model call option price.

2.3.5.2 Information Sets for *CK-Models*

Next, we define the information sets required for each model for calibration or estimation of parameters and for forecasting the call option price scaled by the strike price (C_N/K_N). We implement a single forecasting horizon, that is one-trading-day-ahead forecasts, so we use the information available on day $t = N$ to forecast option prices for day $t = N + 1$. The parametric models are calibrated daily, based only on the data available for day N. In contrast, the MLP models use an expanding window, the LSTM models use a fixed window, and both the MLP and LSTM use data for $t = 1, ..., N$ for estimation and forecast for day $t = N + 1$. Thus the parametric models follow the usual convention of daily calibrations, whereas the expanding (for the MLP) and fixed (for the LSTM) window allows the ANNs to cover a wide range of values for its input variables. In what follows we use ϕ to represent a generic parameter scalar or vector for each model.

2.3.5.2.1 *CK-Models*: Parametric Models (Black–Scholes–Merton, Heston, Heston Jump Diffusion, and Finite Moment Log Stable Model)

For the parametric models that fall under the *CK-Models* category, on day N the information used to calibrate the model parameters for each option is $(C_N/K_N, S_N/K_N, T_N, R_N, Q_N; \phi_N^{Model})$, and we define the in-sample pricing error, $\epsilon_N^{Model_N}$ for each option under each model as:

$$\epsilon_N^{Model_N} = C_N/K_N - (f^{Model}\left(S_N/K_N, T_N, R_N, Q_N; \phi_N^{Model}\right)/K_N) \tag{2.44}$$

where ϕ_N^{Model} and f^{Model} are for each model as follows:

- Black–Scholes–Merton model: $\phi_N^{Model} = \phi_N^{BSM^{CK}} = (\sigma_N^{CALIB^{CK}})$, and $f^{Model}(.)$ is the Black–Scholes–Merton with the characteristic function (see Eq. (2.6)).

- Heston model: $\phi_N^{Model} = (\sigma_N^{CALIB^{CK^2}}; \phi_N^{H^{CK}})$, where $\sigma_N^{CALIB^{CK^2}}$ is the square of $\sigma_N^{CALIB^{CK}}$ which is used as the initial value for the long-term variance parameter and $\phi_N^{H^{CK}} = HParams_N^{CK} = (\kappa_N^{H^{CK}}, \sigma_N^{H^{CK}}, \theta_N^{H^{CK}}, \rho_N^{H^{CK}}, V_{0,N}^{H^{CK}})$, and $f^{Model}(.)$ is the Heston with the characteristic function (see Eq. (2.13)).

- Heston Jump Diffusion model: $\phi_N^{Model} = (\sigma_N^{CALIB^{CK^2}} ; \phi_N^{HJD^{CK}})$, where $\phi_N^{HJD^{CK}} = HJDParams_N^{CK} = (\kappa_N^{HJD^{CK}}, \sigma_N^{HJD^{CK}}, \theta_N^{HJD^{CK}}, \rho_N^{HJD^{CK}}, V_{0,N}^{HJD^{CK}}, \sigma_N^{HJD^{CK}},$ $\mu_N^{HJD^{CK}}, \lambda_N^{HJD^{CK}})$, and $f^{Model}(.)$ is the Heston Jump Diffusion with the characteristic function (see Eq. (2.22)).

- Finite Moment Log Stable model: $\phi_N^{Model} = \phi_N^{FMLS^{CK}} = (\alpha_N^{FMLS^{CK}}, \sigma_N^{FMLS^{CK}})$, and $f^{Model}(.)$ is the Finite Moment Log Stable with the characteristic function (see Eq. (2.25)).

We calibrate each model for each day (over historical empirical call option prices) by choosing ϕ_N^{Model} to minimise the mean square error. In this case, we retain the fitted option prices, and the calibrated parameters for each respective model are as follows:

- $\sigma_N^{CALIB^{CK}}$ for the Black–Scholes–Merton model
- $HParams_N^{CK}$ for the Heston model
- $HJDParams_N^{CK}$ for the Heston Jump Diffusion model
- $\alpha_N^{FMLS^{CK}}$, and $\sigma_N^{FMLS^{CK}}$ for the Finite Moment Log Stable model

We compute the one-trading-day-ahead forecast errors, $\epsilon_{N+1}^{Model_N}$, for each of the respective model as:

$$\epsilon_{N+1}^{Model_N} = C_{N+1}/K_{N+1} - (f^{Model}\left(S_N/K_N, T_N, R_N, Q_N; \phi_N^{Model}\right)/K_N) \tag{2.45}$$

Here we evaluate the option price at the index value on the previous trading day and use the known exercise price and time to maturity, as well as the previous day's interest rate, dividend yield, and respective calibrated parameters for each of the respective model. Finally, for the parametric models that fall under the *CK-Models* category that use one-trading-day-ahead input variables for forecasting the one-trading-day C_{N+1}/K_{N+1}, we compute the one-trading-day-ahead forecast errors for these models as:

$$\epsilon_{N+1}^{Model_{N+1}} = C_{N+1}/K_{N+1} - (f^{Model}(S_{N+1}/K_{N+1}, T_{N+1}, R_{N+1}, Q_{N+1}; \phi_N^{Model})/K_N) \tag{2.46}$$

where f^{Model} is a pricing function under a generic model. We report the root mean square error of these forecast errors.

2.3.5.2.2 Deep Learning Neural Network Models

In this section, we analyse the performance of models that use the homogeneity hint of Merton (1973), i.e. the call price scaled by its strike price (C_N/K_N) as the target (y_N) variable. 72 ANN models (36 MLPs and 36 LSTMs) are trained on empirical call option prices scaled by the strike price of the S&P 500 Index scaled by their respective strike price (C_N/K_N) and forecast the (C_{N+1}/K_{N+1}) for the next trading day. Amongst the 36 MLPs and 36 LSTMs, we analysed the performance of:

- Using the information available on day $t = N$ to forecast one-day-ahead moneyness (C_{N+1}/K_{N+1}) with nine single hidden layer MLP $M1CK_N$-Models ($M1CK1_N$ to $M1CK9_N$), nine single hidden layer LSTM $L1CK_N$-Models ($L1CK1_N$ to $L1CK9_N$), nine double hidden layer MLP $M2CK_N$-Models ($M2CK1_N$ to $M2CK9_N$), nine double hidden layer LSTM $L2CK_N$-Models ($L2CK1_N$ to $L2CK9_N$), nine triple hidden layer MLP $M3CK_N$-Models ($M3CK1_N$ to $M3CK9_N$), and nine triple hidden layer LSTM $L3CK_N$-Models ($L3CK1_N$ to $L3CK9_N$). ($3 \times 9 = 27$ MLPs and $3 \times 9 = 27$ LSTMs)
- Using the information available (except for calibrated model parameters) on day $t = N + 1$ to forecast one-day-ahead moneyness (C_{N+1}/K_{N+1}) with nine triple hidden layer MLP $M3CK_{N+1}$-Models ($M3CK1_{N+1}$ to $M3CK9_{N+1}$) and nine triple hidden layer LSTM $L3CK_{N+1}$-Models ($L3CK1_{N+1}$ to $L3CK9_{N+1}$). (9 MLPs and 9 LSTMs)

The nine MLP and nine LSTM models under each of the categories above are differentiated by the choice of input variables and the network architecture. As in the parametric models, each model here has a set of input variables and a set of parameters, ϕ, called biases and weights. The input variables for the MLP models ($M1CK_N$-Models, $M2CK_N$-Models, and $M3CK_N$-Models) and the LSTM models ($L1CK_N$-Models, $L2CK_N$-Models, and $L3CK_N$-Models) use the information available on day $t = N$ to forecast the C_{N+1}/K_{N+1} for day $t = N+1$ are mentioned in Table A.1.3. Similarly, the input variables for the MLP models ($M3CK_{N+1}$-Models) and the LSTM models ($L3CK_{N+1}$-Models) that use the information available (except for calibrated model parameters) on day $t = N+1$ to forecast the C_{N+1}/K_{N+1} for day $t = N+1$ are mentioned in Table A.1.4. We compute the one-trading-day-ahead forecast errors under the respective models as follows:

1. **MLP $MnCK_N$-Models ($MnCK1_N$ to $MnCK9_N$):**

$$\epsilon_{N+1}^{MnCK_N\text{-}Models} = C_{N+1}/K_{N+1} - f\left(X_N; \phi^{MnCK_N\text{-}Models}\right), \quad \text{where } n = 1,2,3 \tag{2.47}$$

2. **LSTM $LnCK_N$-Models ($LnCK1_N$ to $LnCK9_N$):**

$$\epsilon_{N+1}^{LnCK_N\text{-}Models} = C_{N+1}/K_{N+1} - f\left(X_N; \phi^{LnCK_N\text{-}Models}\right), \quad \text{where } n = 1,2,3 \tag{2.48}$$

3. **MLP $M3CK_{N+1}$-Models ($M3CK1_{N+1}$ to $M3CK9_{N+1}$):**

$$\epsilon_{N+1}^{M3CK_{N+1}\text{-}Models} = C_{N+1}/K_{N+1} - f\left(X_{N+1}; \phi^{M3CK_{N+1}\text{-}Models}\right), \tag{2.49}$$

4. **LSTM $L3CK_{N+1}$-Models ($L3CK1_{N+1}$ to $L3CK9_{N+1}$):**

$$\epsilon_{N+1}^{L3CK_{N+1}\text{-}Models} = C_{N+1}/K_{N+1} - f\left(X_{N+1}; \phi^{L3CK_{N+1}\text{-}Models}\right), \tag{2.50}$$

where $f(.)$ represents a Deep Learning MLP model in Eqs. (2.47) and (2.49), and $f(.)$ represents a Deep Learning LSTM model in Eqs. (2.48), and (2.50). We estimate these models each day (over historical empirical call option prices scaled by the strike prices) by choosing their respective ϕ to minimise the mean square error. We report the root mean square error of these forecast errors. Thus, the above models are defined by identifying the inputs of each model (X_N) for the MLP ($M1CK_N$-Models, $M2CK_N$-Models, and $M3CK_N$-Models) and LSTM ($L1CK_N$-Models, $L2CK_N$-Models, and $L3CK_N$-Models) models. Similarly, models that have been defined by having X_{N+1} as their inputs are the MLP ($M3CK_{N+1}$-Models) and LSTM ($L3CK_{N+1}$-Models) models.

Unlike the parametric models, the MLP models ($M1CK_N$-Models, $M2CK_N$-Models, $M3CK_N$-Models, and $M3CK_{N+1}$-Models) are estimated with an expanding window of observations, whereas, the LSTM models ($L1CK_N$-Models, $L2CK_N$-Models, $L3CK_N$-Models, and $L3CK_{N+1}$-Models) are estimated with a fixed-sliding window of observations, but the forecast horizon remains one trading day for all the models, so we compute the one-trading-day-ahead forecasts and report the root mean square error of the forecast errors. We have hierarchically classified the non-parametric MLP models ($M1CK_N$-Models, $M2CK_N$-Models, $M3CK_N$-Models, and $M3CK_{N+1}$-Models) and the LSTM models ($L1CK_N$-Models, $L2CK_N$-Models, $L3CK_N$-Models, and $L3CK_{N+1}$-Models) into nine categories:

1. **Series 1:** $MnCK1_N$, $M3CK1_{N+1}$, $LnCK1_N$, and $L3CK1_{N+1}$ models, where $n = 1, 2, 3$.
2. **Series 2:** $MnCK2_N$, $M3CK2_{N+1}$, $LnCK2_N$, and $L3CK2_{N+1}$ models, where $n = 1, 2, 3$.
3. **Series 3:** $MnCK3_N$, $M3CK3_{N+1}$, $LnCK3_N$, and $L3CK3_{N+1}$ models, where $n = 1, 2, 3$.
4. **Series 4:** $MnCK4_N$, $M3CK4_{N+1}$, $LnCK4_N$, and $L3CK4_{N+1}$ models, where $n = 1, 2, 3$.
5. **Series 5:** $MnCK5_N$, $M3CK5_{N+1}$, $LnCK5_N$, and $L3CK5_{N+1}$ models, where $n = 1, 2, 3$.
6. **Series 6:** $MnCK6_N$, $M3CK6_{N+1}$, $LnCK6_N$, and $L3CK6_{N+1}$ models, where $n = 1, 2, 3$.
7. **Series 7:** $MnCK7_N$, $M3CK7_{N+1}$, $LnCK7_N$, and $L3CK7_{N+1}$ models, where $n = 1, 2, 3$.
8. **Series 8:** $MnCK8_N$, $M3CK8_{N+1}$, $LnCK8_N$, and $L3CK8_{N+1}$ models, where $n = 1, 2, 3$.
9. **Series 9:** $MnCK9_N$, $M3CK9_{N+1}$, $LnCK9_N$, and $L3CK9_{N+1}$ models, where $n = 1, 2, 3$.

The **Series 1** set of models uses the inputs required to calibrate the Black–Scholes–Merton model (except that the index price is scaled by the strike price, i.e. $S_N/K_N, T_{N+1}$, R_N, Q_N). The input variables are extended further by the **Series 2** set of models by adding the lagged call option price of the S&P 500 Index scaled by the strike price. The **Series 3** set of models extends the input variables of Series 2 models by adding the lagged Black–Scholes–Merton greeks. The **Series 4** set of models extends the input variables of Series 3 models by adding the lagged calibrated Heston model parameters. The **Series 5** set of models extends the input variables of Series 4 models by adding the lagged in-sample Heston model call option price scaled by the strike price. From **Series 6** onwards, apart from the standard information/input vector, we provide input parameters to the ANN models that are specific to a particular parametric model. Thus, in addition to the standard input vector, **Series 6** would be provided with the lagged calibrated Heston model parameters and lagged in-sample Heston model call option price scaled by the strike price. **Series 7** models replicate the Black–Scholes–Merton model, and hence along with the standard input vector, they would be provided with the lagged Black–Scholes–Merton greeks, and the lagged in-sample Black–Scholes–Merton model call option price scaled by the strike price. Similarly, **Series 8** models would replicate the information set available to the Heston Jump Diffusion model, whereby, along with the standard input vector, they would be provided the lagged calibrated Heston Jump Diffusion model parameters, and the lagged in-sample Heston Jump Diffusion model call option price scaled by the strike price. Finally, the **Series 9** models would replicate the information set available to the Finite Moment Log Stable model, whereby, along with the standard input vector, they would be provided the lagged calibrated Finite Moment Log Stable model parameters, and the lagged in-sample Finite Moment Log Stable model call option price scaled by the strike price.

2.3.6 Random Walk Models

It is generally accepted that the time series realisations of many asset price processes are well-modelled by a simple random walk process. In these models, the minimum means square error forecast of the next period price is simply the current period price. We introduce two random walk models to benchmark forecast models for our parametric and non-parametric models. With two definitions of the target variable, we have two models: the δC-$Model$ and the δCK-$Model$. We compute the one trading day ahead forecast errors as,

$$\delta C_N\text{-}Model: \quad \epsilon_{N+1}^{\delta C_N} = C_{N+1} - C_N \tag{2.51}$$

$$\delta CK_N\text{-}Model: \quad \epsilon_{N+1}^{\delta CK_N} = C_{N+1}/K_{N+1} - C_N/K_N. \tag{2.52}$$

We report the root mean square error of the forecast errors from these two models.

2.3.7 Model Calibration and Performance Criteria

2.3.7.1 Performance Criterion

The forecasting performance of each model is measured using Root Mean Square Error (RMSE) in the test sample, that is, in out-of-sample prediction. For each day, as we cycle through the observations, we retain the pricing errors for each model. Below, we use these errors to compute the RMSE on a daily, monthly, and annual basis.[5] Defining the pricing errors as $\epsilon_i = y_i - \hat{y}_i$,

[5] In the Electronic Appendix, the RMSEs of the $C-Models$ that use lagged input variables to forecast the C_{N+1} for the next trading day on a monthly, yearly, and overall basis can be found

where y_i is the target value and $\hat{y}_i$ is its predicted value, then the RMSE for a series of N pricing errors is calculated by

$$RMSE = \sqrt{\frac{1}{N}\sum_{i=1}^{N}\epsilon_i^2}. \tag{2.53}$$

We should choose the model with the lowest out-of-sample RMSE. Diebold and Mariano (1995) have provided a test procedure to determine if the out-of-sample fit of one model is significantly worse than the out-of-sample fit of another model. The Diebold-Mariano (DM) test statistic is distributed as a standard normal distribution under the null hypothesis of no difference in the predictive accuracy of the two models.

To compute the DM statistic from the errors of two competing models, we calculate $d_i = h(\epsilon_{i,1}) - h(\epsilon_{i,2})$, where $h(\cdot)$ can be any loss function. The DM test statistic null hypothesis is $H_0 : \mathbb{E}(d_i) = 0$. The DM test statistic is computed as

$$DM = \frac{\overline{d}}{\sqrt{2\pi \hat{f}_d(0)/T}}, \tag{2.54}$$

$$\tag{2.55}$$

where $\overline{d} = \sum_{i=1}^{N}\left(h(\epsilon_{i,1}) - h(\epsilon_{i,2})\right)/N$ and $f_d(\cdot)$ is the spectral density of $\{d_i\}$.

2.3.7.2 Calibration of Parametric Option Pricing Models

The parametric option pricing models have unknown parameters. To implement the models for in-sample and out-of-sample prediction, values are required for these parameters. These values are calibrated for each day of the sample by choosing the parameter values to minimise the mean squared error of the in-sample pricing errors. This non-linear optimisation exercise is implemented differently and separately for parametric models under the $C - Models$ ($BSMC_N$, HC_N, $HJDC_N$, and $FMLSC_N$ models) and for each model under $CK - Models$ ($BSMCK_N$, HCK_N, $HJDCK_N$, and $FMLSCK_N$ models) using the **Matlab Optimization Toolbox** function *lsqnonlin*. Similarly, To impose inequality restrictions on the parameters,

in Tables 1, 5, and 9, respectively. The RMSEs of the $C - Models$ that use one-trading-day-ahead input variables to forecast the C_{N+1} for the next trading day on a monthly, yearly, and overall basis can be found in Tables 2, 6, and 10, respectively. The RMSEs of the $CK - Models$ that use one-trading-day-ahead input variables to forecast the C_{N+1}/K_{N+1} for the next trading day on a monthly, yearly, and overall basis can be found in Tables 3, 7, and 11, respectively. The RMSEs of the $CK - Models$ that use one-trading-day-ahead input variables to forecast the C_{N+1}/K_{N+1} for the next trading day on a monthly, yearly, and overall basis can be found in Tables 4, 8, and 12, respectively.

the *trustregion* option is employed. For the Black–Scholes–Merton, the calibrated parameter $\sigma_N^{CALIB^C}$ (used by the $BSMC_N$ and $BSMC_{N+1}$ model) and the calibrated parameter $\sigma_N^{CALIB^{CK}}$ (used by the $BSMCK_N$ and the $BSMCK_{N+1}$ model) for day N are retained for use in computing the greeks, and as an input to other parametric and various ANN models. For the Heston model, calibrated parameters $HParams_N^C$ (used by the HC_N and the HC_{N+1} model) and the calibrated parameters $HParams_N^{CK}$ (used by the HCK_N and the HCK_{N+1} model) for day N are retained as inputs for some ANN models. For the Heston Jump Diffusion model, calibrated parameters $HJDParams_N^C$ (used by the $HJDC_N$ and the $HJDC_{N+1}$ model) and the calibrated parameters $HJDParams_N^{CK}$ (used by the $HJDCK_N$ and the $HJDCK_{N+1}$ model) for day N are retained as inputs for some ANN models. Similarly, for the Finite Moment Log Stable model, calibrated parameters $FMLSParams_N^C$ (used by the $FMLSC_N$ and the $FMLSC_{N+1}$ model) and the calibrated parameters $FMLSParams_N^{CK}$ (used by the $FMLSCK_N$ and the $FMLSCK_{N+1}$ model) for day N are retained as inputs for some ANN models. The parametric models under the $C - Models$ category (having target variable C_N) are calibrated separately to the $CK - Models$ (having target variable C_N/K_N) for each of the 1,328 trading days in the sample.

2.3.7.3 Estimating Deep Learning Neural Network Models

2.3.7.3.1 Network Parameters This study seeks to compare various networks by varying the number of neurons in each layer, as well as the number of hidden layers, to find the optimal network architecture size that outperforms the out-of-sample prediction of option prices and option price scaled by the strike price. The various network configurations are listed in Table A.1.1 for models that use the information available on day $t = N$ to forecast the call option price for day $t = N + 1$, in Table A.1.2 for models that use the information available (except for calibrated model parameters) on day $t = N + 1$ to forecast the call option price for day $t = N+1$, in Table A.1.3 for models that use the information available on day $t = N$ to forecast the C_{N+1}/K_{N+1} for day $t = N + 1$, and in Table A.1.4 for models that use the information available (except for calibrated model parameters) on day $t = N+1$ to forecast the C_{N+1}/K_{N+1} for day $t = N+1$. Root mean squared error is the performance evaluation criteria for all the ANN (MLP and LSTM) models. In the MLP models ($M1C_N - Models$, $M2C_N - Models$, $M3C_N - Models$, $M3C_{N+1} - Models$, $M1CK_N - Models$, $M2CK_N - Models$, $M3CK_N - Models$, and $M3CK_{N+1} - Models$) the layer biases and weights of the various network are estimated following using Bayesian Regularisation (see Mackay (1992) and Forsee F.D. (1997)), whereas, for the

LSTM models ($L1C_N-Models$, $L2C_N-Models$, $L3C_N-Models$, $L3C_{N+1}-Models$, $L1CK_N-Models$, $L2CK_N-Models$, $L3CK_N-Models$, and the $L3CK_{N+1}-Models$), Adaptive Moment Estimator (ADAM) (see Kingma and Ba (2005)) has been used. Finally, as Klimasauskas (1991) and Baughman and Liu (1995) state that the hyperbolic tangent function (also called "tanh" function) performs better in ANN forecasting problems, the hyperbolic tangent function is used in our study for the hidden layer squashing functions for all the MLP models. [6] Since the LSTM models were implemented in Python (using TensorFlow), the hyperbolic tangent function is not available. Xavier et al. (2011) showed that the tanh function does not have necessary and desirable properties; moreover, it often does not deactivate, and it is shown both biologically and in deep nets that deactivation (or activation sparsity) is necessary, where L1 regularisation helps with this and rectified linear unit (ReLUs) have it built in. Thus, for the LSTM models the ReLU was used as the squashing function. [7] The output layer for the MLP and LSTM models uses a simple linear transfer function that returns the forecast variable.

2.3.7.3.2 Data Division As mentioned earlier, the data set covers the period from September 2012 to December 2017 and includes 1,328 trading days. The ANN (MLP and LSTM) methodology requires data for a training set, a validation set and a test set. The training set is used to estimate the parameters, the validation set is used to evaluate under-fitting and over-fitting, and the test set is used for out-of-sample prediction. In this study for the MLPs, we utilise an expanding window (in terms of the number of days) for the training and validation sets and a fixed size (of one-trading-day) for the test set, whereas for the LSTMs, we utilise a fixed-

[6] The MLP models designed in Matlab that use the in-built activation functions do not support having the ReLU function for time series forecasting. Only until recently, Nguyen et al. (2022) has implemented custom-built ReLU as the activation function in Matlab in conjunction with Recurrent Neural Networks. The documentation states that the ReLU function in Matlab is used for image classification purposes. The available transfer/activation functions compatible with the MLP networks designed using the Matlab Neural Network Toolbox are the Log-Sigmoid Transfer function(logsig), Tan-Sigmoid Transfer Function(tansig), and Linear Transfer Function(purelin) (refer to the following link). The "tanh" activation function is equivalent to the "tansig" function (refer to the following link). The following studies have used a "tanh" activation function with their MLP networks: Andreevna (2022), Liang et al. (2009a), Liang et al. (2009b), Vejendla and Enke (2013), Liang et al. (2006), Shin and Ryu (2012), Abhishek et al. (2012), and Wang et al. (2012). De Ryck et al. (2021) cites that tanh networks with two hidden layers are at least as expressive as deeper ReLU networks and has improved convergence rate for neural network approximation of analytic functions.

[7] The following studies that have used a "ReLU" activation function with their LSTM networks are: Liu and Zhang (2023), Paredes and Kadry (2022), Chang (2022), Ke and Yang (2019), Zhao et al. (2022), Kavinnilaa et al. (2021), Pathan et al. (2020), Karakoyun and Cibikdiken (2018), and Liang and Cai (2022).

Figure 2.4: MLP Data Division: The data set covering from September 2012 to December 2017 is divided into a training set, a validation set, and a test set. The training set is used to estimate the parameters, the validation set is used to evaluate under- and over-fitting, and the test set is used for out-of-sample prediction. The MLP $M1C_N$-Models ($M1C1_N$ to $M1C9_N$), MLP $M2C_N$-Models ($M2C1_N$ to $M2C9_N$), MLP $M3C_N$-Models ($M3C1_N$ to $M3C9_N$), and the MLP $M3C_{N+1}$-Models ($M3C1_{N+1}$ to $M3C9_{N+1}$) utilise an expanding window (in terms of the number of days) for the training and fixed size (of one trading day) for the validation and test sets. For example, in the first iteration of the expanding window, the observations in 11 days (1 to 10 days as training set and 1 day as validation set) are randomly split into 80%:20% as the training set, and the validation set and the test set is fixed at one trading day. This format of data division is based on Andreou et al. (2008).

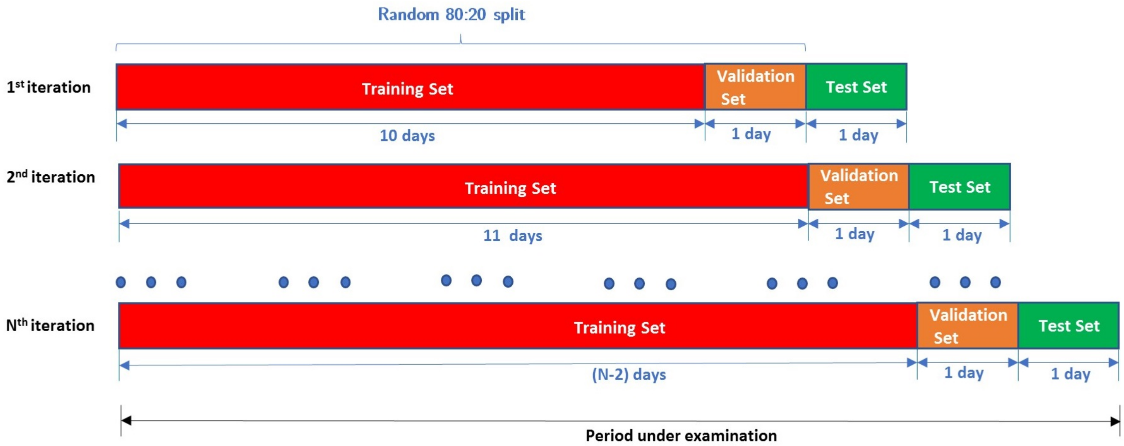

sliding window (in terms of the number of days, 10 trading days) for the training and validation sets and a fixed size (of one-trading-day) for the test set. Due to computational limitations, it was not feasible to have an expanding window for the LSTM models. Thus, the training and validation sets comprise trading days (1 to N) and the test set trading days ($N + 1$). This is repeated for the trading days N = 11, 12,..., 1,327. At each iteration, the observations in days 1 to N are randomly split into 80%:20% as the training and validation sets. The expanding window method for the MLPs is chosen over a fixed number of trading days for the training and validation sets so that the MLPs are exposed to a large variable and parameter space. The pictorial representation of the MLPs data division is presented in Figure 2.4. For the LSTM models, for each iteration, the combined set of training and validation of observations, which consists of trading days from 1 to N, stays fixed, and this fixed window (number of days) keeps sliding on each iteration and is not randomly split, which is the case with MLPs. The test set for the MLPs and the LSTMs is fixed at one trading day as the focus of this study is on one-trading-day-ahead prediction. The pictorial representation of the LSTMs data division is presented in Figure 2.5.

Figure 2.5: LSTM Data Division: The data set covering from September 2012 to December 2017 is divided into a training set, a validation set and a test set. The training set is used to estimate the parameters, the validation set is used to evaluate under- and over-fitting, and the test set is used for out-of-sample prediction. The LSTM $L1C_N$-Models ($L1C1_N$ to $L1C9_N$), LSTM $L2C_N$-Models ($L2C1_N$ to $L2C9_N$), LSTM $L3C_N$-Models ($L3C1_N$ to $L3C9_N$), and LSTM $L3C_{N+1}$-Models ($L3C1_{N+1}$ to $L3C9_{N+1}$) utilise a fixed window (in terms of the number of days) for the training, validation, and test sets. For example, in the first iteration of the fixed window, the observations in 10 days are considered as the training set, 1 day as the validation set, and the test set is fixed at 1 trading day. This procedure is repeated over the entire data set. This format of data division is based on Andreou et al. (2008).

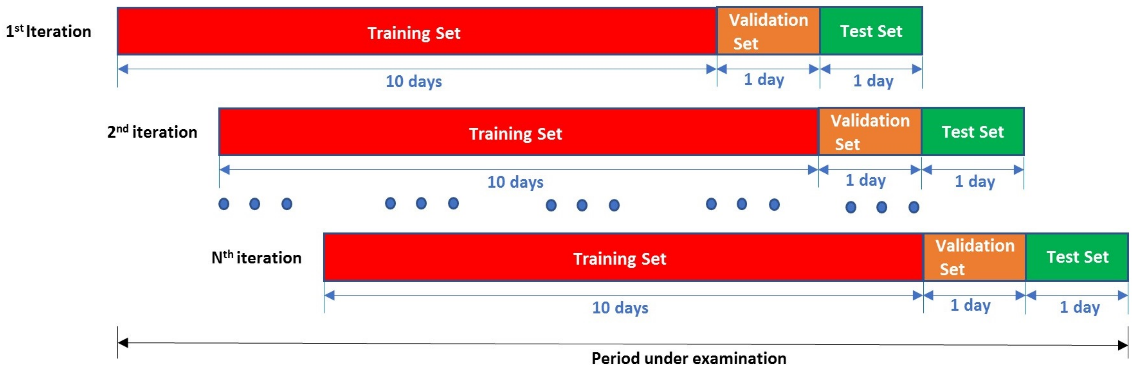

2.3.7.3.3 Training the Neural Network Models A problem that occurs during neural network training is called overfitting. The performance or loss function on the training set is driven to a minimal value, but when test set data is presented to the trained network, the loss function gets large. The network has identified the training examples, but it does not generalise to new data. Early stopping is a method for improving generalisation. The available data is divided into three subsets (i.e. training, validation and test sets). The training set is used for updating the network weights and biases. The validation set is monitored during the training process, and its loss function normally decreases during the initial phase of training, but when the network begins to overfit the data, its loss function typically begins to rise (as illustrated in Figure 2.6). When the validation loss function increases for a specified number of iterations, the training is stopped, and the weights and biases at the minimum of the validation loss function are used to evaluate the loss function in the test data. Another method for improving generalisation is called regularisation. This involves modifying the loss function, which is normally chosen to be the mean square error of the training set. To improve generalisation, the mean square error loss function is modified by adding a term that consists of the mean of the sum of squares of the network weights and biases (ω_k).

Figure 2.6: Early Stopping Method: Training reduces the loss function on the training set with an increase in the number of epochs, while the validation set loss function normally decreases during the initial phase of training. The problem of over-fitting comes into play when the loss function on the validation set begins to rise. In this study, training is stopped when the validation loss function increases consecutively for 100 epochs. The weights and biases at the minimum point of the validation loss function are used for predicting the call option prices in the test set.

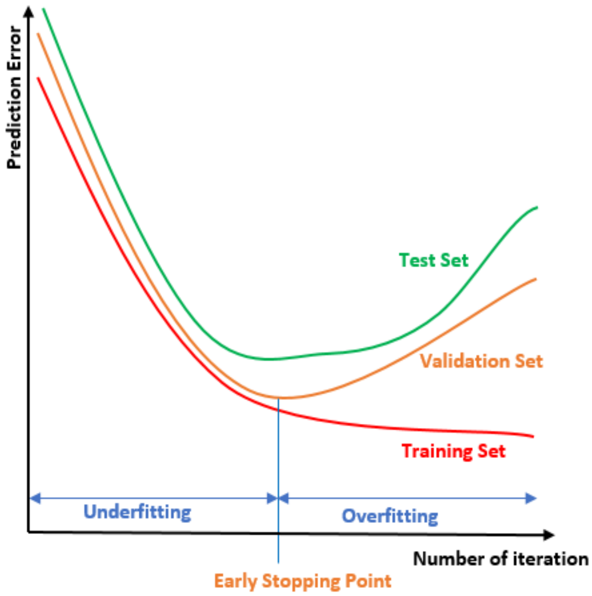

$$MSE = \gamma \times \frac{1}{J}\sum_{j=1}^{J}\epsilon_j^2 + (1-\gamma) \times \frac{1}{K}\sum_{k=1}^{K}\omega_k^2. \tag{2.56}$$

where γ is called the performance ratio (refer to Beale et al. (2010)). Using this loss function causes the network to have smaller weights and biases, with the result that the network is less likely to overfit. The problem with the method is the difficulty in determining the optimum value for the performance ratio parameter. One solution is the Bayesian framework of Mackay (1992). The detail of this Bayesian regularisation method is beyond the scope of this paper, but it has been implemented in MATLAB in the function *trainbr* and has been employed in training the MLP models reported in this paper, whereas for the LSTM models, we use the *adam* function in Python(as the Bayesian regularisation optimiser was not available in Tensorflow), which is an extended version of stochastic gradient descent. Based on several experiments, we set the learning rate to 10^{-3}, and batch size to 10, we train each ANN for 500 epochs, and we set early stopping to 250 epochs.

2.4 Empirical Results

We evaluate the forecasting performance of the various parametric and ANN models and the impact of ANN architecture on the forecasting performance of the network models in predicting one-trading-day-ahead call option prices and moneyness. The out-of-sample forecasting performance of $C\text{-}Models$ and $CK\text{-}Models$ are discussed, together with several robustness tests.

2.4.1 C-Models: Results

All of the studies listed in Table 1.1 and recent studies such as Ruf and Wang (2021) have a look-ahead bias; even though they use a test set, they fail to provide lagged input variables to their models to forecast option prices. Our study tackled this by proposing the following set of $C\text{-}Models$ that use lagged input variables for forecasting one-trading-day-ahead option prices C_{N+1}.

- $C\text{-}Models$ using lagged input variables
  - Parametric models:
    - Black–Scholes–Merton ($BSMC_N$) model
    - Heston (HC_N) model
    - Heston Jump Diffusion ($HJDC_N$) model
    - Finite Moment Log Stable ($FMLSC_N$) model
  - MLP models:
    - Single hidden layer MLP $M1C_N\text{-}Models$ ($M1C1_N$ to $M1C9_N$)
    - Double hidden layer MLP $M2C_N\text{-}Models$ ($M2C1_N$ to $M2C9_N$)
    - Triple hidden layer MLP $M3C_N\text{-}Models$ ($M3C1_N$ to $M3C9_N$)
  - LSTM models:
    - Single hidden layer LSTM $L1C_N\text{-}Models$ ($L1C1_N$ to $L1C9_N$)
    - Double hidden layer LSTM $L2C_N\text{-}Models$ ($L2C1_N$ to $L2C9_N$)
    - Triple hidden layer LSTM $L3C_N\text{-}Models$ ($L3C1_N$ to $L3C9_N$)

Following previous literature and for comparison purposes, we also perform the exercise of using one-trading-day-ahead input variables for forecasting the one-trading-day-ahead call option price

C_{N+1}. For this exercise, we only consider triple hidden layer C-$Models$, as the triple hidden layer models have shown to largely out-perform the single and double layer C-$Models$, that use lagged input variables (see extended results in Appendix A.2). Also, most of the traditional literature[8] focuses on single hidden layer MLP models, aside from Ghaziri et al. (2000), where they studied the double hidden layer MLP models; thus, this analysis provides insights into the performance of higher dimensional ANN models.

- C-$Models$ using one-trading-day-ahead input values
  - Parametric models:
    - Black–Scholes–Merton ($BSMC_{N+1}$) model
    - Heston (HC_{N+1}) model
    - Heston Jump Diffusion ($HJDC_{N+1}$) model
    - Finite Moment Log Stable ($FMLSC_{N+1}$) model
  - MLP models:
    - Triple hidden layer MLP $M3C_{N+1}$-$Models$ ($M3C1_{N+1}$ to $M3C9_{N+1}$)
  - LSTM models:
    - Triple hidden layer LSTM $L3C_{N+1}$-$Models$ ($L3C1_{N+1}$ to $L3C9_{N+1}$)

2.4.1.1 Forecasting Performance of C-$Models$ Using Lagged Input Variables

Table 2.1 presents the relative out-of-sample forecasting performance amongst all parametric and ANN models[9] that use lagged input variables to forecast the one-trading-day-ahead call option prices. The performance metric is the $RMSE$ of the one-trading-day-ahead forecast errors of C_{N+1}, which is computed for each model utilising all of the errors in each day or each month. Amongst all of the models, columns V and VI record the number of months and days, respectively, that each model has the lowest $RMSE$ when including the random walk model

[8] See examples in Table 1.1.

[9] As explained in Section 2.4.1, the models using lagged input variables to forecast the call option price are the random walk model (δC_N), the parametric models ($BSMC_N$, HC_N, $HJDC_N$, and $FMLSC_N$), the single hidden layer MLP models ($M1C_N$-$Models$), the single hidden layer LSTM models ($L1C_N$-$Models$), the double hidden layer MLP models ($M2C_N$-$Models$), the double hidden layer LSTM models ($L2C_N$-$Models$), the triple hidden layer MLP models ($M3C_N$-$Models$), and the triple hidden layer LSTM models ($L3C_N$-$Models$).

(δC_N)), while columns VII and VIII record the number of months and days that each model has the lowest $RMSE$ when excluding the δC_N model.

There are three key findings from these out-of-sample forecasting performance comparisons. Firstly, the triple hidden layer LSTM models typically outperform all the other models, and in particular, the $L3C9_N$ model out-perform all the other models with the lowest $RMSE$ for 122 days. Secondly, collectively out of 1326 forecasting days, the LSTM models outperform for 863 days (65%), the MLP models for 356 days (27%), while the parametric models only for 109 days (8%). Also, from the monthly RMSE from daily forecasts, we find similar out-performance of the LSTM models, where the $L3C8_N$ model outperforms. The daily RMSEs have been the focus of this study since we forecast daily. Note that when comparing results from daily and monthly RMSEs, we do not always obtain consistent results, which highlights the importance of using daily measures when assessing daily forecast. Thirdly, the best performing LSTM model outperforms the random walk model (δC_N) (refer to column V in Table 2.1). However, in various other such comparisons discussed in the Appendix A.2, the random walk model outperforms all the C-$Models$ - except for the $L2C9_N$, $L3C9_N$ and the $FMLSC_N$ models.

We have also performed a more comprehensive analysis by exclusively comparing the parametric models to the single layer ANN (MLP and LSTM) models, the parametric models to the double layer ANN models, and the parametric models to the triple layer ANN models. The associated tables are presented in Appendix A.2 for the sake of brevity. In particular, we consider the following nine comparisons. Firstly, we compare the parametric models with the single hidden layer MLP and LSTM models (in Table A.2.1), the parametric models with the double hidden layer MLP and LSTM models (in Table A.2.4), and the parametric models with the triple hidden layer MLP and LSTM models (in Table A.2.7). We find the LSTM models consistently outperform all other models regardless of the number of layers used by the models. More specifically, the best outperforming LSTM models include the one-layer $L1C8_N$ belonging to the Series 8 set of models that uses an input information set replicating the HJD model, while the other two out-performing LSTM models are the two-layer $L2C9_N$ and the three-layer $L3C9_N$ belonging to Series 9 set of models, which use an input information set replicating the FMLS model.[10] Furthermore, we observe an improvement in forecasting performance of the outperforming LSTM models from a single hidden layer ($L1C8_N$ model) to a double hidden layer ($L2C9_N$ model) by an additional 19.2% and from a double hidden layer to a triple hidden layer ($L3C9_N$ model) by an additional 5%. The LSTM models also outperform on the basis of monthly RMSEs in

[10] See Section 2.3.5.1.2 for the details of each series.

the above-mentioned set of comparisons.[11] The Series 8 set of LSTM models has consistently outperformed when we gauge models based on monthly RMSEs. Thus to summarise, the LSTM models typically outperform other models across various layers with triple layer providing the best performance, and mainly the LSTM models belonging to the Series 8 and Series 9 set of models.

The outperformance of LSTM models (single, double, and triple hidden layers) is also evident when we consider the three combinations of comparing the parametric models with the single hidden layer LSTM models only, the double hidden layer LSTM models only, and the triple hidden layer LSTM models only; see Tables A.2.3, A.2.6, and A.2.9, respectively. We find again that the Series 8 and Series 9 sets of LSTM models outperform the parametric models.[12] However, we lastly compare the MLP models (single, double, and triple hidden layers) with the parametric models; the MLP's show poor performance, as they fail to outperform the parametric models in Tables A.2.2, A.2.5, and A.2.8, respectively. In these tables, the $FMLSC_N$ model has consistently outperformed other parametric and MLP models.[13]

2.4.1.2 Forecasting Performance of C-$Models$ Using One-trading-day-ahead Input Variables

Table 2.2 shows the relative out-of-sample forecasting performance (in $RMSE$) amongst all parametric and triple layer ANN models[14] that use one-trading-day-ahead input variables to forecast the one-trading-day day ahead call option prices. For this analysis, along with the parametric models, we only experiment with triple layer ANN (MLP and LSTM) models because the triple hidden layer LSTM ($L3C9_N$ model) outperforms the single and double hidden layers models, as demonstrated in Section 2.4.1.1. Similarly, columns V and VI record the number

[11] The $L1C8_N$ model outperforms for 11 months (Table A.2.1), $L2C8_N$ for 12 months (Table A.2.4), and $L3C8_N$ for 13 months (Table A.2.7) out of 64 months.

[12] The single hidden layer $L1C8_N$, the double hidden layer $L2C9_N$ and the triple hidden layer $L3C9_N$ models outperformed all the other models, see Tables A.2.3, A.2.6, and A.2.9, respectively.

[13] The $FMLSC_N$ outperforms the single hidden layer MLP models by 229 days, other parametric models and the double hidden layer MLP models by 230 days, and other parametric models and the triple hidden layer MLP models by 229 days.

[14] As explained in Section 2.4.1, the models using one-trading-day-ahead input variables to forecast the call option price are the random walk model (δC_N), the parametric models ($BSMC_{N+1}$, HC_{N+1}, $HJDC_{N+1}$, and $FMLSC_{N+1}$), the triple hidden layer MLP models ($M3C_{N+1}$-$Models$), and the triple hidden layer LSTM models ($L3C_{N+1}$-$Models$).

of months and days, respectively, that each model has the lowest $RMSE$ when including the random walk model (δC_N)), while columns VII and VIII record the number of months and days that each model has the lowest $RMSE$ when excluding the δC_N model (amongst all the models).

This analysis reveals different results. When comparing the parametric models with the triple hidden layer MLP and LSTM models, the MLP model, $M3C4_{N+1}$ has the lowest $RMSE$ for 232 days and outperforms all other models. The out-performance is not just limited to the $M3C4_{N+1}$ model but can be seen across other MLP models (i.e. across $M3C_{N+1}$-$Models$, which consists of models $M3C1_{N+1}$ to $M3C9_{N+1}$) too.

We perform further investigations to compare the use of one-trading-day-ahead input variables with the use of lagged input variables. From Table 2.2, all the nine triple hidden layer MLP models with one-trading-day-ahead input variables significantly outperform all the corresponding nine triple hidden layer MLP models with lagged input variables in Table A.2.7 (this table presents the comparison between the parametric, triple hidden layer MLP and LSTM models that use lagged input variables), with the improvement reaching up to 419% for MLP Series 9 models.[15] Thus, a substantial improvement in forecasting performance can be noticed by using one-trading-day-ahead input variables compared with the use of lagged input variables to forecast C_{N+1}. We also observe an out-performance of the $M3C_{N+1}$-$Models$ when considering monthly RMSEs. The parametric and the LSTM $L3C_{N+1}$-$Models$ from Table 2.2 have fared poorly compared to their counterparts in Table A.2.7.

Tables A.2.16 and Table A.2.17 consider the comparison between the parametric and triple hidden layer MLP only and between the parametric and triple hidden layer LSTM models only, respectively. We find that the MLP $M3C4_{N+1}$ model again has the lowest $RMSE$ for 240 days. The LSTM $L3C_{N+1}$-$Models$ fail to out-perform in any of the comparisons mentioned above and also fail when they are compared to the parametric models, where the $HJDC_{N+1}$ model has the lowest $RMSE$ for 878 days, and none of the LSTM $L3C_{N+1}$-$Models$ has shown any out-performance.

[15] Indeed, the forecasting performance of the MLP models can be summarised as follows: $M3C1_{N+1}$ has an improvement of 74% over the $M3C1_N$, $M3C2_{N+1}$ has an improvement of 300% over $M3C2_N$, $M3C3_{N+1}$ has an improvement of 274% over $M3C3_N$, $M3C4_{N+1}$ has an improvement of 362% over $M3C4_N$, $M3C5_{N+1}$ has an improvement of 300% over $M3C5_N$, $M3C6_{N+1}$ has an improvement of 314% over $M3C6_N$, $M3C7_{N+1}$, however, has a decrease of 3% in forecasting performance compared to $M3C7_N$, $M3C8_{N+1}$ has an improvement of 138% over $M3C8_N$, and $M3C9_{N+1}$ has an improvement of 419% over $M3C9_N$.

The improvement seen in the MLP models that use one-trading-day-ahead input variables rather than lagged input variables may explain why previous studies find MLP models to outperform other parametric models (Andreou et al. (2002), Andreou et al. (2004), Andreou et al. (2008), Ghaziri et al. (2000), Gençay and Gibson (2007), Thomaidis et al. (2006a), and Ghaziri et al. (2000)).[16]

[16] We discuss in depth the relative out-of-sample forecasting performance amongst the models that lagged variables and one-trading-day-ahead input variables to forecast the one-trading-day-ahead C_{N+1} in sections A.2.1 and A.2.2, respectively. The RMSEs for the C-$Models$ that use lagged input variables to forecast the C_{N+1} for the next trading day on a monthly, yearly, and overall basis can be found in Tables 1, 5, and 9, respectively and for the C-$Models$ that use one-trading-day-ahead input variables to forecast the C_{N+1} for the next trading day on a monthly, yearly, and overall basis can be found in Tables 2, 6, and 10, respectively, of the Electronic Appendix.

Table 2.1: This table presents the forecasting performance comparison using both daily and monthly statistics amongst *C-Models* that use lagged input variables to forecast the one-trading-day-ahead call option price (C_{N+1}). The one-day-ahead forecast errors of C_{N+1} are used to compute the Root Mean Square Error (RMSE). Column I identifies the models, and columns II, III, and IV describe the network architecture of the MLP and LSTM models. Forecasts are made for 1,326 trading days, and there are 64 months covered in the sample using the monthly data. When comparing all models simultaneously (i.e. including the random walk model (δC_N)), column V reports the number of months out of the 64 months that each model has the smallest RMSE, while column VI reports the number of days out of the 1,326 days each model has the smallest RMSE. Similarly, when the δC_N model was excluded in the comparison, column VII reports the number of months out of the 64 months that each model has the smallest RMSE, while column VIII reports the number of days out of the 1,326 days each model has the smallest RMSE.

				Incl. random walk		**Excl. random walk**	
(I)	**(II)**	**(III)**	**(IV)**	**(V)**	**(VI)**	**(VII)**	**(VIII)**
Model	**No. of hidden layers**	**No. of hidden nodes per layer**	**Network architecture**	**Performance amongst all models (Monthly)**	**Performance amongst all models (Daily)**	**Performance amongst all models (Monthly)**	**Performance amongst all models (Daily)**
δC_N	-	-	-	6	106	-	-
$BSMC_N$	-	-	-	0	53	0	53
HC_N	-	-	-	1	40	1	40
$HJDC_N$	-	-	-	0	1	0	9
$FMLSC_N$	-	-	-	0	7	0	7
$M1C1_N$	1	6	6	0	6	0	6
$M1C2_N$	1	7	7	1	8	1	8
$M1C3_N$	1	12	12	1	19	1	24
$M1C4_N$	1	17	17	0	20	0	26
$M1C5_N$	1	18	18	2	5	2	6
$M1C6_N$	1	11	11	2	4	3	5
$M1C7_N$	1	12	12	2	14	2	15
$M1C8_N$	1	14	14	0	3	0	6
$M1C9_N$	1	8	8	0	5	0	6
$M2C1_N$	2	6	6 X 6	0	1	0	1
$M2C2_N$	2	7	7 X 7	0	17	0	17
$M2C3_N$	2	12	12 X 12	0	13	0	13
$M2C4_N$	2	17	17 X 17	0	28	0	28
$M2C5_N$	2	18	18 X 18	4	32	4	32
$M2C6_N$	2	11	11 X 11	0	14	0	14
$M2C7_N$	2	12	12 X 12	2	26	3	27
$M2C8_N$	2	14	14 X 14	1	21	1	22
$M2C9_N$	2	8	8 X 8	0	4	0	4
$M3C1_N$	3	6	6 X 6 X 6	0	11	0	11
$M3C2_N$	3	7	7 X 7 X 7	0	13	0	14
$M3C3_N$	3	12	12 X 12 X 12	3	17	3	21
$M3C4_N$	3	17	17 X 17 X 17	1	18	1	24
$M3C5_N$	3	18	18 X 18 X 18	0	2	0	4
$M3C6_N$	3	11	11 X 11 X 11	1	3	2	6
$M3C7_N$	3	12	12 X 12 X 12	1	4	1	8
$M3C8_N$	3	14	14 X 14 X 14	0	1	0	2
$M3C9_N$	3	8	8 X 8 X 8	0	4	0	6
$L1C1_N$	1	6	6	0	3	0	3
$L1C2_N$	1	7	7	0	45	0	45
$L1C3_N$	1	12	12	0	27	0	27
$L1C4_N$	1	17	17	0	28	0	28
$L1C5_N$	1	18	18	1	29	1	33
$L1C6_N$	1	11	11	2	11	2	13
$L1C7_N$	1	12	12	3	21	3	22
$L1C8_N$	1	14	14	2	25	3	27
$L1C9_N$	1	8	8	0	33	0	34
$L2C1_N$	2	6	6 X 6	0	8	0	11
$L2C2_N$	2	7	7 X 7	1	21	1	23
$L2C3_N$	2	12	12 X 12	4	32	4	37
$L2C4_N$	2	17	17 X 17	2	17	2	23
$L2C5_N$	2	18	18 X 18	0	2	0	5
$L2C6_N$	2	11	11 X 11	0	2	0	5
$L2C7_N$	2	12	12 X 12	4	8	4	16
$L2C8_N$	2	14	14 X 14	1	2	2	8
$L2C9_N$	2	8	8 X 8	0	7	1	13
$L3C1_N$	3	6	6 X 6 X 6	0	34	0	34
$L3C2_N$	3	7	7 X 7 X 7	0	86	0	86
$L3C3_N$	3	12	12 X 12 X 12	0	38	0	38
$L3C4_N$	3	17	17 X 17 X 17	0	73	0	73
$L3C5_N$	3	18	18 X 18 X 18	1	39	1	40
$L3C6_N$	3	11	11 X 11 X 11	1	22	1	22
$L3C7_N$	3	12	12 X 12 X 12	5	24	5	25
$L3C8_N$	3	14	14 X 14 X 14	**9**	49	**9**	50
$L3C9_N$	3	8	8 X 8 X 8	0	**122**	0	**122**

Table 2.2: This table presents the forecasting performance comparison using both daily and monthly statistics amongst *C-Models* that use one-trading-day-ahead input variables to forecast the one-trading-day-ahead call option price (C_{N+1}). The one-day-ahead forecast errors of C_{N+1} are used to compute the Root Mean Square Error (RMSE). Column I identifies the models, and columns II, III, and IV describe the network architecture of the MLP and the LSTM model. Forecasts are made for 1,326 trading days, and there are 64 months covered in the sample using the monthly data. When comparing all models simultaneously (i.e. including the random walk model (δC_N)), column V reports the number of months out of the 64 months that each model has the smallest RMSE, while column VI reports the number of days out of the 1,326 days each model has the smallest RMSE. Similarly, when the δC_N model was excluded in the comparison, column VII reports the number of months out of the 64 months that each model has the smallest RMSE, while column VIII reports the number of days out of the 1,326 days each model has the smallest RMSE.

				Incl. random walk		**Excl. random walk**	
(I)	**(II)**	**(III)**	**(IV)**	**(V)**	**(VI)**	**(VII)**	**(VIII)**
Model	**No. of hidden layers**	**No. of hidden nodes per layer**	**Network architecture**	**Performance amongst all models (Monthly)**	**Performance amongst all models (Daily)**	**Performance amongst all models (Monthly)**	**Performance amongst all models (Daily)**
δC_N	-	-	-	0	89	-	-
$BSMC_{N+1}$	-	-	-	0	0	0	0
HC_{N+1}	-	-	-	0	9	0	9
$HJDC_{N+1}$	-	-	-	4	56	4	57
$FMLSC_{N+1}$	-	-	-	0	0	0	0
$M3C1_{N+1}$	3	6	6 X 6 X 6	3	87	3	87
$M3C2_{N+1}$	3	7	7 X 7 X 7	**24**	210	**24**	212
$M3C3_{N+1}$	3	12	12 X 12 X 12	8	228	8	232
$M3C4_{N+1}$	3	17	17 X 17 X 17	16	**232**	16	**245**
$M3C5_{N+1}$	3	18	18 X 18 X 18	4	112	4	124
$M3C6_{N+1}$	3	11	11 X 11 X 11	0	76	0	87
$M3C7_{N+1}$	3	12	12 X 12 X 12	0	21	0	35
$M3C8_{N+1}$	3	14	14 X 14 X 14	0	17	0	38
$M3C9_{N+1}$	3	8	8 X 8 X 8	5	162	5	166
$L3C1_{N+1}$	3	6	6 X 6 X 6	0	0	0	0
$L3C2_{N+1}$	3	7	7 X 7 X 7	0	4	0	4
$L3C3_{N+1}$	3	12	12 X 12 X 12	0	3	0	4
$L3C4_{N+1}$	3	17	17 X 17 X 17	0	5	0	5
$L3C5_{N+1}$	3	18	18 X 18 X 18	0	8	0	9
$L3C6_{N+1}$	3	11	11 X 11 X 11	0	4	0	6
$L3C7_{N+1}$	3	12	12 X 12 X 12	0	2	0	4
$L3C8_{N+1}$	3	14	14 X 14 X 14	0	2	0	3
$L3C9_{N+1}$	3	8	8 X 8 X 8	0	1	0	1

2.4.2 CK-Models: Results

We continue with the evaluation of the forecasting performance of the following set of CK-$Models$, that use lagged and one-trading-day-ahead input variables to forecast one-trading-day-ahead call option prices scaled by the strike price C_{N+1}/K_{N+1}.

- CK-$Models$ using lagged input variables
  - Parametric models:
    - Black–Scholes–Merton ($BSMCK_N$) model
    - Heston (HCK_N) model
    - Heston Jump Diffusion ($HJDCK_N$) model
    - Finite Moment Log Stable ($FMLSCK_N$) model
  - MLP models:
    - Single hidden layer MLP $M1CK_N$-$Models$ ($M1C1K_N$ to $M1C9K_N$)
    - Double hidden layer MLP $M2CK_N$-$Models$ ($M2C1K_N$ to $M2C9K_N$)
    - Triple hidden layer MLP $M3CK_N$-$Models$ ($M3C1K_N$ to $M3C9K_N$)
  - LSTM models:
    - Single hidden layer LSTM $L1CK_N$-$Models$ ($L1C1K_N$ to $L1C9K_N$)
    - Double hidden layer LSTM $L2CK_N$-$Models$ ($L2C1K_N$ to $L2C9K_N$)
    - Triple hidden layer LSTM $L3CK_N$-$Models$ ($L3C1K_N$ to $L3C9K_N$)
- CK-$Models$ using one-trading-day-ahead input values
  - Parametric models:
    - Black–Scholes–Merton ($BSMCK_{N+1}$) model
    - Heston (HCK_{N+1}) model
    - Heston Jump Diffusion ($HJDCK_{N+1}$) model
    - Finite Moment Log Stable ($FMLSCK_{N+1}$) model
  - MLP models:
    - Triple hidden layer MLP $M3CK_{N+1}$-$Models$ ($M3C1K_{N+1}$ to $M3C9K_{N+1}$)

- LSTM models:
    - ∗ Triple hidden layer LSTM $L3CK_{N+1}$-*Models* ($L3C1K_{N+1}$ to $L3C9K_{N+1}$)

In this section, we also discuss the forecasting performance of the *rescaled CK-Models* that involves multiplying the strike price (K_{N+1}) to the forecasted C_{N+1}/K_{N+1} from the *CK-Models* considered above. These models, thereby, provide an evaluation of forecasting one-trading-day-ahead option prices C_{N+1}, which are inferred from the forecasting of C_{N+1}/K_{N+1} prices. The *rescaled CK-Models* makes the forecasts comparable to that of the *C-Models*.

- *Rescaled CK-Models* using lagged input variables
  - MLP models:
    - ∗ Single hidden layer MLP $M1CK_N$-*Models-Rescaled* ($M1C1K_N$-*Rescaled* to $M1C9K_N$-*Rescaled*)
    - ∗ Double hidden layer MLP $M2CK_N$-*Models-Rescaled* ($M2C1K_N$-*Rescaled* to $M2C9K_N$-*Rescaled*)
    - ∗ Triple hidden layer MLP $M3CK_N$-*Models-Rescaled* ($M3C1K_N$-*Rescaled* to $M3C9K_N$-*Rescaled*)
  - LSTM models:
    - ∗ Single hidden layer LSTM $L1CK_N$-*Models-Rescaled* ($L1C1K_N$-*Rescaled* to $L1C9K_N$-*Rescaled*)
    - ∗ Double hidden layer LSTM $L2CK_N$-*Models-Rescaled* ($L2C1K_N$-*Rescaled* to $L2C9K_N$-*Rescaled*)
    - ∗ Triple hidden layer LSTM $L3CK_N$-*Models-Rescaled* ($L3C1K_N$-*Rescaled* to $L3C9K_N$-*Rescaled*)

The benefits of scaling, such as convergence and faster training of ANN models, have been discussed in the literature[17] that forecasts call option prices scaled by the strike price (C_{N+1}/K_{N+1}), but none of these studies have compared the performance of directly forecasting option prices with the re-scaling of the forecasts of C_{N+1}/K_{N+1}.

[17] Examples include Dugas et al. (2001), Andreou et al. (2002), Gençay and Salih (2003), Andreou et al. (2008), Gradojevic et al. (2009), and Andreou et al. (2010).

2.4.2.1 Forecast Performance of CK-$Models$ Using Lagged Input Variables

Table 2.3 summarises the relative out-of-sample forecasting performance amongst the models that use lagged input variables to forecast the one-trading-day-ahead call option prices scaled by the strike price (C_{N+1}/K_{N+1}).[18] The performance metric is the $RMSE$ of the one-trading-day-ahead forecast errors of C_{N+1}/K_{N+1}, which is computed for each model utilising all of the errors in each day or each month. Amongst all of the models, including the random walk model (δCK_N)), columns V and VI record the number of months and days, respectively, that each model has the lowest $RMSE$ and while excluding the δCK_N model amongst the comparison, columns VII and VIII record the number of months and days that each model has the lowest $RMSE$.

From these comparisons, there are two key findings. Firstly, we notice the forecasting outperformance of the double hidden layer LSTM models, and in particular, the $L2CK2_N$ model outperforms all the models and has the lowest $RMSE$ for 96 days out of 1326. When monthly RMSE are used from daily forecasts, we find similar outperformance of the LSTM models, yet, the double hidden layer LSTM model, $L2CK6$ outperforms. Secondly, the LSTM models based on CK-$Models$ perform similarly to LSTM models based on C-$Models$. Out of 1326 forecasting days, the LSTM models collectively outperform for 778 days (59%) compared to the parametric models, where they collectively outperform for only 2 days (0%). The MLP models also collectively outperform for 549 days (41%). However, unlike the C-$Models$, none of the CK-$Models$ could outperform the random walk model.

As we did a comprehensive analysis for C-$Models$, we perform a similar analysis for CK-$Models$, where we consider the following nine comparisons of CK-$Models$. The associated tables are presented in the Appendix A.2 for the sake of brevity. We start with comparing the parametric models to the single hidden layer MLP and LSTM models (in Table A.2.19), double hidden layer MLP and LSTM models (in Table A.2.22), and triple hidden layer MLP and LSTM models (in Table A.2.25) in order to understand the forecasting performance across different layers of the ANN. We find a similar outperformance of all LSTM models compared to

[18] As explained in Section 2.4.2, the models using lagged input variables to forecast C_{N+1}/K_{N+1} are the random walk model (δCK_N), the parametric models ($BSMCK_N$, HCK_N, $HJDCK_N$, and $FMLSCK_N$), the single hidden layer MLP models ($M1CK_N$-$Models$), the single hidden layer LSTM models ($L1CK_N$-$Models$), the double hidden layer MLP models ($M2CK_N$-$Models$), the double hidden layer LSTM models ($L2CK_N$-$Models$), the triple hidden layer MLP models ($M3CK_N$-$Models$), and the triple hidden layer LSTM models ($L3CK_N$-$Models$).

other models, regardless of the number of hidden layers used in the models. More specifically, the single hidden layer LSTM model, $L1CK2_N$ model outperforms all other models and has the lowest $RMSE$ for 218 days (daily bootstrap winning percentage from 14% to 18%), the double hidden layer LSTM model, $L2CK2_N$ model outperforms all other models and has the lowest $RMSE$ for 201 days (daily bootstrap winning percentage from 13% to 17%), and the triple hidden layer LSTM model, $L3CK2_N$ outperforms all other models and has the lowest $RMSE$ for 203 days (daily bootstrap winning percentage from 13% to 17%). These three LSTM models belong to the Series 2 set of models, which uses the lagged call option price of the S&P 500 Index scaled by the strike price as an input along with inputs that replicate the BSM model (refer to Section 2.3.5.2.2).

We also confirm the forecasting performance of the Series 2 set of LSTM models when we compare them exclusively with all the parametric models. Tables A.2.21, A.2.24, and A.2.27 for the single, double and triple hidden layer LSTM models, respectively, show that the single hidden layer $L1CK2_N$ model outperforms the parametric models for 439 days, the two-layer $L2CK2_N$ model outperforms for 408 days, and the three-layer $L3CK2_N$ model outperforms for 410 days. The performance of the parametric models is also compared with MLP models exclusively in Tables A.2.20, A.2.23, and A.2.26 for single, double, and triple hidden layer MLP models, respectively. We find that the single hidden layer $M1CK3_N$ model outperforms all other models and has the lowest $RMSE$ for 216 days; the two-layer $M2CK3_N$ model outperforms all other models and has the lowest $RMSE$ for 179 days, and finally, the triple hidden layer $M3CK3_N$ model outperforms all other models and has the lowest $RMSE$ for 164 days. Thus, the CK-$Models$-based MLP models (single, double and triple hidden layers) have consistently out-performed the CK-$Models$-based parametric models, and moreover, the parametric models have fared poorly in comparison to the CK-$Models$-based LSTM models (as discussed above in this section).

2.4.2.2 Forecast Performance of CK-$Models$ Using One-trading-day-ahead Input Variables

Following the exercise of assessing the forecasting performance of one-trading-day-ahead moneyness ($CN+1/K_{N+1}$) by using lagged variables above, we now asses its forecasting performance by using one-trading-day-ahead input variables, and only for the triple layer ANN (MLP and LSTM) models in order to make results comparable. Table 2.4 presents the relative out-of-sample forecasting performance (in $RMSE$) amongst the models using one-trading-day-ahead input variables.[19] Similarly with the results obtained for the *C-Models* in Section 2.4.1.1 and Table 2.2, the *CK-Models*-based MLP models outperform, with the $M3CK2_{N+1}$ model having the lowest $RMSE$ for 308 days and outperforming all other models.

Furthermore, a substantial improvement of up to 199% (for MLP Series 2 models) in forecasting performance is evident for the models using one-trading-day-ahead input variables in the triple hidden layer MLP $M3CK_{N+1}$-*Models* compared to the $M3CK_N$-*Models* that use lagged input variables (mentioned in Table A.2.25 presenting the comparison between the parametric, and the triple hidden layer MLP and LSTM models using lagged input variables).[20] These results are in line with Garcia and Gençay (2000), Gençay and Qi (2001), Gençay and Salih (2003), Ghosn and Bengio (2002), and Gradojevic et al. (2009) who find that the MLP models typically outperform parametric models.

Next, we consider the comparison between the parametric and triple hidden layer MLP only and between the parametric and triple hidden layer LSTM models only, respectively. We find similar outperformance of the triple hidden layer MLP $M3CK_{N+1}$-*Models* when we compare them to parametric models in Table A.2.34, where the $M3CK2_{N+1}$ model again has the lowest $RMSE$ for 313 days. Furthermore, the triple hidden layer LSTM $L3CK_{N+1}$-*Models* outperform the parametric models when they are compared in Table A.2.35, where the $L3CK2_{N+1}$ model outperforms all the parametric models.

2.4.2.3 Forecast Performance of *Rescaled CK-Models* Using Lagged Input Variables

Furthermore, when we compare the out-of-sample performance of the random walk model, the class of models that use lagged input variables, which are the unscaled *C-Models* (from Section 2.4.1.1) and the rescaled *CK-Models* (called $CK - Models - Rescaled$ in Section 2.4.2), in Table 2.5, we observe that after rescaling the forecast variable, C_{N+1}/K_{N+1}, of the *CK-Models*

[19] Recall that the models using one-trading-day-ahead input variables to forecast the moneyness are the random walk model(δCK_N), the parametric models ($BSMCK_{N+1}$, HCK_{N+1}, $HJDCK_{N+1}$, and $FMLSCK_{N+1}$), the triple hidden layer MLP models ($M3CK_{N+1}$-*Models*), and the triple hidden layer LSTM models ($L3CK_{N+1}$-*Models*).

[20] For example, the forecasting performance of the $M3CK1_{N+1}$ has an improvement of 58% over $M3CK1_N$, $M3CK2_{N+1}$ has an improvement of 199% over $M3CK2_N$, $M3CK3_{N+1}$ has an improvement of 107% over $M3CK3_N$, $M3CK4_{N+1}$ has an improvement of 29% over $M3CK4_N$, $M3CK5_{N+1}$, however, has shown a decrease of 20% in forecasting performance compared to $M3CK5_N$, $M3CK6_{N+1}$ has an improvement of 5% over $M3CK6_N$, $M3CK7_{N+1}$ has a decrement of 56% in forecasting performance compared to $M3CK7_N$, $M3CK8_{N+1}$ has an improvement of 106% over $M3CK8_N$, and $M3CK9_{N+1}$ has an improvement of 82% over $M3CK9_N$.

to C_{N+1}, all of $CK-Models-Rescaled$ fail to out-perform the C-$Models$. The $L3C9_N$ model, which belongs to the category of C-$Models$, outperforms all other models and has the lowest $RMSE$ for 97 days. The $L3C9_N$ is also the out-performing model amongst all the models in Section 2.4.1.1. As a result, we have demonstrated that training and forecasting call option prices using ANN models with the homogeneity hint are inferior to models without it. [21]

To make the results comparable with previous studies that estimate an overall RMSE over their corresponding sample periods,[22] we provide an evaluation of the overall RMSE (for the period from September 2012 to December 2017) of C-$Models$ in Table A.1.6, and for CK-$Models$ in Table A.1.8. We compare only the models that use one-trading-day-ahead input variables to forecast option prices/moneyness since past literature does not use lagged variables in the test set. Andreou et al. (2010) forecast S&P 500 index option prices from January 2002 to August 2004 using an SV and SVJ with an ANN and found that their SV model (has a RMSE of 1.498) outperforms by 2.21% over their best performing ANN enhanced model, namely the CS ePOMP model (has a RMSE of 1.532), and by 1.46% over their best performing ANN enhanced model, namely the BS ePOMP model (RMSE of 1.754). Our best performing ANN model based on overall RMSE for a window spanning from September 2012 to December 2017 is the C-$Models$-based triple hidden layer MLP $M3C2_{N+1}$ model, which has a RMSE of 2.1 (in Table A.1.6), and the CK-$Models$-based triple hidden layer MLP $M3CK4_{N+1}$ model, which has a RMSE of 0.148 (in Table A.1.8).

[21] We also discuss in depth the relative out-of-sample forecasting performance amongst the models that use lagged variables and one-trading-day-ahead input variables to forecast the one-trading-day-ahead C_{N+1}/K_{N+1} in Sections A.2.3 and A.2.4, respectively. The RMSEs for the CK-$Models$ that use lagged input variables to forecast the C_{N+1}/K_{N+1} for the next trading day on a monthly, yearly, and overall basis can be found in Tables 3, 7, and 11, respectively and for the CK-$Models$ that use one-trading-day-ahead input variables to forecast the C_{N+1}/K_{N+1} for the next trading day on a monthly, yearly, and overall basis can be found in Tables 4, 8, and 12, respectively of the Electronic Appendix.

[22] See, for example, Andreou et al. (2010), Andreou et al. (2010) extended the models of Andreou et al. (2004), Andreou et al. (2006), and Andreou et al. (2008).

Table 2.3: This table presents the forecasting performance comparison using both daily and monthly statistics amongst *CK-Models* that use lagged input variables to forecast the one-trading-day-ahead call option price scaled by the strike price(C_{N+1}/K_{N+1}). The one-day-ahead forecast errors of C_{N+1}/K_{N+1} are used to compute the Root Mean Square Error (RMSE). Column I identifies the models, and columns II, III, and IV describe the network architecture of the MLP and LSTM models. Forecasts are made for 1,326 trading days, and there are 64 months covered in the sample using the monthly data. When comparing all models simultaneously (i.e. including the random walk model (δCK_N)), column V reports the number of months out of the 64 months that each model has the smallest RMSE, while column VI reports the number of days out of the 1,326 days each model has the smallest RMSE. Similarly, when the δCK_N model was excluded in the comparison, column VII reports the number of months out of the 64 months that each model has the smallest RMSE, while column VIII reports the number of days out of the 1,326 days each model has the smallest RMSE.

				Incl. random walk		**Excl. random walk**	
(I)	**(II)**	**(III)**	**(IV)**	**(V)**	**(VI)**	**(VII)**	**(VIII)**
Model	**No. of hidden layers**	**No. of hidden nodes per layer**	**Network architecture**	**Performance amongst all models (Monthly)**	**Performance amongst all models (Daily)**	**Performance amongst all models (Monthly)**	**Performance amongst all models (Daily)**
δCK_N	-	-	-	**18**	**202**	-	-
$BSMCK_N$	-	-	-	0	1	0	1
HCK_N	-	-	-	0	0	0	0
$HJDCK_N$	-	-	-	0	1	0	1
$FMLSCK_N$	-	-	-	0	0	0	0
$M1CK1_N$	1	5	5	0	13	0	14
$M1CK2_N$	1	6	6	0	6	1	6
$M1CK3_N$	1	11	11	0	23	0	26
$M1CK4_N$	1	16	16	3	15	3	16
$M1CK5_N$	1	17	17	2	15	2	23
$M1CK6_N$	1	10	10	0	14	1	14
$M1CK7_N$	1	11	11	0	19	0	19
$M1CK8_N$	1	13	13	0	18	0	19
$M1CK9_N$	1	7	7	0	16	0	16
$M2CK1_N$	2	5	5 X 5	0	1	0	1
$M2CK2_N$	2	6	6 X 6	0	89	0	89
$M2CK3_N$	2	11	11 X 11	0	4	0	4
$M2CK4_N$	2	16	16 X 16	0	19	0	20
$M2CK5_N$	2	17	17 X 17	0	16	0	16
$M2CK6_N$	2	10	10 X 10	0	10	0	10
$M2CK7_N$	2	11	11 X 11	1	14	1	14
$M2CK8_N$	2	13	13 X 13	0	0	0	0
$M2CK9_N$	2	7	7 X 7	0	2	0	2
$M3CK1_N$	3	5	5 X 5 X 5	0	25	0	26
$M3CK2_N$	3	6	6 X 6 X 6	0	36	0	40
$M3CK3_N$	3	11	11 X 11 X 11	2	32	3	41
$M3CK4_N$	3	16	16 X 16 X 16	1	20	1	25
$M3CK5_N$	3	17	17 X 17 X 17	0	15	0	17
$M3CK6_N$	3	10	10 X 10 X 10	4	12	5	15
$M3CK7_N$	3	11	11 X 11 X 11	1	21	1	27
$M3CK8_N$	3	13	13 X 13 X 13	2	21	2	27
$M3CK9_N$	3	7	7 X 7 X 7	0	16	0	22
$L1CK1_N$	1	5	5	0	6	0	6
$L1CK2_N$	1	6	6	0	92	0	**96**
$L1CK3_N$	1	11	11	0	8	0	8
$L1CK4_N$	1	16	16	0	18	0	19
$L1CK5_N$	1	17	17	0	28	0	31
$L1CK6_N$	1	10	10	0	15	0	15
$L1CK7_N$	1	11	11	0	17	0	18
$L1CK8_N$	1	13	13	0	0	0	0
$L1CK9_N$	1	7	7	0	10	0	10
$L2CK1_N$	2	5	5 X 5	2	25	2	26
$L2CK2_N$	2	6	6 X 6	2	29	4	40
$L2CK3_N$	2	11	11 X 11	6	41	6	52
$L2CK4_N$	2	16	16 X 16	5	39	7	63
$L2CK5_N$	2	17	17 X 17	3	22	7	55
$L2CK6_N$	2	10	10 X 10	3	30	**8**	52
$L2CK7_N$	2	11	11 X 11	3	24	3	32
$L2CK8_N$	2	13	13 X 13	4	24	4	35
$L2CK9_N$	2	7	7 X 7	1	18	2	28
$L3CK1_N$	3	5	5 X 5 X 5	0	7	0	7
$L3CK2_N$	3	6	6 X 6 X 6	0	76	0	78
$L3CK3_N$	3	11	11 X 11 X 11	1	12	1	12
$L3CK4_N$	3	16	16 X 16 X 16	0	25	0	26
$L3CK5_N$	3	17	17 X 17 X 17	0	25	0	26
$L3CK6_N$	3	10	10 X 10 X 10	0	14	0	14
$L3CK7_N$	3	11	11 X 11 X 11	0	15	0	16
$L3CK8_N$	3	13	13 X 13 X 13	0	0	0	0
$L3CK9_N$	3	7	7 X 7 X 7	0	13	0	13

Table 2.4: This table presents the forecasting performance comparison using both daily and monthly statistics amongst the *CK-Models* that use one-trading-day-ahead input variables to forecast the one-trading-day-ahead call option price scaled by the strike price(C_{N+1}/K_{N+1}). The one-day-ahead forecast errors of C_{N+1}/K_{N+1} are used to compute the Root Mean Square Error (RMSE). Column I identifies the models, and columns II, III, and IV describe the network architecture of the MLP and the LSTM models. Forecasts are made for 1,326 trading days, and there are 64 months covered in the sample using the monthly data. When comparing all models simultaneously (i.e. including the random walk model (δCK_N)), column V reports the number of months out of the 64 months that each model has the smallest RMSE, while column VI reports the number of days out of the 1,326 days each model has the smallest RMSE. Similarly, when the δCK_N model was excluded in the comparison, column VII reports the number of months out of the 64 months that each model has the smallest RMSE, while column VIII reports the number of days out of the 1,326 days each model has the smallest RMSE.

				Incl. random walk		**Excl. random walk**	
(I) Model	**(II)** No. of hidden layers	**(III)** No. of hidden nodes per layer	**(IV)** Network architecture	**(V)** Performance amongst all models (Monthly)	**(VI)** Performance amongst all models (Daily)	**(VII)** Performance amongst all models (Monthly)	**(VIII)** Performance amongst all models (Daily)
δCK_N	-	-	-	0	183	-	-
$BSMCK_{N+1}$	-	-	-	0	0	0	0
HCK_{N+1}	-	-	-	0	2	0	2
$HJDCK_{N+1}$	-	-	-	0	0	0	0
$FMLSCK_{N+1}$	-	-	-	0	0	0	0
$M3CK1_{N+1}$	3	5	5 X 5 X 5	0	117	0	120
$M3CK2_{N+1}$	3	6	6 X 6 X 6	**27**	**291**	**27**	**308**
$M3CK3_{N+1}$	3	11	11 X 11 X 11	12	181	12	203
$M3CK4_{N+1}$	3	16	16 X 16 X 16	18	120	18	143
$M3CK5_{N+1}$	3	17	17 X 17 X 17	0	49	0	71
$M3CK6_{N+1}$	3	10	10 X 10 X 10	3	79	3	106
$M3CK7_{N+1}$	3	11	11 X 11 X 11	0	25	0	52
$M3CK8_{N+1}$	3	13	13 X 13 X 13	2	140	2	165
$M3CK9_{N+1}$	3	7	7 X 7 X 7	2	131	2	140
$L3CK1_{N+1}$	3	5	5 X 5 X 5	0	0	0	0
$L3CK2_{N+1}$	3	6	6 X 6 X 6	0	5	0	10
$L3CK3_{N+1}$	3	11	11 X 11 X 11	0	1	0	2
$L3CK4_{N+1}$	3	16	16 X 16 X 16	0	1	0	2
$L3CK5_{N+1}$	3	17	17 X 17 X 17	0	2	0	2
$L3CK6_{N+1}$	3	10	10 X 10 X 10	0	0	0	0
$L3CK7_{N+1}$	3	11	11 X 11 X 11	0	1	0	2
$L3CK8_{N+1}$	3	13	13 X 13 X 13	0	0	0	0
$L3CK9_{N+1}$	3	7	7 X 7 X 7	0	0	0	0

Table 2.5: This table presents the forecasting performance comparison using both daily and monthly statistics amongst the parametric ($BSMC_N$, HC_N, $HJDC_N$, and $FMLSC_N$) models, MLP $M1C_N$-*Models*, LSTM $L1C_N$-*Models*, MLP $M2C_N$-*Models*, LSTM $L2C_N$-*Models*, MLP $M3C_N$-*Models*, and the LSTM $L3C_N$-*Models*, MLP $M1CK_N - Models - Rescaled$, MLP $M2CK_N - Models - Rescaled$, MLP $M3CK_N - Models - Rescaled$, LSTM $L1CK_N - Models - Rescaled$, LSTM $L2CK_N - Models - Rescaled$, and the LSTM $L3CK_N - Models - Rescaled$. The forecast variable for all the models is the one-day-ahead call option price (C_{N+1}). The models denoted by the $_N$ subscript use lagged input variables for forecasting C_{N+1}. The one-day-ahead forecast errors of C_{N+1} are used to compute the Root Mean Square Error (RMSE). Column I identifies the models, and column II identifies whether the forecast variable of the model has been re-scaled to C_{N+1}. Forecasts are made for 1,326 trading days, and there are 64 months covered in the sample using the monthly data. When comparing all models simultaneously (i.e. including the random walk model (δC_N), column III reports the number of months out of the 64 months that each model has the smallest RMSE, while column IV reports the number of days out of the 1,326 days each model has the smallest RMSE. Similarly, when the δC_N model was excluded in the comparison, column V reports the number of months out of the 64 months that each model has the smallest RMSE, while column VI reports the number of days out of the 1,326 days each model has the smallest RMSE.

		Incl. random walk		**Excl. random walk**	
(I)	**(II)**	**(III)**	**(IV)**	**(V)**	**(VI)**
Model	**Forecast variable re-scaled to call price**	**Performance amongst all models (Monthly)**	**Performance amongst all models (Daily)**	**Performance amongst all models (Monthly)**	**Performance amongst all models (Daily)**
δC_N	-	6	**100**	-	-
$BSMC_N$	-	0	17	0	17
HC_N	-	1	9	1	9
$HJDC_N$	-	0	0	0	6
$FMLSC_N$	-	0	0	0	0
$M1C1_N$	-	0	0	0	0
$M1C2_N$	-	1	1	1	1
$M1C3_N$	-	1	13	1	17
$M1C4_N$	-	0	13	0	19
$M1C5_N$	-	2	4	2	5
$M1C6_N$	-	1	2	2	3
$M1C7_N$	-	1	7	1	8
$M1C8_N$	-	0	2	0	5
$M1C9_N$	-	0	2	0	2
$M2C1_N$	-	0	4	0	4
$M2C2_N$	-	0	8	0	9
$M2C3_N$	-	1	9	1	13
$M2C4_N$	-	1	14	1	19
$M2C5_N$	-	0	1	0	3
$M2C6_N$	-	0	2	1	5
$M2C7_N$	-	0	3	0	6
$M2C8_N$	-	0	0	0	1
$M2C9_N$	-	0	2	0	4
$M3C1_N$	-	0	5	0	8
$M3C2_N$	-	0	13	0	15
$M3C3_N$	-	3	23	3	28
$M3C4_N$	-	2	10	2	16
$M3C5_N$	-	0	1	0	4
$M3C6_N$	-	0	0	0	2
$M3C7_N$	-	3	7	3	15
$M3C8_N$	-	0	1	1	7
$M3C9_N$	-	0	7	1	13
$L1C1_N$	-	0	0	0	0
$L1C2_N$	-	0	4	0	4
$L1C3_N$	-	0	7	0	7
$L1C4_N$	-	0	17	0	17
$L1C5_N$	-	4	27	4	27
$L1C6_N$	-	0	10	0	10
$L1C7_N$	-	0	19	1	20
$L1C8_N$	-	1	16	1	17
$L1C9_N$	-	0	1	0	1
$L2C1_N$	-	0	0	0	0
$L2C2_N$	-	0	28	0	28
$L2C3_N$	-	0	19	0	19
$L2C4_N$	-	0	19	0	19
$L2C5_N$	-	1	25	1	29
$L2C6_N$	-	2	10	2	11
$L2C7_N$	-	3	12	3	13
$L2C8_N$	-	2	24	3	26
$L2C9_N$	-	0	26	0	27
$L3C1_N$	-	0	22	0	22
$L3C2_N$	-	0	57	0	57
$L3C3_N$	-	0	26	0	26
$L3C4_N$	-	0	45	0	45
$L3C5_N$	-	1	34	1	35
$L3C6_N$	-	1	17	1	17
$L3C7_N$	-	4	17	4	18
$L3C8_N$	-	**9**	40	**9**	41
$L3C9_N$	-	0	97	0	**97**
$M1CK1_N - Rescaled$	Yes	0	3	0	3
$M1CK2_N - Rescaled$	Yes	0	1	0	1
$M1CK3_N - Rescaled$	Yes	0	9	0	9
$M1CK4_N - Rescaled$	Yes	1	4	1	4
$M1CK5_N - Rescaled$	Yes	1	4	1	4
$M1CK6_N - Rescaled$	Yes	0	3	0	3
$M1CK7_N - Rescaled$	Yes	0	7	0	7
$M1CK8_N - Rescaled$	Yes	0	2	0	2
$M1CK9_N - Rescaled$	Yes	0	8	0	8
$M2CK1_N - Rescaled$	Yes	0	5	0	5
$M2CK2_N - Rescaled$	Yes	0	18	0	18
$M2CK3_N - Rescaled$	Yes	1	14	1	14
$M2CK4_N - Rescaled$	Yes	0	8	0	8
$M2CK5_N - Rescaled$	Yes	0	8	0	8
$M2CK6_N - Rescaled$	Yes	0	2	0	2
$M2CK7_N - Rescaled$	Yes	0	12	0	12
$M2CK8_N - Rescaled$	Yes	1	5	1	5
$M2CK9_N - Rescaled$	Yes	0	5	0	5
$M3CK1_N - Rescaled$	Yes	2	5	2	5
$M3CK2_N - Rescaled$	Yes	1	12	1	14
$M3CK3_N - Rescaled$	Yes	0	12	0	12
$M3CK4_N - Rescaled$	Yes	1	10	1	10
$M3CK5_N - Rescaled$	Yes	0	3	0	3
$M3CK6_N - Rescaled$	Yes	0	9	0	9
$M3CK7_N - Rescaled$	Yes	1	7	1	7
$M3CK8_N - Rescaled$	Yes	2	10	2	10
$M3CK9_N - Rescaled$	Yes	0	3	0	3
$L1CK1_N - Rescaled$	Yes	0	1	0	1
$L1CK2_N - Rescaled$	Yes	0	37	0	37
$L1CK3_N - Rescaled$	Yes	0	2	0	2
$L1CK4_N - Rescaled$	Yes	0	11	0	11
$L1CK5_N - Rescaled$	Yes	0	7	0	7
$L1CK6_N - Rescaled$	Yes	0	8	0	8
$L1CK7_N - Rescaled$	Yes	1	7	1	7
$L1CK8_N - Rescaled$	Yes	0	0	0	0
$L1CK9_N - Rescaled$	Yes	0	0	0	0
$L2CK1_N - Rescaled$	Yes	0	6	0	6
$L2CK2_N - Rescaled$	Yes	0	22	0	22
$L2CK3_N - Rescaled$	Yes	0	5	0	5
$L2CK4_N - Rescaled$	Yes	0	12	0	12
$L2CK5_N - Rescaled$	Yes	0	14	0	14
$L2CK6_N - Rescaled$	Yes	0	9	0	9
$L2CK7_N - Rescaled$	Yes	0	10	0	10
$L2CK8_N - Rescaled$	Yes	0	0	0	0
$L2CK9_N - Rescaled$	Yes	0	2	0	2
$L3CK1_N - Rescaled$	Yes	0	5	0	5
$L3CK2_N - Rescaled$	Yes	0	27	0	27
$L3CK3_N - Rescaled$	Yes	1	8	1	8
$L3CK4_N - Rescaled$	Yes	0	15	0	15
$L3CK5_N - Rescaled$	Yes	0	12	0	12
$L3CK6_N - Rescaled$	Yes	0	10	0	10
$L3CK7_N - Rescaled$	Yes	0	10	0	10
$L3CK8_N - Rescaled$	Yes	0	0	0	0
$L3CK9_N - Rescaled$	Yes	0	1	0	1

2.4.3 Robustness tests for *C-Models* and *CK-Models*

2.4.3.1 The Diebold–Mariano(DM) Tests

In the DM tests, if the null can be rejected, a positive value (DM test statistic) suggests the rejection may be due to the second model being the better forecast model. In contrast, a negative value suggests the rejection may be due to the first model being the better forecast model. The model pairs with statistically insignificant differences in their prediction accuracy are reported in Table A.1.9. For the 1653 pairs created from models belonging to *C-Models* that use lagged input variables, 1.69% of the pairs is insignificant for the 231 pairs created from models belonging to *C-Models* that use one-trading-day-ahead input variables, 1.30% of the pairs is insignificant, for the 1653 pairs created from models belonging to *CK-Models* that use one-trading-day-ahead input variables, 0.91% of the pairs is insignificant, and for the 231 pairs created from models belonging to *CK-Models* that use one-trading-day-ahead input variables, 0.87% of the pairs is insignificant. Apart from the pairs mentioned in Table A.1.9, all the other pairs have significant forecasting power. Thus, the results are vastly statistically significant.

2.4.3.2 Bootstrap Tests

To further assess the validity of the forecasting performance results, we perform bootstrap tests using the daily and monthly RMSEs and discuss them in Sections A.2.1 through A.2.5, and present them in Tables A.2.1 to A.2.36 in Appendix A.2.[23] In these tables, columns IX (lower bound) and X (upper bound) present the results from the bootstrap (with replacement) using monthly RMSEs at a 95% confidence level and shows the winning percentage out of 64 months for each model (including the δC_N model), and columns XI (lower bound) and XII (upper bound) shows the 95% confidence intervals computed from bootstrapping of the daily RMSEs signifying the winning percentage out of 1328 days for each model. We repeat the exercise of performing the bootstrap by excluding the δC_N model in the comparisons, report the corresponding results in columns XV (lower bound), XVI (upper bound) for monthly RMSEs and columns XVII (lower bound), XVIII (upper bound) for the daily RMSEs. We conclude that the results from

[23]These results are summarised in Tables A.2.1 to A.2.14 for *C-Models* that use lagged input variables, Tables A.2.15 to A.2.18 for *C-Models* that use one-trading-day-ahead input variables, Tables A.2.19 to A.2.32 for *CK-Models* that use lagged input variables, and Tables A.2.33 to A.2.36 for *CK-Models* that use one-trading-day-ahead input variables.

the bootstrap tests typically support the results discussed in Sections 2.4.1 and 2.4.2.

2.4.3.3 Pairwise Test

We complement the model comparisons in this chapter with pairwise comparisons by performing a pairwise bootstrap comparison, which is computed using the respective pair's daily RMSEs. The pairwise bootstrap results for *C-Models* pairs using lagged input variables are presented in Table 17, for the *C-Models* pairs using one-trading-day-ahead input variables are presented in Table 18, for the *CK-Models* pairs using one-trading-day-ahead input variables are presented in Table 19, and for the *CK-Models* pairs using one-trading-day-ahead input variables are presented in Table 20 of the Electronic Appendix. We have summarised the results from all the above-mentioned tables in Table A.1.10. The MLP class of models outperforms for over 68.1%, the LSTM models for 24.2%, and parametric models a meagre 4.3% of the 1711 pairs created from models belonging to *C-Models* that use lagged input variables. For the 253 pairs created from models belonging to *C-Models* using one-trading-day-ahead input variables, the MLP class of models outperforms for over 60.9%, the LSTM models for 17.4%, and parametric models for 17.8% of the pairs. Similar to the *C-Models*, for the 1711 pairs created from models belonging to *CK-Models* that use lagged input variables, again the MLP class of models outperforms for, over 69.4%, the LSTM models outperform for 25.5% and parametric models with the lowest outperformance of 1.7%. Also, similar out-performance of the MLP class of models is evident when we created 253 pairs from models belonging to *CK-Models* that use one-trading-day-ahead input variables, where the MLP class of models outperforms for over 64%, the LSTM models for 25.3%, and parametric models for 5.5% of the pairs. Even though the comparisons performed in Sections 2.4.1 and 2.4.2 show that the LSTM models consistently outperform other models, the pairwise bootstrap comparison cannot reveal conclusive evidence on outperforming models.

2.4.3.4 Computational Effort

This exercise of daily forecasting of index option prices has shown that the models that forecast option prices are able to capture the non-linear dynamics of option prices with a high degree of accuracy but are computationally very intensive compared to models that forecast moneyness. We have documented the number of epochs required for training models which are similar to *C-Models* and *CK-Models* in Table A.1.15. The models belonging to the category of *CK-Models* were faster than their C-$Models$-based counterparts, with typically large RMSE (i.e. when we compare the RMSEs from the rescaled forecasts of CK-$Models$ with the RMSEs of forecasts of call option prices from C-$Models$.

2.5 Conclusion

In this chapter, the daily forecasting performance of European-style index options prices has been empirically evaluated by using parametric (Black–Scholes–Merton, Heston, Heston Jump Diffusion, and the Finite Moment Log Stable), MLP, and LSTM networks. The MLP and LSTM networks are trained using both lagged and one-trading-day-ahead input variables to forecast the one-trading-day-ahead option price and moneyness. An alternative approach is investigated, where MLP and LSTM networks are trained using lagged input variables to forecast moneyness and then via re-scaling option prices. Several robustness tests have also been used to further validate the analysis.

We find that the ANN tends to provide a considerable improvement in daily out-of-sample forecast performance of options prices and moneyness compared to the parametric models. More specifically, LSTM models using lagged input variables to forecast the one trading-day-ahead option price outperform the parametric and MLP models. However, the MLP models outperform the parametric and LSTM models when using one-trading-day ahead input variables for daily forecasts of option prices. Within the parametric models, the Heston Jump Diffusion model has the lowest RMSEs among the other three parametric models. This result holds for both types of inputs, namely lagged and one-trading-day ahead input variables. Moreover, when the models that used lagged input variables to forecast moneyness are rescaled to option prices, the rescaled models fare poorly to the models using lagged input variables to forecast option prices. Also, the LSTM models tend to outperform other parametric and MLP models. The robustness tests further support these results.

Furthermore, from all of these comparisons, it is evident that neither the parametric models nor the non-parametric models (MLP and LSTM models) could improve on a simple random walk forecasting model. This suggests that there may be some innate randomness that cannot be effectively forecasted by either parametric or non-parametric models. Though the out-of-sample performance of parametric models are not necessarily dominated, at least for forecasting, they have an important role in developing inputs for the Deep Learning ANN models (MLPs and LSTMs).

The focus of this study is to perform a comprehensive assessment of the daily forecast of option prices. Even though it is beyond the purpose of this thesis, this ANN methodology can be extended for longer forecast windows. That exercise would involve recursively forecasting one-trading-day-ahead options, using multiple times a one-step model, where the forecast for the prior time step is used as an input for making a forecast on the following time step. Thereby, this multi-step forecast approach would incur higher forecasting errors compared to the one-trading-day forecast. One of the concerns of the approach used in this chapter is that the forecasting performance comparison between models is biased by model and error uncertainty. To improve this in Chapter 5, we also assess the forecasting performance of the models considered in this study based on an averaging error approach as proposed by Gençay and Qi (2001).

Chapter 3

Daily Forecasting of Delta for S&P 500 Index Options Using Deep Learning Models

3.1 Introduction

Risk management practices for options positions are critically important, with delta hedges being the most conventional yet fundamental type of hedges. Hedging short-term price risk for options positions requires dynamic hedges, which may not always be effective, especially during periods of high volatility. Parametric models, such as the Black and Scholes (1973) (BS) option pricing model, and the stochastic volatility models of Heston (1993), Bakshi et al. (1997a), Heston (1993), and Black and Scholes (1973) derive the delta hedge ratio based on the distributional assumptions of the underlying process and have been providing effective hedges (Andreou et al. (2010), Buehler et al. (2019)). However, Artificial Neural Networks (ANNs) provide an alternative approach that does not impose a rigid model structure; instead, they are based on universal function approximators (Gybenko et al. (1989), Hornik et al. (1990), Buehler et al. (2019), Hornik et al. (1989)). Most studies derive the hedge ratios from an ANN fitted to options prices.[1] Chen and Sutcliffe (2012), Carverhill and Cheuk (2003), Buehler et al. (2019), and Ruf and Wang (2021) used ANNs to hedge options by directly training the ANN on hedge ratios rather than prices. An ongoing direction of this research is to extend this literature to

[1]Refer to the list of papers in Table 1.2

daily S&P 500 index call options and to train the ANN models with additional input variables to better capture the relationships between the hedge ratios and the underlying asset and to potentially produce improved hedging performance. Furthermore, most of the existing studies are limited in evaluating hedge ratios and assessing hedging performance using single hidden layer ANN, including Gençay and Qi (2001), Andreou et al. (2008), Andreou et al. (2010), and Ruf and Wang (2020).

This chapter investigates the forecasting performance of deltas[2] for European-style index options using triple hidden layer Deep Learning ANN models, in particular, the MLP and LSTM networks. These multi-layer ANN models have the potential to achieve improved forecasting, pricing, and hedging performance compared to single hidden layer ANN (Hutchinson et al. (1994), Gençay and Qi (2001), Garcia and Gençay (2000), Andreou et al. (2008), Thomaidis et al. (2006a)).[3] We assess the empirical forecasting performance of European-style index options delta of parametric models and ANN models using daily data on S&P 500 index option prices from September 2012 to December 2017. Similarly to the pricing forecasting analysis in Chapter 2, we have used the following four parametric models, Black-Scholes-Merton, Heston, Heston Jump Diffusion, and the Finite Moment Log Stable, and the ANN models are trained on various lagged and one trading-day-ahead input variables. This study focuses on (only) one-trading-day-ahead forecasts aiming to provide an assessment suitable for short-term dynamic hedging relevant to traders who re-balance their portfolios on a daily basis. In practice, dynamic delta hedging requires daily re-balancing of the hedged portfolio.[4]

We obtain daily forecasts of European-style index options delta in two different ways. First, the delta is directly evaluated using ANN models to forecast the one trading-day-ahead delta. For this direct forecasting methodology of the delta, the ANN models may use lagged input variables and also one-trading-day-ahead input variables. The lagged input variables specification allows to incorporate information from longer horizons of input variables and consists of one of the innovations of the current study. The one-trading-day-ahead input variables specifications have

[2]For this paper, the focus is only on delta hedge ratio as we assess only short-term effects (daily forecasting). These ANN approaches can be extended to consider other greeks letters, e.g. gamma, but these approaches require forecasting for longer horizons, which are beyond the purpose of this thesis.

[3]Note that for this exercise, we only consider triple layer ANN (MLP and LSTM) models, because previously in Chapter 2, we saw the triple hidden layer ANN models had broadly outperformed the single and double hidden layers ANN models.

[4]These methodologies can be extended to longer forecast windows, but it is beyond the purpose of this thesis.

been widely used in other studies.[5] Thus, we compare seven MLP models and seven LSTM models having lagged input variables with four parametric models and seven MLP models and seven LSTM models having one-trading-day-ahead input variables with four parametric models. Second, we use the ANN models to forecast the one trading-day-ahead option price, from which the delta is then analytically derived. For this indirect forecasting methodology of deltas, the ANN models are trained on one-trading-day-ahead input variables only. Using lagged input variables to obtain option prices to analytically derive the delta is not feasible because calculating the delta analytically would require the one-trading-day-ahead index price. Therefore, we assess seven MLP models and seven LSTM models having one-trading-day-ahead input variables with four parametric models to forecast the one-trading-day-ahead call option price, from which the delta is then analytically derived.

Lastly, we (re-)assess the daily forecasting performance of the deltas based on their ability to forecast the replicating portfolio value. The replicating portfolio can be constructed by selling one call option at time 0 and dynamically adjusting the number of stocks and bonds throughout the option's life. Thus, at expiration, the combined value of the positions of stocks and bonds should exactly match the value of the call under the assumption that the adjustments can be made continuously and at zero cost. The difference in terminal values between the call, stock, and bond positions is the measure of the option-pricing model's accuracy.[6] Robustness tests based on bounds assessments and DM tests to assess the significance of pairwise comparisons between the corresponding ANN and parametric models have also been performed.

We find that forecasting one trading-day-ahead delta using parametric models, specifically, the BSM model outperforms other parametric models and ANN models (see also Andreou et al. (2010) and Ruf and Wang (2021) for similar conclusions). The ANN models, independent of the inputs used to be trained (lagged or one-trading-day-ahead input variables), have shown no significant improvement in the out-of-sample forecasting performance of these networks. Hence, deep learning models do not improve the forecasting performance of deltas or inferring the replicating portfolio value compared to the parametric models. Indeed, the BSM model typically displays the lowest RMSEs,[7] especially when the comparison is limited to only parametric mod-

[5] Refer to the list of papers in Table 1.2

[6] Practically, continuous hedging is not possible, and hence the process of delta hedging always results in tracking error.

[7] Some works from Table 1.2 have presented their results in an evaluation measure other than RMSE. However, since our study assesses the daily forecast of the hedge ratio and the associated replicating portfolio value, we use RMSE as a measure, as reporting in RMSE provides insight in terms of actual dollar value.

els. We also find that both forecasting assessments –forecasting of the one trading-day-ahead delta and forecasting the replicating portfolio value –provide consistent results in terms of the outperforming models. The results are also robust based on a bound assessment of performance, while the DM tests show that out of the 918 model pairs, only 1.95% of the pairs have insignificant forecasting power. However, when the MLP and LSTM networks are used to predict the one-trading-day-ahead delta indirectly by training the ANN models to predict prices and then analytically infer the one-trading-day-ahead delta, the LSTM models produce forecasts with the lower RMSE's compared the four parametric and the MLP models.

This study makes several key contributions to the literature. Many previous studies have covered the hedging performance of the Black-Scholes-Merton, Heston, Heston Jump Diffusion and the Multi-Layer Perceptron,[8] but this is the first study to assess the performance of the Finite Moment Log Stable and Long Short-Term Memory Networks. There is empirical evidence (Masini et al. (2021)) that these ANNs, except for RNNs, deal with the vanishing or exploding gradient and improve time series forecasting.

Secondly, we introduce lagged input variables to tackle look ahead bias while using a test set for the parametric, MLP, and LSTM models. Much of the associated literature uses input variables, for example, the end-of-day index close prices belonging to the test set to forecast the end-of-day delta or the other associated greeks. Then, the index price is required to compute that it is only available at the close of that trading day, thus inducing look-ahead bias. Except for a few studies (Carverhill and Cheuk (2003), Chen and Sutcliffe (2012), Ruf and Wang (2021), and Buehler et al. (2019)), previous literature[9] has derived the hedge ratios analytically from an ANN fitted to option prices. Thus, another contribution of the study is the assessment of hedging performance using hedge ratios, which are computed directly from the ANN, as well as hedge ratios, which are computed analytically from an ANN fitted to option prices.

Lastly, the economic significance of option pricing models can be assessed by the hedging performance of various replicating portfolios, which can be designed to delta-hedge an option position (Hutchinson et al. (1994)). Amilon (2003) proposed a different exercise for evaluating a pricing model's performance by trading in mispriced options, where the under-priced according to the

[8]For example, Hutchinson et al. (1994) were the first to measure the hedging performance of ANN models by introducing three ANN models, the Radial-Basis Function network, the MLP network, and the Projection Pursuit network, on the S&P Futures 500 options. Herrmann and Narr (1997) followed Hutchinson et al. (1994) by training an ANN model for hedging DAX options.

[9]Refer to the list of papers in Table 1.2.

respective pricing model is bought and is then delta hedged until the overpriced option become under-priced, or if the under-priced option become overpriced, or the option expires. In doing so, a pricing model can identify mispriced options, and the terminal value of the position should be positive. Similarly, Andreou et al. (2008) implemented a trading strategy for delta hedging, whereby they create portfolios by buying (selling) options that are undervalued (overvalued) relative to the option price from the respective pricing model. Out-of-sample pricing performance does not always prove to be better at delta hedging, according to Hutchinson et al. (1994), Garcia and Gençay (2000) and Schittenkopf and Dorffner (2001). Ruf and Wang (2021) compared linear regressions with their newly designed neural network known as 'HedgeNet', which is designed for the hedging of options that was trained to minimise the hedging error instead of the pricing error. This approach reduces the mean squared hedging error of the Black–Scholes benchmark significantly; however, similar results were also obtained using simple linear regressions. Thus, to investigate the economic significance of the option pricing models, we consider a replicated portfolio constructed similar to Ruf and Wang (2021) and further assess the hedging performance via the forecasting performance of the replicating portfolio.

This chapter is structured as follows. Section 3.2 explains the source of the data set, the filters used to refine the data set, the summary statistics of the data set, and the inputs used. Section 3.3 presents the calibration procedures used in the BS, Heston, SVJ, and FMLS model and the data fitting (network parameters, division of data set, the optimisation and generalisation procedures used to improve the accuracy of ANN (MLP and LSTM) models). Section 3.4 compares the forecasting performance of deltas from the proposed deep learning models and the parametric models and includes the findings of several robustness tests. The chapter concludes with Section 3.5.

3.2 Data and Methodology

3.2.1 Optionmetrics and Data Filtering

This study uses the same Optionmetrics data set as mentioned in Section 2.3.1. In addition to the filtering steps mentioned in Section 2.3.2, we also apply an additional filter as the previous trading day's call price is used to calculate the lagged empirical delta, which is an input to the neural networks, and as a result, we remove those observations having no previous day option price (16,716 observations), and thereby the total number of observations on call options used in this study is 547,011.

3.2.2 Summary Statistics

Appendix B.1.12 provides summary statistics for the call option delta used in this study. The monthly summary statistics show that the total number of daily option prices included each month varies from $1,975$ in September 2012 to $8,281$ in December 2017. The average delta has been at around 0.406 from 2012 to 2017. Appendix B.1.13 provides summary statistics for the call option prices used in this study. The monthly average call price varies from \$76.89 to \$156.28, so we see that these average prices have doubled from 2012 to 2017. In contrast, the average bid-ask spread, which varies from \$1.46 in September 2012 to \$1.81 in December 2017, has increased by a smaller percentage. The CBOE reports that the annual average daily volume has increased from $698,000$ SPX contracts in 2012 to $1,163,000$ SPX contracts in 2017.

3.2.3 Forecasting Errors

Using the methodology to decompose the forecasting errors discussed in Section 2.3.4, the errors in forecasting the delta ($\delta C_{N+1}/\delta S_{N+1}$) on day $(N+1)$ can be defined as:

$$\frac{\delta C_{N+1}}{\delta S_{N+1}} = h\left(X_N; \hat{\phi}_{N+1}\right) + u^X_{N+1} + u^{\phi}_{N+1} + u^{g}_{N+1} + u^{r}_{N+1} \tag{3.1}$$

$$= h\left(X_N; \hat{\phi}_{N+1}\right) + \epsilon_{N+1} \tag{3.2}$$

where u^X_{N+1} is the error caused by using X_N rather than X_{N+1}, and is interpreted as forecasting using observations from the previous trading day, rather than the trading day that the delta is observed. In the analysis below, we consider the forecast errors as defined by ϵ_{N+1} so that the forecasts are made for the trading day $(N+1)$ based on information available at the end of the trading day N.

3.2.4 Information Sets (for Computing the Delta)

In this section, we discuss the information sets required for each model that falls under the category of $H-Models$ and $CH-Models$ for calibration and estimation of parameters and for forecasting the one-trading-day-ahead delta.

3.2.4.1 Empirical Delta

The empirical delta is computed using

$$\delta_{N+1}^{EMP} = \frac{C_{N+1} - C_N}{S_{N+1} - S_N} \tag{3.3}$$

where, C_N is the call price and S_N is the index price of the S&P 500 Index.

3.2.4.2 $H - Models$: Parametric Models (Black–Scholes–Merton, Heston, Heston Jump Diffusion, and Finite Moment Log Stable Model)

The focus of this chapter is on the delta forecasting performance of parametric option pricing models relative to Deep Learning ANN models (MLP and LSTM). Here we define the information sets required for each model for calibration or estimation of parameters and for forecasting the hedge ratio (delta). We implement a single forecasting horizon, that is, one-trading-day-ahead forecasts of the delta. We use the information available on day $t = N$ to forecast the delta for day $t = N + 1$, and these models are denoted by an N subscript. Similarly, models that we use the information available on day $t = N + 1$ to forecast the delta for day $t = N + 1$ are denoted by the $N + 1$ subscript. The parametric models are calibrated daily, based only on the data available for day N, whereas the MLP models use an expanding window, using data for $t = 1, ..., N$ for estimation and forecast for day $t = N + 1$ and the LSTM models use a fixed-sliding window, using data for $t = 1, ..., N$ for estimation and forecast for day $t = N + 1$. Thus, the parametric models follow the usual convention of daily calibrations, whereas the expanding window allows the MLP and the fixed-sliding window for the LSTM to cover a wide range of values for its input variables. In what follows, we use ϕ to represent a generic parameter scalar or vector for each model.

For the parametric models that fall under the $H - Models$ category, on day N the information used to calibrate the model parameters for each option is $(C_N, S_N, K_N, T_N, R_N, Q_N; \phi_N^{Model})$, and we define the in-sample error in forecasting the delta, $\epsilon_N^{Model_N}$, for each option under each model as:

$$\epsilon_N^{Model_N} = \delta_N^{EMP} - \delta^{Model}\left(S_N, K_N, T_N, R_N, Q_N; \phi_N^{Model}\right) \tag{3.4}$$

where, ϕ_N^{Model} and δ^{Model} are for each model as follows:

- Black–Scholes–Merton model: $\phi_N^{Model} = \phi_N^{BSMH^C} = (\sigma_N^{CALIB^C})$, and $\delta^{Model}(.)$ is the delta from the Black–Scholes–Merton model.

- Heston model: $\phi_N^{Model} = (\sigma_N^{CALIB^{C^2}};\ \phi_N^{HH^C})$, where $\sigma_N^{CALIB^{C^2}}$ is the square of $\sigma_N^{CALIB^C}$ which is used as the initial value for the long-term variance parameter and $\phi_N^{HH^C} = HHParams_N^C = (\kappa_N^{HH^C}, \sigma_N^{HH^C}, \theta_N^{HH^C}, \rho_N^{HH^C}, V_{0,N}^{HH^C})$, and $\delta^{Model}(.)$ is the delta from the Heston model.

- Heston Jump Diffusion model: $\phi_N^{Model} = (\sigma_N^{CALIB^{C^2}}\ ;\ \phi_N^{HJDH^C})$, where $\phi_N^{HJDH^C} = HJDHParams_N^C = (\kappa_N^{HJDH^C}, \sigma_N^{HJDH^C}, \theta_N^{HJDH^C}, \rho_N^{HJDH^C}, V_{0,N}^{HJDH^C}, \sigma_N^{HJDH^C}, \mu_N^{HJDH^C}, \lambda_N^{HJDH^C})$, and $\delta^{Model}(.)$ is the delta from the Heston Jump Diffusion model.

- Finite Moment Log Stable model: $\phi_N^{Model} = \phi_N^{FMLSH^C} = (\alpha_N^{FMLSH^C}, \sigma_N^{FMLSH^C})$, and $\delta^{Model}(.)$ is the delta from the Finite Moment Log Stable model.

However, the models that have the one-day-ahead delta computed from the call prices (these models are suffixed with CH_{N+1}) are computed as:

$$C_{N+1}^{Model} = \delta^{Model}\left(S_{N+1}, K_{N+1}, T_{N+1}, R_{N+1}, Q_{N+1}; \phi_N^{Model}\right) \tag{3.5}$$

$$\delta_{N+1}^{Model} = \frac{C_{N+1}^{Model} - C_N^{Model}}{S_{N+1} - S_N} \tag{3.6}$$

We calibrate each model for each day (over historical empirical call option prices) by choosing ϕ_N^{Model} to minimise the mean square error. In this case, we retain the fitted option prices and the calibrated parameters for each respective model are as follows:

- $\sigma_N^{CALIB^C}$ for the Black–Scholes–Merton model,
- $HParamsH_N^C$ for the Heston model,
- $HJDParamsH_N^C$ for the Heston Jump Diffusion model,
- $\alpha_N^{FMLSH^C}$, and $\sigma_N^{FMLSH^C}$ for the Finite Moment Log Stable model,

We compute the one-trading-day-ahead forecast errors, $\epsilon_{N+1}^{Model_N}$, for each of the respective models as:

$$\epsilon_{N+1}^{Model_N} = \delta_{N+1}^{EMP} - \delta^{Model}\left(S_N, K_N, T_N, R_N, Q_N; \phi_N^{Model}\right). \tag{3.7}$$

Here we evaluate the delta at the index value on the previous trading day, using the known exercise price and time to maturity, as well as the previous day's interest rate, dividend yield, and respective calibrated parameters for each of the respective models. Finally, for the parametric models that fall under the $H - Models$ category that use one-trading-day-ahead input variables for forecasting the one-trading-day-ahead Δ_{N+1}, we compute the one-trading-day-ahead forecast errors for these models as:

$$\epsilon_{N+1}^{Model_{N+1}} = \delta_{N+1}^{EMP} - \delta^{Model}\left(S_{N+1}, K_{N+1}, T_{N+1}, R_{N+1}, Q_{N+1}; \phi_N^{Model}\right). \tag{3.8}$$

Finally, using the δ_{N+1} computed in Eq. (3.6), the one-trading-day-ahead forecast errors for those models (models that are suffixed with CH_{N+1}) are:

$$\epsilon_{N+1}^{Model} = \delta_{N+1}^{EMP} - \delta_{N+1}^{Model} \tag{3.9}$$

We report the root mean square error of these forecast errors.

3.2.4.3 Deep Learning Neural Network Models

A total of 21 MLPs and 21 LSTMs were estimated and reported in this study to compare the one trading ahead delta. Amongst the 21 MLPs, we analysed the performance of 7 MLPs that use the information available on day $t = N$ to forecast option delta for day $t = N+1$ (referred to as MLP $M3H_N$-Models), 7 MLPs that use use the information available (except for calibrated model parameters) on day $t = N + 1$ to forecast option delta for day $t = N + 1$ (referred to as MLP $M3H_{N+1}$-Models), and the other 7 MLPs that use the information available (except for calibrated model parameters) on day $t = N + 1$ to forecast option prices for day $t = N + 1$ (referred to as MLP $M3CH_{N+1}$-Models), and the delta for these is computed as,

$$\delta_{N+1}^{M3CH_{N+1}\text{-}Models} = \frac{C_{N+1}^{M3CH_{N+1}\text{-}Models} - C_N^{M3CH_{N+1}\text{-}Models}}{S_{N+1} - S_N} \tag{3.10}$$

Similarly, the exercise conducted for MLP $M3H_N$-Models is replicated for the LSTM $L3H_N$-Models and MLP $M3H_{N+1}$-Models for the LSTM $L3H_{N+1}$-Models.

The forecast variable ($\delta C_{N+1}/\delta S_{N+1}$), the target variable ($\delta C_N/\delta S_N$) used while training, and the inputs used to forecast $\delta C_{N+1}/\delta S_{N+1}$ are the same for the MLP $M3H_N$-Models and LSTM $L3H_N$-Models. Similarly, the forecast variable ($\delta C_{N+1}/\delta S_{N+1}$), the target variable ($\delta C_N/\delta S_N$) used while training, and the inputs used to forecast $\delta C_{N+1}/\delta S_{N+1}$ are the same for the MLP $M3H_{N+1}$-Models and LSTM $L3H_{N+1}$-Models. Whereas, the seven MLP $M3CH_{N+1}$-Models, LSTM $L3CH_{N+1}$-Models differ in the forecast variable (C_{N+1}), the target variable (C_N), but the input variable to forecast C_{N+1}, is similar and inline with the $M3H_{N+1}$-Models and $L3H_{N+1}$-Models. The input variables for the MLP $M3H_N$-Models, LSTM $L3H_N$-Models, MLP $M3H_{N+1}$-Models, LSTM $L3H_{N+1}$-Models, MLP $M3CH_{N+1}$-Models, and the LSTM $L3CH_{N+1}$-Models are mentioned in Table B.1.1. All the seven models under each category (i.e. MLP $M3H_N$-Models, LSTM $L3H_N$-Models, MLP $M3H_{N+1}$-Models, LSTM $L3H_{N+1}$-Models, MLP $M3CH_{N+1}$-Models, and the LSTM $L3CH_{N+1}$-Models) are differentiated by the choice of input variables and the network architecture. As in the parametric models, each model here has a set of input variables and a set of parameters, ϕ, called biases and weights. We compute the one-trading-day-ahead forecast errors under the respective models as follows:

1. **MLP $M3H_N$-Models ($M3H1_N$ to $M3H7_N$):**

$$\epsilon_{N+1}^{M3H_N-Models} = \delta_{N+1}^{EMP} - \delta\left(X_N; \phi^{M3H_N-Models}\right) \tag{3.11}$$

2. **LSTM $L3H_N$-Models ($L3H1_N$ to $L3H7_N$):**

$$\epsilon_{N+1}^{L3H_N-Models} = \delta_{N+1}^{EMP} - \delta\left(X_N; \phi^{L3H_N-Models}\right) \tag{3.12}$$

3. **MLP $M3H_{N+1}$-Models ($M3H1_{N+1}$ to $M3H7_{N+1}$):**

$$\epsilon_{N+1}^{M3H_{N+1}-Models} = \delta_{N+1}^{EMP} - \delta\left(X_{N+1}; \phi^{M3H_{N+1}-Models}\right) \tag{3.13}$$

4. **LSTM $L3H_{N+1}$-Models ($L3H1_{N+1}$ to $L3H7_{N+1}$):**

$$\epsilon_{N+1}^{L3H_{N+1}-Models} = \delta_{N+1}^{EMP} - \delta\left(X_{N+1}; \phi^{L3H_{N+1}-Models}\right) \tag{3.14}$$

5. **MLP $M3CH_{N+1}$-Models ($M3CH1_{N+1}$ to $M3CH7_{N+1}$):**

$$\epsilon_{N+1}^{M3CH_{N+1}-Models} = \delta_{N+1}^{EMP} - \delta\left(X_{N+1}; \phi^{M3CH_{N+1}-Models}\right) \tag{3.15}$$

6. **LSTM $L3CH_{N+1}$-Models ($L3CH1_{N+1}$ to $L3CH7_{N+1}$):**

$$\epsilon_{N+1}^{L3CH_{N+1}-Models} = \delta_{N+1}^{EMP} - \delta\left(X_{N+1}; \phi^{L3CH_{N+1}-Models}\right) \tag{3.16}$$

where $f(.)$ represents the delta obtained from a Deep Learning ANN model. We estimate this model each day (over historical empirical call option prices) by choosing ϕ to minimise the mean square error. We report the root mean square error of these forecast errors. Thus, the models above are defined by identifying the inputs of each model X_N for the: MLP $M3H_N$-Models and LSTM $L3H_N$-Models, and X_{N+1} for the: MLP $M3H_{N+1}$-Models, LSTM $L3H_{N+1}$-Models, MLP $M3CH_{N+1}$-Models, and the LSTM $L3CH_{N+1}$-Models.

Unlike the parametric models, the MLP Models ($M3H_N$-Models, $M3H_{N+1}$-Models, and $M3CH_{N+1}$-Models) are estimated with an expanding window of observations, whereas, the LSTM Models ($L3H_N$-Models, $L3H_{N+1}$-Models, and $L3CH_{N+1}$-Models) are estimated with a fixed-sliding window of observations, but the forecast horizon remains one trading day for all the models, so we compute the one-trading-day-ahead forecasts and report the root mean square error of the forecast errors. We denote the daily changes in the call and index prices as $\delta C_N = C_{t+1} - C_N$ and $\delta S_N = S_{t+1} - S_N$, respectively. The empirical delta from the observed call prices C_N and observed index prices S_N is defined as the quotient $\frac{\delta C_N}{\delta S_N}$. The empirical delta as defined above are the target variable in the non-parametric models: $M3H_N$-Models, $L3H_N$-Models, $M3H_{N+1}$-Models, and $L3H_{N+1}$-Models, whereas the target variable for the $M3CH_{N+1}$-Models and the $L3CH_{N+1}$-Models is the C_N. We have classified the non-parametric models ($M3H_N$-Models, $L3H_N$-Models, $M3H_{N+1}$-Models, $L3H_{N+1}$-Models, $M3CH_{N+1}$-Models and $L3CH_{N+1}$-Models) into seven categories:

1. **Series 1:** $M3H1_N$, $L3H1_N$, $M3H1_{N+1}$, $L3H1_{N+1}$, $M3CH1_{N+1}$, and $L3CH1_{N+1}$ models
2. **Series 2:** $M3H2_N$, $L3H2_N$, $M3H2_{N+1}$, $L3H2_{N+1}$, $M3CH2_{N+1}$, and $L3CH2_{N+1}$ models
3. **Series 3:** $M3H3_N$, $L3H3_N$, $M3H3_{N+1}$, $L3H3_{N+1}$, $M3CH3_{N+1}$, and $L3CH3_{N+1}$ models
4. **Series 4:** $M3H4_N$, $L3H4_N$, $M3H4_{N+1}$, $L3H4_{N+1}$, $M3CH4_{N+1}$, and $L3CH4_{N+1}$ models
5. **Series 5:** $M3H5_N$, $L3H5_N$, $M3H5_{N+1}$, $L3H5_{N+1}$, $M3CH5_{N+1}$, and $L3CH5_{N+1}$ models
6. **Series 6:** $M3H6_N$, $L3H6_N$, $M3H6_{N+1}$, $L3H6_{N+1}$, $M3CH6_{N+1}$, and $L3CH6_{N+1}$ models
7. **Series 7:** $M3H7_N$, $L3H7_N$, $M3H7_{N+1}$, $L3H7_{N+1}$, $M3CH7_{N+1}$, and $L3CH7_{N+1}$ models

The **Series 1** set of models uses the inputs required to calibrate the Black–Scholes–Merton model. The input variables are extended further by the **Series 2** set of models by adding the lagged empirical delta. The **Series 3** set of models extends the input variables of Series 1 models by adding the Black–Scholes–Merton delta. The **Series 4** set of models extends the input variables of Series 1 models by adding the Black–Scholes–Merton greeks. The **Series 5** set of models reduces the input variables of Series 1 models by removing the Black–Scholes–Merton implied volatility and extends the input variables of Series 1 models by adding the calibrated parameters and the delta from the Heston model. The **Series 6** set of models reduces the input variables of Series 1 models by removing the Black–Scholes–Merton implied volatility and extends the input variables of the Series 1 set of models by adding the calibrated parameters and the delta from the Heston Jump Diffusion model. The **Series 7** set of models reduces the input variables of Series 1 models by removing the Black–Scholes–Merton implied volatility and extends the input variables of Series 1 models by adding the calibrated parameters and the delta from the Finite Moment Log Stable model.

3.2.5 Information Sets (for Computing the Replicating Portfolio Value)

In the second half of this paper, we focus on comparing the value of the replicated portfolio using the forecasted hedge ratio from the models discussed in Section 3.2.4. Here we define the information sets required for each model for forecasting the value of the replicated portfolio. We implement a single forecasting horizon, that is one-trading-day-ahead forecasts of the replicated portfolio value. We use the information available on day $t = N$ to forecast the replicated portfolio value for day $t = N + 1$, and these models are denoted by an N subscript. Similarly, models that we use the information available on day $t = N+1$ to forecast the replicated portfolio value for day $t = N + 1$ are denoted by the $N + 1$ subscript.

3.2.5.1 Empirical Replicating Portfolio Value

The tracking/hedging error in the empirical replicating portfolio at time N, is computed as,

$$V_N^{EMP} = \delta_N^{EMP} S_N + (1 + R_{\mathrm{N}} \delta t) \left(C_{N-1} - \delta_N^{EMP} S_{N-1} \right) - C_N \qquad (3.17)$$

where, on day N, C_N is observed call price of the S&P 500 Index, S_N is the S&P500 Index price, $\delta t = 1$, R_{N} is the overnight rate, and δ_N^{EMP} is the empirical delta, which is computed using the Eq. (3.3). Similarly, we compute the error of the replicating portfolio value for all the models covered in this study.

3.3 Fitting and Calibrating the Models

3.3.1 Performance Criterion

The hedging performance and the replicating portfolio value performance of each model are measured using Root Mean Square Error (RMSE) in the test sample, that is, in out-of-sample prediction. For each day, as we cycle through the observations, we retain the hedging and replicating portfolio value errors for each model. Below, we use these errors to compute the RMSE on a daily, monthly and annual basis. Defining the hedging and the replicating portfolio value errors as $\epsilon_j = y_j - \hat{y}_j$, where y_j is the target value and $\hat{y}_j$ is its predicted value, the RMSE for a series of J pricing errors is calculated using Eq. (2.53). We should choose the model with the lowest out-of-sample RMSE.

3.3.2 Calibration of Parametric Option Pricing Models

A similar non-linear optimisation exercise mentioned in Section 2.3.7.2 is performed in this chapter and is implemented differently and separately for parametric models under the H-$Models$ ($BSMH_N$, HH_N, $HJDH_N$, and $FMLSH_N$ models) and for each model under CH-$Models$ ($BSMCH_{N+1}$, HCH_{N+1}, $HJDCH_{N+1}$, and the $FMLSCH_{N+1}$ models). For the Black–Scholes–Merton models, the calibrated parameter, $\sigma_N^{CALIB^C}$ (used by the $BSMH_N$ model, $BSMH_{N+1}$ model, and the $BSMCH_{N+1}$ model) for day N, are retained for use in computing the greeks, and as an input to other parametric and various ANN models. For the Heston model, calibrated parameters, $HParams_N^C$ (used by the HH_N model, the HH_{N+1} model, and the HCH_{N+1} model) for day N, are retained as inputs for some ANN models. For the Heston Jump Diffusion model, calibrated parameters, $HJDParams_N^C$ (used by the $HJDH_N$ model, the $HJDH_{N+1}$ model, and the $HJDCH_{N+1}$ model) for day N, are retained as inputs for some ANN models.

Similarly, for the Finite Moment Log Stable model, calibrated parameters, $FMLSParams_N^C$ (used by the $FMLSH_N$ model, the $FMLSH_{N+1}$ model, and the $FMLSCH_{N+1}$ model) for day N, are retained as inputs for some ANN models. The parametric models under the H-$Models$ category (having a forecast variable: H_{N+1}) are calibrated separately to the CH-$Models$ (having a forecast variable: C_{N+1}) for each of the 1,326 trading days in the sample.

3.3.3 Estimating Deep Learning Neural Network Models

3.3.3.1 Network Parameters

The various network configurations to forecast the delta for day $t = N + 1$ are listed in Part I of Table B.1.1 for models using the information available on day $t = N$, in Part II of Table B.1.1 for models using the information available (except for calibrated model parameters) on day $t = N + 1$, and in Part III of Table B.1.1 for models using the information available on day $t = N + 1$ to forecast the C_{N+1} (from which the delta is later analytically derived using Eq. (3.3)). The MLP (MH_N-$Models$, MH_{N+1}-$Models$, MCH_{N+1}-$Models$) and the LSTM (LH_N-$Models$, LH_{N+1}-$Models$, LCH_{N+1}-$Models$) follows the network design of the MLP and LSTM models mentioned in Section 2.3.7.3.1. The only difference in the set of models considered in this chapter is that the MLP MH_N-$Models$, MH_{N+1}-$Models$, LSTM LH_N-$Models$, and LH_{N+1}-$Models$ use a simple linear transfer function, which returns the predicted delta while the MLP MCH_{N+1}-$Models$ and the LSTM LCH_{N+1}-$Models$ returns the predicted call option price.

3.3.3.2 Data Division

Recall that the data set covers the period from September 2012 to December 2017 and includes 1,326 trading days. The MLP and LSTM methodologies require data for a training set, a validation set, and a test set. The training set is used to estimate the parameters, the validation set is used to evaluate under-fitting and over-fitting, and the test set is used for out-of-sample prediction. In this study, for the MLP $M3H_N$-$Models$, MLP $M3H_{N+1}$-$Models$, and the MLP $M3CH_{N+1}$-$Models$, we utilise an expanding window (in terms of the number of trading days) for the training and validation set (of one trading day) and a fixed size (of one trading day) for the test set, and for the LSTM $L3H_N$-$Models$, LSTM $L3H_{N+1}$-$Models$, and the LSTM $L3CH_{N+1}$-$Models$, we utilise a fixed-sliding window (of 10 trading days) for training and validation set (of one trading day) and a fixed test set (of one trading day). Thus, the training and validation set for both MLP ($M3H_N$-$Models$, $M3H_{N+1}$-$Models$, and the $M3CH_{N+1}$-$Models$) and LSTM ($L3H_N$-$Models$, $L3H_{N+1}$-$Models$, and the $L3CH_{N+1}$-$Models$) models comprise of the trading day including (N) and the test set trading day ($N + 1$). This is repeated for the trading days N = 11, 12,..., 1,326. For the MLP models, for each iteration, the combined set of training and validation of observations temporarily consists of trading days from 1 to N but is further randomly split into 80%: 20% as the training set and the validation set. The pictorial representation of the MLP's data division is presented in Figure 2.4. For the LSTM models, for each iteration, the combined set of training and validation of observations, which consists of trading days from 1 to N, stays fixed throughout each iteration and is not randomly split, which is the case with MLPs. The expanding window for the MLP models is chosen over a fixed-sliding window for the training and validation set so that the MLP be exposed to a large variable and parameter space. The fixed-sliding window is chosen for the LSTM models because as the training size keeps expanding, it becomes computationally intensive for the LSTM. The test set for the MLP and LSTM models is fixed at one trading day as the focus of this study is on one-trading-day-ahead prediction. The pictorial representation of the LSTMs data division is presented in Figure 2.5 and is similar for the LSTM ($L3H_N$-$Models$, $L3H_{N+1}$-$Models$, and the $L3CH_{N+1}$-$Models$) models discussed in this chapter.

3.3.3.3 Training the Neural Network Models

The procedure to train the neural network in this chapter is similar to the procedure followed in Section 2.3.7.3.3.

3.4 Empirical Results

In this section, we evaluate the out-of-sample forecasting performance of the various parametric and ANN models in predicting the one-trading-day-ahead delta and associated replicating portfolio value. Accordingly, the out-of-sample forecasting performance of H-$Models$, CH-$Models$, HV-$Models$, and CHV-$Models$ is analysed, together with several robustness tests.

3.4.1 $H-$Models: Results

We consider the following set of H-$Models$ for forecasting one-trading-day-ahead delta (Δ_{N+1}).

- H-$Models$ using lagged input variables:
  - Parametric models:
    * Black–Scholes–Merton ($BSMH_N$) model
    * Heston (HH_N) model
    * Heston Jump Diffusion ($HJDH_N$) model

- Finite Moment Log Stable ($FMLSH_N$) model

- MLP models:
  - Triple hidden layer MLP $M3H_N$-$Models$ ($M3H1_N$ to $M3H7_N$)
- LSTM models:
  - Triple hidden layer LSTM $L3H_N$-$Models$ ($L3H1_N$ to $L3H7_N$)

- H-$Models$ using one-trading-day-ahead input variables to forecast the delta (Δ_{N+1}) for the next trading day:
  - Parametric models:
    - Black–Scholes–Merton ($BSMH_{N+1}$) model
    - Heston (HH_{N+1}) model
    - Heston Jump Diffusion ($HJDH_{N+1}$) model
    - Finite Moment Log Stable ($FMLSH_{N+1}$) model
  - MLP models:
    - Triple hidden layer MLP $M3H_{N+1}$-$Models$ ($M3H1_{N+1}$ to $M3H7_{N+1}$)
  - LSTM models:
    - Triple hidden layer LSTM $L3H_{N+1}$-$Models$ ($L3H1_{N+1}$ to $L3H7_{N+1}$)

3.4.1.1 Forecasting performance of H-$Models$ with lagged input variables

Table 3.1 presents the relative out-of-sample forecasting performance amongst the H-$Models$ that use lagged input variables to forecast the one-trading-day-ahead delta (Δ_{N+1}).[10] Amongst all of the models, columns V and VI record the number of months and days, respectively, that each model has the lowest $RMSE$.[11] For parametric models, the Δ_{N+1} is calculated using each model's characteristic function, while the MLP and LSTM models forecast the Δ_{N+1} directly.

There are two key findings from these investigations. Firstly, the parametric $BSMH_N$ model has the lowest $RMSE$ for the most days compared to other models (166 days out of 1,326 days,

[10]These model include the parametric models ($BSMH_N$, HH_N, $HJDH_N$, and $FMLSH_N$), the triple hidden layer MLP models ($M3H_N$-$Models$), and triple hidden layer LSTM models ($L3H_N$-$Models$), as explained in section above.

[11]The performance metric is the $RMSE$ of the one-trading-day-ahead forecast errors of Δ_{N+1}, which is computed for each model utilising all of the errors in each day or each month.

12.5%). When we compute the monthly RMSE from daily forecasts, similar performance is observed, where the $BSMH_N$ model outperforms for 19 months out of 64 months. Second, out of 1,326 forecasting days, the MLP models collectively outperform the highest number of days, for 685 days (52%), while the parametric models could collectively out-perform for only 463 days (35%) and the LSTM models collectively outperformed the lowest, for 189 days (14%).

Next, we perform a more comprehensive analysis by comparing the parametric models to the triple layer MLP models only, and to the triple layer LSTM models only, as in Tables B.2.2 and B.2.3, respectively. We find that the $BSMH_N$ outperformed all other $M3H_N$-$Models$ for 188 days (having a daily bootstrap winning percentage of 12% to 16%) and all other $L3H_N$-$Models$ for 452 days (having a daily bootstrap winning percentage of 31% to 37%). The outperformance of $BSMH_N$ model is also clear when compared to other parametric models in Table B.2.4 where they have the lowest $RMSE$ for 910 days (having a daily bootstrap winning % of 66% to 71%) out of 1,326 days. Thus, when lagged input variables are used to forecast the one-trading-day-ahead delta, the Black–Scholes–Merton is consistently the best outperforming model (among other models).

3.4.1.2 Forecasting Performance of H-$Models$ with One-trading-day-ahead Input Variables

We also discuss the relative out-of-sample hedging performance (in RMSE)[11] amongst the H-$Models$ using one-trading-day-ahead input variables to forecast the one-trading-day-ahead delta. These results are presented in Table 3.2. We observe that the $BSMH_{N+1}$ model (similar to that of the $BSMH_N$ model) outperforms. Indeed, the $BSMH_{N+1}$ model outperforms other models with the lowest $RMSE$ for 196 days out of 1,326 days and the lowest $RMSE$ for 37 months out of 64 months. This out-performance of the $BSMH_{N+1}$ is also seen in Table B.2.6, where it outperforms other parametric and MLP models for 208 days (having a daily bootstrap winning percentage of 14% to 18%), and in Table B.2.7, where it outperforms other parametric and LSTM models for 486 days (having a daily bootstrap winning percentage of 34% to 39%) out of 1,326 days. The $BSMH_{N+1}$ model also outperforms when the comparison is restricted to only parametric models in Table B.2.8, where the $BSMH_{N+1}$ model has the lowest $RMSE$ for 936 days (having a daily bootstrap winning percentage of 68% to 73%) out of 1,326 days. Thus, irrespective of using lagged or one-trading-ahead input variables to forecast the one-trading-day-ahead delta, the Black–Scholes–Merton is consistently the best-performing model. However, predictions from the H-$Models$-based BSM with one trading-day-ahead input variables (from Table 3.2) provide the best improvement in forecasting performance, which represents an improvement of 18% compared to deltas predicted from BSM *H-Models* with lagged input (from Table 3.1), 11% from Table B.2.6 and 8% from Table B.2.7.[12] The hedging out-performance of the BSM model has also been cited by Andreou et al. (2010) where the delta was inferred using ANNs and by Ruf and Wang (2021) using linear regression.

The scope of this study is limited to daily forecasting, and hence to compare our results with past literature (Andreou et al. (2010), Ruf and Wang (2021)), we perform a comparison based on the overall RMSE (for the period from September 2012 to December 2017), which is computed from daily forecast errors. We compare only the *H-Models*, that use one-trading-day-ahead input variables to forecast the Δ_{N+1}, since past literature does not use lagged variables in the test set to forecast deltas. Based on forecasting S&P 500 index options from January 2002 to August 2004, Andreou et al. (2010) found that their BSM model (with a RMSE of 1.114) has an out-performance of 17.7% over the CS model (RMSE of 1.354); however, the ANN-enhanced CS ePOMP model (RMSE of 1.080) outperforms by 3.3% over the ANN-enhanced BS ePOMP model (RMSE of 1.117). Our best performing model based on overall RMSE for a window spanning from September 2012 to December 2017 is the $BSMH_{N+1}$ model, which has a RMSE of 2.474 (see Table B.1.4). Similarly, based on forecasting S&P 500 index options from January 2010 to June 2019, Ruf and Wang (2021) found that their regression-based BSM model had an out-performance of 21.3% over the standard BSM model, and the ANN-based BSM model has an out-performance of 23.4% over the standard BSM model. Our best-performing model, the standard BSM model, $BSMH_{N+1}$, based on overall RMSE for a window spanning from September 2012 to December 2017, has an average out-performance of 46.3% over MLP models and an average out-performance of 18.5% over LSTM models (see Table B.1.4).

3.4.2 $CH-$Models: Results

We consider the following set of *CH-Models* to forecast firstly the call option price (C_{N+1}) for the next trading day and then derive the delta analytically from the forecasted call option price

[12] We discuss in depth the relative out-of-sample forecasting performance amongst the models that lagged variables and one-trading-day-ahead input variables to forecast the one-trading-day-ahead Δ_{N+1} in Section B.2.1, Section B.2.2, and Section B.2.3 respectively. The RMSEs for the *H-Models* that use lagged input variables to forecast the Δ_{N+1} for the next trading day on a monthly, yearly, and overall basis can be found in tables 21, 27, and 33, for the *H-Models* that use one-trading-day-ahead input variables to forecast the Δ_{N+1} for the next trading day on a monthly, yearly, and overall basis can be found in Tables 22, 28, and 34, and for the *CH-Models* in Tables 23, 29, and 35, respectively of the Electronic Appendix.

(C_{N+1}) as follows $\delta C_{N+1}/\delta S_{N+1}$.

- *CH-Models* using one-trading-day-ahead input variables
  - Parametric models:
    - Black–Scholes–Merton ($BSMCH_{N+1}$) model
    - Heston (HCH_{N+1}) model
    - Heston Jump Diffusion ($HJDCH_{N+1}$) model
    - Finite Moment Log Stable ($FMLSCH_{N+1}$) model
  - MLP models:
    - Triple hidden layer MLP $M3CH_{N+1}$-*Models* ($M3CH1_{N+1}$ to $M3CH7_{N+1}$)
  - LSTM models:
    - Triple hidden layer LSTM $L3CH_{N+1}$-*Models* ($L3CH1_{N+1}$ to $L3CH7_{N+1}$)

3.4.2.1 Forecasting Performance Using *CH-Models*

The *CH-Models* derive analytically the delta ($\delta C_{N+1}/\delta S_{N+1}$) from forecasted call option prices (C_{N+1}). These models use one-trading-day input variables to forecast C_{N+1}, which is the target variable for the MLP $M3CH_{N+1}$-*Models* and the LSTM $L3CH_{N+1}$-*Models*, and later compute the delta ($\delta C_{N+1}/\delta S_{N+1}$) using Eq. (3.3). The computation of $\delta C_{N+1}/\delta S_{N+1}$ requires S_{N+1}, and is only possible if we use one-trading-day input variables. These out-of-sample forecasting results are summarised in Table 3.3.[13]

We find that the triple hidden layer LSTM $L3CH4_{N+1}$ model outperforms other models with the lowest $RMSE$ for 274 days out of 1,326 days. The LSTM model $L3CH4_{N+1}$ however, fails to outperform when the comparison is confined to the parametric and the LSTM $L3CH_{N+1}$-*Models* only, in Table B.2.11, where the parametric $HJDCH_{N+1}$ model outperforms other models for 385 days (having a daily bootstrap winning percentage from 27% to 32%). Similar outperformance of the parametric models is observed when the comparison is made amongst the parametric models and the MLP $M3CH_{N+1}$-*Models* only, in Table B.2.10. Now the parametric model $FMLSCH_{N+1}$ outperforms with the lowest $RMSE$ for 226 days (having a daily bootstrap winning percentage of 15% to 19%) out of 1,326 days. Interestingly, the $HJDCH_{N+1}$

[13]The models considered are the parametric models ($BSMCH_{N+1}$, HCH_{N+1}, $HJDCH_{N+1}$, and $FMLSCH_{N+1}$), the triple hidden layer MLP models ($M3CH_{N+1}$-*Models*), and triple hidden layer LSTM models ($L3CH_{N+1}$-*Models*)

again outperforms if the comparison is only made amongst the parametric models; see Table B.2.12.[14] Thus, when the delta is analytically computed using forecasted option prices, there is no consistent outperforming model.

[14] $HJDCH_{N+1}$ has the lowest $RMSE$ for 475 days (having a daily bootstrap winning percentage of 34% to 39%) out of 1,326 days.

Table 3.1: This table presents the forecasting performance using both daily and monthly statistics amongst the *H-Models* that use lagged input variables to forecast the one-trading-day-ahead delta. The forecast variable for the MLP and LSTM models is the delta that is directly forecasted from the respective model, whereas the delta for the parametric models is computed using their respective characteristic functions. Column I identifies the models, and columns II, III, and IV describe the network architecture of the MLP and the LSTM models. Column V reports the number of months out of the 64 months that each model has the smallest RMSE, while column VI reports the number of days out of the 1,326 days each model has the smallest RMSE. The one-day-ahead forecast errors of the delta are used to compute the Root Mean Square Error (RMSE).

(I) Model	**(II)** No. of hidden layers	**(III)** No. of hidden nodes per layer	**(IV)** Network architecture	**(V)** Performance amongst all models (Monthly)	**(VI)** Performance amongst all models (Daily)
$BSMH_N$	-	-	-	**19**	**166**
HH_N	-	-	-	5	67
$HJDH_N$	-	-	-	0	69
$FMLSH_N$	-	-	-	0	161
$M3H1_N$	3	6	$6 \times 6 \times 6$	15	137
$M3H2_N$	3	7	$7 \times 7 \times 7$	8	105
$M3H3_N$	3	7	$7 \times 7 \times 7$	7	89
$M3H4_N$	3	11	$11 \times 11 \times 11$	0	72
$M3H5_N$	3	11	$11 \times 11 \times 11$	0	93
$M3H6_N$	3	14	$14 \times 14 \times 14$	0	94
$M3H7_N$	3	8	$8 \times 8 \times 8$	7	95
$L3H1_N$	3	6	$6 \times 6 \times 6$	0	19
$L3H2_N$	3	7	$7 \times 7 \times 7$	0	20
$L3H3_N$	3	7	$7 \times 7 \times 7$	0	21
$L3H4_N$	3	11	$11 \times 11 \times 11$	3	78
$L3H5_N$	3	11	$11 \times 11 \times 11$	0	16
$L3H6_N$	3	14	$14 \times 14 \times 14$	0	20
$L3H7_N$	3	8	$8 \times 8 \times 8$	0	15

Table 3.2: This table presents the forecasting performance using both daily and monthly statistics amongst the *H-Models* that use one-trading-day-ahead input variables to forecast the one-trading-day-ahead delta. The forecast variable for the MLP and LSTM models is the delta that is directly forecasted from the respective model, whereas the delta for the parametric models is computed using their respective characteristic functions. Column I identifies the models, and columns II, III, and IV describe the network architecture of the MLP and the LSTM models. Column V reports the number of months out of the 64 months that each model has the smallest RMSE, while column VI reports the number of days out of the 1,326 days each model has the smallest RMSE. The one-day-ahead forecast errors of the delta are used to compute the Root Mean Square Error (RMSE).

(I) Model	**(II)** No. of hidden layers	**(III)** No. of hidden nodes per layer	**(IV)** Network architecture	**(V)** Performance amongst all models (Monthly)	**(VI)** Performance amongst all models (Daily)
$BSMH_{N+1}$	-	-	-	**37**	**196**
HH_{N+1}	-	-	-	4	44
$HJDH_{N+1}$	-	-	-	0	71
$FMLSH_{N+1}$	-	-	-	0	162
$M3H1_{N+1}$	3	6	$6 \times 6 \times 6$	8	157
$M3H2_{N+1}$	3	7	$7 \times 7 \times 7$	6	109
$M3H3_{N+1}$	3	7	$7 \times 7 \times 7$	4	95
$M3H4_{N+1}$	3	11	$11 \times 11 \times 11$	0	66
$M3H5_{N+1}$	3	11	$11 \times 11 \times 11$	0	84
$M3H6_{N+1}$	3	14	$14 \times 14 \times 14$	0	96
$M3H7_{N+1}$	3	8	$8 \times 8 \times 8$	1	98
$L3H1_{N+1}$	3	6	$6 \times 6 \times 6$	0	12
$L3H2_{N+1}$	3	7	$7 \times 7 \times 7$	0	18
$L3H3_{N+1}$	3	7	$7 \times 7 \times 7$	0	15
$L3H4_{N+1}$	3	11	$11 \times 11 \times 11$	3	73
$L3H5_{N+1}$	3	11	$11 \times 11 \times 11$	1	12
$L3H6_{N+1}$	3	14	$14 \times 14 \times 14$	0	15
$L3H7_{N+1}$	3	8	$8 \times 8 \times 8$	0	13

Table 3.3: This table presents the forecasting performance using both daily and monthly statistics amongst the *CH-Models* that use one-trading-day-ahead input variables to forecast the one-trading-day-ahead call option price (C_{N+1}). The delta ($\delta C_{N+1}/\delta S_{N+1}$) is derived analytically from the forecasted C_{N+1} using equation 3.3. The one-day-ahead forecast errors of the delta are used to compute the Root Mean Square Error (RMSE). Column I identifies the models, and columns II, III, and IV describe the network architecture of the MLP and the LSTM models. Column V reports the number of months out of the 64 months that each model has the smallest RMSE, while column VI reports the number of days out of the 1,326 days each model has the smallest RMSE.

(I) Model	**(II)** No. of hidden layers	**(III)** No. of hidden nodes per layer	**(IV)** Network architecture	**(V)** Performance amongst all models (Monthly)	**(VI)** Performance amongst all models (Daily)
$BSMCH_{N+1}$	-	-	-	0	77
HCH_{N+1}	-	-	-	1	77
$HJDCH_{N+1}$	-	-	-	2	39
$FMLSCH_{N+1}$	-	-		0	120
$M3CH1_{N+1}$	3	6	6 X 6 X 6	3	69
$M3CH2_{N+1}$	3	7	7 X 7 X 7	5	72
$M3CH3_{N+1}$	3	7	7 X 7 X 7	4	80
$M3CH4_{N+1}$	3	11	11 X 11 X 11	8	137
$M3CH5_{N+1}$	3	11	11 X 11 X 11	**20**	107
$M3CH6_{N+1}$	3	14	14 X 14 X 14	7	80
$M3CH7_{N+1}$	3	8	8 X 8 X 8	14	87
$L3CH1_{N+1}$	3	6	6 X 6 X 6	0	19
$L3CH2_{N+1}$	3	7	7 X 7 X 7	0	13
$L3CH3_{N+1}$	3	7	7 X 7 X 7	0	15
$L3CH4_{N+1}$	3	11	11 X 11 X 11	0	**274**
$L3CH5_{N+1}$	3	11	11 X 11 X 11	0	19
$L3CH6_{N+1}$	3	14	14 X 14 X 14	0	33
$L3CH7_{N+1}$	3	8	8 X 8 X 8	0	6

3.4.3 *HV-Models* and *CHV-Models*: Results

We evaluate the replicating portfolio value performance of the various parametric and ANN models in terms of their one-trading-day-ahead replicating portfolio value forecast errors. The *HV-Models* comprises the same set of *H-Models* (which uses lagged or one-trading day ahead input variables to forecast delta) as mentioned in Sections 3.4.1.1 and 3.4.1.2, and the V_{N+1} is computed for these *H-Models* using the delta obtained from the respective models. *CHV-Models*, similarly comprises the same set of *CH-Models* in Section 3.4.2.1. Thus, to differentiate these models, we append the end of each model name for which we compute the replicating portfolio value by the letter "V".

3.4.3.1 Forecasting Performance of *HV-Models*

Tables 3.4 and 3.5 present the relative out-of-sample forecasting performance (in $RMSE$) amongst the models that use the delta from *H-Models* to compute the replicating portfolio value (V_{N+1}) using Eq. (3.17).[15] The Table 3.4 is based on *H-Models* using lagged input variables and Table 3.5 is based on *H-Models* using one-trading-day-ahead input to forecast delta. Amongst all of the models, columns V and VI record the number of months and days, respectively, that each model has the lowest $RMSE$.

The results are similar to what we document in Sections 3.4.1.1 and 3.4.1.2 regarding the forecasting of delta. More specifically, for the *HV-Models* in Table 3.4, the $BSMHV_N$ model outperforms all models, with the lowest $RMSE$ in 166 days out of 1326 days. The $BSMHV_N$ model also outperforms other models when the comparison is made amongst the parametric and MLP models only, in Table B.2.14, and the parametric models and LSTM models only, in Table B.2.15, and amongst parametric models, in Table B.2.16.[16] From Table 3.5, we also observe the outperformance of the parametric Black–Scholes $BSMHV_{N+1}$ model produced from *H-Models* using one-trading-day-ahead input to forecast delta. The $BSMHV_{N+1}$ model outperforms with the lowest $RMSE$ for 195 days out of 1,326 days and the lowest $RMSE$ for 17 months out of 64

[15] The performance metric is the $RMSE$ of the one-trading-day-ahead forecast errors of V_{N+1}, which is computed for each model utilising all of the errors in each day or each month.

[16] The $BSMHV_N$ model outperforms other parametric and MLP models for 188 days (having a daily bootstrap winning percentage of 12% to 16%) out of 1,326 days, other parametric and LSTM models for 451 days (having a daily bootstrap winning percentage of 31% to 37%) out of 1,326 days, and all parametric models for 909 days (having a daily bootstrap winning percentage of 66% to 71%) out of 1,326 days.

months. This out-performance of the $BSMHV_{N+1}$ is also seen in Table B.2.18, where it outperforms other parametric and MLP models, in Table B.2.19, where it outperforms parametric and LSTM models, and in Table B.2.20, where it outperforms parametric models.[17] Thus, irrespective of using lagged or one-trading-ahead input variables to forecast the one-trading-day-ahead delta, the $BSMHV_{N+1}$ model has been the most outperforming model.

3.4.3.2 Forecasting Performance of *CHV-Models*

For the *CHV-Models* using delta from *CH-Models* to compute the V_{N+1} from Eq. (3.17), we observe results similar to what is observed for the category of *CH-Models* in Section 3.4.2.1. Table 3.6 compares the out-of-sample forecasting performance of these models, in which the delta is computed analytically from option price forecasts. We find that the LSTM models outperform other models (lowest $RMSE$ for 276 days out of 1,326 days). However, comparing parametric models and the LSTM $L3CHV_{N+1}$-*Models* in Table B.2.23, the parametric $HJDCHV_{N+1}$ model outperforms, when comparing the parametric models and the MLP $M3CHV_{N+1}$-*Models* in Table B.2.22, the $FMLSCHV_{N+1}$ model outperforms and within the parametric models shown in Table B.2.24, the $HJDCHV_{N+1}$ out-perform all other parametric models.[18] Thus, when the value of the replicating portfolio is obtained from the delta that is analytically computed using the forecasted option prices (from *CH-Models*), the results do not reveal a consistently outperforming model. This underscores the economic benefits of such approaches, which imply that ANN models that cannot directly predict delta may not provide robust forecasting performance.

---

[17]The $BSMHV_{N+1}$ model outperforms other parametric and MLP models for 207 days (having a daily bootstrap winning percentage of 14% to 18%), other parametric and LSTM models for 485 days (having a daily bootstrap winning percentage of 34% to 39%) out of 1,326 days, and all parametric models for 934 days (having a daily bootstrap winning percentage of 68% to 73%) out of 1,326 days.

[18]When we compare parametric models and the LSTM $L3CHV_{N+1}$-*Models* only, the parametric $HJDCHV_{N+1}$ model outperforms for 387 days (having a daily bootstrap winning percentage from 27% to 32%) out of 1,326 days, when the parametric models and the MLP $M3CHV_{N+1}$-*Models* are compared, the $FMLSCHV_{N+1}$ model outperforms for 224 days (having a daily bootstrap winning percentage from 15% to 19%) out of 1,326 days, and finally within all parametric models, the $HJDCHV_{N+1}$ outperforms for 479 days (having a daily bootstrap winning percentage from 34% to 39%) out of 1,326 days.

Table 3.4: This table presents the forecasting performance using both daily and monthly statistics amongst the *HV-Models* that uses the delta obtained from *H-Models*. The *H-Models* use lagged input variables to forecast the one-trading-day-ahead delta, and the delta is directly forecasted from the MLP and LSTM models, and whereas for the parametric models, it is computed using their respective characteristic functions. The forecasted delta from a model is later used to compute the replicating portfolio value (V_N) using equation 3.17. The one-day-ahead forecast errors of V_N are used to compute the Root Mean Square Error (RMSE). Column I identifies the models, column II identifies the forecast variable, and columns II, III, and IV describe the network architecture of the MLP and LSTM models. Column V reports the number of months out of the 64 months that each model has the smallest RMSE, while column VI reports the number of days out of the 1,326 days each model has the smallest RMSE.

(I) Model	**(II)** No. of hidden layers	**(III)** No. of hidden nodes per layer	**(IV)** Network architecture	**(V)** Performance amongst all models (Monthly)	**(VI)** Performance amongst all models (Daily)
$BSMHV_N$	-	-	-	3	**166**
HHV_N	-	-	-	6	66
$HJDHV_N$	-	-	-	1	69
$FMLSHV_N$	-	-		1	162
$M3HV1_N$	3	6	6 X 6 X 6	7	137
$M3HV2_N$	3	7	7 X 7 X 7	5	105
$M3HV3_N$	3	7	7 X 7 X 7	5	89
$M3HV4_N$	3	11	11 X 11 X 11	5	72
$M3HV5_N$	3	11	11 X 11 X 11	8	93
$M3HV6_N$	3	14	14 X 14 X 14	4	94
$M3HV7_N$	3	8	8 X 8 X 8	**10**	95
$L3HV1_N$	3	6	6 X 6 X 6	0	18
$L3HV2_N$	3	7	7 X 7 X 7	1	20
$L3HV3_N$	3	7	7 X 7 X 7	0	22
$L3HV4_N$	3	11	11 X 11 X 11	6	77
$L3HV5_N$	3	11	11 X 11 X 11	0	16
$L3HV6_N$	3	14	14 X 14 X 14	1	20
$L3HV7_N$	3	8	8 X 8 X 8	1	15

Table 3.5: This table presents the forecasting performance using both daily and monthly statistics amongst the *HV-Models* that uses the delta obtained from *H-Models*. The *H-Models* use one-trading-day input variables to forecast the one-trading-day-ahead delta and the delta is directly forecasted from the MLP and LSTM models, whereas for the parametric models, it is computed using their respective characteristic functions. The forecasted delta from a model is later used to compute the replicating portfolio value (V_{N+1}) using equation 3.17. The one-day-ahead forecast errors of V_{N+1} are used to compute the Root Mean Square Error (RMSE). Column I identifies the models, column II identifies the forecast variable, and columns II, III, and IV describe the network architecture of the MLP and LSTM models. Column V reports the number of months out of the 64 months that each model has the smallest RMSE, while column VI reports the number of days out of the 1,326 days each model has the smallest RMSE.

(I) Model	**(II)** No. of hidden layers	**(III)** No. of hidden nodes per layer	**(IV)** Network architecture	**(V)** Performance amongst all models (Monthly)	**(VI)** Performance amongst all models (Daily)
$BSMHV_{N+1}$	-	-	-	**17**	**195**
HHV_{N+1}	-	-	-	11	43
$HJDHV_{N+1}$	-	-	-	0	71
$FMLSHV_{N+1}$	-	-		3	165
$M3HV1_{N+1}$	3	6	6 X 6 X 6	9	158
$M3HV2_{N+1}$	3	7	7 X 7 X 7	6	109
$M3HV3_{N+1}$	3	7	7 X 7 X 7	2	95
$M3HV4_{N+1}$	3	11	11 X 11 X 11	2	67
$M3HV5_{N+1}$	3	11	11 X 11 X 11	1	83
$M3HV6_{N+1}$	3	14	14 X 14 X 14	3	95
$M3HV7_{N+1}$	3	8	8 X 8 X 8	0	97
$L3HV1_{N+1}$	3	6	6 X 6 X 6	0	12
$L3HV2_{N+1}$	3	7	7 X 7 X 7	1	18
$L3HV3_{N+1}$	3	7	7 X 7 X 7	0	15
$L3HV4_{N+1}$	3	11	11 X 11 X 11	6	72
$L3HV5_{N+1}$	3	11	11 X 11 X 11	1	12
$L3HV6_{N+1}$	3	14	14 X 14 X 14	0	15
$L3HV7_{N+1}$	3	8	8 X 8 X 8	1	13

Table 3.6: This table presents the forecasting performance using both daily and monthly statistics amongst the *CHV-Models* that uses the delta obtained from *CH-Models*. The *CH-Models* use one-trading-day input variables to forecast the one-trading-day-ahead call option price (C_{N+1}). The delta ($\delta C_{N+1}/\delta S_{N+1}$) is derived analytically from the forecasted C_{N+1} using equation 3.3, and then used to compute the replicating portfolio value V_{N+1} using equation 3.17. The one-day-ahead forecast errors of V_N are used to compute the Root Mean Square Error (RMSE). Column I identifies the models, column II identifies the forecast variable, and columns III and IV describe the network architecture of the ANN models. Column V reports the number of months out of the 64 months that each model has the smallest RMSE, while column VI reports the number of days out of the 1,326 days each model has the smallest RMSE. Forecasts are made for 1,326 trading days, and there are 64 months covered in the sample using the monthly data.

(I) Model	**(II)** No. of hidden layers	**(III)** No. of hidden nodes per layer	**(IV)** Network architecture	**(V)** Performance amongst all models (Monthly)	**(VI)** Performance amongst all models (Daily)
$BSMCHV_{N+1}$	-	-	-	0	77
$HCHV_{N+1}$	-	-	-	0	77
$HJDCHV_{N+1}$	-	-	-	2	39
$FMLSCHV_{N+1}$	-	-		0	116
$M3CHV1_{N+1}$	3	6	6 X 6 X 6	5	70
$M3CHV2_{N+1}$	3	7	7 X 7 X 7	8	73
$M3CHV3_{N+1}$	3	7	7 X 7 X 7	8	82
$M3CHV4_{N+1}$	3	11	11 X 11 X 11	8	141
$M3CHV5_{N+1}$	3	11	11 X 11 X 11	**14**	109
$M3CHV6_{N+1}$	3	14	14 X 14 X 14	5	81
$M3CHV7_{N+1}$	3	8	8 X 8 X 8	**13**	87
$L3CHV1_{N+1}$	3	6	6 X 6 X 6	0	20
$L3CHV2_{N+1}$	3	7	7 X 7 X 7	0	14
$L3CHV3_{N+1}$	3	7	7 X 7 X 7	0	15
$L3CHV4_{N+1}$	3	11	11 X 11 X 11	1	**276**
$L3CHV5_{N+1}$	3	11	11 X 11 X 11	0	20
$L3CHV6_{N+1}$	3	14	14 X 14 X 14	0	34
$L3CHV7_{N+1}$	3	8	8 X 8 X 8	0	7

3.4.4 Robustness tests

3.4.4.1 The Diebold–Mariano (DM) Tests

Similar to the DM tests performed in Chapter 2, the model pairs that are statistically insignificant different in their prediction accuracy have been reported in Table B.1.9. For each model category, 153 pairs are created, and for the models belonging to the category of H-$Models$ that use lagged input variables to forecast Δ_{N+1}, 0% of the pairs are insignificant, for the models belonging to H-$Models$ that use one-trading-day-ahead input variables to forecast the Δ_{N+1}, 2.6% of the pairs are insignificant, for models belonging to CH-$Models$ that use one-trading-day-ahead input variables to forecast the δ_{N+1}, 2.6% of the pairs are insignificant, for the HV-$Models$ computed from the Δ_{N+1} obtained from H-$Models$ (that uses lagged input variables for forecasting), 3.9% of the pairs are insignificant, for the HV-$Models$ computed from the Δ_{N+1} obtained from H-$Models$ (that uses one-trading-day-ahead input variables for forecasting), 0% of the pairs are insignificant, and for the CHV-$Models$ computed from the δ_{N+1}obtained from CH-$Models$, 2.6% of the pairs are insignificant. Apart from the pairs mentioned in Table B.1.9, all the other pairs have significant forecasting power. Thus, the daily delta forecasting results are vastly statistically significant.

3.4.4.2 Bootstrap Tests

To further assess the validity of the forecasting performance results, we perform bootstrap tests using the daily and monthly RMSEs and discuss them in Sections B.2.1 through B.2.6, and present them in Tables B.2.1 to B.2.4 for H-$Models$ that use lagged input variables to forecast the Δ_{N+1}, Tables B.2.5 to B.2.8 for H-$Models$ that use one-trading-day-ahead input variables to forecast the Δ_{N+1}, Tables B.2.9 to B.2.12 for CH-$Models$ that use one-trading-day-ahead input variables to forecast the δ_{N+1}, Tables B.2.13 to B.2.16 for HV-$Models$ computed from the Δ_{N+1} obtained from H-$Models$ (that uses lagged input variables for forecasting), Tables B.2.17 to B.2.20 for HV-$Models$ computed from the Δ_{N+1} obtained from H-$Models$ (that uses one-trading-day-ahead input variables for forecasting), and Tables B.2.21 to B.2.24 for CHV-$Models$ computed from the δ_{N+1}obtained from CH-$Models$ in Appendix B.2, presents the results of the bootstrap performed using the daily and monthly RMSEs. In these tables, columns IX (lower bound) and X (upper bound) present the results from the bootstrap performed (with replacement) using monthly RMSEs at a 95% confidence level and shows the winning percentage out of 64 months for each model and similarly, the 95 % confidence intervals computed from bootstrapping of the daily RMSEs signify the winning percentage out of 1328 days for each model and are reported in columns XI (lower bound) and XII (upper bound). The results from the bootstrap tests typically support the results discussed in Section 3.4.

3.4.4.3 Pairwise Test

In the above comparisons of Section 3.4, a particular model wins against a set of many models. We also perform a pairwise bootstrap comparison which is computed using the respective pair's daily RMSEs. The pairwise bootstrap results for $H\text{-}Models$ pairs that use lagged input variables are presented in Table 45, for $H\text{-}Models$ that use one-trading-day-ahead input variables in Table 46, for $CH\text{-}Models$ that use one-trading-day-ahead input variables in Table 47, for $HV\text{-}Models$ that use delta from $H\text{-}Models$ (using lagged inputs for forecasting) in Table 48, for $HV\text{-}Models$ that use delta from $H\text{-}Models$ (using one-trading-day-ahead inputs for forecasting) in Table 49, and $CHV\text{-}Models$ that use delta from $CH\text{-}Models$ in Table 50 of the Electronic Appendix. We summarise the results from all the above-mentioned tables in Table B.1.10.

The comparisons of Section 3.4 reveal the parametric class of models to be consistently outperforming. When we compare models pair-wise, the results in forecasting performance change. The MLP class of models outperforms for over 47.1%, the LSTM models for 37.9%, and parametric models for 15% of the 153 pairs created from models belonging to $H\text{-}Models$ that use lagged input variables. For the 153 pairs created from models belonging to $H\text{-}Models$ that use one-trading-day-ahead input variables, the MLP class of models outperforms by over 39.2%, the parametric models similar to the MLP models, at 39.9%, and the LSTM models for 20.9% of the pairs. For the 153 pairs created from models belonging to $CH\text{-}Models$ that use one-trading-day-ahead input variables, the MLP class of models outperforms by over 62.7%, the parametric models for 22.9%, and the LSTM models for 14.4% of the pairs. Thus, the pairwise bootstrap comparison does not reveal conclusive evidence of outperforming models. Indeed, the pair-wise bootstrap results for $HV\text{-}Models$ and $CHV\text{-}Models$ are quantitatively similar to the results for $H\text{-}Models$ and $CH\text{-}Models$, respectively.

3.5 Conclusion

This chapter empirically evaluates the daily forecasting performance of deltas for S&P 500 European-style index options using parametric models and triple hidden layer Deep Learning

ANN models, namely the MLP and LSTM networks. One set of MLP and LSTM networks is trained using lagged and one-trading-day-ahead input variables to directly forecast the one-trading-day-ahead delta. Another set of MLP and LSTM networks is trained using one-trading-day-ahead input variables to forecast the one-trading-day-ahead option price and then analytically the one-trading-day-ahead delta. The economic significance of these forecasts are further gauged by assessing the daily forecast performance of the value of the corresponding replicating portfolio.

We find that the Black–Scholes–Merton model produces one-trading-day-ahead delta forecasts with the lower RMSEs than the three parametric (Heston, Heston Jump Diffusion, and the Finite Moment Log Stable) models and the Deep Learning ANN (MLP and LSTM) models. This result holds when the MLP and LSTM networks are used to predict directly the one-trading-day-ahead delta and independent of the input variables used (e.g. for both lagged and one-trading-day-ahead input variables). Based on the assessment of the forecasting performance of the replicating portfolio, we find quantitatively similar results. Thus, deep learning models would not typically improve (statistically or economically) the forecasting performance of deltas compared to the parametric models.

However, we find contradicting results when the MLP and LSTM networks are used to predict the one-trading-day-ahead delta indirectly by training the ANN models to predict prices and then analytically infer the one-trading-day-ahead delta. Then, the LSTM models produced forecasts with lower RMSEs compared to the four parametric and MLP models.

In summary, based on our empirical study, MLP and LSTM networks with a variety of input variables and multiple hidden layers do not provide a clear advantage compared to parametric models. Surprisingly, the most basic options pricing model tends to outperform all parametric and the ANN models considered in this study in terms of predicting delta hedge ratios or the value of corresponding replicating portfolios. This suggests that there may be some innate randomness that confines MLP and LSTM networks from effectively forecasting deltas. As mentioned in Chapter 2, the forecasting performance comparison between models may be biased by model and error uncertainty. Thus, we also assess the forecasting performance of delta based on an averaging error approach (Gençay and Qi (2001)) in the next chapter.

Chapter 4

Can Model Averaging Improve Forecasting Performance?

4.1 Introduction

Previous research has attempted to improve the predictability of non-parametric ANN models by making them more robust, reducing model uncertainty, and increasing predictive power by using a method called bagging introduced by Breiman (1996). This method proposes an aggregate value of the prediction from multiple versions of the model through bootstrapping. According to Gençay and Qi (2001), multiple versions of the ANN are generated using a random seed, and the outputs of these networks are aggregated to get an average predicted call price. We aim to replicate this process of aggregation by using average call prices to infer the prediction error in Chapter 4, which is the most basic form of ensemble learning. Non-parametric ANN models tend to over-estimate or under-estimate forecasts (Andreou et al. (2010), Ruf and Wang (2020), Buehler et al. (2019)). By averaging the forecasts from several models, we could balance the over-estimation and under-estimation, thereby reducing the variance of the forecast and possibly reducing the generalisation error of the pricing/hedging ANN model. The forecasts based on the average of several pricing/hedging models may also be more reliable than a forecast based on a single pricing/hedging model.

In this study, we use averaging methods for forecasting prices and delta. The average call price is employed to infer the call price prediction error, which is computed as the difference between the actual mid-point call price and the average of the forecasted call prices from multiple models. Taking averages is the simplest form of ensemble learning. We effectively use the same method to evaluate the forecasting performance of call price scaled by the strike price, delta, and replicating portfolio values. We thus empirically assess the daily forecasting performance of prices and delta for S&P 500 index options using averaging of parametric and ANN models. For a more comprehensive assessment, we compare between averaging all parametric and all ANN models, as well as between the best performing model and the averaging of all parametric and all ANN models. The best-performing models are selected by the analysis in Chapters 2 and 3, while MLP and LSTM networks are trained using lagged and one-trading-day-ahead input variables to forecast the one-trading-day-ahead prices and delta. Alternatively, MLP and LSTM networks forecast the one trading-day-ahead option price, and then we compute analytically the one-trading-day-ahead delta. Finally, we investigate the economic significance of these forecasts by comparing the daily forecast performance of the value of the corresponding replicating portfolio.

The forecasting performance of daily option prices and moneyness using lagged input variables shows that the simple random walk outperforms all models. When the random walk model is excluded, we find that the average of all the triple hidden layer MLP models outperforms any combination of the average of all the parametric models, the average of all the single, double, or triple hidden layer LSTM models, and the average of all the single, or the double hidden layer MLP models. The average of all the triple hidden layer MLP models, which forecasts the call option price, typically cannot outperform the individually best-outperforming model, an LSTM model, identified in Chapter 2. However, the average of all the triple hidden layer MLP models, which forecasts moneyness, can consistently outperform the individually best-outperforming models in any combination of comparisons. Furthermore, for forecasting the call option price/moneyness using one-trading-day-ahead input variables, we test only the triple hidden layer models, and we find that the average of all triple hidden layer MLP models again is typically the best performing model that also outperforms the random walk forecasting model. However, the average of all triple hidden layer MLP models which forecast call option prices do not consistently outperform the individually best out-performing models listed in Chapter 2, whereas the average of all triple hidden layer MLP models that forecasts moneyness could outperform the individually best out-performing models.

In terms of measuring the forecasting performance of daily delta using lagged/one-trading-day-ahead input variables, we find that the average of all the parametric models produces forecasts with the lowest RMSEs, followed by the average of all the triple hidden layer models. However, the average of all parametric models fails to outperform the best outperforming models identified in Chapter 3. Similar results are also seen while measuring the forecasting performance of daily delta, which is analytically derived from call option prices, where the average of all the parametric models has the lowest RMSEs, but unlike before, it outperforms the best out-performing models identified from Chapter 2. To assess the economic significance of these delta models, we compare the forecasting performance of their corresponding replicating portfolio value. The average of all triple hidden layer MLP models and the average of all parametric models has at-par forecasting performance, yet, the average of all triple hidden layer MLP models outperforms the best out-performing models identified in Chapter 3. Comparatively, we can see that the average of all parametric models has the lowest RMSEs when the performance of replicating portfolio value forecasting is measured from models that use one-trading-day inputs to forecast the delta but cannot outperform the best-performing models. When delta is derived analytically from call option prices, then the average of all triple hidden layer MLP models again displays the lowest RMSEs and could outperform the best-performing models identified in Chapter 3 for replicating portfolio value forecasting performance of models. The results are robust based on a bound assessment of performance, while the DM tests show that out of the 66 model pairs, only 1.52% of the pairs have insignificant forecasting power.

This chapter is organised into four sections. Section 4.2 presents the model averaging approach for parametric and ANN models employed to assess forecasting performance for prices and delta. The empirical results on the daily forecasting performance of S&P 500 index option prices using model averaging are discussed in Section 4.3. The empirical comparison of the daily forecasting performance of S&P 500 index option delta and replicating portfolio value performance is discussed in Section 4.4. Robustness tests are summarised in Section 4.5. Section 4.6 concludes.

4.2 Methodology

We use a variety of models having different sets of predictors to get an average value of the one-day-ahead call price and delta, as averaging can significantly improve the forecasting performance of a model according to Breiman (1996) and Gençay and Qi (2001). We consider two model averaging methods. In the first method, we compare the forecasting performance of averaging for all parametric and ANN models. In the second method, we assess the forecasting performance of the best performing model as indicated from Chapters 2 and 3 and the averaging for corresponding parametric and ANN models.

More specifically, to perform model averaging for the $C\text{-}Models$ using lagged input variables to forecast option prices (defined in Section 2.3.5.1), we take the average call option price of the following models:

- $ParamC_N^{AVG}\text{-}Models$: all the parametric models ($BSMC_N$, HC_N, $HJDC_N$, and $FMLSC_N$)
- $M1C_N^{AVG}\text{-}Models$: all the single hidden MLP models ($M1C1_N$ to $M1C9_N$),
- $M2C_N^{AVG}\text{-}Models$: all the double hidden MLP models ($M2C1_N$ to $M2C9_N$),
- $M3C_N^{AVG}\text{-}Models$: all the triple hidden MLP models ($M3C1_N$ to $M3C9_N$),
- $L1C_N^{AVG}\text{-}Models$: all the single hidden LSTM models ($L1C1_N$ to $L1C9_N$),
- $L2C_N^{AVG}\text{-}Models$: all the double hidden LSTM models ($L2C1_N$ to $L2C9_N$),
- $L3C_N^{AVG}\text{-}Models$: all the triple hidden LSTM models ($L3C1_N$ to $L3C9_N$).

Similarly, for the $C\text{-}Models$, which use one-trading-day-ahead input variables to forecast option prices (defined in Section 2.3.5.1), we take the average of the following models: [1]

- $ParamC_{N+1}^{AVG}\text{-}Models$: all the parametric models ($BSMC_{N+1}$, HC_{N+1}, $HJDC_{N+1}$, and $FMLSC_{N+1}$)
- $M3C_{N+1}^{AVG}\text{-}Models$: all the triple hidden MLP models ($M3C1_{N+1}$ to $M3C9_{N+1}$)
- $L3C_{N+1}^{AVG}\text{-}Models$: all the triple hidden LSTM models ($L3C1_{N+1}$ to $L3C9_{N+1}$).

A similar exercise of computing the average forecast of C_{N+1}/K_{N+1} from $CK\text{-}Models$ using lagged input variables and $CK\text{-}Models$ using one-trading-day-ahead input variables (defined in Section 2.3.5.2) is also examined.

For the $H\text{-}Models$ using lagged input variables to forecast delta (defined in Section 3.2.4), we take the average delta of the following models:

- $ParamH_N^{AVG}\text{-}Models$: all the parametric models ($BSMH_N$, HH_N, $HJDH_N$, and $FMLSH_N$)

[1] Since forecasting using single, and double layer ANN (MLP/LSTM) models is computationally intensive, and as the triple hidden layer ANN models have shown to largely outperform the single and double layer $C\text{-}Models$ which use lagged input variables (see extended results in Appendix A.2), this exercise only considers triple hidden layer $C\text{-}Models$. In a similar manner, we only take into account $CK\text{-}Models$ with triple hidden layers in order to maintain comparability with $C\text{-}Models$.

- $M3H_N^{AVG}$-$Models$: all the triple hidden MLP models ($M3H1_N$ to $M3H7_N$)
- $L3H_N^{AVG}$-$Models$: all the triple hidden LSTM models ($L3H1_N$ to $L3H7_N$)

For the H-$Models$ using one-trading-day-ahead input variables to forecast the Δ_{N+1} (see Section 3.2.4, we consider the average delta of the models below:

- $ParamH_{N+1}^{AVG}$-$Models$: all the parametric models ($BSMH_{N+1}$, HH_{N+1}, $HJDH_{N+1}$, and $FMLSH_{N+1}$)
- $M3H_{N+1}^{AVG}$-$Models$: all the triple hidden MLP models ($M3H1_{N+1}$ to $M3H7_{N+1}$)
- $L3H_{N+1}^{AVG}$-$Models$: all the triple hidden LSTM models ($L3H1_{N+1}$ to $L3H7_{N+1}$)

For the CH-$Models$ using one-trading-day-ahead input variables to forecast the δ_{N+1} (see Section 3.2.4, we take the average delta of the models:

- $ParamCH_{N+1}^{AVG}$-$Models$: all the parametric models ($BSMCH_{N+1}$, HCH_{N+1}, $HJDCH_{N+1}$, and $FMLSCH_{N+1}$)
- $M3CH_{N+1}^{AVG}$-$Models$: all the triple hidden MLP models ($M3CH1_{N+1}$ to $M3CH7_{N+1}$)
- $L3CH_{N+1}^{AVG}$-$Models$: all the triple hidden LSTM models ($L3CH1_{N+1}$ to $L3CH7_{N+1}$)

A similar exercise is done to compute the average replicating portfolio value for the HV-$Models$ and CHV-$Models$ (from Section 3.2.5).

For the second method, we compare the performance of the best out-performing models detected of the analysis in Chapters 2 and 3 with the performance of the corresponding model averaging results. More specifically, we compare the call option prices of the best out-performing C-$Models$ (as detected in Section 2.4.1.1) with the call option prices from averaging the parametric, the single, double, and triple hidden layer MLP/LSTM models. Furthermore, we compare the strike-adjusted option prices of the best out-performing CK-$Models$ discussed in Section 2.4.2 with the adjusted option prices of the corresponding model averages. We perform similar comparisons for the option's delta and the associated replicating portfolios. These comparisons include the delta of the best out-performing H-$Models$, CH-$Models$ (as detected in Sections 3.4.1.1 , 3.4.1.2 and 3.4.2.1, respectively), and the replicating portfolio of the best out-performing HV-$Models$ and CHV-$Models$ (as detected in Sections 3.4.3.1 and 3.4.3.2, respectively) with the delta from the corresponding average parametric, MLP models, and LSTM models. The detailed list of these model averaging options is discussed above. Note that the data used in the analysis are S&P 500 options prices from September 2012 to December 2017; see for more details in Sections 2.3 and 3.2.

4.3 Forecasting of S&P 500 Index Options Prices using Averaging Models

In this section, we evaluate the forecasting performance of the averaging models in predicting one-trading-day-ahead call option prices (C-$Models$) and moneyness (CK-$Models$). We use lagged input variables and one-trading-day-ahead input variables.

4.3.1 Averaging Forecasts from C-$Models$

4.3.2 Using Lagged Input Variables

Table 4.1 shows the relative out-of-sample pricing performance (in $RMSE$) amongst the averaging models that forecast the one-trading-day-ahead call option price using lagged input variables. We compare the averages of the parametric ($ParamC_N^{AVG}$-$Models$), the single ($M1C_N^{AVG}$-$Models$), double ($M2C_N^{AVG}$-$Models$), and triple ($M2C_N^{AVG}$-$Models$) hidden layer MLP models and the single ($L1C_N^{AVG}$-$Models$), double ($L2C_N^{AVG}$-$Models$), and triple ($L2C_N^{AVG}$-$Models$) hidden layer LSTM models belonging to C-$Models$ from Table 2.1, separately, and present them in the top panel of Table 4.1, namely under panel Method A. It is found that none of the averaging models could outperform the random walk (δC_N) model. However, if the random walk model is excluded from the comparison, the triple hidden layer MLP, $M3C_N^{AVG}$-$Models$, is the best-performing model.

We perform further set comparisons for the averages derived from the C-$Models$ from Section 2.4.1 of Chapter 2 (presented in Table C.2.1). We perform 13 combinations of comparisons among the parametric, single, double, and triple hidden layer MLP/LSTM models. There are three key findings in these 13 comparisons. Firstly, none of the models could outperform the random walk model. Secondly, if the random walk model is excluded from the comparisons, and if we compare the average of the parametric models with the averages of the single, double, or triple hidden layer MLP models, the average of the MLP models outperforms all other models (i.e. in Parts II, V, VIII, and XI of Table C.2.1). However, if the comparison is confined between the average of the parametric models and the averages of the single, double, or triple hidden layer LSTM models, the average of the parametric models outperforms all other models (i.e. in Parts III, VI, IX, and XII of Table C.2.1). Third, the outperformance of the average of the MLP models can also be noticed if we compared the average of the parametric models with the averages of the single, double, and triple hidden layer MLP models and the averages of the single, double, and triple hidden layer LSTM models, where the average of the MLP models has outperformed all other models (i.e. in Parts I, IV, X, XIII of Table C.2.1).

We next compare the best-performing *C-Models* (that use lagged input variables) from Section 2.4.1 of Chapter 2 with the model averages discussed above (i.e. in Tables 4.1 and C.2.1), which sums up to 13 different combinations of comparisons. Method B panel of Table 4.1 presents the results of comparing the best-performing model from Table 2.1 of Chapter 2, namely $L3C9_N$ model, with the average of the parametric, and the single, double, and triple hidden layer MLP and LSTM models. We find that this LSTM model ($L3C9_N$ model) outperforms all the above models (for 311 days out of 1,328).

Furthermore, none of the models could outperform the random walk model, except in Parts I and X of Table C.2.2. If the random walk model is excluded, and if we compared the best-performing *C-Models* with the average of the parametric models, the averages of the single, double, or triple hidden layer MLP models, then the average of the MLP models outperforms all other models (i.e. in Parts II, V, and VIII of Table C.2.2).[2] In addition, if the comparison is confined between the best-performing *C-Models* with the average of the parametric models, the averages of the single, double, or triple hidden layer LSTM models, the $L1C8_N$, $L2C9_N$, and $L3C9_N$ model outperforms all other models (in Parts III and XII of Table C.2.2) – except in Parts VI and IX, where the $ParamC_N^{AVG}$-*Models* outperforms all other models. Finally, if the comparison is made between the best-performing *C-Models* with the average of the parametric models, the averages of the single, double, and triple hidden layer MLP models, and the averages of the single, double, and triple hidden layer LSTM models, then the average of the MLP models has outperformed all other models (i.e. in Parts I, IV, and VII of Table C.2.2) – except in Parts X and XIII, where the $L3C9_N$ model outperforms all other models.

[2]Except in Part XI, where the $FMLSC_N$ model outperforms all other models.

4.3.3 Using One-trading-day-ahead Input Variables

The relative out-of-sample performance (in $RMSE$) amongst the averaging C-$Models$ using one-trading-day-ahead input variables is presented in Method A panel of Table 4.2. Method A compares the average option prices of the parametric ($ParamC^{AVG}_{N+1}$-$Models$), the triple ($M2C^{AVG}_{N+1}$-$Models$) hidden layer MLP models and the triple ($L2C^{AVG}_{N+1}$-$Models$) hidden layer LSTM models from Table 2.2, separately. It is shown that the average of the triple hidden layer MLP models outperforms all other models, including the random walk (for 987 days out of 1,328), and when the random walk is excluded (for 1,114 days out of 1,328). This out-performance of the average of the triple hidden layer MLP model is also seen when we compare it only with the parametric models in Part II of Table C.2.3. The average of the parametric models however outperforms only when the comparison is made with the average of the triple hidden layer LSTM models in Part III of Table C.2.3 and for 1065 days out of 1,328.

Method B panel of Table 4.2 presents the comparisons of the best-performing C-$Models$ (using one-trading-day-ahead input variables) from Section 2.4.1 of Chapter 2 with the models discussed above, i.e., models in Method A panel of Table 4.2. Here, the random walk model does not outperform these comparisons. When the random walk model is excluded, and we compare the best-performing model, namely $M3C4_{N+1}$, to the models in Method A panel of Table 4.2, i.e., with the average of the parametric, and average of the triple hidden layer MLP and LSTM models, we find that the $M3C4_{N+1}$ model outperforms all the above models (for 683 days out of 1,328). This is slightly better than the average of all the triple hidden layer MLP models, which outperforms (for 610 days out of 1,328).

Now, if we compare the best-performing model, $M3C4_{N+1}$, with the average of the parametric models, the averages of the triple hidden layer MLP in Part II of Table C.2.4, it shows consistent outperformance for 683 days out of 1,328. Third, if the comparison is made between the best-performing parametric model, HC_{N+1}, with the average of the parametric models, and the averages of the triple hidden layer LSTM models, in Part III of Table C.2.4, the parametric model HC_{N+1} outperforms all other models.

Therefore, forecasting the call option prices derived from averaging models using lagged input variables demonstrates that none of the pricing models could improve or outperform a simple random walk forecasting model. The best approach is to average the forecast from several MLP models, average from several parametric models, or use an individual LSTM model, like the $L3C9N$ model. Forecasting the call option prices derived from averaging models using one-trading-ahead input variables shows that the random walk model does not outperform in any of these comparisons, and the best approach is to use an individual MLP model like the $M3C4_{N+1}$ model, average the forecast from several MLP/parametric models, or use an individual parametric model, like the HC_{N+1} model.

4.3.4 Averaging Forecasts from CK-$Models$

4.3.5 Using Lagged Input Variables

Panel Method A of Table 4.3 compares the average of the CK-$Models$ including parametric ($ParamCK_N^{AVG}$-$Models$), the single ($M1CK_N^{AVG}$-$Models$), double ($M2CK_N^{AVG}$-$Models$), triple ($M3CK_N^{AVG}$-$Models$) hidden layer MLP models and the single ($L1CK_N^{AVG}$-$Models$), double ($L2CK_N^{AVG}$-$Models$), triple ($L3CK_N^{AVG}$-$Models$) hidden layer LSTM models of CK-$Models$ from Table 2.3. None of the models outperforms the random walk, but if the random walk is excluded, then the MLP $M3CK_N^{AVG}$-$Models$ outperform (for 627 days out of 1,328).

Table C.2.5 shows the relative out-of-sample pricing performance (in $RMSE$) amongst the CK-$Models$ (i.e. from section 2.4.2 of Chapter 2) using lagged input variables, which is divided again into thirteen parts as different combinations of comparisons amongst the parametric, single, double, and triple hidden layer MLP/LSTM models are considered. The key findings of these comparisons are summarised next. None of the models could outperform the random walk model. If the random walk model is excluded, and the average of the parametric models are compared with the averages of the single, double, and triple hidden layer MLP and LSTM models (i.e. in Parts I, IV, VII, and X of Table C.2.5), then the average of the MLP models outperforms all other models. The out-performance of the average of the MLP models is also evident when we compare the average of the parametric models with the averages of the single, double, and triple hidden layer MLP models (i.e. in Parts II, V, VIII, and XI of Table C.2.5). Lastly, if the comparison is confined between the average of the parametric models with the averages of the single, double, or triple hidden layer LSTM models (i.e. in Parts III, VI, IX, and XII of Table C.2.5), the average of the parametric models outperforms all other models.

Panel Method B of Table 4.3 compares the best-performing CK-$Models$ (using lagged input variables) from Section 2.4.2 of Chapter 2 (which is the $L1CK2_N$ model) with the the average of the parametric, the single, double, and triple hidden layer MLP and LSTM models. None of the models could outperform the random walk model. If the random walk model is excluded, and the best-performing model compared to the models in Method A of Table 4.3, it is revealed that the average of the triple hidden layer MLP models, namely the $M3CK_N^{AVG}$ model, outperforms all the above models (for 492 days out of 1,328).

Comparing the best-performing *CK-Models* (that use lagged input variables) from Section 2.4.2 of Chapter 2 with the models discussed above in Table C.2.5 and present the comparison in Table C.2.6, we draw the following conclusions (from these thirteen different comparisons). If we compared the best-performing *CK-Models* with the average of the parametric models, the averages of the single, double, and triple hidden layer MLP and LSTM models, then the average of the MLP models outperforms all other models (i.e. in Parts I, II, IV, V, VII, VIII, X, XI, and XIII of Table C.2.6). However, if the comparison is confined between the best-performing *CK-Models* with the average of the parametric models, and the averages of the single, double, or triple hidden layer LSTM models, the $L1CK2_N$, $L2CK2_N$, and $L3CK2_N$ model outperforms all other models (in Parts III, VI, IX, and XII of Table C.2.6).

4.3.6 Using One-trading-day-ahead Input Variables

We summarise the relative out-of-sample performance (in $RMSE$) amongst the *CK-Models* models using one-trading-day-ahead input variables in Table 4.4, where in panel Method A, we compared the average C_{N+1}/K_{N+1} of the parametric ($ParamCK_{N+1}^{AVG}$-*Models*), the triple ($M3CK_{N+1}^{AVG}$-*Models*) hidden layer MLP models and the triple ($L3CK_{N+1}^{AVG}$-*Models*) hidden layer LSTM models of the *CK-Models* in Table 2.4. It is shown that the average of the triple hidden layer MLP models outperforms all other models, including the random walk (for 1076 days out of 1,328) or excluding the random walk (for 1,328 days out of 1,328). This outperformance of the average of the triple hidden layer MLP model is also seen when we compare it only with the parametric models in Part II of Table C.2.7. The average of the parametric models, however, fails to outperform even when the comparison is made with the average of the triple hidden layer LSTM models in Part III of Table C.2.7, where the average of the triple hidden layer LSTM models outperform for 1,328 days out of 1,328.

There are three key findings when we compare the best-performing *CK-Models* (that use one-trading-day-ahead input variables) from Section 2.4.2 of Chapter 2 with the models discussed above in Tables 4.4 and C.2.7. First, the random walk model does not outperform in any of these comparisons. When we exclude the random walk model from the comparisons and compare the $M3CK2_{N+1}$ model (i.e., the best outperforms model when compared to the models in Method

A panel of Table 4.4) with the average of the parametric, and average of the triple hidden layer MLP and LSTM models, the average of the triple hidden layer MLP models outperforms all the above models (840 days out of 1,328). Second, when we compare the best-performing *CK-Models* with the average of the parametric models, the average of the triple hidden layer MLP models in Part II of Table C.2.8, then the best-performing model, the average of the triple hidden layer MLP models, i.e. the $M3CK_{N+1}^{AVG}$ model, consistently outperforms (for 840 days out of 1,328). Third, if the comparisons are made between the best-performing model from *CK-Models*, the $L3CK2_{N+1}$ with the average of the parametric models, and the average of the triple hidden layer LSTM models, in Part III of Table C.2.8, the $L3CK2_{N+1}$ outperforms all other models for 809 days out of 1,328 days.

A comparison between *CK-Models* with lagged input variables and *CK-Models* models with one-trading-day-ahead input variables reveals a substantial improvement in forecasting performance of using one-trading-day-ahead input variables in the $M3C_{N+1}^{AVG}$-*Models* from Table 4.2, when compared to the corresponding $M3C_{N}^{AVG}$-*Models* using lagged input variables from Table 4.1 –similarly for the $M3CK_{N+1}^{AVG}$-*Models* from Table 4.4, when compared to the $M3CK_{N}^{AVG}$-*Models* using lagged input variables from Table 4.3. For example, the forecasting performance of the $M3C_{N+1}^{AVG}$-*Models* has an improvement of 347.5% (based on daily RMSE) / 75.8% (based on monthly RMSE) over $M3C_{N}^{AVG}$-*Models*, and the $M3CK_{N+1}^{AVG}$-*Models* has an improvement of 111.8% (based on daily RMSE) / 25.5% (based on monthly RMSE) over $M3CK_{N}^{AVG}$-*Models*. We also observe that the majority of the models that have outperformed based on daily RMSE have outperformed based on their monthly RMSE.

Therefore, forecasting moneyness derived from averaging models using lagged input variables demonstrates that none of the pricing models could improve or outperform the simple random walk forecasting model. The best approach is to average the forecast from several MLP models, average from several parametric models, or use an individual LSTM model, like the $L1CK2_N$, $L2CK2_N$, and $L3CK2_N$ model. Forecasting moneyness from averaging models using one-trading-ahead input variables also shows that the random walk model does not outperform in any of these comparisons, and the best approach is to use an individual MLP model, like the $M3CK2_{N+1}$ model, average the forecast from several parametric/MLP/LSTM models.

Table 4.1: This table, categorised into two parts, presents the out-of-sample forecasting performance using daily and monthly statistics amongst the set of models, which averages the forecast of the one-day-ahead call option price from models that use lagged input variables. Below, in each of the parts, we compare the out-of-sample performance of the following models: **Method A**: The average call option price from the parametric, the single, double, and triple hidden layer MLP models, and the single, double, and triple hidden layer LSTM models. **Method B**: The best out-performing model ($L3C9_N$) from Table 2.1 with average call option price from the parametric, the single, double, and triple hidden layer MLP models, and the single, double, and triple hidden layer LSTM models. The average one-day-ahead forecast errors of the call option prices are used to compute the Root Mean Square Error (RMSE). Column I identifies the models, and when comparing all models (i.e. including the random walk model (δC_N), column II reports the number of months out of the 64 months that each model has the smallest RMSE, while column III reports the number of days out of the 1,328 days each model has the smallest RMSE. Similarly, when the δC_N model is excluded in the comparison, column IV reports the number of months out of the 64 months that each model has the smallest RMSE, while column V reports the number of days out of the 1,328 days each model has the smallest RMSE. Forecasts are made for 1,328 trading days, and there are 64 months covered in the sample using the monthly data.

	Incl. random walk		**Excl. random walk**	
(I) **Model**	**(II)** **Performance amongst all models (Monthly)**	**(III)** **Performance amongst all models (Daily)**	**(IV)** **Performance amongst all models (Monthly)**	**(V)** **Performance amongst all models (Daily)**
Method A				
δC_N	**34**	**369**	-	-
$ParamC_N^{AVG}$-$Models$	0	174	0	184
$M1C_N^{AVG}$-$Models$	10	126	16	185
$M2C_N^{AVG}$-$Models$	14	97	19	196
$M3C_N^{AVG}$-$Models$	6	86	**29**	**249**
$L1C_N^{AVG}$-$Models$	0	89	0	94
$L2C_N^{AVG}$-$Models$	0	161	0	176
$L3C_N^{AVG}$-$Models$	0	226	0	244
Method B				
$L3C9_N$	0	**311**	0	**333**
$ParamC_N^{AVG}$-$Models$	0	174	0	184
$M1C_N^{AVG}$-$Models$	10	97	16	134
$M2C_N^{AVG}$-$Models$	14	86	19	171
$M3C_N^{AVG}$-$Models$	6	76	**29**	204
$L1C_N^{AVG}$-$Models$	0	64	0	66
$L2C_N^{AVG}$-$Models$	0	116	0	123
$L3C_N^{AVG}$-$Models$	0	105	0	113

Table 4.2: This table, categorised into two parts, presents the out-of-sample forecasting performance using daily and monthly statistics amongst the set of models, which averages the forecast of the one-day-ahead call option price from models that use one-trading-day-ahead input variables. Below, in each of the parts, we compare the out-of-sample performance of the following models: **Method A**: The average call option price from the parametric, the triple hidden layer MLP models, and the triple hidden layer LSTM models. **Method B**: The best out-performing model ($M3C4_{N+1}$) from Table 2.2 with the average call option price from the parametric, the triple hidden layer MLP models, and the triple hidden layer LSTM models. The one-day-ahead forecast errors of the call option prices are used to compute the Root Mean Square Error (RMSE). Column I identifies the models, and when comparing all models (i.e. including the random walk model (δC_N), column II reports the number of months out of the 64 months that each model has the smallest RMSE, while column III reports the number of days out of the 1,326 days each model has the smallest RMSE. Similarly, when the δC_N model was excluded in the comparison, column IV reports the number of months out of the 64 months that each model has the smallest RMSE, while column V reports the number of days out of the 1,326 days each model has the smallest RMSE. Forecasts are made for 1,326 trading days, and there are 64 months covered in the sample using the monthly data.

	Incl. random walk		**Excl. random walk**	
(I) Model	**(II) Performance amongst all models (Monthly)**	**(III) Performance amongst all models (Daily)**	**(IV) Performance amongst all models (Monthly)**	**(V) Performance amongst all models (Daily)**
Method A				
δC_N	0	129	-	-
$ParamC^{AVG}_{N+1}$-$Models$	13	208	13	208
$M3C^{AVG}_{N+1}$-$Models$	**51**	**987**	**51**	**1114**
$L3C^{AVG}_{N+1}$-$Models$	0	4	0	6
Method B				
δ_C	0	119	-	-
$M3C4_{N+1}$	**35**	**650**	**35**	**683**
$ParamC^{AVG}_{N+1}$-$Models$	0	34	0	34
$M3C^{AVG}_{N+1}$-$Models$	29	525	29	610
$L3C^{AVG}_{N+1}$-$Models$	0	0	0	1

Table 4.3: This table, categorised into two parts, presents the out-of-sample forecasting performance using daily and monthly statistics amongst the set of models, which averages the forecast of the one-day-ahead call option price scaled by the exercise price from models that use lagged input variables. Below, in each of the parts, we compare the out-of-sample performance of the following models: **Method A**: The average call option price is scaled by the exercise price from the parametric, single, double, and triple hidden layer MLP models, and the single, double, and triple hidden layer LSTM models. **Method B**: The best out-performing model ($L1CK2_N$) from Table 2.3 with the average call option price scaled by the exercise price from the parametric, the single, double, and triple hidden layer MLP models, and the single, double, and triple hidden layer LSTM models. The one-day-ahead forecast errors of call option prices scaled by the exercise prices are used to compute the Root Mean Square Error (RMSE). Column I identifies the models, and when comparing all models (i.e. including the random walk model (δC_N), column II reports the number of months out of the 64 months that each model has the smallest RMSE, while column III reports the number of days out of the 1,326 days each model has the smallest RMSE. Similarly, when the δC_N model was excluded in the comparison, column IV reports the number of months out of the 64 months that each model has the smallest RMSE, while column V reports the number of days out of the 1,326 days each model has the smallest RMSE. Forecasts are made for 1,326 trading days, and there are 64 months covered in the sample using the monthly data.

	Incl. random walk		**Excl. random walk**	
(I) Model	**(II) Performance amongst all models (Monthly)**	**(III) Performance amongst all models (Daily)**	**(IV) Performance amongst all models (Monthly)**	**(V) Performance amongst all models (Daily)**
Method A				
δCK_N	**48**	**696**	-	-
$ParamCK_N^{AVG}$-$Models$	0	26	0	27
$M1CK_N^{AVG}$-$Models$	1	138	10	264
$M2CK_N^{AVG}$-$Models$	2	227	3	349
$M3CK_N^{AVG}$-$Models$	13	182	**51**	**627**
$L1CK_N^{AVG}$-$Models$	0	7	0	9
$L2CK_N^{AVG}$-$Models$	0	26	0	26
$L3CK_N^{AVG}$-$Models$	0	26	0	26
Method B				
δ_{CK}	**48**	**586**	-	-
$L1CK2_N$	0	250	0	290
$ParamCK_N^{AVG}$-$Models$	0	16	0	16
$M1CK_N^{AVG}$-$Models$	1	115	10	216
$M2CK_N^{AVG}$-$Models$	2	180	3	272
$M3CK_N^{AVG}$-$Models$	13	140	**51**	**492**
$L1CK_N^{AVG}$-$Models$	0	6	0	7
$L2CK_N^{AVG}$-$Models$	0	16	0	16
$L3CK_N^{AVG}$-$Models$	0	19	0	19

Table 4.4: This table, categorised into two parts, presents the out-of-sample forecasting performance using daily and monthly statistics amongst the set of models, which averages the forecast of the one-day-ahead call option price scaled by the exercise price from models that use lagged input variables. Below, in each of the parts, we compare the out-of-sample performance of the following models: **Method A**: The average call option price is scaled by the exercise price from the parametric, the triple hidden layer MLP models, and the triple hidden layer LSTM models. **Method B**: The best out-performing model ($M3CK2_{N+1}$) from Table 2.4 with the average call option price scaled by the exercise price from the parametric, the triple hidden layer MLP models, and the triple hidden layer LSTM models. The one-day-ahead forecast errors of the call option prices scaled by the exercise prices are used to compute the Root Mean Square Error (RMSE). Column I identifies the models, and when comparing all models (i.e. including the random walk model (δC_N), column II reports the number of months out of the 64 months that each model has the smallest RMSE, while column III reports the number of days out of the 1,326 days each model has the smallest RMSE. Similarly, when the δC_N model was excluded in the comparison, column IV reports the number of months out of the 64 months that each model has the smallest RMSE, while column V reports the number of days out of the 1,326 days each model has the smallest RMSE. Forecasts are made for 1,326 trading days, and there are 64 months covered in the sample using the monthly data.

	Incl. random walk		**Excl. random walk**	
(I) **Model**	**(II)** **Performance amongst all models (Monthly)**	**(III)** **Performance amongst all models (Daily)**	**(IV)** **Performance amongst all models (Monthly)**	**(V)** **Performance amongst all models (Daily)**
Method A				
δCK_N	0	252	-	-
$ParamCK_{N+1}^{AVG}$-$Models$	0	0	0	0
$M3CK_{N+1}^{AVG}$-$Models$	**64**	**1076**	**64**	**1328**
$L3CK_{N+1}^{AVG}$-$Models$	0	0	0	0
Method B				
δ_{CK}	0	238	-	-
$M3CK2_{N+1}$	14	443	14	488
$ParamCK_{N+1}^{AVG}$-$Models$	0	0	0	0
$M3CK_{N+1}^{AVG}$-$Models$	**50**	**647**	**50**	**840**
$L3CK_{N+1}^{AVG}$-$Models$	0	0	0	0

4.4 Forecasting of S&P 500 Index Options Delta Using Averaging Models

We next evaluate the forecasting performance of the averaging models in predicting the deltas for the H-$Models$, and CH-$Models$, and then the corresponding average replicating portfolio value for the models HV-$Models$, and CHV-$Models$. We consider lagged and one-trading-day-ahead input variables for the H-$Models$ and the one-trading-day-ahead input variables for the CH-$Models$.

4.4.1 Averaging Forecasts from H-$Models$ and HV-$Models$

4.4.1.1 Using Lagged Input Variables

By following the approach of Section 4.3, we present the relative out-of-sample forecasting performance (in $RMSE$) amongst the H-$Models$ using lagged input variables in panel Method A of Table 4.5. In this table, we compare the average of the parametric ($ParamH_N^{AVG}$-$Models$), the triple ($M3H_N^{AVG}$-$Models$) hidden layer MLP models, and the triple ($L3H_N^{AVG}$-$Models$) hidden layer LSTM models belonging to H-$Models$ from Table 3.1, separately. We find that the average of the parametric models outperforms all other models for 593 days out of 1,326. Furthermore, in Table C.2.9, we compare the average derived from the H-$Models$ from the Section 3.4.1 of Chapter 3. In Part II of this table, we compared the average of the parametric models with the average of the triple hidden layer MLP models, and we find contrasting results. The average of the triple hidden layer MLP models outperforms for 675 days out of 1,326 days, but the average of the parametric models outperforms similarly for 652 days out of 1,326 days. In Part III of this table, we also compared the average of the parametric models with the average of the triple hidden layer LSTM models, and we find that the average of the parametric models outperforms for 907 days out of 1,326 days. Thus, the average of the parametric and the MLP models exhibit similar at-par outperformance.

We summarise three key findings when we compare the best-performing H-$Models$ (using lagged input variables) from Section 3.4.1 of Chapter 3 in Table 3.1, with the models discussed in Method A of Table 4.5. Firstly, in panel Method B of Table 4.5, where we compare the $BSMH_N$ model (i.e. the best-performing model of models in Table 3.1) with the average of the parametric, the triple hidden layer MLP and LSTM models, we conclude that the average of the triple hidden layer MLP models, the $M3H_N^{AVG}$-$Models$, outperforms all the above models (for 450 days out of 1,326). In Part II of Table C.2.10, we compare the $BSMH_N$ model with the average of the parametric models, and the average of the triple hidden layer MLP models and find that the average of the MLP models (again) outperforms all other models. Thirdly, in Part III of Table C.2.10, where the comparison is confined between the $BSMH_N$ model with the average of the parametric models and the average of the triple hidden layer LSTM models, the $BSMH_N$ model outperforms all other models (for 565 days out of 1,326 days).

We observe consistently similar results for the one-trading-day-ahead replicating portfolio value from the averaging HV-$Models$ in Section 3.4.3 of Chapter 3, which is obtained from the H-$Models$ (with lagged inputs). The average of the parametric models, the $ParamHV_N^{AVG}$-$Models$, outperforms all other models for 592 days out of 1,326 (in panel Method A of Table 4.8), and for 907 days out of 1,326 (in Part III of Table C.2.15), the average of the MLP models, the $M3H_N^{AVG}$-$Models$, outperforms all other models for 675 days out of 1,326 days (in Part II of Table C.2.15). Similar results are also observed while comparing the best-performing HV-$Models$ (with lagged input variables) from Section 3.4.3 of Chapter 3) with the models discussed in Tables 4.8 and C.2.15. The average of the MLP models, the $M3HV_N^{AVG}$ model, outperforms for 448 days out of 1,326 days (in Method B of Table 4.8), and for 588 days out of 1,326 days (in Part II of Table C.2.16), the $BSMHV_N$ model out-performs all other models for 561 days out of 1,326 days (in Part III of Table C.2.16).

Therefore, forecasting the one-trading-ahead delta and the associated replicating portfolio value from averaging models using lagged input variables demonstrates that the best approach is to average the forecasts from the triple hidden layer MLP models or the parametric models.

4.4.1.2 Using one-trading-day-ahead Input Variables

Panel Method A of Table 4.6 shows the relative out-of-sample forecasting performance (in $RMSE$) amongst the H-$Models$ using one-trading-day input variables. We compare the average of the parametric ($ParamH_{N+1}^{AVG}$-$Models$), the triple ($M3H_{N+1}^{AVG}$-$Models$) hidden layer MLP models, and the triple ($L3H_{N+1}^{AVG}$-$Models$) hidden layer LSTM models belonging to H-$Models$ from Table 3.2, separately. From these comparisons, we find that the average of the parametric models outperforms all other models (for 653 days out of 1,326). We further compare the averages derived from the H-$Models$ from Section 3.4.1 of Chapter 3 in Table C.2.9. Part II of this table compares the average of the parametric models with the average of the triple hidden layer

MLP models and finds that the average of the parametric models outperforms all other models (for 754 days out of 1,326). The average of the parametric models also outperforms the average of the triple hidden layer LSTM models in Part II of this table (for 907 days out of 1,326).

Comparing the best-performing $H\text{-}Models$ (using one-trading-day input variables) from Section 3.4.1 of Chapter 3 with the models discussed above in Tables 4.6 and C.2.11, we find that in panel Method B of Table 4.6, where we compare the $BSMH_{N+1}$ model (i.e. the best-performing model of the models in Table 3.2) with the average of the parametric, the triple hidden layer MLP and LSTM models, the Black-Scholes $BSMH_{N+1}$ model, outperforms all the above models (for 391 days out of 1,326). The $BSMH_{N+1}$ model also outperforms in Part III of Table C.2.9 (for 595 days out of 1,326 days), where we compare the best-performing $H\text{-}Models$, the $BSMH_{N+1}$ model, with the average of the parametric models and the average of the triple hidden layer LSTM models. The average of the parametric models though outperforms for 595 days out of 1,326 days when the comparison is with the best-performing $H\text{-}Models$, the $BSMH_{N+1}$ model, and the average of the MLP models in Part III of Table C.2.9.

The results regarding the one-trading-day-ahead replicating portfolio value of the averaging $HV\text{-}Models$ - obtained from the $H\text{-}Models$ (using one-trading-day inputs) in Section 3.4.3 of Chapter 3 are presented in Tables 4.9 and C.2.17. Panel Method A of Table 4.9 finds that the average of the parametric models, the $ParamHV^{AVG}_{N+1}\text{-}Models$, outperforms all other models (for 653 days out of 1,326) and for 754 days out of 1,326 (in Part II of Table C.2.17), and 907 days out of 1,326 (in Part III of Table C.2.17). Similar results are also observed when comparing the best-performing $HV\text{-}Models$ (using one-trading-day-ahead input variables) from Section 3.4.3 of Chapter 3, in Table 3.5, with the models discussed in Method A of Table 4.9. The parametric model, $BSMHV_{N+1}$ model, outperforms for 389 days out of 1,326 days (in Method B of Table 4.9), and similar, for 591 days out of 1,326 days (in Part III of Table C.2.18), the average of the MLP models, the $M3HV^{AVG}_{N+1}$ model outperforms all other models for 487 days out of 1,326 days (in Part II of Table C.2.18).

Thus, the best approach towards daily forecasting delta and the associated replicating portfolio value from models using one-trading-ahead input variables is to average the forecasts from the parametric models or use the $BSMH_{N+1}$ model.

4.4.2 Averaging Forecasts from CH-$Models$ and CHV-$Models$

Similar to above exercise, we present the relative out-of-sample forecasting performance (in $RMSE$) amongst the CH-$Models$ that forecast the one-trading-day-ahead average delta ($\delta C_{N+1}/\delta S_{N+1}$) derived analytically from C_{N+1} forecasted from models that use one-trading-day-ahead input variables from Table 4.7. We find similar results as the ones obtained from averaging forecasts of H-$Models$ and HV-$Models$ that use one-trading-day-ahead input variables. The average of the parametric models ($ParamCH^{AVG}_{N+1}$-$Models$) outperforms all other models (for 1290 days out of 1,326) when compared to the triple ($M3CH^{AVG}_{N+1}$-$Models$) hidden layer MLP models and the triple ($L3CH^{AVG}_{N+1}$-$Models$) hidden layer LSTM models in Method A of Table 4.7, and outperforms for 1290 days out of 1,326 when compared only to the average of the triple hidden layer MLP models in Part II of Table C.2.13, and for 1327 days out of 1,326 when compared only to the average of the triple hidden layer LSTM models in Part III of Table C.2.13.

We perform the comparison of the best-performing CH-$Models$ (that use one-trading-day input variables) from Section 3.4.2 of Chapter 3 with the models discussed above in Tables 4.7 and C.2.14. Method B panel of Table 4.7 compares the best-performing model CH-$Models$, namely $L3CH4_{N+1}$ model from Table 3.3, with the average of the parametric, the triple hidden layer MLP and LSTM models. The average of the parametric models, the $ParamCH^{AVG}_{N+1}$ model, outperforms all the above models for 1,285 days out of 1,326, also for 1,289 days out of 1,326 days when comparing the best-performing CH-$Models$, the $FMLSCH_{N+1}$ model, with the average of the parametric models and the average of the triple hidden layer MLP models in Part II of Table C.2.14. Finally, the $ParamCH^{AVG}_{N+1}$ model also outperforms when the comparison is with the best-performing CH-$Models$, the $HJDCH_{N+1}$ model, and the average of the LSTM models in Part III of Table C.2.14.

Contrasting results are observed in Tables 4.10 and C.2.19 when averaging the CHV-$Models$ obtained from the CH-$Models$ (with one-trading-day inputs) in Section 3.4.3 of Chapter 3. The average of the MLP models outperforms all other models for 912 days out of 1,326 (in panel Method A of Table 4.10), and for 1,038 days out of 1,326 (in Part II of Table C.2.19), and 1,134 days out of 1,326 (in Part III of Table C.2.19). Similar results are also observed when comparing the best-performing CHV-$Models$ with the models in Tables 4.10 and C.2.19. The average of the MLP model outperforms for 721 days out of 1,326 days (in panel Method B of Table 4.10) and for 655 days out of 1,326 days (in Part II of Table C.2.20).

Thus, the best approach to daily forecasting of the delta from predicted call prices is to average forecasts from the parametric models, while forecasting the average replicating portfolios would involve averaging forecasts from the MLP models.

Table 4.5: This table, categorised into two parts, presents the out-of-sample forecasting performance using daily and monthly statistics amongst the set of models, which averages the forecast of the one-day-ahead delta from models that lagged input variables. Below, in each of the parts, we compare the out-of-sample performance of the following models: **Method A**: The average delta from the parametric, the triple hidden layer MLP models, and the triple hidden layer LSTM models. **Method B**: The best out-performing model ($BSMH_N$) from Table 3.1 with the average delta from the parametric, the triple hidden layer MLP models, and the triple hidden layer LSTM models. The one-day-ahead forecast errors of the call option prices are used to compute the Root Mean Square Error (RMSE). Column I identifies the models, and when comparing all models, column II reports the number of months out of the 64 months that each model has the smallest RMSE, while column III reports the number of days out of the 1,326 days each model has the smallest RMSE. Forecasts are made for 1,326 trading days, and there are 64 months covered in the sample using the monthly data.

(I) **Model**	**(II)** **Performance amongst all models (Monthly)**	**(III)** **Performance amongst all models (Daily)**
	Method A	
$ParamH_N^{AVG}$-$Models$	**37**	**593**
$M3H_N^{AVG}$-$Models$	25	519
$L3H_N^{AVG}$-$Models$	2	215
	Method B	
$BSMH_N$	**39**	311
$ParamH_N^{AVG}$-$Models$	5	370
$M3H_N^{AVG}$-$Models$	18	**450**
$L3H_N^{AVG}$-$Models$	2	195

Table 4.6: This table, categorised into two parts, presents the out-of-sample forecasting performance using daily and monthly statistics amongst the set of models, which averages the forecast of the one-trading-day delta from models that use one-trading-day-ahead input variables. Below, in each of the parts, we compare the out-of-sample performance of the following models: **Method A**: The average delta from the parametric, the triple hidden layer MLP models, and the triple hidden layer LSTM models. **Method B**: The best out-performing model ($BSMH_{N+1}$) from Table 3.2 with the average delta from the parametric, the triple hidden layer MLP models, and the triple hidden layer LSTM models. The one-day-ahead forecast errors of the delta are used to compute the Root Mean Square Error (RMSE). Column I identifies the models, and when comparing all models, column II reports the number of months out of the 64 months that each model has the smallest RMSE, while column III reports the number of days out of the 1,326 days each model has the smallest RMSE. Forecasts are made for 1,326 trading days, and there are 64 months covered in the sample using the monthly data.

(I) **Model**	**(II)** **Performance amongst all models (Monthly)**	**(III)** **Performance amongst all models (Daily)**
	Method A	
$ParamH_{N+1}^{AVG}$-$Models$	**46**	**653**
$M3H_{N+1}^{AVG}$-$Models$	13	442
$L3H_{N+1}^{AVG}$-$Models$	5	232
	Method B	
$BSMH_{N+1}$	**46**	**391**
$ParamH_{N+1}^{AVG}$-$Models$	6	353
$M3H_{N+1}^{AVG}$-$Models$	10	373
$L3H_{N+1}^{AVG}$-$Models$	2	209

Table 4.7: This table, categorised into two parts, presents the out-of-sample forecasting performance using daily and monthly statistics amongst the set of models, which averages the forecast of the one-trading-day delta from models that use one-trading-day-ahead input variables to forecast one-trading-day-ahead call option price from which the delta is derived analytically. Below, in each of the parts, we compare the out-of-sample performance of the following models: **Method A**: The average delta from the parametric, the triple hidden layer MLP models, and the triple hidden layer LSTM models. **Method B**: The best out-performing model ($L3CH4_{N+1}$) from Table B.2.9 with the average delta from the parametric, the triple hidden layer MLP models, and the triple hidden layer LSTM models. The one-day-ahead forecast errors of the delta are used to compute the Root Mean Square Error (RMSE). Column I identifies the models, and when comparing all models, column II reports the number of months out of the 64 months that each model has the smallest RMSE, while column III reports the number of days out of the 1,326 days each model has the smallest RMSE. Forecasts are made for 1,326 trading days, and there are 64 months covered in the sample using the monthly data.

(I) **Model**	**(II)** **Performance amongst all models (Monthly)**	**(III)** **Performance amongst all models (Daily)**
	Method A	
$ParamCH_{N+1}^{AVG}$-$Models$	**64**	**1290**
$M3CH_{N+1}^{AVG}$-$Models$	0	37
$L3CH_{N+1}^{AVG}$-$Models$	0	0
	Method B	
$L3CH4_{N+1}$	0	4
$ParamCH_{N+1}^{AVG}$-$Models$	**64**	**1285**
$M3CH_{N+1}^{AVG}$-$Models$	0	37
$L3CH_{N+1}^{AVG}$-$Models$	0	0

Table 4.8: This table, categorised into two parts, presents the out-of-sample forecasting performance using daily and monthly statistics amongst the set of models, which averages the forecast of the replicating portfolio value from models that use lagged input variables to forecast the one-trading-day-ahead delta. Below, in each of the parts, we compare the out-of-sample performance of the following models: **Method A**: The average replicating portfolio value from the parametric, the triple hidden layer MLP models, and the triple hidden layer LSTM models. **Method B**: The best out-performing model ($BSMHV_N$) from Table 3.4 with the average replicating portfolio value from the parametric, the triple hidden layer MLP models, and the triple hidden layer LSTM models. The one-day-ahead forecast errors of the replicating portfolio value are used to compute the Root Mean Square Error (RMSE). Column I identifies the models, and when comparing all models, column II reports the number of months out of the 64 months that each model has the smallest RMSE, while column III reports the number of days out of the 1,326 days each model has the smallest RMSE. Forecasts are made for 1,326 trading days, and there are 64 months covered in the sample using the monthly data.

(I) Model	**(II)** Performance amongst all models (Monthly)	**(III)** Performance amongst all models (Daily)
Method A		
$ParamHV_N^{AVG}$-$Models$	17	**592**
$M3HV_N^{AVG}$-$Models$	**39**	519
$L3HV_N^{AVG}$-$Models$	7	215
Method B		
$BSMHV_N$	10	308
$ParamHV_N^{AVG}$-$Models$	13	372
$M3HV_N^{AVG}$-$Models$	**35**	**448**
$L3HV_N^{AVG}$-$Models$	6	198

Table 4.9: This table, categorised into two parts, presents the out-of-sample forecasting performance using daily and monthly statistics amongst the set of models, which averages the forecast of the replicating portfolio value from models that use one-trading-day-ahead input variables to forecast the one-trading-day-ahead delta. Below, in each of the parts, we compare the out-of-sample performance of the following models: **Method A**: The average replicating portfolio value from the parametric, the triple hidden layer MLP models, and the triple hidden layer LSTM models. **Method B**: The best out-performing model ($BSMHV_{N+1}$) from Table 3.5 with the average replicating portfolio value from the parametric, the triple hidden layer MLP models, and the triple hidden layer LSTM models. The one-day-ahead forecast errors of the replicating portfolio value are used to compute the Root Mean Square Error (RMSE). Column I identifies the models, and when comparing all models, column II reports the number of months out of the 64 months that each model has the smallest RMSE, while column III reports the number of days out of the 1,326 days each model has the smallest RMSE. Forecasts are made for 1,326 trading days, and there are 64 months covered in the sample using the monthly data.

(I) **Model**	**(II)** **Performance amongst all models (Monthly)**	**(III)** **Performance amongst all models (Daily)**
Method A		
$ParamHV_{N+1}^{AVG}$-$Models$	**37**	**653**
$M3HV_{N+1}^{AVG}$-$Models$	16	443
$L3HV_{N+1}^{AVG}$-$Models$	10	230
Method B		
$BSMHV_{N+1}$	**29**	**389**
$ParamHV_{N+1}^{AVG}$-$Models$	15	354
$M3HV_{N+1}^{AVG}$-$Models$	12	373
$L3HV_{N+1}^{AVG}$-$Models$	8	210

Table 4.10: This table, categorised into two parts, presents the out-of-sample forecasting performance using daily and monthly statistics amongst the set of models, which averages the forecast of the replicating portfolio value from models that use one-trading-day-ahead input variables to forecast one-trading-day-ahead call option price from which the delta is derived analytically. Below, in each of the parts, we compare the out-of-sample performance of the following models: **Method A**: The average replicating portfolio value from the parametric, the triple hidden layer MLP models, and the triple hidden layer LSTM models. **Method B**: The best out-performing model ($L3CHV4_{N+1}$) from Table 3.6 with the average replicating portfolio value from the parametric, the triple hidden layer MLP models, and the triple hidden layer LSTM models. The one-day-ahead forecast errors of the replicating portfolio value are used to compute the Root Mean Square Error (RMSE). Column I identifies the models, and when comparing all models, column II reports the number of months out of the 64 months that each model has the smallest RMSE, while column III reports the number of days out of the 1,326 days each model has the smallest RMSE. Forecasts are made for 1,326 trading days, and there are 64 months covered in the sample using the monthly data.

(I) Model	**(II)** Performance amongst all models (Monthly)	**(III)** Performance amongst all models (Daily)
Method A		
$ParamCHV^{AVG}_{N+1}$-Models	0	284
$M3CHV^{AVG}_{N+1}$-Models	**63**	**912**
$L3CHV^{AVG}_{N+1}$-Models	0	132
Method B		
$L3CHV4_{N+1}$	1	369
$ParamCHV^{AVG}_{N+1}$-Models	0	153
$M3CHV^{AVG}_{N+1}$-Models	**63**	**721**
$L3CHV^{AVG}_{N+1}$-Models	0	87

4.5 Robustness Tests

4.5.1 The Diebold–Mariano(DM) Tests

Similar to the DM tests performed in Chapters 2 and 3, the model pairs that are statistically insignificant differences in their prediction accuracy have been reported in Table C.1.1. For the 66 pairs created from the averaging of models belonging to *C-Models* (using lagged/one-trading-day-ahead input variables to forecast C_{N+1}), *CK-Models* (using lagged/one-trading-day-ahead input variables to forecast C_{N+1}/K_{N+1}), *H-Models* (using lagged/one-trading-day-ahead input variables to forecast δ_{N+1}), *CH-Models* (using one-trading-day-ahead input variables to forecast δ_{N+1}), *HV-Models* (using the δ_{N+1} from *H-Models*), *CHV-Models* (using the δ_{N+1} from *CH-Models*), only one pair is insignificant, and apart from that all the other pairs have significant forecasting power.

4.5.2 Bootstrap Tests

To further assess the validity of the forecasting performance results, we perform bootstrap tests using the daily and monthly RMSEs and discuss them in Sections C.2.1 through C.2.4, and present them in Tables C.2.1 and C.2.2 for *C-Models* that use lagged input variables to forecast the C_{N+1}, Tables C.2.3 and C.2.4 for *C-Models* that use one-trading-day-ahead input variables to forecast the C_{N+1}, Tables C.2.5 and C.2.6 for *CK-Models* that use one-trading-day-ahead input variables to forecast the C_{N+1}/K_{N+1}, and Tables C.2.7 and C.2.8 for *CK-Models* that use one-trading-day-ahead input variables to forecast the C_{N+1}/K_{N+1}, Tables C.2.9 and C.2.10 for *H-Models* that use lagged input variables to forecast the Δ_{N+1}, Tables C.2.11 and C.2.12 for *H-Models* that use one-trading-day-ahead input variables to forecast the Δ_{N+1}, Tables C.2.13 and C.2.14 for *CH-Models* that use one-trading-day-ahead input variables to forecast the δ_{N+1}, Tables C.2.15 and C.2.16 for *HV-Models* computed from the Δ_{N+1} obtained from *H-Models* (that uses lagged input variables for forecasting), Tables C.2.17 and C.2.18 for *HV-Models* computed from the Δ_{N+1} obtained from *H-Models* (that uses one-trading-day-ahead input variables for forecasting), Tables C.2.19 and C.2.20 for *CHV-Models* computed from the δ_{N+1}obtained from *CH-Models* in Appendix C.2, presents the results of the bootstrap performed using the daily and monthly RMSEs. In Tables C.2.1 to C.2.8, we present the lower/upper bounds from the bootstrap performed (with replacement) using monthly RMSEs at a 95% confidence level and shows the winning percentage out of 64 months for each model including/excluding the δC_N model and similarly, the 95 % confidence intervals computed from bootstrapping of the daily RMSEs signify the winning percentage out of 1328 days for each model and are reported as lower/upper bounds. In Tables C.2.9 to C.2.20, we repeat a similar exercise of performing the bootstrap. The results from the bootstrap tests support the results discussed in Section C.2.

4.5.3 Pairwise Test

In the several comparisons made in Sections 4.3 and 4.4, even though a particular model wins by a higher percentage against other models, we investigate further these models pairwise by performing a pairwise bootstrap comparison which is computed using the respective pair's daily RMSEs. Amongst the several comparisons performed in Sections 4.3, we find that the average of the MLP class of models has consistently out-performed other classes of models, and in Section 4.4, the average of the MLP/Parametric class of models has consistently outperformed other classes of models. We make similar conclusions when we compare the models' average pairwise. We summarise the results from the pairwise bootstrap tests from Table 91 (for the *C-Models* that use lagged ahead input variables), Table 92 (for the *C-Models* that use one-trading-day-ahead input variables), Table 93 (for the *CK-Models* that use lagged ahead input variables), Table 94 (for the *CK-Models* that use one-trading-day-ahead input variables), Table 95 (for the *H-Models* that use lagged input variables), Table 96 (for the *H-Models* that use one-trading-day-ahead input variables), Table 97 (for *CH-Models* that use one-trading-day-ahead input variables), Table 97 (for the *HV-Models* that use delta from *H-Models*, that uses lagged input variables), Table 98 (for the *HV-Models* that use delta from *H-Models*, that uses one-trading-day inputs variables) of the Electronic Appendix in Table C.1.2. We observe similar results for the 28 pairs derived from averaging the models belonging to *C-Models* (that use lagged input variables) and 28 pairs from averaging the models belonging to the *CK-Models* (that use lagged input variables), where the MLP class of models outperforms for over 53.6%, the parametric 10.7%, and the LSTM models for 10.7% of the pairs. Similar results can be seen for the 6 pairs derived from averaging the models belonging to *C-Models* (that use one-trading-day input variables) and the 6 pairs from averaging the models belonging to *CK-Models* (that use one-trading-day input variables), where the MLP class of models outperforms for 50%, the parametric 33.3%, and the LSTM models for 16.7% of the pairs. For the 3 pairs derived from averaging the models belonging to *H-Models* (that use lagged input variables) and the 3 pairs from *HV-Models* (that use lagged input variables), we observe similar results where the MLP class of models outperforms 66.7%, the parametric 33.3%, and the LSTM models for 0% of the pairs. Finally, for the 3 pairs derived from averaging the models belonging to $H\text{-}Models$, 3 pairs averaging the models belonging to $HV\text{-}Models$ (that use one-trading-day input variables), 3 pairs derived from averaging the models belonging to $CH\text{-}Models$, and 3 pairs averaging the models belonging to $CHV\text{-}Models$, we see exactly similar results, where the parametric class of models outperforms 66.7%, the MLP 33.3%, and the LSTM class of models for 0% of the pairs. Thus, the pairwise bootstrap comparison reveals conclusive evidence that a class of models could consistently outperform.

4.6 Conclusion

This chapter introduces averaging methods for forecasting prices and delta and computing the replicating portfolio value of the options positions. Furthermore, this chapter gauges the empirical daily forecasting performance of prices and delta for S&P 500 index options using averaging of parametric and ANN models. These investigations are based on comparisons between averaging all parametric and averaging all the ANN models based on the class of hidden layers, as well as comparing these models with the best performing models (as identified in Chapters 2 and 3). The MLP and LSTM networks used in this study are trained using lagged and one-trading-day-ahead input variables to forecast the one-trading-day-ahead option prices and delta. Alternatively, we also analytically compute the one-trading-day-ahead delta from a class of MLP and LSTM networks that forecasts the one-trading-day-ahead option price. The economic significance of these forecasts is assessed by the daily forecast performance of the value of the corresponding replicating portfolio.

With regards to the forecasting performance of daily option prices and moneyness, we find that simple random walk outperforms all models. Furthermore, when we exclude the random walk, we find that the average of all the triple hidden layer MLP models outperforms any combination of the average of all the models considered in the study.[3] When using one-trading-day-ahead input variables, we test only the triple hidden layer models, and we find that the average of all triple hidden layer MLP models again is typically the best-performing model also outperforming the random walk forecasting model. However, while the average of all the triple hidden layer MLP models typically could not out-perform the individually best out-performing

[3]These models include the parametric models, the average of all the single, or the double, or the triple hidden layer LSTM models, and the average of all the single or the double hidden layer MLP models

LSTM model (identified in Chapter 2) for forecasting prices, it outperforms the individually best out-performing LSTM model when forecasting moneyness. This also holds for models that average the forecasts from models that use one-trade-day ahead inputs to forecast moneyness.

With regards to the forecasting performance of daily delta using lagged/one-trading day ahead input variables, we find that the average of all the parametric models is capable of producing forecasts with the lowest RMSEs, and is closely followed by the average of all the triple hidden layer models. Similar results are also seen while measuring the forecasting performance of daily delta, which was analytically derived from call option prices. However, the average of all parametric models does not perform better than the best outperforming models (identified in Chapter 3) when forecasting daily delta directly but does perform better when forecasting daily delta analytically.

The economic significance of these forecasts is measured by comparing the forecast performance of their corresponding replicating portfolio value. The average replicating portfolio value (with lagged inputs) reveals that the average of all triple hidden layer MLP models and the average of all parametric models perform similarly, while the average of all triple hidden layer LSTM models has the least forecasting accuracy. The out-performance of the average of all triple hidden layer MLP models also remains when compared with the best-performing models identified in Chapter 3, where it has the lowest RMSEs followed by the BSM model. The replicating portfolio value forecasting performance of models that use one-trading-day ahead inputs to forecast the delta reveals that the average of all parametric models has the lowest RMSEs, but when it is compared to the best-performing models, it fails to outperform. For the replicating portfolio value forecasting performance of models that derive the delta analytically from call option prices, we see contrasting results where the average of all triple hidden layer MLP models has the lowest RMSEs and could also perform better than the best-performing models identified in Chapter 3.

Overall, the average triple hidden layer MLP models tend to perform the best for forecasting option prices, with the parametric models performing better in forecasting delta and even better than the best-performing models when delta is computed analytically from prices. For the replicating portfolio, the pricing forecasts seem to dominate the delta forecasts revealing an outperformance for the average triple hidden layer MLP models. Thus, model averaging could potentially benefit forecasting pricing and hedging applications with ANN.

Chapter 5

Optimal Pairs Trading–An Alternate Way of Trading Equity ETF Pairs Using Machine Learning Models

5.1 Introduction

Pairs trading (PT) is a statistical arbitrage method that invests in the spread between two equities whose prices have historically moved in unison (Gatev et al. (2006)). A long position is taken in one stock, and a short position is taken in the other simultaneously. Trading signals are based on deviations from the long-term equilibrium spread, and the spread between the two stocks creates a stationary process. Investors act and profit from the momentary inconsistency created when spreads deviate from their historical equilibrium in the belief that they will revert shortly. PT is a market-neutral strategy because it generates returns regardless of whether the market rises or falls. PT studies have primarily been focused on traditional methods, where statistical and parametric tools are used to improvise the trading strategy (Gatev et al. (2006, 1999), Nath (2003), Vidyamurthy (2011)). This chapter considers the more advanced applications of machine learning-based PT strategies to provide a comprehensive empirical assessment of MS arbitrage methodologies.

In this study, we introduce a new methodology for PT equity ETFs that outperforms existing traditional strategies by implementing several modified versions of the distance method, the cointegration method (using the Johansen and the Engle-Granger tests), the Kalman filter and the ratio method as baselines for comparison with several technical indicators and modified versions of the decision trees (DT) and deep learning ANN models based on the MLP network architecture (Dunis et al. (2006, 2015), Sarmento and Horta (2020)). We perform a comparative analysis based on actual PnL ($ value), returns, Sharpe ratios, and other performance indicators. The modified versions of the aforementioned traditional approaches are formulated by effectively applying commonly used technical indicators, such as the Exponential Moving Averages (EMA), Relative Strength Index (RSI), Moving Average Convergence Divergence (MACD), and Bollinger Bands (BB) to the spread generated by these traditional approaches, thereby generating ways to enhance returns. We effectively apply the traditional and modified approaches to eight equity ETF pairs—four of which are cointegrated/correlated and four of which are not. Finally, we investigate the back-test performance of these eight equity ETF pairs across three rolling windows of 30, 50 and 100 days.

The back-test/forecasting performance of the 3,084 trading strategies across the 30-, 50-, and 100-day rolling windows demonstrates that the modified (MOD) strategies have the potential to provide significant returns over traditional ($TRAD$) strategies. However, the average number of winning/losing trades and the average maximum drawdown (MDD) for the MOD strategies are higher compared to those of the $TRAD$ set of trading strategies. More specifically, out of the 216 methods (i.e. 9 methods, across 3 rolling windows, used for back-testing each of the eight ETF pairs), 8.8% of the methods belonging to $TRAD$ trading strategies outperform the methods belonging to the MOD, and machine learning (ML) strategies, 69.9% of the methods belonging to MOD trading strategies outperform the methods belonging to the $TRAD$ and ML strategies, and 20.8% of the methods belonging to ML trading strategies had out-performed the methods belonging to the MOD and $TRAD$ strategies. Thus, the methods using ML-based strategies tend to have more predictive power than methods using $TRAD$-based strategies.

This study makes three contributions to the literature in that it assesses the sensitivity of rolling windows, uses technical indicators and gauges the impact of cointegration between the pairs of assets. In order to unfold more information on ways to trade ETF pairs in a high-frequency setting, we compute three rolling windows (30, 50 and 100 days). Chaudhuri and Singh (2015) proposed a framework for PT using technical analysis (Momentum, BBs and MACD), but they were applied to the stock prices. This study is extended by Chaudhuri et al. (2017), who used BBs on the ratios of stock prices as an input to the support vector regression (SVR), RF and Adaptive Neuro-Fuzzy Inference System (ANFIS) to infer PT opportunities. The RSI, a technical indicator, is applied to spreads in PTF Pro's software to find investment opportunities.

However, there are no studies that apply these and other technical indicators to the spread/ratio and use them along with machine learning techniques to infer PT opportunities. In addition, the modified machine learning strategies that have been designed in this study have a dynamic stop-loss barrier rather than fixed stop-loss barriers, which is different from traditional strategies (Nath (2003), Huck and Afawubo (2015), Ramos-Requena et al. (2020) and Vidyamurthy (2004)). These modified sets of strategies could also be applied regardless of whether the pairs are cointegrated or correlated, thereby generating unique ways to enhance portfolio returns.

This chapter is organised into four sections. Section 5.2 provides the theoretical aspect of the models and methods used in this study. Section 5.3 elaborates on the source of the dataset, the filters used to refine the dataset, the summary statistics of the dataset, and the inputs used in the models to forecast the spread. Section 5.4 examines the calibration procedures used in the models, the data fitting (network parameters, division of datasets, the optimisation and generalisation procedures used to improve the accuracy of the MLP and DT models and the performance criteria used to evaluate the trading strategies. Section 5.5 discusses the empirical results by comparing the performance of the proposed models, and finally, Section 5.6 concludes the study.

5.2 Models

5.2.1 Distance Methods

There have been several variations on distance method-based pair selection, including Nath (2003), Gatev et al. (2006), Huck (2015), Huck and Afawubo (2015), Ramos-Requena et al. (2017, 2020). Gatev et al. (2006)'s distance method of pair selection can be considered the baseline.

5.2.1.1 The Distance Method - Version 1

Gatev et al. (2006) selected pairs that minimised the distance criteria. The distance measure is calculated by minimising the sum of squared differences between two normalised price series. The Euclidean squared distance is defined as

$$ESD = \sum_{t} \left(P_X(t) - P_Y(t)\right)^2, \tag{5.1}$$

where $P_X(t)$ is the cumulative return of price series X at time t and $P_Y(t)$ is the cumulative return of price series Y at time t. The pairs which minimise (5.1) were selected. The spread is the price difference between series X and Y, and at time t, it is defined as

$$S(t) = P_Y(t) - P_X(t). \tag{5.2}$$

The spread generated using Eq. (5.2) is denoted as '**DIST$^{\mathbf{V1.1}}$-SPRD**' in this chapter. Since the definition of the spread is vaguely mentioned and not written down mathematically, we also follow the definition of spread provided in Ramos-Requena et al. (2017, 2020) as follows:

$$S(t) = log(P_Y(t) - P_Y(0)) - log(P_X(t) - P_X(0)). \tag{5.3}$$

The spread generated using Eq. (5.3) is denoted as '**DIST$^{\mathbf{V1.2}}$-SPRD**'.

5.2.1.2 The Distance Method - Version 2

Huck (2015)'s and Huck and Afawubo (2015)'s interpretations of Gatev et al. (2006)'s distance method were slightly different. Initially, for each pair, they normalise the price series of X and Y to start at \$1, respectively, and then they formed pairs by finding the pairs that minimised the sum of squared differences, as shown in Eq. (5.2). Although, Huck (2015) and Huck and Afawubo (2015) did not specify a mathematical definition, Quantpedia[1] also follows the same interpretation and defines the spread as

$$S(t) = P_Y(t) - P_X(t), \tag{5.4}$$

which is denoted as '**DIST$^{\mathbf{V2}}$-SPRD**'.

5.2.1.3 The Distance Method - Version 3

Nath (2003) approached the distance method differently in terms of pairs selection and the definition of trading signals. The author defined the distance measure as the sum of the square of the daily differences in the normalised prices of the securities, where the price used is the median of the mid-quote for each day. The normalisation of prices for each security is carried out by subtracting the sample mean of the training period and dividing it by the sample standard deviation over the training period. The spread defined by Nath (2003) is as follows:

$$S(t) = P_Y(t) - P_X(t), \tag{5.5}$$

and in this chapter, it is denoted as '**DIST$^{\mathbf{V3}}$-SPRD**'.

[1] Follow the link: https://quantpedia.com/strategies/pairs-trading-with-stocks/

5.2.1.4 The Distance Method - Version 4

The distance approach method proposed by Gatev et al. (2006) was identified as sub-optimal by Krauss (2017). First, minimising the sum of the squared differences between two normalised price series would also minimise the spread. Second, this results in the spread having fewer deviations from the mean. For PT to be profitable, the spread should ideally exhibit some variation. Krauss (2017) expressed the spread variance $S^2_{P_X-P_Y}$ as

$$S^2_{P_X-P_Y} = \frac{1}{T}\sum_{t=1}^{T}(P_X(t) - P_Y(t))^2 - \left(\frac{1}{T}\sum_{t=1}^{T}(P_X(t) - P_Y(t))\right)^2, \tag{5.6}$$

which can be solved for the average sum of squared distances ($\overline{SSD}_{P_X,P_Y}$) as

$$\overline{SSD}_{P_X,P_Y} = \frac{1}{T}\sum_{t=1}^{T}(P_X(t) - P_Y(t))^2 = S^2_{P_X-P_Y} + \left(\frac{1}{T}\sum_{t=1}^{T}(P_X(t) - P_Y(t))\right)^2. \tag{5.7}$$

In this chapter, we denote the spread interpreted by Krauss (2017) in Eq. (5.7) as '**DIST$^{\mathbf{V4}}$-SPRD**'.

5.2.2 The Co-integration Methods

Three methods are used to assess cointegration, as discussed below.

5.2.2.1 Co-integration Method - Using ADF Test

Engle and Granger (1987) set in motion the concept of cointegration, which could be applied to produce a stationary time series ($S(t)$) by forming a specific linear combination of two non-stationary time series (or $I(1)$ processes) P_X and P_Y as

$$S(t) = P_X(t) - \beta P_Y(t) - \mu - \varepsilon(t), \tag{5.8}$$

where, S_t is $I(0)$ and exhibits a mean-reverting behaviour μ denotes the intercept. $\varepsilon(t)$ was further examined using the Dickey and Fuller (1979) test to test for cointegration. We denote the spread in Eq. (5.8) as '**ADF-SPRD**'.

5.2.2.2 The Co-integration Method - Using Johansen's Test

Johansen (1988, 1991) overcame the drawbacks of Engle and Granger (1987) by analysing the cointegration relationship between variables simultaneously in one system by introducing a cointegration test for a multivariate system, known as the Johansen test. This test uses the Vector

Error Correction Model (VECM) to find the cointegration coefficient/vector(β) and considers every time series as an independent variable. Using the eigenvalue statistics and trace statistics, we are able to determine whether the time series is statistically significantly cointegrated. We denote the spread interpreted by Johansen (1988) as '**JOHANSEN-SPRD**'.

5.2.3 Kalman Filter - State Space Regression Method

Drakos (2016) defined the multivariate Kalman filter process as a three-step process comprised of prediction, observation and correction steps. The aim of the Kalman filter is to calculate at each time step the updated hedge ratio $\beta(t)$ of the synthetic asset. Dunis et al. (2010) and Kim (2011) applied the Kalman states space regression method, where the state-space model consists of two matrix equations as shown below:

$$Y(t) = \beta(t)X(t) + \varepsilon(t), \tag{5.9}$$

$$\beta(t) = \beta(t-1) + \eta(t), \tag{5.10}$$

where Eq. (5.9) is known as the measurement equation, and the state variables are shown in Eq. (5.10), which is also known as the state transition equation. They described the change in state variables from one time period to the next. There is a linear dependence on the previous state given by the transition matrix as well as normally distributed system noise. In the general sense, this means that the transition matrix is itself time-dependent. $Y(t)$ is the dependent variable, $\beta(t)$ is time-varying regression coefficient (hedge ratio) and $X(t)$ is the independent variable at time t. $\varepsilon(t)$ and $\eta(t)$ are independent, uncorrelated error terms with standard deviations H and Q, respectively.

Kim (2011) mentioned that the variances of the noise process and other unknown parameters could be estimated by maximising the following likelihood function:

$$\log L = -\frac{NT}{2}\log 2\pi - \frac{1}{2}\sum_{t=1}^{T}\log F(t) - \frac{1}{2}\frac{v(t)'v(t)}{F(t)}, \tag{5.11}$$

where $v(t)$ is the one-step-ahead residual, which is calculated from the difference between $Y(t)$ and its estimate, $F(t)$ is its variance and N and T are the number of columns of $X(t)$ and the number of elements of the time series $Y(t)$, respectively. The set of regressions below is known as the Kalman filter, and it provides an estimate of the coefficient β at time t given the estimate of β at t-1:

$$\begin{aligned}\beta(t|t-1) &= \beta(t), &(5.12)\\ v(t) &= Y(t) - X(t)\beta(t), &(5.13)\\ F(t) &= X(t)P(t)X(t)' + H, &(5.14)\\ \beta(t+1) &= \beta(t) + P(t)X(t)'\frac{v(t)}{F(t)}, &(5.15)\\ P(t+1) &= P(t) - P(t)X(t)'X(t)P(t)\frac{1}{F(t)} + Q. &(5.16)\end{aligned}$$

The parameters H and Q are the error terms of the process. The higher the noise ratio ($\frac{Q}{H}$), the more adaptive the beta, and the lower the ratio, the less adaptive the beta. The most important parameter of the Kalman filter procedure is the noise ratio.
After obtaining the estimate for $\beta(t)$, the spread is calculated using the equation

$$S(t) = P_Y(t) - \beta(t)P_X(t), \tag{5.17}$$

and it is denoted as '**KALMAN-SPRD**'.

5.2.4 The Ratio Method

The ratio method applied by Chaudhuri et al. (2017), Chaudhuri and Singh (2015), and PTF Pro involves finding arbitrage opportunities from the movement in the ratio of the prices of two stocks. The ratio between two stocks or two ETFs in a pair trading strategy can be defined as:

$$R(t) = (P_X(t)/P_Y(t)) \tag{5.18}$$

In this study, we denote the ratio in Eq. (5.18) as '**RATIO-SPRD**'.

5.2.5 Machine Learning Algorithms

5.2.5.1 Decision Trees

We use the Python Scikit package to implement a DT for multi-class classification of trading signals. The Scikit package uses an optimised version of the Classification and Regression Tree (CART) algorithm, which is very similar to the C4.5 algorithm, which is the successor to the ID3 algorithm. As per the documentation on Scikit, the ID3 algorithm builds a multi-way tree and identifies the categorical feature for each node that provides the most information for categorical targets. To enhance a tree's capacity to generalise to new data, trees are typically pruned after reaching their maximum size. As per Seni and Elder (2010) and Bai et al. (2019), an information gain ratio is used by the ID3 algorithm to classify data. The information gain ratio (IGR) for classifying the categorical variable(X) using the training set(T) is given as

$$IGR(T, X) = \frac{IG(T, X)}{H_X(T)}, \tag{5.19}$$

where $IG(T, X)$ is the information gain to the entropy and $H_X(T)$ is the eigenvalue X for the given T. The information gain can be further expanded as

$$IG(T, X) = H(T) - H(T \mid X), \tag{5.20}$$

where H(T) is the entropy of T and $H(T \mid X)$ is the empirical conditional entropy of the training set T under the given condition X. $H(T \mid X)$ can be further expanded as,

$$H(T \mid X) = \sum_{i=1}^{n} P_i H\left(T \mid X = X_i\right), \tag{5.21}$$

$$\therefore H(T) = -\sum_{i=1}^{n} P_i \log_2 P_i, \tag{5.22}$$

where P_i is the probability of classification 'i'. Thus, the entropy of T under the eigenvalue X is given as

$$H_X(T) = -\sum_{i=1}^{n} P_i \log_2 P_i. \tag{5.23}$$

5.2.5.2 Multilayer Perceptron

The theoretical foundations of the MLP model are discussed in detail in Section 2.2.5.1.

5.2.6 Technical Indicators

To offer a comprehensive assessment, several technical indicators are used in the analysis, including SMA, EMA, RSI, MACD, and BBs.

5.2.6.1 The Simple Moving Average

The simple moving average (SMA) calculates an average over a finite size window of n observations. The SMA for a window length (number of periods) of n is

$$SMA_n(t) = \frac{1}{n} \sum_{t=0}^{n} S(t-1),$$

where, in our study, $S(t)$ denotes the spread from the respective parametric models.

5.2.6.2 The Exponential Moving Average

The exponential moving average (EMA) scales each observation exponentially, which the SMA fails to do. The EMA is preferred over the SMA because the SMA's trendline is delayed by a factor proportional to n, as it was calculated using the previous n observations. Moreover, this also delays the detection of a change in the trend. The EMA scales each observation by an exponential factor α, and an n-day EMA is defined as

$$\text{EMA}_n(t) = \alpha \times S(t) + (1 - \alpha) \times EMA(t-1),$$

where $\alpha = \left(\frac{2}{1+n}\right)$ and $S(t)$ denotes the spread from the respective parametric models.

5.2.6.3 The Relative Strength Index

Wilder (1978) developed the RSI momentum oscillator, which measures the extent to which a time series has a positive change to its negative change. The RSI is defined as

$$RSI_n(t) = 100 - \left(\frac{100}{1 + RS_n(t)}\right),$$

where $RS_n(t)$ = the average positive change in the spread ($S(t)$) in the past n days and the average negative change in the spread ($S(t)$) in the past n days, while $S(t)$ denotes the spread from the respective parametric models. According to Wilder (1978), the RSI fluctuates between 0 and 100. When the RSI rises above 70, the upper threshold, it is considered overbought, and when it falls below 30, the lower threshold, it is considered oversold.

5.2.6.4 The Moving Average Convergence/Divergence Oscillator

Appel developed the MACD oscillator to trade the weekly cycles of the stock market. Zakamulin (2017) and Stock Charts stated that the MACD oscillator consists of the MAC (which is a combination of two EMAs) and the $Signal$ (which is an EMA of the MAC). The MAC indicator is defined as

$$MAC_{(s,l)}(t) = EMA_{(s)}(t) - EMA_{(l)}(t),$$

where the default values for s and l are taken as 12 days and 26 days, respectively. The *Signal* indicator is defined as,

$$Signal_{(n)}(t) = EMA_n(MAC_{(s,l)}(t)),$$

where n is 9 days. The $MAC_{(s,l)}(t)$ and the $Signal_{(n)}(t)$ are combined and denoted as $MACD_{(s,l,n)}(t)$.

5.2.6.5 Bollinger Bands

Bollinger (1992) introduced a set of three bands (upper, middle and lower bands) that uses standard deviations to dynamically calculate whether a time series (or stock price) is at its highest (if the price is at the upper band) or lowest (if the price is at the lower band). The n-day Bollinger bands are computed as follows,

- Middle band: n-day simple/weighted moving average.
- Upper band: Middle band + 2 $\times$ $n-$day standard deviation.
- Lower band: Middle band - 2 $\times$ $n-$day standard deviation.

In this chapter, we denote the n-day BBs as $BB_{(n)}$.

5.3 Data

5.3.1 Dataset

According to Chan (2013), one of the biggest advantages of using ETF pairs instead of stock pairs is that once a pair is cointegrated, it is less prone to fall apart due to the fundamental economics of a basket of stocks. Changes in ETFs happen much more slowly compared to the fundamental economics of a single stock. The focus of this paper is on a subset of equity ETFs listed on the NYSE. NYSE Arca has the highest market share of traded volume and liquidity depth and narrowest quoted spreads and quotes the most time at the best prices across all US ETFs, according to the NYSE. Finding the number of possible pairs among the entire universe of equity ETFs is computationally intensive. By limiting the subset to ETFs obtained using the filters applied in Section 5.3.2, we select four ETF pairs with a cointegration and correlation value of greater than 90%, of which we choose four ETF pairs. We also choose four ETF pairs having a cointegration and correlation value lesser than 10%. This makes the strategy computationally faster and allows time for a thorough analysis of the selected pairs. Thus, we choose the following four ETF pairs, **ITOT.N/IXUS.N**, **IWF.N/XLE.N**, **SCHB.N/SCHF.N**, and **SCHF.N/VO.N** which had a cointegration and correlation value of greater than 90% as of 31 January 2022. Similarly, we choose four ETF pairs, namely **QQQ.N/XLE.N**, **USMV.N/XLE.N**, **VO.N/VXUS.N**, and **VWO.N/XLE.N** which had a cointegration and correlation values of less than 10% as on 01 January 2019. We further consider open-high-low-close (OHLC) time-series data with an end-of-day (EOD) frequency for the period from 01 January 2019 to 31 January 2022, which includes 776 trading days for the eight ETF pairs mentioned above. For back-testing, depending on the trading signals generated by the strategies discussed in Section 5.3.4, we initiate a long/short position on the next day's open price of the respective pair, thereby allowing for the precise and practical entry and exit points where EOD data are used. This approach prevents look-ahead bias.

5.3.2 Data Filtering

The following filtering steps are performed before a pair selection is carried out:

- ETFs with fund sizes greater than $500 million.
- After filtering for fund size, 50 ETFs are chosen on the basis of the fund size.
- ETFs traded since 2015 are selected.

After selecting the universe of the top 50 ETFs, we form 1,225 ETF pairs among the 50 individual ETFs. Once 1,225 ETF pairs are formed, we then check for any missing quotes. If an individual ETF in an ETF pair has a missing open, high, low or close value for a given date/time, we consider the previous traded value.

5.3.3 Information Sets

5.3.3.1 Information Sets using Z-Score-Based Trading Models:

The inputs used in Z-Score-based trading strategies are tabulated in Table D.1.2 (refer to the trading strategy codes mentioned in column I), from A1.1 to A1.6, B1.1 to B1.6, C1.1 to C1.6, D1.1 to D1.6, E1.1 to E1.6, F1.1 to F1.6, G1.1 to G1.6, H1.1 to H1.6 and I1.1 to I1.6.

5.3.3.2 Information Sets used for MLP- and DT-Based Trading Strategies:

For the various MLP- and DT-based strategies, we use a variety of variables as inputs, which are modelled from the spreads using the methods mentioned below. We model the spread ($S(t)$) returns as

$$SprdRet(t) = \frac{S(t)}{S(t-1)}, \tag{5.24}$$

and the close price returns of each ETF in a given pair are computed as

$$CloseRet(t) = \frac{Close(t)}{Close(t-1)}. \tag{5.25}$$

We also compute the daily running profit and loss for each trade and denote them as '**PnL()**' in the information sets used in the strategies mentioned below. The close price returns, spread returns and PnL are further categorically encoded as follows:

- a value > 0 is categorised as 1,
- a value < 0 is categorised as -1,
- a value $= 0$ is categorised as 0.

(5.26)

In the information sets used in the strategies mentioned below, we denote the categorical columns as '**CATEG()**'. Creating a target variable for the various MLP- and DT-based trading strategies mentioned below involves a process of merging categorical values from two outputs. We take the categorical values of the average PnL computed based on multiple trading strategies (denoted as $value\_column1$ in Eqs. (5.27), (5.28), 5.29)) and the categorical values of those respective trading strategies underlying spread returns (denoted as $value\_column2$ in Eqs. 5.27, 5.28, 5.29). The multiple trading strategies are used to compute the average PnL and the underlying spread from which the spread returns are computed differently for the A3/A4, B3/B4, C3/C4, F3/F4, G3/G4, H3/H4 and I3/I4 trading strategies. Later, we apply a logical function, which binds these two categorical variable inputs into a single categorical variable (denoted as $value\_output$ in Eqs. (5.27), (5.28) and (5.29)). The logical function has the following rules, where a **buy** is categorised as follows:

- if $value\_column1 = 1$ and $value\_column2 = 1$, then $value\_output = 1$
- if $value\_column1 = 1$ and $value\_column2 = 0$, then $value\_output = 1$
- if $value\_column1 = 0$ and $value\_column2 = 1$, then $value\_output = 1$

(5.27)

a **sell** is categorised as follows:

- if $value\_column1$ = -1 and $value\_column2$ = -1, then $value\_output$ = -1
- if $value\_column1$ = -1 and $value\_column2$ = 0, then $value\_output$ = -1
- if $value\_column1$ = 0 and $value\_column2$ = -1, then $value\_output$ = -1

(5.28)

and a **hold** is categorised as follows:

- if $value\_column1$ = 0 and $value\_column2$ = 0, then $value\_output$ = 0
- if $value\_column1$ = 1 and $value\_column2$ = -1, then $value\_output$ = 0
- if $value\_column1$ = -1 and $value\_column2$ = 1, then $value\_output$ = 0

(5.29)

Below, we denote the first ETF in a given ETF pair as $SYM1$ and the second ETF in that pair as $SYM2$. Also, in the above-mentioned sections, depending on the rolling window, i.e. 30, 50 or 100 days, we select the variables used for the train and test and target sets based on that respective rolling window. The categorical values used as input in these train and test sets are modelled using the logic presented in Eq. (5.26). Similarly, the logic used to model the target variable is presented in Eqs. (5.27), (5.28) and (5.29).

The training set for trading strategies A3 and A4 involves using the categorical values of the close price returns of $SYM1$ and $SYM2$, the difference in close price returns between $SYM1$ and $SYM2$, the categorical values of the daily running PnL values of the trades generated from trading strategies $CLS - SYM1.1$ to $CLS - SYM1.5$ and the categorical values of the daily running PnL values of the trades generated from trading strategies $CLS - SYM2.1$ to $CLS-SYM2.5$. [2] These common inputs are also used for the training set of the B3/B4, C3/C4, F3/F4, G3/G4, H3/H4 and I3/I4 trading strategies. In addition to the above, the training set of the A3 and A4 trading strategies also includes the categorical values of the daily running PnL values of the trades generated from trading strategies $A2.1$ to $A2.5$ and the close price returns of $SYM1$ and $SYM2$. For the other set of trading strategies, which are for the B3/B4, C3/C4, F3/F4, G3/G4, H3/H4 and I3/I4 models, apart from the common set of inputs (mentioned above), the additional set of inputs used in the training set involves the categorical values of the daily running PnL values of the trades generated from trading strategies 2.1 to 2.5 of the

[2] Refer to Section 5.4.3 for further details on $CLS - SYM1.1$ to $CLS - SYM2.6$ trading strategies

respective model category. For example, for the B3/B4 trading strategies, the additional set of inputs used in the training set would involve using the categorical values of the daily running PnL values of the trades generated from trading strategies $B2.1$ to $B2.5$.

The target set for the A3 and A4 trading strategies involves using the categorical values of the average PnL of the daily running PnL values of the trades generated by trading strategies $A1.1$ to $A1.6$ and the categorical values of the underlying spread returns ($DIST^{V1.1} - SPRD$), which are transformed to a single categorical target variable using the logic presented in Eqs. (5.27), (5.28) and (5.29). The target set for the other category of trading strategies, the B3/B4, C3/C4, F3/F4, G3/G4, H3/H4 and I3/I4 trading strategies, involves using the categorical values of the average PnL of the daily running PnL values of the trades generated from trading strategies 1.1 to 1.6 and the categorical values of the underlying spread returns of that respective model category. For example, for the B3/B4 trading strategies, the target set would have the categorical values of the average PnL of the daily running PnL values of the trades generated by trading strategies $B1.1$ to $B1.6$ and the categorical values of the underlying spread returns ($DIST^{V1.2} - SPRD$).

A detailed tabular representation of the variables used in the train, test and target sets for each of the rolling windows, i.e. 30-, 50-, and 100-day, can be found in Table D.1.3.

5.3.4 Entry and Exit Thresholds

In this section, we discuss the entry and exit conditions for the z-score, technical indicator and machine learning-based trading strategies.

5.3.4.1 Conditions for Z-Score-Based Trading Strategies:

The trade entry and exit conditions for the various trading strategies and the spread $S(t)$[3] for each of the trading strategies listed in Table D.1.2 are given below, where ϕ_1^{Model} and ϕ_2^{Model} are the standard deviations for entering and exiting a trade,[4] respectively:

- Long threshold:

[3]Note that $t = i, \ldots, n$, where, n = 30 for a 30-day rolling window, n = 50 for a 50-day rolling window and n = 100 for a 100-day rolling window.

[4]These standard deviations can take the values 0.5, 1, 2, 2.7 and 3. We consider a combination of these values to create scenarios for trading.

- Entry: $\mu_{S(t)} - \phi_1^{Model}\sigma_{S(t)}$
- Exit: $\mu_{S(t)} - \phi_2^{Model}\sigma_{S(t)}$

- Short threshold:
  - Entry: $\mu_{S(t)} + \phi_1^{Model}\sigma_{S(t)}$
  - Exit: $\mu_{S(t)} + \phi_2^{Model}\sigma_{S(t)}$

where

- $\phi_1^{Model} = 3$ and $\phi_2^{Model} = 2$ for the A1.1, B1.1, C1.1, D1.1, E1.1, G1.1, H1.1 and I1.1 trading strategies (i.e. trading strategies with the suffix 1.1).
- $\phi_1^{Model} = 3$ and $\phi_2^{Model} = 1$ for the A1.2, B1.2, C1.2, D1.2, E1.2, G1.2, H1.2 and I1.2 trading strategies (i.e. trading strategies with the suffix 1.2).
- $\phi_1^{Model} = 3$ and $\phi_2^{Model} = 0.5$ for the A1.3, B1.3, C1.3, D1.3, E1.3, G1.3, H1.3 and I1.3 trading strategies (i.e. trading strategies with the suffix 1.3).
- $\phi_1^{Model} = 2.7$ and $\phi_2^{Model} = 2$ for the A1.4, B1.4, C1.4, D1.4, E1.4, G1.4, H1.4 and I1.4 trading strategies (i.e. trading strategies with the suffix 1.4).
- $\phi_1^{Model} = 2.7$ and $\phi_2^{Model} = 1$ for the A1.5, B1.5, C1.5, D1.5, E1.5, G1.5, H1.5 and I1.5 trading strategies (i.e. trading strategies with the suffix 1.5).
- $\phi_1^{Model} = 2.7$ and $\phi_2^{Model} = 0.5$ for the A1.6, B1.6, C1.6, D1.6, E1.6, G1.6, H1.6 and I1.6 trading strategies (i.e. trading strategies with the suffix 1.6).

5.3.4.2 Conditions for Technical Indicator-Based Trading Strategies

For the SMA trading strategies (refer to Section 5.2.6.1), namely A2.1, B2.1, C2.1, D2.1, E2.1, G2.1, H2.1 and I2.1, the trade entry and exit conditions are as follows:[5]

- Long threshold:
  - Entry: $SMA_{(10)}(S(t-1)) \leq SMA_{(20)}(S(t))$ and $SMA_{(10)}(S(t)) \geq SMA_{(20)}(S(t))$

[5]The long threshold refers to initiating a BUY condition, whereas the short threshold refers to initiating a SELL condition.

– Exit: $SMA_{(10)}(S(t-1)) \geq SMA_{(20)}(S(t))$ and $SMA_{(10)}(S(t)) \leq SMA_{(20)}(S(t))$

- Short threshold:
  – Entry: $SMA_{(10)}(S(t-1)) \geq SMA_{(20)}(S(t))$ and $SMA_{(10)}(S(t)) \leq SMA_{(20)}(S(t))$
  – Exit: $SMA_{(10)}(S(t-1)) \leq SMA_{(20)}(S(t))$ and $SMA_{(10)}(S(t)) \geq SMA_{(20)}(S(t))$

For the EMA trading strategies (refer to Section 5.2.6.2), namely A2.2, B2.2, C2.2, D2.2, E2.2, G2.2, H2.2 and I2.2 strategies, the trade entry and exit conditions are as follows:[5]

- Long threshold:
  – Entry: $EMA_{(10)}(S(t-1)) \leq EMA_{(20)}(S(t))$ and $EMA_{(10)}(S(t)) \geq EMA_{(20)}(S(t))$
  – Exit: $EMA_{(10)}(S(t-1)) \geq EMA_{(20)}(S(t))$ and $EMA_{(10)}(S(t)) \leq EMA_{(20)}(S(t))$
- Short threshold:
  – Entry: $EMA_{(10)}(S(t-1)) \geq EMA_{(20)}(S(t))$ and $EMA_{(10)}(S(t)) \leq EMA_{(20)}(S(t))$
  – Exit: $EMA_{(10)}(S(t-1)) \leq EMA_{(20)}(S(t))$ and $EMA_{(10)}(S(t)) \geq EMA_{(20)}(S(t))$

For the RSI trading strategies (refer to Section 5.2.6.3), namely A2.3, B2.3, C2.3, D2.3, E2.3, G2.3, H2.3 and I2.3 strategies, the trade entry and exit conditions are as follows:[5]

- Long threshold:
  – Entry: $RSI_{(14)}(S(t-1)) < Threshold_{30}$ and $RSI_{(14)}(S(t)) > Threshold_{(30)}$
  – Exit: $RSI_{(14)}(S(t-1)) > Threshold_{70}$ and $RSI_{(14)}(S(t)) < Threshold_{(70)}$
- Short threshold:
  – Entry: $RSI_{(14)}(S(t-1)) > Threshold_{70}$ and $RSI_{(14)}(S(t)) < Threshold_{(70)}$

- Exit: $RSI_{(14)}(S(t-1)) < Threshold_{30}$ and $RSI_{(14)}(S(t)) > Threshold_{(30)}$

For the $MACD$ trading strategies (refer to Section 5.2.6.4), namely A2.4, B2.4, C2.4, D2.4, E2.4, G2.4, H2.4 and I2.4 strategies, the trade entry and exit conditions are as follows:[5]

- Long threshold:
  - Entry: $(MAC_{(12,26)}(S(t-1)) < Signal_{(9)}(S(t)))$ and $(MAC_{(12,26)}(S(t-1)) > Signal_{(9)}(S(t)))$
  - Exit: $(MAC_{(12,26)}(S(t-1)) > Signal_{(9)}(S(t)))$ and $(MAC_{(12,26)}(S(t-1)) < Signal_{(9)}(S(t)))$
- Short threshold:
  - Entry: $(MAC_{(12,26)}(S(t-1)) > Signal_{(9)}(S(t)))$ and $(MAC_{(12,26)}(S(t-1)) < Signal_{(9)}(S(t)))$
  - Exit: $(MAC_{(12,26)}(S(t-1)) < Signal_{(9)}(S(t)))$ and $(MAC_{(12,26)}(S(t-1)) > Signal_{(9)}(S(t)))$

Finally, for the $BB_{(20)}$ trading strategies (refer to Section 5.2.6.5), namely A2.5, B2.5, C2.5, D2.5, E2.5, G2.5, H2.5 and I2.5 strategies, the trade entry and exit conditions are:[5]

- Long threshold:
  - Entry: $S(t-1) < Lower - band_{(20)}$ and $S(t) > Lower - band_{(20)}$
  - Exit: $S(t-1) < Middle - band_{(20)}$ and $S(t) >= Middle - band_{(20)}$
- Short threshold:
  - Entry: $S(t-1) > Upper - band_{(20)}$ and $S(t) < Upper - band_{(20)}$
  - Exit: $S(t-1) > Middle - band_{(20)}$ and $S(t) <= Middle - band_{(20)}$

5.3.4.3 Conditions for MLP- and DT-Based Trading Strategies

The MLP and DT strategies, namely A3/A4, B3/B4, C3/C4, F3/F4, G3/G4, H3/H4 and I3/I4, provide output as 0 (Hold), 1 (Buy Pair) or -1 (Sell Pair), and their trade entry and exit conditions are as follows:[5]

- Long threshold:
  - Entry: 1
  - Exit: -1

- Short threshold:
  - Entry: -1
  - Exit: 1

5.4 Model Calibration and Performance Criteria

5.4.1 Performance Criterion

The evaluation metrics used in this study to analyse the eight ETF pairs across the different rolling windows are as follows.

5.4.1.1 The Sharpe Ratio

Sharpe (1994) defined the ratio for a given strategy as

$$Share\ Ratio = \frac{\bar{r}_p - r_f}{\sigma_p}, \tag{5.30}$$

where r_p is the average portfolio return, r_f represents the risk-free rate and σ_p is the standard deviation of the portfolio returns.

5.4.1.2 Maximum Drawdown

The Maximum Drawdown (MDD) calculates the maximum loss from a peak to a trough in a given period to determine the downside risk. de Melo Mendes and Leal (2005) defined draw-down as

$$D_t = \log\left(\frac{V_l}{V_h}\right), \tag{5.31}$$

where $V_{l,t}$ is the local minimum value of the portfolio at time t, and $V_{m,t}$ is the local maximum value of the portfolio at time t. The MDD for a strategy over the entire out-of-sample period $t = 1, 2, \ldots$ is

$$\mathcal{MDD} = \min\left(D_{t=1}, \ldots, D_{t=N}\right). \tag{5.32}$$

5.4.1.3 Other Performance Metrics

To assess the performance of these trading strategies, we use other performance metrics, including the total number of trades, number of winning trades (i.e. trades with a PnL > 0), number of losing trades (i.e. trades with a PnL < 0), total trade capital ($\$10,000$ is the initial capital used for each trade), average profit per trade (i.e. the average profit of all the trades with a PnL > 0), average loss per trade (i.e. the average loss of all the trades with a PnL < 0), gross profit (i.e. the sum of the PnL of all trades having PnL > 0), gross loss (i.e. the sum of the PnL of all trades having PnL < 0), net profit (which is the difference between the gross profit and gross loss), average return, minimum PnL, maximum PnL, the ROI (i.e. the net profit divided by the total capital), hit ratio (i.e. the number of profitable trades divided by the number of unprofitable trades), expectancy ratio,[6] profit factor (i.e. gross profit divided by the gross loss) and the realised risk-reward ratio (i.e. the ratio of the average profit to the average loss).

5.4.2 Estimating Deep Learning MLP Network and DT Models

5.4.2.1 Network Parameters

This study uses a triple hidden layer MLP model (for models A4, B4, C4, D4, E4, F4, G4, H4 and I4, mentioned in Tables D.2.1 to D.2.24), where the number of neurons in each hidden layer is equivalent to the number of inputs to the respective triple hidden layer MLP model. We solve a multi-class classification problem, where the output node of all of these MLP networks has three neurons that predicts or classify the output as 1 (for buy), 0 (for hold) or -1 (for sell). Since there are two or more label classes in these models, the cross-entropy loss function is used as the loss function. The rectified linear unit (ReLU) function is used as the squashing function between the hidden layers. The layer biases and weights of the different networks are also estimated in these MLP models using the adaptive moment estimator (ADAM) (see Kingma and Ba (2005)).

5.4.2.2 Data Division

The dataset covers EOD ETF prices for the period from 01 January 2019 to 31 January 2022 and includes 776 trading days. The MLP methodology requires data for a training set, a validation

[6](average profit per trade × hit ratio) - (average loss per trade × (1 - hit ratio))

set and a test set. The training set is used to estimate the parameters, the validation set is used to evaluate under-fitting and over-fitting, and the test set is used for out-of-sample prediction. In this study, for the MLP and the DT models, we utilise an expanding window (in terms of the number of days) for the training and a fixed size (of one trading day) for the test set. Thus, the training set comprises trading days (1 to N) and the test set trading day ($N + 1$). This is repeated for trading days N = 1, 2, ..., 776. A pictorial representation of the data division is presented in Figure 5.1.

Figure 5.1: MLP and DT Data Division: The dataset spanning from 01 January 2019 to 31 January 2022 is divided into a training set and a test set. The training set is used to estimate the parameters, and the test set is used for out-of-sample prediction.

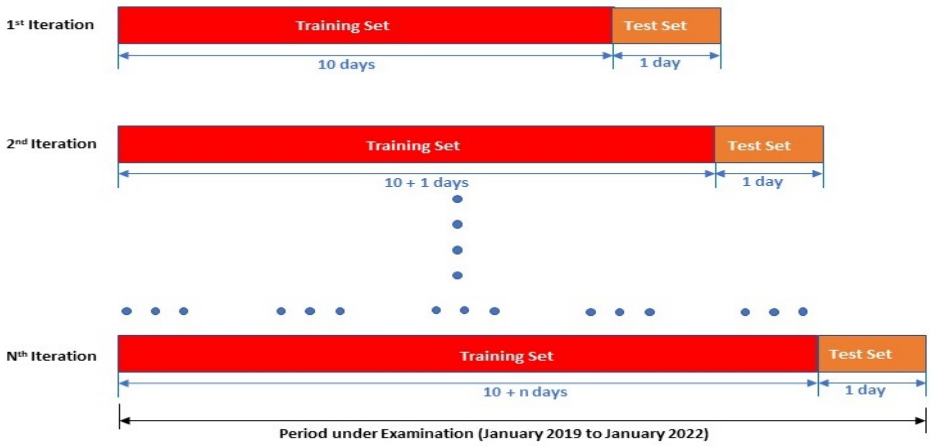

5.4.3 Approach

Each of the eight symbol pairs has been back-tested for three different rolling windows of 30, 50 and 100 days. For each pair and each window, there are 127 trading strategies created using 11 different models, and the bifurcation of these 127 trading strategies is detailed below. Each of these 127 trading strategies has a unique trading strategy code, and these codes are similar across the three different rolling windows.

- Distance Method (Version 1.1), denoted as $DIST^{V1.1} - SPRD$: There are 13 trading strategies that use the spread from $DIST^{V1.1} - SPRD$, and they are denoted by trading strategy codes from A1.1 to A4.
- Distance Method (Version 1.2), denoted as $DIST^{V1.2} - SPRD$: There are 13 trading strategies that use the spread from $DIST^{V1.2} - SPRD$, and they are denoted by trading strategy codes from B1.1 to B4.

- Distance Method (Version 2), denoted as $DIST^{V2}-SPRD$: There are 13 trading strategies that use the spread from $DIST^{V2} - SPRD$, and they are denoted by trading strategy codes from C1.1 to C4.
- Distance Method (Version 3), denoted as $DIST^{V3}-SPRD$: There are 13 trading strategies that use the spread from $DIST^{V1.3} - SPRD$, and they are denoted by trading strategy codes from D1.1 to D4.
- Distance Method (Version 4), denoted as $DIST^{V4}-SPRD$: There are 13 trading strategies that use the spread from $DIST^{V1.4} - SPRD$, and they are denoted by trading strategy codes from E1.1 to E4.
- Co-integration Method using the Johansen's Test approach, denoted as $JOHANSEN - SPRD$: There are 13 trading strategies that use the spread from $JOHANSEN - SPRD$, and they are denoted by trading strategy codes from F1.1 to F4.
- Co-integration Method - using the ADF approach, denoted as $JOHANSEN - SPRD$: There are 13 trading strategies that use the spread from $ADF - SPRD$, and they are denoted by trading strategy codes from G1.1 to G4.
- Kalman Method, denoted as $KALMAN - SPRD$: There are 13 trading strategies that use the spread from $KALMAN - SPRD$, and they are denoted by trading strategy codes from H1.1 to H4.
- Ratio Method, denoted as $RATIO - SPRD$: There are 13 trading strategies that use the spread from $RATIO - SPRD$, and they are denoted by trading strategy codes from I1.1 to I4.
- Using Close Prices of individual instruments:
  - Using close prices of Symbol 1[7] denoted as $CLS - SYM - 1$: There are five trading strategies that use the close price from the first instrument in a given pair, and they are denoted by trading strategy codes from CLS-SYM-1.1 to CLS-SYM-1.5.
  - Using close prices of Symbol 2[7] denoted as $CLS - SYM - 2$: There are five trading strategies that use the close price from the second instrument in a given pair, and they are denoted by trading strategy codes from CLS-SYM-2.1 to CLS-SYM-2.5.

[7]Each pair consists of two ETFs. The first instrument in the pair is called 'Symbol 1', and the second instrument is called 'Symbol 2'.

In this study, we compare two types of strategies, the traditional strategies (TRAD) and the modified strategies (MOD). TRAD strategies are categorised based on the distance method (versions 1.1,1.2,2,3 and 4), the co-integration methods (using the Johansen's Test and the ADF), and the Kalman Filter (refer to Sections 5.2.1, 5.2.2 and 5.2.3). Thus, the trading strategy codes with suffixes 1.1 to 1.6 fall under the TRAD classification. Similarly, the categorisation of the MOD trading strategies is based on machine learning algorithms (refer to Section 5.2.5) and technical indicators (refer to Section 5.2.6), and the trading strategy codes with suffixes 2.1 to 4, fall under this classification.

5.5 Empirical Results

The back-test results of the comparisons of the eight pairs over the 127 trading strategies for the three rolling windows on the basis of the various performance criteria (discussed in Section 5.4.1) are presented in Appendix D.2.[8] To assess the 127 trading strategies for each pair, we summarise the results of the tables from Appendix D.2 according to their trading strategy codes. For example, the trading strategy code 1.1 averages the performance of all the trading strategy codes from $A1.1$ to $I1.1$, i.e. trading strategy codes with the suffixes 1.1. Similar exercises are performed for the other trading strategy codes, namely from 1.2 to 4.

5.5.1 Performance Based on ROI

Table 5.1 presents the relative forecasting performance based on average ROI. We compare nine different methods of obtaining the spread[9] and using the different sets of $TRAD$ (in Panel I) and MOD (in Panel II) trading strategies.

We find that the MOD strategies have consistently superior returns compared to the $TRAD$ strategies. Specifically, for the $DIST^{V1.1} - SPRD$ method, we find the MOD trading strategy

[8] The detailed results are presented as follows: for pair $ITOT.N/IXUS.N$ in Table D.2.1 to D.2.3, for pair $SCHB.N/SCHF.N$ in Table D.2.10 to D.2.12, for pair $SCHF.N/VO.N$ in Table D.2.13 to D.2.15, for pair $VO.N/VXUS.N$ in Table D.2.19 to Table D.2.21, for pair $IWF.N/XLE.N$ in Table D.2.4 to Table D.2.6, for pair $QQQ.N/XLE.N$ in Table D.2.7 to Table D.2.7, for pair $USMV.N/XLE.N$ in Table D.2.16 to Table D.2.18 and for pair $VWO.N/XLE.N$ in Table D.2.22 to Table D.2.24.

[9] These methods are $DIST^{V1.1} - SPRD$, $DIST^{V1.2} - SPRD$, $DIST^{V2} - SPRD$, $DIST^{V3} - SPRD$, $DIST^{V4} - SPRD$, $JOHANSEN - SPRD$, $ADF - SPRD$, $KALMAN - SPRD$, and $RATIO - SPRD$.

2.3 has an excess return of 7.8% compared to the best-performing $TRAD$ strategy.[10] For the $DIST^{V1.2} - SPRD$ ($DIST^{V2} - SPRD$) method, the MOD strategy 4 has an excess return of 15.4% (18%) compared to the the best performing $TRAD$ strategy 1.3.[11] For the $DIST^{V2} - SPRD$, $DIST^{V3} - SPRD$ and $DIST^{V4} - SPRD$ methods, the improvement of the MOD strategies compared to the $TRAD$ is 18%, 23.1% and 23.1%, respectively.[12]

For the cointegration methods $JOHANSEN - SPRD$ (and $ADF - SPRD$), the MOD trading strategy 2.5 (2.3) reaches excess returns of 829.1% (381.5%), respectively, compared to the best performing $TRAD$ strategy 1.6 (1.2). Finally, the $KALMAN - SPRD$ and $RATIO - SPRD$ methods show similar results, where for the MOD strategies, the $KALMAN - SPRD$ method's 2.2 strategy (an ROI of 38.2% in a 100-day rolling window), and $RATIO - SPRD$ method's 2.2 strategy (an ROI of 40.4% in a 30-day rolling window) surpassed their corresponding $TRAD$ trading strategies.

The next step is to compare the above nine methods by aggregating them on the basis of the three rolling windows (30, 50, and 100 days) in Panel I of Table 5.2 presenting the average of the methods aggregated over all the different rolling windows in Panel II of Table 5.2.

Based on these tables, we conclude that the MOD strategies clearly outperform the $TRAD$ strategies. Three MOD methods ($DIST^{V1.2} - SPRD$, $DIST^{V2} - SPRD$ and $DIST^{V3} - SPRD$) perform better in the 30-day rolling window, two methods ($DIST^{V4} - SPRD$, and $ADF - SPRD$) in the 50-day rolling window and four methods ($DIST^{V1.1} - SPRD$, $JOHANSEN - SPRD$, $KALMAN - SPRD$ and $RATIO - SPRD$) in the 100-day rolling window. The 100-day rolling window provides the highest overall returns for MOD strategies. This can also be observed in Panel II of 5.2.[13]

Furthermore, we aim to gauge the ROI performance of the MLP and DT trading strategies separately. Thus, we compare the 216 methods (nine methods to obtain the spreads across

[10] The MOD trading strategy 2.3 has ROI of 20% for a 100-day rolling window. The best-performing $TRAD$ strategy is strategy 1.3 with an ROI of 12.2% in a 50-day rolling window.

[11] The MOD strategy has an ROI of 26.2% in a 30-day rolling window, while the $TRAD$ has an ROI of 10.9% in a 100-day rolling window.

[12] For the $DIST^{V2} - SPRD$ method, the MOD trading strategy 4 is compared to the best performing $TRAD$ strategy 1.3, and for the $DIST^{V3} - SPRD$ and $DIST^{V4} - SPRD$ methods, MOD trading strategy 2.4 is compared to the best-performing $TRAD$ strategy, 1.4.

[13] In Panel I of 5.2, the $TRAD$ strategies have an average ROI of 5.7% in a 30-day rolling window, 5.4% in a 50-day rolling window and 12.8% in a 100-day rolling window. The corresponding MOD strategies have 9.1% in a 30-day rolling window, 44.1% in a 30-day rolling window and 34.5% in a 100-day rolling window.

three rolling windows for eight ETF pairs) by clubbing the $TRAD$ trading strategy codes with the suffixes 1.1 to 1.6, clubbing the MOD trading strategy codes with the suffixes 2.1 to 2.5 and comparing them to the MLP and DT trading strategy codes with the suffixes 3 to 4. These results are summarised in Table D.1.6.

We find that out of the 216 methods, 22 (10.2%) methods belonging to $TRAD$ strategies outperform the MOD strategies, while 193 (89.8%) methods for MOD strategies outperform the $TRAD$ strategies (see columns IV and V). To assess how the ML (MLP and DT) strategies compare to other strategies, see columns VI, VII and VIII. Out of the 216 methods, 19 (8.8%) methods belonging to $TRAD$ strategies outperform the methods used for MOD and ML strategies, while 151 (70%) methods belonging to MOD strategies (excluding the methods used for ML strategies) outperform the methods used for $TRAD$ and ML strategies, and 45 (20.8%) ML strategies outperform the methods used for MOD and $TRAD$ strategies. Thus, a considerable number of methods under the MOD- and ML-based strategies provide improved forecasting power compared to $TRAD$-based strategies.

5.5.2 Performance based on Average Number Winning and Losing Trades

Panel I in Table 5.3 compares the methods based on the average number of winning and losing trades, according to the three rolling windows. On the basis of the winning and losing trades derived from Panel I, the improvement percentages of the MOD-based strategies over the $TRAD$-based strategies are reported in Panel II. In Panel III, the average number of winning and losing trades are aggregated over all the different rolling windows.

We find that the average number of winning trades for the MOD-based strategies is 13.08% higher for the 30-day, 14.31% higher for the 50-day, and 23.61% higher for the 100-day rolling windows (compared to the $TRAD$-based strategies). Similarly, the average losing number of trades for the MOD-based strategies is higher by 20% for the 30-day, 16.36% for the 50-day and 30.72% for the 100-day rolling windows compared to the $TRAD$-based strategies. This high number of trades implies higher transaction costs, but considering the rise of discount brokers, this cost should be manageable. We also find that the overall number of winning and losing trades (across all rolling windows) for MOD-based strategies is considerably higher compared to that of $TRAD$-based strategies, as shown in Panel II of Table 5.3.

5.5.3 Performance Based on the Profit Factor, Realised Risk-Reward Ratio, Average Profit Per Trade and Max Drawdown

We compare the methods on the basis of the profit factor (i.e. the gross profit divided by the gross loss) in Table 5.5, the realised risk-reward ratio (i.e. the ratio of the average profit to the average loss) in Table 5.6, the average profit per trade in Table 5.4 and the Max drawdown in Table 5.7. Panel I presents the aggregated effect over the three rolling windows, and Panel II the aggregated effect over all the rolling windows.

We find contrasting results, where $TRAD$-based strategies may offer a better profit factor and realised risk-reward ratio. Within the $TRAD$-based strategies, the ones back-tested on the 30- and 100-day outperform the 50-day rolling window-based strategies. In Panel I of Table 5.5, for the 30 and 100-day rolling window-based $TRAD$ strategies, seven out of nine methods have a double-digit profit factor. Similarly, in Panel I of Table 5.6, eight out of nine methods have a double-digit realised risk-reward ratio, and for the 100-day rolling window, five methods have a double-digit ratio. This phenomenon is also visible in Panel II of Table 5.5. A double-digit ratio in these cases, however, does not indicate a higher return but rather a return that has been adjusted for risk. This is clearly reflected in Panel I of Table 5.4, where the $TRAD$-based trading strategies (on the 30- and 100-day rolling windows) have higher profit factor/realised risk-reward ratios but fail to yield profitable trading strategies when accounted for dollar value. In Panel I of Table 5.4, the MOD-based 30-day rolling window produces 76% higher average profit per trade compared to the $TRAD$-based 30-day rolling window. Similarly, the MOD-based 50- and 100-day rolling windows have 96% and 175% higher average profits per trade than $TRAD$-based rolling window counterparts, respectively. The same reasoning holds true for the average loss per trade in Panel II of Table 5.4, where the MOD-based 30- and 100-day rolling windows result in a higher loss per trade than their $TRAD$-based rolling window counterparts. This can also be prominently seen when it comes to comparing the average MDDs in Panel I and II of Table 5.7, where the average MDDs are considerably higher for MOD-based strategies across all rolling windows.

5.5.4 Performance of Individual Pairs

We performed further comparisons by reporting the performance of different methods aggregated at the window/pair level by bifurcating the MOD- and $TRAD$-based trading strategies that have positive returns in Table D.1.4, and listing the pair/window method-based comparisons, with aggregation performed across all rolling windows in Table D.1.5.

In Table D.1.4, the numbers of MOD- and $TRAD$-based trading strategies with positive returns are typically the same in columns III and IV, but the number of $TRAD$-based trading strategies having greater returns than the MOD-based trading strategies is virtually less than five or close to zero trading strategies for all the eight ETF pair across all the rolling windows. The number of MOD-based trading strategies having greater returns than the $TRAD$-based trading strategies are prominently highlighted in column VI of this table, and columns VII and VIII show that, even at a window-pair level, we see the MOD-based trading strategies outperforming the $TRAD$-based trading strategies (except in one instance where for the $IWF.N/XLE.N$ pair, where 100-days rolling based $TRAD$ trading strategies have outperformed the MOD trading strategies).

Now for the pair/window method-based comparisons performed in Table D.1.5, we can notice that, for the $ITOT.N/IXUS.N$ pair, out of the 93 $TRAD$ and 71 MOD strategies with positive returns, only 2.2% of the $TRAD$-based strategies have returns greater than MOD-based strategies, while 43.7% MOD-based strategies have positive returns greater than $TRAD$-based strategies. Similarly, for the $IWF.N/XLE.N$ pair, 67.7% of the MOD-based strategies have returns greater than than those of the $TRAD$-based strategies; for the $QQQ.N/XLE.N$ pair, 66.3% of the MOD-based strategies have returns greater than those of the $TRAD$-based strategies; for the $SCHB.N/SCHF.N$ pair, 27% of the MOD-based strategies have returns greater than those of the $TRAD$-based strategies; for the $SCHF.N/VO.N$ pair, 57.7% of the MOD-based strategies have returns greater than those of the $TRAD$-based strategies; for the $USMV.N/XLE.N$ pair, 63.6% of the MOD-based strategies, have returns greater than those of the $TRAD$-based strategies; for the $VO.N/VXUS.N$ pair, 58.3% of the MOD-based strategies have returns greater than those of the $TRAD$-based strategies and for the $VWO.N/XLE.N$ pair 68.8% of the MOD-based strategies have returns greater than those of the $TRAD$-based strategies.

Finally, for all 3,084 back-tested strategies (i.e. back-tests for the eight pairs), we calculate the Sharpe and subsequently the annualised Share ratio and present these results in Appendix D.1 (from Table D.2.1 to Table D.2.24). However, we summarise these results for the trading strategies that have a positive Sharpe ratio in two tables: first in Table 5.8, where we present the results for the various methods and their associated trading strategies categorised on the basis of $TRAD$- and MOD-based trading strategies, and second in Table D.1.7, where these methods and their associated trading strategies are presented on the basis of the eight pairs.

Some trading strategies, despite having excellent returns, have negative Sharpe ratios and higher drawdowns, which could indicate that these strategies are not consistent. However, the trades in these trading strategies with higher drawdowns would or could see their drawdowns reverse when the trade is closed, resulting in that trade having a profit. Thus, strategies that exhibit larger volatility could have negative Sharpe ratios. The annualised Sharpe ratios in this study are calculated based on a risk-free rate postulated as 1.5% (the average 3M treasury bill risk-free rate prevailing from January 2019 to January 2022 was 0.81%). The results summarised in both of the above-mentioned tables are computed before transaction costs. The results from Tables 5.8 and D.1.7 indicate that, for the 30-day rolling window, the highest annualised Sharpe ratio, 18.57 is achieved by the $TRAD$-based trading strategies belonging to the $KALMAN - SPRD$ method (for the QQQ.N/XLE.N pair, which has an ROI of 28.28%), whereas the MOD-based trading strategies can attain a ratio of only 9.37 (for the IWF.N/XLE.N pair, which has an ROI of 55.70%), which belongs to the $DIST^{V2} - SPRD$ method. However, for the 50-day rolling window, the MOD-based trading strategies belonging to the $ADF - SPRD$ method (for the VWO.N/XLE.N pair, which has an ROI of 121.28%) have the highest annualised Sharpe ratio, 30.48, while the $TRAD$-based trading strategies belonging to the $KALMAN - SPRD$ method (for the IWF.N/XLE.N pair, which has an ROI of 11.07%) attain the highest annualised Sharpe ratio, at 56.99.

Lastly, for the 100-day rolling window, the MOD-based trading strategies belonging to the $DIST^{V1.1} - SPRD$ method (for the ITOT.N/IXUS.N pair, which has an ROI of 12.95%) have the highest annualised Sharpe ratio, 16.19, and the highest annualised Sharpe ratio, 18.41 is attained by the $TRAD$-based trading strategies belonging, once again to the $DIST^{V1.1} - SPRD$ method (for the USMV.N/XLE.N pair, which has an ROI of 12.10%). Though across the three rolling windows, $TRAD$-based strategies have better Sharpe ratios than MOD-based strategies in some cases, they have lower returns than the MOD-based strategies. Additionally, in Table D.1.7, there are numerous strategies that do not have the highest Sharpe ratios but are still able to produce higher returns. To compare these results to past literature, Gatev et al. (2006) attained Sharpe ratios of 0.35 and 0.59 for the top 5 and top 20 US stock pairs, respectively, from 1962 until 2002. After accounting for transaction costs, Avellaneda and Lee (2010)'s PCA-based strategies for US securities had an average annual Sharpe ratio of 1.44 from 1997 to 2007, and from 2003–2007, it is 0.9. Their ETF strategies with volume information achieved a Sharpe ratio of 1.51 from 2003 to 2007, while Huck (2009) using an ELECTRE III and neural networks achieved a Sharpe ratio of 1.5. Dunis et al. (2009, 2015) did not report their performance metrics in terms of the Sharpe ratio. For the top five pairs of securities from the NYSE, Lin

(2018) calculated a Sharpe ratio of 0.078. Yang et al. (2017) achieved a Sharpe ratio of 0.94 with pairs based on Chinese commodity futures. Using annualised Sharpe ratios, Stübinger and Bredthauer (2017) reported that the best-performing pairs from the S&P 500 from 1998 to 2015 had an annualised Sharpe ratio of 8.14 (significant returns of 50.50% p.a.) after transaction costs. The results of our back-testing show that our trading strategies have significant returns with a better Sharpe ratio.

Table 5.1: This table is divided into two panels; where in Panel I, we present the forecasting performance comparison on the basis of the average ROIs among the trading strategies with suffixes 1.1 to 1.6, which are classified as '$TRAD$' trading strategies, for the rolling windows of 30, 50 and 100 days. In Panel II, we present the forecasting performance comparison on the basis of the average ROIs among the trading strategies with suffixes 2.1 to 4, which are classified as 'MOD' trading strategies, for the rolling windows of 30, 50 and 100 days.

Panel I

"TRAD" trading strategies (Average ROI)

	30 days						50 days						100 days					
Model Category	**1.1**	**1.2**	**1.3**	**1.4**	**1.5**	**1.6**	**1.1**	**1.2**	**1.3**	**1.4**	**1.5**	**1.6**	**1.1**	**1.2**	**1.3**	**1.4**	**1.5**	**1.6**
$DIST^{V1.1} - SPRD$	1.6%	2.8%	2.4%	3.1%	3.3%	6.6%	2.8%	4.6%	**12.2%**	11.0%	6.5%	10.6%	4.6%	9.7%	9.5%	5.0%	7.3%	9.8%
$DIST^{V1.2} - SPRD$	2.4%	1.7%	3.2%	1.8%	3.8%	5.8%	4.1%	8.3%	7.6%	7.0%	7.7%	2.3%			**10.9%**			6.9%
$DIST^{V2} - SPRD$	1.0%	1.8%	0.8%	3.1%	1.7%	2.2%	1.0%	3.6%	**3.8%**	2.0%	0.6%	1.6%	1.1%	1.4%	2.2%	0.7%	1.7%	2.3%
$DIST^{V3} - SPRD$	2.9%	1.5%	1.5%	**4.6%**	3.3%	3.4%	0.3%	1.1%	2.2%		0.4%	1.5%	3.1%	2.7%	2.9%	2.6%	3.4%	3.7%
$DIST^{V4} - SPRD$	2.9%	1.5%	1.5%	**4.6%**	3.3%	3.4%	0.3%	1.1%	2.2%		0.4%	1.5%	3.1%	2.7%	2.9%	2.6%	3.4%	3.7%
$JOHANSEN - SPRD$	4.9%	9.6%	8.9%	5.6%	14.7%	18.0%	11.7%	20.1%	17.9%	7.5%	16.3%	**24.7%**	5.1%	4.0%	6.9%	7.6%	5.7%	8.2%
$ADF - SPRD$	10.4%	10.9%	15.5%	33.0%	19.0%	17.5%	1.8%	17.9%	14.7%	0.5%	1.5%	2.1%	61.7%	**118.2%**	103.1%	73.3%	70.9%	35.2%
$KALMAN - SPRD$	11.1%	3.0%	8.6%	6.9%	3.9%	6.2%	5.8%	0.2%	1.8%	8.2%	0.2%	0.3%	5.0%	6.1%	8.6%	6.1%	5.7%	**17.4%**
$RATIO - SPRD$	1.2%	1.3%	1.4%	1.5%	2.4%	3.3%	1.9%	2.6%	3.1%	2.6%	4.6%	**5.6%**	1.0%	2.1%	3.2%	2.2%	3.7%	4.3%

Panel II

"MOD" trading strategies (Average ROI)

	30							**50**							**100**						
Model Category	2.1	2.2	2.3	2.4	2.5	3	4	2.1	2.2	2.3	2.4	2.5	3	4	2.1	2.2	2.3	2.4	2.5	3	4
$DIST^{V1.1} - SPRD$	7.8%	6.5%	14.1%	17.8%	10.0%	15.0%	10.9%	5.9%	9.6%	16.5%	18.1%	8.7%	14.5%	13.9%	0.5%	5.9%	**20.0%**	18.9%	11.9%	15.5%	17.2%
$DIST^{V1.2} - SPRD$	6.9%		19.7%	5.4%	9.3%	23.8%	**26.2%**	11.6%	14.4%	9.7%		7.2%	15.1%	11.3%	13.5%	15.7%	10.1%			14.5%	4.2%
$DIST^{V2} - SPRD$	15.5%	8.2%	1.3%	7.4%	7.3%	8.6%	16.6%	13.8%	7.1%	2.5%	7.8%	10.4%	2.7%	12.4%	12.3%	11.2%	1.8%	3.5%	9.9%	9.7%	**21.7%**
$DIST^{V3} - SPRD$	11.5%	12.2%		9.4%	2.9%	24.2%	14.8%	15.7%	2.0%	21.1%	**27.7%**	7.7%		5.3%	4.4%	13.3%	5.4%	2.7%	6.1%	8.1%	9.6%
$DIST^{V4} - SPRD$	11.1%	12.2%		9.4%	2.9%	13.4%	13.0%	13.0%	2.0%	21.1%	**27.7%**	7.7%	9.6%	7.1%	4.4%	13.3%	5.4%	2.7%	6.1%	14.9%	9.6%
$JOHANSEN - SPRD$	19.8%	62.9%	12.9%	141.4%	51.3%	3.5%	12.4%	113.6%	175.1%	256.1%	64.1%	95.0%	16.3%	24.0%	78.8%	150.3%	110.4%	37.0%	**853.9%**	16.7%	13.9%
$ADF - SPRD$	66.7%	44.4%	52.4%	7.8%	29.1%	9.2%	24.8%	210.5%	342.7%	**499.7%**	28.7%	50.9%	15.6%	8.0%	75.2%	36.6%	72.6%	20.9%	138.1%	12.4%	10.0%
$KALMAN - SPRD$	37.5%	16.0%	23.4%	6.6%	7.7%	12.8%	9.0%	18.3%	13.2%	25.9%		21.8%	6.7%	6.9%	19.1%	**38.2%**	7.5%	0.7%	29.4%	20.7%	11.4%
$RATIO - SPRD$	7.3%	**40.4%**	25.5%		4.7%	3.6%	19.0%	7.5%	38.4%	22.0%		4.6%	7.5%	7.0%	11.1%	36.4%	33.7%		3.6%	9.1%	12.5%

Table 5.2: In Panel I, we present the forecasting performance comparison on the basis of the average ROIs among the trading strategies classified as '*TRAD*' from Panel I and the trading strategies classified as '*MOD*' from Panel II of Table 5.1, for the rolling windows of 30, 50 and 100 days. In Panel II of this table, we present the overall forecasting performance comparison on the basis of the average ROI for the '*TRAD*' and '*MOD*' trading strategies presented in Panel I of this table.

	Panel I					
	TRAD(Average ROI)			**MOD(Average ROI)**		
Model Category	30	50	100	30	50	100
$DIST^{V1.1} - SPRD$	3.4%	7.5%	7.3%	12.9%	13.9%	**14.0%**
$DIST^{V1.2} - SPRD$	3.3%	5.8%	8.9%	**14.9%**	11.9%	11.3%
$DIST^{V2} - SPRD$	1.9%	2.3%	1.6%	**10.9%**	9.4%	10.7%
$DIST^{V3} - SPRD$	3.1%	1.4%	3.0%	**11.4%**	11.0%	7.2%
$DIST^{V4} - SPRD$	3.1%	1.4%	3.0%	10.0%	**11.0%**	8.2%
$JOHANSEN - SPRD$	9.5%	15.7%	6.1%	42.9%	129.8%	**165.2%**
$ADF - SPRD$	18.8%	7.6%	74.6%	33.9%	**180.1%**	52.9%
$KALMAN - SPRD$	6.6%	3.2%	7.9%	18.3%	15.0%	**22.6%**
$RATIO - SPRD$	1.8%	3.3%	2.8%	16.9%	14.9%	**17.8%**

	Panel II	
Model-Category	**TRAD (Average ROI)**	**MOD (Average ROI)**
$DIST^{V1.1} - SPRD$	6.1%	**13.6%**
$DIST^{V1.2} - SPRD$	4.4%	**12.5%**
$DIST^{V2} - SPRD$	2.0%	**10.4%**
$DIST^{V3} - SPRD$	2.7%	**9.6%**
$DIST^{V4} - SPRD$	2.7%	**9.7%**
$JOHANSEN - SPRD$	9.3%	**117.6%**
$ADF - SPRD$	42.4%	**93.5%**
$KALMAN - SPRD$	6.4%	**18.7%**
$RATIO - SPRD$	2.6%	**16.5%**

Table 5.3: This table is divided into two panels, where in Panel I, we present the comparison on the basis of the average number of trades amongst the trading strategies classified as '$TRAD$' (i.e. those trading strategies with suffixes 1.1 to 1.6), and the trading strategies which are classified as 'MOD' (i.e. those trading strategies with suffixes 2.1 to 4), for the rolling windows of 30, 50 and 100 days. In Panel II, we present the percentage increase in winning and losing trades when using MOD over TRAD-based strategies. These percentages are inferred from Panel I of this table. In Panel III, we present the overall comparison on the basis of the average number of trades for the '$TRAD$' and 'MOD' trading strategies presented in Panel I of this table.

	Panel I											
	TRAD						**MOD**					
	Avg. Number of Winning Trades			**Avg. Number of Loosing Trades**			**Avg. Number of Winning Trades**			**Avg. Number of Loosing Trades**		
Model-Category	**30**	**50**	**100**	**30**	**50**	**100**	**30**	**50**	**100**	**30**	**50**	**100**
$DIST^{V1.1}-SPRD$	2	2	1	2	2	1	51	49	45	56	53	49
$DIST^{V1.2}-SPRD$	5	4	1	5	4	3	45	42	34	47	41	35
$DIST^{V2}-SPRD$	2	2	1	2	2	1	48	44	40	59	54	51
$DIST^{V3}-SPRD$	6	4	3	2	4	2	43	42	38	54	52	48
$DIST^{V4}-SPRD$	6	4	3	2	4	2	42	41	38	54	52	48
$JOHANSEN-SPRD$	12	8	7	11	9	7	49	47	45	51	48	44
$ADF-SPRD$	3	3	2	4	4	2	46	44	44	46	45	48
$KALMAN-SPRD$	2	2	1	2	2	1	48	43	39	49	47	42
$RATIO-SPRD$	3	3	2	2	3	1	42	37	34	67	58	53

	Panel II					
	Percentage increase in winning and losing trades when using MOD over TRAD strategies					
	Avg. Number of Winning Trades			**Avg. Number of Loosing Trades**		
Model-Category	**30**	**50**	**100**	**30**	**50**	**100**
$DIST^{V1.1}-SPRD$	26.08	28.64	51.24	25.48	24.72	46.16
$DIST^{V1.2}-SPRD$	8.47	10.40	27.68	9.07	9.80	11.27
$DIST^{V2}-SPRD$	21.60	20.40	37.25	30.39	31.22	58.52
$DIST^{V3}-SPRD$	6.45	8.37	9.99	21.54	11.87	24.66
$DIST^{V4}-SPRD$	6.33	8.26	9.99	21.61	11.85	24.71
$JOHANSEN-SPRD$	3.08	5.14	5.80	3.64	4.04	5.69
$ADF-SPRD$	14.34	15.51	28.45	12.13	10.50	21.74
$KALMAN-SPRD$	19.13	20.83	25.76	28.62	21.33	35.26
$RATIO-SPRD$	12.31	11.31	16.43	27.52	21.98	48.53
Average %	**13.09**	**14.32**	**23.62**	**20.00**	**16.37**	**30.73**

	Panel III			
	TRAD		**MOD**	
Model Category	**Avg. Number Of Winning Trades**	**Avg. Number Of Loosing Trades**	**Avg. Number Of Winning Trades**	**Avg. Number Of Loosing Trades**
$DIST^{V1.1}-SPRD$	1	2	48	53
$DIST^{V1.2}-SPRD$	3	4	40	41
$DIST^{V2}-SPRD$	2	1	44	54
$DIST^{V3}-SPRD$	5	3	41	51
$DIST^{V4}-SPRD$	5	3	41	51
$JOHANSEN-SPRD$	9	9	47	47
$ADF-SPRD$	2	3	45	46
$KALMAN-SPRD$	2	2	43	46
$RATIO-SPRD$	3	2	37	59

Table 5.4: This table is divided into two panels, where in Panel I, we present the comparison on the basis of the average profit per trade amongst the trading strategies classified as '$TRAD$' (i.e. those trading strategies with suffixes 1.1 to 1.6), and the trading strategies which are classified as 'MOD' (i.e. those trading strategies with suffixes 2.1 to 4), for the rolling windows of 30, 50 and 100 days. In Panel II, we do a similar exercise by presenting a comparison based on the basis of the average loss per trade.

	Panel I					
	TRAD			**MOD**		
	Avg. Average Profit Per Trade ($)			**Avg. Average Profit Per Trade ($)**		
Model Category	**30**	**50**	**100**	**30**	**50**	**100**
$DIST^{V1.1} - SPRD$	156	180	**397**	264	244	**282**
$DIST^{V1.2} - SPRD$	181	**253**	134	185	220	**278**
$DIST^{V2} - SPRD$	**118**	109	87	245	249	**253**
$DIST^{V3} - SPRD$	136	146	**158**	220	214	**231**
$DIST^{V4} - SPRD$	136	146	**158**	222	214	**231**
$JOHANSEN - SPRD$	132	**157**	139	550	780	**1,670**
$ADF - SPRD$	704	986	**2,326**	512	**1,596**	1,024
$KALMAN - SPRD$	346	252	**375**	**568**	545	504
$RATIO - SPRD$	**173**	146	98	**224**	212	220

	Panel II					
	TRAD			**MOD**		
	Avg. Average Loss Per Trade ($)			**Avg. Average Loss Per Trade ($)**		
Model Category	**30**	**50**	**100**	**30**	**50**	**100**
$DIST^{V1.1} - SPRD$	**118**	109	87	244	248	**251**
$DIST^{V1.2} - SPRD$	154	316	**365**	212	240	**290**
$DIST^{V2} - SPRD$	156	180	**397**	264	244	**273**
$DIST^{V3} - SPRD$	215	201	**265**	217	203	**275**
$DIST^{V4} - SPRD$	215	201	**265**	217	203	**275**
$JOHANSEN - SPRD$	**406**	124	77	873	**1,576**	821
$ADF - SPRD$	646	**2,207**	1,211	1,841	3,700	**11,041**
$KALMAN - SPRD$	399	**408**	291	846	**854**	577
$RATIO - SPRD$	263	230	**553**	311	286	**325**

Table 5.5: This table is divided into two panels, where in Panel I, we present the comparison on the basis of the average profit factor amongst the trading strategies classified as '$TRAD$' (i.e. those trading strategies with suffixes 1.1 to 1.6), and the trading strategies which are classified as 'MOD' (i.e. those trading strategies with suffixes 2.1 to 4), for the rolling windows of 30, 50 and 100 days. In Panel II, we present the overall comparison on the basis of the average number of trades for the '$TRAD$' and 'MOD' trading strategies presented in Panel I of this table.

	Panel I					
	TRAD			**MOD**		
Model Category	**30**	**50**	**100**	**30**	**50**	**100**
$DIST^{V1.1} - SPRD$	32.4	12.9	**226.2**	1.6	2.3	24.7
$DIST^{V1.2} - SPRD$	**1.2**	1.0	0.3	1.0	1.1	1.0
$DIST^{V2} - SPRD$	37.1	**65.1**	60.8	1.4	1.3	1.4
$DIST^{V3} - SPRD$	**34.0**	1.1	21.7	11.1	1.1	1.1
$DIST^{V4} - SPRD$	**34.0**	1.1	21.7	11.1	1.1	1.1
$JOHANSEN - SPRD$	1.8	1.5	**4.1**	1.4	3.2	2.3
$ADF - SPRD$	140.2	10.6	20.9	4.5	**224.0**	54.5
$KALMAN - SPRD$	178.3	44.3	**327.4**	1.2	1.1	1.9
$RATIO - SPRD$	17.8	**68.9**	46.8	1.1	1.0	1.0

	Panel II	
Model Category	**TRAD**	**MOD**
$DIST^{V1.1} - SPRD$	**90.5**	9.5
$DIST^{V1.2} - SPRD$	0.8	**1.0**
$DIST^{V2} - SPRD$	**54.3**	1.4
$DIST^{V3} - SPRD$	**18.9**	4.4
$DIST^{V4} - SPRD$	**18.9**	4.4
$JOHANSEN - SPRD$	**2.5**	2.3
$ADF - SPRD$	57.2	**94.9**
$KALMAN - SPRD$	**180.1**	1.4
$RATIO - SPRD$	**44.5**	1.1

Table 5.6: This table is divided into two panels, where in Panel I, we present the comparison on the basis of the average realised risk-reward ratio amongst the trading strategies classified as '*TRAD*' (i.e. those trading strategies with suffixes 1.1 to 1.6), and the trading strategies which are classified as '*MOD*' (i.e. those trading strategies with suffixes 2.1 to 4), for the rolling windows of 30, 50 and 100 days. In Panel II, we present the overall comparison on the basis of the average number of trades for the '*TRAD*' and '*MOD*' trading strategies presented in Panel I of this table.

	Panel I					
	TRAD			**MOD**		
Model Category	**30**	**50**	**100**	**30**	**50**	**100**
$DIST^{V1.1} - SPRD$	38.9	13.4	**324.3**	1.2	1.4	8.9
$DIST^{V1.2} - SPRD$	**1.1**	1.0	0.6	1.0	1.0	1.0
$DIST^{V2} - SPRD$	28.1	38.1	**69.2**	1.4	1.3	1.5
$DIST^{V3} - SPRD$	6.2	0.8	7.3	**11.3**	1.3	1.3
$DIST^{V4} - SPRD$	6.2	0.8	7.3	**11.4**	1.3	1.3
$JOHANSEN - SPRD$	1.8	1.7	**3.3**	1.2	2.1	2.3
$ADF - SPRD$	43.0	4.4	19.8	4.6	**95.8**	54.5
$KALMAN - SPRD$	140.3	26.5	**258.8**	1.5	1.4	1.6
$RATIO - SPRD$	8.5	**25.8**	25.1	1.3	1.3	1.3

	Panel II	
Model Category	**TRAD**	**MOD**
$DIST^{V1.1} - SPRD$	**114.0**	3.9
$DIST^{V1.2} - SPRD$	0.9	**1.0**
$DIST^{V2} - SPRD$	**44.4**	1.4
$DIST^{V3} - SPRD$	**4.8**	4.7
$DIST^{V4} - SPRD$	**4.8**	4.7
$JOHANSEN - SPRD$	**2.3**	1.9
$ADF - SPRD$	22.5	**52.8**
$KALMAN - SPRD$	**141.8**	1.5
$RATIO - SPRD$	**19.2**	1.3

Table 5.7: This table is divided into two panels, where in Panel I, we present the comparison on the basis of the average max drawdown amongst the trading strategies classified as '$TRAD$' (i.e. those trading strategies with suffixes 1.1 to 1.6), and the trading strategies which are classified as 'MOD' (i.e. those trading strategies with suffixes 2.1 to 4), for the rolling windows of 30, 50 and 100 days. In Panel II, we present the overall comparison on the basis of the average number of trades for the '$TRAD$' and 'MOD' trading strategies presented in Panel I of this table. The number presented below are dollar values.

	Panel I					
	TRAD			**MOD**		
Model Category	**30**	**50**	**100**	**30**	**50**	**100**
$DIST^{V1.1} - SPRD$	-239	-256	-111	**-1,362**	-1,342	-1,255
$DIST^{V1.2} - SPRD$	-434	-646	-772	**-1,779**	-1,283	-1,249
$DIST^{V2} - SPRD$	-316	-411	-473	-1,606	**-1,640**	-1,391
$DIST^{V3} - SPRD$	-547	-718	-490	**-1,873**	-1,713	-1,316
$DIST^{V4} - SPRD$	-547	-718	-490	**-1,891**	-1,758	-1,325
$JOHANSEN - SPRD$	-3,333	-887	-320	-9,521	**-14,914**	-7,676
$ADF - SPRD$	-2,100	-7,424	-2,244	-14,356	**-30,213**	-20,146
$KALMAN - SPRD$	-656	-815	-487	**-2,850**	-2,781	-2,290
$RATIO - SPRD$	-614	-758	-659	**-1,600**	-1,486	-1,333

	Panel II	
Model Category	**TRAD**	**MOD**
$DIST^{V1.1} - SPRD$	-202	**-1,320**
$DIST^{V1.2} - SPRD$	-617	**-1,437**
$DIST^{V2} - SPRD$	-400	**-1,546**
$DIST^{V3} - SPRD$	-585	**-1,634**
$DIST^{V4} - SPRD$	-585	**-1,658**
$JOHANSEN - SPRD$	-1,513	**-10,704**
$ADF - SPRD$	-3,923	**-21,572**
$KALMAN - SPRD$	-653	**-2,640**
$RATIO - SPRD$	-677	**-1,473**

Table 5.8: This table presents the summary of the Sharpe Ratios, which are categorised on the basis of Window- and Method-wise)

		MOD	**TRAD**
Window	**Model Category**	**Max. Annualized Sharpe Ratio**	
30	$DIST^{V1.1} - SPRD$	7.14	2.06
	$DIST^{V2} - SPRD$	**9.37**	
	$DIST^{V3} - SPRD$	4.76	
	$DIST^{V4} - SPRD$	4.76	
	$JOHANSEN - SPRD$	5.87	1.27
	$ADF - SPRD$	5.08	11.91
	$KALMAN - SPRD$	3.81	**18.57**
	$RATIO - SPRD$	4.76	
50	$DIST^{V1.1} - SPRD$	6.67	4.60
	$DIST^{V1.2} - SPRD$	3.97	1.43
	$DIST^{V2} - SPRD$	9.37	9.37
	$DIST^{V3} - SPRD$	6.19	
	$DIST^{V4} - SPRD$	6.19	
	$JOHANSEN - SPRD$	9.05	5.56
	$ADF - SPRD$	**30.48**	
	$KALMAN - SPRD$	3.33	**56.99**
100	$RATIO - SPRD$	4.44	5.87
	$DIST^{V1.1} - SPRD$	**16.19**	**18.41**
	$DIST^{V1.2} - SPRD$	2.38	1.59
	$DIST^{V2} - SPRD$	10.48	13.49
	$DIST^{V3} - SPRD$	0.32	
	$DIST^{V4} - SPRD$	0.32	
	$JOHANSEN - SPRD$	8.25	5.71
	$ADF - SPRD$	7.14	11.43
	$KALMAN - SPRD$	6.83	2.86
	$RATIO - SPRD$	3.49	

Table 5.9: This table presents the back-test metrics for the pair $QQQ.N/XLE.N$ for the 30 days rolling window.The table is subdivided into two parts, where in Part I, we present the back-test metrics for the trading strategies using the spread from the $DIST^{V1.1}$ model, and in Part II, the trading strategies use the $JOHANSEN - SPRD$ model.

(I) Trading Strategy Code	(II) Model Name	(III) Total Number of Trades	(IV) Number of Winning Trades	(V) Number of Loosing Trades	(VI) Average Profit per Trade ($)	(VII) Average Loss per Trade ($)	(VIII) Gross Profit ($)	(IX) Gross Loss ($)	(X) Net Profit ($)	(XI) ROI (%)	(XII) Max P&L ($)	(XIII) Min P&L ($)	(XIV) Daily Sharpe Ratio	(XV) Annualized Sharpe Ratio	(XVI) Hit Ratio	(XVII) Expectancy	(XVIII) Profit Factor	(XIX) Realized Risk Reward Ratio	(XX) Max Drawdown ($)
Part I: Models derived using the spread obtained from $DIST^{V1.1} - SPRD^{30D}$																			
A1.1	$DIST^{V1.1} - ZSPRD^{30D}_{(3,2)}$	-	-	-	-	-	-	-	-	-	-	-	-	-	-	-	-	-	-
A1.2	$DIST^{V1.1} - ZSPRD^{30D}_{(3,1)}$	-	-	-	-	-	-	-	-	-	-	-	-	-	-	-	-	-	-
A1.3	$DIST^{V1.1} - ZSPRD^{30D}_{(3,0.5)}$	-	-	-	-	-	-	-	-	-	-	-	-	-	-	-	-	-	-
A1.4	$DIST^{V1.1} - ZSPRD^{30D}_{(2.7,2)}$	4	1	3	262.05	171.53	262.05	514.6	**-252.55**	-2.53	262.05	-226.15	-0.98	-15.56	25	-63.14	0.51	1.53	-514.6
A1.5	$DIST^{V1.1} - ZSPRD^{30D}_{(2.7,1)}$	3	1	2	325.1	361.47	325.1	722.94	**-397.84**	-3.98	325.1	-623.79	-0.6	-9.52	33.33	-132.64	0.45	0.9	-722.94
A1.6	$DIST^{V1.1} - ZSPRD^{30D}_{(2.7,0.5)}$	3	1	2	318.02	354.12	318.02	708.24	**-390.21**	-3.9	318.02	-374.34	-0.73	-11.59	33.33	-130.09	0.45	0.9	-708.24
A2.1	$DIST^{V1.1} - SPRD^{30D} - SMA_{(10,20)}$	12	7	5	441.77	641.08	3092.42	3205.4	**-112.98**	-1.13	1112.86	-1432.79	-0.22	-3.49	58.33	-9.45	0.96	0.69	-2287.18
A2.2	$DIST^{V1.1} - SPRD^{30D} - EMA_{(10,20)}$	22	16	6	409.95	851.33	6559.27	5107.97	**1451.3**	14.51	2101.89	-2011.03	-0.1	-1.59	72.73	66	1.28	0.48	-2246.75
A2.3	$DIST^{V1.1} - SPRD^{30D} - MACD_{(12,26,9)}$	37	25	12	264.16	281.91	6603.91	3382.98	**3220.94**	32.21	1422.9	-887.69	-0.16	-2.54	67.57	87.07	1.95	0.94	-2533.12
A2.4	$DIST^{V1.1} - SPRD^{30D} - RSI_{(14)}$	5	3	2	1618.7	576.95	4856.11	1153.9	**3702.21**	37.02	4771.09	-1099.04	0.26	4.13	60	740.44	4.21	2.81	-1099.04
A2.5	$DIST^{V1.1} - SPRD^{30D} - BB_{(20)}$	9	6	3	304.87	574.76	1829.24	1724.28	**104.96**	1.05	968.03	-1324.15	-0.23	-3.65	66.67	11.69	1.06	0.53	-1558.57
A3	$DIST^{V1.1} - SPRD^{30D} - DECTREE$	350	166	184	106.66	79.59	17705.79	14645.45	**3060.34**	30.6	673.13	-420.52	-1.05	-16.67	47.43	8.75	1.21	1.34	-1310.27
A4	$DIST^{V1.1} - SPRD^{30D} - MLP$	313	145	168	124.37	87.49	18034.15	14698.76	**3335.39**	33.35	1044.96	-675.27	-0.88	-13.97	46.33	10.66	1.23	1.42	-1229.09
Part VI: Models derived using the spread obtained from $JOHANSEN - SPRD^{30D}$																			
F1.1	$JOHANSEN - ZSPRD^{30D}_{(3,2)}$	21	13	8	42.9	61.55	557.7	492.38	**65.32**	0.65	131.41	-247.04	-0.28	-4.44	61.9	3.11	1.13	0.7	-490.63
F1.2	$JOHANSEN - ZSPRD^{30D}_{(3,1)}$	20	15	5	97.9	123.76	1468.48	618.79	**849.69**	8.5	532.09	-310.42	-0.27	-4.29	75	42.48	2.37	0.79	-617.95
F1.3	$JOHANSEN - ZSPRD^{30D}_{(3,0.5)}$	18	14	4	112.18	154.49	1570.49	617.95	**952.53**	9.53	651.81	-310.42	-0.28	-4.44	77.78	52.92	2.54	0.73	-617.95
F1.4	$JOHANSEN - ZSPRD^{30D}_{(2.7,2)}$	26	15	11	48.16	183.84	722.4	2022.24	**-1299.84**	-13	131.41	-1396.83	-0.32	-5.08	57.69	-50	0.36	0.26	-1984.89
F1.5	$JOHANSEN - ZSPRD^{30D}_{(2.7,1)}$	23	16	7	109.63	1046.69	1754.1	7326.84	**-5572.73**	-55.73	532.09	-6507.09	-0.32	-5.08	69.57	-242.24	0.24	0.1	-7325.99
F1.6	$JOHANSEN - ZSPRD^{30D}_{(2.7,0.5)}$	19	14	5	132.17	1204.29	1850.4	6021.46	**-4171.06**	-41.71	651.81	-5052.73	-0.37	-5.87	73.68	-219.59	0.31	0.11	-6021.46
F2.1	$JOHANSEN - SPRD^{30D} - SMA_{(10,20)}$	24	13	11	767.88	465.92	9982.38	5125.15	**4857.23**	48.57	3360.29	-1056.81	-0.08	-1.27	54.17	202.43	1.95	1.65	-1452.51
F2.2	$JOHANSEN - SPRD^{30D} - EMA_{(10,20)}$	38	18	20	1195.49	401.04	21518.8	8020.86	**13497.94**	134.98	14284.7	-1008.03	0.19	3.02	47.37	355.23	2.68	2.98	-4489.25
F2.3	$JOHANSEN - SPRD^{30D} - MACD_{(12,26,9)}$	40	19	21	652.72	484	12401.66	10163.99	**2237.66**	22.38	6435.11	-2816.45	-0.06	-0.95	47.5	55.94	1.22	1.35	-3560.87
F2.4	$JOHANSEN - SPRD^{30D} - RSI_{(14)}$	7	5	2	901.94	380.31	4509.72	760.62	**3749.1**	37.49	2162.65	-704.89	0.3	4.76	71.43	535.6	5.93	2.37	-704.89
F2.5	$JOHANSEN - SPRD^{30D} - BB_{(20)}$	22	12	10	1059.39	1215.26	12712.67	12152.61	**560.06**	5.6	10190.62	-8935.66	-0.09	-1.43	54.55	25.56	1.05	0.87	-10373.95
F3	$JOHANSEN - SPRD^{30D} - DECTREE$	350	163	187	98.56	92.49	16065.71	17295.28	**-1229.57**	-12.3	547.34	-672.38	-1.11	-17.62	46.57	-3.52	0.93	1.07	-2932.04
F4	$JOHANSEN - SPRD^{30D} - MLP$	236	116	120	114.34	136.11	13263.76	16332.81	**-3069.05**	-30.69	929.85	-1383.47	-0.79	-12.54	49.15	-13.01	0.81	0.84	-3737

Table 5.10: This table presents the back-test metrics for the pair $VO.N/VXUS.N$ for the 30 days rolling window.The table is subdivided into two parts, where in Part I, we present the back-test metrics for the trading strategies using the spread from the $DIST^{V1.1}$ model, and in Part II, the trading strategies use the $JOHANSEN-SPRD$ model.

(I) Trading Strategy Code	(II) Model Name	(III) Total Number of Trades	(IV) Number of Winning Trades	(V) Number of Loosing Trades	(VI) Average Profit per Trade ($)	(VII) Average Loss per Trade ($)	(VIII) Gross Profit ($)	(IX) Gross Loss ($)	(X) Net Profit ($)	(XI) ROI (%)	(XII) Max P&L ($)	(XIII) Min P&L ($)	(XIV) Daily Sharpe Ratio	(XV) Annualized Sharpe Ratio	(XVI) Hit Ratio	(XVII) Expectancy	(XVIII) Profit Factor	(XIX) Realized Risk Reward Ratio	(XX) Max Drawdown ($)
Part I: Models derived using the spread obtained from $DIST^{V1.1}-SPRD^{30D}$																			
A1.1	$DIST^{V1.1}-ZSPRD^{30D}_{(3,2)}$	1	-	1	-	109.23	-	109.23	**-109.23**	-1.09	-	-109.23	-	-	-	-109.23	-	-	-109.23
A1.2	$DIST^{V1.1}-ZSPRD^{30D}_{(3,1)}$	1	1	-	117.28	-	117.28	-	**117.28**	1.17	117.28	-	-	-	100	117.28	117.28	117.28	-
A1.3	$DIST^{V1.1}-ZSPRD^{30D}_{(3,0.5)}$	1	1	-	110.89	-	110.89	-	**110.89**	1.11	110.89	-	-	-	100	110.89	110.89	110.89	-
A1.4	$DIST^{V1.1}-ZSPRD^{30D}_{(2.7,2)}$	4	-	4	-	60.45	-	241.8	**-241.8**	-2.42	-	-90.39	-8.92	-141.6	-	-60.45	-	-	-241.8
A1.5	$DIST^{V1.1}-ZSPRD^{30D}_{(2.7,1)}$	2	1	1	145.11	33.51	145.11	33.51	**111.6**	1.12	145.11	-33.51	-0.76	-12.06	50	55.8	4.33	4.33	-33.51
A1.6	$DIST^{V1.1}-ZSPRD^{30D}_{(2.7,0.5)}$	2	1	1	138.65	67.69	138.65	67.69	**70.96**	0.71	138.65	-67.69	-0.8	-12.7	50	35.48	2.05	2.05	-67.69
A2.1	$DIST^{V1.1}-SPRD^{30D}-SMA_{(10,20)}$	17	7	10	91.49	88.61	640.45	886.11	**-245.66**	-2.46	216.07	-168.73	-1.47	-23.34	41.18	-14.44	0.72	1.03	-466.55
A2.2	$DIST^{V1.1}-SPRD^{30D}-EMA_{(10,20)}$	20	11	9	56.99	92.23	626.86	830.1	**-203.24**	-2.03	159.89	-171.1	-1.75	-27.78	55	-10.16	0.76	0.62	-382.48
A2.3	$DIST^{V1.1}-SPRD^{30D}-MACD_{(12,26,9)}$	31	20	11	57.94	88.12	1158.85	969.31	**189.54**	1.9	108.8	-244.03	-1.74	-27.62	64.52	6.12	1.2	0.66	-649.89
A2.4	$DIST^{V1.1}-SPRD^{30D}-RSI_{(14)}$	3	2	1	713.67	236.17	1427.34	236.17	**1191.17**	11.91	736.97	-236.17	0.45	7.14	66.67	397.09	6.04	3.02	-236.17
A2.5	$DIST^{V1.1}-SPRD^{30D}-BB_{(20)}$	17	9	8	91.57	26.85	824.09	214.81	**609.28**	6.09	222.43	-78.92	-1.45	-23.02	52.94	35.84	3.84	3.41	-145.98
A3	$DIST^{V1.1}-SPRD^{30D}-DECTREE$	385	181	204	27.08	22.44	4900.71	4578.23	**322.48**	3.22	163.09	-133.03	-4.31	-68.42	47.01	0.84	1.07	1.21	-778.42
A4	$DIST^{V1.1}-SPRD^{30D}-MLP$	335	144	191	30.56	25.56	4400.02	4882.35	**-482.33**	-4.82	120.53	-183.49	-3.99	-63.34	42.99	-1.44	0.9	1.2	-1164.63
Part VI: Models derived using the spread obtained from $JOHANSEN-SPRD^{30D}$																			
F1.1	$JOHANSEN-ZSPRD^{30D}_{(3,2)}$	21	9	12	74	20.92	666.04	251.04	**415**	4.15	421.03	-119.75	-0.32	-5.08	42.86	19.76	2.65	3.54	-136.81
F1.2	$JOHANSEN-ZSPRD^{30D}_{(3,1)}$	21	9	12	81.91	24.75	737.2	296.97	**440.23**	4.4	421.03	-119.75	-0.32	-5.08	42.86	20.97	2.48	3.31	-182.59
F1.3	$JOHANSEN-ZSPRD^{30D}_{(3,0.5)}$	21	9	12	87.75	27.21	789.73	326.53	**463.2**	4.63	421.03	-119.75	-0.32	-5.08	42.86	22.06	2.42	3.22	-189.15
F1.4	$JOHANSEN-ZSPRD^{30D}_{(2.7,2)}$	25	11	14	93.56	28.96	1029.2	405.44	**623.76**	6.24	421.03	-130.04	-0.26	-4.13	44	24.95	2.54	3.23	-266.86
F1.5	$JOHANSEN-ZSPRD^{30D}_{(2.7,1)}$	24	11	13	220.16	29.93	2421.81	389.12	**2032.69**	20.33	1621.5	-130.04	0.04	0.63	45.83	84.69	6.22	7.36	-250.39
F1.6	$JOHANSEN-ZSPRD^{30D}_{(2.7,0.5)}$	23	11	12	270.36	32.31	2973.92	387.77	**2586.15**	25.86	2040.55	-130.04	0.08	1.27	47.83	112.45	7.67	8.37	-250.39
F2.1	$JOHANSEN-SPRD^{30D}-SMA_{(10,20)}$	26	15	11	226.66	142.5	3399.89	1567.46	**1832.43**	18.32	772.66	-436.6	-0.27	-4.29	57.69	70.47	2.17	1.59	-436.6
F2.2	$JOHANSEN-SPRD^{30D}-EMA_{(10,20)}$	29	16	13	295.76	227.58	4732.2	2958.55	**1773.65**	17.74	918.25	-800.52	0.18	2.86	55.17	61.15	1.6	1.3	-1365.5
F2.3	$JOHANSEN-SPRD^{30D}-MACD_{(12,26,9)}$	40	25	15	202.35	239.21	5058.68	3588.21	**1470.47**	14.7	2099.09	-652.27	-0.34	-5.4	62.5	36.76	1.41	0.85	-1130.56
F2.4	$JOHANSEN-SPRD^{30D}-RSI_{(14)}$	8	5	3	1319.72	662.16	6598.6	1986.49	**4612.11**	46.12	5338.3	-1622.95	0.26	4.13	62.5	576.51	3.32	1.99	-1622.95
F2.5	$JOHANSEN-SPRD^{30D}-BB_{(20)}$	21	13	8	240.79	538.51	3130.32	4308.11	**-1177.79**	-11.78	1223.09	-2065.71	-0.11	-1.75	61.9	-56.12	0.73	0.45	-3424.52
F3	$JOHANSEN-SPRD^{30D}-DECTREE$	338	160	178	25.5	27.79	4080.33	4946.92	**-866.58**	-8.67	174.23	-144.36	-4.15	-65.88	47.34	-2.56	0.82	0.92	-1154.62
F4	$JOHANSEN-SPRD^{30D}-MLP$	266	117	149	28.33	29.59	3314.44	4409.49	**-1095.05**	-10.95	145.74	-165.24	-3.7	-58.74	43.98	-4.12	0.75	0.96	-1659.48

5.6 Conclusion

This chapter presents a new modified approach for PT equity ETFs formulated by effectively applying commonly used technical indicators and machine learning algorithms (DT and deep learning MLP models) to spreads generated by traditional approaches. This study offers a thorough analysis of this new modified approach which back-tests eight ETF pairs across three rolling windows (30-, 50-, and 100-days) and also provides a detailed back-test of 127 trading strategies using spreads derived from nine approaches, some of which are modified, and some are traditional. Finally, we perform a comparative analysis of these trading strategies based on actual PnL, returns, Sharpe ratios, and other performance indicators.

There are several key takeaways. First, modified strategies provide significant improvement in returns over traditional strategies. Second, the average number of winning/losing trades and the average maximum drawdown of modified strategies are higher than those of traditional strategies, and modified strategies typically surpass traditional strategies when coming to profitability. Third, by bifurcating the methods of modified strategies and gauging the trading performance of methods based on machine learning-based trading strategies, we find that 21% of the machine learning-based strategies outperform the methods belonging to modified and traditional strategies.

These results provide empirical evidence that machine learning-based strategies can be useful in improving the performance of pair trading. Moreover, machine learning and modified strategies are designed to have dynamic stop-loss barriers rather than fixed stop-loss barriers, which are typical of traditional strategies, allowing traders to hold trades for a longer duration. Furthermore, these modified strategies can be applied regardless of whether the pairs are cointegrated or correlated, thereby generating unique ways to enhance portfolio returns. Finally, the approaches discussed in this study are easy to implement and provide practitioners with a variety of profitable opportunities to select from.

Chapter 6

Conclusion

Machine learning algorithms are widely used by practitioners and academicians as risk management tools to improve asset price predictions and hedging applications and to develop effective trading strategies for short- and long-term investing. This thesis analyses the effectiveness of associated financial applications using machine learning approaches.

6.1 Summary of Findings

This thesis starts with an extensive empirical assessment of the daily forecasting performance of S&P 500 call option prices/moneyness from September 9, 2012, through December 31, 2017. We experimented with parametric models and single, double, and triple hidden layered MLP and LSTM models trained on lagged and one-trading-day-ahead input variables. The numerical investigations reveal that ANNs tend to provide an improvement in the daily out-of-sample forecast performance of options prices and moneyness compared to parametric models. More specifically, LSTM models are the best-performing models when using lagged input variables, while MLP models perform best when one-trading-day-ahead input variables are employed. Within the parametric models, the Heston Jump Diffusion model had the lowest RMSEs than the other three parametric models (the Black–Scholes–Merton, Heston, and the Finite Moment Log Stable), and this holds for both types of inputs: lagged and one-trading-day-ahead input variables. In addition, forecasting prices directly offers improved performance compared to forecasting prices with re-scaled models for moneyness (using lagged inputs), with LSTM models outperforming other parametric and MLP models. The robustness tests further support these findings. Finally, it is evident that neither parametric nor non-parametric models (such as MLP and LSTM models) can improve on a simple random walk forecasting model. This suggests that there may be some intrinsic randomness that either parametric or non-parametric models cannot effectively forecast. Although the out-of-sample performance of parametric models is not necessarily dominant, at least for forecasting, they have an essential role in developing inputs for the deep learning ANN models (MLPs and LSTMs).

In the second study, the ability to forecast the daily S&P 500 call option delta and the corresponding replicating portfolio value using triple hidden layer deep learning ANN and parametric models (with lagged and one-trading-day-ahead input variables) is empirically evaluated. Both an analytical inference from option prices using one-trading-day-ahead input variables and a direct forecast of the delta using lagged and one-trading-day-ahead input variables are made, and the economic significance of these forecasts is further gauged by assessing the daily forecast performance of the value of the corresponding replicating portfolio. We find that the Black–Scholes–Merton model outperforms the parametric and ANN (MLP and LSTM) models, whether using lagged or one-trading-day-ahead input variables. We find similar results when evaluating these models' performance in forecasting the replicating portfolio. However, when the delta is estimated analytically from predicted option prices, then the LSTM models display the best performance relative to the other models. Within the parametric models, the Black–Scholes–Merton model demonstrates the best performance in forecasting the delta directly, and the Heston Jump Diffusion model exhibits the best performance in predicting the delta analytically. Thus, MLP and LSTM models typically do not enhance (statistically or economically) the forecasting performance of delta compared to parametric models.

The third study assesses the empirical daily forecasting performance of averaging methods. We compare the models by averaging the forecasts of prices, deltas and replicating portfolios from deep learning ANN and parametric models discussed in the first two studies. We also compare the performance of these models with the best-performing models from Chapters 2 and 3. The models used in this study are trained using lagged and one-trading-day-ahead input variables to forecast option prices/moneyness/delta, and one-trading-day-ahead input variables to forecast the prices from which the delta is then analytically derived. The economic significance of the delta forecasting models is assessed by comparing the forecasting performance of the value of the corresponding replicating portfolio. We find that the simple random walk model provides the best performance in forecasting daily option prices and moneyness (with lagged input variables), while the average of all triple hidden layer MLP models is typically the best performing model, even outperforming the random walk forecasting model (with one-trading-day-ahead input variables). When the random walk is excluded, the average of all the triple hidden layer MLP models outperforms any combination of the average of all the models considered in the study. Furthermore, while the average of all the triple hidden layer MLP models typically cannot outperform the individually best-performing LSTM model (identified in Chapter 2) for forecasting prices, it outperforms the individually best out-performing LSTM model when forecasting moneyness. These results hold for models that average the forecasts from models that use lagged and one-trade-day ahead inputs.

The averages of all parametric models and the average of all triple hidden layer MLP models generate superior forecasts for delta (directly and analytically). Although the average of all parametric models falls short compared to the best-performing models identified in Chapter 3 when forecasting the daily delta directly, it does perform better when forecasting the daily delta analytically. The averages of all triple hidden layer MLP models and the averages of all parametric models typically exhibit similar performance regarding the forecasting of their corresponding replicating portfolio values, even when they are compared to the best-performing models listed in Chapter 3 or when delta is computed analytically from option prices. Thus, ANN model averaging can be advantageous for forecasting, pricing, and hedging applications, but the ideal model depends on the application. Thus it is recommended not to automatically prefer ANN models, as, on occasion, random walk or simple parametric models such as Black-Scholes can provide better predictions in pricing and hedging.

The fourth study presents a new modified approach for PT equity ETFs, which is formulated by effectively applying commonly used technical indicators and machine learning algorithms (decision tree and deep learning MLP models) to the spreads generated by traditional approaches. We carry out an exhaustive comparison of this newly modified approach by back-testing eight ETF pairs over three rolling windows over 127 trading strategies. The actual PnL, returns, Sharpe ratios, and other performance indicators serve as the basis for our comparative analysis. We find that the forecasting performance across the 30-, 50-, and 100-day rolling windows of the MOD-based strategies have provided significant returns over $TRAD$-based strategies, as well as a higher average number of winning and losing trades and a higher average maximum drawdown compared to $TRAD$-based trading strategies. The performance of methods based on machine learning-based trading strategies obtained after bifurcating the performance of methods belonging to MOD-based trading strategies shows that 21% of the machine learning-based strategies outperform the methods belonging to both MOD- and $TRAD$-based trading strategies. Thus, machine learning-based strategies can improve the performance of MOD-based strategies of pair trading. The dynamic stop-loss barriers used by machine learning- and MOD-based strategies, as opposed to the fixed stop-loss barriers used by $TRAD$-based strategies, make it easier for traders to hold positions for extended periods of time. Additionally, MOD-based sets of strategies could be used for correlated and non-correlated pairs, leading to novel ways of increasing portfolio returns. Finally, unlike $TRAD$-based approaches, which limit one to a finite number of opportunities, the proposed MOD-based approaches are simple to use and offer practitioners a wide range of lucrative opportunities.

The four chapters in this thesis provide investors with practical suggestions for improving and managing their investment strategies. The empirical results presented in Chapter 2 could help financial institutions and retail options traders design and adjust their pricing models based on the improved understanding of parametric and non-parametric models covered in this study. Chapter 3 discusses improvised techniques of hedging call options and arriving at the replicating portfolio value for traders to hedge call options more effectively, Chapter 4 discusses methods a trader could deploy to enhance the forecast of a pricing/hedging model through the use of model averaging and Chapter 5 introduces a new approach to PT whereby a pair of ETFs can be traded irrespective of whether they are cointegrated or correlated, thereby enabling hedge funds and institutional investors and retail traders to deploy this strategy as a long/short equity investment tool.

6.2 Avenues for Future Research

The focus of Chapters 2 to 3 is performing a comprehensive assessment of the daily forecasts of option prices. In future research, this methodology could be extended over longer forecast windows by recursively forecasting one-trading-day-ahead options using a multi-step model in which the forecast for the prior time step is used as input for making a forecast on the following time step. Thereby, this multi-step forecasting approach would incur higher forecasting error rates compared to the one-trading-day forecast, and it would be a far more computationally expensive exercise. In addition, the use of a Transformer Neural Network (TNN) could be used to price and hedge options, which could solve sequence-to-sequence tasks, handle dependencies among longer time series than LSTM models, and outperform traditional deep learning ANN models by providing accurate forecasts (Ahmed et al. (2022), Jonsson and Deumic (2022), Li et al. (2022), Nino (2020), Wang et al. (2022), Wen et al. (2022), Woo et al. (2022), Zhang et al. (2022), Zeng et al. (2022), So et al. (2019)). Additionally, for the inputs used in these MLP and LSTM ANN models, a feature selection using a Least Absolute Shrinkage and Selection Operator (LASSO) regularisation which ascertains the importance of each input variable using a random forest model (i.e. computed using Gini importance or mean decrease accuracy) or a dimensionality reduction using Principal Component Analysis (PCA) could be carried out. An expansion of the averaging models discussed in Chapter 4 would involve running each ANN several times and averaging the outputs to obtain an average forecasted call price (see Gençay and Qi (2001)'s method). For example, as shown in Figure 2.4, Iteration 1 could be performed multiple times to arrive at an average call price. Finally, in terms of the PT strategies in Chapter 5, the spread could be further modelled by using a variety of other technical indicators and different machine learning classification algorithms to generate a buy/sell condition. The existing MLP and DT algorithms could be provided with additional features derived from the use of additional technical indicators or lagged variables. These algorithms could then be applied and examined on other market instruments that might provide higher returns or better Sharpe ratios.

Appendix A.1

Appendix for Chapter 2: Tables and Graphs

Table A.1.1: Model Definition for Call Price Comparison: This table presents the models with the N subscript that use lagged input variables for forecasting C_{N+1}. The forecast variable for all the models is the one-day-ahead call option price (C_{N+1}). Column I identifies the models, column II identifies the number of hidden layers used for the MLP and LSTM models, column III identifies the forecast variable, column IV identifies the target variable used while training the respective MLP and LSTM models, column V lists the input variables used by the models to obtain the one-trading-day ahead forecast of C_{N+1}. Forecasts are made for 1,326 trading days, and there are 64 months covered in the sample using the monthly data.

(I) Model	(II) No. of hidden layers	(III) Forecast variable	(IV) Target variable	(V) Inputs for training/forecasting
Black-Scholes-Merton Models				
$BSMC_N$	–	$C_{N+1}^{BSMC_N}$	C_N	$S_N, K_{N+1}, T_{N+1}, R_N, Q_N, \sigma_N^{CALIB^C}$
Finite Moment Log Stable Models				
$FMLS_N$	–	$C_{N+1}^{FMLS_N}$	C_N	$S_N, K_{N+1}, T_{N+1}, R_N, Q_N, FMLSParams_N^C$
$M1C_N$ Multi Layer Perceptron (MLP) Models				
$M1C1_N$	1	$C_{N+1}^{M1C1_N}$	C_N	$S_N, K_{N+1}, T_{N+1}, R_N, Q_N, \sigma_N^{CALIB^C}$
$M1C2_N$	1	$C_{N+1}^{M1C2_N}$	C_N	$S_N, K_{N+1}, T_{N+1}, R_N, Q_N, \sigma_N^{CALIB^C}, C_N$
$M1C3_N$	1	$C_{N+1}^{M1C3_N}$	C_N	$S_N, K_{N+1}, T_{N+1}, R_N, Q_N, \sigma_N^{CALIB^C}, C_N, BSMGreeks_N^C$
$M1C4_N$	1	$C_{N+1}^{M1C4_N}$	C_N	$S_N, K_{N+1}, T_{N+1}, R_N, Q_N, \sigma_N^{CALIB^C}, C_N, BSMGreeks_N^C, HParams_N^C$
$M1C5_N$	1	$C_{N+1}^{M1C5_N}$	C_N	$S_N, K_{N+1}, T_{N+1}, R_N, Q_N, \sigma_N^{CALIB^C}, C_N, BSMGreeks_N^C, HParams_N^C, C_N^{HC}$
$M1C6_N$	1	$C_{N+1}^{M1C6_N}$	C_N	$S_N, K_{N+1}, T_{N+1}, R_N, Q_N, HParams_N^C, C_N^{HC}$
$M1C7_N$	1	$C_{N+1}^{M1C7_N}$	C_N	$S_N, K_{N+1}, T_{N+1}, R_N, Q_N, \sigma_N^{CALIB^C}, BSMGreeks_N^C, C_N^{BSMC}$
$M1C8_N$	1	$C_{N+1}^{M1C8_N}$	C_N	$S_N, K_{N+1}, T_{N+1}, R_N, Q_N, HJDParams_N^C, C_N^{HJDC}$
$M1C9_N$	1	$C_{N+1}^{M1C9_N}$	C_N	$S_N, K_{N+1}, T_{N+1}, R_N, Q_N, FMLSParams_N^C, C_N^{FMLSC}$
$M2C_N$ Multi Layer Perceptron (MLP) Models				
$M2C1_N$	2	$C_{N+1}^{M2C1_N}$	C_N	$S_N, K_{N+1}, T_{N+1}, R_N, Q_N, \sigma_N^{CALIB^C}$
$M2C2_N$	2	$C_{N+1}^{M2C2_N}$	C_N	$S_N, K_{N+1}, T_{N+1}, R_N, Q_N, \sigma_N^{CALIB^C}, C_N$
$M2C3_N$	2	$C_{N+1}^{M2C3_N}$	C_N	$S_N, K_{N+1}, T_{N+1}, R_N, Q_N, \sigma_N^{CALIB^C}, C_N, BSMGreeks_N^C$
$M2C4_N$	2	$C_{N+1}^{M2C4_N}$	C_N	$S_N, K_{N+1}, T_{N+1}, R_N, Q_N, \sigma_N^{CALIB^C}, C_N, BSMGreeks_N^C, HParams_N^C$
$M2C5_N$	2	$C_{N+1}^{M2C5_N}$	C_N	$S_N, K_{N+1}, T_{N+1}, R_N, Q_N, \sigma_N^{CALIB^C}, C_N, BSMGreeks_N^C, HParams_N^C, C_N^{HC}$
$M2C6_N$	2	$C_{N+1}^{M2C6_N}$	C_N	$S_N, K_{N+1}, T_{N+1}, R_N, Q_N, HParams_N^C, C_N^{HC}$
$M2C7_N$	2	$C_{N+1}^{M2C7_N}$	C_N	$S_N, K_{N+1}, T_{N+1}, R_N, Q_N, \sigma_N^{CALIB^C}, BSMGreeks_N^C, C_N^{BSMC}$
$M2C8_N$	2	$C_{N+1}^{M2C8_N}$	C_N	$S_N, K_{N+1}, T_{N+1}, R_N, Q_N, HJDParams_N^C, C_N^{HJDC}$
$M2C9_N$	2	$C_{N+1}^{M2C9_N}$	C_N	$S_N, K_{N+1}, T_{N+1}, R_N, Q_N, FMLSParams_N^C, C_N^{FMLSC}$
$M3C_N$ Multi Layer Perceptron (MLP) Models				
$M3C1_N$	3	$C_{N+1}^{M3C1_N}$	C_N	$S_N, K_{N+1}, T_{N+1}, R_N, Q_N, \sigma_N^{CALIB^C}$
$M3C2_N$	3	$C_{N+1}^{M3C2_N}$	C_N	$S_N, K_{N+1}, T_{N+1}, R_N, Q_N, \sigma_N^{CALIB^C}, C_N$
$M3C3_N$	3	$C_{N+1}^{M3C3_N}$	C_N	$S_N, K_{N+1}, T_{N+1}, R_N, Q_N, \sigma_N^{CALIB^C}, C_N, BSMGreeks_N^C$
$M3C4_N$	3	$C_{N+1}^{M3C4_N}$	C_N	$S_N, K_{N+1}, T_{N+1}, R_N, Q_N, \sigma_N^{CALIB^C}, C_N, BSMGreeks_N^C, HParams_N^C$
$M3C5_N$	3	$C_{N+1}^{M3C5_N}$	C_N	$S_N, K_{N+1}, T_{N+1}, R_N, Q_N, \sigma_N^{CALIB^C}, C_N, BSMGreeks_N^C, HParams_N^C, C_N^{HC}$
$M3C6_N$	3	$C_{N+1}^{M3C6_N}$	C_N	$S_N, K_{N+1}, T_{N+1}, R_N, Q_N, HParams_N^C, C_N^{HC}$
$M3C7_N$	3	$C_{N+1}^{M3C7_N}$	C_N	$S_N, K_{N+1}, T_{N+1}, R_N, Q_N, \sigma_N^{CALIB^C}, BSMGreeks_N^C, C_N^{BSMC}$
$M3C8_N$	3	$C_{N+1}^{M3C8_N}$	C_N	$S_N, K_{N+1}, T_{N+1}, R_N, Q_N, HJDParams_N^C, C_N^{HJDC}$
$M3C9_N$	3	$C_{N+1}^{M3C9_N}$	C_N	$S_N, K_{N+1}, T_{N+1}, R_N, Q_N, FMLSParams_N^C, C_N^{FMLSC}$

(I) Model	(II) No. of hidden layers	(III) Forecast variable	(IV) Target variable	(V) Inputs for training/forecasting
Heston Models				
H_N	–	$C_{N+1}^{H_N}$	C_N	$S_N, K_{N+1}, T_{N+1}, R_N, Q_N, \sigma_N^{CALIB^C}, HParams_N^C$
Heston Jump Diffusion Models				
HJD_N	–	$C_{N+1}^{HJD_N}$	C_N	$S_N, K_{N+1}, T_{N+1}, R_N, Q_N, \sigma_N^{CALIB^C}, HJDParams_N^C$
$L1C_N$ Long Short Term Memory (LSTM) Models				
$L1C1_N$	1	$C_{N+1}^{L1C1_N}$	C_N	$S_N, K_{N+1}, T_{N+1}, R_N, Q_N, \sigma_N^{CALIB^C}$
$L1C2_N$	1	$C_{N+1}^{L1C2_N}$	C_N	$S_N, K_{N+1}, T_{N+1}, R_N, Q_N, \sigma_N^{CALIB^C}, C_N$
$L1C3_N$	1	$C_{N+1}^{L1C3_N}$	C_N	$S_N, K_{N+1}, T_{N+1}, R_N, Q_N, \sigma_N^{CALIB^C}, C_N, BSMGreeks_N^C$
$L1C4_N$	1	$C_{N+1}^{L1C4_N}$	C_N	$S_N, K_{N+1}, T_{N+1}, R_N, Q_N, \sigma_N^{CALIB^C}, C_N, BSMGreeks_N^C, HParams_N^C$
$L1C5_N$	1	$C_{N+1}^{L1C5_N}$	C_N	$S_N, K_{N+1}, T_{N+1}, R_N, Q_N, \sigma_N^{CALIB^C}, C_N, BSMGreeks_N^C, HParams_N^C, C_N^{HC}$
$L1C6_N$	1	$C_{N+1}^{L1C6_N}$	C_N	$S_N, K_{N+1}, T_{N+1}, R_N, Q_N, HParams_N^C, C_N^{HC}$
$L1C7_N$	1	$C_{N+1}^{L1C7_N}$	C_N	$S_N, K_{N+1}, T_{N+1}, R_N, Q_N, \sigma_N^{CALIB^C}, BSMGreeks_N^C, C_N^{BSMC}$
$L1C8_N$	1	$C_{N+1}^{L1C8_N}$	C_N	$S_N, K_{N+1}, T_{N+1}, R_N, Q_N, HJDParams_N^C, C_N^{HJDC}$
$L1C9_N$	1	$C_{N+1}^{L1C9_N}$	C_N	$S_N, K_{N+1}, T_{N+1}, R_N, Q_N, FMLSParams_N^C, C_N^{FMLSC}$
$L2C_N$ Long Short Term Memory (LSTM) Models				
$L2C1_N$	2	$C_{N+1}^{L2C1_N}$	C_N	$S_N, K_{N+1}, T_{N+1}, R_N, Q_N, \sigma_N^{CALIB^C}$
$L2C2_N$	2	$C_{N+1}^{L2C2_N}$	C_N	$S_N, K_{N+1}, T_{N+1}, R_N, Q_N, \sigma_N^{CALIB^C}, C_N$
$L2C3_N$	2	$C_{N+1}^{L2C3_N}$	C_N	$S_N, K_{N+1}, T_{N+1}, R_N, Q_N, \sigma_N^{CALIB^C}, C_N, BSMGreeks_N^C$
$L2C4_N$	2	$C_{N+1}^{L2C4_N}$	C_N	$S_N, K_{N+1}, T_{N+1}, R_N, Q_N, \sigma_N^{CALIB^C}, C_N, BSMGreeks_N^C, HParams_N^C$
$L2C5_N$	2	$C_{N+1}^{L2C5_N}$	C_N	$S_N, K_{N+1}, T_{N+1}, R_N, Q_N, \sigma_N^{CALIB^C}, C_N, BSMGreeks_N^C, HParams_N^C, C_N^{HC}$
$L2C6_N$	2	$C_{N+1}^{L2C6_N}$	C_N	$S_N, K_{N+1}, T_{N+1}, R_N, Q_N, HParams_N^C, C_N^{HC}$
$L2C7_N$	2	$C_{N+1}^{L2C7_N}$	C_N	$S_N, K_{N+1}, T_{N+1}, R_N, Q_N, \sigma_N^{CALIB^C}, BSMGreeks_N^C, C_N^{BSMC}$
$L2C8_N$	2	$C_{N+1}^{L2C8_N}$	C_N	$S_N, K_{N+1}, T_{N+1}, R_N, Q_N, HJDParams_N^C, C_N^{HJDC}$
$L2C9_N$	2	$C_{N+1}^{L2C9_N}$	C_N	$S_N, K_{N+1}, T_{N+1}, R_N, Q_N, FMLSParams_N^C, C_N^{FMLSC}$
$L3C_N$ Long Short Term Memory (LSTM) Models				
$L3C1_N$	3	$C_{N+1}^{L3C1_N}$	C_N	$S_N, K_{N+1}, T_{N+1}, R_N, Q_N, \sigma_N^{CALIB^C}$
$L3C2_N$	3	$C_{N+1}^{L3C2_N}$	C_N	$S_N, K_{N+1}, T_{N+1}, R_N, Q_N, \sigma_N^{CALIB^C}, C_N$
$L3C3_N$	3	$C_{N+1}^{L3C3_N}$	C_N	$S_N, K_{N+1}, T_{N+1}, R_N, Q_N, \sigma_N^{CALIB^C}, C_N, BSMGreeks_N^C$
$L3C4_N$	3	$C_{N+1}^{L3C4_N}$	C_N	$S_N, K_{N+1}, T_{N+1}, R_N, Q_N, \sigma_N^{CALIB^C}, C_N, BSMGreeks_N^C, HParams_N^C$
$L3C5_N$	3	$C_{N+1}^{L3C5_N}$	C_N	$S_N, K_{N+1}, T_{N+1}, R_N, Q_N, \sigma_N^{CALIB^C}, C_N, BSMGreeks_N^C, HParams_N^C, C_N^{HC}$
$L3C6_N$	3	$C_{N+1}^{L3C6_N}$	C_N	$S_N, K_{N+1}, T_{N+1}, R_N, Q_N, HParams_N^C, C_N^{HC}$
$L3C7_N$	3	$C_{N+1}^{L3C7_N}$	C_N	$S_N, K_{N+1}, T_{N+1}, R_N, Q_N, \sigma_N^{CALIB^C}, BSMGreeks_N^C, C_N^{BSMC}$
$L3C8_N$	3	$C_{N+1}^{L3C8_N}$	C_N	$S_N, K_{N+1}, T_{N+1}, R_N, Q_N, HJDParams_N^C, C_N^{HJDC}$
$L3C9_N$	3	$C_{N+1}^{L3C9_N}$	C_N	$S_N, K_{N+1}, T_{N+1}, R_N, Q_N, FMLSParams_N^C, C_N^{FMLSC}$

Table A.1.2: Model Definition for Call Price Comparison: This table presents the models with the $N+1$ subscript that use one-day-ahead input variables for forecasting C_{N+1}. The forecast variable for all the models is the one-day-ahead call option price (C_{N+1}). Column I identifies the models, column II identifies the number of hidden layers used for the MLP and LSTM models, column III identifies the forecast variable, column IV identifies the target variable used while training the respective MLP and LSTM models, column V lists the input variables used by the models to obtain the one-trading-day ahead forecast of C_{N+1}. Forecasts are made for 1,326 trading days, and there are 64 months covered in the sample using the monthly data.

(I) Model	(II) No. of hidden layers	(III) Forecast variable	(IV) Target variable	(V) Inputs for training/forecasting
Black-Scholes-Merton Models				
$BSMC_{N+1}$	–	$C_{N+1}^{BSMC_{N+1}}$	C_N	$S_{N+1}, K_{N+1}, T_{N+1}, R_{N+1}, Q_{N+1}, \sigma_N^{CALIB^C}$
Finite Moment Log Stable Models				
$FMLS_{N+1}$	–	$C_{N+1}^{FMLS_{N+1}}$	C_N	$S_{N+1}, K_{N+1}, T_{N+1}, R_{N+1}, Q_{N+1}, FMLSParams_N^C$
$M3C_{N+1}$ Multi Layer Perceptron (MLP) Models				
$M3C1_{N+1}$	3	$C_{N+1}^{M3C1_{N+1}}$	C_N	$S_{N+1}, K_{N+1}, T_{N+1}, R_{N+1}, Q_{N+1}, \sigma_N^{CALIB^C}$
$M3C2_{N+1}$	3	$C_{N+1}^{M3C2_{N+1}}$	C_N	$S_{N+1}, K_{N+1}, T_{N+1}, R_{N+1}, Q_{N+1}, \sigma_N^{CALIB^C}, C_N$
$M3C3_{N+1}$	3	$C_{N+1}^{M3C3_{N+1}}$	C_N	$S_{N+1}, K_{N+1}, T_{N+1}, R_{N+1}, Q_{N+1}, \sigma_N^{CALIB^C}, C_N, BSMGreeks_N^C$
$M3C4_{N+1}$	3	$C_{N+1}^{M3C4_{N+1}}$	C_N	$S_{N+1}, K_{N+1}, T_{N+1}, R_{N+1}, Q_{N+1}, \sigma_N^{CALIB^C}, C_N, BSMGreeks_N^C, HParams_N^C$
$M3C5_{N+1}$	3	$C_{N+1}^{M3C5_{N+1}}$	C_N	$S_{N+1}, K_{N+1}, T_{N+1}, R_{N+1}, Q_{N+1}, \sigma_N^{CALIB^C}, C_N, BSMGreeks_N^C, HParams_N^C, C_N^{HC}$
$M3C6_{N+1}$	3	$C_{N+1}^{M3C6_{N+1}}$	C_N	$S_{N+1}, K_{N+1}, T_{N+1}, R_{N+1}, Q_{N+1}, HParams_N^C, C_N^{HC}$
$M3C7_{N+1}$	3	$C_{N+1}^{M3C7_{N+1}}$	C_N	$S_{N+1}, K_{N+1}, T_{N+1}, R_{N+1}, Q_{N+1}, \sigma_N^{CALIB^C}, BSMGreeks_N^C, C_N^{BSMC}$
$M3C8_{N+1}$	3	$C_{N+1}^{M3C8_{N+1}}$	C_N	$S_{N+1}, K_{N+1}, T_{N+1}, R_{N+1}, Q_{N+1}, HJDParams_N^C, C_N^{HJDC}$
$M3C9_{N+1}$	3	$C_{N+1}^{M3C9_{N+1}}$	C_N	$S_{N+1}, K_{N+1}, T_{N+1}, R_{N+1}, Q_{N+1}, FMLSParams_N^C, C_N^{FMLSC}$
Heston Models				
H_{N+1}	–	$C_{N+1}^{H_{N+1}}$	C_N	$S_{N+1}, K_{N+1}, T_{N+1}, R_{N+1}, Q_{N+1}, \sigma_N^{CALIB^C}, HParams_N^C$
Heston Jump Diffusion Models				
HJD_{N+1}	–	$C_{N+1}^{HJD_{N+1}}$	C_N	$S_{N+1}, K_{N+1}, T_{N+1}, R_{N+1}, Q_{N+1}, \sigma_N^{CALIB^C}, HJDParams_N^C$
$L3C_{N+1}$ Long Short Term Memory (LSTM) Models				
$L3C1_{N+1}$	3	$C_{N+1}^{L3C1_{N+1}}$	C_N	$S_{N+1}, K_{N+1}, T_{N+1}, R_{N+1}, Q_{N+1}, \sigma_N^{CALIB^C}$
$L3C2_{N+1}$	3	$C_{N+1}^{L3C2_{N+1}}$	C_N	$S_{N+1}, K_{N+1}, T_{N+1}, R_{N+1}, Q_{N+1}, \sigma_N^{CALIB^C}, C_N$
$L3C3_{N+1}$	3	$C_{N+1}^{L3C3_{N+1}}$	C_N	$S_{N+1}, K_{N+1}, T_{N+1}, R_{N+1}, Q_{N+1}, \sigma_N^{CALIB^C}, C_N, BSMGreeks_N^C$
$L3C4_{N+1}$	3	$C_{N+1}^{L3C4_{N+1}}$	C_N	$S_{N+1}, K_{N+1}, T_{N+1}, R_{N+1}, Q_{N+1}, \sigma_N^{CALIB^C}, C_N, BSMGreeks_N^C, HParams_N^C$
$L3C5_{N+1}$	3	$C_{N+1}^{L3C5_{N+1}}$	C_N	$S_{N+1}, K_{N+1}, T_{N+1}, R_{N+1}, Q_{N+1}, \sigma_N^{CALIB^C}, C_N, BSMGreeks_N^C, HParams_N^C, C_N^{HC}$
$L3C6_{N+1}$	3	$C_{N+1}^{L3C6_{N+1}}$	C_N	$S_{N+1}, K_{N+1}, T_{N+1}, R_{N+1}, Q_{N+1}, HParams_N^C, C_N^{HC}$
$L3C7_{N+1}$	3	$C_{N+1}^{L3C7_{N+1}}$	C_N	$S_{N+1}, K_{N+1}, T_{N+1}, R_{N+1}, Q_{N+1}, \sigma_N^{CALIB^C}, BSMGreeks_N^C, C_N^{BSMC}$
$L3C8_{N+1}$	3	$C_{N+1}^{L3C8_{N+1}}$	C_N	$S_{N+1}, K_{N+1}, T_{N+1}, R_{N+1}, Q_{N+1}, HJDParams_N^C, C_N^{HJDC}$
$L3C9_{N+1}$	3	$C_{N+1}^{L3C9_{N+1}}$	C_N	$S_{N+1}, K_{N+1}, T_{N+1}, R_{N+1}, Q_{N+1}, FMLSParams_N^C, C_N^{FMLSC}$

Table A.1.3: Model Definition for Call Price Scaled by the Exercise Price Comparison: This table presents the models with the N subscript that use lagged input variables for forecasting the one-day-ahead call option price scaled by the exercise price (C_{N+1}/K_{N+1}). The forecast variable for all the models is the one-day-ahead C_{N+1}/K_{N+1}. Column I identifies the models, column II identifies the number of hidden layers used for the MLP and LSTM models, column III identifies the forecast variable, column IV identifies the target variable used while training the respective MLP and LSTM models, column V lists the input variables used by the models to obtain the one-trading-day ahead forecast of C_{N+1}/K_{N+1}. Forecasts are made for 1,326 trading days, and there are 64 months covered in the sample using the monthly data.

(I) Model	(II) No. of hidden layers	(III) Forecast variable	(IV) Target variable	(V) Inputs for training/forecasting
Black-Scholes-Merton Models				
$BSMCK_N$	–	$C_{N+1}^{BSMCK_N}/K_{N+1}$	C_N/K_N	$S_N, K_{N+1}, T_{N+1}, R_N, Q_N, \sigma_N^{CALIB^{CK}}$
Finite Moment Log Stable Models				
$FMLSCK_N$	–	$C_{N+1}^{FMLSCK_N}/K_{N+1}$	C_N/K_N	$S_N, K_{N+1}, T_{N+1}, R_N, Q_N, FMLSParams_N^{CK}$
$M1CK_N$ Multi Layer Perceptron (MLP) Models				
$M1CK1_N$	1	$C_{N+1}^{M1CK1_N}/K_{N+1}$	C_N/K_N	$S_N/K_N, T_{N+1}, R_N, Q_N, \sigma_N^{CALIB^{CK}}$
$M1CK2_N$	1	$C_{N+1}^{M1CK2_N}/K_{N+1}$	C_N/K_N	$S_N/K_N, T_{N+1}, R_N, Q_N, \sigma_N^{CALIB^{CK}}, (C_N/K_N)$
$M1CK3_N$	1	$C_{N+1}^{M1CK3_N}/K_{N+1}$	C_N/K_N	$S_N/K_N, T_{N+1}, R_N, Q_N, \sigma_N^{CALIB^{CK}}, (C_N/K_N), BSMGreeks_N^{CK}$
$M1CK4_N$	1	$C_{N+1}^{M1CK4_N}/K_{N+1}$	C_N/K_N	$S_N/K_N, T_{N+1}, R_N, Q_N, \sigma_N^{CALIB^{CK}}, (C_N/K_N), BSMGreeks_N^{CK}, HParams_N^{CK}$
$M1CK5_N$	1	$C_{N+1}^{M1CK5_N}/K_{N+1}$	C_N/K_N	$S_N/K_N, T_{N+1}, R_N, Q_N, \sigma_N^{CALIB^{CK}}, (C_N/K_N), BSMGreeks_N^{CK}, HParams_N^{CK}, (C_N^{HCK}/K_N)$
$M1CK6_N$	1	$C_{N+1}^{M1CK6_N}/K_{N+1}$	C_N/K_N	$S_N/K_N, T_{N+1}, R_N, Q_N, HParams_N^{CK}, (C_N^{HCK}/K_N)$
$M1CK7_N$	1	$C_{N+1}^{M1CK7_N}/K_{N+1}$	C_N/K_N	$S_N/K_N, T_{N+1}, R_N, Q_N, \sigma_N^{CALIB^{CK}}, BSMGreeks_N^{CK}, (C_N^{BSMCK}/K_N)$
$M1CK8_N$	1	$C_{N+1}^{M1CK8_N}/K_{N+1}$	C_N/K_N	$S_N/K_N, T_{N+1}, R_N, Q_N, HJDParams_N^{CK}, (C_N^{HJDCK}/K_N)$
$M1CK9_N$	1	$C_{N+1}^{M1CK9_N}/K_{N+1}$	C_N/K_N	$S_N/K_N, T_{N+1}, R_N, Q_N, FMLSParams_N^{CK}, (C_N^{FMLSCK}/K_N)$
$M2CK_N$ Multi Layer Perceptron (MLP) Models				
$M2CK1_N$	2	$C_{N+1}^{M2CK1_N}/K_{N+1}$	C_N/K_N	$S_N/K_N, T_{N+1}, R_N, Q_N, \sigma_N^{CALIB^{CK}}$
$M2CK2_N$	2	$C_{N+1}^{M2CK2_N}/K_{N+1}$	C_N/K_N	$S_N/K_N, T_{N+1}, R_N, Q_N, \sigma_N^{CALIB^{CK}}, (C_N/K_N)$
$M2CK3_N$	2	$C_{N+1}^{M2CK3_N}/K_{N+1}$	C_N/K_N	$S_N/K_N, T_{N+1}, R_N, Q_N, \sigma_N^{CALIB^{CK}}, (C_N/K_N), BSMGreeks_N^{CK}$
$M2CK4_N$	2	$C_{N+1}^{M2CK4_N}/K_{N+1}$	C_N/K_N	$S_N/K_N, T_{N+1}, R_N, Q_N, \sigma_N^{CALIB^{CK}}, (C_N/K_N), BSMGreeks_N^{CK}, HParams_N^{CK}$
$M2CK5_N$	2	$C_{N+1}^{M2CK5_N}/K_{N+1}$	C_N/K_N	$S_N/K_N, T_{N+1}, R_N, Q_N, \sigma_N^{CALIB^{CK}}, (C_N/K_N), BSMGreeks_N^{CK}, HParams_N^{CK}, (C_N^{HCK}/K_N)$
$M2CK6_N$	2	$C_{N+1}^{M2CK6_N}/K_{N+1}$	C_N/K_N	$S_N/K_N, T_{N+1}, R_N, Q_N, HParams_N^{CK}, (C_N^{HCK}/K_N)$
$M2CK7_N$	2	$C_{N+1}^{M2CK7_N}/K_{N+1}$	C_N/K_N	$S_N/K_N, T_{N+1}, R_N, Q_N, \sigma_N^{CALIB^{CK}}, BSMGreeks_N^{CK}, (C_N^{BSMCK}/K_N)$
$M2CK8_N$	2	$C_{N+1}^{M2CK8_N}/K_{N+1}$	C_N/K_N	$S_N/K_N, T_{N+1}, R_N, Q_N, HJDParams_N^{CK}, (C_N^{HJDCK}/K_N)$
$M2CK9_N$	2	$C_{N+1}^{M2CK9_N}/K_{N+1}$	C_N/K_N	$S_N/K_N, T_{N+1}, R_N, Q_N, FMLSParams_N^{CK}, (C_N^{FMLSCK}/K_N)$
$M3CK_N$ Multi Layer Perceptron (MLP) Models				
$M3CK1_N$	3	$C_{N+1}^{M3CK1_N}/K_{N+1}$	C_N/K_N	$S_N/K_N, T_{N+1}, R_N, Q_N, \sigma_N^{CALIB^{CK}}$
$M3CK2_N$	3	$C_{N+1}^{M3CK2_N}/K_{N+1}$	C_N/K_N	$S_N/K_N, T_{N+1}, R_N, Q_N, \sigma_N^{CALIB^{CK}}, (C_N/K_N)$
$M3CK3_N$	3	$C_{N+1}^{M3CK3_N}/K_{N+1}$	C_N/K_N	$S_N/K_N, T_{N+1}, R_N, Q_N, \sigma_N^{CALIB^{CK}}, (C_N/K_N), BSMGreeks_N^{CK}$
$M3CK4_N$	3	$C_{N+1}^{M3CK4_N}/K_{N+1}$	C_N/K_N	$S_N/K_N, T_{N+1}, R_N, Q_N, \sigma_N^{CALIB^{CK}}, (C_N/K_N), BSMGreeks_N^{CK}, HParams_N^{CK}$
$M3CK5_N$	3	$C_{N+1}^{M3CK5_N}/K_{N+1}$	C_N/K_N	$S_N/K_N, T_{N+1}, R_N, Q_N, \sigma_N^{CALIB^{CK}}, (C_N/K_N), BSMGreeks_N^{CK}, HParams_N^{CK}, (C_N^{HCK}/K_N)$
$M3CK6_N$	3	$C_{N+1}^{M3CK6_N}/K_{N+1}$	C_N/K_N	$S_N/K_N, T_{N+1}, R_N, Q_N, HParams_N^{CK}, (C_N^{HCK}/K_N)$
$M3CK7_N$	3	$C_{N+1}^{M3CK7_N}/K_{N+1}$	C_N/K_N	$S_N/K_N, T_{N+1}, R_N, Q_N, \sigma_N^{CALIB^{CK}}, BSMGreeks_N^{CK}, (C_N^{BSMCK}/K_N)$
$M3CK8_N$	3	$C_{N+1}^{M3CK8_N}/K_{N+1}$	C_N/K_N	$S_N/K_N, T_{N+1}, R_N, Q_N, HJDParams_N^{CK}, (C_N^{HJDCK}/K_N)$
$M3CK9_N$	3	$C_{N+1}^{M3CK9_N}/K_{N+1}$	C_N/K_N	$S_N/K_N, T_{N+1}, R_N, Q_N, FMLSParams_N^{CK}, (C_N^{FMLSCK}/K_N)$

(I) Model	(II) No. of hidden layers	(III) Forecast variable	(IV) Target variable	(V) Inputs for training/forecasting
Heston Models				
HCK_N	–	$C_{N+1}^{HCK_N}/K_{N+1}$	C_N/K_N	$S_N, K_{N+1}, T_{N+1}, R_N, Q_N, \sigma_N^{CALIB^{CK}}, HParams_N^{CK}$
Heston Jump Diffusion Models				
$HJDCK_N$	–	$C_{N+1}^{HJDCK_N}/K_{N+1}$	C_N/K_N	$S_N, K_{N+1}, T_{N+1}, R_N, Q_N, \sigma_N^{CALIB^{CK}}, HJDParams_N^{CK}$
$L1CK_N$ Long Short Term Memory (LSTM) Models				
$L1CK1_N$	1	$C_{N+1}^{L1CK1_N}/K_{N+1}$	C_N/K_N	$S_N/K_N, T_{N+1}, R_N, Q_N, \sigma_N^{CALIB^{CK}}$
$L1CK2_N$	1	$C_{N+1}^{L1CK2_N}/K_{N+1}$	C_N/K_N	$S_N/K_N, T_{N+1}, R_N, Q_N, \sigma_N^{CALIB^{CK}}, (C_N/K_N)$
$L1CK3_N$	1	$C_{N+1}^{L1CK3_N}/K_{N+1}$	C_N/K_N	$S_N/K_N, T_{N+1}, R_N, Q_N, \sigma_N^{CALIB^{CK}}, (C_N/K_N), BSMGreeks_N^{CK}$
$L1CK4_N$	1	$C_{N+1}^{L1CK4_N}/K_{N+1}$	C_N/K_N	$S_N/K_N, T_{N+1}, R_N, Q_N, \sigma_N^{CALIB^{CK}}, (C_N/K_N), BSMGreeks_N^{CK}, HParams_N^{CK}$
$L1CK5_N$	1	$C_{N+1}^{L1CK5_N}/K_{N+1}$	C_N/K_N	$S_N/K_N, T_{N+1}, R_N, Q_N, \sigma_N^{CALIB^{CK}}, (C_N/K_N), BSMGreeks_N^{CK}, HParams_N^{CK}, (C_N^{HCK}/K_N)$
$L1CK6_N$	1	$C_{N+1}^{L1CK6_N}/K_{N+1}$	C_N/K_N	$S_N/K_N, T_{N+1}, R_N, Q_N, HParams_N^{CK}, (C_N^{HCK}/K_N)$
$L1CK7_N$	1	$C_{N+1}^{L1CK7_N}/K_{N+1}$	C_N/K_N	$S_N/K_N, T_{N+1}, R_N, Q_N, \sigma_N^{CALIB^{CK}}, BSMGreeks_N^{CK}, (C_N^{BSMCK}/K_N)$
$L1CK8_N$	1	$C_{N+1}^{L1CK8_N}/K_{N+1}$	C_N/K_N	$S_N/K_N, T_{N+1}, R_N, Q_N, HJDParams_N^{CK}, (C_N^{HJDCK}/K_N)$
$L1CK9_N$	1	$C_{N+1}^{L1CK9_N}/K_{N+1}$	C_N/K_N	$S_N/K_N, T_{N+1}, R_N, Q_N, FMLSParams_N^{CK}, (C_N^{FMLSCK}/K_N)$
$L2CK_N$ Long Short Term Memory (LSTM) Models				
$L2CK1_N$	2	$C_{N+1}^{L2CK1_N}/K_{N+1}$	C_N/K_N	$S_N/K_N, T_{N+1}, R_N, Q_N, \sigma_N^{CALIB^{CK}}$
$L2CK2_N$	2	$C_{N+1}^{L2CK2_N}/K_{N+1}$	C_N/K_N	$S_N/K_N, T_{N+1}, R_N, Q_N, \sigma_N^{CALIB^{CK}}, (C_N/K_N)$
$L2CK3_N$	2	$C_{N+1}^{L2CK3_N}/K_{N+1}$	C_N/K_N	$S_N/K_N, T_{N+1}, R_N, Q_N, \sigma_N^{CALIB^{CK}}, (C_N/K_N), BSMGreeks_N^{CK}$
$L2CK4_N$	2	$C_{N+1}^{L2CK4_N}/K_{N+1}$	C_N/K_N	$S_N/K_N, T_{N+1}, R_N, Q_N, \sigma_N^{CALIB^{CK}}, (C_N/K_N), BSMGreeks_N^{CK}, HParams_N^{CK}$
$L2CK5_N$	2	$C_{N+1}^{L2CK5_N}/K_{N+1}$	C_N/K_N	$S_N/K_N, T_{N+1}, R_N, Q_N, \sigma_N^{CALIB^{CK}}, (C_N/K_N), BSMGreeks_N^{CK}, HParams_N^{CK}, (C_N^{HCK}/K_N)$
$L2CK6_N$	2	$C_{N+1}^{L2CK6_N}/K_{N+1}$	C_N/K_N	$S_N/K_N, T_{N+1}, R_N, Q_N, HParams_N^{CK}, (C_N^{HCK}/K_N)$
$L2CK7_N$	2	$C_{N+1}^{L2CK7_N}/K_{N+1}$	C_N/K_N	$S_N/K_N, T_{N+1}, R_N, Q_N, \sigma_N^{CALIB^{CK}}, BSMGreeks_N^{CK}, (C_N^{BSMCK}/K_N)$
$L2CK8_N$	2	$C_{N+1}^{L2CK8_N}/K_{N+1}$	C_N/K_N	$S_N/K_N, T_{N+1}, R_N, Q_N, HJDParams_N^{CK}, (C_N^{HJDCK}/K_N)$
$L2CK9_N$	2	$C_{N+1}^{L2CK9_N}/K_{N+1}$	C_N/K_N	$S_N/K_N, T_{N+1}, R_N, Q_N, FMLSParams_N^{CK}, (C_N^{FMLSCK}/K_N)$
$L3CK_N$ Long Short Term Memory (LSTM) Models				
$L3CK1_N$	3	$C_{N+1}^{L3CK1_N}/K_{N+1}$	C_N/K_N	$S_N/K_N, T_{N+1}, R_N, Q_N, \sigma_N^{CALIB^{CK}}$
$L3CK2_N$	3	$C_{N+1}^{L3CK2_N}/K_{N+1}$	C_N/K_N	$S_N/K_N, T_{N+1}, R_N, Q_N, \sigma_N^{CALIB^{CK}}, (C_N/K_N)$
$L3CK3_N$	3	$C_{N+1}^{L3CK3_N}/K_{N+1}$	C_N/K_N	$S_N/K_N, T_{N+1}, R_N, Q_N, \sigma_N^{CALIB^{CK}}, (C_N/K_N), BSMGreeks_N^{CK}$
$L3CK4_N$	3	$C_{N+1}^{L3CK4_N}/K_{N+1}$	C_N/K_N	$S_N/K_N, T_{N+1}, R_N, Q_N, \sigma_N^{CALIB^{CK}}, (C_N/K_N), BSMGreeks_N^{CK}, HParams_N^{CK}$
$L3CK5_N$	3	$C_{N+1}^{L3CK5_N}/K_{N+1}$	C_N/K_N	$S_N/K_N, T_{N+1}, R_N, Q_N, \sigma_N^{CALIB^{CK}}, (C_N/K_N), BSMGreeks_N^{CK}, HParams_N^{CK}, (C_N^{HCK}/K_N)$
$L3CK6_N$	3	$C_{N+1}^{L3CK6_N}/K_{N+1}$	C_N/K_N	$S_N/K_N, T_{N+1}, R_N, Q_N, HParams_N^{CK}, (C_N^{HCK}/K_N)$
$L3CK7_N$	3	$C_{N+1}^{L3CK7_N}/K_{N+1}$	C_N/K_N	$S_N/K_N, T_{N+1}, R_N, Q_N, \sigma_N^{CALIB^{CK}}, BSMGreeks_N^{CK}, (C_N^{BSMCK}/K_N)$
$L3CK8_N$	3	$C_{N+1}^{L3CK8_N}/K_{N+1}$	C_N/K_N	$S_N/K_N, T_{N+1}, R_N, Q_N, HJDParams_N^{CK}, (C_N^{HJDCK}/K_N)$
$L3CK9_N$	3	$C_{N+1}^{L3CK9_N}/K_{N+1}$	C_N/K_N	$S_N/K_N, T_{N+1}, R_N, Q_N, FMLSParams_N^{CK}, (C_N^{FMLSCK}/K_N)$

Table A.1.4: Model Definition for Call Price Scaled by the Exercise Price Comparison: This table presents the models with the $N+1$ subscript that use one-day-ahead input variables for forecasting the one-day-ahead call option price scaled by the exercise price (C_{N+1}/K_{N+1}). The forecast variable for all the models is the one-day-ahead C_{N+1}/K_{N+1}. Column I identifies the models, column II identifies the number of hidden layers used for the MLP and LSTM models, column III identifies the forecast variable, column IV identifies the target variable used while training the respective MLP and LSTM models, column V lists the input variables used by the models to obtain the one-trading-day ahead forecast of C_{N+1}/K_{N+1}. Forecasts are made for 1,326 trading days, and there are 64 months covered in the sample using the monthly data.

(I) Model	(II) No. of hidden layers	(III) Forecast variable	(IV) Target variable	(V) Inputs for training/forecasting	(I) Model	(II) No. of hidden layers	(III) Forecast variable	(IV) Target variable	(V) Inputs for training/forecasting
				Black-Scholes-Merton Models					**Heston Models**
$BSMCK_{N+1}$	–	$C_{N+1}^{BSMCK_{N+1}}/K_{N+1}$	C_N/K_N	$S_{N+1}, K_{N+1}, T_{N+1}, R_{N+1}, Q_{N+1}, \sigma_N^{CALIB^{CK}}$	HCK_{N+1}	–	$C_{N+1}^{HCK_{N+1}}/K_{N+1}$	C_N/K_N	$S_{N+1}, K_{N+1}, T_{N+1}, R_{N+1}, Q_{N+1}, \sigma_N^{CALIB^{CK}}, HParams_N^{CK}$
				Finite Moment Log Stable Models					**Heston Jump Diffusion Models**
$FMLSCK_{N+1}$	–	$C_{N+1}^{FMLSCK_{N+1}}/K_{N+1}$	C_N/K_N	$S_{N+1}, K_{N+1}, T_{N+1}, R_{N+1}, Q_{N+1}, FMLSParams_N^{CK}$	$HJDCK_{N+1}$	–	$C_{N+1}^{HJDCK_{N+1}}/K_{N+1}$	C_N/K_N	$S_{N+1}, K_{N+1}, T_{N+1}, R_{N+1}, Q_{N+1}, \sigma_N^{CALIB^{CK}}, HJDParams_N^{CK}$
				$M1CK_{N+1}$ Multi Layer Perceptron (MLP) Models					**$L1CK_{N+1}$ Long Short Term Memory (LSTM) Models**
$M3CK1_{N+1}$	3	$C_{N+1}^{M3CK1_{N+1}}/K_{N+1}$	C_N/K_N	$S_{N+1}/K_{N+1}, T_{N+1}, R_{N+1}, Q_{N+1}, \sigma_N^{CALIB^{CK}}$	$L3CK1_{N+1}$	3	$C_{N+1}^{L3CK1_{N+1}}/K_{N+1}$	C_N/K_N	$S_{N+1}/K_{N+1}, T_{N+1}, R_{N+1}, Q_{N+1}, \sigma_N^{CALIB^{CK}}$
$M3CK2_{N+1}$	3	$C_{N+1}^{M3CK2_{N+1}}/K_{N+1}$	C_N/K_N	$S_{N+1}/K_{N+1}, T_{N+1}, R_{N+1}, Q_{N+1}, \sigma_N^{CALIB^{CK}}, (C_N/K_N)$	$L3CK2_{N+1}$	3	$C_{N+1}^{L3CK2_{N+1}}/K_{N+1}$	C_N/K_N	$S_{N+1}/K_{N+1}, T_{N+1}, R_{N+1}, Q_{N+1}, \sigma_N^{CALIB^{CK}}, (C_N/K_N)$
$M3CK3_{N+1}$	3	$C_{N+1}^{M3CK3_{N+1}}/K_{N+1}$	C_N/K_N	$S_{N+1}/K_{N+1}, T_{N+1}, R_{N+1}, Q_{N+1}, \sigma_N^{CALIB^{CK}}, (C_N/K_N), BSMGreeks_N^{CK}$	$L3CK3_{N+1}$	3	$C_{N+1}^{L3CK3_{N+1}}/K_{N+1}$	C_N/K_N	$S_{N+1}/K_{N+1}, T_{N+1}, R_{N+1}, Q_{N+1}, \sigma_N^{CALIB^{CK}}, (C_N/K_N), BSMGreeks_N^{CK}$
$M3CK4_{N+1}$	3	$C_{N+1}^{M3CK4_{N+1}}/K_{N+1}$	C_N/K_N	$S_{N+1}/K_{N+1}, T_{N+1}, R_{N+1}, Q_{N+1}, \sigma_N^{CALIB^{CK}}, (C_N/K_N), BSMGreeks_N^{CK}, HParams_N^{CK}$	$L3CK4_{N+1}$	3	$C_{N+1}^{L3CK4_{N+1}}/K_{N+1}$	C_N/K_N	$S_{N+1}/K_{N+1}, T_{N+1}, R_{N+1}, Q_{N+1}, \sigma_N^{CALIB^{CK}}, (C_N/K_N), BSMGreeks_N^{CK}, HParams_N^{CK}$
$M3CK5_{N+1}$	3	$C_{N+1}^{M3CK5_{N+1}}/K_{N+1}$	C_N/K_N	$S_{N+1}/K_{N+1}, T_{N+1}, R_{N+1}, Q_{N+1}, \sigma_N^{CALIB^{CK}}, (C_N/K_N), BSMGreeks_N^{CK}, HParams_N^{CK}, (C_N^{HCK}/K_N)$	$L3CK5_{N+1}$	3	$C_{N+1}^{L3CK5_{N+1}}/K_{N+1}$	C_N/K_N	$S_{N+1}/K_{N+1}, T_{N+1}, R_{N+1}, Q_{N+1}, \sigma_N^{CALIB^{CK}}, (C_N/K_N), BSMGreeks_N^{CK}, HParams_N^{CK}, (C_N^{HCK}/K_N)$
$M3CK6_{N+1}$	3	$C_{N+1}^{M3CK6_{N+1}}/K_{N+1}$	C_N/K_N	$S_{N+1}/K_{N+1}, T_{N+1}, R_{N+1}, Q_{N+1}, HParams_N^{CK}, (C_N^{HCK}/K_N)$	$L3CK6_{N+1}$	3	$C_{N+1}^{L3CK6_{N+1}}/K_{N+1}$	C_N/K_N	$S_{N+1}/K_{N+1}, T_{N+1}, R_{N+1}, Q_{N+1}, HParams_N^{CK}, (C_N^{HCK}/K_N)$
$M3CK7_{N+1}$	3	$C_{N+1}^{M3CK7_{N+1}}/K_{N+1}$	C_N/K_N	$S_{N+1}/K_{N+1}, T_{N+1}, R_{N+1}, Q_{N+1}, \sigma_N^{CALIB^{CK}}, BSMGreeks_N^{CK}, (C_N^{BSMCK}/K_N)$	$L3CK7_{N+1}$	3	$C_{N+1}^{L3CK7_{N+1}}/K_{N+1}$	C_N/K_N	$S_{N+1}/K_{N+1}, T_{N+1}, R_{N+1}, Q_{N+1}, \sigma_N^{CALIB^{CK}}, BSMGreeks_N^{CK}, (C_N^{BSMCK}/K_N)$
$M3CK8_{N+1}$	3	$C_{N+1}^{M3CK8_{N+1}}/K_{N+1}$	C_N/K_N	$S_{N+1}/K_{N+1}, T_{N+1}, R_{N+1}, Q_{N+1}, HJDParams_N^{CK}, (C_N^{HJDCK}/K_N)$	$L3CK8_{N+1}$	3	$C_{N+1}^{L3CK8_{N+1}}/K_{N+1}$	C_N/K_N	$S_{N+1}/K_{N+1}, T_{N+1}, R_{N+1}, Q_{N+1}, HJDParams_N^{CK}, (C_N^{HJDCK}/K_N)$
$M3CK9_{N+1}$	3	$C_{N+1}^{M3CK9_{N+1}}/K_{N+1}$	C_N/K_N	$S_{N+1}/K_{N+1}, T_{N+1}, R_{N+1}, Q_{N+1}, FMLSParams_N^{CK}, (C_N^{FMLSCK}/K_N)$	$L3CK9_{N+1}$	3	$C_{N+1}^{L3CK9_{N+1}}/K_{N+1}$	C_N/K_N	$S_{N+1}/K_{N+1}, T_{N+1}, R_{N+1}, Q_{N+1}, FMLSParams_N^{CK}, (C_N^{FMLSCK}/K_N)$

Table A.1.5: Overall Call Price Comparison (amongst Parametric, MLP $M1C_N$-Models, LSTM $L1C_N$-Models, MLP $M2C_N$-Models, LSTM $L2C_N$-Models, MLP $M3C_N$-Models, and LSTM $L3C_N$-Models): This table presents the overall comparison of out-of-sample root mean square error ($RMSE$) amongst the Random Walk (δC_N) model, Black-Scholes-Merton ($BSMC_N$) model, Heston (HC_N) model, Heston Jump Diffusion ($HJDC_N$) model, Finite Moment Log Stable ($FMLSC_N$) model, MLP $M1C_N$-Models ($M1C1_N$ to $M1C9_N$), MLP $M2C_N$-Models ($M2C1_N$ to $M2C9_N$), MLP $M3C_N$-Models ($M3C1_N$ to $M3C9_N$), LSTM $L1C_N$-Models ($L1C1_N$ to $L1C9_N$), LSTM $L2C_N$-Models ($L2C1_N$ to $L2C9_N$), and the LSTM $L3C_N$-Models ($L3C1_N$ to $L3C9_N$) from column IV to column LXII. The forecast variable for all the models is the one-day-ahead call option price (C_{N+1}). The models denoted by the $_N$ subscript use lagged input variables for forecasting C_{N+1}. The one-day-ahead forecast errors of C_{N+1} are used to compute the Root Mean Square Error (RMSE). Forecasts are made for 1,326 trading days. The model having the lowest $RMSE$ has been highlighted in red.

(I) Size	(II) Mean of C_N	(III) Std.Dev. of C_N	(IV) δC_N	(V) $BSMC_N$	(VI) HC_N	(VII) $HJDC_N$	(VIII) $FMLSC_N$	(IX) $M1C1_N$	(X) $M1C2_N$	(XI) $M1C3_N$	(XII) $M1C4_N$	(XIII) $M1C5_N$	(XIV) $M1C6_N$	(XV) $M1C7_N$	(XVI) $M1C8_N$	(XVII) $M1C9_N$	(XVIII) $L1C1_N$	(XIX) $L1C2_N$	(XX) $L1C3_N$	(XXI) $L1C4_N$	(XXII) $L1C5_N$	(XXIII) $L1C6_N$	(XXIV) $L1C7_N$	(XXV) $L1C8_N$	(XXVI) $L1C9_N$	(XXVII) $M2C1_N$	(XXVIII) $M2C2_N$	(XXIX) $M2C3_N$	(XXX) $M2C4_N$	(XXXI) $M2C5_N$
556395	113.541	109.059	**8.809**	13.544	9.076	8.885	9.372	9.118	8.984	8.897	8.845	8.836	8.838	8.871	8.829	8.868	44.623	34.810	15.058	11.258	10.666	20.835	15.380	11.690	33.750	8.899	8.907	8.852	8.843	8.829

(I) Size	(XXXII) $M2C6_N$	(XXXIII) $M2C7_N$	(XXXIV) $M2C8_N$	(XXXV) $M2C9_N$	(XXXVI) $L2C1_N$	(XXXVII) $L2C2_N$	(XXXVIII) $L2C3_N$	(XXXIX) $L2C4_N$	(XL) $L2C5_N$	(XLI) $L2C6_N$	(XLII) $L2C7_N$	(XLIII) $L2C8_N$	(XLIV) $L2C9_N$	(XLV) $M3C1_N$	(XLVI) $M3C2_N$	(XLVII) $M3C3_N$	(XLVIII) $M3C4_N$	(XLIX) $M3C5_N$	(L) $M3C6_N$	(LI) $M3C7_N$	(LII) $M3C8_N$	(LIII) $M3C9_N$	(LIV) $L3C1_N$	(LV) $L3C2_N$	(LVI) $L3C3_N$	(LVII) $L3C4_N$	(LVIII) $L3C5_N$	(LIX) $L3C6_N$	(LX) $L3C7_N$	(LXI) $L3C8_N$	(LXII) $L3C9_N$
556395	8.832	8.835	8.835	8.853	49.144	36.552	16.235	11.567	9.310	16.773	13.186	11.929	29.700	8.889	8.891	8.854	8.856	8.834	8.841	8.839	8.833	8.849	49.803	36.097	13.891	11.335	10.309	15.765	11.879	11.078	26.518

Table A.1.6: Overall Call Price Comparison (amongst Parametric, $M3C_{N+1}$-Models and $L3C_{N+1}$-Models): This table presents the overall comparison of out-of-sample root mean square error ($RMSE$) amongst the Random Walk (δC_N) model, Black-Scholes-Merton ($BSMC_{N+1}$) model, Heston (HC_{N+1}) model, Heston Jump Diffusion ($HJDC_{N+1}$) model, Finite Moment Log Stable ($FMLSC_{N+1}$) model, MLP $M3C_{N+1}$-Models ($M3C1_{N+1}$ to $M3C9_{N+1}$), and the LSTM $L3C_{N+1}$-Models ($L3C1_{N+1}$ to $L3C9_{N+1}$) from column V to column XXVI. The forecast variable for all the models is the one-day-ahead call option price (C_{N+1}). The models denoted by the $_{N+1}$ subscript use one-day-ahead input variables for forecasting C_{N+1}. The one-day-ahead forecast errors of C_{N+1} are used to compute the Root Mean Square Error (RMSE). Forecasts are made for 1,326 trading days. The model having the lowest $RMSE$ has been highlighted in red.

(I) Size	(II) Mean of C_N	(III) Std.Dev. of C_N	(IV) δC_N	(V) $BSMC_{N+1}$	(VI) HC_{N+1}	(VII) $HJDC_{N+1}$	(VIII) $FMLSC_{N+1}$	(IX) $M3C1_{N+1}$	(X) $M3C2_{N+1}$	(XI) $M3C3_{N+1}$	(XII) $M3C4_{N+1}$	(XIII) $M3C5_{N+1}$	(XIV) $M3C6_{N+1}$	(XV) $M3C7_{N+1}$	(XVI) $M3C8_{N+1}$	(XVII) $M3C9_{N+1}$	(XVIII) $L3C1_{N+1}$	(XIX) $L3C2_{N+1}$	(XX) $L3C3_{N+1}$	(XXI) $L3C4_{N+1}$	(XXII) $L3C5_{N+1}$	(XXIII) $L3C6_{N+1}$	(XXIV) $L3C7_{N+1}$	(XXV) $L3C8_{N+1}$	(XXVI) $L3C9_{N+1}$
556395	113.5	109.1	8.8	10.1	2.8	2.3	3.7	2.5	**2.1**	2.4	3.7	4.8	4.4	7.9	7.0	3.1	46.8	36.3	12.9	10.3	10.1	17.8	12.9	11.1	27.9

Table A.1.7: Overall Call Price Scaled by the Exercise Price Comparison (amongst Parametric, MLP $M1CK_N$-Models, LSTM $L1CK_N$-Models, MLP $M2CK_N$-Models, LSTM $L2CK_N$-Models, MLP $M3CK_N$-Models, and LSTM $L3CK_N$-Models): This table presents the overall comparison of out-of-sample root mean square error ($RMSE$) amongst the Random Walk (δCK_N) model, Black-Scholes-Merton ($BSMCK_N$) model, Heston (HCK_N) model, Heston Jump Diffusion ($HJDCK_N$) model, Finite Moment Log Stable ($FMLSCK_N$) model, MLP $M1CK_N$-Models ($M1CK1_N$ to $M1CK9_N$), MLP $M2CK_N$-Models ($M2CK1_N$ to $M2CK9_N$), MLP $M3CK_N$-Models ($M3CK1_N$ to $M3CK9_N$), LSTM $L1CK_N$-Models ($L1CK1_N$ to $L1CK9_N$), LSTM $L2CK_N$-Models ($L2CK1_N$ to $L2CK9_N$), and the LSTM $L3CK_N$-Models ($L3CK1_N$ to $L3CK9_N$) from column V to column LXII. The forecast variable for all the models is the one-day-ahead call option price scaled by the exercise price (C_{N+1}/K_{N+1}). The models denoted by the $_N$ subscript use lagged input variables for forecasting C_{N+1}/K_{N+1}. The one-day-ahead forecast errors of C_{N+1}/K_{N+1} are used to compute the Root Mean Square Error (RMSE). Forecasts are made for 1,326 trading days. The model having the lowest $RMSE$ has been highlighted in red.

(I) Size	(II) Mean of C_N/K_N	(III) Std.Dev. of C_N/K_N	(IV) δCK_N	(V) $BSMCK_N$	(VI) HCK_N	(VII) $HJDCK_N$	(VIII) $FMLSCK_N$	(IX) $M1CK1_N$	(X) $M1CK2_N$	(XI) $M1CK3_N$	(XII) $M1CK4_N$	(XIII) $M1CK5_N$	(XIV) $M1CK6_N$	(XV) $M1CK7_N$	(XVI) $M1CK8_N$	(XVII) $M1CK9_N$	(XVIII) $L1CK1_N$	(XIX) $L1CK2_N$	(XX) $L1CK3_N$	(XXI) $L1CK4_N$	(XXII) $L1CK5_N$	(XXIII) $L1CK6_N$	(XXIV) $L1CK7_N$	(XXV) $L1CK8_N$	(XXVI) $L1CK9_N$	(XXVII) $M2CK1_N$	(XXVIII) $M2CK2_N$	(XXIX) $M2CK3_N$	(XXX) $M2CK4_N$	(XXXI) $M2CK5_N$
556395	6.167	6.052	**0.490**	2.087	3.051	1.571	1.593	0.509	0.502	0.511	0.501	0.501	0.507	0.514	0.530	0.558	3.890	2.397	0.977	0.935	0.872	1.582	0.896	5.739	2.152	0.545	0.519	0.508	0.503	0.501

(I) Size	(XXXII) $M2CK6_N$	(XXXIII) $M2CK7_N$	(XXXIV) $M2CK8_N$	(XXXV) $M2CK9_N$	(XXXVI) $L2CK1_N$	(XXXVII) $L2CK2_N$	(XXXVIII) $L2CK3_N$	(XXXIX) $L2CK4_N$	(XL) $L2CK5_N$	(XLI) $L2CK6_N$	(XLII) $L2CK7_N$	(XLIII) $L2CK8_N$	(XLIV) $L2CK9_N$	(XLV) $M3CK1_N$	(XLVI) $M3CK2_N$	(XLVII) $M3CK3_N$	(XLVIII) $M3CK4_N$	(XLIX) $M3CK5_N$	(L) $M3CK6_N$	(LI) $M3CK7_N$	(LII) $M3CK8_N$	(LIII) $M3CK9_N$	(LIV) $L3CK1_N$	(LV) $L3CK2_N$	(LVI) $L3CK3_N$	(LVII) $L3CK4_N$	(LVIII) $L3CK5_N$	(LIX) $L3CK6_N$	(LX) $L3CK7_N$	(LXI) $L3CK8_N$	(LXII) $L3CK9_N$
556395	0.500	0.507	0.509	0.530	3.557	2.591	0.974	0.903	0.835	1.531	0.942	5.690	2.076	0.525	0.510	0.496	0.495	0.494	0.495	0.503	0.501	0.522	3.528	2.517	1.068	0.944	0.829	1.523	0.980	5.644	2.139

Table A.1.8: Overall Call Price Scaled by the Exercise Price Comparison (amongst Parametric, MLP $M3CK_{N+1}$-Models and LSTM $L3CK_{N+1}$-Models): This table presents the overall comparison of out-of-sample root mean square error ($RMSE$) amongst the Random Walk (δCK_N) model, Black-Scholes-Merton ($BSMCK_{N+1}$) model, Heston (HCK_{N+1}) model, Heston Jump Diffusion ($HJDCK_{N+1}$) model, Finite Moment Log Stable ($FMLSCK_{N+1}$) model, MLP $M3CK_{N+1}$-Models ($M3CK1_{N+1}$ to $M3CK9_{N+1}$), and the LSTM $L3C_{N+1}$-Models ($L3CK1_{N+1}$ to $L3CK9_{N+1}$) from column V to column XXVI. The forecast variable for all the models is the one-day-ahead call option price scaled by the exercise price (C_{N+1}/K_{N+1}). The models denoted by the $_{N+1}$ subscript use one-day-ahead input variables for forecasting C_{N+1}/K_{N+1}. The one-day-ahead forecast errors of C_{N+1}/K_{N+1} are used to compute the Root Mean Square Error (RMSE). Forecasts are made for 1,326 trading days. The model having the lowest $RMSE$ has been highlighted in red.

(I) Size	(II) Mean of C_N/K_N	(III) Std.Dev. of C_N/K_N	(IV) δCK_N	(V) $BSMCK_{N+1}$	(VI) HCK_{N+1}	(VII) $HJDCK_{N+1}$	(VIII) $FMLSCK_{N+1}$	(IX) $M3CK1_{N+1}$	(X) $M3CK2_{N+1}$	(XI) $M3CK3_{N+1}$	(XII) $M3CK4_{N+1}$	(XIII) $M3CK5_{N+1}$	(XIV) $M3CK6_{N+1}$	(XV) $M3CK7_{N+1}$	(XVI) $M3CK8_{N+1}$	(XVII) $M3CK9_{N+1}$	(XVIII) $L3CK1_{N+1}$	(XIX) $L3CK2_{N+1}$	(XX) $L3CK3_{N+1}$	(XXI) $L3CK4_{N+1}$	(XXII) $L3CK5_{N+1}$	(XXIII) $L3CK6_{N+1}$	(XXIV) $L3CK7_{N+1}$	(XXV) $L3CK8_{N+1}$	(XXVI) $L3CK9_{N+1}$
556395	6.167	6.052	0.490	2.048	3.032	1.465	1.488	0.209	0.149	0.162	**0.148**	0.258	0.211	0.402	0.239	0.202	3.589	2.488	1.048	0.941	0.868	1.505	1.039	5.635	2.163

Table A.1.9: This table presents the insignificant pairs for $C - Models$ and $CK - Models$. The complete table consisting of the DM test statistic for $C - Models$, which use lagged input variables to forecast the C_{N+1} can be found in table 13, for $C - Models$ which use one-trading-day ahead input variables to forecast the C_{N+1} in table 14, for $CK - Models$ that use one-trading-day ahead input variables to forecast the C_{N+1}/K_{N+1} in table 15 and for $CK - Models$ that use one-trading-day ahead input variables to forecast the C_{N+1}/K_{N+1} in table 16 of the Electronic Appendix.

Model	Insignificant Pairs
For $C - Models$ which use lagged input variables to forecast the C_{N+1}	$(HJDC_N, M3C1_N)$, $(M1C3_N, M2C1_N)$, $(M1C4_N, M2C4_N)$, $(M1C5_N, M2C7_N)$, $(M1C5_N, M2C8_N)$, $(M1C5_N, M3C8_N)$, $(M1C6_N, M2C7_N)$, $(M1C6_N, M3C7_N)$, $(M1C7_N, M1C9_N)$, $(M1C8_N, M2C5_N)$, $(L1C4_N, L3C4_N)$, $(L1C8_N, L2C4_N)$, $(M2C3_N, M2C9_N)$, $(M2C3_N, M3C3_N)$, $(M2C3_N, M3C9_N)$, $(M2C6_N, M2C7_N)$, $(M2C6_N, M3C5_N)$, $(M2C6_N, M3C8_N)$, $(M2C7_N, M2C8_N)$, $(M2C7_N, M3C5_N)$, $(M2C7_N, M3C8_N)$, $(M2C8_N, M3C5_N)$, $(M2C9_N, M3C3_N)$, $(L2C8_N, L3C7_N)$, $(M3C1_N, M3C2_N)$, $(M3C3_N, M3C4_N)$, $(M3C5_N, M3C8_N)$, and $(M3C6_N, M3C7_N)$
$C - Models$ which use one-trading-day ahead input variables to forecast the C_{N+1}	$(BSMC_{N+1}, L3C5_{N+1})$, $(FMLSC_{N+1}, M3C4_{N+1})$, and $(L3C3_{N+1}, L3C7_{N+1})$
$CK - Models$ that use one-trading-day ahead input variables to forecast the C_{N+1}/K_{N+1}	$(BSMCK_N, L2CK9_N)$, $(M1CK1_N, M2CK8_N)$, $(M1CK4_N, M1CK5_N)$, $(M1CK4_N, M3CK8_N)$, $(M1CK5_N, M3CK8_N)$, $(M1CK6_N, M2CK7_N)$, $(M1CK8_N, M2CK9_N)$, $(L1CK3_N, L2CK3_N)$, $(L1CK3_N, L3CK7_N)$, $(L1CK9_N, L3CK9_N)$, $(M2CK5_N, M3CK8_N)$, $(L2CK3_N, L3CK7_N)$, $(L2CK6_N, L3CK6_N)$, $(L2CK7_N, L3CK4_N)$, and $(M3CK4_N, M3CK6_N)$
$CK - Models$ that use one-trading-day ahead input variables to forecast the C_{N+1}/K_{N+1}	$(M3CK2_{N+1}, M3CK4_{N+1})$, and $(L3CK3_{N+1}, L3CK7_{N+1})$

Table A.1.10: This table presents the summary of the pair-wise bootstrap tests performed for $C-Models$ and $CK-Models$. The complete table consisting of the results for the pair-wise bootstrap for $C-Models$, which use lagged input variables to forecast the C_{N+1} can be found in table 17, for $C-Models$ which use one-trading-day ahead input variables to forecast the C_{N+1} in table 18, for $CK-Models$ that use one-trading-day ahead input variables to forecast the C_{N+1}/K_{N+1} in table 19 and for $CK-Models$ that use one-trading-day ahead input variables to forecast the C_{N+1}/K_{N+1} in table 20 of the Electronic Appendix.

Model	Number of pairs a model wins	Winning %
$C-Models$ (using lagged inputs)		
$M3C_N-Models$	413	24.1%
$M2C_N-Models$	403	23.6%
$M1C_N-Models$	349	20.4%
$L2C_N-Models$	153	8.9%
$L3C_N-Models$	137	8.0%
$L1C_N-Models$	124	7.2%
Parametric	74	4.3%
δC_N	58	3.4%
$CK-Models$ (using lagged inputs)		
$M3CK_N-Models$	450	26.3%
$M2CK_N-Models$	393	23.0%
$M1CK_N-Models$	345	20.2%
$L3CK_N-Models$	154	9.0%
$L2CK_N-Models$	153	8.9%
$L1CK_N-Models$	129	7.5%
δCK_N	58	3.4%
Parametric	29	1.7%
$C-Models$ (using one-trading-day ahead inputs)		
$M3C_{N+1}-Models$	154	60.9%
Parametric	45	17.8%
$L3C_{N+1}-Models$	44	17.4%
δC_N	10	4.0%
$CK-Models$ (using one-trading-day ahead inputs)		
$M3CK_{N+1}-Models$	162	64.0%
$L3CK_{N+1}-Models$	64	25.3%
Parametric	14	5.5%
δCK_N	13	5.1%

A.1.1 Fields from OptionMetrics

The OptionMetric manual is available to WRDS account holders and OptionMetric clients. The direct link to the manual is https://wrds-www.wharton.upenn.edu/documents/755/IvyDB_US_Reference_Manual.pdf

1. **Option_Price File**

   The Options Price file from OptionMetrics contains the historical price, implied volatility, and sensitivity information for the options on an underlying security.

   Field descriptions

   (a) **Security ID** = The Security ID for the underlying security.

   (b) **Date** = The date of this price.

   (c) **Symbol** = The option symbol.

   (d) **Strike** = The strike price of the option times 1000.

   (e) **Expiration** = The expiration date of the option.

   (f) **Call/Put** = C or P, where C is Call, P is Put.

   (g) **Best Bid** = The best, or highest, 15:59 EST bid price across all exchanges on which the option trades.

   (h) **Best Offer** = The best, or lowest, 15:59 EST ask price across all exchanges on which the option trades.

   (i) **Special Settlement** = 0 or 1 or E.

      i. 0 - The option has a standard settlement (100 shares of underlying security are to be delivered at exercise; the strike price and premium multipliers are $ 100 per tick).

      ii. 1 - The option has a non-standard settlement. The number of shares to be delivered may be different from 100 (fractional shares); additional securities and/or cash may be required, and the strike price and premium multipliers may be different than $ 100 per tick.

      iii. E - The option has a non-standard expiration date. This is usually due to an error in the historical data, which has not yet been researched and fixed.

   (j) **Option ID** = Option ID is a unique integer identifier for the options contract. This identifier can be used to track specific options contracts over time.

2. **Zero_Curve File**

   The Zero Curve file contains the current zero-coupon interest rate curve used by OptionMetrics.

   Field descriptions

   (a) **Date** = The date of this zero curve

   (b) **Days** = The number of days to maturity

   (c) **Rate** = The continuously-compounded zero-coupon interest rate

3. **Index_Dividend file**

The Index Dividend file contains the current dividend yield used for implied volatility calculations on index options.

Field descriptions

(a) **Security ID** = The Security ID of the underlying index

(b) **Date** = The date of this dividend yield

(c) **Rate** = The annualized dividend yield

A.1.2 Optimization Methods

Trust-Region method for nonlinear optimization:

According to Yang et al. (2017), in the trust-region algorithm, the first step is to approximate the nonlinear objective function by using truncated Taylor expansions

$$\phi_k(\boldsymbol{x}) \approx f(\boldsymbol{x}_k) + \nabla f(\boldsymbol{x}_k)^{\mathrm{T}} \boldsymbol{u} + \frac{1}{2} \boldsymbol{u}^{\mathrm{T}} \boldsymbol{H}_k \boldsymbol{u}$$

in a so-called trust region Ω_k which is defined by

$$\Omega_k = \{\boldsymbol{x} \in \mathbb{R}^n | \, \|\boldsymbol{\Gamma}(\boldsymbol{x} - \boldsymbol{x}_k)\| \leq \Delta_k\}$$

where Δ_k is the trust-region radius, $\boldsymbol{H}_k$ is the local Hessian matrix, $\boldsymbol{\Gamma}$ is a diagonal scaling matrix that is related to the scalings of the optimization problem,$\boldsymbol{x}_{k+1}$ is the next trial solution from the current solution x_k.

The minimization using trust-region follows a four-step process:

1. Start at an initial guess x_0 and radius 0 of the trust region Ω_0.
2. Initialize algorithm constants: $0 < \alpha_1 \leq \alpha_2 < 1, 0 < \beta_1 \leq \beta_2 < 1$.
3. while (stop criterion)
   Construct an approximate model $\phi_k(x)$ for the objective $f(x_k)$ in Ω_k.
   Find a trial point $\boldsymbol{x}_{k+1}$ with a sufficient model decrease inside Ω_k
   Calculate the ratio γ_k of the achieved versus predicted decrease (This ratio measures how good the approximation ϕ_k is to the actual objective $f(x)$):

   $$\gamma_k = \frac{f(\boldsymbol{x}_k) - f(\boldsymbol{x}_{k+1})}{\phi_k(\boldsymbol{x}_k) - \phi_k(\boldsymbol{X}_{k+1})}$$

   If $\gamma_k \geq \alpha_1$ (i.e. if the above ratio γ_k was close to unity, then we have a good approximation and we should move the trust region to $\boldsymbol{x}_{k+1}$) and perform the following steps:

   - Accept the move and update the trust region: $\boldsymbol{x}_k \leftarrow \boldsymbol{x}_{k+1}$;
   - If $\gamma_k \geq \alpha_2$ (i.e. if γ_k is about $O(1)$ or $\gamma_k \geq \alpha_2 \approx 0.9$, we say that decrease is significant, and we can increase the trust-region radius) then $\Delta_{k+1} \in [\Delta_k, \infty)$; **end if**
   - If $\gamma_k \in [\alpha_1, \alpha_2)$, (i.e. if $\alpha_1 < \gamma_k \leq \alpha_2$, we should shrink the trust region), then $\Delta_{k+1} \in [\beta_2 \Delta_k, \Delta_k]$; **end if**

   else (i.e. if the decrease is too small or $\gamma_k < \alpha_1$, we should abandon the move as the approximation is not good enough over this larger region and seek a better approximation on a smaller region by reducing the trust-region radius)

   - Discard the move and reduce the trust-region radius Δ_{k+1};
   - $\Delta_{k+1} \in [\beta_1 \Delta_k, \beta_2 \Delta_k]$ (where $0 < \beta_1 \leq \beta_2 < 1$, typically $\beta_1 = \beta_2 = 1/2$
4. Update $k = k + 1$.
5. **end**

The typical values of the parameters are $\alpha_1 = 0.01$, $\alpha_2 = 0.9$, $\beta_1 = \beta_2 = \frac{1}{2}$.

A.1.3 Rule-of-Thumb Evaluation

The Tables A.1.11, A.1.12 and A.1.13 contains output from exercises designed to evaluate the performance of the rules-of-thumb proposed Heaton (2008) relative to the architecture proposed for the $C_N - Models$ and $CK_N - Models$. The performance of a two hidden layer MLP over a three hidden layer MLP is mentioned in table A.1.13 from columns IV to IX. Since the three hidden layer MLPs perform marginally better than the two-layered network and are faster to train (as mentioned in table A.1.15, we choose three hidden layered MLPs in this study. Note, the inputs of the MLP models in table A.1.11 are similar to the MLP models used in section 2.4.1, and the inputs of the MLP models in table A.1.14 are similar to the MLP models used in section 2.4.2

Table A.1.11: Overall Call Price Comparison (amongst Parametric and MLP models to evaluate the performance of the rules-of-thumb proposed by Heaton (2008)): This table presents the overall comparison of out-of-sample root mean square error ($RMSE$) amongst the Random Walk (δC_N) model, Black-Scholes-Merton ($BSMC_N$) model, Heston (HC_N) model and the MLP models. The one-day-ahead forecast errors of C_{N+1} are used to compute the Root Mean Square Error (RMSE). Column I identifies the models, column II identifies the forecast variable, column III lists the input variables used by the models to obtain the one-trading-day ahead forecast of C_{N+1}, and columns IV, V and VI describe the network architecture of the MLP models, and column VII describe the overall RMSE. The forecast variable for all the models is the one-day-ahead call option price (C_{N+1}). The models denoted by the $_N$ subscript use lagged input variables for forecasting C_{N+1}. Forecasts are made for 1,326 trading days.

(I) MLP Model	**(II) Forecast Variable**	**(III) Inputs**	**(IV) No. of Hidden Layers**	**(V) No. of Hidden Nodes per layer**	**(VI) Network Architecture**	**(VII) Overall RMSE**
δC_N	C_{N+1}	C_N	-	-	-	8.807
$BSMC_N$	C_{N+1}	$S_N, K_{N+1}, T_{N+1}, R_N, Q_N, \sigma_N^{CALIB^C}$	-	-	-	13.542
HC_N	C_{N+1}	$S_N, K_{N+1}, T_{N+1}, R_N, Q_N, \sigma_N^{CALIB^C}, HParams_N^C$	-	-	-	9.077
$C1_N$	C_{N+1}	$S_N, K_{N+1}, T_{N+1}, R_N, Q_N, \sigma_N^{CALIB^C}$	1	6	6	9.115
$C2_N$	C_{N+1}	$S_N, K_{N+1}, T_{N+1}, R_N, Q_N, \sigma_N^{CALIB^C}, C_N$	1	7	7	8.982
$C3_N$	C_{N+1}	$S_N, K_{N+1}, T_{N+1}, R_N, Q_N, \sigma_N^{CALIB^C}, C_N, BSMGreeks_N^C$	3	12	$12 \times 12 \times 12$	8.852
$C4_N$	C_{N+1}	$S_N, K_{N+1}, T_{N+1}, R_N, Q_N, \sigma_N^{CALIB^C}, C_N, BSMGreeks_N^C, HParams_N^C$	3	17	$17 \times 17 \times 17$	8.854
$C5_N$	C_{N+1}	$S_N, K_{N+1}, T_{N+1}, R_N, Q_N, \sigma_N^{CALIB^C}, C_N, BSMGreeks_N^C, HParams_N^C, C_N^{HC}$	3	18	$18 \times 18 \times 18$	8.831
$C6_N$	C_{N+1}	$S_N, K_{N+1}, T_{N+1}, R_N, Q_N, HParams_N^C, C_N^{HC}$	3	11	$11 \times 11 \times 11$	8.838

Table A.1.12: Heaton (2008) Methodology: This table presents the overall comparison of out-of-sample root mean square error ($RMSE$) amongst the MLP $JC_N - Models$ ($JC1_N$ to $JC6_N$) that follow the methodology of Heaton (2008) in choosing the number of hidden layers and the number of hidden neuron in each hidden layer, on the S&P 500 Index from Sept. 2012 to Dec. 2017. Column I identifies the models, column II identifies the forecast variable, column III lists the input variables used by the models to obtain the one-trading-day ahead forecast of C_{N+1}, and columns IV, V and VI describe the network architecture of the MLP models, and column VII describe the overall RMSE. The forecast variable for all the models is the one-day-ahead call option price (C_{N+1}). The models denoted by the $_N$ subscript use lagged input variables for forecasting C_{N+1}. Forecasts are made for 1,326 trading days.

(I) **Heaton (2008) inspired MLP Model**	**(II)** **Forecast Variable**	**(III)** **Inputs**	**(IV)** **No. of Hidden Layers**	**(V)** **No. of Hidden Nodes per layer**	**(VI)** **Network Architecture**	**(VII)** **Overall RMSE**
$JC1_N$	C_{N+1}	$S_N, K_{N+1}, T_{N+1}, R_N, Q_N, \sigma_N^{CALIB^C}$	1	5	5	9.231
$JC2_N$	C_{N+1}	$S_N, K_{N+1}, T_{N+1}, R_N, Q_N, \sigma_N^{CALIB^C}, C_N$	1	6	6	9.012
$JC3_N$	C_{N+1}	$S_N, K_{N+1}, T_{N+1}, R_N, Q_N, \sigma_N^{CALIB^C}, C_N, BSMGreeks_N^C$	2	9	5 X 4	8.826
$JC4_N$	C_{N+1}	$S_N, K_{N+1}, T_{N+1}, R_N, Q_N, \sigma_N^{CALIB^C}, C_N, BSMGreeks_N^C, HParams_N^C$	2	12	6 X 6	8.860
$JC5_N$	C_{N+1}	$S_N, K_{N+1}, T_{N+1}, R_N, Q_N, \sigma_N^{CALIB^C}, C_N, BSMGreeks_N^C, HParams_N^C, C_N^{HC}$	2	13	7 X 6	8.863
$JC6_N$	C_{N+1}	$S_N, K_{N+1}, T_{N+1}, R_N, Q_N, HParams_N^C, C_N^{HC}$	2	8	4 X 4	8.866

Table A.1.13: Heaton (2008) Methodology: This table presents the overall comparison of out-of-sample root mean square error ($RMSE$) amongst the MLP $JC_N - Models$ models ($JC1_N$ to $JC6_N$) from table A.1.12 with the MLP models in the table A.1.11. The performance of the $JC_N - Models$, measured as a percentage reduction in $RMSE$, relative to $BSMC_N$ model, is reported in column II, relative to the HC_N in column III and relative to the MLP Models from table A.1.11 from column IV to column IX.

(I) **MLP Model**	**(II)** **Performance of $JC_N - Models$ over $BSMC_N$**	**(III)** **Performance of $JC_N - Models$ over HC_N**	**(IV)** **Performance of $JC1_N$ over $C1_N$**	**(V)** **Performance of $JC2_N$ over $C2_N$**	**(VI)** **Performance of $JC3_N$ over $C3_N$**	**(VII)** **Performance of $JC4_N$ over $C4_N$**	**(VIII)** **Performance of $JC5_N$ over $C5_N$**	**(IX)** **Performance of $JC6_N$ over $C6_N$**
$JC1_N$	31.83%	-1.70%	-1.27%	-	-	-	-	-
$JC2_N$	33.45%	0.71%	-	-0.33%	-	-	-	-
$JC3_N$	34.82%	2.76%	-	-	0.06%	-	-	-
$JC4_N$	34.58%	2.39%	-	-	-	-0.24%	-	-
$JC5_N$	34.55%	2.36%	-	-	-	-	-0.10%	-
$JC6_N$	34.53%	2.32%	-	-	-	-	-	-0.16%

A.1.4 Epochs

Table A.1.14: Overall Call Price Scaled by the Exercise Price Comparison (amongst Parametric and MLP models): This table presents the overall comparison of out-of-sample root mean square error ($RMSE$) amongst the Random Walk (δCK_N) model, Black-Scholes-Merton ($BSMCK_N$) model, Heston (HCK_N) model and the MLP models. Column I identifies the models, column II identifies the forecast variable, column III lists the input variables used by the models to obtain the one-trading-day ahead forecast of C_{N+1}/K_{N+1}, and columns IV, V and VI describe the network architecture of the MLP models, and column VII describe the overall RMSE. The forecast variable for all the models is the one-day-ahead call option price scaled by the exercise price (C_{N+1}/K_{N+1}). The models denoted by the $_N$ subscript use lagged input variables for forecasting C_{N+1}/K_{N+1}. The one-day-ahead forecast errors of C_{N+1}/K_{N+1} are used to compute the Root Mean Square Error (RMSE). Forecasts are made for 1,326 trading days.

(I) MLP Model	**(II) Forecast Variable**	**(III) Inputs**	**(IV) No. of Hidden Layers**	**(V) No. of Hidden Nodes per layer**	**(VI) Network Architecture**	**(VII) Overall RMSE**
δCK_N	C_{N+1}/K_{N+1}	C_N/K_N	-	-	-	0.490
$BSMCK_N$	C_{N+1}/K_{N+1}	$S_N/K_N, T_{N+1}, R_N, Q_N, \sigma_N^{CALIB^{CK}}$	-	-	-	0.715
HCK_N	C_{N+1}/K_{N+1}	$S_N/K_N, T_{N+1}, R_N, Q_N, \sigma_N^{CALIB^{CK}}, HParams_N^{CK}$	-	-	-	0.502
$CK1_N$	C_{N+1}/K_{N+1}	$S_N/K_N, T_{N+1}, R_N, Q_N, \sigma_N^{CALIB^{CK}}$	1	5	5	0.509
$CK2_N$	C_{N+1}/K_{N+1}	$S_N/K_N, T_{N+1}, R_N, Q_N, \sigma_N^{CALIB^{CK}}, C_N/K_N$	1	6	6	0.502
$CK3_N$	C_{N+1}/K_{N+1}	$S_N/K_N, T_{N+1}, R_N, Q_N, \sigma_N^{CALIB^{CK}}, C_N/K_N, BSMGreeks_N^{CK}$	3	11	$11 \times 11 \times 11$	0.496
$CK4_N$	C_{N+1}/K_{N+1}	$S_N/K_N, T_{N+1}, R_N, Q_N, \sigma_N^{CALIB^{CK}}, C_N/K_N, BSMGreeks_N^{CK}, HParams_N^{CK}$	3	16	$16 \times 16 \times 16$	0.494
$CK5_N$	C_{N+1}/K_{N+1}	$S_N/K_N, T_{N+1}, R_N, Q_N, \sigma_N^{CALIB^{CK}}, C_N/K_N, BSMGreeks_N^{CK}, HParams_N^{CK}, (C_N^{HCK}/K_N)$	3	17	$17 \times 17 \times 17$	0.494
$CK6_N$	C_{N+1}/K_{N+1}	$S_N/K_N, T_{N+1}, R_N, Q_N, HParams_N^{CK}, (C_N^{HCK}/K_N)$	3	10	$10 \times 10 \times 10$	0.495

Table A.1.15: Observed Average Epochs: This table presents the average number of epochs, over the whole sample, required to train the various MLP models. The number of epochs observed depends on the early stopping criteria. Column I lists the models where the call price ($C_N - Models$) is the forecast variable, and Column II records the average epochs required for training these models. Similarly, column III lists the $JC_N - Models$ which follow the rule of thumb of Heaton (2008), and column IV reports the average epochs required to train the $JC_N - Models$. Column VI presents the average epochs required to train the $CK_N - Models$ listed in Column V.

(I) $C_N - Models$ **from table A.1.11**	**(II)** **Average no. of epochs for models in column I**	**(III)** $JC_N - Models$ **from table A.1.12**	**(IV)** **Average no. of epochs for models in column II**	**(V)** $CK_N - Models$ **from table A.1.14**	**(VI)** **Average no. of epochs for models in column III**
$C1_N$	1,545	$JC1_N$	1,368	$CK1_N$	1,157
$C2_N$	1,563	$JC2_N$	1,542	$CK2_N$	1,884
$C3_N$	1,248	$JC3_N$	1,632	$CK3_N$	10
$C4_N$	25	$JC4_N$	583	$CK4_N$	9
$C5_N$	43	$JC5_N$	205	$CK5_N$	8
$C6_N$	80	$JC6_N$	982	$CK6_N$	9

Table A.1.16: Table of variables for Chapter 2

Symbol	Name	Description
C_t	Call price	Call price calculated by taking the average of the bid and ask call price from OptionMetrics
S_t	S&P 500 Index Price	S&P 500 Index Price from OptionMetrics
K_t	Exercise price	Option exercise price from OptionMetrics
T_t	Time to Maturity	Time to maturity calculated from option expiry date from OptionMetrics
R_t	Risk-free interest rate	The interpolated interest rate using zero interest curves from OptionMetrics
Q_t	Dividend Yield	S&P 500 Index dividend yield from OptionMetrics
S_t/K_t	Moneyness	Moneyness is defined as the ratio of the S&P Index price and the option strike price
σ_t^B	Volatility	Black-Scholes-Merton implied volatility
δ_t^B	Delta	Black-Scholes-Merton Delta.
γ_t^B	Gamma	Black-Scholes-Merton Gamma.
θ_t^B	Theta	Black-Scholes-Merton Theta.
ρ_t^B	Rho	Black-Scholes-Merton Rho.
ν_t^B	Vega	Black-Scholes-Merton Vega.
$V_{0,t}^H$	Initial variance	Initial variance in the Heston model
θ_t^H	Long term variance	Long term variance in the Heston model
κ_t^H	Mean reversion speed	Mean reversion speed in the Heston model
σ_t^H	Volatility	Volatility of variance in the Heston model
ρ_t^H	Correlation	Correlation parameter in the Heston model
$V_{0,t}^{HJD}$	Initial variance	Initial variance in the Heston Jump Diffusion model
θ_t^{HJD}	Long term variance	Long term variance in the Heston Jump Diffusion model
κ_t^{HJD}	Mean reversion speed	Mean reversion speed in the Heston Jump Diffusion model
σ_t^{HJD}	Volatility	Volatility of variance in the Heston Jump Diffusion model
ρ_t^{HJD}	Correlation	Correlation parameter in the Heston Jump Diffusion model
σ_t^{HJD}	Jump Volatility	Jump volatility parameter in the Heston Jump Diffusion model
μ_t^{HJD}	Jump Mean	Jump mean parameter in the Heston Jump Diffusion model
λ_t^{HJD}	Jump Frequency	Jump frequency parameter in the Heston Jump Diffusion model
α_t^{FMLS}	Tail Parameter	Tail parameter in the Finite Moment Log Stable model
σ_t^{FMLS}	Dispersion Parameter	Dispersion parameter in the Finite Moment Log Stable model
$BGreeks_t$	BSM greeks	Black-Scholes-Merton greeks ($\delta_t^B, \gamma_t^B, \rho_t^B, \theta_t^B, \nu_t^B$)
$HParams_t$	Heston parameters	Heston model parameters (κ_t^H , σ_t^H, θ_t^H, ρ_t^H, $V_{0,t}^H$)
$HJDParams_t$	Heston Jump Diffusion parameters	Heston Jump Diffusion model parameters (κ_t^{HJD} , σ_t^{HJD}, θ_t^{HJD}, ρ_t^{HJD}, $V_{0,t}^{HJD}$, σ_t^{HJD},μ_t^{HJD},λ_t^{HJD})
$FMLSParams_t$	Finite Moment Log Stable parameters	FMLS model parameters (α_t^{FMLS} , σ_t^{FMLS})

Table A.1.17: Month-wise summary statistics of the S&P 500 Index call options prices used in Chapter 2.

Month	Number of Observations	Average Call Price	Bid-Ask Spread
September 2012	2,005	$71.25	$1.46
October 2012	7,196	$71.38	$1.24
November 2012	6,918	$67.11	$0.78
December 2012	6,602	$71.51	$0.81
January 2013	6,526	$80.25	$0.87
February 2013	6,324	$81.94	$0.91
March 2013	6,768	$84.58	$0.95
April 2013	7,795	$84.04	$1.07
May 2013	8,189	$87.87	$1.02
June 2013	7,867	$84.84	$1.01
July 2013	8,672	$88.60	$1.13
August 2013	8,338	$85.23	$1.04
September 2013	7,461	$89.32	$1.00
October 2013	7,957	$93.49	$1.03
November 2013	6,884	$99.42	$1.05
December 2013	7,359	$97.48	$0.98
January 2014	7,676	$97.57	$0.98
February 2014	7,392	$96.73	$1.04
March 2014	8,235	$103.58	$1.08
April 2014	8,099	$101.67	$1.16
May 2014	7,809	$107.11	$1.05
June 2014	7,575	$113.44	$1.13
July 2014	8,264	$116.33	$1.28
August 2014	8,392	$109.66	$1.23
September 2014	8,115	$111.10	$1.21
October 2014	9,231	$104.16	$1.23
November 2014	7,070	$122.60	$1.23
December 2014	8,484	$120.37	$1.46
January 2015	8,667	$114.67	$1.39
February 2015	8,567	$120.67	$1.41
March 2015	10,283	$114.19	$1.19
April 2015	9,436	$119.03	$1.24
May 2015	9,082	$122.14	$1.30
June 2015	10,209	$119.98	$1.21
July 2015	9,840	$118.99	$1.32
August 2015	9,467	$112.70	$1.64
September 2015	10,956	$100.27	$1.47
October 2015	9,649	$114.73	$1.43
November 2015	8,575	$119.68	$1.24
December 2015	9,222	$114.99	$1.17
January 2016	8,297	$101.10	$1.02
February 2016	9,561	$105.90	$1.05
March 2016	9,992	$123.42	$1.04
April 2016	9,381	$119.88	$1.00
May 2016	9,820	$113.89	$0.98
June 2016	9,977	$114.51	$0.94
July 2016	9,036	$120.09	$0.95
August 2016	10,629	$121.10	$0.85
September 2016	9,597	$117.80	$0.96
October 2016	9,271	$118.89	$1.01
November 2016	9,542	$117.65	$1.14
December 2016	9,878	$125.01	$1.18
January 2017	9,514	$125.31	$1.14
February 2017	8,353	$132.58	$1.19
March 2017	10,939	$133.36	$1.41
April 2017	9,249	$132.04	$1.24
May 2017	10,424	$137.74	$1.36
June 2017	10,528	$133.50	$1.52
July 2017	10,076	$139.66	$1.41
August 2017	10,937	$141.37	$1.60
September 2017	9,403	$142.40	$1.66
October 2017	10,074	$151.84	$1.74
November 2017	9,833	$152.60	$1.84
December 2017	8,928	$156.71	$1.82

Appendix A.2

Appendix for Chapter 2: Extended Results

A.2.1 Pricing performance of C-Models that use lagged input variables to forecast the call option price (C_{N+1}) for the next trading day:

Table A.2.1 to Table A.2.14 shows the relative out-of-sample pricing performance (in $RMSE$) amongst the models that use lagged input variables to forecast the one-trading-day-ahead call option price(C_{N+1}). For convenience, the models in table A.2.1 to table A.2.13, lists the forecast variable and the input variables in columns II and III, respectively, and the architecture of the MLP and LSTM models in columns IV, V and VI, respectively. The performance metric is the $RMSE$ of the one-trading-day-ahead forecast errors of C_{N+1}, which is computed for each model utilising all of the errors in each day or each month. Amongst all of the models (including the random walk model (δC_N)), columns VII and VIII record the number of months and days, respectively, that each model had the lowest $RMSE$. To be certain of our results, we performed a bootstrap using the daily and monthly RMSEs. Columns IX (lower bound) and X (upper bound) present the results from the bootstrap performed (with replacement) using monthly RMSEs at a 95% confidence level and show the winning percentage out of 64 months for each model (including the δC_N model), and similarly, the 95 % confidence intervals computed from bootstrapping of the daily RMSEs signifies the winning percentage out of 1328 days for each model and are reported in columns XI (lower bound), XII (upper bound). While excluding the δC_N model amongst the comparison, columns XIII and XIV record the number of months and days that each model had the lowest $RMSE$. We repeat the exercise of performing the bootstrap by excluding the δC_N model in the comparison, and thus, columns XV (lower bound) and XVI (upper bound) present the results from the bootstrap performed (with replacement) using monthly RMSEs at a 95% confidence level and shows the winning percentage out of 64 months for each model (excluding the δC_N model), and similarly, the 95 % confidence intervals computed from bootstrapping of the daily RMSEs signifies the winning percentage out of 1328 days for each model and are reported in columns XVII (lower bound), XVIII (upper bound).

In the below several comparisons, even though a particular model wins by a higher percentage against other models, we investigated further these models pairwise by performing a pairwise bootstrap comparison, which was computed using the respective pair's daily RMSEs. The results are presented in Table 17 of the Electronic Appendix. Also, we examined the pairwise Diebold-Mariano(DM) (Diebold and Mariano (1995)) tests on the and have presented the results in Table 13 of the Electronic Appendix. In constructing the DM tests, the model pairs are reported in column I and column II, and the DM test statistics for a particular pair are reported in column III. If the null can be rejected, a positive number suggests the rejection may be due to the second model being the better forecast model. In contrast, a negative value suggests the rejection may be due to the first model being the better forecast model. The model pairs highlighted in a red state that their forecasts have statistically insignificant differences in their prediction accuracy. The following model pairs have been shown to have statistically insignificant differences: ($HJDC_N$, $M3C1_N$), ($M1C3_N$, $M2C1_N$), ($M1C4_N$, $M2C4_N$), ($M1C5_N$, $M2C7_N$), ($M1C5_N$, $M2C8_N$), ($M1C5_N$, $M3C8_N$), ($M1C6_N$, $M2C7_N$), ($M1C6_N$, $M3C7_N$), ($M1C7_N$, $M1C9_N$), ($M1C8_N$, $M2C5_N$), ($L1C4_N$, $L3C4_N$), ($L1C8_N$, $L2C4_N$), ($M2C3_N$, $M2C9_N$), ($M2C3_N$, $M3C3_N$), ($M2C3_N$, $M3C9_N$), ($M2C6_N$, $M2C7_N$), ($M2C6_N$, $M3C5_N$), ($M2C6_N$, $M3C8_N$), ($M2C7_N$, $M2C8_N$), ($M2C7_N$, $M3C5_N$), ($M2C7_N$, $M3C8_N$), ($M2C8_N$, $M3C5_N$), ($M2C9_N$, $M3C3_N$), ($L2C8_N$, $L3C7_N$), ($M3C1_N$, $M3C2_N$), ($M3C3_N$, $M3C4_N$), ($M3C5_N$, $M3C8_N$), and ($M3C6_N$, $M3C7_N$). The RMSEs for the $C-Models$ that use lagged input variables to forecast the C_{N+1} for the next trading day on a monthly, yearly, and overall basis can be found in the Electronic Appendix, in Tables 1, 5, and 9, respectively.

A.2.1.1 Comparison amongst all Parametric Models with Single Hidden Layer ANN Models:

In this section, we compare the out-of-sample pricing performance of the random walk model (δC_N), the parametric models ($BSMC_N$, HC_N, $HJDC_N$, and $FMLSC_N$), the single hidden layer MLP models ($M1C_N - Models$) and single hidden layer LSTM models ($L1C_N - Models$), then the parametric models with the $M1C_N - Models$, and finally the parametric models with the $L1C_N - Models$.

The results for the parametric models with the MLP $M1C_N - Models$ ($M1C1_N$ to $M1C9_N$) and LSTM $L1C_N - Models$ ($L1C1_N$ to $L1C9_N$) are presented in Table A.2.1. If all the models are individually compared, then the δC_N model had the lowest $RMSE$ for 161 days (having a daily bootstrap winning % of 10% to 14%) out of 1,328 days, while other variants of the LSTM model, the $L1C4_N$(118 days), $L1C8_N$(135 days) have had a collective daily bootstrap winning percentage from 7% (lower bound for the $L1C4_N$ model) to 12% (upper bound for the $L1C8_N$ model). When the δC_N was excluded from the comparison, the $L1C8_N$ model outperformed all other models for 142 days (having a daily bootstrap winning % of 9% to 12%) out of 1,328 days. Though the $L1C8_N$ model outperformed, other variants of the LSTM model, like the $L1C4_N$ (120 days), and the $L1C5_N$ (105 days), have shown similar outperformance to $L1C8_N$ model, where they have a collective daily bootstrap winning percentage from 6% (lower bound for the $L1C5_N$ model) to 11% (upper bound for the $L1C4_N$ model).

Table A.2.2 presents the results for the comparison of the parametric models with the MLP $M1C_N - Models$ ($M1C1_N$ to $M1C9_N$). Accordingly, when all the models are compared, the δC_N model had the lowest $RMSE$ for 234 days (having a daily bootstrap winning % of16% to 20%) out of 1,328 days, while another parametric model, the $FMLSC_N$(221 days) had a similar bootstrap winning % of15% to 19%). When the δC_N was excluded from the comparison, the

$FMLSC_N$ model outperformed all other models for 229 days (having a daily bootstrap winning % of 15% to 19%) out of 1,328 days.

We present the comparison results of the parametric models with the LSTM $L1C_N - Models$ ($L1C1_N$ to $L1C9_N$) in Table A.2.3. We find that the δC_N model had the lowest $RMSE$ for 248 (having a daily bootstrap winning % of 17% to 21%) days out of 1,328 days when all the models were compared together. When the δC_N was excluded from the comparison, the $L1C8_N$ model had outperformed all other models for 171 days (having a daily bootstrap winning % of 11% to 15%) out of 1,328 days. Though the $L1C8_N$ model outperformed, other variants of the parametric model, the HC_N (145 days), and the $HJDC_N$ (144 days), and other variants of the LSTM model, the $L1C4_N$ (124 days), $L1C5_N$ (142 days), $L1C6_N$ (118 days), and the $L1C7_N$ (123 days) have shown similar outperformance to $L1C8_N$ model, where they have a collective daily bootstrap winning percentage ranging from 7% (lower bound for the $L1C6_N$ model) to 13%(upper bound for the HC_N, $HJDC_N$ model).

Thus, when the parametric models are compared with the single hidden layer ANN models, we conclude that an LSTM model ($L1C8_N$) could outperform all other models. If the parametric models were compared with the single hidden layer MLP models (in Table A.2.2), a parametric model ($FMLSC_N$) had outperformed all the single hidden layer MLP models, but when the parametric models were compared with the single hidden layer LSTM models (in Table A.2.3), an LSTM model ($L1C8_N$) had still outperformed them all.

A.2.1.2 Comparison amongst all Parametric Models with Double Hidden Layer ANN Models:

In this section, we compare the out-of-sample pricing performance of the random walk model (δC_N), the parametric models ($BSMC_N$, HC_N, $HJDC_N$, and $FMLSC_N$), the double hidden layer MLP models ($M2C_N - Models$) and double hidden layer LSTM models ($L2C_N - Models$), then the parametric models with the $M2C_N - Models$, and finally the parametric models with the $L2C_N - Models$.

The results for the parametric models with the MLP $M2C_N - Models$ ($M2C1_N$ to $M2C9_N$) and the LSTM $L2C_N - Models$ ($L2C1_N$ to $L2C9_N$) are presented in Table A.2.4. If all the models are individually compared, then the $L2C9_N$ model had the lowest $RMSE$ for 160 days (having a daily bootstrap winning % of 10% to 14%) out of 1,328 days, while other variants of the LSTM model, the $L2C2_N$ (126 days), and the $L2C4_N$ (108 days) have had a collective daily bootstrap winning percentage from 7% (lower bound for the $L2C4_N$ model) to 11% (upper bound for the $L2C2_N$ model). When the δC_N was excluded from the comparison, the $L2C9_N$ model still outperformed all other models for 161 days (having a daily bootstrap winning % of 10% to 14%) out of 1,328 days. Though the $L2C9_N$ model outperformed, other variants of the LSTM model, the $L2C2_N$ (126 days), and the $L2C4_N$ (109 days), have shown similar outperformance to $L2C9_N$ model, where they have a collective daily bootstrap winning percentage from 7% (lower bound for the $L2C4_N$ model) to 11% (upper bound for the $L2C2_N$ model).

Table A.2.5 presents the results for the comparison of the parametric models with the MLP $M2C_N - Models$ ($M2C1_N$ to $M2C9_N$). Accordingly, the $FMLSC_N$ model had the lowest $RMSE$ for 223 days (having a daily bootstrap winning % of 15% to 19%) out of 1,328 days. When the δC_N was excluded from the comparison, the $FMLSC_N$ model still outperformed all other models for 230 days (having a daily bootstrap winning % of 15% to 19%) out of 1,328 days.

We present the comparison results of the parametric models with the LSTM $L2C_N - Models$ ($L2C1_N$ to $L2C9_N$) in Table A.2.6. We find that the δC_N model had the lowest $RMSE$ for 231 days (having a daily bootstrap winning % of 15% to 19%) out of 1,328 days, while another variant of the LSTM model, the $L2C9_N$ (164 days) had a daily bootstrap winning percentage of 11% to 14%. When the δC_N was excluded from the comparison, the $L2C9_N$ model outperformed all other models for 165 days (having a daily bootstrap winning % of 11% to 14%) out of 1,328 days. Though the $L2C9_N$ model outperformed, other variants of the parametric model, the HC_N (138 days), and the $HJDC_N$ (114 days), and other variants of the LSTM model, the $L2C2_N$ (127 days), $L2C4_N$ (116 days), $L2C5_N$ (121 days), and the $L2C8_N$ (142 days) have shown similar outperformance to $L2C9_N$ model, where they have a collective daily bootstrap winning percentage from 7% (lower bound for the $L2C4_N$ model) to 12% (upper bound for the HC_N model).

Thus, when the parametric models are compared with the double hidden layer ANN models, we conclude that an LSTM model ($L2C9_N$) could outperform all other models (in Table A.2.4). If the parametric models were compared with the double hidden layer MLP models ($M2C_N - Models$)(in Table A.2.5), a parametric model ($FMLSC_N$) outperformed all the double hidden layer MLP models, but when the parametric models were compared with the double hidden layer LSTM models (in Table A.2.6), an LSTM model ($L2C9_N$) model had still outperformed them all.

A.2.1.3 Comparison amongst all Parametric Models with Triple Hidden Layer ANN Models:

In this section, we compare the out-of-sample pricing performance of the random walk model (δC_N), the parametric models ($BSMC_N$, HC_N, $HJDC_N$, and $FMLSC_N$), the triple hidden layer MLP models ($M3C_N - Models$) and triple hidden layer LSTM models ($L3C_N - Models$), then the parametric models with the $M3C_N - Models$, and finally the parametric models with the $L3C_N - Models$.

The results for the parametric models with the MLP $M3C_N - Models$ ($M3C1_N$ to $M3C9_N$) and the LSTM $L3C_N - Models$ ($L3C1_N$ to $L3C9_N$) are presented in Table A.2.7. If all the models are individually compared, then the $L3C9_N$ model had the lowest $RMSE$ for 169 days (having a daily bootstrap winning % of 11% to 15%) out of 1,328 days, while the δC_N (128 days) and another variant of the LSTM model, the $L3C2_N$ (138 days) have had a collective daily bootstrap winning percentage from 9% (lower bound for the $L3C2_N$ model) to 11% (upper bound for the δC_N model). When the δC_N was excluded from the comparison, the $L3C9_N$ model still outperformed all other models for 169 (having a daily bootstrap winning % of 11% to 15%) days out of 1,328 days. Though the $L3C9_N$ model outperformed, another variant of the LSTM model, the $L3C2_N$ (138 days), had a daily bootstrap winning percentage of 9% to 12%).

Table A.2.8 presents the results for the comparison of the parametric models with the MLP $M3C_N - Models$ ($M3C1_N$ to $M3C9_N$). Accordingly, the $FMLSC_N$ model had the lowest $RMSE$ for 224 days (having a daily bootstrap winning % of 15% to 19%) out of 1,328 days, but the δC_N model similarly out-performed for 206 days and had a daily bootstrap winning percentage of 14% to 17%). When the δC_N was excluded from the comparison, the $FMLSC_N$ model (having a daily bootstrap winning % of 15% to 19%) still outperformed all other models for 229 days out of 1,328 days. Though the $FMLSC_N$ model outperformed, another variant of the parametric model, the HC_N (159 days), had a daily bootstrap winning percentage of 10% to 14%).

We present the comparison results of the parametric models with the LSTM $L3C_N - Models$ ($L3C1_N$ to $L3C9_N$) in Table A.2.9. We find that the δC_N model had the lowest $RMSE$ for 234 days (having a daily bootstrap winning % of 16% to 20%) out of 1,328 days, while another variant of the LSTM model, the $L3C9_N$ (176 days) had a similar daily bootstrap winning percentage of 11% to 15%). When the δC_N was excluded from the comparison, the $L3C9_N$ model outperformed all other models for 180 days (having a daily bootstrap winning % of 12% to 15%) out of 1,328 days. Though the $L3C9_N$ model outperformed other variants of the parametric model, the HC_N (144 days), and the $HJDC_N$ (126 days), and other variants of the LSTM model, the $L3C2_N$ (144 days), $L3C5_N$ (127 days), and the $L3C8_N$ (121 days) have shown similar outperformance to $L3C9_N$ model, where they have a collective daily bootstrap winning percentage from 8% (lower bound for the $HJDC_N$, $L3C5_N$, $L3C8_N$ model) to 13% (upper bound for the HC_N, $L3C2_N$ model)

Thus, when the parametric models are compared with the triple hidden layer ANN models, we conclude that an LSTM model ($L3C9_N$) could outperform all other models. If the parametric models were compared with the triple hidden layer MLP models ($M3C_N - Models$) (in Table A.2.8), a parametric model ($FMLSC_N$) outperforms, but when the parametric models were compared with the triple hidden layer LSTM models (in Table A.2.9), the LSTM model ($L3C9_N$) had still outperformed them all.

A.2.1.4 Comparison amongst all Parametric Models with Single, Double and Triple Hidden Layer ANN Models:

In this section, we compare the out-of-sample pricing performance of the random walk model (δC_N), the parametric models ($BSMC_N$, HC_N, $HJDC_N$, and $FMLSC_N$), the single, double, triple hidden layer MLP models ($M1C_N - Models$, $M2C_N - Models$, and $M3C_N - Models$) and single, double, triple hidden layer LSTM models ($L1C_N - Models$, $L2C_N - Models$, and $L3C_N - Models$), then the parametric models with the $M1C_N - Models$, $M2C_N - Models$, and $M3C_N - Models$, and finally the parametric models with the $L1C_N - Models$, $L2C_N - Models$, and $L3C_N - Models$.

The results for the parametric models with the $M1C_N - Models$ ($M1C1_N$ to $M1C9_N$), $M2C_N - Models$ ($M2C1_N$ to $M2C9_N$), $M3C_N - Models$ ($M3C1_N$ to $M3C9_N$), $L1C_N - Models$ ($L1C1_N$ to $L1C9_N$), $L2C_N - Models$ ($L2C1_N$ to $L2C9_N$), and $L3C_N - Models$ ($L3C1_N$ to $L3C9_N$) are presented in Table A.2.10. If all the models are individually compared, then the $L3C9_N$ model had the lowest $RMSE$ for 122 days (having a daily bootstrap winning % of 8% to 11%) out of 1,328 days. Although the $L3C9_N$ model had outperformed, the δC_N model had similarly out-performed for 106 days (having a daily bootstrap winning % of 7% to 9%) days out of 1,328 days. When the δC_N was excluded from the comparison, the $L3C9_N$ model still outperformed all other models for 122 days (having a daily bootstrap winning % of 8% to 11%) out of 1,328 days, while there was another variant of the LSTM model, the $L3C2_N$(86 days), that had a daily bootstrap winning percentage of 5% to 8%).

Table A.2.11 presents the results for the comparison of the parametric models with the $M1C_N - Models$ ($M1C1_N$ to $M1C9_N$), $M2C_N - Models$ ($M2C1_N$ to $M2C9_N$), $M3C_N - Models$ ($M3C1_N$ to $M3C9_N$). Accordingly, the $FMLSC_N$ model had the lowest $RMSE$ for 195 (having a daily bootstrap winning % of 13% to 17%) days out of 1,328 days, while the δC_N had similarly out-performed for 158 days (having a daily bootstrap winning % of 10% to 14%) out of 1,328 days. When the δC_N was excluded from the comparison, the $FMLSC_N$ model still outperformed all other models for 198 days (having a daily bootstrap winning % of 13% to 17%) out of 1,328 days.

We present the comparison results of the parametric models with the $L1C_N - Models$ ($L1C1_N$ to $L1C9_N$), $L2C_N - Models$ ($L2C1_N$ to $L2C9_N$), and $L3C_N - Models$ ($L3C1_N$ to $L3C9_N$) in Table A.2.12. We find that the δC_N model had the lowest $RMSE$ for 200 days (having a daily bootstrap winning % of 13% to 17%) out of 1,328 days. When the δC_N was excluded from the comparison, the $L3C9_N$ model still outperformed all other models for 130 days (having a daily bootstrap winning % of 8% to 11%) out of 1,328 days, although there were other variants of the parametric model, the HC_N (93 days), and the $HJDC_N$ (87 days) have had a collective daily bootstrap winning percentage from 5% (lower bound for the $HJDC_N$ model) to 8% (upper bound for the HC_N model)).

Thus, when the parametric models are compared with the single, double and triple hidden layer ANN models (in Table A.2.10), we notice that a three-hidden layer LSTM model ($L3C9_N$) had outperformed all other models, including the δC_N model, which had shown similar outperformance to the $L3C9_N$ model. If the parametric models were compared with the single, double and triple hidden layer MLP models (in Table A.2.11), then a parametric model ($FMLSC_N$) outperforms all the single, double and the triple hidden layer MLP models, but when the parametric models were compared with the single, double and the triple hidden layer LSTM models (in Table A.2.12), a three-hidden layer LSTM ($L3C9_N$) model had still outperformed them all.

A.2.1.5 Comparison amongst Single, Double and Triple Hidden Layer ANN Models:

In this section, we compare the out-of-sample pricing performance of the random walk model (δC_N), the single, double, and triple hidden layer MLP models ($M1C_N - Models$ ($M1C1_N$ to $M1C9_N$), $M2C_N - Models$ ($M2C1_N$ to $M2C9_N$), and $M3C_N - Models$ ($M3C1_N$ to $M3C9_N$)) and the single, double, triple hidden layer LSTM models ($L1C_N - Models$ ($L1C1_N$ to $L1C9_N$), $L2C_N - Models$ ($L2C1_N$ to $L2C9_N$), and $L3C_N - Models$ ($L3C1_N$ to $L3C9_N$)), and present the results in Table A.2.13. We find that the $L3C9_N$ model had the lowest $RMSE$ for 125 days (having a daily bootstrap winning % of 8% to 11%) out of 1,328 days. Although the $L3C9_N$ model outperformed, the δC_N (107 days) and other variants of the LSTM model, the $L3C2_N$ (86 days), and the $L3C4_N$ (85 days) have had a collective daily bootstrap winning percentage from 5% (lower bound for the $L3C2_N$, and the $L3C4_N$ model) to 10% (upper bound for the δC_N model). When the δC_N was excluded from the comparison, the $L3C9_N$ model still outperformed all other models for 125 days (having a daily bootstrap winning % of 8% to 11%) out of 1,328 days, while other variants of the LSTM model, the $L3C2_N$ (86 days), and the $L3C4_N$ (85 days) have had a collective daily bootstrap winning percentage from 5% (lower bound for the $L3C2_N$, and the $L3C4_N$ model) to 8% (upper bound for the $L3C2_N$, and the $L3C4_N$ model).

Thus, when comparing the out-of-sample pricing performance amongst the single, double and triple hidden layer ANN models (in Table A.2.13), a triple hidden layer LSTM($L3C9_N$) model outperforms the single, double and the triple hidden layer MLP models and also the single, double hidden layer LSTM models.

A.2.1.6 Comparison amongst all Parametric models:

In this section, we compare the out-of-sample pricing performance of the random walk model (δC_N), and the parametric models ($BSMC_N$, HC_N, $HJDC_N$, and $FMLSC_N$) in Table A.2.14. We find that the δC_N model had the lowest $RMSE$ for 498 days (having a daily bootstrap winning % of 35% to 40%) out of 1,328 days. When the δC_N was excluded from the comparison, the $HJDC_N$ model still outperformed all other models for 458 days (having a daily bootstrap winning % of 32% to 37%) out of 1,328 days. Though the $HJDC_N$ model outperformed other parametric models, other variants of the parametric model, the HC_N (376 days) and the $FMLSC_N$ (362 days), have shown similar outperformance to $HJDC_N$ model, where they have a collective daily bootstrap winning percentage from 25% (lower bound for the $FMLSC_N$ model) to 31% (upper bound for the HC_N model).

Thus, when comparing the out-of-sample pricing performance amongst the parametric models, the $HJDC_N$ model had outperformed all other parametric models, followed by the $FMLSC_N$ and HC_N model (in Table A.2.14).

Table A.2.1: Call Price Comparison (amongst Parametric, MLP $M1C_N - Models$ and LSTM $L1C_N - Models$): This table presents a performance comparison using both daily and monthly statistics amongst the Black-Scholes-Merton ($BSMC_N$) model, Heston (HC_N) model, Heston Jump Diffusion ($HJDC_N$) model, Finite Moment Log Stable ($FMLSC_N$) model, MLP $M1C_N - Models$ ($M1C1_N$ to $M1C9_N$) and the LSTM $L1C_N - Models$ ($L1C1_N$ to $L1C9_N$). The forecast variable for all the models is the one-day-ahead call option price (C_{N+1}). The models denoted by the $_N$ subscript use lagged input variables for forecasting C_{N+1}. The one-day-ahead forecast errors of C_{N+1} are used to compute the Root Mean Square Error (RMSE). Column I identifies the models, column II identifies the forecast variable, column III lists the input variables used by the models to obtain the one-trading-day ahead forecast of C_{N+1}, and columns IV, V and VI describe the network architecture of the MLP $M1C_N - Models$ and the LSTM $L1C_N - Models$. Forecasts are made for 1,328 trading days, and there are 64 months covered in the sample using the monthly data.

When comparing all models simultaneously (i.e. including the random walk model (δC_N), column VII reports the number of months out of the 64 months that each model has the smallest RMSE, while column VIII reports the number of days out of the 1,328 days each model has the smallest RMSE. Columns IX (lower bound) and X (upper bound) present the winning percentage out of 64 months for each model, evaluated using the bootstrap sampling technique. The statistical bootstrap performed (with replacement) at a 95% confidence level is computed from the monthly RMSE values of the respective models below. Columns XI (lower bound), XII (upper bound) presents the winning percentage out of 1326 days for each model computed from bootstrapping the daily RMSE values of the respective models at a 95% confidence level.

Similarly, when the δC_N model was excluded in the comparison, column XIII report the number of months out of the 64 months that each model has the smallest RMSE, while column XIV reports the number of days out of the 1,328 days each model has the smallest RMSE. Columns XV (lower bound) and XVI (upper bound) present the winning percentage out of 64 months for each model, evaluated using the bootstrap sampling technique. The statistical bootstrap performed (with replacement) at a 95% confidence level is computed from the monthly RMSE values of the respective models below. Also, columns XVII (lower bound) and XVIII (upper bound) present the winning percentage out of 1326 days for each model computed from bootstrapping the daily RMSE values of the respective models at a 95% confidence level.

						Including the random walk						Excluding the random walk					
(I) Model	(II) Forecast	(III) Inputs	(IV) No. of hidden layers	(V) No. of hidden nodes per layer	(VI) Network architecture	(VII) Performance amongst all models (Monthly)	(VIII) Performance amongst all models (Daily)	(IX) 2.5% lower bound-(for monthly) (%)	(X) 2.5% upper bound-(for monthly) (%)	(XI) 2.5% lower bound-(for daily) (%)	(XII) 2.5% upper bound-(for daily) (%)	(XIII) Performance amongst all models (Monthly)	(XIV) Performance amongst all models (Daily)	(XV) 2.5% lower bound-(for monthly) (%)	(XVI) 2.5% upper bound-(for monthly) (%)	(XVII) 2.5% lower bound-(for daily) (%)	(XVIII) 2.5% upper bound-(for daily) (%)
δC_N	C_{N+1}	C_N	-	-	-	**13**	**161**	11%	31%	10%	14%	-	-	-	-	-	-
$BSMC_N$	$C_{N+1}^{BSMC_N}$	$S_N, K_{N+1}, T_{N+1}, R_N, Q_N, \sigma_N^{CALIB^C}$	-	-	-	0	70	0%	0%	4%	7%	0	70	0%	0%	4%	6%
HC_N	$C_{N+1}^{HC_N}$	$S_N, K_{N+1}, T_{N+1}, R_N, Q_N, \sigma_N^{CALIB^C}, HParams_N^C$	-	-	-	2	79	0%	8%	5%	7%	2	81	0%	8%	5%	7%
$HJDC_N$	$C_{N+1}^{HJDC_N}$	$S_N, K_{N+1}, T_{N+1}, R_N, Q_N, \sigma_N^{CALIB^C}, HJDParams_N^C$	-	-	-	0	6	0%	0%	0%	1%	0	27	0%	0%	1%	3%
$FMLSC_N$	$C_{N+1}^{FMLSC_N}$	$S_N, K_{N+1}, T_{N+1}, R_N, Q_N, FMLSParams_N^C$	-	-	-	0	45	0%	0%	2%	4%	0	46	0%	0%	2%	4%
$M1C1_N$	$C_{N+1}^{M1C1_N}$	$S_N, K_{N+1}, T_{N+1}, R_N, Q_N, \sigma_N^{CALIB^C}$	1	6	6	0	14	0%	0%	1%	2%	0	14	0%	0%	1%	2%
$M1C2_N$	$C_{N+1}^{M1C2_N}$	$S_N, K_{N+1}, T_{N+1}, R_N, Q_N, \sigma_N^{CALIB^C}, C_N$	1	7	7	4	16	2%	13%	1%	2%	4	16	0%	13%	1%	2%
$M1C3_N$	$C_{N+1}^{M1C3_N}$	$S_N, K_{N+1}, T_{N+1}, R_N, Q_N, \sigma_N^{CALIB^C}, C_N, BSMGreeks_N^C$	1	12	12	1	61	0%	5%	4%	6%	1	73	0%	5%	4%	7%
$M1C4_N$	$C_{N+1}^{M1C4_N}$	$S_N, K_{N+1}, T_{N+1}, R_N, Q_N, \sigma_N^{CALIB^C}, C_N, BSMGreeks_N^C, HParams_N^C$	1	17	17	1	53	0%	5%	3%	5%	6	87	3%	17%	5%	8%
$M1C5_N$	$C_{N+1}^{M1C5_N}$	$S_N, K_{N+1}, T_{N+1}, R_N, Q_N, \sigma_N^{CALIB^C}, C_N, BSMGreeks_N^C, HParams_N^C, C_N^{HC}$	1	18	18	5	16	2%	16%	1%	2%	5	43	2%	16%	2%	4%
$M1C6_N$	$C_{N+1}^{M1C6_N}$	$S_N, K_{N+1}, T_{N+1}, R_N, Q_N, HParams_N^C, C_N^{HC}$	1	11	11	5	12	2%	16%	0%	2%	7	21	5%	19%	1%	2%
$M1C7_N$	$C_{N+1}^{M1C7_N}$	$S_N, K_{N+1}, T_{N+1}, R_N, Q_N, \sigma_N^{CALIB^C}, BSMGreeks_N^C, C_N^{BSMC}$	1	12	12	10	43	8%	25%	2%	4%	10	51	7%	25%	3%	5%
$M1C8_N$	$C_{N+1}^{M1C8_N}$	$S_N, K_{N+1}, T_{N+1}, R_N, Q_N, HJDParams_N^C, C_N^{HJDC}$	1	14	14	2	6	0%	8%	0%	1%	5	24	2%	14%	1%	3%
$M1C9_N$	$C_{N+1}^{M1C9_N}$	$S_N, K_{N+1}, T_{N+1}, R_N, Q_N, FMLSParams_N^C, C_N^{FMLSC}$	1	8	8	0	17	0%	0%	1%	2%	0	22	0%	0%	1%	2%
$L1C1_N$	$C_{N+1}^{L1C1_N}$	$S_N, K_{N+1}, T_{N+1}, R_N, Q_N, \sigma_N^{CALIB^C}$	1	6	6	0	2	0%	0%	0%	0%	0	2	0%	0%	0%	0%
$L1C2_N$	$C_{N+1}^{L1C2_N}$	$S_N, K_{N+1}, T_{N+1}, R_N, Q_N, \sigma_N^{CALIB^C}, C_N$	1	7	7	0	93	0%	0%	6%	8%	0	93	0%	0%	6%	8%
$L1C3_N$	$C_{N+1}^{L1C3_N}$	$S_N, K_{N+1}, T_{N+1}, R_N, Q_N, \sigma_N^{CALIB^C}, C_N, BSMGreeks_N^C$	1	12	12	0	85	0%	0%	5%	8%	0	85	0%	0%	5%	8%
$L1C4_N$	$C_{N+1}^{L1C4_N}$	$S_N, K_{N+1}, T_{N+1}, R_N, Q_N, \sigma_N^{CALIB^C}, C_N, BSMGreeks_N^C, HParams_N^C$	1	17	17	0	118	0%	0%	7%	11%	0	120	0%	0%	7%	11%
$L1C5_N$	$C_{N+1}^{L1C5_N}$	$S_N, K_{N+1}, T_{N+1}, R_N, Q_N, \sigma_N^{CALIB^C}, C_N, BSMGreeks_N^C, HParams_N^C, C_N^{HC}$	1	18	18	6	101	3%	17%	6%	9%	6	105	3%	17%	6%	9%
$L1C6_N$	$C_{N+1}^{L1C6_N}$	$S_N, K_{N+1}, T_{N+1}, R_N, Q_N, HParams_N^C, C_N^{HC}$	1	11	11	2	93	0%	8%	6%	8%	2	96	0%	8%	6%	9%
$L1C7_N$	$C_{N+1}^{L1C7_N}$	$S_N, K_{N+1}, T_{N+1}, R_N, Q_N, \sigma_N^{CALIB^C}, BSMGreeks_N^C, C_N^{BSMC}$	1	12	12	4	67	2%	13%	4%	6%	5	75	2%	16%	4%	7%
$L1C8_N$	$C_{N+1}^{L1C8_N}$	$S_N, K_{N+1}, T_{N+1}, R_N, Q_N, HJDParams_N^C, C_N^{HJDC}$	1	14	14	9	135	6%	23%	9%	12%	**11**	**142**	8%	27%	9%	12%
$L1C9_N$	$C_{N+1}^{L1C9_N}$	$S_N, K_{N+1}, T_{N+1}, R_N, Q_N, FMLSParams_N^C, C_N^{FMLSC}$	1	8	8	0	35	0%	0%	2%	4%	0	35	0%	0%	2%	3%

Table A.2.2: Call Price Comparison (amongst Parametric and MLP $M1C_N - Models$): This table presents a performance comparison using both daily and monthly statistics amongst the Black-Scholes-Merton ($BSMC_N$) model, Heston (HC_N) model, Heston Jump Diffusion ($HJDC_N$) model, Finite Moment Log Stable ($FMLSC_N$) model and the MLP $M1C_N - Models$ ($M1C1_N$ to $M1C9_N$). The forecast variable for all the models is the one-day-ahead call option price (C_{N+1}). The models denoted by the N subscript use lagged input variables for forecasting C_{N+1}. The one-day-ahead forecast errors of C_{N+1} are used to compute the Root Mean Square Error (RMSE). Column I identifies the models, column II identifies the forecast variable, column III lists the input variables used by the models to obtain the one-trading-day ahead forecast of C_{N+1}, and columns IV, V and VI describe the network architecture of the MLP $M1C_N - Models$. Forecasts are made for 1,328 trading days, and there are 64 months covered in the sample using the monthly data.

When comparing all models simultaneously (i.e. including the random walk model (δC_N), column VII reports the number of months out of the 64 months that each model has the smallest RMSE, while column VIII reports the number of days out of the 1,328 days each model has the smallest RMSE. Columns IX (lower bound) and X (upper bound) present the winning percentage out of 64 months for each model, evaluated using the bootstrap sampling technique. The statistical bootstrap performed (with replacement) at a 95% confidence level is computed from the monthly RMSE values of the respective models below. Columns XI (lower bound), XII (upper bound) presents the winning percentage out of 1326 days for each model computed from bootstrapping the daily RMSE values of the respective models at a 95% confidence level.

Similarly, when the δC_N model was excluded in the comparison, column XIII report the number of months out of the 64 months that each model has the smallest RMSE, while column XIV reports the number of days out of the 1,328 days each model has the smallest RMSE. Columns XV (lower bound) and XVI (upper bound) present the winning percentage out of 64 months for each model, evaluated using the bootstrap sampling technique. The statistical bootstrap performed (with replacement) at a 95% confidence level is computed from the monthly RMSE values of the respective models below. Also, columns XVII (lower bound) and XVIII (upper bound) present the winning percentage out of 1326 days for each model computed from bootstrapping the daily RMSE values of the respective models at a 95% confidence level.

						Including the random walk						**Excluding the random walk**					
(I) Model	**(II) Forecast**	**(III) Inputs**	**(IV) No. of hidden layers**	**(V) No. of hidden nodes per layer**	**(VI) Network architecture**	**(VII) Performance amongst all models (Monthly)**	**(VIII) Performance amongst all models (Daily)**	**(IX) 2.5% lower bound- (for monthly) (%)**	**(X) 2.5% upper bound- (for monthly) (%)**	**(XI) 2.5% lower bound- (for daily) (%)**	**(XII) 2.5% upper bound- (for daily) (%)**	**(XIII) Performance amongst all models (Monthly)**	**(XIV) Performance amongst all models (Daily)**	**(XV) 2.5% lower bound- (for monthly) (%)**	**(XVI) 2.5% upper bound- (for monthly) (%)**	**(XVII) 2.5% lower bound- (for daily) (%)**	**(XVIII) 2.5% upper bound- (for daily) (%)**
δC_N	C_{N+1}	C_N	-	-	-	**18**	**234**	17%	39%	16%	20%	-	-	-	-	-	-
$BSMC_N$	$C_{N+1}^{BSMC_N}$	$S_N, K_{N+1}, T_{N+1}, R_N, Q_N, \sigma_N^{CALIB^C}$	-	-	-	0	124	0%	0%	8%	11%	0	124	0%	0%	8%	11%
HC_N	$C_{N+1}^{HC_N}$	$S_N, K_{N+1}, T_{N+1}, R_N, Q_N, \sigma_N^{CALIB^C}, HParams_N^C$	-	-	-	3	163	0%	11%	11%	14%	3	170	0%	11%	11%	15%
$HJDC_N$	$C_{N+1}^{HJDC_N}$	$S_N, K_{N+1}, T_{N+1}, R_N, Q_N, \sigma_N^{CALIB^C}, HJDParams_N^C$	-	-	-	0	16	0%	0%	1%	2%	0	52	0%	0%	3%	5%
$FMLSC_N$	$C_{N+1}^{FMLSC_N}$	$S_N, K_{N+1}, T_{N+1}, R_N, Q_N, FMLSParams_N^C$	-	-	-	0	221	0%	0%	15%	19%	0	**229**	0%	0%	15%	19%
$M1C1_N$	$C_{N+1}^{M1C1_N}$	$S_N, K_{N+1}, T_{N+1}, R_N, Q_N, \sigma_N^{CALIB^C}$	1	6	6	0	50	0%	0%	3%	5%	0	50	0%	0%	3%	5%
$M1C2_N$	$C_{N+1}^{M1C2_N}$	$S_N, K_{N+1}, T_{N+1}, R_N, Q_N, \sigma_N^{CALIB^C}, C_N$	1	7	7	6	49	3%	17%	3%	5%	6	50	3%	17%	3%	5%
$M1C3_N$	$C_{N+1}^{M1C3_N}$	$S_N, K_{N+1}, T_{N+1}, R_N, Q_N, \sigma_N^{CALIB^C}, C_N, BSMGreeks_N^C$	1	12	12	4	124	2%	13%	8%	11%	4	144	2%	13%	9%	13%
$M1C4_N$	$C_{N+1}^{M1C4_N}$	$S_N, K_{N+1}, T_{N+1}, R_N, Q_N, \sigma_N^{CALIB^C}, C_N, BSMGreeks_N^C, HParams_N^C$	1	17	17	3	93	0%	9%	6%	8%	8	140	6%	22%	9%	12%
$M1C5_N$	$C_{N+1}^{M1C5_N}$	$S_N, K_{N+1}, T_{N+1}, R_N, Q_N, \sigma_N^{CALIB^C}, C_N, BSMGreeks_N^C, HParams_N^C, C_N^{HC}$	1	18	18	7	45	5%	19%	3%	4%	11	81	8%	27%	5%	7%
$M1C6_N$	$C_{N+1}^{M1C6_N}$	$S_N, K_{N+1}, T_{N+1}, R_N, Q_N, HParams_N^C, C_N^{HC}$	1	11	11	6	37	3%	17%	2%	4%	8	54	5%	20%	3%	5%
$M1C7_N$	$C_{N+1}^{M1C7_N}$	$S_N, K_{N+1}, T_{N+1}, R_N, Q_N, \sigma_N^{CALIB^C}, BSMGreeks_N^C, C_N^{BSMC}$	1	12	12	13	104	11%	31%	6%	9%	**13**	117	11%	30%	7%	10%
$M1C8_N$	$C_{N+1}^{M1C8_N}$	$S_N, K_{N+1}, T_{N+1}, R_N, Q_N, HJDParams_N^C, C_N^{HJDC}$	1	14	14	3	23	0%	11%	1%	2%	10	59	8%	25%	3%	6%
$M1C9_N$	$C_{N+1}^{M1C9_N}$	$S_N, K_{N+1}, T_{N+1}, R_N, Q_N, FMLSParams_N^C, C_N^{FMLSC}$	1	8	8	1	45	0%	5%	2%	4%	1	58	0%	5%	3%	5%

Table A.2.3: Call Price Comparison (amongst Parametric and LSTM $L1C_N - Models$): This table presents a performance comparison using both daily and monthly statistics amongst the Black-Scholes-Merton ($BSMC_N$) model, Heston (HC_N) model, Heston Jump Diffusion ($HJDC_N$) model, Finite Moment Log Stable ($FMLSC_N$) model and the LSTM $L1C_N - Models$ ($L1C1_N$ to $L1C9_N$). The forecast variable for all the models is the one-day-ahead call option price (C_{N+1}). The models denoted by the $_N$ subscript use lagged input variables for forecasting C_{N+1}. The one-day-ahead forecast errors of C_{N+1} are used to compute the Root Mean Square Error (RMSE). Column I identifies the models, column II identifies the forecast variable, column III lists the input variables used by the models to obtain the one-trading-day ahead forecast of C_{N+1}, and columns IV, V and VI describe the network architecture of the LSTM $L1C_N - Models$. Forecasts are made for 1,328 trading days, and there are 64 months covered in the sample using the monthly data.

When comparing all models simultaneously (i.e. including the random walk model (δC_N), column VII reports the number of months out of the 64 months that each model has the smallest RMSE, while column VIII reports the number of days out of the 1,328 days each model has the smallest RMSE. Columns IX (lower bound) and X (upper bound) present the winning percentage out of 64 months for each model, evaluated using the bootstrap sampling technique. The statistical bootstrap performed (with replacement) at a 95% confidence level is computed from the monthly RMSE values of the respective models below. Columns XI (lower bound) and XII (upper bound) present the winning percentage out of 1326 days for each model computed from bootstrapping the daily RMSE values of the respective models at a 95% confidence level.

Similarly, when the δC_N model was excluded in the comparison, column XIII report the number of months out of the 64 months that each model has the smallest RMSE, while column XIV reports the number of days out of the 1,328 days each model has the smallest RMSE. Columns XV (lower bound) and XVI (upper bound) present the winning percentage out of 64 months for each model, evaluated using the bootstrap sampling technique. The statistical bootstrap performed (with replacement) at a 95% confidence level is computed from the monthly RMSE values of the respective models below. Also, columns XVII (lower bound) and XVIII (upper bound) present the winning percentage out of 1326 days for each model computed from bootstrapping the daily RMSE values of the respective models at a 95% confidence level.

						Including the random walk						**Excluding the random walk**					
(I) Model	**(II) Forecast**	**(III) Inputs**	**(IV) No. of hidden layers**	**(V) No. of hidden nodes per layer**	**(VI) Network architecture**	**(VII) Performance amongst all models (Monthly)**	**(VIII) Performance amongst all models (Daily)**	**(IX) 2.5% lower bound-(for monthly) (%)**	**(X) 2.5% upper bound-(for monthly) (%)**	**(XI) 2.5% lower bound-(for daily) (%)**	**(XII) 2.5% upper bound-(for daily) (%)**	**(XIII) Performance amongst all models (Monthly)**	**(XIV) Performance amongst all models (Daily)**	**(XV) 2.5% lower bound-(for monthly) (%)**	**(XVI) 2.5% upper bound-(for monthly) (%)**	**(XVII) 2.5% lower bound-(for daily) (%)**	**(XVIII) 2.5% upper bound-(for daily) (%)**
δC_N	C_{N+1}	C_N	-	-	-	**27**	**248**	31%	55%	17%	21%	-	-	-	-	-	-
$BSMC_N$	$C_{N+1}^{BSMC_N}$	$S_N, K_{N+1}, T_{N+1}, R_N, Q_N, \sigma_N^{CALIB^C}$	-	-	-	0	72	0%	0%	4%	7%	0	72	0%	0%	4%	7%
HC_N	$C_{N+1}^{HC_N}$	$S_N, K_{N+1}, T_{N+1}, R_N, Q_N, \sigma_N^{CALIB^C}, HParams_N^C$	-	-	-	6	133	3%	17%	8%	12%	7	145	5%	19%	9%	13%
$HJDC_N$	$C_{N+1}^{HJDC_N}$	$S_N, K_{N+1}, T_{N+1}, R_N, Q_N, \sigma_N^{CALIB^C}, HJDParams_N^C$	-	-	-	1	18	0%	5%	1%	2%	**16**	144	15%	36%	9%	13%
$FMLSC_N$	$C_{N+1}^{FMLSC_N}$	$S_N, K_{N+1}, T_{N+1}, R_N, Q_N, FMLSParams_N^C$	-	-	-	0	61	0%	0%	4%	6%	0	65	0%	0%	4%	6%
$L1C1_N$	$C_{N+1}^{L1C1_N}$	$S_N, K_{N+1}, T_{N+1}, R_N, Q_N, \sigma_N^{CALIB^C}$	1	6	6	0	2	0%	0%	0%	0%	0	2	0%	0%	0%	0%
$L1C2_N$	$C_{N+1}^{L1C2_N}$	$S_N, K_{N+1}, T_{N+1}, R_N, Q_N, \sigma_N^{CALIB^C}, C_N$	1	7	7	0	93	0%	0%	6%	8%	0	93	0%	0%	6%	8%
$L1C3_N$	$C_{N+1}^{L1C3_N}$	$S_N, K_{N+1}, T_{N+1}, R_N, Q_N, \sigma_N^{CALIB^C}, C_N, BSMGreeks_N^C$	1	12	12	0	87	0%	0%	5%	8%	0	88	0%	0%	5%	8%
$L1C4_N$	$C_{N+1}^{L1C4_N}$	$S_N, K_{N+1}, T_{N+1}, R_N, Q_N, \sigma_N^{CALIB^C}, C_N, BSMGreeks_N^C, HParams_N^C$	1	17	17	0	122	0%	0%	8%	11%	1	124	0%	5%	8%	11%
$L1C5_N$	$C_{N+1}^{L1C5_N}$	$S_N, K_{N+1}, T_{N+1}, R_N, Q_N, \sigma_N^{CALIB^C}, C_N, BSMGreeks_N^C, HParams_N^C, C_N^{HC}$	1	18	18	8	116	5%	20%	7%	10%	11	142	9%	27%	9%	12%
$L1C6_N$	$C_{N+1}^{L1C6_N}$	$S_N, K_{N+1}, T_{N+1}, R_N, Q_N, HParams_N^C, C_N^{HC}$	1	11	11	5	103	2%	14%	6%	9%	5	118	2%	16%	7%	10%
$L1C7_N$	$C_{N+1}^{L1C7_N}$	$S_N, K_{N+1}, T_{N+1}, R_N, Q_N, \sigma_N^{CALIB^C}, BSMGreeks_N^C, C_N^{BSMC}$	1	12	12	7	92	3%	19%	5%	8%	9	123	6%	22%	8%	11%
$L1C8_N$	$C_{N+1}^{L1C8_N}$	$S_N, K_{N+1}, T_{N+1}, R_N, Q_N, HJDParams_N^C, C_N^{HJDC}$	1	14	14	10	142	8%	25%	9%	12%	15	**171**	14%	34%	11%	15%
$L1C9_N$	$C_{N+1}^{L1C9_N}$	$S_N, K_{N+1}, T_{N+1}, R_N, Q_N, FMLSParams_N^C, C_N^{FMLSC}$	1	8	8	0	39	0%	0%	2%	4%	0	41	0%	0%	2%	4%

Table A.2.4: Call Price Comparison (amongst Parametric, MLP $M2C_N - Models$ and LSTM $L2C_N - Models$): This table presents a performance comparison using both daily and monthly statistics amongst the Black-Scholes-Merton ($BSMC_N$) model, Heston (HC_N) model, Heston Jump Diffusion ($HJDC_N$) model, Finite Moment Log Stable ($FMLSC_N$) model, MLP $M2C_N - Models$ ($M2C1_N$ to $M2C9_N$) and the LSTM $L2C_N - Models$ ($L2C1_N$ to $L2C9_N$). The forecast variable for all the models is the one-day-ahead call option price (C_{N+1}). The models denoted by the $_N$ subscript use lagged input variables for forecasting C_{N+1}. The one-day-ahead forecast errors of C_{N+1} are used to compute the Root Mean Square Error (RMSE). Column I identifies the models, column II identifies the forecast variable, column III lists the input variables used by the models to obtain the one-trading-day ahead forecast of C_{N+1}, and columns IV, V and VI describe the network architecture of the MLP $M2C_N - Models$ and the LSTM $L2C_N - Models$. Forecasts are made for 1,328 trading days, and there are 64 months covered in the sample using the monthly data.

When comparing all models simultaneously (i.e. including the random walk model (δC_N), column VII reports the number of months out of the 64 months that each model has the smallest RMSE, while column VIII reports the number of days out of the 1,328 days each model has the smallest RMSE. Columns IX (lower bound) and X (upper bound) present the winning percentage out of 64 months for each model, evaluated using the bootstrap sampling technique. The statistical bootstrap performed (with replacement) at a 95% confidence level is computed from the monthly RMSE values of the respective models below. Columns XI (lower bound) and XII (upper bound) present the winning percentage out of 1326 days for each model computed from bootstrapping the daily RMSE values of the respective models at a 95% confidence level.

Similarly, when the δC_N model was excluded in the comparison, column XIII report the number of months out of the 64 months that each model has the smallest RMSE, while column XIV reports the number of days out of the 1,328 days each model has the smallest RMSE. Columns XV (lower bound) and XVI (upper bound) present the winning percentage out of 64 months for each model, evaluated using the bootstrap sampling technique. The statistical bootstrap performed (with replacement) at a 95% confidence level is computed from the monthly RMSE values of the respective models below. Also, columns XVII (lower bound) and XVIII (upper bound) present the winning percentage out of 1326 days for each model computed from bootstrapping the daily RMSE values of the respective models at a 95% confidence level.

						Including the random walk						Excluding the random walk					
(I) Model	**(II) Forecast**	**(III) Inputs**	**(IV) No. of hidden layers**	**(V) No. of hidden nodes per layer**	**(VI) Network architecture**	**(VII) Performance amongst all models (Monthly)**	**(VIII) Performance amongst all models (Daily)**	**(IX) 2.5% lower bound- (for monthly) (%)**	**(X) 2.5% upper bound- (for monthly) (%)**	**(XI) 2.5% lower bound- (for daily) (%)**	**(XII) 2.5% upper bound- (for daily) (%)**	**(XIII) Performance amongst all models (Monthly)**	**(XIV) Performance amongst all models (Daily)**	**(XV) 2.5% lower bound- (for monthly) (%)**	**(XVI) 2.5% upper bound- (for monthly) (%)**	**(XVII) 2.5% lower bound- (for daily) (%)**	**(XVIII) 2.5% upper bound- (for daily) (%)**
δC_N	C_{N+1}	C_N	-	-	-	10	142	8%	25%	9%	12%	-	-	-	-	-	-
$BSMC_N$	$C_{N+1}^{BSMC_N}$	$S_N, K_{N+1}, T_{N+1}, R_N, Q_N, \sigma_N^{CALIB^C}$	-	-	-	0	67	0%	0%	4%	6%	0	67	0%	0%	4%	6%
HC_N	$C_{N+1}^{HC_N}$	$S_N, K_{N+1}, T_{N+1}, R_N, Q_N, \sigma_N^{CALIB^C}, HParams_N^C$	-	-	-	3	66	0%	9%	4%	6%	3	67	0%	11%	4%	6%
$HJDC_N$	$C_{N+1}^{HJDC_N}$	$S_N, K_{N+1}, T_{N+1}, R_N, Q_N, \sigma_N^{CALIB^C}, HJDParams_N^C$	-	-	-	0	5	0%	0%	0%	1%	0	21	0%	0%	1%	2%
$FMLSC_N$	$C_{N+1}^{FMLSC_N}$	$S_N, K_{N+1}, T_{N+1}, R_N, Q_N, FMLSParams_N^C$	-	-	-	0	29	0%	0%	1%	3%	0	29	0%	0%	1%	3%
$M2C1_N$	$C_{N+1}^{M2C1_N}$	$S_N, K_{N+1}, T_{N+1}, R_N, Q_N, \sigma_N^{CALIB^C}$	2	6	6 X 6	3	38	0%	11%	2%	4%	3	40	0%	9%	2%	4%
$M2C2_N$	$C_{N+1}^{M2C2_N}$	$S_N, K_{N+1}, T_{N+1}, R_N, Q_N, \sigma_N^{CALIB^C}, C_N$	2	7	7 X 7	0	38	0%	0%	2%	4%	0	43	0%	0%	2%	4%
$M2C3_N$	$C_{N+1}^{M2C3_N}$	$S_N, K_{N+1}, T_{N+1}, R_N, Q_N, \sigma_N^{CALIB^C}, C_N, BSMGreeks_N^C$	2	12	12 X 12	5	54	2%	14%	3%	5%	5	70	2%	14%	4%	7%
$M2C4_N$	$C_{N+1}^{M2C4_N}$	$S_N, K_{N+1}, T_{N+1}, R_N, Q_N, \sigma_N^{CALIB^C}, C_N, BSMGreeks_N^C, HParams_N^C$	2	17	17 X 17	4	43	2%	13%	2%	4%	6	56	3%	17%	3%	5%
$M2C5_N$	$C_{N+1}^{M2C5_N}$	$S_N, K_{N+1}, T_{N+1}, R_N, Q_N, \sigma_N^{CALIB^C}, C_N, BSMGreeks_N^C, HParams_N^C, C_N^{HC}$	2	18	18 X 18	2	16	0%	8%	1%	2%	3	30	0%	11%	2%	3%
$M2C6_N$	$C_{N+1}^{M2C6_N}$	$S_N, K_{N+1}, T_{N+1}, R_N, Q_N, HParams_N^C, C_N^{HC}$	2	11	11 X 11	3	12	0%	11%	0%	1%	4	30	2%	13%	2%	3%
$M2C7_N$	$C_{N+1}^{M2C7_N}$	$S_N, K_{N+1}, T_{N+1}, R_N, Q_N, \sigma_N^{CALIB^C}, BSMGreeks_N^C, C_N^{BSMC}$	2	12	12 X 12	6	26	3%	17%	1%	3%	7	41	3%	19%	2%	4%
$M2C8_N$	$C_{N+1}^{M2C8_N}$	$S_N, K_{N+1}, T_{N+1}, R_N, Q_N, HJDParams_N^C, C_N^{HJDC}$	2	14	14 X 14	0	3	0%	0%	0%	1%	4	15	2%	13%	1%	2%
$M2C9_N$	$C_{N+1}^{M2C9_N}$	$S_N, K_{N+1}, T_{N+1}, R_N, Q_N, FMLSParams_N^C, C_N^{FMLSC}$	2	8	8 X 8	3	16	0%	11%	1%	2%	3	26	0%	11%	1%	3%
$L2C1_N$	$C_{N+1}^{L2C1_N}$	$S_N, K_{N+1}, T_{N+1}, R_N, Q_N, \sigma_N^{CALIB^C}$	2	6	6 X 6	0	22	0%	0%	1%	2%	0	22	0%	0%	1%	2%
$L2C2_N$	$C_{N+1}^{L2C2_N}$	$S_N, K_{N+1}, T_{N+1}, R_N, Q_N, \sigma_N^{CALIB^C}, C_N$	2	7	7 X 7	0	126	0%	0%	8%	11%	0	126	0%	0%	8%	11%
$L2C3_N$	$C_{N+1}^{L2C3_N}$	$S_N, K_{N+1}, T_{N+1}, R_N, Q_N, \sigma_N^{CALIB^C}, C_N, BSMGreeks_N^C$	2	12	12 X 12	0	81	0%	0%	5%	7%	0	83	0%	0%	5%	8%
$L2C4_N$	$C_{N+1}^{L2C4_N}$	$S_N, K_{N+1}, T_{N+1}, R_N, Q_N, \sigma_N^{CALIB^C}, C_N, BSMGreeks_N^C, HParams_N^C$	2	17	17 X 17	0	108	0%	0%	7%	10%	0	109	0%	0%	7%	10%
$L2C5_N$	$C_{N+1}^{L2C5_N}$	$S_N, K_{N+1}, T_{N+1}, R_N, Q_N, \sigma_N^{CALIB^C}, C_N, BSMGreeks_N^C, HParams_N^C, C_N^{HC}$	2	18	18 X 18	2	74	0%	8%	4%	7%	2	79	0%	8%	5%	7%
$L2C6_N$	$C_{N+1}^{L2C6_N}$	$S_N, K_{N+1}, T_{N+1}, R_N, Q_N, HParams_N^C, C_N^{HC}$	2	11	11 X 11	6	57	3%	17%	3%	6%	6	62	3%	17%	4%	6%
$L2C7_N$	$C_{N+1}^{L2C7_N}$	$S_N, K_{N+1}, T_{N+1}, R_N, Q_N, \sigma_N^{CALIB^C}, BSMGreeks_N^C, C_N^{BSMC}$	2	12	12 X 12	5	44	2%	14%	2%	4%	5	47	2%	14%	3%	4%
$L2C8_N$	$C_{N+1}^{L2C8_N}$	$S_N, K_{N+1}, T_{N+1}, R_N, Q_N, HJDParams_N^C, C_N^{HJDC}$	2	14	14 X 14	**11**	101	9%	27%	6%	9%	**12**	104	9%	30%	6%	9%
$L2C9_N$	$C_{N+1}^{L2C9_N}$	$S_N, K_{N+1}, T_{N+1}, R_N, Q_N, FMLSParams_N^C, C_N^{FMLSC}$	2	8	8 X 8	1	**160**	0%	5%	10%	14%	1	**161**	0%	5%	10%	14%

Table A.2.5: Call Price Comparison (amongst Parametric and MLP $M2C_N - Models$): This table presents a performance comparison using both daily and monthly statistics amongst the Black-Scholes-Merton ($BSMC_N$) model, Heston (HC_N) model, Heston Jump Diffusion ($HJDC_N$) model, Finite Moment Log Stable ($FMLSC_N$) model and the MLP $M2C_N - Models$ ($M2C1_N$ to $M2C9_N$). The forecast variable for all the models is the one-day-ahead call option price (C_{N+1}). The models denoted by the $_N$ subscript use lagged input variables for forecasting C_{N+1}. The one-day-ahead forecast errors of C_{N+1} are used to compute the Root Mean Square Error (RMSE). Column I identifies the models, column II identifies the forecast variable, column III lists the input variables used by the models to obtain the one-trading-day ahead forecast of C_{N+1}, and columns IV, V and VI describe the network architecture of the MLP $M2C_N - Models$. Forecasts are made for 1,328 trading days, and there are 64 months covered in the sample using the monthly data.
When comparing all models simultaneously (i.e. including the random walk model (δC_N), column VII reports the number of months out of the 64 months that each model has the smallest RMSE, while column VIII reports the number of days out of the 1,328 days each model has the smallest RMSE. Columns IX (lower bound) and X (upper bound) present the winning percentage out of 64 months for each model, evaluated using the bootstrap sampling technique. The statistical bootstrap performed (with replacement) at a 95% confidence level is computed from the monthly RMSE values of the respective models below. Columns XI (lower bound) and XII (upper bound) present the winning percentage out of 1326 days for each model computed from bootstrapping the daily RMSE values of the respective models at a 95% confidence level.
Similarly, when the δC_N model was excluded in the comparison, column XIII report the number of months out of the 64 months that each model has the smallest RMSE, while column XIV reports the number of days out of the 1,328 days each model has the smallest RMSE. Columns XV (lower bound) and XVI (upper bound) present the winning percentage out of 64 months for each model, evaluated using the bootstrap sampling technique. The statistical bootstrap performed (with replacement) at a 95% confidence level is computed from the monthly RMSE values of the respective models below. Also, columns XVII (lower bound) and XVIII (upper bound) present the winning percentage out of 1326 days for each model computed from bootstrapping the daily RMSE values of the respective models at a 95% confidence level.

						Including the random walk						**Excluding the random walk**					
(I) Model	**(II) Forecast**	**(III) Inputs**	**(IV) No. of hidden layers**	**(V) No. of hidden nodes per layer**	**(VI) Network architecture**	**(VII) Performance amongst all models (Monthly)**	**(VIII) Performance amongst all models (Daily)**	**(IX) 2.5% lower bound- (for monthly) (%)**	**(X) 2.5% upper bound- (for monthly) (%)**	**(XI) 2.5% lower bound- (for daily) (%)**	**(XII) 2.5% upper bound- (for daily) (%)**	**(XIII) Performance amongst all models (Monthly)**	**(XIV) Performance amongst all models (Daily)**	**(XV) 2.5% lower bound- (for monthly) (%)**	**(XVI) 2.5% upper bound- (for monthly) (%)**	**(XVII) 2.5% lower bound- (for daily) (%)**	**(XVIII) 2.5% upper bound- (for daily) (%)**
δC_N	C_{N+1}	C_N	-	-	-	**15**	217	14%	34%	15%	18%	-	-	-	-	-	-
$BSMC_N$	$C_{N+1}^{BSMC_N}$	$S_N, K_{N+1}, T_{N+1}, R_N, Q_N, \sigma_N^{CALIB^C}$	-	-	-	0	122	0%	0%	8%	11%	0	122	0%	0%	8%	11%
HC_N	$C_{N+1}^{HC_N}$	$S_N, K_{N+1}, T_{N+1}, R_N, Q_N, \sigma_N^{CALIB^C}, HParams_N^C$	-	-	-	3	153	0%	10%	10%	13%	3	155	0%	11%	10%	13%
$HJDC_N$	$C_{N+1}^{HJDC_N}$	$S_N, K_{N+1}, T_{N+1}, R_N, Q_N, \sigma_N^{CALIB^C}, HJDParams_N^C$	-	-	-	1	16	0%	5%	1%	2%	2	40	0%	8%	2%	4%
$FMLSC_N$	$C_{N+1}^{FMLSC_N}$	$S_N, K_{N+1}, T_{N+1}, R_N, Q_N, FMLSParams_N^C$	-	-	-	0	**223**	0%	0%	15%	19%	0	**230**	0%	0%	15%	19%
$M2C1_N$	$C_{N+1}^{M2C1_N}$	$S_N, K_{N+1}, T_{N+1}, R_N, Q_N, \sigma_N^{CALIB^C}$	2	6	6 X 6	4	99	2%	13%	6%	9%	4	102	2%	13%	6%	9%
$M2C2_N$	$C_{N+1}^{M2C2_N}$	$S_N, K_{N+1}, T_{N+1}, R_N, Q_N, \sigma_N^{CALIB^C}, C_N$	2	7	7 X 7	0	87	0%	0%	5%	8%	1	97	0%	5%	6%	9%
$M2C3_N$	$C_{N+1}^{M2C3_N}$	$S_N, K_{N+1}, T_{N+1}, R_N, Q_N, \sigma_N^{CALIB^C}, C_N, BSMGreeks_N^C$	2	12	12 X 12	7	96	3%	19%	6%	9%	7	116	5%	19%	7%	10%
$M2C4_N$	$C_{N+1}^{M2C4_N}$	$S_N, K_{N+1}, T_{N+1}, R_N, Q_N, \sigma_N^{CALIB^C}, C_N, BSMGreeks_N^C, HParams_N^C$	2	17	17 X 17	5	91	2%	16%	5%	8%	8	111	5%	22%	7%	10%
$M2C5_N$	$C_{N+1}^{M2C5_N}$	$S_N, K_{N+1}, T_{N+1}, R_N, Q_N, \sigma_N^{CALIB^C}, C_N, BSMGreeks_N^C, HParams_N^C, C_N^{HC}$	2	18	18 X 18	4	45	2%	13%	2%	4%	6	69	3%	17%	4%	6%
$M2C6_N$	$C_{N+1}^{M2C6_N}$	$S_N, K_{N+1}, T_{N+1}, R_N, Q_N, HParams_N^C, C_N^{HC}$	2	11	11 X 11	5	36	2%	16%	2%	4%	6	63	3%	17%	4%	6%
$M2C7_N$	$C_{N+1}^{M2C7_N}$	$S_N, K_{N+1}, T_{N+1}, R_N, Q_N, \sigma_N^{CALIB^C}, BSMGreeks_N^C, C_N^{BSMC}$	2	12	12 X 12	14	78	11%	30%	5%	7%	**16**	99	13%	33%	6%	9%
$M2C8_N$	$C_{N+1}^{M2C8_N}$	$S_N, K_{N+1}, T_{N+1}, R_N, Q_N, HJDParams_N^C, C_N^{HJDC}$	2	14	14 X 14	3	26	0%	11%	1%	3%	7	64	3%	19%	4%	6%
$M2C9_N$	$C_{N+1}^{M2C9_N}$	$S_N, K_{N+1}, T_{N+1}, R_N, Q_N, FMLSParams_N^C, C_N^{FMLSC}$	2	8	8 X 8	4	39	2%	13%	2%	4%	5	60	2%	14%	3%	6%

Table A.2.6: Call Price Comparison (amongst Parametric and LSTM $L2C_N - Models$): This table presents a performance comparison using both daily and monthly statistics amongst the Black-Scholes-Merton ($BSMC_N$) model, Heston (HC_N) model, Heston Jump Diffusion ($HJDC_N$) model, Finite Moment Log Stable ($FMLSC_N$) model and the LSTM $L2C_N - Models$ ($L2C1_N$ to $L2C9_N$). The forecast variable for all the models is the one-day-ahead call option price (C_{N+1}). The models denoted by the $_N$ subscript use lagged input variables for forecasting C_{N+1}. The one-day-ahead forecast errors of C_{N+1} are used to compute the Root Mean Square Error (RMSE). Column I identifies the models, column II identifies the forecast variable, column III lists the input variables used by the models to obtain the one-trading-day ahead forecast of C_{N+1}, and columns IV, V and VI describe the network architecture of the LSTM $L2C_N - Models$. Forecasts are made for 1,328 trading days, and there are 64 months covered in the sample using the monthly data.

When comparing all models simultaneously (i.e. including the random walk model (δC_N), column VII reports the number of months out of the 64 months that each model has the smallest RMSE, while column VIII reports the number of days out of the 1,328 days each model has the smallest RMSE. Columns IX (lower bound) and X (upper bound) present the winning percentage out of 64 months for each model, evaluated using the bootstrap sampling technique. The statistical bootstrap performed (with replacement) at a 95% confidence level is computed from the monthly RMSE values of the respective models below. Columns XI (lower bound) and XII (upper bound) present the winning percentage out of 1326 days for each model computed from bootstrapping the daily RMSE values of the respective models at a 95% confidence level.

Similarly, when the δC_N model was excluded in the comparison, column XIII report the number of months out of the 64 months that each model has the smallest RMSE, while column XIV reports the number of days out of the 1,328 days each model has the smallest RMSE. Columns XV (lower bound) and XVI (upper bound) present the winning percentage out of 64 months for each model, evaluated using the bootstrap sampling technique. The statistical bootstrap performed (with replacement) at a 95% confidence level is computed from the monthly RMSE values of the respective models below. Also, columns XVII (lower bound) and XVIII (upper bound) present the winning percentage out of 1326 days for each model computed from bootstrapping the daily RMSE values of the respective models at a 95% confidence level.

						Including the random walk						**Excluding the random walk**					
(I) Model	**(II) Forecast**	**(III) Inputs**	**(IV) No. of hidden layers**	**(V) No. of hidden nodes per layer**	**(VI) Network architecture**	**(VII) Performance amongst all models (Monthly)**	**(VIII) Performance amongst all models (Daily)**	**(IX) 2.5% lower bound- (for monthly) (%)**	**(X) 2.5% upper bound- (for monthly) (%)**	**(XI) 2.5% lower bound- (for daily) (%)**	**(XII) 2.5% upper bound- (for daily) (%)**	**(XIII) Performance amongst all models (Monthly)**	**(XIV) Performance amongst all models (Daily)**	**(XV) 2.5% lower bound- (for monthly) (%)**	**(XVI) 2.5% upper bound- (for monthly) (%)**	**(XVII) 2.5% lower bound- (for daily) (%)**	**(XVIII) 2.5% upper bound- (for daily) (%)**
δC_N	C_{N+1}	C_N	-	-	-	**22**	**231**	22%	45%	15%	19%	-	-	-	-	-	-
$BSMC_N$	$C_{N+1}^{BSMC_N}$	$S_N, K_{N+1}, T_{N+1}, R_N, Q_N, \sigma_N^{CALIB^C}$	-	-	-	0	68	0%	0%	4%	6%	0	68	0%	0%	4%	6%
HC_N	$C_{N+1}^{HC_N}$	$S_N, K_{N+1}, T_{N+1}, R_N, Q_N, \sigma_N^{CALIB^C}, HParams_N^C$	-	-	-	10	122	8%	25%	8%	11%	11	138	8%	27%	9%	12%
$HJDC_N$	$C_{N+1}^{HJDC_N}$	$S_N, K_{N+1}, T_{N+1}, R_N, Q_N, \sigma_N^{CALIB^C}, HJDParams_N^C$	-	-	-	2	16	0%	8%	1%	2%	15	114	13%	33%	7%	10%
$FMLSC_N$	$C_{N+1}^{FMLSC_N}$	$S_N, K_{N+1}, T_{N+1}, R_N, Q_N, FMLSParams_N^C$	-	-	-	0	38	0%	0%	2%	4%	0	38	0%	0%	2%	4%
$L2C1_N$	$C_{N+1}^{L2C1_N}$	$S_N, K_{N+1}, T_{N+1}, R_N, Q_N, \sigma_N^{CALIB^C}$	2	6	6 X 6	0	22	0%	0%	1%	2%	0	22	0%	0%	1%	2%
$L2C2_N$	$C_{N+1}^{L2C2_N}$	$S_N, K_{N+1}, T_{N+1}, R_N, Q_N, \sigma_N^{CALIB^C}, C_N$	2	7	7 X 7	0	126	0%	0%	8%	11%	0	127	0%	0%	8%	11%
$L2C3_N$	$C_{N+1}^{L2C3_N}$	$S_N, K_{N+1}, T_{N+1}, R_N, Q_N, \sigma_N^{CALIB^C}, C_N, BSMGreeks_N^C$	2	12	12 X 12	0	83	0%	0%	5%	8%	0	86	0%	0%	5%	8%
$L2C4_N$	$C_{N+1}^{L2C4_N}$	$S_N, K_{N+1}, T_{N+1}, R_N, Q_N, \sigma_N^{CALIB^C}, C_N, BSMGreeks_N^C, HParams_N^C$	2	17	17 X 17	0	113	0%	0%	7%	10%	0	116	0%	0%	7%	10%
$L2C5_N$	$C_{N+1}^{L2C5_N}$	$S_N, K_{N+1}, T_{N+1}, R_N, Q_N, \sigma_N^{CALIB^C}, C_N, BSMGreeks_N^C, HParams_N^C, C_N^{HC}$	2	18	18 X 18	4	102	2%	13%	6%	9%	4	121	2%	13%	8%	11%
$L2C6_N$	$C_{N+1}^{L2C6_N}$	$S_N, K_{N+1}, T_{N+1}, R_N, Q_N, HParams_N^C, C_N^{HC}$	2	11	11 X 11	7	66	3%	20%	4%	6%	8	87	5%	20%	5%	8%
$L2C7_N$	$C_{N+1}^{L2C7_N}$	$S_N, K_{N+1}, T_{N+1}, R_N, Q_N, \sigma_N^{CALIB^C}, BSMGreeks_N^C, C_N^{BSMC}$	2	12	12 X 12	6	63	3%	17%	4%	6%	9	104	6%	23%	7%	9%
$L2C8_N$	$C_{N+1}^{L2C8_N}$	$S_N, K_{N+1}, T_{N+1}, R_N, Q_N, HJDParams_N^C, C_N^{HJDC}$	2	14	14 X 14	12	114	9%	28%	7%	10%	**16**	142	16%	36%	9%	12%
$L2C9_N$	$C_{N+1}^{L2C9_N}$	$S_N, K_{N+1}, T_{N+1}, R_N, Q_N, FMLSParams_N^C, C_N^{FMLSC}$	2	8	8 X 8	1	164	0%	5%	11%	14%	1	**165**	0%	5%	11%	14%

Table A.2.7: Call Price Comparison (amongst Parametric, MLP $M3C_N - Models$ and LSTM $L3C_N - Models$): This table presents a performance comparison using both daily and monthly statistics amongst the Black-Scholes-Merton ($BSMC_N$) model, Heston (HC_N) model, Heston Jump Diffusion ($HJDC_N$) model, Finite Moment Log Stable ($FMLSC_N$) model, MLP $M3C_N - Models$ ($M3C1_N$ to $M3C9_N$) and the LSTM $L3C_N - Models$ ($L3C1_N$ to $L3C9_N$). The forecast variable for all the models is the one-day-ahead call option price (C_{N+1}). The models denoted by the $_N$ subscript use lagged input variables for forecasting C_{N+1}. The one-day-ahead forecast errors of C_{N+1} are used to compute the Root Mean Square Error (RMSE). Column I identifies the models, column II identifies the forecast variable, column III lists the input variables used by the models to obtain the one-trading-day ahead forecast of C_{N+1}, and columns IV, V and VI describe the network architecture of the MLP $M3C_N - Models$ and the LSTM $L3C_N - Models$. Forecasts are made for 1,328 trading days, and there are 64 months covered in the sample using the monthly data.

When comparing all models simultaneously (i.e. including the random walk model (δC_N), column VII reports the number of months out of the 64 months that each model has the smallest RMSE, while column VIII reports the number of days out of the 1,328 days each model has the smallest RMSE. Columns IX (lower bound) and X (upper bound) present the winning percentage out of 64 months for each model, evaluated using the bootstrap sampling technique. The statistical bootstrap performed (with replacement) at a 95% confidence level is computed from the monthly RMSE values of the respective models below. Columns XI (lower bound) and XII (upper bound) present the winning percentage out of 1326 days for each model computed from bootstrapping the daily RMSE values of the respective models at a 95% confidence level.

Similarly, when the δC_N model was excluded in the comparison, column XIII report the number of months out of the 64 months that each model has the smallest RMSE, while column XIV reports the number of days out of the 1,328 days each model has the smallest RMSE. Columns XV (lower bound) and XVI (upper bound) present the winning percentage out of 64 months for each model, evaluated using the bootstrap sampling technique. The statistical bootstrap performed (with replacement) at a 95% confidence level is computed from the monthly RMSE values of the respective models below. Also, columns XVII (lower bound) and XVIII (upper bound) present the winning percentage out of 1326 days for each model computed from bootstrapping the daily RMSE values of the respective models at a 95% confidence level.

						Including the random walk						Excluding the random walk					
(I)	**(II)**	**(III)**	**(IV)**	**(V)**	**(VI)**	**(VII)**	**(VIII)**	**(IX)**	**(X)**	**(XI)**	**(XII)**	**(XIII)**	**(XIV)**	**(XV)**	**(XVI)**	**(XVII)**	**(XVIII)**
Model	**Forecast**	**Inputs**	**No. of hidden layers**	**No. of hidden nodes per layer**	**Network architecture**	**Performance amongst all models (Monthly)**	**Performance amongst all models (Daily)**	**2.5% lower bound-(for monthly) (%)**	**2.5% upper bound-(for monthly) (%)**	**2.5% lower bound-(for daily) (%)**	**2.5% upper bound-(for daily) (%)**	**Performance amongst all models (Monthly)**	**Performance amongst all models (Daily)**	**2.5% lower bound-(for monthly) (%)**	**2.5% upper bound-(for monthly) (%)**	**2.5% lower bound-(for daily) (%)**	**2.5% upper bound-(for daily) (%)**
δC_N	C_{N+1}	C_N	-	-	-	9	128	6%	22%	8%	11%	-	-	-	-	-	-
$BSMC_N$	$C_{N+1}^{BSMC_N}$	$S_N, K_{N+1}, T_{N+1}, R_N, Q_N, \sigma_N^{CALIB^C}$	-	-	-	0	55	0%	0%	3%	5%	0	55	0%	0%	3%	5%
HC_N	$C_{N+1}^{HC_N}$	$S_N, K_{N+1}, T_{N+1}, R_N, Q_N, \sigma_N^{CALIB^C}, HParams_N^C$	-	-	-	1	71	0%	5%	4%	7%	1	71	0%	5%	4%	6%
$HJDC_N$	$C_{N+1}^{HJDC_N}$	$S_N, K_{N+1}, T_{N+1}, R_N, Q_N, \sigma_N^{CALIB^C}, HJDParams_N^C$	-	-	-	0	5	0%	0%	0%	1%	1	17	0%	5%	1%	2%
$FMLSC_N$	$C_{N+1}^{FMLSC_N}$	$S_N, K_{N+1}, T_{N+1}, R_N, Q_N, FMLSParams_N^C$	-	-	-	0	13	0%	0%	1%	2%	0	13	0%	0%	0%	2%
$M3C1_N$	$C_{N+1}^{M3C1_N}$	$S_N, K_{N+1}, T_{N+1}, R_N, Q_N, \sigma_N^{CALIB^C}$	3	6	6 X 6 X 6	3	44	0%	11%	2%	4%	3	50	0%	9%	3%	5%
$M3C2_N$	$C_{N+1}^{M3C2_N}$	$S_N, K_{N+1}, T_{N+1}, R_N, Q_N, \sigma_N^{CALIB^C}, C_N$	3	7	7 X 7 X 7	1	45	0%	5%	2%	4%	1	53	0%	5%	3%	5%
$M3C3_N$	$C_{N+1}^{M3C3_N}$	$S_N, K_{N+1}, T_{N+1}, R_N, Q_N, \sigma_N^{CALIB^C}, C_N, BSMGreeks_N^C$	3	12	12 X 12 X 12	7	50	5%	20%	3%	5%	7	62	3%	19%	4%	6%
$M3C4_N$	$C_{N+1}^{M3C4_N}$	$S_N, K_{N+1}, T_{N+1}, R_N, Q_N, \sigma_N^{CALIB^C}, C_N, BSMGreeks_N^C, HParams_N^C$	3	17	17 X 17 X 17	3	40	0%	11%	2%	4%	4	53	2%	13%	3%	5%
$M3C5_N$	$C_{N+1}^{M3C5_N}$	$S_N, K_{N+1}, T_{N+1}, R_N, Q_N, \sigma_N^{CALIB^C}, C_N, BSMGreeks_N^C, HParams_N^C, C_N^{HC}$	3	18	18 X 18 X 18	1	12	0%	5%	0%	1%	3	31	0%	10%	2%	3%
$M3C6_N$	$C_{N+1}^{M3C6_N}$	$S_N, K_{N+1}, T_{N+1}, R_N, Q_N, HParams_N^C, C_N^{HC}$	3	11	11 X 11 X 11	4	13	2%	13%	0%	2%	4	21	2%	13%	1%	2%
$M3C7_N$	$C_{N+1}^{M3C7_N}$	$S_N, K_{N+1}, T_{N+1}, R_N, Q_N, \sigma_N^{CALIB^C}, BSMGreeks_N^C, C_N^{BSMC}$	3	12	12 X 12 X 12	8	21	5%	22%	1%	2%	8	36	5%	22%	2%	4%
$M3C8_N$	$C_{N+1}^{M3C8_N}$	$S_N, K_{N+1}, T_{N+1}, R_N, Q_N, HJDParams_N^C, C_N^{HJDC}$	3	14	14 X 14 X 14	1	6	0%	5%	0%	1%	3	16	0%	11%	1%	2%
$M3C9_N$	$C_{N+1}^{M3C9_N}$	$S_N, K_{N+1}, T_{N+1}, R_N, Q_N, FMLSParams_N^C, C_N^{FMLSC}$	3	8	8 X 8 X 8	2	19	0%	8%	1%	2%	4	32	2%	13%	2%	3%
$L3C1_N$	$C_{N+1}^{L3C1_N}$	$S_N, K_{N+1}, T_{N+1}, R_N, Q_N, \sigma_N^{CALIB^C}$	3	6	6 X 6 X 6	0	37	0%	0%	2%	4%	0	37	0%	0%	2%	4%
$L3C2_N$	$C_{N+1}^{L3C2_N}$	$S_N, K_{N+1}, T_{N+1}, R_N, Q_N, \sigma_N^{CALIB^C}, C_N$	3	7	7 X 7 X 7	0	138	0%	0%	9%	12%	0	138	0%	0%	9%	12%
$L3C3_N$	$C_{N+1}^{L3C3_N}$	$S_N, K_{N+1}, T_{N+1}, R_N, Q_N, \sigma_N^{CALIB^C}, C_N, BSMGreeks_N^C$	3	12	12 X 12 X 12	0	86	0%	0%	5%	8%	0	86	0%	0%	5%	8%
$L3C4_N$	$C_{N+1}^{L3C4_N}$	$S_N, K_{N+1}, T_{N+1}, R_N, Q_N, \sigma_N^{CALIB^C}, C_N, BSMGreeks_N^C, HParams_N^C$	3	17	17 X 17 X 17	0	105	0%	0%	6%	9%	0	105	0%	0%	6%	9%
$L3C5_N$	$C_{N+1}^{L3C5_N}$	$S_N, K_{N+1}, T_{N+1}, R_N, Q_N, \sigma_N^{CALIB^C}, C_N, BSMGreeks_N^C, HParams_N^C, C_N^{HC}$	3	18	18 X 18 X 18	2	89	0%	8%	5%	8%	2	91	0%	8%	6%	8%
$L3C6_N$	$C_{N+1}^{L3C6_N}$	$S_N, K_{N+1}, T_{N+1}, R_N, Q_N, HParams_N^C, C_N^{HC}$	3	11	11 X 11 X 11	3	53	0%	11%	3%	5%	3	55	0%	11%	3%	5%
$L3C7_N$	$C_{N+1}^{L3C7_N}$	$S_N, K_{N+1}, T_{N+1}, R_N, Q_N, \sigma_N^{CALIB^C}, BSMGreeks_N^C, C_N^{BSMC}$	3	12	12 X 12 X 12	6	39	3%	16%	2%	4%	7	41	5%	19%	2%	4%
$L3C8_N$	$C_{N+1}^{L3C8_N}$	$S_N, K_{N+1}, T_{N+1}, R_N, Q_N, HJDParams_N^C, C_N^{HJDC}$	3	14	14 X 14 X 14	**13**	90	11%	31%	5%	8%	**13**	96	11%	30%	6%	9%
$L3C9_N$	$C_{N+1}^{L3C9_N}$	$S_N, K_{N+1}, T_{N+1}, R_N, Q_N, FMLSParams_N^C, C_N^{FMLSC}$	3	8	8 X 8 X 8	0	**169**	0%	0%	11%	15%	0	**169**	0%	0%	11%	15%

Table A.2.8: Call Price Comparison (amongst Parametric and MLP $M3C_N - Models$): This table presents a performance comparison using both daily and monthly statistics amongst the Black-Scholes-Merton ($BSMC_N$) model, Heston (HC_N) model, Heston Jump Diffusion ($HJDC_N$) model, Finite Moment Log Stable ($FMLSC_N$) model and the MLP $M3C_N - Models$ ($M3C1_N$ to $M3C9_N$). The forecast variable for all the models is the one-day-ahead call option price (C_{N+1}). The models denoted by the $_N$ subscript use lagged input variables for forecasting C_{N+1}. The one-day-ahead forecast errors of C_{N+1} are used to compute the Root Mean Square Error (RMSE). Column I identifies the models, column II identifies the forecast variable, column III lists the input variables used by the models to obtain the one-trading-day ahead forecast of C_{N+1}, and columns IV, V and VI describe the network architecture of the MLP $M3C_N - Models$. Forecasts are made for 1,328 trading days, and there are 64 months covered in the sample using the monthly data.

When comparing all models simultaneously (i.e. including the random walk model (δC_N), column VII reports the number of months out of the 64 months that each model has the smallest RMSE, while column VIII reports the number of days out of the 1,328 days each model has the smallest RMSE. Columns IX (lower bound) and X (upper bound) present the winning percentage out of 64 months for each model, evaluated using the bootstrap sampling technique. The statistical bootstrap performed (with replacement) at a 95% confidence level is computed from the monthly RMSE values of the respective models below. Columns XI (lower bound) and XII (upper bound) present the winning percentage out of 1326 days for each model computed from bootstrapping the daily RMSE values of the respective models at a 95% confidence level.

Similarly, when the δC_N model was excluded in the comparison, column XIII report the number of months out of the 64 months that each model has the smallest RMSE, while column XIV reports the number of days out of the 1,328 days each model has the smallest RMSE. Columns XV (lower bound) and XVI (upper bound) present the winning percentage out of 64 months for each model, evaluated using the bootstrap sampling technique. The statistical bootstrap performed (with replacement) at a 95% confidence level is computed from the monthly RMSE values of the respective models below. Also, columns XVII (lower bound) and XVIII (upper bound) present the winning percentage out of 1326 days for each model computed from bootstrapping the daily RMSE values of the respective models at a 95% confidence level.

						Including the random walk						**Excluding the random walk**					
(I) Model	**(II) Forecast**	**(III) Inputs**	**(IV) No. of hidden layers**	**(V) No. of hidden nodes per layer**	**(VI) Network architecture**	**(VII) Performance amongst all models (Monthly)**	**(VIII) Performance amongst all models (Daily)**	**(IX) 2.5% lower bound- (for monthly) (%)**	**(X) 2.5% upper bound- (for monthly) (%)**	**(XI) 2.5% lower bound- (for daily) (%)**	**(XII) 2.5% upper bound- (for daily) (%)**	**(XIII) Performance amongst all models (Monthly)**	**(XIV) Performance amongst all models (Daily)**	**(XV) 2.5% lower bound- (for monthly) (%)**	**(XVI) 2.5% upper bound- (for monthly) (%)**	**(XVII) 2.5% lower bound- (for daily) (%)**	**(XVIII) 2.5% upper bound- (for daily) (%)**
δC_N	C_{N+1}	C_N	-	-	-	**15**	206	13%	36%	14%	17%	-	-	-	-	-	-
$BSMC_N$	$C_{N+1}^{BSMC_N}$	$S_N, K_{N+1}, T_{N+1}, R_N, Q_N, \sigma_N^{CALIB^C}$	-	-	-	0	124	0%	0%	8%	11%	0	124	0%	0%	8%	11%
HC_N	$C_{N+1}^{HC_N}$	$S_N, K_{N+1}, T_{N+1}, R_N, Q_N, \sigma_N^{CALIB^C}, HParams_N^C$	-	-	-	3	157	0%	11%	10%	13%	3	159	0%	11%	10%	14%
$HJDC_N$	$C_{N+1}^{HJDC_N}$	$S_N, K_{N+1}, T_{N+1}, R_N, Q_N, \sigma_N^{CALIB^C}, HJDParams_N^C$	-	-	-	0	19	0%	0%	1%	2%	2	46	0%	8%	3%	5%
$FMLSC_N$	$C_{N+1}^{FMLSC_N}$	$S_N, K_{N+1}, T_{N+1}, R_N, Q_N, FMLSParams_N^C$	-	-	-	0	**224**	0%	0%	15%	19%	0	**229**	0%	0%	15%	19%
$M3C1_N$	$C_{N+1}^{M3C1_N}$	$S_N, K_{N+1}, T_{N+1}, R_N, Q_N, \sigma_N^{CALIB^C}$	3	6	6 X 6 X 6	5	107	2%	15%	7%	9%	5	114	2%	14%	7%	10%
$M3C2_N$	$C_{N+1}^{M3C2_N}$	$S_N, K_{N+1}, T_{N+1}, R_N, Q_N, \sigma_N^{CALIB^C}, C_N$	3	7	7 X 7 X 7	1	91	0%	5%	5%	8%	2	101	0%	8%	6%	9%
$M3C3_N$	$C_{N+1}^{M3C3_N}$	$S_N, K_{N+1}, T_{N+1}, R_N, Q_N, \sigma_N^{CALIB^C}, C_N, BSMGreeks_N^C$	3	12	12 X 12 X 12	10	99	8%	25%	6%	9%	**11**	116	8%	27%	7%	10%
$M3C4_N$	$C_{N+1}^{M3C4_N}$	$S_N, K_{N+1}, T_{N+1}, R_N, Q_N, \sigma_N^{CALIB^C}, C_N, BSMGreeks_N^C, HParams_N^C$	3	17	17 X 17 X 17	6	71	3%	17%	4%	7%	7	90	5%	19%	5%	8%
$M3C5_N$	$C_{N+1}^{M3C5_N}$	$S_N, K_{N+1}, T_{N+1}, R_N, Q_N, \sigma_N^{CALIB^C}, C_N, BSMGreeks_N^C, HParams_N^C, C_N^{HC}$	3	18	18 X 18 X 18	3	38	0%	9%	2%	4%	6	68	3%	17%	4%	7%
$M3C6_N$	$C_{N+1}^{M3C6_N}$	$S_N, K_{N+1}, T_{N+1}, R_N, Q_N, HParams_N^C, C_N^{HC}$	3	11	11 X 11 X 11	6	48	3%	17%	3%	5%	6	65	3%	17%	4%	6%
$M3C7_N$	$C_{N+1}^{M3C7_N}$	$S_N, K_{N+1}, T_{N+1}, R_N, Q_N, \sigma_N^{CALIB^C}, BSMGreeks_N^C, C_N^{BSMC}$	3	12	12 X 12 X 12	11	73	9%	27%	4%	7%	**11**	94	8%	27%	6%	9%
$M3C8_N$	$C_{N+1}^{M3C8_N}$	$S_N, K_{N+1}, T_{N+1}, R_N, Q_N, HJDParams_N^C, C_N^{HJDC}$	3	14	14 X 14 X 14	2	24	0%	8%	1%	3%	6	57	3%	17%	3%	5%
$M3C9_N$	$C_{N+1}^{M3C9_N}$	$S_N, K_{N+1}, T_{N+1}, R_N, Q_N, FMLSParams_N^C, C_N^{FMLSC}$	3	8	8 X 8 X 8	2	47	0%	8%	3%	5%	5	65	2%	16%	4%	6%

Table A.2.9: Call Price Comparison (amongst Parametric and LSTM $L3C_N - Models$): This table presents a performance comparison using both daily and monthly statistics amongst the Black-Scholes-Merton ($BSMC_N$) model, Heston (HC_N) model, Heston Jump Diffusion ($HJDC_N$) model, Finite Moment Log Stable ($FMLSC_N$) model and the LSTM $L3C_N - Models$ ($L3C1_N$ to $L3C9_N$). The forecast variable for all the models is the one-day-ahead call option price (C_{N+1}). The models denoted by the $_N$ subscript use lagged input variables for forecasting C_{N+1}. The one-day-ahead forecast errors of C_{N+1} are used to compute the Root Mean Square Error (RMSE). Column I identifies the models, column II identifies the forecast variable, column III lists the input variables used by the models to obtain the one-trading-day ahead forecast of C_{N+1}, and columns IV, V and VI describe the network architecture of the LSTM $L3C_N - Models$. Forecasts are made for 1,328 trading days, and there are 64 months covered in the sample using the monthly data.

When comparing all models simultaneously (i.e. including the random walk model (δC_N), column VII reports the number of months out of the 64 months that each model has the smallest RMSE, while column VIII reports the number of days out of the 1,328 days each model has the smallest RMSE. Columns IX (lower bound) and X (upper bound) present the winning percentage out of 64 months for each model, evaluated using the bootstrap sampling technique. The statistical bootstrap performed (with replacement) at a 95% confidence level is computed from the monthly RMSE values of the respective models below. Columns XI (lower bound) and XII (upper bound) present the winning percentage out of 1326 days for each model computed from bootstrapping the daily RMSE values of the respective models at a 95% confidence level.

Similarly, when the δC_N model was excluded in the comparison, column XIII report the number of months out of the 64 months that each model has the smallest RMSE, while column XIV reports the number of days out of the 1,328 days each model has the smallest RMSE. Columns XV (lower bound) and XVI (upper bound) present the winning percentage out of 64 months for each model, evaluated using the bootstrap sampling technique. The statistical bootstrap performed (with replacement) at a 95% confidence level is computed from the monthly RMSE values of the respective models below. Also, columns XVII (lower bound) and XVIII (upper bound) present the winning percentage out of 1326 days for each model computed from bootstrapping the daily RMSE values of the respective models at a 95% confidence level.

						Including the random walk						**Excluding the random walk**					
(I) Model	**(II) Forecast**	**(III) Inputs**	**(IV) No. of hidden layers**	**(V) No. of hidden nodes per layer**	**(VI) Network architecture**	**(VII) Performance amongst all models (Monthly)**	**(VIII) Performance amongst all models (Daily)**	**(IX) 2.5% lower bound- (for monthly) (%)**	**(X) 2.5% upper bound- (for monthly) (%)**	**(XI) 2.5% lower bound- (for daily) (%)**	**(XII) 2.5% upper bound- (for daily) (%)**	**(XIII) Performance amongst all models (Monthly)**	**(XIV) Performance amongst all models (Daily)**	**(XV) 2.5% lower bound- (for monthly) (%)**	**(XVI) 2.5% upper bound- (for monthly) (%)**	**(XVII) 2.5% lower bound- (for daily) (%)**	**(XVIII) 2.5% upper bound- (for daily) (%)**
δC_N	C_{N+1}	C_N	-	-	-	**24**	**234**	27%	50%	16%	20%	-	-	-	-	-	-
$BSMC_N$	$C_{N+1}^{BSMC_N}$	$S_N, K_{N+1}, T_{N+1}, R_N, Q_N, \sigma_N^{CALIB^C}$	-	-	-	0	55	0%	0%	3%	5%	0	55	0%	0%	3%	5%
HC_N	$C_{N+1}^{HC_N}$	$S_N, K_{N+1}, T_{N+1}, R_N, Q_N, \sigma_N^{CALIB^C}, HParams_N^C$	-	-	-	8	129	5%	20%	8%	11%	9	144	6%	23%	9%	13%
$HJDC_N$	$C_{N+1}^{HJDC_N}$	$S_N, K_{N+1}, T_{N+1}, R_N, Q_N, \sigma_N^{CALIB^C}, HJDParams_N^C$	-	-	-	0	17	0%	0%	1%	2%	15	126	13%	34%	8%	11%
$FMLSC_N$	$C_{N+1}^{FMLSC_N}$	$S_N, K_{N+1}, T_{N+1}, R_N, Q_N, FMLSParams_N^C$	-	-	-	0	18	0%	0%	1%	2%	0	18	0%	0%	1%	2%
$L3C1_N$	$C_{N+1}^{L3C1_N}$	$S_N, K_{N+1}, T_{N+1}, R_N, Q_N, \sigma_N^{CALIB^C}$	3	6	6 X 6 X 6	0	37	0%	0%	2%	4%	0	37	0%	0%	2%	4%
$L3C2_N$	$C_{N+1}^{L3C2_N}$	$S_N, K_{N+1}, T_{N+1}, R_N, Q_N, \sigma_N^{CALIB^C}, C_N$	3	7	7 X 7 X 7	1	143	0%	5%	9%	12%	1	144	0%	5%	9%	13%
$L3C3_N$	$C_{N+1}^{L3C3_N}$	$S_N, K_{N+1}, T_{N+1}, R_N, Q_N, \sigma_N^{CALIB^C}, C_N, BSMGreeks_N^C$	3	12	12 X 12 X 12	0	92	0%	0%	6%	8%	0	95	0%	0%	6%	9%
$L3C4_N$	$C_{N+1}^{L3C4_N}$	$S_N, K_{N+1}, T_{N+1}, R_N, Q_N, \sigma_N^{CALIB^C}, C_N, BSMGreeks_N^C, HParams_N^C$	3	17	17 X 17 X 17	0	112	0%	0%	7%	10%	0	115	0%	0%	7%	10%
$L3C5_N$	$C_{N+1}^{L3C5_N}$	$S_N, K_{N+1}, T_{N+1}, R_N, Q_N, \sigma_N^{CALIB^C}, C_N, BSMGreeks_N^C, HParams_N^C, C_N^{HC}$	3	18	18 X 18 X 18	3	103	0%	11%	6%	9%	3	127	0%	11%	8%	11%
$L3C6_N$	$C_{N+1}^{L3C6_N}$	$S_N, K_{N+1}, T_{N+1}, R_N, Q_N, HParams_N^C, C_N^{HC}$	3	11	11 X 11 X 11	7	58	5%	19%	3%	6%	11	75	8%	27%	4%	7%
$L3C7_N$	$C_{N+1}^{L3C7_N}$	$S_N, K_{N+1}, T_{N+1}, R_N, Q_N, \sigma_N^{CALIB^C}, BSMGreeks_N^C, C_N^{BSMC}$	3	12	12 X 12 X 12	6	56	3%	17%	3%	5%	9	91	6%	23%	5%	8%
$L3C8_N$	$C_{N+1}^{L3C8_N}$	$S_N, K_{N+1}, T_{N+1}, R_N, Q_N, HJDParams_N^C, C_N^{HJDC}$	3	14	14 X 14 X 14	15	98	14%	33%	6%	9%	**16**	121	16%	36%	8%	11%
$L3C9_N$	$C_{N+1}^{L3C9_N}$	$S_N, K_{N+1}, T_{N+1}, R_N, Q_N, FMLSParams_N^C, C_N^{FMLSC}$	3	8	8 X 8 X 8	0	176	0%	0%	11%	15%	0	**180**	0%	0%	12%	15%

Table A.2.10: Call Price Comparison (amongst Parametric, MLP $M1C_N - Models$, LSTM $L1C_N - Models$, MLP $M2C_N - Models$, LSTM $L2C_N - Models$, MLP $M3C_N - Models$, and LSTM $L3C_N - Models$): This table presents a performance comparison using both daily and monthly statistics amongst the Black-Scholes-Merton ($BSMC_N$) model, Heston (HC_N) model, Heston Jump Diffusion ($HJDC_N$) model, Finite Moment Log Stable ($FMLSC_N$) model, MLP $M1C_N - Models$ ($M1C1_N$ to $M1C9_N$), LSTM $L1C_N - Models$ ($L1C1_N$ to $L1C9_N$), MLP $M2C_N - Models$ ($M2C1_N$ to $M2C9_N$), LSTM $L2C_N - Models$ ($L2C1_N$ to $L2C9_N$), MLP $M3C_N - Models$ ($M3C1_N$ to $M3C9_N$) and the LSTM $L3C_N - Models$ ($L3C1_N$ to $L3C9_N$). The forecast variable for all the models is the one-day-ahead call option price (C_{N+1}). The models denoted by the $_N$ subscript use lagged input variables for forecasting C_{N+1}. The one-day-ahead forecast errors of C_{N+1} are used to compute the Root Mean Square Error (RMSE). Column I identifies the models, column II identifies the forecast variable, column III lists the input variables used by the models to obtain the one-trading-day ahead forecast of C_{N+1}, and columns IV, V and VI describe the network architecture of the MLP $M1C_N - Models$, LSTM $L1C_N - Models$, MLP $M2C_N - Models$, LSTM $L2C_N - Models$, MLP $M3C_N - Models$, and the LSTM $L3C_N - Models$. Forecasts are made for 1,328 trading days, and there are 64 months covered in the sample using the monthly data.

When comparing all models simultaneously (i.e. including the random walk model (δC_N), column VII reports the number of months out of the 64 months that each model has the smallest RMSE, while column VIII reports the number of days out of the 1,328 days each model has the smallest RMSE. Columns IX (lower bound) and X (upper bound) present the winning percentage out of 64 months for each model, evaluated using the bootstrap sampling technique. The statistical bootstrap performed (with replacement) at a 95% confidence level is computed from the monthly RMSE values of the respective models below. Columns XI (lower bound), and XII (upper bound) presents the winning percentage out of 1326 days for each model computed from bootstrapping the daily RMSE values of the respective models at a 95% confidence level.

Similarly, when the δC_N model was excluded in the comparison, column XIII report the number of months out of the 64 months that each model has the smallest RMSE, while column XIV reports the number of days out of the 1,328 days each model has the smallest RMSE. Columns XV (lower bound) and XVI (upper bound) present the winning percentage out of 64 months for each model, evaluated using the bootstrap sampling technique. The statistical bootstrap performed (with replacement) at a 95% confidence level is computed from the monthly RMSE values of the respective models below. Also, columns XVII (lower bound) and XVIII (upper bound) present the winning percentage out of 1326 days for each model computed from bootstrapping the daily RMSE values of the respective models at a 95% confidence level.

						Including the random walk						Excluding the random walk					
(I)	**(II)**	**(III)**	**(IV)**	**(V)**	**(VI)**	**(VII)**	**(VIII)**	**(IX)**	**(X)**	**(XI)**	**(XII)**	**(XIII)**	**(XIV)**	**(XV)**	**(XVI)**	**(XVII)**	**(XVIII)**
Model	**Forecast**	**Inputs**	**No. of hidden layers**	**No. of hidden nodes per layer**	**Network architecture**	**Performance amongst all models (Monthly)**	**Performance amongst all models (Daily)**	**2.5% lower bound- (for monthly) (%)**	**2.5% upper bound- (for monthly) (%)**	**2.5% lower bound- (for daily) (%)**	**2.5% upper bound- (for daily) (%)**	**Performance amongst all models (Monthly)**	**Performance amongst all models (Daily)**	**2.5% lower bound- (for monthly) (%)**	**2.5% upper bound- (for monthly) (%)**	**2.5% lower bound- (for daily) (%)**	**2.5% upper bound- (for daily) (%)**
δC_N	C_{N+1}	C_N	-	-	-	6	106	3%	17%	7%	9%	-	-	-	-	-	-
$BSMC_N$	$C_{N+1}^{BSMC_N}$	$S_N, K_{N+1}, T_{N+1}, R_N, Q_N, \sigma_N^{CALIB^C}$	-	-	-	0	53	0%	0%	3%	5%	0	53	0%	0%	3%	5%
HC_N	$C_{N+1}^{HC_N}$	$S_N, K_{N+1}, T_{N+1}, R_N, Q_N, \sigma_N^{CALIB^C}, HParams_N^C$	-	-	-	1	40	0%	5%	2%	4%	1	40	0%	5%	2%	4%
$HJDC_N$	$C_{N+1}^{HJDC_N}$	$S_N, K_{N+1}, T_{N+1}, R_N, Q_N, \sigma_N^{CALIB^C}, HJDParams_N^C$	-	-	-	0	1	0%	0%	0%	0%	0	9	0%	0%	0%	1%
$FMLSC_N$	$C_{N+1}^{FMLSC_N}$	$S_N, K_{N+1}, T_{N+1}, R_N, Q_N, FMLSParams_N^C$	-	-	-	0	7	0%	0%	0%	1%	0	7	0%	0%	0%	1%
$M1C1_N$	$C_{N+1}^{M1C1_N}$	$S_N, K_{N+1}, T_{N+1}, R_N, Q_N, \sigma_N^{CALIB^C}$	1	6	6	0	6	0%	0%	0%	1%	0	6	0%	0%	0%	1%
$M1C2_N$	$C_{N+1}^{M1C2_N}$	$S_N, K_{N+1}, T_{N+1}, R_N, Q_N, \sigma_N^{CALIB^C}, C_N$	1	7	7	1	8	0%	5%	0%	1%	1	8	0%	5%	0%	1%
$M1C3_N$	$C_{N+1}^{M1C3_N}$	$S_N, K_{N+1}, T_{N+1}, R_N, Q_N, \sigma_N^{CALIB^C}, C_N, BSMGreeks_N^C$	1	12	12	1	19	0%	5%	1%	2%	1	24	0%	5%	1%	3%
$M1C4_N$	$C_{N+1}^{M1C4_N}$	$S_N, K_{N+1}, T_{N+1}, R_N, Q_N, \sigma_N^{CALIB^C}, C_N, BSMGreeks_N^C, HParams_N^C$	1	17	17	0	20	0%	0%	1%	2%	0	26	0%	0%	1%	3%
$M1C5_N$	$C_{N+1}^{M1C5_N}$	$S_N, K_{N+1}, T_{N+1}, R_N, Q_N, \sigma_N^{CALIB^C}, C_N, BSMGreeks_N^C, HParams_N^C, C_N^{HC}$	1	18	18	2	5	0%	8%	0%	1%	2	6	0%	8%	0%	1%
$M1C6_N$	$C_{N+1}^{M1C6_N}$	$S_N, K_{N+1}, T_{N+1}, R_N, Q_N, HParams_N^C, C_N^{HC}$	1	11	11	2	4	0%	8%	0%	1%	3	5	0%	11%	0%	1%
$M1C7_N$	$C_{N+1}^{M1C7_N}$	$S_N, K_{N+1}, T_{N+1}, R_N, Q_N, \sigma_N^{CALIB^C}, BSMGreeks_N^C, C_N^{BSMC}$	1	12	12	2	14	0%	8%	1%	2%	2	15	0%	8%	1%	2%
$M1C8_N$	$C_{N+1}^{M1C8_N}$	$S_N, K_{N+1}, T_{N+1}, R_N, Q_N, HJDParams_N^C, C_N^{HJDC}$	1	14	14	0	3	0%	0%	0%	1%	0	6	0%	0%	0%	1%
$M1C9_N$	$C_{N+1}^{M1C9_N}$	$S_N, K_{N+1}, T_{N+1}, R_N, Q_N, FMLSParams_N^C, C_N^{FMLSC}$	1	8	8	0	5	0%	0%	0%	1%	0	6	0%	0%	0%	1%
$M2C1_N$	$C_{N+1}^{M2C1_N}$	$S_N, K_{N+1}, T_{N+1}, R_N, Q_N, \sigma_N^{CALIB^C}$	2	6	6 X 6	0	1	0%	0%	0%	0%	0	1	0%	0%	0%	0%
$M2C2_N$	$C_{N+1}^{M2C2_N}$	$S_N, K_{N+1}, T_{N+1}, R_N, Q_N, \sigma_N^{CALIB^C}, C_N$	2	7	7 X 7	0	17	0%	0%	1%	2%	0	17	0%	0%	1%	2%
$M2C3_N$	$C_{N+1}^{M2C3_N}$	$S_N, K_{N+1}, T_{N+1}, R_N, Q_N, \sigma_N^{CALIB^C}, C_N, BSMGreeks_N^C$	2	12	12 X 12	0	13	0%	0%	1%	2%	0	13	0%	0%	1%	2%
$M2C4_N$	$C_{N+1}^{M2C4_N}$	$S_N, K_{N+1}, T_{N+1}, R_N, Q_N, \sigma_N^{CALIB^C}, C_N, BSMGreeks_N^C, HParams_N^C$	2	17	17 X 17	0	28	0%	0%	1%	3%	0	28	0%	0%	1%	3%
$M2C5_N$	$C_{N+1}^{M2C5_N}$	$S_N, K_{N+1}, T_{N+1}, R_N, Q_N, \sigma_N^{CALIB^C}, C_N, BSMGreeks_N^C, HParams_N^C, C_N^{HC}$	2	18	18 X 18	4	32	2%	13%	2%	3%	4	32	2%	13%	2%	3%
$M2C6_N$	$C_{N+1}^{M2C6_N}$	$S_N, K_{N+1}, T_{N+1}, R_N, Q_N, HParams_N^C, C_N^{HC}$	2	11	11 X 11	0	14	0%	0%	1%	2%	0	14	0%	0%	1%	2%
$M2C7_N$	$C_{N+1}^{M2C7_N}$	$S_N, K_{N+1}, T_{N+1}, R_N, Q_N, \sigma_N^{CALIB^C}, BSMGreeks_N^C, C_N^{BSMC}$	2	12	12 X 12	2	26	0%	8%	1%	3%	3	27	0%	11%	1%	3%
$M2C8_N$	$C_{N+1}^{M2C8_N}$	$S_N, K_{N+1}, T_{N+1}, R_N, Q_N, HJDParams_N^C, C_N^{HJDC}$	2	14	14 X 14	1	21	0%	5%	1%	2%	1	22	0%	5%	1%	2%
$M2C9_N$	$C_{N+1}^{M2C9_N}$	$S_N, K_{N+1}, T_{N+1}, R_N, Q_N, FMLSParams_N^C, C_N^{FMLSC}$	2	8	8 X 8	0	4	0%	0%	0%	1%	0	4	0%	0%	0%	1%
$M3C1_N$	$C_{N+1}^{M3C1_N}$	$S_N, K_{N+1}, T_{N+1}, R_N, Q_N, \sigma_N^{CALIB^C}$	3	6	6 X 6 X 6	0	11	0%	0%	0%	1%	0	11	0%	0%	0%	1%
$M3C2_N$	$C_{N+1}^{M3C2_N}$	$S_N, K_{N+1}, T_{N+1}, R_N, Q_N, \sigma_N^{CALIB^C}, C_N$	3	7	7 X 7 X 7	0	13	0%	0%	1%	2%	0	14	0%	0%	1%	2%
$M3C3_N$	$C_{N+1}^{M3C3_N}$	$S_N, K_{N+1}, T_{N+1}, R_N, Q_N, \sigma_N^{CALIB^C}, C_N, BSMGreeks_N^C$	3	12	12 X 12 X 12	3	17	0%	11%	1%	2%	3	21	0%	11%	1%	2%
$M3C4_N$	$C_{N+1}^{M3C4_N}$	$S_N, K_{N+1}, T_{N+1}, R_N, Q_N, \sigma_N^{CALIB^C}, C_N, BSMGreeks_N^C, HParams_N^C$	3	17	17 X 17 X 17	1	18	0%	5%	1%	2%	1	24	0%	5%	1%	3%
$M3C5_N$	$C_{N+1}^{M3C5_N}$	$S_N, K_{N+1}, T_{N+1}, R_N, Q_N, \sigma_N^{CALIB^C}, C_N, BSMGreeks_N^C, HParams_N^C, C_N^{HC}$	3	18	18 X 18 X 18	0	2	0%	0%	0%	0%	0	4	0%	0%	0%	1%
$M3C6_N$	$C_{N+1}^{M3C6_N}$	$S_N, K_{N+1}, T_{N+1}, R_N, Q_N, HParams_N^C, C_N^{HC}$	3	11	11 X 11 X 11	1	3	0%	5%	0%	1%	2	6	0%	8%	0%	1%
$M3C7_N$	$C_{N+1}^{M3C7_N}$	$S_N, K_{N+1}, T_{N+1}, R_N, Q_N, \sigma_N^{CALIB^C}, BSMGreeks_N^C, C_N^{BSMC}$	3	12	12 X 12 X 12	1	4	0%	5%	0%	1%	1	8	0%	5%	0%	1%
$M3C8_N$	$C_{N+1}^{M3C8_N}$	$S_N, K_{N+1}, T_{N+1}, R_N, Q_N, HJDParams_N^C, C_N^{HJDC}$	3	14	14 X 14 X 14	0	1	0%	0%	0%	0%	0	2	0%	0%	0%	0%
$M3C9_N$	$C_{N+1}^{M3C9_N}$	$S_N, K_{N+1}, T_{N+1}, R_N, Q_N, FMLSParams_N^C, C_N^{FMLSC}$	3	8	8 X 8 X 8	0	4	0%	0%	0%	1%	0	6	0%	0%	0%	1%
$L1C1_N$	$C_{N+1}^{L1C1_N}$	$S_N, K_{N+1}, T_{N+1}, R_N, Q_N, \sigma_N^{CALIB^C}$	1	6	6	0	3	0%	0%	0%	1%	0	3	0%	0%	0%	1%
$L1C2_N$	$C_{N+1}^{L1C2_N}$	$S_N, K_{N+1}, T_{N+1}, R_N, Q_N, \sigma_N^{CALIB^C}, C_N$	1	7	7	0	45	0%	0%	2%	4%	0	45	0%	0%	2%	4%
$L1C3_N$	$C_{N+1}^{L1C3_N}$	$S_N, K_{N+1}, T_{N+1}, R_N, Q_N, \sigma_N^{CALIB^C}, C_N, BSMGreeks_N^C$	1	12	12	0	27	0%	0%	1%	3%	0	27	0%	0%	1%	3%
$L1C4_N$	$C_{N+1}^{L1C4_N}$	$S_N, K_{N+1}, T_{N+1}, R_N, Q_N, \sigma_N^{CALIB^C}, C_N, BSMGreeks_N^C, HParams_N^C$	1	17	17	0	28	0%	0%	1%	3%	0	28	0%	0%	1%	3%
$L1C5_N$	$C_{N+1}^{L1C5_N}$	$S_N, K_{N+1}, T_{N+1}, R_N, Q_N, \sigma_N^{CALIB^C}, C_N, BSMGreeks_N^C, HParams_N^C, C_N^{HC}$	1	18	18	1	29	0%	5%	1%	3%	1	33	0%	5%	2%	3%
$L1C6_N$	$C_{N+1}^{L1C6_N}$	$S_N, K_{N+1}, T_{N+1}, R_N, Q_N, HParams_N^C, C_N^{HC}$	1	11	11	2	11	0%	8%	0%	1%	2	13	0%	8%	1%	2%
$L1C7_N$	$C_{N+1}^{L1C7_N}$	$S_N, K_{N+1}, T_{N+1}, R_N, Q_N, \sigma_N^{CALIB^C}, BSMGreeks_N^C, C_N^{BSMC}$	1	12	12	3	21	0%	9%	1%	2%	3	22	0%	11%	1%	2%
$L1C8_N$	$C_{N+1}^{L1C8_N}$	$S_N, K_{N+1}, T_{N+1}, R_N, Q_N, HJDParams_N^C, C_N^{HJDC}$	1	14	14	2	25	0%	8%	1%	3%	3	27	0%	11%	1%	3%
$L1C9_N$	$C_{N+1}^{L1C9_N}$	$S_N, K_{N+1}, T_{N+1}, R_N, Q_N, FMLSParams_N^C, C_N^{FMLSC}$	1	8	8	0	33	0%	0%	2%	3%	0	34	0%	0%	2%	3%
$L2C1_N$	$C_{N+1}^{L2C1_N}$	$S_N, K_{N+1}, T_{N+1}, R_N, Q_N, \sigma_N^{CALIB^C}$	2	6	6 X 6	0	8	0%	0%	0%	1%	0	11	0%	0%	0%	1%
$L2C2_N$	$C_{N+1}^{L2C2_N}$	$S_N, K_{N+1}, T_{N+1}, R_N, Q_N, \sigma_N^{CALIB^C}, C_N$	2	7	7 X 7	1	21	0%	5%	1%	2%	1	23	0%	5%	1%	3%
$L2C3_N$	$C_{N+1}^{L2C3_N}$	$S_N, K_{N+1}, T_{N+1}, R_N, Q_N, \sigma_N^{CALIB^C}, C_N, BSMGreeks_N^C$	2	12	12 X 12	4	32	2%	13%	2%	3%	4	37	2%	13%	2%	4%
$L2C4_N$	$C_{N+1}^{L2C4_N}$	$S_N, K_{N+1}, T_{N+1}, R_N, Q_N, \sigma_N^{CALIB^C}, C_N, BSMGreeks_N^C, HParams_N^C$	2	17	17 X 17	2	17	0%	8%	1%	2%	2	23	0%	8%	1%	2%
$L2C5_N$	$C_{N+1}^{L2C5_N}$	$S_N, K_{N+1}, T_{N+1}, R_N, Q_N, \sigma_N^{CALIB^C}, C_N, BSMGreeks_N^C, HParams_N^C, C_N^{HC}$	2	18	18 X 18	0	2	0%	0%	0%	0%	0	5	0%	0%	0%	1%
$L2C6_N$	$C_{N+1}^{L2C6_N}$	$S_N, K_{N+1}, T_{N+1}, R_N, Q_N, HParams_N^C, C_N^{HC}$	2	11	11 X 11	0	2	0%	0%	0%	0%	0	5	0%	0%	0%	1%
$L2C7_N$	$C_{N+1}^{L2C7_N}$	$S_N, K_{N+1}, T_{N+1}, R_N, Q_N, \sigma_N^{CALIB^C}, BSMGreeks_N^C, C_N^{BSMC}$	2	12	12 X 12	4	8	0%	13%	0%	1%	4	16	1%	13%	1%	2%
$L2C8_N$	$C_{N+1}^{L2C8_N}$	$S_N, K_{N+1}, T_{N+1}, R_N, Q_N, HJDParams_N^C, C_N^{HJDC}$	2	14	14 X 14	1	2	0%	6%	0%	0%	2	8	0%	8%	0%	1%
$L2C9_N$	$C_{N+1}^{L2C9_N}$	$S_N, K_{N+1}, T_{N+1}, R_N, Q_N, FMLSParams_N^C, C_N^{FMLSC}$	2	8	8 X 8	0	7	0%	0%	0%	1%	1	13	0%	5%	0%	2%
$L3C1_N$	$C_{N+1}^{L3C1_N}$	$S_N, K_{N+1}, T_{N+1}, R_N, Q_N, \sigma_N^{CALIB^C}$	3	6	6 X 6 X 6	0	34	0%	0%	2%	3%	0	34	0%	0%	2%	3%
$L3C2_N$	$C_{N+1}^{L3C2_N}$	$S_N, K_{N+1}, T_{N+1}, R_N, Q_N, \sigma_N^{CALIB^C}, C_N$	3	7	7 X 7 X 7	0	86	0%	0%	5%	8%	0	86	0%	0%	5%	8%
$L3C3_N$	$C_{N+1}^{L3C3_N}$	$S_N, K_{N+1}, T_{N+1}, R_N, Q_N, \sigma_N^{CALIB^C}, C_N, BSMGreeks_N^C$	3	12	12 X 12 X 12	0	38	0%	0%	2%	4%	0	38	0%	0%	2%	4%
$L3C4_N$	$C_{N+1}^{L3C4_N}$	$S_N, K_{N+1}, T_{N+1}, R_N, Q_N, \sigma_N^{CALIB^C}, C_N, BSMGreeks_N^C, HParams_N^C$	3	17	17 X 17 X 17	0	73	0%	0%	4%	7%	0	73	0%	0%	4%	7%
$L3C5_N$	$C_{N+1}^{L3C5_N}$	$S_N, K_{N+1}, T_{N+1}, R_N, Q_N, \sigma_N^{CALIB^C}, C_N, BSMGreeks_N^C, HParams_N^C, C_N^{HC}$	3	18	18 X 18 X 18	1	39	0%	5%	2%	4%	1	40	0%	5%	2%	4%
$L3C6_N$	$C_{N+1}^{L3C6_N}$	$S_N, K_{N+1}, T_{N+1}, R_N, Q_N, HParams_N^C, C_N^{HC}$	3	11	11 X 11 X 11	1	22	0%	5%	1%	2%	1	22	0%	5%	1%	2%
$L3C7_N$	$C_{N+1}^{L3C7_N}$	$S_N, K_{N+1}, T_{N+1}, R_N, Q_N, \sigma_N^{CALIB^C}, BSMGreeks_N^C, C_N^{BSMC}$	3	12	12 X 12 X 12	5	24	2%	14%	1%	3%	5	25	2%	14%	1%	3%
$L3C8_N$	$C_{N+1}^{L3C8_N}$	$S_N, K_{N+1}, T_{N+1}, R_N, Q_N, HJDParams_N^C, C_N^{HJDC}$	3	14	14 X 14 X 14	**9**	49	6%	23%	3%	5%	**9**	50	6%	23%	3%	5%
$L3C9_N$	$C_{N+1}^{L3C9_N}$	$S_N, K_{N+1}, T_{N+1}, R_N, Q_N, FMLSParams_N^C, C_N^{FMLSC}$	3	8	8 X 8 X 8	0	**122**	0%	0%	8%	11%	0	**122**	0%	0%	8%	11%

Table A.2.11: Call Price Comparison (amongst Parametric, MLP $M1C_N - Models$, MLP $M2C_N - Models$, and MLP $M3C_N - Models$): This table presents a performance comparison using both daily and monthly statistics amongst the Black-Scholes-Merton ($BSMC_N$) model, Heston (HC_N) model, Heston Jump Diffusion ($HJDC_N$) model, Finite Moment Log Stable ($FMLSC_N$) model, MLP $M1C_N - Models$ ($M1C1_N$ to $M1C9_N$), MLP $M2C_N - Models$ ($M2C1_N$ to $M2C9_N$), and the MLP $M3C_N - Models$ ($M3C1_N$ to $M3C9_N$). The forecast variable for all the models is the one-day-ahead call option price (C_{N+1}). The models denoted by the $_N$ subscript use lagged input variables for forecasting C_{N+1}. The one-day-ahead forecast errors of C_{N+1} are used to compute the Root Mean Square Error (RMSE). Column I identifies the models, column II identifies the forecast variable, column III lists the input variables used by the models to obtain the one-trading-day ahead forecast of C_{N+1}, and columns IV, V and VI describe the network architecture of the MLP $M1C_N - Models$, MLP $M2C_N - Models$, and MLP $M3C_N - Models$. Forecasts are made for 1,328 trading days, and there are 64 months covered in the sample using the monthly data.

When comparing all models simultaneously (i.e. including the random walk model (δC_N), column VII reports the number of months out of the 64 months that each model has the smallest RMSE, while column VIII reports the number of days out of the 1,328 days each model has the smallest RMSE. Columns IX (lower bound) and X (upper bound) present the winning percentage out of 64 months for each model, evaluated using the bootstrap sampling technique. The statistical bootstrap performed (with replacement) at a 95% confidence level is computed from the monthly RMSE values of the respective models below. Columns XI (lower bound), and XII (upper bound) presents the winning percentage out of 1326 days for each model computed from bootstrapping the daily RMSE values of the respective models at a 95% confidence level.

Similarly, when the δC_N model was excluded in the comparison, column XIII report the number of months out of the 64 months that each model has the smallest RMSE, while column XIV reports the number of days out of the 1,328 days each model has the smallest RMSE. Columns XV (lower bound) and XVI (upper bound) present the winning percentage out of 64 months for each model, evaluated using the bootstrap sampling technique. The statistical bootstrap performed (with replacement) at a 95% confidence level is computed from the monthly RMSE values of the respective models below. Also, columns XVII (lower bound) and XVIII (upper bound) present the winning percentage out of 1326 days for each model computed from bootstrapping the daily RMSE values of the respective models at a 95% confidence level.

						Including the random walk						**Excluding the random walk**					
(I)	**(II)**	**(III)**	**(IV)**	**(V)**	**(VI)**	**(VII)**	**(VIII)**	**(IX)**	**(X)**	**(XI)**	**(XII)**	**(XIII)**	**(XIV)**	**(XV)**	**(XVI)**	**(XVII)**	**(XVIII)**
Model	**Forecast**	**Inputs**	**No. of hidden layers**	**No. of hidden nodes per layer**	**Network architecture**	**Performance amongst all models (Monthly)**	**Performance amongst all models (Daily)**	**2.5% lower bound- (for monthly) (%)**	**2.5% upper bound- (for monthly) (%)**	**2.5% lower bound- (for daily) (%)**	**2.5% upper bound- (for daily) (%)**	**Performance amongst all models (Monthly)**	**Performance amongst all models (Daily)**	**2.5% lower bound- (for monthly) (%)**	**2.5% upper bound- (for monthly) (%)**	**2.5% lower bound- (for daily) (%)**	**2.5% upper bound- (for daily) (%)**
δC_N	C_{N+1}	C_N	-	-	-	**11**	158	9%	27%	10%	14%	-	-	-	-	-	-
$BSMC_N$	$C_{N+1}^{BSMC_N}$	$S_N, K_{N+1}, T_{N+1}, R_N, Q_N, \sigma_N^{CALIB^C}$	-	-	-	0	121	0%	0%	8%	11%	0	121	0%	0%	8%	11%
HC_N	$C_{N+1}^{HC_N}$	$S_N, K_{N+1}, T_{N+1}, R_N, Q_N, \sigma_N^{CALIB^C}, HParams_N^C$	-	-	-	2	108	0%	8%	7%	10%	2	108	0%	8%	7%	10%
$HJDC_N$	$C_{N+1}^{HJDC_N}$	$S_N, K_{N+1}, T_{N+1}, R_N, Q_N, \sigma_N^{CALIB^C}, HJDParams_N^C$	-	-	-	0	10	0%	0%	0%	1%	0	24	0%	0%	1%	3%
$FMLSC_N$	$C_{N+1}^{FMLSC_N}$	$S_N, K_{N+1}, T_{N+1}, R_N, Q_N, FMLSParams_N^C$	-	-	-	0	**195**	0%	0%	13%	17%	0	**198**	0%	0%	13%	17%
$M1C1_N$	$C_{N+1}^{M1C1_N}$	$S_N, K_{N+1}, T_{N+1}, R_N, Q_N, \sigma_N^{CALIB^C}$	1	6	6	0	35	0%	0%	2%	4%	0	35	0%	0%	2%	4%
$M1C2_N$	$C_{N+1}^{M1C2_N}$	$S_N, K_{N+1}, T_{N+1}, R_N, Q_N, \sigma_N^{CALIB^C}, C_N$	1	7	7	3	28	0%	11%	1%	3%	3	28	0%	9%	1%	3%
$M1C3_N$	$C_{N+1}^{M1C3_N}$	$S_N, K_{N+1}, T_{N+1}, R_N, Q_N, \sigma_N^{CALIB^C}, C_N, BSMGreeks_N^C$	1	12	12	1	50	0%	5%	3%	5%	1	57	0%	6%	3%	5%
$M1C4_N$	$C_{N+1}^{M1C4_N}$	$S_N, K_{N+1}, T_{N+1}, R_N, Q_N, \sigma_N^{CALIB^C}, C_N, BSMGreeks_N^C, HParams_N^C$	1	17	17	0	38	0%	0%	2%	4%	0	46	0%	0%	2%	5%
$M1C5_N$	$C_{N+1}^{M1C5_N}$	$S_N, K_{N+1}, T_{N+1}, R_N, Q_N, \sigma_N^{CALIB^C}, C_N, BSMGreeks_N^C, HParams_N^C, C_N^{HC}$	1	18	18	2	16	0%	8%	1%	2%	2	22	0%	8%	1%	2%
$M1C6_N$	$C_{N+1}^{M1C6_N}$	$S_N, K_{N+1}, T_{N+1}, R_N, Q_N, HParams_N^C, C_N^{HC}$	1	11	11	2	11	0%	8%	0%	1%	3	12	0%	11%	0%	2%
$M1C7_N$	$C_{N+1}^{M1C7_N}$	$S_N, K_{N+1}, T_{N+1}, R_N, Q_N, \sigma_N^{CALIB^C}, BSMGreeks_N^C, C_N^{BSMC}$	1	12	12	5	48	2%	16%	3%	5%	5	50	2%	16%	3%	5%
$M1C8_N$	$C_{N+1}^{M1C8_N}$	$S_N, K_{N+1}, T_{N+1}, R_N, Q_N, HJDParams_N^C, C_N^{HJDC}$	1	14	14	1	12	0%	5%	0%	1%	2	19	0%	8%	1%	2%
$M1C9_N$	$C_{N+1}^{M1C9_N}$	$S_N, K_{N+1}, T_{N+1}, R_N, Q_N, FMLSParams_N^C, C_N^{FMLSC}$	1	8	8	0	16	0%	0%	1%	2%	0	20	0%	0%	1%	2%
$M2C1_N$	$C_{N+1}^{M2C1_N}$	$S_N, K_{N+1}, T_{N+1}, R_N, Q_N, \sigma_N^{CALIB^C}$	2	6	6 X 6	1	39	0%	5%	2%	4%	1	40	0%	5%	2%	4%
$M2C2_N$	$C_{N+1}^{M2C2_N}$	$S_N, K_{N+1}, T_{N+1}, R_N, Q_N, \sigma_N^{CALIB^C}, C_N$	2	7	7 X 7	0	35	0%	0%	2%	4%	0	36	0%	0%	2%	4%
$M2C3_N$	$C_{N+1}^{M2C3_N}$	$S_N, K_{N+1}, T_{N+1}, R_N, Q_N, \sigma_N^{CALIB^C}, C_N, BSMGreeks_N^C$	2	12	12 X 12	4	47	2%	13%	3%	5%	4	53	2%	13%	3%	5%
$M2C4_N$	$C_{N+1}^{M2C4_N}$	$S_N, K_{N+1}, T_{N+1}, R_N, Q_N, \sigma_N^{CALIB^C}, C_N, BSMGreeks_N^C, HParams_N^C$	2	17	17 X 17	3	46	0%	9%	2%	4%	4	53	2%	13%	3%	5%
$M2C5_N$	$C_{N+1}^{M2C5_N}$	$S_N, K_{N+1}, T_{N+1}, R_N, Q_N, \sigma_N^{CALIB^C}, C_N, BSMGreeks_N^C, HParams_N^C, C_N^{HC}$	2	18	18 X 18	1	8	0%	5%	0%	1%	2	12	0%	8%	0%	1%
$M2C6_N$	$C_{N+1}^{M2C6_N}$	$S_N, K_{N+1}, T_{N+1}, R_N, Q_N, HParams_N^C, C_N^{HC}$	2	11	11 X 11	1	10	0%	5%	0%	1%	2	13	0%	8%	0%	2%
$M2C7_N$	$C_{N+1}^{M2C7_N}$	$S_N, K_{N+1}, T_{N+1}, R_N, Q_N, \sigma_N^{CALIB^C}, BSMGreeks_N^C, C_N^{BSMC}$	2	12	12 X 12	4	30	2%	13%	2%	3%	4	36	2%	13%	2%	4%
$M2C8_N$	$C_{N+1}^{M2C8_N}$	$S_N, K_{N+1}, T_{N+1}, R_N, Q_N, HJDParams_N^C, C_N^{HJDC}$	2	14	14 X 14	1	12	0%	5%	0%	1%	3	21	0%	11%	1%	2%
$M2C9_N$	$C_{N+1}^{M2C9_N}$	$S_N, K_{N+1}, T_{N+1}, R_N, Q_N, FMLSParams_N^C, C_N^{FMLSC}$	2	8	8 X 8	2	14	0%	8%	1%	2%	2	20	0%	8%	1%	2%
$M3C1_N$	$C_{N+1}^{M3C1_N}$	$S_N, K_{N+1}, T_{N+1}, R_N, Q_N, \sigma_N^{CALIB^C}$	3	6	6 X 6 X 6	2	27	0%	8%	1%	3%	2	30	0%	8%	2%	3%
$M3C2_N$	$C_{N+1}^{M3C2_N}$	$S_N, K_{N+1}, T_{N+1}, R_N, Q_N, \sigma_N^{CALIB^C}, C_N$	3	7	7 X 7 X 7	1	35	0%	5%	2%	4%	1	38	0%	5%	2%	4%
$M3C3_N$	$C_{N+1}^{M3C3_N}$	$S_N, K_{N+1}, T_{N+1}, R_N, Q_N, \sigma_N^{CALIB^C}, C_N, BSMGreeks_N^C$	3	12	12 X 12 X 12	6	63	3%	17%	4%	6%	**7**	72	5%	19%	4%	7%
$M3C4_N$	$C_{N+1}^{M3C4_N}$	$S_N, K_{N+1}, T_{N+1}, R_N, Q_N, \sigma_N^{CALIB^C}, C_N, BSMGreeks_N^C, HParams_N^C$	3	17	17 X 17 X 17	4	33	2%	13%	2%	3%	4	41	2%	13%	2%	4%
$M3C5_N$	$C_{N+1}^{M3C5_N}$	$S_N, K_{N+1}, T_{N+1}, R_N, Q_N, \sigma_N^{CALIB^C}, C_N, BSMGreeks_N^C, HParams_N^C, C_N^{HC}$	3	18	18 X 18 X 18	1	9	0%	5%	0%	1%	1	14	0%	5%	1%	2%
$M3C6_N$	$C_{N+1}^{M3C6_N}$	$S_N, K_{N+1}, T_{N+1}, R_N, Q_N, HParams_N^C, C_N^{HC}$	3	11	11 X 11 X 11	0	15	0%	0%	1%	2%	0	21	0%	0%	1%	2%
$M3C7_N$	$C_{N+1}^{M3C7_N}$	$S_N, K_{N+1}, T_{N+1}, R_N, Q_N, \sigma_N^{CALIB^C}, BSMGreeks_N^C, C_N^{BSMC}$	3	12	12 X 12 X 12	5	28	2%	16%	1%	3%	5	37	2%	16%	2%	4%
$M3C8_N$	$C_{N+1}^{M3C8_N}$	$S_N, K_{N+1}, T_{N+1}, R_N, Q_N, HJDParams_N^C, C_N^{HJDC}$	3	14	14 X 14 X 14	1	8	0%	5%	0%	1%	2	19	0%	8%	1%	2%
$M3C9_N$	$C_{N+1}^{M3C9_N}$	$S_N, K_{N+1}, T_{N+1}, R_N, Q_N, FMLSParams_N^C, C_N^{FMLSC}$	3	8	8 X 8 X 8	0	23	0%	0%	1%	2%	2	32	0%	8%	2%	3%

Table A.2.12: Call Price Comparison (amongst Parametric, LSTM $L1C_N - Models$, LSTM $L2C_N - Models$, and LSTM $L3C_N - Models$): This table presents a performance comparison using both daily and monthly statistics amongst the Black-Scholes-Merton ($BSMC_N$) model, Heston (HC_N) model, Heston Jump Diffusion ($HJDC_N$) model, Finite Moment Log Stable ($FMLSC_N$) model, LSTM $L1C_N - Models$ ($L1C1_N$ to $L1C9_N$), LSTM $L2C_N - Models$ ($L2C1_N$ to $L2C9_N$), and the LSTM $L3C_N - Models$ ($L3C1_N$ to $L3C9_N$). The forecast variable for all the models is the one-day-ahead call option price (C_{N+1}). The models denoted by the $_N$ subscript use lagged input variables for forecasting C_{N+1}. The one-day-ahead forecast errors of C_{N+1} are used to compute the Root Mean Square Error (RMSE). Column I identifies the models, column II identifies the forecast variable, column III lists the input variables used by the models to obtain the one-trading-day ahead forecast of C_{N+1}, and columns IV, V and VI describe the network architecture of the LSTM $L1C_N - Models$, LSTM $L2C_N - Models$, and LSTM $L3C_N - Models$. Forecasts are made for 1,328 trading days, and there are 64 months covered in the sample using the monthly data.

When comparing all models simultaneously (i.e. including the random walk model (δC_N), column VII reports the number of months out of the 64 months that each model has the smallest RMSE, while column VIII reports the number of days out of the 1,328 days each model has the smallest RMSE. Columns IX (lower bound) and X (upper bound) present the winning percentage out of 64 months for each model, evaluated using the bootstrap sampling technique. The statistical bootstrap performed (with replacement) at a 95% confidence level is computed from the monthly RMSE values of the respective models below. Columns XI (lower bound), and XII (upper bound) presents the winning percentage out of 1326 days for each model computed from bootstrapping the daily RMSE values of the respective models at a 95% confidence level.

Similarly, when the δC_N model was excluded in the comparison, column XIII report the number of months out of the 64 months that each model has the smallest RMSE, while column XIV reports the number of days out of the 1,328 days each model has the smallest RMSE. Columns XV (lower bound) and XVI (upper bound) present the winning percentage out of 64 months for each model, evaluated using the bootstrap sampling technique. The statistical bootstrap performed (with replacement) at a 95% confidence level is computed from the monthly RMSE values of the respective models below. Also, columns XVII (lower bound) and XVIII (upper bound) present the winning percentage out of 1326 days for each model computed from bootstrapping the daily RMSE values of the respective models at a 95% confidence level.

						Including the random walk						Excluding the random walk					
(I) Model	**(II) Forecast**	**(III) Inputs**	**(IV) No. of hidden layers**	**(V) No. of hidden nodes per layer**	**(VI) Network architecture**	**(VII) Performance amongst all models (Monthly)**	**(VIII) Performance amongst all models (Daily)**	**(IX) 2.5% lower bound-(for monthly) (%)**	**(X) 2.5% upper bound-(for monthly) (%)**	**(XI) 2.5% lower bound-(for daily) (%)**	**(XII) 2.5% upper bound-(for daily) (%)**	**(XIII) Performance amongst all models (Monthly)**	**(XIV) Performance amongst all models (Daily)**	**(XV) 2.5% lower bound-(for monthly) (%)**	**(XVI) 2.5% upper bound-(for monthly) (%)**	**(XVII) 2.5% lower bound-(for daily) (%)**	**(XVIII) 2.5% upper bound-(for daily) (%)**
δC_N	C_{N+1}	C_N	-	-	-	**17**	**200**	17%	38%	13%	17%	-	-	-	-	-	-
$BSMC_N$	$C^{BSMC_N}_{N+1}$	$S_N, K_{N+1}, T_{N+1}, R_N, Q_N, \sigma^{CALIB^C}_N$	-	-	-	0	53	0%	0%	3%	5%	0	53	0%	0%	3%	5%
HC_N	$C^{HC_N}_{N+1}$	$S_N, K_{N+1}, T_{N+1}, R_N, Q_N, \sigma^{CALIB^C}_N, HParams^C_N$	-	-	-	5	86	2%	14%	5%	8%	6	93	3%	17%	6%	8%
$HJDC_N$	$C^{HJDC_N}_{N+1}$	$S_N, K_{N+1}, T_{N+1}, R_N, Q_N, \sigma^{CALIB^C}_N, HJDParams^C_N$	-	-	-	0	12	0%	0%	0%	1%	7	87	5%	19%	5%	8%
$FMLSC_N$	$C^{FMLSC_N}_{N+1}$	$S_N, K_{N+1}, T_{N+1}, R_N, Q_N, FMLSParams^C_N$	-	-	-	0	9	0%	0%	0%	1%	0	9	0%	0%	0%	1%
$L1C1_N$	$C^{L1C1_N}_{N+1}$	$S_N, K_{N+1}, T_{N+1}, R_N, Q_N, \sigma^{CALIB^C}_N$	1	6	6	0	1	0%	0%	0%	0%	0	1	0%	0%	0%	0%
$L1C2_N$	$C^{L1C2_N}_{N+1}$	$S_N, K_{N+1}, T_{N+1}, R_N, Q_N, \sigma^{CALIB^C}_N, C_N$	1	7	7	0	17	0%	0%	1%	2%	0	17	0%	0%	1%	2%
$L1C3_N$	$C^{L1C3_N}_{N+1}$	$S_N, K_{N+1}, T_{N+1}, R_N, Q_N, \sigma^{CALIB^C}_N, C_N, BSMGreeks^C_N$	1	12	12	0	13	0%	0%	0%	2%	0	13	0%	0%	0%	2%
$L1C4_N$	$C^{L1C4_N}_{N+1}$	$S_N, K_{N+1}, T_{N+1}, R_N, Q_N, \sigma^{CALIB^C}_N, C_N, BSMGreeks^C_N, HParams^C_N$	1	17	17	0	29	0%	0%	1%	3%	0	29	0%	0%	1%	3%
$L1C5_N$	$C^{L1C5_N}_{N+1}$	$S_N, K_{N+1}, T_{N+1}, R_N, Q_N, \sigma^{CALIB^C}_N, C_N, BSMGreeks^C_N, HParams^C_N, C^{HC}_N$	1	18	18	5	38	2%	14%	2%	4%	6	44	3%	17%	2%	4%
$L1C6_N$	$C^{L1C6_N}_{N+1}$	$S_N, K_{N+1}, T_{N+1}, R_N, Q_N, HParams^C_N, C^{HC}_N$	1	11	11	2	21	0%	8%	1%	2%	2	24	0%	8%	1%	3%
$L1C7_N$	$C^{L1C7_N}_{N+1}$	$S_N, K_{N+1}, T_{N+1}, R_N, Q_N, \sigma^{CALIB^C}_N, BSMGreeks^C_N, C^{BSMC}_N$	1	12	12	4	50	2%	13%	3%	5%	6	60	3%	17%	3%	6%
$L1C8_N$	$C^{L1C8_N}_{N+1}$	$S_N, K_{N+1}, T_{N+1}, R_N, Q_N, HJDParams^C_N, C^{HJDC}_N$	1	14	14	1	23	0%	5%	1%	2%	1	27	0%	5%	1%	3%
$L1C9_N$	$C^{L1C9_N}_{N+1}$	$S_N, K_{N+1}, T_{N+1}, R_N, Q_N, FMLSParams^C_N, C^{FMLSC}_N$	1	8	8	0	4	0%	0%	0%	1%	0	4	0%	0%	0%	1%
$L2C1_N$	$C^{L2C1_N}_{N+1}$	$S_N, K_{N+1}, T_{N+1}, R_N, Q_N, \sigma^{CALIB^C}_N$	2	6	6 X 6	0	3	0%	0%	0%	1%	0	3	0%	0%	0%	1%
$L2C2_N$	$C^{L2C2_N}_{N+1}$	$S_N, K_{N+1}, T_{N+1}, R_N, Q_N, \sigma^{CALIB^C}_N, C_N$	2	7	7 X 7	0	45	0%	0%	2%	4%	0	45	0%	0%	2%	4%
$L2C3_N$	$C^{L2C3_N}_{N+1}$	$S_N, K_{N+1}, T_{N+1}, R_N, Q_N, \sigma^{CALIB^C}_N, C_N, BSMGreeks^C_N$	2	12	12 X 12	0	27	0%	0%	1%	3%	0	29	0%	0%	1%	3%
$L2C4_N$	$C^{L2C4_N}_{N+1}$	$S_N, K_{N+1}, T_{N+1}, R_N, Q_N, \sigma^{CALIB^C}_N, C_N, BSMGreeks^C_N, HParams^C_N$	2	17	17 X 17	0	30	0%	0%	2%	3%	0	31	0%	0%	2%	3%
$L2C5_N$	$C^{L2C5_N}_{N+1}$	$S_N, K_{N+1}, T_{N+1}, R_N, Q_N, \sigma^{CALIB^C}_N, C_N, BSMGreeks^C_N, HParams^C_N, C^{HC}_N$	2	18	18 X 18	2	38	0%	8%	2%	4%	2	47	0%	8%	3%	5%
$L2C6_N$	$C^{L2C6_N}_{N+1}$	$S_N, K_{N+1}, T_{N+1}, R_N, Q_N, HParams^C_N, C^{HC}_N$	2	11	11 X 11	4	15	2%	13%	1%	2%	5	27	2%	16%	1%	3%
$L2C7_N$	$C^{L2C7_N}_{N+1}$	$S_N, K_{N+1}, T_{N+1}, R_N, Q_N, \sigma^{CALIB^C}_N, BSMGreeks^C_N, C^{BSMC}_N$	2	12	12 X 12	3	25	0%	9%	1%	3%	3	39	0%	11%	2%	4%
$L2C8_N$	$C^{L2C8_N}_{N+1}$	$S_N, K_{N+1}, T_{N+1}, R_N, Q_N, HJDParams^C_N, C^{HJDC}_N$	2	14	14 X 14	3	28	0%	11%	1%	3%	6	41	3%	17%	2%	4%
$L2C9_N$	$C^{L2C9_N}_{N+1}$	$S_N, K_{N+1}, T_{N+1}, R_N, Q_N, FMLSParams^C_N, C^{FMLSC}_N$	2	8	8 X 8	0	37	0%	0%	2%	4%	0	38	0%	0%	2%	4%
$L3C1_N$	$C^{L3C1_N}_{N+1}$	$S_N, K_{N+1}, T_{N+1}, R_N, Q_N, \sigma^{CALIB^C}_N$	3	6	6 X 6 X 6	0	34	0%	0%	2%	3%	0	34	0%	0%	2%	3%
$L3C2_N$	$C^{L3C2_N}_{N+1}$	$S_N, K_{N+1}, T_{N+1}, R_N, Q_N, \sigma^{CALIB^C}_N, C_N$	3	7	7 X 7 X 7	0	89	0%	0%	5%	8%	0	90	0%	0%	5%	8%
$L3C3_N$	$C^{L3C3_N}_{N+1}$	$S_N, K_{N+1}, T_{N+1}, R_N, Q_N, \sigma^{CALIB^C}_N, C_N, BSMGreeks^C_N$	3	12	12 X 12 X 12	0	39	0%	0%	2%	4%	0	39	0%	0%	2%	4%
$L3C4_N$	$C^{L3C4_N}_{N+1}$	$S_N, K_{N+1}, T_{N+1}, R_N, Q_N, \sigma^{CALIB^C}_N, C_N, BSMGreeks^C_N, HParams^C_N$	3	17	17 X 17 X 17	0	76	0%	0%	5%	7%	0	77	0%	0%	5%	7%
$L3C5_N$	$C^{L3C5_N}_{N+1}$	$S_N, K_{N+1}, T_{N+1}, R_N, Q_N, \sigma^{CALIB^C}_N, C_N, BSMGreeks^C_N, HParams^C_N, C^{HC}_N$	3	18	18 X 18 X 18	2	49	0%	8%	3%	5%	2	59	0%	8%	3%	6%
$L3C6_N$	$C^{L3C6_N}_{N+1}$	$S_N, K_{N+1}, T_{N+1}, R_N, Q_N, HParams^C_N, C^{HC}_N$	3	11	11 X 11 X 11	1	24	0%	5%	1%	3%	3	30	0%	11%	2%	3%
$L3C7_N$	$C^{L3C7_N}_{N+1}$	$S_N, K_{N+1}, T_{N+1}, R_N, Q_N, \sigma^{CALIB^C}_N, BSMGreeks^C_N, C^{BSMC}_N$	3	12	12 X 12 X 12	5	35	2%	16%	2%	4%	5	50	3%	16%	3%	5%
$L3C8_N$	$C^{L3C8_N}_{N+1}$	$S_N, K_{N+1}, T_{N+1}, R_N, Q_N, HJDParams^C_N, C^{HJDC}_N$	3	14	14 X 14 X 14	10	50	8%	25%	3%	5%	**10**	58	8%	25%	3%	5%
$L3C9_N$	$C^{L3C9_N}_{N+1}$	$S_N, K_{N+1}, T_{N+1}, R_N, Q_N, FMLSParams^C_N, C^{FMLSC}_N$	3	8	8 X 8 X 8	0	128	0%	0%	8%	11%	0	**130**	0%	0%	8%	11%

Table A.2.13: Call Price Comparison (amongst MLP $M1C_N - Models$, LSTM $L1C_N - Models$, MLP $M2C_N - Models$, LSTM $L2C_N - Models$, MLP $M3C_N - Models$, and LSTM $L3C_N - Models$): This table presents a performance comparison using both daily and monthly statistics amongst the MLP $M1C_N - Models$ ($M1C1_N$ to $M1C9_N$), LSTM $L1C_N - Models$ ($L1C1_N$ to $L1C9_N$), MLP $M2C_N - Models$ ($M2C1_N$ to $M2C9_N$), LSTM $L2C_N - Models$ ($L2C1_N$ to $L2C9_N$), MLP $M3C_N - Models$ ($M3C1_N$ to $M3C9_N$) and the LSTM $L3C_N - Models$ ($L3C1_N$ to $L3C9_N$). The forecast variable for all the models is the one-day-ahead call option price (C_{N+1}). The models denoted by the $_N$ subscript use lagged input variables for forecasting C_{N+1}. The one-day-ahead forecast errors of C_{N+1} are used to compute the Root Mean Square Error (RMSE). Column I identifies the models, column II identifies the forecast variable, column III lists the input variables used by the models to obtain the one-trading-day ahead forecast of C_{N+1}, and columns IV, V and VI describe the network architecture of the MLP $M1C_N - Models$ ($M1C1_N$ to $M1C9_N$), LSTM $L1C_N - Models$ ($L1C1_N$ to $L1C9_N$), MLP $M2C_N - Models$ ($M2C1_N$ to $M2C9_N$), LSTM $L2C_N - Models$ ($L2C1_N$ to $L2C9_N$), MLP $M3C_N - Models$ ($M3C1_N$ to $M3C9_N$) and the LSTM $L3C_N - Models$ ($L3C1_N$ to $L3C9_N$). Forecasts are made for 1,328 trading days, and there are 64 months covered in the sample using the monthly data. When comparing all models simultaneously (i.e. including the random walk model (δC_N), column VII reports the number of months out of the 64 months that each model has the smallest RMSE, while column VIII reports the number of days out of the 1,328 days each model has the smallest RMSE. Columns IX (lower bound) and X (upper bound) present the winning percentage out of 64 months for each model, evaluated using the bootstrap sampling technique. The statistical bootstrap performed (with replacement) at a 95% confidence level is computed from the monthly RMSE values of the respective models below. Columns XI (lower bound), and XII (upper bound) presents the winning percentage out of 1326 days for each model computed from bootstrapping the daily RMSE values of the respective models at a 95% confidence level.
Similarly, when the δC_N model was excluded in the comparison, column XIII report the number of months out of the 64 months that each model has the smallest RMSE, while column XIV reports the number of days out of the 1,328 days each model has the smallest RMSE. Columns XV (lower bound) and XVI (upper bound) present the winning percentage out of 64 months for each model, evaluated using the bootstrap sampling technique. The statistical bootstrap performed (with replacement) at a 95% confidence level is computed from the monthly RMSE values of the respective models below. Also, columns XVII (lower bound) and XVIII (upper bound) present the winning percentage out of 1326 days for each model computed from bootstrapping the daily RMSE values of the respective models at a 95% confidence level.

						Including the random walk						Excluding the random walk					
(I) Model	(II) Forecast	(III) Inputs	(IV) No. of hidden layers	(V) No. of hidden nodes per layer	(VI) Network architecture	(VII) Performance amongst all models (Monthly)	(VIII) Performance amongst all models (Daily)	(IX) 2.5% lower bound-(for monthly) (%)	(X) 2.5% upper bound-(for monthly) (%)	(XI) 2.5% lower bound-(for daily) (%)	(XII) 2.5% upper bound-(for daily) (%)	(XIII) Performance amongst all models (Monthly)	(XIV) Performance amongst all models (Daily)	(XV) 2.5% lower bound-(for monthly) (%)	(XVI) 2.5% upper bound-(for monthly) (%)	(XVII) 2.5% lower bound-(for daily) (%)	(XVIII) 2.5% upper bound-(for daily) (%)
δC_N	C_{N+1}	C_N	-	-	-	6	107	3%	17%	7%	10%	-	-	-	-	-	-
$M1C1_N$	$C_{N+1}^{M1C1_N}$	$S_N, K_{N+1}, T_{N+1}, R_N, Q_N, \sigma_N^{CALIB^C}$	1	6	6	0	12	0%	0%	0%	2%	0	12	0%	0%	0%	1%
$M1C2_N$	$C_{N+1}^{M1C2_N}$	$S_N, K_{N+1}, T_{N+1}, R_N, Q_N, \sigma_N^{CALIB^C}, C_N$	1	7	7	1	13	0%	5%	0%	2%	1	13	0%	5%	1%	2%
$M1C3_N$	$C_{N+1}^{M1C3_N}$	$S_N, K_{N+1}, T_{N+1}, R_N, Q_N, \sigma_N^{CALIB^C}, C_N, BSMGreeks_N^C$	1	12	12	1	21	0%	5%	1%	2%	1	26	0%	5%	1%	3%
$M1C4_N$	$C_{N+1}^{M1C4_N}$	$S_N, K_{N+1}, T_{N+1}, R_N, Q_N, \sigma_N^{CALIB^C}, C_N, BSMGreeks_N^C, HParams_N^C$	1	17	17	0	21	0%	0%	1%	2%	0	28	0%	0%	1%	3%
$M1C5_N$	$C_{N+1}^{M1C5_N}$	$S_N, K_{N+1}, T_{N+1}, R_N, Q_N, \sigma_N^{CALIB^C}, C_N, BSMGreeks_N^C, HParams_N^C, C_N^{HC}$	1	18	18	2	6	0%	8%	0%	1%	2	7	0%	8%	0%	1%
$M1C6_N$	$C_{N+1}^{M1C6_N}$	$S_N, K_{N+1}, T_{N+1}, R_N, Q_N, HParams_N^C, C_N^{HC}$	1	11	11	2	4	0%	8%	0%	1%	3	5	0%	11%	0%	1%
$M1C7_N$	$C_{N+1}^{M1C7_N}$	$S_N, K_{N+1}, T_{N+1}, R_N, Q_N, \sigma_N^{CALIB^C}, BSMGreeks_N^C, C_N^{BSMC}$	1	12	12	2	15	0%	8%	1%	2%	2	16	0%	8%	1%	2%
$M1C8_N$	$C_{N+1}^{M1C8_N}$	$S_N, K_{N+1}, T_{N+1}, R_N, Q_N, HJDParams_N^C, C_N^{HJDC}$	1	14	14	0	3	0%	0%	0%	1%	0	7	0%	0%	0%	1%
$M1C9_N$	$C_{N+1}^{M1C9_N}$	$S_N, K_{N+1}, T_{N+1}, R_N, Q_N, FMLSParams_N^C, C_N^{FMLSC}$	1	8	8	0	7	0%	0%	0%	1%	0	8	0%	0%	0%	1%
$M2C1_N$	$C_{N+1}^{M2C1_N}$	$S_N, K_{N+1}, T_{N+1}, R_N, Q_N, \sigma_N^{CALIB^C}$	2	6	6 X 6	0	11	0%	0%	0%	1%	0	11	0%	0%	0%	1%
$M2C2_N$	$C_{N+1}^{M2C2_N}$	$S_N, K_{N+1}, T_{N+1}, R_N, Q_N, \sigma_N^{CALIB^C}, C_N$	2	7	7 X 7	0	17	0%	0%	1%	2%	0	18	0%	0%	1%	2%
$M2C3_N$	$C_{N+1}^{M2C3_N}$	$S_N, K_{N+1}, T_{N+1}, R_N, Q_N, \sigma_N^{CALIB^C}, C_N, BSMGreeks_N^C$	2	12	12 X 12	3	19	0%	11%	1%	2%	3	23	0%	11%	1%	2%
$M2C4_N$	$C_{N+1}^{M2C4_N}$	$S_N, K_{N+1}, T_{N+1}, R_N, Q_N, \sigma_N^{CALIB^C}, C_N, BSMGreeks_N^C, HParams_N^C$	2	17	17 X 17	1	23	0%	5%	1%	2%	1	32	0%	5%	2%	3%
$M2C5_N$	$C_{N+1}^{M2C5_N}$	$S_N, K_{N+1}, T_{N+1}, R_N, Q_N, \sigma_N^{CALIB^C}, C_N, BSMGreeks_N^C, HParams_N^C, C_N^{HC}$	2	18	18 X 18	0	2	0%	0%	0%	0%	0	4	0%	0%	0%	1%
$M2C6_N$	$C_{N+1}^{M2C6_N}$	$S_N, K_{N+1}, T_{N+1}, R_N, Q_N, HParams_N^C, C_N^{HC}$	2	11	11 X 11	1	3	0%	5%	0%	1%	2	6	0%	8%	0%	1%
$M2C7_N$	$C_{N+1}^{M2C7_N}$	$S_N, K_{N+1}, T_{N+1}, R_N, Q_N, \sigma_N^{CALIB^C}, BSMGreeks_N^C, C_N^{BSMC}$	2	12	12 X 12	1	7	0%	5%	0%	1%	1	11	0%	5%	0%	1%
$M2C8_N$	$C_{N+1}^{M2C8_N}$	$S_N, K_{N+1}, T_{N+1}, R_N, Q_N, HJDParams_N^C, C_N^{HJDC}$	2	14	14 X 14	0	1	0%	0%	0%	0%	0	2	0%	0%	0%	0%
$M2C9_N$	$C_{N+1}^{M2C9_N}$	$S_N, K_{N+1}, T_{N+1}, R_N, Q_N, FMLSParams_N^C, C_N^{FMLSC}$	2	8	8 X 8	0	6	0%	0%	0%	1%	0	9	0%	0%	0%	1%
$M3C1_N$	$C_{N+1}^{M3C1_N}$	$S_N, K_{N+1}, T_{N+1}, R_N, Q_N, \sigma_N^{CALIB^C}$	3	6	6 X 6 X 6	0	12	0%	0%	0%	1%	0	15	0%	0%	1%	2%
$M3C2_N$	$C_{N+1}^{M3C2_N}$	$S_N, K_{N+1}, T_{N+1}, R_N, Q_N, \sigma_N^{CALIB^C}, C_N$	3	7	7 X 7 X 7	1	22	0%	5%	1%	2%	1	24	0%	5%	1%	3%
$M3C3_N$	$C_{N+1}^{M3C3_N}$	$S_N, K_{N+1}, T_{N+1}, R_N, Q_N, \sigma_N^{CALIB^C}, C_N, BSMGreeks_N^C$	3	12	12 X 12 X 12	5	33	2%	14%	2%	3%	5	38	2%	16%	2%	4%
$M3C4_N$	$C_{N+1}^{M3C4_N}$	$S_N, K_{N+1}, T_{N+1}, R_N, Q_N, \sigma_N^{CALIB^C}, C_N, BSMGreeks_N^C, HParams_N^C$	3	17	17 X 17 X 17	2	20	0%	8%	1%	2%	2	27	0%	8%	1%	3%
$M3C5_N$	$C_{N+1}^{M3C5_N}$	$S_N, K_{N+1}, T_{N+1}, R_N, Q_N, \sigma_N^{CALIB^C}, C_N, BSMGreeks_N^C, HParams_N^C, C_N^{HC}$	3	18	18 X 18 X 18	0	2	0%	0%	0%	0%	0	5	0%	0%	0%	1%
$M3C6_N$	$C_{N+1}^{M3C6_N}$	$S_N, K_{N+1}, T_{N+1}, R_N, Q_N, HParams_N^C, C_N^{HC}$	3	11	11 X 11 X 11	0	4	0%	0%	0%	1%	0	7	0%	0%	0%	1%
$M3C7_N$	$C_{N+1}^{M3C7_N}$	$S_N, K_{N+1}, T_{N+1}, R_N, Q_N, \sigma_N^{CALIB^C}, BSMGreeks_N^C, C_N^{BSMC}$	3	12	12 X 12 X 12	4	10	2%	13%	0%	1%	4	18	2%	13%	1%	2%
$M3C8_N$	$C_{N+1}^{M3C8_N}$	$S_N, K_{N+1}, T_{N+1}, R_N, Q_N, HJDParams_N^C, C_N^{HJDC}$	3	14	14 X 14 X 14	1	3	0%	6%	0%	0%	2	9	0%	8%	0%	1%
$M3C9_N$	$C_{N+1}^{M3C9_N}$	$S_N, K_{N+1}, T_{N+1}, R_N, Q_N, FMLSParams_N^C, C_N^{FMLSC}$	3	8	8 X 8 X 8	0	9	0%	0%	0%	1%	1	17	0%	5%	1%	2%
$L1C1_N$	$C_{N+1}^{L1C1_N}$	$S_N, K_{N+1}, T_{N+1}, R_N, Q_N, \sigma_N^{CALIB^C}$	1	6	6	0	1	0%	0%	0%	0%	0	1	0%	0%	0%	0%
$L1C2_N$	$C_{N+1}^{L1C2_N}$	$S_N, K_{N+1}, T_{N+1}, R_N, Q_N, \sigma_N^{CALIB^C}, C_N$	1	7	7	0	18	0%	0%	1%	2%	0	18	0%	0%	1%	2%
$L1C3_N$	$C_{N+1}^{L1C3_N}$	$S_N, K_{N+1}, T_{N+1}, R_N, Q_N, \sigma_N^{CALIB^C}, C_N, BSMGreeks_N^C$	1	12	12	0	14	0%	0%	1%	2%	0	14	0%	0%	1%	2%
$L1C4_N$	$C_{N+1}^{L1C4_N}$	$S_N, K_{N+1}, T_{N+1}, R_N, Q_N, \sigma_N^{CALIB^C}, C_N, BSMGreeks_N^C, HParams_N^C$	1	17	17	0	29	0%	0%	1%	3%	0	29	0%	0%	1%	3%
$L1C5_N$	$C_{N+1}^{L1C5_N}$	$S_N, K_{N+1}, T_{N+1}, R_N, Q_N, \sigma_N^{CALIB^C}, C_N, BSMGreeks_N^C, HParams_N^C, C_N^{HC}$	1	18	18	4	33	2%	13%	2%	3%	4	33	2%	13%	2%	3%
$L1C6_N$	$C_{N+1}^{L1C6_N}$	$S_N, K_{N+1}, T_{N+1}, R_N, Q_N, HParams_N^C, C_N^{HC}$	1	11	11	0	17	0%	0%	1%	2%	0	17	0%	0%	1%	2%
$L1C7_N$	$C_{N+1}^{L1C7_N}$	$S_N, K_{N+1}, T_{N+1}, R_N, Q_N, \sigma_N^{CALIB^C}, BSMGreeks_N^C, C_N^{BSMC}$	1	12	12	2	30	0%	8%	2%	3%	3	31	0%	11%	2%	3%
$L1C8_N$	$C_{N+1}^{L1C8_N}$	$S_N, K_{N+1}, T_{N+1}, R_N, Q_N, HJDParams_N^C, C_N^{HJDC}$	1	14	14	1	21	0%	5%	1%	2%	1	22	0%	5%	1%	2%
$L1C9_N$	$C_{N+1}^{L1C9_N}$	$S_N, K_{N+1}, T_{N+1}, R_N, Q_N, FMLSParams_N^C, C_N^{FMLSC}$	1	8	8	0	4	0%	0%	0%	1%	0	4	0%	0%	0%	1%
$L2C1_N$	$C_{N+1}^{L2C1_N}$	$S_N, K_{N+1}, T_{N+1}, R_N, Q_N, \sigma_N^{CALIB^C}$	2	6	6 X 6	0	3	0%	0%	0%	1%	0	3	0%	0%	0%	1%
$L2C2_N$	$C_{N+1}^{L2C2_N}$	$S_N, K_{N+1}, T_{N+1}, R_N, Q_N, \sigma_N^{CALIB^C}, C_N$	2	7	7 X 7	0	46	0%	0%	2%	5%	0	46	0%	0%	2%	5%
$L2C3_N$	$C_{N+1}^{L2C3_N}$	$S_N, K_{N+1}, T_{N+1}, R_N, Q_N, \sigma_N^{CALIB^C}, C_N, BSMGreeks_N^C$	2	12	12 X 12	0	28	0%	0%	1%	3%	0	28	0%	0%	1%	3%
$L2C4_N$	$C_{N+1}^{L2C4_N}$	$S_N, K_{N+1}, T_{N+1}, R_N, Q_N, \sigma_N^{CALIB^C}, C_N, BSMGreeks_N^C, HParams_N^C$	2	17	17 X 17	0	30	0%	0%	1%	3%	0	30	0%	0%	2%	3%
$L2C5_N$	$C_{N+1}^{L2C5_N}$	$S_N, K_{N+1}, T_{N+1}, R_N, Q_N, \sigma_N^{CALIB^C}, C_N, BSMGreeks_N^C, HParams_N^C, C_N^{HC}$	2	18	18 X 18	1	32	0%	5%	2%	3%	1	36	0%	5%	2%	4%
$L2C6_N$	$C_{N+1}^{L2C6_N}$	$S_N, K_{N+1}, T_{N+1}, R_N, Q_N, HParams_N^C, C_N^{HC}$	2	11	11 X 11	2	12	0%	8%	0%	1%	2	14	0%	8%	1%	2%
$L2C7_N$	$C_{N+1}^{L2C7_N}$	$S_N, K_{N+1}, T_{N+1}, R_N, Q_N, \sigma_N^{CALIB^C}, BSMGreeks_N^C, C_N^{BSMC}$	2	12	12 X 12	3	25	0%	11%	1%	3%	3	26	0%	11%	1%	3%
$L2C8_N$	$C_{N+1}^{L2C8_N}$	$S_N, K_{N+1}, T_{N+1}, R_N, Q_N, HJDParams_N^C, C_N^{HJDC}$	2	14	14 X 14	2	26	0%	8%	1%	3%	3	28	0%	9%	1%	3%
$L2C9_N$	$C_{N+1}^{L2C9_N}$	$S_N, K_{N+1}, T_{N+1}, R_N, Q_N, FMLSParams_N^C, C_N^{FMLSC}$	2	8	8 X 8	0	33	0%	0%	2%	3%	0	34	0%	0%	2%	3%
$L3C1_N$	$C_{N+1}^{L3C1_N}$	$S_N, K_{N+1}, T_{N+1}, R_N, Q_N, \sigma_N^{CALIB^C}$	3	6	6 X 6 X 6	0	34	0%	0%	2%	3%	0	34	0%	0%	2%	3%
$L3C2_N$	$C_{N+1}^{L3C2_N}$	$S_N, K_{N+1}, T_{N+1}, R_N, Q_N, \sigma_N^{CALIB^C}, C_N$	3	7	7 X 7 X 7	0	86	0%	0%	5%	8%	0	86	0%	0%	5%	8%
$L3C3_N$	$C_{N+1}^{L3C3_N}$	$S_N, K_{N+1}, T_{N+1}, R_N, Q_N, \sigma_N^{CALIB^C}, C_N, BSMGreeks_N^C$	3	12	12 X 12 X 12	0	41	0%	0%	2%	4%	0	41	0%	0%	2%	4%
$L3C4_N$	$C_{N+1}^{L3C4_N}$	$S_N, K_{N+1}, T_{N+1}, R_N, Q_N, \sigma_N^{CALIB^C}, C_N, BSMGreeks_N^C, HParams_N^C$	3	17	17 X 17 X 17	0	85	0%	0%	5%	8%	0	85	0%	0%	5%	8%
$L3C5_N$	$C_{N+1}^{L3C5_N}$	$S_N, K_{N+1}, T_{N+1}, R_N, Q_N, \sigma_N^{CALIB^C}, C_N, BSMGreeks_N^C, HParams_N^C, C_N^{HC}$	3	18	18 X 18 X 18	1	42	0%	5%	2%	4%	1	43	0%	5%	2%	4%
$L3C6_N$	$C_{N+1}^{L3C6_N}$	$S_N, K_{N+1}, T_{N+1}, R_N, Q_N, HParams_N^C, C_N^{HC}$	3	11	11 X 11 X 11	1	22	0%	5%	1%	2%	1	22	0%	5%	1%	2%
$L3C7_N$	$C_{N+1}^{L3C7_N}$	$S_N, K_{N+1}, T_{N+1}, R_N, Q_N, \sigma_N^{CALIB^C}, BSMGreeks_N^C, C_N^{BSMC}$	3	12	12 X 12 X 12	5	28	2%	16%	1%	3%	5	29	2%	14%	1%	3%
$L3C8_N$	$C_{N+1}^{L3C8_N}$	$S_N, K_{N+1}, T_{N+1}, R_N, Q_N, HJDParams_N^C, C_N^{HJDC}$	3	14	14 X 14 X 14	**9**	50	6%	22%	3%	5%	**9**	51	6%	23%	3%	5%
$L3C9_N$	$C_{N+1}^{L3C9_N}$	$S_N, K_{N+1}, T_{N+1}, R_N, Q_N, FMLSParams_N^C, C_N^{FMLSC}$	3	8	8 X 8 X 8	0	**125**	0%	0%	8%	11%	0	**125**	0%	0%	8%	11%

Table A.2.14: Call Price Comparison (amongst Parametric Models): This table presents a performance comparison using both daily and monthly statistics amongst the Black-Scholes-Merton ($BSMC_N$) model, Heston (HC_N) model, Heston Jump Diffusion ($HJDC_N$) model, and the Finite Moment Log Stable ($FMLSC_N$) model. The forecast variable for all the models is the one-day-ahead call option price (C_{N+1}). The models denoted by the $_N$ subscript use lagged input variables for forecasting C_{N+1}. The one-day-ahead forecast errors of C_{N+1} are used to compute the Root Mean Square Error (RMSE). Column I identifies the models, column II identifies the forecast variable, and column III lists the input variables used by the models to obtain the one-trading-day ahead forecast of C_{N+1}. Forecasts are made for 1,328 trading days, and there are 64 months covered in the sample using the monthly data.

When comparing all models simultaneously (i.e. including the random walk model (δC_N), column VII reports the number of months out of the 64 months that each model has the smallest RMSE, while column VIII reports the number of days out of the 1,328 days each model has the smallest RMSE. Columns IX (lower bound) and X (upper bound) present the winning percentage out of 64 months for each model, evaluated using the bootstrap sampling technique. The statistical bootstrap performed (with replacement) at a 95% confidence level is computed from the monthly RMSE values of the respective models below. Columns XI (lower bound) and XII (upper bound) present the winning percentage out of 1326 days for each model computed from bootstrapping the daily RMSE values of the respective models at a 95% confidence level.

Similarly, when the δC_N model was excluded in the comparison, column XIII report the number of months out of the 64 months that each model has the smallest RMSE, while column XIV reports the number of days out of the 1,328 days each model has the smallest RMSE. Columns XV (lower bound) and XVI (upper bound) present the winning percentage out of 64 months for each model, evaluated using the bootstrap sampling technique. The statistical bootstrap performed (with replacement) at a 95% confidence level is computed from the monthly RMSE values of the respective models below. Also, columns XVII (lower bound) and XVIII (upper bound) present the winning percentage out of 1326 days for each model computed from bootstrapping the daily RMSE values of the respective models at a 95% confidence level.

			Including the random walk						**Excluding the random walk**					
(I)	**(II)**	**(III)**	**(IV)**	**(V)**	**(VI)**	**(VII)**	**(VIII)**	**(IX)**	**(X)**	**(XI)**	**(XII)**	**(XIII)**	**(XIV)**	**(XV)**
Model	**Forecast**	**Inputs**	**Performance amongst all models (Monthly)**	**Performance amongst all models (Daily)**	**2.5% lower bound- (for monthly) (%)**	**2.5% upper bound- (for monthly) (%)**	**2.5% lower bound- (for daily) (%)**	**2.5% upper bound- (for daily) (%)**	**Performance amongst all models (Monthly)**	**Performance amongst all models (Daily)**	**2.5% lower bound- (for monthly) (%)**	**2.5% upper bound- (for monthly) (%)**	**2.5% lower bound- (for daily) (%)**	**2.5% upper bound- (for daily) (%)**
δC_N	C_{N+1}	C_N	**47**	**498**	63%	84%	35%	40%	-	-	-	-	-	-
$BSMC_N$	$C_{N+1}^{BSMC_N}$	$S_N, K_{N+1}, T_{N+1}, R_N, Q_N, \sigma_N^{CALIB^C}$	0	132	0%	0%	8%	11%	0	132	0%	0%	8%	11%
HC_N	$C_{N+1}^{HC_N}$	$S_N, K_{N+1}, T_{N+1}, R_N, Q_N, \sigma_N^{CALIB^C}, HParams_N^C$	13	304	11%	30%	21%	25%	15	376	14%	34%	26%	31%
$HJDC_N$	$C_{N+1}^{HJDC_N}$	$S_N, K_{N+1}, T_{N+1}, R_N, Q_N, \sigma_N^{CALIB^C}, HJDParams_N^C$	4	73	2%	13%	4%	7%	**49**	**458**	66%	86%	32%	37%
$FMLSC_N$	$C_{N+1}^{FMLSC_N}$	$S_N, K_{N+1}, T_{N+1}, R_N, Q_N, FMLSParams_N^C$	0	321	0%	0%	22%	26%	0	362	0%	0%	25%	30%

A.2.2 Pricing performance of C-Models that use one-trading-day-ahead input variables to forecast the call option price C_{N+1} for the next trading day

Table A.2.15 to Table A.2.18 shows the relative out-of-sample pricing performance (in $RMSE$) amongst the models that use one-trading-day-ahead input variables to forecast the one-trading-day-ahead call option price(C_{N+1}). For convenience, the models in table A.2.15 to table A.2.17, list the forecast variable and the input variables in columns II and III, respectively, and the architecture of the MLP and LSTM models in columns IV, V and VI, respectively. The performance metric is the $RMSE$ of the one-trading-day-ahead forecast errors of C_{N+1}, which is computed for each model utilising all of the errors in each day or each month. Amongst all of the models (including the random walk model (δC_N)), columns VII and VIII record the number of months and days, respectively, that each model has the lowest $RMSE$. We performed a bootstrap using the daily and monthly RMSEs to be certain of our results. Columns IX (lower bound) and X (upper bound) present the results from the bootstrap performed (with replacement) using monthly RMSEs at a 95% confidence level and show the winning percentage out of 64 months for each model (including the δC_N model), and similarly, the 95 % confidence intervals computed from bootstrapping of the daily RMSEs signifies the winning percentage out of 1328 days for each model and are reported in columns XI (lower bound), XII (upper bound). While excluding the δC_N model amongst the comparison, columns XIII and XIV record the number of months and days that each model has the lowest $RMSE$. We repeat the exercise of performing the bootstrap by excluding the δC_N model in the comparison, and thus, columns XV (lower bound) and XVI (upper bound) present the results from the bootstrap performed (with replacement) using monthly RMSEs at a 95% confidence level and shows the winning percentage out of 64 months for each model (excluding the δC_N model) and similarly, the 95 % confidence intervals computed from bootstrapping of the daily RMSEs signifies the winning percentage out of 1328 days for each model and are reported in columns XVII (lower bound), XVIII (upper bound).

In the below several comparisons, even though a particular model wins by a higher percentage against other models, we investigated further these models pairwise by performing a pairwise bootstrap comparison, which was computed using the respective pair's daily RMSEs. The results are presented in Table 18 of the Electronic Appendix. Also, we examined the pairwise Diebold-Mariano(DM) (Diebold and Mariano (1995)) tests on the and have presented the results in Table 14 of the Electronic Appendix. In constructing the DM tests, the model pairs are reported in column I and column II, and the DM test statistics for a particular pair are reported in column III. If the null can be rejected, a positive number suggests the rejection may be due to the second model being the better forecast model. In contrast, a negative value suggests the rejection may be due to the first model being the better forecast model. The model pairs highlighted in a red state that their forecasts have statistically insignificant differences in their prediction accuracy. The following model pairs have been shown to have statistically insignificant differences: ($BSMC_{N+1}$, $L3C5_{N+1}$), ($FMLSC_{N+1}$, $M3C4_{N+1}$), and ($L3C3_{N+1}$, $L3C7_{N+1}$). The RMSEs for the $C - Models$ that use one-trading-day-ahead input variables to forecast the C_{N+1} for the next trading day on a monthly, yearly, and overall basis can be found in the Electronic Appendix, in Tables 2, 6, and 10, respectively.

A.2.2.1 Comparison amongst all Parametric Models with Triple Hidden Layer ANN Models:

In this section, we compare the out-of-sample pricing performance of the random walk model (δC_N), the parametric models ($BSMC_{N+1}$, HC_{N+1}, $HJDC_{N+1}$, and $FMLSC_{N+1}$), the triple hidden layer MLP models ($M3C_{N+1} - Models$) and the triple hidden layer LSTM models ($L3C_{N+1} - Models$), then the parametric models with the $M3C_{N+1} - Models$, and finally the parametric models with the $L3C_{N+1} - Models$.

The results for the parametric models with the MLP $M3C_{N+1} - Models$ ($M3C1_{N+1}$ to $M3C9_{N+1}$) and the LSTM $L3C_{N+1} - Models$ ($L3C1_{N+1}$ to $L3C9_{N+1}$) are presented in Table A.2.15. If all the models are individually compared, then the $M3C4_{N+1}$ model had the lowest $RMSE$ for 232 days (having a daily bootstrap winning % of 15% to 20%) out of 1,328 days. Though the $M3C4_{N+1}$ model outperformed, other models like the $M3C2_{N+1}$ (210 days), $M3C3_{N+1}$ (228 days), and the $M3C9_{N+1}$ (162 days) have shown similar outperformance to $M3C4_{N+1}$ model, where they have a collective daily bootstrap winning percentage from 10% (lower bound for the $M3C9_{N+1}$ model) to 19% (upper bound for the $M3C3_{N+1}$ model). When the δC_N was excluded from the comparison, the $M3C4_{N+1}$ model still outperformed all other models for 245 days (having a daily bootstrap winning % of 16% to 21%) out of 1,328 days. Although again the $M3C4_{N+1}$ model outperformed, it was closely followed by the $M3C2_{N+1}$ (212 days), and the $M3C3_{N+1}$ (232 days) which have shown similar outperformance to $M3C4_{N+1}$ model, and they have a collective daily bootstrap winning percentage from 14% (lower bound for the $M3C2_{N+1}$ model) to 20% (upper bound for the $M3C3_{N+1}$ model).

Table A.2.16 presents the results for the comparison of the parametric models with the MLP $M3C_{N+1} - Models$ ($M3C1_{N+1}$ to $M3C9_{N+1}$). Accordingly, $M3C4_{N+1}$ model had the lowest $RMSE$ for 240 days (having a daily bootstrap winning % of 16% to 20%) out of 1,328 days. Though the $M3C4_{N+1}$ model outperformed, other models like the $M3C2_{N+1}$ (213 days), and the $M3C3_{N+1}$ (230 days) have shown similar outperformance to $M3C4_{N+1}$ model, where they have a collective daily bootstrap winning percentage from 14% (lower bound for the $M3C2_{N+1}$ model) to 19% (upper bound for the $M3C3_{N+1}$ model). When the δC_N was excluded from the comparison, the $M3C4_{N+1}$ model still outperformed all other models for 253 days (having a daily bootstrap winning % of 17% to 21%) out of 1,328 days. Although again the $M3C4_{N+1}$ model outperformed, it was closely followed by the $M3C2_{N+1}$ (215 days), and the $M3C3_{N+1}$ (235 days), which have shown similar outperformance to $M3C4_{N+1}$ model, and they have a collective daily bootstrap winning percentage from 14% (lower bound for the $M3C2_{N+1}$ model) to 20% (upper bound for the $M3C3_{N+1}$ model).

We present the comparison results of the parametric models with the LSTM $L3C_{N+1} - Models$ ($L3C1_{N+1}$ to $L3C9_{N+1}$) in Table A.2.17. We find that the $HJDC_{N+1}$ model had the lowest $RMSE$ for 878 days (having a daily bootstrap winning % of 64% to 69%) out of 1,328 days. When the δC_N was excluded from the comparison, the $HJDC_{N+1}$ model still outperformed all other models for 955 days (having a daily bootstrap winning % of 70% to 74%) out of 1,328 days.

Thus, when the parametric models are compared with the triple hidden layer ANN models that use one-trading-day-ahead input variables to forecast C_{N+1}, we conclude that the MLP model ($M3C4_{N+1}$) could outperform all other models, but there were other variants of the MLP model that had similar out-performance. Similar out-performance of the MLP model ($M3C4_{N+1}$) (in Table A.2.16) can be noticed when the parametric models were compared with the triple hidden layer MLP models. However, when the parametric models were compared with the triple hidden layer LSTM models, none of the LSTM models could out-perform the parametric models, particularly the $HJDC_{N+1}$) model (in Table A.2.17).

A.2.2.2 Comparison amongst all Parametric models:

In this section, we compare the out-of-sample pricing performance of the random walk model (δC_N), and the parametric models ($BSMC_{N+1}$, HC_{N+1}, $HJDC_{N+1}$, and $FMLSC_{N+1}$) in Table A.2.18. We find that the $HJDC_{N+1}$ model had the lowest $RMSE$ for 980 days (having a daily bootstrap winning % of 72% to 76%) out of 1,328 days. When the δC_N was excluded from the comparison, the $HJDC_{N+1}$ model still outperformed all other models for 1175 days (having a daily bootstrap winning % of 87% to 90%) out of 1,328 days.

Thus, when comparing the out-of-sample pricing performance amongst the parametric models, the $HJDC_{N+1}$ model had outperformed all other parametric models by a large margin(in Table A.2.18).

Table A.2.15: Call Price Comparison (amongst Parametric, $M3C_{N+1} - Models$ and $L3C_{N+1} - Models$): This table presents a performance comparison using both daily and monthly statistics amongst the Black-Scholes-Merton ($BSMC_{N+1}$) model, Heston (HC_{N+1}) model, Heston Jump Diffusion ($HJDC_{N+1}$) model, Finite Moment Log Stable ($FMLSC_{N+1}$) model, MLP $M3C_{N+1} - Models$ ($M3C1_{N+1}$ to $M3C9_{N+1}$) and the LSTM $L3C_{N+1} - Models$ ($L3C1_{N+1}$ to $L3C9_{N+1}$). The forecast variable for all the models is the one-day-ahead call option price (C_{N+1}). The models denoted by the $_{N+1}$ subscript use one-day-ahead input variables for forecasting C_{N+1}. The one-day-ahead forecast errors of C_{N+1} are used to compute the Root Mean Square Error (RMSE). Column I identifies the models, column II identifies the forecast variable, column III lists the input variables used by the models to obtain the one-trading-day ahead forecast of C_{N+1}, and columns IV, V and VI describe the network architecture of the MLP $M3C_{N+1} - Models$ and the LSTM $L3C_{N+1} - Models$. Forecasts are made for 1,328 trading days, and there are 64 months covered in the sample using the monthly data.

When comparing all models simultaneously (i.e. including the random walk model (δC_N), column VII reports the number of months out of the 64 months that each model has the smallest RMSE, while column VIII reports the number of days out of the 1,328 days each model has the smallest RMSE. Columns IX (lower bound) and X (upper bound) present the winning percentage out of 64 months for each model, evaluated using the bootstrap sampling technique. The statistical bootstrap performed (with replacement) at a 95% confidence level is computed from the monthly RMSE values of the respective models below. Columns XI (lower bound), and XII (upper bound) presents the winning percentage out of 1326 days for each model computed from bootstrapping the daily RMSE values of the respective models at a 95% confidence level.

Similarly, when the δC_N model was excluded in the comparison, column XIII report the number of months out of the 64 months that each model has the smallest RMSE, while column XIV reports the number of days out of the 1,328 days each model has the smallest RMSE. Columns XV (lower bound) and XVI (upper bound) present the winning percentage out of 64 months for each model, evaluated using the bootstrap sampling technique. The statistical bootstrap performed (with replacement) at a 95% confidence level is computed from the monthly RMSE values of the respective models below. Also, columns XVII (lower bound) and XVIII (upper bound) present the winning percentage out of 1326 days for each model computed from bootstrapping the daily RMSE values of the respective models at a 95% confidence level.

						Including the random walk						Excluding the random walk					
(I) Model	**(II) Forecast**	**(III) Inputs**	**(IV) No. of hidden layers**	**(V) No. of hidden nodes per layer**	**(VI) Network architecture**	**(VII) Performance amongst all models (Monthly)**	**(VIII) Performance amongst all models (Daily)**	**(IX) 2.5% lower bound- (for monthly) (%)**	**(X) 2.5% upper bound- (for monthly) (%)**	**(XI) 2.5% lower bound- (for daily) (%)**	**(XII) 2.5% upper bound- (for daily) (%)**	**(XIII) Performance amongst all models (Monthly)**	**(XIV) Performance amongst all models (Daily)**	**(XV) 2.5% lower bound- (for monthly) (%)**	**(XVI) 2.5% upper bound- (for monthly) (%)**	**(XVII) 2.5% lower bound- (for daily) (%)**	**(XVIII) 2.5% upper bound- (for daily) (%)**
δC_N	C_{N+1}	C_N	-	-	-	0	89	0%	0%	5%	8%	-	-	-	-	-	-
$BSMC_{N+1}$	$C_{N+1}^{BSMC_{N+1}}$	$S_{N+1}, K_{N+1}, T_{N+1}, R_{N+1}, Q_{N+1}, \sigma_N^{CALIB^C}$	-	-	-	0	0	0%	0%	0%	0%	0	0	0%	0%	0%	0%
HC_{N+1}	$C_{N+1}^{HC_{N+1}}$	$S_{N+1}, K_{N+1}, T_{N+1}, R_{N+1}, Q_{N+1}, \sigma_N^{CALIB^C}, HParams_N^C$	-	-	-	0	9	0%	0%	0%	1%	0	9	0%	0%	0%	1%
$HJDC_{N+1}$	$C_{N+1}^{HJDC_{N+1}}$	$S_{N+1}, K_{N+1}, T_{N+1}, R_{N+1}, Q_{N+1}, \sigma_N^{CALIB^C}, HJDParams_N^C$	-	-	-	4	56	2%	13%	3%	5%	4	57	2%	13%	3%	5%
$FMLSC_{N+1}$	$C_{N+1}^{FMLSC_{N+1}}$	$S_{N+1}, K_{N+1}, T_{N+1}, R_{N+1}, Q_{N+1}, FMLSParams_N^C$	-	-	-	0	0	0%	0%	0%	0%	0	0	0%	0%	0%	0%
$M3C1_{N+1}$	$C_{N+1}^{M3C1_{N+1}}$	$S_{N+1}, K_{N+1}, T_{N+1}, R_{N+1}, Q_{N+1}, \sigma_N^{CALIB^C}$	3	6	6 X 6 X 6	3	87	0%	11%	5%	8%	3	87	0%	11%	5%	8%
$M3C2_{N+1}$	$C_{N+1}^{M3C2_{N+1}}$	$S_{N+1}, K_{N+1}, T_{N+1}, R_{N+1}, Q_{N+1}, \sigma_N^{CALIB^C}, C_N$	3	7	7 X 7 X 7	**24**	210	25%	50%	14%	18%	**24**	212	26%	48%	14%	18%
$M3C3_{N+1}$	$C_{N+1}^{M3C3_{N+1}}$	$S_{N+1}, K_{N+1}, T_{N+1}, R_{N+1}, Q_{N+1}, \sigma_N^{CALIB^C}, C_N, BSMGreeks_N^C$	3	12	12 X 12 X 12	8	228	5%	22%	15%	19%	8	232	5%	20%	15%	20%
$M3C4_{N+1}$	$C_{N+1}^{M3C4_{N+1}}$	$S_{N+1}, K_{N+1}, T_{N+1}, R_{N+1}, Q_{N+1}, \sigma_N^{CALIB^C}, C_N, BSMGreeks_N^C, HParams_N^C$	3	17	17 X 17 X 17	16	**232**	14%	36%	15%	20%	16	**245**	16%	36%	16%	21%
$M3C5_{N+1}$	$C_{N+1}^{M3C5_{N+1}}$	$S_{N+1}, K_{N+1}, T_{N+1}, R_{N+1}, Q_{N+1}, \sigma_N^{CALIB^C}, C_N, BSMGreeks_N^C, HParams_N^C, C_N^{HC}$	3	18	18 X 18 X 18	4	112	2%	13%	7%	10%	4	124	2%	13%	8%	11%
$M3C6_{N+1}$	$C_{N+1}^{M3C6_{N+1}}$	$S_{N+1}, K_{N+1}, T_{N+1}, R_{N+1}, Q_{N+1}, HParams_N^C, C_N^{HC}$	3	11	11 X 11 X 11	0	76	0%	0%	5%	7%	0	87	0%	0%	5%	8%
$M3C7_{N+1}$	$C_{N+1}^{M3C7_{N+1}}$	$S_{N+1}, K_{N+1}, T_{N+1}, R_{N+1}, Q_{N+1}, \sigma_N^{CALIB^C}, BSMGreeks_N^C, C_N^{BSMC}$	3	12	12 X 12 X 12	0	21	0%	0%	1%	2%	0	35	0%	0%	2%	4%
$M3C8_{N+1}$	$C_{N+1}^{M3C8_{N+1}}$	$S_{N+1}, K_{N+1}, T_{N+1}, R_{N+1}, Q_{N+1}, HJDParams_N^C, C_N^{HJDC}$	3	14	14 X 14 X 14	0	17	0%	0%	1%	2%	0	38	0%	0%	2%	4%
$M3C9_{N+1}$	$C_{N+1}^{M3C9_{N+1}}$	$S_{N+1}, K_{N+1}, T_{N+1}, R_{N+1}, Q_{N+1}, FMLSParams_N^C, C_N^{FMLSC}$	3	8	8 X 8 X 8	5	162	2%	14%	10%	14%	5	166	2%	16%	11%	14%
$L3C1_{N+1}$	$C_{N+1}^{L3C1_{N+1}}$	$S_{N+1}, K_{N+1}, T_{N+1}, R_{N+1}, Q_{N+1}, \sigma_N^{CALIB^C}$	3	6	6 X 6 X 6	0	0	0%	0%	0%	0%	0	0	0%	0%	0%	0%
$L3C2_{N+1}$	$C_{N+1}^{L3C2_{N+1}}$	$S_{N+1}, K_{N+1}, T_{N+1}, R_{N+1}, Q_{N+1}, \sigma_N^{CALIB^C}, C_N$	3	7	7 X 7 X 7	0	4	0%	0%	0%	1%	0	4	0%	0%	0%	1%
$L3C3_{N+1}$	$C_{N+1}^{L3C3_{N+1}}$	$S_{N+1}, K_{N+1}, T_{N+1}, R_{N+1}, Q_{N+1}, \sigma_N^{CALIB^C}, C_N, BSMGreeks_N^C$	3	12	12 X 12 X 12	0	3	0%	0%	0%	1%	0	4	0%	0%	0%	1%
$L3C4_{N+1}$	$C_{N+1}^{L3C4_{N+1}}$	$S_{N+1}, K_{N+1}, T_{N+1}, R_{N+1}, Q_{N+1}, \sigma_N^{CALIB^C}, C_N, BSMGreeks_N^C, HParams_N^C$	3	17	17 X 17 X 17	0	5	0%	0%	0%	1%	0	5	0%	0%	0%	1%
$L3C5_{N+1}$	$C_{N+1}^{L3C5_{N+1}}$	$S_{N+1}, K_{N+1}, T_{N+1}, R_{N+1}, Q_{N+1}, \sigma_N^{CALIB^C}, C_N, BSMGreeks_N^C, HParams_N^C, C_N^{HC}$	3	18	18 X 18 X 18	0	8	0%	0%	0%	1%	0	9	0%	0%	0%	1%
$L3C6_{N+1}$	$C_{N+1}^{L3C6_{N+1}}$	$S_{N+1}, K_{N+1}, T_{N+1}, R_{N+1}, Q_{N+1}, HParams_N^C, C_N^{HC}$	3	11	11 X 11 X 11	0	4	0%	0%	0%	1%	0	6	0%	0%	0%	1%
$L3C7_{N+1}$	$C_{N+1}^{L3C7_{N+1}}$	$S_{N+1}, K_{N+1}, T_{N+1}, R_{N+1}, Q_{N+1}, \sigma_N^{CALIB^C}, BSMGreeks_N^C, C_N^{BSMC}$	3	12	12 X 12 X 12	0	2	0%	0%	0%	0%	0	4	0%	0%	0%	1%
$L3C8_{N+1}$	$C_{N+1}^{L3C8_{N+1}}$	$S_{N+1}, K_{N+1}, T_{N+1}, R_{N+1}, Q_{N+1}, HJDParams_N^C, C_N^{HJDC}$	3	14	14 X 14 X 14	0	2	0%	0%	0%	0%	0	3	0%	0%	0%	1%
$L3C9_{N+1}$	$C_{N+1}^{L3C9_{N+1}}$	$S_{N+1}, K_{N+1}, T_{N+1}, R_{N+1}, Q_{N+1}, FMLSParams_N^C, C_N^{FMLSC}$	3	8	8 X 8 X 8	0	1	0%	0%	0%	0%	0	1	0%	0%	0%	0%

Table A.2.16: Call Price Comparison (amongst Parametric and $M3C_{N+1} - Models$): This table presents a performance comparison using both daily and monthly statistics amongst the Black-Scholes-Merton ($BSMC_{N+1}$) model, Heston (HC_{N+1}) model, Heston Jump Diffusion ($HJDC_{N+1}$) model, Finite Moment Log Stable ($FMLSC_{N+1}$) model and the MLP $M3C_{N+1} - Models$ ($M3C1_{N+1}$ to $M3C9_{N+1}$). The forecast variable for all the models is the one-day-ahead call option price (C_{N+1}). The models denoted by the $_{N+1}$ subscript use one-day-ahead input variables for forecasting C_{N+1}. The one-day-ahead forecast errors of C_{N+1} are used to compute the Root Mean Square Error (RMSE). Column I identifies the models, column II identifies the forecast variable, column III lists the input variables used by the models to obtain the one-trading-day ahead forecast of C_{N+1}, and columns IV, V and VI describe the network architecture of the MLP $M3C_{N+1} - Models$. Forecasts are made for 1,328 trading days, and there are 64 months covered in the sample using the monthly data.

When comparing all models simultaneously (i.e. including the random walk model (δC_N), column VII reports the number of months out of the 64 months that each model has the smallest RMSE, while column VIII reports the number of days out of the 1,328 days each model has the smallest RMSE. Columns IX (lower bound) and X (upper bound) present the winning percentage out of 64 months for each model, evaluated using the bootstrap sampling technique. The statistical bootstrap performed (with replacement) at a 95% confidence level is computed from the monthly RMSE values of the respective models below. Columns XI (lower bound), and XII (upper bound) presents the winning percentage out of 1326 days for each model computed from bootstrapping the daily RMSE values of the respective models at a 95% confidence level.

Similarly, when the δC_N model was excluded in the comparison, column XIII report the number of months out of the 64 months that each model has the smallest RMSE, while column XIV reports the number of days out of the 1,328 days each model has the smallest RMSE. Columns XV (lower bound) and XVI (upper bound) present the winning percentage out of 64 months for each model, evaluated using the bootstrap sampling technique. The statistical bootstrap performed (with replacement) at a 95% confidence level is computed from the monthly RMSE values of the respective models below. Also, columns XVII (lower bound) and XVIII (upper bound) present the winning percentage out of 1326 days for each model computed from bootstrapping the daily RMSE values of the respective models at a 95% confidence level.

						Including the random walk						**Excluding the random walk**					
(I)	**(II)**	**(III)**	**(IV)**	**(V)**	**(VI)**	**(VII)**	**(VIII)**	**(IX)**	**(X)**	**(XI)**	**(XII)**	**(XIII)**	**(XIV)**	**(XV)**	**(XVI)**	**(XVII)**	**(XVIII)**
Model	**Forecast**	**Inputs**	**No. of hidden layers**	**No. of hidden nodes per layer**	**Network architecture**	**Performance amongst all models (Monthly)**	**Performance amongst all models (Daily)**	**2.5% lower bound-(for monthly) (%)**	**2.5% upper bound-(for monthly) (%)**	**2.5% lower bound-(for daily) (%)**	**2.5% upper bound-(for daily) (%)**	**Performance amongst all models (Monthly)**	**Performance amongst all models (Daily)**	**2.5% lower bound-(for monthly) (%)**	**2.5% upper bound-(for monthly) (%)**	**2.5% lower bound-(for daily) (%)**	**2.5% upper bound-(for daily) (%)**
δC_N	C_{N+1}	C_N	-	-	-	0	90	0%	0%	5%	8%	-	-	-	-	-	-
$BSMC_{N+1}$	$C_{N+1}^{BSMC_{N+1}}$	$S_{N+1}, K_{N+1}, T_{N+1}, R_{N+1}, Q_{N+1}, \sigma_N^{CALIB^C}$	-	-	-	0	0	0%	0%	0%	0%	0	0	0%	0%	0%	0%
HC_{N+1}	$C_{N+1}^{HC_{N+1}}$	$S_{N+1}, K_{N+1}, T_{N+1}, R_{N+1}, Q_{N+1}, \sigma_N^{CALIB^C}, HParams_N^C$	-	-	-	0	9	0%	0%	0%	1%	0	9	0%	0%	0%	1%
$HJDC_{N+1}$	$C_{N+1}^{HJDC_{N+1}}$	$S_{N+1}, K_{N+1}, T_{N+1}, R_{N+1}, Q_{N+1}, \sigma_N^{CALIB^C}, HJDParams_N^C$	-	-	-	4	59	2%	13%	3%	6%	4	60	2%	13%	4%	6%
$FMLSC_{N+1}$	$C_{N+1}^{FMLSC_{N+1}}$	$S_{N+1}, K_{N+1}, T_{N+1}, R_{N+1}, Q_{N+1}, FMLSParams_N^C$	-	-	-	0	0	0%	0%	0%	0%	0	0	0%	0%	0%	0%
$M3C1_{N+1}$	$C_{N+1}^{M3C1_{N+1}}$	$S_{N+1}, K_{N+1}, T_{N+1}, R_{N+1}, Q_{N+1}, \sigma_N^{CALIB^C}$	3	6	6 X 6 X 6	3	89	0%	11%	5%	8%	3	89	0%	9%	5%	8%
$M3C2_{N+1}$	$C_{N+1}^{M3C2_{N+1}}$	$S_{N+1}, K_{N+1}, T_{N+1}, R_{N+1}, Q_{N+1}, \sigma_N^{CALIB^C}, C_N$	3	7	7 X 7 X 7	**24**	213	25%	50%	14%	18%	**24**	215	27%	50%	14%	18%
$M3C3_{N+1}$	$C_{N+1}^{M3C3_{N+1}}$	$S_{N+1}, K_{N+1}, T_{N+1}, R_{N+1}, Q_{N+1}, \sigma_N^{CALIB^C}, C_N, BSMGreeks_N^C$	3	12	12 X 12 X 12	8	230	5%	21%	15%	19%	8	235	5%	20%	16%	20%
$M3C4_{N+1}$	$C_{N+1}^{M3C4_{N+1}}$	$S_{N+1}, K_{N+1}, T_{N+1}, R_{N+1}, Q_{N+1}, \sigma_N^{CALIB^C}, C_N, BSMGreeks_N^C, HParams_N^C$	3	17	17 X 17 X 17	16	**240**	16%	36%	16%	20%	16	**253**	16%	36%	17%	21%
$M3C5_{N+1}$	$C_{N+1}^{M3C5_{N+1}}$	$S_{N+1}, K_{N+1}, T_{N+1}, R_{N+1}, Q_{N+1}, \sigma_N^{CALIB^C}, C_N, BSMGreeks_N^C, HParams_N^C, C_N^{HC}$	3	18	18 X 18 X 18	4	114	2%	13%	7%	10%	4	127	1%	13%	8%	11%
$M3C6_{N+1}$	$C_{N+1}^{M3C6_{N+1}}$	$S_{N+1}, K_{N+1}, T_{N+1}, R_{N+1}, Q_{N+1}, HParams_N^C, C_N^{HC}$	3	11	11 X 11 X 11	0	78	0%	0%	5%	7%	0	89	0%	0%	5%	8%
$M3C7_{N+1}$	$C_{N+1}^{M3C7_{N+1}}$	$S_{N+1}, K_{N+1}, T_{N+1}, R_{N+1}, Q_{N+1}, \sigma_N^{CALIB^C}, BSMGreeks_N^C, C_N^{BSMC}$	3	12	12 X 12 X 12	0	22	0%	0%	1%	2%	0	37	0%	0%	2%	4%
$M3C8_{N+1}$	$C_{N+1}^{M3C8_{N+1}}$	$S_{N+1}, K_{N+1}, T_{N+1}, R_{N+1}, Q_{N+1}, HJDParams_N^C, C_N^{HJDC}$	3	14	14 X 14 X 14	0	18	0%	0%	1%	2%	0	44	0%	0%	2%	4%
$M3C9_{N+1}$	$C_{N+1}^{M3C9_{N+1}}$	$S_{N+1}, K_{N+1}, T_{N+1}, R_{N+1}, Q_{N+1}, FMLSParams_N^C, C_N^{FMLSC}$	3	8	8 X 8 X 8	5	166	2%	16%	11%	14%	5	170	2%	14%	11%	15%

Table A.2.17: Call Price Comparison (amongst Parametric and $L3C_{N+1} - Models$): This table presents a performance comparison using both daily and monthly statistics amongst the Black-Scholes-Merton ($BSMC_{N+1}$) model, Heston (HC_{N+1}) model, Heston Jump Diffusion ($HJDC_{N+1}$) model, Finite Moment Log Stable ($FMLSC_{N+1}$) model and the LSTM $L3C_{N+1} - Models$ ($L3C1_{N+1}$ to $L3C9_{N+1}$). The forecast variable for all the models is the one-day-ahead call option price (C_{N+1}). The models denoted by the $_{N+1}$ subscript use one-day-ahead input variables for forecasting C_{N+1}. The one-day-ahead forecast errors of C_{N+1} are used to compute the Root Mean Square Error (RMSE). Column I identifies the models, column II identifies the forecast variable, column III lists the input variables used by the models to obtain the one-trading-day ahead forecast of C_{N+1}, and columns IV, V and VI describe the network architecture of the LSTM $L3C_{N+1} - Models$. Forecasts are made for 1,328 trading days, and there are 64 months covered in the sample using the monthly data.

When comparing all models simultaneously (i.e. including the random walk model (δC_N), column VII reports the number of months out of the 64 months that each model has the smallest RMSE, while column VIII reports the number of days out of the 1,328 days each model has the smallest RMSE. Columns IX (lower bound) and X (upper bound) present the winning percentage out of 64 months for each model, evaluated using the bootstrap sampling technique. The statistical bootstrap performed (with replacement) at a 95% confidence level is computed from the monthly RMSE values of the respective models below. Columns XI (lower bound), and XII (upper bound) presents the winning percentage out of 1326 days for each model computed from bootstrapping the daily RMSE values of the respective models at a 95% confidence level.

Similarly, when the δC_N model was excluded in the comparison, column XIII report the number of months out of the 64 months that each model has the smallest RMSE, while column XIV reports the number of days out of the 1,328 days each model has the smallest RMSE. Columns XV (lower bound) and XVI (upper bound) present the winning percentage out of 64 months for each model, evaluated using the bootstrap sampling technique. The statistical bootstrap performed (with replacement) at a 95% confidence level is computed from the monthly RMSE values of the respective models below. Also, columns XVII (lower bound) and XVIII (upper bound) present the winning percentage out of 1326 days for each model computed from bootstrapping the daily RMSE values of the respective models at a 95% confidence level.

						Including the random walk						**Excluding the random walk**					
(I) Model	**(II)** Forecast	**(III)** Inputs	**(IV)** No. of hidden layers	**(V)** No. of hidden nodes per layer	**(VI)** Network architecture	**(VII)** Performance amongst all models (Monthly)	**(VIII)** Performance amongst all models (Daily)	**(IX)** 2.5% lower bound- (for monthly) (%)	**(X)** 2.5% upper bound- (for monthly) (%)	**(XI)** 2.5% lower bound- (for daily) (%)	**(XII)** 2.5% upper bound- (for daily) (%)	**(XIII)** Performance amongst all models (Monthly)	**(XIV)** Performance amongst all models (Daily)	**(XV)** 2.5% lower bound- (for monthly) (%)	**(XVI)** 2.5% upper bound- (for monthly) (%)	**(XVII)** 2.5% lower bound- (for daily) (%)	**(XVIII)** 2.5% upper bound- (for daily) (%)
δC_N	C_{N+1}	C_N	-	-	-	0	182	0%	0%	12%	16%	-	-	-	-	-	-
$BSMC_{N+1}$	$C_{N+1}^{BSMC_{N+1}}$	$S_{N+1}, K_{N+1}, T_{N+1}, R_{N+1}, Q_{N+1}, \sigma_N^{CALIB^C}$	-	-	-	0	0	0%	0%	0%	0%	0	0	0%	0%	0%	0%
HC_{N+1}	$C_{N+1}^{HC_{N+1}}$	$S_{N+1}, K_{N+1}, T_{N+1}, R_{N+1}, Q_{N+1}, \sigma_N^{CALIB^C}, HParams_N^C$	-	-	-	0	98	0%	0%	6%	9%	0	99	0%	0%	6%	9%
$HJDC_{N+1}$	$C_{N+1}^{HJDC_{N+1}}$	$S_{N+1}, K_{N+1}, T_{N+1}, R_{N+1}, Q_{N+1}, \sigma_N^{CALIB^C}, HJDParams_N^C$	-	-	-	**64**	**878**	100%	100%	64%	69%	**64**	**955**	100%	100%	70%	74%
$FMLSC_{N+1}$	$C_{N+1}^{FMLSC_{N+1}}$	$S_{N+1}, K_{N+1}, T_{N+1}, R_{N+1}, Q_{N+1}, FMLSParams_N^C$	-	-	-	0	15	0%	0%	1%	2%	0	15	0%	0%	1%	2%
$L3C1_{N+1}$	$C_{N+1}^{L3C1_{N+1}}$	$S_{N+1}, K_{N+1}, T_{N+1}, R_{N+1}, Q_{N+1}, \sigma_N^{CALIB^C}$	3	6	6 X 6 X 6	0	0	0%	0%	0%	0%	0	0	0%	0%	0%	0%
$L3C2_{N+1}$	$C_{N+1}^{L3C2_{N+1}}$	$S_{N+1}, K_{N+1}, T_{N+1}, R_{N+1}, Q_{N+1}, \sigma_N^{CALIB^C}, C_N$	3	7	7 X 7 X 7	0	23	0%	0%	1%	2%	0	25	0%	0%	1%	3%
$L3C3_{N+1}$	$C_{N+1}^{L3C3_{N+1}}$	$S_{N+1}, K_{N+1}, T_{N+1}, R_{N+1}, Q_{N+1}, \sigma_N^{CALIB^C}, C_N, BSMGreeks_N^C$	3	12	12 X 12 X 12	0	27	0%	0%	1%	3%	0	30	0%	0%	2%	3%
$L3C4_{N+1}$	$C_{N+1}^{L3C4_{N+1}}$	$S_{N+1}, K_{N+1}, T_{N+1}, R_{N+1}, Q_{N+1}, \sigma_N^{CALIB^C}, C_N, BSMGreeks_N^C, HParams_N^C$	3	17	17 X 17 X 17	0	22	0%	0%	1%	2%	0	26	0%	0%	1%	3%
$L3C5_{N+1}$	$C_{N+1}^{L3C5_{N+1}}$	$S_{N+1}, K_{N+1}, T_{N+1}, R_{N+1}, Q_{N+1}, \sigma_N^{CALIB^C}, C_N, BSMGreeks_N^C, HParams_N^C, C_N^{HC}$	3	18	18 X 18 X 18	0	40	0%	0%	2%	4%	0	59	0%	0%	3%	6%
$L3C6_{N+1}$	$C_{N+1}^{L3C6_{N+1}}$	$S_{N+1}, K_{N+1}, T_{N+1}, R_{N+1}, Q_{N+1}, HParams_N^C, C_N^{HC}$	3	11	11 X 11 X 11	0	14	0%	0%	1%	2%	0	32	0%	0%	2%	3%
$L3C7_{N+1}$	$C_{N+1}^{L3C7_{N+1}}$	$S_{N+1}, K_{N+1}, T_{N+1}, R_{N+1}, Q_{N+1}, \sigma_N^{CALIB^C}, BSMGreeks_N^C, C_N^{BSMC}$	3	12	12 X 12 X 12	0	11	0%	0%	0%	1%	0	42	0%	0%	2%	4%
$L3C8_{N+1}$	$C_{N+1}^{L3C8_{N+1}}$	$S_{N+1}, K_{N+1}, T_{N+1}, R_{N+1}, Q_{N+1}, HJDParams_N^C, C_N^{HJDC}$	3	14	14 X 14 X 14	0	16	0%	0%	1%	2%	0	42	0%	0%	2%	4%
$L3C9_{N+1}$	$C_{N+1}^{L3C9_{N+1}}$	$S_{N+1}, K_{N+1}, T_{N+1}, R_{N+1}, Q_{N+1}, FMLSParams_N^C, C_N^{FMLSC}$	3	8	8 X 8 X 8	0	2	0%	0%	0%	0%	0	3	0%	0%	0%	1%

Table A.2.18: Call Price Comparison (amongst Parametric Models): This table presents a performance comparison using both daily and monthly statistics amongst the Black-Scholes-Merton ($BSMC_{N+1}$) model, Heston (HC_{N+1}) model, Heston Jump Diffusion ($HJDC_{N+1}$) model, and the Finite Moment Log Stable ($FMLSC_{N+1}$) model. The forecast variable for all the models is the one-day-ahead call option price (C_{N+1}). The models denoted by the $_{N+1}$ subscript use one-day-ahead input variables for forecasting C_{N+1}. The one-day-ahead forecast errors of C_{N+1} are used to compute the Root Mean Square Error (RMSE). Column I identifies the models, column II identifies the forecast variable, and column III lists the input variables used by the models to obtain the one-trading-day ahead forecast of C_{N+1}. Forecasts are made for 1,328 trading days, and there are 64 months covered in the sample using the monthly data.
When comparing all models simultaneously (i.e. including the random walk model (δC_N), column VII reports the number of months out of the 64 months that each model has the smallest RMSE, while column VIII reports the number of days out of the 1,328 days each model has the smallest RMSE. Columns IX (lower bound) and X (upper bound) present the winning percentage out of 64 months for each model, evaluated using the bootstrap sampling technique. The statistical bootstrap performed (with replacement) at a 95% confidence level is computed from the monthly RMSE values of the respective models below. Columns XI (lower bound), and XII (upper bound) presents the winning percentage out of 1326 days for each model computed from bootstrapping the daily RMSE values of the respective models at a 95% confidence level.
Similarly, when the δC_N model was excluded in the comparison, column XIII report the number of months out of the 64 months that each model has the smallest RMSE, while column XIV reports the number of days out of the 1,328 days each model has the smallest RMSE. Columns XV (lower bound) and XVI (upper bound) present the winning percentage out of 64 months for each model, evaluated using the bootstrap sampling technique. The statistical bootstrap performed (with replacement) at a 95% confidence level is computed from the monthly RMSE values of the respective models below. Also, columns XVII (lower bound) and XVIII (upper bound) present the winning percentage out of 1326 days for each model computed from bootstrapping the daily RMSE values of the respective models at a 95% confidence level.

			Including the random walk						**Excluding the random walk**					
(I)	**(II)**	**(III)**	**(IV)**	**(V)**	**(VI)**	**(VII)**	**(VIII)**	**(IX)**	**(X)**	**(XI)**	**(XII)**	**(XIII)**	**(XIV)**	**(XV)**
Model	**Forecast**	**Inputs**	**Performance amongst all models (Monthly)**	**Performance amongst all models (Daily)**	**2.5% lower bound-(for monthly) (%)**	**2.5% upper bound-(for monthly) (%)**	**2.5% lower bound-(for daily) (%)**	**2.5% upper bound-(for daily) (%)**	**Performance amongst all models (Monthly)**	**Performance amongst all models (Daily)**	**2.5% lower bound-(for monthly) (%)**	**2.5% upper bound-(for monthly) (%)**	**2.5% lower bound-(for daily) (%)**	**2.5% upper bound-(for daily) (%)**
δC_N	C_{N+1}	C_N	0	217	0%	0%	14%	18%	-	-	-	-	-	-
$BSMC_{N+1}$	$C_{N+1}^{BSMC_{N+1}}$	$S_{N+1}, K_{N+1}, T_{N+1}, R_{N+1}, Q_{N+1}, \sigma_N^{CALIB^C}$	0	0	0%	0%	0%	0%	0	0	0%	0%	0%	0%
HC_{N+1}	$C_{N+1}^{HC_{N+1}}$	$S_{N+1}, K_{N+1}, T_{N+1}, R_{N+1}, Q_{N+1}, \sigma_N^{CALIB^C}, HParams_N^C$	0	116	0%	0%	7%	10%	0	138	0%	0%	9%	12%
$HJDC_{N+1}$	$C_{N+1}^{HJDC_{N+1}}$	$S_{N+1}, K_{N+1}, T_{N+1}, R_{N+1}, Q_{N+1}, \sigma_N^{CALIB^C}, HJDParams_N^C$	**64**	**980**	100%	100%	72%	76%	**64**	**1175**	100%	100%	87%	90%
$FMLSC_{N+1}$	$C_{N+1}^{FMLSC_{N+1}}$	$S_{N+1}, K_{N+1}, T_{N+1}, R_{N+1}, Q_{N+1}, FMLSParams_N^C$	0	15	0%	0%	1%	2%	0	15	0%	0%	1%	2%

A.2.3 Pricing performance of CK-Models that use lagged input variables to forecast the call option price scaled by the strike price (C_{N+1}/K_{N+1}) for the next trading day

Table A.2.19 to Table A.2.32 shows the relative out-of-sample pricing performance (in $RMSE$) amongst the models that use lagged input variables to forecast the one-trading-day-ahead call option price scaled by the strike price(C_{N+1}/K_{N+1}). For convenience, the models in Table A.2.19 to Table A.2.31, lists the forecast variable and the input variables are listed in columns II and III, and the architecture of the MLP and LSTM models in columns IV, V and VI. The performance metric is the $RMSE$ of the one-trading-day-ahead forecast errors, computed for each model utilising all of the errors in each day or each month. Amongst all of the models (including the random walk model (δCK_N)), columns VII and VIII record the number of months and days, respectively, that each model has the lowest $RMSE$. To be certain of our results, we performed a bootstrap using the daily and monthly RMSEs. Columns IX (lower bound) and X (upper bound) present the results from the bootstrap performed (with replacement) using monthly RMSEs at a 95% confidence level and show the winning percentage out of 64 months for each model (including the δCK_N model), and similarly, the 95 % confidence intervals computed from bootstrapping of the daily RMSEs signifies the winning percentage out of 1328 days for each model and are reported in columns XI (lower bound), XII (upper bound). While excluding the δCK_N model amongst the comparison, columns XIII and XIV record the number of months and days, respectively, that each model has the lowest $RMSE$. We repeat the exercise of performing the bootstrap by excluding the δCK_N model in the comparison, and thus, columns XV (lower bound) and XVI (upper bound) present the results from the bootstrap performed (with replacement) using monthly RMSEs at a 95% confidence level and show the winning percentage out of 64 months for each model (excluding the δCK_N model), and similarly, the 95 % confidence intervals computed from bootstrapping of the daily RMSEs signifies the winning percentage out of 1328 days for each model and are reported in columns XVII (lower bound), XVIII (upper bound).

In the below several comparisons, even though a particular model wins by a higher percentage against other models, we investigated further these models pairwise by performing a pairwise bootstrap comparison, which was computed using the respective pair's daily RMSEs. The results are presented in Table 19 of the Electronic Appendix. Also, we examined the pairwise Diebold-Mariano(DM) (Diebold and Mariano (1995)) tests on these models and have presented the results in Table 15 of the Electronic Appendix. In constructing the DM tests, the model pairs are reported in column I and column II, and the DM test statistics for a particular pair are reported in column III. If the null can be rejected, a positive number suggests the rejection may be due to the second model being the better forecast model. In contrast, a negative value suggests the rejection may be due to the first model being the better forecast model. The model pairs highlighted in a red state that their forecasts have statistically insignificant differences in their prediction accuracy. The following model pairs have been shown to have statistically insignificant differences: ($BSMCK_N$, $L2CK9_N$), ($M1CK1_N$, $M2CK8_N$), ($M1CK4_N$, $M1CK5_N$), ($M1CK4_N$, $M3CK8_N$), ($M1CK5_N$, $M3CK8_N$), ($M1CK6_N$, $M2CK7_N$), ($M1CK8_N$, $M2CK9_N$), ($L1CK3_N$, $L2CK3_N$), ($L1CK3_N$, $L3CK7_N$), ($L1CK9_N$, $L3CK9_N$), ($M2CK5_N$, $M3CK8_N$), ($L2CK3_N$, $L3CK7_N$), ($L2CK6_N$, $L3CK6_N$), ($L2CK7_N$, $L3CK4_N$), and ($M3CK4_N$, $M3CK6_N$). The RMSEs for the $CK - Models$ that use lagged input variables to forecast the C_{N+1}/K_{N+1} for the next trading day on a monthly, yearly, and overall basis can be found in the Electronic Appendix, in Tables 3, 7, and 11, respectively.

A.2.3.1 Comparison amongst all Parametric Models with Single Hidden Layer ANN Models:

In this section, we compare the out-of-sample pricing performance of the random walk model (δCK_N), the parametric models ($BSMCK_N$, HCK_N, $HJDCK_N$, and $FMLSCK_N$), the single hidden layer MLP models ($M1CK_N - Models$) and single hidden layer LSTM models ($L1CK_N - Models$), then the parametric models with the $M1CK_N - Models$, and finally the parametric models with the $L1CK_N - Models$.

The results for the parametric models with the MLP $M1CK_N - Models$ ($M1CK1_N$ to $M1CK9_N$) and LSTM $L1CK_N - Models$ ($L1CK1_N$ to $L1CK9_N$) are presented in Table A.2.19. If all the models are individually compared, then the δCK_N model had the lowest $RMSE$ for 374 days (having a daily bootstrap winning % of 26% to 31%) out of 1,328 days. When the δCK_N was excluded from the comparison, the $L1CK2_N$ model outperformed all other models for 218 days (having a daily bootstrap winning % of 14% to 18%) out of 1,328 days, while there was another variant of the MLP model, the $M1CK3_N$ (159 days) had a similar daily bootstrap winning percentage of 10% to 14%.

Table A.2.20 presents the results for the comparison of the parametric models with the MLP $M1CK_N - Models$ ($M1CK1_N$ to $M1CK9_N$). Accordingly, the δCK_N model had the lowest $RMSE$ for 466 days (having a daily bootstrap winning % of 32% to 38%) out of 1,328 days. When the δCK_N was excluded from the comparison, the $M1CK3_N$ model outperformed all other models for 216 days (having a daily bootstrap winning % of 14% to 18%) out of 1,328 days. Though the $M1CK3_N$ model outperformed them all, other variants of the MLP model, the $M1CK4_N$ (146 days), $M1CK5_N$ (169 days), $M1CK7_N$ (161 days), and the $M1CK8_N$ (148 days) have shown similar outperformance to $M1CK3_N$ model, where they have a collective daily bootstrap winning percentage from 9% (lower bound for the $M1CK8_N$ model) to 15% (upper bound for the $M1CK5_N$ model).

We present the comparison results of the parametric models with the LSTM $L1CK_N - Models$ ($L1CK1_N$ to $L1CK9_N$) in Table A.2.21. We find that the δCK_N model had the lowest $RMSE$ for 737 days (having a daily bootstrap winning % of 53% to 58%) out of 1,328 days. When the δCK_N was excluded from the comparison, the $L1CK2_N$ model outperformed all other models for 439 days (having a daily bootstrap winning % of 31% to 36%) out of 1,328 days.

Thus, when the parametric models are compared with the single hidden layer ANN models, we conclude that an LSTM model ($L1CK2_N$) could outperform all other models (in Table A.2.19). If the parametric models were compared with the single hidden layer MLP models (in Table A.2.20), the MLP model ($M1CK3_N$) outperforms them all, but other there were other variants of the MLP model that had similar out-performance. When the parametric models were compared with the single hidden layer LSTM models (in Table A.2.21), the LSTM($L1CK2_N$) model still outperformed them all.

A.2.3.2 Comparison amongst all Parametric Models with Double Hidden Layer ANN Models:

In this section, we compare the out-of-sample pricing performance of the random walk model (δCK_N), the parametric models ($BSMCK_N$, HCK_N, $HJDCK_N$, and $FMLSCK_N$), the double hidden layer MLP models ($M2CK_N - Models$) and double hidden layer LSTM models

($L2CK_N - Models$), then the parametric models with the $M2CK_N - Models$, and finally the parametric models with the $L2CK_N - Models$.

The results for the parametric models with the MLP $M2CK_N - Models$ ($M2CK1_N$ to $M2CK9_N$) and the LSTM $L2CK_N - Models$ ($L2CK1_N$ to $L2CK9_N$) are presented in Table A.2.22. If all the models are individually compared, then the δCK_N model had the lowest $RMSE$ for 334 days (having a daily bootstrap winning % of 23% to 28%) out of 1,328 days. When the δCK_N was excluded from the comparison, the $L2CK2_N$ model outperformed all other models for 201 days (having a daily bootstrap winning % of 13% to 17%) out of 1,328 days.

Table A.2.23 presents the results for the comparison of the parametric models with the MLP $M2CK_N - Models$ ($M2CK1_N$ to $M2CK9_N$). Accordingly, the δCK_N model had the lowest $RMSE$ for 428 days (having a daily bootstrap winning % of 30% to 35%) out of 1,328 days. When the δCK_N was excluded from the comparison, the $M2CK3_N$ model outperformed all other models for 179 days (having a daily bootstrap winning % of 12% to 15%) out of 1,328 days. Though the $M2CK3_N$ model outperformed them all, other variants of the MLP model, the $M2CK2_N$ (178 days), $M2CK4_N$ (131 days), $M2CK6_N$ (168 days), $M2CK7_N$ (145 days), $M2CK8_N$ (160 days), and the $M2CK9_N$ (127 days) have shown similar outperformance to $M2CK3_N$ model, where they have a collective daily bootstrap winning percentage from 8% (lower bound for the $M2CK9_N$ model) to 15% (upper bound for the $M2CK2_N$ model).

We present the comparison results of the parametric models with the LSTM $L2CK_N - Models$ ($L2CK1_N$ to $L2CK9_N$) in Table A.2.24. We find that the δCK_N model had the lowest $RMSE$ for 704 days (having a daily bootstrap winning % of 50% to 56%) out of 1,328 days. When the δCK_N was excluded from the comparison, the $L2CK2_N$ model outperformed all other models for 408 days (having a daily bootstrap winning % of 28% to 33%) out of 1,328 days.

Thus, when the parametric models are compared with the double hidden layer ANN models, we conclude that though an LSTM model ($L2CK2_N$) could outperform all other models (i.e. in Table A.2.22). If the parametric models were compared with the double hidden layer MLP models (in Table A.2.23), the MLP model ($M2CK3_N$) outperforms, but other there were other variants of the MLP model that had similar out-performance, but when the parametric models were compared with the double hidden layer LSTM models (in Table A.2.24), the LSTM($L2CK2_N$) model had still outperformed them all.

A.2.3.3 Comparison amongst all Parametric Models with Triple Hidden Layer ANN Models:

In this section, we compare the out-of-sample pricing performance of the random walk model (δCK_N), the parametric models ($BSMCK_N$, HCK_N, $HJDCK_N$, and $FMLSCK_N$), the triple hidden layer MLP models ($M3CK_N - Models$) and triple hidden layer LSTM models ($L3CK_N - Models$), then the parametric models with the $M3CK_N - Models$, and finally the parametric models with the $L3CK_N - Models$.

The results for the parametric models with the MLP $M3CK_N - Models$ ($M3CK1_N$ to $M3CK9_N$) and the LSTM $L3CK_N - Models$ ($L3CK1_N$ to $L3CK9_N$) are presented in Table A.2.25. If all the models are individually compared, then the δCK_N model had the lowest $RMSE$ for 259 days (having a daily bootstrap winning % of 17% to 22%) out of 1,328 days, while another LSTM model, the $L3CK2_N$ (195 days) had a similar daily bootstrap winning percentage of 13% to 17%). When the δCK_N was excluded from the comparison, the $L3CK2_N$ model outperformed all other models for 203 days (having a daily bootstrap winning % of 13% to 17%) out of 1,328 days.

Table A.2.26 presents the results for the comparison of the parametric models with the MLP $M3CK_N - Models$ ($M3CK1_N$ to $M3CK9_N$). Accordingly, the δCK_N model had the lowest $RMSE$ for 314 days (having a daily bootstrap winning % of 21% to 26%) out of 1,328 days. When the δCK_N was excluded from the comparison, the $M3CK2_N$ model outperformed all other models for 164 days (having a daily bootstrap winning % of 11% to 14%) out of 1,328 days. Though the $M3CK2_N$ model outperformed them all, there were other variants of the MLP model, the $M3CK1_N$ (134 days), $M3CK3_N$ (149 days), $M3CK4_N$ (160 days), $M3CK5_N$ (138 days), $M3CK6_N$ (155 days), $M3CK7_N$ (159 days), $M3CK8_N$ (120 days), and the $M3CK9_N$ (133 days) have shown similar outperformance to $M3CK2_N$ model, where they have a collective daily bootstrap winning percentage from 8% (lower bound for the $M3CK8_N$ model) to 14% (upper bound for the $M3CK4_N$ model).

We present the comparison results of the parametric models with the LSTM $L3CK_N - Models$ ($L3CK1_N$ to $L3CK9_N$) in Table A.2.27. We find that the δCK_N model had the lowest $RMSE$ for 683 days (having a daily bootstrap winning % of 49% to 54%) out of 1,328 days. When the δCK_N was excluded from the comparison, the $L3CK2_N$ model outperformed all other models for 410 days (having a daily bootstrap winning % of 28% to 34%) out of 1,328 days.

Thus, when the parametric models are compared with the triple hidden layer ANN models, we conclude that an LSTM model ($L3CK2_N$) could outperform all other models (i.e. in Table A.2.25). If the parametric models were compared with the triple hidden layer MLP models (in Table A.2.26), the MLP model ($M3CK2_N$) outperforms, but there were other variants of the MLP model that had similar out-performance. When the parametric models were compared with the triple hidden layer LSTM models (in Table A.2.27), the LSTM($L3CK2_N$) model had still outperformed them all.

A.2.3.4 Comparison amongst all Parametric Models with Single, Double and Triple Hidden Layer ANN Models:

In this section, we compare the out-of-sample pricing performance of the random walk model (δCK_N), the parametric models ($BSMCK_N$, HCK_N, $HJDCK_N$, and $FMLSCK_N$), the single, double, triple hidden layer MLP models ($M1CK_N - Models$, $M2CK_N - Models$, and $M3CK_N - Models$) and single, double, triple hidden layer LSTM models ($L1CK_N - Models$, $L2CK_N - Models$, and $L3CK_N - Models$), then the parametric models with the $M1CK_N - Models$, $M2CK_N - Models$, and $M3CK_N - Models$, and finally the parametric models with the $L1CK_N - Models$, $L2CK_N - Models$, and $L3CK_N - Models$.

The results for the parametric models with the $M1CK_N - Models$ ($M1CK1_N$ to $M1CK9_N$), $M2CK_N - Models$ ($M2CK1_N$ to $M2CK9_N$), $M3CK_N - Models$ ($M3CK1_N$ to $M3CK9_N$), $L1CK_N - Models$ ($L1CK1_N$ to $L1CK9_N$), $L2CK_N - Models$ ($L2CK1_N$ to $L2CK9_N$), and $L3CK_N - Models$ ($L3CK1_N$ to $L3CK9_N$) are presented in Table A.2.28. If all the models are individually compared, then the δCK_N model had the lowest $RMSE$ for 202 days (having a daily bootstrap winning % of 13% to 17%) out of 1,328 days. When the δCK_N was excluded from the comparison, the $L1CK2_N$ model outperformed all other models for 96 days (having a daily bootstrap winning % of 6% to 9%) out of 1,328 days, but there was another MLP model, the $M2CK2_N$ (89 days), and there were other variants of the LSTM model, the $L2CK3_N$ (52 days), $L2CK4_N$ (63 days), $L2CK5_N$ (55 days), $L2CK6_N$(52 days), that had a collective daily bootstrap winning percentage from 3% (lower bound for the $L2CK3_N$, $L2CK5_N$, and the $L2CK6_N$ model) to 8% (upper bound for the $M2CK2_N$ model).

Table A.2.29 presents the results for the comparison of the parametric models with the $M1CK_N-Models$ ($M1CK1_N$ to $M1CK9_N$), $M2CK_N - Models$ ($M2CK1_N$ to $M2CK9_N$), $M3CK_N - Models$ ($M3CK1_N$ to $M3CK9_N$). Accordingly, the δCK_N model had the lowest $RMSE$ for 241 days (having a daily bootstrap winning % of 16% to 20%) out of 1,328 days. When the δCK_N was excluded from the comparison, the $M3CK4_N$ model outperformed all other models for 99 days (having a daily bootstrap winning % of 6% to 9%) out of 1,328 days. Though the $M3CK4_N$ model outperformed them all, other variants of the MLP model, the $M2CK1_N$ (51 days), $M2CK2_N$ (64 days), $M2CK3_N$ (65 days), $M3CK1_N$ (61 days), $M3CK2_N$ (62 days), $M3CK3_N$ (79 days), $M3CK5_N$ (73 days), $M3CK6_N$ (87 days), $M3CK8_N$ (59 days), and the $M3CK9_N$ (55 days) have shown similar outperformance to $M3CK4_N$ model, where they have a collective daily bootstrap winning percentage from 3% (lower bound for the $M2CK1_N$ model) to 8% (upper bound for the $M3CK6_N$ model).

We present the comparison results of the parametric models with the $L1CK_N-Models$ ($L1CK1_N$ to $L1CK9_N$), $L2CK_N - Models$ ($L2CK1_N$ to $L2CK9_N$), and $L3CK_N - Models$ ($L3CK1_N$ to $L3CK9_N$) in Table A.2.30. We find that the δCK_N model had the lowest $RMSE$ for 551 days (having a daily bootstrap winning % of 39% to 44%) out of 1,328 days. When the δCK_N was excluded from the comparison, the $L2CK2_N$ model outperformed all other models for 185 days (having a daily bootstrap winning % of 12% to 16%) out of 1,328 days. Though the $L2CK2_N$ model outperformed them all, other variants of the LSTM model, the $L1CK2_N$ (157 days), and the $L3CK2_N$ (158 days) have shown similar outperformance to $L2CK2_N$ model, where they have a collective daily bootstrap winning percentage from 10% (lower bound for the $L1CK2_N$, and the $L3CK2_N$ model) to 14% (upper bound for the $L1CK2_N$, $L3CK2_N$ model)

Thus, when the parametric models are compared with the single, double and triple hidden layer ANN models (in Table A.2.28), we notice that a single-hidden layer LSTM model ($L1CK2_N$) had outperformed all other models. If the parametric models were compared with the single, double and triple hidden layer MLP models (in Table A.2.29), then a triple hidden layer MLP model ($M3CK4_N$) outperforms all other MLP models, but when the parametric models were compared with the single, double and the triple hidden layer LSTM models (in Table A.2.30), a double hidden layer LSTM model ($L2CK2_N$) had outperformed them all, but there were other variants of the triple hidden layer LSTM model that had similar out-performance.

A.2.3.5 Comparison amongst Single, Double and Triple Hidden Layer ANN Models:

In this section, we compare the out-of-sample pricing performance of the random walk model (δCK_N), the single, double, and triple hidden layer MLP models ($M1CK_N-Models$ ($M1CK1_N$ to $M1CK9_N$), $M2CK_N-Models$ ($M2CK1_N$ to $M2CK9_N$), and $M3CK_N-Models$ ($M3CK1_N$ to $M3CK9_N$)) and the single, double, triple hidden layer LSTM models ($L1CK_N - Models$ ($L1CK1_N$ to $L1CK9_N$), $L2CK_N - Models$ ($L2CK1_N$ to $L2CK9_N$), and $L3CK_N - Models$ ($L3CK1_N$ to $L3CK9_N$)), and present the results in Table A.2.31. We find that the δCK_N model had the lowest $RMSE$ for 202 days (having a daily bootstrap winning % of 13% to 17%) out of 1,328 days. When the δCK_N was excluded from the comparison, the $L2CK2_N$ model outperformed all other models for 96 days (having a daily bootstrap winning % of 6% to 9%) out of 1,328 days. Although the $L2CK2_N$ model outperforms, other variants of the triple hidden layer MLP model, the $M3CK3_N$ (52 days), $M3CK4_N$ (63 days), $M3CK5_N$ (55 days), and the $M3CK6_N$ (52 days), and other variants of the LSTM model, the $L1CK2_N$ (89 days), and the $L3C2_N$ (78 days) have shown similar outperformance to $L2CK2_N$ model, where they have a collective daily bootstrap winning percentage from 3% (lower bound for the $M3CK3_N$, $M3CK5_N$, $M3CK6_N$ model) to 8% (upper bound for the $L1CK2_N$ model).

Thus, when comparing the out-of-sample pricing performance amongst the single, double and triple hidden layer ANN models (in Table A.2.31), a double hidden layer LSTM($L2CK2_N$) model outperformed them all, but there were other variants of the MLP, and the LSTM model that had shown similar out-performance to the $L2CK2_N$ model.

A.2.3.6 Comparison amongst all Parametric models:

In this section, we compare the out-of-sample pricing performance of the random walk model (δCK_N), and the parametric models ($BSMCK_N$, HCK_N, $HJDCK_N$, and $FMLSCK_N$) in Table A.2.32. We find that the δCK_N model had the lowest $RMSE$ for 1279 days (having a daily bootstrap winning % of 95% to 97%) out of 1,328 days. When the δCK_N was excluded from the comparison, the $HJDCK_N$ model still outperformed all other models for 540 days (having a daily bootstrap winning % of 38% to 43%) out of 1,328 days.

Thus, when comparing the out-of-sample pricing performance amongst the parametric models, the $HJDCK_N$ model had outperformed all other parametric models, followed by the $BSMCK_N$ and HCK_N model (in Table A.2.32).

Table A.2.19: Call Option Price Scaled by the Exercise Price Comparison (amongst Parametric, MLP $M1CK_N - Models$ and LSTM $L1CK_N - Models$): This table presents a performance comparison using both daily and monthly statistics amongst the Black-Scholes-Merton ($BSMCK_N$) model, Heston (HCK_N) model, Heston Jump Diffusion ($HJDCK_N$) model, Finite Moment Log Stable ($FMLSCK_N$) model, MLP $M1CK_N - Models$ ($M1CK1_N$ to $M1CK9_N$) and the LSTM $L1CK_N - Models$ ($L1CK1_N$ to $L1CK9_N$). The forecast variable for all the models is the one-day-ahead call option price scaled by the exercise price (C_{N+1}/K_{N+1}). The models denoted by the $_N$ subscript use lagged input variables for forecasting C_{N+1}/K_{N+1}. The one-day-ahead forecast errors of C_{N+1}/K_{N+1} are used to compute the Root Mean Square Error (RMSE). Column I identifies the models, column II identifies the forecast variable, column III lists the input variables used by the models to obtain the one-trading-day ahead forecast of C_{N+1}/K_{N+1}, and columns IV, V and VI describe the network architecture of the MLP $M1CK_N - Models$ and the LSTM $L1CK_N - Models$. Forecasts are made for 1,328 trading days, and there are 64 months covered in the sample using the monthly data.
When comparing all models simultaneously (i.e. including the random walk model (δCK_N), column VII reports the number of months out of the 64 months that each model has the smallest RMSE, while column VIII reports the number of days out of the 1,328 days each model has the smallest RMSE. Columns IX (lower bound) and X (upper bound) present the winning percentage out of 64 months for each model, evaluated using the bootstrap sampling technique. The statistical bootstrap performed (with replacement) at a 95% confidence level is computed from the monthly RMSE values of the respective models below. Columns XI (lower bound) and XII (upper bound) present the winning percentage out of 1326 days for each model computed from bootstrapping the daily RMSE values of the respective models at a 95% confidence level.
Similarly, when the δCK_N model was excluded in the comparison, column XIII reports the number of months out of the 64 months that each model has the smallest RMSE, while column XIV reports the number of days out of the 1,328 days each model has the smallest RMSE. Columns XV (lower bound) and XVI (upper bound) present the winning percentage out of 64 months for each model, evaluated using the bootstrap sampling technique. The statistical bootstrap performed (with replacement) at a 95% confidence level is computed from the monthly RMSE values of the respective models below. Also, columns XVII (lower bound) and XVIII (upper bound) present the winning percentage out of 1326 days for each model computed from bootstrapping the daily RMSE values of the respective models at a 95% confidence level.

						Including the random walk						Excluding the random walk					
(I) Model	**(II) Forecast**	**(III) Inputs**	**(IV) No. of hidden layers**	**(V) No. of hidden nodes per layer**	**(VI) Network architecture**	**(VII) Performance amongst all models (Monthly)**	**(VIII) Performance amongst all models (Daily)**	**(IX) 2.5% lower bound- (for monthly) (%)**	**(X) 2.5% upper bound- (for monthly) (%)**	**(XI) 2.5% lower bound- (for daily) (%)**	**(XII) 2.5% upper bound- (for daily) (%)**	**(XIII) Performance amongst all models (Monthly)**	**(XIV) Performance amongst all models (Daily)**	**(XV) 2.5% lower bound- (for monthly) (%)**	**(XVI) 2.5% upper bound- (for monthly) (%)**	**(XVII) 2.5% lower bound- (for daily) (%)**	**(XVIII) 2.5% upper bound- (for daily) (%)**
δCK_N	C_{N+1}/K_{N+1}	C_N, K_N	-	-	-	**41**	**374**	53%	75%	26%	31%	-	-	-	-	-	-
$BSMCK_N$	$C_{N+1}^{BSMCK_N}/K_{N+1}$	$S_N, K_{N+1}, T_{N+1}, R_N, Q_N, \sigma_N^{CALIB^{CK}}$	-	-	-	0	4	0%	0%	0%	1%	0	4	0%	0%	0%	1%
HCK_N	$C_{N+1}^{HCK_N}/K_{N+1}$	$S_N, K_{N+1}, T_{N+1}, R_N, Q_N, \sigma_N^{CALIB^{CK}}, HParams_N^{CK}$	-	-	-	0	0	0%	0%	0%	0%	0	1	0%	0%	0%	0%
$HJDCK_N$	$C_{N+1}^{HJDCK_N}/K_{N+1}$	$S_N, K_{N+1}, T_{N+1}, R_N, Q_N, \sigma_N^{CALIB^{CK}}, HJDParams_N^{CK}$	-	-	-	0	1	0%	0%	0%	0%	0	1	0%	0%	0%	0%
$FMLSCK_N$	$C_{N+1}^{FMLSCK_N}/K_{N+1}$	$S_N, K_{N+1}, T_{N+1}, R_N, Q_N, FMLSParams_N^{CK}$	-	-	-	0	1	0%	0%	0%	0%	0	1	0%	0%	0%	0%
$M1CK1_N$	$C_{N+1}^{M1CK1_N}/K_{N+1}$	$S_N/K_N, T_{N+1}, R_N, Q_N, \sigma_N^{CALIB^{CK}}$	1	5	5	3	31	0%	11%	2%	3%	5	43	2%	14%	2%	4%
$M1CK2_N$	$C_{N+1}^{M1CK2_N}/K_{N+1}$	$S_N/K_N, T_{N+1}, R_N, Q_N, \sigma_N^{CALIB^{CK}}, (C_N/K_N)$	1	6	6	7	34	5%	17%	2%	3%	**15**	76	13%	34%	4%	7%
$M1CK3_N$	$C_{N+1}^{M1CK3_N}/K_{N+1}$	$S_N/K_N, T_{N+1}, R_N, Q_N, \sigma_N^{CALIB^{CK}}, (C_N/K_N), BSMGreeks_N^{CK}$	1	11	11	3	106	0%	11%	7%	9%	6	159	3%	17%	10%	14%
$M1CK4_N$	$C_{N+1}^{M1CK4_N}/K_{N+1}$	$S_N/K_N, T_{N+1}, R_N, Q_N, \sigma_N^{CALIB^{CK}}, (C_N/K_N), BSMGreeks_N^{CK}, HParams_N^{CK}$	1	16	16	4	58	2%	13%	3%	5%	10	110	8%	25%	7%	10%
$M1CK5_N$	$C_{N+1}^{M1CK5_N}/K_{N+1}$	$S_N/K_N, T_{N+1}, R_N, Q_N, \sigma_N^{CALIB^{CK}}, (C_N/K_N), BSMGreeks_N^{CK}, HParams_N^{CK}, (C_N^{HCK}/K_N)$	1	17	17	3	52	0%	11%	3%	5%	10	121	8%	25%	8%	11%
$M1CK6_N$	$C_{N+1}^{M1CK6_N}/K_{N+1}$	$S_N/K_N, T_{N+1}, R_N, Q_N, HParams_N^{CK}, (C_N^{HCK}/K_N)$	1	10	10	1	47	0%	5%	3%	5%	10	75	6%	25%	4%	7%
$M1CK7_N$	$C_{N+1}^{M1CK7_N}/K_{N+1}$	$S_N/K_N, T_{N+1}, R_N, Q_N, \sigma_N^{CALIB^{CK}}, BSMGreeks_N^{CK}, (C_N^{BSMCK}/K_N)$	1	11	11	1	77	0%	5%	5%	7%	4	113	2%	13%	7%	10%
$M1CK8_N$	$C_{N+1}^{M1CK8_N}/K_{N+1}$	$S_N/K_N, T_{N+1}, R_N, Q_N, HJDParams_N^{CK}, (C_N^{HJDCK}/K_N)$	1	13	13	0	57	0%	0%	3%	5%	1	85	0%	5%	5%	8%
$M1CK9_N$	$C_{N+1}^{M1CK9_N}/K_{N+1}$	$S_N/K_N, T_{N+1}, R_N, Q_N, FMLSParams_N^{CK}, (C_N^{FMLSCK}/K_N)$	1	7	7	0	71	0%	0%	4%	6%	1	80	0%	5%	5%	7%
$L1CK1_N$	$C_{N+1}^{L1CK1_N}/K_{N+1}$	$S_N/K_N, T_{N+1}, R_N, Q_N, \sigma_N^{CALIB^{CK}}$	1	5	5	0	5	0%	0%	0%	1%	0	5	0%	0%	0%	1%
$L1CK2_N$	$C_{N+1}^{L1CK2_N}/K_{N+1}$	$S_N/K_N, T_{N+1}, R_N, Q_N, \sigma_N^{CALIB^{CK}}, (C_N/K_N)$	1	6	6	0	196	0%	0%	13%	17%	0	**218**	0%	0%	14%	18%
$L1CK3_N$	$C_{N+1}^{L1CK3_N}/K_{N+1}$	$S_N/K_N, T_{N+1}, R_N, Q_N, \sigma_N^{CALIB^{CK}}, (C_N/K_N), BSMGreeks_N^{CK}$	1	11	11	0	33	0%	0%	2%	3%	0	34	0%	0%	2%	3%
$L1CK4_N$	$C_{N+1}^{L1CK4_N}/K_{N+1}$	$S_N/K_N, T_{N+1}, R_N, Q_N, \sigma_N^{CALIB^{CK}}, (C_N/K_N), BSMGreeks_N^{CK}, HParams_N^{CK}$	1	16	16	0	48	0%	0%	3%	5%	0	51	0%	0%	3%	5%
$L1CK5_N$	$C_{N+1}^{L1CK5_N}/K_{N+1}$	$S_N/K_N, T_{N+1}, R_N, Q_N, \sigma_N^{CALIB^{CK}}, (C_N/K_N), BSMGreeks_N^{CK}, HParams_N^{CK}, (C_N^{HCK}/K_N)$	1	17	17	0	46	0%	0%	2%	4%	1	55	0%	5%	3%	5%
$L1CK6_N$	$C_{N+1}^{L1CK6_N}/K_{N+1}$	$S_N/K_N, T_{N+1}, R_N, Q_N, HParams_N^{CK}, (C_N^{HCK}/K_N)$	1	10	10	0	28	0%	0%	1%	3%	0	29	0%	0%	1%	3%
$L1CK7_N$	$C_{N+1}^{L1CK7_N}/K_{N+1}$	$S_N/K_N, T_{N+1}, R_N, Q_N, \sigma_N^{CALIB^{CK}}, BSMGreeks_N^{CK}, (C_N^{BSMCK}/K_N)$	1	11	11	1	51	0%	5%	3%	5%	1	59	0%	5%	3%	6%
$L1CK8_N$	$C_{N+1}^{L1CK8_N}/K_{N+1}$	$S_N/K_N, T_{N+1}, R_N, Q_N, HJDParams_N^{CK}, (C_N^{HJDCK}/K_N)$	1	13	13	0	0	0%	0%	0%	0%	0	0	0%	0%	0%	0%
$L1CK9_N$	$C_{N+1}^{L1CK9_N}/K_{N+1}$	$S_N/K_N, T_{N+1}, R_N, Q_N, FMLSParams_N^{CK}, (C_N^{FMLSCK}/K_N)$	1	7	7	0	9	0%	0%	0%	1%	0	9	0%	0%	0%	1%

Table A.2.20: Call Option Price Scaled by the Exercise Price Comparison (amongst Parametric and MLP $M1CK_N - Models$): This table presents a performance comparison using both daily and monthly statistics amongst the Black-Scholes-Merton ($BSMCK_N$) model, Heston (HCK_N) model, Heston Jump Diffusion ($HJDCK_N$) model, Finite Moment Log Stable ($FMLSCK_N$) model and the MLP $M1CK_N - Models$ ($M1CK1_N$ to $M1CK9_N$). The forecast variable for all the models is the one-day-ahead call option price scaled by the exercise price (C_{N+1}/K_{N+1}). The models denoted by the $_N$ subscript use lagged input variables for forecasting C_{N+1}/K_{N+1}. The one-day-ahead forecast errors of C_{N+1}/K_{N+1} are used to compute the Root Mean Square Error (RMSE). Column I identifies the models, column II identifies the forecast variable, column III lists the input variables used by the models to obtain the one-trading-day ahead forecast of C_{N+1}/K_{N+1}, and columns IV, V and VI describe the network architecture of the MLP $M1CK_N - Models$. Forecasts are made for 1,328 trading days, and there are 64 months covered in the sample using the monthly data.

When comparing all models simultaneously (i.e. including the random walk model (δCK_N), column VII reports the number of months out of the 64 months that each model has the smallest RMSE, while column VIII reports the number of days out of the 1,328 days each model has the smallest RMSE. Columns IX (lower bound) and X (upper bound) present the winning percentage out of 64 months for each model, evaluated using the bootstrap sampling technique. The statistical bootstrap performed (with replacement) at a 95% confidence level is computed from the monthly RMSE values of the respective models below. Columns XI (lower bound), and XII (upper bound) presents the winning percentage out of 1326 days for each model computed from bootstrapping the daily RMSE values of the respective models at a 95% confidence level.

Similarly, when the δCK_N model was excluded in the comparison, column XIII reports the number of months out of the 64 months that each model has the smallest RMSE, while column XIV reports the number of days out of the 1,328 days each model has the smallest RMSE. Columns XV (lower bound) and XVI (upper bound) present the winning percentage out of 64 months for each model, evaluated using the bootstrap sampling technique. The statistical bootstrap performed (with replacement) at a 95% confidence level is computed from the monthly RMSE values of the respective models below. Also, columns XVII (lower bound) and XVIII (upper bound) present the winning percentage out of 1326 days for each model computed from bootstrapping the daily RMSE values of the respective models at a 95% confidence level.

						Including the random walk						**Excluding the random walk**					
(I)	**(II)**	**(III)**	**(IV)**	**(V)**	**(VI)**	**(VII)**	**(VIII)**	**(IX)**	**(X)**	**(XI)**	**(XII)**	**(XIII)**	**(XIV)**	**(XV)**	**(XVI)**	**(XVII)**	**(XVIII)**
Model	**Forecast**	**Inputs**	**No. of hidden layers**	**No. of hidden nodes per layer**	**Network architecture**	**Performance amongst all models (Monthly)**	**Performance amongst all models (Daily)**	**2.5% lower bound-(for monthly) (%)**	**2.5% upper bound-(for monthly) (%)**	**2.5% lower bound-(for daily) (%)**	**2.5% upper bound-(for daily) (%)**	**Performance amongst all models (Monthly)**	**Performance amongst all models (Daily)**	**2.5% lower bound-(for monthly) (%)**	**2.5% upper bound-(for monthly) (%)**	**2.5% lower bound-(for daily) (%)**	**2.5% upper bound-(for daily) (%)**
δCK_N	C_{N+1}/K_{N+1}	C_N, K_N	-	-	-	**41**	**466**	53%	76%	32%	38%	-	-	-	-	-	-
$BSMCK_N$	$C_{N+1}^{BSMCK_N}/K_{N+1}$	$S_N, K_{N+1}, T_{N+1}, R_N, Q_N, \sigma_N^{CALIB^{CK}}$	-	-	-	0	10	0%	0%	0%	1%	0	12	0%	0%	0%	1%
HCK_N	$C_{N+1}^{HCK_N}/K_{N+1}$	$S_N, K_{N+1}, T_{N+1}, R_N, Q_N, \sigma_N^{CALIB^{CK}}, HParams_N^{CK}$	-	-	-	0	1	0%	0%	0%	0%	0	2	0%	0%	0%	0%
$HJDCK_N$	$C_{N+1}^{HJDCK_N}/K_{N+1}$	$S_N, K_{N+1}, T_{N+1}, R_N, Q_N, \sigma_N^{CALIB^{CK}}, HJDParams_N^{CK}$	-	-	-	0	4	0%	0%	0%	1%	0	4	0%	0%	0%	1%
$FMLSCK_N$	$C_{N+1}^{FMLSCK_N}/K_{N+1}$	$S_N, K_{N+1}, T_{N+1}, R_N, Q_N, FMLSParams_N^{CK}$	-	-	-	0	1	0%	0%	0%	0%	0	1	0%	0%	0%	0%
$M1CK1_N$	$C_{N+1}^{M1CK1_N}/K_{N+1}$	$S_N/K_N, T_{N+1}, R_N, Q_N, \sigma_N^{CALIB^{CK}}$	1	5	5	3	55	0%	9%	3%	5%	5	77	2%	16%	5%	7%
$M1CK2_N$	$C_{N+1}^{M1CK2_N}/K_{N+1}$	$S_N/K_N, T_{N+1}, R_N, Q_N, \sigma_N^{CALIB^{CK}}, (C_N/K_N)$	1	6	6	7	63	3%	19%	4%	6%	**15**	116	14%	34%	7%	10%
$M1CK3_N$	$C_{N+1}^{M1CK3_N}/K_{N+1}$	$S_N/K_N, T_{N+1}, R_N, Q_N, \sigma_N^{CALIB^{CK}}, (C_N/K_N), BSMGreeks_N^{CK}$	1	11	11	3	142	0%	11%	9%	13%	6	**216**	3%	17%	14%	18%
$M1CK4_N$	$C_{N+1}^{M1CK4_N}/K_{N+1}$	$S_N/K_N, T_{N+1}, R_N, Q_N, \sigma_N^{CALIB^{CK}}, (C_N/K_N), BSMGreeks_N^{CK}, HParams_N^{CK}$	1	16	16	4	79	2%	13%	5%	7%	10	146	8%	25%	9%	13%
$M1CK5_N$	$C_{N+1}^{M1CK5_N}/K_{N+1}$	$S_N/K_N, T_{N+1}, R_N, Q_N, \sigma_N^{CALIB^{CK}}, (C_N/K_N), BSMGreeks_N^{CK}, HParams_N^{CK}, (C_N^{HCK}/K_N)$	1	17	17	4	80	2%	13%	5%	7%	12	169	9%	28%	11%	15%
$M1CK6_N$	$C_{N+1}^{M1CK6_N}/K_{N+1}$	$S_N/K_N, T_{N+1}, R_N, Q_N, HParams_N^{CK}, (C_N^{HCK}/K_N)$	1	10	10	1	81	0%	5%	5%	7%	10	136	8%	25%	9%	12%
$M1CK7_N$	$C_{N+1}^{M1CK7_N}/K_{N+1}$	$S_N/K_N, T_{N+1}, R_N, Q_N, \sigma_N^{CALIB^{CK}}, BSMGreeks_N^{CK}, (C_N^{BSMCK}/K_N)$	1	11	11	1	112	0%	5%	7%	10%	4	161	2%	13%	10%	14%
$M1CK8_N$	$C_{N+1}^{M1CK8_N}/K_{N+1}$	$S_N/K_N, T_{N+1}, R_N, Q_N, HJDParams_N^{CK}, (C_N^{HJDCK}/K_N)$	1	13	13	0	108	0%	0%	7%	10%	1	148	0%	5%	9%	13%
$M1CK9_N$	$C_{N+1}^{M1CK9_N}/K_{N+1}$	$S_N/K_N, T_{N+1}, R_N, Q_N, FMLSParams_N^{CK}, (C_N^{FMLSCK}/K_N)$	1	7	7	0	126	0%	0%	8%	11%	1	140	0%	5%	9%	12%

Table A.2.21: Call Option Price Scaled by the Exercise Price Comparison (amongst Parametric and LSTM $L1CK_N - Models$): This table presents a performance comparison using both daily and monthly statistics amongst the Black-Scholes-Merton ($BSMCK_N$) model, Heston (HCK_N) model, Heston Jump Diffusion ($HJDCK_N$) model, Finite Moment Log Stable ($FMLSCK_N$) model and the LSTM $L1CK_N - Models$ ($L1CK1_N$ to $L1CK9_N$). The forecast variable for all the models is the one-day-ahead call option price scaled by the exercise price (C_{N+1}/K_{N+1}). The models denoted by the $_N$ subscript use lagged input variables for forecasting C_{N+1}/K_{N+1}. The one-day-ahead forecast errors of C_{N+1}/K_{N+1} are used to compute the Root Mean Square Error (RMSE). Column I identifies the models, column II identifies the forecast variable, column III lists the input variables used by the models to obtain the one-trading-day ahead forecast of C_{N+1}/K_{N+1}, and columns IV, V and VI describe the network architecture of the LSTM $L1CK_N - Models$. Forecasts are made for 1,328 trading days, and there are 64 months covered in the sample using the monthly data.

When comparing all models simultaneously (i.e. including the random walk model (δCK_N), column VII reports the number of months out of the 64 months that each model has the smallest RMSE, while column VIII reports the number of days out of the 1,328 days each model has the smallest RMSE. Columns IX (lower bound) and X (upper bound) present the winning percentage out of 64 months for each model, evaluated using the bootstrap sampling technique. The statistical bootstrap performed (with replacement) at a 95% confidence level is computed from the monthly RMSE values of the respective models below. Columns XI (lower bound) and XII (upper bound) present the winning percentage out of 1326 days for each model computed from bootstrapping the daily RMSE values of the respective models at a 95% confidence level.

Similarly, when the δCK_N model was excluded in the comparison, column XIII reports the number of months out of the 64 months that each model has the smallest RMSE, while column XIV reports the number of days out of the 1,328 days each model has the smallest RMSE. Columns XV (lower bound) and XVI (upper bound) present the winning percentage out of 64 months for each model, evaluated using the bootstrap sampling technique. The statistical bootstrap performed (with replacement) at a 95% confidence level is computed from the monthly RMSE values of the respective models below. Also, columns XVII (lower bound) and XVIII (upper bound) present the winning percentage out of 1326 days for each model computed from bootstrapping the daily RMSE values of the respective models at a 95% confidence level.

						Including the random walk						**Excluding the random walk**					
(I)	**(II)**	**(III)**	**(IV)**	**(V)**	**(VI)**	**(VII)**	**(VIII)**	**(IX)**	**(X)**	**(XI)**	**(XII)**	**(XIII)**	**(XIV)**	**(XV)**	**(XVI)**	**(XVII)**	**(XVIII)**
Model	**Forecast**	**Inputs**	**No. of hidden layers**	**No. of hidden nodes per layer**	**Network architecture**	**Performance amongst all models (Monthly)**	**Performance amongst all models (Daily)**	**2.5% lower bound- (for monthly) (%)**	**2.5% upper bound- (for monthly) (%)**	**2.5% lower bound- (for daily) (%)**	**2.5% upper bound- (for daily) (%)**	**Performance amongst all models (Monthly)**	**Performance amongst all models (Daily)**	**2.5% lower bound- (for monthly) (%)**	**2.5% upper bound- (for monthly) (%)**	**2.5% lower bound- (for daily) (%)**	**2.5% upper bound- (for daily) (%)**
δCK_N	C_{N+1}/K_{N+1}	C_N, K_N	-	-	-	**63**	**737**	95%	100%	53%	58%	-	-	-	-	-	-
$BSMCK_N$	$C_{N+1}^{BSMCK_N}/K_{N+1}$	$S_N, K_{N+1}, T_{N+1}, R_N, Q_N, \sigma_N^{CALIB^{CK}}$	-	-	-	0	6	0%	0%	0%	1%	0	12	0%	0%	0%	1%
HCK_N	$C_{N+1}^{HCK_N}/K_{N+1}$	$S_N, K_{N+1}, T_{N+1}, R_N, Q_N, \sigma_N^{CALIB^{CK}}, HParams_N^{CK}$	-	-	-	0	2	0%	0%	0%	0%	0	34	0%	0%	2%	3%
$HJDCK_N$	$C_{N+1}^{HJDCK_N}/K_{N+1}$	$S_N, K_{N+1}, T_{N+1}, R_N, Q_N, \sigma_N^{CALIB^{CK}}, HJDParams_N^{CK}$	-	-	-	0	1	0%	0%	0%	0%	0	1	0%	0%	0%	0%
$FMLSCK_N$	$C_{N+1}^{FMLSCK_N}/K_{N+1}$	$S_N, K_{N+1}, T_{N+1}, R_N, Q_N, FMLSParams_N^{CK}$	-	-	-	0	2	0%	0%	0%	0%	1	2	0%	5%	0%	0%
$L1CK1_N$	$C_{N+1}^{L1CK1_N}/K_{N+1}$	$S_N/K_N, T_{N+1}, R_N, Q_N, \sigma_N^{CALIB^{CK}}$	1	5	5	0	6	0%	0%	0%	1%	0	9	0%	0%	0%	1%
$L1CK2_N$	$C_{N+1}^{L1CK2_N}/K_{N+1}$	$S_N/K_N, T_{N+1}, R_N, Q_N, \sigma_N^{CALIB^{CK}}, (C_N/K_N)$	1	6	6	0	248	0%	0%	17%	21%	4	**439**	2%	13%	31%	36%
$L1CK3_N$	$C_{N+1}^{L1CK3_N}/K_{N+1}$	$S_N/K_N, T_{N+1}, R_N, Q_N, \sigma_N^{CALIB^{CK}}, (C_N/K_N), BSMGreeks_N^{CK}$	1	11	11	0	54	0%	0%	3%	5%	5	112	2%	14%	7%	10%
$L1CK4_N$	$C_{N+1}^{L1CK4_N}/K_{N+1}$	$S_N/K_N, T_{N+1}, R_N, Q_N, \sigma_N^{CALIB^{CK}}, (C_N/K_N), BSMGreeks_N^{CK}, HParams_N^{CK}$	1	16	16	0	63	0%	0%	4%	6%	5	116	2%	16%	7%	10%
$L1CK5_N$	$C_{N+1}^{L1CK5_N}/K_{N+1}$	$S_N/K_N, T_{N+1}, R_N, Q_N, \sigma_N^{CALIB^{CK}}, (C_N/K_N), BSMGreeks_N^{CK}, HParams_N^{CK}, (C_N^{HCK}/K_N)$	1	17	17	0	76	0%	0%	4%	7%	**20**	193	20%	44%	12%	16%
$L1CK6_N$	$C_{N+1}^{L1CK6_N}/K_{N+1}$	$S_N/K_N, T_{N+1}, R_N, Q_N, HParams_N^{CK}, (C_N^{HCK}/K_N)$	1	10	10	0	36	0%	0%	2%	4%	4	110	2%	13%	7%	10%
$L1CK7_N$	$C_{N+1}^{L1CK7_N}/K_{N+1}$	$S_N/K_N, T_{N+1}, R_N, Q_N, \sigma_N^{CALIB^{CK}}, BSMGreeks_N^{CK}, (C_N^{BSMCK}/K_N)$	1	11	11	1	87	0%	5%	5%	8%	17	229	16%	38%	15%	19%
$L1CK8_N$	$C_{N+1}^{L1CK8_N}/K_{N+1}$	$S_N/K_N, T_{N+1}, R_N, Q_N, HJDParams_N^{CK}, (C_N^{HJDCK}/K_N)$	1	13	13	0	0	0%	0%	0%	0%	0	0	0%	0%	0%	0%
$L1CK9_N$	$C_{N+1}^{L1CK9_N}/K_{N+1}$	$S_N/K_N, T_{N+1}, R_N, Q_N, FMLSParams_N^{CK}, (C_N^{FMLSCK}/K_N)$	1	7	7	0	11	0%	0%	0%	1%	8	72	5%	22%	4%	7%

Table A.2.22: Call Option Price Scaled by the Exercise Price Comparison (amongst Parametric, MLP $M2CK_N - Models$ and LSTM $L2CK_N - Models$): This table presents a performance comparison using both daily and monthly statistics amongst the Black-Scholes-Merton ($BSMCK_N$) model, Heston (HCK_N) model, Heston Jump Diffusion ($HJDCK_N$) model, Finite Moment Log Stable ($FMLSCK_N$) model, MLP $M2CK_N - Models$ ($M2CK1_N$ to $M2CK9_N$) and the LSTM $L2CK_N - Models$ ($L2CK1_N$ to $L2CK9_N$). The forecast variable for all the models is the one-day-ahead call option price scaled by the exercise price (C_{N+1}/K_{N+1}). The models denoted by the $_N$ subscript use lagged input variables for forecasting C_{N+1}/K_{N+1}. The one-day-ahead forecast errors of C_{N+1}/K_{N+1} are used to compute the Root Mean Square Error (RMSE). Column I identifies the models, column II identifies the forecast variable, column III lists the input variables used by the models to obtain the one-trading-day ahead forecast of C_{N+1}/K_{N+1}, and columns IV, V and VI describe the network architecture of the MLP $M2CK_N - Models$ and the LSTM $L2CK_N - Models$. Forecasts are made for 1,328 trading days, and there are 64 months covered in the sample using the monthly data.

When comparing all models simultaneously (i.e. including the random walk model (δCK_N), column VII reports the number of months out of the 64 months that each model has the smallest RMSE, while column VIII reports the number of days out of the 1,328 days each model has the smallest RMSE. Columns IX (lower bound) and X (upper bound) present the winning percentage out of 64 months for each model, evaluated using the bootstrap sampling technique. The statistical bootstrap performed (with replacement) at a 95% confidence level is computed from the monthly RMSE values of the respective models below. Columns XI (lower bound) and XII (upper bound) present the winning percentage out of 1326 days for each model computed from bootstrapping the daily RMSE values of the respective models at a 95% confidence level.

Similarly, when the δCK_N model was excluded in the comparison, column XIII reports the number of months out of the 64 months that each model has the smallest RMSE, while column XIV reports the number of days out of the 1,328 days each model has the smallest RMSE. Columns XV (lower bound) and XVI (upper bound) present the winning percentage out of 64 months for each model, evaluated using the bootstrap sampling technique. The statistical bootstrap performed (with replacement) at a 95% confidence level is computed from the monthly RMSE values of the respective models below. Also, columns XVII (lower bound) and XVIII (upper bound) present the winning percentage out of 1326 days for each model computed from bootstrapping the daily RMSE values of the respective models at a 95% confidence level.

						Including the random walk						Excluding the random walk					
(I)	**(II)**	**(III)**	**(IV)**	**(V)**	**(VI)**	**(VII)**	**(VIII)**	**(IX)**	**(X)**	**(XI)**	**(XII)**	**(XIII)**	**(XIV)**	**(XV)**	**(XVI)**	**(XVII)**	**(XVIII)**
Model	**Forecast**	**Inputs**	**No. of hidden layers**	**No. of hidden nodes per layer**	**Network architecture**	**Performance amongst all models (Monthly)**	**Performance amongst all models (Daily)**	**2.5% lower bound- (for monthly) (%)**	**2.5% upper bound- (for monthly) (%)**	**2.5% lower bound- (for daily) (%)**	**2.5% upper bound- (for daily) (%)**	**Performance amongst all models (Monthly)**	**Performance amongst all models (Daily)**	**2.5% lower bound- (for monthly) (%)**	**2.5% upper bound- (for monthly) (%)**	**2.5% lower bound- (for daily) (%)**	**2.5% upper bound- (for daily) (%)**
δCK_N	C_{N+1}/K_{N+1}	C_N, K_N	-	-	-	**32**	**334**	38%	61%	23%	28%	-	-	-	-	-	-
$BSMCK_N$	$C_{N+1}^{BSMCK_N}/K_{N+1}$	$S_N, K_{N+1}, T_{N+1}, R_N, Q_N, \sigma_N^{CALIB^{CK}}$	-	-	-	0	3	0%	0%	0%	1%	0	3	0%	0%	0%	1%
HCK_N	$C_{N+1}^{HCK_N}/K_{N+1}$	$S_N, K_{N+1}, T_{N+1}, R_N, Q_N, \sigma_N^{CALIB^{CK}}, HParams_N^{CK}$	-	-	-	0	0	0%	0%	0%	0%	0	1	0%	0%	0%	0%
$HJDCK_N$	$C_{N+1}^{HJDCK_N}/K_{N+1}$	$S_N, K_{N+1}, T_{N+1}, R_N, Q_N, \sigma_N^{CALIB^{CK}}, HJDParams_N^{CK}$	-	-	-	0	1	0%	0%	0%	0%	0	1	0%	0%	0%	0%
$FMLSCK_N$	$C_{N+1}^{FMLSCK_N}/K_{N+1}$	$S_N, K_{N+1}, T_{N+1}, R_N, Q_N, FMLSParams_N^{CK}$	-	-	-	0	0	0%	0%	0%	0%	0	0	0%	0%	0%	0%
$M2CK1_N$	$C_{N+1}^{M2CK1_N}/K_{N+1}$	$S_N/K_N, T_{N+1}, R_N, Q_N, \sigma_N^{CALIB^{CK}}$	2	5	5 X 5	1	56	0%	5%	3%	5%	1	65	0%	5%	4%	6%
$M2CK2_N$	$C_{N+1}^{M2CK2_N}/K_{N+1}$	$S_N/K_N, T_{N+1}, R_N, Q_N, \sigma_N^{CALIB^{CK}}, (C_N/K_N)$	2	6	6 X 6	1	91	0%	5%	6%	8%	4	123	2%	13%	8%	11%
$M2CK3_N$	$C_{N+1}^{M2CK3_N}/K_{N+1}$	$S_N/K_N, T_{N+1}, R_N, Q_N, \sigma_N^{CALIB^{CK}}, (C_N/K_N), BSMGreeks_N^{CK}$	2	11	11 X 11	4	78	2%	13%	5%	7%	6	120	3%	17%	8%	11%
$M2CK4_N$	$C_{N+1}^{M2CK4_N}/K_{N+1}$	$S_N/K_N, T_{N+1}, R_N, Q_N, \sigma_N^{CALIB^{CK}}, (C_N/K_N), BSMGreeks_N^{CK}, HParams_N^{CK}$	2	16	16 X 16	6	46	3%	17%	2%	4%	10	83	6%	23%	5%	8%
$M2CK5_N$	$C_{N+1}^{M2CK5_N}/K_{N+1}$	$S_N/K_N, T_{N+1}, R_N, Q_N, \sigma_N^{CALIB^{CK}}, (C_N/K_N), BSMGreeks_N^{CK}, HParams_N^{CK}, (C_N^{HCK}/K_N)$	2	17	17 X 17	2	42	0%	8%	2%	4%	8	71	5%	22%	4%	6%
$M2CK6_N$	$C_{N+1}^{M2CK6_N}/K_{N+1}$	$S_N/K_N, T_{N+1}, R_N, Q_N, HParams_N^{CK}, (C_N^{HCK}/K_N)$	2	10	10 X 10	8	43	5%	22%	2%	4%	**15**	86	14%	34%	5%	8%
$M2CK7_N$	$C_{N+1}^{M2CK7_N}/K_{N+1}$	$S_N/K_N, T_{N+1}, R_N, Q_N, \sigma_N^{CALIB^{CK}}, BSMGreeks_N^{CK}, (C_N^{BSMCK}/K_N)$	2	11	11 X 11	4	67	2%	13%	4%	6%	7	110	5%	19%	7%	10%
$M2CK8_N$	$C_{N+1}^{M2CK8_N}/K_{N+1}$	$S_N/K_N, T_{N+1}, R_N, Q_N, HJDParams_N^{CK}, (C_N^{HJDCK}/K_N)$	2	13	13 X 13	5	58	2%	16%	3%	5%	10	103	6%	25%	6%	9%
$M2CK9_N$	$C_{N+1}^{M2CK9_N}/K_{N+1}$	$S_N/K_N, T_{N+1}, R_N, Q_N, FMLSParams_N^{CK}, (C_N^{FMLSCK}/K_N)$	2	7	7 X 7	0	61	0%	0%	3%	6%	2	77	0%	8%	5%	7%
$L2CK1_N$	$C_{N+1}^{L2CK1_N}/K_{N+1}$	$S_N/K_N, T_{N+1}, R_N, Q_N, \sigma_N^{CALIB^{CK}}$	2	5	5 X 5	0	7	0%	0%	0%	1%	0	7	0%	0%	0%	1%
$L2CK2_N$	$C_{N+1}^{L2CK2_N}/K_{N+1}$	$S_N/K_N, T_{N+1}, R_N, Q_N, \sigma_N^{CALIB^{CK}}, (C_N/K_N)$	2	6	6 X 6	0	187	0%	0%	12%	16%	0	**201**	0%	0%	13%	17%
$L2CK3_N$	$C_{N+1}^{L2CK3_N}/K_{N+1}$	$S_N/K_N, T_{N+1}, R_N, Q_N, \sigma_N^{CALIB^{CK}}, (C_N/K_N), BSMGreeks_N^{CK}$	2	11	11 X 11	1	28	0%	5%	1%	3%	1	30	0%	5%	2%	3%
$L2CK4_N$	$C_{N+1}^{L2CK4_N}/K_{N+1}$	$S_N/K_N, T_{N+1}, R_N, Q_N, \sigma_N^{CALIB^{CK}}, (C_N/K_N), BSMGreeks_N^{CK}, HParams_N^{CK}$	2	16	16 X 16	0	64	0%	0%	4%	6%	0	67	0%	0%	4%	6%
$L2CK5_N$	$C_{N+1}^{L2CK5_N}/K_{N+1}$	$S_N/K_N, T_{N+1}, R_N, Q_N, \sigma_N^{CALIB^{CK}}, (C_N/K_N), BSMGreeks_N^{CK}, HParams_N^{CK}, (C_N^{HCK}/K_N)$	2	17	17 X 17	0	63	0%	0%	4%	6%	0	71	0%	0%	4%	7%
$L2CK6_N$	$C_{N+1}^{L2CK6_N}/K_{N+1}$	$S_N/K_N, T_{N+1}, R_N, Q_N, HParams_N^{CK}, (C_N^{HCK}/K_N)$	2	10	10 X 10	0	40	0%	0%	2%	4%	0	40	0%	0%	2%	4%
$L2CK7_N$	$C_{N+1}^{L2CK7_N}/K_{N+1}$	$S_N/K_N, T_{N+1}, R_N, Q_N, \sigma_N^{CALIB^{CK}}, BSMGreeks_N^{CK}, (C_N^{BSMCK}/K_N)$	2	11	11 X 11	0	45	0%	0%	2%	4%	0	55	0%	0%	3%	5%
$L2CK8_N$	$C_{N+1}^{L2CK8_N}/K_{N+1}$	$S_N/K_N, T_{N+1}, R_N, Q_N, HJDParams_N^{CK}, (C_N^{HJDCK}/K_N)$	2	13	13 X 13	0	0	0%	0%	0%	0%	0	0	0%	0%	0%	0%
$L2CK9_N$	$C_{N+1}^{L2CK9_N}/K_{N+1}$	$S_N/K_N, T_{N+1}, R_N, Q_N, FMLSParams_N^{CK}, (C_N^{FMLSCK}/K_N)$	2	7	7 X 7	0	14	0%	0%	0%	2%	0	14	0%	0%	1%	2%

Table A.2.23: Call Option Price Scaled by the Exercise Price Comparison (amongst Parametric and MLP $M2CK_N - Models$): This table presents a performance comparison using both daily and monthly statistics amongst the Black-Scholes-Merton ($BSMCK_N$) model, Heston (HCK_N) model, Heston Jump Diffusion ($HJDCK_N$) model, Finite Moment Log Stable ($FMLSCK_N$) model and the MLP $M2CK_N - Models$ ($M2CK1_N$ to $M2CK9_N$). The forecast variable for all the models is the one-day-ahead call option price scaled by the exercise price (C_{N+1}/K_{N+1}). The models denoted by the $_N$ subscript use lagged input variables for forecasting C_{N+1}/K_{N+1}. The one-day-ahead forecast errors of C_{N+1}/K_{N+1} are used to compute the Root Mean Square Error (RMSE). Column I identifies the models, column II identifies the forecast variable, column III lists the input variables used by the models to obtain the one-trading-day ahead forecast of C_{N+1}/K_{N+1}, and columns IV, V and VI describe the network architecture of the MLP $M2CK_N - Models$. Forecasts are made for 1,328 trading days, and there are 64 months covered in the sample using the monthly data.
When comparing all models simultaneously (i.e. including the random walk model (δCK_N), column VII reports the number of months out of the 64 months that each model has the smallest RMSE, while column VIII reports the number of days out of the 1,328 days each model has the smallest RMSE. Columns IX (lower bound) and X (upper bound) present the winning percentage out of 64 months for each model, evaluated using the bootstrap sampling technique. The statistical bootstrap performed (with replacement) at a 95% confidence level is computed from the monthly RMSE values of the respective models below. Columns XI (lower bound) and XII (upper bound) present the winning percentage out of 1326 days for each model computed from bootstrapping the daily RMSE values of the respective models at a 95% confidence level.
Similarly, when the δCK_N model was excluded in the comparison, column XIII reports the number of months out of the 64 months that each model has the smallest RMSE, while column XIV reports the number of days out of the 1,328 days each model has the smallest RMSE. Columns XV (lower bound) and XVI (upper bound) present the winning percentage out of 64 months for each model, evaluated using the bootstrap sampling technique. The statistical bootstrap performed (with replacement) at a 95% confidence level is computed from the monthly RMSE values of the respective models below. Also, columns XVII (lower bound) and XVIII (upper bound) present the winning percentage out of 1326 days for each model computed from bootstrapping the daily RMSE values of the respective models at a 95% confidence level.

						Including the random walk						**Excluding the random walk**					
(I)	**(II)**	**(III)**	**(IV)**	**(V)**	**(VI)**	**(VII)**	**(VIII)**	**(IX)**	**(X)**	**(XI)**	**(XII)**	**(XIII)**	**(XIV)**	**(XV)**	**(XVI)**	**(XVII)**	**(XVIII)**
Model	**Forecast**	**Inputs**	**No. of hidden layers**	**No. of hidden nodes per layer**	**Network architecture**	**Performance amongst all models (Monthly)**	**Performance amongst all models (Daily)**	**2.5% lower bound- (for monthly) (%)**	**2.5% upper bound- (for monthly) (%)**	**2.5% lower bound- (for daily) (%)**	**2.5% upper bound- (for daily) (%)**	**Performance amongst all models (Monthly)**	**Performance amongst all models (Daily)**	**2.5% lower bound- (for monthly) (%)**	**2.5% upper bound- (for monthly) (%)**	**2.5% lower bound- (for daily) (%)**	**2.5% upper bound- (for daily) (%)**
δCK_N	C_{N+1}/K_{N+1}	C_N, K_N	-	-	-	**32**	**428**	38%	63%	30%	35%	-	-	-	-	-	-
$BSMCK_N$	$C_{N+1}^{BSMCK_N}/K_{N+1}$	$S_N, K_{N+1}, T_{N+1}, R_N, Q_N, \sigma_N^{CALIB^{CK}}$	-	-	-	0	12	0%	0%	0%	1%	0	12	0%	0%	0%	1%
HCK_N	$C_{N+1}^{HCK_N}/K_{N+1}$	$S_N, K_{N+1}, T_{N+1}, R_N, Q_N, \sigma_N^{CALIB^{CK}}, HParams_N^{CK}$	-	-	-	0	0	0%	0%	0%	0%	0	1	0%	0%	0%	0%
$HJDCK_N$	$C_{N+1}^{HJDCK_N}/K_{N+1}$	$S_N, K_{N+1}, T_{N+1}, R_N, Q_N, \sigma_N^{CALIB^{CK}}, HJDParams_N^{CK}$	-	-	-	0	4	0%	0%	0%	1%	0	4	0%	0%	0%	1%
$FMLSCK_N$	$C_{N+1}^{FMLSCK_N}/K_{N+1}$	$S_N, K_{N+1}, T_{N+1}, R_N, Q_N, FMLSParams_N^{CK}$	-	-	-	0	1	0%	0%	0%	0%	0	1	0%	0%	0%	0%
$M2CK1_N$	$C_{N+1}^{M2CK1_N}/K_{N+1}$	$S_N/K_N, T_{N+1}, R_N, Q_N, \sigma_N^{CALIB^{CK}}$	2	5	5 X 5	1	104	0%	5%	6%	9%	1	117	0%	5%	7%	10%
$M2CK2_N$	$C_{N+1}^{M2CK2_N}/K_{N+1}$	$S_N/K_N, T_{N+1}, R_N, Q_N, \sigma_N^{CALIB^{CK}}, (C_N/K_N)$	2	6	6 X 6	1	137	0%	5%	9%	12%	4	178	2%	13%	12%	15%
$M2CK3_N$	$C_{N+1}^{M2CK3_N}/K_{N+1}$	$S_N/K_N, T_{N+1}, R_N, Q_N, \sigma_N^{CALIB^{CK}}, (C_N/K_N), BSMGreeks_N^{CK}$	2	11	11 X 11	4	125	2%	13%	8%	11%	6	**179**	3%	17%	12%	15%
$M2CK4_N$	$C_{N+1}^{M2CK4_N}/K_{N+1}$	$S_N/K_N, T_{N+1}, R_N, Q_N, \sigma_N^{CALIB^{CK}}, (C_N/K_N), BSMGreeks_N^{CK}, HParams_N^{CK}$	2	16	16 X 16	6	76	3%	17%	5%	7%	10	131	6%	25%	8%	12%
$M2CK5_N$	$C_{N+1}^{M2CK5_N}/K_{N+1}$	$S_N/K_N, T_{N+1}, R_N, Q_N, \sigma_N^{CALIB^{CK}}, (C_N/K_N), BSMGreeks_N^{CK}, HParams_N^{CK}, (C_N^{HCK}/K_N)$	2	17	17 X 17	2	62	0%	8%	4%	6%	8	105	5%	22%	7%	9%
$M2CK6_N$	$C_{N+1}^{M2CK6_N}/K_{N+1}$	$S_N/K_N, T_{N+1}, R_N, Q_N, HParams_N^{CK}, (C_N^{HCK}/K_N)$	2	10	10 X 10	9	88	6%	23%	5%	8%	**16**	168	14%	36%	11%	14%
$M2CK7_N$	$C_{N+1}^{M2CK7_N}/K_{N+1}$	$S_N/K_N, T_{N+1}, R_N, Q_N, \sigma_N^{CALIB^{CK}}, BSMGreeks_N^{CK}, (C_N^{BSMCK}/K_N)$	2	11	11 X 11	4	88	2%	13%	5%	8%	7	145	3%	19%	9%	13%
$M2CK8_N$	$C_{N+1}^{M2CK8_N}/K_{N+1}$	$S_N/K_N, T_{N+1}, R_N, Q_N, HJDParams_N^{CK}, (C_N^{HJDCK}/K_N)$	2	13	13 X 13	5	96	2%	14%	6%	9%	10	160	8%	25%	10%	14%
$M2CK9_N$	$C_{N+1}^{M2CK9_N}/K_{N+1}$	$S_N/K_N, T_{N+1}, R_N, Q_N, FMLSParams_N^{CK}, (C_N^{FMLSCK}/K_N)$	2	7	7 X 7	0	107	0%	0%	6%	10%	2	127	0%	8%	8%	11%

Table A.2.24: Call Option Price Scaled by the Exercise Price Comparison (amongst Parametric and LSTM $L2CK_N - Models$): This table presents a performance comparison using both daily and monthly statistics amongst the Black-Scholes-Merton ($BSMCK_N$) model, Heston (HCK_N) model, Heston Jump Diffusion ($HJDCK_N$) model, Finite Moment Log Stable ($FMLSCK_N$) model and the LSTM $L2CK_N - Models$ ($L2CK1_N$ to $L2CK9_N$). The forecast variable for all the models is the one-day-ahead call option price scaled by the exercise price (C_{N+1}/K_{N+1}). The models denoted by the $_N$ subscript use lagged input variables for forecasting C_{N+1}/K_{N+1}. The one-day-ahead forecast errors of C_{N+1}/K_{N+1} are used to compute the Root Mean Square Error (RMSE). Column I identifies the models, column II identifies the forecast variable, column III lists the input variables used by the models to obtain the one-trading-day ahead forecast of C_{N+1}/K_{N+1}, and columns IV, V and VI describe the network architecture of the LSTM $L2CK_N - Models$. Forecasts are made for 1,328 trading days, and there are 64 months covered in the sample using the monthly data.

When comparing all models simultaneously (i.e. including the random walk model (δCK_N), column VII reports the number of months out of the 64 months that each model has the smallest RMSE, while column VIII reports the number of days out of the 1,328 days each model has the smallest RMSE. Columns IX (lower bound) and X (upper bound) present the winning percentage out of 64 months for each model, evaluated using the bootstrap sampling technique. The statistical bootstrap performed (with replacement) at a 95% confidence level is computed from the monthly RMSE values of the respective models below. Columns XI (lower bound) and XII (upper bound) present the winning percentage out of 1326 days for each model computed from bootstrapping the daily RMSE values of the respective models at a 95% confidence level.

Similarly, when the δCK_N model was excluded in the comparison, column XIII reports the number of months out of the 64 months that each model has the smallest RMSE, while column XIV reports the number of days out of the 1,328 days each model has the smallest RMSE. Columns XV (lower bound) and XVI (upper bound) present the winning percentage out of 64 months for each model, evaluated using the bootstrap sampling technique. The statistical bootstrap performed (with replacement) at a 95% confidence level is computed from the monthly RMSE values of the respective models below. Also, columns XVII (lower bound) and XVIII (upper bound) present the winning percentage out of 1326 days for each model computed from bootstrapping the daily RMSE values of the respective models at a 95% confidence level.

						Including the random walk						Excluding the random walk					
(I) Model	**(II)** Forecast	**(III)** Inputs	**(IV)** No. of hidden layers	**(V)** No. of hidden nodes per layer	**(VI)** Network architecture	**(VII)** Performance amongst all models (Monthly)	**(VIII)** Performance amongst all models (Daily)	**(IX)** 2.5% lower bound-(for monthly) (%)	**(X)** 2.5% upper bound-(for monthly) (%)	**(XI)** 2.5% lower bound-(for daily) (%)	**(XII)** 2.5% upper bound-(for daily) (%)	**(XIII)** Performance amongst all models (Monthly)	**(XIV)** Performance amongst all models (Daily)	**(XV)** 2.5% lower bound-(for monthly) (%)	**(XVI)** 2.5% upper bound-(for monthly) (%)	**(XVII)** 2.5% lower bound-(for daily) (%)	**(XVIII)** 2.5% upper bound-(for daily) (%)
δCK_N	C_{N+1}/K_{N+1}	C_N, K_N	-	-	-	**63**	**704**	95%	100%	50%	56%	-	-	-	-	-	-
$BSMCK_N$	$C_{N+1}^{BSMCK_N}/K_{N+1}$	$S_N, K_{N+1}, T_{N+1}, R_N, Q_N, \sigma_N^{CALIB^{CK}}$	-	-	-	0	6	0%	0%	0%	1%	0	11	0%	0%	0%	1%
HCK_N	$C_{N+1}^{HCK_N}/K_{N+1}$	$S_N, K_{N+1}, T_{N+1}, R_N, Q_N, \sigma_N^{CALIB^{CK}}, HParams_N^{CK}$	-	-	-	0	1	0%	0%	0%	0%	0	33	0%	0%	2%	3%
$HJDCK_N$	$C_{N+1}^{HJDCK_N}/K_{N+1}$	$S_N, K_{N+1}, T_{N+1}, R_N, Q_N, \sigma_N^{CALIB^{CK}}, HJDParams_N^{CK}$	-	-	-	0	2	0%	0%	0%	0%	1	2	0%	5%	0%	0%
$FMLSCK_N$	$C_{N+1}^{FMLSCK_N}/K_{N+1}$	$S_N, K_{N+1}, T_{N+1}, R_N, Q_N, FMLSParams_N^{CK}$	-	-	-	0	1	0%	0%	0%	0%	1	1	0%	5%	0%	0%
$L2CK1_N$	$C_{N+1}^{L2CK1_N}/K_{N+1}$	$S_N/K_N, T_{N+1}, R_N, Q_N, \sigma_N^{CALIB^{CK}}$	2	5	5 X 5	0	7	0%	0%	0%	1%	0	9	0%	0%	0%	1%
$L2CK2_N$	$C_{N+1}^{L2CK2_N}/K_{N+1}$	$S_N/K_N, T_{N+1}, R_N, Q_N, \sigma_N^{CALIB^{CK}}, (C_N/K_N)$	2	6	6 X 6	0	236	0%	0%	16%	20%	1	**408**	0%	5%	28%	33%
$L2CK3_N$	$C_{N+1}^{L2CK3_N}/K_{N+1}$	$S_N/K_N, T_{N+1}, R_N, Q_N, \sigma_N^{CALIB^{CK}}, (C_N/K_N), BSMGreeks_N^{CK}$	2	11	11 X 11	1	51	0%	5%	3%	5%	2	91	0%	8%	6%	8%
$L2CK4_N$	$C_{N+1}^{L2CK4_N}/K_{N+1}$	$S_N/K_N, T_{N+1}, R_N, Q_N, \sigma_N^{CALIB^{CK}}, (C_N/K_N), BSMGreeks_N^{CK}, HParams_N^{CK}$	2	16	16 X 16	0	82	0%	0%	5%	8%	5	140	3%	16%	9%	12%
$L2CK5_N$	$C_{N+1}^{L2CK5_N}/K_{N+1}$	$S_N/K_N, T_{N+1}, R_N, Q_N, \sigma_N^{CALIB^{CK}}, (C_N/K_N), BSMGreeks_N^{CK}, HParams_N^{CK}, (C_N^{HCK}/K_N)$	2	17	17 X 17	0	99	0%	0%	6%	9%	**32**	246	39%	63%	16%	21%
$L2CK6_N$	$C_{N+1}^{L2CK6_N}/K_{N+1}$	$S_N/K_N, T_{N+1}, R_N, Q_N, HParams_N^{CK}, (C_N^{HCK}/K_N)$	2	10	10 X 10	0	48	0%	0%	3%	5%	3	87	0%	11%	5%	8%
$L2CK7_N$	$C_{N+1}^{L2CK7_N}/K_{N+1}$	$S_N/K_N, T_{N+1}, R_N, Q_N, \sigma_N^{CALIB^{CK}}, BSMGreeks_N^{CK}, (C_N^{BSMCK}/K_N)$	2	11	11 X 11	0	69	0%	0%	4%	6%	16	231	16%	34%	16%	19%
$L2CK8_N$	$C_{N+1}^{L2CK8_N}/K_{N+1}$	$S_N/K_N, T_{N+1}, R_N, Q_N, HJDParams_N^{CK}, (C_N^{HJDCK}/K_N)$	2	13	13 X 13	0	0	0%	0%	0%	0%	0	0	0%	0%	0%	0%
$L2CK9_N$	$C_{N+1}^{L2CK9_N}/K_{N+1}$	$S_N/K_N, T_{N+1}, R_N, Q_N, FMLSParams_N^{CK}, (C_N^{FMLSCK}/K_N)$	2	7	7 X 7	0	22	0%	0%	1%	2%	3	69	0%	11%	4%	6%

Table A.2.25: Call Option Price Scaled by the Exercise Price Comparison (amongst Parametric, MLP $M3CK_N - Models$ and LSTM $L3CK_N - Models$): This table presents a performance comparison using both daily and monthly statistics amongst the Black-Scholes-Merton ($BSMCK_N$) model, Heston (HCK_N) model, Heston Jump Diffusion ($HJDCK_N$) model, Finite Moment Log Stable ($FMLSCK_N$) model, MLP $M3CK_N - Models$ ($M3CK1_N$ to $M3CK9_N$) and the LSTM $L3CK_N - Models$ ($L3CK1_N$ to $L3CK9_N$). The forecast variable for all the models is the one-day-ahead call option price scaled by the exercise price (C_{N+1}/K_{N+1}). The models denoted by the $_N$ subscript use lagged input variables for forecasting C_{N+1}/K_{N+1}. The one-day-ahead forecast errors of C_{N+1}/K_{N+1} are used to compute the Root Mean Square Error (RMSE). Column I identifies the models, column II identifies the forecast variable, column III lists the input variables used by the models to obtain the one-trading-day ahead forecast of C_{N+1}/K_{N+1}, and columns IV, V and VI describe the network architecture of the MLP $M3CK_N - Models$ and the LSTM $L3CK_N - Models$. Forecasts are made for 1,328 trading days, and there are 64 months covered in the sample using the monthly data.
When comparing all models simultaneously (i.e. including the random walk model (δCK_N), column VII reports the number of months out of the 64 months that each model has the smallest RMSE, while column VIII reports the number of days out of the 1,328 days each model has the smallest RMSE. Columns IX (lower bound) and X (upper bound) present the winning percentage out of 64 months for each model, evaluated using the bootstrap sampling technique. The statistical bootstrap performed (with replacement) at a 95% confidence level is computed from the monthly RMSE values of the respective models below. Columns XI (lower bound) and XII (upper bound) present the winning percentage out of 1326 days for each model computed from bootstrapping the daily RMSE values of the respective models at a 95% confidence level.
Similarly, when the δCK_N model was excluded in the comparison, column XIII reports the number of months out of the 64 months that each model has the smallest RMSE, while column XIV reports the number of days out of the 1,328 days each model has the smallest RMSE. Columns XV (lower bound) and XVI (upper bound) present the winning percentage out of 64 months for each model, evaluated using the bootstrap sampling technique. The statistical bootstrap performed (with replacement) at a 95% confidence level is computed from the monthly RMSE values of the respective models below. Also, columns XVII (lower bound) and XVIII (upper bound) present the winning percentage out of 1326 days for each model computed from bootstrapping the daily RMSE values of the respective models at a 95% confidence level.

						Including the random walk						**Excluding the random walk**					
(I)	**(II)**	**(III)**	**(IV)**	**(V)**	**(VI)**	**(VII)**	**(VIII)**	**(IX)**	**(X)**	**(XI)**	**(XII)**	**(XIII)**	**(XIV)**	**(XV)**	**(XVI)**	**(XVII)**	**(XVIII)**
Model	**Forecast**	**Inputs**	**No. of hidden layers**	**No. of hidden nodes per layer**	**Network architecture**	**Performance amongst all models (Monthly)**	**Performance amongst all models (Daily)**	**2.5% lower bound- (for monthly) (%)**	**2.5% upper bound- (for monthly) (%)**	**2.5% lower bound- (for daily) (%)**	**2.5% upper bound- (for daily) (%)**	**Performance amongst all models (Monthly)**	**Performance amongst all models (Daily)**	**2.5% lower bound- (for monthly) (%)**	**2.5% upper bound- (for monthly) (%)**	**2.5% lower bound- (for daily) (%)**	**2.5% upper bound- (for daily) (%)**
δCK_N	C_{N+1}/K_{N+1}	C_N, K_N	-	-	-	**22**	**259**	22%	47%	17%	22%	-	-	-	-	-	-
$BSMCK_N$	$C_{N+1}^{BSMCK_N}/K_{N+1}$	$S_N, K_{N+1}, T_{N+1}, R_N, Q_N, \sigma_N^{CALIB^{CK}}$	-	-	-	0	1	0%	0%	0%	0%	0	1	0%	0%	0%	0%
HCK_N	$C_{N+1}^{HCK_N}/K_{N+1}$	$S_N, K_{N+1}, T_{N+1}, R_N, Q_N, \sigma_N^{CALIB^{CK}}, HParams_N^{CK}$	-	-	-	0	1	0%	0%	0%	0%	0	1	0%	0%	0%	0%
$HJDCK_N$	$C_{N+1}^{HJDCK_N}/K_{N+1}$	$S_N, K_{N+1}, T_{N+1}, R_N, Q_N, \sigma_N^{CALIB^{CK}}, HJDParams_N^{CK}$	-	-	-	0	1	0%	0%	0%	0%	0	1	0%	0%	0%	0%
$FMLSCK_N$	$C_{N+1}^{FMLSCK_N}/K_{N+1}$	$S_N, K_{N+1}, T_{N+1}, R_N, Q_N, FMLSParams_N^{CK}$	-	-	-	0	1	0%	0%	0%	0%	0	1	0%	0%	0%	0%
$M3CK1_N$	$C_{N+1}^{M3CK1_N}/K_{N+1}$	$S_N/K_N, T_{N+1}, R_N, Q_N, \sigma_N^{CALIB^{CK}}$	3	5	5 X 5 X 5	2	70	0%	8%	4%	7%	2	76	0%	8%	4%	7%
$M3CK2_N$	$C_{N+1}^{M3CK2_N}/K_{N+1}$	$S_N/K_N, T_{N+1}, R_N, Q_N, \sigma_N^{CALIB^{CK}}, (C_N/K_N)$	3	6	6 X 6 X 6	2	80	0%	8%	5%	7%	5	103	2%	16%	6%	9%
$M3CK3_N$	$C_{N+1}^{M3CK3_N}/K_{N+1}$	$S_N/K_N, T_{N+1}, R_N, Q_N, \sigma_N^{CALIB^{CK}}, (C_N/K_N), BSMGreeks_N^{CK}$	3	11	11 X 11 X 11	8	79	5%	21%	5%	7%	9	98	6%	22%	6%	9%
$M3CK4_N$	$C_{N+1}^{M3CK4_N}/K_{N+1}$	$S_N/K_N, T_{N+1}, R_N, Q_N, \sigma_N^{CALIB^{CK}}, (C_N/K_N), BSMGreeks_N^{CK}, HParams_N^{CK}$	3	16	16 X 16 X 16	8	71	5%	22%	4%	7%	10	111	8%	25%	7%	10%
$M3CK5_N$	$C_{N+1}^{M3CK5_N}/K_{N+1}$	$S_N/K_N, T_{N+1}, R_N, Q_N, \sigma_N^{CALIB^{CK}}, (C_N/K_N), BSMGreeks_N^{CK}, HParams_N^{CK}, (C_N^{HCK}/K_N)$	3	17	17 X 17 X 17	4	40	0%	13%	2%	4%	10	89	6%	25%	5%	8%
$M3CK6_N$	$C_{N+1}^{M3CK6_N}/K_{N+1}$	$S_N/K_N, T_{N+1}, R_N, Q_N, HParams_N^{CK}, (C_N^{HCK}/K_N)$	3	10	10 X 10 X 10	4	58	2%	13%	3%	6%	**11**	101	8%	27%	6%	9%
$M3CK7_N$	$C_{N+1}^{M3CK7_N}/K_{N+1}$	$S_N/K_N, T_{N+1}, R_N, Q_N, \sigma_N^{CALIB^{CK}}, BSMGreeks_N^{CK}, (C_N^{BSMCK}/K_N)$	3	11	11 X 11 X 11	4	93	2%	13%	6%	8%	5	117	2%	16%	7%	10%
$M3CK8_N$	$C_{N+1}^{M3CK8_N}/K_{N+1}$	$S_N/K_N, T_{N+1}, R_N, Q_N, HJDParams_N^{CK}, (C_N^{HJDCK}/K_N)$	3	13	13 X 13 X 13	7	57	3%	19%	3%	5%	8	80	5%	20%	5%	7%
$M3CK9_N$	$C_{N+1}^{M3CK9_N}/K_{N+1}$	$S_N/K_N, T_{N+1}, R_N, Q_N, FMLSParams_N^{CK}, (C_N^{FMLSCK}/K_N)$	3	7	7 X 7 X 7	2	62	0%	8%	4%	6%	3	77	0%	11%	5%	7%
$L3CK1_N$	$C_{N+1}^{L3CK1_N}/K_{N+1}$	$S_N/K_N, T_{N+1}, R_N, Q_N, \sigma_N^{CALIB^{CK}}$	3	5	5 X 5 X 5	0	12	0%	0%	0%	1%	0	12	0%	0%	0%	1%
$L3CK2_N$	$C_{N+1}^{L3CK2_N}/K_{N+1}$	$S_N/K_N, T_{N+1}, R_N, Q_N, \sigma_N^{CALIB^{CK}}, (C_N/K_N)$	3	6	6 X 6 X 6	0	195	0%	0%	13%	17%	0	**203**	0%	0%	13%	17%
$L3CK3_N$	$C_{N+1}^{L3CK3_N}/K_{N+1}$	$S_N/K_N, T_{N+1}, R_N, Q_N, \sigma_N^{CALIB^{CK}}, (C_N/K_N), BSMGreeks_N^{CK}$	3	11	11 X 11 X 11	1	28	0%	5%	1%	3%	1	28	0%	5%	1%	3%
$L3CK4_N$	$C_{N+1}^{L3CK4_N}/K_{N+1}$	$S_N/K_N, T_{N+1}, R_N, Q_N, \sigma_N^{CALIB^{CK}}, (C_N/K_N), BSMGreeks_N^{CK}, HParams_N^{CK}$	3	16	16 X 16 X 16	0	55	0%	0%	3%	5%	0	57	0%	0%	3%	5%
$L3CK5_N$	$C_{N+1}^{L3CK5_N}/K_{N+1}$	$S_N/K_N, T_{N+1}, R_N, Q_N, \sigma_N^{CALIB^{CK}}, (C_N/K_N), BSMGreeks_N^{CK}, HParams_N^{CK}, (C_N^{HCK}/K_N)$	3	17	17 X 17 X 17	0	62	0%	0%	4%	6%	0	65	0%	0%	4%	6%
$L3CK6_N$	$C_{N+1}^{L3CK6_N}/K_{N+1}$	$S_N/K_N, T_{N+1}, R_N, Q_N, HParams_N^{CK}, (C_N^{HCK}/K_N)$	3	10	10 X 10 X 10	0	35	0%	0%	2%	4%	0	35	0%	0%	2%	4%
$L3CK7_N$	$C_{N+1}^{L3CK7_N}/K_{N+1}$	$S_N/K_N, T_{N+1}, R_N, Q_N, \sigma_N^{CALIB^{CK}}, BSMGreeks_N^{CK}, (C_N^{BSMCK}/K_N)$	3	11	11 X 11 X 11	0	44	0%	0%	2%	4%	0	47	0%	0%	2%	5%
$L3CK8_N$	$C_{N+1}^{L3CK8_N}/K_{N+1}$	$S_N/K_N, T_{N+1}, R_N, Q_N, HJDParams_N^{CK}, (C_N^{HJDCK}/K_N)$	3	13	13 X 13 X 13	0	0	0%	0%	0%	0%	0	0	0%	0%	0%	0%
$L3CK9_N$	$C_{N+1}^{L3CK9_N}/K_{N+1}$	$S_N/K_N, T_{N+1}, R_N, Q_N, FMLSParams_N^{CK}, (C_N^{FMLSCK}/K_N)$	3	7	7 X 7 X 7	0	24	0%	0%	1%	3%	0	25	0%	0%	1%	3%

Table A.2.26: Call Option Price Scaled by the Exercise Price Comparison (amongst Parametric and MLP $M3CK_N - Models$): This table presents a performance comparison using both daily and monthly statistics amongst the Black-Scholes-Merton ($BSMCK_N$) model, Heston (HCK_N) model, Heston Jump Diffusion ($HJDCK_N$) model, Finite Moment Log Stable ($FMLSCK_N$) model and the MLP $M3CK_N - Models$ ($M3CK1_N$ to $M3CK9_N$). The forecast variable for all the models is the one-day-ahead call option price scaled by the exercise price (C_{N+1}/K_{N+1}). The models denoted by the $_N$ subscript use lagged input variables for forecasting C_{N+1}/K_{N+1}. The one-day-ahead forecast errors of C_{N+1}/K_{N+1} are used to compute the Root Mean Square Error (RMSE). Column I identifies the models, column II identifies the forecast variable, column III lists the input variables used by the models to obtain the one-trading-day ahead forecast of C_{N+1}/K_{N+1}, and columns IV, V and VI describe the network architecture of the MLP $M3CK_N - Models$. Forecasts are made for 1,328 trading days, and there are 64 months covered in the sample using the monthly data.
When comparing all models simultaneously (i.e. including the random walk model (δCK_N), column VII reports the number of months out of the 64 months that each model has the smallest RMSE, while column VIII reports the number of days out of the 1,328 days each model has the smallest RMSE. Columns IX (lower bound) and X (upper bound) present the winning percentage out of 64 months for each model, evaluated using the bootstrap sampling technique. The statistical bootstrap performed (with replacement) at a 95% confidence level is computed from the monthly RMSE values of the respective models below. Columns XI (lower bound) and XII (upper bound) present the winning percentage out of 1326 days for each model computed from bootstrapping the daily RMSE values of the respective models at a 95% confidence level.
Similarly, when the δCK_N model was excluded in the comparison, column XIII reports the number of months out of the 64 months that each model has the smallest RMSE, while column XIV reports the number of days out of the 1,328 days each model has the smallest RMSE. Columns XV (lower bound) and XVI (upper bound) present the winning percentage out of 64 months for each model, evaluated using the bootstrap sampling technique. The statistical bootstrap performed (with replacement) at a 95% confidence level is computed from the monthly RMSE values of the respective models below. Also, columns XVII (lower bound) and XVIII (upper bound) present the winning percentage out of 1326 days for each model computed from bootstrapping the daily RMSE values of the respective models at a 95% confidence level.

						Including the random walk						Excluding the random walk					
(I) Model	**(II)** Forecast	**(III)** Inputs	**(IV)** No. of hidden layers	**(V)** No. of hidden nodes per layer	**(VI)** Network architecture	**(VII)** Performance amongst all models (Monthly)	**(VIII)** Performance amongst all models (Daily)	**(IX)** 2.5% lower bound- (for monthly) (%)	**(X)** 2.5% upper bound- (for monthly) (%)	**(XI)** 2.5% lower bound- (for daily) (%)	**(XII)** 2.5% upper bound- (for daily) (%)	**(XIII)** Performance amongst all models (Monthly)	**(XIV)** Performance amongst all models (Daily)	**(XV)** 2.5% lower bound- (for monthly) (%)	**(XVI)** 2.5% upper bound- (for monthly) (%)	**(XVII)** 2.5% lower bound- (for daily) (%)	**(XVIII)** 2.5% upper bound- (for daily) (%)
δCK_N	C_{N+1}/K_{N+1}	C_N, K_N	-	-	-	**23**	**314**	23%	48%	21%	26%	-	-	-	-	-	-
$BSMCK_N$	$C_{N+1}^{BSMCK_N}/K_{N+1}$	$S_N, K_{N+1}, T_{N+1}, R_N, Q_N, \sigma_N^{CALIB^{CK}}$	-	-	-	0	9	0%	0%	0%	1%	0	9	0%	0%	0%	1%
HCK_N	$C_{N+1}^{HCK_N}/K_{N+1}$	$S_N, K_{N+1}, T_{N+1}, R_N, Q_N, \sigma_N^{CALIB^{CK}}, HParams_N^{CK}$	-	-	-	0	2	0%	0%	0%	0%	0	2	0%	0%	0%	0%
$HJDCK_N$	$C_{N+1}^{HJDCK_N}/K_{N+1}$	$S_N, K_{N+1}, T_{N+1}, R_N, Q_N, \sigma_N^{CALIB^{CK}}, HJDParams_N^{CK}$	-	-	-	0	4	0%	0%	0%	1%	0	4	0%	0%	0%	1%
$FMLSCK_N$	$C_{N+1}^{FMLSCK_N}/K_{N+1}$	$S_N, K_{N+1}, T_{N+1}, R_N, Q_N, FMLSParams_N^{CK}$	-	-	-	0	1	0%	0%	0%	0%	0	1	0%	0%	0%	0%
$M3CK1_N$	$C_{N+1}^{M3CK1_N}/K_{N+1}$	$S_N/K_N, T_{N+1}, R_N, Q_N, \sigma_N^{CALIB^{CK}}$	3	5	5 X 5 X 5	2	127	0%	8%	8%	11%	2	134	0%	8%	9%	12%
$M3CK2_N$	$C_{N+1}^{M3CK2_N}/K_{N+1}$	$S_N/K_N, T_{N+1}, R_N, Q_N, \sigma_N^{CALIB^{CK}}, (C_N/K_N)$	3	6	6 X 6 X 6	2	134	0%	8%	9%	12%	5	**164**	2%	16%	11%	14%
$M3CK3_N$	$C_{N+1}^{M3CK3_N}/K_{N+1}$	$S_N/K_N, T_{N+1}, R_N, Q_N, \sigma_N^{CALIB^{CK}}, (C_N/K_N), BSMGreeks_N^{CK}$	3	11	11 X 11 X 11	8	122	5%	20%	8%	11%	9	149	6%	22%	10%	13%
$M3CK4_N$	$C_{N+1}^{M3CK4_N}/K_{N+1}$	$S_N/K_N, T_{N+1}, R_N, Q_N, \sigma_N^{CALIB^{CK}}, (C_N/K_N), BSMGreeks_N^{CK}, HParams_N^{CK}$	3	16	16 X 16 X 16	8	109	5%	20%	7%	10%	10	160	8%	25%	10%	14%
$M3CK5_N$	$C_{N+1}^{M3CK5_N}/K_{N+1}$	$S_N/K_N, T_{N+1}, R_N, Q_N, \sigma_N^{CALIB^{CK}}, (C_N/K_N), BSMGreeks_N^{CK}, HParams_N^{CK}, (C_N^{HCK}/K_N)$	3	17	17 X 17 X 17	4	73	2%	13%	4%	7%	10	138	7%	25%	9%	12%
$M3CK6_N$	$C_{N+1}^{M3CK6_N}/K_{N+1}$	$S_N/K_N, T_{N+1}, R_N, Q_N, HParams_N^{CK}, (C_N^{HCK}/K_N)$	3	10	10 X 10 X 10	4	94	2%	13%	6%	8%	**12**	155	9%	28%	10%	14%
$M3CK7_N$	$C_{N+1}^{M3CK7_N}/K_{N+1}$	$S_N/K_N, T_{N+1}, R_N, Q_N, \sigma_N^{CALIB^{CK}}, BSMGreeks_N^{CK}, (C_N^{BSMCK}/K_N)$	3	11	11 X 11 X 11	4	132	2%	13%	8%	12%	5	159	2%	14%	10%	14%
$M3CK8_N$	$C_{N+1}^{M3CK8_N}/K_{N+1}$	$S_N/K_N, T_{N+1}, R_N, Q_N, HJDParams_N^{CK}, (C_N^{HJDCK}/K_N)$	3	13	13 X 13 X 13	7	91	3%	20%	6%	8%	8	120	5%	20%	8%	11%
$M3CK9_N$	$C_{N+1}^{M3CK9_N}/K_{N+1}$	$S_N/K_N, T_{N+1}, R_N, Q_N, FMLSParams_N^{CK}, (C_N^{FMLSCK}/K_N)$	3	7	7 X 7 X 7	2	116	0%	8%	7%	10%	3	133	0%	11%	8%	12%

Table A.2.27: Call Option Price Scaled by the Exercise Price Comparison (amongst Parametric and LSTM $L3CK_N - Models$): This table presents a performance comparison using both daily and monthly statistics amongst the Black-Scholes-Merton ($BSMCK_N$) model, Heston (HCK_N) model, Heston Jump Diffusion ($HJDCK_N$) model, Finite Moment Log Stable ($FMLSCK_N$) model and the LSTM $L3CK_N - Models$ ($L3CK1_N$ to $L3CK9_N$). The forecast variable for all the models is the one-day-ahead call option price scaled by the exercise price (C_{N+1}/K_{N+1}). The models denoted by the $_N$ subscript use lagged input variables for forecasting C_{N+1}/K_{N+1}. The one-day-ahead forecast errors of C_{N+1}/K_{N+1} are used to compute the Root Mean Square Error (RMSE). Column I identifies the models, column II identifies the forecast variable, column III lists the input variables used by the models to obtain the one-trading-day ahead forecast of C_{N+1}/K_{N+1}, and columns IV, V and VI describe the network architecture of the LSTM $L3CK_N - Models$. Forecasts are made for 1,328 trading days, and there are 64 months covered in the sample using the monthly data.
When comparing all models simultaneously (i.e. including the random walk model (δCK_N), column VII reports the number of months out of the 64 months that each model has the smallest RMSE, while column VIII reports the number of days out of the 1,328 days each model has the smallest RMSE. Columns IX (lower bound) and X (upper bound) present the winning percentage out of 64 months for each model, evaluated using the bootstrap sampling technique. The statistical bootstrap performed (with replacement) at a 95% confidence level is computed from the monthly RMSE values of the respective models below. Columns XI (lower bound) and XII (upper bound) present the winning percentage out of 1326 days for each model computed from bootstrapping the daily RMSE values of the respective models at a 95% confidence level.
Similarly, when the δCK_N model was excluded in the comparison, column XIII reports the number of months out of the 64 months that each model has the smallest RMSE, while column XIV reports the number of days out of the 1,328 days each model has the smallest RMSE. Columns XV (lower bound) and XVI (upper bound) present the winning percentage out of 64 months for each model, evaluated using the bootstrap sampling technique. The statistical bootstrap performed (with replacement) at a 95% confidence level is computed from the monthly RMSE values of the respective models below. Also, columns XVII (lower bound) and XVIII (upper bound) present the winning percentage out of 1326 days for each model computed from bootstrapping the daily RMSE values of the respective models at a 95% confidence level.

						Including the random walk						Excluding the random walk					
(I) Model	(II) Forecast	(III) Inputs	(IV) No. of hidden layers	(V) No. of hidden nodes per layer	(VI) Network architecture	(VII) Performance amongst all models (Monthly)	(VIII) Performance amongst all models (Daily)	(IX) 2.5% lower bound-(for monthly) (%)	(X) 2.5% upper bound-(for monthly) (%)	(XI) 2.5% lower bound-(for daily) (%)	(XII) 2.5% upper bound-(for daily) (%)	(XIII) Performance amongst all models (Monthly)	(XIV) Performance amongst all models (Daily)	(XV) 2.5% lower bound-(for monthly) (%)	(XVI) 2.5% upper bound-(for monthly) (%)	(XVII) 2.5% lower bound-(for daily) (%)	(XVIII) 2.5% upper bound-(for daily) (%)
δCK_N	C_{N+1}/K_{N+1}	C_N, K_N	-	-	-	**61**	**683**	89%	100%	49%	54%	-	-	-	-	-	-
$BSMCK_N$	$C_{N+1}^{BSMCK_N}/K_{N+1}$	$S_N, K_{N+1}, T_{N+1}, R_N, Q_N, \sigma_N^{CALIB^{CK}}$	-	-	-	0	3	0%	0%	0%	1%	0	8	0%	0%	0%	1%
HCK_N	$C_{N+1}^{HCK_N}/K_{N+1}$	$S_N, K_{N+1}, T_{N+1}, R_N, Q_N, \sigma_N^{CALIB^{CK}}, HParams_N^{CK}$	-	-	-	0	2	0%	0%	0%	0%	0	35	0%	0%	2%	4%
$HJDCK_N$	$C_{N+1}^{HJDCK_N}/K_{N+1}$	$S_N, K_{N+1}, T_{N+1}, R_N, Q_N, \sigma_N^{CALIB^{CK}}, HJDParams_N^{CK}$	-	-	-	0	1	0%	0%	0%	0%	0	1	0%	0%	0%	0%
$FMLSCK_N$	$C_{N+1}^{FMLSCK_N}/K_{N+1}$	$S_N, K_{N+1}, T_{N+1}, R_N, Q_N, FMLSParams_N^{CK}$	-	-	-	0	2	0%	0%	0%	0%	0	2	0%	0%	0%	0%
$L3CK1_N$	$C_{N+1}^{L3CK1_N}/K_{N+1}$	$S_N/K_N, T_{N+1}, R_N, Q_N, \sigma_N^{CALIB^{CK}}$	3	5	5 X 5 X 5	0	13	0%	0%	1%	2%	0	15	0%	0%	1%	2%
$L3CK2_N$	$C_{N+1}^{L3CK2_N}/K_{N+1}$	$S_N/K_N, T_{N+1}, R_N, Q_N, \sigma_N^{CALIB^{CK}}, (C_N/K_N)$	3	6	6 X 6 X 6	0	247	0%	0%	17%	21%	2	**410**	0%	8%	28%	34%
$L3CK3_N$	$C_{N+1}^{L3CK3_N}/K_{N+1}$	$S_N/K_N, T_{N+1}, R_N, Q_N, \sigma_N^{CALIB^{CK}}, (C_N/K_N), BSMGreeks_N^{CK}$	3	11	11 X 11 X 11	1	53	0%	5%	3%	5%	2	85	0%	8%	5%	8%
$L3CK4_N$	$C_{N+1}^{L3CK4_N}/K_{N+1}$	$S_N/K_N, T_{N+1}, R_N, Q_N, \sigma_N^{CALIB^{CK}}, (C_N/K_N), BSMGreeks_N^{CK}, HParams_N^{CK}$	3	16	16 X 16 X 16	1	87	0%	5%	5%	8%	8	154	5%	22%	10%	13%
$L3CK5_N$	$C_{N+1}^{L3CK5_N}/K_{N+1}$	$S_N/K_N, T_{N+1}, R_N, Q_N, \sigma_N^{CALIB^{CK}}, (C_N/K_N), BSMGreeks_N^{CK}, HParams_N^{CK}, (C_N^{HCK}/K_N)$	3	17	17 X 17 X 17	1	99	0%	5%	6%	9%	**40**	239	52%	73%	16%	20%
$L3CK6_N$	$C_{N+1}^{L3CK6_N}/K_{N+1}$	$S_N/K_N, T_{N+1}, R_N, Q_N, HParams_N^{CK}, (C_N^{HCK}/K_N)$	3	10	10 X 10 X 10	0	42	0%	0%	2%	4%	4	86	2%	13%	5%	8%
$L3CK7_N$	$C_{N+1}^{L3CK7_N}/K_{N+1}$	$S_N/K_N, T_{N+1}, R_N, Q_N, \sigma_N^{CALIB^{CK}}, BSMGreeks_N^{CK}, (C_N^{BSMCK}/K_N)$	3	11	11 X 11 X 11	0	66	0%	0%	4%	6%	3	238	0%	11%	16%	20%
$L3CK8_N$	$C_{N+1}^{L3CK8_N}/K_{N+1}$	$S_N/K_N, T_{N+1}, R_N, Q_N, HJDParams_N^{CK}, (C_N^{HJDCK}/K_N)$	3	13	13 X 13 X 13	0	0	0%	0%	0%	0%	0	0	0%	0%	0%	0%
$L3CK9_N$	$C_{N+1}^{L3CK9_N}/K_{N+1}$	$S_N/K_N, T_{N+1}, R_N, Q_N, FMLSParams_N^{CK}, (C_N^{FMLSCK}/K_N)$	3	7	7 X 7 X 7	0	30	0%	0%	2%	3%	5	55	2%	16%	3%	5%

Table A.2.28: Call Option Price Scaled by the Exercise Price Comparison (amongst Parametric, MLP $M1CK_N - Models$, LSTM $L1CK_N - Models$, MLP $M2CK_N - Models$, LSTM $L2CK_N - Models$, MLP $M3CK_N - Models$, and the LSTM $L3CK_N - Models$): This table presents a performance comparison using both daily and monthly statistics amongst the Black-Scholes-Merton ($BSMCK_N$) model, Heston (HCK_N) model, Heston Jump Diffusion ($HJDCK_N$) model, Finite Moment Log Stable ($FMLSCK_N$) model, MLP $M1CK_N - Models$ ($M1CK1_N$ to $M1CK9_N$), LSTM $L1CK_N - Models$ ($L1CK1_N$ to $L1CK9_N$), MLP $M2CK_N - Models$ ($M2CK1_N$ to $M2CK9_N$), LSTM $L2CK_N - Models$ ($L2CK1_N$ to $L2CK9_N$), MLP $M3CK_N - Models$ ($M3CK1_N$ to $M3CK9_N$) and the LSTM $L3CK_N - Models$ ($L3CK1_N$ to $L3CK9_N$). The forecast variable for all the models is the one-day-ahead call option price scaled by the exercise price (C_{N+1}/K_{N+1}). The models denoted by the $_N$ subscript use lagged input variables for forecasting C_{N+1}/K_{N+1}. The one-day-ahead forecast errors of C_{N+1}/K_{N+1} are used to compute the Root Mean Square Error (RMSE). Column I identifies the models, column II identifies the forecast variable, column III lists the input variables used by the models to obtain the one-trading-day ahead forecast of C_{N+1}/K_{N+1}, and columns IV, V and VI describe the network architecture of the MLP $M1CK_N - Models$, LSTM $L1CK_N - Models$, MLP $M2CK_N - Models$, LSTM $L2CK_N - Models$, MLP $M3CK_N - Models$, and the LSTM $L3CK_N - Models$. Forecasts are made for 1,328 trading days, and there are 64 months covered in the sample using the monthly data.
When comparing all models simultaneously (i.e. including the random walk model (δCK_N), column VII reports the number of months out of the 64 months that each model has the smallest RMSE, while column VIII reports the number of days out of the 1,328 days each model has the smallest RMSE. Columns IX (lower bound) and X (upper bound) present the winning percentage out of 64 months for each model, evaluated using the bootstrap sampling technique. The statistical bootstrap performed (with replacement) at a 95% confidence level is computed from the monthly RMSE values of the respective models below. Columns XI (lower bound) and XII (upper bound) present the winning percentage out of 1326 days for each model computed from bootstrapping the daily RMSE values of the respective models at a 95% confidence level.
Similarly, when the δCK_N model was excluded in the comparison, column XIII reports the number of months out of the 64 months that each model has the smallest RMSE, while column XIV reports the number of days out of the 1,328 days each model has the smallest RMSE. Columns XV (lower bound) and XVI (upper bound) present the winning percentage out of 64 months for each model, evaluated using the bootstrap sampling technique. The statistical bootstrap performed (with replacement) at a 95% confidence level is computed from the monthly RMSE values of the respective models below. Also, columns XVII (lower bound) and XVIII (upper bound) present the winning percentage out of 1326 days for each model computed from bootstrapping the daily RMSE values of the respective models at a 95% confidence level.

						Including the random walk						Excluding the random walk					
(I) Model	**(II) Forecast**	**(III) Inputs**	**(IV) No. of hidden layers**	**(V) No. of hidden nodes per layer**	**(VI) Network architecture**	**(VII) Performance amongst all models (Monthly)**	**(VIII) Performance amongst all models (Daily)**	**(IX) 2.5% lower bound- (for monthly) (%)**	**(X) 2.5% upper bound- (for monthly) (%)**	**(XI) 2.5% lower bound- (for daily) (%)**	**(XII) 2.5% upper bound- (for daily) (%)**	**(XIII) Performance amongst all models (Monthly)**	**(XIV) Performance amongst all models (Daily)**	**(XV) 2.5% lower bound- (for monthly) (%)**	**(XVI) 2.5% upper bound- (for monthly) (%)**	**(XVII) 2.5% lower bound- (for daily) (%)**	**(XVIII) 2.5% upper bound- (for daily) (%)**
δCK_N	C_{N+1}/K_{N+1}	C_N, K_N	-	-	-	**18**	**202**	17%	40%	13%	17%	-	-	-	-	-	-
$BSMCK_N$	$C_{N+1}^{BSMCK_N}/K_{N+1}$	$S_N, K_{N+1}, T_{N+1}, R_N, Q_N, \sigma_N^{CALIB^{CK}}$	-	-	-	0	1	0%	0%	0%	0%	0	1	0%	0%	0%	0%
HCK_N	$C_{N+1}^{HCK_N}/K_{N+1}$	$S_N, K_{N+1}, T_{N+1}, R_N, Q_N, \sigma_N^{CALIB^{CK}}, HParams_N^{CK}$	-	-	-	0	0	0%	0%	0%	0%	0	0	0%	0%	0%	0%
$HJDCK_N$	$C_{N+1}^{HJDCK_N}/K_{N+1}$	$S_N, K_{N+1}, T_{N+1}, R_N, Q_N, \sigma_N^{CALIB^{CK}}, HJDParams_N^{CK}$	-	-	-	0	1	0%	0%	0%	0%	0	1	0%	0%	0%	0%
$FMLSCK_N$	$C_{N+1}^{FMLSCK_N}/K_{N+1}$	$S_N, K_{N+1}, T_{N+1}, R_N, Q_N, FMLSParams_N^{CK}$	-	-	-	0	0	0%	0%	0%	0%	0	0	0%	0%	0%	0%
$M1CK1_N$	$C_{N+1}^{M1CK1_N}/K_{N+1}$	$S_N/K_N, T_{N+1}, R_N, Q_N, \sigma_N^{CALIB^{CK}}$	1	5	5	0	13	0%	0%	0%	2%	0	14	0%	0%	1%	2%
$M1CK2_N$	$C_{N+1}^{M1CK2_N}/K_{N+1}$	$S_N/K_N, T_{N+1}, R_N, Q_N, \sigma_N^{CALIB^{CK}}, (C_N/K_N)$	1	6	6	0	6	0%	0%	0%	1%	1	6	0%	5%	0%	1%
$M1CK3_N$	$C_{N+1}^{M1CK3_N}/K_{N+1}$	$S_N/K_N, T_{N+1}, R_N, Q_N, \sigma_N^{CALIB^{CK}}, (C_N/K_N), BSMGreeks_N^{CK}$	1	11	11	0	23	0%	0%	1%	3%	0	26	0%	0%	1%	3%
$M1CK4_N$	$C_{N+1}^{M1CK4_N}/K_{N+1}$	$S_N/K_N, T_{N+1}, R_N, Q_N, \sigma_N^{CALIB^{CK}}, (C_N/K_N), BSMGreeks_N^{CK}, HParams_N^{CK}$	1	16	16	3	15	0%	11%	1%	2%	3	16	0%	11%	1%	2%
$M1CK5_N$	$C_{N+1}^{M1CK5_N}/K_{N+1}$	$S_N/K_N, T_{N+1}, R_N, Q_N, \sigma_N^{CALIB^{CK}}, (C_N/K_N), BSMGreeks_N^{CK}, HParams_N^{CK}, (C_N^{HCK}/K_N)$	1	17	17	2	15	0%	8%	1%	2%	2	23	0%	8%	1%	2%
$M1CK6_N$	$C_{N+1}^{M1CK6_N}/K_{N+1}$	$S_N/K_N, T_{N+1}, R_N, Q_N, HParams_N^{CK}, (C_N^{HCK}/K_N)$	1	10	10	0	14	0%	0%	1%	2%	1	14	0%	5%	1%	2%
$M1CK7_N$	$C_{N+1}^{M1CK7_N}/K_{N+1}$	$S_N/K_N, T_{N+1}, R_N, Q_N, \sigma_N^{CALIB^{CK}}, BSMGreeks_N^{CK}, (C_N^{BSMCK}/K_N)$	1	11	11	0	19	0%	0%	1%	2%	0	19	0%	0%	1%	2%
$M1CK8_N$	$C_{N+1}^{M1CK8_N}/K_{N+1}$	$S_N/K_N, T_{N+1}, R_N, Q_N, HJDParams_N^{CK}, (C_N^{HJDCK}/K_N)$	1	13	13	0	18	0%	0%	1%	2%	0	19	0%	0%	1%	2%
$M1CK9_N$	$C_{N+1}^{M1CK9_N}/K_{N+1}$	$S_N/K_N, T_{N+1}, R_N, Q_N, FMLSParams_N^{CK}, (C_N^{FMLSCK}/K_N)$	1	7	7	0	16	0%	0%	1%	2%	0	16	0%	0%	1%	2%
$M2CK1_N$	$C_{N+1}^{M2CK1_N}/K_{N+1}$	$S_N/K_N, T_{N+1}, R_N, Q_N, \sigma_N^{CALIB^{CK}}$	2	5	5 X 5	0	1	0%	0%	0%	0%	0	1	0%	0%	0%	0%
$M2CK2_N$	$C_{N+1}^{M2CK2_N}/K_{N+1}$	$S_N/K_N, T_{N+1}, R_N, Q_N, \sigma_N^{CALIB^{CK}}, (C_N/K_N)$	2	6	6 X 6	0	89	0%	0%	5%	8%	0	89	0%	0%	5%	8%
$M2CK3_N$	$C_{N+1}^{M2CK3_N}/K_{N+1}$	$S_N/K_N, T_{N+1}, R_N, Q_N, \sigma_N^{CALIB^{CK}}, (C_N/K_N), BSMGreeks_N^{CK}$	2	11	11 X 11	0	4	0%	0%	0%	1%	0	4	0%	0%	0%	1%
$M2CK4_N$	$C_{N+1}^{M2CK4_N}/K_{N+1}$	$S_N/K_N, T_{N+1}, R_N, Q_N, \sigma_N^{CALIB^{CK}}, (C_N/K_N), BSMGreeks_N^{CK}, HParams_N^{CK}$	2	16	16 X 16	0	19	0%	0%	1%	2%	0	20	0%	0%	1%	2%
$M2CK5_N$	$C_{N+1}^{M2CK5_N}/K_{N+1}$	$S_N/K_N, T_{N+1}, R_N, Q_N, \sigma_N^{CALIB^{CK}}, (C_N/K_N), BSMGreeks_N^{CK}, HParams_N^{CK}, (C_N^{HCK}/K_N)$	2	17	17 X 17	0	16	0%	0%	1%	2%	0	16	0%	0%	1%	2%
$M2CK6_N$	$C_{N+1}^{M2CK6_N}/K_{N+1}$	$S_N/K_N, T_{N+1}, R_N, Q_N, HParams_N^{CK}, (C_N^{HCK}/K_N)$	2	10	10 X 10	0	10	0%	0%	0%	1%	0	10	0%	0%	0%	1%
$M2CK7_N$	$C_{N+1}^{M2CK7_N}/K_{N+1}$	$S_N/K_N, T_{N+1}, R_N, Q_N, \sigma_N^{CALIB^{CK}}, BSMGreeks_N^{CK}, (C_N^{BSMCK}/K_N)$	2	11	11 X 11	1	14	0%	5%	1%	2%	1	14	0%	5%	1%	2%
$M2CK8_N$	$C_{N+1}^{M2CK8_N}/K_{N+1}$	$S_N/K_N, T_{N+1}, R_N, Q_N, HJDParams_N^{CK}, (C_N^{HJDCK}/K_N)$	2	13	13 X 13	0	0	0%	0%	0%	0%	0	0	0%	0%	0%	0%
$M2CK9_N$	$C_{N+1}^{M2CK9_N}/K_{N+1}$	$S_N/K_N, T_{N+1}, R_N, Q_N, FMLSParams_N^{CK}, (C_N^{FMLSCK}/K_N)$	2	7	7 X 7	0	2	0%	0%	0%	0%	0	2	0%	0%	0%	0%
$M3CK1_N$	$C_{N+1}^{M3CK1_N}/K_{N+1}$	$S_N/K_N, T_{N+1}, R_N, Q_N, \sigma_N^{CALIB^{CK}}$	3	5	5 X 5 X 5	0	25	0%	0%	1%	3%	0	26	0%	0%	1%	3%
$M3CK2_N$	$C_{N+1}^{M3CK2_N}/K_{N+1}$	$S_N/K_N, T_{N+1}, R_N, Q_N, \sigma_N^{CALIB^{CK}}, (C_N/K_N)$	3	6	6 X 6 X 6	0	36	0%	0%	2%	4%	0	40	0%	0%	2%	4%
$M3CK3_N$	$C_{N+1}^{M3CK3_N}/K_{N+1}$	$S_N/K_N, T_{N+1}, R_N, Q_N, \sigma_N^{CALIB^{CK}}, (C_N/K_N), BSMGreeks_N^{CK}$	3	11	11 X 11 X 11	2	32	0%	8%	2%	3%	3	41	0%	11%	2%	4%
$M3CK4_N$	$C_{N+1}^{M3CK4_N}/K_{N+1}$	$S_N/K_N, T_{N+1}, R_N, Q_N, \sigma_N^{CALIB^{CK}}, (C_N/K_N), BSMGreeks_N^{CK}, HParams_N^{CK}$	3	16	16 X 16 X 16	1	20	0%	5%	1%	2%	1	25	0%	5%	1%	3%
$M3CK5_N$	$C_{N+1}^{M3CK5_N}/K_{N+1}$	$S_N/K_N, T_{N+1}, R_N, Q_N, \sigma_N^{CALIB^{CK}}, (C_N/K_N), BSMGreeks_N^{CK}, HParams_N^{CK}, (C_N^{HCK}/K_N)$	3	17	17 X 17 X 17	0	15	0%	0%	1%	2%	0	17	0%	0%	1%	2%
$M3CK6_N$	$C_{N+1}^{M3CK6_N}/K_{N+1}$	$S_N/K_N, T_{N+1}, R_N, Q_N, HParams_N^{CK}, (C_N^{HCK}/K_N)$	3	10	10 X 10 X 10	4	12	2%	13%	0%	1%	5	15	2%	14%	1%	2%
$M3CK7_N$	$C_{N+1}^{M3CK7_N}/K_{N+1}$	$S_N/K_N, T_{N+1}, R_N, Q_N, \sigma_N^{CALIB^{CK}}, BSMGreeks_N^{CK}, (C_N^{BSMCK}/K_N)$	3	11	11 X 11 X 11	1	21	0%	5%	1%	2%	1	27	0%	5%	1%	3%
$M3CK8_N$	$C_{N+1}^{M3CK8_N}/K_{N+1}$	$S_N/K_N, T_{N+1}, R_N, Q_N, HJDParams_N^{CK}, (C_N^{HJDCK}/K_N)$	3	13	13 X 13 X 13	2	21	0%	8%	1%	2%	2	27	0%	8%	1%	3%
$M3CK9_N$	$C_{N+1}^{M3CK9_N}/K_{N+1}$	$S_N/K_N, T_{N+1}, R_N, Q_N, FMLSParams_N^{CK}, (C_N^{FMLSCK}/K_N)$	3	7	7 X 7 X 7	0	16	0%	0%	1%	2%	0	22	0%	0%	1%	2%
$L1CK1_N$	$C_{N+1}^{L1CK1_N}/K_{N+1}$	$S_N/K_N, T_{N+1}, R_N, Q_N, \sigma_N^{CALIB^{CK}}$	1	5	5	0	6	0%	0%	0%	1%	0	6	0%	0%	0%	1%
$L1CK2_N$	$C_{N+1}^{L1CK2_N}/K_{N+1}$	$S_N/K_N, T_{N+1}, R_N, Q_N, \sigma_N^{CALIB^{CK}}, (C_N/K_N)$	1	6	6	0	92	0%	0%	6%	8%	0	**96**	0%	0%	6%	9%
$L1CK3_N$	$C_{N+1}^{L1CK3_N}/K_{N+1}$	$S_N/K_N, T_{N+1}, R_N, Q_N, \sigma_N^{CALIB^{CK}}, (C_N/K_N), BSMGreeks_N^{CK}$	1	11	11	0	8	0%	0%	0%	1%	0	8	0%	0%	0%	1%
$L1CK4_N$	$C_{N+1}^{L1CK4_N}/K_{N+1}$	$S_N/K_N, T_{N+1}, R_N, Q_N, \sigma_N^{CALIB^{CK}}, (C_N/K_N), BSMGreeks_N^{CK}, HParams_N^{CK}$	1	16	16	0	18	0%	0%	1%	2%	0	19	0%	0%	1%	2%
$L1CK5_N$	$C_{N+1}^{L1CK5_N}/K_{N+1}$	$S_N/K_N, T_{N+1}, R_N, Q_N, \sigma_N^{CALIB^{CK}}, (C_N/K_N), BSMGreeks_N^{CK}, HParams_N^{CK}, (C_N^{HCK}/K_N)$	1	17	17	0	28	0%	0%	1%	3%	0	31	0%	0%	2%	3%
$L1CK6_N$	$C_{N+1}^{L1CK6_N}/K_{N+1}$	$S_N/K_N, T_{N+1}, R_N, Q_N, HParams_N^{CK}, (C_N^{HCK}/K_N)$	1	10	10	0	15	0%	0%	1%	2%	0	15	0%	0%	1%	2%
$L1CK7_N$	$C_{N+1}^{L1CK7_N}/K_{N+1}$	$S_N/K_N, T_{N+1}, R_N, Q_N, \sigma_N^{CALIB^{CK}}, BSMGreeks_N^{CK}, (C_N^{BSMCK}/K_N)$	1	11	11	0	17	0%	0%	1%	2%	0	18	0%	0%	1%	2%
$L1CK8_N$	$C_{N+1}^{L1CK8_N}/K_{N+1}$	$S_N/K_N, T_{N+1}, R_N, Q_N, HJDParams_N^{CK}, (C_N^{HJDCK}/K_N)$	1	13	13	0	0	0%	0%	0%	0%	0	0	0%	0%	0%	0%
$L1CK9_N$	$C_{N+1}^{L1CK9_N}/K_{N+1}$	$S_N/K_N, T_{N+1}, R_N, Q_N, FMLSParams_N^{CK}, (C_N^{FMLSCK}/K_N)$	1	7	7	0	10	0%	0%	0%	1%	0	10	0%	0%	0%	1%
$L2CK1_N$	$C_{N+1}^{L2CK1_N}/K_{N+1}$	$S_N/K_N, T_{N+1}, R_N, Q_N, \sigma_N^{CALIB^{CK}}$	2	5	5 X 5	2	25	0%	8%	1%	3%	2	26	0%	8%	1%	3%
$L2CK2_N$	$C_{N+1}^{L2CK2_N}/K_{N+1}$	$S_N/K_N, T_{N+1}, R_N, Q_N, \sigma_N^{CALIB^{CK}}, (C_N/K_N)$	2	6	6 X 6	2	29	0%	8%	1%	3%	4	40	2%	13%	2%	4%
$L2CK3_N$	$C_{N+1}^{L2CK3_N}/K_{N+1}$	$S_N/K_N, T_{N+1}, R_N, Q_N, \sigma_N^{CALIB^{CK}}, (C_N/K_N), BSMGreeks_N^{CK}$	2	11	11 X 11	6	41	3%	17%	2%	4%	6	52	3%	17%	3%	5%
$L2CK4_N$	$C_{N+1}^{L2CK4_N}/K_{N+1}$	$S_N/K_N, T_{N+1}, R_N, Q_N, \sigma_N^{CALIB^{CK}}, (C_N/K_N), BSMGreeks_N^{CK}, HParams_N^{CK}$	2	16	16 X 16	5	39	3%	14%	2%	4%	7	63	5%	19%	4%	6%
$L2CK5_N$	$C_{N+1}^{L2CK5_N}/K_{N+1}$	$S_N/K_N, T_{N+1}, R_N, Q_N, \sigma_N^{CALIB^{CK}}, (C_N/K_N), BSMGreeks_N^{CK}, HParams_N^{CK}, (C_N^{HCK}/K_N)$	2	17	17 X 17	3	22	0%	11%	1%	2%	7	55	5%	19%	3%	5%
$L2CK6_N$	$C_{N+1}^{L2CK6_N}/K_{N+1}$	$S_N/K_N, T_{N+1}, R_N, Q_N, HParams_N^{CK}, (C_N^{HCK}/K_N)$	2	10	10 X 10	3	30	0%	11%	2%	3%	**8**	52	5%	22%	3%	5%
$L2CK7_N$	$C_{N+1}^{L2CK7_N}/K_{N+1}$	$S_N/K_N, T_{N+1}, R_N, Q_N, \sigma_N^{CALIB^{CK}}, BSMGreeks_N^{CK}, (C_N^{BSMCK}/K_N)$	2	11	11 X 11	3	24	0%	11%	1%	3%	3	32	0%	11%	2%	3%
$L2CK8_N$	$C_{N+1}^{L2CK8_N}/K_{N+1}$	$S_N/K_N, T_{N+1}, R_N, Q_N, HJDParams_N^{CK}, (C_N^{HJDCK}/K_N)$	2	13	13 X 13	4	24	2%	13%	1%	3%	4	35	2%	13%	2%	4%
$L2CK9_N$	$C_{N+1}^{L2CK9_N}/K_{N+1}$	$S_N/K_N, T_{N+1}, R_N, Q_N, FMLSParams_N^{CK}, (C_N^{FMLSCK}/K_N)$	2	7	7 X 7	1	18	0%	5%	1%	2%	2	28	0%	8%	1%	3%
$L3CK1_N$	$C_{N+1}^{L3CK1_N}/K_{N+1}$	$S_N/K_N, T_{N+1}, R_N, Q_N, \sigma_N^{CALIB^{CK}}$	3	5	5 X 5 X 5	0	7	0%	0%	0%	1%	0	7	0%	0%	0%	1%
$L3CK2_N$	$C_{N+1}^{L3CK2_N}/K_{N+1}$	$S_N/K_N, T_{N+1}, R_N, Q_N, \sigma_N^{CALIB^{CK}}, (C_N/K_N)$	3	6	6 X 6 X 6	0	76	0%	0%	4%	7%	0	78	0%	0%	5%	7%
$L3CK3_N$	$C_{N+1}^{L3CK3_N}/K_{N+1}$	$S_N/K_N, T_{N+1}, R_N, Q_N, \sigma_N^{CALIB^{CK}}, (C_N/K_N), BSMGreeks_N^{CK}$	3	11	11 X 11 X 11	1	12	0%	5%	0%	1%	1	12	0%	5%	0%	1%
$L3CK4_N$	$C_{N+1}^{L3CK4_N}/K_{N+1}$	$S_N/K_N, T_{N+1}, R_N, Q_N, \sigma_N^{CALIB^{CK}}, (C_N/K_N), BSMGreeks_N^{CK}, HParams_N^{CK}$	3	16	16 X 16 X 16	0	25	0%	0%	1%	3%	0	26	0%	0%	1%	3%
$L3CK5_N$	$C_{N+1}^{L3CK5_N}/K_{N+1}$	$S_N/K_N, T_{N+1}, R_N, Q_N, \sigma_N^{CALIB^{CK}}, (C_N/K_N), BSMGreeks_N^{CK}, HParams_N^{CK}, (C_N^{HCK}/K_N)$	3	17	17 X 17 X 17	0	25	0%	0%	1%	3%	0	26	0%	0%	1%	3%
$L3CK6_N$	$C_{N+1}^{L3CK6_N}/K_{N+1}$	$S_N/K_N, T_{N+1}, R_N, Q_N, HParams_N^{CK}, (C_N^{HCK}/K_N)$	3	10	10 X 10 X 10	0	14	0%	0%	1%	2%	0	14	0%	0%	1%	2%
$L3CK7_N$	$C_{N+1}^{L3CK7_N}/K_{N+1}$	$S_N/K_N, T_{N+1}, R_N, Q_N, \sigma_N^{CALIB^{CK}}, BSMGreeks_N^{CK}, (C_N^{BSMCK}/K_N)$	3	11	11 X 11 X 11	0	15	0%	0%	1%	2%	0	16	0%	0%	1%	2%
$L3CK8_N$	$C_{N+1}^{L3CK8_N}/K_{N+1}$	$S_N/K_N, T_{N+1}, R_N, Q_N, HJDParams_N^{CK}, (C_N^{HJDCK}/K_N)$	3	13	13 X 13 X 13	0	0	0%	0%	0%	0%	0	0	0%	0%	0%	0%
$L3CK9_N$	$C_{N+1}^{L3CK9_N}/K_{N+1}$	$S_N/K_N, T_{N+1}, R_N, Q_N, FMLSParams_N^{CK}, (C_N^{FMLSCK}/K_N)$	3	7	7 X 7 X 7	0	13	0%	0%	1%	2%	0	13	0%	0%	0%	2%

Table A.2.29: Call Option Price Scaled by the Exercise Price Comparison (amongst Parametric, MLP $M1CK_N - Models$, MLP $M2CK_N - Models$, and MLP $M3CK_N - Models$): This table presents a performance comparison using both daily and monthly statistics amongst the Black-Scholes-Merton ($BSMCK_N$) model, Heston (HCK_N) model, Heston Jump Diffusion ($HJDCK_N$) model, Finite Moment Log Stable ($FMLSCK_N$) model, MLP $M1CK_N - Models$ ($M1CK1_N$ to $M1CK9_N$), MLP $M2CK_N - Models$ ($M2CK1_N$ to $M2CK9_N$), and the MLP $M3CK_N - Models$ ($M3CK1_N$ to $M3CK9_N$). The forecast variable for all the models is the one-day-ahead call option price scaled by the exercise price (C_{N+1}/K_{N+1}). The models denoted by the $_N$ subscript use lagged input variables for forecasting C_{N+1}/K_{N+1}. The one-day-ahead forecast errors of C_{N+1}/K_{N+1} are used to compute the Root Mean Square Error (RMSE). Column I identifies the models, column II identifies the forecast variable, column III lists the input variables used by the models to obtain the one-trading-day ahead forecast of C_{N+1}/K_{N+1}, and columns IV, V and VI describe the network architecture of the MLP $M1CK_N - Models$, MLP $M2CK_N - Models$, and the MLP $M3CK_N - Models$. Forecasts are made for 1,328 trading days, and there are 64 months covered in the sample using the monthly data.
When comparing all models simultaneously (i.e. including the random walk model (δCK_N), column VII reports the number of months out of the 64 months that each model has the smallest RMSE, while column VIII reports the number of days out of the 1,328 days each model has the smallest RMSE. Columns IX (lower bound) and X (upper bound) present the winning percentage out of 64 months for each model, evaluated using the bootstrap sampling technique. The statistical bootstrap performed (with replacement) at a 95% confidence level is computed from the monthly RMSE values of the respective models below. Columns XI (lower bound) and XII (upper bound) present the winning percentage out of 1326 days for each model computed from bootstrapping the daily RMSE values of the respective models at a 95% confidence level.
Similarly, when the δCK_N model was excluded in the comparison, column XIII reports the number of months out of the 64 months that each model has the smallest RMSE, while column XIV reports the number of days out of the 1,328 days each model has the smallest RMSE. Columns XV (lower bound) and XVI (upper bound) present the winning percentage out of 64 months for each model, evaluated using the bootstrap sampling technique. The statistical bootstrap performed (with replacement) at a 95% confidence level is computed from the monthly RMSE values of the respective models below. Also, columns XVII (lower bound) and XVIII (upper bound) present the winning percentage out of 1326 days for each model computed from bootstrapping the daily RMSE values of the respective models at a 95% confidence level.

						Including the random walk						Excluding the random walk					
(I) Model	(II) Forecast	(III) Inputs	(IV) No. of hidden layers	(V) No. of hidden nodes per layer	(VI) Network architecture	(VII) Performance amongst all models (Monthly)	(VIII) Performance amongst all models (Daily)	(IX) 2.5% lower bound- (for monthly) (%)	(X) 2.5% upper bound- (for monthly) (%)	(XI) 2.5% lower bound- (for daily) (%)	(XII) 2.5% upper bound- (for daily) (%)	(XIII) Performance amongst all models (Monthly)	(XIV) Performance amongst all models (Daily)	(XV) 2.5% lower bound- (for monthly) (%)	(XVI) 2.5% upper bound- (for monthly) (%)	(XVII) 2.5% lower bound- (for daily) (%)	(XVIII) 2.5% upper bound- (for daily) (%)
δCK_N	C_{N+1}/K_{N+1}	C_N, K_N	-	-	-	**19**	**241**	20%	42%	16%	20%	-	-	-	-	-	-
$BSMCK_N$	$C_{N+1}^{BSMCK_N}/K_{N+1}$	$S_N, K_{N+1}, T_{N+1}, R_N, Q_N, \sigma_N^{CALIB^{CK}}$	-	-	-	0	8	0%	0%	0%	1%	0	8	0%	0%	0%	1%
HCK_N	$C_{N+1}^{HCK_N}/K_{N+1}$	$S_N, K_{N+1}, T_{N+1}, R_N, Q_N, \sigma_N^{CALIB^{CK}}, HParams_N^{CK}$	-	-	-	0	0	0%	0%	0%	0%	0	0	0%	0%	0%	0%
$HJDCK_N$	$C_{N+1}^{HJDCK_N}/K_{N+1}$	$S_N, K_{N+1}, T_{N+1}, R_N, Q_N, \sigma_N^{CALIB^{CK}}, HJDParams_N^{CK}$	-	-	-	0	2	0%	0%	0%	0%	0	2	0%	0%	0%	0%
$FMLSCK_N$	$C_{N+1}^{FMLSCK_N}/K_{N+1}$	$S_N, K_{N+1}, T_{N+1}, R_N, Q_N, FMLSParams_N^{CK}$	-	-	-	0	1	0%	0%	0%	0%	0	1	0%	0%	0%	0%
$M1CK1_N$	$C_{N+1}^{M1CK1_N}/K_{N+1}$	$S_N/K_N, T_{N+1}, R_N, Q_N, \sigma_N^{CALIB^{CK}}$	1	6	6	0	27	0%	0%	1%	3%	0	28	0%	0%	1%	3%
$M1CK2_N$	$C_{N+1}^{M1CK2_N}/K_{N+1}$	$S_N/K_N, T_{N+1}, R_N, Q_N, \sigma_N^{CALIB^{CK}}, (C_N/K_N)$	1	7	7	0	17	0%	0%	1%	2%	1	18	0%	5%	1%	2%
$M1CK3_N$	$C_{N+1}^{M1CK3_N}/K_{N+1}$	$S_N/K_N, T_{N+1}, R_N, Q_N, \sigma_N^{CALIB^{CK}}, (C_N/K_N), BSMGreeks_N^{CK}$	1	12	12	0	40	0%	0%	2%	4%	0	43	0%	0%	2%	4%
$M1CK4_N$	$C_{N+1}^{M1CK4_N}/K_{N+1}$	$S_N/K_N, T_{N+1}, R_N, Q_N, \sigma_N^{CALIB^{CK}}, (C_N/K_N), BSMGreeks_N^{CK}, HParams_N^{CK}$	1	17	17	3	28	0%	9%	1%	3%	3	30	0%	11%	2%	3%
$M1CK5_N$	$C_{N+1}^{M1CK5_N}/K_{N+1}$	$S_N/K_N, T_{N+1}, R_N, Q_N, \sigma_N^{CALIB^{CK}}, (C_N/K_N), BSMGreeks_N^{CK}, HParams_N^{CK}, (C_N^{HCK}/K_N)$	1	18	18	2	22	0%	8%	1%	2%	2	30	0%	8%	2%	3%
$M1CK6_N$	$C_{N+1}^{M1CK6_N}/K_{N+1}$	$S_N/K_N, T_{N+1}, R_N, Q_N, HParams_N^{CK}, (C_N^{HCK}/K_N)$	1	11	11	0	31	0%	0%	2%	3%	1	33	0%	5%	2%	3%
$M1CK7_N$	$C_{N+1}^{M1CK7_N}/K_{N+1}$	$S_N/K_N, T_{N+1}, R_N, Q_N, \sigma_N^{CALIB^{CK}}, BSMGreeks_N^{CK}, (C_N^{BSMCK}/K_N)$	1	12	12	0	34	0%	0%	2%	3%	0	34	0%	0%	2%	3%
$M1CK8_N$	$C_{N+1}^{M1CK8_N}/K_{N+1}$	$S_N/K_N, T_{N+1}, R_N, Q_N, HJDParams_N^{CK}, (C_N^{HJDCK}/K_N)$	1	14	14	0	35	0%	0%	2%	4%	0	37	0%	0%	2%	4%
$M1CK9_N$	$C_{N+1}^{M1CK9_N}/K_{N+1}$	$S_N/K_N, T_{N+1}, R_N, Q_N, FMLSParams_N^{CK}, (C_N^{FMLSCK}/K_N)$	1	8	8	0	42	0%	0%	2%	4%	0	43	0%	0%	2%	4%
$M2CK1_N$	$C_{N+1}^{M2CK1_N}/K_{N+1}$	$S_N/K_N, T_{N+1}, R_N, Q_N, \sigma_N^{CALIB^{CK}}$	3	6	6 X 6	0	50	0%	0%	3%	5%	0	51	0%	0%	3%	5%
$M2CK2_N$	$C_{N+1}^{M2CK2_N}/K_{N+1}$	$S_N/K_N, T_{N+1}, R_N, Q_N, \sigma_N^{CALIB^{CK}}, (C_N/K_N)$	3	7	7 X 7	0	59	0%	0%	3%	6%	0	64	0%	0%	4%	6%
$M2CK3_N$	$C_{N+1}^{M2CK3_N}/K_{N+1}$	$S_N/K_N, T_{N+1}, R_N, Q_N, \sigma_N^{CALIB^{CK}}, (C_N/K_N), BSMGreeks_N^{CK}$	3	12	12 X 12	2	52	0%	8%	3%	5%	3	65	0%	11%	4%	6%
$M2CK4_N$	$C_{N+1}^{M2CK4_N}/K_{N+1}$	$S_N/K_N, T_{N+1}, R_N, Q_N, \sigma_N^{CALIB^{CK}}, (C_N/K_N), BSMGreeks_N^{CK}, HParams_N^{CK}$	3	17	17 X 17	1	34	0%	5%	2%	3%	1	41	0%	5%	2%	4%
$M2CK5_N$	$C_{N+1}^{M2CK5_N}/K_{N+1}$	$S_N/K_N, T_{N+1}, R_N, Q_N, \sigma_N^{CALIB^{CK}}, (C_N/K_N), BSMGreeks_N^{CK}, HParams_N^{CK}, (C_N^{HCK}/K_N)$	3	18	18 X 18	0	22	0%	0%	1%	2%	0	27	0%	0%	1%	3%
$M2CK6_N$	$C_{N+1}^{M2CK6_N}/K_{N+1}$	$S_N/K_N, T_{N+1}, R_N, Q_N, HParams_N^{CK}, (C_N^{HCK}/K_N)$	3	11	11 X 11	4	30	2%	13%	2%	3%	5	36	2%	16%	2%	4%
$M2CK7_N$	$C_{N+1}^{M2CK7_N}/K_{N+1}$	$S_N/K_N, T_{N+1}, R_N, Q_N, \sigma_N^{CALIB^{CK}}, BSMGreeks_N^{CK}, (C_N^{BSMCK}/K_N)$	3	12	12 X 12	1	30	0%	6%	1%	3%	2	36	0%	8%	2%	4%
$M2CK8_N$	$C_{N+1}^{M2CK8_N}/K_{N+1}$	$S_N/K_N, T_{N+1}, R_N, Q_N, HJDParams_N^{CK}, (C_N^{HJDCK}/K_N)$	3	14	14 X 14	2	34	0%	8%	2%	3%	2	41	0%	8%	2%	4%
$M2CK9_N$	$C_{N+1}^{M2CK9_N}/K_{N+1}$	$S_N/K_N, T_{N+1}, R_N, Q_N, FMLSParams_N^{CK}, (C_N^{FMLSCK}/K_N)$	3	8	8 X 8	0	34	0%	0%	2%	3%	0	41	0%	0%	2%	4%
$M3CK1_N$	$C_{N+1}^{M3CK1_N}/K_{N+1}$	$S_N/K_N, T_{N+1}, R_N, Q_N, \sigma_N^{CALIB^{CK}}$	3	6	6 X 6 X 6	2	60	0%	8%	3%	6%	2	61	0%	8%	4%	6%
$M3CK2_N$	$C_{N+1}^{M3CK2_N}/K_{N+1}$	$S_N/K_N, T_{N+1}, R_N, Q_N, \sigma_N^{CALIB^{CK}}, (C_N/K_N)$	3	7	7 X 7 X 7	2	51	0%	8%	3%	5%	4	62	2%	13%	4%	6%
$M3CK3_N$	$C_{N+1}^{M3CK3_N}/K_{N+1}$	$S_N/K_N, T_{N+1}, R_N, Q_N, \sigma_N^{CALIB^{CK}}, (C_N/K_N), BSMGreeks_N^{CK}$	3	12	12 X 12 X 12	6	62	3%	16%	4%	6%	6	79	3%	17%	5%	7%
$M3CK4_N$	$C_{N+1}^{M3CK4_N}/K_{N+1}$	$S_N/K_N, T_{N+1}, R_N, Q_N, \sigma_N^{CALIB^{CK}}, (C_N/K_N), BSMGreeks_N^{CK}, HParams_N^{CK}$	3	17	17 X 17 X 17	5	67	2%	16%	4%	6%	7	**99**	5%	19%	6%	9%
$M3CK5_N$	$C_{N+1}^{M3CK5_N}/K_{N+1}$	$S_N/K_N, T_{N+1}, R_N, Q_N, \sigma_N^{CALIB^{CK}}, (C_N/K_N), BSMGreeks_N^{CK}, HParams_N^{CK}, (C_N^{HCK}/K_N)$	3	18	18 X 18 X 18	3	35	0%	11%	2%	4%	7	73	5%	20%	4%	7%
$M3CK6_N$	$C_{N+1}^{M3CK6_N}/K_{N+1}$	$S_N/K_N, T_{N+1}, R_N, Q_N, HParams_N^{CK}, (C_N^{HCK}/K_N)$	3	11	11 X 11 X 11	4	56	2%	13%	3%	5%	**9**	87	6%	23%	5%	8%
$M3CK7_N$	$C_{N+1}^{M3CK7_N}/K_{N+1}$	$S_N/K_N, T_{N+1}, R_N, Q_N, \sigma_N^{CALIB^{CK}}, BSMGreeks_N^{CK}, (C_N^{BSMCK}/K_N)$	3	12	12 X 12 X 12	3	33	0%	10%	2%	3%	3	44	0%	11%	2%	4%
$M3CK8_N$	$C_{N+1}^{M3CK8_N}/K_{N+1}$	$S_N/K_N, T_{N+1}, R_N, Q_N, HJDParams_N^{CK}, (C_N^{HJDCK}/K_N)$	3	14	14 X 14 X 14	4	47	2%	13%	3%	5%	4	59	2%	13%	3%	6%
$M3CK9_N$	$C_{N+1}^{M3CK9_N}/K_{N+1}$	$S_N/K_N, T_{N+1}, R_N, Q_N, FMLSParams_N^{CK}, (C_N^{FMLSCK}/K_N)$	3	8	8 X 8 X 8	1	44	0%	5%	2%	4%	2	55	0%	8%	3%	5%

Table A.2.30: Call Option Price Scaled by the Exercise Price Comparison (amongst Parametric and LSTM $L1CK_N - Models$, LSTM $L2CK_N - Models$, and LSTM $L3CK_N - Models$): This table presents a performance comparison using both daily and monthly statistics amongst the Black-Scholes-Merton ($BSMCK_N$) model, Heston (HCK_N) model, Heston Jump Diffusion ($HJDCK_N$) model, Finite Moment Log Stable ($FMLSCK_N$) model, LSTM $L1CK_N - Models$ ($L1CK1_N$ to $L1CK9_N$), LSTM $L2CK_N - Models$ ($L2CK1_N$ to $L2CK9_N$), and the LSTM $L3CK_N - Models$ ($L3CK1_N$ to $L3CK9_N$). The forecast variable for all the models is the one-day-ahead call option price scaled by the exercise price (C_{N+1}/K_{N+1}). The models denoted by the $_N$ subscript use lagged input variables for forecasting C_{N+1}/K_{N+1}. The one-day-ahead forecast errors of C_{N+1}/K_{N+1} are used to compute the Root Mean Square Error (RMSE). Column I identifies the models, column II identifies the forecast variable, column III lists the input variables used by the models to obtain the one-trading-day ahead forecast of C_{N+1}/K_{N+1}, and columns IV, V and VI describe the network architecture of the LSTM $L1CK_N - Models$, LSTM $L2CK_N - Models$, and the LSTM $L3CK_N - Models$. Forecasts are made for 1,328 trading days, and there are 64 months covered in the sample using the monthly data.
When comparing all models simultaneously (i.e. including the random walk model (δCK_N), column VII reports the number of months out of the 64 months that each model has the smallest RMSE, while column VIII reports the number of days out of the 1,328 days each model has the smallest RMSE. Columns IX (lower bound) and X (upper bound) present the winning percentage out of 64 months for each model, evaluated using the bootstrap sampling technique. The statistical bootstrap performed (with replacement) at a 95% confidence level is computed from the monthly RMSE values of the respective models below. Columns XI (lower bound) and XII (upper bound) present the winning percentage out of 1326 days for each model computed from bootstrapping the daily RMSE values of the respective models at a 95% confidence level.
Similarly, when the δCK_N model was excluded in the comparison, column XIII reports the number of months out of the 64 months that each model has the smallest RMSE, while column XIV reports the number of days out of the 1,328 days each model has the smallest RMSE. Columns XV (lower bound) and XVI (upper bound) present the winning percentage out of 64 months for each model, evaluated using the bootstrap sampling technique. The statistical bootstrap performed (with replacement) at a 95% confidence level is computed from the monthly RMSE values of the respective models below. Also, columns XVII (lower bound) and XVIII (upper bound) present the winning percentage out of 1326 days for each model computed from bootstrapping the daily RMSE values of the respective models at a 95% confidence level.

						Including the random walk						Excluding the random walk					
(I) Model	**(II) Forecast**	**(III) Inputs**	**(IV) No. of hidden layers**	**(V) No. of hidden nodes per layer**	**(VI) Network architecture**	**(VII) Performance amongst all models (Monthly)**	**(VIII) Performance amongst all models (Daily)**	**(IX) 2.5% lower bound-(for monthly) (%)**	**(X) 2.5% upper bound-(for monthly) (%)**	**(XI) 2.5% lower bound-(for daily) (%)**	**(XII) 2.5% upper bound-(for daily) (%)**	**(XIII) Performance amongst all models (Monthly)**	**(XIV) Performance amongst all models (Daily)**	**(XV) 2.5% lower bound-(for monthly) (%)**	**(XVI) 2.5% upper bound-(for monthly) (%)**	**(XVII) 2.5% lower bound-(for daily) (%)**	**(XVIII) 2.5% upper bound-(for daily) (%)**
δCK_N	C_{N+1}/K_{N+1}	C_N, K_N	-	-	-	**60**	**551**	88%	98%	39%	44%	-	-	-	-	-	-
$BSMCK_N$	$C_{N+1}^{BSMCK_N}/K_{N+1}$	$S_N, K_{N+1}, T_{N+1}, R_N, Q_N, \sigma_N^{CALIB^{CK}}$	-	-	-	0	2	0%	0%	0%	0%	0	5	0%	0%	0%	1%
HCK_N	$C_{N+1}^{HCK_N}/K_{N+1}$	$S_N, K_{N+1}, T_{N+1}, R_N, Q_N, \sigma_N^{CALIB^{CK}}, HParams_N^{CK}$	-	-	-	0	1	0%	0%	0%	0%	0	17	0%	0%	1%	2%
$HJDCK_N$	$C_{N+1}^{HJDCK_N}/K_{N+1}$	$S_N, K_{N+1}, T_{N+1}, R_N, Q_N, \sigma_N^{CALIB^{CK}}, HJDParams_N^{CK}$	-	-	-	0	1	0%	0%	0%	0%	0	1	0%	0%	0%	0%
$FMLSCK_N$	$C_{N+1}^{FMLSCK_N}/K_{N+1}$	$S_N, K_{N+1}, T_{N+1}, R_N, Q_N, FMLSParams_N^{CK}$	-	-	-	0	1	0%	0%	0%	0%	0	1	0%	0%	0%	0%
$L1CK1_N$	$C_{N+1}^{L1CK1_N}/K_{N+1}$	$S_N/K_N, T_{N+1}, R_N, Q_N, \sigma_N^{CALIB^{CK}}$	1	6	6	0	2	0%	0%	0%	0%	0	3	0%	0%	0%	1%
$L1CK2_N$	$C_{N+1}^{L1CK2_N}/K_{N+1}$	$S_N/K_N, T_{N+1}, R_N, Q_N, \sigma_N^{CALIB^{CK}}, (C_N/K_N)$	1	7	7	0	117	0%	0%	7%	10%	2	157	0%	8%	10%	14%
$L1CK3_N$	$C_{N+1}^{L1CK3_N}/K_{N+1}$	$S_N/K_N, T_{N+1}, R_N, Q_N, \sigma_N^{CALIB^{CK}}, (C_N/K_N), BSMGreeks_N^{CK}$	1	12	12	0	9	0%	0%	0%	1%	0	9	0%	0%	0%	1%
$L1CK4_N$	$C_{N+1}^{L1CK4_N}/K_{N+1}$	$S_N/K_N, T_{N+1}, R_N, Q_N, \sigma_N^{CALIB^{CK}}, (C_N/K_N), BSMGreeks_N^{CK}, HParams_N^{CK}$	1	17	17	0	21	0%	0%	1%	2%	0	26	0%	0%	1%	3%
$L1CK5_N$	$C_{N+1}^{L1CK5_N}/K_{N+1}$	$S_N/K_N, T_{N+1}, R_N, Q_N, \sigma_N^{CALIB^{CK}}, (C_N/K_N), BSMGreeks_N^{CK}, HParams_N^{CK}, (C_N^{HCK}/K_N)$	1	18	18	0	23	0%	0%	1%	2%	1	38	0%	5%	2%	4%
$L1CK6_N$	$C_{N+1}^{L1CK6_N}/K_{N+1}$	$S_N/K_N, T_{N+1}, R_N, Q_N, HParams_N^{CK}, (C_N^{HCK}/K_N)$	1	11	11	0	15	0%	0%	1%	2%	3	44	0%	11%	2%	4%
$L1CK7_N$	$C_{N+1}^{L1CK7_N}/K_{N+1}$	$S_N/K_N, T_{N+1}, R_N, Q_N, \sigma_N^{CALIB^{CK}}, BSMGreeks_N^{CK}, (C_N^{BSMCK}/K_N)$	1	12	12	1	33	0%	5%	2%	3%	3	49	0%	9%	3%	5%
$L1CK8_N$	$C_{N+1}^{L1CK8_N}/K_{N+1}$	$S_N/K_N, T_{N+1}, R_N, Q_N, HJDParams_N^{CK}, (C_N^{HJDCK}/K_N)$	1	14	14	0	0	0%	0%	0%	0%	0	0	0%	0%	0%	0%
$L1CK9_N$	$C_{N+1}^{L1CK9_N}/K_{N+1}$	$S_N/K_N, T_{N+1}, R_N, Q_N, FMLSParams_N^{CK}, (C_N^{FMLSCK}/K_N)$	1	8	8	0	4	0%	0%	0%	1%	7	15	4%	19%	1%	2%
$L2CK1_N$	$C_{N+1}^{L2CK1_N}/K_{N+1}$	$S_N/K_N, T_{N+1}, R_N, Q_N, \sigma_N^{CALIB^{CK}}$	3	6	6 X 6	0	6	0%	0%	0%	1%	0	6	0%	0%	0%	1%
$L2CK2_N$	$C_{N+1}^{L2CK2_N}/K_{N+1}$	$S_N/K_N, T_{N+1}, R_N, Q_N, \sigma_N^{CALIB^{CK}}, (C_N/K_N)$	3	7	7 X 7	0	117	0%	0%	7%	10%	1	**185**	0%	5%	12%	16%
$L2CK3_N$	$C_{N+1}^{L2CK3_N}/K_{N+1}$	$S_N/K_N, T_{N+1}, R_N, Q_N, \sigma_N^{CALIB^{CK}}, (C_N/K_N), BSMGreeks_N^{CK}$	3	12	12 X 12	1	11	0%	5%	0%	1%	1	17	0%	5%	1%	2%
$L2CK4_N$	$C_{N+1}^{L2CK4_N}/K_{N+1}$	$S_N/K_N, T_{N+1}, R_N, Q_N, \sigma_N^{CALIB^{CK}}, (C_N/K_N), BSMGreeks_N^{CK}, HParams_N^{CK}$	3	17	17 X 17	0	23	0%	0%	1%	2%	0	35	0%	0%	2%	3%
$L2CK5_N$	$C_{N+1}^{L2CK5_N}/K_{N+1}$	$S_N/K_N, T_{N+1}, R_N, Q_N, \sigma_N^{CALIB^{CK}}, (C_N/K_N), BSMGreeks_N^{CK}, HParams_N^{CK}, (C_N^{HCK}/K_N)$	3	18	18 X 18	0	47	0%	0%	3%	4%	8	96	5%	20%	6%	9%
$L2CK6_N$	$C_{N+1}^{L2CK6_N}/K_{N+1}$	$S_N/K_N, T_{N+1}, R_N, Q_N, HParams_N^{CK}, (C_N^{HCK}/K_N)$	3	11	11 X 11	0	19	0%	0%	1%	2%	1	22	0%	5%	1%	2%
$L2CK7_N$	$C_{N+1}^{L2CK7_N}/K_{N+1}$	$S_N/K_N, T_{N+1}, R_N, Q_N, \sigma_N^{CALIB^{CK}}, BSMGreeks_N^{CK}, (C_N^{BSMCK}/K_N)$	3	12	12 X 12	0	30	0%	0%	2%	3%	3	81	0%	11%	5%	7%
$L2CK8_N$	$C_{N+1}^{L2CK8_N}/K_{N+1}$	$S_N/K_N, T_{N+1}, R_N, Q_N, HJDParams_N^{CK}, (C_N^{HJDCK}/K_N)$	3	14	14 X 14	0	0	0%	0%	0%	0%	0	0	0%	0%	0%	0%
$L2CK9_N$	$C_{N+1}^{L2CK9_N}/K_{N+1}$	$S_N/K_N, T_{N+1}, R_N, Q_N, FMLSParams_N^{CK}, (C_N^{FMLSCK}/K_N)$	3	8	8 X 8	0	12	0%	0%	0%	1%	3	22	0%	11%	1%	2%
$L3CK1_N$	$C_{N+1}^{L3CK1_N}/K_{N+1}$	$S_N/K_N, T_{N+1}, R_N, Q_N, \sigma_N^{CALIB^{CK}}$	3	6	6 X 6 X 6	0	8	0%	0%	0%	1%	0	8	0%	0%	0%	1%
$L3CK2_N$	$C_{N+1}^{L3CK2_N}/K_{N+1}$	$S_N/K_N, T_{N+1}, R_N, Q_N, \sigma_N^{CALIB^{CK}}, (C_N/K_N)$	3	7	7 X 7 X 7	0	106	0%	0%	6%	9%	2	158	0%	8%	10%	14%
$L3CK3_N$	$C_{N+1}^{L3CK3_N}/K_{N+1}$	$S_N/K_N, T_{N+1}, R_N, Q_N, \sigma_N^{CALIB^{CK}}, (C_N/K_N), BSMGreeks_N^{CK}$	3	12	12 X 12 X 12	1	21	0%	5%	1%	2%	1	28	0%	5%	1%	3%
$L3CK4_N$	$C_{N+1}^{L3CK4_N}/K_{N+1}$	$S_N/K_N, T_{N+1}, R_N, Q_N, \sigma_N^{CALIB^{CK}}, (C_N/K_N), BSMGreeks_N^{CK}, HParams_N^{CK}$	3	17	17 X 17 X 17	1	36	0%	5%	2%	4%	3	59	0%	11%	3%	6%
$L3CK5_N$	$C_{N+1}^{L3CK5_N}/K_{N+1}$	$S_N/K_N, T_{N+1}, R_N, Q_N, \sigma_N^{CALIB^{CK}}, (C_N/K_N), BSMGreeks_N^{CK}, HParams_N^{CK}, (C_N^{HCK}/K_N)$	3	18	18 X 18 X 18	0	48	0%	0%	3%	5%	**20**	97	19%	42%	6%	9%
$L3CK6_N$	$C_{N+1}^{L3CK6_N}/K_{N+1}$	$S_N/K_N, T_{N+1}, R_N, Q_N, HParams_N^{CK}, (C_N^{HCK}/K_N)$	3	11	11 X 11 X 11	0	20	0%	0%	1%	2%	1	30	0%	5%	1%	3%
$L3CK7_N$	$C_{N+1}^{L3CK7_N}/K_{N+1}$	$S_N/K_N, T_{N+1}, R_N, Q_N, \sigma_N^{CALIB^{CK}}, BSMGreeks_N^{CK}, (C_N^{BSMCK}/K_N)$	3	12	12 X 12 X 12	0	29	0%	0%	2%	3%	0	98	0%	0%	6%	9%
$L3CK8_N$	$C_{N+1}^{L3CK8_N}/K_{N+1}$	$S_N/K_N, T_{N+1}, R_N, Q_N, HJDParams_N^{CK}, (C_N^{HJDCK}/K_N)$	3	14	14 X 14 X 14	0	0	0%	0%	0%	0%	0	0	0%	0%	0%	0%
$L3CK9_N$	$C_{N+1}^{L3CK9_N}/K_{N+1}$	$S_N/K_N, T_{N+1}, R_N, Q_N, FMLSParams_N^{CK}, (C_N^{FMLSCK}/K_N)$	3	8	8 X 8 X 8	0	16	0%	0%	1%	2%	4	22	2%	13%	1%	2%

Table A.2.31: Call Option Price Scaled by the Exercise Price Comparison (amongst MLP $M1CK_N - Models$, LSTM $L1CK_N - Models$, MLP $M2CK_N - Models$, LSTM $L2CK_N - Models$, MLP $M3CK_N - Models$, and LSTM $L3CK_N - Models$): This table presents a performance comparison using both daily and monthly statistics amongst the MLP $M1CK_N - Models$ ($M1CK1_N$ to $M1CK9_N$), LSTM $L1CK_N - Models$ ($L1CK1_N$ to $L1CK9_N$), MLP $M2CK_N - Models$ ($M2CK1_N$ to $M2CK9_N$), LSTM $L2CK_N - Models$ ($L2CK1_N$ to $L2CK9_N$), MLP $M3CK_N - Models$ ($M3CK1_N$ to $M3CK9_N$) and the LSTM $L3CK_N - Models$ ($L3CK1_N$ to $L3CK9_N$). The forecast variable for all the models is the one-day-ahead call option price scaled by the exercise price (C_{N+1}/K_{N+1}). The models denoted by the $_N$ subscript use lagged input variables for forecasting C_{N+1}/K_{N+1}. The one-day-ahead forecast errors of C_{N+1}/K_{N+1} are used to compute the Root Mean Square Error (RMSE). Column I identifies the models, column II identifies the forecast variable, column III lists the input variables used by the models to obtain the one-trading-day ahead forecast of C_{N+1}/K_{N+1}, and columns IV, V and VI describe the network architecture of the MLP $M1CK_N - Models$, LSTM $L1CK_N - Models$, MLP $M2CK_N - Models$, LSTM $L2CK_N - Models$, MLP $M3CK_N - Models$, and the LSTM $L3CK_N - Models$. Forecasts are made for 1,328 trading days, and there are 64 months covered in the sample using the monthly data.
When comparing all models simultaneously (i.e. including the random walk model (δCK_N), column VII reports the number of months out of the 64 months that each model has the smallest RMSE, while column VIII reports the number of days out of the 1,328 days each model has the smallest RMSE. Columns IX (lower bound) and X (upper bound) present the winning percentage out of 64 months for each model, evaluated using the bootstrap sampling technique. The statistical bootstrap performed (with replacement) at a 95% confidence level is computed from the monthly RMSE values of the respective models below. Columns XI (lower bound) and XII (upper bound) present the winning percentage out of 1326 days for each model computed from bootstrapping the daily RMSE values of the respective models at a 95% confidence level. Similarly, when the δCK_N model was excluded in the comparison, column XIII reports the number of months out of the 64 months that each model has the smallest RMSE, while column XIV reports the number of days out of the 1,328 days each model has the smallest RMSE. Columns XV (lower bound) and XVI (upper bound) present the winning percentage out of 64 months for each model, evaluated using the bootstrap sampling technique. The statistical bootstrap performed (with replacement) at a 95% confidence level is computed from the monthly RMSE values of the respective models below. Also, columns XVII (lower bound) and XVIII (upper bound) present the winning percentage out of 1326 days for each model computed from bootstrapping the daily RMSE values of the respective models at a 95% confidence level.

						Including the random walk						Excluding the random walk					
(I) Model	(II) Forecast	(III) Inputs	(IV) No. of hidden layers	(V) No. of hidden nodes per layer	(VI) Network architecture	(VII) Performance amongst all models (Monthly)	(VIII) Performance amongst all models (Daily)	(IX) 2.5% lower bound- (for monthly) (%)	(X) 2.5% upper bound- (for monthly) (%)	(XI) 2.5% lower bound- (for daily) (%)	(XII) 2.5% upper bound- (for daily) (%)	(XIII) Performance amongst all models (Monthly)	(XIV) Performance amongst all models (Daily)	(XV) 2.5% lower bound- (for monthly) (%)	(XVI) 2.5% upper bound- (for monthly) (%)	(XVII) 2.5% lower bound- (for daily) (%)	(XVIII) 2.5% upper bound- (for daily) (%)
δCK_N	C_{N+1}/K_{N+1}	C_N, K_N	-	-	-	**18**	**202**	17%	40%	13%	17%	-	-	-	-	-	-
$M1CK1_N$	$C_{N+1}^{M1CK1_N}/K_{N+1}$	$S_N/K_N, T_{N+1}, R_N, Q_N, \sigma_N^{CALIB^{CK}}$	1	5	5	0	13	0%	0%	0%	2%	0	14	0%	0%	1%	2%
$M1CK2_N$	$C_{N+1}^{M1CK2_N}/K_{N+1}$	$S_N/K_N, T_{N+1}, R_N, Q_N, \sigma_N^{CALIB^{CK}}, (C_N/K_N)$	1	6	6	0	7	0%	0%	0%	1%	1	7	0%	5%	0%	1%
$M1CK3_N$	$C_{N+1}^{M1CK3_N}/K_{N+1}$	$S_N/K_N, T_{N+1}, R_N, Q_N, \sigma_N^{CALIB^{CK}}, (C_N/K_N), BSMGreeks_N^{CK}$	1	11	11	0	23	0%	0%	1%	2%	0	26	0%	0%	1%	3%
$M1CK4_N$	$C_{N+1}^{M1CK4_N}/K_{N+1}$	$S_N/K_N, T_{N+1}, R_N, Q_N, \sigma_N^{CALIB^{CK}}, (C_N/K_N), BSMGreeks_N^{CK}, HParams_N^{CK}$	1	16	16	3	15	0%	11%	1%	2%	3	16	0%	11%	1%	2%
$M1CK5_N$	$C_{N+1}^{M1CK5_N}/K_{N+1}$	$S_N/K_N, T_{N+1}, R_N, Q_N, \sigma_N^{CALIB^{CK}}, (C_N/K_N), BSMGreeks_N^{CK}, HParams_N^{CK}, (C_N^{HCK}/K_N)$	1	17	17	2	15	0%	8%	1%	2%	2	23	0%	8%	1%	2%
$M1CK6_N$	$C_{N+1}^{M1CK6_N}/K_{N+1}$	$S_N/K_N, T_{N+1}, R_N, Q_N, HParams_N^{CK}, (C_N^{HCK}/K_N)$	1	10	10	0	14	0%	0%	1%	2%	1	14	0%	5%	1%	2%
$M1CK7_N$	$C_{N+1}^{M1CK7_N}/K_{N+1}$	$S_N/K_N, T_{N+1}, R_N, Q_N, \sigma_N^{CALIB^{CK}}, BSMGreeks_N^{CK}, (C_N^{BSMCK}/K_N)$	1	11	11	0	19	0%	0%	1%	2%	0	19	0%	0%	1%	2%
$M1CK8_N$	$C_{N+1}^{M1CK8_N}/K_{N+1}$	$S_N/K_N, T_{N+1}, R_N, Q_N, HJDParams_N^{CK}, (C_N^{HJDCK}/K_N)$	1	13	13	0	18	0%	0%	1%	2%	0	19	0%	0%	1%	2%
$M1CK9_N$	$C_{N+1}^{M1CK9_N}/K_{N+1}$	$S_N/K_N, T_{N+1}, R_N, Q_N, FMLSParams_N^{CK}, (C_N^{FMLSCK}/K_N)$	1	7	7	0	16	0%	0%	1%	2%	0	16	0%	0%	1%	2%
$M2CK1_N$	$C_{N+1}^{M2CK1_N}/K_{N+1}$	$S_N/K_N, T_{N+1}, R_N, Q_N, \sigma_N^{CALIB^{CK}}$	2	5	5 X 5	0	25	0%	0%	1%	3%	0	26	0%	0%	1%	3%
$M2CK2_N$	$C_{N+1}^{M2CK2_N}/K_{N+1}$	$S_N/K_N, T_{N+1}, R_N, Q_N, \sigma_N^{CALIB^{CK}}, (C_N/K_N)$	2	6	6 X 6	0	36	0%	0%	2%	4%	0	40	0%	0%	2%	4%
$M2CK3_N$	$C_{N+1}^{M2CK3_N}/K_{N+1}$	$S_N/K_N, T_{N+1}, R_N, Q_N, \sigma_N^{CALIB^{CK}}, (C_N/K_N), BSMGreeks_N^{CK}$	2	11	11 X 11	2	32	0%	8%	2%	3%	3	41	0%	9%	2%	4%
$M2CK4_N$	$C_{N+1}^{M2CK4_N}/K_{N+1}$	$S_N/K_N, T_{N+1}, R_N, Q_N, \sigma_N^{CALIB^{CK}}, (C_N/K_N), BSMGreeks_N^{CK}, HParams_N^{CK}$	2	16	16 X 16	1	20	0%	5%	1%	2%	1	25	0%	6%	1%	3%
$M2CK5_N$	$C_{N+1}^{M2CK5_N}/K_{N+1}$	$S_N/K_N, T_{N+1}, R_N, Q_N, \sigma_N^{CALIB^{CK}}, (C_N/K_N), BSMGreeks_N^{CK}, HParams_N^{CK}, (C_N^{HCK}/K_N)$	2	17	17 X 17	0	15	0%	0%	1%	2%	0	17	0%	0%	1%	2%
$M2CK6_N$	$C_{N+1}^{M2CK6_N}/K_{N+1}$	$S_N/K_N, T_{N+1}, R_N, Q_N, HParams_N^{CK}, (C_N^{HCK}/K_N)$	2	10	10 X 10	4	12	2%	13%	0%	1%	5	15	2%	16%	1%	2%
$M2CK7_N$	$C_{N+1}^{M2CK7_N}/K_{N+1}$	$S_N/K_N, T_{N+1}, R_N, Q_N, \sigma_N^{CALIB^{CK}}, BSMGreeks_N^{CK}, (C_N^{BSMCK}/K_N)$	2	11	11 X 11	1	21	0%	5%	1%	2%	1	27	0%	5%	1%	3%
$M2CK8_N$	$C_{N+1}^{M2CK8_N}/K_{N+1}$	$S_N/K_N, T_{N+1}, R_N, Q_N, HJDParams_N^{CK}, (C_N^{HJDCK}/K_N)$	2	13	13 X 13	2	21	0%	8%	1%	2%	2	27	0%	8%	1%	3%
$M2CK9_N$	$C_{N+1}^{M2CK9_N}/K_{N+1}$	$S_N/K_N, T_{N+1}, R_N, Q_N, FMLSParams_N^{CK}, (C_N^{FMLSCK}/K_N)$	2	7	7 X 7	0	16	0%	0%	1%	2%	0	22	0%	0%	1%	2%
$M3CK1_N$	$C_{N+1}^{M3CK1_N}/K_{N+1}$	$S_N/K_N, T_{N+1}, R_N, Q_N, \sigma_N^{CALIB^{CK}}$	3	5	5 X 5 X 5	2	25	0%	8%	1%	3%	2	26	0%	8%	1%	3%
$M3CK2_N$	$C_{N+1}^{M3CK2_N}/K_{N+1}$	$S_N/K_N, T_{N+1}, R_N, Q_N, \sigma_N^{CALIB^{CK}}, (C_N/K_N)$	3	6	6 X 6 X 6	2	29	0%	8%	1%	3%	4	40	2%	13%	2%	4%
$M3CK3_N$	$C_{N+1}^{M3CK3_N}/K_{N+1}$	$S_N/K_N, T_{N+1}, R_N, Q_N, \sigma_N^{CALIB^{CK}}, (C_N/K_N), BSMGreeks_N^{CK}$	3	11	11 X 11 X 11	6	41	3%	17%	2%	4%	6	52	3%	17%	3%	5%
$M3CK4_N$	$C_{N+1}^{M3CK4_N}/K_{N+1}$	$S_N/K_N, T_{N+1}, R_N, Q_N, \sigma_N^{CALIB^{CK}}, (C_N/K_N), BSMGreeks_N^{CK}, HParams_N^{CK}$	3	16	16 X 16 X 16	5	39	2%	16%	2%	4%	7	63	3%	19%	4%	6%
$M3CK5_N$	$C_{N+1}^{M3CK5_N}/K_{N+1}$	$S_N/K_N, T_{N+1}, R_N, Q_N, \sigma_N^{CALIB^{CK}}, (C_N/K_N), BSMGreeks_N^{CK}, HParams_N^{CK}, (C_N^{HCK}/K_N)$	3	17	17 X 17 X 17	3	22	0%	11%	1%	2%	7	55	5%	19%	3%	5%
$M3CK6_N$	$C_{N+1}^{M3CK6_N}/K_{N+1}$	$S_N/K_N, T_{N+1}, R_N, Q_N, HParams_N^{CK}, (C_N^{HCK}/K_N)$	3	10	10 X 10 X 10	3	30	0%	11%	1%	3%	**8**	52	5%	20%	3%	5%
$M3CK7_N$	$C_{N+1}^{M3CK7_N}/K_{N+1}$	$S_N/K_N, T_{N+1}, R_N, Q_N, \sigma_N^{CALIB^{CK}}, BSMGreeks_N^{CK}, (C_N^{BSMCK}/K_N)$	3	11	11 X 11 X 11	3	24	0%	9%	1%	3%	3	32	0%	11%	2%	3%
$M3CK8_N$	$C_{N+1}^{M3CK8_N}/K_{N+1}$	$S_N/K_N, T_{N+1}, R_N, Q_N, HJDParams_N^{CK}, (C_N^{HJDCK}/K_N)$	3	13	13 X 13 X 13	4	24	2%	13%	1%	3%	4	35	2%	13%	2%	4%
$M3CK9_N$	$C_{N+1}^{M3CK9_N}/K_{N+1}$	$S_N/K_N, T_{N+1}, R_N, Q_N, FMLSParams_N^{CK}, (C_N^{FMLSCK}/K_N)$	3	7	7 X 7 X 7	1	18	0%	5%	1%	2%	2	28	0%	8%	1%	3%
$L1CK1_N$	$C_{N+1}^{L1CK1_N}/K_{N+1}$	$S_N/K_N, T_{N+1}, R_N, Q_N, \sigma_N^{CALIB^{CK}}$	1	5	5	0	1	0%	0%	0%	0%	0	1	0%	0%	0%	0%
$L1CK2_N$	$C_{N+1}^{L1CK2_N}/K_{N+1}$	$S_N/K_N, T_{N+1}, R_N, Q_N, \sigma_N^{CALIB^{CK}}, (C_N/K_N)$	1	6	6	0	89	0%	0%	5%	8%	0	89	0%	0%	5%	8%
$L1CK3_N$	$C_{N+1}^{L1CK3_N}/K_{N+1}$	$S_N/K_N, T_{N+1}, R_N, Q_N, \sigma_N^{CALIB^{CK}}, (C_N/K_N), BSMGreeks_N^{CK}$	1	11	11	0	4	0%	0%	0%	1%	0	4	0%	0%	0%	1%
$L1CK4_N$	$C_{N+1}^{L1CK4_N}/K_{N+1}$	$S_N/K_N, T_{N+1}, R_N, Q_N, \sigma_N^{CALIB^{CK}}, (C_N/K_N), BSMGreeks_N^{CK}, HParams_N^{CK}$	1	16	16	0	19	0%	0%	1%	2%	0	20	0%	0%	1%	2%
$L1CK5_N$	$C_{N+1}^{L1CK5_N}/K_{N+1}$	$S_N/K_N, T_{N+1}, R_N, Q_N, \sigma_N^{CALIB^{CK}}, (C_N/K_N), BSMGreeks_N^{CK}, HParams_N^{CK}, (C_N^{HCK}/K_N)$	1	17	17	0	16	0%	0%	1%	2%	0	16	0%	0%	1%	2%
$L1CK6_N$	$C_{N+1}^{L1CK6_N}/K_{N+1}$	$S_N/K_N, T_{N+1}, R_N, Q_N, HParams_N^{CK}, (C_N^{HCK}/K_N)$	1	10	10	0	10	0%	0%	0%	1%	0	10	0%	0%	0%	1%
$L1CK7_N$	$C_{N+1}^{L1CK7_N}/K_{N+1}$	$S_N/K_N, T_{N+1}, R_N, Q_N, \sigma_N^{CALIB^{CK}}, BSMGreeks_N^{CK}, (C_N^{BSMCK}/K_N)$	1	11	11	1	14	0%	5%	1%	2%	1	14	0%	5%	0%	2%
$L1CK8_N$	$C_{N+1}^{L1CK8_N}/K_{N+1}$	$S_N/K_N, T_{N+1}, R_N, Q_N, HJDParams_N^{CK}, (C_N^{HJDCK}/K_N)$	1	13	13	0	0	0%	0%	0%	0%	0	0	0%	0%	0%	0%
$L1CK9_N$	$C_{N+1}^{L1CK9_N}/K_{N+1}$	$S_N/K_N, T_{N+1}, R_N, Q_N, FMLSParams_N^{CK}, (C_N^{FMLSCK}/K_N)$	1	7	7	0	2	0%	0%	0%	0%	0	2	0%	0%	0%	0%
$L2CK1_N$	$C_{N+1}^{L2CK1_N}/K_{N+1}$	$S_N/K_N, T_{N+1}, R_N, Q_N, \sigma_N^{CALIB^{CK}}$	2	5	5 X 5	0	6	0%	0%	0%	1%	0	6	0%	0%	0%	1%
$L2CK2_N$	$C_{N+1}^{L2CK2_N}/K_{N+1}$	$S_N/K_N, T_{N+1}, R_N, Q_N, \sigma_N^{CALIB^{CK}}, (C_N/K_N)$	2	6	6 X 6	0	92	0%	0%	6%	8%	0	**96**	0%	0%	6%	9%
$L2CK3_N$	$C_{N+1}^{L2CK3_N}/K_{N+1}$	$S_N/K_N, T_{N+1}, R_N, Q_N, \sigma_N^{CALIB^{CK}}, (C_N/K_N), BSMGreeks_N^{CK}$	2	11	11 X 11	0	8	0%	0%	0%	1%	0	8	0%	0%	0%	1%
$L2CK4_N$	$C_{N+1}^{L2CK4_N}/K_{N+1}$	$S_N/K_N, T_{N+1}, R_N, Q_N, \sigma_N^{CALIB^{CK}}, (C_N/K_N), BSMGreeks_N^{CK}, HParams_N^{CK}$	2	16	16 X 16	0	18	0%	0%	1%	2%	0	19	0%	0%	1%	2%
$L2CK5_N$	$C_{N+1}^{L2CK5_N}/K_{N+1}$	$S_N/K_N, T_{N+1}, R_N, Q_N, \sigma_N^{CALIB^{CK}}, (C_N/K_N), BSMGreeks_N^{CK}, HParams_N^{CK}, (C_N^{HCK}/K_N)$	2	17	17 X 17	0	28	0%	0%	1%	3%	0	31	0%	0%	2%	3%
$L2CK6_N$	$C_{N+1}^{L2CK6_N}/K_{N+1}$	$S_N/K_N, T_{N+1}, R_N, Q_N, HParams_N^{CK}, (C_N^{HCK}/K_N)$	2	10	10 X 10	0	16	0%	0%	1%	2%	0	16	0%	0%	1%	2%
$L2CK7_N$	$C_{N+1}^{L2CK7_N}/K_{N+1}$	$S_N/K_N, T_{N+1}, R_N, Q_N, \sigma_N^{CALIB^{CK}}, BSMGreeks_N^{CK}, (C_N^{BSMCK}/K_N)$	2	11	11 X 11	0	17	0%	0%	1%	2%	0	18	0%	0%	1%	2%
$L2CK8_N$	$C_{N+1}^{L2CK8_N}/K_{N+1}$	$S_N/K_N, T_{N+1}, R_N, Q_N, HJDParams_N^{CK}, (C_N^{HJDCK}/K_N)$	2	13	13 X 13	0	0	0%	0%	0%	0%	0	0	0%	0%	0%	0%
$L2CK9_N$	$C_{N+1}^{L2CK9_N}/K_{N+1}$	$S_N/K_N, T_{N+1}, R_N, Q_N, FMLSParams_N^{CK}, (C_N^{FMLSCK}/K_N)$	2	7	7 X 7	0	10	0%	0%	0%	1%	0	10	0%	0%	0%	1%
$L3CK1_N$	$C_{N+1}^{L3CK1_N}/K_{N+1}$	$S_N/K_N, T_{N+1}, R_N, Q_N, \sigma_N^{CALIB^{CK}}$	3	5	5 X 5 X 5	0	7	0%	0%	0%	1%	0	7	0%	0%	0%	1%
$L3CK2_N$	$C_{N+1}^{L3CK2_N}/K_{N+1}$	$S_N/K_N, T_{N+1}, R_N, Q_N, \sigma_N^{CALIB^{CK}}, (C_N/K_N)$	3	6	6 X 6 X 6	0	76	0%	0%	4%	7%	0	78	0%	0%	4%	7%
$L3CK3_N$	$C_{N+1}^{L3CK3_N}/K_{N+1}$	$S_N/K_N, T_{N+1}, R_N, Q_N, \sigma_N^{CALIB^{CK}}, (C_N/K_N), BSMGreeks_N^{CK}$	3	11	11 X 11 X 11	1	12	0%	5%	0%	2%	1	12	0%	5%	0%	1%
$L3CK4_N$	$C_{N+1}^{L3CK4_N}/K_{N+1}$	$S_N/K_N, T_{N+1}, R_N, Q_N, \sigma_N^{CALIB^{CK}}, (C_N/K_N), BSMGreeks_N^{CK}, HParams_N^{CK}$	3	16	16 X 16 X 16	0	25	0%	0%	1%	3%	0	26	0%	0%	1%	3%
$L3CK5_N$	$C_{N+1}^{L3CK5_N}/K_{N+1}$	$S_N/K_N, T_{N+1}, R_N, Q_N, \sigma_N^{CALIB^{CK}}, (C_N/K_N), BSMGreeks_N^{CK}, HParams_N^{CK}, (C_N^{HCK}/K_N)$	3	17	17 X 17 X 17	0	25	0%	0%	1%	3%	0	26	0%	0%	1%	3%
$L3CK6_N$	$C_{N+1}^{L3CK6_N}/K_{N+1}$	$S_N/K_N, T_{N+1}, R_N, Q_N, HParams_N^{CK}, (C_N^{HCK}/K_N)$	3	10	10 X 10 X 10	0	14	0%	0%	1%	2%	0	14	0%	0%	1%	2%
$L3CK7_N$	$C_{N+1}^{L3CK7_N}/K_{N+1}$	$S_N/K_N, T_{N+1}, R_N, Q_N, \sigma_N^{CALIB^{CK}}, BSMGreeks_N^{CK}, (C_N^{BSMCK}/K_N)$	3	11	11 X 11 X 11	0	15	0%	0%	1%	2%	0	16	0%	0%	1%	2%
$L3CK8_N$	$C_{N+1}^{L3CK8_N}/K_{N+1}$	$S_N/K_N, T_{N+1}, R_N, Q_N, HJDParams_N^{CK}, (C_N^{HJDCK}/K_N)$	3	13	13 X 13 X 13	0	0	0%	0%	0%	0%	0	0	0%	0%	0%	0%
$L3CK9_N$	$C_{N+1}^{L3CK9_N}/K_{N+1}$	$S_N/K_N, T_{N+1}, R_N, Q_N, FMLSParams_N^{CK}, (C_N^{FMLSCK}/K_N)$	3	7	7 X 7 X 7	0	13	0%	0%	0%	2%	0	13	0%	0%	0%	2%

Table A.2.32: Call Option Price Scaled by the Exercise Price Comparison (amongst Parametric Models): This table presents a performance comparison using both daily and monthly statistics amongst the Black-Scholes-Merton ($BSMCK_N$) model, Heston (HCK_N) model, Heston Jump Diffusion ($HJDCK_N$) model, and the Finite Moment Log Stable ($FMLSCK_N$) model. The forecast variable for all the models is the one-day-ahead call option price scaled by the exercise price (C_{N+1}/K_{N+1}). The models denoted by the $_N$ subscript use lagged input variables for forecasting C_{N+1}/K_{N+1}. The one-day-ahead forecast errors of C_{N+1}/K_{N+1} are used to compute the Root Mean Square Error (RMSE). Column I identifies the models, column II identifies the forecast variable, and column III lists the input variables used by the models to obtain the one-trading-day ahead forecast of C_{N+1}. Forecasts are made for 1,328 trading days, and there are 64 months covered in the sample using the monthly data.

When comparing all models simultaneously (i.e. including the random walk model (δCK_N), column VII reports the number of months out of the 64 months that each model has the smallest RMSE, while column VIII reports the number of days out of the 1,328 days each model has the smallest RMSE. Columns IX (lower bound) and X (upper bound) present the winning percentage out of 64 months for each model, evaluated using the bootstrap sampling technique. The statistical bootstrap performed (with replacement) at a 95% confidence level is computed from the monthly RMSE values of the respective models below. Columns XI (lower bound) and XII (upper bound) present the winning percentage out of 1326 days for each model computed from bootstrapping the daily RMSE values of the respective models at a 95% confidence level.

Similarly, when the δCK_N model was excluded in the comparison, column XIII reports the number of months out of the 64 months that each model has the smallest RMSE, while column XIV reports the number of days out of the 1,328 days each model has the smallest RMSE. Columns XV (lower bound) and XVI (upper bound) present the winning percentage out of 64 months for each model, evaluated using the bootstrap sampling technique. The statistical bootstrap performed (with replacement) at a 95% confidence level is computed from the monthly RMSE values of the respective models below. Also, columns XVII (lower bound) and XVIII (upper bound) present the winning percentage out of 1326 days for each model computed from bootstrapping the daily RMSE values of the respective models at a 95% confidence level.

			Including the random walk						**Excluding the random walk**					
(I) Model	**(II) Forecast**	**(III) Inputs**	**(IV) Performance amongst all models (Monthly)**	**(V) Performance amongst all models (Daily)**	**(VI) 2.5% lower bound- (for monthly) (%)**	**(VII) 2.5% upper bound- (for monthly) (%)**	**(VIII) 2.5% lower bound- (for daily) (%)**	**(IX) 2.5% upper bound- (for daily) (%)**	**(X) Performance amongst all models (Monthly)**	**(XI) Performance amongst all models (Daily)**	**(XII) 2.5% lower bound- (for monthly) (%)**	**(XIII) 2.5% upper bound- (for monthly) (%)**	**(XIV) 2.5% lower bound- (for daily) (%)**	**(XV) 2.5% upper bound- (for daily) (%)**
δCK_N	C_{N+1}/K_{N+1}	C_N, K_N	**64**	**1279**	100%	100%	95%	97%	-	-	-	-	-	-
$BSMCK_N$	$C_{N+1}^{BSMCK_N}/K_{N+1}$	$S_N, K_{N+1}, T_{N+1}, R_N, Q_N, \sigma_N^{CALIB^{CK}}$	0	29	0%	0%	2%	3%	17	354	16%	38%	24%	29%
HCK_N	$C_{N+1}^{HCK_N}/K_{N+1}$	$S_N, K_{N+1}, T_{N+1}, R_N, Q_N, \sigma_N^{CALIB^{CK}}, HParams_N^{CK}$	0	9	0%	0%	0%	1%	0	259	0%	0%	17%	22%
$HJDCK_N$	$C_{N+1}^{HJDCK_N}/K_{N+1}$	$S_N, K_{N+1}, T_{N+1}, R_N, Q_N, \sigma_N^{CALIB^{CK}}, HJDParams_N^{CK}$	0	8	0%	0%	0%	1%	**40**	**540**	52%	75%	38%	43%
$FMLSCK_N$	$C_{N+1}^{FMLSCK_N}/K_{N+1}$	$S_N, K_{N+1}, T_{N+1}, R_N, Q_N, FMLSParams_N^{CK}$	0	3	0%	0%	0%	1%	7	178	5%	20%	12%	15%

A.2.4 Pricing performance of CK-Models that use one-trading-day-ahead input variables to forecast the call option price CK_{N+1} for the next trading day

Table A.2.33 to Table A.2.36 shows the relative out-of-sample pricing performance (in $RMSE$) amongst the models that use one-trading-day-ahead input variables to forecast the one-trading-day-ahead call option price scaled by the strike price(C_{N+1}/K_{N+1}). For convenience, the models in Table A.2.33 to Table A.2.35 list the forecast variable and the input variables in columns II and III, respectively, and the architecture of the MLP and LSTM models in columns IV, V and VI, respectively. The performance metric is the $RMSE$ of the one-trading-day-ahead forecast errors of C_{N+1}/K_{N+1}, which is computed for each model utilising all of the errors in each day or each month. Amongst all of the models (including the random walk model (δCK_N)), columns VII and VIII record the number of months and days, respectively, that each model has the lowest $RMSE$. In order to be certain of our results, we performed a bootstrap using the daily and monthly RMSEs. Columns IX (lower bound) and X (upper bound) present the results from the bootstrap performed (with replacement) using monthly RMSEs at a 95% confidence level and show the winning percentage out of 64 months for each model (including the δCK_N model), and similarly, the 95 % confidence intervals computed from bootstrapping of the daily RMSEs signifies the winning percentage out of 1328 days for each model and are reported in columns XI (lower bound), XII (upper bound). While excluding the δCK_N model amongst the comparison, columns XIII and XIV record the number of months and days that each model has the lowest $RMSE$. We repeat the exercise of performing the bootstrap by excluding the δCK_N model in the comparison, and thus, columns XV (lower bound) and XVI (upper bound) present the results from the bootstrap performed (with replacement) using monthly RMSEs at a 95% confidence level, and shows the winning percentage out of 64 months for each model (excluding the δCK_N model) and similarly, the 95 % confidence intervals computed from bootstrapping of the daily RMSEs signifies the winning percentage out of 1328 days for each model and are reported in columns XVII (lower bound), XVIII (upper bound).

In the below several comparisons, even though a particular model wins by a higher percentage against other models, we investigated further these models pairwise by performing a pairwise bootstrap comparison, which was computed using the respective pair's daily RMSEs. The results are presented in Table 20 of the Electronic Appendix. Also, we examined the pairwise Diebold-Mariano(DM) (Diebold and Mariano (1995)) tests on these models and have presented the results in Table 16 of the Electronic Appendix. In constructing the DM tests, the model pairs are reported in column I and column II, and the DM test statistics for a particular pair are reported in column III. If the null can be rejected, a positive number suggests the rejection may be due to the second model being the better forecast model. In contrast, a negative value suggests the rejection may be due to the first model being the better forecast model. The model pairs highlighted in a red state that their forecasts have statistically insignificant differences in their prediction accuracy. The following model pairs have been shown to have statistically insignificant differences:($M3CK2_{N+1}$, $M3CK4_{N+1}$), and ($L3CK3_{N+1}$, $L3CK7_{N+1}$). The RMSEs for the $CK - Models$ that use one-trading-day-ahead input variables to forecast the C_{N+1}/K_{N+1} for the next trading day on a monthly, yearly, and overall basis can be found in the Electronic Appendix, in Tables 4, 8, and 12, respectively.

A.2.4.1 Comparison amongst all Parametric Models with Triple Hidden Layer ANN Models:

In this section, we compare the out-of-sample pricing performance of the random walk model (δCK_N), the parametric models ($BSMCK_{N+1}$, HCK_{N+1}, $HJDCK_{N+1}$, and $FMLSCK_{N+1}$), the triple hidden layer MLP models ($M3CK_{N+1} - Models$) and the triple hidden layer LSTM models ($L3CK_{N+1} - Models$), then the parametric models with the $M3CK_{N+1} - Models$, and finally the parametric models with the $L3CK_{N+1} - Models$.

The results for the parametric models with the MLP $M3CK_{N+1} - Models$ ($M3CK1_{N+1}$ to $M3CK9_{N+1}$) and the LSTM $L3CK_{N+1} - Models$ ($L3CK1_{N+1}$ to $L3CK9_{N+1}$) are presented in Table A.2.33. If all the models are individually compared, then the $M3CK2_{N+1}$ model had the lowest $RMSE$ for 291 days (having a daily bootstrap winning % of 20% to 24%) out of 1,328 days. When the δCK_N was excluded from the comparison, the $M3CK2_{N+1}$ model still outperformed all other models for 308 days (having a daily bootstrap winning % of 21% to 26%) out of 1,328 days.

Table A.2.34 presents the results for the comparison of the parametric models with the MLP $M3CK_{N+1} - Models$ ($M3CK1_{N+1}$ to $M3CK9_{N+1}$). Accordingly, the $M3CK2_{N+1}$ model had the lowest $RMSE$ for 292 days (having a daily bootstrap winning % of 20% to 24%) out of 1,328 days. When the δCK_N was excluded from the comparison, the $M3CK2_{N+1}$ model still outperformed all other models for 313 days (having a daily bootstrap winning % of 21% to 26%) out of 1,328 days.

We present the comparison results of the parametric models with the LSTM $L3CK_{N+1} - Models$ ($L3CK1_{N+1}$ to $L3CK9_{N+1}$) in Table A.2.35. We find that the δCK_N model had the lowest $RMSE$ for 680 days (having a daily bootstrap winning % of 48% to 54%) out of 1,328 days. When the δCK_N was excluded from the comparison, the $L3CK2_{N+1}$ model outperformed all other models for 345 days (having a daily bootstrap winning % of 24% to 28%) out of 1,328 days.

Thus, when the parametric models are compared with the triple hidden layer ANN models that use one-trading-day-ahead input variables to forecast the C_{N+1}/K_{N+1}, we conclude that an MLP model ($M3CK2_{N+1}$) could outperform all other models (in Table A.2.33). Similarly, the out-performance of an MLP model ($M3CK2_{N+1}$ in Table A.2.34) can be noticed when the parametric models were compared with the triple hidden layer MLP models. However, when the parametric models were compared with the triple hidden layer LSTM models, an LSTM model ($L3CK2_{N+1}$) could outperform the parametric models (in Table A.2.35).

A.2.4.2 Comparison amongst all Parametric models:

In this section, we compare the out-of-sample pricing performance of the random walk model (δCK_N), and the parametric models ($BSMCK_{N+1}$, HCK_{N+1}, $HJDCK_{N+1}$, and $FMLSCK_{N+1}$) in Table A.2.36. We find that the δCK_N model had the lowest $RMSE$ for 1158 days (having a daily bootstrap winning % of 85% to 89%) out of 1,328 days. When the δCK_N was excluded from the comparison, the $HJDCK_{N+1}$ model outperformed all other models for 559 days (having a daily bootstrap winning % of 39% to 45%) out of 1,328 days.

Thus, when comparing the out-of-sample pricing performance amongst the parametric models, the $HJDCK_{N+1}$ model had outperformed all other parametric models by a large margin (in

Table A.2.36).

Table A.2.33: Call Option Price Scaled by the Exercise Price Comparison (amongst Parametric, MLP $M3CK_{N+1} - Models$ and LSTM $L3CK_{N+1} - Models$): This table presents a performance comparison using both daily and monthly statistics amongst the Black-Scholes-Merton ($BSMCK_{N+1}$) model, Heston (HCK_{N+1}) model, Heston Jump Diffusion ($HJDCK_{N+1}$) model, Finite Moment Log Stable ($FMLSCK_{N+1}$) model, MLP $M3CK_{N+1} - Models$ ($M3CK1_{N+1}$ to $M3CK9_{N+1}$) and the LSTM $L3CK_{N+1} - Models$ ($L3CK1_{N+1}$ to $L3CK9_{N+1}$). The forecast variable for all the models is the one-day-ahead call option price scaled by the exercise price (C_{N+1}/K_{N+1}). The models denoted by the $_{N+1}$ subscript use one-day-ahead input variables for forecasting C_{N+1}/K_{N+1}. The one-day-ahead forecast errors of C_{N+1}/K_{N+1} are used to compute the Root Mean Square Error (RMSE). Column I identifies the models, column II identifies the forecast variable, column III lists the input variables used by the models to obtain the one-trading-day-ahead forecast of C_{N+1}/K_{N+1}, and columns IV, V and VI describe the network architecture of the MLP $M3CK_{N+1} - Models$ and the LSTM $L3CK_{N+1} - Models$. Forecasts are made for 1,328 trading days, and there are 64 months covered in the sample using the monthly data.

When comparing all models simultaneously (i.e. including the random walk model (δCK_N), column VII reports the number of months out of the 64 months that each model has the smallest RMSE, while column VIII reports the number of days out of the 1,328 days each model has the smallest RMSE. Columns IX (lower bound) and X (upper bound) present the winning percentage out of 64 months for each model, evaluated using the bootstrap sampling technique. The statistical bootstrap performed (with replacement) at a 95% confidence level is computed from the monthly RMSE values of the respective models below. Columns XI (lower bound), and XII (upper bound) present the winning percentage out of 1326 days for each model computed from bootstrapping the daily RMSE values of the respective models at a 95% confidence level.

Similarly, when the δCK_N model was excluded in the comparison, column XIII reports the number of months out of the 64 months that each model has the smallest RMSE, while column XIV reports the number of days out of the 1,328 days each model has the smallest RMSE. Columns XV (lower bound) and XVI (upper bound) present the winning percentage out of 64 months for each model, evaluated using the bootstrap sampling technique. The statistical bootstrap performed (with replacement) at a 95% confidence level is computed from the monthly RMSE values of the respective models below. Also, columns XVII (lower bound) and XVIII (upper bound) present the winning percentage out of 1326 days for each model computed from bootstrapping the daily RMSE values of the respective models at a 95% confidence level.

						Including the random walk						Excluding the random walk					
(I) Model	(II) Forecast	(III) Inputs	(IV) No. of hidden layers	(V) No. of hidden nodes per layer	(VI) Network architecture	(VII) Performance amongst all models (Monthly)	(VIII) Performance amongst all models (Daily)	(IX) 2.5% lower bound- (for monthly) (%)	(X) 2.5% upper bound- (for monthly) (%)	(XI) 2.5% lower bound- (for daily) (%)	(XII) 2.5% upper bound- (for daily) (%)	(XIII) Performance amongst all models (Monthly)	(XIV) Performance amongst all models (Daily)	(XV) 2.5% lower bound- (for monthly) (%)	(XVI) 2.5% upper bound- (for monthly) (%)	(XVII) 2.5% lower bound- (for daily) (%)	(XVIII) 2.5% upper bound- (for daily) (%)
δCK_N	C_{N+1}/K_{N+1}	C_N, K_N	-	-	-	0	183	0%	0%	12%	16%	-	-	-	-	-	-
$BSMCK_{N+1}$	$C_{N+1}^{BSMCK_{N+1}}/K_{N+1}$	$S_{N+1}, K_{N+1}, T_{N+1}, R_{N+1}, Q_{N+1}, \sigma_N^{CALIB^{CK}}$	-	-	-	0	0	0%	0%	0%	0%	0	0	0%	0%	0%	0%
HCK_{N+1}	$C_{N+1}^{HCK_{N+1}}/K_{N+1}$	$S_{N+1}, K_{N+1}, T_{N+1}, R_{N+1}, Q_{N+1}, \sigma_N^{CALIB^{CK}}, HParams_N^{CK}$	-	-	-	0	2	0%	0%	0%	0%	0	2	0%	0%	0%	0%
$HJDCK_{N+1}$	$C_{N+1}^{HJDCK_{N+1}}/K_{N+1}$	$S_{N+1}, K_{N+1}, T_{N+1}, R_{N+1}, Q_{N+1}, \sigma_N^{CALIB^{CK}}, HJDParams_N^{CK}$	-	-	-	0	0	0%	0%	0%	0%	0	0	0%	0%	0%	0%
$FMLSCK_{N+1}$	$C_{N+1}^{FMLSCK_{N+1}}/K_{N+1}$	$S_{N+1}, K_{N+1}, T_{N+1}, R_{N+1}, Q_{N+1}, FMLSParams_N^{CK}$	-	-	-	0	0	0%	0%	0%	0%	0	0	0%	0%	0%	0%
$M3CK1_{N+1}$	$C_{N+1}^{M3CK1_{N+1}}/K_{N+1}$	$S_{N+1}/K_{N+1}, T_{N+1}, R_{N+1}, Q_{N+1}, \sigma_N^{CALIB^{CK}}$	3	5	5 X 5 X 5	0	117	0%	0%	7%	10%	0	120	0%	0%	8%	11%
$M3CK2_{N+1}$	$C_{N+1}^{M3CK2_{N+1}}/K_{N+1}$	$S_{N+1}/K_{N+1}, T_{N+1}, R_{N+1}, Q_{N+1}, \sigma_N^{CALIB^{CK}}, (C_N/K_N)$	3	6	6 X 6 X 6	**27**	**291**	30%	55%	20%	24%	**27**	**308**	30%	55%	21%	26%
$M3CK3_{N+1}$	$C_{N+1}^{M3CK3_{N+1}}/K_{N+1}$	$S_{N+1}/K_{N+1}, T_{N+1}, R_{N+1}, Q_{N+1}, \sigma_N^{CALIB^{CK}}, (C_N/K_N), BSMGreeks_N^{CK}$	3	11	11 X 11 X 11	12	181	11%	28%	12%	16%	12	203	9%	28%	13%	17%
$M3CK4_{N+1}$	$C_{N+1}^{M3CK4_{N+1}}/K_{N+1}$	$S_{N+1}/K_{N+1}, T_{N+1}, R_{N+1}, Q_{N+1}, \sigma_N^{CALIB^{CK}}, (C_N/K_N), BSMGreeks_N^{CK}, HParams_N^{CK}$	3	16	16 X 16 X 16	18	120	17%	39%	8%	11%	18	143	17%	39%	9%	13%
$M3CK5_{N+1}$	$C_{N+1}^{M3CK5_{N+1}}/K_{N+1}$	$S_{N+1}/K_{N+1}, T_{N+1}, R_{N+1}, Q_{N+1}, \sigma_N^{CALIB^{CK}}, (C_N/K_N), BSMGreeks_N^{CK}, HParams_N^{CK}, (C_N^{HCK}/K_N)$	3	17	17 X 17 X 17	0	49	0%	0%	3%	5%	0	71	0%	0%	4%	6%
$M3CK6_{N+1}$	$C_{N+1}^{M3CK6_{N+1}}/K_{N+1}$	$S_{N+1}/K_{N+1}, T_{N+1}, R_{N+1}, Q_{N+1}, HParams_N^{CK}, (C_N^{HCK}/K_N)$	3	10	10 X 10 X 10	3	79	0%	11%	5%	7%	3	106	0%	11%	7%	9%
$M3CK7_{N+1}$	$C_{N+1}^{M3CK7_{N+1}}/K_{N+1}$	$S_{N+1}/K_{N+1}, T_{N+1}, R_{N+1}, Q_{N+1}, \sigma_N^{CALIB^{CK}}, BSMGreeks_N^{CK}, (C_N^{BSMCK}/K_N)$	3	11	11 X 11 X 11	0	25	0%	0%	1%	3%	0	52	0%	0%	3%	5%
$M3CK8_{N+1}$	$C_{N+1}^{M3CK8_{N+1}}/K_{N+1}$	$S_{N+1}/K_{N+1}, T_{N+1}, R_{N+1}, Q_{N+1}, HJDParams_N^{CK}, (C_N^{HJDCK}/K_N)$	3	13	13 X 13 X 13	2	140	0%	8%	9%	12%	2	165	0%	8%	11%	14%
$M3CK9_{N+1}$	$C_{N+1}^{M3CK9_{N+1}}/K_{N+1}$	$S_{N+1}/K_{N+1}, T_{N+1}, R_{N+1}, Q_{N+1}, FMLSParams_N^{CK}, (C_N^{FMLSCK}/K_N)$	3	7	7 X 7 X 7	2	131	0%	8%	8%	11%	2	140	0%	8%	9%	12%
$L3CK1_{N+1}$	$C_{N+1}^{L3CK1_{N+1}}/K_{N+1}$	$S_{N+1}/K_{N+1}, T_{N+1}, R_{N+1}, Q_{N+1}, \sigma_N^{CALIB^{CK}}$	3	5	5 X 5 X 5	0	0	0%	0%	0%	0%	0	0	0%	0%	0%	0%
$L3CK2_{N+1}$	$C_{N+1}^{L3CK2_{N+1}}/K_{N+1}$	$S_{N+1}/K_{N+1}, T_{N+1}, R_{N+1}, Q_{N+1}, \sigma_N^{CALIB^{CK}}, (C_N/K_N)$	3	6	6 X 6 X 6	0	5	0%	0%	0%	1%	0	10	0%	0%	0%	1%
$L3CK3_{N+1}$	$C_{N+1}^{L3CK3_{N+1}}/K_{N+1}$	$S_{N+1}/K_{N+1}, T_{N+1}, R_{N+1}, Q_{N+1}, \sigma_N^{CALIB^{CK}}, (C_N/K_N), BSMGreeks_N^{CK}$	3	11	11 X 11 X 11	0	1	0%	0%	0%	0%	0	2	0%	0%	0%	0%
$L3CK4_{N+1}$	$C_{N+1}^{L3CK4_{N+1}}/K_{N+1}$	$S_{N+1}/K_{N+1}, T_{N+1}, R_{N+1}, Q_{N+1}, \sigma_N^{CALIB^{CK}}, (C_N/K_N), BSMGreeks_N^{CK}, HParams_N^{CK}$	3	16	16 X 16 X 16	0	1	0%	0%	0%	0%	0	2	0%	0%	0%	0%
$L3CK5_{N+1}$	$C_{N+1}^{L3CK5_{N+1}}/K_{N+1}$	$S_{N+1}/K_{N+1}, T_{N+1}, R_{N+1}, Q_{N+1}, \sigma_N^{CALIB^{CK}}, (C_N/K_N), BSMGreeks_N^{CK}, HParams_N^{CK}, (C_N^{HCK}/K_N)$	3	17	17 X 17 X 17	0	2	0%	0%	0%	0%	0	2	0%	0%	0%	0%
$L3CK6_{N+1}$	$C_{N+1}^{L3CK6_{N+1}}/K_{N+1}$	$S_{N+1}/K_{N+1}, T_{N+1}, R_{N+1}, Q_{N+1}, HParams_N^{CK}, (C_N^{HCK}/K_N)$	3	10	10 X 10 X 10	0	0	0%	0%	0%	0%	0	0	0%	0%	0%	0%
$L3CK7_{N+1}$	$C_{N+1}^{L3CK7_{N+1}}/K_{N+1}$	$S_{N+1}/K_{N+1}, T_{N+1}, R_{N+1}, Q_{N+1}, \sigma_N^{CALIB^{CK}}, BSMGreeks_N^{CK}, (C_N^{BSMCK}/K_N)$	3	11	11 X 11 X 11	0	1	0%	0%	0%	0%	0	2	0%	0%	0%	0%
$L3CK8_{N+1}$	$C_{N+1}^{L3CK8_{N+1}}/K_{N+1}$	$S_{N+1}/K_{N+1}, T_{N+1}, R_{N+1}, Q_{N+1}, HJDParams_N^{CK}, (C_N^{HJDCK}/K_N)$	3	13	13 X 13 X 13	0	0	0%	0%	0%	0%	0	0	0%	0%	0%	0%
$L3CK9_{N+1}$	$C_{N+1}^{L3CK9_{N+1}}/K_{N+1}$	$S_{N+1}/K_{N+1}, T_{N+1}, R_{N+1}, Q_{N+1}, FMLSParams_N^{CK}, (C_N^{FMLSCK}/K_N)$	3	7	7 X 7 X 7	0	0	0%	0%	0%	0%	0	0	0%	0%	0%	0%

Table A.2.34: Call Option Price Scaled by the Exercise Price Comparison (amongst Parametric and MLP $M3CK_{N+1} - Models$): This table presents a performance comparison using both daily and monthly statistics amongst the Black-Scholes-Merton ($BSMCK_{N+1}$) model, Heston (HCK_{N+1}) model, Heston Jump Diffusion ($HJDCK_{N+1}$) model, Finite Moment Log Stable ($FMLSCK_{N+1}$) model and the MLP $M3CK_{N+1} - Models$ ($M3CK1_{N+1}$ to $M3CK9_{N+1}$). The forecast variable for all the models is the one-day-ahead call option price scaled by the exercise price (C_{N+1}/K_{N+1}). The models denoted by the $_{N+1}$ subscript use one-day-ahead input variables for forecasting C_{N+1}/K_{N+1}. The one-day-ahead forecast errors of C_{N+1}/K_{N+1} are used to compute the Root Mean Square Error (RMSE). Column I identifies the models, column II identifies the forecast variable, column III lists the input variables used by the models to obtain the one-trading-day-ahead forecast of C_{N+1}/K_{N+1}, and columns IV, V and VI describe the network architecture of the MLP $M3CK_{N+1} - Models$. Forecasts are made for 1,328 trading days, and there are 64 months covered in the sample using the monthly data.

When comparing all models simultaneously (i.e. including the random walk model (δCK_N), column VII reports the number of months out of the 64 months that each model has the smallest RMSE, while column VIII reports the number of days out of the 1,328 days each model has the smallest RMSE. Columns IX (lower bound) and X (upper bound) present the winning percentage out of 64 months for each model, evaluated using the bootstrap sampling technique. The statistical bootstrap performed (with replacement) at a 95% confidence level is computed from the monthly RMSE values of the respective models below. Columns XI (lower bound) and XII (upper bound) present the winning percentage out of 1326 days for each model computed from bootstrapping the daily RMSE values of the respective models at a 95% confidence level.

Similarly, when the δCK_N model was excluded in the comparison, column XIII reports the number of months out of the 64 months that each model has the smallest RMSE, while column XIV reports the number of days out of the 1,328 days each model has the smallest RMSE. Columns XV (lower bound) and XVI (upper bound) present the winning percentage out of 64 months for each model, evaluated using the bootstrap sampling technique. The statistical bootstrap performed (with replacement) at a 95% confidence level is computed from the monthly RMSE values of the respective models below. Also, columns XVII (lower bound) and XVIII (upper bound) present the winning percentage out of 1326 days for each model computed from bootstrapping the daily RMSE values of the respective models at a 95% confidence level.

						Including the random walk						Excluding the random walk					
(I) Model	(II) Forecast	(III) Inputs	(IV) No. of hidden layers	(V) No. of hidden nodes per layer	(VI) Network architecture	(VII) Performance amongst all models (Monthly)	(VIII) Performance amongst all models (Daily)	(IX) 2.5% lower bound- (for monthly) (%)	(X) 2.5% upper bound- (for monthly) (%)	(XI) 2.5% lower bound- (for daily) (%)	(XII) 2.5% upper bound- (for daily) (%)	(XIII) Performance amongst all models (Monthly)	(XIV) Performance amongst all models (Daily)	(XV) 2.5% lower bound- (for monthly) (%)	(XVI) 2.5% upper bound- (for monthly) (%)	(XVII) 2.5% lower bound- (for daily) (%)	(XVIII) 2.5% upper bound- (for daily) (%)
δCK_N	C_{N+1}/K_{N+1}	C_N, K_N	-	-	-	0	185	0%	0%	12%	16%	-	-	-	-	-	-
$BSMCK_{N+1}$	$C_{N+1}^{BSMCK_{N+1}}/K_{N+1}$	$S_{N+1}, K_{N+1}, T_{N+1}, R_{N+1}, Q_{N+1}, \sigma_N^{CALIB^{CK}}$	-	-	-	0	0	0%	0%	0%	0%	0	0	0%	0%	0%	0%
HCK_{N+1}	$C_{N+1}^{HCK_{N+1}}/K_{N+1}$	$S_{N+1}, K_{N+1}, T_{N+1}, R_{N+1}, Q_{N+1}, \sigma_N^{CALIB^{CK}}, HParams_N^{CK}$	-	-	-	0	2	0%	0%	0%	0%	0	2	0%	0%	0%	0%
$HJDCK_{N+1}$	$C_{N+1}^{HJDCK_{N+1}}/K_{N+1}$	$S_{N+1}, K_{N+1}, T_{N+1}, R_{N+1}, Q_{N+1}, \sigma_N^{CALIB^{CK}}, HJDParams_N^{CK}$	-	-	-	0	0	0%	0%	0%	0%	0	0	0%	0%	0%	0%
$FMLSCK_{N+1}$	$C_{N+1}^{FMLSCK_{N+1}}/K_{N+1}$	$S_{N+1}, K_{N+1}, T_{N+1}, R_{N+1}, Q_{N+1}, FMLSParams_N^{CK}$	-	-	-	0	0	0%	0%	0%	0%	0	0	0%	0%	0%	0%
$M3CK1_{N+1}$	$C_{N+1}^{M3CK1_{N+1}}/K_{N+1}$	$S_{N+1}/K_{N+1}, T_{N+1}, R_{N+1}, Q_{N+1}, \sigma_N^{CALIB^{CK}}$	3	5	5 X 5 X 5	0	117	0%	0%	7%	10%	0	121	0%	0%	8%	11%
$M3CK2_{N+1}$	$C_{N+1}^{M3CK2_{N+1}}/K_{N+1}$	$S_{N+1}/K_{N+1}, T_{N+1}, R_{N+1}, Q_{N+1}, \sigma_N^{CALIB^{CK}}, (C_N/K_N)$	3	6	6 X 6 X 6	**27**	**292**	31%	55%	20%	24%	**27**	**313**	31%	55%	21%	26%
$M3CK3_{N+1}$	$C_{N+1}^{M3CK3_{N+1}}/K_{N+1}$	$S_{N+1}/K_{N+1}, T_{N+1}, R_{N+1}, Q_{N+1}, \sigma_N^{CALIB^{CK}}, (C_N/K_N), BSMGreeks_N^{CK}$	3	11	11 X 11 X 11	12	183	9%	30%	12%	16%	12	205	9%	29%	13%	17%
$M3CK4_{N+1}$	$C_{N+1}^{M3CK4_{N+1}}/K_{N+1}$	$S_{N+1}/K_{N+1}, T_{N+1}, R_{N+1}, Q_{N+1}, \sigma_N^{CALIB^{CK}}, (C_N/K_N), BSMGreeks_N^{CK}, HParams_N^{CK}$	3	16	16 X 16 X 16	18	124	17%	39%	8%	11%	18	149	17%	39%	10%	13%
$M3CK5_{N+1}$	$C_{N+1}^{M3CK5_{N+1}}/K_{N+1}$	$S_{N+1}/K_{N+1}, T_{N+1}, R_{N+1}, Q_{N+1}, \sigma_N^{CALIB^{CK}}, (C_N/K_N), BSMGreeks_N^{CK}, HParams_N^{CK}, (C_N^{HCK}/K_N)$	3	17	17 X 17 X 17	0	49	0%	0%	3%	5%	0	72	0%	0%	4%	7%
$M3CK6_{N+1}$	$C_{N+1}^{M3CK6_{N+1}}/K_{N+1}$	$S_{N+1}/K_{N+1}, T_{N+1}, R_{N+1}, Q_{N+1}, HParams_N^{CK}, (C_N^{HCK}/K_N)$	3	10	10 X 10 X 10	3	79	0%	11%	5%	7%	3	106	0%	11%	6%	9%
$M3CK7_{N+1}$	$C_{N+1}^{M3CK7_{N+1}}/K_{N+1}$	$S_{N+1}/K_{N+1}, T_{N+1}, R_{N+1}, Q_{N+1}, \sigma_N^{CALIB^{CK}}, BSMGreeks_N^{CK}, (C_N^{BSMCK}/K_N)$	3	11	11 X 11 X 11	0	26	0%	0%	1%	3%	0	55	0%	0%	3%	5%
$M3CK8_{N+1}$	$C_{N+1}^{M3CK8_{N+1}}/K_{N+1}$	$S_{N+1}/K_{N+1}, T_{N+1}, R_{N+1}, Q_{N+1}, HJDParams_N^{CK}, (C_N^{HJDCK}/K_N)$	3	13	13 X 13 X 13	2	140	0%	8%	9%	12%	2	165	0%	8%	11%	14%
$M3CK9_{N+1}$	$C_{N+1}^{M3CK9_{N+1}}/K_{N+1}$	$S_{N+1}/K_{N+1}, T_{N+1}, R_{N+1}, Q_{N+1}, FMLSParams_N^{CK}, (C_N^{FMLSCK}/K_N)$	3	7	7 X 7 X 7	2	131	0%	8%	8%	12%	2	140	0%	8%	9%	12%

Table A.2.35: Call Option Price Scaled by the Exercise Price Comparison (amongst Parametric and LSTM $L3CK_{N+1} - Models$): This table presents a performance comparison using both daily and monthly statistics amongst the Black-Scholes-Merton ($BSMCK_{N+1}$) model, Heston (HCK_{N+1}) model, Heston Jump Diffusion ($HJDCK_{N+1}$) model, Finite Moment Log Stable ($FMLSCK_{N+1}$) model and the LSTM $L3CK_{N+1} - Models$ ($L3CK1_{N+1}$ to $L3CK9_{N+1}$). The forecast variable for all the models is the one-day-ahead call option price scaled by the exercise price (C_{N+1}/K_{N+1}). The models denoted by the $_{N+1}$ subscript use one-day-ahead input variables for forecasting C_{N+1}/K_{N+1}. The one-day-ahead forecast errors of C_{N+1}/K_{N+1} are used to compute the Root Mean Square Error (RMSE). Column I identifies the models, column II identifies the forecast variable, column III lists the input variables used by the models to obtain the one-trading-day-ahead forecast of C_{N+1}/K_{N+1}, and columns IV, V and VI describe the network architecture of the LSTM $L3CK_{N+1} - Models$. Forecasts are made for 1,328 trading days, and there are 64 months covered in the sample using the monthly data.
When comparing all models simultaneously (i.e. including the random walk model (δCK_N), column VII reports the number of months out of the 64 months that each model has the smallest RMSE, while column VIII reports the number of days out of the 1,328 days each model has the smallest RMSE. Columns IX (lower bound) and X (upper bound) present the winning percentage out of 64 months for each model, evaluated using the bootstrap sampling technique. The statistical bootstrap performed (with replacement) at a 95% confidence level is computed from the monthly RMSE values of the respective models below. Columns XI (lower bound) and XII (upper bound) present the winning percentage out of 1326 days for each model computed from bootstrapping the daily RMSE values of the respective models at a 95% confidence level.
Similarly, when the δCK_N model was excluded in the comparison, column XIII reports the number of months out of the 64 months that each model has the smallest RMSE, while column XIV reports the number of days out of the 1,328 days each model has the smallest RMSE. Columns XV (lower bound) and XVI (upper bound) present the winning percentage out of 64 months for each model, evaluated using the bootstrap sampling technique. The statistical bootstrap performed (with replacement) at a 95% confidence level is computed from the monthly RMSE values of the respective models below. Also, columns XVII (lower bound) and XVIII (upper bound) present the winning percentage out of 1326 days for each model computed from bootstrapping the daily RMSE values of the respective models at a 95% confidence level.

						Including the random walk						Excluding the random walk					
(I)	**(II)**	**(III)**	**(IV)**	**(V)**	**(VI)**	**(VII)**	**(VIII)**	**(IX)**	**(X)**	**(XI)**	**(XII)**	**(XIII)**	**(XIV)**	**(XV)**	**(XVI)**	**(XVII)**	**(XVIII)**
Model	**Forecast**	**Inputs**	**No. of hidden layers**	**No. of hidden nodes per layer**	**Network architecture**	**Performance amongst all models (Monthly)**	**Performance amongst all models (Daily)**	**2.5% lower bound- (for monthly) (%)**	**2.5% upper bound- (for monthly) (%)**	**2.5% lower bound- (for daily) (%)**	**2.5% upper bound- (for daily) (%)**	**Performance amongst all models (Monthly)**	**Performance amongst all models (Daily)**	**2.5% lower bound- (for monthly) (%)**	**2.5% upper bound- (for monthly) (%)**	**2.5% lower bound- (for daily) (%)**	**2.5% upper bound- (for daily) (%)**
δCK_N	C_{N+1}/K_{N+1}	C_N, K_N	-	-	-	**64**	**680**	100%	100%	48%	54%	-	-	-	-	-	-
$BSMCK_{N+1}$	$C_{N+1}^{BSMCK_{N+1}}/K_{N+1}$	$S_{N+1}, K_{N+1}, T_{N+1}, R_{N+1}, Q_{N+1}, \sigma_N^{CALIB^{CK}}$	-	-	-	0	21	0%	0%	1%	2%	0	26	0%	0%	1%	3%
HCK_{N+1}	$C_{N+1}^{HCK_{N+1}}/K_{N+1}$	$S_{N+1}, K_{N+1}, T_{N+1}, R_{N+1}, Q_{N+1}, \sigma_N^{CALIB^{CK}}, HParams_N^{CK}$	-	-	-	0	109	0%	0%	7%	10%	0	141	0%	0%	9%	12%
$HJDCK_{N+1}$	$C_{N+1}^{HJDCK_{N+1}}/K_{N+1}$	$S_{N+1}, K_{N+1}, T_{N+1}, R_{N+1}, Q_{N+1}, \sigma_N^{CALIB^{CK}}, HJDParams_N^{CK}$	-	-	-	0	0	0%	0%	0%	0%	1	1	0%	5%	0%	0%
$FMLSCK_{N+1}$	$C_{N+1}^{FMLSCK_{N+1}}/K_{N+1}$	$S_{N+1}, K_{N+1}, T_{N+1}, R_{N+1}, Q_{N+1}, FMLSParams_N^{CK}$	-	-	-	0	0	0%	0%	0%	0%	2	1	0%	8%	0%	0%
$L3CK1_{N+1}$	$C_{N+1}^{L3CK1_{N+1}}/K_{N+1}$	$S_{N+1}/K_{N+1}, T_{N+1}, R_{N+1}, Q_{N+1}, \sigma_N^{CALIB^{CK}}$	3	5	5 X 5 X 5	0	5	0%	0%	0%	1%	0	7	0%	0%	0%	1%
$L3CK2_{N+1}$	$C_{N+1}^{L3CK2_{N+1}}/K_{N+1}$	$S_{N+1}/K_{N+1}, T_{N+1}, R_{N+1}, Q_{N+1}, \sigma_N^{CALIB^{CK}}, (C_N/K_N)$	3	6	6 X 6 X 6	0	182	0%	0%	12%	15%	0	**345**	0%	0%	24%	28%
$L3CK3_{N+1}$	$C_{N+1}^{L3CK3_{N+1}}/K_{N+1}$	$S_{N+1}/K_{N+1}, T_{N+1}, R_{N+1}, Q_{N+1}, \sigma_N^{CALIB^{CK}}, (C_N/K_N), BSMGreeks_N^{CK}$	3	11	11 X 11 X 11	0	39	0%	0%	2%	4%	4	87	2%	13%	5%	8%
$L3CK4_{N+1}$	$C_{N+1}^{L3CK4_{N+1}}/K_{N+1}$	$S_{N+1}/K_{N+1}, T_{N+1}, R_{N+1}, Q_{N+1}, \sigma_N^{CALIB^{CK}}, (C_N/K_N), BSMGreeks_N^{CK}, HParams_N^{CK}$	3	16	16 X 16 X 16	0	64	0%	0%	4%	6%	5	123	2%	16%	8%	11%
$L3CK5_{N+1}$	$C_{N+1}^{L3CK5_{N+1}}/K_{N+1}$	$S_{N+1}/K_{N+1}, T_{N+1}, R_{N+1}, Q_{N+1}, \sigma_N^{CALIB^{CK}}, (C_N/K_N), BSMGreeks_N^{CK}, HParams_N^{CK}, (C_N^{HCK}/K_N)$	3	17	17 X 17 X 17	0	72	0%	0%	4%	7%	**32**	223	38%	63%	15%	19%
$L3CK6_{N+1}$	$C_{N+1}^{L3CK6_{N+1}}/K_{N+1}$	$S_{N+1}/K_{N+1}, T_{N+1}, R_{N+1}, Q_{N+1}, HParams_N^{CK}, (C_N^{HCK}/K_N)$	3	10	10 X 10 X 10	0	28	0%	0%	1%	3%	4	62	2%	13%	4%	6%
$L3CK7_{N+1}$	$C_{N+1}^{L3CK7_{N+1}}/K_{N+1}$	$S_{N+1}/K_{N+1}, T_{N+1}, R_{N+1}, Q_{N+1}, \sigma_N^{CALIB^{CK}}, BSMGreeks_N^{CK}, (C_N^{BSMCK}/K_N)$	3	11	11 X 11 X 11	0	39	0%	0%	2%	4%	14	195	13%	33%	13%	17%
$L3CK8_{N+1}$	$C_{N+1}^{L3CK8_{N+1}}/K_{N+1}$	$S_{N+1}/K_{N+1}, T_{N+1}, R_{N+1}, Q_{N+1}, HJDParams_N^{CK}, (C_N^{HJDCK}/K_N)$	3	13	13 X 13 X 13	0	0	0%	0%	0%	0%	0	0	0%	0%	0%	0%
$L3CK9_{N+1}$	$C_{N+1}^{L3CK9_{N+1}}/K_{N+1}$	$S_{N+1}/K_{N+1}, T_{N+1}, R_{N+1}, Q_{N+1}, FMLSParams_N^{CK}, (C_N^{FMLSCK}/K_N)$	3	7	7 X 7 X 7	0	89	0%	0%	5%	8%	2	117	0%	8%	7%	10%

Table A.2.36: Call Option Price Scaled by the Exercise Comparison (amongst Parametric Models): This table presents a performance comparison using both daily and monthly statistics amongst the Black-Scholes-Merton ($BSMCK_{N+1}$) model, Heston (HCK_{N+1}) model, Heston Jump Diffusion ($HJDCK_{N+1}$) model, and the Finite Moment Log Stable ($FMLSCK_{N+1}$) model. The forecast variable for all the models is the one-day-ahead call option price scaled by the exercise price (C_{N+1}/K_{N+1}). The models denoted by the $_{N+1}$ subscript use one-day-ahead input variables for forecasting C_{N+1}/K_{N+1}. The one-day-ahead forecast errors of C_{N+1}/K_{N+1} are used to compute the Root Mean Square Error (RMSE). Column I identifies the models, column II identifies the forecast variable, column III lists the input variables used by the models to obtain the one-trading-day-ahead forecast of C_{N+1}. Forecasts are made for 1,328 trading days, and there are 64 months covered in the sample using the monthly data.

When comparing all models simultaneously (i.e. including the random walk model (δCK_N), column VII reports the number of months out of the 64 months that each model has the smallest RMSE, while column VIII reports the number of days out of the 1,328 days each model has the smallest RMSE. Columns IX (lower bound) and X (upper bound) present the winning percentage out of 64 months for each model, evaluated using the bootstrap sampling technique. The statistical bootstrap performed (with replacement) at a 95% confidence level is computed from the monthly RMSE values of the respective models below. Columns XI (lower bound) and XII (upper bound) present the winning percentage out of 1326 days for each model computed from bootstrapping the daily RMSE values of the respective models at a 95% confidence level.

Similarly, when the δCK_N model was excluded in the comparison, column XIII reports the number of months out of the 64 months that each model has the smallest RMSE, while column XIV reports the number of days out of the 1,328 days each model has the smallest RMSE. Columns XV (lower bound) and XVI (upper bound) present the winning percentage out of 64 months for each model, evaluated using the bootstrap sampling technique. The statistical bootstrap performed (with replacement) at a 95% confidence level is computed from the monthly RMSE values of the respective models below. Also, columns XVII (lower bound) and XVIII (upper bound) present the winning percentage out of 1326 days for each model computed from bootstrapping the daily RMSE values of the respective models at a 95% confidence level.

			Including the random walk						**Excluding the random walk**					
(I) Model	**(II) Forecast**	**(III) Inputs**	**(IV) Performance amongst all models (Monthly)**	**(V) Performance amongst all models (Daily)**	**(VI) 2.5% lower bound-(for monthly) (%)**	**(VII) 2.5% upper bound-(for monthly) (%)**	**(VIII) 2.5% lower bound-(for daily) (%)**	**(IX) 2.5% upper bound-(for daily) (%)**	**(X) Performance amongst all models (Monthly)**	**(XI) Performance amongst all models (Daily)**	**(XII) 2.5% lower bound-(for monthly) (%)**	**(XIII) 2.5% upper bound-(for monthly) (%)**	**(XIV) 2.5% lower bound-(for daily) (%)**	**(XV) 2.5% upper bound-(for daily) (%)**
δCK_N	C_{N+1}/K_{N+1}	C_N, K_N	**64**	**1158**	100%	100%	85%	89%	-	-	-	-	-	-
$BSMCK_{N+1}$	$C_{N+1}^{BSMCK_{N+1}}/K_{N+1}$	$S_{N+1}, K_{N+1}, T_{N+1}, R_{N+1}, Q_{N+1}, \sigma_N^{CALIB^{CK}}$	0	36	0%	0%	2%	4%	18	305	17%	39%	21%	25%
HCK_{N+1}	$C_{N+1}^{HCK_{N+1}}/K_{N+1}$	$S_{N+1}, K_{N+1}, T_{N+1}, R_{N+1}, Q_{N+1}, \sigma_N^{CALIB^{CK}}, HParams_N^{CK}$	0	131	0%	0%	8%	11%	0	285	0%	0%	19%	24%
$HJDCK_{N+1}$	$C_{N+1}^{HJDCK_{N+1}}/K_{N+1}$	$S_{N+1}, K_{N+1}, T_{N+1}, R_{N+1}, Q_{N+1}, \sigma_N^{CALIB^{CK}}, HJDParams_N^{CK}$	0	3	0%	0%	0%	1%	**39**	**559**	50%	73%	39%	45%
$FMLSCK_{N+1}$	$C_{N+1}^{FMLSCK_{N+1}}/K_{N+1}$	$S_{N+1}, K_{N+1}, T_{N+1}, R_{N+1}, Q_{N+1}, FMLSParams_N^{CK}$	0	0	0%	0%	0%	0%	7	179	5%	20%	12%	15%

A.2.5 Pricing performance of $C - Models$ that use lagged input variables to forecast the call option price (C_{N+1}) and performance of $CK - Models - Rescaled$ that have re-scaled call option prices from $CK - Models$ that use lagged input variables to forecast the call option prices scaled by the strike price (C_{N+1}/K_{N+1}) for the next trading day

Table A.2.37 shows the relative out-of-sample performance (in $RMSE$) amongst the models that use lagged input variables to forecast the one-trading-day-ahead call option price (C_{N+1}), and the models that use lagged input variables to forecast the one-trading-day-ahead call option price scaled by the strike price(C_{N+1}/K_{N+1}) which is later re-scaled to C_{N+1}. Column II lists whether the forecast variable of the model has been re-scaled to C_{N+1}. The performance metric is the $RMSE$ of the one-trading-day-ahead forecast errors, computed for each model utilising all of the errors in each day or each month. Amongst all of the models (including the random walk model (δC_N)), columns III and IV record the number of months and days, respectively, that each model has the lowest $RMSE$. We performed a bootstrap using the daily and monthly RMSEs to be certain of our results. Columns V (lower bound) and VI (upper bound) present the results from the bootstrap performed (with replacement) using monthly RMSEs at a 95% confidence level and show the winning percentage out of 64 months for each model (including the δC_N model), and similarly, the 95 % confidence intervals computed from bootstrapping of the daily RMSEs signifies the winning percentage out of 1328 days for each model and are reported in columns VII (lower bound), VIII (upper bound). While excluding the δCK_N model amongst the comparison, columns IX and X record the number of months and days, respectively, that each model has the lowest $RMSE$. We repeat the exercise of performing the bootstrap by excluding the δC_N model in the comparison, and thus, the columns XI (lower bound) and XII (upper bound) present the results from the bootstrap performed (with replacement) using monthly RMSEs at a 95% confidence level and shows the winning percentage out of 64 months for each model (excluding the δC_N model) and similarly, the 95 % confidence intervals computed from bootstrapping of the daily RMSEs signifies the winning percentage out of 1328 days for each model and are reported in columns XIII (lower bound), XIV (upper bound).

A.2.5.1 Comparison amongst all Parametric Models with $C - Models$ and $CK - Models - Rescaled$:

In this section, we compare the out-of-sample performance of the random walk model (δC_N), the parametric models ($BSMCK_{N+1}$, HCK_{N+1}, $HJDCK_{N+1}$, and $FMLSCK_{N+1}$), the $C - Models$ which consists of the single, double, triple hidden layer MLP models ($M1C_N - Models(M1C1_N$ to $M1C9_N)$, $M2C_N - Models(M2C1_N$ to $M2C9_N)$, and $M3C_N - Models(M3C1_N$ to $M3C9_N)$), the single, double, triple hidden layer LSTM models ($L1C_N - Models(L1C1_N$ to $L1C9_N)$, $L2C_N - Models(L2C1_N$ to $L2C9_N)$, and $L3C_N - Models(L3C1_N$ to $L3C9_N)$), the $CK - Models - Rescaled$ models which consists of single, double, triple hidden layer MLP models ($M1CK_N - Models - Rescaled(M1CK1_N - Rescaled$ to $M1CK9_N - Rescaled)$, $M2CK_N - Models - Rescaled(M2CK1_N - Rescaled$ to $M2CK9_N - Rescaled)$, and $M3CK_N - Models - Rescaled(M3CK1_N - Rescaled$ to $M3CK9_N - Rescaled)$), the single, double, triple hidden layer

LSTM models ($L1CK_N - Models - Rescaled(L1CK1_N - Rescaled$ to $L1CK9_N - Rescaled)$, $L2CK_N - Models - Rescaled(L2CK1_N - Rescaled$ to $L2CK9_N - Rescaled)$, and $L3CK_N - Models - Rescaled(L3CK1_N - Rescaled$ to $L3CK9_N - Rescaled)$) in Table A.2.37.

We find that the δC_N model had the lowest $RMSE$ for 100 days (having a daily bootstrap winning % of 6% to 9%) out of 1,328 days. When the δC_N was excluded from the comparison, the $L3C9_N$ model outperformed all other models for 97 days (having a daily bootstrap winning % of 6% to 9%) out of 1,328 days.

Thus, when comparing the out-of-sample performance amongst the single, double and triple hidden layer ANN models belonging to the $C - Models$ category and amongst the single, double and triple hidden layer ANN models belonging to the $CK - Models - Rescaled$ category (in Table A.2.37), we notice that only a triple hidden layer LSTM($L3C9_N$) model belonging to the $C - Models$ category could outperform all other models.

Table A.2.37: Call Price Comparison (amongst Parametric, MLP $M1C_N - Models$, MLP $M2C_N - Models$, MLP $M3C_N - Models$, LSTM $L1C_N - Models$, LSTM $L2C_N - Models$, LSTM $L3C_N - Models$, MLP $M1CK_N - Models - Rescaled$, MLP $M2CK_N - Models - Rescaled$, MLP $M3CK_N - Models - Rescaled$, LSTM $L1CK_N - Models - Rescaled$, LSTM $L2CK_N - Models - Rescaled$, and LSTM $L3CK_N - Models - Rescaled$): This table presents a performance comparison using both daily and monthly statistics amongst the Black-Scholes-Merton ($BSMC_N$) model, Heston (HC_N) model, Heston Jump Diffusion ($HJDC_N$) model, Finite Moment Log Stable ($FMLSC_N$) model, MLP $M1C_N - Models$ ($M1C1_N$ to $M1C9_N$), MLP $M2C_N - Models$ ($M2C1_N$ to $M2C9_N$), MLP $M3C_N - Models$ ($M3C1_N$ to $M3C9_N$), LSTM $L1C_N - Models$ ($L1C1_N$ to $L1C9_N$), LSTM $L2C_N - Models$ ($L2C1_N$ to $L2C9_N$), LSTM $L3C_N - Models$ ($L3C1_N$ to $L3C9_N$), MLP $M1CK_N - Models - Rescaled$ ($M1CK1_N$ to $M1CK9_N$), MLP $M2CK_N - Models - Rescaled$ ($M2CK1_N$ to $M2CK9_N$), MLP $M3CK_N - Models - Rescaled$ ($M3CK1_N$ to $M3CK9_N$), LSTM $L1CK_N - Models - Rescaled$ ($L1CK1_N$ to $L1CK9_N$), LSTM $L2CK_N - Models - Rescaled$ ($L2CK1_N$ to $L2CK9_N$), and the LSTM $L3CK_N - Models - Rescaled$ ($L3CK1_N$ to $L3CK9_N$). The forecast variable for all the models is the one-day-ahead call option price (C_{N+1}). The models denoted by the $_N$ subscript use lagged input variables for forecasting C_{N+1}. The one-day-ahead forecast errors of C_{N+1} are used to compute the Root Mean Square Error (RMSE). Column I identifies the models, and column II identifies whether the forecast variable of the model has been re-scaled to C_{N+1}. Forecasts are made for 1,328 trading days, and there are 64 months covered in the sample using the monthly data. When comparing all models simultaneously (i.e. including the random walk model (δC_N), column III reports the number of months out of the 64 months that each model has the smallest RMSE, while column IV reports the number of days out of the 1,328 days each model has the smallest RMSE. Columns V (lower bound) and VI (upper bound) present the winning percentage out of 64 months for each model, evaluated using the bootstrap sampling technique. The statistical bootstrap performed (with replacement) at a 95% confidence level is computed from the monthly RMSE values of the respective models below. Columns VII (lower bound) and VIII (upper bound) present the winning percentage out of 1326 days for each model computed from bootstrapping the daily RMSE values of the respective models at a 95% confidence level. Similarly, when the δC_N model was excluded in the comparison, column IX reports the number of months out of the 64 months that each model has the smallest RMSE, while column X reports the number of days out of the 1,328 days each model has the smallest RMSE. Columns XI (lower bound) and XII (upper bound) present the winning percentage out of 64 months for each model, evaluated using the bootstrap sampling technique. The statistical bootstrap performed (with replacement) at a 95% confidence level is computed from the monthly RMSE values of the respective models below. Also, columns XIII (lower bound) and XIV (upper bound) present the winning percentage out of 1326 days for each model computed from bootstrapping the daily RMSE values of the respective models at a 95% confidence level.

		Including the random walk						Excluding the random walk					
(I) Model	**(II) Forecast variable re-scaled to call price**	**(III) Performance amongst all models (Monthly)**	**(IV) Performance amongst all models (Daily)**	**(V) 2.5% lower bound-(for monthly) (%)**	**(VI) 2.5% upper bound-(for monthly) (%)**	**(VII) 2.5% lower bound-(for daily) (%)**	**(VIII) 2.5% upper bound-(for daily) (%)**	**(IX) Performance amongst all models (Monthly)**	**(X) Performance amongst all models (Daily)**	**(XI) 2.5% lower bound-(for monthly) (%)**	**(XII) 2.5% upper bound-(for monthly) (%)**	**(XIII) 2.5% lower bound-(for daily) (%)**	**(XIV) 2.5% upper bound-(for daily) (%)**
δC_N	-	6	**100**	3%	17%	6%	9%	-	-	-	-	-	-
$BSMC_N$	-	0	17	0%	0%	1%	2%	0	17	0%	0%	1%	2%
HC_N	-	1	9	0%	6%	0%	1%	1	9	0%	5%	0%	1%
$HJDC_N$	-	0	0	0%	0%	0%	0%	0	6	0%	0%	0%	1%
$FMLSC_N$	-	0	0	0%	0%	0%	0%	0	0	0%	0%	0%	0%
$M1C1_N$	-	0	0	0%	0%	0%	0%	0	0	0%	0%	0%	0%
$M1C2_N$	-	1	1	0%	5%	0%	0%	1	1	0%	5%	0%	0%
$M1C3_N$	-	1	13	0%	5%	0%	2%	1	17	0%	5%	1%	2%
$M1C4_N$	-	0	13	0%	0%	1%	2%	0	19	0%	0%	1%	2%
$M1C5_N$	-	2	4	0%	8%	0%	1%	2	5	0%	8%	0%	1%
$M1C6_N$	-	1	2	0%	5%	0%	0%	2	3	0%	8%	0%	1%
$M1C7_N$	-	1	7	0%	5%	0%	1%	1	8	0%	5%	0%	1%
$M1C8_N$	-	0	2	0%	0%	0%	0%	0	5	0%	0%	0%	1%
$M1C9_N$	-	0	2	0%	0%	0%	0%	0	2	0%	0%	0%	0%
$M2C1_N$	-	0	4	0%	0%	0%	1%	0	4	0%	0%	0%	1%
$M2C2_N$	-	0	8	0%	0%	0%	1%	0	9	0%	0%	0%	1%
$M2C3_N$	-	1	9	0%	5%	0%	1%	1	13	0%	5%	1%	2%
$M2C4_N$	-	1	14	0%	5%	1%	2%	1	19	0%	5%	1%	2%
$M2C5_N$	-	0	1	0%	0%	0%	0%	0	3	0%	0%	0%	1%
$M2C6_N$	-	0	2	0%	0%	0%	0%	1	5	0%	5%	0%	1%
$M2C7_N$	-	0	3	0%	0%	0%	1%	0	6	0%	0%	0%	1%
$M2C8_N$	-	0	0	0%	0%	0%	0%	0	1	0%	0%	0%	0%
$M2C9_N$	-	0	2	0%	0%	0%	0%	0	4	0%	0%	0%	1%
$M3C1_N$	-	0	5	0%	0%	0%	1%	0	8	0%	0%	0%	1%
$M3C2_N$	-	0	13	0%	0%	0%	2%	0	15	0%	0%	1%	2%
$M3C3_N$	-	3	23	0%	10%	1%	2%	3	28	0%	11%	1%	3%
$M3C4_N$	-	2	10	0%	8%	0%	1%	2	16	0%	8%	1%	2%
$M3C5_N$	-	0	1	0%	0%	0%	0%	0	4	0%	0%	0%	1%
$M3C6_N$	-	0	0	0%	0%	0%	0%	0	2	0%	0%	0%	0%
$M3C7_N$	-	3	7	0%	11%	0%	1%	3	15	0%	11%	1%	2%
$M3C8_N$	-	0	1	0%	0%	0%	0%	1	7	0%	5%	0%	1%
$M3C9_N$	-	0	7	0%	0%	0%	1%	1	13	0%	5%	0%	2%
$L1C1_N$	-	0	0	0%	0%	0%	0%	0	0	0%	0%	0%	0%
$L1C2_N$	-	0	4	0%	0%	0%	1%	0	4	0%	0%	0%	1%
$L1C3_N$	-	0	7	0%	0%	0%	1%	0	7	0%	0%	0%	1%
$L1C4_N$	-	0	17	0%	0%	1%	2%	0	17	0%	0%	1%	2%
$L1C5_N$	-	4	27	2%	13%	1%	3%	4	27	2%	13%	1%	3%
$L1C6_N$	-	0	10	0%	0%	0%	1%	0	10	0%	0%	0%	1%
$L1C7_N$	-	0	19	0%	0%	1%	2%	1	20	0%	5%	1%	2%
$L1C8_N$	-	1	16	0%	5%	1%	2%	1	17	0%	5%	1%	2%
$L1C9_N$	-	0	1	0%	0%	0%	0%	0	1	0%	0%	0%	0%
$L2C1_N$	-	0	0	0%	0%	0%	0%	0	0	0%	0%	0%	0%
$L2C2_N$	-	0	28	0%	0%	1%	3%	0	28	0%	0%	1%	3%
$L2C3_N$	-	0	19	0%	0%	1%	2%	0	19	0%	0%	1%	2%
$L2C4_N$	-	0	19	0%	0%	1%	2%	0	19	0%	0%	1%	2%
$L2C5_N$	-	1	25	0%	5%	1%	3%	1	29	0%	5%	1%	3%
$L2C6_N$	-	2	10	0%	8%	0%	1%	2	11	0%	8%	0%	1%
$L2C7_N$	-	3	12	0%	9%	0%	1%	3	13	0%	10%	0%	2%
$L2C8_N$	-	2	24	0%	8%	1%	3%	3	26	0%	11%	1%	3%
$L2C9_N$	-	0	26	0%	0%	1%	3%	0	27	0%	0%	1%	3%
$L3C1_N$	-	0	22	0%	0%	1%	2%	0	22	0%	0%	1%	2%
$L3C2_N$	-	0	57	0%	0%	3%	5%	0	57	0%	0%	3%	5%
$L3C3_N$	-	0	26	0%	0%	1%	3%	0	26	0%	0%	1%	3%
$L3C4_N$	-	0	45	0%	0%	2%	4%	0	45	0%	0%	2%	4%
$L3C5_N$	-	1	34	0%	5%	2%	4%	1	35	0%	6%	2%	4%
$L3C6_N$	-	1	17	0%	5%	1%	2%	1	17	0%	5%	1%	2%
$L3C7_N$	-	4	17	2%	13%	1%	2%	4	18	2%	13%	1%	2%
$L3C8_N$	-	**9**	40	6%	23%	2%	4%	**9**	41	6%	23%	2%	4%
$L3C9_N$	-	0	97	0%	0%	6%	9%	0	**97**	0%	0%	6%	9%
$M1CK1_N - Rescaled$	Yes	0	3	0%	0%	0%	1%	0	3	0%	0%	0%	1%
$M1CK2_N - Rescaled$	Yes	0	1	0%	0%	0%	0%	0	1	0%	0%	0%	0%
$M1CK3_N - Rescaled$	Yes	0	9	0%	0%	0%	1%	0	9	0%	0%	0%	1%
$M1CK4_N - Rescaled$	Yes	1	4	0%	6%	0%	1%	1	4	0%	5%	0%	1%
$M1CK5_N - Rescaled$	Yes	1	4	0%	5%	0%	1%	1	4	0%	5%	0%	1%
$M1CK6_N - Rescaled$	Yes	0	3	0%	0%	0%	1%	0	3	0%	0%	0%	0%
$M1CK7_N - Rescaled$	Yes	0	7	0%	0%	0%	1%	0	7	0%	0%	0%	1%
$M1CK8_N - Rescaled$	Yes	0	2	0%	0%	0%	0%	0	2	0%	0%	0%	0%
$M1CK9_N - Rescaled$	Yes	0	8	0%	0%	0%	1%	0	8	0%	0%	0%	1%
$M2CK1_N - Rescaled$	Yes	0	5	0%	0%	0%	1%	0	5	0%	0%	0%	1%
$M2CK2_N - Rescaled$	Yes	0	18	0%	0%	1%	2%	0	18	0%	0%	1%	2%
$M2CK3_N - Rescaled$	Yes	1	14	0%	6%	0%	2%	1	14	0%	5%	0%	2%
$M2CK4_N - Rescaled$	Yes	0	8	0%	0%	0%	1%	0	8	0%	0%	0%	1%
$M2CK5_N - Rescaled$	Yes	0	8	0%	0%	0%	1%	0	8	0%	0%	0%	1%
$M2CK6_N - Rescaled$	Yes	0	2	0%	0%	0%	0%	0	2	0%	0%	0%	0%
$M2CK7_N - Rescaled$	Yes	0	12	0%	0%	0%	1%	0	12	0%	0%	0%	1%
$M2CK8_N - Rescaled$	Yes	1	5	0%	5%	0%	1%	1	5	0%	5%	0%	1%
$M2CK9_N - Rescaled$	Yes	0	5	0%	0%	0%	1%	0	5	0%	0%	0%	1%
$M3CK1_N - Rescaled$	Yes	2	5	0%	8%	0%	1%	2	5	0%	8%	0%	1%
$M3CK2_N - Rescaled$	Yes	1	12	0%	5%	0%	1%	1	14	0%	5%	1%	2%
$M3CK3_N - Rescaled$	Yes	0	12	0%	0%	0%	1%	0	12	0%	0%	0%	1%
$M3CK4_N - Rescaled$	Yes	1	10	0%	5%	0%	1%	1	10	0%	5%	0%	1%
$M3CK5_N - Rescaled$	Yes	0	3	0%	0%	0%	1%	0	3	0%	0%	0%	1%
$M3CK6_N - Rescaled$	Yes	0	9	0%	0%	0%	1%	0	9	0%	0%	0%	1%
$M3CK7_N - Rescaled$	Yes	1	7	0%	5%	0%	1%	1	7	0%	5%	0%	1%
$M3CK8_N - Rescaled$	Yes	2	10	0%	8%	0%	1%	2	10	0%	8%	0%	1%
$M3CK9_N - Rescaled$	Yes	0	3	0%	0%	0%	1%	0	3	0%	0%	0%	0%
$L1CK1_N - Rescaled$	Yes	0	1	0%	0%	0%	0%	0	1	0%	0%	0%	0%
$L1CK2_N - Rescaled$	Yes	0	37	0%	0%	2%	4%	0	37	0%	0%	2%	4%
$L1CK3_N - Rescaled$	Yes	0	2	0%	0%	0%	0%	0	2	0%	0%	0%	0%
$L1CK4_N - Rescaled$	Yes	0	11	0%	0%	0%	1%	0	11	0%	0%	0%	1%
$L1CK5_N - Rescaled$	Yes	0	7	0%	0%	0%	1%	0	7	0%	0%	0%	1%
$L1CK6_N - Rescaled$	Yes	0	8	0%	0%	0%	1%	0	8	0%	0%	0%	1%
$L1CK7_N - Rescaled$	Yes	1	7	0%	5%	0%	1%	1	7	0%	5%	0%	1%
$L1CK8_N - Rescaled$	Yes	0	0	0%	0%	0%	0%	0	0	0%	0%	0%	0%
$L1CK9_N - Rescaled$	Yes	0	0	0%	0%	0%	0%	0	0	0%	0%	0%	0%
$L2CK1_N - Rescaled$	Yes	0	6	0%	0%	0%	1%	0	6	0%	0%	0%	1%
$L2CK2_N - Rescaled$	Yes	0	22	0%	0%	1%	2%	0	22	0%	0%	1%	2%
$L2CK3_N - Rescaled$	Yes	0	5	0%	0%	0%	1%	0	5	0%	0%	0%	1%
$L2CK4_N - Rescaled$	Yes	0	12	0%	0%	0%	1%	0	12	0%	0%	0%	1%
$L2CK5_N - Rescaled$	Yes	0	14	0%	0%	1%	2%	0	14	0%	0%	1%	2%
$L2CK6_N - Rescaled$	Yes	0	9	0%	0%	0%	1%	0	9	0%	0%	0%	1%
$L2CK7_N - Rescaled$	Yes	0	10	0%	0%	0%	1%	0	10	0%	0%	0%	1%
$L2CK8_N - Rescaled$	Yes	0	0	0%	0%	0%	0%	0	0	0%	0%	0%	0%
$L2CK9_N - Rescaled$	Yes	0	2	0%	0%	0%	0%	0	2	0%	0%	0%	0%
$L3CK1_N - Rescaled$	Yes	0	5	0%	0%	0%	1%	0	5	0%	0%	0%	1%
$L3CK2_N - Rescaled$	Yes	0	27	0%	0%	1%	3%	0	27	0%	0%	1%	3%
$L3CK3_N - Rescaled$	Yes	1	8	0%	5%	0%	1%	1	8	0%	5%	0%	1%
$L3CK4_N - Rescaled$	Yes	0	15	0%	0%	1%	2%	0	15	0%	0%	1%	2%
$L3CK5_N - Rescaled$	Yes	0	12	0%	0%	0%	2%	0	12	0%	0%	0%	1%
$L3CK6_N - Rescaled$	Yes	0	10	0%	0%	0%	1%	0	10	0%	0%	0%	1%
$L3CK7_N - Rescaled$	Yes	0	10	0%	0%	0%	1%	0	10	0%	0%	0%	1%
$L3CK8_N - Rescaled$	Yes	0	0	0%	0%	0%	0%	0	0	0%	0%	0%	0%
$L3CK9_N - Rescaled$	Yes	0	1	0%	0%	0%	0%	0	1	0%	0%	0%	0%

Table A.2.38: Out-of-sample out-performance comparison based on average number of days and the total number of days amongst MLP $M1C_N-Models$, MLP $M2C_N-Models$, MLP $M3C_N-Models$, LSTM $L1C_N-Models$, LSTM $L2C_N-Models$, LSTM $L3C_N-Models$, MLP $M1CK_N-Models$, MLP $M2CK_N-Models$, MLP $M3CK_N-Models$, LSTM $L1CK_N-Models$, LSTM $L2CK_N-Models$, LSTM $L3CK_N-Models$, MLP $M1CK_N-Models-Rescaled$, MLP $M2CK_N-Models-Rescaled$, MLP $M3CK_N-Models-Rescaled$, LSTM $L1CK_N-Models-Rescaled$, LSTM $L2CK_N-Models-Rescaled$, and LSTM $L3CK_N-Models-Rescaled$: This table presents the out-of-sample out-performance comparison based on average number of days and the total number of days amongst the MLP $M1C_N-Models$, MLP $M2C_N-Models$, MLP $M3C_N-Models$, LSTM $L1C_N-Models$, LSTM $L2C_N-Models$, LSTM $L3C_N-Models$ in Part I, MLP $M1CK_N-Models$, MLP $M2CK_N-Models$, MLP $M3CK_N-Models$, LSTM $L1CK_N-Models$, LSTM $L2CK_N-Models$, LSTM $L3CK_N-Models$ in Part II, and MLP $M1C_N-Models$, MLP $M2C_N-Models$, MLP $M3C_N-Models$, LSTM $L1C_N-Models$, LSTM $L2C_N-Models$, LSTM $L3C_N-Models$, MLP $M1CK_N-Models-Rescaled$, MLP $M2CK_N-Models-Rescaled$, MLP $M3CK_N-Models-Rescaled$, LSTM $L1CK_N-Models-Rescaled$, LSTM $L2CK_N-Models-Rescaled$, LSTM $L3CK_N-Models-Rescaled$ in Part III. For models in Part I, the average number of days a model out-performed and the total number of days it out-performed was computed from column VIII of Table A.2.10, for models in Part II, the average number of days a model out-performed and the total number of days it out-performed was computed from column VIII of Table A.2.28, and for models in Part III, the average number of days a model out-performed and the total number of days it out-performed was computed from column IV of A.2.38. The forecast variable for the models in Part I is the one-day-ahead call option (C_{N+1}), in Part II is the one-day-ahead call option price scaled by the exercise price (C_{N+1}/K_{N+1}), and in Part III is the one-day-ahead call option price (C_{N+1}) which is re-scaled from C_{N+1}/K_{N+1}). The models denoted by the $_N$ subscript use lagged input variables for forecasting the C_{N+1} in Part I, C_{N+1}/K_{N+1} in Part II and Part III. The one-day-ahead forecast errors are used to compute the Root Mean Square Error (RMSE). Column I identifies the models, column II identifies whether the forecast variable of the model has been re-scaled to C_{N+1}, and column III reports the average number of days each model has out-performed in Part I, II and III, respectively, and similarly, column IV reports the total number of days each model has out-performed in Part I, II and III respectively. Forecasts are made for 1,328 trading days, and there are 64 months covered in the sample using the monthly data.

(I) Model	(II) Forecast variable re-scaled to call price	(III) Avg. number of days out-performed	(IV) Total number of days out-performed
Part I: Performance of $M1C_N-Models$, $M2C_N-Models$, $M3C_N-Models$, $L1C_N-Models$, $L2C_N-Models$, $L3C_N-Models$			
$M1C_N-Models$	-	9	84
$M2C_N-Models$	-	17	156
$M3C_N-Models$	-	8	73
$L1C_N-Models$	-	25	222
$L2C_N-Models$	-	11	99
$L3C_N-Models$	-	**54**	**487**
Part II: Performance of $M1CK_N-Models$, $M2CK_N-Models$, $M3CK_N-Models$, $L1CK_N-Models$, $L2CK_N-Models$, $L3CK_N-Models$			
$M1CK_N-Models$	-	15	139
$M2CK_N-Models$	-	17	155
$M3CK_N-Models$	-	22	198
$L1CK_N-Models$	-	22	194
$L2CK_N-Models$	-	**28**	**252**
$L3CK_N-Models$	-	21	187
Part III: Performance of $M1C_N-Models$, $M2C_N-Models$, $M3C_N-Models$, $L3C_N-Models$, $L2C_N-Models$, $L3C_N-Models$, $M1CK_N-Models-Rescaled$, $M2CK_N-Models-Rescaled$, $M3CK_N-Models-Rescaled$, $L3CK_N-Models-Rescaled$, $L2CK_N-Models-Rescaled$, $L3CK_N-Models-Rescaled$			
$M1C_N-Models$	-	5	44
$M2C_N-Models$	-	5	43
$M3C_N-Models$	-	7	67
$L1C_N-Models$	-	11	101
$L2C_N-Models$	-	18	163
$L3C_N-Models$	-	**39**	**355**
$M1CK_N-Models-Rescaled$	Yes	5	41
$M2CK_N-Models-Rescaled$	Yes	9	77
$M3CK_N-Models-Rescaled$	Yes	8	71
$L1CK_N-Models-Rescaled$	Yes	8	73
$L2CK_N-Models-Rescaled$	Yes	9	80
$L3CK_N-Models-Rescaled$	Yes	10	89

Appendix B.1

Appendix for Chapter 3: Tables

Table B.1.1: Model Definition for Delta Comparison: This table is compartmentalised into III parts. Column I identifies the models, column II identifies the forecast variable, column III identifies the target variable used while training the respective MLP and LSTM models, and column IV list the input variables used by the respective models to obtain the one-trading-day-ahead forecast. Forecasts are made for 1,326 trading days, and there are 64 months covered in the sample using the monthly data. Each sub-section below presents the following set of models: **Part I**: This sub-section presents the models having the N subscript that uses lagged input variables for forecasting the delta. The one-trading-day-ahead forecast errors of the delta are used to compute the Root Mean Square Error (RMSE). The forecast variable for the MLP $M3H_N$-Models and the LSTM $L3H_N$-Models is the delta that is directly forecasted from the respective ANN model, whereas the delta for the $BSMH_N$, HH_N, $HJDH_N$ models are computed using their respective characteristic functions. **Part II**: This sub-section presents the models having the $N+1$ subscript that use one-trading-day-ahead input variables for forecasting the delta. The one-trading-day-ahead forecast errors of the delta are used to compute the Root Mean Square Error (RMSE). The forecast variable for the MLP $M3H_{N+1}$-Models and the LSTM $L3H_{N+1}$-Models is the delta that is directly forecasted from the respective ANN model, whereas the delta for the $BSMH_{N+1}$, HH_{N+1}, $HJDH_{N+1}$ models are computed using their respective characteristic functions. **Part III**: This sub-section presents the models having the $N+1$ subscript that use one-trading-day-ahead input variables for forecasting the one-trading-day-ahead call option price (C_{N+1}), and later using the C_{N+1}, we analytically derive the delta ($\delta C_{N+1}/\delta S_{N+1}$) using equation 3.3. The one-trading-day-ahead forecast errors of $\delta C_{N+1}/\delta S_{N+1}$ are used to compute the Root Mean Square Error (RMSE). The forecast variable, the delta, for all the models in this sub-section is computed as $\delta C_{N+1}/\delta S_{N+1}$.

(I) Model	**(II)** Forecast variable	**(III)** Target variable	**(IV)** Inputs for training/forecasting	**(I)** Model	**(II)** Forecast variable	**(III)** Target variable	**(IV)** Inputs for training/forecasting
Part I							
Black-Scholes-Merton Model				**Heston Model**			
$BSMH_N$	$\Delta_{N+1}^{BSMH_N}$	-	$S_N, K_{N+1}, T_{N+1}, R_N, Q_N, \sigma_N^{CALIB^C}$	HH_N	$\Delta_{N+1}^{HH_N}$	-	$S_N, K_{N+1}, T_{N+1}, R_N, Q_N, \sigma_N^{CALIB^C}, HParams_N^C$
Heston Jump Diffusion Model				**Finite Moment Log Stable Model**			
$HJDH_N$	$\Delta_{N+1}^{HJDH_N}$	-	$S_N, K_{N+1}, T_{N+1}, R_N, Q_N, \sigma_N^{CALIB^C}, HJDParams_N^C$	$FMLSH_N$	$\Delta_{N+1}^{FMLSH_N}$	-	$S_N, K_{N+1}, T_{N+1}, R_N, Q_N, FMLSParams_N^C$
$M3H_N$ **Multi Layer Perceptron (MLP) Models**				$L3H_N$ **Long Short Term Memory (LSTM) Models**			
$M3H1_N$	$\Delta_{N+1}^{M3H1_N}$	$(\delta C_{N+1}^{M3H1_N}/\delta S_{N+1})$	$S_N, K_{N+1}, T_{N+1}, R_N, Q_N, \sigma_N^{CALIB^C}$	$L3H1_N$	$\Delta_{N+1}^{L3H1_N}$	$(\delta C_{N+1}^{L3H1_N}/\delta S_{N+1})$	$S_N, K_{N+1}, T_{N+1}, R_N, Q_N, \sigma_N^{CALIB^C}$
$M3H2_N$	$\Delta_{N+1}^{M3H2_N}$	$(\delta C_{N+1}^{M3H2_N}/\delta S_{N+1})$	$S_N, K_{N+1}, T_{N+1}, R_N, Q_N, \sigma_N^{CALIB^C}, (\delta C_N/\delta S_N)$	$L3H2_N$	$\Delta_{N+1}^{L3H2_N}$	$(\delta C_{N+1}^{L3H2_N}/\delta S_{N+1})$	$S_N, K_{N+1}, T_{N+1}, R_N, Q_N, \sigma_N^{CALIB^C}, (\delta C_N/\delta S_N)$
$M3H3_N$	$\Delta_{N+1}^{M3H3_N}$	$(\delta C_{N+1}^{M3H3_N}/\delta S_{N+1})$	$S_N, K_{N+1}, T_{N+1}, R_N, Q_N, \sigma_N^{CALIB^C}, \Delta_N^{BSMH_N}$	$L3H3_N$	$\Delta_{N+1}^{L3H3_N}$	$(\delta C_{N+1}^{L3H3_N}/\delta S_{N+1})$	$S_N, K_{N+1}, T_{N+1}, R_N, Q_N, \sigma_N^{CALIB^C}, \Delta_N^{BSMH_N}$
$M3H4_N$	$\Delta_{N+1}^{M3H4_N}$	$(\delta C_{N+1}^{M3H4_N}/\delta S_{N+1})$	$S_N, K_{N+1}, T_{N+1}, R_N, Q_N, \sigma_N^{CALIB^C}, BSMGreeks_N^C$	$L3H4_N$	$\Delta_{N+1}^{L3H4_N}$	$(\delta C_{N+1}^{L3H4_N}/\delta S_{N+1})$	$S_N, K_{N+1}, T_{N+1}, R_N, Q_N, \sigma_N^{CALIB^C}, BSMGreeks_N^C$
$M3H5_N$	$\Delta_{N+1}^{M3H5_N}$	$(\delta C_{N+1}^{M3H5_N}/\delta S_{N+1})$	$S_N, K_{N+1}, T_{N+1}, R_N, Q_N, HParams_N^C, \Delta_N^{HH_N}$	$L3H5_N$	$\Delta_{N+1}^{L3H5_N}$	$(\delta C_{N+1}^{L3H5_N}/\delta S_{N+1})$	$S_N, K_{N+1}, T_{N+1}, R_N, Q_N, HParams_N^C, \Delta_N^{HH_N}$
$M3H6_N$	$\Delta_{N+1}^{M3H6_N}$	$(\delta C_{N+1}^{M3H6_N}/\delta S_{N+1})$	$S_N, K_{N+1}, T_{N+1}, R_N, Q_N, HJDParams_N^C, \Delta_N^{HJDH_N}$	$L3H6_N$	$\Delta_{N+1}^{L3H6_N}$	$(\delta C_{N+1}^{L3H6_N}/\delta S_{N+1})$	$S_N, K_{N+1}, T_{N+1}, R_N, Q_N, HJDParams_N^C, \Delta_N^{HJDH_N}$
$M3H7_N$	$\Delta_{N+1}^{M3H7_N}$	$(\delta C_{N+1}^{M3H7_N}/\delta S_{N+1})$	$S_N, K_{N+1}, T_{N+1}, R_N, Q_N, FMLSParams_N^C, \Delta_N^{FMLSH_N}$	$L3H7_N$	$\Delta_{N+1}^{L3H7_N}$	$(\delta C_{N+1}^{L3H7_N}/\delta S_{N+1})$	$S_N, K_{N+1}, T_{N+1}, R_N, Q_N, FMLSParams_N^C, \Delta_N^{FMLSH_N}$
Part II							
Black-Scholes-Merton Model				**Heston Model**			
$BSMH_{N+1}$	$\Delta_{N+1}^{BSMH_{N+1}}$	-	$S_{N+1}, K_{N+1}, T_{N+1}, R_{N+1}, Q_{N+1}, \sigma_N^{CALIB^C}$	HH_{N+1}	$\Delta_{N+1}^{HH_{N+1}}$	-	$S_{N+1}, K_{N+1}, T_{N+1}, R_{N+1}, Q_{N+1}, \sigma_N^{CALIB^C}, HParams_N^C$
Heston Jump Diffusion Model				**Finite Moment Log Stable Model**			
$HJDH_{N+1}$	$\Delta_{N+1}^{HJDH_{N+1}}$	-	$S_{N+1}, K_{N+1}, T_{N+1}, R_{N+1}, Q_{N+1}, \sigma_N^{CALIB^C}, HJDParams_N^C$	$FMLSH_{N+1}$	$\Delta_{N+1}^{FMLSH_{N+1}}$	-	$S_{N+1}, K_{N+1}, T_{N+1}, R_{N+1}, Q_{N+1}, FMLSParams_N^C$
$M3H_{N+1}$ **Multi Layer Perceptron (MLP) Models**				$L3H_{N+1}$ **Long Short Term Memory (LSTM) Models**			
$M3H1_{N+1}$	$\Delta_{N+1}^{M3H1_{N+1}}$	$(\delta C_{N+1}^{M3H1_{N+1}}/\delta S_{N+1})$	$S_{N+1}, K_{N+1}, T_{N+1}, R_{N+1}, Q_{N+1}, \sigma_N^{CALIB^C}$	$L3H1_{N+1}$	$\Delta_{N+1}^{L3H1_{N+1}}$	$(\delta C_{N+1}^{L3H1_{N+1}}/\delta S_{N+1})$	$S_{N+1}, K_{N+1}, T_{N+1}, R_{N+1}, Q_{N+1}, \sigma_N^{CALIB^C}$
$M3H2_{N+1}$	$\Delta_{N+1}^{M3H2_{N+1}}$	$(\delta C_{N+1}^{M3H2_{N+1}}/\delta S_{N+1})$	$S_{N+1}, K_{N+1}, T_{N+1}, R_{N+1}, Q_{N+1}, \sigma_N^{CALIB^C}, (\delta C_N/\delta S_N)$	$L3H2_{N+1}$	$\Delta_{N+1}^{L3H2_{N+1}}$	$(\delta C_{N+1}^{L3H2_{N+1}}/\delta S_{N+1})$	$S_{N+1}, K_{N+1}, T_{N+1}, R_{N+1}, Q_{N+1}, \sigma_N^{CALIB^C}, (\delta C_N/\delta S_N)$
$M3H3_{N+1}$	$\Delta_{N+1}^{M3H3_{N+1}}$	$(\delta C_{N+1}^{M3H3_{N+1}}/\delta S_{N+1})$	$S_{N+1}, K_{N+1}, T_{N+1}, R_{N+1}, Q_{N+1}, \sigma_N^{CALIB^C}, \Delta_N^{BSMH_N}$	$L3H3_{N+1}$	$\Delta_{N+1}^{L3H3_{N+1}}$	$(\delta C_{N+1}^{L3H3_{N+1}}/\delta S_{N+1})$	$S_{N+1}, K_{N+1}, T_{N+1}, R_{N+1}, Q_{N+1}, \sigma_N^{CALIB^C}, \Delta_N^{BSMH_N}$
$M3H4_{N+1}$	$\Delta_{N+1}^{M3H4_{N+1}}$	$(\delta C_{N+1}^{M3H4_{N+1}}/\delta S_{N+1})$	$S_{N+1}, K_{N+1}, T_{N+1}, R_{N+1}, Q_{N+1}, \sigma_N^{CALIB^C}, BSMGreeks_N^C$	$L3H4_{N+1}$	$\Delta_{N+1}^{L3H4_{N+1}}$	$(\delta C_{N+1}^{L3H4_{N+1}}/\delta S_{N+1})$	$S_{N+1}, K_{N+1}, T_{N+1}, R_{N+1}, Q_{N+1}, \sigma_N^{CALIB^C}, BSMGreeks_N^C$
$M3H5_{N+1}$	$\Delta_{N+1}^{M3H5_{N+1}}$	$(\delta C_{N+1}^{M3H5_{N+1}}/\delta S_{N+1})$	$S_{N+1}, K_{N+1}, T_{N+1}, R_{N+1}, Q_{N+1}, HParams_N^C, \Delta_N^{HH_N}$	$L3H5_{N+1}$	$\Delta_{N+1}^{L3H5_{N+1}}$	$(\delta C_{N+1}^{L3H5_{N+1}}/\delta S_{N+1})$	$S_{N+1}, K_{N+1}, T_{N+1}, R_{N+1}, Q_{N+1}, HParams_N^C, \Delta_N^{HH_N}$
$M3H6_{N+1}$	$\Delta_{N+1}^{M3H6_{N+1}}$	$(\delta C_{N+1}^{M3H6_{N+1}}/\delta S_{N+1})$	$S_{N+1}, K_{N+1}, T_{N+1}, R_{N+1}, Q_{N+1}, HJDParams_N^C, \Delta_N^{HJDH_N}$	$L3H6_{N+1}$	$\Delta_{N+1}^{L3H6_{N+1}}$	$(\delta C_{N+1}^{L3H6_{N+1}}/\delta S_{N+1})$	$S_{N+1}, K_{N+1}, T_{N+1}, R_{N+1}, Q_{N+1}, HJDParams_N^C, \Delta_N^{HJDH_N}$
$M3H7_{N+1}$	$\Delta_{N+1}^{M3H7_{N+1}}$	$(\delta C_{N+1}^{M3H7_{N+1}}/\delta S_{N+1})$	$S_{N+1}, K_{N+1}, T_{N+1}, R_{N+1}, Q_{N+1}, FMLSParams_N^C, \Delta_N^{FMLSH_N}$	$L3H7_{N+1}$	$\Delta_{N+1}^{L3H7_{N+1}}$	$(\delta C_{N+1}^{L3H7_{N+1}}/\delta S_{N+1})$	$S_{N+1}, K_{N+1}, T_{N+1}, R_{N+1}, Q_{N+1}, FMLSParams_N^C, \Delta_N^{FMLSH_N}$
Part III							
Black-Scholes-Merton Model				**Heston Model**			
$BSMCH_{N+1}$	$\delta_{N+1}^{BSMCH_{N+1}}$	-	$S_{N+1}, K_{N+1}, T_{N+1}, R_{N+1}, Q_{N+1}, \sigma_N^{CALIB^C}$	HCH_{N+1}	$\delta_{N+1}^{HCH_{N+1}}$	-	$S_{N+1}, K_{N+1}, T_{N+1}, R_{N+1}, Q_{N+1}, \sigma_N^{CALIB^C}, HParams_N^C$
Heston Jump Diffusion Model				**Finite Moment Log Stable Model**			
$HJDCH_{N+1}$	$\delta_{N+1}^{HJDCH_{N+1}}$	-	$S_{N+1}, K_{N+1}, T_{N+1}, R_{N+1}, Q_{N+1}, \sigma_N^{CALIB^C}, HJDParams_N^C$	$FMLSCH_{N+1}$	$\delta_{N+1}^{FMLSCH_{N+1}}$	-	$S_{N+1}, K_{N+1}, T_{N+1}, R_{N+1}, Q_{N+1}, FMLSParams_N^C$
$M3CH_{N+1}$ **Multi Layer Perceptron (MLP) Models**				$L3CH_{N+1}$ **Long Short Term Memory (LSTM) Models**			
$M3CH1_{N+1}$	$(\delta C_{N+1}^{M3CH1_{N+1}}/\delta S_{N+1})$	$C_{N+1}^{M3CH1_{N+1}}$	$S_{N+1}, K_{N+1}, T_{N+1}, R_{N+1}, Q_{N+1}, \sigma_N^{CALIB^C}$	$L3CH1_{N+1}$	$C_{N+1}^{L3CH1_{N+1}}$	$(\delta C_{N+1}^{L3CH1_{N+1}}/\delta S_{N+1})$	$S_{N+1}, K_{N+1}, T_{N+1}, R_{N+1}, Q_{N+1}, \sigma_N^{CALIB^C}$
$M3CH2_{N+1}$	$(\delta C_{N+1}^{M3CH2_{N+1}}/\delta S_{N+1})$	$C_{N+1}^{M3CH2_{N+1}}$	$S_{N+1}, K_{N+1}, T_{N+1}, R_{N+1}, Q_{N+1}, \sigma_N^{CALIB^C}, (\delta C_N/\delta S_N)$	$L3CH2_{N+1}$	$C_{N+1}^{L3CH2_{N+1}}$	$(\delta C_{N+1}^{L3CH2_{N+1}}/\delta S_{N+1})$	$S_{N+1}, K_{N+1}, T_{N+1}, R_{N+1}, Q_{N+1}, \sigma_N^{CALIB^C}, (\delta C_N/\delta S_N)$
$M3CH3_{N+1}$	$(\delta C_{N+1}^{M3CH3_{N+1}}/\delta S_{N+1})$	$C_{N+1}^{M3CH3_{N+1}}$	$S_{N+1}, K_{N+1}, T_{N+1}, R_{N+1}, Q_{N+1}, \sigma_N^{CALIB^C}, \delta_N^{BSMCH_{N+1}}$	$L3CH3_{N+1}$	$C_{N+1}^{L3CH3_{N+1}}$	$(\delta C_{N+1}^{L3CH3_{N+1}}/\delta S_{N+1})$	$S_{N+1}, K_{N+1}, T_{N+1}, R_{N+1}, Q_{N+1}, \sigma_N^{CALIB^C}, \delta_N^{BSMCH_{N+1}}$
$M3CH4_{N+1}$	$(\delta C_{N+1}^{M3CH4_{N+1}}/\delta S_{N+1})$	$C_{N+1}^{M3CH4_{N+1}}$	$S_{N+1}, K_{N+1}, T_{N+1}, R_{N+1}, Q_{N+1}, \sigma_N^{CALIB^C}, BSMGreeks_N^C$	$L3CH4_{N+1}$	$C_{N+1}^{L3CH4_{N+1}}$	$(\delta C_{N+1}^{L3CH4_{N+1}}/\delta S_{N+1})$	$S_{N+1}, K_{N+1}, T_{N+1}, R_{N+1}, Q_{N+1}, \sigma_N^{CALIB^C}, BSMGreeks_N^C$
$M3CH5_{N+1}$	$(\delta C_{N+1}^{M3CH5_{N+1}}/\delta S_{N+1})$	$C_{N+1}^{M3CH5_{N+1}}$	$S_{N+1}, K_{N+1}, T_{N+1}, R_{N+1}, Q_{N+1}, HParams_N^C, \delta_N^{HCH_{N+1}}$	$L3CH5_{N+1}$	$C_{N+1}^{L3CH5_{N+1}}$	$(\delta C_{N+1}^{L3CH5_{N+1}}/\delta S_{N+1})$	$S_{N+1}, K_{N+1}, T_{N+1}, R_{N+1}, Q_{N+1}, HParams_N^C, \delta_N^{HCH_{N+1}}$
$M3CH6_{N+1}$	$(\delta C_{N+1}^{M3CH6_{N+1}}/\delta S_{N+1})$	$C_{N+1}^{M3CH6_{N+1}}$	$S_{N+1}, K_{N+1}, T_{N+1}, R_{N+1}, Q_{N+1}, HJDParams_N^C, \delta_N^{HJDCH_{N+1}}$	$L3CH6_{N+1}$	$C_{N+1}^{L3CH6_{N+1}}$	$(\delta C_{N+1}^{L3CH6_{N+1}}/\delta S_{N+1})$	$S_{N+1}, K_{N+1}, T_{N+1}, R_{N+1}, Q_{N+1}, HJDParams_N^C, \delta_N^{HJDCH_{N+1}}$
$M3CH7_{N+1}$	$(\delta C_{N+1}^{M3CH7_{N+1}}/\delta S_{N+1})$	$C_{N+1}^{M3CH7_{N+1}}$	$S_{N+1}, K_{N+1}, T_{N+1}, R_{N+1}, Q_{N+1}, FMLSParams_N^C, \delta_N^{FMLSCH_{N+1}}$	$L3CH7_{N+1}$	$C_{N+1}^{L3CH7_{N+1}}$	$(\delta C_{N+1}^{L3CH7_{N+1}}/\delta S_{N+1})$	$S_{N+1}, K_{N+1}, T_{N+1}, R_{N+1}, Q_{N+1}, FMLSParams_N^C, \delta_N^{FMLSCH_{N+1}}$

Table B.1.2: Model Definition for Replicating Portfolio Value Comparison: This table is compartmentalized into III parts. Column I identifies the models, column II identifies the computed variable, and column III lists the input variables used by the respective models to compute the one-trading-day-ahead forecast of the replicating portfolio value(V_{N+1}). Forecasts are made for 1,326 trading days, and there are 64 months covered in the sample using the monthly data. Each sub-section below presents the following set of models: **Part I**: This sub-section presents the models having the N subscript that use lagged input variables for forecasting the delta. The forecast variable for the MLP $M3HV_N$-Models and LSTM $L3HV_N$-Models is the delta that is directly forecasted from the respective ANN model, whereas the delta for the $BSMHV_N$, HHV_N, $HJDHV_N$ models are computed using their respective characteristic functions. The forecasted delta is later used to compute the replicating portfolio value V_{N+1} using equation 3.17. The one-trading-day-ahead forecast errors of V_{N+1} are used to compute the Root Mean Square Error (RMSE). **Part II**: This sub-section presents the models having the $N+1$ subscript that use one-trading-day-ahead input variables for forecasting the delta. The forecast variable for the MLP $M3HV_{N+1}$-Models and LSTM $L3HV_{N+1}$-Models is the delta that is directly forecasted from the respective ANN model, whereas the delta for the $BSMHV_{N+1}$, HHV_{N+1}, $HJDHV_{N+1}$ models are computed using their respective characteristic functions. The forecasted delta is later used to compute the replicating portfolio value V_{N+1} using equation 3.17. The one-trading-day-ahead forecast errors of V_{N+1} are used to compute the Root Mean Square Error (RMSE). **Part III**: This sub-section presents the models having the $N+1$ subscript that use one-trading-day-ahead input variables for forecasting the one-trading-day-ahead call option price (C_{N+1}), and later using the C_{N+1}, we analytically derive the delta ($\delta C_{N+1}/\delta S_{N+1}$) using equation 3.3, and used to compute V_{N+1} using equation 3.17. The one-trading-day-ahead forecast errors of V_{N+1} are used to compute the Root Mean Square Error (RMSE).

(I) Model	(II) Computed variable	(III) Inputs for training/forecasting	(I) Model	(II) Computed variable	(III) Inputs for training/forecasting
Part I					
Black-Scholes-Merton Model			**Heston Model**		
$BSMHV_N$	$V_{N+1}^{BSMHV_N}$	$S_{N+1}, S_N, R_{N+1}, \delta t, C_N^{BSMH_N}, C_{N+1}^{BSMH_N}, \Delta_{N+1}^{BSMH_N}$	HHV_N	$V_{N+1}^{HHV_N}$	$S_{N+1}, S_N, R_{N+1}, \delta t, C_N^{HH_N}, C_{N+1}^{HH_N}, \Delta_{N+1}^{HH_N}$
Heston Jump Diffusion Model			**Finite Moment Log Stable Model**		
$FMLSV_N$	$V_{N+1}^{FMLSV_N}$	$S_N, S_{N-1}, R_N, \delta t, C_N^{FMLS_N}, C_{N+1}^{FMLS_N}, \Delta_{N+1}^{FMLS_N}$	$HJDV_N$	$V_{N+1}^{HJDV_N}$	$S_N, S_{N-1}, R_N, \delta t, C_N^{HJD_N}, C_{N+1}^{HJD_N}, \Delta_{N+1}^{HJD_N}$
$M3H_N$ Multi Layer Perceptron (MLP) Models			**$L3H_N$ Long Short Term Memory (LSTM) Models**		
$M3H1V_N$	$V_{N+1}^{M3H1V_N}$	$S_{N+1}, S_N, R_{N+1}, \delta t, C_N^{M3H1_N}, C_{N+1}^{M3H1_N}, \Delta_{N+1}^{M3H1_N}$	$L3H1V_N$	$V_{N+1}^{L3H1V_N}$	$S_{N+1}, S_N, R_{N+1}, \delta t, C_N^{L3H1_N}, C_{N+1}^{L3H1_N}, \Delta_{N+1}^{L3H1_N}$
$M3H2V_N$	$V_{N+1}^{M3H2V_N}$	$S_{N+1}, S_N, R_{N+1}, \delta t, C_N^{M3H2_N}, C_{N+1}^{M3H2_N}, \Delta_{N+1}^{M3H2_N}$	$L3H2V_N$	$V_{N+1}^{L3H2V_N}$	$S_{N+1}, S_N, R_{N+1}, \delta t, C_N^{L3H2_N}, C_{N+1}^{L3H2_N}, \Delta_{N+1}^{L3H2_N}$
$M3H3V_N$	$V_{N+1}^{M3H3V_N}$	$S_{N+1}, S_N, R_{N+1}, \delta t, C_N^{M3H3_N}, C_{N+1}^{M3H3_N}, \Delta_{N+1}^{M3H3_N}$	$L3H3V_N$	$V_{N+1}^{L3H3V_N}$	$S_{N+1}, S_N, R_{N+1}, \delta t, C_N^{L3H3_N}, C_{N+1}^{L3H3_N}, \Delta_{N+1}^{L3H3_N}$
$M3H4V_N$	$V_{N+1}^{M3H4V_N}$	$S_{N+1}, S_N, R_{N+1}, \delta t, C_N^{M3H4_N}, C_{N+1}^{M3H4_N}, \Delta_{N+1}^{M3H4_N}$	$L3H4V_N$	$V_{N+1}^{L3H4V_N}$	$S_{N+1}, S_N, R_{N+1}, \delta t, C_N^{L3H4_N}, C_{N+1}^{L3H4_N}, \Delta_{N+1}^{L3H4_N}$
$M3H5V_N$	$V_{N+1}^{M3H5V_N}$	$S_{N+1}, S_N, R_{N+1}, \delta t, C_N^{M3H5_N}, C_{N+1}^{M3H5_N}, \Delta_{N+1}^{M3H5_N}$	$L3H5V_N$	$V_{N+1}^{L3H5V_N}$	$S_{N+1}, S_N, R_{N+1}, \delta t, C_N^{L3H5_N}, C_{N+1}^{L3H5_N}, \Delta_{N+1}^{L3H5_N}$
$M3H6V_N$	$V_{N+1}^{M3H6V_N}$	$S_{N+1}, S_N, R_{N+1}, \delta t, C_N^{M3H6_N}, C_{N+1}^{M3H6_N}, \Delta_{N+1}^{M3H6_N}$	$L3H6V_N$	$V_{N+1}^{L3H6V_N}$	$S_{N+1}, S_N, R_{N+1}, \delta t, C_N^{L3H6_N}, C_{N+1}^{L3H6_N}, \Delta_{N+1}^{L3H6_N}$
$M3H7V_N$	$V_{N+1}^{M3H7V_N}$	$S_{N+1}, S_N, R_{N+1}, \delta t, C_N^{M3H7_N}, C_{N+1}^{M3H7_N}, \Delta_{N+1}^{M3H7_N}$	$L3H7V_N$	$V_{N+1}^{L3H7V_N}$	$S_{N+1}, S_N, R_{N+1}, \delta t, C_N^{L3H7_N}, C_{N+1}^{L3H7_N}, \Delta_{N+1}^{L3H7_N}$
Part II					
Black-Scholes-Merton Model			**Heston Model**		
$BSMHV_{N+1}$	$V_{N+1}^{BSMHV_{N+1}}$	$S_{N+1}, S_N, R_{N+1}, \delta t, C_N^{BSMH_{N+1}}, C_{N+1}^{BSMH_{N+1}}, \Delta_{N+1}^{BSMH_{N+1}}$	HHV_{N+1}	$V_{N+1}^{HHV_{N+1}}$	$S_{N+1}, S_N, R_{N+1}, \delta t, C_N^{HH_{N+1}}, C_{N+1}^{HH_{N+1}}, \Delta_{N+1}^{HH_{N+1}}$
Heston Jump Diffusion Model			**Finite Moment Log Stable Model**		
$FMLSV_{N+1}$	$V_{N+1}^{FMLSV_{N+1}}$	$S_{N+1}, S_N, R_{N+1}, \delta t, C_N^{FMLS_{N+1}}, C_{N+1}^{FMLS_{N+1}}, \Delta_{N+1}^{FMLS_{N+1}}$	$HJDV_{N+1}$	$V_{N+1}^{HJDV_{N+1}}$	$S_{N+1}, S_N, R_{N+1}, \delta t, C_N^{HJD_{N+1}}, C_{N+1}^{HJD_{N+1}}, \Delta_{N+1}^{HJD_{N+1}}$
$M3H_{N+1}$ Multi Layer Perceptron (MLP) Models			**$L3H_{N+1}$ Long Short Term Memory (LSTM) Models**		
$M3H1V_{N+1}$	$V_{N+1}^{M3H1V_{N+1}}$	$S_{N+1}, S_N, R_{N+1}, \delta t, C_N^{M3H1_{N+1}}, C_{N+1}^{M3H1_{N+1}}, \Delta_{N+1}^{M3H1_{N+1}}$	$L3H1V_{N+1}$	$V_{N+1}^{L3H1V_{N+1}}$	$S_{N+1}, S_N, R_{N+1}, \delta t, C_N^{L3H1_{N+1}}, C_{N+1}^{L3H1_{N+1}}, \Delta_{N+1}^{L3H1_{N+1}}$
$M3H2V_{N+1}$	$V_{N+1}^{M3H2V_{N+1}}$	$S_{N+1}, S_N, R_{N+1}, \delta t, C_N^{M3H2_{N+1}}, C_{N+1}^{M3H2_{N+1}}, \Delta_{N+1}^{M3H2_{N+1}}$	$L3H2V_{N+1}$	$V_{N+1}^{L3H2V_{N+1}}$	$S_{N+1}, S_N, R_{N+1}, \delta t, C_N^{L3H2_{N+1}}, C_{N+1}^{L3H2_{N+1}}, \Delta_{N+1}^{L3H2_{N+1}}$
$M3H3V_{N+1}$	$V_{N+1}^{M3H3V_{N+1}}$	$S_{N+1}, S_N, R_{N+1}, \delta t, C_N^{M3H3_{N+1}}, C_{N+1}^{M3H3_{N+1}}, \Delta_{N+1}^{M3H3_{N+1}}$	$L3H3V_{N+1}$	$V_{N+1}^{L3H3V_{N+1}}$	$S_{N+1}, S_N, R_{N+1}, \delta t, C_N^{L3H3_{N+1}}, C_{N+1}^{L3H3_{N+1}}, \Delta_{N+1}^{L3H3_{N+1}}$
$M3H4V_{N+1}$	$V_{N+1}^{M3H4V_{N+1}}$	$S_{N+1}, S_N, R_{N+1}, \delta t, C_N^{M3H4_{N+1}}, C_{N+1}^{M3H4_{N+1}}, \Delta_{N+1}^{M3H4_{N+1}}$	$L3H4V_{N+1}$	$V_{N+1}^{L3H4V_{N+1}}$	$S_{N+1}, S_N, R_{N+1}, \delta t, C_N^{L3H4_{N+1}}, C_{N+1}^{L3H4_{N+1}}, \Delta_{N+1}^{L3H4_{N+1}}$
$M3H5V_{N+1}$	$V_{N+1}^{M3H5V_{N+1}}$	$S_{N+1}, S_N, R_{N+1}, \delta t, C_N^{M3H5_{N+1}}, C_{N+1}^{M3H5_{N+1}}, \Delta_{N+1}^{M3H5_{N+1}}$	$L3H5V_{N+1}$	$V_{N+1}^{L3H5V_{N+1}}$	$S_{N+1}, S_N, R_{N+1}, \delta t, C_N^{L3H5_{N+1}}, C_{N+1}^{L3H5_{N+1}}, \Delta_{N+1}^{L3H5_{N+1}}$
$M3H6V_{N+1}$	$V_{N+1}^{M3H6V_{N+1}}$	$S_{N+1}, S_N, R_{N+1}, \delta t, C_N^{M3H6_{N+1}}, C_{N+1}^{M3H6_{N+1}}, \Delta_{N+1}^{M3H6_{N+1}}$	$L3H6V_{N+1}$	$V_{N+1}^{L3H6V_{N+1}}$	$S_{N+1}, S_N, R_{N+1}, \delta t, C_N^{L3H6_{N+1}}, C_{N+1}^{L3H6_{N+1}}, \Delta_{N+1}^{L3H6_{N+1}}$
$M3H7V_{N+1}$	$V_{N+1}^{M3H7V_{N+1}}$	$S_{N+1}, S_N, R_{N+1}, \delta t, C_N^{M3H7_{N+1}}, C_{N+1}^{M3H7_{N+1}}, \Delta_{N+1}^{M3H7_{N+1}}$	$L3H7V_{N+1}$	$V_{N+1}^{L3H7V_{N+1}}$	$S_{N+1}, S_N, R_{N+1}, \delta t, C_N^{L3H7_{N+1}}, C_{N+1}^{L3H7_{N+1}}, \Delta_{N+1}^{L3H7_{N+1}}$
Part III					
Black-Scholes-Merton Model			**Heston Model**		
$BSMCHV_{N+1}$	$V_{N+1}^{BSMCHV_{N+1}}$	$S_{N+1}, S_N, R_{N+1}, \delta t, C_N^{BSMCH_{N+1}}, C_{N+1}^{BSMCH_{N+1}}, \delta_{N+1}^{BSMCH_{N+1}}$	$HCHV_{N+1}$	$V_{N+1}^{HCHV_{N+1}}$	$S_{N+1}, S_N, R_{N+1}, \delta t, C_N^{HCH_{N+1}}, C_{N+1}^{HCH_{N+1}}, \delta_{N+1}^{HCH_{N+1}}$
Heston Jump Diffusion Model			**Finite Moment Log Stable Model**		
$FMLSCHV_{N+1}$	$V_{N+1}^{FMLSCHV_{N+1}}$	$S_{N+1}, S_N, R_{N+1}, \delta t, C_N^{FMLSCH_{N+1}}, C_{N+1}^{FMLSCH_{N+1}}, \delta_{N+1}^{FMLSCH_{N+1}}$	$HJDCHV_{N+1}$	$V_{N+1}^{HJDCHV_{N+1}}$	$S_{N+1}, S_N, R_{N+1}, \delta t, C_N^{HJDCH_{N+1}}, C_{N+1}^{HJDCH_{N+1}}, \delta_{N+1}^{HJDCH_{N+1}}$
$M3CH_{N+1}$ Multi Layer Perceptron (MLP) Models			**$L3CH_{N+1}$ Long Short Term Memory (LSTM) Models**		
$M3CH1V_{N+1}$	$V_{N+1}^{M3CH1V_{N+1}}$	$S_{N+1}, S_N, R_{N+1}, \delta t, C_N^{M3CH1_{N+1}}, C_{N+1}^{M3CH1_{N+1}}, \delta_{N+1}^{M3CH1_{N+1}}$	$L3CH1V_{N+1}$	$V_{N+1}^{L3CH1V_{N+1}}$	$S_{N+1}, S_N, R_{N+1}, \delta t, C_N^{L3CH1_{N+1}}, C_{N+1}^{L3CH1_{N+1}}, \delta_{N+1}^{L3CH1_{N+1}}$
$M3CH2V_{N+1}$	$V_{N+1}^{M3CH2V_{N+1}}$	$S_{N+1}, S_N, R_{N+1}, \delta t, C_N^{M3CH2_{N+1}}, C_{N+1}^{M3CH2_{N+1}}, \delta_{N+1}^{M3CH2_{N+1}}$	$L3CH2V_{N+1}$	$V_{N+1}^{L3CH2V_{N+1}}$	$S_{N+1}, S_N, R_{N+1}, \delta t, C_N^{L3CH2_{N+1}}, C_{N+1}^{L3CH2_{N+1}}, \delta_{N+1}^{L3CH2_{N+1}}$
$M3CH3V_{N+1}$	$V_{N+1}^{M3CH3V_{N+1}}$	$S_{N+1}, S_N, R_{N+1}, \delta t, C_N^{M3CH3_{N+1}}, C_{N+1}^{M3CH3_{N+1}}, \delta_{N+1}^{M3CH3_{N+1}}$	$L3CH3V_{N+1}$	$V_{N+1}^{L3CH3V_{N+1}}$	$S_{N+1}, S_N, R_{N+1}, \delta t, C_N^{L3CH3_{N+1}}, C_{N+1}^{L3CH3_{N+1}}, \delta_{N+1}^{L3CH3_{N+1}}$
$M3CH4V_{N+1}$	$V_{N+1}^{M3CH4V_{N+1}}$	$S_{N+1}, S_N, R_{N+1}, \delta t, C_N^{M3CH4_{N+1}}, C_{N+1}^{M3CH4_{N+1}}, \delta_{N+1}^{M3CH4_{N+1}}$	$L3CH4V_{N+1}$	$V_{N+1}^{L3CH4V_{N+1}}$	$S_{N+1}, S_N, R_{N+1}, \delta t, C_N^{L3CH4_{N+1}}, C_{N+1}^{L3CH4_{N+1}}, \delta_{N+1}^{L3CH4_{N+1}}$
$M3CH5V_{N+1}$	$V_{N+1}^{M3CH5V_{N+1}}$	$S_{N+1}, S_N, R_{N+1}, \delta t, C_N^{M3CH5_{N+1}}, C_{N+1}^{M3CH5_{N+1}}, \delta_{N+1}^{M3CH5_{N+1}}$	$L3CH5V_{N+1}$	$V_{N+1}^{L3CH5V_{N+1}}$	$S_{N+1}, S_N, R_{N+1}, \delta t, C_N^{L3CH5_{N+1}}, C_{N+1}^{L3CH5_{N+1}}, \delta_{N+1}^{L3CH5_{N+1}}$
$M3CH6V_{N+1}$	$V_{N+1}^{M3CH6V_{N+1}}$	$S_{N+1}, S_N, R_{N+1}, \delta t, C_N^{M3CH6_{N+1}}, C_{N+1}^{M3CH6_{N+1}}, \delta_{N+1}^{M3CH6_{N+1}}$	$L3CH6V_{N+1}$	$V_{N+1}^{L3CH6V_{N+1}}$	$S_{N+1}, S_N, R_{N+1}, \delta t, C_N^{L3CH6_{N+1}}, C_{N+1}^{L3CH6_{N+1}}, \delta_{N+1}^{L3CH6_{N+1}}$
$M3CH7V_{N+1}$	$V_{N+1}^{M3CH7V_{N+1}}$	$S_{N+1}, S_N, R_{N+1}, \delta t, C_N^{M3CH7_{N+1}}, C_{N+1}^{M3CH7_{N+1}}, \delta_{N+1}^{M3CH7_{N+1}}$	$L3CH7V_{N+1}$	$V_{N+1}^{L3CH7V_{N+1}}$	$S_{N+1}, S_N, R_{N+1}, \delta t, C_N^{L3CH7_{N+1}}, C_{N+1}^{L3CH7_{N+1}}, \delta_{N+1}^{L3CH7_{N+1}}$

Table B.1.3: This table presents the overall comparison of out-of-sample root mean square error ($RMSE$) amongst the MLP $M3H_N$-Models ($M3H1_N$ to $M3H7_N$), LSTM $L3H_N$-Models ($L3H1_N$ to $L3H7_N$), Black-Scholes-Merton ($BSMH_N$) model, Heston (HH_N) model, Heston Jump Diffusion ($HJDH_N$) model and the Finite Moment Log Stable ($FMLSH_N$) model. The forecast variable for the MLP $M3H_N$-Models and LSTM $L3H_N$-Models is the delta that is directly forecasted from the respective ANN model, whereas the delta for the $BSMH_N$, HH_N, $HJDH_N$ models are computed using their respective characteristic functions. The models denoted by the $_N$ subscript use lagged input variables for forecasting the delta. The one-trading-day-ahead forecast errors of the delta are used to compute the Root Mean Square Error (RMSE). Forecasts are made for 1,326 trading days.

(I) **Size**	**(II)** **Mean of** δ_N	**(III)** **Std.Dev. of** δ_N	**(IV)** $BSMH_N$	**(V)** HH_N	**(VI)** $HJDH_N$	**(VII)** $FMLSH_N$	**(VIII)** $M1H1_N$	**(IX)** $M1H2_N$	**(X)** $M1H3_N$	**(XI)** $M1H4_N$	**(XII)** $M1H5_N$	**(XIII)** $M1H6_N$	**(XIV)** $M1H7_N$	**(XV)** $L1H1_N$	**(XVI)** $L1H2_N$	**(XVII)** $L1H3_N$	**(XVIII)** $L1H4_N$	**(XIX)** $L1H5_N$	**(XX)** $L1H6_N$	**(XXI)** $L1H7_N$
543255	0.49962	0.37312	**0.2494**	0.25598	0.25937	0.2614	0.26121	0.27071	0.27368	0.29036	0.28967	0.29395	0.27452	0.31418	0.30771	0.31361	0.27235	0.30855	0.31142	0.30812

Table B.1.4: Overall Delta Comparison (amongst Parametric, $M3H_{N+1}$-Models and $L3H_{N+1}$-Models): This table presents the overall comparison of out-of-sample root mean square error ($RMSE$) amongst the MLP $M3H_{N+1}$-Models ($M3H1_{N+1}$ to $M3H7_{N+1}$), LSTM $L3H_{N+1}$-Models ($L3H1_{N+1}$ to $L3H7_{N+1}$), Black-Scholes-Merton ($BSMH_{N+1}$) model, Heston (HH_{N+1}) model, Heston Jump Diffusion ($HJDH_{N+1}$) model and the Finite Moment Log Stable ($FMLSH_{N+1}$) model. The forecast variable for the MLP $M3H_{N+1}$-Models and LSTM $L3H_{N+1}$-Models is the delta that is directly forecasted from the respective ANN model, whereas the delta for the $BSMH_{N+1}$, HH_{N+1}, $HJDH_{N+1}$ models are computed using their respective characteristic functions. The models denoted by the $_{N+1}$ subscript use one-trading-day-ahead input variables for forecasting the delta. The one-trading-day-ahead forecast errors of the delta are used to compute the Root Mean Square Error (RMSE). Forecasts are made for 1,326 trading days.

(I) **Size**	**(II)** **Mean of** δ_N	**(III)** **Std.Dev. of** δ_N	**(IV)** $BSMH_{N+1}$	**(V)** HH_{N+1}	**(VI)** $HJDH_{N+1}$	**(VII)** $FMLSH_{N+1}$	**(VIII)** $M1H1_{N+1}$	**(IX)** $M1H2_{N+1}$	**(X)** $M1H3_{N+1}$	**(XI)** $M1H4_{N+1}$	**(XII)** $M1H5_{N+1}$	**(XIII)** $M1H6_{N+1}$	**(XIV)** $M1H7_{N+1}$	**(XV)** $L1H1_{N+1}$	**(XVI)** $L1H2_{N+1}$	**(XVII)** $L1H3_{N+1}$	**(XVIII)** $L1H4_{N+1}$	**(XIX)** $L1H5_{N+1}$	**(XX)** $L1H6_{N+1}$	**(XXI)** $L1H7_{N+1}$
543255	0.49962	0.37312	**0.2474**	0.25414	0.25746	0.25935	0.64811	0.31258	0.96403	0.82149	0.36591	0.32038	0.42534	0.31331	0.3069	0.31265	0.27201	0.30768	0.31034	0.30712

Table B.1.5: Overall Delta Comparison (amongst Parametric, $M3CH_{N+1}$-Models and $L3CH_{N+1}$-Models): This table presents the overall comparison of out-of-sample root mean square error ($RMSE$) amongst the MLP $M3CH_{N+1}$-Models ($M3CH1_{N+1}$ to $M3CH7_{N+1}$), LSTM $L3CH_{N+1}$-Models ($L3CH1_{N+1}$ to $L3CH7_{N+1}$), Black-Scholes-Merton ($BSMCH_{N+1}$) model, Heston (HCH_{N+1}) model, Heston Jump Diffusion ($HJDCH_{N+1}$) model and the Finite Moment Log Stable ($FMLSCH_{N+1}$) model. The forecast variable for all the models is the call option price (C_{N+1}). The models denoted by the $_{N+1}$ subscript use one-trading-day-ahead input variables. The delta ($\delta C_{N+1}/\delta S_{N+1}$) is then derived analytically from the forecasted call option price (C_{N+1}) using equation 3.3. The one-trading-day-ahead forecast errors of the delta are used to compute the Root Mean Square Error (RMSE). Forecasts are made for 1,326 trading days.

(I) **Size**	**(II)** **Mean of** δ_N	**(III)** **Std.Dev. of** δ_N	**(IV)** $BSMCH_{N+1}$	**(V)** HCH_{N+1}	**(VI)** $HJDCH_{N+1}$	**(VII)** $FMLSCH_{N+1}$	**(VIII)** $M1CH1_{N+1}$	**(IX)** $M1CH2_{N+1}$	**(X)** $M1CH3_{N+1}$	**(XI)** $M1CH4_{N+1}$	**(XII)** $M1CH5_{N+1}$	**(XIII)** $M1CH6_{N+1}$	**(XIV)** $M1CH7_{N+1}$	**(XV)** $L1CH1_{N+1}$	**(XVI)** $L1CH2_{N+1}$	**(XVII)** $L1CH3_{N+1}$	**(XVIII)** $L1CH4_{N+1}$	**(XIX)** $L1CH5_{N+1}$	**(XX)** $L1CH6_{N+1}$	**(XXI)** $L1CH7_{N+1}$
542456	0.49986	0.37301	41.747	9.8384	8.0976	13.6301	7.7184	7.8624	8.5897	8.6353	**6.8567**	9.216	8.2547	87.6469	63.1143	333.702	30.6275	65.2476	57.3935	59.4208

Table B.1.6: Overall Replicating Portfolio Value Comparison (amongst Parametric, $M3HV_N$-Models and $L3HV_N$-Models): This table presents the overall comparison of out-of-sample root mean square error ($RMSE$) amongst the MLP $M3HV_N$-Models ($M3HV1_N$ to $M3HV7_N$), LSTM $L3HV_N$-Models ($L3HV1_N$ to $L3HV7_N$), Black-Scholes-Merton ($BSMHV_N$) model, Heston (HHV_N) model, Heston Jump Diffusion ($HJDHV_N$) model and the Finite Moment Log Stable ($FMLSHV_N$) model. The forecast variable for the MLP $M3HV_N$-Models and LSTM $L3HV_N$-Models is the delta that is directly forecasted from the respective ANN model, whereas the delta for the $BSMHV_N$, HHV_N, $HJDHV_N$ models are computed using their respective characteristic functions. The models denoted by the $_N$ subscript use lagged input variables for forecasting the delta. The forecasted delta is later used to compute the replicating portfolio value V_{N+1} using equation 3.17. The one-trading-day-ahead forecast errors of V_{N+1} are used to compute the Root Mean Square Error (RMSE). Forecasts are made for 1,326 trading days.

(I) **Size**	**(II)** **Mean of** V_N	**(III)** **Std.Dev. of** V_N	**(IV)** $BSMHV_N$	**(V)** HHV_N	**(VI)** $HJDHV_N$	**(VII)** $FMLSHV_N$	**(VIII)** $M1HV1_N$	**(IX)** $M1HV2_N$	**(X)** $M1HV3_N$	**(XI)** $M1HV4_N$	**(XII)** $M1HV5_N$	**(XIII)** $M1HV6_N$	**(XIV)** $M1HV7_N$	**(XV)** $L1HV1_N$	**(XVI)** $L1HV2_N$	**(XVII)** $L1HV3_N$	**(XVIII)** $L1HV4_N$	**(XIX)** $L1HV5_N$	**(XX)** $L1HV6_N$	**(XXI)** $L1HV7_N$
543255	0.32637	3.5141	3.6292	3.7628	3.8124	3.8517	**3.5073**	3.634	3.6042	3.6073	3.5684	3.5641	3.5703	4.4059	4.2652	4.3184	3.77	4.2146	4.2344	4.2018

Table B.1.7: Overall Replicating Portfolio Value Comparison (amongst Parametric, $M3HV_{N+1}$-Models and $L3HV_{N+1}$-Models): This table presents the overall comparison of out-of-sample root mean square error ($RMSE$) amongst the MLP $M3HV_{N+1}$-Models ($M3HV1_{N+1}$ to $M3HV7_{N+1}$), LSTM $L3HV_{N+1}$-Models ($L3HV1_{N+1}$ to $L3HV7_{N+1}$), Black-Scholes-Merton ($BSMHV_{N+1}$) model, Heston (HHV_{N+1}) model, Heston Jump Diffusion ($HJDHV_{N+1}$) model and the Finite Moment Log Stable ($FMLSHV_{N+1}$) model. The forecast variable for the MLP $M3HV_{N+1}$-Models and LSTM $L3HV_{N+1}$-Models is the delta that is directly forecasted from the respective ANN model, whereas the delta for the $BSMHV_{N+1}$, HHV_{N+1}, $HJDHV_{N+1}$ models are computed using their respective characteristic functions. The models denoted by the $_{N+1}$ subscript use one-trading-day-ahead input variables for forecasting the delta. The forecasted delta is later used to compute the replicating portfolio value V_{N+1} using equation 3.17. The one-trading-day-ahead forecast errors of V_{N+1} are used to compute the Root Mean Square Error (RMSE). Forecasts are made for 1,326 trading days.

(I) **Size**	**(II)** **Mean of** V_N	**(III)** **Std.Dev. of** V_N	**(IV)** $BSMHV_{N+1}$	**(V)** HHV_{N+1}	**(VI)** $HJDHV_{N+1}$	**(VII)** $FMLSHV_{N+1}$	**(VIII)** $M1HV1_{N+1}$	**(IX)** $M1HV2_{N+1}$	**(X)** $M1HV3_{N+1}$	**(XI)** $M1HV4_{N+1}$	**(XII)** $M1HV5_{N+1}$	**(XIII)** $M1HV6_{N+1}$	**(XIV)** $M1HV7_{N+1}$	**(XV)** $L1HV1_{N+1}$	**(XVI)** $L1HV2_{N+1}$	**(XVII)** $L1HV3_{N+1}$	**(XVIII)** $L1HV4_{N+1}$	**(XIX)** $L1HV5_{N+1}$	**(XX)** $L1HV6_{N+1}$	**(XXI)** $L1HV7_{N+1}$
543255	0.32637	3.5141	**0.2474**	0.25414	0.25746	0.25935	0.64811	0.31258	0.96403	0.82149	0.36591	0.32038	0.42534	0.31331	0.3069	0.31265	0.27201	0.30768	0.31034	0.30712

Table B.1.8: Overall Replicating Portfolio Value Comparison (amongst Parametric, $M3CHV_{N+1}$-Models and $L3CHV_{N+1}$-Models): This table presents the overall comparison of out-of-sample root mean square error ($RMSE$) amongst the MLP $M3CHV_{N+1}$-Models ($M3CHV1_{N+1}$ to $M3CHV7_{N+1}$), LSTM $L3CHV_{N+1}$-Models ($L3CHV1_{N+1}$ to $L3CHV7_{N+1}$), Black-Scholes-Merton ($BSMCHV_{N+1}$) model, Heston ($HCHV_{N+1}$) model, Heston Jump Diffusion ($HJDCHV_{N+1}$) model and the Finite Moment Log Stable ($FMLSCHV_{N+1}$) model. The forecast variable for all the models is the call option price (C_{N+1}). The models denoted by the $_{N+1}$ subscript use one-trading-day-ahead input variables for forecasting the call option price. The delta ($\delta C_{N+1}/\delta S_{N+1}$) is derived analytically from the forecasted call option price (C_{N+1}) using equation 3.3 and then used to compute the replicating portfolio value V_{N+1} using equation 3.17. The one-trading-day-ahead forecast errors of V_{N+1} are used to compute the Root Mean Square Error (RMSE).

(I) **Size**	**(II)** **Mean of** V_N	**(III)** **Std.Dev. of** V_N	**(IV)** $BSMCHV_{N+1}$	**(V)** $HCHV_{N+1}$	**(VI)** $HJDCHV_{N+1}$	**(VII)** $FMLSCHV_{N+1}$	**(VIII)** $M1CHV1_{N+1}$	**(IX)** $M1CHV2_{N+1}$	**(X)** $M1CHV3_{N+1}$	**(XI)** $M1CHV4_{N+1}$	**(XII)** $M1CHV5_{N+1}$	**(XIII)** $M1CHV6_{N+1}$	**(XIV)** $M1CHV7_{N+1}$	**(XV)** $L1CHV1_{N+1}$	**(XVI)** $L1CHV2_{N+1}$	**(XVII)** $L1CHV3_{N+1}$	**(XVIII)** $L1CHV4_{N+1}$	**(XIX)** $L1CHV5_{N+1}$	**(XX)** $L1CHV6_{N+1}$	**(XXI)** $L1CHV7_{N+1}$
543255	0.32637	3.5141	826.11	207.0706	164.5071	232.8291	156.9775	159.5832	189.3558	147.0468	**132.6154**	192.4877	164.7324	1427.6376	1113.023	7027.106	459.8463	1189.366	1148.76	1142.848

Table B.1.9: Diebold-Mariano(DM) test-based insignificant pairs: This table presents the insignificant pairs for $H-Models$, $CH-Models$, $HV-Models$, and $CHV-Models$. The complete table consisting of the DM test statistic for $H-Models$, which use lagged input variables to forecast the $Delta_{N+1}$ can be found in Table 39, for $H-Models$ which use one-trading-day-ahead input variables to forecast the Δ_{N+1} in Table 40, for $CH-Models$ that use one-trading-day-ahead input variables to forecast the δ_{N+1} in Table 41, for $HV-Models$ which use delta from $H-Models$ (using lagged inputs for forecasting) in Table 42, for $HV-Models$ which use delta from $H-Models$ (using one-trading-day-ahead inputs for forecasting) in Table 43, and $CHV-Models$ which use delta from $CH-Models$ in Table 44 of the Electronic Appendix.

Model	Insignificant Pairs
For $H-Models$ (using lagged inputs)	None
For $H-Models$ (using one-trading-day-ahead inputs)	$(M3H2_{N+1}, L3H1_{N+1})$, $(M3H2_{N+1}, L3H3_{N+1})$, $(M3H2_{N+1}, L3H6_{N+1})$, $(L3H2_{N+1}, L3H7_{N+1})$
For $CH-Models$ (using one-trading-day-ahead inputs)	$(M3CH3_{N+1}, M3CH4_{N+1})$, $(M3CH4_{N+1}, M3CH6_{N+1})$, $(M3CH4_{N+1}, M3CH7_{N+1})$, and $(HJDCH_{N+1}, M3CH7_{N+1})$
For $HV-Models$ computed from the Δ_{N+1} obtained from $H-Models$ that uses lagged input variables for forecasting	$(BSMHV_N, M3HV2_N)$, $(M3HV3_N, M3HV4_N)$, $(M3HV5_N, M3HV6_N)$, $(M3HV5_N, M3HV7_N)$, $(M3HV6_N, M3HV7_N)$, and $(HHV_N, L3HV4N_N)$
For $HV-Models$ computed from the Δ_{N+1} obtained from $H-Models$ that uses one-trading-day input variables for forecasting	None
For $CHV-Models$ computed from the δ_{N+1} obtained from $CH-Models$ that uses one-trading-day input variables for forecasting	$(M3CHV1_{N+1}, M3CHV2_{N+1})$, $(M3CHV3_{N+1}, M3CHV6_{N+1})$, $(HJDCHV_{N+1}, M3CHV7_{N+1})$, and $(L3CHV6_{N+1}, L3CHV7_{N+1})$

Table B.1.10: This table presents the summary of the pair-wise bootstrap tests performed for $H-Models$, $CH-Models$, $HV-Models$, and $CHV-Models$. The complete table consisting of the results for the pair-wise bootstrap for $H-Models$, which use lagged input variables to forecast the Δ_{N+1} can be found in Table 45, for $H-Models$ which use one-trading-day-ahead input variables to forecast the Δ_{N+1} in Table 46, for $CH-Models$ that use one-trading-day-ahead input variables to forecast the δ_{N+1} in Table 47, for $HV-Models$ which use delta from $H-Models$ (using lagged inputs for forecasting) in Table 48, for $HV-Models$ which use delta from $H-Models$ (using one-trading-day-ahead inputs for forecasting) in Table 49, and $CHV-Models$ which use delta from $CH-Models$ in Table 50 of the Electronic Appendix.

Model	Number of pairs a model wins	Winning %
$H-Models$ (using lagged inputs)		
$M3H_N$-Models	72	47.1%
Parametric	58	37.9%
$L3H_N$-Models	23	15.0%
$H-Models$(using one-trading-day-ahead inputs)		
$M3H_{N+1}$-Models	60	39.2%
Parametric	61	39.9%
$L3H_{N+1}$-Models	32	20.9%
$CH-Models$ (using one-trading-day-ahead inputs)		
$M3CH_{N+1}$-Models	96	62.7%
Parametric	35	22.9%
$L3CH_{N+1}$-Models	22	14.4%
$HV-Models$ (computed from the Δ_{N+1} obtained from $H-Models$ that use lagged input variables for forecasting)		
$M3HV_N$-Models	72	47.1%
Parametric	58	37.9%
$L3HV_N$-Models	23	15.0%
$HV-Models$ (computed from the Δ_{N+1} obtained from $H-Models$ that use one-trading-day-ahead input variables for forecasting		
$M3HV_{N+1}$-Models	60	39.2%
Parametric	61	39.9%
$L3HV_{N+1}$-Models	32	20.9%
$CHV-Models$ (computed from the δ_{N+1} obtained from $CH-Models$ that use one-trading-day-ahead input variables for forecasting)		
$M3CHV_{N+1}$-Models	96	62.7%
Parametric	35	22.9%
$L3CHV_{N+1}$-Models	22	14.4%

Table B.1.11: Table of variables for Chapter 3

Symbol	Name	Description
C_t	Call price	Call price calculated by taking the average of the bid and ask call price from OptionMetrics
S_t	S&P500 Index Price	S&P500 Index Price from OptionMetrics
K_t	Exercise price	Option exercise price from OptionMetrics
T_t	Time to Maturity	Time to maturity calculated from option expiry date from OptionMetrics
R_t	Risk-free interest rate	The interpolated interest rate using zero interest curves from OptionMetrics
Q_t	Dividend Yield	S&P500 Index dividend yield from OptionMetrics
S_t/K_t	Moneyness	Moneyness is defined as the ratio of the S&P Index price and the option strike price
σ_t^B	Volatility	Black-Scholes-Merton implied volatility
δ_t^B	Delta	Black-Scholes-Merton Delta.
γ_t^B	Gamma	Black-Scholes-Merton Gamma.
θ_t^B	Theta	Black-Scholes-Merton Theta.
ρ_t^B	Rho	Black-Scholes-Merton Rho.
ν_t^B	Vega	Black-Scholes-Merton Vega.
$V_{0,t}^H$	Initial variance	Initial variance in the Heston model
θ_t^H	Long term variance	Long term variance in the Heston model
κ_t^H	Mean reversion speed	Mean reversion speed in the Heston model
σ_t^H	Volatility	Volatility of variance in the Heston model
ρ_t^H	Correlation	Correlation parameter in the Heston model
$V_{0,t}^{HJD}$	Initial variance	Initial variance in the Heston Jump Diffusion model
θ_t^{HJD}	Long term variance	Long term variance in the Heston Jump Diffusion model
κ_t^{HJD}	Mean reversion speed	Mean reversion speed in the Heston Jump Diffusion model
σ_t^{HJD}	Volatility	Volatility of variance in the Heston Jump Diffusion model
ρ_t^{HJD}	Correlation	Correlation parameter in the Heston Jump Diffusion model
σ_t^{HJD}	Jump Volatility	Jump volatility parameter in the Heston Jump Diffusion model
μ_t^{HJD}	Jump Mean	Jump mean parameter in the Heston Jump Diffusion model
λ_t^{HJD}	Jump Frequency	Jump frequency parameter in the Heston Jump Diffusion model
α_t^{FMLS}	Tail Parameter	Tail parameter in the Finite Moment Log Stable model
σ_t^{FMLS}	Dispersion Parameter	Dispersion parameter in the Finite Moment Log Stable model
$BGreeks_t$	BSM greeks	Black-Scholes-Merton greeks ($\delta_t^B, \gamma_t^B, \rho_t^B, \theta_t^B, \nu_t^B$)
$HParams_t$	Heston parameters	Heston model parameters (κ_t^H , σ_t^H, θ_t^H, ρ_t^H, $V_{0,t}^H$)
$HJDParams_t$	Heston Jump Diffusion parameters	Heston Jump Diffusion model parameters (κ_t^{HJD} , σ_t^{HJD}, θ_t^{HJD}, ρ_t^{HJD}, $V_{0,t}^{HJD}$, σ_t^{HJD},μ_t^{HJD},λ_t^{HJD})
$FMLSParams_t$	Finite Moment Log Stable parameters	FMLS model parameters (α_t^{FMLS} , σ_t^{FMLS})

Table B.1.12: Month-wise statistics of the S&P 500 Index call options delta used in Chapter 3

Month	**Number of Observations**	**Mean**	**Variance**
September 2012	1975	0.406	0.104
October 2012	7010	0.474	0.154
November 2012	6716	0.416	0.142
December 2012	6425	0.438	0.130
January 2013	6387	0.480	0.167
February 2013	6187	0.434	0.126
March 2013	6637	0.484	0.126
April 2013	7625	0.494	0.126
May 2013	8034	0.568	0.129
June 2013	7677	0.476	0.115
July 2013	8468	0.446	0.141
August 2013	8177	0.502	0.129
September 2013	7286	0.483	0.132
October 2013	7769	0.437	0.133
November 2013	6741	0.560	0.139
December 2013	7176	0.491	0.138
January 2014	7505	0.542	0.142
February 2014	7213	0.510	0.155
March 2014	8048	0.462	0.141
April 2014	7909	0.494	0.127
May 2014	7626	0.542	0.132
June 2014	7396	0.623	0.141
July 2014	8092	0.492	0.121
August 2014	8195	0.502	0.144
September 2014	7943	0.487	0.134
October 2014	8955	0.437	0.131
November 2014	6917	0.480	0.158
December 2014	8268	0.526	0.146
January 2015	8429	0.470	0.114
February 2015	8381	0.533	0.143
March 2015	10037	0.541	0.129
April 2015	9216	0.522	0.132
May 2015	8892	0.536	0.132
June 2015	9982	0.482	0.122
July 2015	9610	0.522	0.145
August 2015	9089	0.492	0.109
September 2015	10643	0.429	0.118
October 2015	9396	0.445	0.131
November 2015	8381	0.494	0.129
December 2015	8920	0.534	0.118
January 2016	8008	0.403	0.117
February 2016	9246	0.504	0.123
March 2016	9783	0.486	0.138
April 2016	9217	0.497	0.135
May 2016	9619	0.498	0.156
June 2016	9722	0.501	0.130
July 2016	8864	0.566	0.152
August 2016	10459	0.552	0.145
September 2016	9374	0.518	0.140
October 2016	9111	0.505	0.153
November 2016	9345	0.490	0.143
December 2016	9673	0.527	0.144
January 2017	9282	0.515	0.147
February 2017	8141	0.520	0.141
March 2017	10758	0.571	0.155
April 2017	9078	0.527	0.142
May 2017	10219	0.466	0.151
June 2017	10373	0.473	0.145
July 2017	9899	0.493	0.156
August 2017	10704	0.487	0.153
September 2017	9241	0.495	0.138
October 2017	9895	0.523	0.136
November 2017	9630	0.539	0.163
December 2017	8281	0.503	0.145

Table B.1.13: Month-wise statistics of the S&P 500 Index call options delta used in Chapter 3

Month	**Number of Observations**	**Average Call Price**	**Bid-Ask spread**
September 2012	1,975	$76.89	$1.46
October 2012	7,010	$71.52	$1.25
November 2012	6,716	$66.67	$0.78
December 2012	6,425	$70.79	$0.81
January 2013	6,387	$79.55	$0.87
February 2013	6,187	$81.37	$0.91
March 2013	6,637	$83.69	$0.95
April 2013	7,625	$83.11	$1.08
May 2013	8,034	$87.16	$1.02
June 2013	7,677	$84.54	$1.01
July 2013	8,468	$87.70	$1.13
August 2013	8,177	$85.66	$1.04
September 2013	7,286	$88.26	$1.00
October 2013	7,769	$92.46	$1.03
November 2013	6,741	$98.83	$1.05
December 2013	7,176	$96.65	$0.98
January 2014	7,505	$98.04	$0.99
February 2014	7,213	$95.37	$1.04
March 2014	8,048	$102.83	$1.08
April 2014	7,909	$100.98	$1.14
May 2014	7,626	$106.56	$1.06
June 2014	7,396	$113.06	$1.14
July 2014	8,092	$116.21	$1.29
August 2014	8,195	$109.09	$1.23
September 2014	7,943	$111.36	$1.21
October 2014	8,955	$102.64	$1.23
November 2014	6,917	$122.20	$1.24
December 2014	8,268	$120.01	$1.47
January 2015	8,429	$114.74	$1.41
February 2015	8,381	$119.10	$1.40
March 2015	10,037	$114.03	$1.20
April 2015	9,216	$118.89	$1.25
May 2015	8,892	$121.37	$1.30
June 2015	9,982	$119.67	$1.22
July 2015	9,610	$118.28	$1.32
August 2015	9,089	$113.15	$1.66
September 2015	10,643	$100.33	$1.47
October 2015	9,396	$112.53	$1.42
November 2015	8,381	$119.86	$1.24
December 2015	8,920	$115.18	$1.17
January 2016	8,008	$101.51	$1.03
February 2016	9,246	$105.11	$1.04
March 2016	9,783	$122.04	$1.04
April 2016	9,217	$119.39	$0.99
May 2016	9,619	$113.45	$0.98
June 2016	9,722	$113.40	$0.93
July 2016	8,864	$118.95	$0.94
August 2016	10,459	$120.93	$0.85
September 2016	9,374	$117.73	$0.96
October 2016	9,111	$118.89	$1.01
November 2016	9,345	$115.96	$1.14
December 2016	9,673	$123.69	$1.18
January 2017	9,282	$125.04	$1.14
February 2017	8,141	$130.89	$1.18
March 2017	10,758	$133.35	$1.41
April 2017	9,078	$131.80	$1.24
May 2017	10,219	$137.02	$1.36
June 2017	10,373	$133.19	$1.49
July 2017	9,899	$138.71	$1.40
August 2017	10,704	$140.97	$1.58
September 2017	9,241	$141.28	$1.66
October 2017	9,895	$150.71	$1.74
November 2017	9,630	$151.53	$1.83
December 2017	8,281	$156.28	$1.81

Appendix B.2

Appendix for Chapter 3: Extended Results

B.2.1 Hedging performance of H-Models that use lagged input variables to forecast the delta (Δ_{N+1}) for the next trading day:

Tables B.2.1, B.2.2, B.2.3 and B.2.4 shows the relative out-of-sample hedging performance (in $RMSE$) amongst the models that use lagged input variables to forecast the one-trading-day-ahead delta Δ_{N+1}. For convenience, the models in Tables B.2.1, B.2.2, B.2.3, lists the forecast variable and the input variables are listed in columns II and III, and, the architecture of the MLP and LSTM models in columns IV, V and VI. The performance metric is the $RMSE$ of the one-trading-day-ahead forecast errors of the delta, which is computed for each model utilising all of the errors in each day or each month. Amongst all models, columns VII and VIII record the number of months and days, respectively, that each model has the lowest $RMSE$. To be certain of our results, we performed a bootstrap using the daily and monthly RMSEs. Columns IX (lower bound) and X (upper bound) present the results from the bootstrap performed (with replacement) using monthly RMSEs at a 95% confidence level and show the winning percentage out of 64 months for each model, and similarly, the 95 % confidence intervals computed from bootstrapping of the daily RMSEs signifies the winning percentage out of 1326 days for each model and are reported in columns XI (lower bound), XII (upper bound).

In the below several comparisons, even though a particular model wins by a higher percentage against other models, we investigated further these models pairwise by performing a pairwise bootstrap comparison, which was computed using the respective pair's daily RMSEs. The results are presented in Table 45 of the Electronic Appendix. Also, we examined the pairwise Diebold-Mariano(DM) (Diebold and Mariano (1995)) tests on these models and have presented the results in Table 39 of the Electronic Appendix. In constructing the DM test statistics, the models listed in the left column represent Model 1, and the models in the first row represent Model 2 in Table 39 of the Electronic Appendix. If the null can be rejected, a positive number suggests the rejection may be due to the second model being the better forecast model. In contrast, a negative value suggests the rejection may be due to the first model being the better forecast model. The model pairs highlighted in a red state that their forecasts have statistically insignificant differences in their prediction accuracy. Considering the DM-Test statistics in Table 39 of the Electronic Appendix, all the model pairs lead to the rejection of the null of equal forecasting performance. The RMSEs for the models that use lagged input variables to forecast the Δ_{N+1} on a monthly, yearly, and overall basis can be found in the Electronic Appendix, in Tables 21, 27, and 33, respectively.

In this section, we compare the out-of-sample hedging performance of the parametric models ($BSMH_N$, HH_N, $HJDH_N$ and $FMLSH_N$), the triple hidden layer MLP models ($M3H_N - Models$) and triple hidden layer LSTM models ($L3H_N - Models$), then the parametric models with the $M3H_N - Models$, and finally the parametric models with the $L3H_N - Models$.

The results for the parametric models with the triple hidden layer MLP $M3H_N - Models$ ($M3H1_N$ to $M3H7_N$) and the triple hidden layer LSTM $L3H_N - Models$ ($L3H1_N$ to $L3H7_N$) are presented in Table B.2.1. If all the models are compared together, then the $BSMH_N$ model had the lowest $RMSE$ for 166 days (having a daily bootstrap winning % of 11% to 14%) out of 1,326 days. Although the $BSMH_N$ model had outperformed other models, the $FMLSH_N$(161 days) and the $M3H1_N$(137 days) have shown similar outperformance, where they have a collective daily bootstrap winning percentage from 9% (lower bound for the $M3H1_N$ model) to 14%. (upper bound for the $FMLSH_N$ model). Table B.2.2 presents the results for the comparison of the parametric models with the triple hidden layer MLP $M3H_N - Models$ ($M3H1_N$ to $M3H7_N$), and the $BSMH_N$ model had the lowest $RMSE$ for 188 days (having a daily bootstrap winning % of 12% to 16%) out of 1,326 days. Though the $BSMH_N$ model had outperformed other models, the $FMLSH_N$(165 days), $M3H1_N$(169 days), and the $M3H2_N$(143 days) have shown similar outperformance, where they have a collective daily bootstrap winning percentage from 9% (lower bound for the $M3H2_N$ model) to 15%. (upper bound for the $M3H1_N$ model). We present the comparison results of the parametric models with the triple hidden layer LSTM $L3H_N - Models$ ($L3H1_N$ to $L3H7_N$) in Table B.2.3. We find that the $BSMH_N$ model had the lowest $RMSE$ for 452 days (having a daily bootstrap winning % of 31% to 37%) out of 1,326 days. Finally, we compare amongst the parametric models in Table B.2.4 and find that the $BSMH_N$ model still had the lowest $RMSE$ for 910 days (having a daily bootstrap winning % of 66% to 71%) out of 1,326 days.

Thus, when the parametric models are compared with the triple hidden layer ANN models that use lagged input variables to forecast the delta (in Table B.2.1), we conclude that a parametric model ($BSMH_N$) could outperform all other models. If the parametric models were compared with the triple hidden layer MLP models (in Table B.2.2), a parametric model ($BSMH_N$) outperforms all the triple hidden layer MLP models, also when the parametric models were compared with the triple hidden layer LSTM models (in Table B.2.3), a parametric model ($BSMH_N$) still outperforms them all. Finally, when a comparison is made amongst the parametric models, the $BSMH_N$ model has been shown to outperform the rest of the parametric models.

Table B.2.1: Delta Comparison (amongst Parametric, $M3H_N$-Models and $L3H_N$-Models): This table presents a performance comparison using both daily and monthly statistics amongst the Black-Scholes-Merton ($BSMH_N$) model, Heston (HH_N) model, Heston Jump Diffusion ($HJDH_N$) model, Finite Moment Log Stable ($FMLSH_N$) model, MLP $M3H_N$-Models ($M3H1_N$ to $M3H7_N$) and the LSTM $L3H_N$-Models ($L3H1_N$ to $L3H7_N$). The forecast variable for the MLP $M3H_N$-Models and LSTM $L3H_N$-Models is the delta that is directly forecasted from the respective ANN model, whereas the delta for the $BSMH_N$, HH_N, $HJDH_N$ models are computed using their respective characteristic functions. The models denoted by the $_N$ subscript use lagged input variables for forecasting the delta. Column I identifies the models, column II identifies the forecast variable, column III lists the input variables used by the models to obtain the one-trading-day-ahead forecast of the delta and columns IV, V and VI describe the network architecture of the MLP $M3H_N$-Models and the LSTM $L3H_N$-Models. The one-trading-day-ahead forecast errors of the delta are used to compute the Root Mean Square Error (RMSE). Forecasts are made for 1,326 trading days, and there are 64 months covered in the sample using the monthly data. Column VII reports the number of months out of the 64 months that each model has the smallest RMSE, while column VIII reports the number of days out of the 1,326 days each model has the smallest RMSE. Columns IX (lower bound) and X (upper bound) present the winning percentage out of 64 months for each model, evaluated using the bootstrap sampling technique. The statistical bootstrap performed (with replacement) at a 95% confidence level is computed from the monthly RMSE values of the respective models below. Similarly, columns XI (lower bound) and XII (upper bound) present the winning percentage out of 1326 days for each model computed from bootstrapping the daily RMSE values of the respective models at a 95% confidence level.

(I) Model	**(II)** Forecast	**(III)** Inputs	**(IV)** No. of hidden Layers	**(V)** No. of hidden nodes per layer	**(VI)** Network architecture	**(VII)** Performance amongst all models (Monthly)	**(VIII)** Performance amongst all models (Daily)	**(IX)** 2.5% lower bound-(for monthly) (%)	**(X)** 2.5% upper bound-(for monthly) (%)	**(XI)** 2.5% lower bound-(for daily) (%)	**(XII)** 2.5% upper bound-(for daily) (%)
$BSMH_N$	$\Delta_{N+1}^{BSMH_N}$	$S_N, K_{N+1}, T_{N+1}, R_N, Q_N, \sigma_N^{CALIB^C}$	-	-	-	**19**	**166**	19%	41%	11%	14%
HH_N	$\Delta_{N+1}^{HH_N}$	$S_N, K_{N+1}, T_{N+1}, R_N, Q_N, \sigma_N^{CALIB^C}, HParams_N^C$	-	-	-	5	67	2%	16%	4%	6%
$HJDH_N$	$\Delta_{N+1}^{HJDH_N}$	$S_N, K_{N+1}, T_{N+1}, R_N, Q_N, \sigma_N^{CALIB^C}, HJDParams_N^C$	-	-	-	0	69	0%	0%	4%	6%
$FMLSH_N$	$\Delta_{N+1}^{FMLSH_N}$	$S_N, K_{N+1}, T_{N+1}, R_N, Q_N, FMLSParams_N^C$	-	-	-	0	161	0%	0%	10%	14%
$M3H1_N$	$\Delta_{N+1}^{M3H1_N}$	$S_N, K_{N+1}, T_{N+1}, R_N, Q_N, \sigma_N^{CALIB^C}$	3	6	6 ×6 × 6	15	137	14%	34%	9%	12%
$M3H2_N$	$\Delta_{N+1}^{M3H2_N}$	$S_N, K_{N+1}, T_{N+1}, R_N, Q_N, \sigma_N^{CALIB^C}, (\delta C_N/\delta S_N)$	3	7	7 × 7 × 7	8	105	5%	20%	6%	9%
$M3H3_N$	$\Delta_{N+1}^{M3H3_N}$	$(S_N, K_{N+1}, T_{N+1}, R_N, Q_N, \sigma_N^{CALIB^C}, \Delta_N^{BSMH_N}$	3	7	7 ×7 × 7	7	89	5%	19%	5%	8%
$M3H4_N$	$\Delta_{N+1}^{M3H4_N}$	$S_N, K_{N+1}, T_{N+1}, R_N, Q_N, \sigma_N^{CALIB^C}, BSMGreeks_N^C$	3	11	11 × 11× 11	0	72	0%	0%	4%	7%
$M3H5_N$	$\Delta_{N+1}^{M3H5_N}$	$S_N, K_{N+1}, T_{N+1}, R_N, Q_N, HParams_N^C, \Delta_N^{HH_N}$	3	11	11 × 11× 11	0	93	0%	0%	6%	8%
$M3H6_N$	$\Delta_{N+1}^{M3H6_N}$	$S_N, K_{N+1}, T_{N+1}, R_N, Q_N, HJDParams_N^C, \Delta_N^{HJDH_N}$	3	14	14 × 14 × 14	0	94	0%	0%	6%	9%
$M3H7_N$	$\Delta_{N+1}^{M3H7_N}$	$S_N, K_{N+1}, T_{N+1}, R_N, Q_N, FMLSParams_N^C, \Delta_N^{FMLSH_N}$	3	8	8 × 8 × 8	7	95	3%	19%	6%	9%
$L3H1_N$	$\Delta_{N+1}^{L3H1_N}$	$S_N, K_{N+1}, T_{N+1}, R_N, Q_N, \sigma_N^{CALIB^C}$	3	6	6 × 6 × 6	0	19	0%	0%	1%	2%
$L3H2_N$	$\Delta_{N+1}^{L3H2_N}$	$S_N, K_{N+1}, T_{N+1}, R_N, Q_N, \sigma_N^{CALIB^C}, (\delta C_N/\delta S_N)$	3	7	7 × 7 × 7	0	20	0%	0%	1%	2%
$L3H3_N$	$\Delta_{N+1}^{L3H3_N}$	$S_N, K_{N+1}, T_{N+1}, R_N, Q_N, \sigma_N^{CALIB^C}, \Delta_N^{BSMH_N}$	3	7	7 × 7 × 7	0	21	0%	0%	1%	2%
$L3H4_N$	$\Delta_{N+1}^{L3H4_N}$	$S_N, K_{N+1}, T_{N+1}, R_N, Q_N, \sigma_N^{CALIB^C}, BSMGreeks_N^C$	3	11	11 × 11× 11	3	78	0%	11%	5%	7%
$L3H5_N$	$\Delta_{N+1}^{L3H5_N}$	$S_N, K_{N+1}, T_{N+1}, R_N, Q_N, HParams_N^C, \Delta_N^{HH_N}$	3	11	11 × 11× 11	0	16	0%	0%	1%	2%
$L3H6_N$	$\Delta_{N+1}^{L3H6_N}$	$S_N, K_{N+1}, T_{N+1}, R_N, Q_N, HJDParams_N^C, \Delta_N^{HJDH_N}$	3	14	14 × 14 × 14	0	20	0%	0%	1%	2%
$L3H7_N$	$\Delta_{N+1}^{L3H7_N}$	$S_N, K_{N+1}, T_{N+1}, R_N, Q_N, FMLSParams_N^C, \Delta_N^{FMLSH_N}$	3	8	8 × 8 × 8	0	15	0%	0%	0%	2%

Table B.2.2: Delta Comparison (amongst Parametric and $M3H_N$-Models): This table presents a performance comparison using both daily and monthly statistics amongst the Black-Scholes-Merton ($BSMH_N$) model, Heston (HH_N) model, Heston Jump Diffusion ($HJDH_N$) model, Finite Moment Log Stable ($FMLSH_N$) model, and the MLP $M3H_N$-Models ($M3H1_N$ to $M3H7_N$). The forecast variable for the MLP $M3H_N$-Models is the delta that is directly forecasted from the respective MLP model, whereas the delta for the $BSMH_N$, HH_N, $HJDH_N$ models are computed using their respective characteristic functions. The models denoted by the $_N$ subscript use lagged input variables for forecasting the delta. Column I identifies the models, column II identifies the forecast variable, column III lists the input variables used by the models to obtain the one-trading-day-ahead forecast of the delta, and columns IV, V and VI describe the network architecture of the MLP $M3H_N$-Models. The one-trading-day-ahead forecast errors of the delta are used to compute the Root Mean Square Error (RMSE). Forecasts are made for 1,326 trading days, and there are 64 months covered in the sample using the monthly data. Column VII reports the number of months out of the 64 months that each model has the smallest RMSE, while column VIII reports the number of days out of the 1,326 days each model has the smallest RMSE. Columns IX (lower bound) and X (upper bound) present the winning percentage out of 64 months for each model, evaluated using the bootstrap sampling technique. The statistical bootstrap performed (with replacement) at a 95% confidence level is computed from the monthly RMSE values of the respective models below. Similarly, columns XI (lower bound) and XII (upper bound) present the winning percentage out of 1326 days for each model computed from bootstrapping the daily RMSE values of the respective models at a 95% confidence level.

(I) Model	**(II)** Forecast	**(III)** Inputs	**(IV)** No. of hidden Layers	**(V)** No. of hidden nodes per layer	**(VI)** Network architecture	**(VII)** Performance amongst all models (Monthly)	**(VIII)** Performance amongst all models (Daily)	**(IX)** 2.5% lower bound- (for monthly) (%)	**(X)** 2.5% upper bound- (for monthly) (%)	**(XI)** 2.5% lower bound- (for daily) (%)	**(XII)** 2.5% upper bound- (for daily) (%)
$BSMH_N$	$\Delta_{N+1}^{BSMH_N}$	$S_N, K_{N+1}, T_{N+1}, R_N, Q_N, \sigma_N^{CALIB^C}$	-	-	-	**20**	**188**	20%	44%	12%	16%
HH_N	$\Delta_{N+1}^{HH_N}$	$S_N, K_{N+1}, T_{N+1}, R_N, Q_N, \sigma_N^{CALIB^C}, HParams_N^C$	-	-	-	5	68	2%	16%	4%	6%
$HJDH_N$	$\Delta_{N+1}^{HJDH_N}$	$S_N, K_{N+1}, T_{N+1}, R_N, Q_N, \sigma_N^{CALIB^C}, HJDParams_N^C$	-	-	-	0	69	0%	0%	4%	7%
$FMLSH_N$	$\Delta_{N+1}^{FMLSH_N}$	$S_N, K_{N+1}, T_{N+1}, R_N, Q_N, FMLSParams_N^C$	-	-	-	0	165	0%	0%	11%	14%
$M3H1_N$	$\Delta_{N+1}^{M3H1_N}$	$S_N, K_{N+1}, T_{N+1}, R_N, Q_N, \sigma_N^{CALIB^C}$	3	6	$6 \times 6 \times 6$	16	169	14%	36%	11%	15%
$M3H2_N$	$\Delta_{N+1}^{M3H2_N}$	$S_N, K_{N+1}, T_{N+1}, R_N, Q_N, \sigma_N^{CALIB^C}, (\delta C_N/\delta S_N)$	3	7	$7 \times 7 \times 7$	9	143	6%	23%	9%	12%
$M3H3_N$	$\Delta_{N+1}^{M3H3_N}$	$S_N, K_{N+1}, T_{N+1}, R_N, Q_N, \sigma_N^{CALIB^C}, \Delta_N^{BSMH_N}$	3	7	$7 \times 7 \times 7$	7	111	5%	19%	7%	10%
$M3H4_N$	$\Delta_{N+1}^{M3H4_N}$	$S_N, K_{N+1}, T_{N+1}, R_N, Q_N, \sigma_N^{CALIB^C}, BSMGreeks_N^C$	3	11	$11 \times 11 \times 11$	0	87	0%	0%	5%	8%
$M3H5_N$	$\Delta_{N+1}^{M3H5_N}$	$S_N, K_{N+1}, T_{N+1}, R_N, Q_N, HParams_N^C, \Delta_N^{HH_N}$	3	11	$11 \times 11 \times 11$	0	108	0%	0%	7%	10%
$M3H6_N$	$\Delta_{N+1}^{M3H6_N}$	$S_N, K_{N+1}, T_{N+1}, R_N, Q_N, HJDParams_N^C, \Delta_N^{HJDH_N}$	3	14	$14 \times 14 \times 14$	0	105	0%	0%	6%	9%
$M3H7_N$	$\Delta_{N+1}^{M3H7_N}$	$S_N, K_{N+1}, T_{N+1}, R_N, Q_N, FMLSParams_N^C, \Delta_N^{FMLSH_N}$	3	8	$8 \times 8 \times 8$	7	113	3%	19%	7%	10%

Table B.2.3: Delta Comparison (amongst Parametric and $L3H_N$-Models): This table presents a performance comparison using both daily and monthly statistics amongst the Black-Scholes-Merton ($BSMH_N$) model, Heston (HH_N) model, Heston Jump Diffusion ($HJDH_N$) model, Finite Moment Log Stable ($FMLSH_N$) model, and the LSTM $L3H_N$-Models ($L3H1_N$ to $L3H7_N$). The forecast variable for the LSTM $L3H_N$-Models is the delta that is directly forecasted from the respective LSTM model, whereas the delta for the $BSMH_N$, HH_N, $HJDH_N$ models are computed using their respective characteristic functions. The models denoted by the $_N$ subscript use lagged input variables for forecasting the delta. Column I identifies the models, column II identifies the forecast variable, column III lists the input variables used by the models to obtain the one-trading-day-ahead forecast of the delta, and columns IV, V and VI describe the network architecture of the LSTM $L3H_N$-Models. The one-trading-day-ahead forecast errors of the delta are used to compute the Root Mean Square Error (RMSE). Forecasts are made for 1,326 trading days, and there are 64 months covered in the sample using the monthly data. Column VII reports the number of months out of the 64 months that each model has the smallest RMSE, while column VIII reports the number of days out of the 1,326 days each model has the smallest RMSE. Columns IX (lower bound) and X (upper bound) present the winning percentage out of 64 months for each model, evaluated using the bootstrap sampling technique. The statistical bootstrap performed (with replacement) at a 95% confidence level is computed from the monthly RMSE values of the respective models below. Similarly, in columns XI (lower bound) and XII (upper bound) presents the winning percentage out of 1326 days for each model computed from bootstrapping the daily RMSE values of the respective models at a 95% confidence level.

(I) Model	**(II)** Forecast	**(III)** Inputs	**(IV)** No. of hidden Layers	**(V)** No. of hidden nodes per layer	**(VI)** Network architecture	**(VII)** Performance amongst all models (Monthly)	**(VIII)** Performance amongst all models (Daily)	**(IX)** 2.5% lower bound-(for monthly) (%)	**(X)** 2.5% upper bound-(for monthly) (%)	**(XI)** 2.5% lower bound-(for daily) (%)	**(XII)** 2.5% upper bound-(for daily) (%)
$BSMH_N$	$\Delta_{N+1}^{BSMH_N}$	$S_N, K_{N+1}, T_{N+1}, R_N, Q_N, \sigma_N^{CALIB^C}$	-	-	-	**48**	**452**	64%	84%	31%	37%
HH_N	$\Delta_{N+1}^{HH_N}$	$S_N, K_{N+1}, T_{N+1}, R_N, Q_N, \sigma_N^{CALIB^C}, HParams_N^C$	-	-	-	8	95	5%	22%	6%	9%
$HJDH_N$	$\Delta_{N+1}^{HJDH_N}$	$S_N, K_{N+1}, T_{N+1}, R_N, Q_N, \sigma_N^{CALIB^C}, HJDParams_N^C$	-	-	-	0	78	0%	0%	5%	7%
$FMLSH_N$	$\Delta_{N+1}^{FMLSH_N}$	$S_N, K_{N+1}, T_{N+1}, R_N, Q_N, FMLSParams_N^C$	-	-	-	0	197	0%	0%	13%	17%
$L3H1_N$	$\Delta_{N+1}^{L3H1_N}$	$S_N, K_{N+1}, T_{N+1}, R_N, Q_N, \sigma_N^{CALIB^C}$	3	6	$6 \times 6 \times 6$	0	38	0%	0%	2%	4%
$L3H2_N$	$\Delta_{N+1}^{L3H2_N}$	$S_N, K_{N+1}, T_{N+1}, R_N, Q_N, \sigma_N^{CALIB^C}, (\delta C_N/\delta S_N)$	3	7	$7 \times 7 \times 7$	1	55	0%	5%	3%	5%
$L3H3_N$	$\Delta_{N+1}^{L3H3_N}$	$S_N, K_{N+1}, T_{N+1}, R_N, Q_N, \sigma_N^{CALIB^C}, \Delta_N^{BSMH_N}$	3	7	$7 \times 7 \times 7$	0	40	0%	0%	2%	4%
$L3H4_N$	$\Delta_{N+1}^{L3H4_N}$	$S_N, K_{N+1}, T_{N+1}, R_N, Q_N, \sigma_N^{CALIB^C}, BSMGreeks_N^C$	3	11	$11 \times 11 \times 11$	5	251	2%	14%	17%	21%
$L3H5_N$	$\Delta_{N+1}^{L3H5_N}$	$S_N, K_{N+1}, T_{N+1}, R_N, Q_N, HParams_N^C, \Delta_N^{HH_N}$	3	11	$11 \times 11 \times 11$	1	49	0%	6%	3%	5%
$L3H6_N$	$\Delta_{N+1}^{L3H6_N}$	$S_N, K_{N+1}, T_{N+1}, R_N, Q_N, HJDParams_N^C, \Delta_N^{HJDH_N}$	3	14	$14 \times 14 \times 14$	1	52	0%	5%	3%	5%
$L3H7_N$	$\Delta_{N+1}^{L3H7_N}$	$S_N, K_{N+1}, T_{N+1}, R_N, Q_N, FMLSParams_N^C, \Delta_N^{FMLSH_N}$	3	8	$8 \times 8 \times 8$	0	31	0%	0%	1%	3%

Table B.2.4: Delta Comparison (amongst Parametric Models): This table presents a performance comparison using both daily and monthly statistics amongst the Black-Scholes-Merton ($BSMH_N$) model, Heston (HH_N) model, Heston Jump Diffusion ($HJDH_N$) model, and the Finite Moment Log Stable ($FMLSH_N$) model. The delta for the $BSMH_N$, HH_N, $HJDH_N$ models are computed using their respective characteristic functions. The models denoted by the $_N$ subscript use lagged input variables for forecasting the delta. The one-trading-day-ahead forecast errors of the delta are used to compute the Root Mean Square Error (RMSE). Forecasts are made for 1,326 trading days, and there are 64 months covered in the sample using the monthly data. Column I identifies the models, column II identifies the forecast variable, and column III lists the input variables used by the models to obtain the one-trading-day-ahead forecast of the delta. Column IV reports the number of months out of the 64 months that each model has the smallest RMSE, while column V reports lists the number of days out of the 1,326 days that each model has the smallest RMSE. Columns VI (lower bound) and VII (upper bound) present the winning percentage out of 64 months for each model, evaluated using the bootstrap sampling technique. The statistical bootstrap performed (with replacement) at a 95% confidence level is computed from the monthly RMSE values of the respective models below. Similarly, columns VIII (lower bound) and IX (upper bound) present the winning percentage out of 1326 days for each model computed from bootstrapping the daily RMSE values of the respective models at a 95% confidence level.

(I) Model	**(II) Forecast**	**(III) Inputs**	**(IV) Performance amongst all models (Monthly)**	**(V) Performance amongst all models (Daily)**	**(VI) 2.5% lower bound- (for monthly) (%)**	**(VII) 2.5% upper bound- (for monthly) (%)**	**(VIII) 2.5% lower bound- (for daily) (%)**	**(IX) 2.5% upper bound- (for daily) (%)**
$BSMH_N$	$\Delta_{N+1}^{BSMH_N}$	$S_N, K_{N+1}, T_{N+1}, R_N, Q_N, \sigma_N^{CALIB^C}$	**55**	**910**	77%	94%	66%	71%
HH_N	$\Delta_{N+1}^{HH_N}$	$S_N, K_{N+1}, T_{N+1}, R_N, Q_N, \sigma_N^{CALIB^C}, HParams_N^C$	9	131	6%	23%	8%	12%
$HJDH_N$	$\Delta_{N+1}^{HJDH_N}$	$S_N, K_{N+1}, T_{N+1}, R_N, Q_N, \sigma_N^{CALIB^C}, HJDParams_N^C$	0	79	0%	0%	5%	7%
$FMLSH_N$	$\Delta_{N+1}^{FMLSH_N}$	$S_N, K_{N+1}, T_{N+1}, R_N, Q_N, FMLSParams_N^C$	0	206	0%	0%	14%	17%

B.2.2 Hedging performance of H-Models that use one-trading-day-ahead input variables to forecast the delta (Δ_{N+1}) for the next trading day:

Tables B.2.5, B.2.6, B.2.7 and B.2.8 shows the relative out-of-sample hedging performance (in $RMSE$) amongst the models that use one-trading-day-ahead input variables to forecast the one-trading-day-ahead delta Δ_{N+1}. For convenience, the models in Tables B.2.5, B.2.6, B.2.7, lists the forecast variable and the input variables are listed in columns II and III, and, the architecture of the MLP and LSTM models in columns IV, V and VI. The performance metric is the $RMSE$ of the one-trading-day-ahead forecast errors of the delta, which is computed for each model utilising all of the errors in each day or each month. Amongst all models, columns VII and VIII record the number of months and days, respectively, that each model has the lowest $RMSE$. To be certain of our results, we performed a bootstrap using the daily and monthly RMSEs. Columns IX (lower bound) and X (upper bound) present the results from the bootstrap performed (with replacement) using monthly RMSEs at a 95% confidence level and show the winning percentage out of 64 months for each model, and similarly, the 95 % confidence intervals computed from bootstrapping of the daily RMSEs signifies the winning percentage out of 1326 days for each model and are reported in columns XI (lower bound), XII (upper bound).

In the below several comparisons, even though a particular model wins by a higher percentage against other models, we investigated further these models pairwise by performing a pairwise bootstrap comparison, which was computed using the respective pair's daily RMSEs. The results are presented in Table 46 of the Electronic Appendix. Also, we examined the pairwise Diebold-Mariano(DM) (Diebold and Mariano (1995)) tests on these models and have presented the results in Table 40 of the Electronic Appendix. In constructing the DM test statistics, the models listed in the left column represent Model 1, and the models in the first row represent Model 2 in Table 40 of the Electronic Appendix. If the null can be rejected, a positive number suggests the rejection may be due to the second model being the better forecast model. In contrast, a negative value suggests the rejection may be due to the first model being the better forecast model. The model pairs highlighted in a red state that their forecasts have statistically insignificant differences in their prediction accuracy. The following model pairs have been shown to have statistically insignificant differences: ($M3H2_{N+1}$, $L3H1_{N+1}$), ($M3H2_{N+1}$, $L3H3_{N+1}$), ($M3H2_{N+1}$, $L3H6_{N+1}$), ($L3H2_{N+1}$, $L3H7_{N+1}$). The RMSEs for the models that use one-trading-day-ahead input variables to forecast the Δ_{N+1} for the next trading day on a monthly, yearly, and overall basis can be found in the Electronic Appendix, in Tables 22, 28, and 34, respectively.

In this section, we compare the out-of-sample hedging performance of the parametric models ($BSMH_{N+1}$, HH_{N+1}, $HJDH_{N+1}$, and $FMLSH_{N+1}$), the triple hidden layer MLP models ($M3H_{N+1} - Models$) and triple hidden layer LSTM models ($L3H_{N+1} - Models$), then the parametric models with the $M3H_{N+1} - Models$, and finally the parametric models with the $L3H_{N+1} - Models$.

The results for the parametric models with the triple hidden layer MLP $M3H_{N+1} - Models$ ($M3H1_{N+1}$ to $M3H7_{N+1}$) and the triple hidden layer LSTM $L3H_{N+1} - Models$ ($L3H1_{N+1}$ to $L3H7_{N+1}$) are presented in Table B.2.5. If all the models are compared together, then the $BSMH_{N+1}$ model had the lowest $RMSE$ for 196 days (having a daily bootstrap winning % of 13% to 17%) out of 1,326 days. Although the $BSMH_{N+1}$ model had outperformed other models, the $FMLSH_{N+1}$(162 days), and the $M3H1_{N+1}$(157 days) have shown similar outperformance, where they have a collective daily bootstrap winning percentage from 10% (lower bound for the $M3H1_{N+1}$ model) to 14%. (upper bound for the $FMLSH_{N+1}$ model). Table B.2.6 presents the results for the comparison of the parametric models with the triple hidden layer MLP $M3H_{N+1} - Models$ ($M3H1_{N+1}$ to $M3H7_{N+1}$), and the $BSMH_{N+1}$ model had the lowest $RMSE$ for 208 days (having a daily bootstrap winning % of 14% to 18%) out of 1,326 days. Though the $BSMH_{N+1}$ model had outperformed other models, the $FMLSH_{N+1}$(167 days), and the $M3H1_{N+1}$(192 days) have shown similar outperformance, where they have a collective daily bootstrap winning percentage from 11% (lower bound for the $FMLSH_{N+1}$ model) to 16%. (upper bound for the $M3H1_{N+1}$ model). We present the comparison results of the parametric models with the triple hidden layer LSTM $L3H_{N+1} - Models$ ($L3H1_{N+1}$ to $L3H7_{N+1}$) in Table B.2.7. We find that the $BSMH_{N+1}$ model had the lowest $RMSE$ for 486 days (having a daily bootstrap winning % of 34% to 39%) out of 1,326 days. Finally, we compare amongst the parametric models in Table B.2.8 and find that the $BSMH_{N+1}$ still model had the lowest $RMSE$ for 936 days (having a daily bootstrap winning % of 68% to 73%) out of 1,326 days.

Thus, when the parametric models are compared with the triple hidden layer ANN models that use one-trading-day-ahead input variables to forecast the delta(in Table B.2.5), we conclude that a parametric model ($BSMH_{N+1}$) could outperform all other models. If the parametric models were compared with the triple hidden layer MLP models (in Table B.2.6), a parametric model ($BSMH_{N+1}$) outperforms all the triple hidden layer MLP models, also when the parametric models were compared with the triple hidden layer LSTM models (in Table B.2.7), a parametric model ($BSMH_{N+1}$) still outperforms them all. Finally, when a comparison is made amongst the parametric models, the $BSMH_{N+1}$ model has been shown to outperform the rest of the parametric models.

Table B.2.5: Delta Comparison (amongst Parametric, $M3H_{N+1}$-Models and $L3H_{N+1}$-Models): This table presents a performance comparison using both daily and monthly statistics amongst the Black-Scholes-Merton ($BSMH_{N+1}$) model, Heston (HH_{N+1}) model, Heston Jump Diffusion ($HJDH_{N+1}$) model, Finite Moment Log Stable ($FMLSH_{N+1}$) model, MLP $M3H_{N+1}$-Models ($M3H1_{N+1}$ to $M3H7_{N+1}$) and the LSTM $L3H_{N+1}$-Models ($L3H1_{N+1}$ to $L3H7_{N+1}$). The forecast variable for the MLP $M3H_{N+1}$-Models and LSTM $L3H_{N+1}$-Models is the delta that is directly forecasted from the respective ANN model, whereas the delta for the $BSMH_{N+1}$, HH_{N+1}, $HJDH_{N+1}$ models are computed using their respective characteristic functions. The models denoted by the $_{N+1}$ subscript use one-trading-day-ahead input variables for forecasting the delta. Column I identifies the models, column II identifies the forecast variable, column III lists the input variables used by the models to obtain the one-trading-day-ahead forecasts of the delta, and columns IV, V and VI describe the network architecture of the MLP $M3H_{N+1}$-Models and the LSTM $L3H_{N+1}$-Models. The one-trading-day-ahead forecast errors of the delta are used to compute the Root Mean Square Error (RMSE). Forecasts are made for 1,326 trading days, and there are 64 months covered in the sample using the monthly data. Column VII reports the number of months out of the 64 months that each model has the smallest RMSE, while column VIII reports the number of days out of the 1,326 days each model has the smallest RMSE. Columns IX (lower bound) and X (upper bound) present the winning percentage out of 64 months for each model, evaluated using the bootstrap sampling technique. The statistical bootstrap performed (with replacement) at a 95% confidence level is computed from the monthly RMSE values of the respective models below. Similarly, in columns XI (lower bound) and XII (upper bound) presents the winning percentage out of 1326 days for each model computed from bootstrapping the daily RMSE values of the respective models at a 95% confidence level.

(I) Model	**(II)** Forecast	**(III)** Inputs	**(IV)** No. of hidden Layers	**(V)** No. of hidden nodes per layer	**(VI)** Network architecture	**(VII)** Performance amongst all models (Monthly)	**(VIII)** Performance amongst all models (Daily)	**(IX)** 2.5% lower bound-(for monthly) (%)	**(X)** 2.5% upper bound-(for monthly) (%)	**(XI)** 2.5% lower bound-(for daily) (%)	**(XII)** 2.5% upper bound-(for daily) (%)
$BSMH_{N+1}$	$\Delta_{N+1}^{BSMH_{N+1}}$	$S_{N+1}, K_{N+1}, T_{N+1}, R_{N+1}, Q_{N+1}, \sigma_N^{CALIB^C}$	-	-	-	**37**	**196**	45%	70%	13%	17%
HH_{N+1}	$\Delta_{N+1}^{HH_{N+1}}$	$S_{N+1}, K_{N+1}, T_{N+1}, R_{N+1}, Q_{N+1}, \sigma_N^{CALIB^C}, HParams_N^C$	-	-	-	4	44	2%	13%	2%	4%
$HJDH_{N+1}$	$\Delta_{N+1}^{HJDH_{N+1}}$	$S_{N+1}, K_{N+1}, T_{N+1}, R_{N+1}, Q_{N+1}, \sigma_N^{CALIB^C}, HJDParams_N^C$	-	-	-	0	71	0%	0%	4%	7%
$FMLSH_{N+1}$	$\Delta_{N+1}^{FMLSH_{N+1}}$	$S_{N+1}, K_{N+1}, T_{N+1}, R_{N+1}, Q_{N+1}, FMLSParams_N^C$	-	-	-	0	162	0%	0%	10%	14%
$M3H1_{N+1}$	$\Delta_{N+1}^{M3H1_{N+1}}$	$S_{N+1}, K_{N+1}, T_{N+1}, R_{N+1}, Q_{N+1}, \sigma_N^{CALIB^C}$	3	6	$6 \times 6 \times 6$	8	157	5%	21%	10%	14%
$M3H2_{N+1}$	$\Delta_{N+1}^{M3H2_{N+1}}$	$S_{N+1}, K_{N+1}, T_{N+1}, R_{N+1}, Q_{N+1}, \sigma_N^{CALIB^C}, (\delta C_N/\delta S_N)$	3	7	$7 \times 7 \times 7$	6	109	3%	17%	7%	10%
$M3H3_{N+1}$	$\Delta_{N+1}^{M3H3_{N+1}}$	$S_{N+1}, K_{N+1}, T_{N+1}, R_{N+1}, Q_{N+1}, \sigma_N^{CALIB^C}, \Delta_N^{BSMH_{N+1}}$	3	7	$7 \times 7 \times 7$	4	95	2%	13%	6%	9%
$M3H4_{N+1}$	$\Delta_{N+1}^{M3H4_{N+1}}$	$S_{N+1}, K_{N+1}, T_{N+1}, R_{N+1}, Q_{N+1}, \sigma_N^{CALIB^C}, BSMGreeks_N^C$	3	11	$11 \times 11 \times 11$	0	66	0%	0%	4%	6%
$M3H5_{N+1}$	$\Delta_{N+1}^{M3H5_{N+1}}$	$S_{N+1}, K_{N+1}, T_{N+1}, R_{N+1}, Q_{N+1}, HParams_N^C, \Delta_N^{HH_{N+1}}$	3	11	$11 \times 11 \times 11$	0	84	0%	0%	5%	8%
$M3H6_{N+1}$	$\Delta_{N+1}^{M3H6_{N+1}}$	$S_{N+1}, K_{N+1}, T_{N+1}, R_{N+1}, Q_{N+1}, HJDParams_N^C, \Delta_N^{HJDH_{N+1}}$	3	14	$14 \times 14 \times 14$	0	96	0%	0%	6%	9%
$M3H7_{N+1}$	$\Delta_{N+1}^{M3H7_{N+1}}$	$S_{N+1}, K_{N+1}, T_{N+1}, R_{N+1}, Q_{N+1}, FMLSParams_N^C, \Delta_N^{FMLSH_{N+1}}$	3	8	$8 \times 8 \times 8$	1	98	0%	5%	6%	9%
$L3H1_{N+1}$	$\Delta_{N+1}^{L3H1_{N+1}}$	$S_{N+1}, K_{N+1}, T_{N+1}, R_{N+1}, Q_{N+1}, \sigma_N^{CALIB^C}$	3	6	$6 \times 6 \times 6$	0	12	0%	0%	0%	1%
$L3H2_{N+1}$	$\Delta_{N+1}^{L3H2_{N+1}}$	$S_{N+1}, K_{N+1}, T_{N+1}, R_{N+1}, Q_{N+1}, \sigma_N^{CALIB^C}, (\delta C_N/\delta S_N)$	3	7	$7 \times 7 \times 7$	0	18	0%	0%	1%	2%
$L3H3_{N+1}$	$\Delta_{N+1}^{L3H3_{N+1}}$	$S_{N+1}, K_{N+1}, T_{N+1}, R_{N+1}, Q_{N+1}, \sigma_N^{CALIB^C}, \Delta_N^{BSMH_{N+1}}$	3	7	$7 \times 7 \times 7$	0	15	0%	0%	0%	1%
$L3H4_{N+1}$	$\Delta_{N+1}^{L3H4_{N+1}}$	$S_{N+1}, K_{N+1}, T_{N+1}, R_{N+1}, Q_{N+1}, \sigma_N^{CALIB^C}, BSMGreeks_N^C$	3	11	$11 \times 11 \times 11$	3	73	0%	11%	4%	7%
$L3H5_{N+1}$	$\Delta_{N+1}^{L3H5_{N+1}}$	$S_{N+1}, K_{N+1}, T_{N+1}, R_{N+1}, Q_{N+1}, HParams_N^C, \Delta_N^{HH_{N+1}}$	3	11	$11 \times 11 \times 11$	1	12	0%	5%	0%	1%
$L3H6_{N+1}$	$\Delta_{N+1}^{L3H6_{N+1}}$	$S_{N+1}, K_{N+1}, T_{N+1}, R_{N+1}, Q_{N+1}, HJDParams_N^C, \Delta_N^{HJDH_{N+1}}$	3	14	$14 \times 14 \times 14$	0	15	0%	0%	0%	1%
$L3H7_{N+1}$	$\Delta_{N+1}^{L3H7_{N+1}}$	$S_{N+1}, K_{N+1}, T_{N+1}, R_{N+1}, Q_{N+1}, FMLSParams_N^C, \Delta_N^{FMLSH_{N+1}}$	3	8	$8 \times 8 \times 8$	0	13	0%	0%	0%	1%

Table B.2.6: Delta Comparison (amongst Parametric and $M3H_{N+1}$-Models): This table presents a performance comparison using both daily and monthly statistics amongst the Black-Scholes-Merton ($BSMH_{N+1}$) model, Heston (HH_{N+1}) model, Heston Jump Diffusion ($HJDH_{N+1}$) model, Finite Moment Log Stable ($FMLSH_{N+1}$) model, and the MLP $M3H_{N+1}$-Models ($M3H1_{N+1}$ to $M3H7_{N+1}$). The forecast variable for the MLP $M3H_{N+1}$-Models is the delta that is directly forecasted from the respective MLP model, whereas the delta for the $BSMH_{N+1}$, HH_{N+1}, $HJDH_{N+1}$ models are computed using their respective characteristic functions. The models denoted by the $_{N+1}$ subscript use one-trading-day-ahead input variables for forecasting the delta. Column I identifies the models, column II identifies the forecast variable, column III lists the input variables used by the models to obtain the one-trading-day-ahead forecasts of the delta, and columns IV, V and VI describe the network architecture of the MLP $M3H_{N+1}$-Models. The one-trading-day-ahead forecast errors of the delta are used to compute the Root Mean Square Error (RMSE). Forecasts are made for 1,326 trading days, and there are 64 months covered in the sample using the monthly data. Column VII reports the number of months out of the 64 months that each model has the smallest RMSE, while column VIII reports the number of days out of the 1,326 days each model has the smallest RMSE. Columns IX (lower bound) and X (upper bound) present the winning percentage out of 64 months for each model, evaluated using the bootstrap sampling technique. The statistical bootstrap performed (with replacement) at a 95% confidence level is computed from the monthly RMSE values of the respective models below. Similarly, columns XI (lower bound) and XII (upper bound) present the winning percentage out of 1326 days for each model computed from bootstrapping the daily RMSE values of the respective models at a 95% confidence level.

(I) Model	**(II)** Forecast	**(III)** Inputs	**(IV)** No. of hidden Layers	**(V)** No. of hidden nodes per layer	**(VI)** Network architecture	**(VII)** Performance amongst all models (Monthly)	**(VIII)** Performance amongst all models (Daily)	**(IX)** 2.5% lower bound-(for monthly) (%)	**(X)** 2.5% upper bound-(for monthly) (%)	**(XI)** 2.5% lower bound-(for daily) (%)	**(XII)** 2.5% upper bound-(for daily) (%)
$BSMH_{N+1}$	$\Delta_{N+1}^{BSMH_{N+1}}$	$S_{N+1}, K_{N+1}, T_{N+1}, R_{N+1}, Q_{N+1}, \sigma_N^{CALIB^C}$	-	-	-	**39**	**208**	48%	73%	14%	18%
HH_{N+1}	$\Delta_{N+1}^{HH_{N+1}}$	$S_{N+1}, K_{N+1}, T_{N+1}, R_{N+1}, Q_{N+1}, \sigma_N^{CALIB^C}, HParams_N^C$	-	-	-	4	46	2%	13%	2%	5%
$HJDH_{N+1}$	$\Delta_{N+1}^{HJDH_{N+1}}$	$S_{N+1}, K_{N+1}, T_{N+1}, R_{N+1}, Q_{N+1}, \sigma_N^{CALIB^C}, HJDParams_N^C$	-	-	-	0	72	0%	0%	4%	7%
$FMLSH_{N+1}$	$\Delta_{N+1}^{FMLSH_{N+1}}$	$S_{N+1}, K_{N+1}, T_{N+1}, R_{N+1}, Q_{N+1}, FMLSParams_N^C$	-	-	-	0	167	0%	0%	11%	15%
$M3H1_{N+1}$	$\Delta_{N+1}^{M3H1_{N+1}}$	$S_{N+1}, K_{N+1}, T_{N+1}, R_{N+1}, Q_{N+1}, \sigma_N^{CALIB^C}$	3	6	$6 \times 6 \times 6$	10	192	8%	25%	13%	16%
$M3H2_{N+1}$	$\Delta_{N+1}^{M3H2_{N+1}}$	$S_{N+1}, K_{N+1}, T_{N+1}, R_{N+1}, Q_{N+1}, \sigma_N^{CALIB^C}, (\delta C_N/\delta S_N)$	3	7	$7 \times 7 \times 7$	6	135	3%	17%	9%	12%
$M3H3_{N+1}$	$\Delta_{N+1}^{M3H3_{N+1}}$	$S_{N+1}, K_{N+1}, T_{N+1}, R_{N+1}, Q_{N+1}, \sigma_N^{CALIB^C}, \Delta_N^{BSMH_{N+1}}$	3	7	$7 \times 7 \times 7$	4	117	2%	13%	7%	10%
$M3H4_{N+1}$	$\Delta_{N+1}^{M3H4_{N+1}}$	$S_{N+1}, K_{N+1}, T_{N+1}, R_{N+1}, Q_{N+1}, \sigma_N^{CALIB^C}, BSMGreeks_N^C$	3	11	$11 \times 11 \times 11$	0	72	0%	0%	4%	7%
$M3H5_{N+1}$	$\Delta_{N+1}^{M3H5_{N+1}}$	$S_{N+1}, K_{N+1}, T_{N+1}, R_{N+1}, Q_{N+1}, HParams_N^C, \Delta_N^{HH_{N+1}}$	3	11	$11 \times 11 \times 11$	0	102	0%	0%	6%	9%
$M3H6_{N+1}$	$\Delta_{N+1}^{M3H6_{N+1}}$	$S_{N+1}, K_{N+1}, T_{N+1}, R_{N+1}, Q_{N+1}, HJDParams_N^C, \Delta_N^{HJDH_{N+1}}$	3	14	$14 \times 14 \times 14$	0	105	0%	0%	6%	9%
$M3H7_{N+1}$	$\Delta_{N+1}^{M3H7_{N+1}}$	$S_{N+1}, K_{N+1}, T_{N+1}, R_{N+1}, Q_{N+1}, FMLSParams_N^C, \Delta_N^{FMLSH_{N+1}}$	3	8	$8 \times 8 \times 8$	1	110	0%	5%	7%	10%

Table B.2.7: Delta Comparison (amongst Parametric and $L3H_{N+1}$-Models): This table presents a performance comparison using both daily and monthly statistics amongst the Black-Scholes-Merton ($BSMH_{N+1}$) model, Heston (HH_{N+1}) model, Heston Jump Diffusion ($HJDH_{N+1}$) model, Finite Moment Log Stable ($FMLSH_{N+1}$) model, and the LSTM $L3H_{N+1}$-Models ($L3H1_{N+1}$ to $L3H7_{N+1}$). The forecast variable for the LSTM $L3H_{N+1}$-Models is the delta that is directly forecasted from the respective LSTM model, whereas the delta for the $BSMH_{N+1}$, HH_{N+1}, $HJDH_{N+1}$ models are computed using their respective characteristic functions. The models denoted by the $_{N+1}$ subscript use one-trading-day-ahead input variables for forecasting the delta. Column I identifies the models, column II identifies the forecast variable, column III lists the input variables used by the models to obtain the one-trading-day-ahead forecasts of the delta, and columns IV, V and VI describe the network architecture of the LSTM $L3H_{N+1}$-Models. The one-trading-day-ahead forecast errors of the delta are used to compute the Root Mean Square Error (RMSE). Forecasts are made for 1,326 trading days, and there are 64 months covered in the sample using the monthly data. Column VII reports the number of months out of the 64 months that each model has the smallest RMSE, while column VIII reports the number of days out of the 1,326 days each model has the smallest RMSE. Columns IX (lower bound) and X (upper bound) present the winning percentage out of 64 months for each model, evaluated using the bootstrap sampling technique. The statistical bootstrap performed (with replacement) at a 95% confidence level is computed from the monthly RMSE values of the respective models below. Similarly, in columns XI (lower bound) and XII (upper bound) present the winning percentage out of 1326 days for each model computed from bootstrapping the daily RMSE values of the respective models at a 95% confidence level.

(I) Model	**(II)** Forecast	**(III)** Inputs	**(IV)** No. of hidden Layers	**(V)** No. of hidden nodes per layer	**(VI)** Network architecture	**(VII)** Performance amongst all models (Monthly)	**(VIII)** Performance amongst all models (Daily)	**(IX)** 2.5% lower bound-(for monthly) (%)	**(X)** 2.5% upper bound-(for monthly) (%)	**(XI)** 2.5% lower bound-(for daily) (%)	**(XII)** 2.5% upper bound-(for daily) (%)
$BSMH_{N+1}$	$\Delta_{N+1}^{BSMH_{N+1}}$	$S_{N+1}, K_{N+1}, T_{N+1}, R_{N+1}, Q_{N+1}, \sigma_N^{CALIB^C}$	-	-	-	**50**	**486**	67%	88%	34%	39%
HH_{N+1}	$\Delta_{N+1}^{HH_{N+1}}$	$S_{N+1}, K_{N+1}, T_{N+1}, R_{N+1}, Q_{N+1}, \sigma_N^{CALIB^C}, HParams_N^C$	-	-	-	6	68	3%	17%	4%	6%
$HJDH_{N+1}$	$\Delta_{N+1}^{HJDH_{N+1}}$	$S_{N+1}, K_{N+1}, T_{N+1}, R_{N+1}, Q_{N+1}, \sigma_N^{CALIB^C}, HJDParams_N^C$	-	-	-	0	78	0%	0%	5%	7%
$FMLSH_{N+1}$	$\Delta_{N+1}^{FMLSH_{N+1}}$	$S_{N+1}, K_{N+1}, T_{N+1}, R_{N+1}, Q_{N+1}, FMLSParams_N^C$	-	-	-	0	198	0%	0%	13%	17%
$L3H1_{N+1}$	$\Delta_{N+1}^{L3H1_{N+1}}$	$S_{N+1}, K_{N+1}, T_{N+1}, R_{N+1}, Q_{N+1}, \sigma_N^{CALIB^C}$	3	6	$6 \times 6 \times 6$	0	37	0%	0%	2%	4%
$L3H2_{N+1}$	$\Delta_{N+1}^{L3H2_{N+1}}$	$S_{N+1}, K_{N+1}, T_{N+1}, R_{N+1}, Q_{N+1}, \sigma_N^{CALIB^C}, (\delta C_N/\delta S_N)$	3	7	$7 \times 7 \times 7$	1	49	0%	5%	3%	5%
$L3H3_{N+1}$	$\Delta_{N+1}^{L3H3_{N+1}}$	$S_{N+1}, K_{N+1}, T_{N+1}, R_{N+1}, Q_{N+1}, \sigma_N^{CALIB^C}, \Delta_N^{BSMH_{N+1}}$	3	7	$7 \times 7 \times 7$	0	43	0%	0%	2%	4%
$L3H4_{N+1}$	$\Delta_{N+1}^{L3H4_{N+1}}$	$S_{N+1}, K_{N+1}, T_{N+1}, R_{N+1}, Q_{N+1}, \sigma_N^{CALIB^C}, BSMGreeks_N^C$	3	11	$11 \times 11 \times 11$	5	248	2%	16%	17%	21%
$L3H5_{N+1}$	$\Delta_{N+1}^{L3H5_{N+1}}$	$S_{N+1}, K_{N+1}, T_{N+1}, R_{N+1}, Q_{N+1}, HParams_N^C, \Delta_N^{HH_{N+1}}$	3	11	$11 \times 11 \times 11$	1	51	0%	5%	3%	5%
$L3H6_{N+1}$	$\Delta_{N+1}^{L3H6_{N+1}}$	$S_{N+1}, K_{N+1}, T_{N+1}, R_{N+1}, Q_{N+1}, HJDParams_N^C, \Delta_N^{HJDH_{N+1}}$	3	14	$14 \times 14 \times 14$	1	53	0%	5%	3%	5%
$L3H7_{N+1}$	$\Delta_{N+1}^{L3H7_{N+1}}$	$S_{N+1}, K_{N+1}, T_{N+1}, R_{N+1}, Q_{N+1}, FMLSParams_N^C, \Delta_N^{FMLSH_{N+1}}$	3	8	$8 \times 8 \times 8$	0	28	0%	0%	1%	3%

Table B.2.8: Delta Comparison (amongst Parametric Models): This table presents a performance comparison using both daily and monthly statistics amongst the Black-Scholes-Merton ($BSMH_{N+1}$) model, Heston (HH_{N+1}) model, Heston Jump Diffusion ($HJDH_{N+1}$) model, and the Finite Moment Log Stable ($FMLSH_{N+1}$) model. The delta for the $BSMH_{N+1}$, HH_{N+1}, $HJDH_{N+1}$ models are computed using their respective characteristic functions. The models denoted by the $_{N+1}$ subscript use one-trading-day-ahead input variables for forecasting the delta. The one-trading-day-ahead forecast errors of the delta are used to compute the Root Mean Square Error (RMSE). Forecasts are made for 1,326 trading days, and there are 64 months covered in the sample using the monthly data. Column I identifies the models, column II identifies the forecast variable, and column III lists the input variables used by the models to obtain the one-trading-day-ahead forecasts of the delta. Column IV reports the number of months out of the 64 months that each model has the smallest RMSE, while column V reports lists the number of days out of the 1,326 days that each model has the smallest RMSE. Columns VI (lower bound) and VII (upper bound) present the winning percentage out of 64 months for each model, evaluated using the bootstrap sampling technique. The statistical bootstrap performed (with replacement) at a 95% confidence level is computed from the monthly RMSE values of the respective models below. Similarly, columns VIII (lower bound) and IX (upper bound) present the winning percentage out of 1326 days for each model computed from bootstrapping the daily RMSE values of the respective models at a 95% confidence level.

(I) Model	**(II)** Forecast	**(III)** Inputs	**(IV)** Performance amongst all models (Monthly)	**(V)** Performance amongst all models (Daily)	**(VI)** 2.5% lower bound- (for monthly) (%)	**(VII)** 2.5% upper bound- (for monthly) (%)	**(VIII)** 2.5% lower bound- (for daily) (%)	**(IX)** 2.5% upper bound- (for daily) (%)
$BSMH_{N+1}$	$\Delta_{N+1}^{BSMH_{N+1}}$	$S_{N+1}, K_{N+1}, T_{N+1}, R_{N+1}, Q_{N+1}, \sigma_N^{CALIB^C}$	**58**	**936**	83%	97%	68%	73%
HH_{N+1}	$\Delta_{N+1}^{HH_{N+1}}$	$S_{N+1}, K_{N+1}, T_{N+1}, R_{N+1}, Q_{N+1}, \sigma_N^{CALIB^C}, HParams_N^C$	6	103	3%	17%	6%	9%
$HJDH_{N+1}$	$\Delta_{N+1}^{HJDH_{N+1}}$	$S_{N+1}, K_{N+1}, T_{N+1}, R_{N+1}, Q_{N+1}, \sigma_N^{CALIB^C}, HJDParams_N^C$	0	79	0%	0%	5%	7%
$FMLSH_{N+1}$	$\Delta_{N+1}^{FMLSH_{N+1}}$	$S_{N+1}, K_{N+1}, T_{N+1}, R_{N+1}, Q_{N+1}, FMLSParams_N^C$	0	208	0%	0%	14%	18%

B.2.3 Hedging performance of CH-Models that have analytically derived the delta ($\delta C_{N+1}/\delta S_{N+1}$) from the call option price (C_{N+1}), which is forecasted from models that use one-trading-day-ahead input variables:

Tables B.2.9, B.2.10, B.2.11 and B.2.12 shows the relative out-of-sample hedging performance (in $RMSE$) amongst the models that have analytically derived the delta ($\delta C_{N+1}/\delta S_{N+1}$) using the C_{N+1} which is forecasted from models that use one-trading-day-ahead input variables. For convenience, the models in Tables B.2.9, B.2.10, B.2.11, lists the forecast variable and the input variables are listed in columns II and III, and, the architecture of the MLP and LSTM models in columns IV, V and VI. The performance metric is the $RMSE$ of the one-trading-day-ahead forecast errors of the delta, which is computed for each model utilising all of the errors in each day or each month. Amongst all models, columns VII and VIII record the number of months and days, respectively, that each model has the lowest $RMSE$. To be certain of our results, we performed a bootstrap using the daily and monthly RMSEs. Columns IX (lower bound) and X (upper bound) present the results from the bootstrap performed (with replacement) using monthly RMSEs at a 95% confidence level and show the winning percentage out of 64 months for each model, and similarly, the 95 % confidence intervals computed from bootstrapping of the daily RMSEs signifies the winning percentage out of 1326 days for each model and are reported in columns XI (lower bound), XII (upper bound).

In the below several comparisons, even though a particular model wins by a higher percentage against other models, we investigated further these models pairwise by performing a pairwise bootstrap comparison, which was computed using the respective pair's daily RMSEs. The results are presented in Table 47 of the Electronic Appendix.

Also, we examined the pairwise Diebold-Mariano(DM) (Diebold and Mariano (1995)) tests on these models and have presented the results in Table 41 of the Electronic Appendix. In constructing the DM test statistics, the models listed in the left column represent Model 1, and the models in the first row represent Model 2 in Table 41 of the Electronic Appendix. If the null can be rejected, a positive number suggests the rejection may be due to the second model being the better forecast model. In contrast, a negative value suggests the rejection may be due to the first model being the better forecast model. The model pairs highlighted in a red state that their forecasts have statistically insignificant differences in their prediction accuracy. The following model pairs have been shown to have statistically insignificant differences: ($M3CH3_{N+1}$, $M3CH4_{N+1}$), ($M3CH4_{N+1}$, $M3CH6_{N+1}$), ($M3CH4_{N+1}$, $M3CH7_{N+1}$), and ($HJDCH_{N+1}$, $M3CH7_{N+1}$).

The RMSEs for the models that have analytically derived the $\delta C_{N+1}/\delta S_{N+1}$ from C_{N+1} which is forecasted from models that use one-trading-day-ahead input variables on a monthly, yearly, and overall basis can be found in the Electronic Appendix, in Tables 23, 29, and 35, respectively.

In this section, we compare the out-of-sample hedging performance of the parametric models ($BSMCH_{N+1}$, HCH_{N+1}, $HJDCH_{N+1}$, and $FMLSCH_{N+1}$), the triple hidden layer MLP models ($M3CH_{N+1} - Models$) and triple hidden layer LSTM models ($L3CH_{N+1} - Models$), then the parametric models with the $M3CH_{N+1} - Models$, and finally the parametric models with the $L3CH_{N+1} - Models$. The results for the parametric models with the triple hidden layer MLP $M3CH_{N+1} - Models$ ($M3CH1_{N+1}$ to $M3CH7_{N+1}$) and the triple hidden layer LSTM $L3CH_{N+1} - Models$ ($L3CH1_{N+1}$ to $L3CH7_{N+1}$) are presented in Table B.2.9. If all the models are compared together, then the $L3CH4_{N+1}$ model had the lowest $RMSE$ for 274 days (having a daily bootstrap winning % of 19% to 23%) out of 1,326 days. Table B.2.10 presents the results for the comparison of the parametric models with the triple hidden layer MLP $M3CH_N - Models$ ($M3CH1_N$ to $M3CH7_N$), and the $FMLSCH_{N+1}$ model had the lowest $RMSE$ for 226 days (having a daily bootstrap winning % of 15% to 19%) out of 1,326 days. Though the $FMLSCH_{N+1}$ model had out-performed other models, a variant of the MLP model, the $M3CH4_{N+1}$(182 days) had shown a daily bootstrap winning percentage from 12% to 16%. We present the comparison results of the parametric models with the triple hidden layer LSTM $L3CH_{N+1}-Models$ ($L3CH1_{N+1}$ to $L3CH7_{N+1}$) in Table B.2.11. We find that the $HDJCH_{N+1}$ model had the lowest $RMSE$ for 385 days (having a daily bootstrap winning % of 27% to 32%) out of 1,326 days. Though the $HJDCH_{N+1}$ model had out-performed other models, a variant of the LSTM model, the $L3CH4_{N+1}$(307 days), have shown similar out-performance, where it had a daily bootstrap winning percentage from 21% to 25%. Finally, we compare amongst the parametric models in Table B.2.12, and find that, yet again the $HJDCH_{N+1}$ model had the lowest $RMSE$ for 475 days (having a daily bootstrap winning % of 34% to 39%) out of 1,326 days.

Thus, when the parametric models are compared with the triple hidden layer ANN models that use one-trading-day-ahead input variables to forecast the call option price (C_{N+1}), from which the delta($\delta C_{N+1}/\delta S_{N+1}$) is analytically computed using the forecasted C_{N+1} (in Table B.2.9), we conclude that an LSTM model ($L3CH4_{N+1}$) could outperform all other models. If the parametric models were compared with the triple hidden layer MLP models (in Table B.2.10), a parametric model ($FMLSCH_{N+1}$) outperforms all other triple hidden layer MLP models, also when the parametric models were compared with the triple hidden layer LSTM models (in Table B.2.11), a parametric model ($HJDCH_{N+1}$) outperforms them all. Finally, when a comparison is made amongst the parametric models, the $HJDCH_{N+1}$ model has been shown to outperform the rest of the parametric models.

Table B.2.9: Delta Comparison (amongst Parametric, $M3CH_{N+1}$-Models and $L3CH_{N+1}$-Models): This table presents a performance comparison using both daily and monthly statistics amongst the Black-Scholes-Merton ($BSMCH_{N+1}$) model, Heston (HCH_{N+1}) model, Heston Jump Diffusion ($HJDCH_{N+1}$) model, Finite Moment Log Stable ($FMLSCH_{N+1}$) model, MLP $M3CH_{N+1}$-Models ($M3CH1_{N+1}$ to $M3CH7_{N+1}$) and the LSTM $L3CH_{N+1}$-Models ($L3CH1_{N+1}$ to $L3CH7_{N+1}$). The forecast variable for all the models is the call option price (C_{N+1}). The models denoted by the $_{N+1}$ subscript use one-trading-day-ahead input variables to forecast the C_{N+1}. The delta ($\delta C_{N+1}/\delta S_{N+1}$) is then derived analytically from the forecasted call option price (C_{N+1}) using equation 3.3. The one-trading-day-ahead forecast errors of the delta are used to compute the Root Mean Square Error (RMSE). Column I identifies the models, column II identifies the forecast variable, column III lists the input variables used by the models to obtain the one-trading-day-ahead forecast of C_{N+1}, and columns IV, V and VI describe the network architecture of the MLP $M3CH_{N+1}$-Models and the LSTM $L3CH_{N+1}$-Models. Forecasts are made for 1,326 trading days, and there are 64 months covered in the sample using the monthly data. Column VII reports the number of months out of the 64 months that each model has the smallest RMSE, while column VIII reports the number of days out of the 1,326 days each model has the smallest RMSE. Columns IX (lower bound) and X (upper bound) present the winning percentage out of 64 months for each model, evaluated using the bootstrap sampling technique. The statistical bootstrap performed (with replacement) at a 95% confidence level is computed from the monthly RMSE values of the respective models below. Similarly, columns XI (lower bound) and XII (upper bound) present the winning percentage out of 1326 days for each model computed from bootstrapping the daily RMSE values of the respective models at a 95% confidence level.

(I) Model	**(II)** Forecast	**(III)** Inputs	**(IV)** No. of hidden Layers	**(V)** No. of hidden nodes per layer	**(VI)** Network architecture	**(VII)** Performance amongst all models (Monthly)	**(VIII)** Performance amongst all models (Daily)	**(IX)** 2.5% lower bound-(for monthly) (%)	**(X)** 2.5% upper bound-(for monthly) (%)	**(XI)** 2.5% lower bound-(for daily) (%)	**(XII)** 2.5% upper bound-(for daily) (%)
$BSMCH_{N+1}$	$C_{N+1}^{BSMCH_{N+1}}$	$S_{N+1}, K_{N+1}, T_{N+1}, R_{N+1}, Q_{N+1}, \sigma_N^{CALIB^C}$	-	-	-	0	77	0%	0%	4%	7%
HCH_{N+1}	$C_{N+1}^{HCH_{N+1}}$	$S_{N+1}, K_{N+1}, T_{N+1}, R_{N+1}, Q_{N+1}, \sigma_N^{CALIB^C}, HParams_N^C$	-	-	-	1	77	0%	5%	5%	7%
$HJDCH_{N+1}$	$C_{N+1}^{HJDCH_{N+1}}$	$S_{N+1}, K_{N+1}, T_{N+1}, R_{N+1}, Q_{N+1}, \sigma_N^{CALIB^C}, HJDParams_N^C$	-	-	-	2	39	0%	8%	2%	4%
$FMLSCH_{N+1}$	$C_{N+1}^{FMLSCH_{N+1}}$	$S_{N+1}, K_{N+1}, T_{N+1}, R_{N+1}, Q_{N+1}, FMLSParams_N^C$	-	-		0	120	0%	0%	8%	11%
$M3CH1_{N+1}$	$C_{N+1}^{M3CH1_{N+1}}$	$S_{N+1}, K_{N+1}, T_{N+1}, R_{N+1}, Q_{N+1}, \sigma_N^{CALIB^C}$	3	6	6 X 6 X 6	3	69	0%	11%	4%	6%
$M3CH2_{N+1}$	$C_{N+1}^{M3CH2_{N+1}}$	$S_{N+1}, K_{N+1}, T_{N+1}, R_{N+1}, Q_{N+1}, \sigma_N^{CALIB^C}, (\delta C_N/\delta S_N)$	3	7	7 X 7 X 7	5	72	2%	16%	4%	7%
$M3CH3_{N+1}$	$C_{N+1}^{M3CH3_{N+1}}$	$S_{N+1}, K_{N+1}, T_{N+1}, R_{N+1}, Q_{N+1}, \sigma_N^{CALIB^C}, \delta_N^{BSMCH_{N+1}}$	3	7	7 X 7 X 7	4	80	2%	13%	5%	7%
$M3CH4_{N+1}$	$C_{N+1}^{M3CH4_{N+1}}$	$S_{N+1}, K_{N+1}, T_{N+1}, R_{N+1}, Q_{N+1}, \sigma_N^{CALIB^C}, BSMGreeks_N^C$	3	11	11 X 11 X 11	8	137	5%	22%	9%	12%
$M3CH5_{N+1}$	$C_{N+1}^{M3CH5_{N+1}}$	$S_{N+1}, K_{N+1}, T_{N+1}, R_{N+1}, Q_{N+1}, HParams_N^C, \delta_N^{HCH_{N+1}}$	3	11	11 X 11 X 11	**20**	107	20%	44%	7%	10%
$M3CH6_{N+1}$	$C_{N+1}^{M3CH6_{N+1}}$	$S_{N+1}, K_{N+1}, T_{N+1}, R_{N+1}, Q_{N+1}, HJDParams_N^C, \delta_N^{HJDCH_{N+1}}$	3	14	14 X 14 X 14	7	80	5%	19%	5%	7%
$M3CH7_{N+1}$	$C_{N+1}^{M3CH7_{N+1}}$	$S_{N+1}, K_{N+1}, T_{N+1}, R_{N+1}, Q_{N+1}, FMLSParams_N^C, \delta_N^{FMLSCH_{N+1}}$	3	8	8 X 8 X 8	14	87	12%	33%	5%	8%
$L3CH1_{N+1}$	$C_{N+1}^{L3CH1_{N+1}}$	$S_{N+1}, K_{N+1}, T_{N+1}, R_{N+1}, Q_{N+1}, \sigma_N^{CALIB^C}$	3	6	6 X 6 X 6	0	19	0%	0%	1%	2%
$L3CH2_{N+1}$	$C_{N+1}^{L3CH2_{N+1}}$	$S_{N+1}, K_{N+1}, T_{N+1}, R_{N+1}, Q_{N+1}, \sigma_N^{CALIB^C}, (\delta C_N/\delta S_N)$	3	7	7 X 7 X 7	0	13	0%	0%	1%	2%
$L3CH3_{N+1}$	$C_{N+1}^{L3CH3_{N+1}}$	$S_{N+1}, K_{N+1}, T_{N+1}, R_{N+1}, Q_{N+1}, \sigma_N^{CALIB^C}, \delta_N^{BSMCH_{N+1}}$	3	7	7 X 7 X 7	0	15	0%	0%	1%	2%
$L3CH4_{N+1}$	$C_{N+1}^{L3CH4_{N+1}}$	$S_{N+1}, K_{N+1}, T_{N+1}, R_{N+1}, Q_{N+1}, \sigma_N^{CALIB^C}, BSMGreeks_N^C$	3	11	11 X 11 X 11	0	**274**	0%	0%	19%	23%
$L3CH5_{N+1}$	$C_{N+1}^{L3CH5_{N+1}}$	$S_{N+1}, K_{N+1}, T_{N+1}, R_{N+1}, Q_{N+1}, HParams_N^C, \delta_N^{HCH_{N+1}}$	3	11	11 X 11 X 11	0	19	0%	0%	1%	2%
$L3CH6_{N+1}$	$C_{N+1}^{L3CH6_{N+1}}$	$S_{N+1}, K_{N+1}, T_{N+1}, R_{N+1}, Q_{N+1}, HJDParams_N^C, \delta_N^{HJDCH_{N+1}}$	3	14	14 X 14 X 14	0	33	0%	0%	2%	3%
$L3CH7_{N+1}$	$C_{N+1}^{L3CH7_{N+1}}$	$S_{N+1}, K_{N+1}, T_{N+1}, R_{N+1}, Q_{N+1}, FMLSParams_N^C, \delta_N^{FMLSCH_{N+1}}$	3	8	8 X 8 X 8	0	6	0%	0%	0%	1%

Table B.2.10: Delta Comparison (amongst Parametric and $M3CH_{N+1}$-Models): This table presents a performance comparison using both daily and monthly statistics amongst the Black-Scholes-Merton ($BSMCH_{N+1}$) model, Heston (HCH_{N+1}) model, Heston Jump Diffusion ($HJDCH_{N+1}$) model, Finite Moment Log Stable ($FMLSCH_{N+1}$) model, and the MLP $M3CH_{N+1}$-Models ($M3CH1_{N+1}$ to $M3CH7_{N+1}$). The forecast variable for all the models is the call option price (C_{N+1}). The models denoted by the $_{N+1}$ subscript use one-trading-day-ahead input variables to forecast the C_{N+1}. The delta ($\delta C_{N+1}/\delta S_{N+1}$) is then derived analytically from the forecasted call option price (C_{N+1}) using equation 3.3. The one-trading-day-ahead forecast errors of the delta are used to compute the Root Mean Square Error (RMSE). Column I identifies the models, column II identifies the forecast variable, column III lists the input variables used by the models to obtain the one-trading-day-ahead forecast of C_{N+1}, and columns IV, V and VI describe the network architecture of the MLP $M3CH_{N+1}$-Models and the LSTM $L3CH_{N+1}$-Models. Forecasts are made for 1,326 trading days, and there are 64 months covered in the sample using the monthly data. Column VII reports the number of months out of the 64 months that each model has the smallest RMSE, while column VIII reports the number of days out of the 1,326 days each model has the smallest RMSE. Columns IX (lower bound) and X (upper bound) present the winning percentage out of 64 months for each model, evaluated using the bootstrap sampling technique. The statistical bootstrap performed (with replacement) at a 95% confidence level is computed from the monthly RMSE values of the respective models below. Similarly, in columns XI (lower bound), XII (upper bound) presents the winning percentage out of 1326 days for each model computed from bootstrapping the daily RMSE values of the respective models at a 95% confidence level.

(I) Model	**(II)** Forecast	**(III)** Inputs	**(IV)** No. of hidden Layers	**(V)** No. of hidden nodes per layer	**(VI)** Network architecture	**(VII)** Performance amongst all models (Monthly)	**(VIII)** Performance amongst all models (Daily)	**(IX)** 2.5% lower bound- (for monthly) (%)	**(X)** 2.5% upper bound- (for monthly) (%)	**(XI)** 2.5% lower bound- (for daily) (%)	**(XII)** 2.5% upper bound- (for daily) (%)
$BSMCH_{N+1}$	$C_{N+1}^{BSMCH_{N+1}}$	$S_{N+1}, K_{N+1}, T_{N+1}, R_{N+1}, Q_{N+1}, \sigma_N^{CALIB^C}$	-	-	-	0	122	0%	0%	8%	11%
HCH_{N+1}	$C_{N+1}^{HCH_{N+1}}$	$S_{N+1}, K_{N+1}, T_{N+1}, R_{N+1}, Q_{N+1}, \sigma_N^{CALIB^C}, HParams_N^C$	-	-	-	1	112	0%	5%	7%	10%
$HJDCH_{N+1}$	$C_{N+1}^{HJDCH_{N+1}}$	$S_{N+1}, K_{N+1}, T_{N+1}, R_{N+1}, Q_{N+1}, \sigma_N^{CALIB^C}, HJDParams_N^C$	-	-	-	2	50	0%	8%	3%	5%
$FMLSCH_{N+1}$	$C_{N+1}^{FMLSCH_{N+1}}$	$S_{N+1}, K_{N+1}, T_{N+1}, R_{N+1}, Q_{N+1}, FMLSParams_N^C$	-	-		0	**226**	0%	0%	15%	19%
$M3CH1_{N+1}$	$C_{N+1}^{M3CH1_{N+1}}$	$S_{N+1}, K_{N+1}, T_{N+1}, R_{N+1}, Q_{N+1}, \sigma_N^{CALIB^C}$	3	6	6 X 6 X 6	3	92	0%	11%	6%	8%
$M3CH2_{N+1}$	$C_{N+1}^{M3CH2_{N+1}}$	$S_{N+1}, K_{N+1}, T_{N+1}, R_{N+1}, Q_{N+1}, \sigma_N^{CALIB^C}, (\delta C_N/\delta S_N)$	3	7	7 X 7 X 7	5	97	2%	14%	6%	9%
$M3CH3_{N+1}$	$C_{N+1}^{M3CH3_{N+1}}$	$S_{N+1}, K_{N+1}, T_{N+1}, R_{N+1}, Q_{N+1}, \sigma_N^{CALIB^C}, \delta_N^{BSMCH_{N+1}}$	3	7	7 X 7 X 7	4	116	2%	13%	7%	10%
$M3CH4_{N+1}$	$C_{N+1}^{M3CH4_{N+1}}$	$S_{N+1}, K_{N+1}, T_{N+1}, R_{N+1}, Q_{N+1}, \sigma_N^{CALIB^C}, BSMGreeks_N^C$	3	11	11 X 11 X 11	8	182	5%	22%	12%	16%
$M3CH5_{N+1}$	$C_{N+1}^{M3CH5_{N+1}}$	$S_{N+1}, K_{N+1}, T_{N+1}, R_{N+1}, Q_{N+1}, HParams_N^C, \delta_N^{HCH_{N+1}}$	3	11	11 X 11 X 11	**20**	128	20%	44%	8%	11%
$M3CH6_{N+1}$	$C_{N+1}^{M3CH6_{N+1}}$	$S_{N+1}, K_{N+1}, T_{N+1}, R_{N+1}, Q_{N+1}, HJDParams_N^C, \delta_N^{HJDCH_{N+1}}$	3	14	14 X 14 X 14	7	94	5%	19%	6%	8%
$M3CH7_{N+1}$	$C_{N+1}^{M3CH7_{N+1}}$	$S_{N+1}, K_{N+1}, T_{N+1}, R_{N+1}, Q_{N+1}, FMLSParams_N^C, \delta_N^{FMLSCH_{N+1}}$	3	8	8 X 8 X 8	14	105	13%	33%	6%	9%

Table B.2.11: Delta Comparison (amongst Parametric and $L3CH_{N+1}$-Models): This table presents a performance comparison using both daily and monthly statistics amongst the Black-Scholes-Merton ($BSMCH_{N+1}$) model, Heston (HCH_{N+1}) model, Heston Jump Diffusion ($HJDCH_{N+1}$) model, Finite Moment Log Stable ($FMLSCH_{N+1}$) model, and the LSTM $L3CH_{N+1}$-Models ($L3CH1_{N+1}$ to $L3CH7_{N+1}$). The forecast variable for all the models is the call option price (C_{N+1}). The models denoted by the $_{N+1}$ subscript use one-trading-day-ahead input variables to forecast the C_{N+1}. The delta ($\delta C_{N+1}/\delta S_{N+1}$) is then derived analytically from the forecasted call option price (C_{N+1}) using equation 3.3. The one-trading-day-ahead forecast errors of the delta are used to compute the Root Mean Square Error (RMSE). Column I identifies the models, column II identifies the forecast variable, column III lists the input variables used by the models to obtain the one-trading-day-ahead forecast of C_{N+1}, and columns IV, V and VI describe the network architecture of the MLP $M3CH_{N+1}$-Models and the LSTM $L3CH_{N+1}$-Models. Forecasts are made for 1,326 trading days, and there are 64 months covered in the sample using the monthly data. Column VII reports the number of months out of the 64 months that each model has the smallest RMSE, while column VIII reports the number of days out of the 1,326 days each model has the smallest RMSE. Columns IX (lower bound) and X (upper bound) present the winning percentage out of 64 months for each model, evaluated using the bootstrap sampling technique. The statistical bootstrap performed (with replacement) at a 95% confidence level is computed from the monthly RMSE values of the respective models below. Similarly, in columns XI (lower bound), XII (upper bound) presents the winning percentage out of 1326 days for each model computed from bootstrapping the daily RMSE values of the respective models at a 95% confidence level.

(I) Model	**(II)** Forecast	**(III)** Inputs	**(IV)** No. of hidden Layers	**(V)** No. of hidden nodes per layer	**(VI)** Network architecture	**(VII)** Performance amongst all models (Monthly)	**(VIII)** Performance amongst all models (Daily)	**(IX)** 2.5% lower bound-(for monthly) (%)	**(X)** 2.5% upper bound-(for monthly) (%)	**(XI)** 2.5% lower bound-(for daily) (%)	**(XII)** 2.5% upper bound-(for daily) (%)
$BSMCH_{N+1}$	$C_{N+1}^{BSMCH_{N+1}}$	$S_{N+1}, K_{N+1}, T_{N+1}, R_{N+1}, Q_{N+1}, \sigma_N^{CALIB^C}$	-	-	-	0	84	0%	0%	5%	8%
HCH_{N+1}	$C_{N+1}^{HCH_{N+1}}$	$S_{N+1}, K_{N+1}, T_{N+1}, R_{N+1}, Q_{N+1}, \sigma_N^{CALIB^C}, HParams_N^C$	-	-	-	4	255	2%	13%	17%	21%
$HJDCH_{N+1}$	$C_{N+1}^{HJDCH_{N+1}}$	$S_{N+1}, K_{N+1}, T_{N+1}, R_{N+1}, Q_{N+1}, \sigma_N^{CALIB^C}, HJDParams_N^C$	-	-	-	**60**	**385**	88%	98%	27%	32%
$FMLSCH_{N+1}$	$C_{N+1}^{FMLSCH_{N+1}}$	$S_{N+1}, K_{N+1}, T_{N+1}, R_{N+1}, Q_{N+1}, FMLSParams_N^C$	-	-		0	186	0%	0%	12%	16%
$L3CH1_{N+1}$	$C_{N+1}^{L3CH1_{N+1}}$	$S_{N+1}, K_{N+1}, T_{N+1}, R_{N+1}, Q_{N+1}, \sigma_N^{CALIB^C}$	3	6	6 X 6 X 6	0	20	0%	0%	1%	2%
$L3CH2_{N+1}$	$C_{N+1}^{L3CH2_{N+1}}$	$S_{N+1}, K_{N+1}, T_{N+1}, R_{N+1}, Q_{N+1}, \sigma_N^{CALIB^C}, (\delta C_N/\delta S_N)$	3	7	7 X 7 X 7	0	13	0%	0%	1%	2%
$L3CH3_{N+1}$	$C_{N+1}^{L3CH3_{N+1}}$	$S_{N+1}, K_{N+1}, T_{N+1}, R_{N+1}, Q_{N+1}, \sigma_N^{CALIB^C}, \delta_N^{BSMCH_{N+1}}$	3	7	7 X 7 X 7	0	15	0%	0%	1%	2%
$L3CH4_{N+1}$	$C_{N+1}^{L3CH4_{N+1}}$	$S_{N+1}, K_{N+1}, T_{N+1}, R_{N+1}, Q_{N+1}, \sigma_N^{CALIB^C}, BSMGreeks_N^C$	3	11	11 X 11 X 11	0	307	0%	0%	21%	25%
$L3CH5_{N+1}$	$C_{N+1}^{L3CH5_{N+1}}$	$S_{N+1}, K_{N+1}, T_{N+1}, R_{N+1}, Q_{N+1}, HParams_N^C, \delta_N^{HCH_{N+1}}$	3	11	11 X 11 X 11	0	20	0%	0%	1%	2%
$L3CH6_{N+1}$	$C_{N+1}^{L3CH6_{N+1}}$	$S_{N+1}, K_{N+1}, T_{N+1}, R_{N+1}, Q_{N+1}, HJDParams_N^C, \delta_N^{HJDCH_{N+1}}$	3	14	14 X 14 X 14	0	33	0%	0%	2%	3%
$L3CH7_{N+1}$	$C_{N+1}^{L3CH7_{N+1}}$	$S_{N+1}, K_{N+1}, T_{N+1}, R_{N+1}, Q_{N+1}, FMLSParams_N^C, \delta_N^{FMLSCH_{N+1}}$	3	8	8 X 8 X 8	0	6	0%	0%	0%	1%

Table B.2.12: Delta Comparison (amongst Parametric Models): This table presents a performance comparison using both daily and monthly statistics amongst the Black-Scholes-Merton ($BSMCH_{N+1}$) model, Heston (HCH_{N+1}) model, Heston Jump Diffusion ($HJDCH_{N+1}$) model, and the Finite Moment Log Stable ($FMLSCH_{N+1}$) model. The forecast variable for all the models is the call option price (C_{N+1}). The models denoted by the $_{N+1}$ subscript use one-trading-day-ahead input variables to forecast the C_{N+1}. The delta ($\delta C_{N+1}/\delta S_{N+1}$) is then derived analytically from the forecasted call option price (C_{N+1}) using equation 3.3. The one-trading-day-ahead forecast errors of the delta are used to compute the Root Mean Square Error (RMSE). Column I identifies the models, column II identifies the forecast variable, column III lists the input variables used by the models to obtain the one-trading-day-ahead forecast of C_{N+1}. Forecasts are made for 1,326 trading days, and there are 64 months covered in the sample using the monthly data. Column IV reports the number of months out of the 64 months that each model has the smallest RMSE, while column V reports the number of days out of the 1,326 days each model has the smallest RMSE. Columns VI (lower bound) and VII (upper bound) present the winning percentage out of 64 months for each model, evaluated using the bootstrap sampling technique. The statistical bootstrap performed (with replacement) at a 95% confidence level is computed from the monthly RMSE values of the respective models below. Similarly, in columns VIII (lower bound), IX (upper bound) presents the winning percentage out of 1326 days for each model computed from bootstrapping the daily RMSE values of the respective models at a 95% confidence level.

(I) Model	**(II)** Forecast	**(III)** Inputs	**(IV)** Performance amongst all models (Monthly)	**(V)** Performance amongst all models (Daily)	**(VI)** 2.5% lower bound- (for monthly) (%)	**(VII)** 2.5% upper bound- (for monthly) (%)	**(VIII)** 2.5% lower bound- (for daily) (%)	**(IX)** 2.5% upper bound- (for daily) (%)
$BSMCH_{N+1}$	$C_{N+1}^{BSMCH_{N+1}}$	$S_{N+1}, K_{N+1}, T_{N+1}, R_{N+1}, Q_{N+1}, \sigma_N^{CALIB^C}$	0	135	0%	0%	9%	12%
HCH_{N+1}	$C_{N+1}^{HCH_{N+1}}$	$S_{N+1}, K_{N+1}, T_{N+1}, R_{N+1}, Q_{N+1}, \sigma_N^{CALIB^C}, HParams_N^C$	4	361	2%	13%	25%	30%
$HJDCH_{N+1}$	$C_{N+1}^{HJDCH_{N+1}}$	$S_{N+1}, K_{N+1}, T_{N+1}, R_{N+1}, Q_{N+1}, \sigma_N^{CALIB^C}, HJDParams_N^C$	**60**	**475**	88%	98%	34%	39%
$FMLSCH_{N+1}$	$C_{N+1}^{FMLSCH_{N+1}}$	$S_{N+1}, K_{N+1}, T_{N+1}, R_{N+1}, Q_{N+1}, FMLSParams_N^C$	0	353	0%	0%	24%	29%

B.2.4 Replicating portfolio value performance of HV-Models that forecast the replicating portfolio value(V_{N+1}), computed using the delta from H-Models that use lagged input variables:

Tables B.2.13, B.2.14, B.2.15 and B.2.16 shows the relative out-of-sample replicating portfolio value performance (in $RMSE$) amongst the models that forecast the one-trading-day-ahead replicating portfolio value (V_{N+1}). The V_{N+1} is computed from equation 3.17 using the forecasted one-trading-day-ahead delta from models that use lagged input variables. For convenience, the models in Tables B.2.13, B.2.14, B.2.15, lists the forecast variable and the input variables are listed in columns II and III, and the architecture of the MLP and LSTM models in columns IV, V and VI. The performance metric is the $RMSE$ of the one-trading-day-ahead forecast errors of V_{N+1}, which is computed for each model utilising all of the errors in each day or each month. Amongst all models, columns VII and VIII record the number of months and days, respectively, that each model has the lowest $RMSE$. We performed a bootstrap using the daily and monthly RMSEs to be certain of our results. Columns IX (lower bound) and X (upper bound) present the results from the bootstrap performed (with replacement) using monthly RMSEs at a 95% confidence level and show the winning percentage out of 64 months for each model, and similarly, the 95 % confidence intervals computed from bootstrapping of the daily RMSEs signifies the winning percentage out of 1326 days for each model and are reported in columns XI (lower bound), XII (upper bound).

In the below several comparisons, even though a particular model wins by a higher percentage against other models, we investigated further these models pairwise by performing a pairwise bootstrap comparison, which was computed using the respective pair's daily RMSEs. The results are presented in Table 48 of the Electronic Appendix. Also, we examined the pairwise Diebold-Mariano(DM) (Diebold and Mariano (1995)) tests on these models and have presented the results in Table 42 of the Electronic Appendix. In constructing the DM test statistics, the models listed in the left column represent Model 1, and the models in the first row represent Model 2 in Table 42 of the Electronic Appendix. If the null can be rejected, a positive number suggests the rejection may be due to the second model being the better forecast model. In contrast, a negative value suggests the rejection may be due to the first model being the better forecast model. The model pairs highlighted in a red state that their forecasts have statistically insignificant differences in their prediction accuracy. The following model pairs have been shown to have statistically insignificant differences: ($BSMHV_N$, $M3HV2_N$), and (HHV_N, $L3HV4N_N$). The RMSEs for the models that use lagged input variables to forecast the V_{N+1} on a monthly, yearly, and overall basis can be found in the Electronic Appendix, in Tables 24, 30, and 36, respectively.

In this section, we compare the out-of-sample replicating portfolio value performance of the parametric models ($BSMHV_N$, HHV_N, $HJDHV_N$, and $FMLSHV_N$), the triple hidden layer MLP models ($M3HV_N - Models$) and triple hidden layer LSTM models ($L3HV_N - Models$), then the parametric models with the $M3HV_N - Models$, and finally the parametric models with the $L3HV_N - Models$.

The results for the parametric models with the triple hidden layer MLP $M3HV_N - Models$ ($M3HV1_N$ to $M3HV7_N$) and the triple hidden layer LSTM $L3HV_N - Models$ ($L3HV1_N$ to $L3HV7_N$) are presented in Table B.2.13. If all the models are compared together, then the $BSMHV_N$ model had the lowest $RMSE$ for 166 days (having a daily bootstrap winning % of

11% to 14%) out of 1,326 days. Although the $BSMHV_N$ model had outperformed other models, the $FMLSHV_N$(162 days), and the $M3HV1_N$(137 days) have shown similar outperformance, where they have a collective daily bootstrap winning percentage from 9% (lower bound for the $M3HV1_N$ model) to 14%. (upper bound for the $FMLSHV_N$ model). Table B.2.14 presents the results for the comparison of the parametric models with the triple hidden layer MLP $M3HV_N - Models$ ($M3HV1_N$ to $M3HV7_N$), and the $BSMHV_N$ model had the lowest $RMSE$ for 188 days (having a daily bootstrap winning % of 12% to 16%) out of 1,326 days. Though the $BSMHV_N$ model had outperformed other models, the $FMLSHV_N$(166 days), $M3HV1_N$(169 days), and the $M3HV2_N$(143 days) have shown similar outperformance, where they have a collective daily bootstrap winning percentage from 9% (lower bound for the $M3H2V_N$ model) to 14%. (upper bound for the $M3HV1_N$ model). We present the comparison results of the parametric models with the triple hidden layer LSTM $L3HV_N - Models$ ($L3HV1_N$ to $L3HV7_N$) in Table B.2.15. We find that the $BSMHV_N$ model had the lowest $RMSE$ for 451 days (having a daily bootstrap winning % of 31% to 37%) out of 1,326 days. Finally, we compare amongst the parametric models in Table B.2.16 and find that the $BSMHV_N$ model had the lowest $RMSE$ for 909 days (having a daily bootstrap winning % of 66% to 71%) out of 1,326 days.

Thus, when the parametric models are compared with the triple hidden layer ANN models that use lagged input variables to forecast the replicating portfolio value(in Table B.2.13), we conclude that a parametric model ($BSMHV_N$) could outperform all models. If the parametric models were compared with the triple hidden layer MLP models (in Table B.2.14), a parametric model ($BSMHV_N$) outperforms all the triple hidden layer MLP models, also when the parametric models were compared with the triple hidden layer LSTM models (in Table B.2.15), a parametric model ($BSMHV_N$) still outperforms them all. Finally, when a comparison is made amongst parametric models, the $BSMHV_N$ model has been shown to outperform the rest of the parametric models.

Table B.2.13: Replicating Portfolio Value Comparison (amongst Parametric, $M3HV_N$-Models and $L3HV_N$-Models): This table presents a performance comparison using both daily and monthly statistics amongst the Black-Scholes-Merton ($BSMHV_N$) model, Heston (HHV_N) model, Heston Jump Diffusion ($HJDHV_N$) model, Finite Moment Log Stable ($FMLSHV_N$) model, MLP $M3HV_N$-Models ($M3HV1_N$ to $M3HV7_N$) and the LSTM $L3HV_N$-Models ($L3HV1_N$ to $L3HV7_N$). The forecast variable for the MLP $M3HV_N$-Models and LSTM $L3HV_N$-Models is the delta that is directly forecasted from the respective ANN model, whereas the delta for the $BSMHV_N$, HHV_N, $HJDHV_N$ models are computed using their respective characteristic functions. The models denoted by the $_N$ subscript use lagged input variables for forecasting the delta. The forecasted delta is later used to compute the replicating portfolio value V_{N+1} using equation 3.17. The one-trading-day-ahead forecast errors of V_{N+1} are used to compute the Root Mean Square Error (RMSE). Column I identifies the models, column II identifies the forecast variable, and column III lists the input variables used by the models to obtain the V_{N+1}. Forecasts are made for 1,326 trading days, and there are 64 months covered in the sample using the monthly data. Column VII reports the number of months out of the 64 months that each model has the smallest RMSE, while column VIII reports the number of days out of the 1,326 days each model has the smallest RMSE. Columns IX (lower bound) and X (upper bound) present the winning percentage out of 64 months for each model, evaluated using the bootstrap sampling technique. The statistical bootstrap performed (with replacement) at a 95% confidence level is computed from the monthly RMSE values of the respective models below. Similarly, columns XI (lower bound) and XII (upper bound) present the winning percentage out of 1326 days for each model computed from bootstrapping the daily RMSE values of the respective models at a 95% confidence level.

(I) Model	**(II) Forecast**	**(III) Inputs**	**(IV) Performance amongst all models (Monthly)**	**(V) Performance amongst all models (Daily)**	**(VI) 2.5% lower bound-(for monthly) (%)**	**(VII) 2.5% upper bound-(for monthly) (%)**	**(VIII) 2.5% lower bound-(for daily) (%)**	**(IX) 2.5% upper bound-(for daily) (%)**
$BSMHV_N$	$V_{N+1}^{BSMHV_N}$	$S_{N+1}, S_N, R_{N+1}, \delta t, C_N^{BSMH_N}, C_{N+1}^{BSMH_N}, \Delta_{N+1}^{BSMH_N}$	3	**166**	0%	10%	11%	14%
HHV_N	$V_{N+1}^{HHV_N}$	$S_{N+1}, S_N, R_{N+1}, \delta t, C_N^{HH_N}, C_{N+1}^{HH_N}, \Delta_{N+1}^{HH_N}$	6	66	3%	17%	4%	6%
$HJDHV_N$	$V_{N+1}^{HJDV_N}$	$S_N, S_{N-1}, R_N, \delta t, C_N^{HJD_N}, C_{N+1}^{HJD_N}, \Delta_{N+1}^{HJD_N}$	1	69	0%	5%	4%	6%
$FMLSHV_N$	$V_{N+1}^{FMLSV_N}$	$S_N, S_{N-1}, R_N, \delta t, C_N^{FMLS_N}, C_{N+1}^{FMLS_N}, \Delta_{N+1}^{FMLS_N}$	1	162	0%	5%	10%	14%
$M3HV1_N$	$V_{N+1}^{M3HV1_N}$	$S_{N+1}, S_N, R_{N+1}, \delta t, C_N^{M3H1_N}, C_{N+1}^{M3H1_N}, \Delta_{N+1}^{M3H1_N}$	7	137	3%	19%	9%	12%
$M3HV2_N$	$V_{N+1}^{M3HV2_N}$	$S_{N+1}, S_N, R_{N+1}, \delta t, C_N^{M3H2_N}, C_{N+1}^{M3H2_N}, \Delta_{N+1}^{M3H2_N}$	5	105	2%	16%	7%	9%
$M3HV3_N$	$V_{N+1}^{M3HV3_N}$	$S_{N+1}, S_N, R_{N+1}, \delta t, C_N^{M3H3_N}, C_{N+1}^{M3H3_N}, \Delta_{N+1}^{M3H3_N}$	5	89	2%	16%	5%	8%
$M3HV4_N$	$V_{N+1}^{M3HV4_N}$	$S_{N+1}, S_N, R_{N+1}, \delta t, C_N^{M3H4_N}, C_{N+1}^{M3H4_N}, \Delta_{N+1}^{M3H4_N}$	5	72	2%	16%	4%	7%
$M3HV5_N$	$V_{N+1}^{M3HV5_N}$	$S_{N+1}, S_N, R_{N+1}, \delta t, C_N^{M3H5_N}, C_{N+1}^{M3H5_N}, \Delta_{N+1}^{M3H5_N}$	8	93	5%	20%	6%	8%
$M3HV6_N$	$V_{N+1}^{M3HV6_N}$	$S_{N+1}, S_N, R_{N+1}, \delta t, C_N^{M3H6_N}, C_{N+1}^{M3H6_N}, \Delta_{N+1}^{M3H6_N}$	4	94	2%	13%	6%	9%
$M3HV7_N$	$V_{N+1}^{M3HV7_N}$	$S_{N+1}, S_N, R_{N+1}, \delta t, C_N^{M3H7_N}, C_{N+1}^{M3H7_N}, \Delta_{N+1}^{M3H7_N}$	**10**	95	8%	25%	6%	9%
$L3HV1_N$	$V_{N+1}^{L3HV1_N}$	$S_{N+1}, S_N, R_{N+1}, \delta t, C_N^{L3H1_N}, C_{N+1}^{L3H1_N}, \Delta_{N+1}^{L3H1_N}$	0	18	0%	0%	1%	2%
$L3HV2_N$	$V_{N+1}^{L3HV2_N}$	$S_{N+1}, S_N, R_{N+1}, \delta t, C_N^{L3H2_N}, C_{N+1}^{L3H2_N}, \Delta_{N+1}^{L3H2_N}$	1	20	0%	5%	1%	2%
$L3HV3_N$	$V_{N+1}^{L3HV3_N}$	$S_{N+1}, S_N, R_{N+1}, \delta t, C_N^{L3H3_N}, C_{N+1}^{L3H3_N}, \Delta_{N+1}^{L3H3_N}$	0	22	0%	0%	1%	2%
$L3HV4_N$	$V_{N+1}^{L3HV4_N}$	$S_{N+1}, S_N, R_{N+1}, \delta t, C_N^{L3H4_N}, C_{N+1}^{L3H4_N}, \Delta_{N+1}^{L3H4_N}$	6	77	3%	16%	5%	7%
$L3HV5_N$	$V_{N+1}^{L3HV5_N}$	$S_{N+1}, S_N, R_{N+1}, \delta t, C_N^{L3H5_N}, C_{N+1}^{L3H5_N}, \Delta_{N+1}^{L3H5_N}$	0	16	0%	0%	1%	2%
$L3HV6_N$	$V_{N+1}^{L3HV6_N}$	$S_{N+1}, S_N, R_{N+1}, \delta t, C_N^{L3H6_N}, C_{N+1}^{L3H6_N}, \Delta_{N+1}^{L3H6_N}$	1	20	0%	5%	1%	2%
$L3HV7_N$	$V_{N+1}^{L3HV7_N}$	$S_{N+1}, S_N, R_{N+1}, \delta t, C_N^{L3H7_N}, C_{N+1}^{L3H7_N}, \Delta_{N+1}^{L3H7_N}$	1	15	0%	5%	0%	2%

Table B.2.14: Replicating Portfolio Value Comparison (amongst Parametric and $M3HV_N$-Models): This table presents a performance comparison using both daily and monthly statistics amongst the Black-Scholes-Merton ($BSMHV_N$) model, Heston (HHV_N) model, Heston Jump Diffusion ($HJDHV_N$) model, Finite Moment Log Stable ($FMLSHV_N$) model, and the MLP $M3HV_N$-Models ($M3HV1_N$ to $M3HV7_N$). The forecast variable for the MLP $M3HV_N$-Models and LSTM $L3HV_N$-Models is the delta that is directly forecasted from the respective MLP model, whereas the delta for the $BSMHV_N$, HHV_N, $HJDHV_N$ models are computed using their respective characteristic functions. The models denoted by the $_N$ subscript use lagged input variables for forecasting the delta. The forecasted delta is later used to compute the replicating portfolio value V_{N+1} using equation 3.17. The one-trading-day-ahead forecast errors of V_{N+1} are used to compute the Root Mean Square Error (RMSE). Column I identifies the models, column II identifies the forecast variable, and column III lists the input variables used by the models to obtain the V_{N+1}. Forecasts are made for 1,326 trading days, and there are 64 months covered in the sample using the monthly data. Column VII reports the number of months out of the 64 months that each model has the smallest RMSE, while column VIII reports the number of days out of the 1,326 days each model has the smallest RMSE. Columns IX (lower bound) and X (upper bound) present the winning percentage out of 64 months for each model, evaluated using the bootstrap sampling technique. The statistical bootstrap performed (with replacement) at a 95% confidence level is computed from the monthly RMSE values of the respective models below. Similarly, columns XI (lower bound) and XII (upper bound) present the winning percentage out of 1326 days for each model computed from bootstrapping the daily RMSE values of the respective models at a 95% confidence level.

(I) Model	**(II) Forecast**	**(III) Inputs**	**(IV) Performance amongst all models (Monthly)**	**(V) Performance amongst all models (Daily)**	**(VI) 2.5% lower bound-(for monthly) (%)**	**(VII) 2.5% upper bound-(for monthly) (%)**	**(VIII) 2.5% lower bound-(for daily) (%)**	**(IX) 2.5% upper bound-(for daily) (%)**
$BSMHV_N$	$V_{N+1}^{BSMHV_N}$	$S_{N+1}, S_N, R_{N+1}, \delta t, C_N^{BSMH_N}, C_{N+1}^{BSMH_N}, \Delta_{N+1}^{BSMH_N}$	4	**188**	2%	13%	12%	16%
HHV_N	$V_{N+1}^{HHV_N}$	$S_{N+1}, S_N, R_{N+1}, \delta t, C_N^{HH_N}, C_{N+1}^{HH_N}, \Delta_{N+1}^{HH_N}$	6	67	3%	17%	4%	6%
$HJDHV_N$	$V_{N+1}^{HJDV_N}$	$S_N, S_{N-1}, R_N, \delta t, C_N^{HJD_N}, C_{N+1}^{HJD_N}, \Delta_{N+1}^{HJD_N}$	1	69	0%	5%	4%	6%
$FMLSHV_N$	$V_{N+1}^{FMLSV_N}$	$S_N, S_{N-1}, R_N, \delta t, C_N^{FMLS_N}, C_{N+1}^{FMLS_N}, \Delta_{N+1}^{FMLS_N}$	1	166	0%	5%	11%	14%
$M3HV1_N$	$V_{N+1}^{M3HV1_N}$	$S_{N+1}, S_N, R_{N+1}, \delta t, C_N^{M3H1_N}, C_{N+1}^{M3H1_N}, \Delta_{N+1}^{M3H1_N}$	9	169	6%	23%	11%	14%
$M3HV2_N$	$V_{N+1}^{M3HV2_N}$	$S_{N+1}, S_N, R_{N+1}, \delta t, C_N^{M3H2_N}, C_{N+1}^{M3H2_N}, \Delta_{N+1}^{M3H2_N}$	6	143	3%	17%	9%	12%
$M3HV3_N$	$V_{N+1}^{M3HV3_N}$	$S_{N+1}, S_N, R_{N+1}, \delta t, C_N^{M3H3_N}, C_{N+1}^{M3H3_N}, \Delta_{N+1}^{M3H3_N}$	5	111	2%	16%	7%	10%
$M3HV4_N$	$V_{N+1}^{M3HV4_N}$	$S_{N+1}, S_N, R_{N+1}, \delta t, C_N^{M3H4_N}, C_{N+1}^{M3H4_N}, \Delta_{N+1}^{M3H4_N}$	5	87	2%	16%	5%	8%
$M3HV5_N$	$V_{N+1}^{M3HV5_N}$	$S_{N+1}, S_N, R_{N+1}, \delta t, C_N^{M3H5_N}, C_{N+1}^{M3H5_N}, \Delta_{N+1}^{M3H5_N}$	9	108	6%	24%	7%	10%
$M3HV6_N$	$V_{N+1}^{M3HV6_N}$	$S_{N+1}, S_N, R_{N+1}, \delta t, C_N^{M3H6_N}, C_{N+1}^{M3H6_N}, \Delta_{N+1}^{M3H6_N}$	7	105	3%	19%	6%	9%
$M3HV7_N$	$V_{N+1}^{M3HV7_N}$	$S_{N+1}, S_N, R_{N+1}, \delta t, C_N^{M3H7_N}, C_{N+1}^{M3H7_N}, \Delta_{N+1}^{M3H7_N}$	**11**	113	9%	27%	7%	10%

Table B.2.15: Replicating Portfolio Value Comparison (amongst Parametric and $L3HV_N$-Models): This table presents a performance comparison using both daily and monthly statistics amongst the Black-Scholes-Merton ($BSMHV_N$) model, Heston (HHV_N) model, Heston Jump Diffusion ($HJDHV_N$) model, Finite Moment Log Stable ($FMLSHV_N$) model, and the LSTM $L3HV_N$-Models ($L3HV1_N$ to $L3HV7_N$). The forecast variable for the MLP $M3HV_N$-Models and LSTM $L3HV_N$-Models is the delta that is directly forecasted from the respective LSTM model, whereas the delta for the $BSMHV_N$, HHV_N, $HJDHV_N$ models are computed using their respective characteristic functions. The models denoted by the $_N$ subscript use lagged input variables for forecasting the delta. The forecasted delta is later used to compute the replicating portfolio value V_{N+1} using equation 3.17. The one-trading-day-ahead forecast errors of V_{N+1} are used to compute the Root Mean Square Error (RMSE). Column I identifies the models, column II identifies the forecast variable, and column III lists the input variables used by the models to obtain the V_{N+1}. Forecasts are made for 1,326 trading days, and there are 64 months covered in the sample using the monthly data. Column VII reports the number of months out of the 64 months that each model has the smallest RMSE, while column VIII reports the number of days out of the 1,326 days each model has the smallest RMSE. Columns IX (lower bound) and X (upper bound) present the winning percentage out of 64 months for each model, evaluated using the bootstrap sampling technique. The statistical bootstrap performed (with replacement) at a 95% confidence level is computed from the monthly RMSE values of the respective models below. Similarly, columns XI (lower bound) and XII (upper bound) present the winning percentage out of 1326 days for each model computed from bootstrapping the daily RMSE values of the respective models at a 95% confidence level.

(I) Model	**(II) Forecast**	**(III) Inputs**	**(IV) Performance amongst all models (Monthly)**	**(V) Performance amongst all models (Daily)**	**(VI) 2.5% lower bound-(for monthly) (%)**	**(VII) 2.5% upper bound-(for monthly) (%)**	**(VIII) 2.5% lower bound-(for daily) (%)**	**(IX) 2.5% upper bound-(for daily) (%)**
$BSMHV_N$	$V_{N+1}^{BSMHV_N}$	$S_{N+1}, S_N, R_{N+1}, \delta t, C_N^{BSMH_N}, C_{N+1}^{BSMH_N}, \Delta_{N+1}^{BSMH_N}$	**27**	**451**	31%	55%	31%	37%
HHV_N	$V_{N+1}^{HHV_N}$	$S_{N+1}, S_N, R_{N+1}, \delta t, C_N^{HH_N}, C_{N+1}^{HH_N}, \Delta_{N+1}^{HH_N}$	13	95	11%	30%	6%	9%
$HJDHV_N$	$V_{N+1}^{HJDV_N}$	$S_N, S_{N-1}, R_N, \delta t, C_N^{HJD_N}, C_{N+1}^{HJD_N}, \Delta_{N+1}^{HJD_N}$	1	78	0%	5%	5%	7%
$FMLSHV_N$	$V_{N+1}^{FMLSV_N}$	$S_N, S_{N-1}, R_N, \delta t, C_N^{FMLS_N}, C_{N+1}^{FMLS_N}, \Delta_{N+1}^{FMLS_N}$	2	198	0%	8%	13%	17%
$L3HV1_N$	$V_{N+1}^{L3HV1_N}$	$S_{N+1}, S_N, R_{N+1}, \delta t, C_N^{L3H1_N}, C_{N+1}^{L3H1_N}, \Delta_{N+1}^{L3H1_N}$	0	37	0%	0%	2%	4%
$L3HV2_N$	$V_{N+1}^{L3HV2_N}$	$S_{N+1}, S_N, R_{N+1}, \delta t, C_N^{L3H2_N}, C_{N+1}^{L3H2_N}, \Delta_{N+1}^{L3H2_N}$	1	55	0%	6%	3%	5%
$L3HV3_N$	$V_{N+1}^{L3HV3_N}$	$S_{N+1}, S_N, R_{N+1}, \delta t, C_N^{L3H3_N}, C_{N+1}^{L3H3_N}, \Delta_{N+1}^{L3H3_N}$	0	41	0%	0%	2%	4%
$L3HV4_N$	$V_{N+1}^{L3HV4_N}$	$S_{N+1}, S_N, R_{N+1}, \delta t, C_N^{L3H4_N}, C_{N+1}^{L3H4_N}, \Delta_{N+1}^{L3H4_N}$	18	250	17%	40%	17%	21%
$L3HV5_N$	$V_{N+1}^{L3HV5_N}$	$S_{N+1}, S_N, R_{N+1}, \delta t, C_N^{L3H5_N}, C_{N+1}^{L3H5_N}, \Delta_{N+1}^{L3H5_N}$	0	49	0%	0%	3%	5%
$L3HV6_N$	$V_{N+1}^{L3HV6_N}$	$S_{N+1}, S_N, R_{N+1}, \delta t, C_N^{L3H6_N}, C_{N+1}^{L3H6_N}, \Delta_{N+1}^{L3H6_N}$	1	52	0%	5%	3%	5%
$L3HV7_N$	$V_{N+1}^{L3HV7_N}$	$S_{N+1}, S_N, R_{N+1}, \delta t, C_N^{L3H7_N}, C_{N+1}^{L3H7_N}, \Delta_{N+1}^{L3H7_N}$	1	31	0%	5%	1%	3%

Table B.2.16: Replicating Portfolio Value Comparison (amongst Parametric models): This table presents a performance comparison using both daily and monthly statistics amongst the Black-Scholes-Merton ($BSMHV_N$) model, Heston (HHV_N) model, Heston Jump Diffusion ($HJDHV_N$) model, and the Finite Moment Log Stable ($FMLSHV_N$) model. The delta for the $BSMHV_N$, HHV_N, $HJDHV_N$ models are computed using their respective characteristic functions. The models denoted by the $_N$ subscript use lagged input variables for forecasting the delta. The forecasted delta is later used to compute the replicating portfolio value V_{N+1} using equation 3.17. The one-trading-day-ahead forecast errors of V_{N+1} are used to compute the Root Mean Square Error (RMSE). Column I identifies the models, column II identifies the forecast variable, and column III lists the input variables used by the models to obtain the V_{N+1}. Forecasts are made for 1,326 trading days, and there are 64 months covered in the sample using the monthly data. Column IV reports the number of months out of the 64 months that each model has the smallest RMSE, while column V reports the number of days out of the 1,326 days each model has the smallest RMSE. Columns VI (lower bound) and VII (upper bound) present the winning percentage out of 64 months for each model, evaluated using the bootstrap sampling technique. The statistical bootstrap performed (with replacement) at a 95% confidence level is computed from the monthly RMSE values of the respective models below. Similarly, columns VIII (lower bound) and IX (upper bound) present the winning percentage out of 1326 days for each model computed from bootstrapping the daily RMSE values of the respective models at a 95% confidence level.

(I) Model	(II) Forecast	(III) Inputs	(IV) Performance amongst all models (Monthly)	(V) Performance amongst all models (Daily)	(VI) 2.5% lower bound- (for monthly) (%)	(VII) 2.5% upper bound- (for monthly) (%)	(VIII) 2.5% lower bound- (for daily) (%)	(IX) 2.5% upper bound- (for daily) (%)
$BSMHV_N$	$V_{N+1}^{BSMHV_N}$	$S_{N+1}, S_N, R_{N+1}, \delta t, C_N^{BSMH_N}, C_{N+1}^{BSMH_N}, \Delta_{N+1}^{BSMH_N}$	**46**	**909**	61%	83%	66%	71%
HHV_N	$V_{N+1}^{HHV_N}$	$S_{N+1}, S_N, R_{N+1}, \delta t, C_N^{HH_N}, C_{N+1}^{HH_N}, \Delta_{N+1}^{HH_N}$	15	131	13%	34%	8%	12%
$HJDHV_N$	$V_{N+1}^{HJDV_N}$	$S_N, S_{N-1}, R_N, \delta t, C_N^{HJD_N}, C_{N+1}^{HJD_N}, \Delta_{N+1}^{HJD_N}$	1	79	0%	5%	5%	7%
$FMLSHV_N$	$V_{N+1}^{FMLSV_N}$	$S_N, S_{N-1}, R_N, \delta t, C_N^{FMLS_N}, C_{N+1}^{FMLS_N}, \Delta_{N+1}^{FMLS_N}$	2	207	0%	8%	14%	18%

B.2.5 Replicating portfolio value performance of HV-Models that forecast the replicating portfolio value(V_{N+1}), computed using the delta from H-Models that use one-trading-day-ahead input variables:

Tables B.2.17, B.2.18, B.2.19 and B.2.20 shows the relative out-of-sample replicating portfolio value performance (in $RMSE$) amongst the models that forecast the one-trading-day-ahead replicating portfolio value (V_{N+1}). The V_{N+1} is computed from equation 3.17 using the forecasted one-trading-day-ahead delta from models that use one-trading-day-ahead input variables. For convenience, the models in Tables B.2.17, B.2.18, B.2.19, lists the forecast variable and the input variables are listed in columns II and III, and, the architecture of the MLP and LSTM models in columns IV, V and VI. The performance metric is the $RMSE$ of the one-trading-day-ahead forecast errors of V_{N+1}, which is computed for each model utilising all of the errors in each day or each month. Amongst all models, columns VII and VIII record the number of months and days, respectively, that each model has the lowest $RMSE$. To be certain of our results, we performed a bootstrap using the daily and monthly RMSEs. Columns IX (lower bound) and X (upper bound) present the results from the bootstrap performed (with replacement) using monthly RMSEs at a 95% confidence level and show the winning percentage out of 64 months for each model, and similarly, the 95 % confidence intervals computed from bootstrapping of the daily RMSEs signifies the winning percentage out of 1326 days for each model and are reported in columns XI (lower bound), XII (upper bound).

In the below several comparisons, even though a particular model wins by a higher percentage against other models, we investigated further these models pairwise by performing a pairwise bootstrap comparison, which was computed using the respective pair's daily RMSEs. The results are presented in Table 49 of the Electronic Appendix. Also, we examined the pairwise Diebold-Mariano(DM) (Diebold and Mariano (1995)) tests on these models and have presented the results in Table 43 of the Electronic Appendix. In constructing the DM test statistics, the models listed in the left column represent Model 1, and the models in the first row represent Model 2 in Table 43 of the Electronic Appendix. If the null can be rejected, a positive number suggests the rejection may be due to the second model being the better forecast model. In contrast, a negative value suggests the rejection may be due to the first model being the better forecast model. The model pairs highlighted in a red state that their forecasts have statistically insignificant differences in their prediction accuracy. Considering the DM-Test statistics in Table 43 of the Electronic Appendix, all the model pairs lead to the rejection of the null of equal forecasting performance. The RMSEs for the models that use one-trading-day-ahead input variables to forecast the V_{N+1} on a monthly, yearly, and overall basis can be found in the Electronic Appendix, in Tables 25, 31, and 37, respectively.

In this section, we compare the out-of-sample replicating portfolio value performance of the parametric models ($BSMHV_{N+1}$, HHV_{N+1}, $HJDHV_{N+1}$, and $FMLSHV_{N+1}$), the triple hidden layer MLP models ($M3HV_{N+1} - Models$) and triple hidden layer LSTM models ($L3HV_{N+1} - Models$), then the parametric models with the $M3HV_{N+1} - Models$, and finally the parametric models with the $L3HV_{N+1} - Models$.

The results for the parametric models with the triple hidden layer MLP $M3HV_{N+1} - Models$ ($M3HV1_{N+1}$ to $M3HV7_{N+1}$) and the triple hidden layer LSTM $L3HV_{N+1} - Models$ ($L3HV1_{N+1}$ to $L3HV7_{N+1}$) are presented in Table B.2.17. If all the models are compared together, then the $BSMHV_{N+1}$ model had the lowest $RMSE$ for 195 (having a daily bootstrap winning % of 13% to 17%) days out of 1,326 days. Although the $BSMHV_{N+1}$ model had outperformed other models, the $FMLSHV_{N+1}$(165 days), and the $M3HV1_{N+1}$(158 days) had shown similar outperformance, where they had a collective daily bootstrap winning percentage from 10% (lower bound for the $M3HV1_{N+1}$ model) to 14%. (upper bound for the $FMLSHV_{N+1}$ model). Table B.2.18 presents the results for the comparison of the parametric models with the triple hidden layer MLP $M3HV_N - Models$ ($M3HV1_{N+1}$ to $M3HV7_{N+1}$), and the $BSMHV_{N+1}$ model had the lowest $RMSE$ for 207 days (having a daily bootstrap winning % of 14% to 18%) out of 1,326 days. Though the $BSMHV_{N+1}$ model had outperformed other models, the $FMLSHV_{N+1}$(170 days), and the $M3HV1_{N+1}$(193 days) have shown similar outperformance, where they had a collective daily bootstrap winning percentage from 11% (lower bound for the $FMLSHV_{N+1}$ model) to 17%. (upper bound for the $M3HV1_{N+1}$ model). We present the comparison results of the parametric models with the triple hidden layer LSTM $L3HV_{N+1} - Models$ ($L3HV1_{N+1}$ to $L3HV7_{N+1}$) in Table B.2.19. We find that the $BSMHV_{N+1}$ model had the lowest $RMSE$ for 485 days (having a daily bootstrap winning % of 34% to 39%) out of 1,326 days. Finally, we compare amongst the parametric models in Table B.2.20, and find that the $BSMHV_{N+1}$ model still had the lowest $RMSE$ for 934 days (having a daily bootstrap winning % of 68% to 73%) out of 1,326 days.

Thus, when the parametric models are compared with the triple hidden layer ANN models that use one-trading-day-ahead input variables to forecast the replicating portfolio value(in Table B.2.17), we conclude that a parametric model ($BSMHV_{N+1}$) could outperform all other models. If the parametric models were compared with the triple hidden layer MLP models (in Table B.2.18), a parametric model ($BSMHV_{N+1}$) outperforms all the triple hidden layer MLP models, also when the parametric models were compared with the triple hidden layer LSTM models (in Table B.2.19), a parametric model ($BSMHV_{N+1}$) still outperforms all the triple hidden layer, LSTM models. Finally, when the comparison is made amongst parametric models, the $BSMHV_{N+1}$ model has been shown to outperform the rest of the parametric models.

Table B.2.17: Replicating Portfolio Value Comparison (amongst Parametric, $M3HV_{N+1}$-Models and $L3HV_{N+1}$-Models): This table presents a performance comparison using both daily and monthly statistics amongst the Black-Scholes-Merton ($BSMHV_{N+1}$) model, Heston (HHV_{N+1}) model, Heston Jump Diffusion ($HJDHV_{N+1}$) model, Finite Moment Log Stable ($FMLSHV_{N+1}$) model, MLP $M3HV_{N+1}$-Models ($M3HV1_{N+1}$ to $M3HV7_{N+1}$) and the LSTM $L3HV_{N+1}$-Models ($L3HV1_{N+1}$ to $L3HV7_{N+1}$). The forecast variable for the MLP $M3HV_{N+1}$-Models and LSTM $L3HV_{N+1}$-Models is the delta that is directly forecasted from the respective ANN model, whereas the delta for the $BSMHV_{N+1}$, HHV_{N+1}, $HJDHV_{N+1}$ models are computed using their respective characteristic functions. The models denoted by the $_{N+1}$ subscript use one-trading-day-ahead input variables for forecasting the delta. The forecasted delta is later used to compute the replicating portfolio value V_{N+1} using equation 3.17. The one-trading-day-ahead forecast errors of V_{N+1} are used to compute the Root Mean Square Error (RMSE). Column I identifies the models, column II identifies the forecast variable, and column III lists the input variables used by the models to obtain the V_{N+1}. Forecasts are made for 1,326 trading days, and there are 64 months covered in the sample using the monthly data. Column VII reports the number of months out of the 64 months that each model has the smallest RMSE, while column VIII reports the number of days out of the 1,326 days each model has the smallest RMSE. Columns IX (lower bound) and X (upper bound) present the winning percentage out of 64 months for each model, evaluated using the bootstrap sampling technique. The statistical bootstrap performed (with replacement) at a 95% confidence level is computed from the monthly RMSE values of the respective models below. Similarly, columns XI (lower bound) and XII (upper bound) present the winning percentage out of 1326 days for each model computed from bootstrapping the daily RMSE values of the respective models at a 95% confidence level.

(I) Model	(II) Forecast	(III) Inputs	(IV) Performance amongst all models (Monthly)	(V) Performance amongst all models (Daily)	(VI) 2.5% lower bound- (for monthly) (%)	(VII) 2.5% upper bound- (for monthly) (%)	(VIII) 2.5% lower bound- (for daily) (%)	(IX) 2.5% upper bound- (for daily) (%)
$BSMHV_{N+1}$	$V_{N+1}^{BSMHV_{N+1}}$	$S_{N+1}, S_N, R_{N+1}, \delta t, C_N^{BSMH_{N+1}}, C_{N+1}^{BSMH_{N+1}}, \Delta_{N+1}^{BSMH_{N+1}}$	**17**	**195**	17%	39%	13%	17%
HHV_{N+1}	$V_{N+1}^{HHV_{N+1}}$	$S_{N+1}, S_N, R_{N+1}, \delta t, C_N^{HH_{N+1}}, C_{N+1}^{HH_{N+1}}, \Delta_{N+1}^{HH_{N+1}}$	11	43	9%	27%	2%	4%
$HJDHV_{N+1}$	$V_{N+1}^{HJDHV_{N+1}}$	$S_{N+1}, S_N, R_{N+1}, \delta t, C_N^{HJD_{N+1}}, C_{N+1}^{HJD_{N+1}}, \Delta_{N+1}^{HJD_{N+1}}$	0	71	0%	0%	4%	7%
$FMLSHV_{N+1}$	$V_{N+1}^{FMLSHV_{N+1}}$	$S_{N+1}, S_N, R_{N+1}, \delta t, C_N^{FMLS_{N+1}}, C_{N+1}^{FMLS_{N+1}}, \Delta_{N+1}^{FMLS_{N+1}}$	3	165	0%	11%	11%	14%
$M3HV1_{N+1}$	$V_{N+1}^{M3HV1_{N+1}}$	$S_{N+1}, S_N, R_{N+1}, \delta t, C_N^{M3H1_{N+1}}, C_{N+1}^{M3H1_{N+1}}, \Delta_{N+1}^{M3H1_{N+1}}$	9	158	6%	23%	10%	14%
$M3HV2_{N+1}$	$V_{N+1}^{M3HV2_{N+1}}$	$S_{N+1}, S_N, R_{N+1}, \delta t, C_N^{M3H2_{N+1}}, C_{N+1}^{M3H2_{N+1}}, \Delta_{N+1}^{M3H2_{N+1}}$	6	109	3%	17%	7%	10%
$M3HV3_{N+1}$	$V_{N+1}^{M3HV3_{N+1}}$	$S_{N+1}, S_N, R_{N+1}, \delta t, C_N^{M3H3_{N+1}}, C_{N+1}^{M3H3_{N+1}}, \Delta_{N+1}^{M3H3_{N+1}}$	2	95	0%	8%	6%	9%
$M3HV4_{N+1}$	$V_{N+1}^{M3HV4_{N+1}}$	$S_{N+1}, S_N, R_{N+1}, \delta t, C_N^{M3H4_{N+1}}, C_{N+1}^{M3H4_{N+1}}, \Delta_{N+1}^{M3H4_{N+1}}$	2	67	0%	8%	4%	6%
$M3HV5_{N+1}$	$V_{N+1}^{M3HV5_{N+1}}$	$S_{N+1}, S_N, R_{N+1}, \delta t, C_N^{M3H5_{N+1}}, C_{N+1}^{M3H5_{N+1}}, \Delta_{N+1}^{M3H5_{N+1}}$	1	83	0%	5%	5%	8%
$M3HV6_{N+1}$	$V_{N+1}^{M3HV6_{N+1}}$	$S_{N+1}, S_N, R_{N+1}, \delta t, C_N^{M3H6_{N+1}}, C_{N+1}^{M3H6_{N+1}}, \Delta_{N+1}^{M3H6_{N+1}}$	3	95	0%	11%	6%	9%
$M3HV7_{N+1}$	$V_{N+1}^{M3HV7_{N+1}}$	$S_{N+1}, S_N, R_{N+1}, \delta t, C_N^{M3H7_{N+1}}, C_{N+1}^{M3H7_{N+1}}, \Delta_{N+1}^{M3H7_{N+1}}$	0	97	0%	0%	6%	9%
$L3HV1_{N+1}$	$V_{N+1}^{L3HV1_{N+1}}$	$S_{N+1}, S_N, R_{N+1}, \delta t, C_N^{L3H1_{N+1}}, C_{N+1}^{L3H1_{N+1}}, \Delta_{N+1}^{L3H1_{N+1}}$	0	12	0%	0%	0%	1%
$L3HV2_{N+1}$	$V_{N+1}^{L3HV2_{N+1}}$	$S_{N+1}, S_N, R_{N+1}, \delta t, C_N^{L3H2_{N+1}}, C_{N+1}^{L3H2_{N+1}}, \Delta_{N+1}^{L3H2_{N+1}}$	1	18	0%	5%	1%	2%
$L3HV3_{N+1}$	$V_{N+1}^{L3HV3_{N+1}}$	$S_{N+1}, S_N, R_{N+1}, \delta t, C_N^{L3H3_{N+1}}, C_{N+1}^{L3H3_{N+1}}, \Delta_{N+1}^{L3H3_{N+1}}$	0	15	0%	0%	0%	1%
$L3HV4_{N+1}$	$V_{N+1}^{L3HV4_{N+1}}$	$S_{N+1}, S_N, R_{N+1}, \delta t, C_N^{L3H4_{N+1}}, C_{N+1}^{L3H4_{N+1}}, \Delta_{N+1}^{L3H4_{N+1}}$	6	72	3%	17%	4%	7%
$L3HV5_{N+1}$	$V_{N+1}^{L3HV5_{N+1}}$	$S_{N+1}, S_N, R_{N+1}, \delta t, C_N^{L3H5_{N+1}}, C_{N+1}^{L3H5_{N+1}}, \Delta_{N+1}^{L3H5_{N+1}}$	1	12	0%	5%	0%	1%
$L3HV6_{N+1}$	$V_{N+1}^{L3HV6_{N+1}}$	$S_{N+1}, S_N, R_{N+1}, \delta t, C_N^{L3H6_{N+1}}, C_{N+1}^{L3H6_{N+1}}, \Delta_{N+1}^{L3H6_{N+1}}$	0	15	0%	0%	0%	1%
$L3HV7_{N+1}$	$V_{N+1}^{L3HV7_{N+1}}$	$S_{N+1}, S_N, R_{N+1}, \delta t, C_N^{L3H7_{N+1}}, C_{N+1}^{L3H7_{N+1}}, \Delta_{N+1}^{L3H7_{N+1}}$	1	13	0%	5%	0%	1%

Table B.2.18: Replicating Portfolio Value Comparison (amongst Parametric and $M3HV_{N+1}$-Models): This table presents a performance comparison using both daily and monthly statistics amongst the Black-Scholes-Merton ($BSMHV_{N+1}$) model, Heston (HHV_{N+1}) model, Heston Jump Diffusion ($HJDHV_{N+1}$) model, Finite Moment Log Stable ($FMLSHV_{N+1}$) model, and the MLP $M3HV_{N+1}$-Models ($M3HV1_{N+1}$ to $M3HV7_{N+1}$). The forecast variable for the MLP $M3HV_{N+1}$-Models and LSTM $L3HV_{N+1}$-Models is the delta that is directly forecasted from the respective MLP model, whereas the delta for the $BSMHV_{N+1}$, HHV_{N+1}, $HJDHV_{N+1}$ models are computed using their respective characteristic functions. The models denoted by the $_{N+1}$ subscript use one-trading-day-ahead input variables for forecasting the delta. The forecasted delta is later used to compute the replicating portfolio value V_{N+1} using equation 3.17. The one-trading-day-ahead forecast errors of V_{N+1} are used to compute the Root Mean Square Error (RMSE). Column I identifies the models, column II identifies the forecast variable, and column III lists the input variables used by the models to obtain the V_{N+1}. Forecasts are made for 1,326 trading days, and there are 64 months covered in the sample using the monthly data. Column VII reports the number of months out of the 64 months that each model has the smallest RMSE, while column VIII reports the number of days out of the 1,326 days each model has the smallest RMSE. Columns IX (lower bound) and X (upper bound) present the winning percentage out of 64 months for each model, evaluated using the bootstrap sampling technique. The statistical bootstrap performed (with replacement) at a 95% confidence level is computed from the monthly RMSE values of the respective models below. Similarly, columns XI (lower bound) and XII (upper bound) present the winning percentage out of 1326 days for each model computed from bootstrapping the daily RMSE values of the respective models at a 95% confidence level.'

(I) Model	**(II) Forecast**	**(III) Inputs**	**(IV) Performance amongst all models (Monthly)**	**(V) Performance amongst all models (Daily)**	**(VI) 2.5% lower bound-(for monthly) (%)**	**(VII) 2.5% upper bound-(for monthly) (%)**	**(VIII) 2.5% lower bound-(for daily) (%)**	**(IX) 2.5% upper bound-(for daily) (%)**
$BSMHV_{N+1}$	$V_{N+1}^{BSMHV_{N+1}}$	$S_{N+1}, S_N, R_{N+1}, \delta t, C_N^{BSMH_{N+1}}, C_{N+1}^{BSMH_{N+1}}, \Delta_{N+1}^{BSMH_{N+1}}$	**20**	**207**	22%	44%	14%	18%
HHV_{N+1}	$V_{N+1}^{HHV_{N+1}}$	$S_{N+1}, S_N, R_{N+1}, \delta t, C_N^{HH_{N+1}}, C_{N+1}^{HH_{N+1}}, \Delta_{N+1}^{HH_{N+1}}$	11	45	8%	27%	2%	4%
$HJDHV_{N+1}$	$V_{N+1}^{HJDHV_{N+1}}$	$S_{N+1}, S_N, R_{N+1}, \delta t, C_N^{HJD_{N+1}}, C_{N+1}^{HJD_{N+1}}, \Delta_{N+1}^{HJD_{N+1}}$	0	72	0%	0%	4%	7%
$FMLSHV_{N+1}$	$V_{N+1}^{FMLSHV_{N+1}}$	$S_{N+1}, S_N, R_{N+1}, \delta t, C_N^{FMLS_{N+1}}, C_{N+1}^{FMLS_{N+1}}, \Delta_{N+1}^{FMLS_{N+1}}$	3	170	0%	11%	11%	15%
$M3HV1_{N+1}$	$V_{N+1}^{M3HV1_{N+1}}$	$S_{N+1}, S_N, R_{N+1}, \delta t, C_N^{M3H1_{N+1}}, C_{N+1}^{M3H1_{N+1}}, \Delta_{N+1}^{M3H1_{N+1}}$	11	193	8%	27%	13%	17%
$M3HV2_{N+1}$	$V_{N+1}^{M3HV2_{N+1}}$	$S_{N+1}, S_N, R_{N+1}, \delta t, C_N^{M3H2_{N+1}}, C_{N+1}^{M3H2_{N+1}}, \Delta_{N+1}^{M3H2_{N+1}}$	6	134	3%	17%	8%	12%
$M3HV3_{N+1}$	$V_{N+1}^{M3HV3_{N+1}}$	$S_{N+1}, S_N, R_{N+1}, \delta t, C_N^{M3H3_{N+1}}, C_{N+1}^{M3H3_{N+1}}, \Delta_{N+1}^{M3H3_{N+1}}$	2	117	0%	8%	7%	10%
$M3HV4_{N+1}$	$V_{N+1}^{M3HV4_{N+1}}$	$S_{N+1}, S_N, R_{N+1}, \delta t, C_N^{M3H4_{N+1}}, C_{N+1}^{M3H4_{N+1}}, \Delta_{N+1}^{M3H4_{N+1}}$	3	73	0%	11%	4%	7%
$M3HV5_{N+1}$	$V_{N+1}^{M3HV5_{N+1}}$	$S_{N+1}, S_N, R_{N+1}, \delta t, C_N^{M3H5_{N+1}}, C_{N+1}^{M3H5_{N+1}}, \Delta_{N+1}^{M3H5_{N+1}}$	1	101	0%	5%	6%	9%
$M3HV6_{N+1}$	$V_{N+1}^{M3HV6_{N+1}}$	$S_{N+1}, S_N, R_{N+1}, \delta t, C_N^{M3H6_{N+1}}, C_{N+1}^{M3H6_{N+1}}, \Delta_{N+1}^{M3H6_{N+1}}$	5	104	2%	16%	6%	9%
$M3HV7_{N+1}$	$V_{N+1}^{M3HV7_{N+1}}$	$S_{N+1}, S_N, R_{N+1}, \delta t, C_N^{M3H7_{N+1}}, C_{N+1}^{M3H7_{N+1}}, \Delta_{N+1}^{M3H7_{N+1}}$	1	109	0%	5%	7%	10%

Table B.2.19: Replicating Portfolio Value Comparison (amongst Parametric and $L3HV_{N+1}$-Models): This table presents a performance comparison using both daily and monthly statistics amongst the Black-Scholes-Merton ($BSMHV_{N+1}$) model, Heston (HHV_{N+1}) model, Heston Jump Diffusion ($HJDHV_{N+1}$) model, Finite Moment Log Stable ($FMLSHV_{N+1}$) model, and the LSTM $L3HV_{N+1}$-Models ($L3HV1_{N+1}$ to $L3HV7_{N+1}$). The forecast variable for the MLP $M3HV_{N+1}$-Models and LSTM $L3HV_{N+1}$-Models is the delta that is directly forecasted from the respective LSTM model, whereas the delta for the $BSMHV_{N+1}$, HHV_{N+1}, $HJDHV_{N+1}$ models are computed using their respective characteristic functions. The models denoted by the $_{N+1}$ subscript use one-trading-day-ahead input variables for forecasting the delta. The forecasted delta is later used to compute the replicating portfolio value V_{N+1} using equation 3.17. The one-trading-day-ahead forecast errors of V_{N+1} are used to compute the Root Mean Square Error (RMSE). Column I identifies the models, column II identifies the forecast variable, and column III lists the input variables used by the models to obtain the V_{N+1}. Forecasts are made for 1,326 trading days, and there are 64 months covered in the sample using the monthly data. Column VII reports the number of months out of the 64 months that each model has the smallest RMSE, while column VIII reports the number of days out of the 1,326 days each model has the smallest RMSE. Columns IX (lower bound) and X (upper bound) present the winning percentage out of 64 months for each model, evaluated using the bootstrap sampling technique. The statistical bootstrap performed (with replacement) at a 95% confidence level is computed from the monthly RMSE values of the respective models below. Similarly, columns XI (lower bound) and XII (upper bound) present the winning percentage out of 1326 days for each model computed from bootstrapping the daily RMSE values of the respective models at a 95% confidence level.

(I) Model	**(II) Forecast**	**(III) Inputs**	**(IV) Performance amongst all models (Monthly)**	**(V) Performance amongst all models (Daily)**	**(VI) 2.5% lower bound- (for monthly) (%)**	**(VII) 2.5% upper bound- (for monthly) (%)**	**(VIII) 2.5% lower bound- (for daily) (%)**	**(IX) 2.5% upper bound- (for daily) (%)**
$BSMHV_{N+1}$	$V_{N+1}^{BSMHV_{N+1}}$	$S_{N+1}, S_N, R_{N+1}, \delta t, C_N^{BSMH_{N+1}}, C_{N+1}^{BSMH_{N+1}}, \Delta_{N+1}^{BSMH_{N+1}}$	**31**	**485**	38%	63%	34%	39%
HHV_{N+1}	$V_{N+1}^{HHV_{N+1}}$	$S_{N+1}, S_N, R_{N+1}, \delta t, C_N^{HH_{N+1}}, C_{N+1}^{HH_{N+1}}, \Delta_{N+1}^{HH_{N+1}}$	12	68	9%	28%	4%	6%
$HJDHV_{N+1}$	$V_{N+1}^{HJDHV_{N+1}}$	$S_{N+1}, S_N, R_{N+1}, \delta t, C_N^{HJD_{N+1}}, C_{N+1}^{HJD_{N+1}}, \Delta_{N+1}^{HJD_{N+1}}$	0	78	0%	0%	5%	7%
$FMLSHV_{N+1}$	$V_{N+1}^{FMLSHV_{N+1}}$	$S_{N+1}, S_N, R_{N+1}, \delta t, C_N^{FMLS_{N+1}}, C_{N+1}^{FMLS_{N+1}}, \Delta_{N+1}^{FMLS_{N+1}}$	3	199	0%	11%	13%	17%
$L3HV1_{N+1}$	$V_{N+1}^{L3HV1_{N+1}}$	$S_{N+1}, S_N, R_{N+1}, \delta t, C_N^{L3H1_{N+1}}, C_{N+1}^{L3H1_{N+1}}, \Delta_{N+1}^{L3H1_{N+1}}$	0	37	0%	0%	2%	4%
$L3HV2_{N+1}$	$V_{N+1}^{L3HV2_{N+1}}$	$S_{N+1}, S_N, R_{N+1}, \delta t, C_N^{L3H2_{N+1}}, C_{N+1}^{L3H2_{N+1}}, \Delta_{N+1}^{L3H2_{N+1}}$	1	49	0%	5%	3%	5%
$L3HV3_{N+1}$	$V_{N+1}^{L3HV3_{N+1}}$	$S_{N+1}, S_N, R_{N+1}, \delta t, C_N^{L3H3_{N+1}}, C_{N+1}^{L3H3_{N+1}}, \Delta_{N+1}^{L3H3_{N+1}}$	0	43	0%	0%	2%	4%
$L3HV4_{N+1}$	$V_{N+1}^{L3HV4_{N+1}}$	$S_{N+1}, S_N, R_{N+1}, \delta t, C_N^{L3H4_{N+1}}, C_{N+1}^{L3H4_{N+1}}, \Delta_{N+1}^{L3H4_{N+1}}$	12	247	9%	28%	17%	21%
$L3HV5_{N+1}$	$V_{N+1}^{L3HV5_{N+1}}$	$S_{N+1}, S_N, R_{N+1}, \delta t, C_N^{L3H5_{N+1}}, C_{N+1}^{L3H5_{N+1}}, \Delta_{N+1}^{L3H5_{N+1}}$	1	51	0%	5%	3%	5%
$L3HV6_{N+1}$	$V_{N+1}^{L3HV6_{N+1}}$	$S_{N+1}, S_N, R_{N+1}, \delta t, C_N^{L3H6_{N+1}}, C_{N+1}^{L3H6_{N+1}}, \Delta_{N+1}^{L3H6_{N+1}}$	1	53	0%	5%	3%	5%
$L3HV7_{N+1}$	$V_{N+1}^{L3HV7_{N+1}}$	$S_{N+1}, S_N, R_{N+1}, \delta t, C_N^{L3H7_{N+1}}, C_{N+1}^{L3H7_{N+1}}, \Delta_{N+1}^{L3H7_{N+1}}$	2	28	0%	8%	1%	3%

Table B.2.20: Replicating Portfolio Value Comparison (amongst Parametric models): This table presents a performance comparison using both daily and monthly statistics amongst the Black-Scholes-Merton ($BSMHV_{N+1}$) model, Heston (HHV_{N+1}) model, Heston Jump Diffusion ($HJDHV_{N+1}$) model, and the Finite Moment Log Stable ($FMLSHV_{N+1}$) model. The delta for the $BSMHV_{N+1}$, HHV_{N+1}, $HJDHV_{N+1}$ models are computed using their respective characteristic functions. The models denoted by the $_{N+1}$ subscript use one-trading-day-ahead input variables for forecasting the delta. The forecasted delta is later used to compute the replicating portfolio value V_{N+1} using equation 3.17. The one-trading-day-ahead forecast errors of V_{N+1} are used to compute the Root Mean Square Error (RMSE). Column I identifies the models, column II identifies the forecast variable, and column III lists the input variables used by the models to obtain the V_{N+1}. Forecasts are made for 1,326 trading days, and there are 64 months covered in the sample using the monthly data. Column IV reports the number of months out of the 64 months that each model has the smallest RMSE, while column V reports the number of days out of the 1,326 days each model has the smallest RMSE. Columns VI (lower bound) and VII (upper bound) present the winning percentage out of 64 months for each model, evaluated using the bootstrap sampling technique. The statistical bootstrap performed (with replacement) at a 95% confidence level is computed from the monthly RMSE values of the respective models below. Similarly, columns VIII (lower bound) and IX (upper bound) present the winning percentage out of 1326 days for each model computed from bootstrapping the daily RMSE values of the respective models at a 95% confidence level.

(I) Model	**(II) Forecast**	**(III) Inputs**	**(IV) Performance amongst all models (Monthly)**	**(V) Performance amongst all models (Daily)**	**(VI) 2.5% lower bound- (for monthly) (%)**	**(VII) 2.5% upper bound- (for monthly) (%)**	**(VIII) 2.5% lower bound- (for daily) (%)**	**(IX) 2.5% upper bound- (for daily) (%)**
$BSMHV_{N+1}$	$V_{N+1}^{BSMHV_{N+1}}$	$S_{N+1}, S_N, R_{N+1}, \delta t, C_N^{BSMH_{N+1}}, C_{N+1}^{BSMH_{N+1}}, \Delta_{N+1}^{BSMH_{N+1}}$	**46**	**934**	63%	84%	68%	73%
HHV_{N+1}	$V_{N+1}^{HHV_{N+1}}$	$S_{N+1}, S_N, R_{N+1}, \delta t, C_N^{HH_{N+1}}, C_{N+1}^{HH_{N+1}}, \Delta_{N+1}^{HH_{N+1}}$	14	103	13%	33%	6%	9%
$HJDHV_{N+1}$	$V_{N+1}^{HJDHV_{N+1}}$	$S_{N+1}, S_N, R_{N+1}, \delta t, C_N^{HJD_{N+1}}, C_{N+1}^{HJD_{N+1}}, \Delta_{N+1}^{HJD_{N+1}}$	0	79	0%	0%	5%	7%
$FMLSHV_{N+1}$	$V_{N+1}^{FMLSHV_{N+1}}$	$S_{N+1}, S_N, R_{N+1}, \delta t, C_N^{FMLS_{N+1}}, C_{N+1}^{FMLS_{N+1}}, \Delta_{N+1}^{FMLS_{N+1}}$	3	209	0%	11%	14%	18%

B.2.6 Replicating portfolio value performance of CHV-Models that forecast the replicating portfolio value(V_{N+1}) computed using the analytically derived delta ($\delta C_{N+1}/\delta S_{N+1}$), and where the $\delta C_{N+1}/\delta S_{N+1}$ is inferred from models that forecast the call option price (C_{N+1}) using one-trading-day-ahead input variables:

Tables B.2.21, B.2.22, B.2.23 and B.2.24 shows the relative out-of-sample replicating portfolio value performance (in $RMSE$) amongst the models that forecast the one-trading-day-ahead replicating portfolio value (V_{N+1}). The V_{N+1} is computed from equation 3.17 using the analytically derived delta ($\delta C_{N+1}/\delta S_{N+1}$). The $\delta C_{N+1}/\delta S_{N+1}$ is computed from models that forecast the call option price (C_{N+1}) using one-trading-day-ahead input variables. For convenience, the models in Tables B.2.21, B.2.22, B.2.23, lists the forecast variable and the input variables are listed in columns II and III, and, the architecture of the MLP and LSTM models in columns IV, V and VI. The performance metric is the $RMSE$ of the one-trading-day-ahead forecast errors of V_{N+1}, which is computed for each model utilising all of the errors in each day or each month. Amongst all of the models, columns VII and VIII record the number of months and days, respectively, that each model has the lowest $RMSE$. In order to be certain of our results, we performed a bootstrap using the daily and monthly RMSEs. Columns IX (lower bound) and X (upper bound) present the results from the bootstrap performed (with replacement) using monthly RMSEs at a 95% confidence level and show the winning percentage out of 64 months for each model, and similarly, the 95 % confidence intervals computed from bootstrapping of the daily RMSEs signifies the winning percentage out of 1326 days for each model and are reported in columns XI (lower bound), XII (upper bound).

In the below several comparisons, even though a particular model wins by a higher percentage against other models, we investigated further these models pairwise by performing a pairwise bootstrap comparison, which was computed using the respective pair's daily RMSEs. The results are presented in Table 50 of the Electronic Appendix. Also, we examined the pairwise Diebold-Mariano(DM) (Diebold and Mariano (1995)) tests on these models and have presented the results in Table 44 of the Electronic Appendix. In constructing the DM test statistics, the models listed in the left column represent Model 1, and the models in the first row represent Model 2 in Table 44 of the Electronic Appendix. If the null can be rejected, a positive number suggests the rejection may be due to the second model being the better forecast model. In contrast, a negative value suggests the rejection may be due to the first model being the better forecast model. The model pairs highlighted in a red state that their forecasts have statistically insignificant differences in their prediction accuracy. The following model pairs have been shown to have statistically insignificant differences: ($M3CHV1_{N+1}$, $M3CHV2_{N+1}$), ($M3CHV3_{N+1}$, $M3CHV6_{N+1}$), ($HJDCHV_{N+1}$, $M3CHV7_{N+1}$), and ($L3CHV6_{N+1}$, $L3CHV7_{N+1}$). The RMSEs for the models that forecast the V_{N+1} computed using the analytically derived $\delta C_{N+1}/\delta S_{N+1}$ (where the $\delta C_{N+1}/\delta S_{N+1}$ is inferred from models that forecast the C_{N+1} using one-trading-day-ahead input variables) on a monthly, yearly, and overall basis can be found in the Electronic Appendix, in Tables 26, 32, and 38, respectively.

In this section, we compare the out-of-sample replicating portfolio value performance of the parametric models ($BSMCHV_{N+1}$, $HCHV_{N+1}$, $HJDCHV_{N+1}$, and $FMLSCHV_{N+1}$), the triple hidden layer MLP models ($M3CHV_{N+1} - Models$) and triple hidden layer LSTM models ($L3CHV_{N+1} - Models$), then the parametric models with the $M3CHV_{N+1} - Models$, and finally the parametric models with the $L3CHV_{N+1} - Models$.

The results for the parametric models with the triple hidden layer MLP $M3CHV_{N+1} - Models$ ($M3CHV1_{N+1}$ to $M3CHV7_{N+1}$) and the triple hidden layer LSTM $L3CHV_{N+1} - Models$ ($L3CHV1_{N+1}$ to $L3CHV7_{N+1}$) are presented in Table B.2.21. If all the models are compared together, then the $L3CHV4_{N+1}$ model had the lowest $RMSE$ for 276 days (having a daily bootstrap winning % of 18% to 23%) out of 1,326 days. Table B.2.22 presents the results for the comparison of the parametric models with the triple hidden layer MLP $M3CHV_N - Models$ ($M3CHV1_{N+1}$ to $M3CHV7_{N+1}$), and the $FMLSCHV_{N+1}$ model had the lowest $RMSE$ for 224 days (having a daily bootstrap winning % of 15% to 19%) out of 1,326 days. Though the $FMLSCHV_{N+1}$ model had outperformed other models, another MLP model, the $M3CHV4_{N+1}$(185 days) had shown similar outperformance, where it had a daily bootstrap winning percentage from 12% to 16%. We present the comparison results of the parametric models with the triple hidden layer LSTM $L3CHV_{N+1} - Models$ ($L3CHV1_{N+1}$ to $L3CHV7_{N+1}$) in Table B.2.23. We find that the $HDJCHV_{N+1}$ model had the lowest $RMSE$ for 387 days (having a daily bootstrap winning % of 27% to 32%) out of 1,326 days. Though the $HJDCHV_{N+1}$ model had outperformed other models, another LSTM model, the $L3CHV4_{N+1}$(311 days), had shown similar outperformance, where it had a daily bootstrap winning percentage from 21% to 26%. Finally, we compare amongst the parametric models in Table B.2.24, and find that the $HJDCHV_{N+1}$ model had the lowest $RMSE$ for 479 days (having a daily bootstrap winning % of 34% to 39%) out of 1,326 days.

Thus, when the parametric models are compared with the triple hidden layer ANN models that use one-trading-day-ahead input variables to forecast the call option price (C_{N+1}), from which the delta($\delta C_{N+1}/\delta S_{N+1}$) is analytically computed using the forecasted C_{N+1}, and then the one-trading-day-ahead replicating portfolio value is computed (in Table B.2.21), we conclude that an LSTM model ($L3CHV4_{N+1}$) could outperform all other models. If the parametric models were compared with the triple hidden layer MLP models (in Table B.2.22), a parametric model ($FMLSCHV_{N+1}$) outperforms all other triple hidden layer MLP models, also when the parametric models were compared with the triple hidden layer LSTM models (in Table B.2.23), a parametric model ($HJDCHV_{N+1}$) outperforms all other triple hidden layer LSTM models. Finally, when a comparison is made amongst the parametric models, the $HJDCHV_{N+1}$ model has been shown to outperform the rest of the parametric models.

Table B.2.21: Replicating Portfolio Value Comparison (amongst Parametric, $M3CHV_{N+1}$-Models and $L3CHV_{N+1}$-Models): This table presents a performance comparison using both daily and monthly statistics amongst the Black-Scholes-Merton ($BSMCHV_{N+1}$) model, Heston ($HCHV_{N+1}$) model, Heston Jump Diffusion ($HJDCHV_{N+1}$) model, Finite Moment Log Stable ($FMLSCHV_{N+1}$) model, MLP $M3CHV_{N+1}$-Models ($M3CHV1_{N+1}$ to $M3CHV7_{N+1}$) and the LSTM $L3CHV_{N+1}$-Models ($L3CHV1_{N+1}$ to $L3CHV7_{N+1}$). The forecast variable for all the models is the call option price (C_{N+1}). The models denoted by the $_{N+1}$ subscript use one-trading-day-ahead input variables for forecasting the call option price. The delta ($\delta C_{N+1}/\delta S_{N+1}$) is derived analytically from the forecasted call option price (C_{N+1}) using equation 3.3 and then used to compute the replicating portfolio value V_{N+1} using equation 3.17. The one-trading-day-ahead forecast errors of V_{N+1} are used to compute the Root Mean Square Error (RMSE). Column I identifies the models, column II identifies the forecast variable, and column III lists the input variables used by the models to obtain the V_{N+1}. Forecasts are made for 1,326 trading days, and there are 64 months covered in the sample using the monthly data. Column VII reports the number of months out of the 64 months that each model has the smallest RMSE, while column VIII reports the number of days out of the 1,326 days each model has the smallest RMSE. Columns IX (lower bound) and X (upper bound) present the winning percentage out of 64 months for each model, evaluated using the bootstrap sampling technique. The statistical bootstrap performed (with replacement) at a 95% confidence level is computed from the monthly RMSE values of the respective models below. Similarly, columns XI (lower bound) and XII (upper bound) present the winning percentage out of 1326 days for each model computed from bootstrapping the daily RMSE values of the respective models at a 95% confidence level.

(I) Model	**(II)** Forecast	**(III)** Inputs	**(IV)** Performance amongst all models (Monthly)	**(V)** Performance amongst all models (Daily)	**(VI)** 2.5% lower bound-(for monthly) (%)	**(VII)** 2.5% upper bound-(for monthly) (%)	**(VIII)** 2.5% lower bound-(for daily) (%)	**(IX)** 2.5% upper bound-(for daily) (%)
$BSMCHV_{N+1}$	$V_{N+1}^{BSMCHV_{N+1}}$	$S_{N+1}, S_N, R_{N+1}, \delta t, C_N^{BSMCH_{N+1}}, C_{N+1}^{BSMCH_{N+1}}, \delta_{N+1}^{BSMCH_{N+1}}$	0	77	0%	5%	5%	7%
$HCHV_{N+1}$	$V_{N+1}^{HCHV_{N+1}}$	$S_{N+1}, S_N, R_{N+1}, \delta t, C_N^{HCH_{N+1}}, C_{N+1}^{HCH_{N+1}}, \delta_{N+1}^{HCH_{N+1}}$	0	77	0%	0%	5%	7%
$HJDCHV_{N+1}$	$V_{N+1}^{HJDCHV_{N+1}}$	$S_{N+1}, S_N, R_{N+1}, \delta t, C_N^{HJDCH_{N+1}}, C_{N+1}^{HJDCH_{N+1}}, \delta_{N+1}^{HJDCH_{N+1}}$	2	39	0%	8%	2%	4%
$FMLSCHV_{N+1}$	$V_{N+1}^{FMLSCHV_{N+1}}$	$S_{N+1}, S_N, R_{N+1}, \delta t, C_N^{FMLSCH_{N+1}}, C_{N+1}^{FMLSCH_{N+1}}, \delta_{N+1}^{FMLSCH_{N+1}}$	0	116	0%	0%	7%	10%
$M3CHV1_{N+1}$	$V_{N+1}^{M3CHV1_{N+1}}$	$S_{N+1}, S_N, R_{N+1}, \delta t, C_N^{M3CH1_{N+1}}, C_{N+1}^{M3CH1_{N+1}}, \delta_{N+1}^{M3CH1_{N+1}}$	5	70	2%	14%	4%	6%
$M3CHV2_{N+1}$	$V_{N+1}^{M3CHV2_{N+1}}$	$S_{N+1}, S_N, R_{N+1}, \delta t, C_N^{M3CH2_{N+1}}, C_{N+1}^{M3CH2_{N+1}}, \delta_{N+1}^{M3CH2_{N+1}}$	8	73	5%	22%	4%	7%
$M3CHV3_{N+1}$	$V_{N+1}^{M3CHV3_{N+1}}$	$S_{N+1}, S_N, R_{N+1}, \delta t, C_N^{M3CH3_{N+1}}, C_{N+1}^{M3CH3_{N+1}}, \delta_{N+1}^{M3CH3_{N+1}}$	8	82	5%	20%	5%	7%
$M3CHV4_{N+1}$	$V_{N+1}^{M3CHV4_{N+1}}$	$S_{N+1}, S_N, R_{N+1}, \delta t, C_N^{M3CH4_{N+1}}, C_{N+1}^{M3CH4_{N+1}}, \delta_{N+1}^{M3CH4_{N+1}}$	8	141	6%	20%	9%	12%
$M3CHV5_{N+1}$	$V_{N+1}^{M3CHV5_{N+1}}$	$S_{N+1}, S_N, R_{N+1}, \delta t, C_N^{M3CH5_{N+1}}, C_{N+1}^{M3CH5_{N+1}}, \delta_{N+1}^{M3CH5_{N+1}}$	**14**	109	11%	31%	7%	10%
$M3CHV6_{N+1}$	$V_{N+1}^{M3CHV6_{N+1}}$	$S_{N+1}, S_N, R_{N+1}, \delta t, C_N^{M3CH6_{N+1}}, C_{N+1}^{M3CH6_{N+1}}, \delta_{N+1}^{M3CH6_{N+1}}$	5	81	2%	14%	5%	7%
$M3CHV7_{N+1}$	$V_{N+1}^{M3CHV7_{N+1}}$	$S_{N+1}, S_N, R_{N+1}, \delta t, C_N^{M3CH7_{N+1}}, C_{N+1}^{M3CH7_{N+1}}, \delta_{N+1}^{M3CH7_{N+1}}$	**13**	87	11%	31%	5%	8%
$L3CHV1_{N+1}$	$V_{N+1}^{L3CHV1_{N+1}}$	$S_{N+1}, S_N, R_{N+1}, \delta t, C_N^{L3CH1_{N+1}}, C_{N+1}^{L3CH1_{N+1}}, \delta_{N+1}^{L3CH1_{N+1}}$	0	20	0%	0%	1%	2%
$L3CHV2_{N+1}$	$V_{N+1}^{L3CHV2_{N+1}}$	$S_{N+1}, S_N, R_{N+1}, \delta t, C_N^{L3CH2_{N+1}}, C_{N+1}^{L3CH2_{N+1}}, \delta_{N+1}^{L3CH2_{N+1}}$	0	14	0%	0%	0%	2%
$L3CHV3_{N+1}$	$V_{N+1}^{L3CHV3_{N+1}}$	$S_{N+1}, S_N, R_{N+1}, \delta t, C_N^{L3CH3_{N+1}}, C_{N+1}^{L3CH3_{N+1}}, \delta_{N+1}^{L3CH3_{N+1}}$	0	15	0%	0%	1%	2%
$L3CHV4_{N+1}$	$V_{N+1}^{L3CHV4_{N+1}}$	$S_{N+1}, S_N, R_{N+1}, \delta t, C_N^{L3CH4_{N+1}}, C_{N+1}^{L3CH4_{N+1}}, \delta_{N+1}^{L3CH4_{N+1}}$	1	**276**	0%	5%	18%	23%
$L3CHV5_{N+1}$	$V_{N+1}^{L3CHV5_{N+1}}$	$S_{N+1}, S_N, R_{N+1}, \delta t, C_N^{L3CH5_{N+1}}, C_{N+1}^{L3CH5_{N+1}}, \delta_{N+1}^{L3CH5_{N+1}}$	0	20	0%	0%	1%	2%
$L3CHV6_{N+1}$	$V_{N+1}^{L3CHV6_{N+1}}$	$S_{N+1}, S_N, R_{N+1}, \delta t, C_N^{L3CH6_{N+1}}, C_{N+1}^{L3CH6_{N+1}}, \delta_{N+1}^{L3CH6_{N+1}}$	0	34	0%	0%	2%	3%
$L3CHV7_{N+1}$	$V_{N+1}^{L3CHV7_{N+1}}$	$S_{N+1}, S_N, R_{N+1}, \delta t, C_N^{L3CH7_{N+1}}, C_{N+1}^{L3CH7_{N+1}}, \delta_{N+1}^{L3CH7_{N+1}}$	0	7	0%	0%	0%	1%

Table B.2.22: Replicating Portfolio Value Comparison (amongst Parametric and $M3CHV_{N+1}$-Models): This table presents a performance comparison using both daily and monthly statistics amongst the Black-Scholes-Merton ($BSMCHV_{N+1}$) model, Heston ($HCHV_{N+1}$) model, Heston Jump Diffusion ($HJDCHV_{N+1}$) model, Finite Moment Log Stable ($FMLSCHV_{N+1}$) model, and the MLP $M3CHV_{N+1}$-Models ($M3CHV1_{N+1}$ to $M3CHV7_{N+1}$). The forecast variable for all the models is the call option price (C_{N+1}). The models denoted by the $_{N+1}$ subscript use one-trading-day-ahead input variables for forecasting the call option price. The delta ($\delta C_{N+1}/\delta S_{N+1}$) is derived analytically from the forecasted call option price (C_{N+1}) using equation 3.3 and then used to compute the replicating portfolio value V_{N+1} using equation 3.17. The one-trading-day-ahead forecast errors of V_{N+1} are used to compute the Root Mean Square Error (RMSE). Column I identifies the models, column II identifies the forecast variable, and column III lists the input variables used by the models to obtain the V_{N+1}. Forecasts are made for 1,326 trading days, and there are 64 months covered in the sample using the monthly data. Column VII reports the number of months out of the 64 months that each model has the smallest RMSE, while column VIII reports the number of days out of the 1,326 days each model has the smallest RMSE. Columns IX (lower bound) and X (upper bound) present the winning percentage out of 64 months for each model, evaluated using the bootstrap sampling technique. The statistical bootstrap performed (with replacement) at a 95% confidence level is computed from the monthly RMSE values of the respective models below. Similarly, columns XI (lower bound) and XII (upper bound) present the winning percentage out of 1326 days for each model computed from bootstrapping the daily RMSE values of the respective models at a 95% confidence level.

(I) Model	**(II) Forecast**	**(III) Inputs**	**(IV) Performance amongst all models (Monthly)**	**(V) Performance amongst all models (Daily)**	**(VI) 2.5% lower bound-(for monthly) (%)**	**(VII) 2.5% upper bound-(for monthly) (%)**	**(VIII) 2.5% lower bound-(for daily) (%)**	**(IX) 2.5% upper bound-(for daily) (%)**
$BSMCHV_{N+1}$	$V_{N+1}^{BSMCHV_{N+1}}$	$S_{N+1}, S_N, R_{N+1}, \delta t, C_N^{BSMCH_{N+1}}, C_{N+1}^{BSMCH_{N+1}}, \delta_{N+1}^{BSMCH_{N+1}}$	0	123	0%	5%	8%	11%
$HCHV_{N+1}$	$V_{N+1}^{HCHV_{N+1}}$	$S_{N+1}, S_N, R_{N+1}, \delta t, C_N^{HCH_{N+1}}, C_{N+1}^{HCH_{N+1}}, \delta_{N+1}^{HCH_{N+1}}$	0	110	0%	0%	7%	10%
$HJDCHV_{N+1}$	$V_{N+1}^{HJDCHV_{N+1}}$	$S_{N+1}, S_N, R_{N+1}, \delta t, C_N^{HJDCH_{N+1}}, C_{N+1}^{HJDCH_{N+1}}, \delta_{N+1}^{HJDCH_{N+1}}$	2	50	0%	8%	3%	5%
$FMLSCHV_{N+1}$	$V_{N+1}^{FMLSCHV_{N+1}}$	$S_{N+1}, S_N, R_{N+1}, \delta t, C_N^{FMLSCH_{N+1}}, C_{N+1}^{FMLSCH_{N+1}}, \delta_{N+1}^{FMLSCH_{N+1}}$	0	**224**	0%	0%	15%	19%
$M3CHV1_{N+1}$	$V_{N+1}^{M3CHV1_{N+1}}$	$S_{N+1}, S_N, R_{N+1}, \delta t, C_N^{M3CH1_{N+1}}, C_{N+1}^{M3CH1_{N+1}}, \delta_{N+1}^{M3CH1_{N+1}}$	5	93	2%	16%	6%	8%
$M3CHV2_{N+1}$	$V_{N+1}^{M3CHV2_{N+1}}$	$S_{N+1}, S_N, R_{N+1}, \delta t, C_N^{M3CH2_{N+1}}, C_{N+1}^{M3CH2_{N+1}}, \delta_{N+1}^{M3CH2_{N+1}}$	8	98	5%	20%	6%	9%
$M3CHV3_{N+1}$	$V_{N+1}^{M3CHV3_{N+1}}$	$S_{N+1}, S_N, R_{N+1}, \delta t, C_N^{M3CH3_{N+1}}, C_{N+1}^{M3CH3_{N+1}}, \delta_{N+1}^{M3CH3_{N+1}}$	8	116	5%	20%	7%	10%
$M3CHV4_{N+1}$	$V_{N+1}^{M3CHV4_{N+1}}$	$S_{N+1}, S_N, R_{N+1}, \delta t, C_N^{M3CH4_{N+1}}, C_{N+1}^{M3CH4_{N+1}}, \delta_{N+1}^{M3CH4_{N+1}}$	8	185	5%	22%	12%	16%
$M3CHV5_{N+1}$	$V_{N+1}^{M3CHV5_{N+1}}$	$S_{N+1}, S_N, R_{N+1}, \delta t, C_N^{M3CH5_{N+1}}, C_{N+1}^{M3CH5_{N+1}}, \delta_{N+1}^{M3CH5_{N+1}}$	**15**	130	13%	33%	8%	11%
$M3CHV6_{N+1}$	$V_{N+1}^{M3CHV6_{N+1}}$	$S_{N+1}, S_N, R_{N+1}, \delta t, C_N^{M3CH6_{N+1}}, C_{N+1}^{M3CH6_{N+1}}, \delta_{N+1}^{M3CH6_{N+1}}$	5	97	2%	16%	6%	9%
$M3CHV7_{N+1}$	$V_{N+1}^{M3CHV7_{N+1}}$	$S_{N+1}, S_N, R_{N+1}, \delta t, C_N^{M3CH7_{N+1}}, C_{N+1}^{M3CH7_{N+1}}, \delta_{N+1}^{M3CH7_{N+1}}$	13	105	11%	30%	6%	9%

Table B.2.23: Replicating Portfolio Value Comparison (amongst Parametric and $L3CHV_{N+1}$-Models): This table presents a performance comparison using both daily and monthly statistics amongst the Black-Scholes-Merton ($BSMCHV_{N+1}$) model, Heston ($HCHV_{N+1}$) model, Heston Jump Diffusion ($HJDCHV_{N+1}$) model, Finite Moment Log Stable ($FMLSCHV_{N+1}$) model, and the LSTM $L3CHV_{N+1}$-Models ($L3CHV1_{N+1}$ to $L3CHV7_{N+1}$). The forecast variable for all the models is the call option price (C_{N+1}). The models denoted by the $_{N+1}$ subscript use one-trading-day-ahead input variables for forecasting the call option price. The delta ($\delta C_{N+1}/\delta S_{N+1}$) is derived analytically from the forecasted call option price (C_{N+1}) using equation 3.3 and then used to compute the replicating portfolio value V_{N+1} using equation 3.17. The one-trading-day-ahead forecast errors of V_{N+1} are used to compute the Root Mean Square Error (RMSE). Column I identifies the models, column II identifies the forecast variable, and column III lists the input variables used by the models to obtain the V_{N+1}. Forecasts are made for 1,326 trading days, and there are 64 months covered in the sample using the monthly data. Column VII reports the number of months out of the 64 months that each model has the smallest RMSE, while column VIII reports the number of days out of the 1,326 days each model has the smallest RMSE. Columns IX (lower bound) and X (upper bound) present the winning percentage out of 64 months for each model, evaluated using the bootstrap sampling technique. The statistical bootstrap performed (with replacement) at a 95% confidence level is computed from the monthly RMSE values of the respective models below. Similarly, columns XI (lower bound) and XII (upper bound) present the winning percentage out of 1326 days for each model computed from bootstrapping the daily RMSE values of the respective models at a 95% confidence level.

(I) Model	**(II)** Forecast	**(III)** Inputs	**(IV)** Performance amongst all models (Monthly)	**(V)** Performance amongst all models (Daily)	**(VI)** 2.5% lower bound-(for monthly) (%)	**(VII)** 2.5% upper bound-(for monthly) (%)	**(VIII)** 2.5% lower bound-(for daily) (%)	**(IX)** 2.5% upper bound-(for daily) (%)
$BSMCHV_{N+1}$	$V_{N+1}^{BSMCHV_{N+1}}$	$S_{N+1}, S_N, R_{N+1}, \delta t, C_N^{BSMCH_{N+1}}, C_{N+1}^{BSMCH_{N+1}}, \delta_{N+1}^{BSMCH_{N+1}}$	0	84	0%	5%	5%	8%
$HCHV_{N+1}$	$V_{N+1}^{HCHV_{N+1}}$	$S_{N+1}, S_N, R_{N+1}, \delta t, C_N^{HCH_{N+1}}, C_{N+1}^{HCH_{N+1}}, \delta_{N+1}^{HCH_{N+1}}$	7	254	3%	17%	17%	21%
$HJDCHV_{N+1}$	$V_{N+1}^{HJDCHV_{N+1}}$	$S_{N+1}, S_N, R_{N+1}, \delta t, C_N^{HJDCH_{N+1}}, C_{N+1}^{HJDCH_{N+1}}, \delta_{N+1}^{HJDCH_{N+1}}$	**56**	**387**	80%	95%	27%	32%
$FMLSCHV_{N+1}$	$V_{N+1}^{FMLSCHV_{N+1}}$	$S_{N+1}, S_N, R_{N+1}, \delta t, C_N^{FMLSCH_{N+1}}, C_{N+1}^{FMLSCH_{N+1}}, \delta_{N+1}^{FMLSCH_{N+1}}$	0	182	0%	0%	12%	16%
$L3CHV1_{N+1}$	$V_{N+1}^{L3CHV1_{N+1}}$	$S_{N+1}, S_N, R_{N+1}, \delta t, C_N^{L3CH1_{N+1}}, C_{N+1}^{L3CH1_{N+1}}, \delta_{N+1}^{L3CH1_{N+1}}$	0	21	0%	0%	1%	2%
$L3CHV2_{N+1}$	$V_{N+1}^{L3CHV2_{N+1}}$	$S_{N+1}, S_N, R_{N+1}, \delta t, C_N^{L3CH2_{N+1}}, C_{N+1}^{L3CH2_{N+1}}, \delta_{N+1}^{L3CH2_{N+1}}$	0	14	0%	0%	1%	2%
$L3CHV3_{N+1}$	$V_{N+1}^{L3CHV3_{N+1}}$	$S_{N+1}, S_N, R_{N+1}, \delta t, C_N^{L3CH3_{N+1}}, C_{N+1}^{L3CH3_{N+1}}, \delta_{N+1}^{L3CH3_{N+1}}$	0	15	0%	0%	1%	2%
$L3CHV4_{N+1}$	$V_{N+1}^{L3CHV4_{N+1}}$	$S_{N+1}, S_N, R_{N+1}, \delta t, C_N^{L3CH4_{N+1}}, C_{N+1}^{L3CH4_{N+1}}, \delta_{N+1}^{L3CH4_{N+1}}$	1	311	0%	5%	21%	26%
$L3CHV5_{N+1}$	$V_{N+1}^{L3CHV5_{N+1}}$	$S_{N+1}, S_N, R_{N+1}, \delta t, C_N^{L3CH5_{N+1}}, C_{N+1}^{L3CH5_{N+1}}, \delta_{N+1}^{L3CH5_{N+1}}$	0	21	0%	0%	1%	2%
$L3CHV6_{N+1}$	$V_{N+1}^{L3CHV6_{N+1}}$	$S_{N+1}, S_N, R_{N+1}, \delta t, C_N^{L3CH6_{N+1}}, C_{N+1}^{L3CH6_{N+1}}, \delta_{N+1}^{L3CH6_{N+1}}$	0	35	0%	0%	2%	3%
$L3CHV7_{N+1}$	$V_{N+1}^{L3CHV7_{N+1}}$	$S_{N+1}, S_N, R_{N+1}, \delta t, C_N^{L3CH7_{N+1}}, C_{N+1}^{L3CH7_{N+1}}, \delta_{N+1}^{L3CH7_{N+1}}$	0	7	0%	0%	0%	1%

Table B.2.24: Replicating Portfolio Value Comparison (amongst Parametric models): This table presents a performance comparison using both daily and monthly statistics amongst the Black-Scholes-Merton ($BSMCHV_{N+1}$) model, Heston ($HCHV_{N+1}$) model, Heston Jump Diffusion ($HJDCHV_{N+1}$) model, and the Finite Moment Log Stable ($FMLSCHV_{N+1}$) model. The forecast variable for all the models is the call option price (C_{N+1}). The models denoted by the $_{N+1}$ subscript use one-trading-day-ahead input variables for forecasting the call option price. The delta ($\delta C_{N+1}/\delta S_{N+1}$) is derived analytically from the forecasted call option price (C_{N+1}) using equation 3.3 and then used to compute the replicating portfolio value V_{N+1} using equation 3.17. The one-trading-day-ahead forecast errors of V_{N+1} are used to compute the Root Mean Square Error (RMSE). Column I identifies the models, column II identifies the forecast variable, and column III lists the input variables used by the models to obtain the V_{N+1}. Forecasts are made for 1,326 trading days, and there are 64 months covered in the sample using the monthly data. Column IV reports the number of months out of the 64 months that each model has the smallest RMSE, while column V reports the number of days out of the 1,326 days each model has the smallest RMSE. Columns VI (lower bound) and VII (upper bound) present the winning percentage out of 64 months for each model, evaluated using the bootstrap sampling technique. The statistical bootstrap performed (with replacement) at a 95% confidence level is computed from the monthly RMSE values of the respective models below. Similarly, columns VIII (lower bound) and IX (upper bound) present the winning percentage out of 1326 days for each model computed from bootstrapping the daily RMSE values of the respective models at a 95% confidence level.

(I) Model	**(II)** Forecast	**(III)** Inputs	**(IV)** Performance amongst all models (Monthly)	**(V)** Performance amongst all models (Daily)	**(VI)** 2.5% lower bound- (for monthly) (%)	**(VII)** 2.5% upper bound- (for monthly) (%)	**(VIII)** 2.5% lower bound- (for daily) (%)	**(IX)** 2.5% upper bound- (for daily) (%)
$BSMCHV_{N+1}$	$V_{N+1}^{BSMCHV_{N+1}}$	$S_{N+1}, S_N, R_{N+1}, \delta t, C_N^{BSMCH_{N+1}}, C_{N+1}^{BSMCH_{N+1}}, \delta_{N+1}^{BSMCH_{N+1}}$	0	136	0%	5%	9%	12%
$HCHV_{N+1}$	$V_{N+1}^{HCHV_{N+1}}$	$S_{N+1}, S_N, R_{N+1}, \delta t, C_N^{HCH_{N+1}}, C_{N+1}^{HCH_{N+1}}, \delta_{N+1}^{HCH_{N+1}}$	8	360	3%	19%	25%	29%
$HJDCHV_{N+1}$	$V_{N+1}^{HJDCHV_{N+1}}$	$S_{N+1}, S_N, R_{N+1}, \delta t, C_N^{HJDCH_{N+1}}, C_{N+1}^{HJDCH_{N+1}}, \delta_{N+1}^{HJDCH_{N+1}}$	**56**	**479**	80%	95%	34%	39%
$FMLSCHV_{N+1}$	$V_{N+1}^{FMLSCHV_{N+1}}$	$S_{N+1}, S_N, R_{N+1}, \delta t, C_N^{FMLSCH_{N+1}}, C_{N+1}^{FMLSCH_{N+1}}, \delta_{N+1}^{FMLSCH_{N+1}}$	0	350	0%	0%	24%	29%

Appendix C.1

Appendix for Chapter 4: Tables

Table C.1.1: Diebold-Mariano(DM) test-based insignificant pairs: This table presents the insignificant pairs for models discussed in 4, where the averaging was done for the $C-Models$, $CK-Models$, $H-Models$, $CH-Models$, $HV-Models$, $CHV-Models$. The complete table consisting of the DM test statistic for $C-Models$ which use lagged input variables to forecast the C_{N+1} can be found in table 81, for $C-Models$ which use one-trading-day-ahead input variables to forecast the C_{N+1} in table 83, for $CK-Models$ that use one-trading-day-ahead input variables to forecast the C_{N+1}/K_{N+1} in table 82 and for $CK-Models$ that use one-trading-day-ahead input variables to forecast the C_{N+1}/K_{N+1} in table 84, for the $H-Models$ which use lagged input variables to forecast the Δ_{N+1} can be found in table 85, for $H-Models$ which use one-trading-day-ahead input variables to forecast the Δ_{N+1} in table 86, for $CH-Models$ that use one-trading-day-ahead input variables to forecast the δ_{N+1} in table 87, for $HV-Models$ which use delta from $H-Models$ (using lagged inputs for forecasting) in table 88, for $HV-Models$ which use delta from $H-Models$ (using one-trading-day-ahead inputs for forecasting) in table 89, and $CHV-Models$ which use delta from $CH-Models$ in table 90 of the Electronic Appendix.

Model	Insignificant Pairs
For $C-Models$ which use lagged input variables to forecast the C_{N+1}	$(L1C_N^{AVG}-Models\ ,\ L2C_N^{AVG}-Models)$
$C-Models$ which use one-trading-day-ahead input variables to forecast the C_{N+1}	None
$CK-Models$ that use one-trading-day-ahead input variables to forecast the C_{N+1}/K_{N+1}	None
$CK-Models$ that use one-trading-day-ahead input variables to forecast the C_{N+1}/K_{N+1}	None
For $H-Models$ (using lagged inputs)	None
For $H-Models$ (using one-trading-day-ahead inputs)	None
For $CH-Models$ (using one-trading-day-ahead inputs)	None
For $HV-Models$ computed from the Δ_{N+1} obtained from $H-Models$ that uses lagged input variables for forecasting	None
For $HV-Models$ computed from the Δ_{N+1} obtained from $H-Models$ that uses one-trading-day input variables for forecasting	None
For $CHV-Models$ computed from the δ_{N+1} obtained from $CH-Models$ that uses one-trading-day input variables for forecasting	None

Table C.1.2: This table presents the summary of the pair-wise bootstrap tests performed for models in 4, where the averaging was done for the $C-Models$, $CK-Models$, $H-Models$, $CH-Models$, $HV-Models$, $CHV-Models$. The complete table consisting of the results for the pair-wise bootstrap for $C-Models$ which use lagged input variables to forecast the C_{N+1} can be found in Table 91, for $C-Models$ which use one-trading-day-ahead input variables to forecast the C_{N+1} in Table 92, for $CK-Models$ that use one-trading-day-ahead input variables to forecast the C_{N+1}/K_{N+1} in Table 93 and for $CK-Models$ that use one-trading-day-ahead input variables to forecast the C_{N+1}/K_{N+1} in Table 94, for the $H-Models$ which use lagged input variables to forecast the Δ_{N+1} can be found in Table 95, for $H-Models$ which use one-trading-day-ahead input variables to forecast the Δ_{N+1} in Table 96, for $CH-Models$ that use one-trading-day-ahead input variables to forecast the δ_{N+1} in Table 97, for $HV-Models$ which use delta from $H-Models$ (that uses lagged inputs for forecasting δ_{N+1}) in Table 98, for $HV-Models$ which use delta from $H-Models$ (that uses one-trading-day-ahead inputs for forecasting δ_{N+1}) in Table 99, and $CHV-Models$ which use delta from $CH-Models$ in Table 100 of the Electronic Appendix.

Model	Number of pairs a model wins	Winning %
$C-Models$ (using lagged inputs)		
δC_N	7	25.0%
$M2C_N^{AVG}-Models$	6	21.4%
$M3C_N^{AVG}-Models$	5	17.9%
$M1C_N^{AVG}-Models$	4	14.3%
$ParamC_N^{AVG}-Models$	3	10.7%
$L2C_N^{AVG}-Models$	2	7.1%
$L3C_N^{AVG}-Models$	1	3.6%
$L1C_N^{AVG}-Models$	0	0.0%
$CK-Models$ (using lagged inputs)		
δCK_N	7	25.0%
$M3CK_N^{AVG}-Models$	6	21.4%
$M2CK_N^{AVG}-Models$	5	17.9%
$M1CK_N^{AVG}-Models$	4	14.3%
$ParamCK_N^{AVG}-Models$	3	10.7%
$L3CK_N^{AVG}-Models$	2	7.1%
$L2CK_N^{AVG}-Models$	1	3.6%
$L1CK_N^{AVG}-Models$	0	0.0%
$C-Models$ (using one-trading-day-ahead inputs)		
$M3C_{N+1}^{AVG}-Models$	3	50.0%
$ParamC_{N+1}^{AVG}-Models$	2	33.3%
δC_{N+1}	1	16.7%
$L3C_{N+1}^{AVG}-Models$	0	0.0%
$CK-Models$ (using one-trading-day-ahead inputs)		
$M3CK_{N+1}^{AVG}-Models$	3	50.0%
δCK_{N+1}	2	33.3%
$ParamCK_{N+1}^{AVG}-Models$	1	16.7%
$L3CK_{N+1}^{AVG}-Models$	0	0.0%
$H-Models$ (using lagged inputs)		
$M3H_N^{AVG}-Models$	2	66.7%
$ParamH_N^{AVG}-Models$	1	33.3%
$L3H_N^{AVG}-Models$	0	0.0%
$H-Models$(using one-trading-day-ahead inputs)		
$ParamH_{N+1}^{AVG}-Models$	2	66.7%
$M3H_{N+1}^{AVG}-Models$	1	33.3%
$L3H_{N+1}^{AVG}-Models$	0	0.0%
$CH-Models$ (using one-trading-day-ahead inputs)		
$ParamCH_{N+1}^{AVG}-Models$	2	66.7%
$M3CH_{N+1}^{AVG}-Models$	1	33.3%
$L3CH_{N+1}^{AVG}-Models$	0	0.0%
$HV-Models$ (computed from the Δ_{N+1} obtained from $H-Models$ that use lagged input variables for forecasting)		
$M3HV_N^{AVG}-Models$	2	66.7%
$ParamHV_N^{AVG}-Models$	1	33.3%
$L3HV_N^{AVG}-Models$	0	0.0%
$HV-Models$ (computed from the Δ_{N+1} obtained from $H-Models$ that use one-trading-day-ahead input variables for forecasting		
$ParamHV_{N+1}^{AVG}-Models$	2	66.7%
$M3HV_{N+1}^{AVG}-Models$	1	33.3%
$L3HV_{N+1}^{AVG}-Models$	0	0.0%
$CHV-Models$ (computed from the δ_{N+1} obtained from $CH-Models$ that use one-trading-day-ahead input variables for forecasting)		
$ParamCHV_{N+1}^{AVG}-Models$	2	66.7%
$M3CHV_{N+1}^{AVG}-Models$	1	33.3%
$L3CHV_{N+1}^{AVG}-Models$	0	0.0%

Table C.1.3: Model Definition for Parametric, MLP and LSTM models discussed in Chapter 4

(I) Model	(II) Inputs
Average of $C-Models$ which use lagged input variables to forecast the C_{N+1}	
$ParamC_N^{AVG}-Models$	$BSMC_N$, HC_N, $HJDC_N$, and $FMLSC_N$
$M1C_N^{AVG}-Models$	$M1C1_N$, $M1C2_N$, $M1C3_N$, $M1C4_N$, $M1C5_N$, $M1C6_N$, $M1C7_N$, $M1C8_N$, and $M1C9_N$
$M2C_N^{AVG}-Models$	$M2C1_N$, $M2C2_N$, $M2C3_N$, $M2C4_N$, $M2C5_N$, $M2C6_N$, $M2C7_N$, $M2C8_N$, and $M2C9_N$
$M3C_N^{AVG}-Models$	$M3C1_N$, $M3C2_N$, $M3C3_N$, $M3C4_N$, $M3C5_N$, $M3C6_N$, $M3C7_N$, $M3C8_N$, and $M3C9_N$
$L1C_N^{AVG}-Models$	$L1C1_N$, $L1C2_N$, $L1C3_N$, $L1C4_N$, $L1C5_N$, $L1C6_N$, $L1C7_N$, $L1C8_N$, and $L1C9_N$
$L2C_N^{AVG}-Models$	$L2C1_N$, $L2C2_N$, $L2C3_N$, $L2C4_N$, $L2C5_N$, $L2C6_N$, $L2C7_N$, $L2C8_N$, and $L2C9_N$
$L3C_N^{AVG}-Models$	$L3C1_N$, $L3C2_N$, $L3C3_N$, $L3C4_N$, $L3C5_N$, $L3C6_N$, $L3C7_N$, $L3C8_N$, and $L3C9_N$
Average of $C-Models$ which use one-trading-day-ahead input variables to forecast the C_{N+1}	
$ParamC_{N+1}^{AVG}-Models$	$BSMC_{N+1}$, HC_{N+1}, $HJDC_{N+1}$, and $FMLSC_{N+1}$
$M3C_{N+1}^{AVG}-Models$	$M3C1_{N+1}$, $M3C2_{N+1}$, $M3C3_{N+1}$, $M3C4_{N+1}$, $M3C5_{N+1}$, $M3C6_{N+1}$, $M3C7_{N+1}$, $M3C8_{N+1}$, and $M3C9_{N+1}$
$L3C_{N+1}^{AVG}-Models$	$L3C1_{N+1}$, $L3C2_{N+1}$, $L3C3_{N+1}$, $L3C4_{N+1}$, $L3C5_{N+1}$, $L3C6_{N+1}$, $L3C7_{N+1}$, $L3C8_{N+1}$, and $L3C9_{N+1}$
Average of $CK-Models$ that use lagged ahead input variables to forecast the C_{N+1}/K_{N+1}	
$ParamCK_N^{AVG}-Models$	$BSMCK_N$, HCK_N, $HJDCK_N$, and $FMLSCK_N$
$M1CK_N^{AVG}-Models$	$M1CK1_N$, $M1CK2_N$, $M1CK3_N$, $M1CK4_N$, $M1CK5_N$, $M1CK6_N$, $M1CK7_N$, $M1CK8_N$, and $M1CK9_N$
$M2CK_N^{AVG}-Models$	$M2CK1_N$, $M2CK2_N$, $M2CK3_N$, $M2CK4_N$, $M2CK5_N$, $M2CK6_N$, $M2CK7_N$, $M2CK8_N$, and $M2CK9_N$
$M3CK_N^{AVG}-Models$	$M3CK1_N$, $M3CK2_N$, $M3CK3_N$, $M3CK4_N$, $M3CK5_N$, $M3CK6_N$, $M3CK7_N$, $M3CK8_N$, and $M3CK9_N$
$L1CK_N^{AVG}-Models$	$L1CK1_N$, $L1CK2_N$, $L1CK3_N$, $L1CK4_N$, $L1CK5_N$, $L1CK6_N$, $L1CK7_N$, $L1CK8_N$, and $L1CK9_N$
$L2CK_N^{AVG}-Models$	$L2CK1_N$, $L2CK2_N$, $L2CK3_N$, $L2CK4_N$, $L2CK5_N$, $L2CK6_N$, $L2CK7_N$, $L2CK8_N$, and $L2CK9_N$
$L3CK_N^{AVG}-Models$	$L3CK1_N$, $L3CK2_N$, $L3CK3_N$, $L3CK4_N$, $L3CK5_N$, $L3CK6_N$, $L3CK7_N$, $L3CK8_N$, and $L3CK9_N$
Average of $CK-Models$ that use one-trading-day-ahead input variables to forecast the C_{N+1}/K_{N+1}	
$ParamCK_{N+1}^{AVG}-Models$	$BSMCK_{N+1}$, HCK_{N+1}, $HJDCK_{N+1}$, and $FMLSCK_{N+1}$
$M3CK_{N+1}^{AVG}-Models$	$M3CK1_{N+1}$, $M3CK2_{N+1}$, $M3CK3_{N+1}$, $M3CK4_{N+1}$, $M3CK5_{N+1}$, $M3CK6_{N+1}$, $M3CK7_{N+1}$, $M3CK8_{N+1}$, and $M3CK9_{N+1}$
$L3CK_{N+1}^{AVG}-Models$	$L3CK1_{N+1}$, $L3CK2_{N+1}$, $L3CK3_{N+1}$, $L3CK4_{N+1}$, $L3CK5_{N+1}$, $L3CK6_{N+1}$, $L3CK7_{N+1}$, $L3CK8_{N+1}$, and $L3CK9_{N+1}$
$H-Models$ (using lagged inputs)	
$ParamH_N^{AVG}-Models$	$BSMH_N$, HH_N, $HJDH_N$, and $FMLSH_N$
$M3H_N^{AVG}-Models$	$M3H1_N$, $M3H2_N$, $M3H3_N$, $M3H4_N$, $M3H5_N$, $M3H6_N$, $M3H7_N$
$L3H_N^{AVG}-Models$	$L3H1_N$, $L3H2_N$, $L3H3_N$, $L3H4_N$, $L3H5_N$, $L3H6_N$, $L3H7_N$
$H-Models$(using one-trading-day-ahead inputs)	
$ParamH_{N+1}^{AVG}-Models$	$BSMH_{N+1}$, HH_{N+1}, $HJDH_{N+1}$, and $FMLSH_{N+1}$
$M3H_{N+1}^{AVG}-Models$	$M3H1_{N+1}$, $M3H2_{N+1}$, $M3H3_{N+1}$, $M3H4_{N+1}$, $M3H5_{N+1}$, $M3H6_{N+1}$, $M3H7_{N+1}$
$L3H_{N+1}^{AVG}-Models$	$L3H1_{N+1}$, $L3H2_{N+1}$, $L3H3_{N+1}$, $L3H4_{N+1}$, $L3H5_{N+1}$, $L3H6_{N+1}$, $L3H7_{N+1}$
$CH-Models$ (using one-trading-day-ahead inputs)	
$ParamCH_{N+1}^{AVG}-Models$	$BSMCH_{N+1}$, $CHCH_{N+1}$, $CHJDCH_{N+1}$, and $FMLSCH_{N+1}$
$M3CH_{N+1}^{AVG}-Models$	$M3CH1_{N+1}$, $M3CH2_{N+1}$, $M3CH3_{N+1}$, $M3CH4_{N+1}$, $M3CH5_{N+1}$, $M3CH6_{N+1}$, $M3CH7_{N+1}$
$L3CH_{N+1}^{AVG}-Models$	$L3CH1_{N+1}$, $L3CH2_{N+1}$, $L3CH3_{N+1}$, $L3CH4_{N+1}$, $L3CH5_{N+1}$, $L3CH6_{N+1}$, $L3CH7_{N+1}$
$HV-Models$ (computed from the Δ_{N+1} obtained from $H-Models$ that use lagged input variables for forecasting)	
$ParamHV_N^{AVG}-Models$	$BSMHV_N$, $HVHV_N$, $HVJDHV_N$, and $FMLSHV_N$
$M3HV_N^{AVG}-Models$	$M3HV1_N$, $M3HV2_N$, $M3HV3_N$, $M3HV4_N$, $M3HV5_N$, $M3HV6_N$, $M3HV7_N$
$L3HV_N^{AVG}-Models$	$L3HV1_N$, $L3HV2_N$, $L3HV3_N$, $L3HV4_N$, $L3HV5_N$, $L3HV6_N$, $L3HV7_N$
$HV-Models$ (computed from the Δ_{N+1} obtained from $H-Models$ that use one-trading-day-ahead input variables for forecasting	
$ParamHV_{N+1}^{AVG}-Models$	$BSMHV_{N+1}$, $HVHV_{N+1}$, $HVJDHV_{N+1}$, and $FMLSHV_{N+1}$
$M3HV_{N+1}^{AVG}-Models$	$M3HV1_{N+1}$, $M3HV2_{N+1}$, $M3HV3_{N+1}$, $M3HV4_{N+1}$, $M3HV5_{N+1}$, $M3HV6_{N+1}$, $M3HV7_{N+1}$
$L3HV_{N+1}^{AVG}-Models$	$L3HV1_{N+1}$, $L3HV2_{N+1}$, $L3HV3_{N+1}$, $L3HV4_{N+1}$, $L3HV5_{N+1}$, $L3HV6_{N+1}$, $L3HV7_{N+1}$
$CHV-Models$ (computed from the δ_{N+1} obtained from $CH-Models$ that use one-trading-day-ahead input variables for forecasting)	
$ParamCHV_{N+1}^{AVG}-Models$	$BSMCHV_{N+1}$, $CHVCHV_{N+1}$, $CHVJDCHV_{N+1}$, and $FMLSCHV_{N+1}$
$M3CHV_{N+1}^{AVG}-Models$	$M3CHV1_{N+1}$, $M3CHV2_{N+1}$, $M3CHV3_{N+1}$, $M3CHV4_{N+1}$, $M3CHV5_{N+1}$, $M3CHV6_{N+1}$, $M3CHV7_{N+1}$
$L3CHV_{N+1}^{AVG}-Models$	$L3CHV1_{N+1}$, $L3CHV2_{N+1}$, $L3CHV3_{N+1}$, $L3CHV4_{N+1}$, $L3CHV5_{N+1}$, $L3CHV6_{N+1}$, $L3CHV7_{N+1}$

Appendix C.2

Appendix for Chapter 4: Extended Results

C.2.1 Results - $C^{AVG} - Models$ - Model Averaging

C.2.1.1 $C^{AVG} - Models$: Model averaging pricing performance of models that use lagged input variables to forecast the call option price (C_{N+1}) for the next trading day:

Table C.2.1 shows the relative out-of-sample pricing performance (in $RMSE$) amongst the models that forecast the one-trading-day-ahead average call option price(C_{N+1}) using lagged input variables. In column II of table C.2.1, we list the several models used as input to obtain the average one-trading-day-ahead forecast of C_{N+1}. The performance metric is the $RMSE$ of the one-trading-day-ahead forecast errors of the average C_{N+1}, which is computed for each averaging model utilising all of the errors in each day or each month. Amongst all of the models (including the random walk model (δC_N)), columns III and IV record the number of months and days, respectively, that each model had the lowest $RMSE$. We performed a bootstrap using the daily and monthly RMSEs to be certain of our results. The columns V (lower bound) and VI (upper bound) present the results from the bootstrap performed (with replacement) using monthly RMSEs at a 95% confidence level and shows the winning percentage out of 64 months for each model (including the δC_N model) and similarly, the 95 % confidence intervals computed from bootstrapping of the daily RMSEs signifies the winning percentage out of 1,328 days for each model and are reported in columns VII (lower bound), VIII (upper bound). While excluding the δC_N model amongst the comparison, columns IX and X record the number of months and days that each model had the lowest $RMSE$. We repeat the exercise of performing the bootstrap by excluding the δC_N model in the comparison, and thus, the columns XI (lower bound) and XII (upper bound) present the results from the bootstrap performed (with replacement) using monthly RMSEs at a 95% confidence level and shows the winning percentage out of 64 months for each model (excluding the δC_N model) and similarly, the 95 % confidence intervals computed from bootstrapping of the daily RMSEs signifies the winning percentage out of 1,328 days for each model and are reported in columns XIII (lower bound), XIV (upper bound). After a model is found to out-perform other individual parametric models, MLP and LSTM models in each of the several comparisons below, we look into whether that out-performing model individually can out-perform the average call option price of all the parametric models combinedly, MLP models combinedly or LSTM models combinedly, covered in that section.

In the below several comparisons, even though a particular model wins by a higher percentage against other models, we investigated further these models pairwise by performing a pairwise bootstrap comparison, which was computed using the respective pair's daily RMSEs. The results are presented in Table 91 of the Electronic Appendix.

The Diebold-Mariano(DM) (Diebold and Mariano (1995)) test was performed on pairs amongst the Random Walk (δC_N) model, the average call option price of all parametric models ($ParamC_N^{AVG}-Models$), the average call option price of all single hidden layer MLP models ($M1C_N^{AVG}-Models$), the average call option price of all single hidden layer LSTM models ($L1C_N^{AVG}-Models$), the average option price of all double hidden layer MLP models ($M2C_N^{AVG}-Models$), the average call option price of all double hidden layer LSTM models ($L3C_N^{AVG}-Models$), the average call option price of all triple hidden layer MLP models ($M3C_N^{AVG}-Models$), and the average call option price of all triple hidden layer LSTM models ($L3C_N^{AVG}-Models$) are reported in Table 81 of the Electronic Appendix. In constructing the DM tests, the model pairs are reported in column I and column II, and the DM test statistics for a particular pair are reported in column III. If the null can be rejected, a positive number suggests the rejection may be due to the second model being the better forecast model. In contrast, a negative value suggests the rejection may be due to the first model being the better forecast model. The model pairs highlighted in a red state that their forecasts have statistically insignificant differences in their prediction accuracy. The following model pairs have been shown to have statistically insignificant differences: ($M3C_N^{AVG}-Models$, $MC_N^{AVG}-Models$), ($L1C_N^{AVG}-Models$, $L2C_N^{AVG}-Models$).

The RMSEs for the models under the $C^{AVG}-Models$ category, which averages the forecasted C_{N+1} from models belonging to the $C-Models$ category (which uses lagged input variables to forecast the C_{N+1} for the next trading day) on a monthly, yearly, and overall basis can be found in the Electronic Appendix, in Tables 51, 61, and 71, respectively.

C.2.1.1.1 Comparison amongst all Parametric Models with Single Hidden Layer ANN Models:

In this section, we compare the out-of-sample pricing performance of the random walk model (δC_N), the parametric models ($ParamC_N^{AVG}-Models$), the single hidden layer MLP models ($M1C_N^{AVG}-Models$), and the single hidden layer LSTM models ($L1C_N^{AVG}-Models$), and then $ParamC_N^{AVG}-Models$ with the $M1C_N^{AVG}-Models$, and Accordingly the $ParamC_N^{AVG}-Models$ with the $L1C_N^{AVG}-Models$.

Initially, in Part I of Table C.2.1, when we compared the $ParamC_N^{AVG}-Models$ with the $M1C_N^{AVG}-Models$ and the $L1C_N^{AVG}-Models$, and found that none of the models could outperform the δC_N model, where the δC_N model had the lowest $RMSE$ for 566 days (having a daily bootstrap winning % of 40% to 45%) out of 1,328, but if the δC_N model was excluded from the comparison, the $M1C_N^{AVG}-Models$ outperformed for 815 days (having a daily bootstrap winning % of 59% to 64%) out of 1,328. Accordingly, we now compare the $L1C8_N$ model (i.e. the best-performing model when compared to the models in column XIV of Table A.2.1) with the $ParamC_N^{AVG}-Models$, $M1C_N^{AVG}-Models$ and the $L1C_N^{AVG}-Models$ in Part I of Table

C.2.2, we found that the $L1C8_N$ could only marginally outperform the δC_N model on 375 days (having a daily bootstrap winning % of 26% to 31%) out of 1,328, where the δC_N had a similar out-performance for 347 days (having a daily bootstrap winning % of 24% to 29%), but if the δC_N model was excluded from this comparison, the $M1C_N^{AVG} - Models$ had outperformed for 477 days (having a daily bootstrap winning % of 33% to 39%) out of 1,328. Although the $M1C_N^{AVG} - Models$ outperformed, the LSTM model, $L1C_N^{AVG} - Models$ (440 days) had a similar daily bootstrap winning percentage from 31% to 36%.

Secondly, in Part II of Table C.2.1, we compared the $ParamC_N^{AVG} - Models$ with the $M1C_N^{AVG} - Models$ and found that none of the models could outperform the δC_N model, where the δC_N model had the lowest $RMSE$ for 661 days (having a daily bootstrap winning % of 47% to 52%) out of 1,328, but if the δC_N model was excluded from the comparison, the $M1C_N^{AVG} - Models$ outperformed for 1,018 days (having a daily bootstrap winning % of 74% to 79%) out of 1,328. Accordingly, we now compare the $FMLSC_N$ model (i.e. the best-performing model when compared to the models in column XIV of Table A.2.2) with the $ParamC_N^{AVG} - Models$, and the $M1C_N^{AVG} - Models$ in Part II of Table C.2.2, and found that none of the models could outperform the δC_N model, which had the lowest $RMSE$ for 465 days (having a daily bootstrap winning % of 32% to 37%) out of 1,328, but if the δC_N model was excluded from this comparison, the $M1C_N^{AVG} - Models$ had outperformed for 646 days (having a daily bootstrap winning % of 46% to 51%) out of 1,328.

Finally, in Part III of Table C.2.1, we compared the $ParamC_N^{AVG} - Models$ with the $L1C_N^{AVG} - Models$ and found that none of the models could outperform the δC_N model, where the δC_N model had the lowest $RMSE$ for 842 days (having a daily bootstrap winning of 61% to 66%) out of 1,328, but if the δC_N model was excluded from the comparison, the $ParamC_N^{AVG} - Models$ outperformed for 788 days (having a daily bootstrap winning % of 57% to 62%) out of 1,328. Accordingly, we now compare the $L1C8_N$ model (i.e. the best-performing model when compared to the models in column XIV of Table A.2.3) with the $ParamC_N^{AVG} - Models$, and the $L1C_N^{AVG} - Models$ in Part III of Table C.2.2, and found that none of the models could outperform the δC_N model, which had the lowest $RMSE$ for 506 days (having a daily bootstrap winning % of 35% to 41%) out of 1,328, but if the δC_N model was excluded from this comparison, the $L1C8_N$ model had outperformed for 766 days (having a daily bootstrap winning % of 55% to 60%) out of 1,328.

Thus, when the best individually performing model, the $L1C8_N$ model (from Table A.2.1) was compared to the average of all the parametric models, and the averages of all the single hidden layer ANN models (in Part I of Table C.2.2), we conclude that an individual LSTM could not out-perform the model averages, where the averages of all the single hidden layer MLP models (i.e. $M1C_N^{AVG} - Models$) had out-performed them all. Similarly, when the best individually performing model, the $FMLSC_N$ model (from Table A.2.2) was compared to the average of all the parametric models, and the averages of all the single hidden layer MLP models (in Part II of Table C.2.2), the averages of all the single hidden layer MLP models (i.e. $M1C_N^{AVG} - Models$) had yet again out-performed them all. Lastly, when the best individually performing model, the $L1C8_N$ model (from Table A.2.3) was compared to the average of all the parametric models, and the averages of all the single hidden layer LSTM models (in Part III of Table C.2.2), an individual LSTM model (i.e. the $L1C8_N$ model) could out-perform them all.

C.2.1.1.2 Comparison amongst all Parametric Models with Double Hidden Layer ANN Models:

In this section, we compare the out-of-sample pricing performance of the random walk model (δC_N), the parametric models ($ParamC_N^{AVG} - Models$), the double hidden layer MLP models ($M2C_N^{AVG} - Models$), and the double hidden layer LSTM models ($L2C_N^{AVG} - Models$), and then $ParamC_N^{AVG} - Models$ with the $M2C_N^{AVG} - Models$, and Accordingly the $ParamC_N^{AVG} - Models$ with the $L2C_N^{AVG} - Models$.

Initially, in Part IV of Table C.2.1, we compared the $ParamC_N^{AVG} - Models$ with the $M2C_N^{AVG} - Models$ and the $L2C_N^{AVG} - Models$, and found that none of the models could outperform the δC_N model, where the δC_N model had the lowest $RMSE$ for 511 days (having a daily bootstrap winning % of 36% to 41%) out of 1,328, but if the δC_N model was excluded from the comparison, the $M2C_N^{AVG} - Models$ outperformed for 763 days (having a daily bootstrap winning % of 55% to 60%) out of 1,328. Accordingly, we now compare the $L2C9_N$ model (i.e. the best-performing model when compared to the models in column XIV of Table A.2.4) with the $ParamC_N^{AVG} - Models$, $M2C_N^{AVG} - Models$, and the $L2C_N^{AVG} - Models$ in Part IV of Table C.2.2, and found that none of the models could outperform the δC_N model, which had the lowest $RMSE$ for 376 days (having a daily bootstrap winning % of 26% to 31%) out of 1,328, where the $L2C9_N$ models also had a similar out-performance for 319 days (having a daily bootstrap winning % of 22% to 26%), but if the δC_N model was excluded from this comparison, the $M2C_N^{AVG} - Models$ had outperformed for 542 days (having a daily bootstrap winning % of 38% to 43%) out of 1,328.

Secondly, in Part V of Table C.2.1, we compared the $ParamC_N^{AVG} - Models$ with the $M2C_N^{AVG} - Models$, and found that none of the models could outperform the δC_N model, where the δC_N model had the lowest $RMSE$ for 653 days (having a daily bootstrap winning % of 46% to 52%) out of 1,328, but if the δC_N model was excluded from the comparison, the $M2C_N^{AVG} - Models$ outperformed for 1,022 days (having a daily bootstrap winning % of 75% to 79%) out of 1,328. Accordingly, we now compare the $FMLSC_N$ model (i.e. the best-performing model when compared to the models in column XIV of Table A.2.5) with the $ParamC_N^{AVG} - Models$, and the $M2C_N^{AVG} - Models$ in Part V of Table C.2.2, and found that none of the models could outperform the δC_N model, which had the lowest $RMSE$ for 452 days (having a daily bootstrap winning % of 32% to 37%) out of 1,328, but if the δC_N model was excluded from this comparison, the $M2C_N^{AVG} - Models$ had outperformed for 653 days (having a daily bootstrap winning % of 47% to 52%) out of 1,328.

Finally, in Part VI of Table C.2.1, we compared the $ParamC_N^{AVG} - Models$ with the $L2C_N^{AVG} - Models$ and found that none of the models could outperform the δC_N model, where the δC_N model had the lowest $RMSE$ for 781 days (having a daily bootstrap winning % of 56% to 61%) out of 1,328, but if the δC_N model was excluded from the comparison, the $ParamC_N^{AVG} - Models$ outperformed for 778 days (having a daily bootstrap winning % of 56% to 61%) out of 1,328. Accordingly, we now compare the $L2C9_N$ model (i.e. the best-performing model when compared to the models in column XIV of Table A.2.6) with the $ParamC_N^{AVG} - Models$, and the $L2C_N^{AVG} - Models$ in Part VI of Table C.2.2, and found that none of the models could outperform the δC_N model, which had the lowest $RMSE$ for 569 days (having a daily bootstrap winning % of 40% to 46%) out of 1,328, but if the δC_N model was excluded from this comparison, the $ParamC_N^{AVG} - Models$ had outperformed for 534 days (having a daily bootstrap winning % of 38% to 43%) out of 1,328. Though the $ParamC_N^{AVG} - Models$ outperformed, the LSTM model, $L2C9_N$ (476 days) had a similar daily bootstrap winning percentage from 33% to 39%.

Thus, when the best individually performing model, the $L2C9_N$ model (from Table A.2.4) was compared to the average of all the parametric models, and the averages of all the double hidden layer ANN models (in Part IV of Table C.2.2), we conclude that an individual LSTM could not out-perform the model averages, where the averages of all the double hidden layer MLP models (i.e. $M2C_N^{AVG} - Models$) had out-performed them all. Similarly, when the best individually performing model, the $FMLSC_N$ model (from Table A.2.5) was compared to the average of all the parametric models, and the averages of all the double hidden layer MLP models (in Part V of Table C.2.2), the averages of all the double hidden layer MLP models (i.e. $M2C_N^{AVG} - Models$) had yet again out-performed them all. Lastly, when the best individually performing model, the $L2C9_N$ model (from Table A.2.6) was compared to the average of all the parametric models, and the averages of all the double hidden layer LSTM models (in Part VI of Table C.2.2), an individual LSTM model (i.e. the $L2C9_N$ model) could not out-perform other models, and the averages of all the parametric models (i.e. $ParamC_N^{AVG} - Models$) could out-perform them all.

C.2.1.1.3 Comparison amongst all Parametric Models with Triple Hidden Layer ANN Models:

In this section, we compare the out-of-sample pricing performance of the random walk model (δC_N), the parametric models ($ParamC_N^{AVG} - Models$), the triple hidden layer MLP models ($M3C_N^{AVG} - Models$), and the triple hidden layer LSTM models ($L3C_N^{AVG} - Models$), and then $ParamC_N^{AVG} - Models$ with the $M3C_N^{AVG} - Models$, and finally the $ParamC_N^{AVG} - Models$ with the $L3C_N^{AVG} - Models$.

Initially, in Part VII of Table C.2.1, we compared the $ParamC_N^{AVG} - Models$ with the $M3C_N^{AVG} - Models$ and the $L3C_N^{AVG} - Models$, and found that none of the models could outperform the δC_N model, where the δC_N model had the lowest $RMSE$ for 481 days (having a daily bootstrap winning % of 33% to 39%) out of 1,328, but if the δC_N model was excluded from the comparison, the $M3C_N^{AVG} - Models$ outperformed for 730 days (having a daily bootstrap winning % of 52% to 57%) out of 1,328. Accordingly, we now compare the $L3C9_N$ model (i.e. the best-performing model when compared to the models in column XIV of Table A.2.7) with the $ParamC_N^{AVG} - Models$ with the $M3C_N^{AVG} - Models$ in Part VII of Table C.2.2, and found that none of the models could outperform the δC_N model, which had the lowest $RMSE$ for 354 days (having a daily bootstrap winning % of 24% to 29%) out of 1,328. Though the δC_N model outperformed, the $L3C9_N$ model had similar out-performance, where it outperforms for 344 days (having a daily bootstrap winning % of 24% to 28%) out of 1,328, but if the δC_N model was excluded from this comparison, the $M3C_N^{AVG} - Models$ had outperformed for 528 days (having a daily bootstrap winning % of 37% to 42%) out of 1,328.

Secondly, in Part VIII of Table C.2.1, we compared the $ParamC_N^{AVG} - Models$ with the $M3C_N^{AVG} - Models$, and found that none of the models could outperform the δC_N model, where the δC_N model had the lowest $RMSE$ for 651 days (having a daily bootstrap winning % of 46% to 52%) out of 1,328, but if the δC_N model was excluded from the comparison, the $M3C_N^{AVG} - Models$ outperformed for 1,022 days (having a daily bootstrap winning % of 75% to 79%) out of 1,328. Accordingly, we now compare the $FMLSC_N$ model (i.e. the best-performing model when compared to the models in column XIV of Table A.2.8) with the $ParamC_N^{AVG} - Models$, and the $M3C_N^{AVG} - Models$ in Part VIII of Table C.2.2, and found that none of the models could outperform the δC_N model, which had the lowest $RMSE$ for 454 days (having a daily bootstrap winning % of 32% to 37%) out of 1,328, but if the δC_N model was excluded from this comparison, the $M3C_N^{AVG} - Models$ had outperformed for 655 days (having a daily bootstrap winning % of 47% to 52%) out of 1,328.

Finally, in Part IX of Table C.2.1, we compared the $ParamC_N^{AVG} - Models$ with the $L3C_N^{AVG} - Models$, and found that none of the models could outperform the δC_N model, where the δC_N model had the lowest $RMSE$ for 740 days (having a daily bootstrap winning % of 53% to 58%) out of 1,328, but if the δC_N model was excluded from the comparison, the $ParamC_N^{AVG} - Models$ outperformed for 796 days (having a daily bootstrap winning % of 57% to 63%) out of 1,328.

Accordingly, we now compare the $L3C9_N$ model (i.e. the best-performing model when compared to the models in column XIV of Table A.2.9) with the $ParamC_N^{AVG} - Models$, and the $L3C_N^{AVG} - Models$ in Part IX of Table C.2.2, and found that none of the models could outperform the δC_N model, which had the lowest $RMSE$ for 558 days (having a daily bootstrap winning % of 39% to 45%) out of 1,328, but if the δC_N model was excluded from this comparison, the $L3C8_N$ model had outperformed for 564 days (having a daily bootstrap winning % of 40% to 45%) out of 1,328.

Thus, when the best individually performing model, the $L3C9_N$ model (from Table A.2.7) was compared to the average of all the parametric models, and the averages of all the triple hidden layer ANN models (in Part VII of Table C.2.2), we conclude that an individual LSTM could not out-perform the model averages, where the averages of all the triple hidden layer MLP models (i.e. $M3C_N^{AVG} - Models$) had out-performed them all. Similarly, when the best individually performing model, the $FMLSC_N$ model (from Table A.2.8) was compared to the average of all the parametric models, and the averages of all the triple hidden layer MLP models (in Part VIII of Table C.2.2), the averages of all the triple hidden layer MLP models (i.e. $M3C_N^{AVG} - Models$) had yet again out-performed them all. Lastly, when the best individually performing model, the $L3C9_N$ model (from Table A.2.9) was compared to the average of all the parametric models, and the averages of all the triple hidden layer LSTM models (in Part IX of Table C.2.2), an individual LSTM model (i.e. the $L3C9_N$ model) could not out-perform other models, and the averages of all the parametric models (i.e. $ParamC_N^{AVG} - Models$) could out-perform them all.

C.2.1.1.4 Comparison amongst all Parametric Models with Single, Double and Triple Hidden Layer ANN Models:

In this section, we compare the out-of-sample pricing performance of the random walk model (δC_N), the parametric models ($ParamC_N^{AVG} - Models$), with the single hidden layer MLP models ($M1C_N^{AVG} - Models$), the single hidden layer LSTM models ($L1C_N^{AVG} - Models$), the double hidden layer MLP models ($M2C_N^{AVG} - Models$), the double hidden layer LSTM models ($L2C_N^{AVG} - Models$), the triple hidden layer MLP models ($M3C_N^{AVG} - Models$), and the triple hidden layer LSTM models ($L3C_N^{AVG} - Models$), and then $ParamC_N^{AVG} - Models$ with the $M1C_N^{AVG} - Models$, $M2C_N^{AVG} - Models$ and the $M3C_N^{AVG} - Models$, and finally the $ParamC_N^{AVG} - Models$ with the $L1C_N^{AVG} - Models$, $L2C_N^{AVG} - Models$ and the $L3C_N^{AVG} - Models$.

Initially, in Part X of Table C.2.1, we compared the $ParamC_N^{AVG} - Models$ with the $M1C_N^{AVG} - Models$, $M2C_N^{AVG} - Models$, $M3C_N^{AVG} - Models$, $L1C_N^{AVG} - Models$, $L2C_N^{AVG} - Models$ and the $L3C_N^{AVG} - Models$, and found that none of the models could outperform the δC_N model, where the δC_N model had the lowest $RMSE$ for 369 days (having a daily bootstrap winning % of 25% to 30%) out of 1,328, but if the δC_N model was excluded from the comparison, the $M3C_N^{AVG} - Models$ outperformed for 249 days (having a daily bootstrap winning % of 17% to 21%) out of 1,328. Although the $M3C_N^{AVG} - Models$ outperformed, the parametric model, the $ParamC_N^{AVG} - Models$ (184 days) and other variants of the MLP model, the $M1C_N^{AVG} - Models$ (185 days), $M2C_N^{AVG} - Models$ (196 days), and the LSTM model, $L3C_N^{AVG} - Models$

(244 days) have had a collective daily bootstrap winning percentage from 12% (lower bound for the $ParamC_N^{AVG} - Models$, and the $M1C_N^{AVG} - Models$) to 21% (upper bound for the $L3C_N^{AVG} - Models$). Accordingly, we now compare the $L3C9_N$ model (i.e. the best-performing model when compared to the models in column XIV of Table A.2.10) with the $ParamC_N^{AVG} - Models$, $M1C_N^{AVG} - Models$, $M2C_N^{AVG} - Models$, $M3C_N^{AVG} - Models$, $L1C_N^{AVG} - Models$, $L2C_N^{AVG} - Models$ and the $L3C_N^{AVG} - Models$ in Part X of Table C.2.2, and found that $L3C9_N$ model had outperformed other models on 311 days (having a daily bootstrap winning % of 21% to 26%) out of 1,328, which was closely followed by the δC_N model, which had a similar out-performance for 299 days (having a daily bootstrap winning % of 20% to 25%), but if the δC_N model was excluded from this comparison, the $L3C9_N$ model still outperformed for 333 days (having a daily bootstrap winning % of 23% to 27%) out of 1,328.

Secondly, in Part XI of Table C.2.1, we compared the $ParamC_N^{AVG} - Models$ with the $M1C_N^{AVG} - Models$, $M2C_N^{AVG} - Models$, and the $M3C_N^{AVG} - Models$, and found that none of the models could outperform the δC_N model, where the δC_N model had the lowest $RMSE$ for 574 days (having a daily bootstrap winning % of 40% to 46%) out of 1,328, but if the δC_N model was excluded from the comparison, the $M3C_N^{AVG} - Models$ outperformed for 386 days (having a daily bootstrap winning % of 27% to 31%) out of 1,328. Although the $M3C_N^{AVG} - Models$ outperformed, the parametric model, the $ParamC_N^{AVG} - Models$ (294 days) and other variants of the MLP model, the $M1C_N^{AVG} - Models$ (341 days), $M2C_N^{AVG} - Models$ (308 days), have had a collective daily bootstrap winning percentage from 20% (lower bound for the $ParamC_N^{AVG} - Models$) to 28% (upper bound for the $M1C_N^{AVG} - Models$). Accordingly, we now compare the $FMLSC_N$ (i.e. the best-performing model when compared to the models in column XIV of Table A.2.11) with the $ParamC_N^{AVG} - Models$, $M1C_N^{AVG} - Models$, $M2C_N^{AVG} - Models$, and the $M3C_N^{AVG} - Models$ in Part XI of Table C.2.2, and found that none of the models could outperform the δC_N model, which had the lowest $RMSE$ for 402 days (having a daily bootstrap winning % of 28% to 33%) out of 1,328, but if the δC_N model was excluded from this comparison, the $FMLSC_N$ had outperformed for 346 days (having a daily bootstrap winning % of 24% to 28%) out of 1,328, which was closely followed by the $ParamC_N^{AVG} - Models$, which had similar out-performance for 294 days (having a daily bootstrap winning % of 20% to 24%).

Finally, initially in Part XII of Table C.2.1, we compared the $ParamC_N^{AVG} - Models$ with the $L1C_N^{AVG} - Models$, $L2C_N^{AVG} - Models$, and the $L3C_N^{AVG} - Models$, and found that none of the models could outperform the δC_N model, where the δC_N model had the lowest $RMSE$ for 631 days (having a daily bootstrap winning % of 45% to 50%) out of 1,328, but if the δC_N model was excluded from the comparison, the $ParamC_N^{AVG} - Models$ outperformed for 480 days (having a daily bootstrap winning % of 34% to 39%) out of 1,328. Accordingly, we now compare the $L3C9_N$ model (i.e. the best-performing model when compared to the models in column XIV of Table A.2.12) with the $ParamC_N^{AVG} - Models$, $L1C_N^{AVG} - Models$, $L2C_N^{AVG} - Models$, and the $L3C_N^{AVG} - Models$ in Part XII of Table C.2.2, and found that none of the models could outperform the δC_N model, which had the lowest $RMSE$ for 520 days (having a daily bootstrap winning % of 37% to 42%) out of 1,328, but if the δC_N model was excluded from this comparison, the $L3C9_N^{AVG} - Models$ had outperformed for 417 days (having a daily bootstrap winning % of 29% to 34%) out of 1,328, which was closely followed by the $ParamC_N^{AVG} - Models$, which had similar out-performance for 400 days (having a daily bootstrap winning % of 28% to 33%).

Thus, when the best individually performing model, the $L3C9_N$ model (from Table A.2.10) was compared to the average of all the parametric models, the averages of all the single hidden layer ANN models, the averages of all the double hidden layer ANN models, and the averages of all the triple hidden layer ANN models (in Part X of Table C.2.2), we conclude that an individual LSTM could out-perform all the model averages. Similarly, when the best individually performing model, the $FMLSC_N$ model (from Table A.2.11) was compared to the average of all the parametric models, the averages of all the single hidden layer MLP models, the averages of all the double hidden layer MLP models, and the averages of all the triple hidden layer MLP models (in Part XI of Table C.2.2), the $FMLSC_N$ model had out-performed them all. Lastly, when the best individually performing model, the $L3C9_N$ model (from Table A.2.12) was compared to the average of all the parametric models, the averages of all the single hidden layer LSTM models, the averages of all the double hidden layer LSTM models, and the averages of all the triple hidden layer LSTM models (in Part XII of Table C.2.2), an individual LSTM model (i.e. the $L3C9_N$ model) could out-perform all other models.

C.2.1.1.5 Comparison amongst Single, Double and Triple Hidden Layer ANN Models:

In this section, we compare the out-of-sample pricing performance amongst the random walk model (δC_N), the single hidden layer MLP models ($M1C_N^{AVG} - Models$), the single hidden layer LSTM models ($L1C_N^{AVG} - Models$), the double hidden layer MLP models ($M2C_N^{AVG} - Models$), the double hidden layer LSTM models ($L2C_N^{AVG} - Models$), the triple hidden layer MLP models ($M3C_N^{AVG} - Models$), and the triple hidden layer LSTM models ($L3C_N^{AVG} - Models$).

In Part XIII of Table C.2.1, we compared within the $M1C_N^{AVG} - Models$, $M2C_N^{AVG} - Models$, $M3C_N^{AVG} - Models$, $L1C_N^{AVG} - Models$, $L2C_N^{AVG} - Models$ and the $L3C_N^{AVG} - Models$, and found that none of the models could outperform the δC_N model, where the δC_N model had the lowest $RMSE$ for 403 days (having a daily bootstrap winning % of 28% to 33%) out of 1,328, but if the δC_N model was excluded from the comparison, the $M3C_N^{AVG} - Models$ outperformed for 311 days (having a daily bootstrap winning % of 21% to 26%) out of 1,328. Although the $M3C_N^{AVG} - Models$ outperformed, other variants of the MLP model, the $M1C_N^{AVG} - Models$ (235 days), $M2C_N^{AVG} - Models$ (239 days), and the LSTM model, $L3C_N^{AVG} - Models$ (247 days) have had a collective daily bootstrap winning percentage from 16% (lower bound for the $M1C_N^{AVG} - Models$, and the $M2C_N^{AVG} - Models$) to 21% (upper bound for the $L3C_N^{AVG} - Models$). Accordingly, we now compare the $L3C9_N$ model (i.e. the best-performing model when compared to the models in column XIV of Table A.2.13) with the $M1C_N^{AVG} - Models$, $M2C_N^{AVG} - Models$, $M3C_N^{AVG} - Models$, $L1C_N^{AVG} - Models$, $L2C_N^{AVG} - Models$ and the $L3C_N^{AVG} - Models$ in Part XIII of Table C.2.2, and found that none of the models could outperform the δC_N model, which had the lowest $RMSE$ for 333 days (having a daily bootstrap winning % of 23% to 27%) out of 1,328, which was closely followed by the $L3C9_N$ model, which had similar out-performance for 312 days (having a daily bootstrap winning % of 21% to 26%), but if the δC_N model was excluded from this comparison, the $L3C9_N^{AVG} - Models$ had outperformed for 334 days (having a daily bootstrap winning % of 23% to 27%) out of 1,328, which was closely followed by the $M3C_N^{AVG} - Models$, which had similar out-performance for 266 days (having a daily bootstrap winning % of 18% to 22%).

Thus, when the best individually performing model, the $L3C9_N$ model (from Table A.2.7) was compared to the averages of all the single hidden layer ANN models, the averages of all the double hidden layer ANN models, and the averages of all the triple hidden layer ANN models (in Part XIII of Table C.2.2), we conclude that an individual LSTM could out-perform all the model averages.

C.2.1.1.6 Comparison amongst all Parametric models:

We now compare the $HJDC_N$ model (i.e. the best-performing model when compared to the models in column XI of Table A.2.14) with the $ParamC_N^{AVG} - Models$ in Part XIV of Table C.2.2, and found that none of the models could outperform the δC_N model, which had the lowest $RMSE$ for 746 days (having a daily bootstrap winning % of 54% to 59%) out of 1,328, but if the δC_N model was excluded from this comparison, the $HJDC_N$ model had outperformed for 972 days (having a daily bootstrap winning % of 71% to 76%) out of 1,328.

Thus, when the best individually performing model, the $HJDC_N$ model (from Table A.2.14) was compared to the average of all the parametric models (in Part XIV of Table C.2.2), we can conclude that the $HJDC_N$ model could outperform the average of all the parametric models.

Table C.2.1: Call Option Price Comparison (Model Averaging): This table is compartmentalised into XVII parts, where each part presents a performance comparison using both daily and monthly statistics amongst the set of models mentioned in that part. The forecast variable for all the models is the one-trading-day-ahead call option price (C_{N+1}). The models denoted by the $_N$ subscript use lagged input variables for forecasting the average call option price C_{N+1}. In the parts mentioned below, we compare the out-of-sample performance of the following models: **In Part I**: $ParamC_N^{AVG}-Models$, $M1C_N^{AVG}-Models$, $L1C_N^{AVG}-Models$, **in Part II**: $ParamC_N^{AVG}-Models$, $M1C_N^{AVG}-Models$, **in Part III**: $ParamC_N^{AVG}-Models$, $L1C_N^{AVG}-Models$, **in Part IV**: $ParamC_N^{AVG}-Models$, $M2C_N^{AVG}-Models$, $L2C_N^{AVG}-Models$, **in Part V**: $ParamC_N^{AVG}-Models$, $M2C_N^{AVG}-Models$, **in Part VI**: $ParamC_N^{AVG}-Models$, $L2C_N^{AVG}-Models$, **in Part VII**: $ParamC_N^{AVG}-Models$, $M3C_N^{AVG}-Models$, $L3C_N^{AVG}-Models$,**in Part VIII**: $ParamC_N^{AVG}-Models$, $M3C_N^{AVG}-Models$, **in Part IX**: $ParamC_N^{AVG}-Models$, $L3C_N^{AVG}-Models$, **in Part X**: $ParamC_N^{AVG}-Models$, $M1C_N^{AVG}-Models$, $M2C_N^{AVG}-Models$, $M3C_N^{AVG}-Models$, $L1C_N^{AVG}-Models$, $L2C_N^{AVG}-Models$, $L3C_N^{AVG}-Models$, **in Part XI**: $ParamC_N^{AVG}-Models$, $M1C_N^{AVG}-Models$, $M2C_N^{AVG}-Models$, $M3C_N^{AVG}-Models$, **in Part XII**: $ParamC_N^{AVG}-Models$, $L1C_N^{AVG}-Models$, $L2C_N^{AVG}-Models$, $L3C_N^{AVG}-Models$, **in Part XIII**: $M1C_N^{AVG}-Models$, $M2C_N^{AVG}-Models$, $M3C_N^{AVG}-Models$, $L1C_N^{AVG}-Models$, $L2C_N^{AVG}-Models$, $L3C_N^{AVG}-Models$. The one-trading-day-ahead forecast errors of C_{N+1} are used to compute the Root Mean Square Error (RMSE). Column I identifies the models, and column II lists the models used as input to obtain the average one-trading-day-ahead forecast of C_{N+1}. Forecasts are made for 1,328 trading days, and there are 64 months covered in the sample using the monthly data. When comparing all models simultaneously (i.e. including the random walk model (δC_N), column III reports the number of months out of the 64 months that each model has the smallest RMSE, while column IV reports the number of days out of the 1,328 days each model has the smallest RMSE. Columns V (lower bound) and VI (upper bound) present the winning percentage out of 64 months for each model, evaluated using the bootstrap sampling technique. The statistical bootstrap performed (with replacement) at a 95% confidence level is computed from the monthly RMSE values of the respective models below. Columns VII (lower bound) and VIII (upper bound) present the winning percentage out of 1326 days for each model computed from bootstrapping the daily RMSE values of the respective models at a 95% confidence level. Similarly, when the δC_N model was excluded in the comparison, column IX report the number of months out of the 64 months that each model has the smallest RMSE, while column X reports the number of days out of the 1,328 days each model has the smallest RMSE. Columns XI (lower bound) and XII (upper bound) present the winning percentage out of 64 months for each model, evaluated using the bootstrap sampling technique. The statistical bootstrap performed (with replacement) at a 95% confidence level is computed from the monthly RMSE values of the respective models below. Also, columns XIII (lower bound) and XIV (upper bound) present the winning percentage out of 1326 days for each model computed from bootstrapping the daily RMSE values of the respective models at a 95% confidence level.

		Including the random walk						**Excluding the random walk**					
(I) **Model**	**(II)** **Inputs**	**(III)** **Performance amongst all models (Monthly)**	**(IV)** **Performance amongst all models (Daily)**	**(V)** **2.5% lower bound-(for monthly) (%)**	**(VI)** **2.5% upper bound-(for monthly) (%)**	**(VII)** **2.5% lower bound-(for daily) (%)**	**(VIII)** **2.5% upper bound-(for daily) (%)**	**(IX)** **Performance amongst all models (Monthly)**	**(X)** **Performance amongst all models (Daily)**	**(XI)** **2.5% lower bound-(for monthly) (%)**	**(XII)** **2.5% upper bound-(for monthly) (%)**	**(XIII)** **2.5% lower bound-(for daily) (%)**	**(XIV)** **2.5% upper bound-(for daily) (%)**
Part I: $ParamC_N^{AVG}-Models$ v/s $M1C_N^{AVG}-Models$ v/s $L1C_N^{AVG}-Models$													
δC_N	-	**41**	**566**	52%	75%	40%	45%	-	-	-	-	-	-
$ParamC_N^{AVG}-Models$	$BSMC_N ,HC_N ,HJDC_N ,FMLSC_N$	0	219	0%	0%	15%	19%	0	239	0%	0%	16%	20%
$M1C_N^{AVG}-Models$	$M1C1_N ,M1C2_N ,M1C3_N ,M1C4_N ,M1C5_N ,M1C6_N ,M1C7_N ,M1C8_N ,M1C9_N$	23	314	25%	48%	21%	26%	**64**	**815**	100%	100%	59%	64%
$L1C_N^{AVG}-Models$	$L1C1_N ,L1C2_N ,L1C3_N ,L1C4_N ,L1C5_N ,L1C6_N ,L1C7_N ,L1C8_N ,L1C9_N$	0	230	0%	0%	15%	19%	0	275	0%	0%	19%	23%
Part II: $ParamC_N^{AVG}-Models$ v/s $M1C_N^{AVG}-Models$													
δC_N	-	**41**	**661**	52%	75%	47%	52%	-	-	-	-	-	-
$ParamC_N^{AVG}-Models$	$BSMC_N ,HC_N ,HJDC_N ,FMLSC_N$	0	285	0%	0%	19%	24%	0	310	0%	0%	21%	26%
$M1C_N^{AVG}-Models$	$M1C1_N ,M1C2_N ,M1C3_N ,M1C4_N ,M1C5_N ,M1C6_N ,M1C7_N ,M1C8_N ,M1C9_N$	23	382	25%	48%	26%	31%	**64**	**1018**	100%	100%	74%	79%
Part III: $ParamC_N^{AVG}-Models$ v/s $L1C_N^{AVG}-Models$													
δC_N	-	**64**	**842**	100%	100%	61%	66%	-	-	-	-	-	-
$ParamC_N^{AVG}-Models$	$BSMC_N ,HC_N ,HJDC_N ,FMLSC_N$	0	244	0%	0%	16%	20%	**64**	**788**	100%	100%	57%	62%
$L1C_N^{AVG}-Models$	$L1C1_N ,L1C2_N ,L1C3_N ,L1C4_N ,L1C5_N ,L1C6_N ,L1C7_N ,L1C8_N ,L1C9_N$	0	242	0%	0%	16%	20%	0	540	0%	0%	38%	43%
Part IV: $ParamC_N^{AVG}-Models$ v/s $M2C_N^{AVG}-Models$ v/s $L2C_N^{AVG}-Models$													
δC_N	-	**37**	**511**	45%	70%	36%	41%	-	-	-	-	-	-
$ParamC_N^{AVG}-Models$	$BSMC_N ,HC_N ,HJDC_N ,FMLSC_N$	0	231	0%	0%	15%	20%	0	248	0%	0%	17%	21%
$M2C_N^{AVG}-Models$	$M2C1_N ,M2C2_N ,M2C3_N ,M2C4_N ,M2C5_N ,M2C6_N ,M2C7_N ,M2C8_N ,M2C9_N$	27	305	30%	55%	21%	25%	**64**	**763**	100%	100%	55%	60%
$L2C_N^{AVG}-Models$	$L2C1_N ,L2C2_N ,L2C3_N ,L2C4_N ,L2C5_N ,L2C6_N ,L2C7_N ,L2C8_N ,L2C9_N$	0	281	0%	0%	19%	23%	0	317	0%	0%	21%	26%
Part V: $ParamC_N^{AVG}-Models$ v/s $M2C_N^{AVG}-Models$													
δC_N	-	**37**	**653**	45%	69%	46%	52%	-	-	-	-	-	-
$ParamC_N^{AVG}-Models$	$BSMC_N ,HC_N ,HJDC_N ,FMLSC_N$	0	288	0%	0%	20%	24%	0	306	0%	0%	21%	25%
$M2C_N^{AVG}-Models$	$M2C1_N ,M2C2_N ,M2C3_N ,M2C4_N ,M2C5_N ,M2C6_N ,M2C7_N ,M2C8_N ,M2C9_N$	27	387	31%	55%	27%	32%	**64**	**1022**	100%	100%	75%	79%
Part VI: $ParamC_N^{AVG}-Models$ v/s $L2C_N^{AVG}-Models$													
δC_N	-	**63**	**781**	95%	100%	56%	61%	-	-	-	-	-	-
$ParamC_N^{AVG}-Models$	$BSMC_N ,HC_N ,HJDC_N ,FMLSC_N$	0	252	0%	0%	17%	21%	**62**	**778**	92%	100%	56%	61%
$L2C_N^{AVG}-Models$	$L2C1_N ,L2C2_N ,L2C3_N ,L2C4_N ,L2C5_N ,L2C6_N ,L2C7_N ,L2C8_N ,L2C9_N$	1	295	0%	5%	20%	24%	2	550	0%	8%	39%	44%
Part VII: $ParamC_N^{AVG}-Models$ v/s $M3C_N^{AVG}-Models$ v/s $L3C_N^{AVG}-Models$													
δC_N	-	**44**	**481**	57%	80%	33%	39%	-	-	-	-	-	-
$ParamC_N^{AVG}-Models$	$BSMC_N ,HC_N ,HJDC_N ,FMLSC_N$	0	244	0%	0%	16%	21%	0	255	0%	0%	17%	21%
$M3C_N^{AVG}-Models$	$M3C1_N ,M3C2_N ,M3C3_N ,M3C4_N ,M3C5_N ,M3C6_N ,M3C7_N ,M3C8_N ,M3C9_N$	20	291	20%	43%	20%	24%	**64**	**730**	100%	100%	52%	57%
$L3C_N^{AVG}-Models$	$L3C1_N ,L3C2_N ,L3C3_N ,L3C4_N ,L3C5_N ,L3C6_N ,L3C7_N ,L3C8_N ,L3C9_N$	0	312	0%	0%	21%	26%	0	343	0%	0%	24%	28%
Part VIII: $ParamC_N^{AVG}-Models$ v/s $M3C_N^{AVG}-Models$													
δC_N	-	**44**	**651**	56%	80%	46%	52%	-	-	-	-	-	-
$ParamC_N^{AVG}-Models$	$BSMC_N ,HC_N ,HJDC_N ,FMLSC_N$	0	293	0%	0%	20%	24%	0	306	0%	0%	21%	25%
$M3C_N^{AVG}-Models$	$M3C1_N ,M3C2_N ,M3C3_N ,M3C4_N ,M3C5_N ,M3C6_N ,M3C7_N ,M3C8_N ,M3C9_N$	20	384	20%	44%	27%	32%	**64**	**1022**	100%	100%	75%	79%
Part IX: $ParamC_N^{AVG}-Models$ v/s $L3C_N^{AVG}-Models$													
δC_N	-	**64**	**740**	100%	100%	53%	58%	-	-	-	-	-	-
$ParamC_N^{AVG}-Models$	$BSMC_N ,HC_N ,HJDC_N ,FMLSC_N$	0	264	0%	0%	18%	22%	**64**	**796**	100%	100%	57%	63%
$L3C_N^{AVG}-Models$	$L3C1_N ,L3C2_N ,L3C3_N ,L3C4_N ,L3C5_N ,L3C6_N ,L3C7_N ,L3C8_N ,L3C9_N$	0	324	0%	0%	22%	27%	0	532	0%	0%	38%	43%
Part X: $ParamC_N^{AVG}-Models$ v/s $M1C_N^{AVG}-Models$ v/s $M2C_N^{AVG}-Models$ $M3C_N^{AVG}-Models$ v/s $L1C_N^{AVG}-Models$ v/s $L2C_N^{AVG}-Models$ v/s $L3C_N^{AVG}-Models$													
δC_N	-	**34**	**369**	41%	64%	25%	30%	-	-	-	-	-	-
$ParamC_N^{AVG}-Models$	$BSMC_N ,HC_N ,HJDC_N ,FMLSC_N$	0	174	0%	0%	11%	15%	0	184	0%	0%	12%	16%
$M1C_N^{AVG}-Models$	$M1C1_N ,M1C2_N ,M1C3_N ,M1C4_N ,M1C5_N ,M1C6_N ,M1C7_N ,M1C8_N ,M1C9_N$	10	126	8%	25%	8%	11%	16	185	14%	36%	12%	16%
$M2C_N^{AVG}-Models$	$M2C1_N ,M2C2_N ,M2C3_N ,M2C4_N ,M2C5_N ,M2C6_N ,M2C7_N ,M2C8_N ,M2C9_N$	14	97	13%	33%	6%	9%	19	196	19%	41%	13%	17%
$M3C_N^{AVG}-Models$	$M3C1_N ,M3C2_N ,M3C3_N ,M3C4_N ,M3C5_N ,M3C6_N ,M3C7_N ,M3C8_N ,M3C9_N$	6	86	3%	17%	5%	8%	**29**	**249**	33%	58%	17%	21%
$L1C_N^{AVG}-Models$	$L1C1_N ,L1C2_N ,L1C3_N ,L1C4_N ,L1C5_N ,L1C6_N ,L1C7_N ,L1C8_N ,L1C9_N$	0	89	0%	0%	5%	8%	0	94	0%	0%	6%	8%
$L2C_N^{AVG}-Models$	$L2C1_N ,L2C2_N ,L2C3_N ,L2C4_N ,L2C5_N ,L2C6_N ,L2C7_N ,L2C8_N ,L2C9_N$	0	161	0%	0%	10%	14%	0	176	0%	0%	11%	15%
$L3C_N^{AVG}-Models$	$L3C1_N ,L3C2_N ,L3C3_N ,L3C4_N ,L3C5_N ,L3C6_N ,L3C7_N ,L3C8_N ,L3C9_N$	0	226	0%	0%	15%	19%	0	244	0%	0%	16%	21%
Part XI: $ParamC_N^{AVG}-Models$ v/s $M1C_N^{AVG}-Models$ v/s $M2C_N^{AVG}-Models$ v/s $M3C_N^{AVG}-Models$													
δC_N	-	**34**	**574**	41%	64%	40%	46%	-	-	-	-	-	-
$ParamC_N^{AVG}-Models$	$BSMC_N ,HC_N ,HJDC_N ,FMLSC_N$	0	282	0%	0%	19%	24%	0	294	0%	0%	20%	24%
$M1C_N^{AVG}-Models$	$M1C1_N ,M1C2_N ,M1C3_N ,M1C4_N ,M1C5_N ,M1C6_N ,M1C7_N ,M1C8_N ,M1C9_N$	10	206	8%	25%	13%	18%	16	341	14%	36%	23%	28%
$M2C_N^{AVG}-Models$	$M2C1_N ,M2C2_N ,M2C3_N ,M2C4_N ,M2C5_N ,M2C6_N ,M2C7_N ,M2C8_N ,M2C9_N$	14	141	13%	33%	9%	12%	19	308	19%	41%	21%	25%
$M3C_N^{AVG}-Models$	$M3C1_N ,M3C2_N ,M3C3_N ,M3C4_N ,M3C5_N ,M3C6_N ,M3C7_N ,M3C8_N ,M3C9_N$	6	126	3%	17%	8%	11%	**29**	**386**	33%	58%	27%	31%
Part XII: $ParamC_N^{AVG}-Models$ v/s $L1C_N^{AVG}-Models$ v/s $L2C_N^{AVG}-Models$ v/s $L3C_N^{AVG}-Models$													
δC_N	-	**63**	**631**	95%	100%	45%	50%	-	-	-	-	-	-
$ParamC_N^{AVG}-Models$	$BSMC_N ,HC_N ,HJDC_N ,FMLSC_N$	0	198	0%	0%	13%	17%	**62**	**480**	92%	100%	34%	39%
$L1C_N^{AVG}-Models$	$L1C1_N ,L1C2_N ,L1C3_N ,L1C4_N ,L1C5_N ,L1C6_N ,L1C7_N ,L1C8_N ,L1C9_N$	0	94	0%	0%	6%	8%	0	176	0%	0%	11%	15%
$L2C_N^{AVG}-Models$	$L2C1_N ,L2C2_N ,L2C3_N ,L2C4_N ,L2C5_N ,L2C6_N ,L2C7_N ,L2C8_N ,L2C9_N$	1	167	0%	5%	11%	14%	2	307	0%	8%	21%	25%
$L3C_N^{AVG}-Models$	$L3C1_N ,L3C2_N ,L3C3_N ,L3C4_N ,L3C5_N ,L3C6_N ,L3C7_N ,L3C8_N ,L3C9_N$	0	238	0%	0%	16%	20%	0	365	0%	0%	25%	30%
Part XIII: $M1C_N^{AVG}-Models$ v/s $M2C_N^{AVG}-Models$ $M3C_N^{AVG}-Models$ v/s $L1C_N^{AVG}-Models$ v/s $L2C_N^{AVG}-Models$ v/s $L3C_N^{AVG}-Models$													
δC_N	-	**34**	**403**	42%	66%	28%	33%	-	-	-	-	-	-
$M1C_N^{AVG}-Models$	$M1C1_N ,M1C2_N ,M1C3_N ,M1C4_N ,M1C5_N ,M1C6_N ,M1C7_N ,M1C8_N ,M1C9_N$	10	171	6%	25%	11%	15%	16	235	16%	36%	16%	20%
$M2C_N^{AVG}-Models$	$M2C1_N ,M2C2_N ,M2C3_N ,M2C4_N ,M2C5_N ,M2C6_N ,M2C7_N ,M2C8_N ,M2C9_N$	14	125	13%	33%	8%	11%	19	239	19%	41%	16%	20%
$M3C_N^{AVG}-Models$	$M3C1_N ,M3C2_N ,M3C3_N ,M3C4_N ,M3C5_N ,M3C6_N ,M3C7_N ,M3C8_N ,M3C9_N$	6	124	2%	17%	8%	11%	**29**	**311**	33%	58%	21%	26%
$L1C_N^{AVG}-Models$	$L1C1_N ,L1C2_N ,L1C3_N ,L1C4_N ,L1C5_N ,L1C6_N ,L1C7_N ,L1C8_N ,L1C9_N$	0	106	0%	0%	7%	9%	0	111	0%	0%	7%	10%
$L2C_N^{AVG}-Models$	$L2C1_N ,L2C2_N ,L2C3_N ,L2C4_N ,L2C5_N ,L2C6_N ,L2C7_N ,L2C8_N ,L2C9_N$	0	170	0%	0%	11%	15%	0	185	0%	0%	12%	16%
$L3C_N^{AVG}-Models$	$L3C1_N ,L3C2_N ,L3C3_N ,L3C4_N ,L3C5_N ,L3C6_N ,L3C7_N ,L3C8_N ,L3C9_N$	0	229	0%	0%	15%	19%	0	247	0%	0%	17%	21%

Table C.2.2: Call Option Price Comparison (Model Averaging): This table is compartmentalised into XVII parts. Each part presents a performance comparison using daily and monthly statistics amongst the set of models mentioned in that part. The forecast variable for all the models is the one-trading-day-ahead call option price (C_{N+1}). The models denoted by the $_N$ subscript use lagged input variables for forecasting the call option price C_{N+1}. In the parts mentioned below, we compare the out-of-sample performance of the best performing model (based on the total number of days out of 1326 days that a particular model had the lowest RMSE) with the average of parametric models ($ParamC_N^{AVG}-Models$), the average of single ($M1C_N^{AVG}-Models$), double ($M2C_N^{AVG}-Models$) and triple ($M3C_N^{AVG}-Models$) hidden layer MLP models, and the average of single ($L1C_N^{AVG}-Models$), double ($L2C_N^{AVG}-Models$) and triple ($L3C_N^{AVG}-Models$) hidden layer LSTM models. **In Part I**: The best performing model ($L1C8_N$) from Table A.2.1 with $ParamC_N^{AVG}-Models$, $M1C_N^{AVG}-Models$, $L1C_N^{AVG}-Models$, **in Part II**: The best performing model ($FMLSC_N$) from Table A.2.2 with $ParamC_N^{AVG}-Models$, $M1C_N^{AVG}-Models$, **in Part III**: The best performing model ($L1C8_N$) from Table A.2.3 with $ParamC_N^{AVG}-Models$, $L1C_N^{AVG}-Models$, **in Part IV**: The best performing model ($L2C9_N$) from Table A.2.4 with $ParamC_N^{AVG}-Models$, $M2C_N^{AVG}-Models$, $L2C_N^{AVG}-Models$, **in Part V**: The best performing model ($FMLSC_N$) from Table A.2.5 with $ParamC_N^{AVG}-Models$, $M2C_N^{AVG}-Models$, **in Part VI**: The best performing model ($L2C9_N$) from Table A.2.6 with $ParamC_N^{AVG}-Models$, $L2C_N^{AVG}-Models$, **in Part VII**: The best performing model ($L3C9_N$) from Table A.2.7 with $ParamC_N^{AVG}-Models$, $M3C_N^{AVG}-Models$, $L3C_N^{AVG}-Models$, **in Part VIII**: The best performing model ($FMLSC_N$) from Table A.2.8 with $ParamC_N^{AVG}-Models$, $M3C_N^{AVG}-Models$, **in Part IX**: The best performing model ($L3C9_N$) from Table A.2.9 with $ParamC_N^{AVG}-Models$, $L3C_N^{AVG}-Models$, **in Part X**: The best performing model ($L3C9_N$) from Table A.2.10 with $ParamC_N^{AVG}-Models$, $M1C_N^{AVG}-Models$, $M2C_N^{AVG}-Models$, $M3C_N^{AVG}-Models$, $L1C_N^{AVG}-Models$, $L2C_N^{AVG}-Models$, $L3C_N^{AVG}-Models$, **in Part XI**: The best performing model ($FMLSC_N$) from Table A.2.11 with $ParamC_N^{AVG}-Models$, $M1C_N^{AVG}-Models$, $M2C_N^{AVG}-Models$, $M3C_N^{AVG}-Models$, **in Part XII**: The best performing model ($L3C9_N$) from Table A.2.12 with $ParamC_N^{AVG}-Models$, $L1C_N^{AVG}-Models$, $L2C_N^{AVG}-Models$, $L3C_N^{AVG}-Models$, **in Part XIII**: The best performing model ($L3C9_N$) from Table A.2.13 with $M1C_N^{AVG}-Models$, $M2C_N^{AVG}-Models$, $M3C_N^{AVG}-Models$, $L1C_N^{AVG}-Models$, $L2C_N^{AVG}-Models$, $L3C_N^{AVG}-Models$, **in Part XIV**: The best performing model ($HJDC_N$) from Table A.2.14 with $ParamC_N^{AVG}-Models$. The one-trading-day-ahead forecast errors of C_{N+1} are used to compute the Root Mean Square Error (RMSE). Forecasts are made for 1,326 trading days, and there are 64 months covered in the sample using the monthly data. Column I identifies the models. When comparing all models simultaneously (i.e. including the random walk model (δC_N)), column II reports the number of months out of the 64 months that each model has the smallest RMSE, while column III reports the number of days out of the 1,326 days each model has the smallest RMSE. Columns IV (lower bound) and V (upper bound) present the winning percentage out of 64 months for each model, evaluated using the bootstrap sampling technique. The statistical bootstrap performed (with replacement) at a 95% confidence level is computed from the monthly RMSE values of the respective models below. Columns VI (lower bound) and VII (upper bound) present the winning percentage out of 1326 days for each model computed from bootstrapping the daily RMSE values of the respective models at a 95% confidence level. Similarly, when the δC_N model was excluded in the comparison, column VIII report the number of months out of the 64 months that each model has the smallest RMSE, while column IX reports the number of days out of the 1,326 days each model has the smallest RMSE. Columns X (lower bound) and XI (upper bound) present the winning percentage out of 64 months for each model, evaluated using the bootstrap sampling technique. The statistical bootstrap performed (with replacement) at a 95% confidence level is computed from the monthly RMSE values of the respective models below. Also, columns XII (lower bound) and XIII (upper bound) present the winning percentage out of 1326 days for each model computed from bootstrapping the daily RMSE values of the respective models at a 95% confidence level.

	Including the random walk						Excluding the random walk					
(I) Model	**(II) Performance amongst all models (Monthly)**	**(III) Performance amongst all models (Daily)**	**(IV) 2.5% lower bound-(for monthly) (%)**	**(V) 2.5% upper bound-(for monthly) (%)**	**(VI) 2.5% lower bound-(for daily) (%)**	**(VII) 2.5% upper bound-(for daily) (%)**	**(VIII) Performance amongst all models (Monthly)**	**(IX) Performance amongst all models (Daily)**	**(X) 2.5% lower bound-(for monthly) (%)**	**(XI) 2.5% upper bound-(for monthly) (%)**	**(XII) 2.5% lower bound-(for daily) (%)**	**(XIII) 2.5% upper bound-(for daily) (%)**
Part I: $L1C8_N$ v/s $ParamC_N^{AVG}-Models$ v/s $M1C_N^{AVG}-Models$ v/s $L1C_N^{AVG}-Models$												
δ_C	**30**	347	34%	59%	24%	29%	-	-	-	-	-	-
$L1C8_N$	17	**375**	17%	38%	26%	31%	26	440	28%	52%	31%	36%
$ParamC_N^{AVG}-Models$	0	211	0%	0%	14%	18%	0	228	0%	0%	15%	19%
$M1C_N^{AVG}-Models$	17	220	16%	38%	15%	19%	**38**	**477**	48%	72%	33%	39%
$L1C_N^{AVG}-Models$	0	176	0%	0%	11%	15%	0	184	0%	0%	12%	16%
Part II: $FMLSC_N$ v/s $ParamC_N^{AVG}-Models$ v/s $M1C_N^{AVG}-Models$												
δ_C	**41**	**465**	53%	75%	32%	37%	-	-	-	-	-	-
$FMLSC_N$	0	306	0%	0%	21%	25%	0	372	0%	0%	26%	30%
$ParamC_N^{AVG}-Models$	0	285	0%	0%	19%	24%	0	310	0%	0%	21%	26%
$M1C_N^{AVG}-Models$	23	272	25%	47%	18%	23%	**64**	**646**	100%	100%	46%	51%
Part III: $L1C8_N$ v/s $ParamC_N^{AVG}-Models$ v/s $L1C_N^{AVG}-Models$												
δ_C	**47**	**506**	63%	84%	35%	41%	-	-	-	-	-	-
$L1C8_N$	17	405	16%	38%	28%	33%	**51**	**766**	70%	89%	55%	60%
$ParamC_N^{AVG}-Models$	0	234	0%	0%	16%	20%	13	342	11%	30%	23%	28%
$L1C_N^{AVG}-Models$	0	183	0%	0%	12%	16%	0	220	0%	0%	15%	19%
Part IV: $L2C9_N$ v/s $ParamC_N^{AVG}-Models$ v/s $M2C_N^{AVG}-Models$ v/s $L2C_N^{AVG}-Models$												
δ_C	**37**	**376**	47%	70%	26%	31%	-	-	-	-	-	-
$L2C9_N$	2	319	0%	8%	22%	26%	3	350	0%	11%	24%	29%
$ParamC_N^{AVG}-Models$	0	231	0%	0%	15%	19%	0	248	0%	0%	16%	21%
$M2C_N^{AVG}-Models$	25	226	27%	50%	15%	19%	**61**	**542**	89%	100%	38%	43%
$L2C_N^{AVG}-Models$	0	176	0%	0%	11%	15%	0	188	0%	0%	12%	16%
Part V: $FMLSC_N$ v/s $ParamC_N^{AVG}-Models$ v/s $M2C_N^{AVG}-Models$												
δ_C	**37**	**452**	45%	69%	32%	37%	-	-	-	-	-	-
$FMLSC_N$	0	307	0%	0%	21%	25%	0	369	0%	0%	25%	30%
$ParamC_N^{AVG}-Models$	0	288	0%	0%	19%	24%	0	306	0%	0%	21%	25%
$M2C_N^{AVG}-Models$	27	281	31%	55%	19%	23%	**64**	**653**	100%	100%	47%	52%
Part VI: $L2C9_N$ v/s $ParamC_N^{AVG}-Models$ v/s $L2C_N^{AVG}-Models$												
δ_C	**61**	**569**	89%	100%	40%	46%	-	-	-	-	-	-
$L2C9_N$	2	326	0%	8%	22%	27%	5	476	2%	14%	33%	39%
$ParamC_N^{AVG}-Models$	0	251	0%	0%	17%	21%	**57**	**534**	81%	95%	38%	43%
$L2C_N^{AVG}-Models$	1	182	0%	5%	12%	16%	2	318	0%	8%	22%	26%
Part VII: $L3C9_N$ v/s $ParamC_N^{AVG}-Models$ v/s $M3C_N^{AVG}-Models$ v/s $L3C_N^{AVG}-Models$												
δ_C	**43**	**354**	55%	78%	24%	29%	-	-	-	-	-	-
$L3C9_N$	1	344	0%	5%	24%	28%	2	373	0%	8%	26%	31%
$ParamC_N^{AVG}-Models$	0	244	0%	0%	16%	20%	0	255	0%	0%	17%	21%
$M3C_N^{AVG}-Models$	20	229	20%	44%	15%	19%	**62**	**528**	92%	100%	37%	42%
$L3C_N^{AVG}-Models$	0	157	0%	0%	10%	14%	0	172	0%	0%	11%	15%
Part VIII: $FMLSC_N$ v/s $ParamC_N^{AVG}-Models$ v/s $M3C_N^{AVG}-Models$												
δ_C	**44**	**454**	58%	80%	32%	37%	-	-	-	-	-	-
$FMLSC_N$	0	307	0%	0%	21%	25%	1	367	0%	5%	25%	30%
$ParamC_N^{AVG}-Models$	0	293	0%	0%	20%	24%	0	306	0%	0%	21%	25%
$M3C_N^{AVG}-Models$	20	274	20%	42%	19%	23%	**63**	**655**	95%	100%	47%	52%
Part IX: $L3C9_N$ v/s $ParamC_N^{AVG}-Models$ v/s $L3C_N^{AVG}-Models$												
δ_C	**63**	**558**	95%	100%	39%	45%	-	-	-	-	-	-
$L3C9_N$	1	348	0%	5%	24%	28%	9	486	6%	23%	34%	39%
$ParamC_N^{AVG}-Models$	0	264	0%	0%	18%	22%	**55**	**564**	77%	94%	40%	45%
$L3C_N^{AVG}-Models$	0	158	0%	0%	10%	14%	0	278	0%	0%	19%	23%
Part X: $L3C9_N$ v/s $ParamC_N^{AVG}-Models$ v/s $M1C_N^{AVG}-Models$ v/s $M2C_N^{AVG}-Models$ $M3C_N^{AVG}-Models$ v/s $L1C_N^{AVG}-Models$ v/s $L2C_N^{AVG}-Models$ v/s $L3C_N^{AVG}-Models$												
δ_C	**34**	299	41%	66%	20%	25%	-	-	-	-	-	-
$L3C9_N$	0	**311**	0%	0%	21%	26%	0	**333**	0%	0%	23%	27%
$ParamC_N^{AVG}-Models$	0	174	0%	0%	11%	15%	0	184	0%	0%	12%	16%
$M1C_N^{AVG}-Models$	10	97	6%	25%	6%	9%	16	134	14%	36%	9%	12%
$M2C_N^{AVG}-Models$	14	86	13%	33%	5%	8%	19	171	19%	42%	11%	15%
$M3C_N^{AVG}-Models$	6	76	3%	16%	5%	7%	**29**	204	34%	58%	13%	17%
$L1C_N^{AVG}-Models$	0	64	0%	0%	4%	6%	0	66	0%	0%	4%	6%
$L2C_N^{AVG}-Models$	0	116	0%	0%	7%	10%	0	123	0%	0%	8%	11%
$L3C_N^{AVG}-Models$	0	105	0%	0%	7%	9%	0	113	0%	0%	7%	10%
Part XI: $FMLSC_N$ v/s $ParamC_N^{AVG}-Models$ v/s $M1C_N^{AVG}-Models$ v/s $M2C_N^{AVG}-Models$ v/s $M3C_N^{AVG}-Models$												
δ_C	**34**	**402**	41%	65%	28%	33%	-	-	-	-	-	-
$FMLSC_N$	0	298	0%	0%	20%	25%	0	**346**	0%	0%	24%	28%
$ParamC_N^{AVG}-Models$	0	282	0%	0%	19%	23%	0	294	0%	0%	20%	24%
$M1C_N^{AVG}-Models$	10	145	8%	25%	9%	13%	16	209	16%	36%	14%	18%
$M2C_N^{AVG}-Models$	14	109	13%	33%	7%	10%	19	215	19%	41%	14%	18%
$M3C_N^{AVG}-Models$	6	92	3%	17%	5%	8%	**29**	264	33%	58%	18%	22%
Part XII: $L3C9_N$ v/s $ParamC_N^{AVG}-Models$ v/s $L1C_N^{AVG}-Models$ v/s $L2C_N^{AVG}-Models$ v/s $L3C_N^{AVG}-Models$												
δ_C	**62**	**520**	92%	100%	37%	42%	-	-	-	-	-	-
$L3C9_N$	1	316	0%	5%	22%	26%	9	**417**	6%	23%	29%	34%
$ParamC_N^{AVG}-Models$	0	198	0%	0%	13%	17%	**53**	400	73%	92%	28%	33%
$L1C_N^{AVG}-Models$	0	67	0%	0%	4%	6%	0	125	0%	0%	8%	11%
$L2C_N^{AVG}-Models$	1	119	0%	5%	7%	10%	2	212	0%	8%	14%	18%
$L3C_N^{AVG}-Models$	0	108	0%	0%	7%	10%	0	174	0%	0%	11%	15%
Part XIII: $L3C9_N$ v/s $M1C_N^{AVG}-Models$ v/s $M2C_N^{AVG}-Models$ $M3C_N^{AVG}-Models$ v/s $L1C_N^{AVG}-Models$ v/s $L2C_N^{AVG}-Models$ v/s $L3C_N^{AVG}-Models$												
δ_C	**34**	**333**	41%	66%	23%	27%	-	-	-	-	-	-
$L3C9_N$	0	312	0%	0%	21%	26%	0	**334**	0%	0%	23%	27%
$M1C_N^{AVG}-Models$	10	141	8%	25%	9%	12%	16	183	16%	36%	12%	16%
$M2C_N^{AVG}-Models$	14	114	13%	33%	7%	10%	19	214	19%	42%	14%	18%
$M3C_N^{AVG}-Models$	6	114	3%	17%	7%	10%	**29**	266	34%	56%	18%	22%
$L1C_N^{AVG}-Models$	0	81	0%	0%	5%	7%	0	83	0%	0%	5%	8%
$L2C_N^{AVG}-Models$	0	125	0%	0%	8%	11%	0	132	0%	0%	8%	12%
$L3C_N^{AVG}-Models$	0	108	0%	0%	7%	10%	0	116	0%	0%	7%	10%
Part XIV: $HJDC_N$ v/s $ParamC_N^{AVG}-Models$												
δ_C	**57**	**746**	81%	95%	54%	59%	-	-	-	-	-	-
$HJDC_N$	7	267	5%	19%	18%	23%	**63**	**972**	95%	100%	71%	76%
$ParamC_N^{AVG}-Models$	0	315	0%	0%	21%	26%	1	356	0%	5%	24%	29%

C.2.1.2 $C^{AVG} - Models$: Model averaging pricing performance of models that use one-trading-day-ahead input variables to forecast the call option price (C_{N+1}) for the next trading day:

Table C.2.3 shows the relative out-of-sample performance (in $RMSE$) amongst the models that forecast the one-trading-day-ahead average call option price(C_{N+1}) using one-trading-day-ahead input variables. In column II of table C.2.3, we list the several models used as an input to obtain the average one-trading-day-ahead forecast of C_{N+1}. The performance metric is the $RMSE$ of the one-trading-day-ahead forecast errors of the average C_{N+1}, which is computed for each averaging model utilising all of the errors in each day or each month. Amongst all of the models (including the random walk model (δC_N)), columns III and IV record the number of months and days, respectively, that each model has the lowest $RMSE$. We performed a bootstrap using the daily and monthly RMSEs to be certain of our results. The columns V (lower bound) and VI (upper bound) present the results from the bootstrap performed (with replacement) using monthly RMSEs at a 95% confidence level and shows the winning percentage out of 64 months for each model (including the δC_N model) and similarly, the 95 % confidence intervals computed from bootstrapping of the daily RMSEs signifies the winning percentage out of 1,328 days for each model and are reported in columns VII (lower bound), VIII (upper bound). While excluding the δC_N model amongst the comparison, columns IX and X record the number of months and days that each model has the lowest $RMSE$. We repeat the exercise of performing the bootstrap by excluding the δC_N model in the comparison, and thus, the columns XI (lower bound) and XII (upper bound) present the results from the bootstrap performed (with replacement) using monthly RMSEs at a 95% confidence level and shows the winning percentage out of 64 months for each model (excluding the δC_N model) and similarly, the 95 % confidence intervals computed from bootstrapping of the daily RMSEs signifies the winning percentage out of 1,328 days for each model and are reported in columns XIII (lower bound), XIV (upper bound). After a model is found to outperform other individual parametric models, MLP and LSTM models in each of the several comparisons below, we look into whether that out-performing model individually can outperform the average call option price of all the parametric models combinedly, MLP models combinedly or LSTM models combinedly, covered in that section.

In the below several comparisons, even though a particular model wins by a higher percentage against other models, we investigated further these models pairwise by performing a pairwise bootstrap comparison, which was computed using the respective pair's daily RMSEs. The results are presented in Table 92 of the Electronic Appendix.

The Diebold-Mariano(DM) (Diebold and Mariano (1995)) test was performed on pairs amongst the Random Walk (δC_N) model, the average call option price of all parametric models ($ParamC^{AVG}_{N+1} - Models$), the average call option price of all single hidden layer MLP models ($M1C^{AVG}_{N+1} - Models$), the average call option price of all single hidden layer LSTM models ($L1C^{AVG}_{N+1} - Models$), the average call option price of all double hidden layer MLP models ($M2C^{AVG}_{N+1} - Models$), the average call option price of all double hidden layer LSTM models ($L3C^{AVG}_{N+1} - Models$), the average call option price of all triple hidden layer MLP models ($M3C^{AVG}_{N+1} - Models$), and the average call option price of all triple hidden layer LSTM models ($L3C^{AVG}_{N+1} - Models$) are reported in Table 83 of the Electronic Appendix. In constructing the DM tests, the model pairs are reported in column I and column II, and the DM test statistics for a particular pair are reported in column III. If the null can be rejected, a positive number suggests the rejection may be due to the second model being the better forecast model. In contrast, a negative value suggests the rejection may be due to the first model being the better forecast model. The model pairs highlighted in a red state that their forecasts have statistically insignificant differences in their prediction accuracy. Considering the DM-Test statistics in Table 83 of the Electronic Appendix, all the model pairs lead to the rejection of the null of equal forecasting performance.

The RMSEs for the models under the $C^{AVG} - Models$ category, which averages the forecasted C_{N+1} from models belonging to the $C - Models$ category(which uses one-trading-day-ahead input variables to forecast the C_{N+1} for the next trading day) on a monthly, yearly, and overall basis can be found in the Electronic Appendix, in Tables 52, 62, and 72, respectively.

C.2.1.2.1 Comparison amongst all Parametric Models with Triple Hidden Layer ANN Models:

In this section, we compare the out-of-sample performance of the random walk model (δC_{N+1}), the parametric models ($ParamC^{AVG}_{N+1} - Models$), the triple hidden layer MLP models ($M3C^{AVG}_{N+1} - Models$), and the triple hidden layer LSTM models ($L3C^{AVG}_{N+1} - Models$), and then $ParamC^{AVG}_{N+1} - Models$ with the $M3C^{AVG}_{N+1} - Models$, and finally the $ParamC^{AVG}_{N+1} - Models$ with the $L3C^{AVG}_{N+1} - Models$.

Initially in Part I of Table C.2.3, we compared the $ParamC^{AVG}_{N+1} - Models$ with the $M3C^{AVG}_{N+1} - Models$ and the $L3C^{AVG}_{N+1} - Models$ and found that the $M3C^{AVG}_{N+1} - Models$ had the lowest $RMSE$ for 987 days (having a daily bootstrap winning % of 72% to 77%) out of 1,328, but if the δC_N model was excluded from the comparison, the $M3C^{AVG}_{N+1} - Models$ still outperformed for 1,114 days (having a daily bootstrap winning % of 82% to 86%) out of 1,328. Accordingly, we now compare the $M3C4_{N+1}$ model (i.e. the best-performing model when compared to the models in column XIV of Table A.2.15) with the $ParamC^{AVG}_{N+1} - Models$, $M3C^{AVG}_{N+1} - Models$, and the $L3C^{AVG}_{N+1} - Models$ in Part I of Table C.2.4 and found that $M3C4_{N+1}$ model had the lowest $RMSE$ for 650 days (having a daily bootstrap winning % of 46% to 52%) out of 1,328, but if the δC_N model was excluded from this comparison, the $M3C4_{N+1}$ model had still outperformed for 683 days (having a daily bootstrap winning % of 49% to 54%) out of 1,328, which was closely followed by the $M3C^{AVG}_{N+1} - Models$, which had similar out-performance for 610 days (having a daily bootstrap winning % of 43% to 49%).

Secondly, in Part II of Table C.2.3, we compared the $ParamC^{AVG}_{N+1} - Models$ with the $M3C^{AVG}_{N+1} - Models$, and found that the $M3C^{AVG}_{N+1} - Models$ model had the lowest $RMSE$ for 991 days (having a daily bootstrap winning % of 72% to 77%) out of 1,328, and even if the δC_N model was excluded from the comparison, the $M3C^{AVG}_{N+1} - Models$ could still outperform for 1,120 days (having a daily bootstrap winning % of 82 % to 86%) out of 1,328. Accordingly, we now compare the $M3C4_{N+1}$ model (i.e. the best-performing model when compared to the models in column XIV of Table A.2.16) with the $ParamC^{AVG}_{N+1} - Models$, and the $M3C^{AVG}_{N+1} - Models$ in Part II of Table C.2.4, and found that the $M3C4_{N+1}$ model had the lowest $RMSE$ for 650 days (having a daily bootstrap winning % of 46% to 52%) out of 1,328, but if the δC_N model was excluded from this comparison, the $M3C^{AVG}_{N+1} - Models$ still outperformed for 683 days (having a daily bootstrap winning % of 49% to 54%) out of 1,328, which was closely followed by the $M3C^{AVG}_{N+1} - Models$, which had similar out-performance for 610 days (having a daily bootstrap winning % of 43% to 49%).

Finally, in Part III of Table C.2.3, we compared the $ParamC^{AVG}_{N+1} - Models$ with the $L3C^{AVG}_{N+1} - Models$, and found that the $ParamC^{AVG}_{N+1} - Models$ had the lowest $RMSE$ for 788 days (having a daily bootstrap winning % of 57% to 62%) out of 1,328, but if the δC_N model was excluded from the comparison, the $ParamC_{N+1}^{AVG} - Models$ outperformed for 1,065 days (having a daily bootstrap winning % of 78% to 82%) out of 1,328.

Accordingly, we now compare the $HJDC^{N+1}$ model (i.e. the best-performing model when compared to the models in column XIV of Table A.2.17) with the $ParamC_{N+1}^{AVG} - Models$, and the $L3C_{N+1}^{AVG} - Models$ in Part III of Table C.2.4, and found that the $HJDC^{N+1}$ model had the lowest $RMSE$ for 456 days (having a daily bootstrap winning % of 32% to 37%) out of 1,328. Even though the $HJDC^{N+1}$ model outperformed, the $ParamC_{N+1}^{AVG} - Models$ also had similar out-performance, where it outperformed for 384 days (having a daily bootstrap winning % of 27% to 31%), but if the δC_N model was excluded from this comparison, the $HJDC_{N+1}$ model had still outperformed for 594 days (having a daily bootstrap winning % of 42% to 48%) out of 1,328, which was closely followed by the $ParamC_{N}^{AVG} - Models$, which had similar out-performance for 517 days (having a daily bootstrap winning % of 36% to 42%).

Thus, when the individually out-performing model, the $M3C4_{N+1}$ model (from Table A.2.15) was compared to the average of all the parametric models, and the averages of all the triple hidden layer ANN models (in Part I of Table C.2.4), we conclude that an individual MLP model (i.e. $M3C4_{N+1}$) could outperform all the models. Similarly, when the individually out-performing model, the $M3C4_{N+1}$ model (from Table A.2.16) was compared to the average of all the parametric models, and the averages of all the triple hidden layer MLP models (in Part II of Table C.2.4), an individual MLP model (i.e. $M3C4_{N+1}$) had yet again outperformed them all. Lastly, when the individually out-performing model, the $HJDC_{N+1}$ model (from Table A.2.17) was compared to the average of all the parametric models, and the averages of all the triple hidden layer LSTM models (in Part III of Table C.2.4), the $HJDC_{N+1}$ model could outperform other models, and even the averages of all the LSTM models (i.e. $L3C_{N+1}^{AVG} - Models$).

C.2.1.2.2 Comparison amongst all Parametric models:

Lastly, we compare the $HJDC_{N+1}$ model (i.e. the best-performing model when compared to the models in column XI of Table A.2.18) with the $ParamC_{N+1}^{AVG} - Models$ in Part IV of Table C.2.4 and found that the $HJDC_{N+1}$ model had the lowest $RMSE$ for 1,050 days (having a daily bootstrap winning % of 77% to 81%) out of 1,328, but if the δC_N model was excluded from this comparison, the $HJDC_{N+1}^{AVG} - Models$ had still outperformed for 1,262 days (having a daily bootstrap winning % of 94% to 96%) out of 1,328.

Thus, when the individually out-performing model, the $HJDC_{N+1}$ model (from Table A.2.18) was compared to the average of all the parametric models (in Part IV of Table C.2.4), we can conclude that the $HJDC_{N+1}$ model could outperform the average of all the parametric models.

Table C.2.3: Call Option Price Comparison (Model Averaging): This table is compartmentalised into III parts, where each part presents a performance comparison using both daily and monthly statistics amongst the set of models mentioned in that part. The forecast variable for all the models is the one-trading-day-ahead call option price (C_{N+1}). The models denoted by the $_{N+1}$ subscript use one-trading-day-ahead input variables for forecasting C_{N+1}. In the parts mentioned below, we compare the out-of-sample performance of the following models: **In Part I**: $ParamC^{AVG}_{N+1} - Models$, $M3C^{AVG}_{N+1} - Models$, $L3C^{AVG}_{N+1} - Models$, **in Part II**: $ParamC^{AVG}_{N+1} - Models$, $M3C^{AVG}_{N+1} - Models$, **in Part III**: $ParamC^{AVG}_{N+1} - Models$, $L3C^{AVG}_{N+1} - Models$. The one-trading-day-ahead forecast errors of C_{N+1} are used to compute the Root Mean Square Error (RMSE). Column I identifies the models, and column II lists the models used as input to obtain the average one-trading-day-ahead forecast of C_{N+1}. Forecasts are made for 1,328 trading days, and there are 64 months covered in the sample using the monthly data. When comparing all models simultaneously (i.e. including the random walk model (δC_N), column III reports the number of months out of the 64 months that each model has the smallest RMSE, while column IV reports the number of days out of the 1,328 days each model has the smallest RMSE. Columns V (lower bound) and VI (upper bound) present the winning percentage out of 64 months for each model, evaluated using the bootstrap sampling technique. The statistical bootstrap performed (with replacement) at a 95% confidence level is computed from the monthly RMSE values of the respective models below. Columns VII (lower bound) and VIII (upper bound) present the winning percentage out of 1326 days for each model computed from bootstrapping the daily RMSE values of the respective models at a 95% confidence level. Similarly, when the δC_N model was excluded in the comparison, column IX report the number of months out of the 64 months that each model has the smallest RMSE, while column X reports the number of days out of the 1,328 days each model has the smallest RMSE. Columns XI (lower bound) and XII (upper bound) present the winning percentage out of 64 months for each model, evaluated using the bootstrap sampling technique. The statistical bootstrap performed (with replacement) at a 95% confidence level is computed from the monthly RMSE values of the respective models below. Also, columns XIII (lower bound) and XIV (upper bound) present the winning percentage out of 1326 days for each model computed from bootstrapping the daily RMSE values of the respective models at a 95% confidence level.

		Including the random walk						**Excluding the random walk**					
(I) Model	**(II) Inputs**	**(III) Performance amongst all models (Monthly)**	**(IV) Performance amongst all models (Daily)**	**(V) 2.5% lower bound- (for monthly) (%)**	**(VI) 2.5% upper bound- (for monthly) (%)**	**(VII) 2.5% lower bound- (for daily) (%)**	**(VIII) 2.5% upper bound- (for daily) (%)**	**(IX) Performance amongst all models (Monthly)**	**(X) Performance amongst all models (Daily)**	**(XI) 2.5% lower bound- (for monthly) (%)**	**(XII) 2.5% upper bound- (for monthly) (%)**	**(XIII) 2.5% lower bound- (for daily) (%)**	**(XIV) 2.5% upper bound- (for daily) (%)**
Part I: $ParamC^{AVG}_{N+1} - Models$ v/s $M3C^{AVG}_{N+1} - Models$ v/s $L3C^{AVG}_{N+1} - Models$													
δC_N	-	0	129	0%	0%	8%	11%	-	-	-	-	-	-
$ParamC^{AVG}_{N+1} - Models$	$BSMC_{N+1}$,HC_{N+1} ,$HJDC_{N+1}$,$FMLSC_{N+1}$	13	208	11%	31%	14%	18%	13	208	11%	30%	14%	18%
$M3C^{AVG}_{N+1} - Models$	$M3C1_{N+1}$,$M3C2_{N+1}$,$M3C3_{N+1}$,$M3C4_{N+1}$,$M3C5_{N+1}$,$M3C6_{N+1}$,$M3C7_{N+1}$,$M3C8_{N+1}$,$M3C9_{N+1}$	**51**	**987**	69%	89%	72%	77%	**51**	**1114**	70%	89%	82%	86%
$L3C^{AVG}_{N+1} - Models$	$L3C1_{N+1}$,$L3C2_{N+1}$,$L3C3_{N+1}$,$L3C4_{N+1}$,$L3C5_{N+1}$,$L3C6_{N+1}$,$L3C7_{N+1}$,$L3C8_{N+1}$,$L3C9_{N+1}$	0	4	0%	0%	0%	1%	0	6	0%	0%	0%	1%
Part II: $ParamC^{AVG}_{N+1} - Models$ v/s $M3C^{AVG}_{N+1} - Models$													
δC_N	-	0	129	0%	0%	8%	11%	-	-	-	-	-	-
$ParamC^{AVG}_{N+1} - Models$	$BSMC_{N+1}$,HC_{N+1} ,$HJDC_{N+1}$,$FMLSC_{N+1}$	13	208	11%	30%	14%	18%	13	208	11%	30%	14%	18%
$M3C^{AVG}_{N+1} - Models$	$M3C1_{N+1}$,$M3C2_{N+1}$,$M3C3_{N+1}$,$M3C4_{N+1}$,$M3C5_{N+1}$,$M3C6_{N+1}$,$M3C7_{N+1}$,$M3C8_{N+1}$,$M3C9_{N+1}$	**51**	**991**	70%	89%	72%	77%	**51**	**1120**	70%	89%	82%	86%
Part III: $ParamC^{AVG}_{N+1} - Models$ v/s $L3C^{AVG}_{N+1} - Models$													
δC_N	-	0	443	0%	0%	31%	36%	-	-	-	-	-	-
$ParamC^{AVG}_{N+1} - Models$	$BSMC_{N+1}$,HC_{N+1} ,$HJDC_{N+1}$,$FMLSC_{N+1}$	**64**	**788**	100%	100%	57%	62%	**64**	**1065**	100%	100%	78%	82%
$L3C^{AVG}_{N+1} - Models$	$L3C1_{N+1}$,$L3C2_{N+1}$,$L3C3_{N+1}$,$L3C4_{N+1}$,$L3C5_{N+1}$,$L3C6_{N+1}$,$L3C7_{N+1}$,$L3C8_{N+1}$,$L3C9_{N+1}$	0	97	0%	0%	6%	9%	0	263	0%	0%	18%	22%

Table C.2.4: Call Option Price Comparison (Model Averaging): This table is compartmentalised into IV parts. Each part presents a performance comparison using daily and monthly statistics amongst the models mentioned in that part. The forecast variable for all the models is the one-trading-day-ahead call option price (C_{N+1}). The models denoted by the $_{N+1}$ subscript use one-trading-day-ahead input variables for forecasting the call option price C_{N+1}. In the parts mentioned below, we compare the out-of-sample performance of the best performing model (based on the total number of days out of 1326 days that a particular model had the lowest RMSE) with the average of parametric models ($ParamC^{AVG}_{N+1} - Models$), the average of triple ($M3C^{AVG}_{N+1} - Models$) hidden layer MLP models, and the average of triple ($L3C^{AVG}_{N+1} - Models$) hidden layer LSTM models. **In Part I**: The best performing model ($M3C4_{N+1}$) from Table A.2.15 with $ParamC^{AVG}_{N+1} - Models$, $M3C^{AVG}_{N+1} - Models$, $L3C^{AVG}_{N+1} - Models$, **in Part II**: The best performing model ($M3C4_{N+1}$) from Table A.2.16 with $ParamC^{AVG}_{N+1} - Models$, $M3C^{AVG}_{N+1} - Models$, **in Part III**: The best performing model (HC_{N+1}) from Table A.2.17 with $ParamC^{AVG}_{N+1} - Models$, $L3C^{AVG}_{N+1} - Models$, **in Part IV**: The best performing model ($HJDC_{N+1}$) from Table A.2.18 with $ParamC^{AVG}_{N+1} - Models$. The one-trading-day-ahead forecast errors of C_{N+1} are used to compute the Root Mean Square Error (RMSE). Forecasts are made for 1,328 trading days, and there are 64 months covered in the sample using the monthly data. Column I identifies the models. When comparing all models simultaneously (i.e. including the random walk model (δC_N), column II reports the number of months out of the 64 months that each model has the smallest RMSE, while column III reports the number of days out of the 1,328 days each model has the smallest RMSE. Columns IV (lower bound) and V (upper bound) present the winning percentage out of 64 months for each model, evaluated using the bootstrap sampling technique. The statistical bootstrap performed (with replacement) at a 95% confidence level is computed from the monthly RMSE values of the respective models below. Columns VI (lower bound) and VII (upper bound) present the winning percentage out of 1326 days for each model computed from bootstrapping the daily RMSE values of the respective models at a 95% confidence level. Similarly, when the δC_N model was excluded in the comparison, column VIII report the number of months out of the 64 months that each model has the smallest RMSE, while column IX reports the number of days out of the 1,328 days each model has the smallest RMSE. Columns X (lower bound) and XI (upper bound) present the winning percentage out of 64 months for each model, evaluated using the bootstrap sampling technique. The statistical bootstrap performed (with replacement) at a 95% confidence level is computed from the monthly RMSE values of the respective models below. Also, columns XII (lower bound) and XIII (upper bound) present the winning percentage out of 1326 days for each model computed from bootstrapping the daily RMSE values of the respective models at a 95% confidence level.

	Including the random walk						**Excluding the random walk**					
(I)	**(II)**	**(III)**	**(IV)**	**(V)**	**(VI)**	**(VII)**	**(VIII)**	**(IX)**	**(X)**	**(XI)**	**(XII)**	**(XIII)**
Model	**Performance amongst all models (Monthly)**	**Performance amongst all models (Daily)**	**2.5% lower bound-(for monthly) (%)**	**2.5% upper bound-(for monthly) (%)**	**2.5% lower bound-(for daily) (%)**	**2.5% upper bound-(for daily) (%)**	**Performance amongst all models (Monthly)**	**Performance amongst all models (Daily)**	**2.5% lower bound-(for monthly) (%)**	**2.5% upper bound-(for monthly) (%)**	**2.5% lower bound-(for daily) (%)**	**2.5% upper bound-(for daily) (%)**
Part I: $M3C4_{N+1}$ v/s $ParamC^{AVG}_{N+1} - Models$ v/s $M3C^{AVG}_{N+1} - Models$ v/s $L3C^{AVG}_{N+1} - Models$												
δ_C	0	119	0%	0%	7%	11%	-	-	-	-	-	-
$M3C4_{N+1}$	**35**	**650**	44%	67%	46%	52%	**35**	**683**	42%	66%	49%	54%
$ParamC^{AVG}_{N+1} - Models$	0	34	0%	0%	2%	3%	0	34	0%	0%	2%	3%
$M3C^{AVG}_{N+1} - Models$	29	525	33%	56%	37%	42%	29	610	34%	58%	43%	49%
$L3C^{AVG}_{N+1} - Models$	0	0	0%	0%	0%	0%	0	1	0%	0%	0%	0%
Part II: $M3C4_{N+1}$ v/s $ParamC^{AVG}_{N+1} - Models$ v/s $M3C^{AVG}_{N+1} - Models$												
δ_C	0	119	0%	0%	7%	10%	-	-	-	-	-	-
$M3C4_{N+1}$	**35**	**650**	42%	66%	46%	52%	**35**	**683**	44%	66%	49%	54%
$ParamC^{AVG}_{N+1} - Models$	0	34	0%	0%	2%	3%	0	34	0%	0%	2%	3%
$M3C^{AVG}_{N+1} - Models$	29	525	34%	58%	37%	42%	29	611	34%	56%	43%	49%
Part III: HC_{N+1} v/s $ParamC^{AVG}_{N+1} - Models$ v/s $L3C^{AVG}_{N+1} - Models$												
δ_C	0	403	0%	0%	28%	33%	-	-	-	-	-	-
$HJDC_{N+1}$	**39**	**456**	48%	73%	32%	37%	**39**	**594**	48%	73%	42%	48%
$ParamC^{AVG}_{N+1} - Models$	25	384	27%	52%	27%	31%	25	517	27%	52%	36%	42%
$L3C^{AVG}_{N+1} - Models$	0	85	0%	0%	5%	8%	0	217	0%	0%	14%	18%
Part IV: $HJDC_{N+1}$ v/s $ParamC^{AVG}_{N+1} - Models$ v/s $L3C^{AVG}_{N+1} - Models$												
δ_C	0	218	0%	0%	14%	18%	-	-	-	-	-	-
$HJDC_{N+1}$	**64**	**1050**	100%	100%	77%	81%	**64**	**1262**	100%	100%	94%	96%
$ParamC^{AVG}_{N+1} - Models$	0	60	0%	0%	3%	6%	0	66	0%	0%	4%	6%

C.2.2 Results - $CK - Models$ - Model Averaging

C.2.2.1 $CK^{AVG}-Models$: Model averaging pricing performance of models that use lagged input variables to forecast the call option price scaled by the strike price (C_{N+1}/K_{N+1}) for the next trading day

Table C.2.5 shows the relative out-of-sample pricing performance (in $RMSE$) amongst the models that forecast the one-trading-day-ahead average call option price scaled by the strike price(C_{N+1}/K_{N+1}) using lagged input variables. In column II of table C.2.5, we list the several models used as an input to obtain the average one-trading-day-ahead forecast of C_{N+1}/K_{N+1}. The performance metric is the $RMSE$ of the one-trading-day-ahead forecast errors of the average C_{N+1}/K_{N+1}, which is computed for each averaging model utilising all of the errors in each day or each month. Amongst all of the models (including the random walk model (δCK_N)), columns III and IV record the number of months and days, respectively, that each model has the lowest $RMSE$. We performed a bootstrap using the daily and monthly RMSEs to be certain of our results. The columns V (lower bound) and VI (upper bound) present the results from the bootstrap performed (with replacement) using monthly RMSEs at a 95% confidence level and show the winning percentage out of 64 months for each model (including the δCK_N model) and similarly, the 95 % confidence intervals computed from bootstrapping of the daily RMSEs signifies the winning percentage out of 1,328 days for each model and are reported in columns VII (lower bound), VIII (upper bound). While excluding the δCK_N model amongst the comparison, columns IX and X record the number of months and days that each model has the lowest $RMSE$.e repeat the exercise of performing the bootstrap by excluding the δCK_N model in the comparison, and thus, the columns XI (lower bound), XII (upper bound) presents the results from the bootstrap performed (with replacement) using monthly RMSEs at a 95% confidence level and shows the winning percentage out of 64 months for each model (excluding the δCK_N model) and similarly, the 95 % confidence intervals computed from bootstrapping of the daily RMSEs signifies the winning percentage out of 1,328 days for each model and are reported in columns XIII (lower bound), XIV (upper bound). After a model is found to outperform other individual parametric models, MLP and LSTM models in each of the several comparisons below, we look into whether that out-performing model individually can outperform the average call option price of all the parametric models combinedly, MLP models combinedly or LSTM models combinedly, covered in that section.

In the below several comparisons, even though a particular model wins by a higher percentage against other models, we investigated further these models pairwise by performing a pairwise bootstrap comparison, which was computed using the respective pair's daily RMSEs. The results are presented in Table 93 of the Electronic Appendix.

The Diebold-Mariano(DM) (Diebold and Mariano (1995)) test was performed on pairs amongst the Random Walk (δCK_N) model, the average C_{N+1}/K_{N+1} of all parametric models ($ParamCK_N^{AVG}-Models$), the average C_{N+1}/K_{N+1} of all single hidden layer MLP models ($M1CK_N^{AVG}-Models$), the average C_{N+1}/K_{N+1} of all single hidden layer LSTM models ($L1CK_N^{AVG} - Models$), the average C_{N+1}/K_{N+1} of all double hidden layer MLP models ($M2CK_N^{AVG} - Models$), the average C_{N+1}/K_{N+1} of all double hidden layer LSTM models ($L3CK_N^{AVG} - Models$), the average C_{N+1}/K_{N+1} of all triple hidden layer MLP models ($M3CK_N^{AVG} - Models$), and the average C_{N+1}/K_{N+1} of all triple hidden layer LSTM models ($L3CK_N^{AVG}-Models$) are reported in Table 82 of the Electronic Appendix. In constructing the DM tests, the model pairs are reported in column I and column II, and the DM test statistics for a particular pair are reported in column

III. If the null can be rejected, a positive number suggests the rejection may be due to the second model being the better forecast model. In contrast, a negative value suggests the rejection may be due to the first model being the better forecast model. The model pairs highlighted in a red state that their forecasts have statistically insignificant differences in their prediction accuracy. Considering the DM-Test statistics in Table 82 of the Electronic Appendix, all the model pairs lead to the rejection of the null of equal forecasting performance.

The RMSEs for the models under the $CK^{AVG} - Models$ category, which averages the forecasted C_{N+1}/K_{N+1} from models belonging to the $CK - Models$ category (which uses lagged input variables to forecast the C_{N+1}/K_{N+1} for the next trading day) on a monthly, yearly, and overall basis can be found in the Electronic Appendix, in Tables 53, 63, and 73, respectively.

C.2.2.1.1 Comparison amongst all Parametric Models with Single Hidden Layer ANN Models:

In this section, we compare the out-of-sample pricing performance of the random walk model (δCK_N), the parametric models ($ParamCK_N^{AVG} - Models$), the single hidden layer MLP models ($M1CK_N^{AVG} - Models$), and the single hidden layer LSTM models ($L1CK_N^{AVG} - Models$), and then $ParamCK_N^{AVG} - Models$ with the $M1CK_N^{AVG} - Models$, and Accordingly the $ParamCK_N^{AVG} - Models$ with the $L1CK_N^{AVG} - Models$.

Initially, in Part I of Table C.2.5, when we compared the $ParamCK_N^{AVG} - Models$ with the $M1CK_N^{AVG} - Models$ and the $L1CK_N^{AVG} - Models$, and found that none of the models could outperform the δCK_N model, where the δCK_N model had the lowest $RMSE$ for 849 days (having a daily bootstrap winning % of 61% to 66%) out of 1,328, but if the δCK_N model was excluded from the comparison, the $M1CK_N^{AVG} - Models$ outperformed for 1,260 days (having a daily bootstrap winning % of 94% to 96%) out of 1,328. Accordingly, we now compare the $L1CK2_N$ model (i.e. the best-performing model when compared to the models in column XIV of Table A.2.19) with the $ParamCK_N^{AVG} - Models$, $M1CK_N^{AVG} - Models$ and the $L1CK_N^{AVG} - Models$ in Part I of Table C.2.6 and found that the δCK_N model still outperformed for 685 days (having a daily bootstrap winning % of 49% to 54%) out of 1,328, but if the δCK_N model was excluded from this comparison, the $M1CK_N^{AVG} - Models$ had outperformed for 937 days (having a daily bootstrap winning % of 68% to 73%) out of 1,328.

Secondly, in Part II of Table C.2.5, we compared the $ParamCK_N^{AVG} - Models$ with the $M1CK_N^{AVG} - Models$ and found that none of the models could outperform the δCK_N model, where the δCK_N model had the lowest $RMSE$ for 853 days (having a daily bootstrap winning % of 62% to 67%) out of 1,328, but if the δCK_N model was excluded from the comparison, the $M1CK_N^{AVG} - Models$ outperformed for 1,281 days (having a daily bootstrap winning % of 95% to 97%) out of 1,328. Accordingly, we now compare the $M1CK3_N$ model (i.e. the best-performing model when compared to the models in column XIV of Table A.2.20) with the $ParamCK_N^{AVG} - Models$, and the $M1CK_N^{AVG} - Models$ in Part II of Table C.2.6 and found that none of the models could outperform the the δCK_N model, which had the lowest $RMSE$ for 765 days (having a daily bootstrap winning % of 55% to 60%) out of 1,328, but if the δCK_N model was excluded from this comparison, the $M1CK_N^{AVG} - Models$ had outperformed for 753 days (having a daily bootstrap winning % of 54% to 59%) out of 1,328.

Finally, in Part III of Table C.2.5, we compared the $ParamCK_N^{AVG} - Models$ with the $L1CK_N^{AVG} - Models$ and found that none of the models could outperform the δCK_N model, where the δCK_N model had the lowest $RMSE$ for 1,263 days (having a daily bootstrap winning % of 94% to 96%)

out of 1,328, but if the δCK_N model was excluded from the comparison, the $L1CK_N^{AVG} - Models$ outperformed for 946 days (having a daily bootstrap winning % of 69% to 74%) out of 1,328. Accordingly, we now compare the $L1CK2_N$ model (i.e. the best-performing model when compared to the models in column XIV of Table A.2.21) with the $ParamCK_N^{AVG} - Models$, and the $L1CK_N^{AVG} - Models$ in Part III of Table C.2.6 and found that none of the models could outperform the δCK_N model, which had the lowest $RMSE$ for 987 days (having a daily bootstrap winning % of 72% to 77%) out of 1,328, but if the δCK_N model was excluded from this comparison, the $L1CK2_N$ model had outperformed for 912 days (having a daily bootstrap winning % of 66% to 71%) out of 1,328.

Thus, when the individually out-performing model, the $L1CK2_N$ model (from Table A.2.19) was compared to the average of all the parametric models, and the averages of all the single hidden layer ANN models (in Part I of Table C.2.6), we conclude that an individual LSTM could not outperform the model averages, where the averages of all the single hidden layer MLP models (i.e. $M1CK_N^{AVG} - Models$) had out-performed them all. Similarly, when the individually out-performing model, the $M1CK3_N$ model (from Table A.2.20) was compared to the average of all the parametric models, and the averages of all the single hidden layer MLP models (in Part II of Table C.2.6), the averages of all the single hidden layer MLP models (i.e. $M1CK_N^{AVG} - Models$) had yet again out-performed them all. Lastly, when the individually out-performing model, the $L1CK2_N$ model (from Table A.2.21) was compared to the average of all the parametric models, and the averages of all the single hidden layer LSTM models (in Part III of Table C.2.6), an individual LSTM model (i.e. the $L1CK2_N$ model) could outperform them all.

C.2.2.1.2 Comparison amongst all Parametric Models with Double Hidden Layer ANN Models:

In this section, we compare the out-of-sample pricing performance of the random walk model (δCK_N), the parametric models ($ParamCK_N^{AVG} - Models$), the double hidden layer MLP models ($M2CK_N^{AVG} - Models$), and the double hidden layer LSTM models ($L2CK_N^{AVG} - Models$), and then $ParamCK_N^{AVG} - Models$ with the $M2CK_N^{AVG} - Models$, and Accordingly the $ParamCK_N^{AVG} - Models$ with the $L2CK_N^{AVG} - Models$.

Initially, in Part IV of Table C.2.5, we compared the $ParamCK_N^{AVG} - Models$ with the $M2CK_N^{AVG} - Models$ and the $L2CK_N^{AVG} - Models$, and found that none of the models could outperform the δCK_N model, where the δCK_N model had the lowest $RMSE$ for 805 days (having a daily bootstrap winning % of 58% to 63%) out of 1,328, but if the δCK_N model was excluded from the comparison, the $M2CK_N^{AVG} - Models$ outperformed for 1,248 days (having a daily bootstrap winning % of 93% to 95%) out of 1,328. Accordingly, we now compare the $L2CK2_N$ model (i.e. the best-performing model when compared to the models in column XIV of Table A.2.22) with the $ParamCK_N^{AVG} - Models$, $M2CK_N^{AVG} - Models$, and the $L2CK_N^{AVG} - Models$ in Part IV of Table C.2.6 and found that none of the models could outperform the δCK_N model, which had the lowest $RMSE$ for 656 days (having a daily bootstrap winning % of 47% to 52%) out of 1,328, but if the δCK_N model was excluded from this comparison, the $M2CK_N^{AVG} - Models$ had outperformed for 934 days (having a daily bootstrap winning % of 68% to 73%) out of 1,328.

Secondly, in Part V of Table C.2.5, we compared the $ParamCK_N^{AVG} - Models$ with the $M2CK_N^{AVG} - Models$, and found that none of the models could outperform the δCK_N model, where the δCK_N model had the lowest $RMSE$ for 816 days (having a daily bootstrap winning % of 59% to 64%) out of 1,328, but if the δCK_N model was excluded from the comparison, the $M2CK_N^{AVG} - Models$ outperformed for 1,284 days (having a daily bootstrap winning % of 96% to 98%) out of 1,328. Accordingly, we now compare the $M2CK3_N$ model (i.e. the best-performing model when compared to the models in column XIV of Table A.2.23) with the $ParamCK_N^{AVG} - Models$, and the $M2CK_N^{AVG} - Models$ in Part V of Table C.2.6 and found that none of the models could outperform the δCK_N model, which had the lowest $RMSE$ for 704 days (having a daily bootstrap winning % of 50% to 56%) out of 1,328, but if the δCK_N model was excluded from this comparison, the $M2CK_N^{AVG} - Models$ had outperformed for 733 days (having a daily bootstrap winning % of 52% to 58%) out of 1,328.

Finally, in Part VI of Table C.2.5, we compared the $ParamCK_N^{AVG} - Models$ with the $L2CK_N^{AVG} - Models$ and found that none of the models could outperform the δCK_N model, where the δCK_N model had the lowest $RMSE$ for 1,242 days (having a daily bootstrap winning % of 92% to 95%) out of 1,328, but if the δCK_N model was excluded from the comparison, the $ParamCK_N^{AVG} - Models$ outperformed for 855 days (having a daily bootstrap winning % of 62% to 67%) out of 1,328. Accordingly, we now compare the $L2CK2_N$ model (i.e. the best-performing model when compared to the models in column XIV of Table A.2.24) with the $ParamCK_N^{AVG} - Models$, and the $L2CK_N^{AVG} - Models$ in Part VI of Table C.2.6 and found that none of the models could outperform the δCK_N model, which had the lowest $RMSE$ for 970 days (having a daily bootstrap winning % of 71% to 75%) out of 1,328, but if the δCK_N model was excluded from this comparison, the $L2CK2_N$ model had outperformed for 873 days (having a daily bootstrap winning % of 63% to 68%) out of 1,328.

Thus, when the individually out-performing model, the $L2CK2_N$ model (from Table A.2.22) was compared to the average of all the parametric models, and the averages of all the double hidden layer ANN models (in Part IV of Table C.2.6), we conclude that an individual LSTM could not outperform the model averages, where the averages of all the double hidden layer MLP models (i.e. $M2CK_N^{AVG} - Models$) had out-performed them all. Similarly, when the individually out-performing model, the $M2CK3_N$ model (from Table A.2.23) was compared to the average of all the parametric models, and the averages of all the double hidden layer MLP models (in Part V of Table C.2.6), the averages of all the double hidden layer MLP models (i.e. $M2CK_N^{AVG} - Models$) had yet again out-performed them all. Lastly, when the individually out-performing model, the $L2CK2_N$ model (from Table A.2.24) was compared to the average of all the parametric models, and the averages of all the double hidden layer LSTM models (in Part VI of Table C.2.6), an individual LSTM model (i.e. the $L2C9_N$ model) could outperform other models.

C.2.2.1.3 Comparison amongst all Parametric Models with Triple Hidden Layer ANN Models:

In this section, we compare the out-of-sample pricing performance of the random walk model (δCK_N), the parametric models ($ParamCK_N^{AVG} - Models$), the triple hidden layer MLP models ($M3CK_N^{AVG} - Models$), and the triple hidden layer LSTM models ($L3CK_N^{AVG} - Models$), and then $ParamCK_N^{AVG} - Models$ with the $M3CK_N^{AVG} - Models$, and finally the $ParamCK_N^{AVG} - Models$ with the $L3CK_N^{AVG} - Models$.

Initially, in Part VII of Table C.2.5, we compared the $ParamCK_N^{AVG} - Models$ with the $M3CK_N^{AVG} - Models$ and the $L3CK_N^{AVG} - Models$, and found that none of the models could outperform the δCK_N model, where the δCK_N model had the lowest $RMSE$ for 797 days (having a daily bootstrap winning % of 57% to 62%) out of 1,328, but if the δCK_N model was excluded from the comparison, the $M3CK_N^{AVG} - Models$ outperformed for 1,244 days (having a daily bootstrap winning % of 92% to 95%) out of 1,328. Accordingly, we now compare the $L3CK2_N$ model (i.e. the best-performing model when compared to the models in column XIV of Table A.2.25) with the $ParamCK_N^{AVG} - Models$ with the $M3CK_N^{AVG} - Models$ in Part VII of Table C.2.6 and found that none of the models could outperform the δCK_N model, which had the lowest $RMSE$ for 656 days (having a daily bootstrap winning % of 47% to 52%) out of 1,328, but if the δCK_N model was excluded from this comparison, the $M3CK_N^{AVG} - Models$ had outperformed for 930 days (having a daily bootstrap winning % of 68% to 72%) out of 1,328.

Secondly, in Part VIII of Table C.2.5, we compared the $ParamCK_N^{AVG} - Models$ with the $M3CK_N^{AVG} - Models$, and found that none of the models could outperform the δCK_N model, where the δCK_N model had the lowest $RMSE$ for 810 days (having a daily bootstrap winning % of 58% to 64%) out of 1,328, but if the δCK_N model was excluded from the comparison, the $M3CK_N^{AVG} - Models$ outperformed for 1,283 days (having a daily bootstrap winning % of 96% to 98%) out of 1,328. Accordingly, we now compare the $M3CK2_N$ model (i.e. the best-performing model when compared to the models in column XIV of Table A.2.26) with the $ParamCK_N^{AVG} - Models$, and the $M3CK_N^{AVG} - Models$ in Part VIII of Table C.2.6 and found that none of the models could outperform the δCK_N model, which had the lowest $RMSE$ for 714 days (having a daily bootstrap winning % of 51% to 57%) out of 1,328, but if the δCK_N model was excluded from this comparison, the $M3CK_N^{AVG} - Models$ had outperformed for 785 days (having a daily bootstrap winning % of 56% to 62%) out of 1,328.

Finally, in Part IX of Table C.2.5, we compared the $ParamCK_N^{AVG} - Models$ with the $L3CK_N^{AVG} - Models$ and found that none of the models could outperform the δCK_N model, where the δCK_N model had the lowest $RMSE$ for 1,241 days (having a daily bootstrap winning % of 92% to 95%) out of 1,328, but if the δCK_N model was excluded from the comparison, the $ParamCK_N^{AVG} - Models$ outperformed for 862 days (having a daily bootstrap winning % of 62% to 68%) out of 1,328. Accordingly, we now compare the $L3CK2_N$ model (i.e. the best-performing model when compared to the models in column XIV of Table A.2.27) with the $ParamCK_N^{AVG} - Models$, and the $L3CK_N^{AVG} - Models$ in Part IX of Table C.2.6 and found that none of the models could outperform the δCK_N model, which had the lowest $RMSE$ for 957 days (having a daily bootstrap winning % of 70% to 74%) out of 1,328, but if the δCK_N model was excluded from this comparison, the $L3CK2_N$ model had outperformed for 907 days (having a daily bootstrap winning % of 66% to 71%) out of 1,328.

Thus, when the individually out-performing model, the $L3CK2_N$ model (from Table A.2.25) was compared to the average of all the parametric models, and the averages of all the triple hidden layer ANN models (in Part VII of Table C.2.6), we conclude that an individual LSTM could not outperform the model averages, where the averages of all the triple hidden layer MLP models (i.e. $M3CK_N^{AVG} - Models$) had out-performed them all. Similarly, when the individually out-performing model, the $M3CK2_N$ model (from Table A.2.26) was compared to the average of all the parametric models, and the averages of all the triple hidden layer MLP models (in Part VIII of Table C.2.6), the averages of all the triple hidden layer MLP models (i.e. $M3CK_N^{AVG} - Models$) had yet again out-performed them all. Lastly, when the best individually performing model, the $L3CK2_N$ model (from Table A.2.27) was compared to the average of all the parametric models, and the averages of all the triple hidden layer LSTM models (in Part IX of Table C.2.6), an individual LSTM model (i.e. the $L3CK2_N$ model) had outperformed other models.

C.2.2.1.4 Comparison amongst all Parametric Models with Single, Double and Triple Hidden Layer ANN Models:

In this section, we compare the out-of-sample pricing performance of the random walk model (δCK_N), the parametric models ($ParamCK_N^{AVG} - Models$), with the single hidden layer MLP models ($M1CK_N^{AVG} - Models$), the single hidden layer LSTM models ($L1CK_N^{AVG} - Models$), the double hidden layer MLP models ($M2CK_N^{AVG} - Models$), the double hidden layer LSTM models ($L2CK_N^{AVG} - Models$), the triple hidden layer MLP models ($M3CK_N^{AVG} - Models$), and the triple hidden layer LSTM models ($L3CK_N^{AVG} - Models$), and then $ParamCK_N^{AVG} - Models$ with the $M1CK_N^{AVG} - Models$, $M2CK_N^{AVG} - Models$ and the $M3CK_N^{AVG} - Models$, and finally the $ParamCK_N^{AVG} - Models$ with the $L1CK_N^{AVG} - Models$, $L2CK_N^{AVG} - Models$ and the $L3CK_N^{AVG} - Models$.

Initially, in Part X of Table C.2.5, we compared the $ParamCK_N^{AVG} - Models$ with the $M1CK_N^{AVG} - Models$, $M2CK_N^{AVG} - Models$, $M3CK_N^{AVG} - Models$, $L1CK_N^{AVG} - Models$, $L2CK_N^{AVG} - Models$ and the $L3CK_N^{AVG} - Models$, and found that none of the models could outperform the δCK_N model, where the δCK_N model had the lowest $RMSE$ for 696 days (having a daily bootstrap winning % of 50% to 55%) out of 1,328, but if the δCK_N model was excluded from the comparison, the $M3CK_N^{AVG} - Models$ outperformed for 627 days (having a daily bootstrap winning % of 44% to 50%) out of 1,328. Accordingly, we now compare the $L1CK2_N$ model (i.e. the best-performing model when compared to the models in column XIV of Table A.2.28) with the $ParamCK_N^{AVG} - Models$, $M1CK_N^{AVG} - Models$, $M2CK_N^{AVG} - Models$, $M3CK_N^{AVG} - Models$, $L1CK_N^{AVG} - Models$, $L2CK_N^{AVG} - Models$ and the $L3CK_N^{AVG} - Models$ in Part X of Table C.2.6, and found that none of the models could outperform the δCK_N model, which had the lowest $RMSE$ for 586 days (having a daily bootstrap winning % of 41% to 47%) out of 1,328, but if the δCK_N model was excluded from this comparison, the $M3CK_N^{AVG} - Models$ model had outperformed for 492 days (having a daily bootstrap winning % of 34% to 40%) out of 1,328.

Secondly, in Part XI of Table C.2.5, we compared the $ParamCK_N^{AVG} - Models$ with the $M1CK_N^{AVG} - Models$, $M2CK_N^{AVG} - Models$, and the $M3CK_N^{AVG} - Models$, and found that none of the models could outperform the δCK_N model, where the δCK_N model had the lowest $RMSE$ for 708 days (having a daily bootstrap winning % of 51% to 56%) out of 1,328, but if the δCK_N model was excluded from the comparison, the $M3CK_N^{AVG} - Models$ outperformed for 651 days (having a daily bootstrap winning % of 47% to 52%) out of 1,328. Accordingly, we now compare the $M3CK4_N$ model (i.e. the best-performing model when compared to the models in column XIV of Table A.2.29) with the $ParamCK_N^{AVG} - Models$, $M1CK_N^{AVG} - Models$, $M2CK_N^{AVG} - Models$, and the $M3CK_N^{AVG} - Models$ in Part XI of Table C.2.6, and found that none of the models could outperform the δCK_N model, which had the lowest $RMSE$ for 536 days (having a daily bootstrap winning % of 38% to 43%) out of 1,328, but if the δCK_N model was excluded from this comparison, the $M3CK4_N$ had outperformed for 539 days (having a daily bootstrap winning % of 38% to 43%) out of 1,328.

Finally, initially in Part XII of Table C.2.5, we compared the $ParamCK_N^{AVG} - Models$ with the $L1CK_N^{AVG} - Models$, $L2CK_N^{AVG} - Models$, and the $L3CK_N^{AVG} - Models$, and found that none of the models could outperform the δCK_N model, where the δCK_N model had the lowest $RMSE$ for 1,225 days (having a daily bootstrap winning % of 91% to 94%) out of 1,328, but if the δCK_N model was excluded from the comparison, the $ParamCK_N^{AVG} - Models$ outperformed for 622 days (having a daily bootstrap winning % of 44% to 50%) out of 1,328. Accordingly, we now compare the $L2CK2_N$ model (i.e. the best-performing model when compared to the models in column XIV of Table A.2.30) with the $ParamCK_N^{AVG} - Models$, $L1CK_N^{AVG} - Models$,

$L2CK_N^{AVG} - Models$, and the $L3CK_N^{AVG} - Models$ in Part XII of Table C.2.6, and found that none of the models could outperform the δCK_N model, which had the lowest $RMSE$ for 957 days (having a daily bootstrap winning % of 70% to 74%) out of 1,328, but if the δCK_N model was excluded from this comparison, the $L2CK2_N$ had outperformed for 847 days (having a daily bootstrap winning % of 61% to 66%) out of 1,328.

Thus, when the individually out-performing model, the $L1CK2_N$ model (from Table A.2.28) was compared to the average of all the parametric models, the averages of all the single hidden layer ANN models, the averages of all the double hidden layer ANN models, and the averages of all the triple hidden layer ANN models (in Part X of Table C.2.6), we conclude that the averages of all the triple hidden layer MLP models (i.e. the $M3CK_N^{AVG} - Models$) had out-performed other models. Similarly, when the individually out-performing model, the $M3CK4_N$ model (from Table A.2.29) was compared to the average of all the parametric models, the averages of all the single hidden layer MLP models, the averages of all the double hidden layer MLP models, and the averages of all the triple hidden layer MLP models (in Part XI of Table C.2.6), the $M3CK4_N$ model had out-performed them all. Lastly, when the individually out-performing model, the $L2CK2_N$ model (from Table A.2.30) was compared to the average of all the parametric models, the averages of all the single hidden layer LSTM models, the averages of all the double hidden layer LSTM models, and the averages of all the triple hidden layer LSTM models (in Part XII of Table C.2.6), an individual LSTM model (i.e. the $L2CK2_N$ model) could outperform all other models.

C.2.2.1.5 Comparison amongst Single, Double and Triple Hidden Layer ANN Models:

In this section, we compare the out-of-sample pricing performance amongst the random walk model (δCK_N), the single hidden layer MLP models ($M1CK_N^{AVG} - Models$), the single hidden layer LSTM models ($L1CK_N^{AVG} - Models$), the double hidden layer MLP models ($M2CK_N^{AVG} - Models$), the double hidden layer LSTM models ($L2CK_N^{AVG} - Models$), the triple hidden layer MLP models ($M3CK_N^{AVG} - Models$), and the triple hidden layer LSTM models ($L3CK_N^{AVG} - Models$).

In Part XIII of Table C.2.5, we compared within the $M1CK_N^{AVG} - Models$, $M2CK_N^{AVG} - Models$, $M3CK_N^{AVG} - Models$, $L1CK_N^{AVG} - Models$, $L2CK_N^{AVG} - Models$ and the $L3CK_N^{AVG} - Models$, and found that none of the models could outperform the δCK_N model, where the δCK_N model had the lowest $RMSE$ for 706 days (having a daily bootstrap winning % of 51% to 56%) out of 1,328, but if the δCK_N model was excluded from the comparison, the $M3CK_N^{AVG} - Models$ outperformed for 636 days (having a daily bootstrap winning % of 45% to 51%) out of 1,328. Accordingly, we now compare the $L2CK2_N$ model (i.e. the best-performing model when compared to the models in column XIV of Table A.2.31) with the $M1CK_N^{AVG} - Models$, $M2CK_N^{AVG} - Models$, $M3CK_N^{AVG} - Models$, $L1CK_N^{AVG} - Models$, $L2CK_N^{AVG} - Models$ and the $L3CK_N^{AVG} - Models$ in Part XIII of Table C.2.6, and found that none of the models could outperform the δCK_N model, which had the lowest $RMSE$ for 584 days (having a daily bootstrap winning % of 41% to 46%) out of 1,328, but if the δCK_N model was excluded from this comparison, the $M3CK_N^{AVG} - Models$ had outperformed for 497 days (having a daily bootstrap winning % of 35% to 40%) out of 1,328.

Thus, when the individually out-performing model, the $L2CK2_N$ model (from Table A.2.25) was compared to the averages of all the single hidden layer ANN models, the averages of all the double hidden layer ANN models, and the averages of all the triple hidden layer ANN models (in Part XIII of Table C.2.6), we conclude that an individual LSTM could not outperform other model averages, but the averages of all the triple hidden layer MLP models (i.e. the $M3CK_N^{AVG} - Models$) had out-performed all models.

C.2.2.1.6 Comparison amongst all Parametric models:

We now compare the $HJDCK_N$ model (i.e. the best-performing model when compared to the models in column XI of Table A.2.32) with the $ParamCK_N^{AVG} - Models$ in Part XIV of Table C.2.6 and found that none of the models could outperform the δCK_N model, which had the lowest $RMSE$ for 1,272 days (having a daily bootstrap winning % of 95% to 97%) out of 1,328, but if the δCK_N model was excluded from this comparison, the $ParamCK_N^{AVG} - Models$ had outperformed for 1,077 days (having a daily bootstrap winning % of 79% to 83%) out of 1,328.

Thus, when the best individually performing model, the $HJDCK_N$ model (from Table A.2.32) was compared to the average of all the parametric models (in Part XIV of Table C.2.6), we can conclude that the average of all the parametric models (i.e. the $ParamCK_N^{AVG} - Models$) could outperform the $HJDCK_N$ model.

Table C.2.5: Call Option Price Scaled by the Exercise Price Comparison (Model Averaging): This table is compartmentalised into XVII parts, where each part presents a performance comparison using daily and monthly statistics amongst the set of models mentioned in that part. The forecast variable for all the models is the one-trading-day-ahead call option price scaled by the exercise price (C_{N+1}/K_{N+1}). The models denoted by the $_N$ subscript use lagged input variables for forecasting C_{N+1}/K_{N+1}. In the parts mentioned below, we compare the out-of-sample performance of the following models: **In Part I**: $ParamCK_N^{AVG}-Models$, $M1CK_N^{AVG}-Models$, $L1CK_N^{AVG}-Models$, **in Part II**: $ParamCK_N^{AVG}-Models$, $M1CK_N^{AVG}-Models$, **in Part III**: $ParamCK_N^{AVG}-Models$, $L1CK_N^{AVG}-Models$, **in Part IV**: $ParamCK_N^{AVG}-Models$, $M2CK_N^{AVG}-Models$, $L2CK_N^{AVG}-Models$, **in Part V**: $ParamCK_N^{AVG}-Models$, $M2CK_N^{AVG}-Models$, **in Part VI**: $ParamCK_N^{AVG}-Models$, $L2CK_N^{AVG}-Models$, **in Part VII**: $ParamCK_N^{AVG}-Models$, $M3CK_N^{AVG}-Models$, $L3CK_N^{AVG}-Models$,**in Part VIII**: $ParamCK_N^{AVG}-Models$, $M3CK_N^{AVG}-Models$, **in Part IX**: $ParamCK_N^{AVG}-Models$, $L3CK_N^{AVG}-Models$, **in Part X**: $ParamCK_N^{AVG}-Models$, $M1CK_N^{AVG}-Models$, $M2CK_N^{AVG}-Models$, $M3CK_N^{AVG}-Models$, $L1CK_N^{AVG}-Models$, $L2CK_N^{AVG}-Models$, $L3CK_N^{AVG}-Models$, **in Part XI**: $ParamCK_N^{AVG}-Models$, $M1CK_N^{AVG}-Models$, $M2CK_N^{AVG}-Models$, $M3CK_N^{AVG}-Models$, **in Part XII**: $ParamCK_N^{AVG}-Models$, $L1CK_N^{AVG}-Models$, $L2CK_N^{AVG}-Models$, $L3CK_N^{AVG}-Models$, **in Part XIII**: $M1CK_N^{AVG}-Models$, $M2CK_N^{AVG}-Models$, $M3CK_N^{AVG}-Models$, $L1CK_N^{AVG}-Models$, $L2CK_N^{AVG}-Models$, $L3CK_N^{AVG}-Models$. The one-trading-day-ahead forecast errors of C_{N+1}/K_{N+1} are used to compute the Root Mean Square Error (RMSE). Column I identifies the models, and column II lists the models used as input to obtain the average one-trading-day-ahead forecast of C_{N+1}/K_{N+1}. Forecasts are made for 1,328 trading days, and there are 64 months covered in the sample using the monthly data. When comparing all models simultaneously (i.e. including the random walk model (δCK_N), column III reports the number of months out of the 64 months that each model has the smallest RMSE, while column IV reports the number of days out of the 1,328 days each model has the smallest RMSE. Columns V (lower bound) and VI (upper bound) present the winning percentage out of 64 months for each model, evaluated using the bootstrap sampling technique. The statistical bootstrap performed (with replacement) at a 95% confidence level is computed from the monthly RMSE values of the respective models below. Columns VII (lower bound) and VIII (upper bound) present the winning percentage out of 1326 days for each model computed from bootstrapping the daily RMSE values of the respective models at a 95% confidence level. Similarly, when the δCK_N model was excluded in the comparison, column IX report the number of months out of the 64 months that each model has the smallest RMSE, while column X reports the number of days out of the 1,328 days each model has the smallest RMSE. Columns XI (lower bound) and XII (upper bound) present the winning percentage out of 64 months for each model, evaluated using the bootstrap sampling technique. The statistical bootstrap performed (with replacement) at a 95% confidence level is computed from the monthly RMSE values of the respective models below. Also, columns XIII (lower bound) and XIV (upper bound) present the winning percentage out of 1326 days for each model computed from bootstrapping the daily RMSE values of the respective models at a 95% confidence level.

		Including the random walk						**Excluding the random walk**					
(I) Model	**(II) Inputs**	**(III) Performance amongst all models (Monthly)**	**(IV) Performance amongst all models (Daily)**	**(V) 2.5% lower bound-(for monthly) (%)**	**(VI) 2.5% upper bound-(for monthly) (%)**	**(VII) 2.5% lower bound-(for daily) (%)**	**(VIII) 2.5% upper bound-(for daily) (%)**	**(IX) Performance amongst all models (Monthly)**	**(X) Performance amongst all models (Daily)**	**(XI) 2.5% lower bound-(for monthly) (%)**	**(XII) 2.5% upper bound-(for monthly) (%)**	**(XIII) 2.5% lower bound-(for daily) (%)**	**(XIV) 2.5% upper bound-(for daily) (%)**
Part I: $ParamCK_N^{AVG}-Models$ v/s $M1CK_N^{AVG}-Models$ v/s $L1CK_N^{AVG}-Models$													
δCK_N	-	**59**	**849**	85%	98%	61%	66%	-	-	-	-	-	-
$ParamCK_N^{AVG}-Models$	$BSMCK_N$,HCK_N ,$HJDCK_N$,$FMLSCK_N$	0	36	0%	0%	2%	4%	0	46	0%	0%	3%	5%
$M1CK_N^{AVG}-Models$	$M1CK1_N$,$M1CK2_N$,$M1CK3_N$,$M1CK4_N$,$M1CK5_N$,$M1CK6_N$,$M1CK7_N$,$M1CK8_N$,$M1CK9_N$	5	425	2%	15%	30%	35%	**64**	**1260**	100%	100%	94%	96%
$L1CK_N^{AVG}-Models$	$L1CK1_N$,$L1CK2_N$,$L1CK3_N$,$L1CK4_N$,$L1CK5_N$,$L1CK6_N$,$L1CK7_N$,$L1CK8_N$,$L1CK9_N$	0	18	0%	0%	1%	2%	0	22	0%	0%	1%	2%
Part II: $ParamCK_N^{AVG}-Models$ v/s $M1CK_N^{AVG}-Models$													
δCK_N	-	**59**	**853**	84%	98%	62%	67%	-	-	-	-	-	-
$ParamCK_N^{AVG}-Models$	$BSMCK_N$,HCK_N ,$HJDCK_N$,$FMLSCK_N$	0	37	0%	0%	2%	4%	0	47	0%	0%	3%	5%
$M1CK_N^{AVG}-Models$	$M1CK1_N$,$M1CK2_N$,$M1CK3_N$,$M1CK4_N$,$M1CK5_N$,$M1CK6_N$,$M1CK7_N$,$M1CK8_N$,$M1CK9_N$	5	438	2%	16%	31%	36%	**64**	**1281**	100%	100%	95%	97%
Part III: $ParamCK_N^{AVG}-Models$ v/s $L1CK_N^{AVG}-Models$													
δCK_N	-	**64**	**1263**	100%	100%	94%	96%	-	-	-	-	-	-
$ParamCK_N^{AVG}-Models$	$BSMCK_N$,HCK_N ,$HJDCK_N$,$FMLSCK_N$	0	46	0%	0%	2%	5%	**62**	**946**	92%	100%	69%	74%
$L1CK_N^{AVG}-Models$	$L1CK1_N$,$L1CK2_N$,$L1CK3_N$,$L1CK4_N$,$L1CK5_N$,$L1CK6_N$,$L1CK7_N$,$L1CK8_N$,$L1CK9_N$	0	19	0%	0%	1%	2%	2	382	0%	8%	26%	31%
Part IV: $ParamCK_N^{AVG}-Models$ v/s $M2CK_N^{AVG}-Models$ v/s $L2CK_N^{AVG}-Models$													
δCK_N	-	**57**	**805**	81%	95%	58%	63%	-	-	-	-	-	-
$ParamCK_N^{AVG}-Models$	$BSMCK_N$,HCK_N ,$HJDCK_N$,$FMLSCK_N$	0	29	0%	0%	1%	3%	0	36	0%	0%	2%	4%
$M2CK_N^{AVG}-Models$	$M2CK1_N$,$M2CK2_N$,$M2CK3_N$,$M2CK4_N$,$M2CK5_N$,$M2CK6_N$,$M2CK7_N$,$M2CK8_N$,$M2CK9_N$	7	452	5%	19%	32%	37%	**64**	**1248**	100%	100%	93%	95%
$L2CK_N^{AVG}-Models$	$L2CK1_N$,$L2CK2_N$,$L2CK3_N$,$L2CK4_N$,$L2CK5_N$,$L2CK6_N$,$L2CK7_N$,$L2CK8_N$,$L2CK9_N$	0	42	0%	0%	2%	4%	0	44	0%	0%	2%	4%
Part V: $ParamCK_N^{AVG}-Models$ v/s $M2CK_N^{AVG}-Models$													
δCK_N	-	**57**	**816**	81%	97%	59%	64%	-	-	-	-	-	-
$ParamCK_N^{AVG}-Models$	$BSMCK_N$,HCK_N ,$HJDCK_N$,$FMLSCK_N$	0	36	0%	0%	2%	4%	0	44	0%	0%	2%	4%
$M2CK_N^{AVG}-Models$	$M2CK1_N$,$M2CK2_N$,$M2CK3_N$,$M2CK4_N$,$M2CK5_N$,$M2CK6_N$,$M2CK7_N$,$M2CK8_N$,$M2CK9_N$	7	476	3%	19%	33%	38%	**64**	**1284**	100%	100%	96%	98%
Part VI: $ParamCK_N^{AVG}-Models$ v/s $L2CK_N^{AVG}-Models$													
δCK_N	-	**64**	**1242**	100%	100%	92%	95%	-	-	-	-	-	-
$ParamCK_N^{AVG}-Models$	$BSMCK_N$,HCK_N ,$HJDCK_N$,$FMLSCK_N$	0	39	0%	0%	2%	4%	**61**	**855**	89%	100%	62%	67%
$L2CK_N^{AVG}-Models$	$L2CK1_N$,$L2CK2_N$,$L2CK3_N$,$L2CK4_N$,$L2CK5_N$,$L2CK6_N$,$L2CK7_N$,$L2CK8_N$,$L2CK9_N$	0	47	0%	0%	3%	5%	3	473	0%	11%	33%	38%
Part VII: $ParamCK_N^{AVG}-Models$ v/s $M3CK_N^{AVG}-Models$ v/s $L3CK_N^{AVG}-Models$													
δCK_N	-	**49**	**797**	66%	86%	57%	62%	-	-	-	-	-	-
$ParamCK_N^{AVG}-Models$	$BSMCK_N$,HCK_N ,$HJDCK_N$,$FMLSCK_N$	0	35	0%	0%	2%	4%	0	39	0%	0%	2%	4%
$M3CK_N^{AVG}-Models$	$M3CK1_N$,$M3CK2_N$,$M3CK3_N$,$M3CK4_N$,$M3CK5_N$,$M3CK6_N$,$M3CK7_N$,$M3CK8_N$,$M3CK9_N$	15	452	14%	34%	31%	37%	**64**	**1244**	100%	100%	92%	95%
$L3CK_N^{AVG}-Models$	$L3CK1_N$,$L3CK2_N$,$L3CK3_N$,$L3CK4_N$,$L3CK5_N$,$L3CK6_N$,$L3CK7_N$,$L3CK8_N$,$L3CK9_N$	0	44	0%	0%	2%	4%	0	45	0%	0%	2%	4%
Part VIII: $ParamCK_N^{AVG}-Models$ v/s $M3CK_N^{AVG}-Models$													
δCK_N	-	**49**	**810**	66%	86%	58%	64%	-	-	-	-	-	-
$ParamCK_N^{AVG}-Models$	$BSMCK_N$,HCK_N ,$HJDCK_N$,$FMLSCK_N$	0	40	0%	0%	2%	4%	0	45	0%	0%	2%	4%
$M3CK_N^{AVG}-Models$	$M3CK1_N$,$M3CK2_N$,$M3CK3_N$,$M3CK4_N$,$M3CK5_N$,$M3CK6_N$,$M3CK7_N$,$M3CK8_N$,$M3CK9_N$	15	478	14%	34%	33%	39%	**64**	**1283**	100%	100%	96%	98%
Part IX: $ParamCK_N^{AVG}-Models$ v/s $L3CK_N^{AVG}-Models$													
δCK_N	-	**64**	**1241**	100%	100%	92%	95%	-	-	-	-	-	-
$ParamCK_N^{AVG}-Models$	$BSMCK_N$,HCK_N ,$HJDCK_N$,$FMLSCK_N$	0	41	0%	0%	2%	4%	**62**	**862**	92%	100%	62%	68%
$L3CK_N^{AVG}-Models$	$L3CK1_N$,$L3CK2_N$,$L3CK3_N$,$L3CK4_N$,$L3CK5_N$,$L3CK6_N$,$L3CK7_N$,$L3CK8_N$,$L3CK9_N$	0	46	0%	0%	3%	4%	2	466	0%	8%	32%	38%
Part X: $ParamCK_N^{AVG}-Models$ v/s $M1CK_N^{AVG}-Models$ v/s $M2CK_N^{AVG}-Models$ $M3CK_N^{AVG}-Models$ v/s $L1CK_N^{AVG}-Models$ v/s $L2CK_N^{AVG}-Models$ v/s $L3CK_N^{AVG}-Models$													
δCK_N	-	**48**	**696**	64%	86%	50%	55%	-	-	-	-	-	-
$ParamCK_N^{AVG}-Models$	$BSMCK_N$,HCK_N ,$HJDCK_N$,$FMLSCK_N$	0	26	0%	0%	1%	3%	0	27	0%	0%	1%	3%
$M1CK_N^{AVG}-Models$	$M1CK1_N$,$M1CK2_N$,$M1CK3_N$,$M1CK4_N$,$M1CK5_N$,$M1CK6_N$,$M1CK7_N$,$M1CK8_N$,$M1CK9_N$	1	138	0%	5%	9%	12%	10	264	8%	25%	18%	22%
$M2CK_N^{AVG}-Models$	$M2CK1_N$,$M2CK2_N$,$M2CK3_N$,$M2CK4_N$,$M2CK5_N$,$M2CK6_N$,$M2CK7_N$,$M2CK8_N$,$M2CK9_N$	2	227	0%	8%	15%	19%	3	349	0%	10%	24%	29%
$M3CK_N^{AVG}-Models$	$M3CK1_N$,$M3CK2_N$,$M3CK3_N$,$M3CK4_N$,$M3CK5_N$,$M3CK6_N$,$M3CK7_N$,$M3CK8_N$,$M3CK9_N$	13	182	11%	31%	12%	16%	**51**	**627**	69%	89%	44%	50%
$L1CK_N^{AVG}-Models$	$L1CK1_N$,$L1CK2_N$,$L1CK3_N$,$L1CK4_N$,$L1CK5_N$,$L1CK6_N$,$L1CK7_N$,$L1CK8_N$,$L1CK9_N$	0	7	0%	0%	0%	1%	0	9	0%	0%	0%	1%
$L2CK_N^{AVG}-Models$	$L2CK1_N$,$L2CK2_N$,$L2CK3_N$,$L2CK4_N$,$L2CK5_N$,$L2CK6_N$,$L2CK7_N$,$L2CK8_N$,$L2CK9_N$	0	26	0%	0%	1%	3%	0	26	0%	0%	1%	3%
$L3CK_N^{AVG}-Models$	$L3CK1_N$,$L3CK2_N$,$L3CK3_N$,$L3CK4_N$,$L3CK5_N$,$L3CK6_N$,$L3CK7_N$,$L3CK8_N$,$L3CK9_N$	0	26	0%	0%	1%	3%	0	26	0%	0%	1%	3%
Part XI: $ParamCK_N^{AVG}-Models$ v/s $M1CK_N^{AVG}-Models$ v/s $M2CK_N^{AVG}-Models$ v/s $M3CK_N^{AVG}-Models$													
δCK_N	-	**48**	**708**	64%	86%	51%	56%	-	-	-	-	-	-
$ParamCK_N^{AVG}-Models$	$BSMCK_N$,HCK_N ,$HJDCK_N$,$FMLSCK_N$	0	34	0%	0%	2%	3%	0	35	0%	0%	2%	4%
$M1CK_N^{AVG}-Models$	$M1CK1_N$,$M1CK2_N$,$M1CK3_N$,$M1CK4_N$,$M1CK5_N$,$M1CK6_N$,$M1CK7_N$,$M1CK8_N$,$M1CK9_N$	1	153	0%	5%	10%	13%	10	282	8%	24%	19%	23%
$M2CK_N^{AVG}-Models$	$M2CK1_N$,$M2CK2_N$,$M2CK3_N$,$M2CK4_N$,$M2CK5_N$,$M2CK6_N$,$M2CK7_N$,$M2CK8_N$,$M2CK9_N$	2	236	0%	8%	16%	20%	3	360	0%	11%	25%	29%
$M3CK_N^{AVG}-Models$	$M3CK1_N$,$M3CK2_N$,$M3CK3_N$,$M3CK4_N$,$M3CK5_N$,$M3CK6_N$,$M3CK7_N$,$M3CK8_N$,$M3CK9_N$	13	197	11%	31%	13%	17%	**51**	**651**	69%	89%	47%	52%
Part XII: $ParamCK_N^{AVG}-Models$ v/s $L1CK_N^{AVG}-Models$ v/s $L2CK_N^{AVG}-Models$ v/s $L3CK_N^{AVG}-Models$													
δCK_N	-	**64**	**1225**	100%	100%	91%	94%	-	-	-	-	-	-
$ParamCK_N^{AVG}-Models$	$BSMCK_N$,HCK_N ,$HJDCK_N$,$FMLSCK_N$	0	35	0%	0%	2%	4%	**60**	**622**	88%	98%	44%	50%
$L1CK_N^{AVG}-Models$	$L1CK1_N$,$L1CK2_N$,$L1CK3_N$,$L1CK4_N$,$L1CK5_N$,$L1CK6_N$,$L1CK7_N$,$L1CK8_N$,$L1CK9_N$	0	7	0%	0%	0%	1%	2	157	0%	8%	10%	13%
$L2CK_N^{AVG}-Models$	$L2CK1_N$,$L2CK2_N$,$L2CK3_N$,$L2CK4_N$,$L2CK5_N$,$L2CK6_N$,$L2CK7_N$,$L2CK8_N$,$L2CK9_N$	0	32	0%	0%	2%	3%	2	274	0%	8%	19%	23%
$L3CK_N^{AVG}-Models$	$L3CK1_N$,$L3CK2_N$,$L3CK3_N$,$L3CK4_N$,$L3CK5_N$,$L3CK6_N$,$L3CK7_N$,$L3CK8_N$,$L3CK9_N$	0	29	0%	0%	1%	3%	0	275	0%	0%	19%	23%
Part XIII: $M1CK_N^{AVG}-Models$ v/s $M2CK_N^{AVG}-Models$ $M3CK_N^{AVG}-Models$ v/s $L1CK_N^{AVG}-Models$ v/s $L2CK_N^{AVG}-Models$ v/s $L3CK_N^{AVG}-Models$													
δCK_N	-	**48**	**706**	63%	84%	51%	56%	-	-	-	-	-	-
$M1CK_N^{AVG}-Models$	$M1CK1_N$,$M1CK2_N$,$M1CK3_N$,$M1CK4_N$,$M1CK5_N$,$M1CK6_N$,$M1CK7_N$,$M1CK8_N$,$M1CK9_N$	1	139	0%	5%	9%	12%	10	267	8%	25%	18%	22%
$M2CK_N^{AVG}-Models$	$M2CK1_N$,$M2CK2_N$,$M2CK3_N$,$M2CK4_N$,$M2CK5_N$,$M2CK6_N$,$M2CK7_N$,$M2CK8_N$,$M2CK9_N$	2	232	0%	8%	15%	19%	3	356	0%	11%	25%	29%
$M3CK_N^{AVG}-Models$	$M3CK1_N$,$M3CK2_N$,$M3CK3_N$,$M3CK4_N$,$M3CK5_N$,$M3CK6_N$,$M3CK7_N$,$M3CK8_N$,$M3CK9_N$	13	184	13%	31%	12%	16%	**51**	**636**	69%	89%	45%	51%
$L1CK_N^{AVG}-Models$	$L1CK1_N$,$L1CK2_N$,$L1CK3_N$,$L1CK4_N$,$L1CK5_N$,$L1CK6_N$,$L1CK7_N$,$L1CK8_N$,$L1CK9_N$	0	7	0%	0%	0%	1%	0	9	0%	0%	0%	1%
$L2CK_N^{AVG}-Models$	$L2CK1_N$,$L2CK2_N$,$L2CK3_N$,$L2CK4_N$,$L2CK5_N$,$L2CK6_N$,$L2CK7_N$,$L2CK8_N$,$L2CK9_N$	0	29	0%	0%	1%	3%	0	29	0%	0%	1%	3%
$L3CK_N^{AVG}-Models$	$L3CK1_N$,$L3CK2_N$,$L3CK3_N$,$L3CK4_N$,$L3CK5_N$,$L3CK6_N$,$L3CK7_N$,$L3CK8_N$,$L3CK9_N$	0	31	0%	0%	2%	3%	0	31	0%	0%	2%	3%

Table C.2.6: Call Option Price Scaled by the Exercise Price Comparison (Model Averaging): This table is compartmentalised into XVII parts. Each part presents a performance comparison using daily and monthly statistics amongst the models mentioned in that part. The forecast variable for all the models is the one-trading-day-ahead call option price scaled by the exercise price (CK_{N+1}/K_{N+1}). The models denoted by the $_N$ subscript use lagged input variables for forecasting CK_{N+1}/K_{N+1}. In the parts mentioned below, we compare the out-of-sample performance of the best performing model (based on the total number of days out of 1326 days that a particular model had the lowest RMSE) with the average of parametric models ($ParamCK_N^{AVG} - Models$), the average of single ($M1CK_N^{AVG} - Models$), double ($M2CK_N^{AVG} - Models$) and triple ($M3CK_N^{AVG} - Models$) hidden layer MLP models, and the average of single ($L1CK_N^{AVG} - Models$), double ($L2CK_N^{AVG} - Models$) and triple ($L3CK_N^{AVG} - Models$) hidden layer LSTM models. **In Part I**: The best performing model ($L1CK2_N$) from Table A.2.19 with $ParamCK_N^{AVG} - Models$, $M1CK_N^{AVG} - Models$, $L1CK_N^{AVG} - Models$, **in Part II**: The best performing model ($M1CK3_N$) from Table A.2.20 with $ParamCK_N^{AVG} - Models$, $M1CK_N^{AVG} - Models$, **in Part III**: The best performing model ($L1CK2_N$) from Table A.2.21 with $ParamCK_N^{AVG} - Models$, $L1CK_N^{AVG} - Models$, **in Part IV**: The best performing model ($L2CK2_N$) from Table A.2.22 with $ParamCK_N^{AVG} - Models$, $M2CK_N^{AVG} - Models$, $L2CK_N^{AVG} - Models$, **in Part V**: The best performing model ($M2CK3_N$) from Table A.2.23 with $ParamCK_N^{AVG} - Models$, $M2CK_N^{AVG} - Models$, **in Part VI**: The best performing model ($L2CK2_N$) from Table A.2.24 with $ParamCK_N^{AVG} - Models$, $L2CK_N^{AVG} - Models$, **in Part VII**: The best performing model ($L3CK2_N$) from Table A.2.25 with $ParamCK_N^{AVG} - Models$, $M3CK_N^{AVG} - Models$, $L3CK_N^{AVG} - Models$, **in Part VIII**: The best performing model ($M3CK2_N$) from Table A.2.26 with $ParamCK_N^{AVG} - Models$, $M3CK_N^{AVG} - Models$, **in Part IX**: The best performing model ($L3CK2_N$) from Table A.2.27 with $ParamCK_N^{AVG} - Models$, $L3CK_N^{AVG} - Models$, **in Part X**: The best performing model ($L1CK2_N$) from Table A.2.28 with $ParamCK_N^{AVG} - Models$, $M1CK_N^{AVG} - Models$, $M2CK_N^{AVG} - Models$, $M3CK_N^{AVG} - Models$, $L1CK_N^{AVG} - Models$, $L2CK_N^{AVG} - Models$, $L3CK_N^{AVG} - Models$, **in Part XI**: The best performing model ($M3CK4_N$) from Table A.2.29 with $ParamCK_N^{AVG} - Models$, $M1CK_N^{AVG} - Models$, $M2CK_N^{AVG} - Models$, $M3CK_N^{AVG} - Models$, **in Part XII**: The best performing model ($L2CK2_N$) from Table A.2.30 with $ParamCK_N^{AVG} - Models$, $L1CK_N^{AVG} - Models$, $L2CK_N^{AVG} - Models$, $L3CK_N^{AVG} - Models$, **in Part XIII**: The best performing model ($L2CK2_N$) from Table A.2.31 with $M1CK_N^{AVG} - Models$, $M2CK_N^{AVG} - Models$, $M3CK_N^{AVG} - Models$, $L1CK_N^{AVG} - Models$, $L2CK_N^{AVG} - Models$, $L3CK_N^{AVG} - Models$, **in Part XIV**: The best performing model ($HJDCK_N$) from Table A.2.32 with $ParamCK_N^{AVG} - Models$. The one-trading-day-ahead forecast errors of CK_{N+1}/K_{N+1} are used to compute the Root Mean Square Error (RMSE). Forecasts are made for 1,328 trading days, and there are 64 months covered in the sample using the monthly data. Column I identifies the models. When comparing all models simultaneously (i.e. including the random walk model (δCK_N), column II reports the number of months out of the 64 months that each model has the smallest RMSE, while column III reports the number of days out of the 1,328 days each model has the smallest RMSE. Columns IV (lower bound) and V (upper bound) present the winning percentage out of 64 months for each model, evaluated using the bootstrap sampling technique. The statistical bootstrap performed (with replacement) at a 95% confidence level is computed from the monthly RMSE values of the respective models below. Columns VI (lower bound) and VII (upper bound) present the winning percentage out of 1326 days for each model computed from bootstrapping the daily RMSE values of the respective models at a 95% confidence level. Similarly, when the δCK_N model was excluded in the comparison, column VIII report the number of months out of the 64 months that each model has the smallest RMSE, while column IX reports the number of days out of the 1,328 days each model has the smallest RMSE. Columns X (lower bound) and XI (upper bound) present the winning percentage out of 64 months for each model, evaluated using the bootstrap sampling technique. The statistical bootstrap performed (with replacement) at a 95% confidence level is computed from the monthly RMSE values of the respective models below. Also, columns XII (lower bound) and XIII (upper bound) present the winning percentage out of 1326 days for each model computed from bootstrapping the daily RMSE values of the respective models at a 95% confidence level.

	Including the random walk						**Excluding the random walk**					
(I) Model	**(II) Performance amongst all models (Monthly)**	**(III) Performance amongst all models (Daily)**	**(IV) 2.5% lower bound- (for monthly) (%)**	**(V) 2.5% upper bound- (for monthly) (%)**	**(VI) 2.5% lower bound- (for daily) (%)**	**(VII) 2.5% upper bound- (for daily) (%)**	**(VIII) Performance amongst all models (Monthly)**	**(IX) Performance amongst all models (Daily)**	**(X) 2.5% lower bound- (for monthly) (%)**	**(XI) 2.5% upper bound- (for monthly) (%)**	**(XII) 2.5% lower bound- (for daily) (%)**	**(XIII) 2.5% upper bound- (for daily) (%)**
Part I: $L1CK2_N$ v/s $ParamCK_N^{AVG} - Models$ v/s $M1CK_N^{AVG} - Models$ v/s $L1CK_N^{AVG} - Models$												
δ_{CK}	**59**	**685**	84%	98%	49%	54%	-	-	-	-	-	-
$L1CK2_N$	0	273	0%	0%	18%	23%	0	353	0%	0%	24%	29%
$ParamCK_N^{AVG} - Models$	0	20	0%	0%	1%	2%	0	24	0%	0%	1%	2%
$M1CK_N^{AVG} - Models$	5	339	2%	16%	23%	28%	**64**	**937**	100%	100%	68%	73%
$L1CK_N^{AVG} - Models$	0	11	0%	0%	0%	1%	0	14	0%	0%	1%	2%
Part II: $M1CK3_N$ v/s $ParamCK_N^{AVG} - Models$ v/s $M1CK_N^{AVG} - Models$												
δ_{CK}	**56**	**765**	78%	95%	55%	60%	-	-	-	-	-	-
$M1CK3_N$	5	309	2%	15%	21%	26%	14	538	13%	33%	38%	43%
$ParamCK_N^{AVG} - Models$	0	29	0%	0%	2%	3%	0	37	0%	0%	2%	4%
$M1CK_N^{AVG} - Models$	3	225	0%	11%	15%	19%	**50**	**753**	67%	88%	54%	59%
Part III: $L1CK2_N$ v/s $ParamCK_N^{AVG} - Models$ v/s $L1CK_N^{AVG} - Models$												
δ_{CK}	**64**	**987**	100%	100%	72%	77%	-	-	-	-	-	-
$L1CK2_N$	0	301	0%	0%	21%	25%	5	**912**	2%	14%	66%	71%
$ParamCK_N^{AVG} - Models$	0	28	0%	0%	1%	3%	**58**	345	83%	97%	24%	28%
$L1CK_N^{AVG} - Models$	0	12	0%	0%	0%	1%	1	71	0%	5%	4%	7%
Part IV: $L2CK2_N$ v/s $ParamCK_N^{AVG} - Models$ v/s $M2CK_N^{AVG} - Models$ v/s $L2CK_N^{AVG} - Models$												
δ_{CK}	**57**	**656**	81%	95%	47%	52%	-	-	-	-	-	-
$L2CK2_N$	0	278	0%	0%	19%	23%	0	340	0%	0%	23%	28%
$ParamCK_N^{AVG} - Models$	0	21	0%	0%	1%	2%	0	24	0%	0%	1%	2%
$M2CK_N^{AVG} - Models$	7	345	5%	19%	24%	28%	**64**	**934**	100%	100%	68%	73%
$L2CK_N^{AVG} - Models$	0	28	0%	0%	1%	3%	0	30	0%	0%	1%	3%
Part V: $M2CK3_N$ v/s $ParamCK_N^{AVG} - Models$ v/s $M2CK_N^{AVG} - Models$												
δ_{CK}	**54**	**704**	75%	92%	50%	56%	-	-	-	-	-	-
$M2CK3_N$	7	322	3%	19%	22%	27%	19	560	19%	41%	40%	45%
$ParamCK_N^{AVG} - Models$	0	29	0%	0%	1%	3%	0	35	0%	0%	2%	4%
$M2CK_N^{AVG} - Models$	3	273	0%	9%	18%	23%	**45**	**733**	59%	81%	52%	58%
Part VI: $L2CK2_N$ v/s $ParamCK_N^{AVG} - Models$ v/s $L2CK_N^{AVG} - Models$												
δ_{CK}	**64**	**970**	100%	100%	71%	75%	-	-	-	-	-	-
$L2CK2_N$	0	300	0%	0%	20%	25%	2	**873**	0%	8%	63%	68%
$ParamCK_N^{AVG} - Models$	0	27	0%	0%	1%	3%	**59**	350	86%	98%	24%	29%
$L2CK_N^{AVG} - Models$	0	31	0%	0%	2%	3%	3	105	0%	11%	6%	9%
Part VII: $L3CK2_N$ v/s $ParamCK_N^{AVG} - Models$ v/s $M3CK_N^{AVG} - Models$ v/s $L3CK_N^{AVG} - Models$												
δ_{CK}	**49**	**656**	66%	86%	47%	52%	-	-	-	-	-	-
$L3CK2_N$	0	298	0%	0%	20%	25%	0	344	0%	0%	23%	28%
$ParamCK_N^{AVG} - Models$	0	21	0%	0%	1%	2%	0	24	0%	0%	1%	3%
$M3CK_N^{AVG} - Models$	15	324	14%	34%	22%	27%	**64**	**930**	100%	100%	68%	72%
$L3CK_N^{AVG} - Models$	0	29	0%	0%	1%	3%	0	30	0%	0%	2%	3%
Part VIII: $M3CK2_N$ v/s $ParamCK_N^{AVG} - Models$ v/s $M3CK_N^{AVG} - Models$												
δ_{CK}	**49**	**714**	66%	87%	51%	57%	-	-	-	-	-	-
$M3CK2_N$	4	384	2%	13%	26%	31%	6	507	3%	17%	36%	41%
$ParamCK_N^{AVG} - Models$	0	32	0%	0%	2%	3%	0	36	0%	0%	2%	4%
$M3CK_N^{AVG} - Models$	11	198	8%	27%	13%	17%	**58**	**785**	83%	97%	56%	62%
Part IX: $L3CK2_N$ v/s $ParamCK_N^{AVG} - Models$ v/s $L3CK_N^{AVG} - Models$												
δ_{CK}	**64**	**957**	100%	100%	70%	74%	-	-	-	-	-	-
$L3CK2_N$	0	315	0%	0%	21%	26%	2	**907**	0%	8%	66%	71%
$ParamCK_N^{AVG} - Models$	0	26	0%	0%	1%	3%	**60**	320	88%	98%	22%	26%
$L3CK_N^{AVG} - Models$	0	30	0%	0%	2%	3%	2	101	0%	8%	6%	9%
Part X: $L1CK2_N$ v/s $ParamCK_N^{AVG} - Models$ v/s $M1CK_N^{AVG} - Models$ v/s $M2CK_N^{AVG} - Models$ $M3CK_N^{AVG} - Models$ v/s $L1CK_N^{AVG} - Models$ v/s $L2CK_N^{AVG} - Models$ v/s $L3CK_N^{AVG} - Models$												
δ_{CK}	**48**	**586**	64%	85%	41%	47%	-	-	-	-	-	-
$L1CK2_N$	0	250	0%	0%	17%	21%	0	290	0%	0%	20%	24%
$ParamCK_N^{AVG} - Models$	0	16	0%	0%	1%	2%	0	16	0%	0%	1%	2%
$M1CK_N^{AVG} - Models$	1	115	0%	5%	7%	10%	10	216	8%	25%	14%	18%
$M2CK_N^{AVG} - Models$	2	180	0%	8%	12%	15%	3	272	0%	11%	18%	23%
$M3CK_N^{AVG} - Models$	13	140	11%	30%	9%	12%	**51**	**492**	69%	89%	34%	40%
$L1CK_N^{AVG} - Models$	0	6	0%	0%	0%	1%	0	7	0%	0%	0%	1%
$L2CK_N^{AVG} - Models$	0	16	0%	0%	1%	2%	0	16	0%	0%	1%	2%
$L3CK_N^{AVG} - Models$	0	19	0%	0%	1%	2%	0	19	0%	0%	1%	2%
Part XI: $M3CK4_N$ v/s $ParamCK_N^{AVG} - Models$ v/s $M1CK_N^{AVG} - Models$ v/s $M2CK_N^{AVG} - Models$ v/s $M3CK_N^{AVG} - Models$												
δ_{CK}	**35**	**536**	42%	66%	38%	43%	-	-	-	-	-	-
$M3CK4_N$	16	283	16%	36%	19%	24%	**30**	**539**	34%	59%	38%	43%
$ParamCK_N^{AVG} - Models$	0	32	0%	0%	2%	3%	0	33	0%	0%	2%	3%
$M1CK_N^{AVG} - Models$	1	130	0%	5%	8%	11%	3	183	0%	9%	12%	16%
$M2CK_N^{AVG} - Models$	1	216	0%	5%	14%	18%	2	290	0%	8%	20%	24%
$M3CK_N^{AVG} - Models$	11	131	9%	27%	8%	12%	29	284	34%	56%	19%	24%
Part XII: $L2CK2_N$ v/s $ParamCK_N^{AVG} - Models$ v/s $L1CK_N^{AVG} - Models$ v/s $L2CK_N^{AVG} - Models$ v/s $L3CK_N^{AVG} - Models$												
δ_{CK}	**64**	**957**	100%	100%	70%	74%	-	-	-	-	-	-
$L2CK2_N$	0	297	0%	0%	20%	25%	2	**847**	0%	8%	61%	66%
$ParamCK_N^{AVG} - Models$	0	24	0%	0%	1%	3%	**58**	253	83%	97%	17%	21%
$L1CK_N^{AVG} - Models$	0	7	0%	0%	0%	1%	2	60	0%	8%	3%	6%
$L2CK_N^{AVG} - Models$	0	18	0%	0%	1%	2%	2	58	0%	8%	3%	5%
$L3CK_N^{AVG} - Models$	0	25	0%	0%	1%	3%	0	110	0%	0%	7%	10%
Part XIII: $L2CK2_N$ v/s $M1CK_N^{AVG} - Models$ v/s $M2CK_N^{AVG} - Models$ $M3CK_N^{AVG} - Models$ v/s $L1CK_N^{AVG} - Models$ v/s $L2CK_N^{AVG} - Models$ v/s $L3CK_N^{AVG} - Models$												
δ_{CK}	**48**	**584**	64%	84%	41%	46%	-	-	-	-	-	-
$L2CK2_N$	0	272	0%	0%	18%	23%	0	308	0%	0%	21%	25%
$M1CK_N^{AVG} - Models$	1	110	0%	5%	7%	10%	10	206	8%	25%	14%	17%
$M2CK_N^{AVG} - Models$	2	177	0%	8%	12%	15%	3	270	0%	11%	18%	23%
$M3CK_N^{AVG} - Models$	13	139	11%	30%	9%	12%	**51**	**497**	69%	89%	35%	40%
$L1CK_N^{AVG} - Models$	0	7	0%	0%	0%	1%	0	8	0%	0%	0%	1%
$L2CK_N^{AVG} - Models$	0	16	0%	0%	1%	2%	0	16	0%	0%	1%	2%
$L3CK_N^{AVG} - Models$	0	23	0%	0%	1%	2%	0	23	0%	0%	1%	2%
Part XIV: $HJDCK_N$ v/s $ParamCK_N^{AVG} - Models$												
δ_{CK}	**64**	**1272**	100%	100%	95%	97%	-	-	-	-	-	-
$HJDCK_N$	0	8	0%	0%	0%	1%	6	251	3%	19%	17%	21%
$ParamCK_N^{AVG} - Models$	0	48	0%	0%	3%	5%	**58**	**1077**	81%	97%	79%	83%

C.2.2.2 $CK^{AVG} - Models$: Model averaging pricing performance of models that use one-trading-day input variables to forecast the call option price scaled by the strike price (C_{N+1}/K_{N+1}) for the next trading day

C.2.2.2.1 Comparison amongst all Parametric Models with Triple Hidden Layer ANN Models:

Table C.2.7 shows the relative out-of-sample pricing performance (in $RMSE$) amongst the models that forecast the one-trading-day-ahead average call option price scaled by the strike price(C_{N+1}/K_{N+1}) using one-trading-day-ahead input variables. In column II of Table C.2.7, we list the several models used as an input to obtain the average one-trading-day-ahead forecast of C_{N+1}/K_{N+1}. The performance metric is the $RMSE$ of the one-trading-day-ahead forecast errors of the average C_{N+1}/K_{N+1}, which is computed for each averaging model utilising all of the errors in each day or each month. Amongst all of the models (including the random walk model (δCK_N)), columns III and IV record the number of months and days, respectively, that each model has the lowest $RMSE$. We performed a bootstrap using the daily and monthly RMSEs to be certain of our results. The columns V (lower bound) and VI (upper bound) present the results from the bootstrap performed (with replacement) using monthly RMSEs at a 95% confidence level and show the winning percentage out of 64 months for each model (including the δCK_N model) and similarly, the 95 % confidence intervals computed from bootstrapping of the daily RMSEs signifies the winning percentage out of 1326 days for each model and are reported in columns VII (lower bound), VIII (upper bound). While excluding the δCK_N model amongst the comparison, columns IX and X record the number of months and days that each model has the lowest $RMSE$.e repeat the exercise of performing the bootstrap by excluding the δCK_N model in the comparison, and thus, the columns XI (lower bound), XII (upper bound) presents the results from the bootstrap performed (with replacement) using monthly RMSEs at a 95% confidence level and shows the winning percentage out of 64 months for each model (excluding the δCK_N model) and similarly, the 95 % confidence intervals computed from bootstrapping of the daily RMSEs signifies the winning percentage out of 1326 days for each model and are reported in columns XIII (lower bound), XIV (upper bound). After a model is found to outperform other individual parametric models, MLP and LSTM models in each of the several comparisons below, we look into whether that out-performing model individually can outperform the average call option price of all the parametric models combinedly, MLP models combinedly or LSTM models combinedly, covered in that section.

In the below several comparisons, even though a particular model wins by a higher percentage against other models, we investigated further these models pairwise by performing a pairwise bootstrap comparison, which was computed using the respective pair's daily RMSEs. The results are presented in Table 94 of the Electronic Appendix.

The Diebold-Mariano(DM) (Diebold and Mariano (1995)) test was performed on pairs amongst the Random Walk (δCK_N) model, the average C_{N+1}/K_{N+1} of all parametric models ($ParamCK_{N+1}^{AVG} - Models$), the average C_{N+1}/K_{N+1} of all triple hidden layer MLP models ($M3CK_{N+1}^{AVG} - Models$), and the average C_{N+1}/K_{N+1} of all triple hidden layer LSTM models ($L3CK_{N+1}^{AVG} - Models$) are reported in Table 84 of the Electronic Appendix. In constructing the DM tests, the model pairs are reported in column I and column II, and the DM test statistics for a particular pair are reported in column III. If the null can be rejected, a positive number suggests the rejection may be due to the second model being the better forecast model. In contrast, a negative value suggests the rejection may be due to the first model being the better forecast model. The model pairs highlighted in a red state that their forecasts have statistically insignificant differences in their prediction accuracy. Considering the DM-Test statistics in Table 84 of the Electronic Appendix, all the model pairs lead to the rejection of the null of equal forecasting performance.

The RMSEs for the models under the $CK^{AVG} - Models$ category, which averages the forecasted C_{N+1}/K_{N+1} from models belonging to the $CK - Models$ category(which uses one-trading-day-ahead input variables to forecast the C_{N+1}/K_{N+1} for the next trading day) on a monthly, yearly, and overall basis can be found in the Electronic Appendix, in Tables 54, 64, and 74, respectively.

C.2.2.2.2 Comparison amongst all Parametric Models with Triple Hidden Layer ANN Models:

In this section, we compare the out-of-sample pricing performance of the random walk model (δCK_{N+1}), the parametric models ($ParamCK_{N+1}^{AVG} - Models$), the triple hidden layer MLP models ($M3CK_{N+1}^{AVG} - Models$), and the triple hidden layer LSTM models ($L3CK_{N+1}^{AVG} - Models$), and then $ParamCK_{N+1}^{AVG} - Models$ with the $M3CK_{N+1}^{AVG} - Models$, and finally the $ParamCK_{N+1}^{AVG} - Models$ with the $L3CK_{N+1}^{AVG} - Models$.

Initially, in Part I of Table C.2.7, we compared the $ParamCK_{N+1}^{AVG} - Models$ with the $M3CK_{N+1}^{AVG} - Models$ and the $L3CK_{N+1}^{AVG} - Models$ and found that the $M3CK_{N+1}^{AVG} - Models$ had the lowest $RMSE$ for 1,076 days (having a daily bootstrap winning % of 79% to 83%) out of 1,328, but if the δCK_N model was excluded from the comparison, the $M3CK_{N+1}^{AVG} - Models$ still outperformed for 1,328 days (having a daily bootstrap winning % of 100% to 100%) out of 1,328. Accordingly, we now compare the $M3CK2_{N+1}$ model (i.e. the best-performing model when compared to the models in column XIV of Table A.2.33) to the average call option price scaled by the exercise price of all the parametric models ($ParamCK_{N+1}^{AVG} - Models$), all the triple hidden layer MLP models ($M3CK_{N+1}^{AVG} - Models$) in Part I of Table C.2.8 and found that $M3CK_{N+1}^{AVG} - Models$ had the lowest $RMSE$ for 647 days (having a daily bootstrap winning % of 46% to 51%) out of 1,328, but if the δCK_N model was excluded from this comparison, the $M3CK_{N+1}^{AVG} - Models$ had still outperformed for 840 days (having a daily bootstrap winning % of 61% to 66%) out of 1,328.

Secondly, in Part II of Table C.2.7, we compared the $ParamCK_{N+1}^{AVG} - Models$ with the $M3CK_{N+1}^{AVG} - Models$ and found that the $M3CK_{N+1}^{AVG} - Models$ model had the lowest $RMSE$ for 1,076 days (having a daily bootstrap winning % of 79% to 83%) out of 1,328, and even if the δCK_N model was excluded from the comparison, the $M3CK_{N+1}^{AVG} - Models$ could still outperform for 1,328 days (having a daily bootstrap winning % of 100% to 100%) out of 1,328. Accordingly, we now compare the $M3CK2_{N+1}$ model (i.e. the best-performing model when compared to the models in column XIV of Table A.2.34) with the $ParamCK_{N+1}^{AVG} - Models$, and the $M3CK_{N+1}^{AVG} - Models$ in Part II of Table C.2.8, and found that the $M3CK_{N+1}^{AVG} - Models$ had the lowest $RMSE$ for 647 days (having a daily bootstrap winning % of 46% to 51%) out of 1,328, but if the δCK_N model was excluded from this comparison, the $M3CK_{N+1}^{AVG} - Models$ still outperformed for 840 days (having a daily bootstrap winning % of 61% to 66%) out of 1,328.

Finally, in Part III of Table C.2.7, we compared the $ParamCK_{N+1}^{AVG} - Models$ with the $L3CK_{N+1}^{AVG} - Models$, and found that the δCK_N had the lowest $RMSE$ for 1,121 days (having a daily bootstrap winning % of 82% to 86%) out of 1,328, but if the δCK_N model was excluded from the comparison, the $L3CK_{N+1}^{AVG} - Models$ outperformed for 1,328 days (having a daily bootstrap winning % of 100% to 100%) out of 1,328. Accordingly, we now compare the $L3CK2_{N+1}$ model (i.e. the best-performing model when compared to the models in column XIV of Table A.2.35) with the $ParamCK_{N+1}^{AVG} - Models$, and the $L3CK_{N+1}^{AVG} - Models$ in Part III of Table C.2.8, and found that the δCK_N had the lowest $RMSE$ for 914 days (having a daily bootstrap winning % of 67% to 71%) out of 1,328, but if the δCK_N model was excluded from this comparison, the $L3CK2_{N+1}$ model had still outperformed for 809 days (having a daily bootstrap winning % of 58% to 64%) out of 1,328.

Thus, when the individually out-performing model, the $M3CK2_{N+1}$ model (from Table A.2.33) was compared to the average of all the parametric models, and the averages of all the triple hidden layer ANN models (in Part I of Table C.2.8), we conclude that the average of all triple hidden layer MLP models (i.e. the $M3CK_{N+1}^{AVG} - Models$) could outperform all other models. Similarly, when the individually out-performing model, the $M3CK2_{N+1}$ model (from Table A.2.34) was compared to the average of all the parametric models, and the averages of all the triple hidden layer MLP models (in Part II of Table C.2.8), yet again the average of all triple hidden layer MLP models (i.e. the $M3CK_{N+1}^{AVG} - Models$) could outperform all other models. Lastly, when the individually out-performing model, the $L3CK2_{N+1}$ model (from Table A.2.35) was compared to the average of all the parametric models, and the averages of all the triple hidden layer LSTM models (in Part III of Table C.2.8), we conclude that an individual LSTM model (i.e. the $L3CK2_{N+1}$ model) could outperform all other models.

C.2.2.2.3 Comparison amongst all Parametric models:

We now compare the $HJDCK_{N+1}$ model (i.e. the best-performing model when compared to the models in column XI of Table A.2.36) with the $ParamCK_{N+1}^{AVG} - Models$ in Part IV of Table C.2.8, and found that the δCK_N model had the lowest $RMSE$ for 1,143 days (having a daily bootstrap winning % of 84% to 88%) out of 1,328, but if the δCK_N model was excluded from this comparison, the $ParamCK_{N+1}^{AVG} - Models$ had outperformed for 1,097 days (having a daily bootstrap winning % of 80% to 84%) out of 1,328.

Thus, when the individually out-performing model, the $HJDCK_{N+1}$ model (from Table A.2.36) was compared to the average of all the parametric models (in Part IV of Table C.2.8), we can conclude that the $ParamCK_{N+1}^{AVG} - Models$ model could again outperform other parametric models.

Table C.2.7: Call Option Price Scaled by the Exercise Price Comparison (Model Averaging): This table is compartmentalised into III parts, where each part presents a performance comparison using both daily and monthly statistics amongst the set of models mentioned in that part. The models denoted by the $_{N+1}$ subscript use one-trading-day-ahead input variables for forecasting C_{N+1}/K_{N+1}. In the parts mentioned below, we compare the out-of-sample performance of the following models: **In Part I**: $ParamCK^{AVG}_{N+1} - Models$, $M3CK^{AVG}_{N+1} - Models$, $L3CK^{AVG}_{N+1} - Models$, **in Part II**: $ParamCK^{AVG}_{N+1} - Models$, $M3CK^{AVG}_{N+1} - Models$, **in Part III**: $ParamCK^{AVG}_{N+1} - Models$, $L3CK^{AVG}_{N+1} - Models$. The one-trading-day-ahead forecast errors of C_{N+1}/K_{N+1} are used to compute the Root Mean Square Error (RMSE). Column I identifies the models, and column II lists the models used as input to obtain the average one-trading-day-ahead forecast of C_{N+1}/K_{N+1}. Forecasts are made for 1,328 trading days, and there are 64 months covered in the sample using the monthly data. When comparing all models simultaneously (i.e. including the random walk model (δCK_N), column III reports the number of months out of the 64 months that each model has the smallest RMSE, while column IV reports the number of days out of the 1,328 days each model has the smallest RMSE. Columns V (lower bound) and VI (upper bound) present the winning percentage out of 64 months for each model, evaluated using the bootstrap sampling technique. The statistical bootstrap performed (with replacement) at a 95% confidence level is computed from the monthly RMSE values of the respective models below. Columns VII (lower bound) and VIII (upper bound) present the winning percentage out of 1326 days for each model computed from bootstrapping the daily RMSE values of the respective models at a 95% confidence level. Similarly, when the δCK_N model was excluded in the comparison, column IX report the number of months out of the 64 months that each model has the smallest RMSE, while column X reports the number of days out of the 1,328 days each model has the smallest RMSE. Columns XI (lower bound) and XII (upper bound) present the winning percentage out of 64 months for each model, evaluated using the bootstrap sampling technique. The statistical bootstrap performed (with replacement) at a 95% confidence level is computed from the monthly RMSE values of the respective models below. Also, columns XIII (lower bound) and XIV (upper bound) present the winning percentage out of 1326 days for each model computed from bootstrapping the daily RMSE values of the respective models at a 95% confidence level.

		Including the random walk						**Excluding the random walk**					
(I) Model	**(II) Inputs**	**(III) Performance amongst all models (Monthly)**	**(IV) Performance amongst all models (Daily)**	**(V) 2.5% lower bound- (for monthly) (%)**	**(VI) 2.5% upper bound- (for monthly) (%)**	**(VII) 2.5% lower bound- (for daily) (%)**	**(VIII) 2.5% upper bound- (for daily) (%)**	**(IX) Performance amongst all models (Monthly)**	**(X) Performance amongst all models (Daily)**	**(XI) 2.5% lower bound- (for monthly) (%)**	**(XII) 2.5% upper bound- (for monthly) (%)**	**(XIII) 2.5% lower bound- (for daily) (%)**	**(XIV) 2.5% upper bound- (for daily) (%)**
Part I: $ParamCK^{AVG}_{N+1} - Models$ v/s $M3CK^{AVG}_{N+1} - Models$ v/s $L3CK^{AVG}_{N+1} - Models$													
δCK_N	-	0	252	0%	0%	17%	21%	-	-	-	-	-	-
$ParamCK^{AVG}_{N+1} - Models$	$BSMCK_{N+1}$,HCK_{N+1} ,$HJDCK_{N+1}$,$FMLSCK_{N+1}$	0	0	0%	0%	0%	0%	0	0	0%	0%	0%	0%
$M3CK^{AVG}_{N+1} - Models$	$M3CK1_{N+1}$,$M3CK2_{N+1}$,$M3CK3_{N+1}$,$M3CK4_{N+1}$,$M3CK5_{N+1}$,$M3CK6_{N+1}$,$M3CK7_{N+1}$,$M3CK8_{N+1}$,$M3CK9_{N+1}$	**64**	**1076**	100%	100%	79%	83%	**64**	**1328**	100%	100%	100%	100%
$L3CK^{AVG}_{N+1} - Models$	$L3CK1_{N+1}$,$L3CK2_{N+1}$,$L3CK3_{N+1}$,$L3CK4_{N+1}$,$L3CK5_{N+1}$,$L3CK6_{N+1}$,$L3CK7_{N+1}$,$L3CK8_{N+1}$,$L3CK9_{N+1}$	0	0	0%	0%	0%	0%	0	0	0%	0%	0%	0%
Part II: $ParamCK^{AVG}_{N+1} - Models$ v/s $M3CK^{AVG}_{N+1} - Models$													
δCK_N	-	0	252	0%	0%	17%	21%	-	-	-	-	-	-
$ParamCK^{AVG}_{N+1} - Models$	$BSMCK_{N+1}$,HCK_{N+1} ,$HJDCK_{N+1}$,$FMLSCK_{N+1}$	0	0	0%	0%	0%	0%	0	0	0%	0%	0%	0%
$M3CK^{AVG}_{N+1} - Models$	$M3CK1_{N+1}$,$M3CK2_{N+1}$,$M3CK3_{N+1}$,$M3CK4_{N+1}$,$M3CK5_{N+1}$,$M3CK6_{N+1}$,$M3CK7_{N+1}$,$M3CK8_{N+1}$,$M3CK9_{N+1}$	**64**	**1076**	100%	100%	79%	83%	**64**	**1328**	100%	100%	100%	100%
Part III: $ParamCK^{AVG}_{N+1} - Models$ v/s $L3CK^{AVG}_{N+1} - Models$													
δCK_N	-	**60**	**1121**	88%	98%	82%	86%	-	-	-	-	-	-
$ParamCK^{AVG}_{N+1} - Models$	$BSMCK_{N+1}$,HCK_{N+1} ,$HJDCK_{N+1}$,$FMLSCK_{N+1}$	4	174	2%	13%	11%	15%	0	0	0%	0%	0%	0%
$L3CK^{AVG}_{N+1} - Models$	$L3CK1_{N+1}$,$L3CK2_{N+1}$,$L3CK3_{N+1}$,$L3CK4_{N+1}$,$L3CK5_{N+1}$,$L3CK6_{N+1}$,$L3CK7_{N+1}$,$L3CK8_{N+1}$,$L3CK9_{N+1}$	0	33	0%	0%	2%	3%	**64**	**1328**	100%	100%	100%	100%

Table C.2.8: Call Option Price Scaled by the Exercise Price Comparison (Model Averaging): This table is compartmentalised into IV parts. Each part presents a performance comparison using daily and monthly statistics amongst the models mentioned in that part. The forecast variable for all the models is the one-trading-day-ahead call option price scaled by the exercise price (CK_{N+1}/K_{N+1}). The models denoted by the $_{N+1}$ subscript use one-trading-day-ahead input variables for forecasting CK_{N+1}/K_{N+1}. In the parts mentioned below, we compare the out-of-sample performance of the best performing model (based on the total number of days out of 1326 days that a particular model had the lowest RMSE) with the average of parametric models ($ParamCK^{AVG}_{N+1} - Models$), the average of the triple ($M3CK^{AVG}_{N+1} - Models$) hidden layer MLP models, and the average of the triple ($L3CK^{AVG}_{N+1} - Models$) hidden layer LSTM models. **In Part I**: The best performing model ($M3CK2_{N+1}$) from Table A.2.33 with $ParamCK^{AVG}_{N+1} - Models$, $M3CK^{AVG}_{N+1} - Models$, $L3CK^{AVG}_{N+1} - Models$, **in Part II**: The best performing model ($M3CK2_{N+1}$) from Table A.2.34 with $ParamCK^{AVG}_{N+1} - Models$, $M3CK^{AVG}_{N+1} - Models$, **in Part III**: The best performing model ($L3CK2_{N+1}$) from Table A.2.35 with $ParamCK^{AVG}_{N+1} - Models$, $L3CK^{AVG}_{N+1} - Models$, **in Part IV**: The best performing model ($HJDCK_{N+1}$) from Table A.2.36 with $ParamCK^{AVG}_{N+1} - Models$. The one-trading-day-ahead forecast errors of CK_{N+1}/K_{N+1} are used to compute the Root Mean Square Error (RMSE). Forecasts are made for 1,328 trading days, and there are 64 months covered in the sample using the monthly data. Column I identifies the models. When comparing all models simultaneously (i.e. including the random walk model (δCK_N), column II reports the number of months out of the 64 months that each model has the smallest RMSE, while column III reports the number of days out of the 1,328 days each model has the smallest RMSE. Columns IV (lower bound) and V (upper bound) present the winning percentage out of 64 months for each model, evaluated using the bootstrap sampling technique. The statistical bootstrap performed (with replacement) at a 95% confidence level is computed from the monthly RMSE values of the respective models below. Columns VI (lower bound) and VII (upper bound) present the winning percentage out of 1326 days for each model computed from bootstrapping the daily RMSE values of the respective models at a 95% confidence level. Similarly, when the δCK_N model was excluded in the comparison, column VIII report the number of months out of the 64 months that each model has the smallest RMSE, while column IX reports the number of days out of the 1,328 days each model has the smallest RMSE. Columns X (lower bound) and XI (upper bound) present the winning percentage out of 64 months for each model, evaluated using the bootstrap sampling technique. The statistical bootstrap performed (with replacement) at a 95% confidence level is computed from the monthly RMSE values of the respective models below. Also, columns XII (lower bound) and XIII (upper bound) present the winning percentage out of 1326 days for each model computed from bootstrapping the daily RMSE values of the respective models at a 95% confidence level.

	Including the random walk						**Excluding the random walk**					
(I) Model	**(II) Performance amongst all models (Monthly)**	**(III) Performance amongst all models (Daily)**	**(IV) 2.5% lower bound- (for monthly) (%)**	**(V) 2.5% upper bound- (for monthly) (%)**	**(VI) 2.5% lower bound- (for daily) (%)**	**(VII) 2.5% upper bound- (for daily) (%)**	**(VIII) Performance amongst all models (Monthly)**	**(IX) Performance amongst all models (Daily)**	**(X) 2.5% lower bound- (for monthly) (%)**	**(XI) 2.5% upper bound- (for monthly) (%)**	**(XII) 2.5% lower bound- (for daily) (%)**	**(XIII) 2.5% upper bound- (for daily) (%)**
Part I: $M3CK2_{N+1}$ v/s $ParamCK^{AVG}_{N+1} - Models$ v/s $M3CK^{AVG}_{N+1} - Models$ v/s $L3CK^{AVG}_{N+1} - Models$												
δ_{CK}	0	238	0%	0%	16%	20%	-	-	-	-	-	-
$M3CK2_{N+1}$	14	443	13%	31%	31%	36%	14	488	13%	31%	34%	39%
$ParamCK^{AVG}_{N+1} - Models$	0	0	0%	0%	0%	0%	0	0	0%	0%	0%	0%
$M3CK^{AVG}_{N+1} - Models$	**50**	**647**	69%	88%	46%	51%	**50**	**840**	69%	88%	61%	66%
$L3CK^{AVG}_{N+1} - Models$	0	0	0%	0%	0%	0%	0	0	0%	0%	0%	0%
Part II: $M3CK2_{N+1}$ v/s $ParamCK^{AVG}_{N+1} - Models$ v/s $M3CK^{AVG}_{N+1} - Models$												
δ_{CK}	0	238	0%	0%	16%	20%	-	-	-	-	-	-
$M3CK2_{N+1}$	14	443	13%	33%	31%	36%	14	488	13%	33%	34%	39%
$ParamCK^{AVG}_{N+1} - Models$	0	0	0%	0%	0%	0%	0	0	0%	0%	0%	0%
$M3CK^{AVG}_{N+1} - Models$	**50**	**647**	67%	88%	46%	51%	**50**	**840**	67%	88%	61%	66%
Part III: $L3CK2_{N+1}$ v/s $ParamCK^{AVG}_{N+1} - Models$ v/s $L3CK^{AVG}_{N+1} - Models$												
δ_{CK}	**60**	**914**	88%	98%	67%	71%	-	-	-	-	-	-
$L3CK2_{N+1}$	0	237	0%	0%	16%	20%	1	**809**	0%	6%	58%	64%
$ParamCK^{AVG}_{N+1} - Models$	4	150	2%	13%	10%	13%	**59**	434	84%	97%	30%	35%
$L3CK^{AVG}_{N+1} - Models$	0	27	0%	0%	1%	3%	4	85	2%	13%	5%	8%
Part IV: $HJDCK_{N+1}$ v/s $ParamCK^{AVG}_{N+1} - Models$ v/s $L3CK^{AVG}_{N+1} - Models$												
δ_{CK}	**60**	**1143**	86%	98%	84%	88%	-	-	-	-	-	-
$HJDCK_{N+1}$	0	0	0%	0%	0%	0%	9	231	6%	23%	16%	20%
$ParamCK^{AVG}_{N+1} - Models$	4	185	2%	14%	12%	16%	**55**	**1097**	77%	94%	80%	84%

C.2.3 Results - Model Averaging for Hedging

C.2.3.1 $H^{AVG} - Models$: Model averaging hedging performance of models that use lagged input variables to forecast the delta (Δ_{N+1}) for the next trading day:

Table C.2.9 shows the relative out-of-sample hedging performance (in $RMSE$) amongst the models that forecast the one-trading-day-ahead average empirical delta Δ_{N+1} using lagged input variables. In column II of table C.2.9, we list the several models used as input to obtain the average one-trading-day-ahead forecast of Δ_{N+1}. The performance metric is the $RMSE$ of the one-trading-day-ahead forecast errors of the average Δ_{N+1}, which is computed for each averaging model utilising all of the errors in each day or each month. Amongst all of the models, columns III and IV record the number of months and days, respectively, that each model has the lowest $RMSE$. We performed a bootstrap using the daily and monthly RMSEs to be certain of our results. Columns V (lower bound) and VI (upper bound) present the results from the bootstrap performed (with replacement) using monthly RMSEs at a 95% confidence level and show the winning percentage out of 64 months for each model, and similarly, the 95 % confidence intervals computed from bootstrapping of the daily RMSEs signifies the winning percentage out of 1326 days for each model and are reported in columns VII (lower bound), VIII (upper bound). After a model is found to outperform other individual parametric models, MLP and LSTM models in each of the several comparisons below, we look into whether that out-performing model individually can outperform the average Δ_{N+1} of all the parametric models combinedly, MLP models combinedly or LSTM models combinedly covered in that section.

In the below several comparisons, even though a particular model wins by a higher percentage against other models, we investigated further these models pairwise by performing a pairwise bootstrap comparison, which was computed using the respective pair's daily RMSEs. The results are presented in Table 95 of the Electronic Appendix.

The Diebold-Mariano statistics were also performed on pairs amongst the average Δ_{N+1} of all parametric models ($ParamH_N^{AVG} - Models$), the average Δ_{N+1} of all triple hidden layer MLP models ($M3H_N^{AVG} - Models$), and the average Δ_{N+1} of all triple hidden layer LSTM models ($L3H_N^{AVG} - Models$) are reported in Table 85 of the Electronic Appendix. In constructing the DM tests, the model pairs are reported in column I and column II, and the DM test statistics for a particular pair are reported in column III. If the null can be rejected, a positive number suggests the rejection may be due to the second model being the better forecast model. In contrast, a negative value suggests the rejection may be due to the first model being the better forecast model. The model pairs highlighted in a red state that their forecasts have statistically insignificant differences in their prediction accuracy. Considering the DM-Test statistics in Table 85 of the Electronic Appendix, all the model pairs lead to the rejection of the null of equal forecasting performance.

The RMSEs for the models under the $H^{AVG} - Models$ category, which averages the forecasted Δ_{N+1} from models belonging to the $H - Models$ category(which uses lagged input variables to forecast the Δ_{N+1} for the next trading day) on a monthly, yearly, and overall basis can be found in the Electronic Appendix, in Tables 55, 65, and 75, respectively.

C.2.3.1.1 Comparison amongst all Parametric Models with Triple Hidden Layer ANN Models:

In this section, we compare the out-of-sample hedging performance of the parametric models ($ParamH_N^{AVG} - Models$), the triple hidden layer MLP models ($M3H_N^{AVG} - Models$), and the triple hidden layer LSTM models ($L3H_N^{AVG} - Models$), and then $ParamH_N^{AVG} - Models$ with the $M3H_N^{AVG} - Models$, and finally the $ParamH_N^{AVG} - Models$ with the $L3H_N^{AVG} - Models$.

Initially, in Part I of Table C.2.9, we compared the $ParamH_N^{AVG} - Models$ with the $M3H_N^{AVG} - Models$ and the $L3H_N^{AVG} - Models$ and found that the $ParamH_N^{AVG} - Models$ had the lowest $RMSE$ for 593 days (having a daily bootstrap winning % of 42% to 47%) out of 1,326, which was closely followed by the $M3H_N^{AVG} - Models$, which had similar out-performance for 519 days (having a daily bootstrap winning % of 37% to 42%). Accordingly, we now compare the $BSMH_N$ model (i.e. the best-performing model when compared to the models in column VIII of Table B.2.1) with the $ParamH_N^{AVG} - Models$, $M3H_N^{AVG} - Models$, and the $L3H_N^{AVG} - Models$ in Part I of Table C.2.10, and found that $M3H_N^{AVG} - Models$ had the lowest $RMSE$ for 450 days (having a daily bootstrap winning % of 31% to 37%) out of 1,326.

Secondly, in Part II of Table C.2.9, we compared the $ParamH_N^{AVG} - Models$ with the $M3H_N^{AVG} - Models$ and found that the $M3H_N^{AVG} - Models$ had the lowest $RMSE$ for 675 days (having a daily bootstrap winning % of 48% to 54%) out of 1,326, which was closely followed by the $ParamH_N^{AVG} - Models$, which had similar out-performance for 652 days (having a daily bootstrap winning % of 46% to 52%). Accordingly, we now compare the $BSMH_N$ model (i.e. the best-performing model when compared to the models in column VIII of Table B.2.2) with the $ParamH_N^{AVG} - Models$, and the $M3H_N^{AVG} - Models$ in Part II of Table C.2.10, and found that the $M3H_N^{AVG} - Models$ had the lowest $RMSE$ for 589 days (having a daily bootstrap winning % of 42% to 47%) out of 1,326.

Finally, in Part III of Table C.2.9, we compared the $ParamH_N^{AVG} - Models$ with the $L3H_N^{AVG} - Models$, and found that the $ParamH_N^{AVG} - Models$ had the lowest $RMSE$ for 907 days (having a daily bootstrap winning % of 66% to 71%) out of 1,326. Accordingly, we now compare the $BSMH_N$ model (i.e. the best-performing model when compared to the models in column VIII of Table B.2.3) with the $ParamH_N^{AVG} - Models$, and the $L3H_N^{AVG} - Models$ in Part III of Table C.2.10, and found that the $BSMH_N$ model had the lowest $RMSE$ for 565 days (having a daily bootstrap winning % of 40% to 45%) out of 1,326.

Thus, when the individually out-performing model, the $BSMH_N$ model (from Table B.2.1) was compared to the average of all the parametric models, and the averages of all the triple hidden layer ANN models (in Part I of Table C.2.10), we conclude that the average of all triple hidden layer MLP models (i.e. the $M3H_N^{AVG} - Models$) could outperform all other models. Similarly, when the individually out-performing model, the $BSMH_N$ model (from Table B.2.2) was compared to the average of all the parametric models, and the averages of all the triple hidden layer MLP models (in Part II of Table C.2.10), yet again the average of all triple hidden layer MLP models (i.e. the $M3H_N^{AVG} - Models$) could outperform all other models. Lastly, when the individually out-performing model, the $BSMH_N$ model (from Table B.2.3) was compared to the average of all the parametric models, and the averages of all the triple hidden layer LSTM models (in Part III of Table C.2.10), we conclude that $BSMH_N$ model could outperform all other models.

C.2.3.1.2 Comparison amongst all Parametric models:

We now compare the $BSMH_N$ model (i.e. the best-performing model when compared to the models in column V of Table B.2.4) $ParamH_N^{AVG}-Models$ in Part IV of Table C.2.10, and found that the $BSMH_N$ model still had the lowest $RMSE$ for 892 days (having a daily bootstrap winning % of 64% to 70%) out of 1,326.

Thus, when the best individually out-performing model, the $BSMH_N$ model (from Table B.2.4) was compared to the average of all the parametric models (in Part IV of Table C.2.10), we can conclude that the $BSMH_N$ model could outperform the average of all the parametric models.

Table C.2.9: Model Averaging for Delta Comparison (amongst $ParamH_N^{AVG}-Models$, $M3H_N^{AVG}-Models$, and $L3H_N^{AVG}-Models$): This table is compartmentalised into III parts, where each part presents a performance comparison using both daily and monthly statistics amongst the set of models mentioned in that part. The forecast variable for all the models is the one-trading-day-ahead delta. The $_N$ subscript denotes models that take an average of the delta from models that forecast the delta using lagged input variables. In the parts mentioned below, we compare the out-of-sample performance of the following models: **In Part I**: $ParamH_N^{AVG}-Models$, MLP $M3H_N^{AVG}-Models$, and LSTM $L3H_N^{AVG}-Models$, **in Part II**: $ParamH_N^{AVG}-Models$, and MLP $M3H_N^{AVG}-Models$, **in Part III**: $ParamH_N^{AVG}-Models$, and LSTM $L3H_N^{AVG}-Models$. The one-trading-day-ahead forecast errors of the delta are used to compute the Root Mean Square Error (RMSE). Column I identifies the models, and column II lists the models used as input to obtain the average one-trading-day-ahead forecast of the delta. Forecasts are made for 1,326 trading days, and there are 64 months covered in the sample using the monthly data. When comparing all models simultaneously, column III reports the number of months out of the 64 months that each model has the smallest RMSE, while column IV reports the number of days out of the 1,326 days each model has the smallest RMSE. Columns V (lower bound) and VI (upper bound) present the winning percentage out of 64 months for each model, evaluated using the bootstrap sampling technique. The statistical bootstrap performed (with replacement) at a 95% confidence level is computed from the monthly RMSE values of the respective models below. Columns VII (lower bound) and VIII (upper bound) present the winning percentage out of 1326 days for each model computed from bootstrapping the daily RMSE values of the respective models at a 95% confidence level.

(I) Model	**(II) Inputs**	**(III) Performance amongst all models (Monthly)**	**(IV) Performance amongst all models (Daily)**	**(V) 2.5% lower bound- (for monthly) (%)**	**(VI) 2.5% upper bound- (for monthly) (%)**	**(VII) 2.5% lower bound- (for daily) (%)**	**(VIII) 2.5% upper bound- (for daily) (%)**
	Part I: $ParamH_N^{AVG}-Models$ v/s $M3H_N^{AVG}-Models$ v/s $L3H_N^{AVG}-Models$						
$ParamH_N^{AVG}-Models$	$BSMH_N$, HH_N , $HJDH_N$, $FMLSH_N$	**37**	**593**	45%	70%	42%	47%
$M3H_N^{AVG}-Models$	$M3H1_N$, $M3H2_N$, $M3H3_N$, $M3H4_N$, $M3H5_N$, $M3H6_N$, $M3H7_N$	25	519	28%	50%	37%	42%
$L3H_N^{AVG}-Models$	$L3H1_N$, $L3H2_N$, $L3H3_N$, $L3H4_N$, $L3H5_N$, $L3H6_N$, $L3H7_N$	2	215	0%	8%	14%	18%
	Part II: $ParamH_N^{AVG}-Models$ v/s $M3H_N^{AVG}-Models$						
$ParamH_N^{AVG}-Models$	$BSMH_N$, HH_N , $HJDH_N$, $FMLSH_N$	**37**	652	45%	69%	46%	52%
$M3H_N^{AVG}-Models$	$M3H1_N$, $M3H2_N$, $M3H3_N$, $M3H4_N$, $M3H5_N$, $M3H6_N$, $M3H7_N$	27	**675**	31%	55%	48%	54%
	Part III: $ParamH_N^{AVG}-Models$ v/s $L3H_N^{AVG}-Models$						
$ParamH_N^{AVG}-Models$	$BSMH_N$, HH_N , $HJDH_N$, $FMLSH_N$	**59**	**907**	84%	98%	66%	71%
$L3H_N^{AVG}-Models$	$L3H1_N$, $L3H2_N$, $L3H3_N$, $L3H4_N$, $L3H5_N$, $L3H6_N$, $L3H7_N$	5	420	2%	16%	29%	34%

Table C.2.10: Model Averaging for Delta Comparison: This table is compartmentalised into IV parts. Each part presents a performance comparison using daily and monthly statistics amongst the models mentioned in that part. The forecast variable for all the models is the one-trading-day-ahead delta. The $_N$ subscript denotes models that take an average of the delta from models that forecast the delta using lagged input variables. In the parts mentioned below, we compare the out-of-sample performance of the best performing model (based on the total number of days out of 1326 days that a particular model had the lowest RMSE) with the average of parametric models ($ParamH_N^{AVG} - Models$), the average of the triple ($M3H_N^{AVG} - Models$) hidden layer MLP models, and the average of the triple ($L3H_N^{AVG} - Models$) hidden layer LSTM models. **In Part I**: The best performing model ($BSMH_N$) from Table B.2.5 with $ParamH_N^{AVG} - Models$, $M3H_N^{AVG} - Models$, $L3H_N^{AVG} - Models$, **in Part II**: The best performing model ($BSMH_N$) from Table B.2.6 with $ParamH_N^{AVG} - Models$, $M3H_N^{AVG} - Models$, **in Part III**: The best performing model ($BSMH_N$) from Table B.2.7 with $ParamH_N^{AVG} - Models$, $L3H_N^{AVG} - Models$, **in Part IV**: The best performing model ($BSMH_N$) from Table B.2.8 with $ParamH_N^{AVG} - Models$. The one-trading-day-ahead forecast errors of the delta are used to compute the Root Mean Square Error (RMSE). Forecasts are made for 1,326 trading days, and there are 64 months covered in the sample using the monthly data. Column I identifies the models. When comparing all models simultaneously, column II reports the number of months out of the 64 months that each model has the smallest RMSE, while column III reports the number of days out of the 1,326 days each model has the smallest RMSE. Columns IV (lower bound) and V (upper bound) present the winning percentage out of 64 months for each model, evaluated using the bootstrap sampling technique. The statistical bootstrap performed (with replacement) at a 95% confidence level is computed from the monthly RMSE values of the respective models below. Columns VI (lower bound) and VII (upper bound) present the winning percentage out of 1326 days for each model computed from bootstrapping the daily RMSE values of the respective models at a 95% confidence level.

(I) Model	**(II) Performance amongst all models (Monthly)**	**(III) Performance amongst all models (Daily)**	**(IV) 2.5% lower bound-(for monthly) (%)**	**(V) 2.5% upper bound-(for monthly) (%)**	**(VI) 2.5% lower bound-(for daily) (%)**	**(VII) 2.5% upper bound-(for daily) (%)**
Part I: $BSMH_N$ v/s $ParamH_N^{AVG} - Models$ v/s $M3H_N^{AVG} - Models$ v/s $L3H_N^{AVG} - Models$						
$BSMH_N$	**39**	311	49%	73%	21%	26%
$ParamH_N^{AVG} - Models$	5	370	3%	14%	25%	30%
$M3H_N^{AVG} - Models$	18	**450**	17%	39%	31%	37%
$L3H_N^{AVG} - Models$	2	195	0%	8%	13%	17%
Part II: $BSMH_N$ v/s $ParamH_N^{AVG} - Models$ v/s $M3H_N^{AVG} - Models$						
$BSMH_N$	**40**	353	50%	75%	24%	29%
$ParamH_N^{AVG} - Models$	5	384	2%	16%	27%	31%
$M3H_N^{AVG} - Models$	19	**589**	19%	41%	42%	47%
Part III: $BSMH_N$ v/s $ParamH_N^{AVG} - Models$ v/s $L3H_N^{AVG} - Models$						
$BSMH_N$	**55**	**565**	77%	94%	40%	45%
$ParamH_N^{AVG} - Models$	6	402	3%	17%	28%	33%
$L3H_N^{AVG} - Models$	3	359	0%	11%	25%	29%
Part IV: $BSMH_N$ v/s $ParamH_N^{AVG} - Models$						
$BSMH_N$	**58**	**892**	83%	97%	64%	70%
$ParamH_N^{AVG} - Models$	6	434	3%	17%	30%	36%

C.2.3.2 $H^{AVG} - Models$: Model averaging hedging performance of models that use one-trading-day input variables to forecast the delta (Δ_{N+1}) for the next trading day:

Table C.2.11 shows the relative out-of-sample performance (in $RMSE$) amongst the models that forecast the one-trading-day-ahead average empirical delta Δ_{N+1} using one-trading-day-ahead input variables. In column II of table C.2.11, we list the several models used as an input to obtain the average one-trading-day-ahead forecast of Δ_{N+1}. The performance metric is the $RMSE$ of the one-trading-day-ahead forecast errors of the average Δ_{N+1}, which is computed for each averaging model utilising all of the errors in each day or each month. Amongst all models, columns III and IV record the number of months and days, respectively, that each model has the lowest $RMSE$. We performed a bootstrap using the daily and monthly RMSEs to be certain of our results. Columns V (lower bound) and VI (upper bound) present the results from the bootstrap performed (with replacement) using monthly RMSEs at a 95% confidence level and show the winning percentage out of 64 months for each model, and similarly, the 95 % confidence intervals computed from bootstrapping of the daily RMSEs signifies the winning percentage out of 1326 days for each model and are reported in columns VII (lower bound), VIII (upper bound). After a model is found to outperform other individual parametric models, MLP and LSTM models in each of the several comparisons below, we look into whether that out-performing model individually can outperform the average Δ_{N+1} of all the parametric models combinedly, MLP models combinedly or LSTM models combinedly covered in that section.

In the below several comparisons, even though a particular model wins by a higher percentage against other models, we investigated further these models pairwise by performing a pairwise bootstrap comparison, which was computed using the respective pair's daily RMSEs. The results are presented in Table 96 of the Electronic Appendix.

The Diebold-Mariano statistics were also performed on pairs amongst the average Δ_{N+1} of all parametric models ($ParamH^{AVG}_{N+1} - Models$), the average Δ_{N+1} of all triple hidden layer MLP models ($M3H^{AVG}_{N+1} - Models$), and the average Δ_{N+1} of all triple hidden layer LSTM models ($L3H^{AVG}_{N+1} - Models$) are reported in Table 86 of the Electronic Appendix. In constructing the DM tests, the model pairs are reported in column I and column II, and the DM test statistics for a particular pair are reported in column III. If the null can be rejected, a positive number suggests the rejection may be due to the second model being the better forecast model. In contrast, a negative value suggests the rejection may be due to the first model being the better forecast model. The model pairs highlighted in a red state that their forecasts have statistically insignificant differences in their prediction accuracy. Considering the DM-Test statistics in Table 86 of the Electronic Appendix, all the model pairs lead to the rejection of the null of equal forecasting performance.

The RMSEs for the models under the $H^{AVG} - Models$ category, which averages the forecasted Δ_{N+1} from models belonging to the $H - Models$ category(which uses one-trading-day-ahead input variables to forecast the Δ_{N+1} for the next trading day) on a monthly, yearly, and overall basis can be found in the Electronic Appendix, in Tables 56, 66, and 76, respectively.

C.2.3.2.1 Comparison amongst all Parametric Models with Triple Hidden Layer ANN Models:

In this section, we compare the out-of-sample hedging performance of the parametric models ($ParamH_{N+1}^{AVG} - Models$), the triple hidden layer MLP models ($M3H_{N+1}^{AVG} - Models$), and the triple hidden layer LSTM models ($L3H_{N+1}^{AVG} - Models$), and then $ParamH_{N+1}^{AVG} - Models$ with the $M3H_{N+1}^{AVG} - Models$, and finally the $ParamH_{N+1}^{AVG} - Models$ with the $L3H_{N+1}^{AVG} - Models$.

Initially in Part I of Table C.2.11, we compared the $ParamH_{N+1}^{AVG} - Models$ with the $M3H_{N+1}^{AVG} - Models$ and the $L3H_{N+1}^{AVG} - Models$, and find that the $ParamH_{N+1}^{AVG} - Models$ had the lowest $RMSE$ for 653 days (having a daily bootstrap winning % of 47% to 52%) out of 1,326. Accordingly, we now compare the $BSMH_{N+1}$ model (i.e. the best-performing model when compared to the models in column VIII of Table B.2.5) with the $ParamH_{N+1}^{AVG} - Models$, $M3H_{N+1}^{AVG} - Models$, and the $L3H_{N+1}^{AVG} - Models$ in Part I of Table C.2.12, and find that $BSMH_{N+1}$ model had the lowest $RMSE$ for 391 days (having a daily bootstrap winning % of 27% to 32%) out of 1,326. Though the $BSMH_{N+1}$ model outperformed, the parametric model, $ParamH_{N+1}^{AVG} - Models$ (353 days), and the MLP model, $M3H_{N+1}^{AVG} - Models$ (373 days) have shown similar out-performance and have a collective daily bootstrap winning percentage from 24% (lower bound for the $ParamH_{N+1}^{AVG} - Models$) to 31% (upper bound for the $M3H_{N+1}^{AVG} - Models$).

Secondly, in Part II of Table C.2.11, we compared the $ParamH_{N+1}^{AVG} - Models$ with the $M3H_{N+1}^{AVG} - Models$, and find that the $ParamH_{N+1}^{AVG} - Models$ had the lowest $RMSE$ for 754 days (having a daily bootstrap winning % of 54% to 59%) out of 1,326. Accordingly, we now compare the $BSMH_{N+1}$ model (i.e. the best-performing model when compared to the models in column VIII of Table B.2.6) with the $ParamH_{N+1}^{AVG} - Models$, and the $M3H_{N+1}^{AVG} - Models$ in Part II of Table C.2.12, and find that the $M3H_{N+1}^{AVG} - Models$ model had the lowest $RMSE$ for 487 days (having a daily bootstrap winning % of 34% to 39%) out of 1,326.

Finally, in Part III of Table C.2.11, we compared the $ParamH_{N+1}^{AVG} - Models$ with the $L3H_{N+1}^{AVG} - Models$, and find that the $ParamH_{N+1}^{AVG} - Models$ had the lowest $RMSE$ for 907 days (having a daily bootstrap winning % of 66% to 71%) out of 1,326. Accordingly, we now compare the $BSMH_{N+1}$ model (i.e. the best-performing model when compared to the models in column VIII of Table B.2.7) with the $ParamH_{N+1}^{AVG} - Models$, and the $L3H_{N+1}^{AVG} - Models$ in Part III of Table C.2.12, and find that the $BSMH_{N+1}$ model had the lowest $RMSE$ for 595 days (having a daily bootstrap winning % of 42% to 48%) out of 1,326.

Thus, when the individually out-performing model, the $BSMH_{N+1}$ model (from Table B.2.5) was compared to the average of all the parametric models, and the averages of all the triple hidden layer ANN models (in Part I of Table C.2.12), we conclude that $BSMH_{N+1}$ model could outperform all other models. Similarly, when the individually out-performing model, the $BSMH_{N+1}$ model (from Table B.2.6) was compared to the average of all the parametric models, and the averages of all the triple hidden layer MLP models (in Part II of Table C.2.12), the average of all triple hidden layer MLP models (i.e. the $M3H_{N+1}^{AVG} - Models$) could outperform all other models. Lastly, when the individually out-performing model, the $BSMH_{N+1}$ model (from Table B.2.7) was compared to the average of all the parametric models, and the averages of all the triple hidden layer LSTM models (in Part III of Table C.2.12), yet again the $BSMH_{N+1}$ model could outperform all other models.

C.2.3.2.2 Comparison amongst all Parametric models:

We now compare the $BSMH_{N+1}$ model (i.e. the best-performing model when compared to the models in column V of Table B.2.8) with the $ParamH_{N+1}^{AVG} - Models$ in Part IV of Table C.2.12, and find that the $BSMH_{N+1}$ model still had the lowest $RMSE$ for 912 days (having a daily bootstrap winning % of 66% to 71%) out of 1,326.

Thus, when the best individually out-performing model, the $BSMH_{N+1}$ model (from Table B.2.8) was compared to the average of all the parametric models (in Part IV of Table C.2.12), we can conclude that the $BSMH_{N+1}$ model could outperform the average of all the parametric models.

Table C.2.11: Model Averaging for Delta Comparison (amongst $ParamH^{AVG}_{N+1} - Models$, $M3H^{AVG}_{N+1} - Models$, and $L3H^{AVG}_{N+1} - Models$): This table is compartmentalised into III parts, where each part presents a performance comparison using both daily and monthly statistics amongst the set of models mentioned in that part. The forecast variable for all the models is the one-trading-day-ahead delta. The $_{N+1}$ subscript denotes models that take an average of the delta from models that forecast the delta using one-trading-day-ahead input variables. In the parts mentioned below, we compare the out-of-sample performance of the following models: **In Part I**: $ParamH^{AVG}_{N+1} - Models$, MLP $M3H^{AVG}_{N+1} - Models$, and LSTM $L3H^{AVG}_{N+1} - Models$, **in Part II**: $ParamH^{AVG}_{N+1} - Models$, and MLP $M3H^{AVG}_{N+1} - Models$, **in Part III**: $ParamH^{AVG}_{N+1} - Models$, and LSTM $L3H^{AVG}_{N+1} - Models$. The one-trading-day-ahead forecast errors of the delta are used to compute the Root Mean Square Error (RMSE). Column I identifies the models, and column II lists the models used as input to obtain the average one-trading-day-ahead forecast of the delta. Forecasts are made for 1,326 trading days, and there are 64 months covered in the sample using the monthly data. When comparing all models simultaneously, column III reports the number of months out of the 64 months that each model has the smallest RMSE, while column IV reports the number of days out of the 1,326 days each model has the smallest RMSE. Columns V (lower bound) and VI (upper bound) present the winning percentage out of 64 months for each model, evaluated using the bootstrap sampling technique. The statistical bootstrap performed (with replacement) at a 95% confidence level is computed from the monthly RMSE values of the respective models below. Columns VII (lower bound) and VIII (upper bound) present the winning percentage out of 1326 days for each model computed from bootstrapping the daily RMSE values of the respective models at a 95% confidence level.

(I) Model	**(II)** Inputs	**(III)** Performance amongst all models (Monthly)	**(IV)** Performance amongst all models (Daily)	**(V)** 2.5% lower bound- (for monthly) (%)	**(VI)** 2.5% upper bound- (for monthly) (%)	**(VII)** 2.5% lower bound- (for daily) (%)	**(VIII)** 2.5% upper bound- (for daily) (%)
Part I: $ParamH^{AVG}_{N+1} - Models$ v/s $M3H^{AVG}_{N+1} - Models$ v/s $L3H^{AVG}_{N+1} - Models$							
$ParamH^{AVG}_{N+1} - Models$	$BSMH_{N+1}$, HH_{N+1} , $HJDH_{N+1}$, $FMLSH_{N+1}$	**46**	**653**	61%	81%	47%	52%
$M3H^{AVG}_{N+1} - Models$	$M3H1_{N+1}$, $M3H2_{N+1}$, $M3H3_{N+1}$, $M3H4_{N+1}$, $M3H5_{N+1}$, $M3H6_{N+1}$, $M3H7_{N+1}$	13	442	11%	30%	31%	36%
$L3H^{AVG}_{N+1} - Models$	$L3H1_{N+1}$, $L3H2_{N+1}$, $L3H3_{N+1}$, $L3H4_{N+1}$, $L3H5_{N+1}$, $L3H6_{N+1}$, $L3H7_{N+1}$	5	232	2%	14%	15%	20%
Part II: $ParamH^{AVG}_{N+1} - Models$ v/s $M3H^{AVG}_{N+1} - Models$							
$ParamH^{AVG}_{N+1} - Models$	$BSMH_{N+1}$, HH_{N+1} , $HJDH_{N+1}$, $FMLSH_{N+1}$	**51**	**754**	70%	89%	54%	59%
$M3H^{AVG}_{N+1} - Models$	$M3H1_{N+1}$, $M3H2_{N+1}$, $M3H3_{N+1}$, $M3H4_{N+1}$, $M3H5_{N+1}$, $M3H6_{N+1}$, $M3H7_{N+1}$	13	573	11%	30%	41%	46%
Part III: $ParamH^{AVG}_{N+1} - Models$ v/s $L3H^{AVG}_{N+1} - Models$							
$ParamH^{AVG}_{N+1} - Models$	$BSMH_{N+1}$, HH_{N+1} , $HJDH_{N+1}$, $FMLSH_{N+1}$	**58**	**907**	83%	97%	66%	71%
$L3H^{AVG}_{N+1} - Models$	$L3H1_{N+1}$, $L3H2_{N+1}$, $L3H3_{N+1}$, $L3H4_{N+1}$, $L3H5_{N+1}$, $L3H6_{N+1}$, $L3H7_{N+1}$	6	420	3%	17%	29%	34%

Table C.2.12: Model Averaging for Delta Comparison: This table is compartmentalised into IV parts. Each part presents a performance comparison using daily and monthly statistics amongst the models mentioned in that part. The forecast variable for all the models is the one-trading-day-ahead delta. The $_{N+1}$ subscript denotes models that take an average of the delta from models that forecast the delta using one-trading-day-ahead input variables. In the parts mentioned below, we compare the out-of-sample performance of the best performing model (based on the total number of days out of 1326 days that a particular model had the lowest RMSE) with the average of parametric models ($ParamH_{N+1}^{AVG} - Models$), the average of the triple ($M3H_{N+1}^{AVG} - Models$) hidden layer MLP models, and the average of the triple ($L3H_{N+1}^{AVG} - Models$) hidden layer LSTM models. **In Part I**: The best performing model ($BSMH_{N+1}$) from Table B.2.5 with $ParamH_{N+1}^{AVG} - Models$, $M3H_{N+1}^{AVG} - Models$, $L3H_{N+1}^{AVG} - Models$, **in Part II**: The best performing model ($BSMH_{N+1}$) from Table B.2.6 with $ParamH_{N+1}^{AVG} - Models$, $M3H_{N+1}^{AVG} - Models$, **in Part III**: The best performing model ($BSMH_{N+1}$) from Table B.2.7 with $ParamH_{N+1}^{AVG} - Models$, $L3H_{N+1}^{AVG} - Models$, **in Part IV**: The best performing model ($BSMH_{N+1}$) from Table B.2.8 with $ParamH_{N+1}^{AVG} - Models$. The one-trading-day-ahead forecast errors of the delta are used to compute the Root Mean Square Error (RMSE). Forecasts are made for 1,326 trading days, and there are 64 months covered in the sample using the monthly data. Column I identifies the models. When comparing all models simultaneously, column II reports the number of months out of the 64 months that each model has the smallest RMSE, while column III reports the number of days out of the 1,326 days each model has the smallest RMSE. Columns IV (lower bound) and V (upper bound) present the winning percentage out of 64 months for each model, evaluated using the bootstrap sampling technique. The statistical bootstrap performed (with replacement) at a 95% confidence level is computed from the monthly RMSE values of the respective models below. Columns VI (lower bound) and VII (upper bound) present the winning percentage out of 1326 days for each model computed from bootstrapping the daily RMSE values of the respective models at a 95% confidence level.

(I) Model	**(II) Performance amongst all models (Monthly)**	**(III) Performance amongst all models (Daily)**	**(IV) 2.5% lower bound- (for monthly) (%)**	**(V) 2.5% upper bound- (for monthly) (%)**	**(VI) 2.5% lower bound- (for daily) (%)**	**(VII) 2.5% upper bound- (for daily) (%)**
Part I: $BSMH_{N+1}$ v/s $ParamH_{N+1}^{AVG} - Models$ v/s $M3H_{N+1}^{AVG} - Models$ v/s $L3H_{N+1}^{AVG} - Models$						
$BSMH_{N+1}$	**46**	**391**	61%	83%	27%	32%
$ParamH_{N+1}^{AVG} - Models$	6	353	3%	17%	24%	29%
$M3H_{N+1}^{AVG} - Models$	10	373	8%	25%	26%	31%
$L3H_{N+1}^{AVG} - Models$	2	209	0%	8%	14%	18%
Part II: $BSMH_{N+1}$ v/s $ParamH_{N+1}^{AVG} - Models$ v/s $M3H_{N+1}^{AVG} - Models$						
$BSMH_{N+1}$	**48**	474	64%	85%	33%	38%
$ParamH_{N+1}^{AVG} - Models$	6	365	3%	17%	25%	30%
$M3H_{N+1}^{AVG} - Models$	10	**487**	7%	25%	34%	39%
Part III: $BSMH_{N+1}$ v/s $ParamH_{N+1}^{AVG} - Models$ v/s $L3H_{N+1}^{AVG} - Models$						
$BSMH_{N+1}$	**55**	**595**	77%	92%	42%	48%
$ParamH_{N+1}^{AVG} - Models$	6	383	3%	17%	27%	32%
$L3H_{N+1}^{AVG} - Models$	3	348	0%	11%	24%	29%
Part IV: $BSMH_{N+1}$ v/s $ParamH_{N+1}^{AVG} - Models$						
$BSMH_{N+1}$	**58**	**912**	83%	97%	66%	71%
$ParamH_{N+1}^{AVG} - Models$	6	414	3%	17%	29%	34%

C.2.3.3 $CH^{AVG} - Models$: Model averaging hedging performance of models that have analytically derived the delta ($\delta C_{N+1}/\delta S_{N+1}$) from the call option price (C_{N+1}), which is forecasted from models that use one-trading-day ahead input variables:

Table C.2.13 shows the relative out-of-sample performance (in $RMSE$) amongst the models that forecast the one-trading-day-ahead average delta ($\delta C_{N+1}/\delta S_{N+1}$) derived analytically from C_{N+1} which is forecasted from models that use one-trading-day-ahead input variables. In column II of Table C.2.13, we list the several models used as an input to obtain the average one-trading-day-ahead forecast of $\delta C_{N+1}/\delta S_{N+1}$. The performance metric is the $RMSE$ of the one-trading-day-ahead forecast errors of the average $\delta C_{N+1}/\delta S_{N+1}$, which is computed for each averaging model utilising all of the errors in each day or each month. Amongst all of the models, columns III and IV record the number of months and days, respectively, that each model has the lowest $RMSE$. We performed a bootstrap using the daily and monthly RMSEs to be certain of our results. Columns V (lower bound) and VI (upper bound) present the results from the bootstrap performed (with replacement) using monthly RMSEs at a 95% confidence level and show the winning percentage out of 64 months for each model, and similarly, the 95 % confidence intervals computed from bootstrapping of the daily RMSEs signifies the winning percentage out of 1,326 days for each model and are reported in columns VII (lower bound), VIII (upper bound). After a model is found to outperform other individual parametric models, MLP and LSTM models in each of the several comparisons below, we look into whether that out-performing model individually can outperform the average $\delta C_{N+1}/\delta S_{N+1}$ of all the parametric models combinedly, MLP models combinedly or LSTM models combinedly covered in that section.

In the below several comparisons, even though a particular model wins by a higher percentage against other models, we investigated further these models pairwise by performing a pairwise bootstrap comparison, which was computed using the respective pair's daily RMSEs. The results are presented in Table 97 of the Electronic Appendix.

The Diebold-Mariano statistics were also performed on pairs amongst the average $\delta C_{N+1}/\delta S_{N+1}$ of all parametric models ($ParamCH^{AVG}_{N+1} - Models$), the average $\delta C_{N+1}/\delta S_{N+1}$ of all triple hidden layer MLP models ($M3CH^{AVG}_{N+1} - Models$), and the average $\delta C_{N+1}/\delta S_{N+1}$ of all triple hidden layer LSTM models ($L3CH^{AVG}_{N+1} - Models$) are reported in Table 87 of the Electronic Appendix. In constructing the DM tests, the model pairs are reported in column I and column II, and the DM test statistics for a particular pair are reported in column III. If the null can be rejected, a positive number suggests the rejection may be due to the second model being the better forecast model. In contrast, a negative value suggests the rejection may be due to the first model being the better forecast model. The model pairs highlighted in a red state that their forecasts have statistically insignificant differences in their prediction accuracy. Considering the DM-Test statistics in Table 87 of the Electronic Appendix, all the model pairs lead to the rejection of the null of equal forecasting performance.

The RMSEs for the models under the $CH^{AVG} - Models$ category, which averages the analytically computed $\delta C_{N+1}/\delta S_{N+1}$ from models belonging to the $CH - Models$ category(which uses one-trading-day-ahead input variables to forecast the C_{N+1} for the next trading day) on a monthly, yearly, and overall basis can be found in the Electronic Appendix, in Tables 57, 67, and 77, respectively.

C.2.3.3.1 Comparison amongst all Parametric Models with Triple Hidden Layer ANN Models:

In this section, we compare the out-of-sample hedging performance of the parametric models ($ParamCH_{N+1}^{AVG} - Models$), the triple hidden layer MLP models ($M3CH_{N+1}^{AVG} - Models$), and the triple hidden layer LSTM models ($L3CH_{N+1}^{AVG} - Models$), and then $ParamCH_{N+1}^{AVG} - Models$ with the $M3CH_{N+1}^{AVG} - Models$, and finally the $ParamCH_{N+1}^{AVG} - Models$ with the $L3CH_{N+1}^{AVG} - Models$.

Initially, in Part I of Table C.2.13, we compared the $ParamCH_{N+1}^{AVG} - Models$ with the $M3CH_{N+1}^{AVG} - Models$ and the $L3CH_{N+1}^{AVG} - Models$, and found that the $ParamCH_{N+1}^{AVG} - Models$ had the lowest $RMSE$ for 1,290 days (having a daily bootstrap winning % of 96% to 98%) out of 1,326. Accordingly, we now compare the $L3CH4_{N+1}$ model (i.e. the best-performing model when compared to the models in column VIII of Table B.2.9) with the $ParamCH_{N+1}^{AVG} - Models$, $M3CH_{N+1}^{AVG} - Models$, and the $L3CH_{N+1}^{AVG} - Models$ in Part I of Table C.2.14, and found that $ParamCH_{N+1}^{AVG} - Models$ had the lowest $RMSE$ for 1,285 days (having a daily bootstrap winning % of 96% to 98%) out of 1,326.

Secondly, in Part II of Table C.2.13, we compared the $ParamCH_{N+1}^{AVG} - Models$ with the $M3CH_{N+1}^{AVG} - Models$, and found that the $ParamCH_{N+1}^{AVG} - Models$ had the lowest $RMSE$ for 1,290 days (having a daily bootstrap winning % of 96% to 98%) out of 1,326. Accordingly, we now compare the $FMLSCH_{N+1}$ model (i.e. the best-performing model when compared to the models in column VIII of Table B.2.10) with the $ParamCH_{N+1}^{AVG} - Models$, and the $M3CH_{N+1}^{AVG} - Models$ in Part II of Table C.2.14, and found that $ParamCH_{N+1}^{AVG} - Models$ had the lowest $RMSE$ for 1,289 days (having a daily bootstrap winning % of 96% to 98%) out of 1,326.

Finally, in Part III of Table C.2.13, we compared the $ParamCH_{N+1}^{AVG} - Models$ with the $L3CH_{N+1}^{AVG} - Models$, and found that the $ParamCH_{N+1}^{AVG} - Models$ had the lowest $RMSE$ for 1,327 days (having a daily bootstrap winning % of 100% to 100%) out of 1,326. Accordingly, we now compare the $HDJCH_{N+1}$ model (i.e. the best-performing model when compared to the models in column VIII of Table B.2.11) with the $ParamCH_{N+1}^{AVG} - Models$, and the $L3CH_{N+1}^{AVG} - Models$ in Part III of Table C.2.14, and found that the $ParamCH_{N+1}^{AVG} - Models$ had the lowest $RMSE$ for 1,306 days (having a daily bootstrap winning % of 98% to 99%) out of 1,326.

Thus, when the best individually out-performing model, the $L3CH4_{N+1}$ model (from Table B.2.9) was compared to the average of all the parametric models, and the averages of all the triple hidden layer ANN models (in Part I of Table C.2.14), we conclude that the average of all the parametric models (i.e. $ParamCH_{N+1}^{AVG} - Models$) could outperform all other models. Similarly, when the best individually out-performing model, the $FMLSCH_{N+1}$ model (from Table B.2.10) was compared to the average of all the parametric models, and the averages of all the triple hidden layer MLP models (in Part II of Table C.2.14), yet again the average of all the parametric models (i.e. $ParamCH_{N+1}^{AVG} - Models$) could outperform all other models. Lastly, when the best individually out-performing model, the $HJDCH_{N+1}$ model (from Table B.2.11) was compared to the average of all the parametric models, and the averages of all the triple hidden layer LSTM models (in Part III of Table C.2.14), again the average of all the parametric models (i.e. $ParamCH_{N+1}^{AVG} - Models$) could outperform all other models.

C.2.3.3.2 Comparison amongst all Parametric models:

We now compare the $HJDCH_{N+1}$ model (i.e. the best-performing model when compared to the models in column V of Table B.2.12) with the $ParamCH_{N+1}^{AVG} - Models$ in Part IV of Table C.2.14 and found that the $ParamCH_{N+1}^{AVG} - Models$ had the lowest $RMSE$ for 1,306 days (having a daily bootstrap winning % of 98% to 99%) out of 1,326.

Thus, when the best individually out-performing model, the $HJDCH_{N+1}$ model (from Table B.2.12) was compared to the average of all the parametric models (in Part IV of Table C.2.14), the average of all the parametric models (i.e. $ParamCH_{N+1}^{AVG} - Models$) could outperform the $HJDCH_{N+1}$ model.

Table C.2.13: Model Averaging for Delta Comparison (amongst $ParamCH^{AVG}_{N+1} - Models$, $M3CH^{AVG}_{N+1} - Models$, and $L3CH^{AVG}_{N+1} - Models$): This table is compartmentalised into III parts, where each part presents a performance comparison using both daily and monthly statistics amongst the set of models mentioned in that part. The forecast variable for all the models is the one-trading-day-ahead delta. The $_{N+1}$ subscript denotes models that take an average of the delta from models that forecast the delta using one-trading-day-ahead input variables. In the parts mentioned below, we compare the out-of-sample performance of the following models: **In Part I**: $ParamCH^{AVG}_{N+1} - Models$, MLP $M3CH^{AVG}_{N+1} - Models$, and LSTM $L3CH^{AVG}_{N+1} - Models$, **in Part II**: $ParamCH^{AVG}_{N+1} - Models$, and MLP $M3CH^{AVG}_{N+1} - Models$, **in Part III**: $ParamCH^{AVG}_{N+1} - Models$, and LSTM $L3CH^{AVG}_{N+1} - Models$. The one-trading-day-ahead forecast errors of the delta are used to compute the Root Mean Square Error (RMSE). Column I identifies the models, and column II lists the models used as input to obtain the average one-trading-day-ahead forecast of the delta. Forecasts are made for 1,326 trading days, and there are 64 months covered in the sample using the monthly data. When comparing all models simultaneously, column III reports the number of months out of the 64 months that each model has the smallest RMSE, while column IV reports the number of days out of the 1,326 days each model has the smallest RMSE. Columns V (lower bound) and VI (upper bound) present the winning percentage out of 64 months for each model, evaluated using the bootstrap sampling technique. The statistical bootstrap performed (with replacement) at a 95% confidence level is computed from the monthly RMSE values of the respective models below. Columns VII (lower bound) and VIII (upper bound) present the winning percentage out of 1326 days for each model computed from bootstrapping the daily RMSE values of the respective models at a 95% confidence level.

(I) Model	**(II) Inputs**	**(III) Performance amongst all models (Monthly)**	**(IV) Performance amongst all models (Daily)**	**(V) 2.5% lower bound-(for monthly) (%)**	**(VI) 2.5% upper bound-(for monthly) (%)**	**(VII) 2.5% lower bound-(for daily) (%)**	**(VIII) 2.5% upper bound-(for daily) (%)**
Part I: $ParamCH^{AVG}_{N+1} - Models$ v/s $M3CH^{AVG}_{N+1} - Models$ v/s $L3CH^{AVG}_{N+1} - Models$							
$ParamCH^{AVG}_{N+1} - Models$	$BSMCH_{N+1}$, HCH_{N+1} , $HJDCH_{N+1}$, $FMLSCH_{N+1}$	**64**	**1290**	100%	100%	96%	98%
$M3CH^{AVG}_{N+1} - Models$	$M3CH1_{N+1}$, $M3CH2_{N+1}$, $M3CH3_{N+1}$, $M3CH4_{N+1}$, $M3CH5_{N+1}$, $M3CH6_{N+1}$, $M3CH7_{N+1}$	0	37	0%	0%	2%	4%
$L3CH^{AVG}_{N+1} - Models$	$L3CH1_{N+1}$, $L3CH2_{N+1}$, $L3CH3_{N+1}$, $L3CH4_{N+1}$, $L3CH5_{N+1}$, $L3CH6_{N+1}$, $L3CH7_{N+1}$	0	0	0%	0%	0%	0%
Part II: $ParamCH^{AVG}_{N+1} - Models$ v/s $M3CH^{AVG}_{N+1} - Models$							
$ParamCH^{AVG}_{N+1} - Models$	$BSMCH_{N+1}$, HCH_{N+1} , $HJDCH_{N+1}$, $FMLSCH_{N+1}$	**64**	**1290**	100%	100%	96%	98%
$M3CH^{AVG}_{N+1} - Models$	$M3CH1_{N+1}$, $M3CH2_{N+1}$, $M3CH3_{N+1}$, $M3CH4_{N+1}$, $M3CH5_{N+1}$, $M3CH6_{N+1}$, $M3CH7_{N+1}$	0	37	0%	0%	2%	4%
Part III: $ParamCH^{AVG}_{N+1} - Models$ v/s $L3CH^{AVG}_{N+1} - Models$							
$ParamCH^{AVG}_{N+1} - Models$	$BSMCH_{N+1}$, HCH_{N+1} , $HJDCH_{N+1}$, $FMLSCH_{N+1}$	**64**	**1327**	100%	100%	100%	100%
$L3CH^{AVG}_{N+1} - Models$	$L3CH1_{N+1}$, $L3CH2_{N+1}$, $L3CH3_{N+1}$, $L3CH4_{N+1}$, $L3CH5_{N+1}$, $L3CH6_{N+1}$, $L3CH7_{N+1}$	0	0	0%	0%	0%	0%

Table C.2.14: Model Averaging for Delta Comparison: This table is compartmentalised into IV parts. Each part presents a performance comparison using daily and monthly statistics amongst the models mentioned in that part. The forecast variable for all the models is the one-trading-day-ahead delta. The $_{N+1}$ subscript denotes models that take an average of the delta from models that forecast the delta using one-trading-day-ahead input variables. In the parts mentioned below, we compare the out-of-sample performance of the best performing model (based on the total number of days out of 1326 days that a particular model had the lowest RMSE) with the average of parametric models ($ParamCH^{AVG}_{N+1} - Models$), the average of the triple ($M3CH^{AVG}_{N+1} - Models$) hidden layer MLP models, and the average of the triple ($L3CH^{AVG}_{N+1} - Models$) hidden layer LSTM models. **In Part I**: The best performing model ($L3CH4_{N+1}$) from Table B.2.9 with $ParamCH^{AVG}_{N+1} - Models$, $M3CH^{AVG}_{N+1} - Models$, $L3CH^{AVG}_{N+1} - Models$, **in Part II**: The best performing model ($FMLSCCH_{N+1}$) from Table B.2.10 with $ParamCH^{AVG}_{N+1} - Models$, $M3CH^{AVG}_{N+1} - Models$, **in Part III**: The best performing model ($HJDCCH_{N+1}$) from Table B.2.11 with $ParamCH^{AVG}_{N+1} - Models$, $L3CH^{AVG}_{N+1} - Models$, **in Part IV**: The best performing model ($HJDCCH_{N+1}$) from Table B.2.12 with $ParamCH^{AVG}_{N+1} - Models$. The one-trading-day-ahead forecast errors of the delta are used to compute the Root Mean Square Error (RMSE). Forecasts are made for 1,326 trading days, and there are 64 months covered in the sample using the monthly data. Column I identifies the models. When comparing all models simultaneously, column II reports the number of months out of the 64 months that each model has the smallest RMSE, while column III reports the number of days out of the 1,326 days each model has the smallest RMSE. Columns IV (lower bound) and V (upper bound) present the winning percentage out of 64 months for each model, evaluated using the bootstrap sampling technique. The statistical bootstrap performed (with replacement) at a 95% confidence level is computed from the monthly RMSE values of the respective models below. Columns VI (lower bound) and VII (upper bound) present the winning percentage out of 1326 days for each model computed from bootstrapping the daily RMSE values of the respective models at a 95% confidence level.

(I) Model	**(II) Performance amongst all models (Monthly)**	**(III) Performance amongst all models (Daily)**	**(IV) 2.5% lower bound- (for monthly) (%)**	**(V) 2.5% upper bound- (for monthly) (%)**	**(VI) 2.5% lower bound- (for daily) (%)**	**(VII) 2.5% upper bound- (for daily) (%)**
Part I: $L3CH4_{N+1}$ v/s $ParamCH^{AVG}_{N+1} - Models$ v/s $M3CH^{AVG}_{N+1} - Models$ v/s $L3CH^{AVG}_{N+1} - Models$						
$L3CH4_{N+1}$	0	4	0%	0%	0%	1%
$ParamCH^{AVG}_{N+1} - Models$	**64**	**1285**	100%	100%	96%	98%
$M3CH^{AVG}_{N+1} - Models$	0	37	0%	0%	2%	4%
$L3CH^{AVG}_{N+1} - Models$	0	0	0%	0%	0%	0%
Part II: $FMLSCH_{N+1}$ v/s $ParamCH^{AVG}_{N+1} - Models$ v/s $M3CH^{AVG}_{N+1} - Models$						
$FMLSCH_{N+1}$	0	1	0%	0%	0%	0%
$ParamCH^{AVG}_{N+1} - Models$	**64**	**1289**	100%	100%	96%	98%
$M3CH^{AVG}_{N+1} - Models$	0	36	0%	0%	2%	4%
Part III: $HJDCH_{N+1}$ v/s $ParamCH^{AVG}_{N+1} - Models$ v/s $L3CH^{AVG}_{N+1} - Models$						
$HJDCH_{N+1}$	0	20	0%	0%	1%	2%
$ParamCH^{AVG}_{N+1} - Models$	**64**	**1306**	100%	100%	98%	99%
$L3CH^{AVG}_{N+1} - Models$	0	0	0%	0%	0%	0%
Part IV: $HJDCH_{N+1}$ v/s $ParamCH^{AVG}_{N+1} - Models$						
$HJDCH_{N+1}$	0	20	0%	0%	1%	2%
$ParamCH^{AVG}_{N+1} - Models$	**64**	**1306**	100%	100%	98%	99%

C.2.4 Results - Model Averaging for computing the Replicating Portfolio

C.2.4.1 $HV^{AVG} - Models$: Model averaging replicating portfolio value performance of models that forecast the replicating portfolio value(V_{N+1}), computed using the delta from H-Models, that use lagged input variables:

Table C.2.15 shows the relative out-of-sample replicating portfolio value performance (in $RMSE$) amongst the models that forecast the average one-trading-day-ahead replicating portfolio value (V_{N+1}). The V_{N+1} is computed from equation 3.17 using the forecasted one-trading-day-ahead delta (Δ_{N+1}) from models that use lagged input variables. In column II of table C.2.15, we list the several models used as input to obtain the average one-trading-day-ahead forecast of V_{N+1}. The performance metric is the $RMSE$ of the one-trading-day-ahead forecast errors of the average V_{N+1}, which is computed for each averaging model utilising all of the errors in each day or each month. Amongst all of the models, columns III and IV record the number of months and days, respectively, that each model has the lowest $RMSE$. We performed a bootstrap using the daily and monthly RMSEs to be certain of our results. Columns V (lower bound) and VI (upper bound) present the results from the bootstrap performed (with replacement) using monthly RMSEs at a 95% confidence level and show the winning percentage out of 64 months for each model, and similarly, the 95 % confidence intervals computed from bootstrapping of the daily RMSEs signifies the winning percentage out of 1326 days for each model and are reported in columns VII (lower bound), VIII (upper bound). After a model is found to outperform other individual parametric models, MLP and LSTM models in each of the several comparisons below, we look into whether that out-performing model individually can outperform the average V_{N+1} of all the parametric models combinedly, MLP models combinedly or LSTM models combinedly, covered in that section.

In the below several comparisons, even though a particular model wins by a higher percentage against other models, we investigated further these models pairwise by performing a pairwise bootstrap comparison, which was computed using the respective pair's daily RMSEs. The results are presented in Table 98 of the Electronic Appendix.

The Diebold-Mariano(DM) (Diebold and Mariano (1995)) test was performed on pairs amongst the average V_{N+1} of all parametric models ($ParamHV_N^{AVG} - Models$), the average V_{N+1} of all triple hidden layer MLP models ($M3HV_N^{AVG} - Models$), and the average V_{N+1} of all triple hidden layer LSTM models ($L3HV_N^{AVG} - Models$) are reported in Table 88 of the Electronic Appendix. In constructing the DM tests, the model pairs are reported in column I and column II, and the DM test statistics for a particular pair are reported in column III. If the null can be rejected, a positive number suggests the rejection may be due to the second model being the better forecast model. In contrast, a negative value suggests the rejection may be due to the first model being the better forecast model. The model pairs highlighted in a red state that their forecasts have statistically insignificant differences in their prediction accuracy. Considering the DM-Test statistics in Table 88 of the Electronic Appendix, all the model pairs lead to the rejection of the null of equal forecasting performance.

The RMSEs for the models under the $HV^{AVG} - Models$ category, which averages the forecasted V_{N+1} from models belonging to the $HV - Models$ category(which uses lagged input variables to forecast the V_{N+1} for the next trading day) on a monthly, yearly, and overall basis can be found in the Electronic Appendix, in Tables 58, 68, and 78, respectively.

C.2.4.1.1 Comparison amongst all Parametric Models with Triple Hidden Layer ANN Models:

In this section, we compare the out-of-sample hedging performance of the parametric models ($ParamHV_N^{AVG} - Models$), the triple hidden layer MLP models ($M3HV_N^{AVG} - Models$), and the triple hidden layer LSTM models ($L3HV_N^{AVG} - Models$), and then $ParamHV_N^{AVG} - Models$ with the $M3HV_N^{AVG} - Models$, and finally the $ParamHV_N^{AVG} - Models$ with the $L3HV_N^{AVG} - Models$.

Initially in Part I of Table C.2.15, we compared the $ParamHV_N^{AVG} - Models$ with the $M3HV_N^{AVG} - Models$ and the $L3HV_N^{AVG} - Models$, and found that the $ParamHV_N^{AVG} - Models$ had the lowest $RMSE$ for 592 days (having a daily bootstrap winning % of 42% to 47%) out of 1,326. Accordingly, we now compare the $BSMHV_N$ model (i.e. the best-performing model when compared to the models in column V of Table B.2.13) with the $ParamHV_N^{AVG} - Models$, $M3HV_N^{AVG} - Models$, and the $L3HV_N^{AVG} - Models$ in Part I of Table C.2.16, and found that $M3HV_N^{AVG} - Models$ had the lowest $RMSE$ for 448 days (having a daily bootstrap winning % of 31% to 36%) out of 1,326, which was closely followed by the $ParamH_N^{AVG} - Models$, which had similar out-performance for 372 days (having a daily bootstrap winning % of 26% to 30%).

Secondly, in Part II of Table C.2.15, we compared the $ParamHV_N^{AVG} - Models$ with the $M3HV_N^{AVG} - Models$ and found that the $M3HV_N^{AVG} - Models$ had the lowest $RMSE$ for 675 days (having a daily bootstrap winning % of 48% to 54%) out of 1,326, which was closely followed by the $ParamH_N^{AVG} - Models$, which had similar out-performance for 651 days (having a daily bootstrap winning % of 46% to 52%). Accordingly, we now compare the $BSMHV_N$ model (i.e. the best-performing model when compared to the models in column V of Table B.2.14) with the $ParamHV_N^{AVG} - Models$, and the $M3HV_N^{AVG} - Models$ in Part II of Table C.2.16, and found that the $M3HV_N^{AVG} - Models$ had the lowest $RMSE$ for 588 days (having a daily bootstrap winning % of 42% to 47%) out of 1,326.

Finally, in Part III of Table C.2.15, we compared the $ParamHV_N^{AVG} - Models$ with the $L3HV_N^{AVG} - Models$, and found that the $ParamHV_N^{AVG} - Models$ had the lowest $RMSE$ for 907 days (having a daily bootstrap winning % of 66% to 71%) out of 1,326. Accordingly, we now compare the $BSMHV_N$ model (i.e. the best-performing model when compared to the models in column V of Table B.2.15) with the $ParamHV_N^{AVG} - Models$ in Part III of Table C.2.16, and the $L3HV_N^{AVG} - Models$ and found that the $BSMHV_N$ model had the lowest $RMSE$ for 561 days (having a daily bootstrap winning % of 40% to 45%) out of 1,326.

Thus, when the best individually out-performing model, the $BSMHV_N$ model (from Table B.2.13) was compared to the average of all the parametric models, and the averages of all the triple hidden layer ANN models (in Part I of Table C.2.16), we conclude that the average of all triple hidden layer MLP models (i.e. the $M3HV_N^{AVG} - Models$) could outperform all other models. Similarly, when the best individually out-performing model, the $BSMHV_N$ model (from Table B.2.14) was compared to the average of all the parametric models, and the averages of all the triple hidden layer MLP models (in Part II of Table C.2.16), yet again the average of all triple hidden layer MLP models (i.e. the $M3HV_N^{AVG} - Models$) could outperform all other models. Lastly, when the best individually out-performing model, the $BSMHV_N$ model (from Table B.2.15) was compared to the average of all the parametric models, and the averages of all the triple hidden layer LSTM models (in Part III of Table C.2.16), we conclude that $BSMHV_N$ model could outperform all other models.

C.2.4.1.2 Comparison amongst all Parametric models:

We now compare the $BSMHV_N$ model (i.e. the best-performing model when compared to the models in column V of Table B.2.16) with the $ParamHV_N^{AVG} - Models$ in Part IV of Table C.2.16, and found that the $BSMHV_N$ model still had the lowest $RMSE$ for 890 days (having a daily bootstrap winning % of 65% to 70%) out of 1,326.

Thus, when the best individually out-performing model, the $BSMHV_N$ model (from Table B.2.16) was compared to the average of all the parametric models (in Part IV of Table C.2.16), we can conclude that the $BSMHV_N$ model could outperform the average of all the parametric models.

Table C.2.15: Model Averaging for Replicating Portfolio Value Comparison (amongst $ParamHV_N^{AVG}-Models$, $M3HV_N^{AVG}-Models$, and $L3HV_N^{AVG}-Models$): This table is compartmentalised into III parts, where each part presents a performance comparison using both daily and monthly statistics amongst the set of models mentioned in that part. The forecast variable for all the models is the one-trading-day-ahead replicating portfolio value (V_{N+1}). The $_N$ subscript denotes models that take an average of the V_{N+1} from models that forecast V_{N+1} using lagged input variables. In the parts mentioned below, we compare the out-of-sample performance of the following models: **In Part I**: $ParamHV_N^{AVG}-Models$, MLP $M3HV_N^{AVG}-Models$, and LSTM $L3HV_N^{AVG}-Models$, **in Part II**: $ParamHV_N^{AVG}-Models$, and MLP $M3HV_N^{AVG}-Models$, **in Part III**: $ParamHV_N^{AVG}-Models$, and LSTM $L3HV_N^{AVG}-Models$. The one-trading-day-ahead forecast errors of the V_{N+1} are used to compute the Root Mean Square Error (RMSE). Column I identifies the models, and column II lists the models used as input to obtain the average one-trading-day-ahead forecast of the V_{N+1}. Forecasts are made for 1,326 trading days, and there are 64 months covered in the sample using the monthly data. When comparing all models simultaneously, column III reports the number of months out of the 64 months that each model has the smallest RMSE, while column IV reports the number of days out of the 1,326 days each model has the smallest RMSE. Columns V (lower bound) and VI (upper bound) present the winning percentage out of 64 months for each model, evaluated using the bootstrap sampling technique. The statistical bootstrap performed (with replacement) at a 95% confidence level is computed from the monthly RMSE values of the respective models below. Columns VII (lower bound) and VIII (upper bound) present the winning percentage out of 1326 days for each model computed from bootstrapping the daily RMSE values of the respective models at a 95% confidence level.

(I) Model	**(II)** Inputs	**(III)** Performance amongst all models (Monthly)	**(IV)** Performance amongst all models (Daily)	**(V)** 2.5% lower bound- (for monthly) (%)	**(VI)** 2.5% upper bound- (for monthly) (%)	**(VII)** 2.5% lower bound- (for daily) (%)	**(VIII)** 2.5% upper bound- (for daily) (%)
	Part I: $ParamHV_N^{AVG}-Models$ v/s $M3HV_N^{AVG}-Models$ v/s $L3HV_N^{AVG}-Models$						
$ParamHV_N^{AVG}-Models$	$BSMHV_N$, HHV_N , $HJDHV_N$, $FMLSHV_N$	17	**592**	19%	39%	42%	47%
$M3HV_N^{AVG}-Models$	$M3HV1_N$, $M3HV2_N$, $M3HV3_N$, $M3HV4_N$, $M3HV5_N$, $M3HV6_N$, $M3HV7_N$	**39**	519	50%	72%	37%	42%
$L3HV_N^{AVG}-Models$	$L3HV1_N$, $L3HV2_N$, $L3HV3_N$, $L3HV4_N$, $L3HV5_N$, $L3HV6_N$, $L3HV7_N$	7	215	4%	19%	14%	18%
	Part II: $ParamHV_N^{AVG}-Models$ v/s $M3HV_N^{AVG}-Models$						
$ParamHV_N^{AVG}-Models$	$BSMHV_N$, HHV_N , $HJDHV_N$, $FMLSHV_N$	17	651	17%	41%	46%	52%
$M3HV_N^{AVG}-Models$	$M3HV1_N$, $M3HV2_N$, $M3HV3_N$, $M3HV4_N$, $M3HV5_N$, $M3HV6_N$, $M3HV7_N$	**46**	**675**	59%	83%	48%	54%
	Part III: $ParamHV_N^{AVG}-Models$ v/s $L3HV_N^{AVG}-Models$						
$ParamHV_N^{AVG}-Models$	$BSMHV_N$, HHV_N , $HJDHV_N$, $FMLSHV_N$	**44**	**907**	58%	81%	66%	71%
$L3HV_N^{AVG}-Models$	$L3HV1_N$, $L3HV2_N$, $L3HV3_N$, $L3HV4_N$, $L3HV5_N$, $L3HV6_N$, $L3HV7_N$	19	419	19%	42%	29%	34%

Table C.2.16: Model Averaging for Replicating Portfolio Value Comparison: This table is compartmentalised into IV parts. Each part presents a performance comparison using daily and monthly statistics amongst the models mentioned in that part. The forecast variable for all the models is the one-trading-day-ahead replicating portfolio value (V_{N+1}). The $_N$ subscript denotes models that take an average of the V_{N+1} from models that forecast V_{N+1} using lagged input variables. In the parts mentioned below, we compare the out-of-sample performance of the best model (based on the total number of days out of 1326 days that a particular model had the lowest RMSE) with the average of parametric models ($ParamHV_N^{AVG} - Models$), the average of the triple ($M3HV_N^{AVG} - Models$) hidden layer MLP models, and the average of the triple ($L3HV_N^{AVG} - Models$) hidden layer LSTM models. **In Part I**: The best model ($BSMHV_N$) from Table B.2.13 with $ParamHV_N^{AVG} - Models$, $M3HV_N^{AVG} - Models$, $L3HV_N^{AVG} - Models$, **in Part II**: The best model ($BSMHV_N$) from Table B.2.14 with $ParamHV_N^{AVG} - Models$, $M3HV_N^{AVG} - Models$, **in Part III**: The best model ($BSMHV_N$) from Table B.2.15 with $ParamHV_N^{AVG} - Models$, $L3HV_N^{AVG} - Models$, **in Part IV**: The best model ($BSMHV_N$) from Table B.2.16 with $ParamHV_N^{AVG} - Models$. The one-trading-day-ahead forecast errors of the V_{N+1} are used to compute the Root Mean Square Error (RMSE). Forecasts are made for 1,326 trading days, and there are 64 months covered in the sample using the monthly data. Column I identifies the models. When comparing all models simultaneously, column II reports the number of months out of the 64 months that each model has the smallest RMSE, while column III reports the number of days out of the 1,326 days each model has the smallest RMSE. Columns IV (lower bound) and V (upper bound) present the winning percentage out of 64 months for each model, evaluated using the bootstrap sampling technique. The statistical bootstrap performed (with replacement) at a 95% confidence level is computed from the monthly RMSE values of the respective models below. Columns VI (lower bound) and VII (upper bound) present the winning percentage out of 1326 days for each model computed from bootstrapping the daily RMSE values of the respective models at a 95% confidence level.

(I) Model	**(II) Performance amongst all models (Monthly)**	**(III) Performance amongst all models (Daily)**	**(IV) 2.5% lower bound-(for monthly) (%)**	**(V) 2.5% upper bound-(for monthly) (%)**	**(VI) 2.5% lower bound-(for daily) (%)**	**(VII) 2.5% upper bound-(for daily) (%)**
Part I: $BSMHV_N$ v/s $ParamHV_N^{AVG} - Models$ v/s $M3HV_N^{AVG} - Models$ v/s $L3HV_N^{AVG} - Models$						
$BSMHV_N$	10	308	6%	25%	21%	25%
$ParamHV_N^{AVG} - Models$	13	372	12%	30%	26%	30%
$M3HV_N^{AVG} - Models$	**35**	**448**	42%	66%	31%	36%
$L3HV_N^{AVG} - Models$	6	198	3%	17%	13%	17%
Part II: $BSMHV_N$ v/s $ParamHV_N^{AVG} - Models$ v/s $M3HV_N^{AVG} - Models$						
$BSMHV_N$	10	352	8%	25%	24%	29%
$ParamHV_N^{AVG} - Models$	13	386	11%	31%	27%	32%
$M3HV_N^{AVG} - Models$	**41**	**588**	53%	75%	42%	47%
Part III: $BSMHV_N$ v/s $ParamHV_N^{AVG} - Models$ v/s $L3HV_N^{AVG} - Models$						
$BSMHV_N$	**36**	**561**	42%	69%	40%	45%
$ParamHV_N^{AVG} - Models$	15	404	14%	34%	28%	33%
$L3HV_N^{AVG} - Models$	13	361	11%	31%	25%	29%
Part IV: $BSMHV_N$ v/s $ParamHV_N^{AVG} - Models$						
$BSMHV_N$	**48**	**890**	64%	84%	65%	70%
$ParamHV_N^{AVG} - Models$	16	436	16%	36%	30%	35%

C.2.4.2 $HV^{AVG} - Models$: Model averaging replicating portfolio value performance of models that forecast the replicating portfolio value(V_{N+1}), computed using the delta from H-Models, that use one-trading-day input variables:

Table C.2.17 shows the relative out-of-sample replicating portfolio value performance (in $RMSE$) amongst the models that forecast the average one-trading-day-ahead replicating portfolio value (V_{N+1}). The V_{N+1} is computed from equation 3.17 using the forecasted one-trading-day-ahead delta (Δ_{N+1}) from models that use one-trading-day input variables. In column II of Table C.2.17, we list the several models used as an input to obtain the average one-trading-day-ahead forecast of V_{N+1}. The performance metric is the $RMSE$ of the one-trading-day-ahead forecast errors of the average V_{N+1}, which is computed for each averaging model utilising all of the errors in each day or each month. Amongst all of the models, columns III and IV record the number of months and days, respectively, that each model has the lowest $RMSE$. We performed a bootstrap using the daily and monthly RMSEs to be certain of our results. Columns V (lower bound) and VI (upper bound) present the results from the bootstrap performed (with replacement) using monthly RMSEs at a 95% confidence level and show the winning percentage out of 64 months for each model, and similarly, the 95 % confidence intervals computed from bootstrapping of the daily RMSEs signifies the winning percentage out of 1326 days for each model and are reported in columns VII (lower bound), VIII (upper bound). After a model is found to outperform other individual parametric models, MLP and LSTM models in each of the several comparisons below, we look into whether that out-performing model individually can outperform the average V_{N+1} of all the parametric models combinedly, MLP models combinedly or LSTM models combinedly, covered in that section.

In the below several comparisons, even though a particular model wins by a higher percentage against other models, we investigated further these models pairwise by performing a pairwise bootstrap comparison, which was computed using the respective pair's daily RMSEs. The results are presented in Table 99 of the Electronic Appendix.

The Diebold-Mariano(DM) (Diebold and Mariano (1995)) test was performed on pairs amongst the average V_{N+1} of all parametric models ($ParamHV_{N+1}^{AVG} - Models$), the average V_{N+1} of all triple hidden layer MLP models ($M3HV_{N+1}^{AVG} - Models$), and the average V_{N+1} of all triple hidden layer LSTM models ($L3HV_{N+1}^{AVG} - Models$) are reported in Table 89 of the Electronic Appendix. In constructing the DM tests, the model pairs are reported in column I and column II, and the DM test statistics for a particular pair are reported in column III. If the null can be rejected, a positive number suggests the rejection may be due to the second model being the better forecast model. In contrast, a negative value suggests the rejection may be due to the first model being the better forecast model. The model pairs highlighted in a red state that their forecasts have statistically insignificant differences in their prediction accuracy. Considering the DM-Test statistics in Table 89 of the Electronic Appendix, all the model pairs lead to the rejection of the null of equal forecasting performance.

The RMSEs for the models under the $HV^{AVG} - Models$ category, which averages the forecasted V_{N+1} from models belonging to the $HV - Models$ category(which uses one-trading-day-ahead input variables to forecast the V_{N+1} for the next trading day) on a monthly, yearly, and overall basis can be found in the Electronic Appendix, in Tables 59, 69, and 79, respectively.

C.2.4.2.1 Comparison amongst all Parametric Models with Triple Hidden Layer ANN Models:

In this section, we compare the out-of-sample hedging performance of the parametric models ($ParamHV_{N+1}^{AVG} - Models$), the triple hidden layer MLP models ($M3HV_{N+1}^{AVG} - Models$), and the triple hidden layer LSTM models ($L3HV_{N+1}^{AVG} - Models$), and then $ParamHV_{N+1}^{AVG} - Models$ with the $M3HV_{N+1}^{AVG} - Models$, and finally the $ParamHV_{N+1}^{AVG} - Models$ with the $L3HV_{N+1}^{AVG} - Models$.

Initially in Part I of Table C.2.17, we compared the $ParamHV_{N+1}^{AVG} - Models$ with the $M3HV_{N+1}^{AVG} - Models$ and the $L3HV_{N+1}^{AVG} - Models$, and found that the $ParamHV_{N+1}^{AVG} - Models$ had the lowest $RMSE$ for 653 days (having a daily bootstrap winning % of 47% to 52%) out of 1,326. Accordingly, we now compare the $BSMHV_{N+1}$ model (i.e. the best-performing model when compared to the models in column V of Table B.2.17) with the $ParamHV_{N+1}^{AVG} - Models$, $M3HV_{N+1}^{AVG} - Models$, and the $L3HV_{N+1}^{AVG} - Models$ in Part I of Table C.2.18, and found that $BSMHV_{N+1}$ model had the lowest $RMSE$ for 389 days (having a daily bootstrap winning % of 27% to 32%) out of 1,326. Though the $BSMHV_{N+1}$ model outperformed, the parametric model, $ParamHV_{N+1}^{AVG} - Models$ (354 days), and the MLP model, $M3HV_{N+1}^{AVG} - Models$ (373 days) have shown similar out-performance and have a collective daily bootstrap winning percentage from 24% (lower bound for the $ParamHV_{N+1}^{AVG} - Models$) to 30% (upper bound for the $M3HV_{N+1}^{AVG} - Models$).

Secondly, in Part II of Table C.2.17, we compared the $ParamHV_{N+1}^{AVG} - Models$ with the $M3HV_{N+1}^{AVG} - Models$, and found that the $ParamHV_{N+1}^{AVG} - Models$ had the lowest $RMSE$ for 754 days (having a daily bootstrap winning % of 54% to 60%) out of 1,326. Accordingly, we now compare the $BSMHV_{N+1}$ model (i.e. the best-performing model when compared to the models in column V of Table B.2.18) with the $ParamHV_{N+1}^{AVG} - Models$, and the $M3HV_{N+1}^{AVG} - Models$ in Part II of Table C.2.18, and found that the $M3HV_{N+1}^{AVG} - Models$ had the lowest $RMSE$ for 487 days (having a daily bootstrap winning % of 34% to 39%) out of 1,326. Though the $M3HV_{N+1}^{AVG} - Models$ outperformed, the parametric models, $BSMHV_{N+1}$ model (473 days), and $ParamHV_{N+1}^{AVG} - Models$ (366 days) have shown similar out-performance, and have a collective daily bootstrap winning percentage from 25% (lower bound for the $ParamHV_{N+1}^{AVG} - Models$) to 38% (upper bound for the $BSMHV_{N+1}$ model).

Finally, in Part III of Table C.2.17, we compared the $ParamHV_{N+1}^{AVG} - Models$ with the $L3HV_{N+1}^{AVG} - Models$, and found that the $ParamHV_{N+1}^{AVG} - Models$ had the lowest $RMSE$ for 907 days (having a daily bootstrap winning % of 66% to 71%) out of 1,326. Accordingly, we now compare the $BSMHV_{N+1}$ model (i.e. the best-performing model when compared to the models in column V of Table B.2.19) with the $ParamHV_{N+1}^{AVG} - Models$ and the $L3HV_{N+1}^{AVG} - Models$ in Part III of Table C.2.18, and found that the $BSMHV_{N+1}$ model had the lowest $RMSE$ for 591 days (having a daily bootstrap winning % of 42% to 47%) out of 1,326.

Thus, when the best individually out-performing model, the $BSMHV_{N+1}$ model (from Table B.2.17) was compared to the average of all the parametric models, and the averages of all the triple hidden layer ANN models (in Part I of Table C.2.18), we conclude that $BSMHV_{N+1}$ model could outperform all other models. Similarly, when the best individually out-performing model, the $BSMHV_{N+1}$ model (from Table B.2.18) was compared to the average of all the parametric models, and the averages of all the triple hidden layer MLP models (in Part II of Table C.2.18), the average of all triple hidden layer MLP models (i.e. the $M3HV_{N+1}^{AVG} - Models$) could outperform all other models. Lastly, when the best individually out-performing model, the $BSMHV_{N+1}$ model (from Table B.2.19) was compared to the average of all the parametric models, and the averages of all the triple hidden layer LSTM models (in Part III of Table C.2.18), yet again the $BSMHV_{N+1}$ model could outperform all other models.

C.2.4.2.2 Comparison amongst all Parametric models:

We now compare the $BSMHV_{N+1}$ model (i.e. the best-performing model when compared to the models in column V of Table B.2.20) to the average V_{N+1} of all the parametric models ($ParamHV_{N+1}^{AVG} - Models$) in Part IV of Table C.2.18, and found that the $BSMHV_{N+1}$ model still had the lowest $RMSE$ for 910 days (having a daily bootstrap winning % of 66% to 71%) out of 1,326.

Thus, when the best individually out-performing model, the $BSMHV_{N+1}$ model (from Table B.2.20) was compared to the average of all the parametric models (in Part IV of Table C.2.18), we can conclude that the $BSMHV_{N+1}$ model could outperform the average of all the parametric models.

Table C.2.17: Model Averaging for Replicating Portfolio Value Comparison (amongst $ParamHV^{AVG}_{N+1} - Models$, $M3HV^{AVG}_{N+1} - Models$, and $L3HV^{AVG}_{N+1} - Models$): This table is compartmentalised into III parts, where each part presents a performance comparison using both daily and monthly statistics amongst the set of models mentioned in that part. The forecast variable for all the models is the one-trading-day-ahead replicating portfolio value (V_{N+1}). The $_{N+1}$ subscript denotes models that take an average of the V_{N+1} from models that forecast V_{N+1} using one-trading-day-ahead input variables. In the parts mentioned below, we compare the out-of-sample performance of the following models: **In Part I**: $ParamHV^{AVG}_{N+1} - Models$, MLP $M3HV^{AVG}_{N+1} - Models$, and LSTM $L3HV^{AVG}_{N+1} - Models$, **in Part II**: $ParamHV^{AVG}_{N+1} - Models$, and MLP $M3HV^{AVG}_{N+1} - Models$, **in Part III**: $ParamHV^{AVG}_{N+1} - Models$, and LSTM $L3HV^{AVG}_{N+1} - Models$. The one-trading-day-ahead forecast errors of V_{N+1} are used to compute the Root Mean Square Error (RMSE). Column I identifies the models, and column II lists the models used as input to obtain the average one-trading-day-ahead forecast of V_{N+1}. Forecasts are made for 1,326 trading days, and there are 64 months covered in the sample using the monthly data. When comparing all models simultaneously, column III reports the number of months out of the 64 months that each model has the smallest RMSE, while column IV reports the number of days out of the 1,326 days each model has the smallest RMSE. Columns V (lower bound) and VI (upper bound) present the winning percentage out of 64 months for each model, evaluated using the bootstrap sampling technique. The statistical bootstrap performed (with replacement) at a 95% confidence level is computed from the monthly RMSE values of the respective models below. Columns VII (lower bound) and VIII (upper bound) present the winning percentage out of 1326 days for each model computed from bootstrapping the daily RMSE values of the respective models at a 95% confidence level.

(I) Model	**(II)** Inputs	**(III)** Performance amongst all models (Monthly)	**(IV)** Performance amongst all models (Daily)	**(V)** 2.5% lower bound- (for monthly) (%)	**(VI)** 2.5% upper bound- (for monthly) (%)	**(VII)** 2.5% lower bound- (for daily) (%)	**(VIII)** 2.5% upper bound- (for daily) (%)
Part I: $ParamHV^{AVG}_{N+1} - Models$ v/s $M3HV^{AVG}_{N+1} - Models$ v/s $L3HV^{AVG}_{N+1} - Models$							
$ParamHV^{AVG}_{N+1} - Models$	$BSMHV_{N+1}$, HHV_{N+1} , $HJDHV_{N+1}$, $FMLSHV_{N+1}$	**37**	**653**	47%	70%	47%	52%
$M3HV^{AVG}_{N+1} - Models$	$M3HV1_{N+1}$, $M3HV2_{N+1}$, $M3HV3_{N+1}$, $M3HV4_{N+1}$, $M3HV5_{N+1}$, $M3HV6_{N+1}$, $M3HV7_{N+1}$	16	443	14%	36%	31%	36%
$L3HV^{AVG}_{N+1} - Models$	$L3HV1_{N+1}$, $L3HV2_{N+1}$, $L3HV3_{N+1}$, $L3HV4_{N+1}$, $L3HV5_{N+1}$, $L3HV6_{N+1}$, $L3HV7_{N+1}$	10	230	8%	25%	15%	19%
Part II: $ParamHV^{AVG}_{N+1} - Models$ v/s $M3HV^{AVG}_{N+1} - Models$							
$ParamHV^{AVG}_{N+1} - Models$	$BSMHV_{N+1}$, HHV_{N+1} , $HJDHV_{N+1}$, $FMLSHV_{N+1}$	**42**	**754**	55%	78%	54%	60%
$M3HV^{AVG}_{N+1} - Models$	$M3HV1_{N+1}$, $M3HV2_{N+1}$, $M3HV3_{N+1}$, $M3HV4_{N+1}$, $M3HV5_{N+1}$, $M3HV6_{N+1}$, $M3HV7_{N+1}$	21	572	22%	45%	40%	46%
Part III: $ParamHV^{AVG}_{N+1} - Models$ v/s $L3HV^{AVG}_{N+1} - Models$							
$ParamHV^{AVG}_{N+1} - Models$	$BSMHV_{N+1}$, HHV_{N+1} , $HJDHV_{N+1}$, $FMLSHV_{N+1}$	**49**	**907**	67%	88%	66%	71%
$L3HV^{AVG}_{N+1} - Models$	$L3HV1_{N+1}$, $L3HV2_{N+1}$, $L3HV3_{N+1}$, $L3HV4_{N+1}$, $L3HV5_{N+1}$, $L3HV6_{N+1}$, $L3HV7_{N+1}$	14	419	13%	33%	29%	34%

Table C.2.18: Model Averaging for Replicating Portfolio Value Comparison: This table is compartmentalised into IV parts. Each part presents a performance comparison using daily and monthly statistics amongst the models mentioned in that part. The forecast variable for all the models is the one-trading-day-ahead replicating portfolio value (V_{N+1}). The $_{N+1}$ subscript denotes models that take an average of the V_{N+1} from models that forecast V_{N+1} using one-trading-day-ahead input variables. In the parts mentioned below, we compare the out-of-sample performance of the best model (based on the total number of days out of 1326 days that a particular model had the lowest RMSE) with the average of parametric models ($ParamHV_{N+1}^{AVG} - Models$), the average of the triple ($M3HV_{N+1}^{AVG} - Models$) hidden layer MLP models, and the average of the triple ($L3HV_{N+1}^{AVG} - Models$) hidden layer LSTM models. **In Part I**: The best model ($BSMHV_{N+1}$) from Table B.2.17 with $ParamHV_{N+1}^{AVG} - Models$, $M3HV_{N+1}^{AVG} - Models$, $L3HV_{N+1}^{AVG} - Models$, **in Part II**: The best model ($BSMHV_{N+1}$) from Table B.2.18 with $ParamHV_{N+1}^{AVG} - Models$, $M3HV_{N+1}^{AVG} - Models$, **in Part III**: The best model ($BSMHV_{N+1}$) from Table B.2.19 with $ParamHV_{N+1}^{AVG} - Models$, $L3HV_{N+1}^{AVG} - Models$, **in Part IV**: The best model ($BSMHV_{N+1}$) from Table B.2.20 with $ParamHV_{N+1}^{AVG} - Models$. The one-trading-day-ahead forecast errors of the V_{N+1} are used to compute the Root Mean Square Error (RMSE). Forecasts are made for 1,326 trading days, and there are 64 months covered in the sample using the monthly data. Column I identifies the models. When comparing all models simultaneously, column II reports the number of months out of the 64 months that each model has the smallest RMSE, while column III reports the number of days out of the 1,326 days each model has the smallest RMSE. Columns IV (lower bound) and V (upper bound) present the winning percentage out of 64 months for each model, evaluated using the bootstrap sampling technique. The statistical bootstrap performed (with replacement) at a 95% confidence level is computed from the monthly RMSE values of the respective models below. Columns VI (lower bound) and VII (upper bound) present the winning percentage out of 1326 days for each model computed from bootstrapping the daily RMSE values of the respective models at a 95% confidence level.

(I) Model	**(II) Performance amongst all models (Monthly)**	**(III) Performance amongst all models (Daily)**	**(IV) 2.5% lower bound-(for monthly) (%)**	**(V) 2.5% upper bound-(for monthly) (%)**	**(VI) 2.5% lower bound-(for daily) (%)**	**(VII) 2.5% upper bound-(for daily) (%)**
Part I: $BSMHV_{N+1}$ v/s $ParamHV_{N+1}^{AVG} - Models$ v/s $M3HV_{N+1}^{AVG} - Models$ v/s $L3HV_{N+1}^{AVG} - Models$						
$BSMHV_{N+1}$	**29**	**389**	33%	58%	27%	32%
$ParamHV_{N+1}^{AVG} - Models$	15	354	14%	34%	24%	29%
$M3HV_{N+1}^{AVG} - Models$	12	373	9%	30%	26%	30%
$L3HV_{N+1}^{AVG} - Models$	8	210	5%	20%	14%	18%
Part II: $BSMHV_{N+1}$ v/s $ParamHV_{N+1}^{AVG} - Models$ v/s $M3HV_{N+1}^{AVG} - Models$						
$BSMHV_{N+1}$	**33**	473	39%	63%	33%	38%
$ParamHV_{N+1}^{AVG} - Models$	15	366	14%	34%	25%	30%
$M3HV_{N+1}^{AVG} - Models$	16	**487**	14%	35%	34%	39%
Part III: $BSMHV_{N+1}$ v/s $ParamHV_{N+1}^{AVG} - Models$ v/s $L3HV_{N+1}^{AVG} - Models$						
$BSMHV_{N+1}$	**37**	**591**	45%	70%	42%	47%
$ParamHV_{N+1}^{AVG} - Models$	16	385	15%	36%	27%	32%
$L3HV_{N+1}^{AVG} - Models$	11	350	8%	27%	24%	29%
Part IV: $BSMHV_{N+1}$ v/s $ParamHV_{N+1}^{AVG} - Models$						
$BSMHV_{N+1}$	**47**	**910**	63%	84%	66%	71%
$ParamHV_{N+1}^{AVG} - Models$	17	416	16%	38%	29%	34%

C.2.4.3 $CHV^{AVG} - Models$: Model averaging replicating portfolio value performance of models that forecast the replicating portfolio value(V_{N+1}) computed using the analytically derived delta ($\delta C_{N+1}/\delta S_{N+1}$), and where the $\delta C_{N+1}/\delta S_{N+1}$ is inferred from models that forecast the call option price (C_{N+1}) using one-trading-day ahead input variables:

Table C.2.19 shows the relative out-of-sample replicating portfolio value performance (in $RMSE$) amongst the models that forecast the average one-trading-day-ahead replicating portfolio value (V_{N+1}). The V_{N+1} is computed from equation 3.17 using the forecasted one-trading-day-ahead delta ($\delta C_{N+1}/\delta S_{N+1}$), which is in turn derived analytically from C_{N+1} that were forecasted from models that use one-trading-day-ahead input variables. In column II of table C.2.19, we list the several models used as an input to obtain the average one-trading-day-ahead forecast of V_{N+1}. The performance metric is the $RMSE$ of the one-trading-day-ahead forecast errors of the average V_{N+1}, which is computed for each averaging model utilising all of the errors in each day or each month. Amongst all of the models, columns III and IV record the number of months and days, respectively, that each model has the lowest $RMSE$. We performed a bootstrap using the daily and monthly RMSEs to be certain of our results. Columns V (lower bound) and VI (upper bound) present the results from the bootstrap performed (with replacement) using monthly RMSEs at a 95% confidence level and show the winning percentage out of 64 months for each model, and similarly, the 95 % confidence intervals computed from bootstrapping of the daily RMSEs signifies the winning percentage out of 1326 days for each model and are reported in columns VII (lower bound), VIII (upper bound). After a model is found to outperform other individual parametric models, MLP and LSTM models in each of the several comparisons below, we look into whether that out-performing model individually can outperform the average V_{N+1} of all the parametric models combinedly, MLP models combinedly or LSTM models combinedly, covered in that section.

In the below several comparisons, even though a particular model wins by a higher percentage against other models, we investigated further these models pairwise by performing a pairwise bootstrap comparison, which was computed using the respective pair's daily RMSEs. The results are presented in Table 100 of the Electronic Appendix.

The Diebold-Mariano(DM) (Diebold and Mariano (1995)) test was performed on pairs amongst the average V_{N+1} of all parametric models ($ParamCHV_{N+1}^{AVG} - Models$), the average V_{N+1} of all triple hidden layer MLP models ($M3CHV_{N+1}^{AVG} - Models$), and the average V_{N+1} of all triple hidden layer LSTM models ($L3CHV_{N+1}^{AVG} - Models$) are reported in Table 90 of the Electronic Appendix. In constructing the DM tests, the model pairs are reported in column I and column II, and the DM test statistics for a particular pair are reported in column III. If the null can be rejected, a positive number suggests the rejection may be due to the second model being the better forecast model. In contrast, a negative value suggests the rejection may be due to the first model being the better forecast model. The model pairs highlighted in a red state that their forecasts have statistically insignificant differences in their prediction accuracy. Considering the DM-Test statistics in Table 90 of the Electronic Appendix, all the model pairs lead to the rejection of the null of equal forecasting performance.

The RMSEs for the models under the $CHV^{AVG} - Models$ category, which averages the forecasted V_{N+1} from models belonging to the $CHV - Models$ category(which uses the inferred $\delta C_{N+1}/\delta S_{N+1}$ to forecast the V_{N+1}, from models that forecast the C_{N+1} for the next trading day, using one-trading-day-ahead input variables) on a monthly, yearly, and overall basis can be found in the Electronic Appendix, in Tables 60, 70, and 80, respectively.

C.2.4.3.1 Comparison amongst all Parametric Models with Triple Hidden Layer ANN Models:

In this section, we compare the out-of-sample hedging performance of the parametric models ($ParamCHV_{N+1}^{AVG} - Models$), the triple hidden layer MLP models ($M3CHV_{N+1}^{AVG} - Models$), and the triple hidden layer LSTM models ($L3CHV_{N+1}^{AVG} - Models$), and then $ParamCHV_{N+1}^{AVG} - Models$ with the $M3CHV_{N+1}^{AVG} - Models$, and finally the $ParamCHV_{N+1}^{AVG} - Models$ with the $L3CHV_{N+1}^{AVG} - Models$.

Initially in Part I of Table C.2.19, we compared the $ParamCHV_{N+1}^{AVG} - Models$ with the $M3CHV_{N+1}^{AVG} - Models$ and the $L3CHV_{N+1}^{AVG} - Models$, and found that the $M3CHV_{N+1}^{AVG} - Models$ had the lowest $RMSE$ for 912 days (having a daily bootstrap winning % of 66% to 71%) out of 1,326. Accordingly, we now compare the $L3CHV4_{N+1}$ model (i.e. the best-performing model when compared to the models in column V of Table B.2.21) with the $ParamCHV_{N+1}^{AVG} - Models$, $M3CHV_{N+1}^{AVG} - Models$, and the $L3CHV_{N+1}^{AVG} - Models$ in Part I of Table C.2.20, and found that $M3CHV_{N+1}^{AVG} - Models$ had the lowest $RMSE$ for 721 days (having a daily bootstrap winning % of 51% to 57%) out of 1,326.

Secondly, in Part II of Table C.2.19, we compared the $ParamCHV_{N+1}^{AVG} - Models$ with the $M3CHV_{N+1}^{AVG} - Models$, and found that the $M3CHV_{N+1}^{AVG} - Models$ had the lowest $RMSE$ for 1,038 days (having a daily bootstrap winning % of 76% to 81%) out of 1,326. Accordingly, we now compare the $FMLSCHV_{N+1}$ model (i.e. the best-performing model when compared to the models in column V of Table B.2.22) with the $ParamCHV_{N+1}^{AVG} - Models$, and the $M3CHV_{N+1}^{AVG} - Models$ in Part II of Table C.2.20, and found that $M3CHV_{N+1}^{AVG} - Models$ had the lowest $RMSE$ for 655 days (having a daily bootstrap winning % of 47% to 52%) out of 1,326.

Finally, in Part III of Table C.2.19, we compared the $ParamCHV_{N+1}^{AVG} - Models$ with the $L3CHV_{N+1}^{AVG} - Models$, and found that the $ParamCHV_{N+1}^{AVG} - Models$ had the lowest $RMSE$ for 1134 days (having a daily bootstrap winning % of 84% to 87%) out of 1,326. Accordingly, we now compare the $HDJCHV_{N+1}$ model (i.e. the best-performing model when compared to the models in column V of Table B.2.23) with the $ParamCHV_{N+1}^{AVG} - Models$, and the $L3CHV_{N+1}^{AVG} - Models$ in Part III of Table C.2.20, and found that the $HDJCHV_{N+1}$ model had the lowest $RMSE$ for 839 days (having a daily bootstrap winning % of 60% to 66%) out of 1,326.

Thus, when the best individually out-performing model, the $L3CHV4_{N+1}$ model (from Table B.2.21) was compared to the average of all the parametric models, and the averages of all the triple hidden layer ANN models (in Part I of Table C.2.20), we conclude that the average of all the triple hidden layer models (i.e. $M3CHV_{N+1}^{AVG} - Models$) could outperform all other models. Similarly, when the best individually out-performing model, the $FMLSCHV_{N+1}$ model (from Table B.2.22) was compared to the average of all the parametric models, and the averages of all the triple hidden layer MLP models (in Part II of Table C.2.20), yet again the average of all the triple hidden layer models (i.e. $M3CHV_{N+1}^{AVG} - Models$) could outperform all other models. Lastly, when the best individually out-performing model, the $HJDCHV_{N+1}$ model (from Table B.2.23) was compared to the average of all the parametric models, and the averages of all the triple hidden layer LSTM models (in Part III of Table C.2.20), the $HJDCHV_{N+1}$ model could outperform all other models.

C.2.4.3.2 Comparison amongst all Parametric models:

We now compare the $HJDCHV_{N+1}$ model (i.e. the best-performing model when compared to the models in column V of Table B.2.24) with the $ParamCHV_{N+1}^{AVG} - Models$ in Part IV of Table C.2.20 and found that the $HJDCHV_{N+1}$ model had the lowest $RMSE$ for 962 days (having a daily bootstrap winning % of 70% to 75%) out of 1,326.

Thus, when the best individually out-performing model, the $HJDCHV_{N+1}$ model (from Table B.2.24) was compared to the average of all the parametric models (in Part IV of Table C.2.20), the $HJDCHV_{N+1}$ model could outperform the average of all the parametric models.

Table C.2.19: Monthly Replicating Portfolio Value Comparison (amongst $ParamCHV_{N+1}^{AVG} - Models$, $M3CHV_{N+1}^{AVG} - Models$, and $L3CHV_{N+1}^{AVG} - Models$): This table is compartmentalized into III parts, where each part presents a performance comparison using both daily and monthly statistics amongst the set of models mentioned in that part. The forecast variable for all the models is the one-trading-day-ahead replicating portfolio value (V_{N+1}). The $_{N+1}$ subscript denotes models that take an average of the V_{N+1} from models that forecast V_{N+1} using one-trading-day-ahead input variables. In the parts mentioned below, we compare the out-of-sample performance of the following models: **In Part I**: $ParamCHV_{N+1}^{AVG} - Models$, MLP $M3CHV_{N+1}^{AVG} - Models$, and LSTM $L3CHV_{N+1}^{AVG} - Models$, **in Part II**: $ParamCHV_{N+1}^{AVG} - Models$, and MLP $M3CHV_{N+1}^{AVG} - Models$, **in Part III**: $ParamCHV_{N+1}^{AVG} - Models$, and LSTM $L3CHV_{N+1}^{AVG} - Models$. The one-trading-day-ahead forecast errors of V_{N+1} are used to compute the Root Mean Square Error (RMSE). Column I identifies the models, and column II lists the models used as input to obtain the average one-trading-day-ahead forecast of V_{N+1}. Forecasts are made for 1,326 trading days, and there are 64 months covered in the sample using the monthly data. When comparing all models simultaneously, column III reports the number of months out of the 64 months that each model has the smallest RMSE, while column IV reports the number of days out of the 1,326 days each model has the smallest RMSE. Columns V (lower bound) and VI (upper bound) present the winning percentage out of 64 months for each model, evaluated using the bootstrap sampling technique. The statistical bootstrap performed (with replacement) at a 95% confidence level is computed from the monthly RMSE values of the respective models below. Columns VII (lower bound) and VIII (upper bound) present the winning percentage out of 1326 days for each model computed from bootstrapping the daily RMSE values of the respective models at a 95% confidence level.

(I) Model	**(II) Inputs**	**(III) Performance amongst all models (Monthly)**	**(IV) Performance amongst all models (Daily)**	**(V) 2.5% lower bound-(for monthly) (%)**	**(VI) 2.5% upper bound-(for monthly) (%)**	**(VII) 2.5% lower bound-(for daily) (%)**	**(VIII) 2.5% upper bound-(for daily) (%)**
Part I: $ParamCHV_{N+1}^{AVG} - Models$ v/s $M3CHV_{N+1}^{AVG} - Models$ v/s $L3CHV_{N+1}^{AVG} - Models$							
$ParamCHV_{N+1}^{AVG} - Models$	$BSMCHV_{N+1}$, $HCHV_{N+1}$, $HJDCHV_{N+1}$, $FMLSCHV_{N+1}$	0	284	0%	5%	19%	24%
$M3CHV_{N+1}^{AVG} - Models$	$M3CHV1_{N+1}$, $M3CHV2_{N+1}$, $M3CHV3_{N+1}$, $M3CHV4_{N+1}$, $M3CHV5_{N+1}$, $M3CHV6_{N+1}$, $M3CHV7_{N+1}$	**63**	**912**	95%	100%	66%	71%
$L3CHV_{N+1}^{AVG} - Models$	$L3CHV1_{N+1}$, $L3CHV2_{N+1}$, $L3CHV3_{N+1}$, $L3CHV4_{N+1}$, $L3CHV5_{N+1}$, $L3CHV6_{N+1}$, $L3CHV7_{N+1}$	0	132	0%	0%	8%	11%
Part II: $ParamCHV_{N+1}^{AVG} - Models$ v/s $M3CHV_{N+1}^{AVG} - Models$							
$ParamCHV_{N+1}^{AVG} - Models$	$BSMCHV_{N+1}$, $HCHV_{N+1}$, $HJDCHV_{N+1}$, $FMLSCHV_{N+1}$	0	288	0%	5%	19%	24%
$M3CHV_{N+1}^{AVG} - Models$	$M3CHV1_{N+1}$, $M3CHV2_{N+1}$, $M3CHV3_{N+1}$, $M3CHV4_{N+1}$, $M3CHV5_{N+1}$, $M3CHV6_{N+1}$, $M3CHV7_{N+1}$	**63**	**1038**	95%	100%	76%	81%
Part III: $ParamCHV_{N+1}^{AVG} - Models$ v/s $L3CHV_{N+1}^{AVG} - Models$							
$ParamCHV_{N+1}^{AVG} - Models$	$BSMCHV_{N+1}$, $HCHV_{N+1}$, $HJDCHV_{N+1}$, $FMLSCHV_{N+1}$	**63**	**1134**	100%	100%	84%	87%
$L3CHV_{N+1}^{AVG} - Models$	$L3CHV1_{N+1}$, $L3CHV2_{N+1}$, $L3CHV3_{N+1}$, $L3CHV4_{N+1}$, $L3CHV5_{N+1}$, $L3CHV6_{N+1}$, $L3CHV7_{N+1}$	0	192	0%	0%	13%	16%

Table C.2.20: Model Averaging for Replicating Portfolio Value Comparison: This table is compartmentalised into IV parts. Each part presents a performance comparison using daily and monthly statistics amongst the models mentioned in that part. The forecast variable for all the models is the one-trading-day-ahead replicating portfolio value (V_{N+1}). The $_{N+1}$ subscript denotes models that take an average of the V_{N+1} from models that forecast V_{N+1} using one-trading-day-ahead input variables. In the parts mentioned below, we compare the out-of-sample performance of the best model (based on the total number of days out of 1326 days that a particular model had the lowest RMSE) with the average of parametric models ($ParamCHV_{N+1}^{AVG} - Models$), the average of the triple ($M3CHV_{N+1}^{AVG} - Models$) hidden layer MLP models, and the average of the triple ($L3CHV_{N+1}^{AVG} - Models$) hidden layer LSTM models. **In Part I**: The best model ($L3CHV4_{N+1}$) from Table B.2.21 with $ParamCHV_{N+1}^{AVG} - Models$, $M3CHV_{N+1}^{AVG} - Models$, $L3CHV_{N+1}^{AVG} - Models$, **in Part II**: The best model ($FMLSCCHV_{N+1}$) from Table B.2.22 with $ParamCHV_{N+1}^{AVG} - Models$, $M3CHV_{N+1}^{AVG} - Models$, **in Part III**: The best model ($HJDCCHV_{N+1}$) from Table B.2.23 with $ParamCHV_{N+1}^{AVG} - Models$, $L3CHV_{N+1}^{AVG} - Models$, **in Part IV**: The best model ($HJDCCHV_{N+1}$) from Table B.2.24 with $ParamCHV_{N+1}^{AVG} - Models$. The one-trading-day-ahead forecast errors of the V_{N+1} are used to compute the Root Mean Square Error (RMSE). Forecasts are made for 1,326 trading days, and there are 64 months covered in the sample using the monthly data. Column I identifies the models. When comparing all models simultaneously, column II reports the number of months out of the 64 months that each model has the smallest RMSE, while column III reports the number of days out of the 1,326 days each model has the smallest RMSE. Columns IV (lower bound) and V (upper bound) present the winning percentage out of 64 months for each model, evaluated using the bootstrap sampling technique. The statistical bootstrap performed (with replacement) at a 95% confidence level is computed from the monthly RMSE values of the respective models below. Columns VI (lower bound) and VII (upper bound) present the winning percentage out of 1326 days for each model computed from bootstrapping the daily RMSE values of the respective models at a 95% confidence level.

(I) Model	**(II)** Performance amongst all models (Monthly)	**(III)** Performance amongst all models (Daily)	**(IV)** 2.5% lower bound (for monthly) (%)	**(V)** 2.5% upper bound (for monthly) (%)	**(VI)** 2.5% lower bound (for daily) (%)	**(VII)** 2.5% upper bound (for daily) (%)
Part I: $L3CHV4_{N+1}$ v/s $ParamCHV_{N+1}^{AVG} - Models$ v/s $M3CHV_{N+1}^{AVG} - Models$ v/s $L3CHV_{N+1}^{AVG} - Models$						
$L3CHV4_{N+1}$	1	369	0%	5%	25%	30%
$ParamCHV_{N+1}^{AVG} - Models$	0	153	0%	0%	10%	13%
$M3CHV_{N+1}^{AVG} - Models$	**63**	**721**	95%	100%	51%	57%
$L3CHV_{N+1}^{AVG} - Models$	0	87	0%	0%	5%	8%
Part II: $FMLSCHV_{N+1}$ v/s $ParamCHV_{N+1}^{AVG} - Models$ v/s $M3CHV_{N+1}^{AVG} - Models$						
$FMLSCHV_{N+1}$	0	384	0%	0%	27%	31%
$ParamCHV_{N+1}^{AVG} - Models$	0	287	0%	0%	19%	24%
$M3CHV_{N+1}^{AVG} - Models$	**64**	**655**	100%	100%	47%	52%
Part III: $HJDCHV_{N+1}$ v/s $ParamCHV_{N+1}^{AVG} - Models$ v/s $L3CHV_{N+1}^{AVG} - Models$						
$HJDCHV_{N+1}$	**63**	**839**	95%	100%	60%	66%
$ParamCHV_{N+1}^{AVG} - Models$	1	360	0%	5%	25%	30%
$L3CHV_{N+1}^{AVG} - Models$	0	127	0%	0%	8%	11%
Part IV: $HJDCHV_{N+1}$ v/s $ParamCHV_{N+1}^{AVG} - Models$						
$HJDCHV_{N+1}$	**63**	**962**	95%	100%	70%	75%
$ParamCHV_{N+1}^{AVG} - Models$	1	364	0%	5%	25%	30%

Appendix D.1

Appendix for Chapter 5: Tables and Graphs

Table D.1.1: This table presents the summary statistics of the 11 Equity ETFs from which 8 ETF pairs have been formed and back-tested in Chapter 5

(I) **Symbol**	**(II)** **ETF Name**	**(III)** **Asset Class**	**(IV)** **Total Assets ($, Million)**	**(V)** **Avg. Daily Volume**
QQQ	Invesco QQQ Trust	Equity	177,010	39,229,028
VWO	Vanguard FTSE Emerging Markets ETF	Equity	84,079	8,201,537
IWF	iShares Russell 1000 Growth ETF	Equity	69,189	1,308,928
VO	Vanguard Mid-Cap ETF	Equity	49,891	550,526
VXUS	Vanguard Total International Stock ETF	Equity	48,255	2,933,415
ITOT	iShares Core S&P Total U.S. Stock Market ETF	Equity	40,106	1,463,958
IXUS	iShares Core MSCI Total International Stock ETF	Equity	29,536	1,460,634
USMV	iShares MSCI USA Min Vol Factor ETF	Equity	27,559	3,037,369
SCHF	Schwab International Equity ETF	Equity	26,988	2,650,951
XLE	Energy Select Sector SPDR Fund	Equity	25,467	28,604,568
SCHB	Schwab U.S. Broad Market ETF	Equity	21,501	451,023

Table D.1.2: This table is compartmentalized into IX parts, where each part mentions the inputs used for the respective trading strategies. In Part I, the spread that is used as an input for these trading strategies is derived from the $DIST^{V1.1}$ model, in Part II from the $DIST^{V1.2}$ model, in Part III from the $DIST^{V2}$ model, in Part IV from the $DIST^{V3}$ model, in Part V from the $DIST^{V4}$ model, in Part VI from the $JOHANSEN - SPRD$ model, in Part VIII from the $ADF - SPRD$ model, in from the $DIST^{V2}$ model, in Part VIII from the $KALMAN - SPRD$ model, and in Part IX from the $RATIO - SPRD$ model. Column I identifies the strategy code, column II, III and IV mentions the trading strategies based on the 30, 50 and 100-day rolling windows, respectively, and Column V mentions the input used for computing the trading strategies mentioned in column II, III and IV.

(I) **Strategy Code**	**(II)** **30-day rolling window based trading strategies**	**(III)** **50-day rolling window based trading strategies**	**(IV)** **100-day rolling window based trading strategies**	**(V)** **Underlying spread used for 30, 50 and 100-day rolling window based trading strategies**
		Part I: Models based on $DIST^{V1.1} - SPRD$		
A1.1	$DIST^{V1.1} - ZSPRD^{30D}_{(3,2)}$	$DIST^{V1.1} - ZSPRD^{50D}_{(3,2)}$	$DIST^{V1.1} - ZSPRD^{100D}_{(3,2)}$	
A1.2	$DIST^{V1.1} - ZSPRD^{30D}_{(3,1)}$	$DIST^{V1.1} - ZSPRD^{50D}_{(3,1)}$	$DIST^{V1.1} - ZSPRD^{100D}_{(3,1)}$	
A1.3	$DIST^{V1.1} - ZSPRD^{30D}_{(3,0.5)}$	$DIST^{V1.1} - ZSPRD^{50D}_{(3,0.5)}$	$DIST^{V1.1} - ZSPRD^{100D}_{(3,0.5)}$	
A1.4	$DIST^{V1.1} - ZSPRD^{30D}_{(2,7,2)}$	$DIST^{V1.1} - ZSPRD^{50D}_{(2,7,2)}$	$DIST^{V1.1} - ZSPRD^{100D}_{(2,7,2)}$	
A1.5	$DIST^{V1.1} - ZSPRD^{30D}_{(2,7,1)}$	$DIST^{V1.1} - ZSPRD^{50D}_{(2,7,1)}$	$DIST^{V1.1} - ZSPRD^{100D}_{(2,7,1)}$	
A1.6	$DIST^{V1.1} - ZSPRD^{30D}_{(2,7,0.5)}$	$DIST^{V1.1} - ZSPRD^{50D}_{(2,7,0.5)}$	$DIST^{V1.1} - ZSPRD^{100D}_{(2,7,0.5)}$	$DIST^{V1.1} - SPRD$
A2.1	$DIST^{V1.1} - SPRD^{30D} - SMA_{(10,20)}$	$DIST^{V1.1} - SPRD^{50D} - SMA_{(10,20)}$	$DIST^{V1.1} - SPRD^{100D} - SMA_{(10,20)}$	
A2.2	$DIST^{V1.1} - SPRD^{30D} - EMA_{(10,20)}$	$DIST^{V1.1} - SPRD^{50D} - EMA_{(10,20)}$	$DIST^{V1.1} - SPRD^{100D} - EMA_{(10,20)}$	
A2.3	$DIST^{V1.1} - SPRD^{30D} - MACD_{(12,26,9)}$	$DIST^{V1.1} - SPRD^{50D} - MACD_{(12,26,9)}$	$DIST^{V1.1} - SPRD^{100D} - MACD_{(12,26,9)}$	
A2.4	$DIST^{V1.1} - SPRD^{30D} - RSI_{(14)}$	$DIST^{V1.1} - SPRD^{50D} - RSI_{(14)}$	$DIST^{V1.1} - SPRD^{100D} - RSI_{(14)}$	
A2.5	$DIST^{V1.1} - SPRD^{30D} - BB_{(20)}$	$DIST^{V1.1} - SPRD^{50D} - BB_{(20)}$	$DIST^{V1.1} - SPRD^{100D} - BB_{(20)}$	
A3	$DIST^{V1.1} - SPRD^{30D} - DECTREE$	$DIST^{V1.1} - SPRD^{50D} - DECTREE$	$DIST^{V1.1} - SPRD^{100D} - DECTREE$	Discussed in Table D.1.3
A4	$DIST^{V1.1} - SPRD^{30D} - MLP$	$DIST^{V1.1} - SPRD^{50D} - MLP$	$DIST^{V1.1} - SPRD^{100D} - MLP$	Discussed in Table D.1.3
		Part II: Models based on $DIST^{V1.2} - SPRD$		
B1.1	$DIST^{V1.2} - ZSPRD^{30D}_{(3,2)}$	$DIST^{V1.2} - ZSPRD^{50D}_{(3,2)}$	$DIST^{V1.2} - ZSPRD^{100D}_{(3,2)}$	
B1.2	$DIST^{V1.2} - ZSPRD^{30D}_{(3,1)}$	$DIST^{V1.2} - ZSPRD^{50D}_{(3,1)}$	$DIST^{V1.2} - ZSPRD^{100D}_{(3,1)}$	
B1.3	$DIST^{V1.2} - ZSPRD^{30D}_{(3,0.5)}$	$DIST^{V1.2} - ZSPRD^{50D}_{(3,0.5)}$	$DIST^{V1.2} - ZSPRD^{100D}_{(3,0.5)}$	
B1.4	$DIST^{V1.2} - ZSPRD^{30D}_{(2,7,2)}$	$DIST^{V1.2} - ZSPRD^{50D}_{(2,7,2)}$	$DIST^{V1.2} - ZSPRD^{100D}_{(2,7,2)}$	
B1.5	$DIST^{V1.2} - ZSPRD^{30D}_{(2,7,1)}$	$DIST^{V1.2} - ZSPRD^{50D}_{(2,7,1)}$	$DIST^{V1.2} - ZSPRD^{100D}_{(2,7,1)}$	
B1.6	$DIST^{V1.2} - ZSPRD^{30D}_{(2,7,0.5)}$	$DIST^{V1.2} - ZSPRD^{50D}_{(2,7,0.5)}$	$DIST^{V1.2} - ZSPRD^{100D}_{(2,7,0.5)}$	$DIST^{V1.2} - SPRD$
B2.1	$DIST^{V1.2} - SPRD^{30D} - SMA_{(10,20)}$	$DIST^{V1.2} - SPRD^{50D} - SMA_{(10,20)}$	$DIST^{V1.2} - SPRD^{100D} - SMA_{(10,20)}$	
B2.2	$DIST^{V1.2} - SPRD^{30D} - EMA_{(10,20)}$	$DIST^{V1.2} - SPRD^{50D} - EMA_{(10,20)}$	$DIST^{V1.2} - SPRD^{100D} - EMA_{(10,20)}$	
B2.3	$DIST^{V1.2} - SPRD^{30D} - MACD_{(12,26,9)}$	$DIST^{V1.2} - SPRD^{50D} - MACD_{(12,26,9)}$	$DIST^{V1.2} - SPRD^{100D} - MACD_{(12,26,9)}$	
B2.4	$DIST^{V1.2} - SPRD^{30D} - RSI_{(14)}$	$DIST^{V1.2} - SPRD^{50D} - RSI_{(14)}$	$DIST^{V1.2} - SPRD^{100D} - RSI_{(14)}$	
B2.5	$DIST^{V1.2} - SPRD^{30D} - BB_{(20)}$	$DIST^{V1.2} - SPRD^{50D} - BB_{(20)}$	$DIST^{V1.2} - SPRD^{100D} - BB_{(20)}$	
B3	$DIST^{V1.2} - SPRD^{30D} - DECTREE$	$DIST^{V1.2} - SPRD^{50D} - DECTREE$	$DIST^{V1.2} - SPRD^{100D} - DECTREE$	Discussed in Table D.1.3
B4	$DIST^{V1.2} - SPRD^{30D} - MLP$	$DIST^{V1.2} - SPRD^{50D} - MLP$	$DIST^{V1.2} - SPRD^{100D} - MLP$	Discussed in Table D.1.3
		Part III: Models based on $DIST^{V2} - SPRD$		
C1.1	$DIST^{V2} - ZSPRD^{30D}_{(3,2)}$	$DIST^{V2} - ZSPRD^{50D}_{(3,2)}$	$DIST^{V2} - ZSPRD^{100D}_{(3,2)}$	
C1.2	$DIST^{V2} - ZSPRD^{30D}_{(3,1)}$	$DIST^{V2} - ZSPRD^{50D}_{(3,1)}$	$DIST^{V2} - ZSPRD^{100D}_{(3,1)}$	
C1.3	$DIST^{V2} - ZSPRD^{30D}_{(3,0.5)}$	$DIST^{V2} - ZSPRD^{50D}_{(3,0.5)}$	$DIST^{V2} - ZSPRD^{100D}_{(3,0.5)}$	
C1.4	$DIST^{V2} - ZSPRD^{30D}_{(2,7,2)}$	$DIST^{V2} - ZSPRD^{50D}_{(2,7,2)}$	$DIST^{V2} - ZSPRD^{100D}_{(2,7,2)}$	
C1.5	$DIST^{V2} - ZSPRD^{30D}_{(2,7,1)}$	$DIST^{V2} - ZSPRD^{50D}_{(2,7,1)}$	$DIST^{V2} - ZSPRD^{100D}_{(2,7,1)}$	
C1.6	$DIST^{V2} - ZSPRD^{30D}_{(2,7,0.5)}$	$DIST^{V2} - ZSPRD^{50D}_{(2,7,0.5)}$	$DIST^{V2} - ZSPRD^{100D}_{(2,7,0.5)}$	$DIST^{V2} - SPRD$
C2.1	$DIST^{V2} - SPRD^{30D} - SMA_{(10,20)}$	$DIST^{V2} - SPRD^{50D} - SMA_{(10,20)}$	$DIST^{V2} - SPRD^{100D} - SMA_{(10,20)}$	
C2.2	$DIST^{V2} - SPRD^{30D} - EMA_{(10,20)}$	$DIST^{V2} - SPRD^{50D} - EMA_{(10,20)}$	$DIST^{V2} - SPRD^{100D} - EMA_{(10,20)}$	
C2.3	$DIST^{V2} - SPRD^{30D} - MACD_{(12,26,9)}$	$DIST^{V2} - SPRD^{50D} - MACD_{(12,26,9)}$	$DIST^{V2} - SPRD^{100D} - MACD_{(12,26,9)}$	
C2.4	$DIST^{V2} - SPRD^{30D} - RSI_{(14)}$	$DIST^{V2} - SPRD^{50D} - RSI_{(14)}$	$DIST^{V2} - SPRD^{100D} - RSI_{(14)}$	
C2.5	$DIST^{V2} - SPRD^{30D} - BB_{(20)}$	$DIST^{V2} - SPRD^{50D} - BB_{(20)}$	$DIST^{V2} - SPRD^{100D} - BB_{(20)}$	
C3	$DIST^{V2} - SPRD^{30D} - DECTREE$	$DIST^{V2} - SPRD^{50D} - DECTREE$	$DIST^{V2} - SPRD^{100D} - DECTREE$	Discussed in Table D.1.3
C4	$DIST^{V2} - SPRD^{30D} - MLP$	$DIST^{V2} - SPRD^{50D} - MLP$	$DIST^{V2} - SPRD^{100D} - MLP$	Discussed in Table D.1.3
		Part IV: Models based on $DIST^{V3} - SPRD$		
D1.1	$DIST^{V3} - ZSPRD^{30D}_{(3,2)}$	$DIST^{V3} - ZSPRD^{50D}_{(3,2)}$	$DIST^{V3} - ZSPRD^{100D}_{(3,2)}$	
D1.2	$DIST^{V3} - ZSPRD^{30D}_{(3,1)}$	$DIST^{V3} - ZSPRD^{50D}_{(3,1)}$	$DIST^{V3} - ZSPRD^{100D}_{(3,1)}$	
D1.3	$DIST^{V3} - ZSPRD^{30D}_{(3,0.5)}$	$DIST^{V3} - ZSPRD^{50D}_{(3,0.5)}$	$DIST^{V3} - ZSPRD^{100D}_{(3,0.5)}$	
D1.4	$DIST^{V3} - ZSPRD^{30D}_{(2,7,2)}$	$DIST^{V3} - ZSPRD^{50D}_{(2,7,2)}$	$DIST^{V3} - ZSPRD^{100D}_{(2,7,2)}$	
D1.5	$DIST^{V3} - ZSPRD^{30D}_{(2,7,1)}$	$DIST^{V3} - ZSPRD^{50D}_{(2,7,1)}$	$DIST^{V3} - ZSPRD^{100D}_{(2,7,1)}$	
D1.6	$DIST^{V3} - ZSPRD^{30D}_{(2,7,0.5)}$	$DIST^{V3} - ZSPRD^{50D}_{(2,7,0.5)}$	$DIST^{V3} - ZSPRD^{100D}_{(2,7,0.5)}$	$DIST^{V3} - SPRD$
D2.1	$DIST^{V3} - SPRD^{30D} - SMA_{(10,20)}$	$DIST^{V3} - SPRD^{50D} - SMA_{(10,20)}$	$DIST^{V3} - SPRD^{100D} - SMA_{(10,20)}$	
D2.2	$DIST^{V3} - SPRD^{30D} - EMA_{(10,20)}$	$DIST^{V3} - SPRD^{50D} - EMA_{(10,20)}$	$DIST^{V3} - SPRD^{100D} - EMA_{(10,20)}$	
D2.3	$DIST^{V3} - SPRD^{30D} - MACD_{(12,26,9)}$	$DIST^{V3} - SPRD^{50D} - MACD_{(12,26,9)}$	$DIST^{V3} - SPRD^{100D} - MACD_{(12,26,9)}$	
D2.4	$DIST^{V3} - SPRD^{30D} - RSI_{(14)}$	$DIST^{V3} - SPRD^{50D} - RSI_{(14)}$	$DIST^{V3} - SPRD^{100D} - RSI_{(14)}$	
D2.5	$DIST^{V3} - SPRD^{30D} - BB_{(20)}$	$DIST^{V3} - SPRD^{50D} - BB_{(20)}$	$DIST^{V3} - SPRD^{100D} - BB_{(20)}$	
D3	$DIST^{V3} - SPRD^{30D} - DECTREE$	$DIST^{V3} - SPRD^{50D} - DECTREE$	$DIST^{V3} - SPRD^{100D} - DECTREE$	Discussed in Table D.1.3
D4	$DIST^{V3} - SPRD^{30D} - MLP$	$DIST^{V3} - SPRD^{50D} - MLP$	$DIST^{V3} - SPRD^{100D} - MLP$	Discussed in Table D.1.3
		Part V: Models based on $DIST^{V4} - SPRD$		
E1.1	$DIST^{V4} - ZSPRD^{30D}_{(3,2)}$	$DIST^{V4} - ZSPRD^{50D}_{(3,2)}$	$DIST^{V4} - ZSPRD^{100D}_{(3,2)}$	
E1.2	$DIST^{V4} - ZSPRD^{30D}_{(3,1)}$	$DIST^{V4} - ZSPRD^{50D}_{(3,1)}$	$DIST^{V4} - ZSPRD^{100D}_{(3,1)}$	
E1.3	$DIST^{V4} - ZSPRD^{30D}_{(3,0.5)}$	$DIST^{V4} - ZSPRD^{50D}_{(3,0.5)}$	$DIST^{V4} - ZSPRD^{100D}_{(3,0.5)}$	
E1.4	$DIST^{V4} - ZSPRD^{30D}_{(2,7,2)}$	$DIST^{V4} - ZSPRD^{50D}_{(2,7,2)}$	$DIST^{V4} - ZSPRD^{100D}_{(2,7,2)}$	
E1.5	$DIST^{V4} - ZSPRD^{30D}_{(2,7,1)}$	$DIST^{V4} - ZSPRD^{50D}_{(2,7,1)}$	$DIST^{V4} - ZSPRD^{100D}_{(2,7,1)}$	
E1.6	$DIST^{V4} - ZSPRD^{30D}_{(2,7,0.5)}$	$DIST^{V4} - ZSPRD^{50D}_{(2,7,0.5)}$	$DIST^{V4} - ZSPRD^{100D}_{(2,7,0.5)}$	$DIST^{V4} - SPRD$
E2.1	$DIST^{V4} - SPRD^{30D} - SMA_{(10,20)}$	$DIST^{V4} - SPRD^{50D} - SMA_{(10,20)}$	$DIST^{V4} - SPRD^{100D} - SMA_{(10,20)}$	
E2.2	$DIST^{V4} - SPRD^{30D} - EMA_{(10,20)}$	$DIST^{V4} - SPRD^{50D} - EMA_{(10,20)}$	$DIST^{V4} - SPRD^{100D} - EMA_{(10,20)}$	
E2.3	$DIST^{V4} - SPRD^{30D} - MACD_{(12,26,9)}$	$DIST^{V4} - SPRD^{50D} - MACD_{(12,26,9)}$	$DIST^{V4} - SPRD^{100D} - MACD_{(12,26,9)}$	
E2.4	$DIST^{V4} - SPRD^{30D} - RSI_{(14)}$	$DIST^{V4} - SPRD^{50D} - RSI_{(14)}$	$DIST^{V4} - SPRD^{100D} - RSI_{(14)}$	
E2.5	$DIST^{V4} - SPRD^{30D} - BB_{(20)}$	$DIST^{V4} - SPRD^{50D} - BB_{(20)}$	$DIST^{V4} - SPRD^{100D} - BB_{(20)}$	
E3	$DIST^{V4} - SPRD^{30D} - DECTREE$	$DIST^{V4} - SPRD^{50D} - DECTREE$	$DIST^{V4} - SPRD^{100D} - DECTREE$	Discussed in Table D.1.3
E4	$DIST^{V4} - SPRD^{30D} - MLP$	$DIST^{V4} - SPRD^{50D} - MLP$	$DIST^{V4} - SPRD^{100D} - MLP$	Discussed in Table D.1.3
		Part VI: Models based on $JOHANSEN - SPRD$		
F1.1	$JOHANSEN - ZSPRD^{30D}_{(3,2)}$	$JOHANSEN - ZSPRD^{50D}_{(3,2)}$	$JOHANSEN - ZSPRD^{100D}_{(3,2)}$	
F1.2	$JOHANSEN - ZSPRD^{30D}_{(3,1)}$	$JOHANSEN - ZSPRD^{50D}_{(3,1)}$	$JOHANSEN - ZSPRD^{100D}_{(3,1)}$	
F1.3	$JOHANSEN - ZSPRD^{30D}_{(3,0.5)}$	$JOHANSEN - ZSPRD^{50D}_{(3,0.5)}$	$JOHANSEN - ZSPRD^{100D}_{(3,0.5)}$	
F1.4	$JOHANSEN - ZSPRD^{30D}_{(2,7,2)}$	$JOHANSEN - ZSPRD^{50D}_{(2,7,2)}$	$JOHANSEN - ZSPRD^{100D}_{(2,7,2)}$	
F1.5	$JOHANSEN - ZSPRD^{30D}_{(2,7,1)}$	$JOHANSEN - ZSPRD^{50D}_{(2,7,1)}$	$JOHANSEN - ZSPRD^{100D}_{(2,7,1)}$	
F1.6	$JOHANSEN - ZSPRD^{30D}_{(2,7,0.5)}$	$JOHANSEN - ZSPRD^{50D}_{(2,7,0.5)}$	$JOHANSEN - ZSPRD^{100D}_{(2,7,0.5)}$	$JOHANSEN - SPRD$
F2.1	$JOHANSEN - SPRD^{30D} - SMA_{(10,20)}$	$JOHANSEN - SPRD^{50D} - SMA_{(10,20)}$	$JOHANSEN - SPRD^{100D} - SMA_{(10,20)}$	
F2.2	$JOHANSEN - SPRD^{30D} - EMA_{(10,20)}$	$JOHANSEN - SPRD^{50D} - EMA_{(10,20)}$	$JOHANSEN - SPRD^{100D} - EMA_{(10,20)}$	
F2.3	$JOHANSEN - SPRD^{30D} - MACD_{(12,26,9)}$	$JOHANSEN - SPRD^{50D} - MACD_{(12,26,9)}$	$JOHANSEN - SPRD^{100D} - MACD_{(12,26,9)}$	
F2.4	$JOHANSEN - SPRD^{30D} - RSI_{(14)}$	$JOHANSEN - SPRD^{50D} - RSI_{(14)}$	$JOHANSEN - SPRD^{100D} - RSI_{(14)}$	
F2.5	$JOHANSEN - SPRD^{30D} - BB_{(20)}$	$JOHANSEN - SPRD^{50D} - BB_{(20)}$	$JOHANSEN - SPRD^{100D} - BB_{(20)}$	
F3	$JOHANSEN - SPRD^{30D} - DECTREE$	$JOHANSEN - SPRD^{50D} - DECTREE$	$JOHANSEN - SPRD^{100D} - DECTREE$	Discussed in Table D.1.3
F4	$JOHANSEN - SPRD^{30D} - MLP$	$JOHANSEN - SPRD^{50D} - MLP$	$JOHANSEN - SPRD^{100D} - MLP$	Discussed in Table D.1.3
		Part VII: Models based on $ADF - SPRD$		
G1.1	$ADF - ZSPRD^{30D}_{(3,2)}$	$ADF - ZSPRD^{50D}_{(3,2)}$	$ADF - ZSPRD^{100D}_{(3,2)}$	
G1.2	$ADF - ZSPRD^{30D}_{(3,1)}$	$ADF - ZSPRD^{50D}_{(3,1)}$	$ADF - ZSPRD^{100D}_{(3,1)}$	
G1.3	$ADF - ZSPRD^{30D}_{(3,0.5)}$	$ADF - ZSPRD^{50D}_{(3,0.5)}$	$ADF - ZSPRD^{100D}_{(3,0.5)}$	
G1.4	$ADF - ZSPRD^{30D}_{(2,7,2)}$	$ADF - ZSPRD^{50D}_{(2,7,2)}$	$ADF - ZSPRD^{100D}_{(2,7,2)}$	
G1.5	$ADF - ZSPRD^{30D}_{(2,7,1)}$	$ADF - ZSPRD^{50D}_{(2,7,1)}$	$ADF - ZSPRD^{100D}_{(2,7,1)}$	
G1.6	$ADF - ZSPRD^{30D}_{(2,7,0.5)}$	$ADF - ZSPRD^{50D}_{(2,7,0.5)}$	$ADF - ZSPRD^{100D}_{(2,7,0.5)}$	$ADF - SPRD$
G2.1	$ADF - SPRD^{30D} - SMA_{(10,20)}$	$ADF - SPRD^{50D} - SMA_{(10,20)}$	$ADF - SPRD^{100D} - SMA_{(10,20)}$	
G2.2	$ADF - SPRD^{30D} - EMA_{(10,20)}$	$ADF - SPRD^{50D} - EMA_{(10,20)}$	$ADF - SPRD^{100D} - EMA_{(10,20)}$	
G2.3	$ADF - SPRD^{30D} - MACD_{(12,26,9)}$	$ADF - SPRD^{50D} - MACD_{(12,26,9)}$	$ADF - SPRD^{100D} - MACD_{(12,26,9)}$	
G2.4	$ADF - SPRD^{30D} - RSI_{(14)}$	$ADF - SPRD^{50D} - RSI_{(14)}$	$ADF - SPRD^{100D} - RSI_{(14)}$	
G2.5	$ADF - SPRD^{30D} - BB_{(20)}$	$ADF - SPRD^{50D} - BB_{(20)}$	$ADF - SPRD^{100D} - BB_{(20)}$	
G3	$ADF - SPRD^{30D} - DECTREE$	$ADF - SPRD^{50D} - DECTREE$	$ADF - SPRD^{100D} - DECTREE$	Discussed in Table D.1.3
G4	$ADF - SPRD^{30D} - MLP$	$ADF - SPRD^{50D} - MLP$	$ADF - SPRD^{100D} - MLP$	Discussed in Table D.1.3
		Part VIII: Models based on $KALMAN - SPRD$		
H1.1	$KALMAN - ZSPRD^{30D}_{(3,2)}$	$KALMAN - ZSPRD^{50D}_{(3,2)}$	$KALMAN - ZSPRD^{100D}_{(3,2)}$	
H1.2	$KALMAN - ZSPRD^{30D}_{(3,1)}$	$KALMAN - ZSPRD^{50D}_{(3,1)}$	$KALMAN - ZSPRD^{100D}_{(3,1)}$	
H1.3	$KALMAN - ZSPRD^{30D}_{(3,0.5)}$	$KALMAN - ZSPRD^{50D}_{(3,0.5)}$	$KALMAN - ZSPRD^{100D}_{(3,0.5)}$	
H1.4	$KALMAN - ZSPRD^{30D}_{(2,7,2)}$	$KALMAN - ZSPRD^{50D}_{(2,7,2)}$	$KALMAN - ZSPRD^{100D}_{(2,7,2)}$	
H1.5	$KALMAN - ZSPRD^{30D}_{(2,7,1)}$	$KALMAN - ZSPRD^{50D}_{(2,7,1)}$	$KALMAN - ZSPRD^{100D}_{(2,7,1)}$	
H1.6	$KALMAN - ZSPRD^{30D}_{(2,7,0.5)}$	$KALMAN - ZSPRD^{50D}_{(2,7,0.5)}$	$KALMAN - ZSPRD^{100D}_{(2,7,0.5)}$	$KALMAN - SPRD$
H2.1	$KALMAN - SPRD^{30D} - SMA_{(10,20)}$	$KALMAN - SPRD^{50D} - SMA_{(10,20)}$	$KALMAN - SPRD^{100D} - SMA_{(10,20)}$	
H2.2	$KALMAN - SPRD^{30D} - EMA_{(10,20)}$	$KALMAN - SPRD^{50D} - EMA_{(10,20)}$	$KALMAN - SPRD^{100D} - EMA_{(10,20)}$	
H2.3	$KALMAN - SPRD^{30D} - MACD_{(12,26,9)}$	$KALMAN - SPRD^{50D} - MACD_{(12,26,9)}$	$KALMAN - SPRD^{100D} - MACD_{(12,26,9)}$	
H2.4	$KALMAN - SPRD^{30D} - RSI_{(14)}$	$KALMAN - SPRD^{50D} - RSI_{(14)}$	$KALMAN - SPRD^{100D} - RSI_{(14)}$	
H2.5	$KALMAN - SPRD^{30D} - BB_{(20)}$	$KALMAN - SPRD^{50D} - BB_{(20)}$	$KALMAN - SPRD^{100D} - BB_{(20)}$	
H3	$KALMAN - SPRD^{30D} - DECTREE$	$KALMAN - SPRD^{50D} - DECTREE$	$KALMAN - SPRD^{100D} - DECTREE$	Discussed in Table D.1.3
H4	$KALMAN - SPRD^{30D} - MLP$	$KALMAN - SPRD^{50D} - MLP$	$KALMAN - SPRD^{100D} - MLP$	Discussed in Table D.1.3
		Part IX: Models based on $RATIO - SPRD$		
I1.1	$RATIO - ZSPRD^{30D}_{(3,2)}$	$RATIO - ZSPRD^{50D}_{(3,2)}$	$RATIO - ZSPRD^{100D}_{(3,2)}$	
I1.2	$RATIO - ZSPRD^{30D}_{(3,1)}$	$RATIO - ZSPRD^{50D}_{(3,1)}$	$RATIO - ZSPRD^{100D}_{(3,1)}$	
I1.3	$RATIO - ZSPRD^{30D}_{(3,0.5)}$	$RATIO - ZSPRD^{50D}_{(3,0.5)}$	$RATIO - ZSPRD^{100D}_{(3,0.5)}$	
I1.4	$RATIO - ZSPRD^{30D}_{(2,7,2)}$	$RATIO - ZSPRD^{50D}_{(2,7,2)}$	$RATIO - ZSPRD^{100D}_{(2,7,2)}$	
I1.5	$RATIO - ZSPRD^{30D}_{(2,7,1)}$	$RATIO - ZSPRD^{50D}_{(2,7,1)}$	$RATIO - ZSPRD^{100D}_{(2,7,1)}$	
I1.6	$RATIO - ZSPRD^{30D}_{(2,7,0.5)}$	$RATIO - ZSPRD^{50D}_{(2,7,0.5)}$	$RATIO - ZSPRD^{100D}_{(2,7,0.5)}$	$RATIO - SPRD$
I2.1	$RATIO - SPRD^{30D} - SMA_{(10,20)}$	$RATIO - SPRD^{50D} - SMA_{(10,20)}$	$RATIO - SPRD^{100D} - SMA_{(10,20)}$	
I2.2	$RATIO - SPRD^{30D} - EMA_{(10,20)}$	$RATIO - SPRD^{50D} - EMA_{(10,20)}$	$RATIO - SPRD^{100D} - EMA_{(10,20)}$	
I2.3	$RATIO - SPRD^{30D} - MACD_{(12,26,9)}$	$RATIO - SPRD^{50D} - MACD_{(12,26,9)}$	$RATIO - SPRD^{100D} - MACD_{(12,26,9)}$	
I2.4	$RATIO - SPRD^{30D} - RSI_{(14)}$	$RATIO - SPRD^{50D} - RSI_{(14)}$	$RATIO - SPRD^{100D} - RSI_{(14)}$	
I2.5	$RATIO - SPRD^{30D} - BB_{(20)}$	$RATIO - SPRD^{50D} - BB_{(20)}$	$RATIO - SPRD^{100D} - BB_{(20)}$	
I3	$RATIO - SPRD^{30D} - DECTREE$	$RATIO - SPRD^{50D} - DECTREE$	$RATIO - SPRD^{100D} - DECTREE$	Discussed in Table D.1.3
I4	$RATIO - SPRD^{30D} - MLP$	$RATIO - SPRD^{50D} - MLP$	$RATIO - SPRD^{100D} - MLP$	Discussed in Table D.1.3

Table D.1.3: This table is compartmentalized into IX parts, each mentioning the inputs used for the respective ML-based trading strategies. Column I identifies the strategy code, column II the rolling window used for these models, column III the inputs used in the train and test set of these ML-based trading strategies, and column IV the target variable used for these ML-based trading strategies.

(I) **Strategy Code**	**(II)** **Rolling Window (in days)**	**(III)** **Train and Test Set Input Variables**	**(IV)** **Target Set Input Variables**	**(V)** **Note**
			Part I: A3 and A4 models	
A3 and *A4*	30	CATEG(PnL(**A2.1**), CATEG(PnL(**A2.2**), CATEG(PnL(**A2.3**), CATEG(PnL(**A2.4**), CATEG(PnL(**A2.5**), CATEG(DifferenceinCloseRet(**SYM1-SYM2**)), CATEG(PnL(**CLS-SYM1.1**), CATEG(PnL(**CLS-SYM1.2**), CATEG(PnL(**CLS-SYM1.3**), CATEG(PnL(**CLS-SYM1.4**), CATEG(PnL(**CLS-SYM1.5**), CATEG(PnL(**CLS-SYM2.1**), CATEG(PnL(**CLS-SYM2.2**), CATEG(PnL(**CLS-SYM2.3**), CATEG(PnL(**CLS-SYM2.4**) , CATEG(PnL(**CLS-SYM2.5**)	$TARGET^{30D}_{A3,A4} = LOGIC(\text{CATEG}(\text{AVG}(\text{PnL}(\mathbf{A1.1}), PnL(\mathbf{A1.2}), \text{PnL}(\mathbf{A1.3}), PnL(\mathbf{A1.4}), \text{PnL}(\mathbf{A1.5}), PnL(\mathbf{A1.6})), CATEG(DIST^{V1.1} - SPRD^{30D}))$	The train/test and target input variables used in columns III and IV belong to the 30 day rolling window. ETF pairs belonging to the 30 day rolling window are tables D.2.1, D.2.10, D.2.13, D.2.19, D.2.4, D.2.7, D.2.16, D.2.22
A3 and *A4*	50	CATEG(PnL(**A2.1**), CATEG(PnL(**A2.2**), CATEG(PnL(**A2.3**), CATEG(PnL(**A2.4**), CATEG(PnL(**A2.5**), CATEG(DifferenceinCloseRet(**SYM1-SYM2**)), CATEG(PnL(**CLS-SYM1.1**), CATEG(PnL(**CLS-SYM1.2**), CATEG(PnL(**CLS-SYM1.3**), CATEG(PnL(**CLS-SYM1.4**), CATEG(PnL(**CLS-SYM1.5**), CATEG(PnL(**CLS-SYM2.1**), CATEG(PnL(**CLS-SYM2.2**), CATEG(PnL(**CLS-SYM2.3**), CATEG(PnL(**CLS-SYM2.4**) , CATEG(PnL(**CLS-SYM2.5**)	$TARGET^{50D}_{A3,A4} = LOGIC(\text{CATEG}(\text{AVG}(\text{PnL}(\mathbf{A1.1}), PnL(\mathbf{A1.2}), \text{PnL}(\mathbf{A1.3}), PnL(\mathbf{A1.4}), \text{PnL}(\mathbf{A1.5}), PnL(\mathbf{A1.6})), CATEG(DIST^{V1.1} - SPRD^{50D}))$	The train/test and target input variables used in columns III and IV belong to the 50 day rolling window. ETF pairs belonging to the 50 day rolling window are tables D.2.2, D.2.11, D.2.14, D.2.20, D.2.5, D.2.8, D.2.17, D.2.23
A3 and *A4*	100	CATEG(PnL(**A2.1**), CATEG(PnL(**A2.2**), CATEG(PnL(**A2.3**), CATEG(PnL(**A2.4**), CATEG(PnL(**A2.5**), CATEG(DifferenceinCloseRet(**SYM1-SYM2**)), CATEG(PnL(**CLS-SYM1.1**), CATEG(PnL(**CLS-SYM1.2**), CATEG(PnL(**CLS-SYM1.3**), CATEG(PnL(**CLS-SYM1.4**), CATEG(PnL(**CLS-SYM1.5**), CATEG(PnL(**CLS-SYM2.1**), CATEG(PnL(**CLS-SYM2.2**), CATEG(PnL(**CLS-SYM2.3**), CATEG(PnL(**CLS-SYM2.4**) , CATEG(PnL(**CLS-SYM2.5**)	$TARGET^{100D}_{A3,A4} = LOGIC(\text{CATEG}(\text{AVG}(\text{PnL}(\mathbf{A1.1}), PnL(\mathbf{A1.2}), \text{PnL}(\mathbf{A1.3}), PnL(\mathbf{A1.4}), \text{PnL}(\mathbf{A1.5}), PnL(\mathbf{A1.6})), CATEG(DIST^{V1.1} - SPRD^{100D}))$	The train/test and target input variables used in columns III and IV belong to the 100 day rolling window. ETF pairs belonging to the 100 day rolling window are tables D.2.3, D.2.12, D.2.15, D.2.21, D.2.6, D.2.9, D.2.18, D.2.24
			Part II: B3 and B4 models	
B3 and *B4*	30	CATEG(PnL(**B2.1**), CATEG(PnL(**B2.2**), CATEG(PnL(**B2.3**), CATEG(PnL(**B2.4**), CATEG(PnL(**B2.5**), CATEG(DifferenceinCloseRet(**SYM1-SYM2**)), CATEG(PnL(**CLS-SYM1.1**), CATEG(PnL(**CLS-SYM1.2**), CATEG(PnL(**CLS-SYM1.3**), CATEG(PnL(**CLS-SYM1.4**), CATEG(PnL(**CLS-SYM1.5**), CATEG(PnL(**CLS-SYM2.1**), CATEG(PnL(**CLS-SYM2.2**), CATEG(PnL(**CLS-SYM2.3**), CATEG(PnL(**CLS-SYM2.4**) , CATEG(PnL(**CLS-SYM2.5**)	$TARGET^{30D}_{B3,B4} = LOGIC(\text{CATEG}(\text{AVG}(\text{PnL}(\mathbf{B1.1}), PnL(\mathbf{B1.2}), \text{PnL}(\mathbf{B1.3}), PnL(\mathbf{B1.4}), \text{PnL}(\mathbf{B1.5}), PnL(\mathbf{B1.6})), CATEG(DIST^{V1.2} - SPRD^{30D}))$	The train/test and target input variables used in columns III and IV belong to the 30 day rolling window. ETF pairs belonging to the 30 day rolling window are tables D.2.1, D.2.10, D.2.13, D.2.19, D.2.4, D.2.7, D.2.16, D.2.22
B3 and *B4*	50	CATEG(PnL(**B2.1**), CATEG(PnL(**B2.2**), CATEG(PnL(**B2.3**), CATEG(PnL(**B2.4**), CATEG(PnL(**B2.5**), CATEG(DifferenceinCloseRet(**SYM1-SYM2**)), CATEG(PnL(**CLS-SYM1.1**), CATEG(PnL(**CLS-SYM1.2**), CATEG(PnL(**CLS-SYM1.3**), CATEG(PnL(**CLS-SYM1.4**), CATEG(PnL(**CLS-SYM1.5**), CATEG(PnL(**CLS-SYM2.1**), CATEG(PnL(**CLS-SYM2.2**), CATEG(PnL(**CLS-SYM2.3**), CATEG(PnL(**CLS-SYM2.4**) , CATEG(PnL(**CLS-SYM2.5**)	$TARGET^{50D}_{B3,B4} = LOGIC(\text{CATEG}(\text{AVG}(\text{PnL}(\mathbf{B1.1}), PnL(\mathbf{B1.2}), \text{PnL}(\mathbf{B1.3}), PnL(\mathbf{B1.4}), \text{PnL}(\mathbf{B1.5}), PnL(\mathbf{B1.6})), CATEG(DIST^{V1.2} - SPRD^{50D}))$	The train/test and target input variables used in columns III and IV belong to the 50 day rolling window. ETF pairs belonging to the 50 day rolling window are tables D.2.2, D.2.11, D.2.14, D.2.20, D.2.5, D.2.8, D.2.17, D.2.23
B3 and *B4*	100	CATEG(PnL(**B2.1**), CATEG(PnL(**B2.2**), CATEG(PnL(**B2.3**), CATEG(PnL(**B2.4**), CATEG(PnL(**B2.5**), CATEG(DifferenceinCloseRet(**SYM1-SYM2**)), CATEG(PnL(**CLS-SYM1.1**), CATEG(PnL(**CLS-SYM1.2**), CATEG(PnL(**CLS-SYM1.3**), CATEG(PnL(**CLS-SYM1.4**), CATEG(PnL(**CLS-SYM1.5**), CATEG(PnL(**CLS-SYM2.1**), CATEG(PnL(**CLS-SYM2.2**), CATEG(PnL(**CLS-SYM2.3**), CATEG(PnL(**CLS-SYM2.4**) , CATEG(PnL(**CLS-SYM2.5**)	$TARGET^{100D}_{B3,B4} = LOGIC(\text{CATEG}(\text{AVG}(\text{PnL}(\mathbf{B1.1}), PnL(\mathbf{B1.2}), \text{PnL}(\mathbf{B1.3}), PnL(\mathbf{B1.4}), \text{PnL}(\mathbf{B1.5}), PnL(\mathbf{B1.6})), CATEG(DIST^{V1.2} - SPRD^{100D}))$	The train/test and target input variables used in columns III and IV belong to the 100 day rolling window. ETF pairs belonging to the 100 day rolling window are tables D.2.3, D.2.12, D.2.15, D.2.21, D.2.6, D.2.9, D.2.18, D.2.24
			Part III: C3 and C4 models	
C3 and *C4*	30	CATEG(PnL(**C2.1**), CATEG(PnL(**C2.2**), CATEG(PnL(**C2.3**), CATEG(PnL(**C2.4**), CATEG(PnL(**C2.5**), CATEG(DifferenceinCloseRet(**SYM1-SYM2**)), CATEG(PnL(**CLS-SYM1.1**), CATEG(PnL(**CLS-SYM1.2**), CATEG(PnL(**CLS-SYM1.3**), CATEG(PnL(**CLS-SYM1.4**), CATEG(PnL(**CLS-SYM1.5**), CATEG(PnL(**CLS-SYM2.1**), CATEG(PnL(**CLS-SYM2.2**), CATEG(PnL(**CLS-SYM2.3**), CATEG(PnL(**CLS-SYM2.4**) , CATEG(PnL(**CLS-SYM2.5**)	$TARGET^{30D}_{C3,C4} = LOGIC(\text{CATEG}(\text{AVG}(\text{PnL}(\mathbf{C1.1}), PnL(\mathbf{C1.2}), \text{PnL}(\mathbf{C1.3}), PnL(\mathbf{C1.4}), \text{PnL}(\mathbf{C1.5}), PnL(\mathbf{C1.6})), CATEG(DIST^{V2} - SPRD^{30D}))$	The train/test and target input variables used in columns III and IV belong to the 30 day rolling window. ETF pairs belonging to the 30 day rolling window are tables D.2.1, D.2.10, D.2.13, D.2.19, D.2.4, D.2.7, D.2.16, D.2.22
C3 and *C4*	50	CATEG(PnL(**C2.1**), CATEG(PnL(**C2.2**), CATEG(PnL(**C2.3**), CATEG(PnL(**C2.4**), CATEG(PnL(**C2.5**), CATEG(DifferenceinCloseRet(**SYM1-SYM2**)), CATEG(PnL(**CLS-SYM1.1**), CATEG(PnL(**CLS-SYM1.2**), CATEG(PnL(**CLS-SYM1.3**), CATEG(PnL(**CLS-SYM1.4**), CATEG(PnL(**CLS-SYM1.5**), CATEG(PnL(**CLS-SYM2.1**), CATEG(PnL(**CLS-SYM2.2**), CATEG(PnL(**CLS-SYM2.3**), CATEG(PnL(**CLS-SYM2.4**) , CATEG(PnL(**CLS-SYM2.5**)	$TARGET^{50D}_{C3,C4} = LOGIC(\text{CATEG}(\text{AVG}(\text{PnL}(\mathbf{C1.1}), PnL(\mathbf{C1.2}), \text{PnL}(\mathbf{C1.3}), PnL(\mathbf{C1.4}), \text{PnL}(\mathbf{C1.5}), PnL(\mathbf{C1.6})), CATEG(DIST^{V2} - SPRD^{50D}))$	The train/test and target input variables used in columns III and IV belong to the 50 day rolling window. ETF pairs belonging to the 50 day rolling window are tables D.2.2, D.2.11, D.2.14, D.2.20, D.2.5, D.2.8, D.2.17, D.2.23
C3 and *C4*	100	CATEG(PnL(**C2.1**), CATEG(PnL(**C2.2**), CATEG(PnL(**C2.3**), CATEG(PnL(**C2.4**), CATEG(PnL(**C2.5**), CATEG(DifferenceinCloseRet(**SYM1-SYM2**)), CATEG(PnL(**CLS-SYM1.1**), CATEG(PnL(**CLS-SYM1.2**), CATEG(PnL(**CLS-SYM1.3**), CATEG(PnL(**CLS-SYM1.4**), CATEG(PnL(**CLS-SYM1.5**), CATEG(PnL(**CLS-SYM2.1**), CATEG(PnL(**CLS-SYM2.2**), CATEG(PnL(**CLS-SYM2.3**), CATEG(PnL(**CLS-SYM2.4**) , CATEG(PnL(**CLS-SYM2.5**)	$TARGET^{100D}_{C3,C4} = LOGIC(\text{CATEG}(\text{AVG}(\text{PnL}(\mathbf{C1.1}), PnL(\mathbf{C1.2}), \text{PnL}(\mathbf{C1.3}), PnL(\mathbf{C1.4}), \text{PnL}(\mathbf{C1.5}), PnL(\mathbf{C1.6})), CATEG(DIST^{V2} - SPRD^{100D}))$	The train/test and target input variables used in columns III and IV belong to the 100 day rolling window. ETF pairs belonging to the 100 day rolling window are tables D.2.3, D.2.12, D.2.15, D.2.21, D.2.6, D.2.9, D.2.18, D.2.24
			Part IV: D3 and D4 models	
D3 and *D4*	30	CATEG(PnL(**D2.1**), CATEG(PnL(**D2.2**), CATEG(PnL(**D2.3**), CATEG(PnL(**D2.4**), CATEG(PnL(**D2.5**), CATEG(DifferenceinCloseRet(**SYM1-SYM2**)), CATEG(PnL(**CLS-SYM1.1**), CATEG(PnL(**CLS-SYM1.2**), CATEG(PnL(**CLS-SYM1.3**), CATEG(PnL(**CLS-SYM1.4**), CATEG(PnL(**CLS-SYM1.5**), CATEG(PnL(**CLS-SYM2.1**), CATEG(PnL(**CLS-SYM2.2**), CATEG(PnL(**CLS-SYM2.3**), CATEG(PnL(**CLS-SYM2.4**) , CATEG(PnL(**CLS-SYM2.5**)	$TARGET^{30D}_{D3,D4} = LOGIC(\text{CATEG}(\text{AVG}(\text{PnL}(\mathbf{D1.1}), PnL(\mathbf{D1.2}), \text{PnL}(\mathbf{D1.3}), PnL(\mathbf{D1.4}), \text{PnL}(\mathbf{D1.5}), PnL(\mathbf{D1.6})), CATEG(DIST^{V3} - SPRD^{30D}))$	The train/test and target input variables used in columns III and IV belong to the 30 day rolling window. ETF pairs belonging to the 30 day rolling window are tables D.2.1, D.2.10, D.2.13, D.2.19, D.2.4, D.2.7, D.2.16, D.2.22
D3 and *D4*	50	CATEG(PnL(**D2.1**), CATEG(PnL(**D2.2**), CATEG(PnL(**D2.3**), CATEG(PnL(**D2.4**), CATEG(PnL(**D2.5**), CATEG(DifferenceinCloseRet(**SYM1-SYM2**)), CATEG(PnL(**CLS-SYM1.1**), CATEG(PnL(**CLS-SYM1.2**), CATEG(PnL(**CLS-SYM1.3**), CATEG(PnL(**CLS-SYM1.4**), CATEG(PnL(**CLS-SYM1.5**), CATEG(PnL(**CLS-SYM2.1**), CATEG(PnL(**CLS-SYM2.2**), CATEG(PnL(**CLS-SYM2.3**), CATEG(PnL(**CLS-SYM2.4**) , CATEG(PnL(**CLS-SYM2.5**)	$TARGET^{50D}_{D3,D4} = LOGIC(\text{CATEG}(\text{AVG}(\text{PnL}(\mathbf{D1.1}), PnL(\mathbf{D1.2}), \text{PnL}(\mathbf{D1.3}), PnL(\mathbf{D1.4}), \text{PnL}(\mathbf{D1.5}), PnL(\mathbf{D1.6})), CATEG(DIST^{V3} - SPRD^{50D}))$	The train/test and target input variables used in columns III and IV belong to the 50 day rolling window. ETF pairs belonging to the 50 day rolling window are tables D.2.2, D.2.11, D.2.14, D.2.20, D.2.5, D.2.8, D.2.17, D.2.23
D3 and *D4*	100	CATEG(PnL(**D2.1**), CATEG(PnL(**D2.2**), CATEG(PnL(**D2.3**), CATEG(PnL(**D2.4**), CATEG(PnL(**D2.5**), CATEG(DifferenceinCloseRet(**SYM1-SYM2**)), CATEG(PnL(**CLS-SYM1.1**), CATEG(PnL(**CLS-SYM1.2**), CATEG(PnL(**CLS-SYM1.3**), CATEG(PnL(**CLS-SYM1.4**), CATEG(PnL(**CLS-SYM1.5**), CATEG(PnL(**CLS-SYM2.1**), CATEG(PnL(**CLS-SYM2.2**), CATEG(PnL(**CLS-SYM2.3**), CATEG(PnL(**CLS-SYM2.4**) , CATEG(PnL(**CLS-SYM2.5**)	$TARGET^{100D}_{D3,D4} = LOGIC(\text{CATEG}(\text{AVG}(\text{PnL}(\mathbf{D1.1}), PnL(\mathbf{D1.2}), \text{PnL}(\mathbf{D1.3}), PnL(\mathbf{D1.4}), \text{PnL}(\mathbf{D1.5}), PnL(\mathbf{D1.6})), CATEG(DIST^{V3} - SPRD^{100D}))$	The train/test and target input variables used in columns III and IV belong to the 100 day rolling window. ETF pairs belonging to the 100 day rolling window are tables D.2.3, D.2.12, D.2.15, D.2.21, D.2.6, D.2.9, D.2.18, D.2.24
			Part V: E3 and E4 models	
E3 and *E4*	30	CATEG(PnL(**E2.1**), CATEG(PnL(**E2.2**), CATEG(PnL(**E2.3**), CATEG(PnL(**E2.4**), CATEG(PnL(**E2.5**), CATEG(DifferenceinCloseRet(**SYM1-SYM2**)), CATEG(PnL(**CLS-SYM1.1**), CATEG(PnL(**CLS-SYM1.2**), CATEG(PnL(**CLS-SYM1.3**), CATEG(PnL(**CLS-SYM1.4**), CATEG(PnL(**CLS-SYM1.5**), CATEG(PnL(**CLS-SYM2.1**), CATEG(PnL(**CLS-SYM2.2**), CATEG(PnL(**CLS-SYM2.3**), CATEG(PnL(**CLS-SYM2.4**) , CATEG(PnL(**CLS-SYM2.5**)	$TARGET^{30D}_{E3,E4} = LOGIC(\text{CATEG}(\text{AVG}(\text{PnL}(\mathbf{E1.1}), PnL(\mathbf{E1.2}), \text{PnL}(\mathbf{E1.3}), PnL(\mathbf{E1.4}), \text{PnL}(\mathbf{E1.5}), PnL(\mathbf{E1.6})), CATEG(DIST^{V4} - SPRD^{30D}))$	The train/test and target input variables used in columns III and IV belong to the 30 day rolling window. ETF pairs belonging to the 30 day rolling window are tables D.2.1, D.2.10, D.2.13, D.2.19, D.2.4, D.2.7, D.2.16, D.2.22
E3 and *E4*	50	CATEG(PnL(**E2.1**), CATEG(PnL(**E2.2**), CATEG(PnL(**E2.3**), CATEG(PnL(**E2.4**), CATEG(PnL(**E2.5**), CATEG(DifferenceinCloseRet(**SYM1-SYM2**)), CATEG(PnL(**CLS-SYM1.1**), CATEG(PnL(**CLS-SYM1.2**), CATEG(PnL(**CLS-SYM1.3**), CATEG(PnL(**CLS-SYM1.4**), CATEG(PnL(**CLS-SYM1.5**), CATEG(PnL(**CLS-SYM2.1**), CATEG(PnL(**CLS-SYM2.2**), CATEG(PnL(**CLS-SYM2.3**), CATEG(PnL(**CLS-SYM2.4**) , CATEG(PnL(**CLS-SYM2.5**)	$TARGET^{50D}_{E3,E4} = LOGIC(\text{CATEG}(\text{AVG}(\text{PnL}(\mathbf{E1.1}), PnL(\mathbf{E1.2}), \text{PnL}(\mathbf{E1.3}), PnL(\mathbf{E1.4}), \text{PnL}(\mathbf{E1.5}), PnL(\mathbf{E1.6})), CATEG(DIST^{V4} - SPRD^{50D}))$	The train/test and target input variables used in columns III and IV belong to the 50 day rolling window. ETF pairs belonging to the 50 day rolling window are tables D.2.2, D.2.11, D.2.14, D.2.20, D.2.5, D.2.8, D.2.17, D.2.23
E3 and *E4*	100	CATEG(PnL(**E2.1**), CATEG(PnL(**E2.2**), CATEG(PnL(**E2.3**), CATEG(PnL(**E2.4**), CATEG(PnL(**E2.5**), CATEG(DifferenceinCloseRet(**SYM1-SYM2**)), CATEG(PnL(**CLS-SYM1.1**), CATEG(PnL(**CLS-SYM1.2**), CATEG(PnL(**CLS-SYM1.3**), CATEG(PnL(**CLS-SYM1.4**), CATEG(PnL(**CLS-SYM1.5**), CATEG(PnL(**CLS-SYM2.1**), CATEG(PnL(**CLS-SYM2.2**), CATEG(PnL(**CLS-SYM2.3**), CATEG(PnL(**CLS-SYM2.4**) , CATEG(PnL(**CLS-SYM2.5**)	$TARGET^{100D}_{E3,E4} = LOGIC(\text{CATEG}(\text{AVG}(\text{PnL}(\mathbf{E1.1}), PnL(\mathbf{E1.2}), \text{PnL}(\mathbf{E1.3}), PnL(\mathbf{E1.4}), \text{PnL}(\mathbf{E1.5}), PnL(\mathbf{E1.6})), CATEG(DIST^{V4} - SPRD^{100D}))$	The train/test and target input variables used in columns III and IV belong to the 100 day rolling window. ETF pairs belonging to the 100 day rolling window are tables D.2.3, D.2.12, D.2.15, D.2.21, D.2.6, D.2.9, D.2.18, D.2.24
			Part VI: F3 and F4 models	
F3 and *F4*	30	CATEG(PnL(**F2.1**), CATEG(PnL(**F2.2**), CATEG(PnL(**F2.3**), CATEG(PnL(**F2.4**), CATEG(PnL(**F2.5**), CATEG(DifferenceinCloseRet(**SYM1-SYM2**)), CATEG(PnL(**CLS-SYM1.1**), CATEG(PnL(**CLS-SYM1.2**), CATEG(PnL(**CLS-SYM1.3**), CATEG(PnL(**CLS-SYM1.4**), CATEG(PnL(**CLS-SYM1.5**), CATEG(PnL(**CLS-SYM2.1**), CATEG(PnL(**CLS-SYM2.2**), CATEG(PnL(**CLS-SYM2.3**), CATEG(PnL(**CLS-SYM2.4**) , CATEG(PnL(**CLS-SYM2.5**)	$TARGET^{30D}_{F3,F4} = LOGIC(\text{CATEG}(\text{AVG}(\text{PnL}(\mathbf{F1.1}), PnL(\mathbf{F1.2}), \text{PnL}(\mathbf{F1.3}), PnL(\mathbf{F1.4}), \text{PnL}(\mathbf{F1.5}), PnL(\mathbf{F1.6})), CATEG(JOHANSEN - SPRD^{30D}))$	The train/test and target input variables used in columns III and IV belong to the 30 day rolling window. ETF pairs belonging to the 30 day rolling window are tables D.2.1, D.2.10, D.2.13, D.2.19, D.2.4, D.2.7, D.2.16, D.2.22
F3 and *F4*	50	CATEG(PnL(**F2.1**), CATEG(PnL(**F2.2**), CATEG(PnL(**F2.3**), CATEG(PnL(**F2.4**), CATEG(PnL(**F2.5**), CATEG(DifferenceinCloseRet(**SYM1-SYM2**)), CATEG(PnL(**CLS-SYM1.1**), CATEG(PnL(**CLS-SYM1.2**), CATEG(PnL(**CLS-SYM1.3**), CATEG(PnL(**CLS-SYM1.4**), CATEG(PnL(**CLS-SYM1.5**), CATEG(PnL(**CLS-SYM2.1**), CATEG(PnL(**CLS-SYM2.2**), CATEG(PnL(**CLS-SYM2.3**), CATEG(PnL(**CLS-SYM2.4**) , CATEG(PnL(**CLS-SYM2.5**)	$TARGET^{50D}_{F3,F4} = LOGIC(\text{CATEG}(\text{AVG}(\text{PnL}(\mathbf{F1.1}), PnL(\mathbf{F1.2}), \text{PnL}(\mathbf{F1.3}), PnL(\mathbf{F1.4}), \text{PnL}(\mathbf{F1.5}), PnL(\mathbf{F1.6})), CATEG(JOHANSEN - SPRD^{50D}))$	The train/test and target input variables used in columns III and IV belong to the 50 day rolling window. ETF pairs belonging to the 50 day rolling window are tables D.2.2, D.2.11, D.2.14, D.2.20, D.2.5, D.2.8, D.2.17, D.2.23
F3 and *F4*	100	CATEG(PnL(**F2.1**), CATEG(PnL(**F2.2**), CATEG(PnL(**F2.3**), CATEG(PnL(**F2.4**), CATEG(PnL(**F2.5**), CATEG(DifferenceinCloseRet(**SYM1-SYM2**)), CATEG(PnL(**CLS-SYM1.1**), CATEG(PnL(**CLS-SYM1.2**), CATEG(PnL(**CLS-SYM1.3**), CATEG(PnL(**CLS-SYM1.4**), CATEG(PnL(**CLS-SYM1.5**), CATEG(PnL(**CLS-SYM2.1**), CATEG(PnL(**CLS-SYM2.2**), CATEG(PnL(**CLS-SYM2.3**), CATEG(PnL(**CLS-SYM2.4**) , CATEG(PnL(**CLS-SYM2.5**)	$TARGET^{100D}_{F3,F4} = LOGIC(\text{CATEG}(\text{AVG}(\text{PnL}(\mathbf{F1.1}), PnL(\mathbf{F1.2}), \text{PnL}(\mathbf{F1.3}), PnL(\mathbf{F1.4}), \text{PnL}(\mathbf{F1.5}), PnL(\mathbf{F1.6})), CATEG(JOHANSEN - SPRD^{100D}))$	The train/test and target input variables used in columns III and IV belong to the 100 day rolling window. ETF pairs belonging to the 100 day rolling window are tables D.2.3, D.2.12, D.2.15, D.2.21, D.2.6, D.2.9, D.2.18, D.2.24
			Part VII: G3 and G4 models	
G3 and *G4*	30	CATEG(PnL(**G2.1**), CATEG(PnL(**G2.2**), CATEG(PnL(**G2.3**), CATEG(PnL(**G2.4**), CATEG(PnL(**G2.5**), CATEG(DifferenceinCloseRet(**SYM1-SYM2**)), CATEG(PnL(**CLS-SYM1.1**), CATEG(PnL(**CLS-SYM1.2**), CATEG(PnL(**CLS-SYM1.3**), CATEG(PnL(**CLS-SYM1.4**), CATEG(PnL(**CLS-SYM1.5**), CATEG(PnL(**CLS-SYM2.1**), CATEG(PnL(**CLS-SYM2.2**), CATEG(PnL(**CLS-SYM2.3**), CATEG(PnL(**CLS-SYM2.4**) , CATEG(PnL(**CLS-SYM2.5**)	$TARGET^{30D}_{G3,G4} = LOGIC(\text{CATEG}(\text{AVG}(\text{PnL}(\mathbf{G1.1}), PnL(\mathbf{G1.2}), \text{PnL}(\mathbf{G1.3}), PnL(\mathbf{G1.4}), \text{PnL}(\mathbf{G1.5}), PnL(\mathbf{G1.6})), CATEG(ADF - SPRD^{30D}))$	The train/test and target input variables used in columns III and IV belong to the 30 day rolling window. ETF pairs belonging to the 30 day rolling window are tables D.2.1, D.2.10, D.2.13, D.2.19, D.2.4, D.2.7, D.2.16, D.2.22
G3 and *G4*	50	CATEG(PnL(**G2.1**), CATEG(PnL(**G2.2**), CATEG(PnL(**G2.3**), CATEG(PnL(**G2.4**), CATEG(PnL(**G2.5**), CATEG(DifferenceinCloseRet(**SYM1-SYM2**)), CATEG(PnL(**CLS-SYM1.1**), CATEG(PnL(**CLS-SYM1.2**), CATEG(PnL(**CLS-SYM1.3**), CATEG(PnL(**CLS-SYM1.4**), CATEG(PnL(**CLS-SYM1.5**), CATEG(PnL(**CLS-SYM2.1**), CATEG(PnL(**CLS-SYM2.2**), CATEG(PnL(**CLS-SYM2.3**), CATEG(PnL(**CLS-SYM2.4**) , CATEG(PnL(**CLS-SYM2.5**)	$TARGET^{50D}_{G3,G4} = LOGIC(\text{CATEG}(\text{AVG}(\text{PnL}(\mathbf{G1.1}), PnL(\mathbf{G1.2}), \text{PnL}(\mathbf{G1.3}), PnL(\mathbf{G1.4}), \text{PnL}(\mathbf{G1.5}), PnL(\mathbf{G1.6})), CATEG(ADF - SPRD^{50D}))$	The train/test and target input variables used in columns III and IV belong to the 50 day rolling window. ETF pairs belonging to the 50 day rolling window are tables D.2.2, D.2.11, D.2.14, D.2.20, D.2.5, D.2.8, D.2.17, D.2.23
G3 and *G4*	100	CATEG(PnL(**G2.1**), CATEG(PnL(**G2.2**), CATEG(PnL(**G2.3**), CATEG(PnL(**G2.4**), CATEG(PnL(**G2.5**), CATEG(DifferenceinCloseRet(**SYM1-SYM2**)), CATEG(PnL(**CLS-SYM1.1**), CATEG(PnL(**CLS-SYM1.2**), CATEG(PnL(**CLS-SYM1.3**), CATEG(PnL(**CLS-SYM1.4**), CATEG(PnL(**CLS-SYM1.5**), CATEG(PnL(**CLS-SYM2.1**), CATEG(PnL(**CLS-SYM2.2**), CATEG(PnL(**CLS-SYM2.3**), CATEG(PnL(**CLS-SYM2.4**) , CATEG(PnL(**CLS-SYM2.5**)	$TARGET^{100D}_{G3,G4} = LOGIC(\text{CATEG}(\text{AVG}(\text{PnL}(\mathbf{G1.1}), PnL(\mathbf{G1.2}), \text{PnL}(\mathbf{G1.3}), PnL(\mathbf{G1.4}), \text{PnL}(\mathbf{G1.5}), PnL(\mathbf{G1.6})), CATEG(ADF - SPRD^{100D}))$	The train/test and target input variables used in columns III and IV belong to the 100 day rolling window. ETF pairs belonging to the 100 day rolling window are tables D.2.3, D.2.12, D.2.15, D.2.21, D.2.6, D.2.9, D.2.18, D.2.24
			Part VIII: H3 and H4 models	
H3 and *H4*	30	CATEG(PnL(**H2.1**), CATEG(PnL(**H2.2**), CATEG(PnL(**H2.3**), CATEG(PnL(**H2.4**), CATEG(PnL(**H2.5**), CATEG(DifferenceinCloseRet(**SYM1-SYM2**)), CATEG(PnL(**CLS-SYM1.1**), CATEG(PnL(**CLS-SYM1.2**), CATEG(PnL(**CLS-SYM1.3**), CATEG(PnL(**CLS-SYM1.4**), CATEG(PnL(**CLS-SYM1.5**), CATEG(PnL(**CLS-SYM2.1**), CATEG(PnL(**CLS-SYM2.2**), CATEG(PnL(**CLS-SYM2.3**), CATEG(PnL(**CLS-SYM2.4**) , CATEG(PnL(**CLS-SYM2.5**)	$TARGET^{30D}_{H3,H4} = LOGIC(\text{CATEG}(\text{AVG}(\text{PnL}(\mathbf{H1.1}), PnL(\mathbf{H1.2}), \text{PnL}(\mathbf{H1.3}), PnL(\mathbf{H1.4}), \text{PnL}(\mathbf{H1.5}), PnL(\mathbf{H1.6})), CATEG(KALMAN - SPRD^{30D}))$	The train/test and target input variables used in columns III and IV belong to the 30 day rolling window. ETF pairs belonging to the 30 day rolling window are tables D.2.1, D.2.10, D.2.13, D.2.19, D.2.4, D.2.7, D.2.16, D.2.22
H3 and *H4*	50	CATEG(PnL(**H2.1**), CATEG(PnL(**H2.2**), CATEG(PnL(**H2.3**), CATEG(PnL(**H2.4**), CATEG(PnL(**H2.5**), CATEG(DifferenceinCloseRet(**SYM1-SYM2**)), CATEG(PnL(**CLS-SYM1.1**), CATEG(PnL(**CLS-SYM1.2**), CATEG(PnL(**CLS-SYM1.3**), CATEG(PnL(**CLS-SYM1.4**), CATEG(PnL(**CLS-SYM1.5**), CATEG(PnL(**CLS-SYM2.1**), CATEG(PnL(**CLS-SYM2.2**), CATEG(PnL(**CLS-SYM2.3**), CATEG(PnL(**CLS-SYM2.4**) , CATEG(PnL(**CLS-SYM2.5**)	$TARGET^{50D}_{H3,H4} = LOGIC(\text{CATEG}(\text{AVG}(\text{PnL}(\mathbf{H1.1}), PnL(\mathbf{H1.2}), \text{PnL}(\mathbf{H1.3}), PnL(\mathbf{H1.4}), \text{PnL}(\mathbf{H1.5}), PnL(\mathbf{H1.6})), CATEG(KALMAN - SPRD^{50D}))$	The train/test and target input variables used in columns III and IV belong to the 50 day rolling window. ETF pairs belonging to the 50 day rolling window are tables D.2.2, D.2.11, D.2.14, D.2.20, D.2.5, D.2.8, D.2.17, D.2.23
H3 and *H4*	100	CATEG(PnL(**H2.1**), CATEG(PnL(**H2.2**), CATEG(PnL(**H2.3**), CATEG(PnL(**H2.4**), CATEG(PnL(**H2.5**), CATEG(DifferenceinCloseRet(**SYM1-SYM2**)), CATEG(PnL(**CLS-SYM1.1**), CATEG(PnL(**CLS-SYM1.2**), CATEG(PnL(**CLS-SYM1.3**), CATEG(PnL(**CLS-SYM1.4**), CATEG(PnL(**CLS-SYM1.5**), CATEG(PnL(**CLS-SYM2.1**), CATEG(PnL(**CLS-SYM2.2**), CATEG(PnL(**CLS-SYM2.3**), CATEG(PnL(**CLS-SYM2.4**) , CATEG(PnL(**CLS-SYM2.5**)	$TARGET^{100D}_{H3,H4} = LOGIC(\text{CATEG}(\text{AVG}(\text{PnL}(\mathbf{H1.1}), PnL(\mathbf{H1.2}), \text{PnL}(\mathbf{H1.3}), PnL(\mathbf{H1.4}), \text{PnL}(\mathbf{H1.5}), PnL(\mathbf{H1.6})), CATEG(KALMAN - SPRD^{100D}))$	The train/test and target input variables used in columns III and IV belong to the 100 day rolling window. ETF pairs belonging to the 100 day rolling window are tables D.2.3, D.2.12, D.2.15, D.2.21, D.2.6, D.2.9, D.2.18, D.2.24
			Part IX: I3 and I4 models	
I3 and *I4*	30	CATEG(PnL(**I2.1**), CATEG(PnL(**I2.2**), CATEG(PnL(**I2.3**), CATEG(PnL(**I2.4**), CATEG(PnL(**I2.5**), CATEG(DifferenceinCloseRet(**SYM1-SYM2**)), CATEG(PnL(**CLS-SYM1.1**), CATEG(PnL(**CLS-SYM1.2**), CATEG(PnL(**CLS-SYM1.3**), CATEG(PnL(**CLS-SYM1.4**), CATEG(PnL(**CLS-SYM1.5**), CATEG(PnL(**CLS-SYM2.1**), CATEG(PnL(**CLS-SYM2.2**), CATEG(PnL(**CLS-SYM2.3**), CATEG(PnL(**CLS-SYM2.4**) , CATEG(PnL(**CLS-SYM2.5**)	$TARGET^{30D}_{I3,I4} = LOGIC(\text{CATEG}(\text{AVG}(\text{PnL}(\mathbf{I1.1}), PnL(\mathbf{I1.2}), \text{PnL}(\mathbf{I1.3}), PnL(\mathbf{I1.4}), \text{PnL}(\mathbf{I1.5}), PnL(\mathbf{I1.6})), CATEG(RATIO - SPRD^{30D}))$	The train/test and target input variables used in columns III and IV belong to the 30 day rolling window. ETF pairs belonging to the 30 day rolling window are tables D.2.1, D.2.10, D.2.13, D.2.19, D.2.4, D.2.7, D.2.16, D.2.22
I3 and *I4*	50	CATEG(PnL(**I2.1**), CATEG(PnL(**I2.2**), CATEG(PnL(**I2.3**), CATEG(PnL(**I2.4**), CATEG(PnL(**I2.5**), CATEG(DifferenceinCloseRet(**SYM1-SYM2**)), CATEG(PnL(**CLS-SYM1.1**), CATEG(PnL(**CLS-SYM1.2**), CATEG(PnL(**CLS-SYM1.3**), CATEG(PnL(**CLS-SYM1.4**), CATEG(PnL(**CLS-SYM1.5**), CATEG(PnL(**CLS-SYM2.1**), CATEG(PnL(**CLS-SYM2.2**), CATEG(PnL(**CLS-SYM2.3**), CATEG(PnL(**CLS-SYM2.4**) , CATEG(PnL(**CLS-SYM2.5**)	$TARGET^{50D}_{I3,I4} = LOGIC(\text{CATEG}(\text{AVG}(\text{PnL}(\mathbf{I1.1}), PnL(\mathbf{I1.2}), \text{PnL}(\mathbf{I1.3}), PnL(\mathbf{I1.4}), \text{PnL}(\mathbf{I1.5}), PnL(\mathbf{I1.6})), CATEG(RATIO - SPRD^{50D}))$	The train/test and target input variables used in columns III and IV belong to the 50 day rolling window. ETF pairs belonging to the 50 day rolling window are tables D.2.2, D.2.11, D.2.14, D.2.20, D.2.5, D.2.8, D.2.17, D.2.23
I3 and *I4*	100	CATEG(PnL(**I2.1**), CATEG(PnL(**I2.2**), CATEG(PnL(**I2.3**), CATEG(PnL(**I2.4**), CATEG(PnL(**I2.5**), CATEG(DifferenceinCloseRet(**SYM1-SYM2**)), CATEG(PnL(**CLS-SYM1.1**), CATEG(PnL(**CLS-SYM1.2**), CATEG(PnL(**CLS-SYM1.3**), CATEG(PnL(**CLS-SYM1.4**), CATEG(PnL(**CLS-SYM1.5**), CATEG(PnL(**CLS-SYM2.1**), CATEG(PnL(**CLS-SYM2.2**), CATEG(PnL(**CLS-SYM2.3**), CATEG(PnL(**CLS-SYM2.4**) , CATEG(PnL(**CLS-SYM2.5**)	$TARGET^{100D}_{I3,I4} = LOGIC(\text{CATEG}(\text{AVG}(\text{PnL}(\mathbf{I1.1}), PnL(\mathbf{I1.2}), \text{PnL}(\mathbf{I1.3}), PnL(\mathbf{I1.4}), \text{PnL}(\mathbf{I1.5}), PnL(\mathbf{I1.6})), CATEG(RATIO - SPRD^{100D}))$	The train/test and target input variables used in columns III and IV belong to the 100 day rolling window. ETF pairs belonging to the 100 day rolling window are tables D.2.3, D.2.12, D.2.15, D.2.21, D.2.6, D.2.9, D.2.18, D.2.24

Figure D.1.1: These charts present the rolling correlation from 01 January 2019 to 31 January 2022 for the eight ETF pairs (**ITOT.N/IXUS.N**, **IWF.N/XLE.N**, **SCHB.N/SCHF.N**, **SCHF.N/VO.N**, **QQQ.N/XLE.N**, **USMV.N/XLE.N**, **VO.N/VXUS.N**, and **VWO.N/XLE.N**) covered in Chapter 5

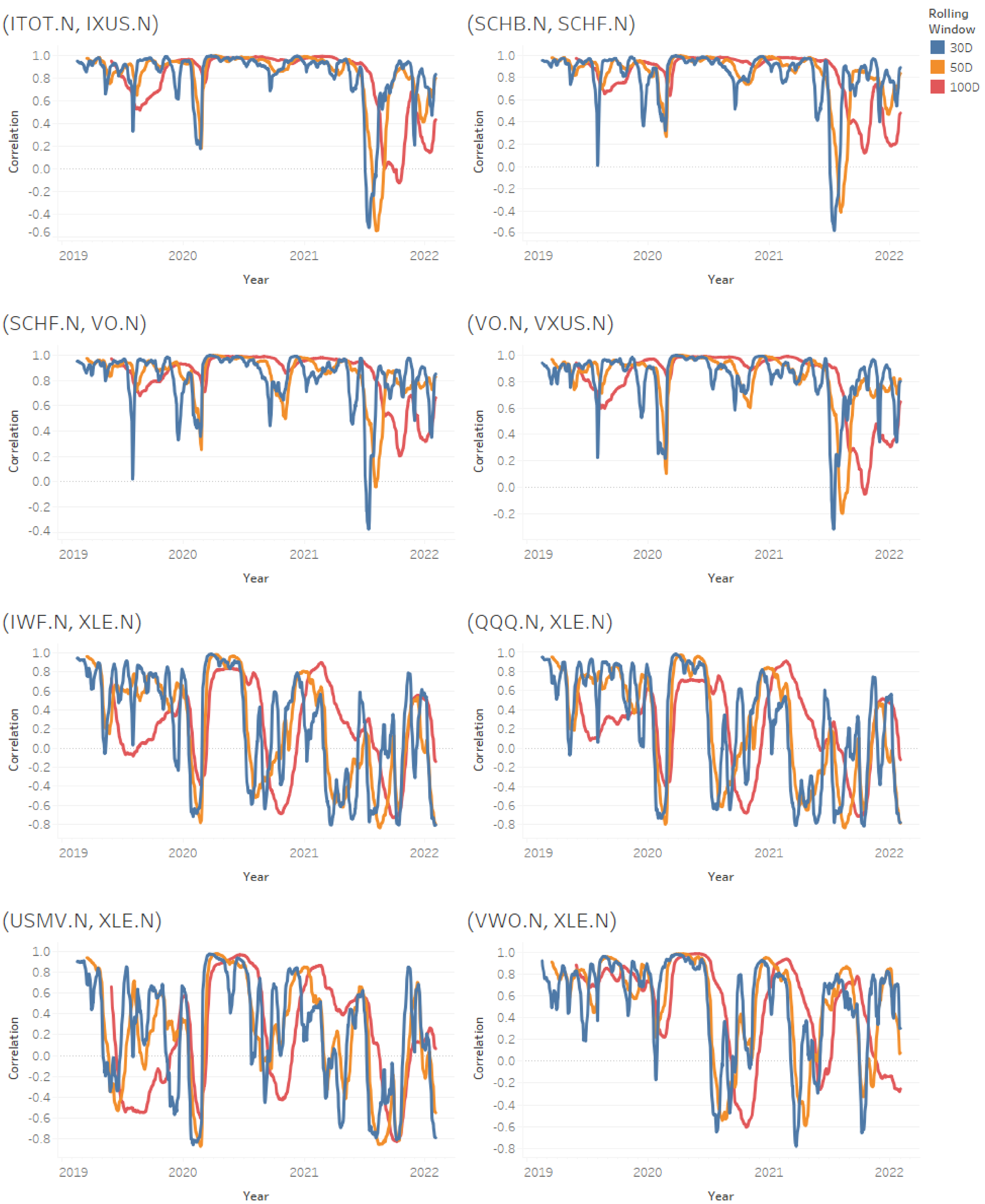

Figure D.1.2: These charts present the rolling cointegration from 01 January 2019 to 31 January 2022 for the eight ETF pairs (**ITOT.N/IXUS.N**, **IWF.N/XLE.N**, **SCHB.N/SCHF.N**, **SCHF.N/VO.N**, **QQQ.N/XLE.N**, **USMV.N/XLE.N**, **VO.N/VXUS.N**, and **VWO.N/XLE.N**) covered in Chapter 5

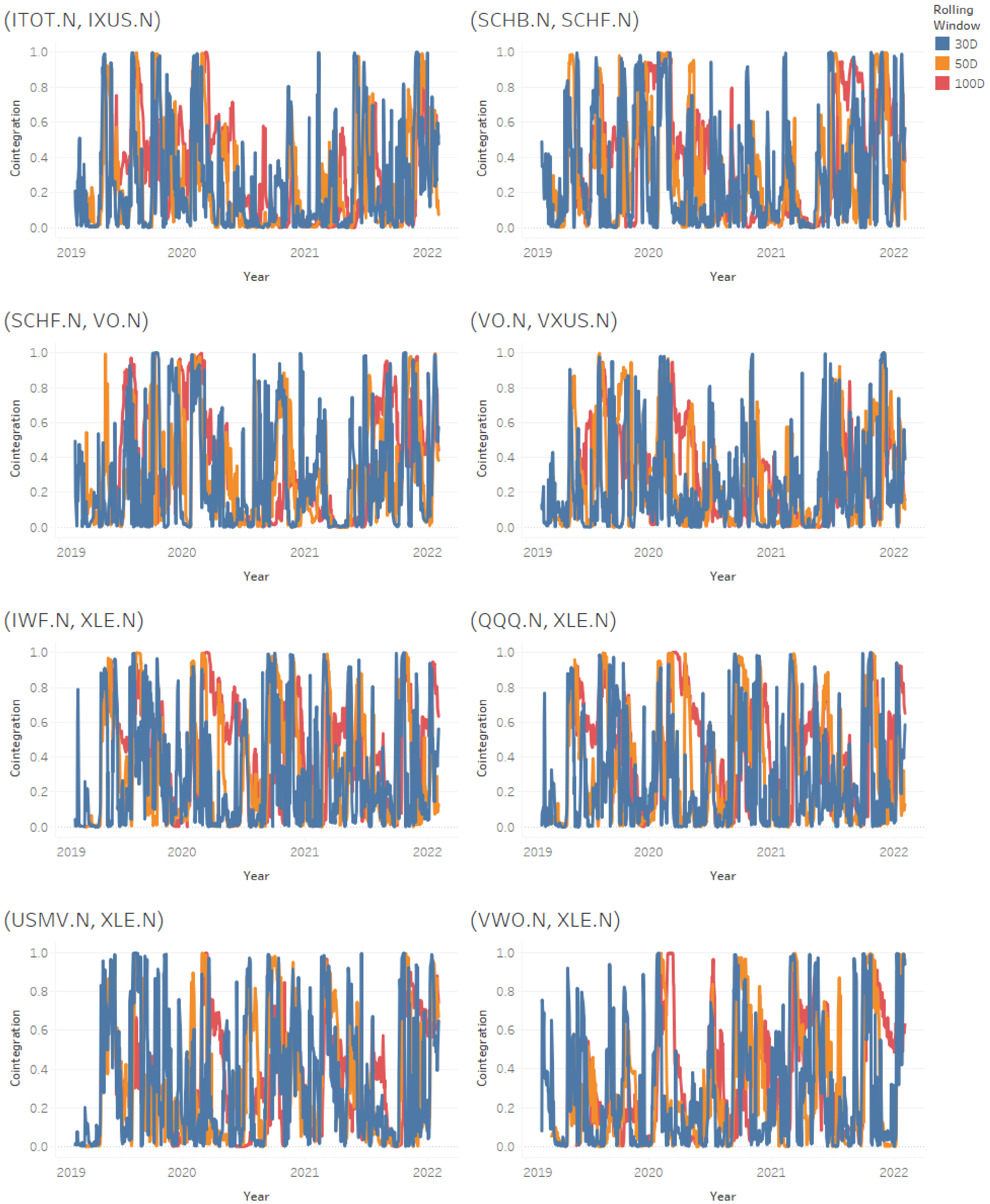

Table D.1.4: This table presents the summary of ROI bifurcated window-wise and then pair-wise. Column I identifies the rolling window, column II the pair name, column III the number of $TRAD$-based trading strategies that have had a positive ROI, column IV the number of MOD-based trading strategies that have had a positive ROI, column V the number of $TRAD$-based trading strategies having an ROI greater than the ROI of MOD-based strategies, column VI the number of MOD-based trading strategies having an ROI greater than the ROI of $TRAD$-based strategies, column VII the average ROI of $TRAD$-based trading strategies, and column VIII the average ROI of MOD-based trading strategies.

(I) Rolling Window	**(II) Pair Name**	**(III) No. of TRAD Strategies having +ve ROI**	**(IV) No. of MOD Strategies having +ve ROI**	**(V) ROI of TRAD Strategies >ROI of MOD Strategies**	**(VI) ROI of MOD Strategies >ROI of TRAD Strategies**	**(VII) Average ROI of TRAD Strategies**	**(VIII) Average ROI of MOD Strategies**
30	ITOT.N/IXUS.N	37	23	0	**11**	1.07%	**10.89%**
	IWF.N/XLE.N	29	26	0	**17**	8.28%	**25.66%**
	QQQ.N/XLE.N	21	28	0	**21**	10.02%	**29.38%**
	SCHB.N/SCHF.N	34	16	2	**4**	4.63%	**17.25%**
	SCHF.N/VO.N	38	31	0	**20**	3.14%	**11.42%**
	USMV.N/XLE.N	29	25	1	**17**	10.33%	**30.44%**
	VO.N/VXUS.N	36	23	2	**14**	3.22%	**13.28%**
	VWO.N/XLE.N	20	29	0	**18**	4.62%	**17.57%**
50	ITOT.N/IXUS.N	23	25	0	**11**	1.29%	**10.24%**
	IWF.N/XLE.N	19	32	0	**21**	4.73%	**62.37%**
	QQQ.N/XLE.N	11	33	0	**20**	4.65%	**105.06%**
	SCHB.N/SCHF.N	22	24	4	**6**	2.41%	**21.89%**
	SCHF.N/VO.N	25	30	0	**17**	1.50%	**21.78%**
	USMV.N/XLE.N	21	30	0	**21**	19.33%	**53.87%**
	VO.N/VXUS.N	23	28	5	**18**	1.93%	**21.77%**
	VWO.N/XLE.N	14	31	0	**22**	6.36%	**41.70%**
100	ITOT.N/IXUS.N	33	23	2	**9**	3.31%	**8.24%**
	IWF.N/XLE.N	17	35	0	**25**	**47.29%**	35.60%
	QQQ.N/XLE.N	21	34	0	**22**	43.06%	**49.53%**
	SCHB.N/SCHF.N	36	23	**10**	7	4.80%	**13.87%**
	SCHF.N/VO.N	36	36	0	**19**	4.32%	**21.09%**
	USMV.N/XLE.N	19	33	2	**18**	15.21%	**122.10%**
	VO.N/VXUS.N	28	21	4	**10**	2.15%	**8.03%**
	VWO.N/XLE.N	24	33	0	**24**	5.49%	**23.90%**

Table D.1.5: This table presents the summary of ROI bifurcated pair-wise, window-wise and then model-wise. Column I identifies the pair, column II the rolling window, column III the model name, column IV the number of $TRAD$-based trading strategies that have had a positive ROI, column V the number of MOD-based trading strategies that have had a positive ROI, column VI the number of $TRAD$-based trading strategies having an ROI greater than the ROI of MOD-based strategies, column VII the number of MOD-based trading strategies having an ROI greater than the ROI of $TRAD$-based strategies, column VIII the average ROI of $TRAD$-based trading strategies, and column IX the average ROI of MOD-based trading strategies.

(I) Pair Name	**(II)** Rolling Window	**(III)** Model	**(IV)** No. of TRAD Strategies having +ve ROI	**(V)** No. of MOD Strategies having +ve ROI	**(VI)** ROI of TRAD Strategies > ROI of MOD Strategies	**(VII)** ROI of MOD Strategies > ROI of TRAD Strategies	**(VIII)** Average ROI of TRAD Strategies	**(IX)** Average ROI of MOD Strategies
ITOT.N/IXUS.N	30	$DIST^{V1.1} - SPRD$	**5**	2	0	**1**	1.61%	**6.04%**
		$DIST^{V1.2} - SPRD$	**4**	**4**	0	**3**	0.96%	**4.75%**
		$DIST^{V2} - SPRD$	1	**3**	0	**1**	0.15%	**2.13%**
		$DIST^{V3} - SPRD$	**6**	2	0	**2**	0.76%	**5.51%**
		$DIST^{V4} - SPRD$	**6**	2	0	**2**	0.76%	**4.73%**
		$JOHANSEN - SPRD$	**3**	**3**	0	0	1.29%	**4.62%**
		$ADF - SPRD$	0	**3**	0	0		**52.77%**
		$KALMAN - SPRD$	**6**	3	0	**2**	1.97%	**5.76%**
		$RATIO - SPRD$	**6**	1	0	0	0.43%	**3.06%**
		Total	**37**	23	0	**11**		
	50	$DIST^{V1.1} - SPRD$	**3**	2	0	**1**	0.54%	**6.92%**
		$DIST^{V1.2} - SPRD$	**4**	1	0	0	**1.75%**	0.22%
		$DIST^{V2} - SPRD$	**3**	**3**	0	**1**	1.38%	**2.54%**
		$DIST^{V3} - SPRD$	**4**	3	0	**1**	1.64%	**2.57%**
		$DIST^{V4} - SPRD$	**4**	3	0	**1**	1.64%	**2.57%**
		$JOHANSEN - SPRD$	1	**5**	0	**3**	1.10%	**30.67%**
		$ADF - SPRD$	0	**3**	0	0		**11.06%**
		$KALMAN - SPRD$	2	**4**	0	**4**	1.06%	**7.24%**
		$RATIO - SPRD$	**2**	1	0	0	0.26%	**3.36%**
		Total	23	**25**	0	**11**		
	100	$DIST^{V1.1} - SPRD$	1	**2**	0	**1**	0.06%	**7.92%**
		$DIST^{V1.2} - SPRD$	0	**2**	0	**1**		**2.93%**
		$DIST^{V2} - SPRD$	**5**	3	0	0	1.92%	**2.21%**
		$DIST^{V3} - SPRD$	**6**	3	0	**1**	2.33%	**3.66%**
		$DIST^{V4} - SPRD$	**6**	3	0	**1**	2.33%	**3.66%**
		$JOHANSEN - SPRD$	**6**	5	0	**2**	8.03%	**21.26%**
		$ADF - SPRD$	**0**	**0**	0	0		
		$KALMAN - SPRD$	**5**	4	0	**3**	2.35%	**7.32%**
		$RATIO - SPRD$	**4**	1	**2**	0	2.96%	**3.64%**
		Total	**33**	23	2	**9**		
IWF.N/XLE.N	30	$DIST^{V1.1} - SPRD$	3	**5**	0	**3**	2.62%	**20.05%**
		$DIST^{V1.2} - SPRD$	**4**	2	0	**2**	2.41%	**18.85%**
		$DIST^{V2} - SPRD$	3	**4**	0	**2**	2.24%	**19.99%**
		$DIST^{V3} - SPRD$	**5**	3	0	**2**	3.86%	**13.60%**
		$DIST^{V4} - SPRD$	**5**	3	0	**2**	3.86%	**13.60%**
		$JOHANSEN - SPRD$	0	**2**	0	**2**		**30.86%**
		$ADF - SPRD$	**4**	2	0	0	32.14%	**97.42%**
		$KALMAN - SPRD$	**4**	2	0	**1**	12.12%	**17.26%**
		$RATIO - SPRD$	1	**3**	0	**3**	0.38%	**25.54%**
		Total	**29**	26	0	**17**		
	50	$DIST^{V1.1} - SPRD$	1	**5**	0	**4**	5.77%	**23.78%**
		$DIST^{V1.2} - SPRD$	3	**4**	0	**2**	8.03%	**11.39%**
		$DIST^{V2} - SPRD$	**5**	2	0	**1**	3.31%	**27.92%**
		$DIST^{V3} - SPRD$	2	**3**	0	**2**	3.42%	**14.80%**
		$DIST^{V4} - SPRD$	2	**4**	0	**2**	3.42%	**12.35%**
		$JOHANSEN - SPRD$	**3**	**3**	0	**3**	6.11%	**144.65%**
		$ADF - SPRD$	0	**2**	0	**1**		**507.63%**
		$KALMAN - SPRD$	3	**5**	0	**2**	3.81%	**32.24%**
		$RATIO - SPRD$	0	**4**	0	**4**		**17.80%**
		Total	19	**32**	0	**21**		
	100	$DIST^{V1.1} - SPRD$	4	**7**	0	**5**	14.07%	**22.37%**
		$DIST^{V1.2} - SPRD$	0	**3**	0	**2**		**19.21%**
		$DIST^{V2} - SPRD$	**2**	1	0	**1**	0.52%	**58.23%**
		$DIST^{V3} - SPRD$	1	**4**	0	**2**	0.18%	**6.57%**
		$DIST^{V4} - SPRD$	1	**4**	0	**2**	0.18%	**6.57%**
		$JOHANSEN - SPRD$	2	**4**	0	**4**	0.84%	**52.69%**
		$ADF - SPRD$	**6**	4	0	**2**	123.35%	**129.52%**
		$KALMAN - SPRD$	1	**4**	0	**3**	4.45%	**27.52%**
		$RATIO - SPRD$	0	**4**	0	**4**		**20.55%**
		Total	17	**35**	0	**25**		
QQQ.N/XLE.N	30	$DIST^{V1.1} - SPRD$	0	**6**	0	**4**		**24.79%**
		$DIST^{V1.2} - SPRD$	**5**	1	0	**1**	4.52%	**9.71%**
		$DIST^{V2} - SPRD$	**3**	**3**	0	**3**	3.47%	**21.16%**
		$DIST^{V3} - SPRD$	**2**	**2**	0	**2**	7.51%	**27.15%**
		$DIST^{V4} - SPRD$	**2**	**2**	0	**2**	7.51%	**23.97%**
		$JOHANSEN - SPRD$	3	**5**	0	**4**	6.23%	**49.80%**
		$ADF - SPRD$	**2**	**2**	0	0	**35.56%**	3.06%
		$KALMAN - SPRD$	**4**	3	0	**1**	14.37%	**39.55%**
		$RATIO - SPRD$	0	**4**	0	**4**		**31.16%**
		Total	21	**28**	0	**21**		
	50	$DIST^{V1.1} - SPRD$	2	**6**	0	**3**	7.42%	**22.94%**
		$DIST^{V1.2} - SPRD$	0	**4**	0	**3**		**18.52%**
		$DIST^{V2} - SPRD$	1	**3**	0	**2**	6.04%	**8.26%**
		$DIST^{V3} - SPRD$	0	**4**	0	**2**		**24.06%**
		$DIST^{V4} - SPRD$	0	**4**	0	**2**		**24.06%**
		$JOHANSEN - SPRD$	**5**	1	0	**1**	2.88%	**41.90%**
		$ADF - SPRD$	0	**4**	0	**2**		**719.80%**
		$KALMAN - SPRD$	**2**	**2**	0	0	**7.60%**	4.25%
		$RATIO - SPRD$	1	**5**	0	**5**	0.65%	**21.73%**
		Total	11	**33**	0	**20**		
	100	$DIST^{V1.1} - SPRD$	2	**6**	0	**4**	15.31%	**21.53%**
		$DIST^{V1.2} - SPRD$	0	**2**	0	**1**		**14.57%**
		$DIST^{V2} - SPRD$	1	**3**	0	**2**	1.60%	**19.93%**
		$DIST^{V3} - SPRD$	**2**	**2**	0	**1**	4.33%	**9.60%**
		$DIST^{V4} - SPRD$	**2**	**2**	0	**1**	4.33%	**20.03%**
		$JOHANSEN - SPRD$	**4**	**4**	0	**4**	8.38%	**141.49%**
		$ADF - SPRD$	**6**	5	0	**1**	**125.37%**	94.84%
		$KALMAN - SPRD$	4	**5**	0	**3**	17.27%	**48.55%**
		$RATIO - SPRD$	0	**5**	0	**5**		**24.77%**
		Total	21	**34**	0	**22**		
SCHB.N/SCHF.N	30	$DIST^{V1.1} - SPRD$	0	**2**	0	**2**		**8.96%**
		$DIST^{V1.2} - SPRD$	**3**	0	0	0	**1.94%**	
		$DIST^{V2} - SPRD$	**6**	3	0	**1**	2.28%	**4.54%**
		$DIST^{V3} - SPRD$	**6**	0	0	0	**1.99%**	
		$DIST^{V4} - SPRD$	**6**	0	0	0	**1.99%**	
		$JOHANSEN - SPRD$	**6**	2	0	0	**14.59%**	7.27%
		$ADF - SPRD$	0	**4**	0	0		**42.15%**
		$KALMAN - SPRD$	1	**3**	0	**1**	3.29%	**18.41%**
		$RATIO - SPRD$	**6**	2	**2**	0	**3.86%**	3.03%
		Total	**34**	16	2	**4**		
	50	$DIST^{V1.1} - SPRD$	0	**3**	0	**2**		**6.71%**
		$DIST^{V1.2} - SPRD$	1	**3**	0	0	**1.37%**	0.76%
		$DIST^{V2} - SPRD$	**6**	2	0	**1**	0.82%	**3.79%**
		$DIST^{V3} - SPRD$	**3**	**3**	0	0	1.37%	**2.23%**
		$DIST^{V4} - SPRD$	**3**	**3**	0	0	1.37%	**2.23%**
		$JOHANSEN - SPRD$	0	**3**	0	**3**		**38.08%**
		$ADF - SPRD$	0	**3**	0	0		**116.09%**
		$KALMAN - SPRD$	**3**	**3**	0	0	3.18%	**5.09%**
		$RATIO - SPRD$	**6**	1	**4**	0	**4.82%**	4.27%
		Total	22	**24**	4	**6**		
	100	$DIST^{V1.1} - SPRD$	**4**	**4**	0	**2**	2.27%	**5.87%**
		$DIST^{V1.2} - SPRD$	0	**1**	0	**1**		**5.89%**
		$DIST^{V2} - SPRD$	**2**	1	0	**1**	0.27%	**14.23%**
		$DIST^{V3} - SPRD$	**6**	4	**4**	0	**4.39%**	2.15%
		$DIST^{V4} - SPRD$	**6**	4	**4**	0	**4.39%**	2.15%
		$JOHANSEN - SPRD$	**6**	2	0	**2**	0.78%	**24.77%**
		$ADF - SPRD$	0	**3**	0	0		**53.60%**
		$KALMAN - SPRD$	**6**	3	0	**1**	13.88%	**14.73%**
		$RATIO - SPRD$	**6**	1	**2**	0	3.75%	**3.77%**
		Total	**36**	23	**10**	7		
SCHF.N/VO.N	30	$DIST^{V1.1} - SPRD$	3	**5**	0	**3**	1.90%	**5.03%**
		$DIST^{V1.2} - SPRD$	**2**	1	0	**1**	1.43%	**2.22%**
		$DIST^{V2} - SPRD$	**3**	**3**	0	**3**	0.70%	**7.94%**
		$DIST^{V3} - SPRD$	**6**	3	0	**2**	2.02%	**3.63%**
		$DIST^{V4} - SPRD$	**6**	3	0	**2**	2.02%	**3.63%**
		$JOHANSEN - SPRD$	**6**	4	0	**2**	8.69%	**44.17%**
		$ADF - SPRD$	**6**	**6**	0	**2**	3.64%	**7.18%**
		$KALMAN - SPRD$	1	**5**	0	**4**	0.06%	**10.70%**
		$RATIO - SPRD$	**5**	1	0	**1**	2.08%	**7.74%**
		Total	**38**	31	0	**20**		
	50	$DIST^{V1.1} - SPRD$	2	**4**	0	**1**	1.43%	**4.51%**
		$DIST^{V1.2} - SPRD$	0	**3**	0	**3**		**4.04%**
		$DIST^{V2} - SPRD$	**4**	**4**	0	**2**	0.31%	**4.50%**
		$DIST^{V3} - SPRD$	**3**	2	0	0	0.61%	**3.32%**
		$DIST^{V4} - SPRD$	3	**4**	0	**2**	0.61%	**6.59%**
		$JOHANSEN - SPRD$	0	**3**	0	**2**		**145.51%**
		$ADF - SPRD$	4	**6**	0	**4**	2.16%	**16.22%**
		$KALMAN - SPRD$	**3**	**3**	0	**2**	1.20%	**10.26%**
		$RATIO - SPRD$	**6**	1	0	**1**	2.92%	**7.74%**
		Total	25	**30**	0	**17**		
	100	$DIST^{V1.1} - SPRD$	2	**4**	0	**3**	0.80%	**6.49%**
		$DIST^{V1.2} - SPRD$	0	**4**	0	**1**		**1.45%**
		$DIST^{V2} - SPRD$	**4**	**4**	0	**3**	1.81%	**5.63%**
		$DIST^{V3} - SPRD$	**6**	4	0	**2**	2.67%	**5.09%**
		$DIST^{V4} - SPRD$	**6**	4	0	**2**	2.67%	**4.83%**
		$JOHANSEN - SPRD$	**6**	5	0	**2**	14.32%	**113.51%**
		$ADF - SPRD$	1	**5**	0	**3**	0.59%	**11.67%**
		$KALMAN - SPRD$	**5**	**5**	0	**2**	3.48%	**6.31%**
		$RATIO - SPRD$	**6**	1	0	**1**	1.78%	**7.73%**
		Total	**36**	**36**	0	**19**		
USMV.N/XLE.N	30	$DIST^{V1.1} - SPRD$	**5**	3	0	0	6.98%	**14.22%**
		$DIST^{V1.2} - SPRD$	**5**	2	0	**1**	6.66%	**22.56%**
		$DIST^{V2} - SPRD$	1	**3**	0	**3**	0.08%	**14.60%**
		$DIST^{V3} - SPRD$	3	**4**	0	**3**	6.08%	**16.35%**
		$DIST^{V4} - SPRD$	3	**4**	0	**2**	6.08%	**12.52%**
		$JOHANSEN - SPRD$	0	**2**	0	**1**		**176.69%**
		$ADF - SPRD$	**6**	0	**1**	0	**27.20%**	
		$KALMAN - SPRD$	**6**	3	0	**3**	5.27%	**25.93%**
		$RATIO - SPRD$	0	**4**	0	**4**		**20.68%**
		Total	**29**	25	1	**17**		
	50	$DIST^{V1.1} - SPRD$	**6**	3	0	**1**	13.05%	**23.85%**
		$DIST^{V1.2} - SPRD$	**6**	2	0	**1**	7.54%	**22.80%**
		$DIST^{V2} - SPRD$	0	**3**	0	**3**		**14.51%**
		$DIST^{V3} - SPRD$	0	**4**	0	**3**		**15.03%**
		$DIST^{V4} - SPRD$	0	**4**	0	**3**		**15.03%**
		$JOHANSEN - SPRD$	**6**	2	0	**2**	39.66%	**539.38%**
		$ADF - SPRD$	3	**4**	0	0	14.84%	**25.01%**
		$KALMAN - SPRD$	0	**4**	0	**4**		**20.82%**
		$RATIO - SPRD$	0	**4**	0	**4**		**18.30%**
		Total	21	**30**	0	**21**		
	100	$DIST^{V1.1} - SPRD$	**6**	4	0	**1**	9.85%	**13.59%**
		$DIST^{V1.2} - SPRD$	**2**	**2**	0	0	**8.91%**	7.00%
		$DIST^{V2} - SPRD$	0	**3**	0	**3**		**9.37%**
		$DIST^{V3} - SPRD$	0	**5**	0	**3**		**11.66%**
		$DIST^{V4} - SPRD$	0	**5**	0	**3**		**12.88%**
		$JOHANSEN - SPRD$	**4**	**4**	0	**2**	1.91%	**891.01%**
		$ADF - SPRD$	**6**	4	**2**	0	**34.07%**	24.42%
		$KALMAN - SPRD$	0	**3**	0	**3**		**24.97%**
		$RATIO - SPRD$	1	**3**	0	**3**	0.04%	**24.53%**
		Total	19	**33**	2	**18**		
VO.N/VXUS.N	30	$DIST^{V1.1} - SPRD$	**4**	**4**	0	**4**	1.03%	**5.78%**
		$DIST^{V1.2} - SPRD$	**4**	3	0	**3**	0.98%	**10.66%**
		$DIST^{V2} - SPRD$	**2**	**2**	0	0	1.76%	**2.25%**
		$DIST^{V3} - SPRD$	**6**	2	0	**1**	2.06%	**4.29%**
		$DIST^{V4} - SPRD$	**6**	2	0	**1**	2.06%	**4.29%**
		$JOHANSEN - SPRD$	**6**	4	0	**1**	10.94%	**24.22%**
		$ADF - SPRD$	0	**3**	0	**2**		**40.05%**
		$KALMAN - SPRD$	**2**	**2**	0	**2**	2.77%	**4.91%**
		$RATIO - SPRD$	**6**	1	**2**	0	1.44%	**1.76%**
		Total	**36**	23	2	**14**		
	50	$DIST^{V1.1} - SPRD$	2	**5**	0	**5**	1.15%	**5.32%**
		$DIST^{V1.2} - SPRD$	0	**5**	0	**2**		**1.99%**
		$DIST^{V2} - SPRD$	**4**	2	0	**1**	1.06%	**2.58%**
		$DIST^{V3} - SPRD$	**4**	3	0	**2**	0.63%	**4.28%**
		$DIST^{V4} - SPRD$	**4**	3	0	**2**	0.63%	**4.28%**
		$JOHANSEN - SPRD$	**3**	**3**	0	**1**	3.71%	**40.65%**
		$ADF - SPRD$	0	**3**	0	**3**		**127.57%**
		$KALMAN - SPRD$	0	**3**	0	**2**		**12.19%**
		$RATIO - SPRD$	**6**	1	**5**	0	**3.60%**	1.04%
		Total	23	**28**	5	**18**		
	100	$DIST^{V1.1} - SPRD$	2	**4**	0	**3**	0.21%	**5.61%**
		$DIST^{V1.2} - SPRD$	0	**3**	0	**2**		**5.26%**
		$DIST^{V2} - SPRD$	**4**	3	0	**1**	2.30%	**2.36%**
		$DIST^{V3} - SPRD$	**5**	2	0	**1**	2.40%	**5.87%**
		$DIST^{V4} - SPRD$	**5**	2	0	**1**	2.40%	**6.51%**
		$JOHANSEN - SPRD$	**4**	3	0	0	0.16%	**13.28%**
		$ADF - SPRD$	**1**	**1**	0	0	**6.55%**	2.68%
		$KALMAN - SPRD$	**2**	**2**	0	**2**	1.80%	**27.65%**
		$RATIO - SPRD$	**5**	1	**4**	0	**3.16%**	0.75%
		Total	**28**	21	4	**10**		
VWO.N/XLE.N	30	$DIST^{V1.1} - SPRD$	**3**	**3**	0	0	**5.76%**	5.26%
		$DIST^{V1.2} - SPRD$	2	**5**	0	**4**	6.47%	**24.35%**
		$DIST^{V2} - SPRD$	3	**4**	0	**1**	2.08%	**9.38%**
		$DIST^{V3} - SPRD$	**4**	1	0	0	**5.68%**	3.42%
		$DIST^{V4} - SPRD$	**4**	2	0	**1**	5.68%	**6.42%**
		$JOHANSEN - SPRD$	0	**3**	0	**2**		**35.08%**
		$ADF - SPRD$	**3**	**3**	0	**2**	3.18%	**29.30%**
		$KALMAN - SPRD$	0	**4**	0	**4**		**22.62%**
		$RATIO - SPRD$	1	**4**	0	**4**	0.85%	**8.62%**
		Total	20	**29**	0	**18**		
	50	$DIST^{V1.1} - SPRD$	**4**	**4**	0	0	**11.29%**	9.30%
		$DIST^{V1.2} - SPRD$	2	**6**	0	**5**	7.29%	**23.73%**
		$DIST^{V2} - SPRD$	2	**4**	0	**2**	9.58%	**13.27%**
		$DIST^{V3} - SPRD$	**3**	2	0	**1**	1.69%	**14.42%**
		$DIST^{V4} - SPRD$	**3**	1	0	**1**	1.69%	**25.86%**
		$JOHANSEN - SPRD$	0	**4**	0	**3**		**183.86%**
		$ADF - SPRD$	0	**3**	0	**3**		**62.04%**
		$KALMAN - SPRD$	0	**4**	0	**4**		**13.66%**
		$RATIO - SPRD$	0	**3**	0	**3**		**9.72%**
		Total	14	**31**	0	**22**		
	100	$DIST^{V1.1} - SPRD$	**6**	3	0	**1**	6.86%	**16.47%**
		$DIST^{V1.2} - SPRD$	0	**4**	0	**4**		**25.90%**
		$DIST^{V2} - SPRD$	0	**5**	0	**2**		**10.06%**
		$DIST^{V3} - SPRD$	**4**	3	0	**2**	3.43%	**13.30%**
		$DIST^{V4} - SPRD$	**4**	3	0	**2**	3.43%	**13.30%**
		$JOHANSEN - SPRD$	**6**	**6**	0	**5**	8.32%	**58.13%**
		$ADF - SPRD$	3	**4**	0	**3**	4.13%	**15.90%**
		$KALMAN - SPRD$	1	**3**	0	**3**	0.75%	**22.49%**
		$RATIO - SPRD$	0	**2**	0	**2**		**12.86%**
		Total	24	**33**	0	**24**		

Table D.1.6: This table presents the summary of ROI bifurcated pair-wise, window-wise and model-wise. The trading strategies are bifurcated based on two sets of comparisons. We compare the average ROI of $TRAD$ and MOD-based trading strategies in columns I and II, respectively. Similarly, in columns III, IV, and V, we compare the average ROI of $TRAD$, MOD-based trading strategies (excluding the ML-based trading strategies) and the ML-based trading strategies, respectively. Please note that we have bifurcated the average ROI of MOD-based trading strategies into MOD-based trading strategies without ML-based trading strategies and the average ROI of ML-based trading strategies in columns VII and VIII, respectively.

(I) Pair Name	(II) Rolling Window	(III) Model	(IV) Average ROI of TRAD Strategies	(V) Average ROI of MOD Strategies (Incl ML Strategies)	(VI) Average ROI of TRAD Strategies	(VII) Average ROI of MOD Strategies (Excl ML Strategies)	(VIII) Average ROI of ML Strategies
		$DIST^{V1.1}-SPRD$	1.61%	**6.04%**	1.61%	**6.04%**	
		$DIST^{V1.2}-SPRD$	0.96%	**4.75%**	0.96%	2.80%	**10.60%**
		$DIST^{V2}-SPRD$	0.15%	**2.13%**	0.15%	**2.13%**	
		$DIST^{V3}-SPRD$	0.76%	**5.51%**	0.76%	**5.51%**	
	30	$DIST^{V4}-SPRD$	0.76%	**4.73%**	0.76%	**4.73%**	
		$JOHANSEN-SPRD$	1.29%	**4.62%**	1.29%	**6.78%**	0.30%
		$ADF-SPRD$		**52.77%**		**52.77%**	
		$KALMAN-SPRD$	1.97%	**5.76%**	1.97%	1.60%	**7.85%**
		$RATIO-SPRD$	0.43%	**3.06%**	0.43%	**3.06%**	
		$DIST^{V1.1}-SPRD$	0.54%	**6.92%**	0.54%	**6.92%**	
		$DIST^{V1.2}-SPRD$	**1.75%**	0.22%	**1.75%**		0.22%
		$DIST^{V2}-SPRD$	1.38%	**2.54%**	1.38%	**2.54%**	
		$DIST^{V3}-SPRD$	1.64%	**2.57%**	1.64%	**2.57%**	
ITOT.N/IXUS.N	50	$DIST^{V4}-SPRD$	1.64%	**2.57%**	1.64%	**2.57%**	
		$JOHANSEN-SPRD$	1.10%	**30.67%**	1.10%	**36.69%**	6.60%
		$ADF-SPRD$		**11.06%**		**11.06%**	
		$KALMAN-SPRD$	1.06%	**7.24%**	1.06%	6.63%	**7.86%**
		$RATIO-SPRD$	0.26%	**3.36%**	0.26%	**3.36%**	
		$DIST^{V1.1}-SPRD$	0.06%	**7.92%**	0.06%	**7.92%**	
		$DIST^{V1.2}-SPRD$		**2.93%**		**3.47%**	2.38%
		$DIST^{V2}-SPRD$	1.92%	**2.21%**	1.92%	**2.21%**	
		$DIST^{V3}-SPRD$	2.33%	**3.66%**	2.33%	**3.66%**	
	100	$DIST^{V4}-SPRD$	2.33%	**3.66%**	2.33%	**3.66%**	
		$JOHANSEN-SPRD$	8.03%	**21.26%**	8.03%	**24.87%**	6.83%
		$ADF-SPRD$					
		$KALMAN-SPRD$	2.35%	**7.32%**	2.35%	3.51%	**11.13%**
		$RATIO-SPRD$	2.96%	**3.64%**	2.96%	**3.64%**	
		$DIST^{V1.1}-SPRD$	2.62%	**20.05%**	2.62%	**27.42%**	8.99%
		$DIST^{V1.2}-SPRD$	2.41%	**18.85%**	2.41%	16.83%	**20.86%**
		$DIST^{V2}-SPRD$	2.24%	**19.99%**	2.24%	**27.99%**	11.99%
		$DIST^{V3}-SPRD$	3.86%	**13.60%**	3.86%	**13.60%**	
	30	$DIST^{V4}-SPRD$	3.86%	**13.60%**	3.86%	**13.60%**	
		$JOHANSEN-SPRD$		**30.86%**		**52.76%**	8.95%
		$ADF-SPRD$	32.14%	**97.42%**	32.14%	**97.42%**	
		$KALMAN-SPRD$	12.12%	**17.26%**	12.12%	**17.26%**	
		$RATIO-SPRD$	0.38%	**25.54%**	0.38%	**25.54%**	
		$DIST^{V1.1}-SPRD$	5.77%	**23.78%**	5.77%	**28.80%**	16.27%
		$DIST^{V1.2}-SPRD$	8.03%	**11.39%**	8.03%	**14.83%**	7.95%
		$DIST^{V2}-SPRD$	3.31%	**27.92%**	3.31%	**27.92%**	
		$DIST^{V3}-SPRD$	3.42%	**14.80%**	3.42%	**14.80%**	
IWF.N/XLE.N	50	$DIST^{V4}-SPRD$	3.42%	**12.35%**	3.42%	**14.80%**	4.98%
		$JOHANSEN-SPRD$	6.11%	**144.65%**	6.11%	**355.24%**	39.36%
		$ADF-SPRD$		**507.63%**		**507.63%**	
		$KALMAN-SPRD$	3.81%	**32.24%**	3.81%	**51.03%**	4.06%
		$RATIO-SPRD$		**17.80%**		**22.99%**	2.20%
		$DIST^{V1.1}-SPRD$	14.07%	**22.37%**	14.07%	17.76%	**33.91%**
		$DIST^{V1.2}-SPRD$		**19.21%**		**28.75%**	0.14%
		$DIST^{V2}-SPRD$	0.52%	**58.23%**	0.52%	**58.23%**	
		$DIST^{V3}-SPRD$	0.18%	**6.57%**	0.18%	**8.00%**	2.25%
	100	$DIST^{V4}-SPRD$	0.18%	**6.57%**	0.18%	**8.00%**	2.25%
		$JOHANSEN-SPRD$	0.84%	**52.69%**	0.84%	**83.05%**	22.33%
		$ADF-SPRD$	123.35%	**129.52%**	123.35%	**249.09%**	9.94%
		$KALMAN-SPRD$	4.45%	**27.52%**	4.45%	**34.96%**	20.09%
		$RATIO-SPRD$		**20.55%**		**25.40%**	5.99%
		$DIST^{V1.1}-SPRD$		**24.79%**		21.20%	**31.98%**
		$DIST^{V1.2}-SPRD$	4.52%	**9.71%**	4.52%	**9.71%**	
		$DIST^{V2}-SPRD$	3.47%	**21.16%**	3.47%	13.69%	**24.89%**
		$DIST^{V3}-SPRD$	7.51%	**27.15%**	7.51%	21.39%	**32.91%**
	30	$DIST^{V4}-SPRD$	7.51%	**23.97%**	7.51%	21.39%	**26.54%**
		$JOHANSEN-SPRD$	6.23%	**49.80%**	6.23%	**49.80%**	
		$ADF-SPRD$	**35.56%**	3.06%	**35.56%**		3.06%
		$KALMAN-SPRD$	14.37%	**39.55%**	14.37%	**58.51%**	1.63%
		$RATIO-SPRD$		**31.16%**		29.88%	**35.00%**
		$DIST^{V1.1}-SPRD$	7.42%	**22.94%**	7.42%	**24.23%**	20.35%
		$DIST^{V1.2}-SPRD$		**18.52%**		**19.90%**	14.38%
		$DIST^{V2}-SPRD$	6.04%	**8.26%**	6.04%	**13.69%**	5.54%
		$DIST^{V3}-SPRD$		**24.06%**		**24.06%**	
QQQ.N/XLE.N	50	$DIST^{V4}-SPRD$		**24.06%**		**24.06%**	
		$JOHANSEN-SPRD$	2.88%	**41.90%**	2.88%	**41.90%**	
		$ADF-SPRD$		**719.80%**		**955.48%**	12.75%
		$KALMAN-SPRD$	**7.60%**	4.25%	**7.60%**	4.25%	
		$RATIO-SPRD$	0.65%	**21.73%**	0.65%	**29.13%**	10.63%
		$DIST^{V1.1}-SPRD$	15.31%	**21.53%**	15.31%	**21.84%**	20.91%
		$DIST^{V1.2}-SPRD$		**14.57%**		**14.57%**	
		$DIST^{V2}-SPRD$	1.60%	**19.93%**	1.60%	3.40%	**28.19%**
		$DIST^{V3}-SPRD$	4.33%	**9.60%**	4.33%		**9.60%**
	100	$DIST^{V4}-SPRD$	4.33%	**20.03%**	4.33%		**20.03%**
		$JOHANSEN-SPRD$	8.38%	**141.49%**	8.38%	**174.28%**	43.12%
		$ADF-SPRD$	**125.37%**	94.84%	125.37%	**144.76%**	19.97%
		$KALMAN-SPRD$	17.27%	**48.55%**	17.27%	**64.83%**	24.13%
		$RATIO-SPRD$		**24.77%**		**33.06%**	12.34%
		$DIST^{V1.1}-SPRD$		**8.96%**		**8.96%**	
		$DIST^{V1.2}-SPRD$	**1.94%**		**1.94%**		
		$DIST^{V2}-SPRD$	2.28%	**4.54%**	2.28%	**4.54%**	
		$DIST^{V3}-SPRD$	**1.99%**		**1.99%**		
	30	$DIST^{V4}-SPRD$	**1.99%**		**1.99%**		
		$JOHANSEN-SPRD$	**14.59%**	7.27%	**14.59%**	7.27%	
		$ADF-SPRD$		**42.15%**		**50.80%**	16.20%
		$KALMAN-SPRD$	3.29%	**18.41%**	3.29%	**18.41%**	
		$RATIO-SPRD$	**3.86%**	3.03%	**3.86%**	3.03%	
		$DIST^{V1.1}-SPRD$		**6.71%**		**6.71%**	
		$DIST^{V1.2}-SPRD$	**1.37%**	0.76%	**1.37%**	0.97%	0.34%
		$DIST^{V2}-SPRD$	0.82%	**3.79%**	0.82%	**3.79%**	
		$DIST^{V3}-SPRD$	1.37%	**2.23%**	1.37%	**2.23%**	
SCHB.N/SCHF.N	50	$DIST^{V4}-SPRD$	1.37%	**2.23%**	1.37%	**2.23%**	
		$JOHANSEN-SPRD$		**38.08%**		**38.08%**	
		$ADF-SPRD$		**116.09%**		**116.09%**	
		$KALMAN-SPRD$	3.18%	**5.09%**	3.18%	**5.09%**	
		$RATIO-SPRD$	**4.82%**	4.27%	**4.82%**	4.27%	
		$DIST^{V1.1}-SPRD$	2.27%	**5.87%**	2.27%	**5.87%**	
		$DIST^{V1.2}-SPRD$		**5.89%**			**5.89%**
		$DIST^{V2}-SPRD$	0.27%	**14.23%**	0.27%	**14.23%**	
		$DIST^{V3}-SPRD$	**4.39%**	2.15%	**4.39%**	2.15%	
	100	$DIST^{V4}-SPRD$	**4.39%**	2.15%	**4.39%**	2.15%	
		$JOHANSEN-SPRD$	0.78%	**24.77%**	0.78%	**24.77%**	
		$ADF-SPRD$		**53.60%**		**53.60%**	
		$KALMAN-SPRD$	13.88%	**14.73%**	13.88%	**14.73%**	
		$RATIO-SPRD$	3.75%	**3.77%**	3.75%	**3.77%**	
		$DIST^{V1.1}-SPRD$	1.90%	**5.03%**	1.90%	4.34%	**7.79%**
		$DIST^{V1.2}-SPRD$	1.43%	**2.22%**	1.43%	**2.22%**	
		$DIST^{V2}-SPRD$	0.70%	**7.94%**	0.70%	**11.54%**	6.14%
		$DIST^{V3}-SPRD$	2.02%	**3.63%**	2.02%	3.07%	**4.76%**
	30	$DIST^{V4}-SPRD$	2.02%	**3.63%**	2.02%	3.07%	**4.76%**
		$JOHANSEN-SPRD$	8.69%	**44.17%**	8.69%	**58.52%**	1.12%
		$ADF-SPRD$	3.64%	**7.18%**	3.64%	5.82%	**9.89%**
		$KALMAN-SPRD$	0.06%	**10.70%**	0.06%	9.03%	**13.21%**
		$RATIO-SPRD$	2.08%	**7.74%**	2.08%	**7.74%**	
		$DIST^{V1.1}-SPRD$	1.43%	**4.51%**	1.43%	**5.38%**	1.92%
		$DIST^{V1.2}-SPRD$		**4.04%**		3.48%	**4.32%**
		$DIST^{V2}-SPRD$	0.31%	**4.50%**	0.31%	3.78%	**5.23%**
		$DIST^{V3}-SPRD$	0.61%	**3.32%**	0.61%	**3.92%**	2.71%
SCHF.N/VO.N	50	$DIST^{V4}-SPRD$	0.61%	**6.59%**	0.61%	3.18%	**10.00%**
		$JOHANSEN-SPRD$		**145.51%**		**213.01%**	10.53%
		$ADF-SPRD$	2.16%	**16.22%**	2.16%	**19.44%**	9.78%
		$KALMAN-SPRD$	1.20%	**10.26%**	1.20%	**11.48%**	9.66%
		$RATIO-SPRD$	2.92%	**7.74%**	2.92%	**7.74%**	
		$DIST^{V1.1}-SPRD$	0.80%	**6.49%**	0.80%	6.20%	**7.37%**
		$DIST^{V1.2}-SPRD$		**1.45%**		**1.74%**	0.57%
		$DIST^{V2}-SPRD$	1.81%	**5.63%**	1.81%	3.93%	**7.34%**
		$DIST^{V3}-SPRD$	2.67%	**5.09%**	2.67%	4.02%	**6.17%**
	100	$DIST^{V4}-SPRD$	2.67%	**4.83%**	2.67%	4.02%	**5.64%**
		$JOHANSEN-SPRD$	14.32%	**113.51%**	14.32%	**140.28%**	6.40%
		$ADF-SPRD$	0.59%	**11.67%**	0.59%	10.42%	**13.54%**
		$KALMAN-SPRD$	3.48%	**6.31%**	3.48%	**6.70%**	5.73%
		$RATIO-SPRD$	1.78%	**7.73%**	1.78%	**7.73%**	
		$DIST^{V1.1}-SPRD$	6.98%	**14.22%**	6.98%	**18.93%**	4.82%
		$DIST^{V1.2}-SPRD$	6.66%	**22.56%**	6.66%	**22.56%**	
		$DIST^{V2}-SPRD$	0.08%	**14.60%**	0.08%	**14.60%**	
		$DIST^{V3}-SPRD$	6.08%	**16.35%**	6.08%	12.57%	**20.13%**
	30	$DIST^{V4}-SPRD$	6.08%	**12.52%**	6.08%	**12.57%**	12.47%
		$JOHANSEN-SPRD$		**176.69%**		**340.65%**	12.72%
		$ADF-SPRD$	**27.20%**		**27.20%**		
		$KALMAN-SPRD$	5.27%	**25.93%**	5.27%	**32.25%**	13.30%
		$RATIO-SPRD$		**20.68%**		**20.68%**	
		$DIST^{V1.1}-SPRD$	13.05%	**23.85%**	13.05%	19.71%	**32.14%**
		$DIST^{V1.2}-SPRD$	7.54%	**22.80%**	7.54%	8.19%	**37.41%**
		$DIST^{V2}-SPRD$		**14.51%**		**14.51%**	
		$DIST^{V3}-SPRD$		**15.03%**		**15.94%**	12.30%
USMV.N/XLE.N	50	$DIST^{V4}-SPRD$		**15.03%**		**15.94%**	12.30%
		$JOHANSEN-SPRD$	39.66%	**539.38%**	39.66%	**539.38%**	
		$ADF-SPRD$	14.84%	**25.01%**	14.84%	**26.03%**	21.94%
		$KALMAN-SPRD$		**20.82%**		**20.82%**	
		$RATIO-SPRD$		**18.30%**		**18.30%**	
		$DIST^{V1.1}-SPRD$	9.85%	**13.59%**	9.85%	**26.83%**	0.36%
		$DIST^{V1.2}-SPRD$	**8.91%**	7.00%	**8.91%**	8.57%	5.43%
		$DIST^{V2}-SPRD$		**9.37%**		**9.37%**	
		$DIST^{V3}-SPRD$		**11.66%**		**11.78%**	11.47%
	100	$DIST^{V4}-SPRD$		**12.88%**		11.78%	**14.54%**
		$JOHANSEN-SPRD$	1.91%	**891.01%**	1.91%	**1182.22%**	17.35%
		$ADF-SPRD$	**34.07%**	24.42%	**34.07%**	24.42%	
		$KALMAN-SPRD$		**24.97%**		**24.97%**	
		$RATIO-SPRD$	0.04%	**24.53%**	0.04%	**24.53%**	
		$DIST^{V1.1}-SPRD$	1.03%	**5.78%**	1.03%	**6.63%**	3.22%
		$DIST^{V1.2}-SPRD$	0.98%	**10.66%**	0.98%	7.04%	**12.47%**
		$DIST^{V2}-SPRD$	1.76%	**2.25%**	1.76%	**2.25%**	
		$DIST^{V3}-SPRD$	2.06%	**4.29%**	2.06%	**4.29%**	
	30	$DIST^{V4}-SPRD$	2.06%	**4.29%**	2.06%	**4.29%**	
		$JOHANSEN-SPRD$	10.94%	**24.22%**	10.94%	**24.22%**	
		$ADF-SPRD$		**40.05%**		**40.05%**	
		$KALMAN-SPRD$	2.77%	**4.91%**	2.77%	**4.91%**	
		$RATIO-SPRD$	1.44%	**1.76%**	1.44%	**1.76%**	
		$DIST^{V1.1}-SPRD$	1.15%	**5.32%**	1.15%	**6.90%**	2.94%
		$DIST^{V1.2}-SPRD$		**1.99%**		1.39%	**2.90%**
		$DIST^{V2}-SPRD$	1.06%	**2.58%**	1.06%	**2.58%**	
		$DIST^{V3}-SPRD$	0.63%	**4.28%**	0.63%	**4.92%**	3.02%
VO.N/VXUS.N	50	$DIST^{V4}-SPRD$	0.63%	**4.28%**	0.63%	**4.92%**	3.02%
		$JOHANSEN-SPRD$	3.71%	**40.65%**	3.71%	**40.65%**	
		$ADF-SPRD$		**127.57%**		**127.57%**	
		$KALMAN-SPRD$		**12.19%**		**12.19%**	
		$RATIO-SPRD$	**3.60%**	1.04%	**3.60%**	1.04%	
		$DIST^{V1.1}-SPRD$	0.21%	**5.61%**	0.21%	**6.88%**	1.81%
		$DIST^{V1.2}-SPRD$		**5.26%**		**5.26%**	
		$DIST^{V2}-SPRD$	2.30%	**2.36%**	2.30%	**2.36%**	
		$DIST^{V3}-SPRD$	2.40%	**5.87%**	2.40%	**9.57%**	2.17%
	100	$DIST^{V4}-SPRD$	2.40%	**6.51%**	2.40%	**9.57%**	3.45%
		$JOHANSEN-SPRD$	0.16%	**13.28%**	0.16%	**19.77%**	0.29%
		$ADF-SPRD$	**6.55%**	2.68%	**6.55%**		2.68%
		$KALMAN-SPRD$	1.80%	**27.65%**	1.80%	**27.65%**	
		$RATIO-SPRD$	**3.16%**	0.75%	**3.16%**	0.75%	
		$DIST^{V1.1}-SPRD$	**5.76%**	5.26%	5.76%	**7.05%**	1.68%
		$DIST^{V1.2}-SPRD$	6.47%	**24.35%**	6.47%	9.30%	**46.92%**
		$DIST^{V2}-SPRD$	2.08%	**9.38%**	2.08%	**10.51%**	5.98%
		$DIST^{V3}-SPRD$	**5.68%**	3.42%	**5.68%**	3.42%	
	30	$DIST^{V4}-SPRD$	5.68%	**6.42%**	5.68%	3.42%	**9.42%**
		$JOHANSEN-SPRD$		**35.08%**		**46.61%**	12.02%
		$ADF-SPRD$	3.18%	**29.30%**	3.18%	13.92%	**60.07%**
		$KALMAN-SPRD$		**22.62%**		21.78%	**25.14%**
		$RATIO-SPRD$	0.85%	**8.62%**	0.85%	**13.92%**	3.32%
		$DIST^{V1.1}-SPRD$	**11.29%**	9.30%	11.29%	4.62%	**13.99%**
		$DIST^{V1.2}-SPRD$	7.29%	**23.73%**	7.29%	16.70%	**37.79%**
		$DIST^{V2}-SPRD$	9.58%	**13.27%**	9.58%	10.66%	**21.11%**
		$DIST^{V3}-SPRD$	1.69%	**14.42%**	1.69%	**25.86%**	2.97%
VWO.N/XLE.N	50	$DIST^{V4}-SPRD$	1.69%	**25.86%**	1.69%	**25.86%**	
		$JOHANSEN-SPRD$		**183.86%**		**242.28%**	8.61%
		$ADF-SPRD$		**62.04%**		**88.74%**	8.64%
		$KALMAN-SPRD$		**13.66%**		**21.72%**	5.60%
		$RATIO-SPRD$		**9.72%**		**11.80%**	5.58%
		$DIST^{V1.1}-SPRD$	6.86%	**16.47%**	6.86%	5.55%	**21.93%**
		$DIST^{V1.2}-SPRD$		**25.90%**		**28.92%**	22.89%
		$DIST^{V2}-SPRD$		**10.06%**		9.17%	**13.64%**
		$DIST^{V3}-SPRD$	3.43%	**13.30%**	3.43%	9.23%	**21.43%**
	100	$DIST^{V4}-SPRD$	3.43%	**13.30%**	3.43%	9.23%	**21.43%**
		$JOHANSEN-SPRD$	8.32%	**58.13%**	8.32%	**80.77%**	12.85%
		$ADF-SPRD$	4.13%	**15.90%**	4.13%	**21.08%**	0.35%
		$KALMAN-SPRD$	0.75%	**22.49%**	0.75%	**24.88%**	17.72%
		$RATIO-SPRD$		**12.86%**		**12.86%**	

Table D.1.7: This table presents the summary of the Sharpe ratio bifurcated window-wise, model-wise and pair-wise. Column I identifies the rolling window, column II the model name, column III the pair name, column IV the maximum annualized Sharpe ratio for MOD-based trading strategies, column V the maximum average ROI for MOD-based trading strategies, column VI the maximum annualized Sharpe ratio for $TRAD$-based trading strategies, column VII the maximum average ROI for $TRAD$-based trading strategies.

			MOD		TRAD	
(I) Window	**(II) Model Category**	**(III) Pair Name**	**(IV) Max. Annualized Sharpe Ratio**	**(V) Max. Roi**	**(VI) Max. Annualized Sharpe Ratio**	**(VII) Max. Roi**
30	$DIST^{V1.1}-SPRD$	ITOT.N/IXUS.N	3.33	9.35		
		IWF.N/XLE.N	2.70	27.29		
		QQQ.N/XLE.N	4.13	37.02		
		SCHF.N/VO.N	6.67	12.87		
		USMV.N/XLE.N	1.90	15.68	2.06	20.04
		VO.N/VXUS.N	7.14	11.91		
		VWO.N/XLE.N			1.11	9.24
	$DIST^{V2}-SPRD$	IWF.N/XLE.N	**9.37**	55.70		
		USMV.N/XLE.N	0.16	34.48		
		VWO.N/XLE.N	0.48	7.36		
	$DIST^{V3}-SPRD$	IWF.N/XLE.N	4.76	22.26		
	$DIST^{V4}-SPRD$	IWF.N/XLE.N	4.76	22.26		
	$JOHANSEN-SPRD$	IWF.N/XLE.N	2.38	52.76		
		QQQ.N/XLE.N	4.76	134.98		
		SCHF.N/VO.N	5.87	139.00	1.11	13.29
		USMV.N/XLE.N	4.29	**340.65**		
		VO.N/VXUS.N	4.13	46.12	1.27	25.86
	$ADF-SPRD$	ITOT.N/IXUS.N	1.90	142.15		
		IWF.N/XLE.N	3.02	137.67	8.10	**74.44**
		QQQ.N/XLE.N			6.35	58.05
		SCHF.N/VO.N			3.65	9.47
		USMV.N/XLE.N			11.91	39.52
		VO.N/VXUS.N	1.59	106.85		
		VWO.N/XLE.N	5.08	25.41	2.54	6.06
	$KALMAN-SPRD$	IWF.N/XLE.N	1.75	27.96	3.02	16.16
		QQQ.N/XLE.N	3.81	116.27	**18.57**	28.28
		USMV.N/XLE.N	1.11	39.55		
		VWO.N/XLE.N	3.17	37.37		
	$RATIO-SPRD$	IWF.N/XLE.N	1.27	40.95		
		QQQ.N/XLE.N	3.17	49.11		
		USMV.N/XLE.N	4.76	53.77		
50	$DIST^{V1.1}-SPRD$	ITOT.N/IXUS.N	6.67	11.50		
		IWF.N/XLE.N	2.22	24.62	1.59	5.77
		QQQ.N/XLE.N	5.24	39.87	1.11	8.09
		SCHF.N/VO.N	6.67	12.87		
		USMV.N/XLE.N	2.22	16.45	4.60	24.86
		VO.N/VXUS.N	5.56	11.44		
		VWO.N/XLE.N			2.54	20.69
	$DIST^{V1.2}-SPRD$	QQQ.N/XLE.N	3.97	29.91		
		USMV.N/XLE.N			1.43	9.54
	$DIST^{V2}-SPRD$	IWF.N/XLE.N	9.37	55.70	9.37	6.79
		USMV.N/XLE.N	0.00	33.73		
		VWO.N/XLE.N	0.16	7.83	0.32	12.57
	$DIST^{V3}-SPRD$	IWF.N/XLE.N	0.16	26.74		
		QQQ.N/XLE.N	6.19	58.53		
		USMV.N/XLE.N	1.43	30.43		
	$DIST^{V4}-SPRD$	IWF.N/XLE.N	0.16	26.74		
		QQQ.N/XLE.N	6.19	58.53		
		USMV.N/XLE.N	1.43	30.43		
	$JOHANSEN-SPRD$	ITOT.N/IXUS.N	3.17	75.17	2.38	1.10
		IWF.N/XLE.N	3.49	355.24		
		QQQ.N/XLE.N	1.90	41.90		
		SCHF.N/VO.N	9.05	311.34		
		USMV.N/XLE.N	5.08	1,009.54	5.56	**56.92**
		VO.N/VXUS.N	2.38	94.96		
		VWO.N/XLE.N	4.13	358.69		
	$ADF-SPRD$	ITOT.N/IXUS.N	11.91	13.17		
		QQQ.N/XLE.N	4.44	**1,578.35**		
		SCHF.N/VO.N	6.03	16.91		
		USMV.N/XLE.N	5.71	38.67		
		VO.N/VXUS.N	15.56	177.00		
		VWO.N/XLE.N	**30.48**	121.28		
	$KALMAN-SPRD$	IWF.N/XLE.N	3.33	72.27	**56.99**	11.07
		QQQ.N/XLE.N			3.97	13.70
		USMV.N/XLE.N	2.38	48.75		
		VO.N/VXUS.N	0.32	25.16		
		VWO.N/XLE.N	0.79	29.65		
	$RATIO-SPRD$	IWF.N/XLE.N	1.11	39.73		
		QQQ.N/XLE.N	3.02	47.35		
		USMV.N/XLE.N	4.44	52.38		
		VO.N/VXUS.N			5.87	4.26
100	$DIST^{V1.1}-SPRD$	ITOT.N/IXUS.N	**16.19**	12.95		
		IWF.N/XLE.N	2.38	25.39		
		QQQ.N/XLE.N	4.76	37.35		
		SCHF.N/VO.N	4.60	12.41		
		USMV.N/XLE.N	3.49	31.95	**18.41**	12.10
		VO.N/VXUS.N	5.08	11.12		
		VWO.N/XLE.N			2.54	12.70
	$DIST^{V1.2}-SPRD$	IWF.N/XLE.N	2.22	27.05		
		QQQ.N/XLE.N	0.48	21.88		
		USMV.N/XLE.N			1.59	10.88
		VWO.N/XLE.N	2.38	33.17		
	$DIST^{V2}-SPRD$	ITOT.N/IXUS.N			13.49	3.59
		IWF.N/XLE.N	10.48	58.23		
		VWO.N/XLE.N	0.00	19.69		
	$DIST^{V3}-SPRD$	USMV.N/XLE.N	0.32	34.35		
	$DIST^{V4}-SPRD$	USMV.N/XLE.N	0.32	34.35		
	$JOHANSEN-SPRD$	IWF.N/XLE.N	3.17	150.01	1.11	0.84
		QQQ.N/XLE.N	5.40	215.16	1.11	15.80
		SCHF.N/VO.N	4.44	**353.41**	1.90	15.35
		USMV.N/XLE.N	7.78	134.29		
		VWO.N/XLE.N	8.25	278.59	5.71	9.06
	$ADF-SPRD$	IWF.N/XLE.N	5.24	328.45	10.95	159.69
		QQQ.N/XLE.N	6.19	338.79	11.43	**181.69**
		USMV.N/XLE.N	7.14	36.35	10.95	46.18
		VWO.N/XLE.N	3.49	26.00	7.46	3.24
	$KALMAN-SPRD$	ITOT.N/IXUS.N			2.86	3.02
		IWF.N/XLE.N	2.54	40.59		
		QQQ.N/XLE.N	6.83	110.62		
		USMV.N/XLE.N	3.97	31.19		
		VO.N/VXUS.N	1.75	36.86	0.00	1.99
		VWO.N/XLE.N	0.95	31.06		
	$RATIO-SPRD$	IWF.N/XLE.N	0.32	34.18		
		QQQ.N/XLE.N	2.54	43.59		
		USMV.N/XLE.N	3.49	47.08		

Appendix D.2

Appendix for Chapter 5: Extended Results

Table D.2.1: This table presents the back-test metrics for the pair $ITOT.N/IXUS.N$ based on a 30-day rolling window. The table is subdivided into eleven parts, and in each of these parts, we present the back-test metrics and the trading strategies which use the spread derived from various models. In Part I, the spread is derived from the $DIST^{V1.1}$ model, in Part II from the $DIST^{V1.2}$ model, in Part III from the $DIST^{V2}$ model, in Part IV from the $DIST^{V3}$ model, in Part V from the $DIST^{V4}$ model, in Part VI from the $JOHANSEN - SPRD$ model, in Part VIII from the $ADF - SPRD$ model, in from the $DIST^{V2}$ model, in Part VIII from the $KALMAN - SPRD$ model, and in Part IX from the $RATIO - SPRD$ model. In Part X and XI, we present the back-test metrics of the trading strategies which use the close price of ITOT.N, and IXUS.N, respectively. All $ numbers reported below are in USD.

(I) Trading Strategy Code	(II) Model Name	(III) Total Number of Trades	(IV) Number of Winning Trades	(V) Number of Loosing Trades	(VI) Average Profit per Trade ($)	(VII) Average Loss per Trade ($)	(VIII) Gross Profit ($)	(IX) Gross Loss ($)	(X) Net Profit ($)	(XI) ROI (%)	(XII) Max P&L ($)	(XIII) Min P&L ($)	(XIV) Daily Sharpe Ratio	(XV) Annualized Sharpe Ratio	(XVI) Hit Ratio	(XVII) Expectancy	(XVIII) Profit Factor	(XIX) Realized Risk Reward Ratio	(XX) Max Drawdown ($)
Part I: Models derived using the spread obtained from $DIST^{V1.1} - SPRD^{30D}$																			
A1.1	$DIST^{V1.1} - ZSPRD^{30D}_{(3,2)}$	2	1	1	11.24	26.03	11.24	26.03	**-14.79**	-0.15	11.24	-26.03	-6.05	-96.04	50	-7.39	0.43	0.43	-26.03
A1.2	$DIST^{V1.1} - ZSPRD^{30D}_{(3,1)}$	2	2	-	13.33	-	26.66	-	**26.66**	0.27	17.12	-	-25.88	-410.83	100	13.33	26.66	13.33	-
A1.3	$DIST^{V1.1} - ZSPRD^{30D}_{(3,0.5)}$	2	2	-	2.37	-	4.73	-	**4.73**	0.05	3.5	-	-93.47	-1483.79	100	2.37	4.73	2.37	-
A1.4	$DIST^{V1.1} - ZSPRD^{30D}_{(2.7,2)}$	8	3	5	64.6	34.79	193.79	173.95	**19.84**	0.2	160.91	-64.57	-2.14	-33.97	37.5	2.48	1.11	1.86	-98.14
A1.5	$DIST^{V1.1} - ZSPRD^{30D}_{(2.7,1)}$	7	5	2	93.84	46.34	469.19	92.67	**376.52**	3.77	228.57	-81.55	-0.96	-15.24	71.43	53.79	5.06	2.03	-92.67
A1.6	$DIST^{V1.1} - ZSPRD^{30D}_{(2.7,0.5)}$	7	5	2	93.64	45.2	468.18	90.41	**377.77**	3.78	225.04	-81.55	-0.9	-14.29	71.43	53.97	5.18	2.07	-81.55
A2.1	$DIST^{V1.1} - SPRD^{30D} - SMA_{(10,20)}$	17	8	9	53.13	80.12	425.02	721.05	**-296.04**	-2.96	121.26	-254.5	-1.87	-29.69	47.06	-17.41	0.59	0.66	-449
A2.2	$DIST^{V1.1} - SPRD^{30D} - EMA_{(10,20)}$	24	17	7	73.3	139.09	1246.1	973.66	**272.45**	2.72	201.75	-279.78	-1.17	-18.57	70.83	11.34	1.28	0.53	-377.78
A2.3	$DIST^{V1.1} - SPRD^{30D} - MACD_{(12,26,9)}$	33	20	13	61.12	110.44	1222.34	1435.69	**-213.35**	-2.13	149.06	-272.02	-1.47	-23.34	60.61	-6.46	0.85	0.55	-432.94
A2.4	$DIST^{V1.1} - SPRD^{30D} - RSI_{(14)}$	4	3	1	373.47	185.16	1120.42	185.16	**935.26**	9.35	738.43	-185.16	0.21	3.33	75	233.82	6.05	2.02	-185.16
A2.5	$DIST^{V1.1} - SPRD^{30D} - BB_{(20)}$	20	8	12	62.54	44.18	500.29	530.12	**-29.83**	-0.3	159.4	-136.41	-2.24	-35.56	40	-1.49	0.94	1.42	-284.68
A3	$DIST^{V1.1} - SPRD^{30D} - DECTREE$	327	117	210	24.17	23.17	2827.99	4865.09	**-2037.1**	-20.37	191.36	-127.55	-4.82	-76.52	35.78	-6.23	0.58	1.04	-2526.49
A4	$DIST^{V1.1} - SPRD^{30D} - MLP$	337	124	213	24.13	21.71	2992.22	4624.19	**-1631.97**	-16.32	200.31	-127.55	-4.78	-75.88	36.8	-4.84	0.65	1.11	-1846.19
Part II: Models derived using the spread obtained from $DIST^{V1.2} - SPRD^{30D}$																			
B1.1	$DIST^{V1.2} - ZSPRD^{30D}_{(3,2)}$	9	6	3	38.44	19.46	230.66	58.39	**172.28**	1.72	112.26	-33.69	-3.09	-49.05	66.67	19.14	3.95	1.98	-56.34
B1.2	$DIST^{V1.2} - ZSPRD^{30D}_{(3,1)}$	8	4	4	71.09	68.88	284.38	275.51	**8.87**	0.09	143.35	-193.8	-1.52	-24.13	50	1.11	1.03	1.03	-193.8
B1.3	$DIST^{V1.2} - ZSPRD^{30D}_{(3,0.5)}$	8	4	4	94.68	57.53	378.73	230.1	**148.63**	1.49	183.55	-98.19	-1.38	-21.91	50	18.58	1.65	1.65	-138.43
B1.4	$DIST^{V1.2} - ZSPRD^{30D}_{(2.7,2)}$	10	6	4	27.7	28.64	166.21	114.55	**51.66**	0.52	53.61	-39.87	-4.44	-70.48	60	5.17	1.45	0.97	-90.43
B1.5	$DIST^{V1.2} - ZSPRD^{30D}_{(2.7,1)}$	9	4	5	31.51	62.6	126.02	313.02	**-187**	-1.87	61.09	-159.07	-2.57	-40.8	44.44	-20.78	0.4	0.5	-211.52
B1.6	$DIST^{V1.2} - ZSPRD^{30D}_{(2.7,0.5)}$	9	4	5	57.49	53.46	229.96	267.3	**-37.35**	-0.37	87.76	-98.19	-2.39	-37.94	44.44	-4.15	0.86	1.08	-138.43
B2.1	$DIST^{V1.2} - SPRD^{30D} - SMA_{(10,20)}$	15	9	6	118.59	87.81	1067.28	526.85	**540.43**	5.4	312.84	-279.57	-0.79	-12.54	60	36.03	2.03	1.35	-179.01
B2.2	$DIST^{V1.2} - SPRD^{30D} - EMA_{(10,20)}$	25	12	13	79.97	105.47	959.62	1371.13	**-411.51**	-4.12	275.42	-204.41	-1.39	-22.07	48	-16.46	0.7	0.76	-688.9
B2.3	$DIST^{V1.2} - SPRD^{30D} - MACD_{(12,26,9)}$	27	15	12	72.63	67.27	1089.46	807.18	**282.28**	2.82	191.97	-158.53	-1.58	-25.08	55.56	10.46	1.35	1.08	-527.38
B2.4	$DIST^{V1.2} - SPRD^{30D} - RSI_{(14)}$	9	2	7	150.14	205.98	300.27	1441.84	**-1141.56**	-11.42	226.99	-469.1	-1.24	-19.68	22.22	-126.85	0.21	0.73	-715.87
B2.5	$DIST^{V1.2} - SPRD^{30D} - BB_{(20)}$	15	7	8	79.52	67.46	556.67	539.66	**17.01**	0.17	218.15	-158.16	-1.54	-24.45	46.67	1.14	1.03	1.18	-283.11
B3	$DIST^{V1.2} - SPRD^{30D} - DECTREE$	303	157	146	27.44	22.24	4307.85	3247.48	**1060.37**	10.6	195.59	-100.04	-4.16	-66.04	51.82	3.5	1.33	1.23	-433.4
B4	$DIST^{V1.2} - SPRD^{30D} - MLP$	214	109	105	28.52	32.7	3109.12	3433.38	**-324.25**	-3.24	222.87	-105.09	-3.48	-55.24	50.93	-1.52	0.91	0.87	-673.87
Part III: Models derived using the spread obtained from $DIST^{V2} - SPRD^{30D}$																			
C1.1	$DIST^{V2} - ZSPRD^{30D}_{(3,2)}$	2	1	1	26.03	11.24	26.03	11.24	**14.79**	0.15	26.03	-11.24	-5.49	-87.15	50	7.39	2.32	2.32	-11.24
C1.2	$DIST^{V2} - ZSPRD^{30D}_{(3,1)}$	2	-	2	-	13.33	-	26.66	**-26.66**	-0.27	-	-17.12	-30.85	-489.73	-	-13.33	-	-	-26.66
C1.3	$DIST^{V2} - ZSPRD^{30D}_{(3,0.5)}$	2	-	2	-	2.37	-	4.73	**-4.73**	-0.05	-	-3.5	-96.43	-1530.78	-	-2.37	-	-	-4.73
C1.4	$DIST^{V2} - ZSPRD^{30D}_{(2.7,2)}$	8	5	3	34.79	64.6	173.95	193.79	**-19.84**	-0.2	64.57	-160.91	-2.21	-35.08	62.5	-2.48	0.9	0.54	-182.55
C1.5	$DIST^{V2} - ZSPRD^{30D}_{(2.7,1)}$	7	2	5	46.34	93.84	92.67	469.19	**-376.52**	-3.77	81.55	-228.57	-2.01	-31.91	28.57	-53.79	0.2	0.49	-459.65
C1.6	$DIST^{V2} - ZSPRD^{30D}_{(2.7,0.5)}$	7	2	5	45.2	93.64	90.41	468.18	**-377.77**	-3.78	81.55	-225.04	-1.89	-30	28.57	-53.97	0.19	0.48	-458.09
C2.1	$DIST^{V2} - SPRD^{30D} - SMA_{(10,20)}$	17	9	8	87.36	48.74	786.22	389.93	**396.29**	3.96	254.5	-121.26	-1.41	-22.38	52.94	23.31	2.02	1.79	-208.64
C2.2	$DIST^{V2} - SPRD^{30D} - EMA_{(10,20)}$	24	7	17	139.09	73.3	973.66	1246.1	**-272.45**	-2.72	279.78	-201.75	-1.36	-21.59	29.17	-11.34	0.78	1.9	-706.65
C2.3	$DIST^{V2} - SPRD^{30D} - MACD_{(12,26,9)}$	33	13	20	110.44	61.12	1435.69	1222.34	**213.35**	2.13	272.02	-149.06	-1.35	-21.43	39.39	6.46	1.17	1.81	-455.41
C2.4	$DIST^{V2} - SPRD^{30D} - RSI_{(14)}$	4	1	3	185.16	373.47	185.16	1120.42	**-935.26**	-9.35	185.16	-738.43	-1.01	-16.03	25	-233.82	0.17	0.5	-961.65
C2.5	$DIST^{V2} - SPRD^{30D} - BB_{(20)}$	20	12	8	44.18	62.54	530.12	500.29	**29.83**	0.3	136.41	-159.4	-2.2	-34.92	60	1.49	1.06	0.71	-169.33
C3	$DIST^{V2} - SPRD^{30D} - DECTREE$	330	120	210	24.34	22.65	2920.8	4756.1	**-1835.3**	-18.35	191.36	-127.55	-4.79	-76.04	36.36	-5.56	0.61	1.07	-2126
C4	$DIST^{V2} - SPRD^{30D} - MLP$	327	120	207	22.96	22.89	2755.73	4738.94	**-1983.2**	-19.83	191.36	-127.55	-5.06	-80.33	36.7	-6.06	0.58	1	-2083.9
Part IV: Models derived using the spread obtained from $DIST^{V3} - SPRD^{30D}$																			
D1.1	$DIST^{V3} - ZSPRD^{30D}_{(3,2)}$	8	5	3	45.23	31.6	226.16	94.8	**131.36**	1.31	84.77	-38.35	-3.1	-49.21	62.5	16.42	2.39	1.43	-38.35
D1.2	$DIST^{V3} - ZSPRD^{30D}_{(3,1)}$	8	5	3	53.91	46.29	269.54	138.87	**130.67**	1.31	84.77	-67.91	-2.48	-39.37	62.5	16.33	1.94	1.16	-67.91
D1.3	$DIST^{V3} - ZSPRD^{30D}_{(3,0.5)}$	8	5	3	49.44	65.15	247.21	195.46	**51.74**	0.52	84.77	-133.71	-2.06	-32.7	62.5	6.47	1.26	0.76	-133.74
D1.4	$DIST^{V3} - ZSPRD^{30D}_{(2.7,2)}$	10	6	4	41.13	59.91	246.78	239.64	**7.14**	0.07	84.77	-177.87	-2.11	-33.5	60	0.71	1.03	0.69	-210.48
D1.5	$DIST^{V3} - ZSPRD^{30D}_{(2.7,1)}$	10	6	4	50.44	48.41	302.62	193.64	**108.99**	1.09	84.77	-87.81	-2.47	-39.21	60	10.9	1.56	1.04	-120.41
D1.6	$DIST^{V3} - ZSPRD^{30D}_{(2.7,0.5)}$	10	6	4	46.23	62.56	277.36	250.23	**27.13**	0.27	84.77	-133.71	-2.18	-34.61	60	2.71	1.11	0.74	-133.71
D2.1	$DIST^{V3} - SPRD^{30D} - SMA_{(10,20)}$	22	11	11	106.82	60.25	1175.01	662.74	**512.27**	5.12	257.62	-212.65	-1.24	-19.68	50	23.28	1.77	1.77	-212.65
D2.2	$DIST^{V3} - SPRD^{30D} - EMA_{(10,20)}$	44	13	31	100.95	66.36	1312.41	2057.06	**-744.65**	-7.45	264.76	-215.43	-1.73	-27.46	29.55	-16.92	0.64	1.52	-1089.18
D2.3	$DIST^{V3} - SPRD^{30D} - MACD_{(12,26,9)}$	48	12	36	76.57	49.3	918.85	1774.86	**-856.01**	-8.56	240.53	-152.77	-2.15	-34.13	25	-17.83	0.52	1.55	-1291.33
D2.4	$DIST^{V3} - SPRD^{30D} - RSI_{(14)}$	5	4	1	216.79	277.47	867.14	277.47	**589.68**	5.9	487.34	-277.47	-0.12	-1.9	80	117.94	3.13	0.78	-277.47
D2.5	$DIST^{V3} - SPRD^{30D} - BB_{(20)}$	16	11	5	29.36	74.69	323	373.45	**-50.45**	-0.5	94.86	-172.61	-2.29	-36.35	68.75	-3.15	0.86	0.39	-172.61
D3	$DIST^{V3} - SPRD^{30D} - DECTREE$	314	150	164	25.91	24.31	3886.11	3986.78	**-100.67**	-1.01	225.05	-214.49	-3.96	-62.86	47.77	-0.32	0.97	1.07	-545.17
D4	$DIST^{V3} - SPRD^{30D} - MLP$	125	54	71	26.02	46.49	1405.13	3301.12	**-1895.99**	-18.96	165.28	-213.23	-2.95	-46.83	43.2	-15.17	0.43	0.56	-2079.3
Part V: Models derived using the spread obtained from $DIST^{V4} - SPRD^{30D}$																			
E1.1	$DIST^{V4} - ZSPRD^{30D}_{(3,2)}$	8	5	3	45.23	31.6	226.16	94.8	**131.36**	1.31	84.77	-38.35	-3.1	-49.21	62.5	16.42	2.39	1.43	-38.35
E1.2	$DIST^{V4} - ZSPRD^{30D}_{(3,1)}$	8	5	3	53.91	46.29	269.54	138.87	**130.67**	1.31	84.77	-67.91	-2.48	-39.37	62.5	16.33	1.94	1.16	-67.91
E1.3	$DIST^{V4} - ZSPRD^{30D}_{(3,0.5)}$	8	5	3	49.44	65.15	247.21	195.46	**51.74**	0.52	84.77	-133.71	-2.06	-32.7	62.5	6.47	1.26	0.76	-133.74
E1.4	$DIST^{V4} - ZSPRD^{30D}_{(2.7,2)}$	10	6	4	41.13	59.91	246.78	239.64	**7.14**	0.07	84.77	-177.87	-2.11	-33.5	60	0.71	1.03	0.69	-210.48
E1.5	$DIST^{V4} - ZSPRD^{30D}_{(2.7,1)}$	10	6	4	50.44	48.41	302.62	193.64	**108.99**	1.09	84.77	-87.81	-2.47	-39.21	60	10.9	1.56	1.04	-120.41
E1.6	$DIST^{V4} - ZSPRD^{30D}_{(2.7,0.5)}$	10	6	4	46.23	62.56	277.36	250.23	**27.13**	0.27	84.77	-133.71	-2.18	-34.61	60	2.71	1.11	0.74	-133.71
E2.1	$DIST^{V4} - SPRD^{30D} - SMA_{(10,20)}$	22	11	11	92.56	60.25	1018.2	662.74	**355.46**	3.55	257.62	-212.65	-1.36	-21.59	50	16.16	1.54	1.54	-212.65
E2.2	$DIST^{V4} - SPRD^{30D} - EMA_{(10,20)}$	44	13	31	100.95	66.36	1312.41	2057.06	**-744.65**	-7.45	264.76	-215.43	-1.73	-27.46	29.55	-16.92	0.64	1.52	-1089.18
E2.3	$DIST^{V4} - SPRD^{30D} - MACD_{(12,26,9)}$	48	12	36	76.57	49.3	918.85	1774.86	**-856.01**	-8.56	240.53	-152.77	-2.15	-34.13	25	-17.83	0.52	1.55	-1291.33
E2.4	$DIST^{V4} - SPRD^{30D} - RSI_{(14)}$	5	4	1	216.79	277.47	867.14	277.47	**589.68**	5.9	487.34	-277.47	-0.12	-1.9	80	117.94	3.13	0.78	-277.47
E2.5	$DIST^{V4} - SPRD^{30D} - BB_{(20)}$	16	11	5	29.36	74.69	323	373.45	**-50.45**	-0.5	94.86	-172.61	-2.29	-36.35	68.75	-3.15	0.86	0.39	-172.61
E3	$DIST^{V4} - SPRD^{30D} - DECTREE$	329	147	182	25	23.68	3674.36	4308.86	**-634.5**	-6.34	132.54	-219.24	-4.32	-68.58	44.68	-1.93	0.85	1.06	-714.89
E4	$DIST^{V4} - SPRD^{30D} - MLP$	146	68	78	33.56	40.99	2281.84	3197.08	**-915.23**	-9.15	254.38	-286.26	-2.6	-41.27	46.58	-6.27	0.71	0.82	-1716.9
Part VI: Models derived using the spread obtained from $JOHANSEN - SPRD^{30D}$																			
F1.1	$JOHANSEN - ZSPRD^{30D}_{(3,2)}$	24	14	10	50.93	53.06	712.97	530.56	**182.41**	1.82	248.2	-317.44	-0.47	-7.46	58.33	7.6	1.34	0.96	-339.29
F1.2	$JOHANSEN - ZSPRD^{30D}_{(3,1)}$	23	11	12	58.37	63.07	642.06	756.82	**-114.76**	-1.15	248.2	-317.44	-0.42	-6.67	47.83	-4.98	0.85	0.93	-457.43
F1.3	$JOHANSEN - ZSPRD^{30D}_{(3,0.5)}$	23	12	11	60.22	58.31	722.61	641.44	**81.17**	0.81	248.2	-317.44	-0.47	-7.46	52.17	3.52	1.13	1.03	-339.29
F1.4	$JOHANSEN - ZSPRD^{30D}_{(2.7,2)}$	28	15	13	46.21	43.84	693.14	569.91	**123.23**	1.23	248.2	-317.44	-0.42	-6.67	53.57	4.4	1.22	1.05	-339.29
F1.5	$JOHANSEN - ZSPRD^{30D}_{(2.7,1)}$	26	12	14	53.3	56.04	639.62	784.56	**-144.94**	-1.45	215.83	-317.44	-0.25	-3.97	46.15	-5.58	0.82	0.95	-453.89
F1.6	$JOHANSEN - ZSPRD^{30D}_{(2.7,0.5)}$	25	12	13	53.59	62.54	643.05	812.99	**-169.94**	-1.7	215.83	-317.44	-0.26	-4.13	48	-6.8	0.79	0.86	-400.81
F2.1	$JOHANSEN - SPRD^{30D} - SMA_{(10,20)}$	28	11	17	461.65	271.19	5078.14	4610.18	**467.97**	4.68	2405.82	-2376.23	-0.24	-3.81	39.29	16.74	1.1	1.7	-2803.96
F2.2	$JOHANSEN - SPRD^{30D} - EMA_{(10,20)}$	33	13	20	208.97	291.2	2716.58	5823.96	**-3107.39**	-31.07	1046.7	-1433.97	-0.17	-2.7	39.39	-94.18	0.47	0.72	-3711.31
F2.3	$JOHANSEN - SPRD^{30D} - MACD_{(12,26,9)}$	41	20	21	290.44	234.39	5808.71	4922.17	**886.54**	8.87	1591.29	-2213.68	-0.1	-1.59	48.78	21.62	1.18	1.24	-3329.2
F2.4	$JOHANSEN - SPRD^{30D} - RSI_{(14)}$	9	2	7	23.9	283.17	47.81	1982.22	**-1934.41**	-19.34	41.41	-934.16	-0.3	-4.76	22.22	-214.94	0.02	0.08	-1898.87
F2.5	$JOHANSEN - SPRD^{30D} - BB_{(20)}$	27	14	13	203.66	309.81	2851.3	4027.57	**-1176.27**	-11.76	1538.43	-1330.8	0.21	3.33	51.85	-43.58	0.71	0.66	-1513.2
F3	$JOHANSEN - SPRD^{30D} - DECTREE$	327	152	175	26.08	22.48	3964.47	3934.03	**30.44**	0.3	251.52	-139.61	-4.18	-66.36	46.48	0.09	1.01	1.16	-619.69
F4	$JOHANSEN - SPRD^{30D} - MLP$	190	84	106	22.85	36.93	1919.64	3914.64	**-1994.99**	-19.95	124.52	-254.69	-3.52	-55.88	44.21	-10.5	0.49	0.62	-2037.37
Part VII: Models derived using the spread obtained from $ADF - SPRD^{30D}$																			
G1.1	$ADF - ZSPRD^{30D}_{(3,2)}$	4	1	3	17.84	539.62	17.84	1618.87	**-1601.02**	-16.01	17.84	-1220.26	-0.82	-13.02	25	-400.26	0.01	0.03	-1618.87
G1.2	$ADF - ZSPRD^{30D}_{(3,1)}$	4	1	3	207.8	400.91	207.8	1202.72	**-994.92**	-9.95	207.8	-728.25	-0.82	-13.02	25	-248.73	0.17	0.52	-1202.72
G1.3	$ADF - ZSPRD^{30D}_{(3,0.5)}$	4	2	2	129.69	743.22	259.38	1486.44	**-1227.07**	-12.27	253.76	-1037.21	-0.71	-11.27	50	-306.77	0.17	0.17	-1480.83
G1.4	$ADF - ZSPRD^{30D}_{(2.7,2)}$	9	2	7	78.69	327.15	157.37	2290.04	**-2132.67**	-21.33	139.53	-1220.26	-0.81	-12.86	22.22	-236.97	0.07	0.24	-2132.67
G1.5	$ADF - ZSPRD^{30D}_{(2.7,1)}$	8	2	6	119.68	315.55	239.36	1893.28	**-1653.93**	-16.54	207.8	-728.25	-0.85	-13.49	25	-206.74	0.13	0.38	-1874.06
G1.6	$ADF - ZSPRD^{30D}_{(2.7,0.5)}$	8	2	6	129.69	399.27	259.38	2395.65	**-2136.27**	-21.36	253.76	-1037.21	-0.87	-13.81	25	-267.03	0.11	0.32	-2137.95
G2.1	$ADF - SPRD^{30D} - SMA_{(10,20)}$	22	13	9	207.18	1000.85	2693.4	9007.68	**-6314.28**	-63.14	944.22	-7256.1	-0.23	-3.65	59.09	-287.02	0.3	0.21	-7504.17
G2.2	$ADF - SPRD^{30D} - EMA_{(10,20)}$	52	31	21	193.66	210.83	6003.43	4427.46	**1575.98**	15.76	1118.17	-826.58	-0.16	-2.54	59.62	30.33	1.36	0.92	-1240.89
G2.3	$ADF - SPRD^{30D} - MACD_{(12,26,9)}$	45	27	18	623.16	145	16825.42	2610.03	**14215.39**	142.15	12532.27	-474.63	0.12	1.9	60	315.9	6.45	4.3	-911.54
G2.4	$ADF - SPRD^{30D} - RSI_{(14)}$	1	1	-	40.37	-	40.37	-	**40.37**	0.4	40.37	-	-	-	100	40.37	40.37	40.37	-
G2.5	$ADF - SPRD^{30D} - BB_{(20)}$	21	8	13	61.5	135.96	492.02	1767.48	**-1275.45**	-12.75	151.68	-406.99	-0.96	-15.24	38.1	-60.73	0.28	0.45	-1382.51
G3	$ADF - SPRD^{30D} - DECTREE$	327	142	185	25.02	22.48	3553.15	4159.62	**-606.47**	-6.06	157.15	-188.03	-4.32	-68.58	43.43	-1.85	0.85	1.11	-953.08
G4	$ADF - SPRD^{30D} - MLP$	194	78	116	20.65	28.46	1610.63	3301.56	**-1690.94**	-16.91	131.9	-160.17	-4.27	-67.78	40.21	-8.71	0.49	0.73	-1690.94
Part VIII: Models derived using the spread obtained from $KALMAN - SPRD^{30D}$																			
H1.1	$KALMAN - ZSPRD^{30D}_{(3,2)}$	1	1	-	133.29	-	133.29	-	**133.29**	1.33	133.29	-	-	-	100	133.29	133.29	133.29	-
H1.2	$KALMAN - ZSPRD^{30D}_{(3,1)}$	1	1	-	125.1	-	125.1	-	**125.1**	1.25	125.1	-	-	-	100	125.1	125.1	125.1	-
H1.3	$KALMAN - ZSPRD^{30D}_{(3,0.5)}$	1	1	-	123.33	-	123.33	-	**123.33**	1.23	123.33	-	-	-	100	123.33	123.33	123.33	-
H1.4	$KALMAN - ZSPRD^{30D}_{(2.7,2)}$	5	5	-	53.17	-	265.85	-	**265.85**	2.66	132.33	-	-1.8	-28.57	100	53.17	265.85	53.17	-
H1.5	$KALMAN - ZSPRD^{30D}_{(2.7,1)}$	5	4	1	83.33	23.57	333.33	23.57	**309.76**	3.1	124.01	-23.57	-1.26	-20	80	61.95	14.14	3.54	-23.57
H1.6	$KALMAN - ZSPRD^{30D}_{(2.7,0.5)}$	4	3	1	79.14	12.47	237.42	12.47	**224.95**	2.25	122.41	-12.47	-1.39	-22.07	75	56.24	19.04	6.35	-12.47
H2.1	$KALMAN - SPRD^{30D} - SMA_{(10,20)}$	17	4	13	80.37	104.56	321.49	1359.28	**-1037.79**	-10.38	153.92	-227.57	-1.84	-29.21	23.53	-61.05	0.24	0.77	-1033.42
H2.2	$KALMAN - SPRD^{30D} - EMA_{(10,20)}$	24	6	18	76.06	102.14	456.35	1838.56	**-1382.2**	-13.82	130.99	-196.35	-2.06	-32.7	25	-57.59	0.25	0.74	-1381.62
H2.3	$KALMAN - SPRD^{30D} - MACD_{(12,26,9)}$	34	14	20	89.77	72.23	1256.83	1444.54	**-187.71**	-1.88	254.66	-365.55	-1.28	-20.32	41.18	-5.52	0.87	1.24	-596.41
H2.4	$KALMAN - SPRD^{30D} - RSI_{(14)}$	2	1	1	107.31	1799.17	107.31	1799.17	**-1691.86**	-16.92	107.31	-1799.17	-0.73	-11.59	50	-845.93	0.06	0.06	-1799.17
H2.5	$KALMAN - SPRD^{30D} - BB_{(20)}$	19	10	9	52.52	40.56	525.22	365.01	**160.21**	1.6	123.05	-135.75	-2.09	-33.18	52.63	8.43	1.44	1.3	-188.38
H3	$KALMAN - SPRD^{30D} - DECTREE$	336	178	158	22.86	21	4069.67	3317.81	**751.87**	7.52	152.77	-104.27	-4.66	-73.98	52.98	2.24	1.23	1.09	-425.42
H4	$KALMAN - SPRD^{30D} - MLP$	278	163	115	24.28	27.31	3957.38	3140.15	**817.23**	8.17	127.55	-286.07	-3.87	-61.43	58.63	2.94	1.26	0.89	-507.39
Part IX: Models derived using the spread obtained from $RATIO - SPRD^{30D}$																			
I1.1	$RATIO - ZSPRD^{30D}_{(3,2)}$	2	2	-	33.65	-	67.29	-	**67.29**	0.67	41.26	-	-10.98	-174.3	100	33.65	67.29	33.65	-
I1.2	$RATIO - ZSPRD^{30D}_{(3,1)}$	2	1	1	38.33	1.24	38.33	1.24	**37.09**	0.37	38.33	-1.24	-4.77	-75.72	50	18.55	31.03	31.03	-1.24
I1.3	$RATIO - ZSPRD^{30D}_{(3,0.5)}$	2	1	1	8.86	1.24	8.86	1.24	**7.62**	0.08	8.86	-1.24	-20.77	-329.71	50	3.81	7.17	7.17	-1.24
I1.4	$RATIO - ZSPRD^{30D}_{(2.7,2)}$	5	4	1	31.21	1.08	124.84	1.08	**123.76**	1.24	41.26	-1.08	-7.3	-115.88	80	24.75	115.8	28.95	-1.08
I1.5	$RATIO - ZSPRD^{30D}_{(2.7,1)}$	5	3	2	44	58.29	132.01	116.57	**15.44**	0.15	53.91	-115.34	-2.15	-34.13	60	3.09	1.13	0.75	-116.57
I1.6	$RATIO - ZSPRD^{30D}_{(2.7,0.5)}$	5	3	2	30.94	43.78	92.81	87.57	**5.24**	0.05	44.18	-86.33	-2.87	-45.56	60	1.05	1.06	0.71	-87.57
I2.1	$RATIO - SPRD^{30D} - SMA_{(10,20)}$	18	6	12	139.47	103.26	836.84	1239.12	**-402.29**	-4.02	580.16	-248.57	-0.97	-15.4	33.33	-22.36	0.68	1.35	-1047.84
I2.2	$RATIO - SPRD^{30D} - EMA_{(10,20)}$	26	7	19	149.21	84.36	1044.47	1602.79	**-558.32**	-5.58	290.66	-406.79	-1.23	-19.53	26.92	-21.48	0.65	1.77	-1357.01
I2.3	$RATIO - SPRD^{30D} - MACD_{(12,26,9)}$	37	12	25	92.37	47.61	1108.4	1190.32	**-81.92**	-0.82	218.33	-271.45	-1.71	-27.15	32.43	-2.22	0.93	1.94	-497.89
I2.4	$RATIO - SPRD^{30D} - RSI_{(14)}$	4	2	2	172.79	798.48	345.57	1596.96	**-1251.39**	-12.51	231.19	-1417.3	-0.61	-9.68	50	-312.85	0.22	0.22	-1417.3
I2.5	$RATIO - SPRD^{30D} - BB_{(20)}$	21	16	5	53.78	110.87	860.56	554.35	**306.21**	3.06	132.81	-244.77	-1.62	-25.72	76.19	14.58	1.55	0.49	-259.78
I3	$RATIO - SPRD^{30D} - DECTREE$	368	127	241	22.69	19.96	2881.7	4809.66	**-1927.96**	-19.28	138.71	-127.55	-5.38	-85.4	34.51	-5.24	0.6	1.14	-2318.17
I4	$RATIO - SPRD^{30D} - MLP$	329	122	207	24.29	21.94	2963.23	4541.57	**-1578.34**	-15.78	132.54	-127.55	-4.95	-78.58	37.08	-4.8	0.65	1.11	-1809.68
Part X: Models derived using the close price of ITOT.N																			
CLS-SYM-1.1	$CLOSE^{ITOT.N} - SMA_{(10,20)}$	12	7	5	349.7	110.23	2447.92	551.13	**1896.79**	18.97	1275.51	-231.05	0.2	3.17	58.33	158.05	4.44	3.17	-320.08
CLS-SYM-1.2	$CLOSE^{ITOT.N} - EMA_{(10,20)}$	18	8	10	320.51	242.25	2564.09	2422.52	**141.57**	1.42	1107.76	-798.87	-0.17	-2.7	44.44	7.84	1.06	1.32	-637.32
CLS-SYM-1.3	$CLOSE^{ITOT.N} - MACD_{(12,26,9)}$	38	15	23	136.98	113.32	2054.75	2606.43	**-551.68**	-5.52	565.03	-354.83	-0.56	-8.89	39.47	-14.53	0.79	1.21	-1373.77
CLS-SYM-1.4	$CLOSE^{ITOT.N} - RSI_{(14)}$	6	3	3	350.41	842.6	1051.24	2527.79	**-1476.55**	-14.77	576.4	-2049.07	-0.34	-5.4	50	-246.09	0.42	0.42	-2049.07
CLS-SYM-1.5	$CLOSE^{ITOT.N} - BB_{(20)}$	12	9	3	93.75	445.83	843.77	1337.49	**-493.72**	-4.94	226.17	-778.78	-0.39	-6.19	75	-41.14	0.63	0.21	-778.78
Part XI: Models derived using the close price of IXUS.N																			
CLS-SYM-2.1	$CLOSE^{IXUS.N} - SMA_{(10,20)}$	14	6	8	191.25	153.22	1147.51	1225.77	**-78.26**	-0.78	563.95	-480.15	-0.33	-5.24	42.86	-5.58	0.94	1.25	-673.35
CLS-SYM-2.2	$CLOSE^{IXUS.N} - EMA_{(10,20)}$	23	8	15	370.89	149.39	2967.1	2240.79	**726.3**	7.26	1091.8	-556.4	-0.12	-1.9	34.78	31.56	1.32	2.48	-790.14
CLS-SYM-2.3	$CLOSE^{IXUS.N} - MACD_{(12,26,9)}$	38	11	27	188.47	95.85	2073.12	2587.91	**-514.79**	-5.15	932.53	-366.94	-0.45	-7.14	28.95	-13.54	0.8	1.97	-1634.42
CLS-SYM-2.4	$CLOSE^{IXUS.N} - RSI_{(14)}$	6	3	3	307.42	280.97	922.25	842.92	**79.33**	0.79	405.82	-589.96	-0.17	-2.7	50	13.22	1.09	1.09	-589.96
CLS-SYM-2.5	$CLOSE^{IXUS.N} - BB_{(20)}$	20	14	6	66.01	208.54	924.11	1251.26	**-327.15**	-3.27	209.32	-831.57	-0.43	-6.83	70	-16.36	0.74	0.32	-837.17

Table D.2.2: This table presents the back-test metrics for the pair $ITOT.N/IXUS.N$ based on a 50-day rolling window. The table is subdivided into eleven parts, and in each of these parts, we present the back-test metrics and the trading strategies which use the spread derived from various models. In Part I, the spread is derived from the $DIST^{V1.1}$ model, in Part II from the $DIST^{V1.2}$ model, in Part III from the $DIST^{V2}$ model, in Part IV from the $DIST^{V3}$ model, in Part V from the $DIST^{V4}$ model, in Part VI from the $JOHANSEN-SPRD$ model, in Part VIII from the $ADF-SPRD$ model, in from the $DIST^{V2}$ model, in Part VIII from the $KALMAN-SPRD$ model, and in Part IX from the $RATIO-SPRD$ model. In Part X and XI, we present the back-test metrics of the trading strategies which use the close price of ITOT.N, and IXUS.N, respectively. All $ numbers reported below are in USD.

(I) Trading Strategy Code	(II) Model Name	(III) Total Number of Trades	(IV) Number of Winning Trades	(V) Number of Loosing Trades	(VI) Average Profit per Trade ($)	(VII) Average Loss per Trade ($)	(VIII) Gross Profit ($)	(IX) Gross Loss ($)	(X) Net Profit ($)	(XI) ROI (%)	(XII) Max P&L ($)	(XIII) Min P&L ($)	(XIV) Daily Sharpe Ratio	(XV) Annualized Sharpe Ratio	(XVI) Hit Ratio	(XVII) Expectancy	(XVIII) Profit Factor	(XIX) Realized Risk Reward Ratio	(XX) Max Drawdown ($)
Part I: Models derived using the spread obtained from $DIST^{V1.1}-SPRD^{50D}$																			
A1.1	$DIST^{V1.1}-ZSPRD^{50D}_{(3,2)}$	2	-	2	-	73.58	-	147.17	**-147.17**	-1.47	-	-121.14	-3.35	-53.18	-	-73.58	-	-	-147.17
A1.2	$DIST^{V1.1}-ZSPRD^{50D}_{(3,1)}$	1	1	-	1.24	-	1.24	-	**1.24**	0.01	1.24	-	-	-	100	1.24	1.24	1.24	-
A1.3	$DIST^{V1.1}-ZSPRD^{50D}_{(3,0.5)}$	1	-	1	-	6.71	-	6.71	**-6.71**	-0.07	-	-6.71	-	-	-	-6.71	-	-	-6.71
A1.4	$DIST^{V1.1}-ZSPRD^{50D}_{(2.7,2)}$	8	2	6	32.5	54.18	64.99	325.11	**-260.12**	-2.6	41.39	-121.14	-3.71	-58.89	25	-32.51	0.2	0.6	-260.11
A1.5	$DIST^{V1.1}-ZSPRD^{50D}_{(2.7,1)}$	6	3	3	71.7	45.21	215.11	135.63	**79.49**	0.79	122.45	-88.31	-1.74	-27.62	50	13.25	1.59	1.59	-135.63
A1.6	$DIST^{V1.1}-ZSPRD^{50D}_{(2.7,0.5)}$	6	2	4	127.54	43.31	255.08	173.24	**81.85**	0.82	174.74	-87.12	-1.4	-22.22	33.33	13.64	1.47	2.94	-173.24
A2.1	$DIST^{V1.1}-SPRD^{50D}-SMA_{(10,20)}$	16	8	8	73.87	85.5	590.98	683.98	**-93**	-0.93	205.74	-254.5	-1.46	-23.18	50	-5.81	0.86	0.86	-411.92
A2.2	$DIST^{V1.1}-SPRD^{50D}-EMA_{(10,20)}$	24	17	7	71.05	139.09	1207.85	973.66	**234.19**	2.34	201.75	-279.78	-1.21	-19.21	70.83	9.75	1.24	0.51	-377.78
A2.3	$DIST^{V1.1}-SPRD^{50D}-MACD_{(12,26,9)}$	32	19	13	64.79	111.6	1230.98	1450.74	**-219.77**	-2.2	149.06	-272.02	-1.44	-22.86	59.38	-6.86	0.85	0.58	-450.53
A2.4	$DIST^{V1.1}-SPRD^{50D}-RSI_{(14)}$	4	3	1	392.31	26.47	1176.93	26.47	**1150.46**	11.5	738.43	-26.47	0.42	6.67	75	287.62	44.46	14.82	-26.47
A2.5	$DIST^{V1.1}-SPRD^{50D}-BB_{(20)}$	19	7	12	67.98	44.18	475.83	530.12	**-54.29**	-0.54	159.4	-136.41	-2.21	-35.08	36.84	-2.86	0.9	1.54	-284.68
A3	$DIST^{V1.1}-SPRD^{50D}-DECTREE$	340	141	199	22.07	20.86	3111.64	4151.44	**-1039.8**	-10.4	191.36	-127.55	-4.93	-78.26	41.47	-3.06	0.75	1.06	-1660.31
A4	$DIST^{V1.1}-SPRD^{50D}-MLP$	323	123	200	23.46	22.83	2885.43	4565.16	**-1679.73**	-16.8	200.31	-127.55	-4.64	-73.66	38.08	-5.2	0.63	1.03	-2080.66
Part II: Models derived using the spread obtained from $DIST^{V1.2}-SPRD^{50D}$																			
B1.1	$DIST^{V1.2}-ZSPRD^{50D}_{(3,2)}$	5	4	1	44.53	103.19	178.12	103.19	**74.94**	0.75	93.25	-103.19	-1.79	-28.42	80	14.99	1.73	0.43	-103.19
B1.2	$DIST^{V1.2}-ZSPRD^{50D}_{(3,1)}$	5	2	3	168.96	152.4	337.91	457.19	**-119.27**	-1.19	183.55	-238.93	-0.95	-15.08	40	-23.85	0.74	1.11	-368.2
B1.3	$DIST^{V1.2}-ZSPRD^{50D}_{(3,0.5)}$	5	2	3	200.44	153.6	400.88	460.81	**-59.92**	-0.6	270.19	-305.99	-0.74	-11.75	40	-11.98	0.87	1.3	-355.1
B1.4	$DIST^{V1.2}-ZSPRD^{50D}_{(2.7,2)}$	11	7	4	63.76	62.21	446.32	248.82	**197.5**	1.97	99.64	-139.49	-1.75	-27.78	63.64	17.96	1.79	1.02	-139.49
B1.5	$DIST^{V1.2}-ZSPRD^{50D}_{(2.7,1)}$	9	5	4	176.21	157.77	881.05	631.1	**249.95**	2.5	225.21	-185.13	-0.7	-11.11	55.56	27.79	1.4	1.12	-308.58
B1.6	$DIST^{V1.2}-ZSPRD^{50D}_{(2.7,0.5)}$	9	5	4	188.22	190.94	941.08	763.78	**177.3**	1.77	290.05	-296.61	-0.6	-9.52	55.56	19.72	1.23	0.99	-425.68
B2.1	$DIST^{V1.2}-SPRD^{50D}-SMA_{(10,20)}$	10	3	7	235.33	144.64	706	1012.47	**-306.47**	-3.06	499.96	-328.58	-0.77	-12.22	30	-30.65	0.7	1.63	-405.12
B2.2	$DIST^{V1.2}-SPRD^{50D}-EMA_{(10,20)}$	19	8	11	144.15	119.88	1153.17	1318.66	**-165.49**	-1.65	328.18	-390.07	-0.93	-14.76	42.11	-8.7	0.87	1.2	-539.09
B2.3	$DIST^{V1.2}-SPRD^{50D}-MACD_{(12,26,9)}$	28	15	13	61.65	83.76	924.82	1088.87	**-164.05**	-1.64	168.56	-301.11	-1.5	-23.81	53.57	-5.86	0.85	0.74	-586.08
B2.4	$DIST^{V1.2}-SPRD^{50D}-RSI_{(14)}$	9	2	7	31.95	152.75	63.89	1069.24	**-1005.35**	-10.05	53.96	-503.94	-1.49	-23.65	22.22	-111.71	0.06	0.21	-731.8
B2.5	$DIST^{V1.2}-SPRD^{50D}-BB_{(20)}$	10	4	6	55.08	143.12	220.3	858.69	**-638.39**	-6.38	84.48	-217.46	-1.81	-28.73	40	-63.84	0.26	0.38	-641.23
B3	$DIST^{V1.2}-SPRD^{50D}-DECTREE$	268	131	137	23.19	22.02	3038.53	3016.45	**22.08**	0.22	109.21	-104.51	-4.91	-77.94	48.88	0.08	1.01	1.05	-713.7
B4	$DIST^{V1.2}-SPRD^{50D}-MLP$	262	130	132	25.49	29.2	3314.2	3853.86	**-539.66**	-5.4	171.32	-205.58	-3.86	-61.28	49.62	-2.06	0.86	0.87	-1406.06
Part III: Models derived using the spread obtained from $DIST^{V2}-SPRD^{50D}$																			
C1.1	$DIST^{V2}-ZSPRD^{50D}_{(3,2)}$	2	2	-	73.58	-	147.17	-	**147.17**	1.47	121.14	-	-1.17	-18.57	100	73.58	147.17	73.58	-
C1.2	$DIST^{V2}-ZSPRD^{50D}_{(3,1)}$	1	-	1	-	1.24	-	1.24	**-1.24**	-0.01	-	-1.24	-	-	-	-1.24	-	-	-1.24
C1.3	$DIST^{V2}-ZSPRD^{50D}_{(3,0.5)}$	1	1	-	6.71	-	6.71	-	**6.71**	0.07	6.71	-	-	-	100	6.71	6.71	6.71	-
C1.4	$DIST^{V2}-ZSPRD^{50D}_{(2.7,2)}$	8	6	2	54.18	32.5	325.11	64.99	**260.12**	2.6	121.14	-41.39	-2.4	-38.1	75	32.51	5	1.67	-64.99
C1.5	$DIST^{V2}-ZSPRD^{50D}_{(2.7,1)}$	6	3	3	45.21	71.7	135.63	215.11	**-79.49**	-0.79	88.31	-122.45	-2.08	-33.02	50	-13.25	0.63	0.63	-213.88
C1.6	$DIST^{V2}-ZSPRD^{50D}_{(2.7,0.5)}$	6	4	2	43.31	127.54	173.24	255.08	**-81.85**	-0.82	87.12	-174.74	-1.68	-26.67	66.67	-13.64	0.68	0.34	-255.08
C2.1	$DIST^{V2}-SPRD^{50D}-SMA_{(10,20)}$	16	9	7	97.09	55.03	873.77	385.24	**488.53**	4.89	254.5	-121.26	-1.2	-19.05	56.25	30.53	2.27	1.76	-208.64
C2.2	$DIST^{V2}-SPRD^{50D}-EMA_{(10,20)}$	24	7	17	139.09	71.05	973.66	1207.85	**-234.19**	-2.34	279.78	-201.75	-1.38	-21.91	29.17	-9.75	0.81	1.96	-706.65
C2.3	$DIST^{V2}-SPRD^{50D}-MACD_{(12,26,9)}$	32	13	19	111.6	64.79	1450.74	1230.98	**219.77**	2.2	272.02	-149.06	-1.32	-20.95	40.62	6.86	1.18	1.72	-455.41
C2.4	$DIST^{V2}-SPRD^{50D}-RSI_{(14)}$	4	1	3	26.47	392.31	26.47	1176.93	**-1150.46**	-11.5	26.47	-738.43	-1.35	-21.43	25	-287.62	0.02	0.07	-1020.81
C2.5	$DIST^{V2}-SPRD^{50D}-BB_{(20)}$	19	12	7	44.18	67.98	530.12	475.83	**54.29**	0.54	136.41	-159.4	-2.13	-33.81	63.16	2.86	1.11	0.65	-169.33
C3	$DIST^{V2}-SPRD^{50D}-DECTREE$	317	123	194	24.23	20.82	2980.13	4038.16	**-1058.03**	-10.58	125.99	-127.55	-4.9	-77.79	38.8	-3.34	0.74	1.16	-1555.53
C4	$DIST^{V2}-SPRD^{50D}-MLP$	253	99	154	29.34	23.28	2904.88	3585.74	**-680.86**	-6.81	259.94	-136.59	-3.92	-62.23	39.13	-2.69	0.81	1.26	-1221.87
Part IV: Models derived using the spread obtained from $DIST^{V3}-SPRD^{50D}$																			
D1.1	$DIST^{V3}-ZSPRD^{50D}_{(3,2)}$	8	5	3	35.46	41.68	177.31	125.04	**52.27**	0.52	61.57	-47.5	-3.35	-53.18	62.5	6.53	1.42	0.85	-47.5
D1.2	$DIST^{V3}-ZSPRD^{50D}_{(3,1)}$	8	6	2	32.92	67.41	197.54	134.81	**62.73**	0.63	97.07	-67.41	-2.64	-41.91	75	7.84	1.47	0.49	-67.41
D1.3	$DIST^{V3}-ZSPRD^{50D}_{(3,0.5)}$	8	6	2	58.32	22.01	349.93	44.02	**305.91**	3.06	92.03	-42.78	-2.55	-40.48	75	38.24	7.95	2.65	-44.02
D1.4	$DIST^{V3}-ZSPRD^{50D}_{(2.7,2)}$	9	4	5	41.35	48.32	165.41	241.62	**-76.21**	-0.76	61.57	-104.36	-2.98	-47.31	44.44	-8.47	0.68	0.86	-104.36
D1.5	$DIST^{V3}-ZSPRD^{50D}_{(2.7,1)}$	9	5	4	38.89	60.19	194.47	240.78	**-46.31**	-0.46	97.07	-134.65	-2.32	-36.83	55.56	-5.14	0.81	0.65	-134.65
D1.6	$DIST^{V3}-ZSPRD^{50D}_{(2.7,0.5)}$	9	6	3	59.43	40.26	356.58	120.78	**235.8**	2.36	92.03	-47.71	-2.32	-36.83	66.67	26.2	2.95	1.48	-73.07
D2.1	$DIST^{V3}-SPRD^{50D}-SMA_{(10,20)}$	23	11	12	82.27	84.71	904.92	1016.52	**-111.6**	-1.12	240.65	-212.23	-1.51	-23.97	47.83	-4.85	0.89	0.97	-439.24
D2.2	$DIST^{V3}-SPRD^{50D}-EMA_{(10,20)}$	32	13	19	94.48	59.5	1228.18	1130.54	**97.64**	0.98	269.72	-157.17	-1.51	-23.97	40.62	3.04	1.09	1.59	-294.85
D2.3	$DIST^{V3}-SPRD^{50D}-MACD_{(12,26,9)}$	38	18	20	93.77	51.31	1687.91	1026.16	**661.75**	6.62	258.77	-189.36	-1.38	-21.91	47.37	17.42	1.64	1.83	-497.17
D2.4	$DIST^{V3}-SPRD^{50D}-RSI_{(14)}$	6	2	4	32.27	160.81	64.53	643.25	**-578.72**	-5.79	50.49	-401	-1.49	-23.65	33.33	-96.46	0.1	0.2	-436.64
D2.5	$DIST^{V3}-SPRD^{50D}-BB_{(20)}$	19	11	8	42.98	57.89	472.8	463.14	**9.66**	0.1	71.25	-108.13	-2.62	-41.59	57.89	0.5	1.02	0.74	-242.92
D3	$DIST^{V3}-SPRD^{50D}-DECTREE$	324	129	195	25.29	24.16	3262.73	4710.38	**-1447.65**	-14.48	179.14	-146.74	-4.51	-71.59	39.81	-4.47	0.69	1.05	-1619.27
D4	$DIST^{V3}-SPRD^{50D}-MLP$	252	106	146	25.86	28.11	2741.31	4103.8	**-1362.49**	-13.62	182.26	-219.24	-4.08	-64.77	42.06	-5.41	0.67	0.92	-1777.4
Part V: Models derived using the spread obtained from $DIST^{V4}-SPRD^{50D}$																			
E1.1	$DIST^{V4}-ZSPRD^{50D}_{(3,2)}$	8	5	3	35.46	41.68	177.31	125.04	**52.27**	0.52	61.57	-47.5	-3.35	-53.18	62.5	6.53	1.42	0.85	-47.5
E1.2	$DIST^{V4}-ZSPRD^{50D}_{(3,1)}$	8	6	2	32.92	67.41	197.54	134.81	**62.73**	0.63	97.07	-67.41	-2.64	-41.91	75	7.84	1.47	0.49	-67.41
E1.3	$DIST^{V4}-ZSPRD^{50D}_{(3,0.5)}$	8	6	2	58.32	22.01	349.93	44.02	**305.91**	3.06	92.03	-42.78	-2.55	-40.48	75	38.24	7.95	2.65	-44.02
E1.4	$DIST^{V4}-ZSPRD^{50D}_{(2.7,2)}$	9	4	5	41.35	48.32	165.41	241.62	**-76.21**	-0.76	61.57	-104.36	-2.98	-47.31	44.44	-8.47	0.68	0.86	-104.36
E1.5	$DIST^{V4}-ZSPRD^{50D}_{(2.7,1)}$	9	5	4	38.89	60.19	194.47	240.78	**-46.31**	-0.46	97.07	-134.65	-2.32	-36.83	55.56	-5.14	0.81	0.65	-134.65
E1.6	$DIST^{V4}-ZSPRD^{50D}_{(2.7,0.5)}$	9	6	3	59.43	40.26	356.58	120.78	**235.8**	2.36	92.03	-47.71	-2.32	-36.83	66.67	26.2	2.95	1.48	-73.07
E2.1	$DIST^{V4}-SPRD^{50D}-SMA_{(10,20)}$	23	11	12	65.63	84.71	721.92	1016.52	**-294.59**	-2.95	145.19	-212.23	-1.82	-28.89	47.83	-12.8	0.71	0.77	-439.24
E2.2	$DIST^{V4}-SPRD^{50D}-EMA_{(10,20)}$	32	13	19	94.48	59.5	1228.18	1130.54	**97.64**	0.98	269.72	-157.17	-1.51	-23.97	40.62	3.04	1.09	1.59	-294.85
E2.3	$DIST^{V4}-SPRD^{50D}-MACD_{(12,26,9)}$	38	18	20	93.77	51.31	1687.91	1026.16	**661.75**	6.62	258.77	-189.36	-1.38	-21.91	47.37	17.42	1.64	1.83	-497.17
E2.4	$DIST^{V4}-SPRD^{50D}-RSI_{(14)}$	6	2	4	32.27	160.81	64.53	643.25	**-578.72**	-5.79	50.49	-401	-1.49	-23.65	33.33	-96.46	0.1	0.2	-436.64
E2.5	$DIST^{V4}-SPRD^{50D}-BB_{(20)}$	19	11	8	42.98	57.89	472.8	463.14	**9.66**	0.1	71.25	-108.13	-2.62	-41.59	57.89	0.5	1.02	0.74	-242.92
E3	$DIST^{V4}-SPRD^{50D}-DECTREE$	321	132	189	24.94	22.67	3292.51	4285.19	**-992.68**	-9.93	179.14	-244.2	-4.45	-70.64	41.12	-3.09	0.77	1.1	-1115.06
E4	$DIST^{V4}-SPRD^{50D}-MLP$	224	87	137	24.4	28.13	2122.69	3854.09	**-1731.4**	-17.31	141.45	-161.53	-4.19	-66.51	38.84	-7.73	0.55	0.87	-1891.66
Part VI: Models derived using the spread obtained from $JOHANSEN-SPRD^{50D}$																			
F1.1	$JOHANSEN-ZSPRD^{50D}_{(3,2)}$	13	7	6	72.37	90.69	506.58	544.12	**-37.54**	-0.38	243.29	-381.14	0.17	2.7	53.85	-2.88	0.93	0.8	-456.99
F1.2	$JOHANSEN-ZSPRD^{50D}_{(3,1)}$	13	6	7	88.25	163.66	529.5	1145.65	**-616.16**	-6.16	243.29	-662.73	0.18	2.86	46.15	-47.41	0.46	0.54	-1009.25
F1.3	$JOHANSEN-ZSPRD^{50D}_{(3,0.5)}$	12	4	8	55.04	142.02	220.14	1136.12	**-915.98**	-9.16	178.53	-666.41	0.3	4.76	33.33	-76.34	0.19	0.39	-1040.05
F1.4	$JOHANSEN-ZSPRD^{50D}_{(2.7,2)}$	15	9	6	73.54	92.01	661.84	552.06	**109.79**	1.1	243.29	-381.14	0.15	2.38	60	7.32	1.2	0.8	-381.14
F1.5	$JOHANSEN-ZSPRD^{50D}_{(2.7,1)}$	14	8	6	85.96	195.95	687.66	1175.7	**-488.03**	-4.88	243.29	-662.73	0.17	2.7	57.14	-34.87	0.58	0.44	-857.66
F1.6	$JOHANSEN-ZSPRD^{50D}_{(2.7,0.5)}$	13	5	8	45.34	163.17	226.72	1305.38	**-1078.66**	-10.79	178.53	-666.41	0.3	4.76	38.46	-82.98	0.17	0.28	-1181.74
F2.1	$JOHANSEN-SPRD^{50D}-SMA_{(10,20)}$	21	12	9	477.38	276.84	5728.57	2491.53	**3237.03**	32.37	1070.09	-817.45	0.19	3.02	57.14	154.12	2.3	1.72	-1117.08
F2.2	$JOHANSEN-SPRD^{50D}-EMA_{(10,20)}$	24	18	6	545.25	382.88	9814.58	2297.26	**7517.32**	75.17	1937.07	-1476.6	0.2	3.17	75	313.22	4.27	1.42	-1566.66
F2.3	$JOHANSEN-SPRD^{50D}-MACD_{(12,26,9)}$	32	18	14	275.51	134.59	4959.17	1884.2	**3074.97**	30.75	1656.55	-302.9	-0.28	-4.44	56.25	96.09	2.63	2.05	-765.31
F2.4	$JOHANSEN-SPRD^{50D}-RSI_{(14)}$	7	3	4	447.72	124.34	1343.15	497.38	**845.77**	8.46	873.74	-244.62	-0.59	-9.37	42.86	120.84	2.7	3.6	-244.62
F2.5	$JOHANSEN-SPRD^{50D}-BB_{(20)}$	18	3	15	1058.45	264.58	3175.34	3968.73	**-793.38**	-7.93	2850.94	-2317.88	-0.31	-4.92	16.67	-44.03	0.8	4	-2462.55
F3	$JOHANSEN-SPRD^{50D}-DECTREE$	279	151	128	24.68	23.96	3727	3066.74	**660.26**	6.6	215.62	-161.09	-4.15	-65.88	54.12	2.37	1.22	1.03	-333.38
F4	$JOHANSEN-SPRD^{50D}-MLP$	253	120	133	24.39	26.23	2926.82	3488.04	**-561.22**	-5.61	201.78	-152.24	-4.04	-64.13	47.43	-2.22	0.84	0.93	-880.74
Part VII: Models derived using the spread obtained from $ADF-SPRD^{50D}$																			
G1.1	$ADF-ZSPRD^{50D}_{(3,2)}$	5	2	3	104.63	1460.57	209.26	4381.71	**-4172.44**	-41.72	204.37	-4023.22	-0.51	-8.1	40	-834.49	0.05	0.07	-4364.47
G1.2	$ADF-ZSPRD^{50D}_{(3,1)}$	5	2	3	150.56	1133.49	301.12	3400.48	**-3099.36**	-30.99	157.43	-3312.74	-0.48	-7.62	40	-619.87	0.09	0.13	-3374.69
G1.3	$ADF-ZSPRD^{50D}_{(3,0.5)}$	5	2	3	184.64	1064.55	369.27	3193.65	**-2824.38**	-28.24	191.21	-3078.6	-0.47	-7.46	40	-564.88	0.12	0.17	-3140.54
G1.4	$ADF-ZSPRD^{50D}_{(2.7,2)}$	10	5	5	131.65	888.53	658.23	4442.65	**-3784.42**	-37.84	224.71	-4023.22	-0.37	-5.87	50	-378.44	0.15	0.15	-4297.23
G1.5	$ADF-ZSPRD^{50D}_{(2.7,1)}$	9	4	5	172.88	725.21	691.51	3626.07	**-2934.56**	-29.35	267.09	-3312.74	-0.38	-6.03	44.44	-326.1	0.19	0.24	-3538.34
G1.6	$ADF-ZSPRD^{50D}_{(2.7,0.5)}$	9	4	5	176.89	694.28	707.56	3471.4	**-2763.84**	-27.64	267.09	-3078.6	-0.38	-6.03	44.44	-307.13	0.2	0.25	-3356.35
G2.1	$ADF-SPRD^{50D}-SMA_{(10,20)}$	20	9	11	258.85	128.9	2329.67	1417.9	**911.77**	9.12	651.05	-272.18	-0.22	-3.49	45	45.59	1.64	2.01	-678.66
G2.2	$ADF-SPRD^{50D}-EMA_{(10,20)}$	34	19	15	461.93	794.56	8776.69	11918.46	**-3141.77**	-31.42	5298.68	-9656.92	-0.09	-1.43	55.88	-92.43	0.74	0.58	-9729.89
G2.3	$ADF-SPRD^{50D}-MACD_{(12,26,9)}$	37	18	19	135.36	241.05	2436.41	4580.01	**-2143.61**	-21.44	644.19	-994.59	-0.47	-7.46	48.65	-57.93	0.53	0.56	-2396.51
G2.4	$ADF-SPRD^{50D}-RSI_{(14)}$	3	2	1	680.54	44.14	1361.09	44.14	**1316.95**	13.17	718.51	-44.14	0.75	11.91	66.67	439.01	30.84	15.42	-
G2.5	$ADF-SPRD^{50D}-BB_{(20)}$	17	9	8	218.82	109.94	1969.37	879.54	**1089.83**	10.9	572.59	-195.65	-0.2	-3.17	52.94	64.1	2.24	1.99	-527.32
G3	$ADF-SPRD^{50D}-DECTREE$	304	129	175	24.78	24.83	3196.03	4344.97	**-1148.94**	-11.49	149.06	-177.12	-4.28	-67.94	42.43	-3.78	0.74	1	-1511.47
G4	$ADF-SPRD^{50D}-MLP$	246	108	138	23.36	30.71	2523.29	4238.2	**-1714.91**	-17.15	187.92	-279.43	-3.83	-60.8	43.9	-6.97	0.6	0.76	-2087.11
Part VIII: Models derived using the spread obtained from $KALMAN-SPRD^{50D}$																			
H1.1	$KALMAN-ZSPRD^{50D}_{(3,2)}$	2	1	1	31.46	167	31.46	167	**-135.54**	-1.36	31.46	-167	-1.48	-23.49	50	-67.77	0.19	0.19	-167
H1.2	$KALMAN-ZSPRD^{50D}_{(3,1)}$	2	1	1	35.2	3.61	35.2	3.61	**31.59**	0.32	35.2	-3.61	-4.61	-73.18	50	15.8	9.76	9.76	-3.61
H1.3	$KALMAN-ZSPRD^{50D}_{(3,0.5)}$	2	2	-	89.84	-	179.67	-	**179.67**	1.8	121.63	-	-1.07	-16.99	100	89.84	179.67	89.84	-
H1.4	$KALMAN-ZSPRD^{50D}_{(2.7,2)}$	6	3	3	25.09	131.93	75.27	395.79	**-320.52**	-3.21	65.78	-170.34	-1.95	-30.96	50	-53.42	0.19	0.19	-388.11
H1.5	$KALMAN-ZSPRD^{50D}_{(2.7,1)}$	6	3	3	37.64	80.8	112.92	242.4	**-129.48**	-1.29	79.43	-220.28	-1.51	-23.97	50	-21.58	0.47	0.47	-238.79
H1.6	$KALMAN-ZSPRD^{50D}_{(2.7,0.5)}$	6	4	2	63.93	187.56	255.73	375.12	**-119.39**	-1.19	121.63	-253.39	-1.11	-17.62	66.67	-19.89	0.68	0.34	-375.12
H2.1	$KALMAN-SPRD^{50D}-SMA_{(10,20)}$	13	7	6	180.86	95.15	1266.04	570.9	**695.15**	6.95	354.17	-220.08	-0.46	-7.3	53.85	53.48	2.22	1.9	-232.1
H2.2	$KALMAN-SPRD^{50D}-EMA_{(10,20)}$	25	9	16	155.54	89.37	1399.82	1429.88	**-30.06**	-0.3	350.48	-196.57	-0.91	-14.45	36	-1.2	0.98	1.74	-693.32
H2.3	$KALMAN-SPRD^{50D}-MACD_{(12,26,9)}$	37	16	21	83.92	89.48	1342.75	1878.98	**-536.22**	-5.36	245.13	-215.92	-1.36	-21.59	43.24	-14.5	0.71	0.94	-992.52
H2.4	$KALMAN-SPRD^{50D}-RSI_{(14)}$	2	1	1	39.94	1803.12	39.94	1803.12	**-1763.18**	-17.63	39.94	-1803.12	-0.78	-12.38	50	-881.59	0.02	0.02	-1803.12
H2.5	$KALMAN-SPRD^{50D}-BB_{(20)}$	20	15	5	54.62	37.65	819.24	188.24	**631**	6.31	123.07	-63.98	-1.97	-31.27	75	31.55	4.35	1.45	-118
H3	$KALMAN-SPRD^{50D}-DECTREE$	316	165	151	24.57	23.64	4054.44	3568.96	**485.48**	4.85	184.53	-137.43	-4.26	-67.63	52.22	1.54	1.14	1.04	-672.21
H4	$KALMAN-SPRD^{50D}-MLP$	260	153	107	25.82	26.77	3950.04	2864.33	**1085.71**	10.86	204.7	-310.67	-3.55	-56.35	58.85	4.18	1.38	0.96	-531.74
Part IX: Models derived using the spread obtained from $RATIO-SPRD^{50D}$																			
I1.1	$RATIO-ZSPRD^{50D}_{(3,2)}$	1	1	-	26.03	-	26.03	-	**26.03**	0.26	26.03	-	-	-	100	26.03	26.03	26.03	-
I1.2	$RATIO-ZSPRD^{50D}_{(3,1)}$	1	-	1	-	1.24	-	1.24	**-1.24**	-0.01	-	-1.24	-	-	-	-1.24	-	-	-1.24
I1.3	$RATIO-ZSPRD^{50D}_{(3,0.5)}$	1	1	-	24.54	-	24.54	-	**24.54**	0.25	24.54	-	-	-	100	24.54	24.54	24.54	-
I1.4	$RATIO-ZSPRD^{50D}_{(2.7,2)}$	5	2	3	27.6	35.61	55.2	106.84	**-51.64**	-0.52	29.17	-97.39	-3.16	-50.16	40	-10.33	0.52	0.78	-97.39
I1.5	$RATIO-ZSPRD^{50D}_{(2.7,1)}$	5	1	4	38.46	68.1	38.47	272.39	**-233.93**	-2.34	38.46	-158.84	-2.65	-42.07	20	-46.79	0.14	0.56	-233.93
I1.6	$RATIO-ZSPRD^{50D}_{(2.7,0.5)}$	5	3	2	33.84	107.13	101.51	214.25	**-112.74**	-1.13	67.99	-120.43	-2.16	-34.29	60	-22.55	0.47	0.32	-214.25
I2.1	$RATIO-SPRD^{50D}-SMA_{(10,20)}$	17	6	11	139.47	109.78	836.84	1207.56	**-370.72**	-3.71	580.16	-248.57	-0.94	-14.92	35.29	-21.82	0.69	1.27	-1003.86
I2.2	$RATIO-SPRD^{50D}-EMA_{(10,20)}$	25	7	18	154.25	83.79	1079.77	1508.26	**-428.49**	-4.28	290.66	-406.79	-1.16	-18.41	28	-17.14	0.72	1.84	-1357.01
I2.3	$RATIO-SPRD^{50D}-MACD_{(12,26,9)}$	37	12	25	86.67	54.11	1040.03	1352.78	**-312.75**	-3.13	218.33	-271.45	-1.73	-27.46	32.43	-8.46	0.77	1.6	-538.82
I2.4	$RATIO-SPRD^{50D}-RSI_{(14)}$	3	1	2	83.63	747.25	83.63	1494.51	**-1410.88**	-14.11	83.63	-1338.39	-0.82	-13.02	33.33	-470.32	0.06	0.11	-1338.39
I2.5	$RATIO-SPRD^{50D}-BB_{(20)}$	20	16	4	53.78	131.04	860.56	524.16	**336.4**	3.36	132.81	-244.77	-1.56	-24.76	80	16.82	1.64	0.41	-259.78
I3	$RATIO-SPRD^{50D}-DECTREE$	339	121	218	24.45	20.81	2958.67	4536.71	**-1578.04**	-15.78	132.54	-127.55	-5.1	-80.96	35.69	-4.66	0.65	1.17	-1913.09
I4	$RATIO-SPRD^{50D}-MLP$	239	101	138	22.7	21.1	2292.5	2912.17	**-619.67**	-6.2	114.65	-187.92	-4.71	-74.77	42.26	-2.59	0.79	1.08	-825.33
Part X: Models derived using the close price of ITOT.N																			
CLS-SYM-1.1	$CLOSE^{ITOT.N}-SMA_{(10,20)}$	12	7	5	349.7	110.23	2447.92	551.13	**1896.79**	18.97	1275.51	-231.05	0.2	3.17	58.33	158.05	4.44	3.17	-320.08
CLS-SYM-1.2	$CLOSE^{ITOT.N}-EMA_{(10,20)}$	18	8	10	320.51	242.25	2564.09	2422.52	**141.57**	1.42	1107.76	-798.87	-0.17	-2.7	44.44	7.84	1.06	1.32	-637.32
CLS-SYM-1.3	$CLOSE^{ITOT.N}-MACD_{(12,26,9)}$	38	15	23	136.98	113.32	2054.75	2606.43	**-551.68**	-5.52	565.03	-354.83	-0.56	-8.89	39.47	-14.53	0.79	1.21	-1373.77
CLS-SYM-1.4	$CLOSE^{ITOT.N}-RSI_{(14)}$	6	3	3	350.41	842.6	1051.24	2527.79	**-1476.55**	-14.77	576.4	-2049.07	-0.34	-5.4	50	-246.09	0.42	0.42	-2049.07
CLS-SYM-1.5	$CLOSE^{ITOT.N}-BB_{(20)}$	12	9	3	93.75	445.83	843.77	1337.49	**-493.72**	-4.94	226.17	-778.78	-0.39	-6.19	75	-41.14	0.63	0.21	-778.78
Part XI: Models derived using the close price of IXUS.N																			
CLS-SYM-2.1	$CLOSE^{IXUS.N}-SMA_{(10,20)}$	14	6	8	191.25	153.22	1147.51	1225.77	**-78.26**	-0.78	563.95	-480.15	-0.33	-5.24	42.86	-5.58	0.94	1.25	-673.35
CLS-SYM-2.2	$CLOSE^{IXUS.N}-EMA_{(10,20)}$	23	8	15	370.89	149.39	2967.1	2240.79	**726.3**	7.26	1091.8	-556.4	-0.12	-1.9	34.78	31.56	1.32	2.48	-790.14
CLS-SYM-2.3	$CLOSE^{IXUS.N}-MACD_{(12,26,9)}$	38	11	27	188.47	95.85	2073.12	2587.91	**-514.79**	-5.15	932.53	-366.94	-0.45	-7.14	28.95	-13.54	0.8	1.97	-1634.42
CLS-SYM-2.4	$CLOSE^{IXUS.N}-RSI_{(14)}$	6	3	3	307.42	280.97	922.25	842.92	**79.33**	0.79	405.82	-589.96	-0.17	-2.7	50	13.22	1.09	1.09	-589.96
CLS-SYM-2.5	$CLOSE^{IXUS.N}-BB_{(20)}$	20	14	6	66.01	208.54	924.11	1251.26	**-327.15**	-3.27	209.32	-831.57	-0.43	-6.83	70	-16.36	0.74	0.32	-837.17

Table D.2.3: This table presents the back-test metrics for the pair $ITOT.N/IXUS.N$ based on a 100-day rolling window. The table is subdivided into eleven parts, and in each of these parts, we present the back-test metrics and the trading strategies which use the spread derived from various models. In Part I, the spread is derived from the $DIST^{V1.1}$ model, in Part II from the $DIST^{V1.2}$ model, in Part III from the $DIST^{V2}$ model, in Part IV from the $DIST^{V3}$ model, in Part V from the $DIST^{V4}$ model, in Part VI from the $JOHANSEN-SPRD$ model, in Part VIII from the $ADF-SPRD$ model, in from the $DIST^{V2}$ model, in Part VIII from the $KALMAN-SPRD$ model, and in Part IX from the $RATIO-SPRD$ model. In Part X and XI, we present the back-test metrics of the trading strategies which use the close price of ITOT.N, and IXUS.N, respectively. All $ numbers reported below are in USD.

(I) Trading Strategy Code	(II) Model Name	(III) Total Number of Trades	(IV) Number of Winning Trades	(V) Number of Loosing Trades	(VI) Average Profit per Trade ($)	(VII) Average Loss per Trade ($)	(VIII) Gross Profit ($)	(IX) Gross Loss ($)	(X) Net Profit ($)	(XI) ROI (%)	(XII) Max P&L ($)	(XIII) Min P&L ($)	(XIV) Daily Sharpe Ratio	(XV) Annualized Sharpe Ratio	(XVI) Hit Ratio	(XVII) Expectancy	(XVIII) Profit Factor	(XIX) Realized Risk Reward Ratio	(XX) Max Drawdown ($)
Part I: Models derived using the spread obtained from $DIST^{V1.1}-SPRD^{100D}$																			
A1.1	$DIST^{V1.1}-ZSPRD^{100D}_{(3,2)}$	2	-	2	-	73.16	-	146.32	**-146.32**	-1.46	-	-86.7	-11.76	-186.68	-	-73.16	-	-	-146.31
A1.2	$DIST^{V1.1}-ZSPRD^{100D}_{(3,1)}$	2	-	2	-	114.75	-	229.5	**-229.5**	-2.3	-	-149.72	-5.39	-85.56	-	-114.75	-	-	-229.5
A1.3	$DIST^{V1.1}-ZSPRD^{100D}_{(3,0.5)}$	2	-	2	-	179.4	-	358.8	**-358.8**	-3.59	-	-202.2	-10.28	-163.19	-	-179.4	-	-	-358.8
A1.4	$DIST^{V1.1}-ZSPRD^{100D}_{(2.7,2)}$	4	1	3	115.34	46.04	115.34	138.14	**-22.8**	-0.23	115.34	-55.57	-1.94	-30.8	25	-5.7	0.83	2.5	-138.13
A1.5	$DIST^{V1.1}-ZSPRD^{100D}_{(2.7,1)}$	3	2	1	51.1	96.1	102.19	96.1	**6.09**	0.06	86.33	-96.1	-1.63	-25.88	66.67	2.04	1.06	0.53	-96.1
A1.6	$DIST^{V1.1}-ZSPRD^{100D}_{(2.7,0.5)}$	3	1	2	6.09	103.02	6.09	206.04	**-199.95**	-2	6.09	-148.54	-2.81	-44.61	33.33	-66.65	0.03	0.06	-206.05
A2.1	$DIST^{V1.1}-SPRD^{100D}-SMA_{(10,20)}$	15	7	8	55.03	85.5	385.24	683.98	**-298.73**	-2.99	121.26	-254.5	-1.8	-28.57	46.67	-19.91	0.56	0.64	-330.93
A2.2	$DIST^{V1.1}-SPRD^{100D}-EMA_{(10,20)}$	24	17	7	75.9	143.19	1290.25	1002.32	**287.93**	2.88	262.66	-279.78	-1.11	-17.62	70.83	11.99	1.29	0.53	-377.78
A2.3	$DIST^{V1.1}-SPRD^{100D}-MACD_{(12,26,9)}$	31	17	14	64.89	104.24	1103.05	1459.31	**-356.26**	-3.56	149.06	-272.02	-1.5	-23.81	54.84	-11.49	0.76	0.62	-489.4
A2.4	$DIST^{V1.1}-SPRD^{100D}-RSI_{(14)}$	3	3	-	431.75	-	1295.24	-	**1295.24**	12.95	738.43	-	1.02	16.19	100	431.75	1295.24	431.75	-
A2.5	$DIST^{V1.1}-SPRD^{100D}-BB_{(20)}$	18	7	11	67.98	43.99	475.83	483.9	**-8.07**	-0.08	159.4	-136.41	-2.14	-33.97	38.89	-0.45	0.98	1.55	-284.68
A3	$DIST^{V1.1}-SPRD^{100D}-DECTREE$	320	121	199	24.05	22.06	2909.93	4389.63	**-1479.71**	-14.8	191.36	-127.55	-4.8	-76.2	37.81	-4.63	0.66	1.09	-1827.23
A4	$DIST^{V1.1}-SPRD^{100D}-MLP$	284	110	174	25.03	23.58	2753.74	4102.52	**-1348.77**	-13.49	191.36	-107.68	-4.63	-73.5	38.73	-4.75	0.67	1.06	-1487.79
Part II: Models derived using the spread obtained from $DIST^{V1.2}-SPRD^{100D}$																			
B1.1	$DIST^{V1.2}-ZSPRD^{100D}_{(3,2)}$	6	2	4	21.97	77.24	43.93	308.98	**-265.04**	-2.65	31.41	-115.34	-3.16	-50.16	33.33	-44.18	0.14	0.28	-265.04
B1.2	$DIST^{V1.2}-ZSPRD^{100D}_{(3,1)}$	5	2	3	62.55	61.22	125.09	183.67	**-58.58**	-0.59	96.1	-140.08	-1.88	-29.84	40	-11.72	0.68	1.02	-177.58
B1.3	$DIST^{V1.2}-ZSPRD^{100D}_{(3,0.5)}$	5	2	3	116.7	80.21	233.4	240.63	**-7.24**	-0.07	181.33	-134.63	-1.22	-19.37	40	-1.45	0.97	1.45	-234.54
B1.4	$DIST^{V1.2}-ZSPRD^{100D}_{(2.7,2)}$	8	4	4	38.49	63.48	153.96	253.92	**-99.97**	-1	91.08	-115.34	-2.45	-38.89	50	-12.5	0.61	0.61	-191.05
B1.5	$DIST^{V1.2}-ZSPRD^{100D}_{(2.7,1)}$	7	4	3	56.17	107.06	224.7	321.17	**-96.47**	-0.96	96.1	-183.38	-1.56	-24.76	57.14	-13.79	0.7	0.52	-315.07
B1.6	$DIST^{V1.2}-ZSPRD^{100D}_{(2.7,0.5)}$	6	2	4	116.7	83.21	233.4	332.82	**-99.43**	-0.99	181.33	-147.72	-1.38	-21.91	33.33	-16.58	0.7	1.4	-326.73
B2.1	$DIST^{V1.2}-SPRD^{100D}-SMA_{(10,20)}$	18	8	10	87.69	112.38	701.49	1123.75	**-422.26**	-4.22	170.2	-372.55	-1.29	-20.48	44.44	-23.47	0.62	0.78	-376.12
B2.2	$DIST^{V1.2}-SPRD^{100D}-EMA_{(10,20)}$	24	10	14	101.45	114.23	1014.47	1599.17	**-584.7**	-5.85	233.53	-252.22	-1.29	-20.48	41.67	-24.36	0.63	0.89	-759.98
B2.3	$DIST^{V1.2}-SPRD^{100D}-MACD_{(12,26,9)}$	26	14	12	97.8	85.17	1369.25	1022.05	**347.19**	3.47	263.26	-204.49	-1.13	-17.94	53.85	13.36	1.34	1.15	-798.53
B2.4	$DIST^{V1.2}-SPRD^{100D}-RSI_{(14)}$	6	4	2	164.49	480.7	657.95	961.4	**-303.45**	-3.03	326.9	-536.53	-0.58	-9.21	66.67	-50.55	0.68	0.34	-424.87
B2.5	$DIST^{V1.2}-SPRD^{100D}-BB_{(20)}$	9	4	5	55.34	197.62	221.36	988.12	**-766.77**	-7.67	79.34	-436.28	-1.26	-20	44.44	-85.21	0.22	0.28	-373.02
B3	$DIST^{V1.2}-SPRD^{100D}-DECTREE$	264	124	140	23.04	22.51	2856.4	3151.99	**-295.59**	-2.96	109.95	-146.74	-4.67	-74.13	46.97	-1.12	0.91	1.02	-1196.66
B4	$DIST^{V1.2}-SPRD^{100D}-MLP$	220	118	102	22.24	23.4	2623.86	2386.35	**237.51**	2.38	152.77	-103.9	-4.67	-74.13	53.64	1.08	1.1	0.95	-701.18
Part III: Models derived using the spread obtained from $DIST^{V2}-SPRD^{100D}$																			
C1.1	$DIST^{V2}-ZSPRD^{100D}_{(3,2)}$	2	2	-	73.16	-	146.32	-	**146.32**	1.46	86.7	-	-4.12	-65.4	100	73.16	146.32	73.16	-
C1.2	$DIST^{V2}-ZSPRD^{100D}_{(3,1)}$	2	2	-	114.75	-	229.5	-	**229.5**	2.3	149.72	-	-0.75	-11.91	100	114.75	229.5	114.75	-
C1.3	$DIST^{V2}-ZSPRD^{100D}_{(3,0.5)}$	2	2	-	179.4	-	358.8	-	**358.8**	3.59	202.2	-	0.85	13.49	100	179.4	358.8	179.4	-
C1.4	$DIST^{V2}-ZSPRD^{100D}_{(2.7,2)}$	4	3	1	46.04	115.34	138.14	115.34	**22.8**	0.23	55.57	-115.34	-1.8	-28.57	75	5.7	1.2	0.4	-115.34
C1.5	$DIST^{V2}-ZSPRD^{100D}_{(2.7,1)}$	3	1	2	96.1	51.1	96.1	102.19	**-6.09**	-0.06	96.1	-86.33	-1.67	-26.51	33.33	-2.04	0.94	1.88	-86.33
C1.6	$DIST^{V2}-ZSPRD^{100D}_{(2.7,0.5)}$	3	2	1	103.02	6.09	206.04	6.09	**199.95**	2	148.54	-6.09	-1.1	-17.46	66.67	66.65	33.82	16.91	-6.09
C2.1	$DIST^{V2}-SPRD^{100D}-SMA_{(10,20)}$	15	8	7	85.5	55.03	683.98	385.24	**298.73**	2.99	254.5	-121.26	-1.39	-22.07	53.33	19.91	1.78	1.55	-208.64
C2.2	$DIST^{V2}-SPRD^{100D}-EMA_{(10,20)}$	24	7	17	143.19	75.9	1002.32	1290.25	**-287.93**	-2.88	279.78	-262.66	-1.3	-20.64	29.17	-11.99	0.78	1.89	-706.65
C2.3	$DIST^{V2}-SPRD^{100D}-MACD_{(12,26,9)}$	31	14	17	104.24	64.89	1459.31	1103.05	**356.26**	3.56	272.02	-149.06	-1.29	-20.48	45.16	11.49	1.32	1.61	-455.41
C2.4	$DIST^{V2}-SPRD^{100D}-RSI_{(14)}$	3	-	3	-	431.75	-	1295.24	**-1295.24**	-12.95	-	-738.43	-2.12	-33.65	-	-431.75	-	-	-1087.03
C2.5	$DIST^{V2}-SPRD^{100D}-BB_{(20)}$	18	11	7	43.99	67.98	483.9	475.83	**8.07**	0.08	136.41	-159.4	-2.12	-33.65	61.11	0.45	1.02	0.65	-169.33
C3	$DIST^{V2}-SPRD^{100D}-DECTREE$	308	119	189	25.32	22.25	3013.48	4206.19	**-1192.7**	-11.93	191.36	-127.55	-4.61	-73.18	38.64	-3.87	0.72	1.14	-1487.11
C4	$DIST^{V2}-SPRD^{100D}-MLP$	294	103	191	21.04	23.97	2167.05	4578.32	**-2411.27**	-24.11	120.54	-202.03	-4.96	-78.74	35.03	-8.2	0.47	0.88	-2449.99
Part IV: Models derived using the spread obtained from $DIST^{V3}-SPRD^{100D}$																			
D1.1	$DIST^{V3}-ZSPRD^{100D}_{(3,2)}$	4	4	-	73.69	-	294.75	-	**294.75**	2.95	148.58	-	-1.15	-18.26	100	73.69	294.75	73.69	-
D1.2	$DIST^{V3}-ZSPRD^{100D}_{(3,1)}$	4	3	1	76.13	2.11	228.38	2.11	**226.28**	2.26	92.03	-2.11	-2.34	-37.15	75	56.57	108.44	36.14	-2.11
D1.3	$DIST^{V3}-ZSPRD^{100D}_{(3,0.5)}$	4	3	1	84.21	60.69	252.63	60.69	**191.94**	1.92	92.03	-60.69	-1.42	-22.54	75	47.98	4.16	1.39	-60.69
D1.4	$DIST^{V3}-ZSPRD^{100D}_{(2.7,2)}$	7	6	1	56.26	19.57	337.53	19.57	**317.96**	3.18	148.58	-19.57	-1.74	-27.62	85.71	45.42	17.25	2.87	-19.57
D1.5	$DIST^{V3}-ZSPRD^{100D}_{(2.7,1)}$	7	5	2	60.36	34.63	301.82	69.25	**232.56**	2.33	92.03	-67.15	-2.2	-34.92	71.43	33.22	4.36	1.74	-67.15
D1.6	$DIST^{V3}-ZSPRD^{100D}_{(2.7,0.5)}$	6	4	2	77.63	87.63	310.51	175.26	**135.25**	1.35	92.03	-114.57	-1.47	-23.34	66.67	22.55	1.77	0.89	-114.57
D2.1	$DIST^{V3}-SPRD^{100D}-SMA_{(10,20)}$	16	7	9	177.73	61.66	1244.08	554.91	**689.17**	6.89	347.93	-131.59	-0.74	-11.75	43.75	43.07	2.24	2.88	-297.24
D2.2	$DIST^{V3}-SPRD^{100D}-EMA_{(10,20)}$	30	12	18	87.23	61.14	1046.77	1100.47	**-53.7**	-0.54	240.23	-192.58	-1.59	-25.24	40	-1.79	0.95	1.43	-639.2
D2.3	$DIST^{V3}-SPRD^{100D}-MACD_{(12,26,9)}$	37	14	23	73.86	53.12	1034.03	1221.66	**-187.63**	-1.88	192.9	-161.53	-2.05	-32.54	37.84	-5.07	0.85	1.39	-392.53
D2.4	$DIST^{V3}-SPRD^{100D}-RSI_{(14)}$	6	3	3	270.14	236.44	810.41	709.33	**101.08**	1.01	446.3	-266.64	-0.46	-7.3	50	16.85	1.14	1.14	-266.64
D2.5	$DIST^{V3}-SPRD^{100D}-BB_{(20)}$	14	9	5	64.83	55.3	583.48	276.5	**306.98**	3.07	316.73	-143.6	-1.26	-20	64.29	21.93	2.11	1.17	-219.16
D3	$DIST^{V3}-SPRD^{100D}-DECTREE$	306	122	184	24.28	23.13	2962.05	4255.59	**-1293.53**	-12.94	191.36	-104.51	-4.8	-76.2	39.87	-4.23	0.7	1.05	-1465.87
D4	$DIST^{V3}-SPRD^{100D}-MLP$	229	91	138	28.38	24.79	2582.27	3420.67	**-838.39**	-8.38	161.09	-144.51	-3.91	-62.07	39.74	-3.66	0.75	1.14	-1143.35
Part V: Models derived using the spread obtained from $DIST^{V4}-SPRD^{100D}$																			
E1.1	$DIST^{V4}-ZSPRD^{100D}_{(3,2)}$	4	4	-	73.69	-	294.75	-	**294.75**	2.95	148.58	-	-1.15	-18.26	100	73.69	294.75	73.69	-
E1.2	$DIST^{V4}-ZSPRD^{100D}_{(3,1)}$	4	3	1	76.13	2.11	228.38	2.11	**226.28**	2.26	92.03	-2.11	-2.34	-37.15	75	56.57	108.44	36.14	-2.11
E1.3	$DIST^{V4}-ZSPRD^{100D}_{(3,0.5)}$	4	3	1	84.21	60.69	252.63	60.69	**191.94**	1.92	92.03	-60.69	-1.42	-22.54	75	47.98	4.16	1.39	-60.69
E1.4	$DIST^{V4}-ZSPRD^{100D}_{(2.7,2)}$	7	6	1	56.26	19.57	337.53	19.57	**317.96**	3.18	148.58	-19.57	-1.74	-27.62	85.71	45.42	17.25	2.87	-19.57
E1.5	$DIST^{V4}-ZSPRD^{100D}_{(2.7,1)}$	7	5	2	60.36	34.63	301.82	69.25	**232.56**	2.33	92.03	-67.15	-2.2	-34.92	71.43	33.22	4.36	1.74	-67.15
E1.6	$DIST^{V4}-ZSPRD^{100D}_{(2.7,0.5)}$	6	4	2	77.63	87.63	310.51	175.26	**135.25**	1.35	92.03	-114.57	-1.47	-23.34	66.67	22.55	1.77	0.89	-114.57
E2.1	$DIST^{V4}-SPRD^{100D}-SMA_{(10,20)}$	16	7	9	177.73	61.66	1244.08	554.91	**689.17**	6.89	347.93	-131.59	-0.74	-11.75	43.75	43.07	2.24	2.88	-297.24
E2.2	$DIST^{V4}-SPRD^{100D}-EMA_{(10,20)}$	30	12	18	87.23	61.14	1046.77	1100.47	**-53.7**	-0.54	240.23	-192.58	-1.59	-25.24	40	-1.79	0.95	1.43	-639.2
E2.3	$DIST^{V4}-SPRD^{100D}-MACD_{(12,26,9)}$	37	14	23	73.86	53.12	1034.03	1221.66	**-187.63**	-1.88	192.9	-161.53	-2.05	-32.54	37.84	-5.07	0.85	1.39	-392.53
E2.4	$DIST^{V4}-SPRD^{100D}-RSI_{(14)}$	6	3	3	270.14	236.44	810.41	709.33	**101.08**	1.01	446.3	-266.64	-0.46	-7.3	50	16.85	1.14	1.14	-266.64
E2.5	$DIST^{V4}-SPRD^{100D}-BB_{(20)}$	14	9	5	64.83	55.3	583.48	276.5	**306.98**	3.07	316.73	-143.6	-1.26	-20	64.29	21.93	2.11	1.17	-219.16
E3	$DIST^{V4}-SPRD^{100D}-DECTREE$	304	124	180	23.75	24.13	2944.73	4344.06	**-1399.33**	-13.99	191.36	-127.55	-4.67	-74.13	40.79	-4.6	0.68	0.98	-1530.78
E4	$DIST^{V4}-SPRD^{100D}-MLP$	229	91	138	28.38	24.79	2582.27	3420.67	**-838.39**	-8.38	161.09	-144.51	-3.91	-62.07	39.74	-3.66	0.75	1.14	-1143.35
Part VI: Models derived using the spread obtained from $JOHANSEN-SPRD^{100D}$																			
F1.1	$JOHANSEN-ZSPRD^{100D}_{(3,2)}$	17	8	9	38.15	19.32	305.17	173.85	**131.32**	1.31	88.07	-53.39	-4.02	-63.82	47.06	7.73	1.76	1.97	-118.67
F1.2	$JOHANSEN-ZSPRD^{100D}_{(3,1)}$	15	8	7	102.21	23.46	817.68	164.22	**653.45**	6.53	601.6	-53.39	-0.45	-7.14	53.33	43.56	4.98	4.36	-118.67
F1.3	$JOHANSEN-ZSPRD^{100D}_{(3,0.5)}$	15	8	7	115.94	23.46	927.56	164.22	**763.33**	7.63	701.48	-53.39	-0.43	-6.83	53.33	50.88	5.65	4.94	-118.67
F1.4	$JOHANSEN-ZSPRD^{100D}_{(2.7,2)}$	20	11	9	67.43	19.32	741.78	173.85	**567.94**	5.68	318.35	-53.39	-0.75	-11.91	55	28.4	4.27	3.49	-109.19
F1.5	$JOHANSEN-ZSPRD^{100D}_{(2.7,1)}$	18	11	7	131.16	23.46	1442.74	164.22	**1278.52**	12.79	601.6	-53.39	-0.58	-9.21	61.11	71.03	8.79	5.59	-109.19
F1.6	$JOHANSEN-ZSPRD^{100D}_{(2.7,0.5)}$	17	10	7	158.81	23.46	1588.13	164.22	**1423.91**	14.24	701.48	-53.39	-0.5	-7.94	58.82	83.75	9.67	6.77	-109.19
F2.1	$JOHANSEN-SPRD^{100D}-SMA_{(10,20)}$	17	13	4	176.11	100.49	2289.41	401.95	**1887.46**	18.87	638.97	-186.03	-0.34	-5.4	76.47	111.03	5.7	1.75	-186.03
F2.2	$JOHANSEN-SPRD^{100D}-EMA_{(10,20)}$	25	11	14	2031.49	1031.97	22346.36	14447.57	**7898.79**	78.99	20030.2	-6957	-0.1	-1.59	44	315.95	1.55	1.97	-7770.64
F2.3	$JOHANSEN-SPRD^{100D}-MACD_{(12,26,9)}$	25	15	10	497.05	818.71	7455.71	8187.14	**-731.42**	-7.31	3558.59	-7152.92	-0.25	-3.97	60	-29.26	0.91	0.61	-7358.32
F2.4	$JOHANSEN-SPRD^{100D}-RSI_{(14)}$	4	3	1	278.62	782.64	835.85	782.64	**53.2**	0.53	610.63	-782.64	-0.38	-6.03	75	13.3	1.07	0.36	-782.64
F2.5	$JOHANSEN-SPRD^{100D}-BB_{(20)}$	18	9	9	224.11	211.96	2016.95	1907.62	**109.32**	1.09	649.86	-869.13	-0.3	-4.76	50	6.07	1.06	1.06	-869.13
F3	$JOHANSEN-SPRD^{100D}-DECTREE$	271	144	127	28.16	26.55	4054.55	3371.6	**682.95**	6.83	222.87	-101.66	-3.79	-60.16	53.14	2.52	1.2	1.06	-531.07
F4	$JOHANSEN-SPRD^{100D}-MLP$	154	71	83	27.77	27.28	1971.46	2264.2	**-292.74**	-2.93	203.35	-205.91	-3.28	-52.07	46.1	-1.9	0.87	1.02	-609.13
Part VII: Models derived using the spread obtained from $ADF-SPRD^{100D}$																			
G1.1	$ADF-ZSPRD^{100D}_{(3,2)}$	3	1	2	135.42	313.73	135.42	627.46	**-492.05**	-4.92	135.42	-342.96	-1.03	-16.35	33.33	-164.03	0.22	0.43	-627.46
G1.2	$ADF-ZSPRD^{100D}_{(3,1)}$	2	1	1	55	1553.76	55	1553.76	**-1498.76**	-14.99	55	-1553.76	-0.75	-11.91	50	-749.38	0.04	0.04	-1553.76
G1.3	$ADF-ZSPRD^{100D}_{(3,0.5)}$	2	1	1	126.58	1858.45	126.58	1858.45	**-1731.87**	-17.32	126.58	-1858.45	-0.69	-10.95	50	-865.94	0.07	0.07	-1858.45
G1.4	$ADF-ZSPRD^{100D}_{(2.7,2)}$	5	1	4	87.09	199.95	87.09	799.8	**-712.72**	-7.13	87.09	-342.96	-1.45	-23.02	20	-142.54	0.11	0.44	-799.8
G1.5	$ADF-ZSPRD^{100D}_{(2.7,1)}$	4	1	3	3.52	610.61	3.52	1831.83	**-1828.31**	-18.28	3.52	-1553.76	-0.77	-12.22	25	-457.08	-	0.01	-1831.83
G1.6	$ADF-ZSPRD^{100D}_{(2.7,0.5)}$	4	1	3	80.31	706.36	80.31	2119.09	**-2038.78**	-20.39	80.31	-1858.45	-0.68	-10.79	25	-509.7	0.04	0.11	-2119.09
G2.1	$ADF-SPRD^{100D}-SMA_{(10,20)}$	15	9	6	303.69	1112.73	2733.24	6676.36	**-3943.13**	-39.43	676.6	-5028.17	-0.29	-4.6	60	-262.88	0.41	0.27	-6676.36
G2.2	$ADF-SPRD^{100D}-EMA_{(10,20)}$	34	22	12	124.97	1968.85	2749.39	23626.22	**-20876.83**	-208.77	493.92	-9630.2	-0.36	-5.71	64.71	-613.94	0.12	0.06	-23225.01
G2.3	$ADF-SPRD^{100D}-MACD_{(12,26,9)}$	32	17	15	149.53	563.27	2542.05	8449.05	**-5907**	-59.07	1338.52	-4445.34	-0.29	-4.6	53.12	-184.63	0.3	0.27	-7887.61
G2.4	$ADF-SPRD^{100D}-RSI_{(14)}$	5	2	3	364.87	738.13	729.74	2214.39	**-1484.64**	-14.85	520.6	-1163.82	-0.66	-10.48	40	-296.93	0.33	0.49	-2018.12
G2.5	$ADF-SPRD^{100D}-BB_{(20)}$	15	4	11	95.86	261.92	383.44	2881.17	**-2497.74**	-24.98	191.59	-1760.34	-0.49	-7.78	26.67	-166.5	0.13	0.37	-2698.8
G3	$ADF-SPRD^{100D}-DECTREE$	309	138	171	27.37	24.92	3777.34	4261.14	**-483.8**	-4.84	148.42	-127.55	-4.23	-67.15	44.66	-1.57	0.89	1.1	-998.96
G4	$ADF-SPRD^{100D}-MLP$	286	135	151	24.04	24.48	3245.7	3696.9	**-451.2**	-4.51	114.48	-141.96	-4.64	-73.66	47.2	-1.58	0.88	0.98	-731.34
Part VIII: Models derived using the spread obtained from $KALMAN-SPRD^{100D}$																			
H1.1	$KALMAN-ZSPRD^{100D}_{(3,2)}$	2	2	-	150.88	-	301.75	-	**301.75**	3.02	221.63	-	0.18	2.86	100	150.88	301.75	150.88	-
H1.2	$KALMAN-ZSPRD^{100D}_{(3,1)}$	2	1	1	270.27	79.74	270.27	79.74	**190.53**	1.91	270.27	-79.74	-0.15	-2.38	50	95.26	3.39	3.39	-79.74
H1.3	$KALMAN-ZSPRD^{100D}_{(3,0.5)}$	2	1	1	319.99	20.36	319.99	20.36	**299.62**	3	319.99	-20.36	0.07	1.11	50	149.81	15.71	15.72	-20.36
H1.4	$KALMAN-ZSPRD^{100D}_{(2.7,2)}$	5	4	1	103.64	90.18	414.57	90.18	**324.4**	3.24	176.01	-90.18	-0.67	-10.64	80	64.88	4.6	1.15	-90.18
H1.5	$KALMAN-ZSPRD^{100D}_{(2.7,1)}$	4	2	2	130.69	102.34	261.37	204.68	**56.69**	0.57	224.22	-111.77	-0.76	-12.06	50	14.17	1.28	1.28	-204.68
H1.6	$KALMAN-ZSPRD^{100D}_{(2.7,0.5)}$	3	1	2	273.58	175.19	273.58	350.38	**-76.8**	-0.77	273.58	-316.66	-0.54	-8.57	33.33	-25.61	0.78	1.56	-350.38
H2.1	$KALMAN-SPRD^{100D}-SMA_{(10,20)}$	16	7	9	98.75	49.42	691.23	444.77	**246.46**	2.46	276.3	-104.26	-1.2	-19.05	43.75	15.4	1.55	2	-360.74
H2.2	$KALMAN-SPRD^{100D}-EMA_{(10,20)}$	27	10	17	129.58	107.91	1295.83	1834.42	**-538.59**	-5.39	312.22	-322.44	-1	-15.87	37.04	-19.94	0.71	1.2	-1299.98
H2.3	$KALMAN-SPRD^{100D}-MACD_{(12,26,9)}$	29	10	19	95.9	87.39	958.99	1660.33	**-701.34**	-7.01	255.1	-216.1	-1.44	-22.86	34.48	-24.19	0.58	1.1	-1193.92
H2.4	$KALMAN-SPRD^{100D}-RSI_{(14)}$	2	-	2	-	846.13	-	1692.27	**-1692.27**	-16.92	-	-1671.34	-0.84	-13.33	-	-846.13	-	-	-1671.34
H2.5	$KALMAN-SPRD^{100D}-BB_{(20)}$	11	6	5	110.38	41.23	662.28	206.16	**456.13**	4.56	195.65	-64.03	-1.06	-16.83	54.55	41.47	3.21	2.68	-118.13
H3	$KALMAN-SPRD^{100D}-DECTREE$	271	145	126	26.13	24.94	3788.3	3142.57	**645.73**	6.46	135.08	-215.62	-4.03	-63.97	53.51	2.39	1.21	1.05	-529.11
H4	$KALMAN-SPRD^{100D}-MLP$	253	150	103	24.62	20.53	3693.17	2114.24	**1578.93**	15.79	104.51	-130.93	-4.67	-74.13	59.29	6.24	1.75	1.2	-301.21
Part IX: Models derived using the spread obtained from $RATIO-SPRD^{100D}$																			
I1.1	$RATIO-ZSPRD^{100D}_{(3,2)}$	4	3	1	72.87	12.55	218.6	12.55	**206.05**	2.06	94.86	-12.55	-2.21	-35.08	75	51.51	17.42	5.81	-12.55
I1.2	$RATIO-ZSPRD^{100D}_{(3,1)}$	4	4	-	91.68	-	366.74	-	**366.74**	3.67	149.72	-	-1.42	-22.54	100	91.68	366.74	91.68	-
I1.3	$RATIO-ZSPRD^{100D}_{(3,0.5)}$	4	4	-	124.69	-	498.77	-	**498.77**	4.99	149.72	-	-1.49	-23.65	100	124.69	498.77	124.69	-
I1.4	$RATIO-ZSPRD^{100D}_{(2.7,2)}$	5	3	2	47.98	89.52	143.95	179.04	**-35.1**	-0.35	87.2	-115.34	-1.92	-30.48	60	-7.02	0.8	0.54	-122.3
I1.5	$RATIO-ZSPRD^{100D}_{(2.7,1)}$	5	3	2	65.54	41.58	196.62	83.17	**113.45**	1.13	138.33	-77.08	-1.64	-26.03	60	22.69	2.36	1.58	-77.08
I1.6	$RATIO-ZSPRD^{100D}_{(2.7,0.5)}$	4	3	1	75.64	338.47	226.92	338.47	**-111.55**	-1.12	138.33	-338.47	-0.85	-13.49	75	-27.89	0.67	0.22	-338.47
I2.1	$RATIO-SPRD^{100D}-SMA_{(10,20)}$	16	6	10	140.11	134.8	840.65	1348.04	**-507.39**	-5.07	580.16	-382.68	-0.89	-14.13	37.5	-31.71	0.62	1.04	-891.54
I2.2	$RATIO-SPRD^{100D}-EMA_{(10,20)}$	25	7	18	160.35	89.21	1122.46	1605.86	**-483.4**	-4.83	290.66	-406.79	-1.15	-18.26	28	-19.34	0.7	1.8	-1357.01
I2.3	$RATIO-SPRD^{100D}-MACD_{(12,26,9)}$	34	13	21	75.59	47.18	982.71	990.81	**-8.1**	-0.08	218.33	-271.45	-1.74	-27.62	38.24	-0.23	0.99	1.6	-497.89
I2.4	$RATIO-SPRD^{100D}-RSI_{(14)}$	2	-	2	-	864.53	-	1729.05	**-1729.05**	-17.29	-	-1520.84	-1.1	-17.46	-	-864.53	-	-	-1520.84
I2.5	$RATIO-SPRD^{100D}-BB_{(20)}$	18	15	3	51.83	137.94	777.45	413.81	**363.65**	3.64	132.81	-244.77	-1.55	-24.61	83.33	20.2	1.88	0.38	-244.77
I3	$RATIO-SPRD^{100D}-DECTREE$	300	111	189	21.99	20.49	2441.34	3872.54	**-1431.2**	-14.31	109.95	-101	-5.64	-89.53	37	-4.77	0.63	1.07	-1804.7
I4	$RATIO-SPRD^{100D}-MLP$	194	79	115	26.96	22.83	2130.15	2625.7	**-495.55**	-4.96	183.9	-218.3	-3.97	-63.02	40.72	-2.56	0.81	1.18	-785.29
Part X: Models derived using the close price of ITOT.N																			
CLS-SYM-1.1	$CLOSE^{ITOT.N}-SMA_{(10,20)}$	12	7	5	349.7	110.23	2447.92	551.13	**1896.79**	18.97	1275.51	-231.05	0.2	3.17	58.33	158.05	4.44	3.17	-320.08
CLS-SYM-1.2	$CLOSE^{ITOT.N}-EMA_{(10,20)}$	18	8	10	320.51	242.25	2564.09	2422.52	**141.57**	1.42	1107.76	-798.87	-0.17	-2.7	44.44	7.84	1.06	1.32	-637.32
CLS-SYM-1.3	$CLOSE^{ITOT.N}-MACD_{(12,26,9)}$	38	15	23	136.98	113.32	2054.75	2606.43	**-551.68**	-5.52	565.03	-354.83	-0.56	-8.89	39.47	-14.53	0.79	1.21	-1373.77
CLS-SYM-1.4	$CLOSE^{ITOT.N}-RSI_{(14)}$	6	3	3	350.41	842.6	1051.24	2527.79	**-1476.55**	-14.77	576.4	-2049.07	-0.34	-5.4	50	-246.09	0.42	0.42	-2049.07
CLS-SYM-1.5	$CLOSE^{ITOT.N}-BB_{(20)}$	12	9	3	93.75	445.83	843.77	1337.49	**-493.72**	-4.94	226.17	-778.78	-0.39	-6.19	75	-41.14	0.63	0.21	-778.78
Part XI: Models derived using the close price of IXUS.N																			
CLS-SYM-2.1	$CLOSE^{IXUS.N}-SMA_{(10,20)}$	14	6	8	191.25	153.22	1147.51	1225.77	**-78.26**	-0.78	563.95	-480.15	-0.33	-5.24	42.86	-5.58	0.94	1.25	-673.35
CLS-SYM-2.2	$CLOSE^{IXUS.N}-EMA_{(10,20)}$	23	8	15	370.89	149.39	2967.1	2240.79	**726.3**	7.26	1091.8	-556.4	-0.12	-1.9	34.78	31.56	1.32	2.48	-790.14
CLS-SYM-2.3	$CLOSE^{IXUS.N}-MACD_{(12,26,9)}$	38	11	27	188.47	95.85	2073.12	2587.91	**-514.79**	-5.15	932.53	-366.94	-0.45	-7.14	28.95	-13.54	0.8	1.97	-1634.42
CLS-SYM-2.4	$CLOSE^{IXUS.N}-RSI_{(14)}$	6	3	3	307.42	280.97	922.25	842.92	**79.33**	0.79	405.82	-589.96	-0.17	-2.7	50	13.22	1.09	1.09	-589.96
CLS-SYM-2.5	$CLOSE^{IXUS.N}-BB_{(20)}$	20	14	6	66.01	208.54	924.11	1251.26	**-327.15**	-3.27	209.32	-831.57	-0.43	-6.83	70	-16.36	0.74	0.32	-837.17

Table D.2.4: This table presents the back-test metrics for the pair $IWF.N/XLE.N$ based on a 30-day rolling window. The table is subdivided into eleven parts, and in each of these parts, we present the back-test metrics and the trading strategies which use the spread derived from various models. In Part I, the spread is derived from the $DIST^{V1.1}$ model, in Part II from the $DIST^{V1.2}$ model, in Part III from the $DIST^{V2}$ model, in Part IV from the $DIST^{V3}$ model, in Part V from the $DIST^{V4}$ model, in Part VI from the $JOHANSEN - SPRD$ model, in Part VIII from the $ADF - SPRD$ model, in from the $DIST^{V2}$ model, in Part VIII from the $KALMAN - SPRD$ model, and in Part IX from the $RATIO - SPRD$ model. In Part X and XI, we present the back-test metrics of the trading strategies which use the close price of IWF.N, and XLE.N, respectively. All $ numbers reported below are in USD.

(I) Trading Strategy Code	(II) Model Name	(III) Total Number of Trades	(IV) Number of Winning Trades	(V) Number of Loosing Trades	(VI) Average Profit per Trade ($)	(VII) Average Loss per Trade ($)	(VIII) Gross Profit ($)	(IX) Gross Loss ($)	(X) Net Profit ($)	(XI) ROI (%)	(XII) Max P&L ($)	(XIII) Min P&L ($)	(XIV) Daily Sharpe Ratio	(XV) Annualized Sharpe Ratio	(XVI) Hit Ratio	(XVII) Expectancy	(XVIII) Profit Factor	(XIX) Realized Risk Reward Ratio	(XX) Max Drawdown ($)
Part I: Models derived using the spread obtained from $DIST^{V1.1} - SPRD^{30D}$																			
A1.1	$DIST^{V1.1} - ZSPRD^{30D}_{(3,2)}$	1	1	-	181.84	-	181.84	-	**181.84**	1.82	181.84	-	-	-	100	181.84	181.84	181.84	-
A1.2	$DIST^{V1.1} - ZSPRD^{30D}_{(3,1)}$	1	1	-	310.87	-	310.87	-	**310.87**	3.11	310.87	-	-	-	100	310.87	310.87	310.87	-
A1.3	$DIST^{V1.1} - ZSPRD^{30D}_{(3,0.5)}$	1	1	-	294.06	-	294.06	-	**294.06**	2.94	294.06	-	-	-	100	294.06	294.06	294.06	-
A1.4	$DIST^{V1.1} - ZSPRD^{30D}_{(2.7,2)}$	4	1	3	181.84	157.05	181.84	471.15	**-289.3**	-2.89	181.84	-204.95	-1.3	-20.64	25	-72.33	0.39	1.16	-471.15
A1.5	$DIST^{V1.1} - ZSPRD^{30D}_{(2.7,1)}$	3	1	2	310.87	191.11	310.87	382.23	**-71.35**	-0.71	310.87	-286.6	-0.58	-9.21	33.33	-23.8	0.81	1.63	-382.23
A1.6	$DIST^{V1.1} - ZSPRD^{30D}_{(2.7,0.5)}$	3	1	2	294.06	303.13	294.06	606.26	**-312.2**	-3.12	294.06	-319.66	-0.74	-11.75	33.33	-104.08	0.49	0.97	-606.25
A2.1	$DIST^{V1.1} - SPRD^{30D} - SMA_{(10,20)}$	10	4	6	168.35	911.79	673.38	5470.77	**-4797.39**	-47.97	377.05	-1545.23	-0.87	-13.81	40	-479.74	0.12	0.18	-5026.8
A2.2	$DIST^{V1.1} - SPRD^{30D} - EMA_{(10,20)}$	23	15	8	375.4	707.37	5631.01	5659	**-27.99**	-0.28	1055.98	-1756.39	-0.22	-3.49	65.22	-1.19	1	0.53	-2365.42
A2.3	$DIST^{V1.1} - SPRD^{30D} - MACD_{(12,26,9)}$	40	25	15	279.61	223.58	6990.33	3353.69	**3636.64**	36.37	735.56	-766.66	-0.18	-2.86	62.5	90.92	2.08	1.25	-1067.68
A2.4	$DIST^{V1.1} - SPRD^{30D} - RSI_{(14)}$	5	3	2	1556.52	970.29	4669.55	1940.57	**2728.98**	27.29	4483.68	-1083.69	0.17	2.7	60	545.8	2.41	1.6	-1884.62
A2.5	$DIST^{V1.1} - SPRD^{30D} - BB_{(20)}$	15	7	8	545.7	244.97	3819.9	1959.77	**1860.12**	18.6	1007.29	-1121.7	-0.05	-0.79	46.67	124.03	1.95	2.23	-1121.7
A3	$DIST^{V1.1} - SPRD^{30D} - DECTREE$	340	147	193	110.9	78.75	16302.63	15198.6	**1104.02**	11.04	580.21	-890.7	-1.04	-16.51	43.24	3.26	1.07	1.41	-1967.41
A4	$DIST^{V1.1} - SPRD^{30D} - MLP$	330	145	185	114.53	86.02	16607.4	15913.4	**694.01**	6.94	631.69	-890.7	-1.02	-16.19	43.94	2.1	1.04	1.33	-2041.18
Part II: Models derived using the spread obtained from $DIST^{V1.2} - SPRD^{30D}$																			
B1.1	$DIST^{V1.2} - ZSPRD^{30D}_{(3,2)}$	7	4	3	192.74	161.32	770.96	483.95	**287**	2.87	301.81	-350.57	-0.49	-7.78	57.14	40.99	1.59	1.19	-445.28
B1.2	$DIST^{V1.2} - ZSPRD^{30D}_{(3,1)}$	7	4	3	287.04	381.5	1148.16	1144.49	**3.68**	0.04	769.02	-822.51	-0.32	-5.08	57.14	0.51	1	0.75	-941.57
B1.3	$DIST^{V1.2} - ZSPRD^{30D}_{(3,0.5)}$	7	3	4	494.27	405.7	1482.82	1622.8	**-139.98**	-1.4	790.67	-765.93	-0.31	-4.92	42.86	-19.97	0.91	1.22	-884.99
B1.4	$DIST^{V1.2} - ZSPRD^{30D}_{(2.7,2)}$	12	7	5	102.86	152.39	720	761.96	**-41.97**	-0.42	274.77	-350.57	-0.97	-15.4	58.33	-3.51	0.94	0.67	-445.28
B1.5	$DIST^{V1.2} - ZSPRD^{30D}_{(2.7,1)}$	12	6	6	270.77	254.1	1624.64	1524.6	**100.04**	1	769.02	-822.51	-0.38	-6.03	50	8.34	1.07	1.07	-941.57
B1.6	$DIST^{V1.2} - ZSPRD^{30D}_{(2.7,0.5)}$	11	7	4	354.48	477.36	2481.35	1909.44	**571.91**	5.72	790.67	-765.93	-0.2	-3.17	63.64	52.02	1.3	0.74	-989.1
B2.1	$DIST^{V1.2} - SPRD^{30D} - SMA_{(10,20)}$	16	6	10	259.41	600.24	1556.44	6002.35	**-4445.91**	-44.46	815.43	-1270.72	-0.76	-12.06	37.5	-277.87	0.26	0.43	-4662.81
B2.2	$DIST^{V1.2} - SPRD^{30D} - EMA_{(10,20)}$	23	11	12	353.18	621.24	3884.96	7454.93	**-3569.97**	-35.7	1016.48	-1888.86	-0.44	-6.98	47.83	-155.18	0.52	0.57	-5408.31
B2.3	$DIST^{V1.2} - SPRD^{30D} - MACD_{(12,26,9)}$	34	17	17	304.13	308.3	5170.15	5241.14	**-70.99**	-0.71	702.34	-1025.84	-0.37	-5.87	50	-2.09	0.99	0.99	-2359.39
B2.4	$DIST^{V1.2} - SPRD^{30D} - RSI_{(14)}$	9	5	4	552.44	742.5	2762.21	2970.01	**-207.8**	-2.08	1177.72	-1407.44	-0.22	-3.49	55.56	-23.03	0.93	0.74	-1407.44
B2.5	$DIST^{V1.2} - SPRD^{30D} - BB_{(20)}$	16	10	6	345.64	295.64	3456.37	1773.86	**1682.52**	16.83	1131.58	-699.73	-0.11	-1.75	62.5	105.16	1.95	1.17	-929.37
B3	$DIST^{V1.2} - SPRD^{30D} - DECTREE$	299	126	173	101.32	99.98	12766.14	17296.92	**-4530.78**	-45.31	504.13	-653.33	-1.16	-18.41	42.14	-15.15	0.74	1.01	-5253.46
B4	$DIST^{V1.2} - SPRD^{30D} - MLP$	228	111	117	133.19	108.54	14784.43	12698.62	**2085.81**	20.86	673.85	-569.86	-0.85	-13.49	48.68	9.14	1.16	1.23	-3063.02
Part III: Models derived using the spread obtained from $DIST^{V2} - SPRD^{30D}$																			
C1.1	$DIST^{V2} - ZSPRD^{30D}_{(3,2)}$	1	-	1	-	181.84	-	181.84	**-181.84**	-1.82	-	-181.84	-	-	-	-181.84	-	-	-181.84
C1.2	$DIST^{V2} - ZSPRD^{30D}_{(3,1)}$	1	-	1	-	310.87	-	310.87	**-310.87**	-3.11	-	-310.87	-	-	-	-310.87	-	-	-310.87
C1.3	$DIST^{V2} - ZSPRD^{30D}_{(3,0.5)}$	1	-	1	-	294.06	-	294.06	**-294.06**	-2.94	-	-294.06	-	-	-	-294.06	-	-	-294.06
C1.4	$DIST^{V2} - ZSPRD^{30D}_{(2.7,2)}$	4	3	1	157.05	181.84	471.15	181.84	**289.3**	2.89	204.95	-181.84	-0.46	-7.3	75	72.33	2.59	0.86	-181.84
C1.5	$DIST^{V2} - ZSPRD^{30D}_{(2.7,1)}$	3	2	1	191.11	310.87	382.23	310.87	**71.35**	0.71	286.6	-310.87	-0.42	-6.67	66.67	23.8	1.23	0.61	-310.87
C1.6	$DIST^{V2} - ZSPRD^{30D}_{(2.7,0.5)}$	3	2	1	303.13	294.06	606.26	294.06	**312.2**	3.12	319.66	-294.06	-0.14	-2.22	66.67	104.08	2.06	1.03	-294.06
C2.1	$DIST^{V2} - SPRD^{30D} - SMA_{(10,20)}$	10	7	3	867.17	166.9	6070.2	500.7	**5569.5**	55.7	1545.23	-377.05	0.59	9.37	70	556.95	12.12	5.2	-377.05
C2.2	$DIST^{V2} - SPRD^{30D} - EMA_{(10,20)}$	23	8	15	707.37	375.4	5659	5631.01	**27.99**	0.28	1756.39	-1055.98	-0.22	-3.49	34.78	1.19	1	1.88	-3541.35
C2.3	$DIST^{V2} - SPRD^{30D} - MACD_{(12,26,9)}$	40	15	25	223.58	279.61	3353.69	6990.33	**-3636.64**	-36.37	766.66	-735.56	-0.73	-11.59	37.5	-90.92	0.48	0.8	-4292.48
C2.4	$DIST^{V2} - SPRD^{30D} - RSI_{(14)}$	5	2	3	970.29	1556.52	1940.57	4669.55	**-2728.98**	-27.29	1083.69	-4483.68	-0.31	-4.92	40	-545.8	0.42	0.62	-4483.68
C2.5	$DIST^{V2} - SPRD^{30D} - BB_{(20)}$	15	8	7	244.97	545.7	1959.77	3819.9	**-1860.12**	-18.6	1121.7	-1007.29	-0.51	-8.1	53.33	-124.03	0.51	0.45	-1992.14
C3	$DIST^{V2} - SPRD^{30D} - DECTREE$	358	152	206	108.59	78.62	16506.27	16195.42	**310.85**	3.11	548.97	-890.7	-1.1	-17.46	42.46	0.87	1.02	1.38	-1712.87
C4	$DIST^{V2} - SPRD^{30D} - MLP$	323	147	176	112.55	82.15	16544.9	14458.3	**2086.6**	20.87	700.5	-890.7	-1	-15.87	45.51	6.46	1.14	1.37	-2295.68
Part IV: Models derived using the spread obtained from $DIST^{V3} - SPRD^{30D}$																			
D1.1	$DIST^{V3} - ZSPRD^{30D}_{(3,2)}$	7	6	1	109.36	206.4	656.17	206.4	**449.77**	4.5	208.26	-206.4	-0.64	-10.16	85.71	64.24	3.18	0.53	-206.4
D1.2	$DIST^{V3} - ZSPRD^{30D}_{(3,1)}$	7	4	3	432.54	523.48	1730.14	1570.44	**159.7**	1.6	1097.39	-700.62	-0.21	-3.33	57.14	22.79	1.1	0.83	-1570.44
D1.3	$DIST^{V3} - ZSPRD^{30D}_{(3,0.5)}$	7	4	3	532.58	762.69	2130.31	2288.06	**-157.75**	-1.58	1250.37	-863.78	-0.22	-3.49	57.14	-22.57	0.93	0.7	-2288.06
D1.4	$DIST^{V3} - ZSPRD^{30D}_{(2.7,2)}$	10	7	3	126.11	98.63	882.8	295.88	**586.92**	5.87	252.76	-206.4	-0.69	-10.95	70	58.69	2.98	1.28	-206.4
D1.5	$DIST^{V3} - ZSPRD^{30D}_{(2.7,1)}$	9	5	4	418.85	393.11	2094.24	1572.43	**521.81**	5.22	1100.73	-700.62	-0.17	-2.7	55.56	58.02	1.33	1.07	-1209.69
D1.6	$DIST^{V3} - ZSPRD^{30D}_{(2.7,0.5)}$	9	6	3	416.66	762.69	2499.94	2288.06	**211.87**	2.12	1243.23	-863.78	-0.19	-3.02	66.67	23.58	1.09	0.55	-1927.31
D2.1	$DIST^{V3} - SPRD^{30D} - SMA_{(10,20)}$	17	7	10	816.16	429.66	5713.11	4296.61	**1416.51**	14.17	3471.98	-1242.37	-0.07	-1.11	41.18	83.37	1.33	1.9	-3865.26
D2.2	$DIST^{V3} - SPRD^{30D} - EMA_{(10,20)}$	39	14	25	480.47	251.62	6726.64	6290.45	**436.2**	4.36	1129.59	-1286.53	-0.3	-4.76	35.9	11.2	1.07	1.91	-2905.78
D2.3	$DIST^{V3} - SPRD^{30D} - MACD_{(12,26,9)}$	39	11	28	411.73	260.09	4528.99	7282.62	**-2753.63**	-27.54	1220.5	-1241.46	-0.51	-8.1	28.21	-70.57	0.62	1.58	-5791.91
D2.4	$DIST^{V3} - SPRD^{30D} - RSI_{(14)}$	5	3	2	966.64	336.89	2899.92	673.78	**2226.14**	22.26	1991.46	-543.85	0.3	4.76	60	445.23	4.3	2.87	-543.85
D2.5	$DIST^{V3} - SPRD^{30D} - BB_{(20)}$	18	12	6	133.01	518.04	1596.12	3108.26	**-1512.14**	-15.12	241.35	-977.01	-0.6	-9.52	66.67	-83.99	0.51	0.26	-2886.46
D3	$DIST^{V3} - SPRD^{30D} - DECTREE$	305	135	170	95.46	89.79	12887.12	15264.49	**-2377.36**	-23.77	544.14	-603.01	-1.2	-19.05	44.26	-7.8	0.84	1.06	-3391.25
D4	$DIST^{V3} - SPRD^{30D} - MLP$	247	89	158	133.5	101.67	11881.89	16064.35	**-4182.46**	-41.82	1560.82	-1083.67	-0.89	-14.13	36.03	-16.94	0.74	1.31	-5702.28
Part V: Models derived using the spread obtained from $DIST^{V4} - SPRD^{30D}$																			
E1.1	$DIST^{V4} - ZSPRD^{30D}_{(3,2)}$	7	6	1	109.36	206.4	656.17	206.4	**449.77**	4.5	208.26	-206.4	-0.64	-10.16	85.71	64.24	3.18	0.53	-206.4
E1.2	$DIST^{V4} - ZSPRD^{30D}_{(3,1)}$	7	4	3	432.54	523.48	1730.14	1570.44	**159.7**	1.6	1097.39	-700.62	-0.21	-3.33	57.14	22.79	1.1	0.83	-1570.44
E1.3	$DIST^{V4} - ZSPRD^{30D}_{(3,0.5)}$	7	4	3	532.58	762.69	2130.31	2288.06	**-157.75**	-1.58	1250.37	-863.78	-0.22	-3.49	57.14	-22.57	0.93	0.7	-2288.06
E1.4	$DIST^{V4} - ZSPRD^{30D}_{(2.7,2)}$	10	7	3	126.11	98.63	882.8	295.88	**586.92**	5.87	252.76	-206.4	-0.69	-10.95	70	58.69	2.98	1.28	-206.4
E1.5	$DIST^{V4} - ZSPRD^{30D}_{(2.7,1)}$	9	5	4	418.85	393.11	2094.24	1572.43	**521.81**	5.22	1100.73	-700.62	-0.17	-2.7	55.56	58.02	1.33	1.07	-1209.69
E1.6	$DIST^{V4} - ZSPRD^{30D}_{(2.7,0.5)}$	9	6	3	416.66	762.69	2499.94	2288.06	**211.87**	2.12	1243.23	-863.78	-0.19	-3.02	66.67	23.58	1.09	0.55	-1927.31
E2.1	$DIST^{V4} - SPRD^{30D} - SMA_{(10,20)}$	17	7	10	816.16	429.66	5713.11	4296.61	**1416.51**	14.17	3471.98	-1242.37	-0.07	-1.11	41.18	83.37	1.33	1.9	-3865.26
E2.2	$DIST^{V4} - SPRD^{30D} - EMA_{(10,20)}$	39	14	25	480.47	251.62	6726.64	6290.45	**436.2**	4.36	1129.59	-1286.53	-0.3	-4.76	35.9	11.2	1.07	1.91	-2905.78
E2.3	$DIST^{V4} - SPRD^{30D} - MACD_{(12,26,9)}$	39	11	28	411.73	260.09	4528.99	7282.62	**-2753.63**	-27.54	1220.5	-1241.46	-0.51	-8.1	28.21	-70.57	0.62	1.58	-5791.91
E2.4	$DIST^{V4} - SPRD^{30D} - RSI_{(14)}$	5	3	2	966.64	336.89	2899.92	673.78	**2226.14**	22.26	1991.46	-543.85	0.3	4.76	60	445.23	4.3	2.87	-543.85
E2.5	$DIST^{V4} - SPRD^{30D} - BB_{(20)}$	18	12	6	133.01	518.04	1596.12	3108.26	**-1512.14**	-15.12	241.35	-977.01	-0.6	-9.52	66.67	-83.99	0.51	0.26	-2886.46
E3	$DIST^{V4} - SPRD^{30D} - DECTREE$	297	127	170	97.91	93.42	12434.04	15880.73	**-3446.7**	-34.47	631.69	-603.01	-1.2	-19.05	42.76	-11.61	0.78	1.05	-4178.46
E4	$DIST^{V4} - SPRD^{30D} - MLP$	247	89	158	133.5	101.67	11881.89	16064.35	**-4182.46**	-41.82	1560.82	-1083.67	-0.89	-14.13	36.03	-16.94	0.74	1.31	-5702.28
Part VI: Models derived using the spread obtained from $JOHANSEN - SPRD^{30D}$																			
F1.1	$JOHANSEN - ZSPRD^{30D}_{(3,2)}$	19	12	7	81.48	433.17	977.8	3032.21	**-2054.41**	-20.54	254.59	-2865.69	-0.26	-4.13	63.16	-108.12	0.32	0.19	-2879.26
F1.2	$JOHANSEN - ZSPRD^{30D}_{(3,1)}$	18	12	6	116.58	2082.17	1399	12493.01	**-11094.01**	-110.94	254.59	-12311.2	-0.25	-3.97	66.67	-616.26	0.11	0.06	-12436.16
F1.3	$JOHANSEN - ZSPRD^{30D}_{(3,0.5)}$	17	12	5	141.13	2150.34	1693.61	10751.71	**-9058.1**	-90.58	289.24	-10519.85	-0.26	-4.13	70.59	-532.79	0.16	0.07	-10732.64
F1.4	$JOHANSEN - ZSPRD^{30D}_{(2.7,2)}$	21	12	9	91.89	353.38	1102.73	3180.41	**-2077.68**	-20.78	274.74	-2865.69	-0.19	-3.02	57.14	-98.95	0.35	0.26	-2879.26
F1.5	$JOHANSEN - ZSPRD^{30D}_{(2.7,1)}$	20	12	8	96.37	1779.72	1156.4	14237.78	**-13081.38**	-130.81	254.59	-12311.2	-0.33	-5.24	60	-654.07	0.08	0.05	-14186.61
F1.6	$JOHANSEN - ZSPRD^{30D}_{(2.7,0.5)}$	19	12	7	116.75	1978.64	1401.02	13850.45	**-12449.43**	-124.49	289.24	-10519.85	-0.35	-5.56	63.16	-655.19	0.1	0.06	-13831.39
F2.1	$JOHANSEN - SPRD^{30D} - SMA_{(10,20)}$	25	12	13	1221.04	1132.3	14652.45	14719.85	**-67.4**	-0.67	10520.18	-9055.58	0.04	0.63	48	-2.7	1	1.08	-13701.88
F2.2	$JOHANSEN - SPRD^{30D} - EMA_{(10,20)}$	42	23	19	917.84	833.4	21110.23	15834.64	**5275.59**	52.76	8978.31	-3126.95	0.15	2.38	54.76	125.58	1.33	1.1	-7692
F2.3	$JOHANSEN - SPRD^{30D} - MACD_{(12,26,9)}$	42	22	20	520.75	834.05	11456.57	16681.08	**-5224.51**	-52.25	4848.38	-10217.21	0.07	1.11	52.38	-124.41	0.69	0.62	-11856.63
F2.4	$JOHANSEN - SPRD^{30D} - RSI_{(14)}$	6	4	2	143.59	649.1	574.37	1298.2	**-723.84**	-7.24	358.65	-1120.42	-0.25	-3.97	66.67	-120.61	0.44	0.22	-1120.42
F2.5	$JOHANSEN - SPRD^{30D} - BB_{(20)}$	21	10	11	242.23	999.92	2422.27	10999.1	**-8576.83**	-85.77	1316.96	-7488.45	-0.3	-4.76	47.62	-408.41	0.22	0.24	-9204.6
F3	$JOHANSEN - SPRD^{30D} - DECTREE$	338	166	172	94.17	85.68	15631.88	14736.76	**895.11**	8.95	365.41	-683.07	-1.16	-18.41	49.11	2.64	1.06	1.1	-1510.75
F4	$JOHANSEN - SPRD^{30D} - MLP$	227	115	112	101.3	131.29	11649.92	14704.59	**-3054.67**	-30.55	530.25	-945.8	-0.94	-14.92	50.66	-13.46	0.79	0.77	-3519.76
Part VII: Models derived using the spread obtained from $ADF - SPRD^{30D}$																			
G1.1	$ADF - ZSPRD^{30D}_{(3,2)}$	6	3	3	807.55	204.06	2422.65	612.19	**1810.46**	18.1	2252.42	-330.39	0.24	3.81	50	301.74	3.96	3.96	-532.04
G1.2	$ADF - ZSPRD^{30D}_{(3,1)}$	5	1	4	3125.4	888.94	3125.4	3555.76	**-430.36**	-4.3	3125.4	-2329.85	-0.1	-1.59	20	-86.07	0.88	3.52	-3555.77
G1.3	$ADF - ZSPRD^{30D}_{(3,0.5)}$	5	2	3	1816.16	1151.07	3632.33	3453.22	**179.11**	1.79	3529.33	-1717.55	-0.03	-0.48	40	35.82	1.05	1.58	-3350.22
G1.4	$ADF - ZSPRD^{30D}_{(2.7,2)}$	8	5	3	1600.9	186.94	8004.5	560.81	**7443.69**	74.44	4428.5	-330.39	0.51	8.1	62.5	930.46	14.27	8.56	-480.66
G1.5	$ADF - ZSPRD^{30D}_{(2.7,1)}$	7	3	4	1983.88	632.53	5951.63	2530.12	**3421.51**	34.22	3125.4	-1350.63	0.26	4.13	42.86	488.86	2.35	3.14	-1350.63
G1.6	$ADF - ZSPRD^{30D}_{(2.7,0.5)}$	7	2	5	1816.16	905.06	3632.33	4525.28	**-892.96**	-8.93	3529.33	-1639.92	-0.13	-2.06	28.57	-127.6	0.8	2.01	-4422.28
G2.1	$ADF - SPRD^{30D} - SMA_{(10,20)}$	19	13	6	1914.04	1852.54	24882.49	11115.24	**13767.25**	137.67	13347.99	-5577.36	0.19	3.02	68.42	724.55	2.24	1.03	-5577.36
G2.2	$ADF - SPRD^{30D} - EMA_{(10,20)}$	44	26	18	830.48	1587.74	21592.39	28579.27	**-6986.88**	-69.87	6472.84	-6211.73	-0.08	-1.27	59.09	-158.81	0.76	0.52	-11760.07
G2.3	$ADF - SPRD^{30D} - MACD_{(12,26,9)}$	43	25	18	1314.7	5077.58	32867.46	91396.37	**-58528.91**	-585.29	15250.87	-57480.81	-0.16	-2.54	58.14	-1361.11	0.36	0.26	-59702.13
G2.4	$ADF - SPRD^{30D} - RSI_{(14)}$	1	-	1	-	7567.48	-	7567.48	**-7567.48**	-75.67	-	-7567.48	-	-	-	-7567.48	-	-	-7567.48
G2.5	$ADF - SPRD^{30D} - BB_{(20)}$	21	7	14	2218.48	700.89	15529.37	9812.46	**5716.91**	57.17	4953.19	-5952.17	0.09	1.43	33.33	272.14	1.58	3.17	-6456.32
G3	$ADF - SPRD^{30D} - DECTREE$	293	133	160	110.14	92.79	14648.61	14846.86	**-198.24**	-1.98	700.5	-822.93	-0.99	-15.72	45.39	-0.68	0.99	1.19	-2424.79
G4	$ADF - SPRD^{30D} - MLP$	140	60	80	149.52	153.02	8971.13	12241.8	**-3270.67**	-32.71	1088.52	-1232.16	-0.67	-10.64	42.86	-23.35	0.73	0.98	-5026.17
Part VIII: Models derived using the spread obtained from $KALMAN - SPRD^{30D}$																			
H1.1	$KALMAN - ZSPRD^{30D}_{(3,2)}$	1	1	-	857.18	-	857.18	-	**857.18**	8.57	857.18	-	-	-	100	857.18	857.18	857.18	-
H1.2	$KALMAN - ZSPRD^{30D}_{(3,1)}$	1	1	-	632.57	-	632.57	-	**632.57**	6.33	632.57	-	-	-	100	632.57	632.57	632.57	-
H1.3	$KALMAN - ZSPRD^{30D}_{(3,0.5)}$	1	1	-	1742.14	-	1742.14	-	**1742.14**	17.42	1742.14	-	-	-	100	1742.14	1742.14	1742.14	-
H1.4	$KALMAN - ZSPRD^{30D}_{(2.7,2)}$	8	4	4	357.16	397	1428.66	1587.99	**-159.33**	-1.59	857.18	-1006.13	-0.21	-3.33	50	-19.92	0.9	0.9	-1372.79
H1.5	$KALMAN - ZSPRD^{30D}_{(2.7,1)}$	7	5	2	320.75	830.09	1603.75	1660.17	**-56.43**	-0.56	632.57	-1193.31	-0.14	-2.22	71.43	-8.04	0.97	0.39	-1193.31
H1.6	$KALMAN - ZSPRD^{30D}_{(2.7,0.5)}$	7	4	3	731.72	436.94	2926.88	1310.81	**1616.07**	16.16	1742.14	-912.5	0.19	3.02	57.14	230.83	2.23	1.67	-982.62
H2.1	$KALMAN - SPRD^{30D} - SMA_{(10,20)}$	14	5	9	921.72	715.59	4608.6	6440.3	**-1831.7**	-18.32	3175.97	-1410.62	-0.21	-3.33	35.71	-130.91	0.72	1.29	-5770.2
H2.2	$KALMAN - SPRD^{30D} - EMA_{(10,20)}$	19	6	13	2304.17	1145.25	13825.02	14888.25	**-1063.23**	-10.63	8538.22	-2681.58	-0.08	-1.27	31.58	-55.92	0.93	2.01	-10109.42
H2.3	$KALMAN - SPRD^{30D} - MACD_{(12,26,9)}$	27	13	14	887.01	953.32	11531.08	13346.51	**-1815.43**	-18.15	2944.39	-3265.78	-0.13	-2.06	48.15	-67.2	0.86	0.93	-6937.81
H2.4	$KALMAN - SPRD^{30D} - RSI_{(14)}$	3	2	1	4247.28	7838.11	8494.57	7838.11	**656.46**	6.56	4355.58	-7838.11	0.09	1.43	66.67	219.22	1.08	0.54	-7838.11
H2.5	$KALMAN - SPRD^{30D} - BB_{(20)}$	14	9	5	708.75	716.57	6378.72	3582.84	**2795.88**	27.96	2599.3	-1331.03	0.11	1.75	64.29	199.77	1.78	0.99	-1497.15
H3	$KALMAN - SPRD^{30D} - DECTREE$	322	144	178	98.06	97.13	14121.08	17289.63	**-3168.55**	-31.69	542.97	-822.93	-1.13	-17.94	44.72	-9.84	0.82	1.01	-3961.64
H4	$KALMAN - SPRD^{30D} - MLP$	183	76	107	131.13	105.22	9965.59	11258.74	**-1293.16**	-12.93	742.67	-1033.87	-0.82	-13.02	41.53	-7.07	0.89	1.25	-3514.95
Part IX: Models derived using the spread obtained from $RATIO - SPRD^{30D}$																			
I1.1	$RATIO - ZSPRD^{30D}_{(3,2)}$	7	3	4	314.92	358.02	944.76	1432.1	**-487.33**	-4.87	473.7	-584.89	-0.54	-8.57	42.86	-69.6	0.66	0.88	-662.42
I1.2	$RATIO - ZSPRD^{30D}_{(3,1)}$	6	3	3	281.81	328.97	845.44	986.91	**-141.47**	-1.41	473.7	-546.4	-0.45	-7.14	50	-23.58	0.86	0.86	-546.4
I1.3	$RATIO - ZSPRD^{30D}_{(3,0.5)}$	6	3	3	333.61	320.97	1000.82	962.91	**37.91**	0.38	631.69	-401.5	-0.35	-5.56	50	6.32	1.04	1.04	-561.41
I1.4	$RATIO - ZSPRD^{30D}_{(2.7,2)}$	10	5	5	226.84	376.26	1134.21	1881.3	**-747.09**	-7.47	473.7	-584.89	-0.62	-9.84	50	-74.71	0.6	0.6	-1111.62
I1.5	$RATIO - ZSPRD^{30D}_{(2.7,1)}$	9	4	5	238.16	332.99	952.65	1664.98	**-712.32**	-7.12	473.7	-673.04	-0.61	-9.68	44.44	-79.17	0.57	0.72	-1219.43
I1.6	$RATIO - ZSPRD^{30D}_{(2.7,0.5)}$	8	5	3	241.37	700.25	1206.86	2100.74	**-893.88**	-8.94	631.69	-1539.34	-0.4	-6.35	62.5	-111.74	0.57	0.34	-1539.34
I2.1	$RATIO - SPRD^{30D} - SMA_{(10,20)}$	15	6	9	563.09	293.2	3378.56	2638.77	**739.79**	7.4	1837.22	-688.58	-0.17	-2.7	40	49.32	1.28	1.92	-1684.01
I2.2	$RATIO - SPRD^{30D} - EMA_{(10,20)}$	20	8	12	786.55	183.08	6292.39	2196.98	**4095.41**	40.95	1882.7	-488.63	0.08	1.27	40	204.77	2.86	4.3	-1003.86
I2.3	$RATIO - SPRD^{30D} - MACD_{(12,26,9)}$	31	13	18	498.62	203.05	6482.03	3654.91	**2827.12**	28.27	1267.96	-548.25	-0.13	-2.06	41.94	91.23	1.77	2.46	-1970.71
I2.4	$RATIO - SPRD^{30D} - RSI_{(14)}$	5	3	2	633.17	2043.39	1899.5	4086.78	**-2187.27**	-21.87	1076.55	-3956.85	-0.29	-4.6	60	-437.45	0.46	0.31	-3956.85
I2.5	$RATIO - SPRD^{30D} - BB_{(20)}$	14	9	5	195.98	510.32	1763.78	2551.59	**-787.81**	-7.88	561.22	-1073.5	-0.45	-7.14	64.29	-56.24	0.69	0.38	-1518.5
I3	$RATIO - SPRD^{30D} - DECTREE$	322	122	200	108.4	68.97	13224.36	13794.35	**-569.99**	-5.7	706.84	-504.13	-1.21	-19.21	37.89	-1.77	0.96	1.57	-2333.28
I4	$RATIO - SPRD^{30D} - MLP$	280	113	167	107.22	85.77	12115.6	14323.98	**-2208.38**	-22.08	770.61	-728.55	-1.11	-17.62	40.36	-7.88	0.85	1.25	-3428.01
Part X: Models derived using the close price of IWF.N																			
CLS-SYM-1.1	$CLOSE^{IWF.N} - SMA_{(10,20)}$	12	6	6	356.71	189.67	2140.24	1138.02	**1002.23**	10.02	555.73	-253.08	0.02	0.32	50	83.52	1.88	1.88	-501.5
CLS-SYM-1.2	$CLOSE^{IWF.N} - EMA_{(10,20)}$	21	7	14	379.1	169.37	2653.72	2371.16	**282.56**	2.83	1556.82	-381.44	-0.15	-2.38	33.33	13.44	1.12	2.24	-1078.61
CLS-SYM-1.3	$CLOSE^{IWF.N} - MACD_{(12,26,9)}$	30	8	22	188.24	130.91	1505.94	2880.12	**-1374.18**	-13.74	760.82	-320.06	-0.61	-9.68	26.67	-45.8	0.52	1.44	-1432.72
CLS-SYM-1.4	$CLOSE^{IWF.N} - RSI_{(14)}$	6	2	4	490.13	759	980.26	3036	**-2055.74**	-20.56	767.73	-2215.65	-0.41	-6.51	33.33	-342.67	0.32	0.65	-2215.65
CLS-SYM-1.5	$CLOSE^{IWF.N} - BB_{(20)}$	12	7	5	112.1	284.97	784.69	1424.86	**-640.17**	-6.4	257.89	-668.35	-0.48	-7.62	58.33	-53.36	0.55	0.39	-1142.05
Part XI: Models derived using the close price of XLE.N																			
CLS-SYM-2.1	$CLOSE^{XLE.N} - SMA_{(10,20)}$	19	9	10	492.93	337.96	4436.4	3379.63	**1056.77**	10.57	1969.29	-993.26	-0.03	-0.48	47.37	55.63	1.31	1.46	-2390.02
CLS-SYM-2.2	$CLOSE^{XLE.N} - EMA_{(10,20)}$	26	11	15	546.32	161.14	6009.56	2417.09	**3592.47**	35.92	2197.81	-326.2	0.12	1.9	42.31	138.19	2.49	3.39	-711.67
CLS-SYM-2.3	$CLOSE^{XLE.N} - MACD_{(12,26,9)}$	27	10	17	637.2	211.29	6372.04	3591.96	**2780.08**	27.8	1931.38	-613.01	0.05	0.79	37.04	102.99	1.77	3.02	-645.92
CLS-SYM-2.4	$CLOSE^{XLE.N} - RSI_{(14)}$	5	3	2	314.75	1213.82	944.26	2427.64	**-1483.38**	-14.83	365.04	-1229.73	-0.44	-6.98	60	-296.68	0.39	0.26	-2062.6
CLS-SYM-2.5	$CLOSE^{XLE.N} - BB_{(20)}$	20	17	3	198.62	500.07	3376.55	1500.22	**1876.33**	18.76	822.47	-1185.85	0.05	0.79	85	93.82	2.25	0.4	-1185.85

Table D.2.5: This table presents the back-test metrics for the pair $IWF.N/XLE.N$ based on a 50-day rolling window. The table is subdivided into eleven parts, and in each of these parts, we present the back-test metrics and the trading strategies which use the spread derived from various models. In Part I, the spread is derived from the $DIST^{V1.1}$ model, in Part II from the $DIST^{V1.2}$ model, in Part III from the $DIST^{V2}$ model, in Part IV from the $DIST^{V3}$ model, in Part V from the $DIST^{V4}$ model, in Part VI from the $JOHANSEN-SPRD$ model, in Part VIII from the $ADF-SPRD$ model, in from the $DIST^{V2}$ model, in Part VIII from the $KALMAN-SPRD$ model, and in Part IX from the $RATIO-SPRD$ model. In Part X and XI, we present the back-test metrics of the trading strategies which use the close price of IWF.N, and XLE.N, respectively. All $ numbers reported below are in USD.

(I) Trading Strategy Code	(II) Model Name	(III) Total Number of Trades	(IV) Number of Winning Trades	(V) Number of Loosing Trades	(VI) Average Profit per Trade ($)	(VII) Average Loss per Trade ($)	(VIII) Gross Profit ($)	(IX) Gross Loss ($)	(X) Net Profit ($)	(XI) ROI (%)	(XII) Max P&L ($)	(XIII) Min P&L ($)	(XIV) Daily Sharpe Ratio	(XV) Annualized Sharpe Ratio	(XVI) Hit Ratio	(XVII) Expectancy	(XVIII) Profit Factor	(XIX) Realized Risk Reward Ratio	(XX) Max Drawdown ($)
	Part I: Models derived using the spread obtained from $DIST^{V1.1}-SPRD^{50D}$																		
A1.1	$DIST^{V1.1}-ZSPRD^{50D}_{(3,2)}$	3	1	2	251.16	150.17	251.16	300.34	**-49.17**	-0.49	251.16	-164.49	-0.73	-11.59	33.33	-16.4	0.84	1.67	-300.34
A1.2	$DIST^{V1.1}-ZSPRD^{50D}_{(3,1)}$	2	-	2	-	184.65	-	369.3	**-369.3**	-3.69	-	-319.66	-1.76	-27.94	-	-184.65	-	-	-369.29
A1.3	$DIST^{V1.1}-ZSPRD^{50D}_{(3,0.5)}$	2	-	2	-	339.37	-	678.74	**-678.74**	-6.79	-	-565.11	-1.54	-24.45	-	-339.37	-	-	-678.74
A1.4	$DIST^{V1.1}-ZSPRD^{50D}_{(2.7,2)}$	3	2	1	370.84	164.49	741.69	164.49	**577.2**	5.77	623.98	-164.49	0.1	1.59	66.67	192.42	4.51	2.25	-164.49
A1.5	$DIST^{V1.1}-ZSPRD^{50D}_{(2.7,1)}$	2	-	2	-	58.75	-	117.5	**-117.5**	-1.17	-	-67.86	-16.35	-259.55	-	-58.75	-	-	-117.5
A1.6	$DIST^{V1.1}-ZSPRD^{50D}_{(2.7,0.5)}$	2	-	2	-	219.87	-	439.74	**-439.74**	-4.4	-	-326.11	-2.48	-39.37	-	-219.87	-	-	-439.74
A2.1	$DIST^{V1.1}-SPRD^{50D}-SMA_{(10,20)}$	10	4	6	168.35	911.79	673.38	5470.77	**-4797.39**	-47.97	377.05	-1545.23	-0.87	-13.81	40	-479.74	0.12	0.18	-5026.8
A2.2	$DIST^{V1.1}-SPRD^{50D}-EMA_{(10,20)}$	23	15	8	378.82	711.93	5682.29	5695.47	**-13.18**	-0.13	1055.98	-1756.39	-0.22	-3.49	65.22	-0.54	1	0.53	-2401.89
A2.3	$DIST^{V1.1}-SPRD^{50D}-MACD_{(12,26,9)}$	40	27	13	282.19	254.01	7619.14	3302.19	**4316.95**	43.17	735.56	-766.66	-0.13	-2.06	67.5	107.92	2.31	1.11	-1067.68
A2.4	$DIST^{V1.1}-SPRD^{50D}-RSI_{(14)}$	6	3	3	1474.62	653.95	4423.86	1961.85	**2462.01**	24.62	4124.57	-1083.69	0.14	2.22	50	410.34	2.25	2.25	-1884.62
A2.5	$DIST^{V1.1}-SPRD^{50D}-BB_{(20)}$	15	7	8	545.7	244.97	3819.9	1959.77	**1860.12**	18.6	1007.29	-1121.7	-0.05	-0.79	46.67	124.03	1.95	2.23	-1121.7
A3	$DIST^{V1.1}-SPRD^{50D}-DECTREE$	340	153	187	114.43	76.9	17507.41	14379.78	**3127.64**	31.28	585.71	-890.7	-1	-15.87	45	9.2	1.22	1.49	-2134.27
A4	$DIST^{V1.1}-SPRD^{50D}-MLP$	306	135	171	110.92	86.84	14974.4	14849.42	**124.98**	1.25	571.7	-890.7	-1.05	-16.67	44.12	0.41	1.01	1.28	-2506.82
	Part II: Models derived using the spread obtained from $DIST^{V1.2}-SPRD^{50D}$																		
B1.1	$DIST^{V1.2}-ZSPRD^{50D}_{(3,2)}$	8	5	3	155.21	161.92	776.03	485.77	**290.26**	2.9	247.6	-283.85	-0.62	-9.84	62.5	36.28	1.6	0.96	-396.06
B1.2	$DIST^{V1.2}-ZSPRD^{50D}_{(3,1)}$	8	3	5	651.82	502.54	1955.45	2512.69	**-557.24**	-5.57	875.82	-1159.04	-0.31	-4.92	37.5	-69.65	0.78	1.3	-1231.76
B1.3	$DIST^{V1.2}-ZSPRD^{50D}_{(3,0.5)}$	6	2	4	503.5	718.7	1006.99	2874.8	**-1867.81**	-18.68	802.46	-1075.55	-0.63	-10	33.33	-311.34	0.35	0.7	-1867.81
B1.4	$DIST^{V1.2}-ZSPRD^{50D}_{(2.7,2)}$	11	7	4	264.27	210.66	1849.89	842.64	**1007.25**	10.07	1006	-356.88	-0.17	-2.7	63.64	91.59	2.2	1.25	-396.06
B1.5	$DIST^{V1.2}-ZSPRD^{50D}_{(2.7,1)}$	10	5	5	724.64	502.54	3623.21	2512.69	**1110.52**	11.11	1006	-1159.04	-0.06	-0.95	50	111.05	1.44	1.44	-1159.04
B1.6	$DIST^{V1.2}-ZSPRD^{50D}_{(2.7,0.5)}$	8	4	4	534.62	718.7	2138.46	2874.8	**-736.34**	-7.36	1006	-1075.55	-0.31	-4.92	50	-92.04	0.74	0.74	-1075.55
B2.1	$DIST^{V1.2}-SPRD^{50D}-SMA_{(10,20)}$	11	5	6	361.92	582.27	1809.61	3493.6	**-1683.99**	-16.84	559.42	-1544.84	-0.45	-7.14	45.45	-153.13	0.52	0.62	-2800.23
B2.2	$DIST^{V1.2}-SPRD^{50D}-EMA_{(10,20)}$	16	10	6	544.35	729.64	5443.54	4377.83	**1065.71**	10.66	1276.86	-1445.23	-0.11	-1.75	62.5	66.61	1.24	0.75	-3056.42
B2.3	$DIST^{V1.2}-SPRD^{50D}-MACD_{(12,26,9)}$	26	15	11	287.05	218.71	4305.7	2405.79	**1899.92**	19	623.18	-814.67	-0.22	-3.49	57.69	73.06	1.79	1.31	-887.77
B2.4	$DIST^{V1.2}-SPRD^{50D}-RSI_{(14)}$	9	5	4	740.34	935.41	3701.71	3741.66	**-39.95**	-0.4	1262	-1284.67	-0.17	-2.7	55.56	-4.36	0.99	0.79	-2180.26
B2.5	$DIST^{V1.2}-SPRD^{50D}-BB_{(20)}$	13	6	7	331.78	390.35	1990.66	2732.44	**-741.78**	-7.42	749	-617.27	-0.49	-7.78	46.15	-57.09	0.73	0.85	-1112.83
B3	$DIST^{V1.2}-SPRD^{50D}-DECTREE$	239	122	117	100.67	101.19	12281.57	11838.81	**442.76**	4.43	631.69	-1521.9	-0.87	-13.81	51.05	1.86	1.04	0.99	-2091.98
B4	$DIST^{V1.2}-SPRD^{50D}-MLP$	239	123	116	107.05	103.62	13166.87	12019.77	**1147.1**	11.47	700.48	-433.74	-0.96	-15.24	51.46	4.79	1.1	1.03	-2269.6
	Part III: Models derived using the spread obtained from $DIST^{V2}-SPRD^{50D}$																		
C1.1	$DIST^{V2}-ZSPRD^{50D}_{(3,2)}$	3	2	1	150.17	251.16	300.34	251.16	**49.17**	0.49	164.49	-251.16	-0.58	-9.21	66.67	16.4	1.2	0.6	-251.16
C1.2	$DIST^{V2}-ZSPRD^{50D}_{(3,1)}$	2	2	-	184.65	-	369.3	-	**369.3**	3.69	319.66	-	0.17	2.7	100	184.65	369.3	184.65	-
C1.3	$DIST^{V2}-ZSPRD^{50D}_{(3,0.5)}$	2	2	-	339.37	-	678.74	-	**678.74**	6.79	565.11	-	0.59	9.37	100	339.37	678.74	339.37	-
C1.4	$DIST^{V2}-ZSPRD^{50D}_{(2.7,2)}$	3	1	2	164.49	370.84	164.49	741.69	**-577.2**	-5.77	164.49	-623.98	-0.86	-13.65	33.33	-192.42	0.22	0.44	-623.98
C1.5	$DIST^{V2}-ZSPRD^{50D}_{(2.7,1)}$	2	2	-	58.75	-	117.5	-	**117.5**	1.17	67.86	-	-7.24	-114.93	100	58.75	117.5	58.75	-
C1.6	$DIST^{V2}-ZSPRD^{50D}_{(2.7,0.5)}$	2	2	-	219.87	-	439.74	-	**439.74**	4.4	326.11	-	0.45	7.14	100	219.87	439.74	219.87	-
C2.1	$DIST^{V2}-SPRD^{50D}-SMA_{(10,20)}$	10	7	3	867.17	166.9	6070.2	500.7	**5569.5**	55.7	1545.23	-377.05	0.59	9.37	70	556.95	12.12	5.2	-377.05
C2.2	$DIST^{V2}-SPRD^{50D}-EMA_{(10,20)}$	23	8	15	711.93	378.82	5695.47	5682.29	**13.18**	0.13	1756.39	-1055.98	-0.22	-3.49	34.78	0.54	1	1.88	-3541.35
C2.3	$DIST^{V2}-SPRD^{50D}-MACD_{(12,26,9)}$	40	13	27	254.01	282.19	3302.19	7619.14	**-4316.95**	-43.17	766.66	-735.56	-0.77	-12.22	32.5	-107.92	0.43	0.9	-4942.15
C2.4	$DIST^{V2}-SPRD^{50D}-RSI_{(14)}$	6	3	3	653.95	1474.62	1961.85	4423.86	**-2462.01**	-24.62	1083.69	-4124.57	-0.3	-4.76	50	-410.34	0.44	0.44	-4124.57
C2.5	$DIST^{V2}-SPRD^{50D}-BB_{(20)}$	15	8	7	244.97	545.7	1959.77	3819.9	**-1860.12**	-18.6	1121.7	-1007.29	-0.51	-8.1	53.33	-124.03	0.51	0.45	-1992.14
C3	$DIST^{V2}-SPRD^{50D}-DECTREE$	350	151	199	107.37	83.23	16212.68	16562.75	**-350.08**	-3.5	571.7	-890.7	-1.09	-17.3	43.14	-1.01	0.98	1.29	-2126.06
C4	$DIST^{V2}-SPRD^{50D}-MLP$	302	137	165	106.34	92.18	14569.05	15209.16	**-640.11**	-6.4	631.69	-890.7	-1.03	-16.35	45.36	-2.13	0.96	1.15	-3612.53
	Part IV: Models derived using the spread obtained from $DIST^{V3}-SPRD^{50D}$																		
D1.1	$DIST^{V3}-ZSPRD^{50D}_{(3,2)}$	8	4	4	171.59	306.25	686.37	1225.01	**-538.64**	-5.39	234.51	-582.03	-0.67	-10.64	50	-67.33	0.56	0.56	-1143.71
D1.2	$DIST^{V3}-ZSPRD^{50D}_{(3,1)}$	6	3	3	464.91	398.35	1394.74	1195.05	**199.69**	2	536.33	-727.18	-0.23	-3.65	50	33.28	1.17	1.17	-1141.23
D1.3	$DIST^{V3}-ZSPRD^{50D}_{(3,0.5)}$	6	4	2	351.15	460.22	1404.61	920.44	**484.16**	4.84	535.21	-670.05	-0.15	-2.38	66.67	80.72	1.53	0.76	-920.44
D1.4	$DIST^{V3}-ZSPRD^{50D}_{(2.7,2)}$	13	6	7	182.09	295.34	1092.52	2067.38	**-974.86**	-9.75	288.94	-768.24	-0.7	-11.11	46.15	-75.01	0.53	0.62	-1350.26
D1.5	$DIST^{V3}-ZSPRD^{50D}_{(2.7,1)}$	9	3	6	322.08	317.07	966.25	1902.43	**-936.18**	-9.36	473.7	-782.94	-0.65	-10.32	33.33	-104.04	0.51	1.02	-1360.68
D1.6	$DIST^{V3}-ZSPRD^{50D}_{(2.7,0.5)}$	9	4	5	276.22	407.59	1104.88	2037.94	**-933.05**	-9.33	473.7	-726.76	-0.61	-9.68	44.44	-103.7	0.54	0.68	-1510.88
D2.1	$DIST^{V3}-SPRD^{50D}-SMA_{(10,20)}$	17	9	8	519.98	250.76	4679.78	2006.06	**2673.72**	26.74	1936.61	-535.03	0.01	0.16	52.94	157.27	2.33	2.07	-647.91
D2.2	$DIST^{V3}-SPRD^{50D}-EMA_{(10,20)}$	35	13	22	470.37	314.6	6114.85	6921.25	**-806.39**	-8.06	1455.29	-1501.74	-0.32	-5.08	37.14	-23.06	0.88	1.5	-3188.62
D2.3	$DIST^{V3}-SPRD^{50D}-MACD_{(12,26,9)}$	34	14	20	454.72	239.68	6366.13	4793.64	**1572.5**	15.72	1336.24	-1356.61	-0.21	-3.33	41.18	46.27	1.33	1.9	-2602.19
D2.4	$DIST^{V3}-SPRD^{50D}-RSI_{(14)}$	5	2	3	880.78	1557.06	1761.55	4671.18	**-2909.62**	-29.1	1171.42	-2525.26	-0.46	-7.3	40	-581.93	0.38	0.57	-3242.48
D2.5	$DIST^{V3}-SPRD^{50D}-BB_{(20)}$	18	12	6	255.12	477.69	3061.42	2866.16	**195.26**	1.95	1195.01	-993.18	-0.29	-4.6	66.67	10.87	1.07	0.53	-1856.68
D3	$DIST^{V3}-SPRD^{50D}-DECTREE$	315	132	183	115.47	84.54	15241.71	15470.54	**-228.83**	-2.29	604.61	-997.97	-1.04	-16.51	41.9	-0.74	0.99	1.37	-2357.54
D4	$DIST^{V3}-SPRD^{50D}-MLP$	107	41	66	155.6	152.5	6379.64	10065.21	**-3685.57**	-36.86	1057.92	-895.17	-0.72	-11.43	38.32	-34.44	0.63	1.02	-6073.31
	Part V: Models derived using the spread obtained from $DIST^{V4}-SPRD^{50D}$																		
E1.1	$DIST^{V4}-ZSPRD^{50D}_{(3,2)}$	8	4	4	171.59	306.25	686.37	1225.01	**-538.64**	-5.39	234.51	-582.03	-0.67	-10.64	50	-67.33	0.56	0.56	-1143.71
E1.2	$DIST^{V4}-ZSPRD^{50D}_{(3,1)}$	6	3	3	464.91	398.35	1394.74	1195.05	**199.69**	2	536.33	-727.18	-0.23	-3.65	50	33.28	1.17	1.17	-1141.23
E1.3	$DIST^{V4}-ZSPRD^{50D}_{(3,0.5)}$	6	4	2	351.15	460.22	1404.61	920.44	**484.16**	4.84	535.21	-670.05	-0.15	-2.38	66.67	80.72	1.53	0.76	-920.44
E1.4	$DIST^{V4}-ZSPRD^{50D}_{(2.7,2)}$	13	6	7	182.09	295.34	1092.52	2067.38	**-974.86**	-9.75	288.94	-768.24	-0.7	-11.11	46.15	-75.01	0.53	0.62	-1350.26
E1.5	$DIST^{V4}-ZSPRD^{50D}_{(2.7,1)}$	9	3	6	322.08	317.07	966.25	1902.43	**-936.18**	-9.36	473.7	-782.94	-0.65	-10.32	33.33	-104.04	0.51	1.02	-1360.68
E1.6	$DIST^{V4}-ZSPRD^{50D}_{(2.7,0.5)}$	9	4	5	276.22	407.59	1104.88	2037.94	**-933.05**	-9.33	473.7	-726.76	-0.61	-9.68	44.44	-103.7	0.54	0.68	-1510.88
E2.1	$DIST^{V4}-SPRD^{50D}-SMA_{(10,20)}$	17	9	8	519.98	250.76	4679.78	2006.06	**2673.72**	26.74	1936.61	-535.03	0.01	0.16	52.94	157.27	2.33	2.07	-647.91
E2.2	$DIST^{V4}-SPRD^{50D}-EMA_{(10,20)}$	35	13	22	470.37	314.6	6114.85	6921.25	**-806.39**	-8.06	1455.29	-1501.74	-0.32	-5.08	37.14	-23.06	0.88	1.5	-3188.62
E2.3	$DIST^{V4}-SPRD^{50D}-MACD_{(12,26,9)}$	34	14	20	454.72	239.68	6366.13	4793.64	**1572.5**	15.72	1336.24	-1356.61	-0.21	-3.33	41.18	46.27	1.33	1.9	-2602.19
E2.4	$DIST^{V4}-SPRD^{50D}-RSI_{(14)}$	5	2	3	880.78	1557.06	1761.55	4671.18	**-2909.62**	-29.1	1171.42	-2525.26	-0.46	-7.3	40	-581.93	0.38	0.57	-3242.48
E2.5	$DIST^{V4}-SPRD^{50D}-BB_{(20)}$	18	12	6	255.12	477.69	3061.42	2866.16	**195.26**	1.95	1195.01	-993.18	-0.29	-4.6	66.67	10.87	1.07	0.53	-1856.68
E3	$DIST^{V4}-SPRD^{50D}-DECTREE$	299	130	169	116.71	86.83	15171.68	14673.86	**497.83**	4.98	604.61	-1157.69	-0.96	-15.24	43.48	1.67	1.03	1.34	-2127.32
E4	$DIST^{V4}-SPRD^{50D}-MLP$	107	41	66	155.6	152.5	6379.64	10065.21	**-3685.57**	-36.86	1057.92	-895.17	-0.72	-11.43	38.32	-34.44	0.63	1.02	-6073.31
	Part VI: Models derived using the spread obtained from $JOHANSEN-SPRD^{50D}$																		
F1.1	$JOHANSEN-ZSPRD^{50D}_{(3,2)}$	18	9	9	109.43	60.02	984.9	540.18	**444.72**	4.45	364.47	-160.33	-0.28	-4.44	50	24.71	1.82	1.82	-250.88
F1.2	$JOHANSEN-ZSPRD^{50D}_{(3,1)}$	15	7	8	167.59	73.04	1173.16	584.33	**588.83**	5.89	364.47	-160.33	-0.23	-3.65	46.67	39.26	2.01	2.29	-332.09
F1.3	$JOHANSEN-ZSPRD^{50D}_{(3,0.5)}$	14	6	8	221.77	66.45	1330.62	531.59	**799.03**	7.99	454.91	-131.79	-0.16	-2.54	42.86	57.08	2.5	3.34	-279.35
F1.4	$JOHANSEN-ZSPRD^{50D}_{(2.7,2)}$	21	10	11	158.37	233.13	1583.66	2564.43	**-980.77**	-9.81	1082.11	-1967.62	-0.28	-4.44	47.62	-46.7	0.62	0.68	-2158.54
F1.5	$JOHANSEN-ZSPRD^{50D}_{(2.7,1)}$	18	8	10	233.38	274.59	1867.07	2745.86	**-878.79**	-8.79	1082.11	-1967.62	-0.4	-6.35	44.44	-48.84	0.68	0.85	-2161.52
F1.6	$JOHANSEN-ZSPRD^{50D}_{(2.7,0.5)}$	17	7	10	294.44	252.69	2061.06	2526.87	**-465.81**	-4.66	1082.11	-1967.62	-0.44	-6.98	41.18	-27.38	0.82	1.17	-1995.28
F2.1	$JOHANSEN-SPRD^{50D}-SMA_{(10,20)}$	20	10	10	618.31	1254.93	6183.09	12549.32	**-6366.23**	-63.66	3047.85	-8147.9	-0.11	-1.75	50	-318.31	0.49	0.49	-9870.3
F2.2	$JOHANSEN-SPRD^{50D}-EMA_{(10,20)}$	26	9	17	4532.07	309.69	40788.64	5264.68	**35523.96**	355.24	34416.23	-2188.41	0.22	3.49	34.62	1366.53	7.75	14.63	-2750.65
F2.3	$JOHANSEN-SPRD^{50D}-MACD_{(12,26,9)}$	34	10	24	1410.5	1342.77	14105.03	32226.46	**-18121.42**	-181.21	5965.43	-27871.68	-0.05	-0.79	29.41	-533.03	0.44	1.05	-30786.44
F2.4	$JOHANSEN-SPRD^{50D}-RSI_{(14)}$	7	4	3	395.36	685.54	1581.43	2056.61	**-475.18**	-4.75	924.7	-1424.88	-0.3	-4.76	57.14	-67.91	0.77	0.58	-1470.3
F2.5	$JOHANSEN-SPRD^{50D}-BB_{(20)}$	18	6	12	216.08	947.86	1296.47	11374.3	**-10077.83**	-100.78	502.93	-7271.21	-0.27	-4.29	33.33	-559.92	0.11	0.23	-10617.07
F3	$JOHANSEN-SPRD^{50D}-DECTREE$	327	174	153	103.51	100.73	18011.32	15411.13	**2600.19**	26	690.46	-890.7	-0.93	-14.76	53.21	7.95	1.17	1.03	-2787.58
F4	$JOHANSEN-SPRD^{50D}-MLP$	211	117	94	129.31	104.88	15128.93	9858.37	**5270.56**	52.71	821.29	-421.38	-0.75	-11.91	55.45	24.98	1.53	1.23	-1104.89
	Part VII: Models derived using the spread obtained from $ADF-SPRD^{50D}$																		
G1.1	$ADF-ZSPRD^{50D}_{(3,2)}$	4	1	3	226.74	1197.21	226.74	3591.63	**-3364.89**	-33.65	226.74	-1937.61	-0.91	-14.45	25	-841.22	0.06	0.19	-3364.89
G1.2	$ADF-ZSPRD^{50D}_{(3,1)}$	4	1	3	2997.93	2391.3	2997.93	7173.9	**-4175.97**	-41.76	2997.93	-3385.06	-0.17	-2.7	25	-1043.99	0.42	1.25	-4175.97
G1.3	$ADF-ZSPRD^{50D}_{(3,0.5)}$	4	1	3	4499.45	2610.14	4499.45	7830.43	**-3330.98**	-33.31	4499.45	-3986.09	-0.04	-0.63	25	-832.74	0.57	1.72	-4946.02
G1.4	$ADF-ZSPRD^{50D}_{(2.7,2)}$	9	2	7	1518.91	1673.85	3037.82	11716.97	**-8679.15**	-86.79	2200.87	-4344.98	-0.49	-7.78	22.22	-964.42	0.26	0.91	-8679.15
G1.5	$ADF-ZSPRD^{50D}_{(2.7,1)}$	7	3	4	3097.13	3414.18	9291.38	13656.72	**-4365.33**	-43.65	5624.01	-6793.04	-0.1	-1.59	42.86	-623.43	0.68	0.91	-10216.84
G1.6	$ADF-ZSPRD^{50D}_{(2.7,0.5)}$	7	3	4	3285.21	3579.98	9855.63	14319.91	**-4464.28**	-44.64	4840.21	-6793.04	-0.07	-1.11	42.86	-637.56	0.69	0.92	-9677.45
G2.1	$ADF-SPRD^{50D}-SMA_{(10,20)}$	17	9	8	14791.94	4776.78	133127.43	38214.21	**94913.22**	949.13	123127.22	-26941.5	0.18	2.86	52.94	5582.9	3.48	3.1	-28807.82
G2.2	$ADF-SPRD^{50D}-EMA_{(10,20)}$	40	23	17	2339.57	3879.64	53810.2	65953.91	**-12143.71**	-121.44	38773.83	-22910.02	-0.05	-0.79	57.5	-303.59	0.82	0.6	-34142.02
G2.3	$ADF-SPRD^{50D}-MACD_{(12,26,9)}$	32	22	10	645.14	1817.89	14193.17	18178.91	**-3985.74**	-39.86	3683.72	-9944.39	-0.11	-1.75	68.75	-124.55	0.78	0.35	-10144.87
G2.4	$ADF-SPRD^{50D}-RSI_{(14)}$	6	1	5	951.5	6035.22	951.5	30176.12	**-29224.62**	-292.25	951.5	-20125.84	-0.61	-9.68	16.67	-4870.54	0.03	0.16	-30176.12
G2.5	$ADF-SPRD^{50D}-BB_{(20)}$	17	4	13	7621.67	1836.54	30486.7	23875.03	**6611.66**	66.12	15268.11	-14458.37	0.07	1.11	23.53	388.98	1.28	4.15	-19631.48
G3	$ADF-SPRD^{50D}-DECTREE$	342	142	200	94.75	92.19	13455.15	18437.69	**-4982.54**	-49.83	572.24	-622.13	-1.22	-19.37	41.52	-14.57	0.73	1.03	-5421.5
G4	$ADF-SPRD^{50D}-MLP$	147	69	78	123.18	135.39	8499.67	10560.46	**-2060.79**	-20.61	1006.54	-826.78	-0.81	-12.86	46.94	-14.02	0.8	0.91	-4603.24
	Part VIII: Models derived using the spread obtained from $KALMAN-SPRD^{50D}$																		
H1.1	$KALMAN-ZSPRD^{50D}_{(3,2)}$	3	3	-	368.95	-	1106.84	-	**1106.84**	11.07	425.64	-	3.59	56.99	100	368.95	1106.84	368.95	-
H1.2	$KALMAN-ZSPRD^{50D}_{(3,1)}$	1	-	1	-	343.56	-	343.56	**-343.56**	-3.44	-	-343.56	-	-	-	-343.56	-	-	-343.56
H1.3	$KALMAN-ZSPRD^{50D}_{(3,0.5)}$	1	1	-	11.48	-	11.48	-	**11.48**	0.11	11.48	-	-	-	100	11.48	11.48	11.48	-
H1.4	$KALMAN-ZSPRD^{50D}_{(2.7,2)}$	4	2	2	237.76	583.37	475.52	1166.73	**-691.21**	-6.91	396.78	-1006.13	-0.44	-6.98	50	-172.8	0.41	0.41	-1166.73
H1.5	$KALMAN-ZSPRD^{50D}_{(2.7,1)}$	2	-	2	-	321.08	-	642.16	**-642.16**	-6.42	-	-343.56	-14.1	-223.83	-	-321.08	-	-	-642.16
H1.6	$KALMAN-ZSPRD^{50D}_{(2.7,0.5)}$	2	2	-	12.67	-	25.34	-	**25.34**	0.25	13.86	-	-44.06	-699.43	100	12.67	25.34	12.67	-
H2.1	$KALMAN-SPRD^{50D}-SMA_{(10,20)}$	14	8	6	1984.17	1464.27	15873.36	8785.62	**7087.75**	70.88	5308.74	-2299.32	0.17	2.7	57.14	506.17	1.81	1.36	-5622.63
H2.2	$KALMAN-SPRD^{50D}-EMA_{(10,20)}$	21	6	15	2459.15	917.49	14754.9	13762.28	**992.61**	9.93	8190.64	-2401.53	-0.03	-0.48	28.57	47.22	1.07	2.68	-7731.56
H2.3	$KALMAN-SPRD^{50D}-MACD_{(12,26,9)}$	30	12	18	849.6	679.17	10195.15	12225.03	**-2029.88**	-20.3	2444.04	-2962.07	-0.16	-2.54	40	-67.66	0.83	1.25	-6925.73
H2.4	$KALMAN-SPRD^{50D}-RSI_{(14)}$	3	2	1	3034.8	8389.35	6069.61	8389.35	**-2319.74**	-23.2	3346	-8389.35	-0.07	-1.11	66.67	-772.87	0.72	0.36	-8389.35
H2.5	$KALMAN-SPRD^{50D}-BB_{(20)}$	18	13	5	982.27	1108.61	12769.56	5543.03	**7226.53**	72.27	2805.47	-4689.56	0.21	3.33	72.22	401.43	2.3	0.89	-4689.56
H3	$KALMAN-SPRD^{50D}-DECTREE$	346	151	195	109.36	83.18	16513.72	16220.29	**293.43**	2.93	906.91	-890.7	-1.03	-16.35	43.64	0.84	1.02	1.31	-2661.24
H4	$KALMAN-SPRD^{50D}-MLP$	278	117	161	125.98	88.32	14739.33	14219.96	**519.37**	5.19	633.2	-367.39	-1.01	-16.03	42.09	1.88	1.04	1.43	-2323.54
	Part IX: Models derived using the spread obtained from $RATIO-SPRD^{50D}$																		
I1.1	$RATIO-ZSPRD^{50D}_{(3,2)}$	5	1	4	367.51	426.54	367.51	1706.18	**-1338.66**	-13.39	367.51	-673.44	-0.98	-15.56	20	-267.73	0.22	0.86	-1338.66
I1.2	$RATIO-ZSPRD^{50D}_{(3,1)}$	4	2	2	273.66	282.35	547.31	564.7	**-17.38**	-0.17	536.33	-401.5	-0.39	-6.19	50	-4.35	0.97	0.97	-401.5
I1.3	$RATIO-ZSPRD^{50D}_{(3,0.5)}$	4	-	4	-	356.92	-	1427.67	**-1427.67**	-14.28	-	-883.99	-1.33	-21.11	-	-356.92	-	-	-1427.67
I1.4	$RATIO-ZSPRD^{50D}_{(2.7,2)}$	9	3	6	58.41	379.06	175.24	2274.35	**-2099.11**	-20.99	90.46	-792.02	-1.21	-19.21	33.33	-233.25	0.08	0.15	-2099.11
I1.5	$RATIO-ZSPRD^{50D}_{(2.7,1)}$	7	4	3	93.94	518.53	375.76	1555.6	**-1179.84**	-11.8	186.68	-1363.51	-0.59	-9.37	57.14	-168.57	0.24	0.18	-1363.51
I1.6	$RATIO-ZSPRD^{50D}_{(2.7,0.5)}$	7	2	5	76.64	577.77	153.29	2888.87	**-2735.58**	-27.36	113.5	-1496.57	-0.83	-13.18	28.57	-390.81	0.05	0.13	-2770.06
I2.1	$RATIO-SPRD^{50D}-SMA_{(10,20)}$	15	5	10	610.85	268.81	3054.25	2688.08	**366.16**	3.66	1837.22	-688.58	-0.21	-3.33	33.33	24.38	1.14	2.27	-1684.01
I2.2	$RATIO-SPRD^{50D}-EMA_{(10,20)}$	20	8	12	786.55	193.24	6292.39	2318.92	**3973.47**	39.73	1882.7	-488.63	0.07	1.11	40	198.67	2.71	4.07	-1003.86
I2.3	$RATIO-SPRD^{50D}-MACD_{(12,26,9)}$	28	12	16	548.57	251.51	6582.86	4024.16	**2558.7**	25.59	1267.96	-632.86	-0.12	-1.9	42.86	91.41	1.64	2.18	-1970.71
I2.4	$RATIO-SPRD^{50D}-RSI_{(14)}$	6	4	2	495.71	2100.09	1982.85	4200.19	**-2217.34**	-22.17	1076.55	-3956.85	-0.29	-4.6	66.67	-369.47	0.47	0.24	-3956.85
I2.5	$RATIO-SPRD^{50D}-BB_{(20)}$	13	8	5	208.83	510.32	1670.63	2551.59	**-880.96**	-8.81	561.22	-1073.5	-0.46	-7.3	61.54	-67.75	0.65	0.41	-1518.5
I3	$RATIO-SPRD^{50D}-DECTREE$	273	113	160	101.62	70.39	11483	11262.89	**220.11**	2.2	770.61	-504.13	-1.23	-19.53	41.39	0.8	1.02	1.44	-2512.23
I4	$RATIO-SPRD^{50D}-MLP$	34	14	20	143.59	129.95	2010.33	2599.06	**-588.73**	-5.89	590.25	-761.39	-0.8	-12.7	41.18	-17.31	0.77	1.1	-1654.09
	Part X: Models derived using the close price of IWF.N																		
CLS-SYM-1.1	$CLOSE^{IWF.N}-SMA_{(10,20)}$	12	6	6	356.71	189.67	2140.24	1138.02	**1002.23**	10.02	555.73	-253.08	0.02	0.32	50	83.52	1.88	1.88	-501.5
CLS-SYM-1.2	$CLOSE^{IWF.N}-EMA_{(10,20)}$	21	7	14	379.1	169.37	2653.72	2371.16	**282.56**	2.83	1556.82	-381.44	-0.15	-2.38	33.33	13.44	1.12	2.24	-1078.61
CLS-SYM-1.3	$CLOSE^{IWF.N}-MACD_{(12,26,9)}$	30	8	22	188.24	130.91	1505.94	2880.12	**-1374.18**	-13.74	760.82	-320.06	-0.61	-9.68	26.67	-45.8	0.52	1.44	-1432.72
CLS-SYM-1.4	$CLOSE^{IWF.N}-RSI_{(14)}$	6	2	4	490.13	759	980.26	3036	**-2055.74**	-20.56	767.73	-2215.65	-0.41	-6.51	33.33	-342.67	0.32	0.65	-2215.65
CLS-SYM-1.5	$CLOSE^{IWF.N}-BB_{(20)}$	12	7	5	112.1	284.97	784.69	1424.86	**-640.17**	-6.4	257.89	-668.35	-0.48	-7.62	58.33	-53.36	0.55	0.39	-1142.05
	Part XI: Models derived using the close price of XLE.N																		
CLS-SYM-2.1	$CLOSE^{XLE.N}-SMA_{(10,20)}$	19	9	10	492.93	337.96	4436.4	3379.63	**1056.77**	10.57	1969.29	-993.26	-0.03	-0.48	47.37	55.63	1.31	1.46	-2390.02
CLS-SYM-2.2	$CLOSE^{XLE.N}-EMA_{(10,20)}$	26	11	15	546.32	161.14	6009.56	2417.09	**3592.47**	35.92	2197.81	-326.2	0.12	1.9	42.31	138.19	2.49	3.39	-711.67
CLS-SYM-2.3	$CLOSE^{XLE.N}-MACD_{(12,26,9)}$	27	10	17	637.2	211.29	6372.04	3591.96	**2780.08**	27.8	1931.38	-613.01	0.05	0.79	37.04	102.99	1.77	3.02	-645.92
CLS-SYM-2.4	$CLOSE^{XLE.N}-RSI_{(14)}$	5	3	2	314.75	1213.82	944.26	2427.64	**-1483.38**	-14.83	365.04	-1229.73	-0.44	-6.98	60	-296.68	0.39	0.26	-2062.6
CLS-SYM-2.5	$CLOSE^{XLE.N}-BB_{(20)}$	20	17	3	198.62	500.07	3376.55	1500.22	**1876.33**	18.76	822.47	-1185.85	0.05	0.79	85	93.82	2.25	0.4	-1185.85

Table D.2.6: This table presents the back-test metrics for the pair $IWF.N/XLE.N$ based on a 100-day rolling window. The table is subdivided into eleven parts, and in each of these parts, we present the back-test metrics and the trading strategies which use the spread derived from various models. In Part I, the spread is derived from the $DIST^{V1.1}$ model, in Part II from the $DIST^{V1.2}$ model, in Part III from the $DIST^{V2}$ model, in Part IV from the $DIST^{V3}$ model, in Part V from the $DIST^{V4}$ model, in Part VI from the $JOHANSEN-SPRD$ model, in Part VIII from the $ADF-SPRD$ model, in from the $DIST^{V2}$ model, in Part VIII from the $KALMAN-SPRD$ model, and in Part IX from the $RATIO-SPRD$ model. In Part X and XI, we present the back-test metrics of the trading strategies which use the close price of IWF.N, and XLE.N, respectively. All $ numbers reported below are in USD.

(I) Trading Strategy Code	(II) Model Name	(III) Total Number of Trades	(IV) Number of Winning Trades	(V) Number of Loosing Trades	(VI) Average Profit per Trade ($)	(VII) Average Loss per Trade ($)	(VIII) Gross Profit ($)	(IX) Gross Loss ($)	(X) Net Profit ($)	(XI) ROI (%)	(XII) Max P&L ($)	(XIII) Min P&L ($)	(XIV) Daily Sharpe Ratio	(XV) Annualized Sharpe Ratio	(XVI) Hit Ratio	(XVII) Expectancy	(XVIII) Profit Factor	(XIX) Realized Risk Reward Ratio	(XX) Max Drawdown ($)
	Part I: Models derived using the spread obtained from $DIST^{V1.1}-SPRD^{100D}$																		
A1.1	$DIST^{V1.1}-ZSPRD^{100D}_{(3,2)}$	1	-	1	-	80.32	-	80.32	**-80.32**	-0.8	-	-80.32	-	-	-	-80.32	-	-	-80.32
A1.2	$DIST^{V1.1}-ZSPRD^{100D}_{(3,1)}$	1	1	-	1073.26	-	1073.26	-	**1073.26**	10.73	1073.26	-	-	-	100	1073.26	1073.26	1073.26	-
A1.3	$DIST^{V1.1}-ZSPRD^{100D}_{(3,0.5)}$	1	1	-	1704.59	-	1704.58	-	**1704.58**	17.05	1704.59	-	-	-	100	1704.59	1704.58	1704.59	-
A1.4	$DIST^{V1.1}-ZSPRD^{100D}_{(2.7,2)}$	1	-	1	-	23.79	-	23.79	**-23.79**	-0.24	-	-23.79	-	-	-	-23.79	-	-	-23.79
A1.5	$DIST^{V1.1}-ZSPRD^{100D}_{(2.7,1)}$	1	1	-	1115.55	-	1115.55	-	**1115.55**	11.16	1115.55	-	-	-	100	1115.55	1115.55	1115.55	-
A1.6	$DIST^{V1.1}-ZSPRD^{100D}_{(2.7,0.5)}$	1	1	-	1731.54	-	1731.54	-	**1731.54**	17.32	1731.54	-	-	-	100	1731.54	1731.54	1731.54	-
A2.1	$DIST^{V1.1}-SPRD^{100D}-SMA_{(10,20)}$	8	6	2	444.54	1301.75	2667.22	2603.49	**63.72**	0.64	1185.1	-1612.36	-0.16	-2.54	75	7.97	1.02	0.34	-2479.85
A2.2	$DIST^{V1.1}-SPRD^{100D}-EMA_{(10,20)}$	23	15	8	406.03	712.58	6090.47	5700.68	**389.79**	3.9	1055.98	-1756.39	-0.19	-3.02	65.22	16.98	1.07	0.57	-2407.1
A2.3	$DIST^{V1.1}-SPRD^{100D}-MACD_{(12,26,9)}$	40	26	14	267.03	238.09	6942.7	3333.25	**3609.46**	36.09	735.56	-766.66	-0.19	-3.02	65	90.24	2.08	1.12	-1067.68
A2.4	$DIST^{V1.1}-SPRD^{100D}-RSI_{(14)}$	6	3	3	1518.12	671.94	4554.35	2015.81	**2538.54**	25.39	3734.81	-1083.69	0.15	2.38	50	423.09	2.26	2.26	-1884.62
A2.5	$DIST^{V1.1}-SPRD^{100D}-BB_{(20)}$	13	7	6	574.14	290.02	4018.99	1740.09	**2278.9**	22.79	1007.29	-1121.7	0.04	0.63	53.85	175.33	2.31	1.98	-1121.7
A3	$DIST^{V1.1}-SPRD^{100D}-DECTREE$	300	137	163	119.31	79.26	16346.14	12919.62	**3426.52**	34.27	608.33	-421.38	-0.99	-15.72	45.67	11.43	1.27	1.51	-1704.45
A4	$DIST^{V1.1}-SPRD^{100D}-MLP$	249	116	133	132.97	90.76	15424.61	12070.63	**3353.98**	33.54	631.69	-637.18	-0.87	-13.81	46.59	13.48	1.28	1.47	-1213.19
	Part II: Models derived using the spread obtained from $DIST^{V1.2}-SPRD^{100D}$																		
B1.1	$DIST^{V1.2}-ZSPRD^{100D}_{(3,2)}$	2	1	1	204.38	414.88	204.38	414.88	**-210.5**	-2.1	204.38	-414.88	-0.59	-9.37	50	-105.25	0.49	0.49	-414.88
B1.2	$DIST^{V1.2}-ZSPRD^{100D}_{(3,1)}$	2	1	1	196.83	783.92	196.83	783.92	**-587.09**	-5.87	196.83	-783.92	-0.64	-10.16	50	-293.54	0.25	0.25	-783.92
B1.3	$DIST^{V1.2}-ZSPRD^{100D}_{(3,0.5)}$	2	1	1	796.8	1199.47	796.8	1199.47	**-402.67**	-4.03	796.8	-1199.47	-0.25	-3.97	50	-201.34	0.66	0.66	-1199.47
B1.4	$DIST^{V1.2}-ZSPRD^{100D}_{(2.7,2)}$	2	-	2	-	256	-	511.99	**-511.99**	-5.12	-	-414.88	-1.82	-28.89	-	-256	-	-	-511.99
B1.5	$DIST^{V1.2}-ZSPRD^{100D}_{(2.7,1)}$	2	-	2	-	452.33	-	904.67	**-904.67**	-9.05	-	-783.92	-1.29	-20.48	-	-452.33	-	-	-904.67
B1.6	$DIST^{V1.2}-ZSPRD^{100D}_{(2.7,0.5)}$	2	1	1	481.22	1199.47	481.22	1199.47	**-718.26**	-7.18	481.22	-1199.47	-0.43	-6.83	50	-359.13	0.4	0.4	-1199.47
B2.1	$DIST^{V1.2}-SPRD^{100D}-SMA_{(10,20)}$	7	4	3	1151.55	633.74	4606.22	1901.21	**2705.01**	27.05	3908.58	-1003.74	0.14	2.22	57.14	386.38	2.42	1.82	-1901.21
B2.2	$DIST^{V1.2}-SPRD^{100D}-EMA_{(10,20)}$	16	9	7	445.57	685.27	4010.17	4796.87	**-786.69**	-7.87	1316.82	-1731.89	-0.26	-4.13	56.25	-49.17	0.84	0.65	-3593.62
B2.3	$DIST^{V1.2}-SPRD^{100D}-MACD_{(12,26,9)}$	23	16	7	352.51	370.87	5640.16	2596.11	**3044.05**	30.44	845.37	-1244.86	-0.04	-0.63	69.57	132.38	2.17	0.95	-2237.82
B2.4	$DIST^{V1.2}-SPRD^{100D}-RSI_{(14)}$	6	3	3	971.41	1516.5	2914.24	4549.5	**-1635.27**	-16.35	1777.02	-1877.72	-0.29	-4.6	50	-272.54	0.64	0.64	-3439.69
B2.5	$DIST^{V1.2}-SPRD^{100D}-BB_{(20)}$	11	3	8	887.97	390.08	2663.91	3120.6	**-456.7**	-4.57	1550.53	-960.37	-0.26	-4.13	27.27	-41.55	0.85	2.28	-1866.99
B3	$DIST^{V1.2}-SPRD^{100D}-DECTREE$	290	142	148	98.05	93.98	13923.68	13909.58	**14.1**	0.14	536.52	-877.12	-1.08	-17.14	48.97	0.06	1	1.04	-1994.9
B4	$DIST^{V1.2}-SPRD^{100D}-MLP$	199	93	106	106.5	104.65	9904.71	11092.74	**-1188.03**	-11.88	501.96	-784.84	-1.04	-16.51	46.73	-5.98	0.89	1.02	-2147.15
	Part III: Models derived using the spread obtained from $DIST^{V2}-SPRD^{100D}$																		
C1.1	$DIST^{V2}-ZSPRD^{100D}_{(3,2)}$	1	1	-	80.32	-	80.32	-	**80.32**	0.8	80.32	-	-	-	100	80.32	80.32	80.32	-
C1.2	$DIST^{V2}-ZSPRD^{100D}_{(3,1)}$	1	-	1	-	1073.26	-	1073.26	**-1073.26**	-10.73	-	-1073.26	-	-	-	-1073.26	-	-	-1073.26
C1.3	$DIST^{V2}-ZSPRD^{100D}_{(3,0.5)}$	1	-	1	-	1704.59	-	1704.58	**-1704.58**	-17.05	-	-1704.59	-	-	-	-1704.59	-	-	-1704.59
C1.4	$DIST^{V2}-ZSPRD^{100D}_{(2.7,2)}$	1	1	-	23.79	-	23.79	-	**23.79**	0.24	23.79	-	-	-	100	23.79	23.79	23.79	-
C1.5	$DIST^{V2}-ZSPRD^{100D}_{(2.7,1)}$	1	-	1	-	1115.55	-	1115.55	**-1115.55**	-11.16	-	-1115.55	-	-	-	-1115.55	-	-	-1115.55
C1.6	$DIST^{V2}-ZSPRD^{100D}_{(2.7,0.5)}$	1	-	1	-	1731.54	-	1731.54	**-1731.54**	-17.32	-	-1731.54	-	-	-	-1731.54	-	-	-1731.54
C2.1	$DIST^{V2}-SPRD^{100D}-SMA_{(10,20)}$	9	6	3	1053.92	166.9	6323.51	500.7	**5822.82**	58.23	1545.23	-377.05	0.66	10.48	66.67	647.02	12.63	6.31	-377.05
C2.2	$DIST^{V2}-SPRD^{100D}-EMA_{(10,20)}$	23	8	15	712.58	406.03	5700.68	6090.47	**-389.79**	-3.9	1756.39	-1055.98	-0.24	-3.81	34.78	-16.98	0.94	1.75	-3541.35
C2.3	$DIST^{V2}-SPRD^{100D}-MACD_{(12,26,9)}$	40	14	26	238.09	267.03	3333.25	6942.7	**-3609.46**	-36.09	766.66	-735.56	-0.73	-11.59	35	-90.24	0.48	0.89	-4265.71
C2.4	$DIST^{V2}-SPRD^{100D}-RSI_{(14)}$	6	3	3	671.94	1518.12	2015.81	4554.35	**-2538.54**	-25.39	1083.69	-3734.81	-0.33	-5.24	50	-423.09	0.44	0.44	-3734.81
C2.5	$DIST^{V2}-SPRD^{100D}-BB_{(20)}$	13	6	7	290.02	574.14	1740.09	4018.99	**-2278.9**	-22.79	1121.7	-1007.29	-0.56	-8.89	46.15	-175.33	0.43	0.51	-1992.14
C3	$DIST^{V2}-SPRD^{100D}-DECTREE$	307	132	175	115.41	90.57	15233.84	15849.71	**-615.87**	-6.16	631.69	-890.7	-1.02	-16.19	43	-2	0.96	1.27	-2081.68
C4	$DIST^{V2}-SPRD^{100D}-MLP$	176	77	99	111.55	92.18	8589.2	9126.15	**-536.95**	-5.37	640.74	-673.98	-0.97	-15.4	43.75	-3.05	0.94	1.21	-1775.28
	Part IV: Models derived using the spread obtained from $DIST^{V3}-SPRD^{100D}$																		
D1.1	$DIST^{V3}-ZSPRD^{100D}_{(3,2)}$	3	1	2	120.63	93.32	120.63	186.64	**-66.02**	-0.66	120.63	-181.62	-1.15	-18.26	33.33	-22.01	0.65	1.29	-186.64
D1.2	$DIST^{V3}-ZSPRD^{100D}_{(3,1)}$	3	1	2	286.86	523.17	286.86	1046.34	**-759.49**	-7.59	286.86	-741.86	-0.78	-12.38	33.33	-253.19	0.27	0.55	-1046.34
D1.3	$DIST^{V3}-ZSPRD^{100D}_{(3,0.5)}$	3	1	2	312	601.1	312	1202.2	**-890.2**	-8.9	312	-627.94	-0.85	-13.49	33.33	-296.76	0.26	0.52	-1202.2
D1.4	$DIST^{V3}-ZSPRD^{100D}_{(2.7,2)}$	4	2	2	131.91	122.86	263.82	245.71	**18.11**	0.18	196.42	-240.69	-0.8	-12.7	50	4.53	1.07	1.07	-245.71
D1.5	$DIST^{V3}-ZSPRD^{100D}_{(2.7,1)}$	4	2	2	274.24	551.31	548.48	1102.61	**-554.13**	-5.54	312.55	-741.86	-0.58	-9.21	50	-138.53	0.5	0.5	-1102.61
D1.6	$DIST^{V3}-ZSPRD^{100D}_{(2.7,0.5)}$	4	2	2	350.48	622.44	700.96	1244.89	**-543.92**	-5.44	439.38	-627.94	-0.51	-8.1	50	-135.98	0.56	0.56	-1244.89
D2.1	$DIST^{V3}-SPRD^{100D}-SMA_{(10,20)}$	12	5	7	643.13	331.86	3215.64	2323.04	**892.59**	8.93	973.31	-634.28	-0.14	-2.22	41.67	74.42	1.38	1.94	-635.76
D2.2	$DIST^{V3}-SPRD^{100D}-EMA_{(10,20)}$	30	14	16	423.95	339.07	5935.27	5425.09	**510.18**	5.1	1001.79	-1032.37	-0.27	-4.29	46.67	17.03	1.09	1.25	-1596.97
D2.3	$DIST^{V3}-SPRD^{100D}-MACD_{(12,26,9)}$	30	11	19	505.62	240.19	5561.79	4563.6	**998.19**	9.98	1256.96	-1326.53	-0.24	-3.81	36.67	33.3	1.22	2.11	-2059.29
D2.4	$DIST^{V3}-SPRD^{100D}-RSI_{(14)}$	7	4	3	926.23	1581.6	3704.92	4744.79	**-1039.87**	-10.4	1366.77	-3351.42	-0.19	-3.02	57.14	-148.62	0.78	0.59	-1393.36
D2.5	$DIST^{V3}-SPRD^{100D}-BB_{(20)}$	14	9	5	221.19	589.82	1990.72	2949.11	**-958.4**	-9.58	871.09	-993.18	-0.44	-6.98	64.29	-68.42	0.68	0.38	-2658.17
D3	$DIST^{V3}-SPRD^{100D}-DECTREE$	292	119	173	111.93	81.58	13320.08	14113.6	**-793.52**	-7.94	878.84	-448.31	-1.06	-16.83	40.75	-2.72	0.94	1.37	-3107.42
D4	$DIST^{V3}-SPRD^{100D}-MLP$	145	66	79	133.01	108.27	8778.62	8553.13	**225.5**	2.25	679.87	-462.73	-0.86	-13.65	45.52	1.56	1.03	1.23	-2754.39
	Part V: Models derived using the spread obtained from $DIST^{V4}-SPRD^{100D}$																		
E1.1	$DIST^{V4}-ZSPRD^{100D}_{(3,2)}$	3	1	2	120.63	93.32	120.63	186.64	**-66.02**	-0.66	120.63	-181.62	-1.15	-18.26	33.33	-22.01	0.65	1.29	-186.64
E1.2	$DIST^{V4}-ZSPRD^{100D}_{(3,1)}$	3	1	2	286.86	523.17	286.86	1046.34	**-759.49**	-7.59	286.86	-741.86	-0.78	-12.38	33.33	-253.19	0.27	0.55	-1046.34
E1.3	$DIST^{V4}-ZSPRD^{100D}_{(3,0.5)}$	3	1	2	312	601.1	312	1202.2	**-890.2**	-8.9	312	-627.94	-0.85	-13.49	33.33	-296.76	0.26	0.52	-1202.2
E1.4	$DIST^{V4}-ZSPRD^{100D}_{(2.7,2)}$	4	2	2	131.91	122.86	263.82	245.71	**18.11**	0.18	196.42	-240.69	-0.8	-12.7	50	4.53	1.07	1.07	-245.71
E1.5	$DIST^{V4}-ZSPRD^{100D}_{(2.7,1)}$	4	2	2	274.24	551.31	548.48	1102.61	**-554.13**	-5.54	312.55	-741.86	-0.58	-9.21	50	-138.53	0.5	0.5	-1102.61
E1.6	$DIST^{V4}-ZSPRD^{100D}_{(2.7,0.5)}$	4	2	2	350.48	622.44	700.96	1244.89	**-543.92**	-5.44	439.38	-627.94	-0.51	-8.1	50	-135.98	0.56	0.56	-1244.89
E2.1	$DIST^{V4}-SPRD^{100D}-SMA_{(10,20)}$	12	5	7	643.13	331.86	3215.64	2323.04	**892.59**	8.93	973.31	-634.28	-0.14	-2.22	41.67	74.42	1.38	1.94	-635.76
E2.2	$DIST^{V4}-SPRD^{100D}-EMA_{(10,20)}$	30	14	16	423.95	339.07	5935.27	5425.09	**510.18**	5.1	1001.79	-1032.37	-0.27	-4.29	46.67	17.03	1.09	1.25	-1596.97
E2.3	$DIST^{V4}-SPRD^{100D}-MACD_{(12,26,9)}$	30	11	19	505.62	240.19	5561.79	4563.6	**998.19**	9.98	1256.96	-1326.53	-0.24	-3.81	36.67	33.3	1.22	2.11	-2059.29
E2.4	$DIST^{V4}-SPRD^{100D}-RSI_{(14)}$	7	4	3	926.23	1581.6	3704.92	4744.79	**-1039.87**	-10.4	1366.77	-3351.42	-0.19	-3.02	57.14	-148.62	0.78	0.59	-1393.36
E2.5	$DIST^{V4}-SPRD^{100D}-BB_{(20)}$	14	9	5	221.19	589.82	1990.72	2949.11	**-958.4**	-9.58	871.09	-993.18	-0.44	-6.98	64.29	-68.42	0.68	0.38	-2658.17
E3	$DIST^{V4}-SPRD^{100D}-DECTREE$	302	121	181	104.77	83.5	12676.75	15113.54	**-2436.79**	-24.37	548.97	-448.31	-1.21	-19.21	40.07	-8.06	0.84	1.25	-3857.08
E4	$DIST^{V4}-SPRD^{100D}-MLP$	145	66	79	133.01	108.27	8778.62	8553.13	**225.5**	2.25	679.87	-462.73	-0.86	-13.65	45.52	1.56	1.03	1.23	-2754.39
	Part VI: Models derived using the spread obtained from $JOHANSEN-SPRD^{100D}$																		
F1.1	$JOHANSEN-ZSPRD^{100D}_{(3,2)}$	17	5	12	114.87	58.4	574.34	700.75	**-126.41**	-1.26	317.93	-307.77	0.04	0.63	29.41	-7.44	0.82	1.97	-369.61
F1.2	$JOHANSEN-ZSPRD^{100D}_{(3,1)}$	16	4	12	136.35	38.41	545.42	460.97	**84.45**	0.84	317.93	-100.08	0.07	1.11	25	5.28	1.18	3.55	-208.91
F1.3	$JOHANSEN-ZSPRD^{100D}_{(3,0.5)}$	14	5	9	136.36	102.02	681.79	918.15	**-236.35**	-2.36	317.93	-424.82	0.09	1.43	35.71	-16.89	0.74	1.34	-569.98
F1.4	$JOHANSEN-ZSPRD^{100D}_{(2.7,2)}$	17	5	12	114.87	58.4	574.34	700.75	**-126.41**	-1.26	317.93	-307.77	0.04	0.63	29.41	-7.44	0.82	1.97	-369.61
F1.5	$JOHANSEN-ZSPRD^{100D}_{(2.7,1)}$	16	4	12	136.35	38.41	545.42	460.97	**84.45**	0.84	317.93	-100.08	0.07	1.11	25	5.28	1.18	3.55	-208.91
F1.6	$JOHANSEN-ZSPRD^{100D}_{(2.7,0.5)}$	14	5	9	136.36	102.02	681.79	918.15	**-236.35**	-2.36	317.93	-424.82	0.09	1.43	35.71	-16.89	0.74	1.34	-569.98
F2.1	$JOHANSEN-SPRD^{100D}-SMA_{(10,20)}$	20	12	8	638.18	756.11	7658.11	6048.84	**1609.26**	16.09	2288.63	-3259.26	0.08	1.27	60	80.46	1.27	0.84	-3259.26
F2.2	$JOHANSEN-SPRD^{100D}-EMA_{(10,20)}$	31	16	15	1500.92	600.92	24014.73	9013.73	**15001**	150.01	8108.57	-4131.66	0.2	3.17	51.61	483.84	2.66	2.5	-4171.68
F2.3	$JOHANSEN-SPRD^{100D}-MACD_{(12,26,9)}$	30	12	18	436.93	875.65	5243.2	15761.79	**-10518.58**	-105.19	2194.82	-3668.96	-0.15	-2.38	40	-350.62	0.33	0.5	-10707.64
F2.4	$JOHANSEN-SPRD^{100D}-RSI_{(14)}$	5	2	3	91.56	595.09	183.12	1785.27	**-1602.15**	-16.02	159.45	-1413.73	-0.44	-6.98	40	-320.43	0.1	0.15	-1602.15
F2.5	$JOHANSEN-SPRD^{100D}-BB_{(20)}$	16	8	8	235.89	415.51	1887.14	3324.06	**-1436.92**	-14.37	683.56	-931.03	-0.16	-2.54	50	-89.81	0.57	0.57	-2035.55
F3	$JOHANSEN-SPRD^{100D}-DECTREE$	318	180	138	96.5	102.34	17370.08	14123.32	**3246.75**	32.47	480.47	-1083.39	-0.96	-15.24	56.6	10.2	1.23	0.94	-1255.91
F4	$JOHANSEN-SPRD^{100D}-MLP$	268	137	131	97.29	92.44	13328.65	12109.64	**1219**	12.19	741.01	-474.91	-1.1	-17.46	51.12	4.55	1.1	1.05	-1536.1
	Part VII: Models derived using the spread obtained from $ADF-SPRD^{100D}$																		
G1.1	$ADF-ZSPRD^{100D}_{(3,2)}$	3	2	1	7160.76	319.83	14321.53	319.83	**14001.69**	140.02	12836.58	-319.83	0.66	10.48	66.67	4667.48	44.78	22.39	-319.83
G1.2	$ADF-ZSPRD^{100D}_{(3,1)}$	3	2	1	8378.24	787.17	16756.48	787.17	**15969.31**	159.69	14507.22	-787.17	0.68	10.79	66.67	5323.41	21.29	10.64	-787.17
G1.3	$ADF-ZSPRD^{100D}_{(3,0.5)}$	3	2	1	6753.3	787.17	13506.61	787.17	**12719.44**	127.19	11426.33	-787.17	0.69	10.95	66.67	4240.06	17.16	8.58	-787.17
G1.4	$ADF-ZSPRD^{100D}_{(2.7,2)}$	4	2	2	7160.76	1270.94	14321.53	2541.87	**11779.66**	117.8	12836.58	-2222.04	0.44	6.98	50	2944.91	5.63	5.63	-2222.04
G1.5	$ADF-ZSPRD^{100D}_{(2.7,1)}$	4	2	2	8378.24	1504.61	16756.48	3009.21	**13747.27**	137.47	14507.22	-2222.04	0.47	7.46	50	3436.82	5.57	5.57	-2222.04
G1.6	$ADF-ZSPRD^{100D}_{(2.7,0.5)}$	4	2	2	6753.3	3856.53	13506.61	7713.06	**5793.55**	57.94	11426.33	-6925.89	0.22	3.49	50	1448.39	1.75	1.75	-6925.89
G2.1	$ADF-SPRD^{100D}-SMA_{(10,20)}$	20	14	6	3061.55	1669.45	42861.75	10016.73	**32845.02**	328.45	17893.45	-3889.86	0.33	5.24	70	1642.25	4.28	1.83	-5771.11
G2.2	$ADF-SPRD^{100D}-EMA_{(10,20)}$	34	23	11	1308.59	3074.04	30097.48	33814.47	**-3716.99**	-37.17	5007.81	-11276.49	-0.08	-1.27	67.65	-109.19	0.89	0.43	-12986.02
G2.3	$ADF-SPRD^{100D}-MACD_{(12,26,9)}$	26	13	13	1024.25	3078.89	13315.3	40025.56	**-26710.25**	-267.1	3169.8	-12836.58	-0.31	-4.92	50	-1027.32	0.33	0.33	-26710.25
G2.4	$ADF-SPRD^{100D}-RSI_{(14)}$	5	3	2	4729.38	188174.11	14188.15	376348.22	**-362160.08**	-3621.6	6835.42	-373120.26	-0.43	-6.83	60	-72432.02	0.04	0.03	-376348.22
G2.5	$ADF-SPRD^{100D}-BB_{(20)}$	20	6	14	4883.48	880.54	29300.89	12327.51	**16973.39**	169.73	11905.9	-2739.4	0.23	3.65	30	848.67	2.38	5.55	-5970.1
G3	$ADF-SPRD^{100D}-DECTREE$	321	154	167	109.5	91.53	16863.72	15285.88	**1577.84**	15.78	890.7	-561.35	-0.98	-15.56	47.98	4.93	1.1	1.2	-2498.08
G4	$ADF-SPRD^{100D}-MLP$	225	103	122	125.59	102.67	12935.71	12525.87	**409.85**	4.1	890.7	-585.71	-0.9	-14.29	45.78	1.83	1.03	1.22	-3064.54
	Part VIII: Models derived using the spread obtained from $KALMAN-SPRD^{100D}$																		
H1.1	$KALMAN-ZSPRD^{100D}_{(3,2)}$	-	-	-	-	-	-	-	-	-	-	-	-	-	-	-	-	-	-
H1.2	$KALMAN-ZSPRD^{100D}_{(3,1)}$	-	-	-	-	-	-	-	-	-	-	-	-	-	-	-	-	-	-
H1.3	$KALMAN-ZSPRD^{100D}_{(3,0.5)}$	-	-	-	-	-	-	-	-	-	-	-	-	-	-	-	-	-	-
H1.4	$KALMAN-ZSPRD^{100D}_{(2.7,2)}$	1	1	-	445.07	-	445.07	-	**445.07**	4.45	445.07	-	-	-	100	445.07	445.07	445.07	-
H1.5	$KALMAN-ZSPRD^{100D}_{(2.7,1)}$	-	-	-	-	-	-	-	-	-	-	-	-	-	-	-	-	-	-
H1.6	$KALMAN-ZSPRD^{100D}_{(2.7,0.5)}$	-	-	-	-	-	-	-	-	-	-	-	-	-	-	-	-	-	-
H2.1	$KALMAN-SPRD^{100D}-SMA_{(10,20)}$	10	5	5	663.54	1251.62	3317.7	6258.11	**-2940.4**	-29.4	2345.48	-2003.28	-0.35	-5.56	50	-294.04	0.53	0.53	-5610.39
H2.2	$KALMAN-SPRD^{100D}-EMA_{(10,20)}$	18	9	9	1514.11	1063.13	13627.03	9568.13	**4058.9**	40.59	8263.98	-1976.24	0.04	0.63	50	225.49	1.42	1.42	-6767.21
H2.3	$KALMAN-SPRD^{100D}-MACD_{(12,26,9)}$	29	8	21	676.54	607.52	5412.3	12757.83	**-7345.54**	-73.46	1340.66	-1607.97	-0.46	-7.3	27.59	-253.25	0.42	1.11	-8075.52
H2.4	$KALMAN-SPRD^{100D}-RSI_{(14)}$	5	3	2	2261.66	5779.69	6784.99	11559.38	**-4774.39**	-47.74	3810.61	-7608.22	-0.2	-3.17	60	-954.88	0.59	0.39	-11559.38
H2.5	$KALMAN-SPRD^{100D}-BB_{(20)}$	11	7	4	967.81	960.7	6774.67	3842.8	**2931.87**	29.32	2604.17	-1689.41	0.16	2.54	63.64	266.6	1.76	1.01	-1894.78
H3	$KALMAN-SPRD^{100D}-DECTREE$	298	140	158	126.98	87.56	17776.78	13835.15	**3941.63**	39.42	654.13	-890.7	-0.88	-13.97	46.98	13.23	1.28	1.45	-1827.32
H4	$KALMAN-SPRD^{100D}-MLP$	189	81	108	131.42	97.87	10645.34	10569.42	**75.92**	0.76	877.12	-535.93	-0.88	-13.97	42.86	0.41	1.01	1.34	-2001.03
	Part IX: Models derived using the spread obtained from $RATIO-SPRD^{100D}$																		
I1.1	$RATIO-ZSPRD^{100D}_{(3,2)}$	2	-	2	-	405.02	-	810.04	**-810.04**	-8.1	-	-408.53	-112.07	-1779.06	-	-405.02	-	-	-810.04
I1.2	$RATIO-ZSPRD^{100D}_{(3,1)}$	1	-	1	-	1411.09	-	1411.09	**-1411.09**	-14.11	-	-1411.09	-	-	-	-1411.09	-	-	-1411.09
I1.3	$RATIO-ZSPRD^{100D}_{(3,0.5)}$	1	-	1	-	1469.88	-	1469.88	**-1469.88**	-14.7	-	-1469.88	-	-	-	-1469.88	-	-	-1469.88
I1.4	$RATIO-ZSPRD^{100D}_{(2.7,2)}$	4	1	3	69.04	360.96	69.04	1082.87	**-1013.83**	-10.14	69.04	-507.22	-1.56	-24.76	25	-253.46	0.06	0.19	-1082.87
I1.5	$RATIO-ZSPRD^{100D}_{(2.7,1)}$	3	2	1	37.13	1484.04	74.27	1484.04	**-1409.78**	-14.1	39.78	-1484.04	-0.71	-11.27	66.67	-469.87	0.05	0.03	-1484.04
I1.6	$RATIO-ZSPRD^{100D}_{(2.7,0.5)}$	3	2	1	256.79	1549.27	513.58	1549.27	**-1035.69**	-10.36	381.89	-1549.27	-0.47	-7.46	66.67	-345.17	0.33	0.17	-1549.27
I2.1	$RATIO-SPRD^{100D}-SMA_{(10,20)}$	14	5	9	610.85	290.61	3054.25	2615.52	**438.72**	4.39	1837.22	-688.58	-0.2	-3.17	35.71	31.3	1.17	2.1	-1684.01
I2.2	$RATIO-SPRD^{100D}-EMA_{(10,20)}$	21	8	13	786.67	221.15	6293.35	2875	**3418.35**	34.18	1882.7	-684.13	0.02	0.32	38.1	162.83	2.19	3.56	-1003.86
I2.3	$RATIO-SPRD^{100D}-MACD_{(12,26,9)}$	28	12	16	602.03	216.35	7224.31	3461.58	**3762.73**	37.63	1267.96	-548.25	-0.04	-0.63	42.86	134.41	2.09	2.78	-1970.71
I2.4	$RATIO-SPRD^{100D}-RSI_{(14)}$	5	3	2	633.17	2437.21	1899.5	4874.43	**-2974.92**	-29.75	1076.55	-4110.84	-0.36	-5.71	60	-594.98	0.39	0.26	-4110.84
I2.5	$RATIO-SPRD^{100D}-BB_{(20)}$	11	7	4	233.22	610.89	1632.52	2443.55	**-811.03**	-8.11	561.22	-1073.5	-0.43	-6.83	63.64	-73.7	0.67	0.38	-1410.47
I3	$RATIO-SPRD^{100D}-DECTREE$	279	110	169	117.45	72.91	12919.84	12320.95	**598.89**	5.99	770.61	-504.13	-1.14	-18.1	39.43	2.15	1.05	1.61	-1949.22
I4	$RATIO-SPRD^{100D}-MLP$	54	25	29	170.35	234.64	4258.69	6804.62	**-2545.93**	-25.46	882.57	-1367.31	-0.61	-9.68	46.3	-47.13	0.63	0.73	-3193.86
	Part X: Models derived using the close price of IWF.N																		
CLS-SYM-1.1	$CLOSE^{IWF.N}-SMA_{(10,20)}$	12	6	6	356.71	189.67	2140.24	1138.02	**1002.23**	10.02	555.73	-253.08	0.02	0.32	50	83.52	1.88	1.88	-501.5
CLS-SYM-1.2	$CLOSE^{IWF.N}-EMA_{(10,20)}$	21	7	14	379.1	169.37	2653.72	2371.16	**282.56**	2.83	1556.82	-381.44	-0.15	-2.38	33.33	13.44	1.12	2.24	-1078.61
CLS-SYM-1.3	$CLOSE^{IWF.N}-MACD_{(12,26,9)}$	30	8	22	188.24	130.91	1505.94	2880.12	**-1374.18**	-13.74	760.82	-320.06	-0.61	-9.68	26.67	-45.8	0.52	1.44	-1432.72
CLS-SYM-1.4	$CLOSE^{IWF.N}-RSI_{(14)}$	6	2	4	490.13	759	980.26	3036	**-2055.74**	-20.56	767.73	-2215.65	-0.41	-6.51	33.33	-342.67	0.32	0.65	-2215.65
CLS-SYM-1.5	$CLOSE^{IWF.N}-BB_{(20)}$	12	7	5	112.1	284.97	784.69	1424.86	**-640.17**	-6.4	257.89	-668.35	-0.48	-7.62	58.33	-53.36	0.55	0.39	-1142.05
	Part XI: Models derived using the close price of XLE.N																		
CLS-SYM-2.1	$CLOSE^{XLE.N}-SMA_{(10,20)}$	19	9	10	492.93	337.96	4436.4	3379.63	**1056.77**	10.57	1969.29	-993.26	-0.03	-0.48	47.37	55.63	1.31	1.46	-2390.02
CLS-SYM-2.2	$CLOSE^{XLE.N}-EMA_{(10,20)}$	26	11	15	546.32	161.14	6009.56	2417.09	**3592.47**	35.92	2197.81	-326.2	0.12	1.9	42.31	138.19	2.49	3.39	-711.67
CLS-SYM-2.3	$CLOSE^{XLE.N}-MACD_{(12,26,9)}$	27	10	17	637.2	211.29	6372.04	3591.96	**2780.08**	27.8	1931.38	-613.01	0.05	0.79	37.04	102.99	1.77	3.02	-645.92
CLS-SYM-2.4	$CLOSE^{XLE.N}-RSI_{(14)}$	5	3	2	314.75	1213.82	944.26	2427.64	**-1483.38**	-14.83	365.04	-1229.73	-0.44	-6.98	60	-296.68	0.39	0.26	-2062.6
CLS-SYM-2.5	$CLOSE^{XLE.N}-BB_{(20)}$	20	17	3	198.62	500.07	3376.55	1500.22	**1876.33**	18.76	822.47	-1185.85	0.05	0.79	85	93.82	2.25	0.4	-1185.85

Table D.2.7: This table presents the back-test metrics for the pair $QQQ.N/XLE.N$ based on a 30-day rolling window. The table is subdivided into eleven parts, and in each of these parts, we present the back-test metrics and the trading strategies which use the spread derived from various models. In Part I, the spread is derived from the $DIST^{V1.1}$ model, in Part II from the $DIST^{V1.2}$ model, in Part III from the $DIST^{V2}$ model, in Part IV from the $DIST^{V3}$ model, in Part V from the $DIST^{V4}$ model, in Part VI from the $JOHANSEN-SPRD$ model, in Part VIII from the $ADF-SPRD$ model, in from the $DIST^{V2}$ model, in Part VIII from the $KALMAN-SPRD$ model, and in Part IX from the $RATIO-SPRD$ model. In Part X and XI, we present the back-test metrics of the trading strategies which use the close price of QQQ.N, and XLE.N, respectively. All $ numbers reported below are in USD.

(I) Trading Strategy Code	(II) Model Name	(III) Total Number of Trades	(IV) Number of Winning Trades	(V) Number of Loosing Trades	(VI) Average Profit per Trade ($)	(VII) Average Loss per Trade ($)	(VIII) Gross Profit ($)	(IX) Gross Loss ($)	(X) Net Profit ($)	(XI) ROI (%)	(XII) Max P&L ($)	(XIII) Min P&L ($)	(XIV) Daily Sharpe Ratio	(XV) Annualized Sharpe Ratio	(XVI) Hit Ratio	(XVII) Expectancy	(XVIII) Profit Factor	(XIX) Realized Risk Reward Ratio	(XX) Max Drawdown ($)
Part I: Models derived using the spread obtained from $DIST^{V1.1}-SPRD^{30D}$																			
A1.1	$DIST^{V1.1}-ZSPRD^{30D}_{(3,2)}$	-	-	-	-	-	-	-	-	-	-	-	-	-	-	-	-	-	-
A1.2	$DIST^{V1.1}-ZSPRD^{30D}_{(3,1)}$	-	-	-	-	-	-	-	-	-	-	-	-	-	-	-	-	-	-
A1.3	$DIST^{V1.1}-ZSPRD^{30D}_{(3,0.5)}$	-	-	-	-	-	-	-	-	-	-	-	-	-	-	-	-	-	-
A1.4	$DIST^{V1.1}-ZSPRD^{30D}_{(2.7,2)}$	4	1	3	262.05	171.53	262.05	514.6	**-252.55**	-2.53	262.05	-226.15	-0.98	-15.56	25	-63.14	0.51	1.53	-514.6
A1.5	$DIST^{V1.1}-ZSPRD^{30D}_{(2.7,1)}$	3	1	2	325.1	361.47	325.1	722.94	**-397.84**	-3.98	325.1	-623.79	-0.6	-9.52	33.33	-132.64	0.45	0.9	-722.94
A1.6	$DIST^{V1.1}-ZSPRD^{30D}_{(2.7,0.5)}$	3	1	2	318.02	354.12	318.02	708.24	**-390.21**	-3.9	318.02	-374.34	-0.73	-11.59	33.33	-130.09	0.45	0.9	-708.24
A2.1	$DIST^{V1.1}-SPRD^{30D}-SMA_{(10,20)}$	12	7	5	441.77	641.08	3092.42	3205.4	**-112.98**	-1.13	1112.86	-1432.79	-0.22	-3.49	58.33	-9.45	0.96	0.69	-2287.18
A2.2	$DIST^{V1.1}-SPRD^{30D}-EMA_{(10,20)}$	22	16	6	409.95	851.33	6559.27	5107.97	**1451.3**	14.51	2101.89	-2011.03	-0.1	-1.59	72.73	66	1.28	0.48	-2246.75
A2.3	$DIST^{V1.1}-SPRD^{30D}-MACD_{(12,26,9)}$	37	25	12	264.16	281.91	6603.91	3382.98	**3220.94**	32.21	1422.9	-887.69	-0.16	-2.54	67.57	87.07	1.95	0.94	-2533.12
A2.4	$DIST^{V1.1}-SPRD^{30D}-RSI_{(14)}$	5	3	2	1618.7	576.95	4856.11	1153.9	**3702.21**	37.02	4771.09	-1099.04	0.26	4.13	60	740.44	4.21	2.81	-1099.04
A2.5	$DIST^{V1.1}-SPRD^{30D}-BB_{(20)}$	9	6	3	304.87	574.76	1829.24	1724.28	**104.96**	1.05	968.03	-1324.15	-0.23	-3.65	66.67	11.69	1.06	0.53	-1558.57
A3	$DIST^{V1.1}-SPRD^{30D}-DECTREE$	350	166	184	106.66	79.59	17705.79	14645.45	**3060.34**	30.6	673.13	-420.52	-1.05	-16.67	47.43	8.75	1.21	1.34	-1310.27
A4	$DIST^{V1.1}-SPRD^{30D}-MLP$	313	145	168	124.37	87.49	18034.15	14698.76	**3335.39**	33.35	1044.96	-675.27	-0.88	-13.97	46.33	10.66	1.23	1.42	-1229.09
Part II: Models derived using the spread obtained from $DIST^{V1.2}-SPRD^{30D}$																			
B1.1	$DIST^{V1.2}-ZSPRD^{30D}_{(3,2)}$	8	4	4	252.62	148.57	1010.49	594.28	**416.22**	4.16	345.03	-353.67	-0.41	-6.51	50	52.03	1.7	1.7	-463.39
B1.2	$DIST^{V1.2}-ZSPRD^{30D}_{(3,1)}$	8	4	4	370.42	362.28	1481.68	1449.12	**32.56**	0.33	809.58	-756.79	-0.31	-4.92	50	4.07	1.02	1.02	-870.57
B1.3	$DIST^{V1.2}-ZSPRD^{30D}_{(3,0.5)}$	8	4	4	677.97	511.06	2711.89	2044.23	**667.66**	6.68	1082.85	-885.28	-0.09	-1.43	50	83.46	1.33	1.33	-1130.34
B1.4	$DIST^{V1.2}-ZSPRD^{30D}_{(2.7,2)}$	11	6	5	140.12	131.88	840.75	659.38	**181.36**	1.81	285.25	-353.67	-0.74	-11.75	54.55	16.5	1.28	1.06	-463.39
B1.5	$DIST^{V1.2}-ZSPRD^{30D}_{(2.7,1)}$	11	6	5	219.87	298.87	1319.24	1494.36	**-175.12**	-1.75	809.58	-756.79	-0.44	-6.98	54.55	-15.9	0.88	0.74	-870.57
B1.6	$DIST^{V1.2}-ZSPRD^{30D}_{(2.7,0.5)}$	10	6	4	501.17	511.06	3007.01	2044.23	**962.78**	9.63	823.22	-885.28	-0.09	-1.43	60	96.28	1.47	0.98	-1130.34
B2.1	$DIST^{V1.2}-SPRD^{30D}-SMA_{(10,20)}$	14	6	8	300.02	568.46	1800.14	4547.65	**-2747.51**	-27.48	1048.33	-1515.23	-0.51	-8.1	42.86	-196.23	0.4	0.53	-4360.06
B2.2	$DIST^{V1.2}-SPRD^{30D}-EMA_{(10,20)}$	19	9	10	463.18	654.03	4168.61	6540.27	**-2371.66**	-23.72	1533.97	-1953.51	-0.32	-5.08	47.37	-124.81	0.64	0.71	-4477.8
B2.3	$DIST^{V1.2}-SPRD^{30D}-MACD_{(12,26,9)}$	34	13	21	348.57	312.18	4531.41	6555.76	**-2024.35**	-20.24	882.63	-1107.03	-0.47	-7.46	38.24	-59.51	0.69	1.12	-4641.34
B2.4	$DIST^{V1.2}-SPRD^{30D}-RSI_{(14)}$	9	3	6	655.79	751.35	1967.38	4508.1	**-2540.72**	-25.41	1507.75	-1495.67	-0.5	-7.94	33.33	-282.35	0.44	0.87	-2226.76
B2.5	$DIST^{V1.2}-SPRD^{30D}-BB_{(20)}$	16	9	7	369.68	336.58	3327.14	2356.08	**971.06**	9.71	1044.96	-762.21	-0.19	-3.02	56.25	60.69	1.41	1.1	-954.17
B3	$DIST^{V1.2}-SPRD^{30D}-DECTREE$	285	136	149	95.8	106.46	13029.34	15862.76	**-2833.42**	-28.33	672.38	-1410.01	-1	-15.87	47.72	-9.94	0.82	0.9	-4158.65
B4	$DIST^{V1.2}-SPRD^{30D}-MLP$	277	136	141	96.71	123.4	13153.05	17399.83	**-4246.78**	-42.47	390.44	-843.47	-1.05	-16.67	49.1	-15.33	0.76	0.78	-5325.21
Part III: Models derived using the spread obtained from $DIST^{V2}-SPRD^{30D}$																			
C1.1	$DIST^{V2}-ZSPRD^{30D}_{(3,2)}$	-	-	-	-	-	-	-	-	-	-	-	-	-	-	-	-	-	-
C1.2	$DIST^{V2}-ZSPRD^{30D}_{(3,1)}$	-	-	-	-	-	-	-	-	-	-	-	-	-	-	-	-	-	-
C1.3	$DIST^{V2}-ZSPRD^{30D}_{(3,0.5)}$	-	-	-	-	-	-	-	-	-	-	-	-	-	-	-	-	-	-
C1.4	$DIST^{V2}-ZSPRD^{30D}_{(2.7,2)}$	4	3	1	171.53	262.05	514.6	262.05	**252.55**	2.53	226.15	-262.05	-0.4	-6.35	75	63.14	1.96	0.65	-262.05
C1.5	$DIST^{V2}-ZSPRD^{30D}_{(2.7,1)}$	3	2	1	361.47	325.1	722.94	325.1	**397.84**	3.98	623.79	-325.1	-0.04	-0.63	66.67	132.64	2.22	1.11	-325.1
C1.6	$DIST^{V2}-ZSPRD^{30D}_{(2.7,0.5)}$	3	2	1	354.12	318.02	708.24	318.02	**390.21**	3.9	374.34	-318.02	-0.06	-0.95	66.67	130.09	2.23	1.11	-318.02
C2.1	$DIST^{V2}-SPRD^{30D}-SMA_{(10,20)}$	12	7	5	580.52	538.87	4063.67	2694.37	**1369.3**	13.69	1449.08	-1112.86	-0.05	-0.79	58.33	114.07	1.51	1.08	-2275.06
C2.2	$DIST^{V2}-SPRD^{30D}-EMA_{(10,20)}$	22	6	16	851.33	409.95	5107.97	6559.27	**-1451.3**	-14.51	2011.03	-2101.89	-0.26	-4.13	27.27	-66	0.78	2.08	-3917.86
C2.3	$DIST^{V2}-SPRD^{30D}-MACD_{(12,26,9)}$	37	12	25	281.91	264.16	3382.98	6603.91	**-3220.94**	-32.21	887.69	-1422.9	-0.61	-9.68	32.43	-87.07	0.51	1.07	-5804.97
C2.4	$DIST^{V2}-SPRD^{30D}-RSI_{(14)}$	5	2	3	576.95	1618.7	1153.9	4856.11	**-3702.21**	-37.02	1099.04	-4771.09	-0.39	-6.19	40	-740.44	0.24	0.36	-4826.88
C2.5	$DIST^{V2}-SPRD^{30D}-BB_{(20)}$	9	3	6	574.76	304.87	1724.28	1829.24	**-104.96**	-1.05	1324.15	-968.03	-0.27	-4.29	33.33	-11.69	0.94	1.89	-695.5
C3	$DIST^{V2}-SPRD^{30D}-DECTREE$	350	164	186	109.72	86.15	17993.77	16023.63	**1970.14**	19.7	817.79	-918.24	-0.92	-14.6	46.86	5.63	1.12	1.27	-1432.36
C4	$DIST^{V2}-SPRD^{30D}-MLP$	323	156	167	118.97	93.12	18558.6	15550.76	**3007.84**	30.08	778.86	-918.24	-0.88	-13.97	48.3	9.32	1.19	1.28	-1605.36
Part IV: Models derived using the spread obtained from $DIST^{V3}-SPRD^{30D}$																			
D1.1	$DIST^{V3}-ZSPRD^{30D}_{(3,2)}$	5	4	1	158.1	176.53	632.4	176.53	**455.86**	4.56	379.06	-176.53	-0.31	-4.92	80	91.17	3.58	0.9	-176.53
D1.2	$DIST^{V3}-ZSPRD^{30D}_{(3,1)}$	5	2	3	258.04	505.45	516.09	1516.36	**-1000.27**	-10	379.06	-726.84	-0.76	-12.06	40	-200.05	0.34	0.51	-1516.36
D1.3	$DIST^{V3}-ZSPRD^{30D}_{(3,0.5)}$	5	2	3	304.99	788.89	609.98	2366.66	**-1756.68**	-17.57	379.06	-899.43	-0.83	-13.18	40	-351.34	0.26	0.39	-2366.66
D1.4	$DIST^{V3}-ZSPRD^{30D}_{(2.7,2)}$	11	7	4	193.76	77.62	1356.31	310.5	**1045.81**	10.46	419.43	-176.53	-0.31	-4.92	63.64	95.08	4.37	2.5	-179.23
D1.5	$DIST^{V3}-ZSPRD^{30D}_{(2.7,1)}$	10	6	4	205.83	428.82	1234.96	1715.27	**-480.31**	-4.8	401.05	-726.84	-0.53	-8.41	60	-48.03	0.72	0.48	-1516.36
D1.6	$DIST^{V3}-ZSPRD^{30D}_{(2.7,0.5)}$	10	6	4	234.44	711.48	1406.63	2845.94	**-1439.31**	-14.39	401.05	-899.43	-0.58	-9.21	60	-143.93	0.49	0.33	-2366.66
D2.1	$DIST^{V3}-SPRD^{30D}-SMA_{(10,20)}$	22	12	10	481.75	364.19	5781.04	3641.95	**2139.1**	21.39	1176.77	-818.23	-0.1	-1.59	54.55	97.27	1.59	1.32	-1594.37
D2.2	$DIST^{V3}-SPRD^{30D}-EMA_{(10,20)}$	43	13	30	512.35	256.28	6660.56	7688.52	**-1027.96**	-10.28	1067.69	-1438.24	-0.37	-5.87	30.23	-23.93	0.87	2	-4047.8
D2.3	$DIST^{V3}-SPRD^{30D}-MACD_{(12,26,9)}$	38	10	28	544.29	227.52	5442.88	6370.44	**-927.56**	-9.28	1296.34	-1609.76	-0.36	-5.71	26.32	-24.38	0.85	2.39	-4144.93
D2.4	$DIST^{V3}-SPRD^{30D}-RSI_{(14)}$	5	3	2	749.16	1293.98	2247.49	2587.97	**-340.48**	-3.4	945.5	-2515.7	-0.15	-2.38	60	-68.1	0.87	0.58	-2515.7
D2.5	$DIST^{V3}-SPRD^{30D}-BB_{(20)}$	19	12	7	230.33	467.54	2763.98	3272.79	**-508.81**	-5.09	1292.35	-941.24	-0.37	-5.87	63.16	-26.76	0.84	0.49	-3118.36
D3	$DIST^{V3}-SPRD^{30D}-DECTREE$	306	143	163	122.77	87.52	17556.81	14266.3	**3290.51**	32.91	709.77	-579.63	-0.93	-14.76	46.73	10.75	1.23	1.4	-2349.28
D4	$DIST^{V3}-SPRD^{30D}-MLP$	240	93	147	117.58	104.77	10935.31	15401.62	**-4466.31**	-44.66	856.9	-843.47	-0.98	-15.56	38.75	-18.61	0.71	1.12	-6995.95
Part V: Models derived using the spread obtained from $DIST^{V4}-SPRD^{30D}$																			
E1.1	$DIST^{V4}-ZSPRD^{30D}_{(3,2)}$	5	4	1	158.1	176.53	632.4	176.53	**455.86**	4.56	379.06	-176.53	-0.31	-4.92	80	91.17	3.58	0.9	-176.53
E1.2	$DIST^{V4}-ZSPRD^{30D}_{(3,1)}$	5	2	3	258.04	505.45	516.09	1516.36	**-1000.27**	-10	379.06	-726.84	-0.76	-12.06	40	-200.05	0.34	0.51	-1516.36
E1.3	$DIST^{V4}-ZSPRD^{30D}_{(3,0.5)}$	5	2	3	304.99	788.89	609.98	2366.66	**-1756.68**	-17.57	379.06	-899.43	-0.83	-13.18	40	-351.34	0.26	0.39	-2366.66
E1.4	$DIST^{V4}-ZSPRD^{30D}_{(2.7,2)}$	11	7	4	193.76	77.62	1356.31	310.5	**1045.81**	10.46	419.43	-176.53	-0.31	-4.92	63.64	95.08	4.37	2.5	-179.23
E1.5	$DIST^{V4}-ZSPRD^{30D}_{(2.7,1)}$	10	6	4	205.83	428.82	1234.96	1715.27	**-480.31**	-4.8	401.05	-726.84	-0.53	-8.41	60	-48.03	0.72	0.48	-1516.36
E1.6	$DIST^{V4}-ZSPRD^{30D}_{(2.7,0.5)}$	10	6	4	234.44	711.48	1406.63	2845.94	**-1439.31**	-14.39	401.05	-899.43	-0.58	-9.21	60	-143.93	0.49	0.33	-2366.66
E2.1	$DIST^{V4}-SPRD^{30D}-SMA_{(10,20)}$	22	12	10	481.75	364.19	5781.04	3641.95	**2139.1**	21.39	1176.77	-818.23	-0.1	-1.59	54.55	97.27	1.59	1.32	-1594.37
E2.2	$DIST^{V4}-SPRD^{30D}-EMA_{(10,20)}$	43	13	30	512.35	256.28	6660.56	7688.52	**-1027.96**	-10.28	1067.69	-1438.24	-0.37	-5.87	30.23	-23.93	0.87	2	-4047.8
E2.3	$DIST^{V4}-SPRD^{30D}-MACD_{(12,26,9)}$	38	10	28	544.29	227.52	5442.88	6370.44	**-927.56**	-9.28	1296.34	-1609.76	-0.36	-5.71	26.32	-24.38	0.85	2.39	-4144.93
E2.4	$DIST^{V4}-SPRD^{30D}-RSI_{(14)}$	5	3	2	749.16	1293.98	2247.49	2587.97	**-340.48**	-3.4	945.5	-2515.7	-0.15	-2.38	60	-68.1	0.87	0.58	-2515.7
E2.5	$DIST^{V4}-SPRD^{30D}-BB_{(20)}$	19	12	7	230.33	467.54	2763.98	3272.79	**-508.81**	-5.09	1292.35	-941.24	-0.37	-5.87	63.16	-26.76	0.84	0.49	-3118.36
E3	$DIST^{V4}-SPRD^{30D}-DECTREE$	305	139	166	121.08	85.4	16830.25	14176.67	**2653.58**	26.54	651.07	-419.43	-0.96	-15.24	45.57	8.69	1.19	1.42	-2951.86
E4	$DIST^{V4}-SPRD^{30D}-MLP$	240	93	147	117.58	104.77	10935.31	15401.62	**-4466.31**	-44.66	856.9	-843.47	-0.98	-15.56	38.75	-18.61	0.71	1.12	-6995.95
Part VI: Models derived using the spread obtained from $JOHANSEN-SPRD^{30D}$																			
F1.1	$JOHANSEN-ZSPRD^{30D}_{(3,2)}$	21	13	8	42.9	61.55	557.7	492.38	**65.32**	0.65	131.41	-247.04	-0.28	-4.44	61.9	3.11	1.13	0.7	-490.63
F1.2	$JOHANSEN-ZSPRD^{30D}_{(3,1)}$	20	15	5	97.9	123.76	1468.48	618.79	**849.69**	8.5	532.09	-310.42	-0.27	-4.29	75	42.48	2.37	0.79	-617.95
F1.3	$JOHANSEN-ZSPRD^{30D}_{(3,0.5)}$	18	14	4	112.18	154.49	1570.49	617.95	**952.53**	9.53	651.81	-310.42	-0.28	-4.44	77.78	52.92	2.54	0.73	-617.95
F1.4	$JOHANSEN-ZSPRD^{30D}_{(2.7,2)}$	26	15	11	48.16	183.84	722.4	2022.24	**-1299.84**	-13	131.41	-1396.83	-0.32	-5.08	57.69	-50	0.36	0.26	-1984.89
F1.5	$JOHANSEN-ZSPRD^{30D}_{(2.7,1)}$	23	16	7	109.63	1046.69	1754.1	7326.84	**-5572.73**	-55.73	532.09	-6507.09	-0.32	-5.08	69.57	-242.24	0.24	0.1	-7325.99
F1.6	$JOHANSEN-ZSPRD^{30D}_{(2.7,0.5)}$	19	14	5	132.17	1204.29	1850.4	6021.46	**-4171.06**	-41.71	651.81	-5052.73	-0.37	-5.87	73.68	-219.59	0.31	0.11	-6021.46
F2.1	$JOHANSEN-SPRD^{30D}-SMA_{(10,20)}$	24	13	11	767.88	465.92	9982.38	5125.15	**4857.23**	48.57	3360.29	-1056.81	-0.08	-1.27	54.17	202.43	1.95	1.65	-1452.51
F2.2	$JOHANSEN-SPRD^{30D}-EMA_{(10,20)}$	38	18	20	1195.49	401.04	21518.8	8020.86	**13497.94**	134.98	14284.7	-1008.03	0.19	3.02	47.37	355.23	2.68	2.98	-4489.25
F2.3	$JOHANSEN-SPRD^{30D}-MACD_{(12,26,9)}$	40	19	21	652.72	484	12401.66	10163.99	**2237.66**	22.38	6435.11	-2816.45	-0.06	-0.95	47.5	55.94	1.22	1.35	-3560.87
F2.4	$JOHANSEN-SPRD^{30D}-RSI_{(14)}$	7	5	2	901.94	380.31	4509.72	760.62	**3749.1**	37.49	2162.65	-704.89	0.3	4.76	71.43	535.6	5.93	2.37	-704.89
F2.5	$JOHANSEN-SPRD^{30D}-BB_{(20)}$	22	12	10	1059.39	1215.26	12712.67	12152.61	**560.06**	5.6	10190.62	-8935.66	-0.09	-1.43	54.55	25.56	1.05	0.87	-10373.95
F3	$JOHANSEN-SPRD^{30D}-DECTREE$	350	163	187	98.56	92.49	16065.71	17295.28	**-1229.57**	-12.3	547.34	-672.38	-1.11	-17.62	46.57	-3.52	0.93	1.07	-2932.04
F4	$JOHANSEN-SPRD^{30D}-MLP$	236	116	120	114.34	136.11	13263.76	16332.81	**-3069.05**	-30.69	929.85	-1383.47	-0.79	-12.54	49.15	-13.01	0.81	0.84	-3737
Part VII: Models derived using the spread obtained from $ADF-SPRD^{30D}$																			
G1.1	$ADF-ZSPRD^{30D}_{(3,2)}$	6	3	3	949.42	513.97	2848.27	1541.9	**1306.36**	13.06	2390.54	-1188.28	0.12	1.9	50	217.73	1.85	1.85	-1243.71
G1.2	$ADF-ZSPRD^{30D}_{(3,1)}$	5	2	3	1905.63	2702.28	3811.25	8106.84	**-4295.59**	-42.96	3420.68	-4408.28	-0.3	-4.76	40	-859.12	0.47	0.71	-7716.27
G1.3	$ADF-ZSPRD^{30D}_{(3,0.5)}$	5	1	4	3928.05	2047.38	3928.06	8189.51	**-4261.46**	-42.61	3928.05	-3677.6	-0.33	-5.24	20	-852.29	0.48	1.92	-8189.51
G1.4	$ADF-ZSPRD^{30D}_{(2.7,2)}$	9	5	4	1510.98	437.36	7554.91	1749.42	**5805.49**	58.05	3233.56	-1188.28	0.4	6.35	55.56	645.14	4.32	3.45	-1451.22
G1.5	$ADF-ZSPRD^{30D}_{(2.7,1)}$	8	4	4	1498.01	1703.14	5992.05	6812.57	**-820.52**	-8.21	3420.68	-3677.6	-0.09	-1.43	50	-102.57	0.88	0.88	-5767.02
G1.6	$ADF-ZSPRD^{30D}_{(2.7,0.5)}$	8	2	6	2291.52	1726.46	4583.04	10358.76	**-5775.72**	-57.76	3928.05	-3677.6	-0.37	-5.87	25	-721.96	0.44	1.33	-9703.77
G2.1	$ADF-SPRD^{30D}-SMA_{(10,20)}$	19	10	9	1676.64	9738.27	16766.39	87644.43	**-70878.04**	-708.78	5716.48	-46621.85	-0.31	-4.92	52.63	-3730.6	0.19	0.17	-78506.74
G2.2	$ADF-SPRD^{30D}-EMA_{(10,20)}$	39	24	15	2803.78	29216.23	67290.7	438243.42	**-370952.72**	-3709.53	23401.6	-292177.53	-0.19	-3.02	61.54	-9511.12	0.15	0.1	-409479.77
G2.3	$ADF-SPRD^{30D}-MACD_{(12,26,9)}$	37	18	19	1228.56	2393.57	22114	45477.74	**-23363.74**	-233.64	3714.07	-11021.16	-0.22	-3.49	48.65	-631.4	0.49	0.51	-24298.22
G2.4	$ADF-SPRD^{30D}-RSI_{(14)}$	2	-	2	-	26538.65	-	53077.3	**-53077.3**	-530.77	-	-40142.08	-1.32	-20.95	-	-26538.65	-	-	-53077.3
G2.5	$ADF-SPRD^{30D}-BB_{(20)}$	18	7	11	3400.33	2492.23	23802.34	27414.52	**-3612.18**	-36.12	9240.83	-12456.83	-0.06	-0.95	38.89	-200.61	0.87	1.36	-14858.64
G3	$ADF-SPRD^{30D}-DECTREE$	328	155	173	104.83	91.36	16248.52	15805.63	**442.89**	4.43	697.93	-869.07	-1.01	-16.03	47.26	1.36	1.03	1.15	-1776.12
G4	$ADF-SPRD^{30D}-MLP$	219	109	110	130.61	127.89	14236.18	14067.45	**168.73**	1.69	955.67	-843.47	-0.73	-11.59	49.77	0.77	1.01	1.02	-2125.55
Part VIII: Models derived using the spread obtained from $KALMAN-SPRD^{30D}$																			
H1.1	$KALMAN-ZSPRD^{30D}_{(3,2)}$	3	3	-	942.56	-	2827.67	-	**2827.67**	28.28	1585.08	-	1.17	18.57	100	942.56	2827.67	942.56	-
H1.2	$KALMAN-ZSPRD^{30D}_{(3,1)}$	1	1	-	184.59	-	184.59	-	**184.59**	1.85	184.59	-	-	-	100	184.59	184.59	184.59	-
H1.3	$KALMAN-ZSPRD^{30D}_{(3,0.5)}$	1	1	-	1061.44	-	1061.44	-	**1061.44**	10.61	1061.44	-	-	-	100	1061.44	1061.44	1061.44	-
H1.4	$KALMAN-ZSPRD^{30D}_{(2.7,2)}$	4	2	2	1338.77	501.56	2677.54	1003.12	**1674.42**	16.74	1585.08	-792.82	0.31	4.92	50	418.61	2.67	2.67	-792.82
H1.5	$KALMAN-ZSPRD^{30D}_{(2.7,1)}$	2	1	1	184.59	1468.54	184.59	1468.54	**-1283.96**	-12.84	184.59	-1468.54	-0.62	-9.84	50	-641.98	0.13	0.13	-1468.54
H1.6	$KALMAN-ZSPRD^{30D}_{(2.7,0.5)}$	2	1	1	1061.44	1468.54	1061.44	1468.54	**-407.1**	-4.07	1061.44	-1468.54	-0.13	-2.06	50	-203.55	0.72	0.72	-1468.54
H2.1	$KALMAN-SPRD^{30D}-SMA_{(10,20)}$	12	6	6	3300.27	1362.49	19801.61	8174.92	**11626.7**	116.27	9953.38	-2923.46	0.24	3.81	50	968.89	2.42	2.42	-2923.46
H2.2	$KALMAN-SPRD^{30D}-EMA_{(10,20)}$	25	7	18	3055.34	1346.18	21387.37	24231.31	**-2843.94**	-28.44	10592.66	-3588.92	-0.08	-1.27	28	-113.76	0.88	2.27	-13703.86
H2.3	$KALMAN-SPRD^{30D}-MACD_{(12,26,9)}$	35	13	22	572.81	988.63	7446.57	21749.95	**-14303.38**	-143.03	1894.46	-5752.25	-0.39	-6.19	37.14	-408.71	0.34	0.58	-14558.94
H2.4	$KALMAN-SPRD^{30D}-RSI_{(14)}$	1	-	1	-	13346.62	-	13346.62	**-13346.62**	-133.47	-	-13346.62	-	-	-	-13346.62	-	-	-13346.62
H2.5	$KALMAN-SPRD^{30D}-BB_{(20)}$	14	8	6	607.29	797.46	4858.34	4784.78	**73.55**	0.74	1996.35	-2420.01	-0.07	-1.11	57.14	5.21	1.02	0.76	-4449.21
H3	$KALMAN-SPRD^{30D}-DECTREE$	344	165	179	101.13	92.31	16685.66	16522.85	**162.81**	1.63	716.36	-591.33	-1.06	-16.83	47.97	0.48	1.01	1.1	-2899.28
H4	$KALMAN-SPRD^{30D}-MLP$	277	131	146	112.71	113.09	14765.1	16511.14	**-1746.04**	-17.46	566.01	-682.51	-1.01	-16.03	47.29	-6.31	0.89	1	-3000.1
Part IX: Models derived using the spread obtained from $RATIO-SPRD^{30D}$																			
I1.1	$RATIO-ZSPRD^{30D}_{(3,2)}$	6	3	3	190.87	480.51	572.61	1441.52	**-868.91**	-8.69	315.01	-717.1	-0.72	-11.43	50	-144.82	0.4	0.4	-897.48
I1.2	$RATIO-ZSPRD^{30D}_{(3,1)}$	5	1	4	530.69	460.01	530.69	1840.04	**-1309.35**	-13.09	530.69	-887.67	-0.76	-12.06	20	-261.87	0.29	1.15	-1519.9
I1.3	$RATIO-ZSPRD^{30D}_{(3,0.5)}$	4	1	3	530.69	806.25	530.69	2418.76	**-1888.08**	-18.88	530.69	-1860.29	-0.62	-9.84	25	-472.02	0.22	0.66	-1888.08
I1.4	$RATIO-ZSPRD^{30D}_{(2.7,2)}$	11	6	5	153.23	396.27	919.41	1981.34	**-1061.94**	-10.62	315.01	-717.1	-0.73	-11.59	54.55	-96.51	0.46	0.39	-1180.61
I1.5	$RATIO-ZSPRD^{30D}_{(2.7,1)}$	9	4	5	281.5	373.26	1126	1866.32	**-740.32**	-7.4	530.69	-887.67	-0.52	-8.25	44.44	-82.29	0.6	0.75	-1519.9
I1.6	$RATIO-ZSPRD^{30D}_{(2.7,0.5)}$	8	5	3	242.73	806.25	1213.66	2418.76	**-1205.1**	-12.05	530.69	-1860.29	-0.41	-6.51	62.5	-150.64	0.5	0.3	-1860.29
I2.1	$RATIO-SPRD^{30D}-SMA_{(10,20)}$	14	8	6	495.01	413.33	3960.1	2479.96	**1480.14**	14.8	1983.68	-670.84	-0.07	-1.11	57.14	105.7	1.6	1.2	-1519.65
I2.2	$RATIO-SPRD^{30D}-EMA_{(10,20)}$	15	7	8	1058.95	312.73	7412.64	2501.81	**4910.83**	49.11	2524.4	-468.08	0.2	3.17	46.67	327.43	2.96	3.39	-965.51
I2.3	$RATIO-SPRD^{30D}-MACD_{(12,26,9)}$	35	13	22	534.93	199.09	6954.07	4379.95	**2574.12**	25.74	1366.95	-564.35	-0.17	-2.7	37.14	73.53	1.59	2.69	-1919.03
I2.4	$RATIO-SPRD^{30D}-RSI_{(14)}$	5	3	2	613.91	2494.67	1841.73	4989.34	**-3147.6**	-31.48	999.24	-4917.07	-0.32	-5.08	60	-629.52	0.37	0.25	-4917.07
I2.5	$RATIO-SPRD^{30D}-BB_{(20)}$	13	6	7	226.02	540.82	1356.12	3785.77	**-2429.65**	-24.3	428.2	-1889.83	-0.55	-8.73	46.15	-186.93	0.36	0.42	-2061.04
I3	$RATIO-SPRD^{30D}-DECTREE$	317	124	193	109.65	70.8	13597	13664.62	**-67.63**	-0.68	731.42	-508.22	-1.15	-18.26	39.12	-0.21	1	1.55	-1774.19
I4	$RATIO-SPRD^{30D}-MLP$	252	118	134	130.59	88.88	15409.59	11910.01	**3499.58**	35	811.5	-508.22	-0.85	-13.49	46.83	13.9	1.29	1.47	-1648.25
Part X: Models derived using the close price of QQQ.N																			
CLS-SYM-1.1	$CLOSE^{QQQ.N}-SMA_{(10,20)}$	13	6	7	194.37	151.12	1166.2	1057.82	**108.38**	1.08	605.78	-255.49	-0.28	-4.44	46.15	8.32	1.1	1.29	-788.38
CLS-SYM-1.2	$CLOSE^{QQQ.N}-EMA_{(10,20)}$	20	5	15	606.51	147.26	3032.57	2208.83	**823.74**	8.24	1524.27	-363.38	-0.08	-1.27	25	41.19	1.37	4.12	-712.96
CLS-SYM-1.3	$CLOSE^{QQQ.N}-MACD_{(12,26,9)}$	35	16	19	198.63	140.31	3178.11	2665.81	**512.3**	5.12	695.53	-296.02	-0.29	-4.6	45.71	14.62	1.19	1.42	-1251.08
CLS-SYM-1.4	$CLOSE^{QQQ.N}-RSI_{(14)}$	7	3	4	938.66	707.17	2815.99	2828.67	**-12.68**	-0.13	1724.49	-1923.52	-0.07	-1.11	42.86	-1.76	1	1.33	-1923.52
CLS-SYM-1.5	$CLOSE^{QQQ.N}-BB_{(20)}$	15	10	5	79.54	186.14	795.4	930.7	**-135.3**	-1.35	153.41	-575.2	-0.46	-7.3	66.67	-9.01	0.85	0.43	-600.51
Part XI: Models derived using the close price of XLE.N																			
CLS-SYM-2.1	$CLOSE^{XLE.N}-SMA_{(10,20)}$	19	9	10	492.93	337.96	4436.4	3379.63	**1056.77**	10.57	1969.29	-993.26	-0.03	-0.48	47.37	55.63	1.31	1.46	-2390.02
CLS-SYM-2.2	$CLOSE^{XLE.N}-EMA_{(10,20)}$	26	11	15	546.32	161.14	6009.56	2417.09	**3592.47**	35.92	2197.81	-326.2	0.12	1.9	42.31	138.19	2.49	3.39	-711.67
CLS-SYM-2.3	$CLOSE^{XLE.N}-MACD_{(12,26,9)}$	27	10	17	637.2	211.29	6372.04	3591.96	**2780.08**	27.8	1931.38	-613.01	0.05	0.79	37.04	102.99	1.77	3.02	-645.92
CLS-SYM-2.4	$CLOSE^{XLE.N}-RSI_{(14)}$	5	3	2	314.75	1213.82	944.26	2427.64	**-1483.38**	-14.83	365.04	-1229.73	-0.44	-6.98	60	-296.68	0.39	0.26	-2062.6
CLS-SYM-2.5	$CLOSE^{XLE.N}-BB_{(20)}$	20	17	3	198.62	500.07	3376.55	1500.22	**1876.33**	18.76	822.47	-1185.85	0.05	0.79	85	93.82	2.25	0.4	-1185.85

Table D.2.8: This table presents the back-test metrics for the pair $QQQ.N/XLE.N$ based on a 50-day rolling window. The table is subdivided into eleven parts, and in each of these parts, we present the back-test metrics and the trading strategies which use the spread derived from various models. In Part I, the spread is derived from the $DIST^{V1.1}$ model, in Part II from the $DIST^{V1.2}$ model, in Part III from the $DIST^{V2}$ model, in Part IV from the $DIST^{V3}$ model, in Part V from the $DIST^{V4}$ model, in Part VI from the $JOHANSEN - SPRD$ model, in Part VIII from the $ADF - SPRD$ model, in from the $DIST^{V2}$ model, in Part VIII from the $KALMAN - SPRD$ model, and in Part IX from the $RATIO - SPRD$ model. In Part X and XI, we present the back-test metrics of the trading strategies which use the close price of QQQ.N, and XLE.N, respectively. All $ numbers reported below are in USD.

(I) Trading Strategy Code	(II) Model Name	(III) Total Number of Trades	(IV) Number of Winning Trades	(V) Number of Loosing Trades	(VI) Average Profit per Trade ($)	(VII) Average Loss per Trade ($)	(VIII) Gross Profit ($)	(IX) Gross Loss ($)	(X) Net Profit ($)	(XI) ROI (%)	(XII) Max P&L ($)	(XIII) Min P&L ($)	(XIV) Daily Sharpe Ratio	(XV) Annualized Sharpe Ratio	(XVI) Hit Ratio	(XVII) Expectancy	(XVIII) Profit Factor	(XIX) Realized Risk Reward Ratio	(XX) Max Drawdown ($)
	Part I: Models derived using the spread obtained from $DIST^{V1.1} - SPRD^{50D}$																		
A1.1	$DIST^{V1.1} - ZSPRD^{50D}_{(3,2)}$	-	-	-	-	-	-	-	-	-	-	-	-	-	-	-	-	-	-
A1.2	$DIST^{V1.1} - ZSPRD^{50D}_{(3,1)}$	-	-	-	-	-	-	-	-	-	-	-	-	-	-	-	-	-	-
A1.3	$DIST^{V1.1} - ZSPRD^{50D}_{(3,0.5)}$	-	-	-	-	-	-	-	-	-	-	-	-	-	-	-	-	-	-
A1.4	$DIST^{V1.1} - ZSPRD^{50D}_{(2.7,2)}$	4	-	4	-	150.9	-	603.59	**-603.59**	-6.04	-	-226.15	-4.59	-72.86	-	-150.9	-	-	-603.59
A1.5	$DIST^{V1.1} - ZSPRD^{50D}_{(2.7,1)}$	4	1	3	1240.03	188.6	1240.03	565.79	**674.24**	6.74	1240.03	-365.13	0.02	0.32	25	168.56	2.19	6.58	-565.79
A1.6	$DIST^{V1.1} - ZSPRD^{50D}_{(2.7,0.5)}$	4	1	3	1276.35	155.9	1276.35	467.7	**808.65**	8.09	1276.35	-308.51	0.07	1.11	25	202.16	2.73	8.19	-467.7
A2.1	$DIST^{V1.1} - SPRD^{50D} - SMA_{(10,20)}$	12	7	5	441.77	641.08	3092.42	3205.4	**-112.98**	-1.13	1112.86	-1432.79	-0.22	-3.49	58.33	-9.45	0.96	0.69	-2287.18
A2.2	$DIST^{V1.1} - SPRD^{50D} - EMA_{(10,20)}$	22	16	6	424.08	851.33	6785.24	5107.97	**1677.27**	16.77	2101.89	-2011.03	-0.09	-1.43	72.73	76.27	1.33	0.5	-2246.75
A2.3	$DIST^{V1.1} - SPRD^{50D} - MACD_{(12,26,9)}$	38	28	10	254.25	319.62	7119.03	3196.2	**3922.83**	39.23	1422.9	-887.69	-0.12	-1.9	73.68	103.21	2.23	0.8	-2533.12
A2.4	$DIST^{V1.1} - SPRD^{50D} - RSI_{(14)}$	4	3	1	1695.22	1099.04	5085.67	1099.04	**3986.63**	39.87	4771.09	-1099.04	0.33	5.24	75	996.66	4.63	1.54	-1099.04
A2.5	$DIST^{V1.1} - SPRD^{50D} - BB_{(20)}$	9	6	3	304.87	574.76	1829.24	1724.28	**104.96**	1.05	968.03	-1324.15	-0.23	-3.65	66.67	11.69	1.06	0.53	-1558.57
A3	$DIST^{V1.1} - SPRD^{50D} - DECTREE$	335	156	179	108.19	87.44	16878.02	15652.62	**1225.4**	12.25	844.69	-918.24	-0.94	-14.92	46.57	3.66	1.08	1.24	-2085.64
A4	$DIST^{V1.1} - SPRD^{50D} - MLP$	315	151	164	114.95	88.49	17357.06	14512.08	**2844.99**	28.45	811.5	-368.59	-0.96	-15.24	47.94	9.04	1.2	1.3	-1830.84
	Part II: Models derived using the spread obtained from $DIST^{V1.2} - SPRD^{50D}$																		
B1.1	$DIST^{V1.2} - ZSPRD^{50D}_{(3,2)}$	5	3	2	122.54	214.89	367.63	429.78	**-62.15**	-0.62	168.56	-309.86	-0.8	-12.7	60	-12.43	0.86	0.57	-309.86
B1.2	$DIST^{V1.2} - ZSPRD^{50D}_{(3,1)}$	5	2	3	661.81	839.79	1323.62	2519.37	**-1195.75**	-11.96	830.28	-1285.49	-0.43	-6.83	40	-239.15	0.53	0.79	-1285.49
B1.3	$DIST^{V1.2} - ZSPRD^{50D}_{(3,0.5)}$	5	2	3	412.98	923.22	825.96	2769.66	**-1943.7**	-19.44	767.37	-1096.83	-0.69	-10.95	40	-388.74	0.3	0.45	-1943.7
B1.4	$DIST^{V1.2} - ZSPRD^{50D}_{(2.7,2)}$	9	5	4	113.85	233.88	569.25	935.52	**-366.27**	-3.66	168.56	-309.86	-0.98	-15.56	55.56	-40.68	0.61	0.49	-570.72
B1.5	$DIST^{V1.2} - ZSPRD^{50D}_{(2.7,1)}$	7	4	3	618.98	839.79	2475.94	2519.37	**-43.43**	-0.43	830.28	-1285.49	-0.19	-3.02	57.14	-6.25	0.98	0.74	-1285.49
B1.6	$DIST^{V1.2} - ZSPRD^{50D}_{(2.7,0.5)}$	6	2	4	412.98	761.96	825.96	3047.83	**-2221.87**	-22.22	767.37	-1096.83	-0.74	-11.75	33.33	-370.35	0.27	0.54	-2221.87
B2.1	$DIST^{V1.2} - SPRD^{50D} - SMA_{(10,20)}$	8	6	2	752.79	763.08	4516.72	1526.17	**2990.55**	29.91	1777.44	-1106.35	0.25	3.97	75	373.82	2.96	0.99	-1106.35
B2.2	$DIST^{V1.2} - SPRD^{50D} - EMA_{(10,20)}$	11	6	5	989.76	747.84	5938.58	3739.21	**2199.36**	21.99	1460.54	-1375.49	0.05	0.79	54.55	200.02	1.59	1.32	-1375.49
B2.3	$DIST^{V1.2} - SPRD^{50D} - MACD_{(12,26,9)}$	24	13	11	172.77	524.73	2246.02	5772.06	**-3526.04**	-35.26	304.33	-1381.54	-0.62	-9.84	54.17	-146.9	0.39	0.33	-4453.91
B2.4	$DIST^{V1.2} - SPRD^{50D} - RSI_{(14)}$	8	4	4	783.23	1056.11	3132.92	4224.46	**-1091.53**	-10.92	1526.8	-1736.59	-0.26	-4.13	50	-136.44	0.74	0.74	-2237.33
B2.5	$DIST^{V1.2} - SPRD^{50D} - BB_{(20)}$	8	4	4	467.19	271.94	1868.76	1087.76	**781**	7.81	1066	-673.51	-0.1	-1.59	50	97.62	1.72	1.72	-673.51
B3	$DIST^{V1.2} - SPRD^{50D} - DECTREE$	238	125	113	96.01	125.96	12000.94	14233.94	**-2233**	-22.33	477.5	-950.21	-0.94	-14.92	52.52	-9.38	0.84	0.76	-3950.91
B4	$DIST^{V1.2} - SPRD^{50D} - MLP$	222	109	113	122.07	105.02	13305.74	11867.5	**1438.24**	14.38	547.34	-502.99	-0.92	-14.6	49.1	6.48	1.12	1.16	-2074.78
	Part III: Models derived using the spread obtained from $DIST^{V2} - SPRD^{50D}$																		
C1.1	$DIST^{V2} - ZSPRD^{50D}_{(3,2)}$	-	-	-	-	-	-	-	-	-	-	-	-	-	-	-	-	-	-
C1.2	$DIST^{V2} - ZSPRD^{50D}_{(3,1)}$	-	-	-	-	-	-	-	-	-	-	-	-	-	-	-	-	-	-
C1.3	$DIST^{V2} - ZSPRD^{50D}_{(3,0.5)}$	-	-	-	-	-	-	-	-	-	-	-	-	-	-	-	-	-	-
C1.4	$DIST^{V2} - ZSPRD^{50D}_{(2.7,2)}$	4	4	-	150.9	-	603.59	-	**603.59**	6.04	226.15	-	-0.02	-0.32	100	150.9	603.59	150.9	-
C1.5	$DIST^{V2} - ZSPRD^{50D}_{(2.7,1)}$	4	3	1	188.6	1240.03	565.79	1240.03	**-674.24**	-6.74	365.13	-1240.03	-0.44	-6.98	75	-168.56	0.46	0.15	-1240.03
C1.6	$DIST^{V2} - ZSPRD^{50D}_{(2.7,0.5)}$	4	3	1	155.9	1276.35	467.7	1276.35	**-808.65**	-8.09	308.51	-1276.35	-0.49	-7.78	75	-202.16	0.37	0.12	-1276.35
C2.1	$DIST^{V2} - SPRD^{50D} - SMA_{(10,20)}$	12	7	5	580.52	538.87	4063.67	2694.37	**1369.3**	13.69	1449.08	-1112.86	-0.05	-0.79	58.33	114.07	1.51	1.08	-2275.06
C2.2	$DIST^{V2} - SPRD^{50D} - EMA_{(10,20)}$	22	6	16	851.33	424.08	5107.97	6785.24	**-1677.27**	-16.77	2011.03	-2101.89	-0.27	-4.29	27.27	-76.27	0.75	2.01	-3917.86
C2.3	$DIST^{V2} - SPRD^{50D} - MACD_{(12,26,9)}$	38	10	28	319.62	254.25	3196.2	7119.03	**-3922.83**	-39.23	887.69	-1422.9	-0.65	-10.32	26.32	-103.21	0.45	1.26	-6300.07
C2.4	$DIST^{V2} - SPRD^{50D} - RSI_{(14)}$	4	1	3	1099.04	1695.22	1099.04	5085.67	**-3986.63**	-39.87	1099.04	-4771.09	-0.44	-6.98	25	-996.66	0.22	0.65	-4826.88
C2.5	$DIST^{V2} - SPRD^{50D} - BB_{(20)}$	9	3	6	574.76	304.87	1724.28	1829.24	**-104.96**	-1.05	1324.15	-968.03	-0.27	-4.29	33.33	-11.69	0.94	1.89	-695.5
C3	$DIST^{V2} - SPRD^{50D} - DECTREE$	331	147	184	105.02	82.09	15438.28	15103.69	**334.59**	3.35	716.36	-508.22	-1.07	-16.99	44.41	1.01	1.02	1.28	-2004.83
C4	$DIST^{V2} - SPRD^{50D} - MLP$	201	107	94	101.78	107.62	10889.96	10116.61	**773.36**	7.73	859.41	-791.59	-0.93	-14.76	53.23	3.84	1.08	0.95	-2042.44
	Part IV: Models derived using the spread obtained from $DIST^{V3} - SPRD^{50D}$																		
D1.1	$DIST^{V3} - ZSPRD^{50D}_{(3,2)}$	8	3	5	130.1	287.47	390.3	1437.35	**-1047.05**	-10.47	221.06	-569.17	-0.95	-15.08	37.5	-130.88	0.27	0.45	-1140.08
D1.2	$DIST^{V3} - ZSPRD^{50D}_{(3,1)}$	7	3	4	390.31	422.17	1170.93	1688.68	**-517.75**	-5.18	487.23	-737.02	-0.47	-7.46	42.86	-73.94	0.69	0.92	-1183.11
D1.3	$DIST^{V3} - ZSPRD^{50D}_{(3,0.5)}$	7	4	3	352.8	493.39	1411.19	1480.16	**-68.97**	-0.69	580.37	-712.63	-0.33	-5.24	57.14	-9.88	0.95	0.72	-979.54
D1.4	$DIST^{V3} - ZSPRD^{50D}_{(2.7,2)}$	11	5	6	186.47	291.81	932.34	1750.86	**-818.52**	-8.19	315.01	-652.17	-0.72	-11.43	45.45	-74.43	0.53	0.64	-1213.05
D1.5	$DIST^{V3} - ZSPRD^{50D}_{(2.7,1)}$	9	4	5	305.4	372.79	1221.61	1863.95	**-642.34**	-6.42	530.69	-821.64	-0.5	-7.94	44.44	-71.4	0.66	0.82	-1358.38
D1.6	$DIST^{V3} - ZSPRD^{50D}_{(2.7,0.5)}$	9	5	4	319.55	402.5	1597.75	1610.01	**-12.26**	-0.12	530.69	-799.27	-0.34	-5.4	55.56	-1.33	0.99	0.79	-1109.39
D2.1	$DIST^{V3} - SPRD^{50D} - SMA_{(10,20)}$	22	9	13	430.78	291.22	3876.98	3785.85	**91.13**	0.91	964.67	-1289.14	-0.29	-4.6	40.91	4.15	1.02	1.48	-2031.52
D2.2	$DIST^{V3} - SPRD^{50D} - EMA_{(10,20)}$	36	10	26	561.22	266.85	5612.19	6938.13	**-1325.94**	-13.26	1347.19	-1657.64	-0.36	-5.71	27.78	-36.81	0.81	2.1	-3106
D2.3	$DIST^{V3} - SPRD^{50D} - MACD_{(12,26,9)}$	33	16	17	571.51	193.62	9144.23	3291.6	**5852.63**	58.53	1660.16	-741.41	0.05	0.79	48.48	177.32	2.78	2.95	-1640.8
D2.4	$DIST^{V3} - SPRD^{50D} - RSI_{(14)}$	7	5	2	705.35	378	3526.73	756.01	**2770.73**	27.71	1310.06	-497.21	0.39	6.19	71.43	395.83	4.66	1.87	-497.21
D2.5	$DIST^{V3} - SPRD^{50D} - BB_{(20)}$	20	14	6	243.53	416.83	3409.42	2501	**908.42**	9.08	697.93	-1035.66	-0.26	-4.13	70	45.42	1.36	0.58	-1345.49
D3	$DIST^{V3} - SPRD^{50D} - DECTREE$	345	149	196	93.46	83.97	13924.87	16458.49	**-2533.62**	-25.34	771.58	-675.27	-1.23	-19.53	43.19	-7.34	0.85	1.11	-3951.02
D4	$DIST^{V3} - SPRD^{50D} - MLP$	295	125	170	107.19	97.82	13398.43	16629.98	**-3231.55**	-32.32	547.34	-843.47	-1.09	-17.3	42.37	-10.96	0.81	1.1	-5296.2
	Part V: Models derived using the spread obtained from $DIST^{V4} - SPRD^{50D}$																		
E1.1	$DIST^{V4} - ZSPRD^{50D}_{(3,2)}$	8	3	5	130.1	287.47	390.3	1437.35	**-1047.05**	-10.47	221.06	-569.17	-0.95	-15.08	37.5	-130.88	0.27	0.45	-1140.08
E1.2	$DIST^{V4} - ZSPRD^{50D}_{(3,1)}$	7	3	4	390.31	422.17	1170.93	1688.68	**-517.75**	-5.18	487.23	-737.02	-0.47	-7.46	42.86	-73.94	0.69	0.92	-1183.11
E1.3	$DIST^{V4} - ZSPRD^{50D}_{(3,0.5)}$	7	4	3	352.8	493.39	1411.19	1480.16	**-68.97**	-0.69	580.37	-712.63	-0.33	-5.24	57.14	-9.88	0.95	0.72	-979.54
E1.4	$DIST^{V4} - ZSPRD^{50D}_{(2.7,2)}$	11	5	6	186.47	291.81	932.34	1750.86	**-818.52**	-8.19	315.01	-652.17	-0.72	-11.43	45.45	-74.43	0.53	0.64	-1213.05
E1.5	$DIST^{V4} - ZSPRD^{50D}_{(2.7,1)}$	9	4	5	305.4	372.79	1221.61	1863.95	**-642.34**	-6.42	530.69	-821.64	-0.5	-7.94	44.44	-71.4	0.66	0.82	-1358.38
E1.6	$DIST^{V4} - ZSPRD^{50D}_{(2.7,0.5)}$	9	5	4	319.55	402.5	1597.75	1610.01	**-12.26**	-0.12	530.69	-799.27	-0.34	-5.4	55.56	-1.33	0.99	0.79	-1109.39
E2.1	$DIST^{V4} - SPRD^{50D} - SMA_{(10,20)}$	22	9	13	430.78	291.22	3876.98	3785.85	**91.13**	0.91	964.67	-1289.14	-0.29	-4.6	40.91	4.15	1.02	1.48	-2031.52
E2.2	$DIST^{V4} - SPRD^{50D} - EMA_{(10,20)}$	36	10	26	561.22	266.85	5612.19	6938.13	**-1325.94**	-13.26	1347.19	-1657.64	-0.36	-5.71	27.78	-36.81	0.81	2.1	-3106
E2.3	$DIST^{V4} - SPRD^{50D} - MACD_{(12,26,9)}$	33	16	17	571.51	193.62	9144.23	3291.6	**5852.63**	58.53	1660.16	-741.41	0.05	0.79	48.48	177.32	2.78	2.95	-1640.8
E2.4	$DIST^{V4} - SPRD^{50D} - RSI_{(14)}$	7	5	2	705.35	378	3526.73	756.01	**2770.73**	27.71	1310.06	-497.21	0.39	6.19	71.43	395.83	4.66	1.87	-497.21
E2.5	$DIST^{V4} - SPRD^{50D} - BB_{(20)}$	20	14	6	243.53	416.83	3409.42	2501	**908.42**	9.08	697.93	-1035.66	-0.26	-4.13	70	45.42	1.36	0.58	-1345.49
E3	$DIST^{V4} - SPRD^{50D} - DECTREE$	345	145	200	95.02	84.84	13777.9	16968.38	**-3190.48**	-31.9	771.58	-390.44	-1.27	-20.16	42.03	-9.25	0.81	1.12	-3970.57
E4	$DIST^{V4} - SPRD^{50D} - MLP$	295	125	170	107.19	97.82	13398.43	16629.98	**-3231.55**	-32.32	547.34	-843.47	-1.09	-17.3	42.37	-10.96	0.81	1.1	-5296.2
	Part VI: Models derived using the spread obtained from $JOHANSEN - SPRD^{50D}$																		
F1.1	$JOHANSEN - ZSPRD^{50D}_{(3,2)}$	21	10	11	49.52	42.13	495.15	463.44	**31.71**	0.32	144.01	-95.16	-1.49	-23.65	47.62	1.51	1.07	1.18	-122.4
F1.2	$JOHANSEN - ZSPRD^{50D}_{(3,1)}$	20	11	9	56.17	93.09	617.82	837.85	**-220.03**	-2.2	197.29	-378.29	-0.89	-14.13	55	-11	0.74	0.6	-423.82
F1.3	$JOHANSEN - ZSPRD^{50D}_{(3,0.5)}$	19	11	8	66.3	58.17	729.26	465.39	**263.87**	2.64	197.29	-167.41	-0.86	-13.65	57.89	13.88	1.57	1.14	-228
F1.4	$JOHANSEN - ZSPRD^{50D}_{(2.7,2)}$	24	13	11	56.99	44.91	740.88	494.05	**246.84**	2.47	161.2	-95.16	-1.48	-23.49	54.17	10.29	1.5	1.27	-153.01
F1.5	$JOHANSEN - ZSPRD^{50D}_{(2.7,1)}$	23	14	9	78.7	93.36	1101.8	840.26	**261.55**	2.62	399.45	-378.29	-0.83	-13.18	60.87	11.37	1.31	0.84	-426.23
F1.6	$JOHANSEN - ZSPRD^{50D}_{(2.7,0.5)}$	20	14	6	85.23	93.01	1193.29	558.07	**635.22**	6.35	399.45	-184.98	-0.79	-12.54	70	31.76	2.14	0.92	-352.39
F2.1	$JOHANSEN - SPRD^{50D} - SMA_{(10,20)}$	24	12	12	450.45	533.34	5405.45	6400.03	**-994.57**	-9.95	2529.96	-1375.28	-0.11	-1.75	50	-41.44	0.84	0.84	-2481.22
F2.2	$JOHANSEN - SPRD^{50D} - EMA_{(10,20)}$	29	14	15	568.51	718.4	7959.17	10776.03	**-2816.86**	-28.17	3767.65	-6466.61	-0.05	-0.79	48.28	-97.08	0.74	0.79	-8345.48
F2.3	$JOHANSEN - SPRD^{50D} - MACD_{(12,26,9)}$	34	14	20	922.64	436.35	12916.94	8727.07	**4189.87**	41.9	8576.92	-2378.66	0.12	1.9	41.18	123.28	1.48	2.11	-5878.18
F2.4	$JOHANSEN - SPRD^{50D} - RSI_{(14)}$	10	6	4	342.75	1531.62	2056.47	6126.47	**-4070**	-40.7	840.7	-5714.41	-0.37	-5.87	60	-407	0.34	0.22	-5935.06
F2.5	$JOHANSEN - SPRD^{50D} - BB_{(20)}$	23	12	11	834.34	34388.05	10012.13	378268.57	**-368256.44**	-3682.56	6943.82	-366873.55	-0.21	-3.33	52.17	-16012.53	0.03	0.02	-368985.29
F3	$JOHANSEN - SPRD^{50D} - DECTREE$	310	159	151	91	107.49	14469.42	16231.28	**-1761.86**	-17.62	716.36	-682.51	-1.1	-17.46	51.29	-5.68	0.89	0.85	-4213.12
F4	$JOHANSEN - SPRD^{50D} - MLP$	270	125	145	95.55	129	11943.79	18705.49	**-6761.7**	-67.62	766.92	-706.4	-1.02	-16.19	46.3	-25.04	0.64	0.74	-8212.8
	Part VII: Models derived using the spread obtained from $ADF - SPRD^{50D}$																		
G1.1	$ADF - ZSPRD^{50D}_{(3,2)}$	5	2	3	133.29	3144.52	266.58	9433.56	**-9166.98**	-91.67	161.5	-5366.21	-0.87	-13.81	40	-1833.4	0.03	0.04	-9272.06
G1.2	$ADF - ZSPRD^{50D}_{(3,1)}$	4	1	3	5345.19	4834.78	5345.19	14504.33	**-9159.14**	-91.59	5345.19	-6550.89	-0.28	-4.44	25	-2289.79	0.37	1.11	-9159.15
G1.3	$ADF - ZSPRD^{50D}_{(3,0.5)}$	4	1	3	5345.19	5497.88	5345.19	16493.64	**-11148.46**	-111.48	5345.19	-7492.56	-0.34	-5.4	25	-2787.11	0.32	0.97	-11148.46
G1.4	$ADF - ZSPRD^{50D}_{(2.7,2)}$	9	2	7	244.41	3129.23	488.82	21904.58	**-21415.76**	-214.16	327.32	-9831.32	-0.75	-11.91	22.22	-2379.6	0.02	0.08	-21743.08
G1.5	$ADF - ZSPRD^{50D}_{(2.7,1)}$	8	2	6	2739.28	5512.58	5478.57	33075.5	**-27596.93**	-275.97	5345.19	-12770.75	-0.54	-8.57	25	-3449.62	0.17	0.5	-27596.93
G1.6	$ADF - ZSPRD^{50D}_{(2.7,0.5)}$	8	2	6	3014.27	6505.13	6028.54	39030.79	**-33002.25**	-330.02	5345.19	-18103.75	-0.53	-8.41	25	-4125.28	0.15	0.46	-33002.25
G2.1	$ADF - SPRD^{50D} - SMA_{(10,20)}$	20	11	9	20055.86	150466.16	220614.51	1354195.48	**-1133580.98**	-11335.81	212050.53	-1345283.82	-0.18	-2.86	55	-56679.05	0.16	0.13	-1350163.17
G2.2	$ADF - SPRD^{50D} - EMA_{(10,20)}$	37	25	12	6623.26	3795.36	165581.49	45544.27	**120037.22**	1200.37	95809.15	-19354.91	0.18	2.86	67.57	3244.5	3.64	1.75	-30977.99
G2.3	$ADF - SPRD^{50D} - MACD_{(12,26,9)}$	31	21	10	8347.99	1747.23	175307.83	17472.35	**157835.48**	1578.35	83618.08	-5345.19	0.28	4.44	67.74	5091.27	10.03	4.78	-7527.07
G2.4	$ADF - SPRD^{50D} - RSI_{(14)}$	4	1	3	1447.85	16190.39	1447.85	48571.17	**-47123.32**	-471.23	1447.85	-29969.36	-0.88	-13.97	25	-11780.83	0.03	0.09	-48571.17
G2.5	$ADF - SPRD^{50D} - BB_{(20)}$	17	5	12	3825.62	863.12	19128.11	10357.44	**8770.67**	87.71	10177.53	-2823.91	0.17	2.7	29.41	515.84	1.85	4.43	-6851.03
G3	$ADF - SPRD^{50D} - DECTREE$	302	139	163	116.98	91.93	16260.18	14984.98	**1275.21**	12.75	918.24	-768.37	-0.96	-15.24	46.03	4.23	1.09	1.27	-2250.32
G4	$ADF - SPRD^{50D} - MLP$	140	72	68	151.71	181.59	10922.92	12348.28	**-1425.36**	-14.25	1262.9	-1455.41	-0.58	-9.21	51.43	-10.18	0.88	0.84	-3075.43
	Part VIII: Models derived using the spread obtained from $KALMAN - SPRD^{50D}$																		
H1.1	$KALMAN - ZSPRD^{50D}_{(3,2)}$	1	1	-	150.18	-	150.18	-	**150.18**	1.5	150.18	-	-	-	100	150.18	150.18	150.18	-
H1.2	$KALMAN - ZSPRD^{50D}_{(3,1)}$	-	-	-	-	-	-	-	-	-	-	-	-	-	-	-	-	-	-
H1.3	$KALMAN - ZSPRD^{50D}_{(3,0.5)}$	-	-	-	-	-	-	-	-	-	-	-	-	-	-	-	-	-	-
H1.4	$KALMAN - ZSPRD^{50D}_{(2.7,2)}$	4	3	1	685.34	686.16	2056.01	686.16	**1369.85**	13.7	1586.97	-686.16	0.25	3.97	75	342.46	3	1	-686.16
H1.5	$KALMAN - ZSPRD^{50D}_{(2.7,1)}$	3	1	2	2515.71	1541.06	2515.71	3082.11	**-566.4**	-5.66	2515.71	-2482.48	-0.11	-1.75	33.33	-188.94	0.82	1.63	-2482.48
H1.6	$KALMAN - ZSPRD^{50D}_{(2.7,0.5)}$	3	1	2	3118.21	2233.52	3118.21	4467.03	**-1348.82**	-13.49	3118.21	-2418.95	-0.16	-2.54	33.33	-449.78	0.7	1.4	-2418.95
H2.1	$KALMAN - SPRD^{50D} - SMA_{(10,20)}$	15	6	9	1535.71	1006.43	9214.28	9057.88	**156.4**	1.56	3246.16	-2819.47	-0.05	-0.79	40	10.43	1.02	1.53	-3852.88
H2.2	$KALMAN - SPRD^{50D} - EMA_{(10,20)}$	21	7	14	2317.48	1109.23	16222.39	15529.15	**693.24**	6.93	11503.72	-3333.91	-0.03	-0.48	33.33	32.9	1.04	2.09	-14278.43
H2.3	$KALMAN - SPRD^{50D} - MACD_{(12,26,9)}$	29	12	17	801.02	851.21	9612.2	14470.56	**-4858.36**	-48.58	2693.84	-1990.68	-0.24	-3.81	41.38	-167.52	0.66	0.94	-7445.43
H2.4	$KALMAN - SPRD^{50D} - RSI_{(14)}$	2	1	1	1454.44	11697.95	1454.44	11697.95	**-10243.51**	-102.44	1454.44	-11697.95	-0.54	-8.57	50	-5121.75	0.12	0.12	-11697.95
H2.5	$KALMAN - SPRD^{50D} - BB_{(20)}$	14	7	7	720.54	1159.02	5043.75	8113.11	**-3069.36**	-30.69	1997.01	-3505.85	-0.2	-3.17	50	-219.24	0.62	0.62	-6139.95
H3	$KALMAN - SPRD^{50D} - DECTREE$	330	153	177	101.27	101.82	15494.53	18022.59	**-2528.05**	-25.28	716.36	-918.24	-1.04	-16.51	46.36	-7.67	0.86	0.99	-4027.82
H4	$KALMAN - SPRD^{50D} - MLP$	156	73	83	99.21	124.6	7242.43	10341.64	**-3099.21**	-30.99	572.08	-1565.91	-0.84	-13.33	46.79	-19.88	0.7	0.8	-5532.94
	Part IX: Models derived using the spread obtained from $RATIO - SPRD^{50D}$																		
I1.1	$RATIO - ZSPRD^{50D}_{(3,2)}$	5	2	3	240.84	608.66	481.69	1825.97	**-1344.28**	-13.44	370.84	-836.11	-0.83	-13.18	40	-268.86	0.26	0.4	-1344.28
I1.2	$RATIO - ZSPRD^{50D}_{(3,1)}$	4	2	2	378.87	346.53	757.74	693.06	**64.68**	0.65	580.37	-518.47	-0.29	-4.6	50	16.17	1.09	1.09	-518.47
I1.3	$RATIO - ZSPRD^{50D}_{(3,0.5)}$	4	2	2	259.68	293.36	519.36	586.72	**-67.36**	-0.67	509.22	-529.77	-0.4	-6.35	50	-16.84	0.89	0.89	-529.77
I1.4	$RATIO - ZSPRD^{50D}_{(2.7,2)}$	10	4	6	49.05	442.91	196.18	2657.47	**-2461.29**	-24.61	79.67	-836.11	-1.22	-19.37	40	-246.13	0.07	0.11	-2498.38
I1.5	$RATIO - ZSPRD^{50D}_{(2.7,1)}$	8	5	3	180.17	574.57	900.86	1723.71	**-822.85**	-8.23	387.24	-1544.66	-0.42	-6.67	62.5	-102.86	0.52	0.31	-1544.66
I1.6	$RATIO - ZSPRD^{50D}_{(2.7,0.5)}$	8	6	2	200.51	900.54	1203.08	1801.08	**-598**	-5.98	585.45	-1711.81	-0.33	-5.24	75	-74.75	0.67	0.22	-1711.81
I2.1	$RATIO - SPRD^{50D} - SMA_{(10,20)}$	14	8	6	495.01	413.33	3960.1	2479.96	**1480.14**	14.8	1983.68	-670.84	-0.07	-1.11	57.14	105.7	1.6	1.2	-1519.65
I2.2	$RATIO - SPRD^{50D} - EMA_{(10,20)}$	15	7	8	1033.8	312.73	7236.58	2501.81	**4734.77**	47.35	2524.4	-468.08	0.19	3.02	46.67	315.7	2.89	3.31	-965.51
I2.3	$RATIO - SPRD^{50D} - MACD_{(12,26,9)}$	32	13	19	545.08	240.17	7086.05	4563.26	**2522.79**	25.23	1366.95	-564.35	-0.15	-2.38	40.62	78.8	1.55	2.27	-1919.03
I2.4	$RATIO - SPRD^{50D} - RSI_{(14)}$	6	4	2	479.04	2428.88	1916.17	4857.76	**-2941.6**	-29.42	999.24	-4598.97	-0.31	-4.92	66.67	-490.17	0.39	0.2	-4598.97
I2.5	$RATIO - SPRD^{50D} - BB_{(20)}$	13	6	7	226.02	540.82	1356.12	3785.77	**-2429.65**	-24.3	428.2	-1889.83	-0.55	-8.73	46.15	-186.93	0.36	0.42	-2061.04
I3	$RATIO - SPRD^{50D} - DECTREE$	307	128	179	111.22	72.36	14235.61	12952.06	**1283.55**	12.84	734.68	-508.22	-1.09	-17.3	41.69	4.17	1.1	1.54	-1569.69
I4	$RATIO - SPRD^{50D} - MLP$	256	113	143	123.39	91.62	13942.75	13101.32	**841.43**	8.41	734.68	-508.22	-0.97	-15.4	44.14	3.29	1.06	1.35	-2575.75
	Part X: Models derived using the close price of QQQ.N																		
CLS-SYM-1.1	$CLOSE^{QQQ.N} - SMA_{(10,20)}$	13	6	7	194.37	151.12	1166.2	1057.82	**108.38**	1.08	605.78	-255.49	-0.28	-4.44	46.15	8.32	1.1	1.29	-788.38
CLS-SYM-1.2	$CLOSE^{QQQ.N} - EMA_{(10,20)}$	20	5	15	606.51	147.26	3032.57	2208.83	**823.74**	8.24	1524.27	-363.38	-0.08	-1.27	25	41.19	1.37	4.12	-712.96
CLS-SYM-1.3	$CLOSE^{QQQ.N} - MACD_{(12,26,9)}$	35	16	19	198.63	140.31	3178.11	2665.81	**512.3**	5.12	695.53	-296.02	-0.29	-4.6	45.71	14.62	1.19	1.42	-1251.08
CLS-SYM-1.4	$CLOSE^{QQQ.N} - RSI_{(14)}$	7	3	4	938.66	707.17	2815.99	2828.67	**-12.68**	-0.13	1724.49	-1923.52	-0.07	-1.11	42.86	-1.76	1	1.33	-1923.52
CLS-SYM-1.5	$CLOSE^{QQQ.N} - BB_{(20)}$	15	10	5	79.54	186.14	795.4	930.7	**-135.3**	-1.35	153.41	-575.2	-0.46	-7.3	66.67	-9.01	0.85	0.43	-600.51
	Part XI: Models derived using the close price of XLE.N																		
CLS-SYM-2.1	$CLOSE^{XLE.N} - SMA_{(10,20)}$	19	9	10	492.93	337.96	4436.4	3379.63	**1056.77**	10.57	1969.29	-993.26	-0.03	-0.48	47.37	55.63	1.31	1.46	-2390.02
CLS-SYM-2.2	$CLOSE^{XLE.N} - EMA_{(10,20)}$	26	11	15	546.32	161.14	6009.56	2417.09	**3592.47**	35.92	2197.81	-326.2	0.12	1.9	42.31	138.19	2.49	3.39	-711.67
CLS-SYM-2.3	$CLOSE^{XLE.N} - MACD_{(12,26,9)}$	27	10	17	637.2	211.29	6372.04	3591.96	**2780.08**	27.8	1931.38	-613.01	0.05	0.79	37.04	102.99	1.77	3.02	-645.92
CLS-SYM-2.4	$CLOSE^{XLE.N} - RSI_{(14)}$	5	3	2	314.75	1213.82	944.26	2427.64	**-1483.38**	-14.83	365.04	-1229.73	-0.44	-6.98	60	-296.68	0.39	0.26	-2062.6
CLS-SYM-2.5	$CLOSE^{XLE.N} - BB_{(20)}$	20	17	3	198.62	500.07	3376.55	1500.22	**1876.33**	18.76	822.47	-1185.85	0.05	0.79	85	93.82	2.25	0.4	-1185.85

Table D.2.9: This table presents the back-test metrics for the pair $QQQ.N/XLE.N$ based on a 100-day rolling window. The table is subdivided into eleven parts, and in each of these parts, we present the back-test metrics and the trading strategies which use the spread derived from various models. In Part I, the spread is derived from the $DIST^{V1.1}$ model, in Part II from the $DIST^{V1.2}$ model, in Part III from the $DIST^{V2}$ model, in Part IV from the $DIST^{V3}$ model, in Part V from the $DIST^{V4}$ model, in Part VI from the $JOHANSEN-SPRD$ model, in Part VIII from the $ADF-SPRD$ model, in from the $DIST^{V2}$ model, in Part VIII from the $KALMAN-SPRD$ model, and in Part IX from the $RATIO-SPRD$ model. In Part X and XI, we present the back-test metrics of the trading strategies which use the close price of QQQ.N, and XLE.N, respectively. All $ numbers reported below are in USD.

(I) Trading Strategy Code	(II) Model Name	(III) Total Number of Trades	(IV) Number of Winning Trades	(V) Number of Loosing Trades	(VI) Average Profit per Trade ($)	(VII) Average Loss per Trade ($)	(VIII) Gross Profit ($)	(IX) Gross Loss ($)	(X) Net Profit ($)	(XI) ROI (%)	(XII) Max P&L ($)	(XIII) Min P&L ($)	(XIV) Daily Sharpe Ratio	(XV) Annualized Sharpe Ratio	(XVI) Hit Ratio	(XVII) Expectancy	(XVIII) Profit Factor	(XIX) Realized Risk Reward Ratio	(XX) Max Drawdown ($)
Part I: Models derived using the spread obtained from $DIST^{V1.1}-SPRD^{100D}$																			
A1.1	$DIST^{V1.1}-ZSPRD^{100D}_{(3,2)}$	-	-	-	-	-	-	-	-	-	-	-	-	-	-	-	-	-	-
A1.2	$DIST^{V1.1}-ZSPRD^{100D}_{(3,1)}$	-	-	-	-	-	-	-	-	-	-	-	-	-	-	-	-	-	-
A1.3	$DIST^{V1.1}-ZSPRD^{100D}_{(3,0.5)}$	-	-	-	-	-	-	-	-	-	-	-	-	-	-	-	-	-	-
A1.4	$DIST^{V1.1}-ZSPRD^{100D}_{(2.7,2)}$	1	-	1	-	159.92	-	159.92	**-159.92**	-1.6	-	-159.92	-	-	-	-159.92	-	-	-159.92
A1.5	$DIST^{V1.1}-ZSPRD^{100D}_{(2.7,1)}$	1	1	-	1190.07	-	1190.07	-	**1190.07**	11.9	1190.07	-	-	-	100	1190.07	1190.07	1190.07	-
A1.6	$DIST^{V1.1}-ZSPRD^{100D}_{(2.7,0.5)}$	1	1	-	1871.51	-	1871.51	-	**1871.51**	18.72	1871.51	-	-	-	100	1871.51	1871.51	1871.51	-
A2.1	$DIST^{V1.1}-SPRD^{100D}-SMA_{(10,20)}$	11	6	5	477.49	641.08	2864.92	3205.4	**-340.48**	-3.4	1112.86	-1432.79	-0.24	-3.81	54.55	-30.9	0.89	0.74	-2287.18
A2.2	$DIST^{V1.1}-SPRD^{100D}-EMA_{(10,20)}$	22	16	6	441.54	849.29	7064.57	5095.72	**1968.85**	19.69	2101.89	-2011.03	-0.07	-1.11	72.73	89.53	1.39	0.52	-2246.75
A2.3	$DIST^{V1.1}-SPRD^{100D}-MACD_{(12,26,9)}$	37	23	14	272.55	238.65	6268.64	3341.12	**2927.52**	29.28	1422.9	-887.69	-0.19	-3.02	62.16	79.11	1.88	1.14	-2533.12
A2.4	$DIST^{V1.1}-SPRD^{100D}-RSI_{(14)}$	5	3	2	1640.03	592.73	4920.09	1185.47	**3734.62**	37.35	4133.83	-1099.04	0.3	4.76	60	746.92	4.15	2.77	-1099.04
A2.5	$DIST^{V1.1}-SPRD^{100D}-BB_{(20)}$	9	6	3	304.87	574.76	1829.24	1724.28	**104.96**	1.05	968.03	-1324.15	-0.23	-3.65	66.67	11.69	1.06	0.53	-1558.57
A3	$DIST^{V1.1}-SPRD^{100D}-DECTREE$	321	149	172	114.35	83.63	17037.85	14384.92	**2652.93**	26.53	716.36	-420.52	-0.97	-15.4	46.42	8.27	1.18	1.37	-2429.43
A4	$DIST^{V1.1}-SPRD^{100D}-MLP$	271	129	142	109.93	89.1	14181.39	12652.42	**1528.96**	15.29	673.13	-306.2	-1.01	-16.03	47.6	5.64	1.12	1.23	-2641.37
Part II: Models derived using the spread obtained from $DIST^{V1.2}-SPRD^{100D}$																			
B1.1	$DIST^{V1.2}-ZSPRD^{100D}_{(3,2)}$	2	1	1	302.72	489.82	302.72	489.82	**-187.1**	-1.87	302.72	-489.82	-0.44	-6.98	50	-93.55	0.62	0.62	-489.82
B1.2	$DIST^{V1.2}-ZSPRD^{100D}_{(3,1)}$	2	1	1	239.68	479.77	239.68	479.77	**-240.09**	-2.4	239.68	-479.77	-0.53	-8.41	50	-120.05	0.5	0.5	-479.77
B1.3	$DIST^{V1.2}-ZSPRD^{100D}_{(3,0.5)}$	2	1	1	875.55	983.86	875.54	983.86	**-108.31**	-1.08	875.55	-983.86	-0.16	-2.54	50	-54.15	0.89	0.89	-983.86
B1.4	$DIST^{V1.2}-ZSPRD^{100D}_{(2.7,2)}$	3	-	3	-	238.08	-	714.23	**-714.23**	-7.14	-	-489.82	-1.62	-25.72	-	-238.08	-	-	-714.23
B1.5	$DIST^{V1.2}-ZSPRD^{100D}_{(2.7,1)}$	3	-	3	-	631.26	-	1893.78	**-1893.78**	-18.94	-	-1324.84	-1.24	-19.68	-	-631.26	-	-	-1893.78
B1.6	$DIST^{V1.2}-ZSPRD^{100D}_{(2.7,0.5)}$	3	1	2	551.03	1272.51	551.03	2545.03	**-1994**	-19.94	551.03	-1561.17	-0.75	-11.91	33.33	-664.73	0.22	0.43	-2545.03
B2.1	$DIST^{V1.2}-SPRD^{100D}-SMA_{(10,20)}$	8	4	4	547.31	738.1	2189.26	2952.41	**-763.16**	-7.63	1137.14	-1091.31	-0.32	-5.08	50	-95.39	0.74	0.74	-1545.35
B2.2	$DIST^{V1.2}-SPRD^{100D}-EMA_{(10,20)}$	12	7	5	720.14	570.53	5040.96	2852.63	**2188.33**	21.88	2272.11	-1226.64	0.03	0.48	58.33	182.32	1.77	1.26	-1789.81
B2.3	$DIST^{V1.2}-SPRD^{100D}-MACD_{(12,26,9)}$	22	12	10	394.47	400.75	4733.65	4007.54	**726.11**	7.26	1010.72	-1217.21	-0.22	-3.49	54.55	33.04	1.18	0.98	-2697.45
B2.4	$DIST^{V1.2}-SPRD^{100D}-RSI_{(14)}$	5	2	3	1285.34	1545.7	2570.68	4637.11	**-2066.44**	-20.66	1343.94	-3224.51	-0.3	-4.76	40	-413.29	0.55	0.83	-1297.98
B2.5	$DIST^{V1.2}-SPRD^{100D}-BB_{(20)}$	10	2	8	955.91	299.1	1911.83	2392.77	**-480.94**	-4.81	961.62	-944.06	-0.33	-5.24	20	-48.09	0.8	3.2	-1022.1
B3	$DIST^{V1.2}-SPRD^{100D}-DECTREE$	276	128	148	109.75	98.18	14047.85	14530.84	**-482.99**	-4.83	682.51	-895.06	-1.01	-16.03	46.38	-1.74	0.97	1.12	-1923.5
B4	$DIST^{V1.2}-SPRD^{100D}-MLP$	127	59	68	107.97	116.73	6370.22	7937.68	**-1567.45**	-15.67	513.65	-432.07	-1.09	-17.3	46.46	-12.33	0.8	0.92	-2418.02
Part III: Models derived using the spread obtained from $DIST^{V2}-SPRD^{100D}$																			
C1.1	$DIST^{V2}-ZSPRD^{100D}_{(3,2)}$	-	-	-	-	-	-	-	-	-	-	-	-	-	-	-	-	-	-
C1.2	$DIST^{V2}-ZSPRD^{100D}_{(3,1)}$	-	-	-	-	-	-	-	-	-	-	-	-	-	-	-	-	-	-
C1.3	$DIST^{V2}-ZSPRD^{100D}_{(3,0.5)}$	-	-	-	-	-	-	-	-	-	-	-	-	-	-	-	-	-	-
C1.4	$DIST^{V2}-ZSPRD^{100D}_{(2.7,2)}$	1	1	-	159.92	-	159.92	-	**159.92**	1.6	159.92	-	-	-	100	159.92	159.92	159.92	-
C1.5	$DIST^{V2}-ZSPRD^{100D}_{(2.7,1)}$	1	-	1	-	1190.07	-	1190.07	**-1190.07**	-11.9	-	-1190.07	-	-	-	-1190.07	-	-	-1190.07
C1.6	$DIST^{V2}-ZSPRD^{100D}_{(2.7,0.5)}$	1	-	1	-	1871.51	-	1871.51	**-1871.51**	-18.72	-	-1871.51	-	-	-	-1871.51	-	-	-1871.51
C2.1	$DIST^{V2}-SPRD^{100D}-SMA_{(10,20)}$	11	5	6	641.08	477.49	3205.4	2864.92	**340.48**	3.4	1432.79	-1112.86	-0.16	-2.54	45.45	30.9	1.12	1.34	-2275.06
C2.2	$DIST^{V2}-SPRD^{100D}-EMA_{(10,20)}$	22	6	16	849.29	441.54	5095.72	7064.57	**-1968.85**	-19.69	2011.03	-2101.89	-0.29	-4.6	27.27	-89.53	0.72	1.92	-3917.86
C2.3	$DIST^{V2}-SPRD^{100D}-MACD_{(12,26,9)}$	37	14	23	238.65	272.55	3341.12	6268.64	**-2927.52**	-29.28	887.69	-1422.9	-0.59	-9.37	37.84	-79.11	0.53	0.88	-5372.95
C2.4	$DIST^{V2}-SPRD^{100D}-RSI_{(14)}$	5	2	3	592.73	1640.03	1185.47	4920.09	**-3734.62**	-37.35	1099.04	-4133.83	-0.45	-7.14	40	-746.92	0.24	0.36	-4189.62
C2.5	$DIST^{V2}-SPRD^{100D}-BB_{(20)}$	9	3	6	574.76	304.87	1724.28	1829.24	**-104.96**	-1.05	1324.15	-968.03	-0.27	-4.29	33.33	-11.69	0.94	1.89	-695.5
C3	$DIST^{V2}-SPRD^{100D}-DECTREE$	320	147	173	117.57	91.69	17282.9	15861.65	**1421.25**	14.21	716.36	-918.24	-0.92	-14.6	45.94	4.45	1.09	1.28	-2170.69
C4	$DIST^{V2}-SPRD^{100D}-MLP$	266	134	132	121.66	91.55	16301.98	12085.14	**4216.83**	42.17	716.36	-420.52	-0.87	-13.81	50.38	15.86	1.35	1.33	-2101.63
Part IV: Models derived using the spread obtained from $DIST^{V3}-SPRD^{100D}$																			
D1.1	$DIST^{V3}-ZSPRD^{100D}_{(3,2)}$	4	3	1	124.27	375.49	372.82	375.49	**-2.66**	-0.03	164.67	-375.49	-0.61	-9.68	75	-0.67	0.99	0.33	-375.49
D1.2	$DIST^{V3}-ZSPRD^{100D}_{(3,1)}$	3	2	1	162.39	357.33	324.79	357.33	**-32.55**	-0.33	188.34	-357.33	-0.54	-8.57	66.67	-10.83	0.91	0.45	-357.33
D1.3	$DIST^{V3}-ZSPRD^{100D}_{(3,0.5)}$	3	1	2	270.69	994.17	270.69	1988.33	**-1717.64**	-17.18	270.69	-1406.01	-0.86	-13.65	33.33	-572.59	0.14	0.27	-1988.33
D1.4	$DIST^{V3}-ZSPRD^{100D}_{(2.7,2)}$	6	5	1	160.14	412.12	800.69	412.12	**388.57**	3.89	221.67	-412.12	-0.37	-5.87	83.33	64.74	1.94	0.39	-412.12
D1.5	$DIST^{V3}-ZSPRD^{100D}_{(2.7,1)}$	4	3	1	290	394.13	870	394.13	**475.87**	4.76	545.22	-394.13	-0.09	-1.43	75	118.97	2.21	0.74	-394.13
D1.6	$DIST^{V3}-ZSPRD^{100D}_{(2.7,0.5)}$	4	2	2	381.87	994.47	763.74	1988.94	**-1225.2**	-12.25	493.05	-1406.62	-0.53	-8.41	50	-306.3	0.38	0.38	-1988.94
D2.1	$DIST^{V3}-SPRD^{100D}-SMA_{(10,20)}$	17	5	12	604.68	402.79	3023.4	4833.43	**-1810.03**	-18.1	970.38	-1516.61	-0.43	-6.83	29.41	-106.49	0.63	1.5	-3269.66
D2.2	$DIST^{V3}-SPRD^{100D}-EMA_{(10,20)}$	29	12	17	490.49	361.93	5885.85	6152.74	**-266.89**	-2.67	1121.85	-1455.18	-0.28	-4.44	41.38	-9.2	0.96	1.36	-3187.54
D2.3	$DIST^{V3}-SPRD^{100D}-MACD_{(12,26,9)}$	29	10	19	394	267.29	3940.05	5078.52	**-1138.47**	-11.38	849.89	-1328.51	-0.43	-6.83	34.48	-39.28	0.78	1.47	-3329.71
D2.4	$DIST^{V3}-SPRD^{100D}-RSI_{(14)}$	6	5	1	609.78	3646.2	3048.89	3646.2	**-597.31**	-5.97	910.29	-3646.2	-0.14	-2.22	83.33	-99.69	0.84	0.17	-
D2.5	$DIST^{V3}-SPRD^{100D}-BB_{(20)}$	16	8	8	142.95	292.86	1143.58	2342.87	**-1199.29**	-11.99	332.27	-817.41	-0.72	-11.43	50	-74.96	0.49	0.49	-1416.39
D3	$DIST^{V3}-SPRD^{100D}-DECTREE$	299	135	164	111.42	83.68	15041.81	13723.44	**1318.37**	13.18	699.95	-843.47	-1	-15.87	45.15	4.41	1.1	1.33	-1736.9
D4	$DIST^{V3}-SPRD^{100D}-MLP$	223	93	130	134.37	91.49	12496.29	11894.04	**602.25**	6.02	1000.7	-498.26	-0.91	-14.45	41.7	2.69	1.05	1.47	-1333.47
Part V: Models derived using the spread obtained from $DIST^{V4}-SPRD^{100D}$																			
E1.1	$DIST^{V4}-ZSPRD^{100D}_{(3,2)}$	4	3	1	124.27	375.49	372.82	375.49	**-2.66**	-0.03	164.67	-375.49	-0.61	-9.68	75	-0.67	0.99	0.33	-375.49
E1.2	$DIST^{V4}-ZSPRD^{100D}_{(3,1)}$	3	2	1	162.39	357.33	324.79	357.33	**-32.55**	-0.33	188.34	-357.33	-0.54	-8.57	66.67	-10.83	0.91	0.45	-357.33
E1.3	$DIST^{V4}-ZSPRD^{100D}_{(3,0.5)}$	3	1	2	270.69	994.17	270.69	1988.33	**-1717.64**	-17.18	270.69	-1406.01	-0.86	-13.65	33.33	-572.59	0.14	0.27	-1988.33
E1.4	$DIST^{V4}-ZSPRD^{100D}_{(2.7,2)}$	6	5	1	160.14	412.12	800.69	412.12	**388.57**	3.89	221.67	-412.12	-0.37	-5.87	83.33	64.74	1.94	0.39	-412.12
E1.5	$DIST^{V4}-ZSPRD^{100D}_{(2.7,1)}$	4	3	1	290	394.13	870	394.13	**475.87**	4.76	545.22	-394.13	-0.09	-1.43	75	118.97	2.21	0.74	-394.13
E1.6	$DIST^{V4}-ZSPRD^{100D}_{(2.7,0.5)}$	4	2	2	381.87	994.47	763.74	1988.94	**-1225.2**	-12.25	493.05	-1406.62	-0.53	-8.41	50	-306.3	0.38	0.38	-1988.94
E2.1	$DIST^{V4}-SPRD^{100D}-SMA_{(10,20)}$	17	5	12	604.68	402.79	3023.4	4833.43	**-1810.03**	-18.1	970.38	-1516.61	-0.43	-6.83	29.41	-106.49	0.63	1.5	-3269.66
E2.2	$DIST^{V4}-SPRD^{100D}-EMA_{(10,20)}$	29	12	17	490.49	361.93	5885.85	6152.74	**-266.89**	-2.67	1121.85	-1455.18	-0.28	-4.44	41.38	-9.2	0.96	1.36	-3187.54
E2.3	$DIST^{V4}-SPRD^{100D}-MACD_{(12,26,9)}$	29	10	19	394	267.29	3940.05	5078.52	**-1138.47**	-11.38	849.89	-1328.51	-0.43	-6.83	34.48	-39.28	0.78	1.47	-3329.71
E2.4	$DIST^{V4}-SPRD^{100D}-RSI_{(14)}$	6	5	1	609.78	3646.2	3048.89	3646.2	**-597.31**	-5.97	910.29	-3646.2	-0.14	-2.22	83.33	-99.69	0.84	0.17	-
E2.5	$DIST^{V4}-SPRD^{100D}-BB_{(20)}$	16	8	8	142.95	292.86	1143.58	2342.87	**-1199.29**	-11.99	332.27	-817.41	-0.72	-11.43	50	-74.96	0.49	0.49	-1416.39
E3	$DIST^{V4}-SPRD^{100D}-DECTREE$	296	142	154	115.15	84.07	16351.48	12947.47	**3404.01**	34.04	699.95	-843.47	-0.9	-14.29	47.97	11.49	1.26	1.37	-1684.66
E4	$DIST^{V4}-SPRD^{100D}-MLP$	223	93	130	134.37	91.49	12496.29	11894.04	**602.25**	6.02	1000.7	-498.26	-0.91	-14.45	41.7	2.69	1.05	1.47	-1333.47
Part VI: Models derived using the spread obtained from $JOHANSEN-SPRD^{100D}$																			
F1.1	$JOHANSEN-ZSPRD^{100D}_{(3,2)}$	15	7	8	63.99	71.54	447.92	572.34	**-124.43**	-1.24	330.57	-249.39	-0.75	-11.91	46.67	-8.29	0.78	0.89	-382.54
F1.2	$JOHANSEN-ZSPRD^{100D}_{(3,1)}$	13	6	7	62.33	38.24	373.96	267.66	**106.3**	1.06	190.9	-111.5	-0.98	-15.56	46.15	8.17	1.4	1.63	-192.41
F1.3	$JOHANSEN-ZSPRD^{100D}_{(3,0.5)}$	13	6	7	306.3	38.24	1837.77	267.66	**1570.11**	15.7	1457.02	-111.5	0.07	1.11	46.15	120.76	6.87	8.01	-192.41
F1.4	$JOHANSEN-ZSPRD^{100D}_{(2.7,2)}$	16	7	9	66.39	66.81	464.7	601.3	**-136.6**	-1.37	330.57	-249.39	-0.78	-12.38	43.75	-8.54	0.77	0.99	-382.54
F1.5	$JOHANSEN-ZSPRD^{100D}_{(2.7,1)}$	14	6	8	65.12	37.08	390.75	296.62	**94.12**	0.94	190.9	-111.5	-1.05	-16.67	42.86	6.73	1.32	1.76	-192.41
F1.6	$JOHANSEN-ZSPRD^{100D}_{(2.7,0.5)}$	14	6	8	312.84	37.08	1877.01	296.62	**1580.39**	15.8	1457.02	-111.5	0.05	0.79	42.86	112.9	6.33	8.44	-192.41
F2.1	$JOHANSEN-SPRD^{100D}-SMA_{(10,20)}$	20	10	10	1406.59	499.24	14065.88	4992.43	**9073.44**	90.73	5991.07	-3106.22	0.29	4.6	50	453.67	2.82	2.82	-4177.38
F2.2	$JOHANSEN-SPRD^{100D}-EMA_{(10,20)}$	28	15	13	1791.94	412.55	26879.16	5363.08	**21516.07**	215.16	8330.39	-1654.5	0.34	5.4	53.57	768.4	5.01	4.34	-2242.66
F2.3	$JOHANSEN-SPRD^{100D}-MACD_{(12,26,9)}$	31	13	18	3067.59	1010.17	39878.65	18183.02	**21695.63**	216.96	34658.26	-4141.92	0.09	1.43	41.94	700.04	2.19	3.04	-13009.89
F2.4	$JOHANSEN-SPRD^{100D}-RSI_{(14)}$	6	4	2	196.82	560.51	787.28	1121.01	**-333.73**	-3.34	551.08	-588.1	-0.59	-9.37	66.67	-55.6	0.7	0.35	-1121.01
F2.5	$JOHANSEN-SPRD^{100D}-BB_{(20)}$	15	4	11	519.95	468.35	2079.78	5151.85	**-3072.06**	-30.72	1302.24	-2717.97	-0.2	-3.17	26.67	-204.77	0.4	1.11	-3072.06
F3	$JOHANSEN-SPRD^{100D}-DECTREE$	307	161	146	109.24	90.93	17588.43	13276.07	**4312.35**	43.12	716.36	-913.64	-0.88	-13.97	52.44	14.04	1.32	1.2	-1567.07
F4	$JOHANSEN-SPRD^{100D}-MLP$	277	144	133	104.35	114.58	15026.91	15239.09	**-212.18**	-2.12	716.36	-918.24	-0.91	-14.45	51.99	-0.76	0.99	0.91	-2509.4
Part VII: Models derived using the spread obtained from $ADF-SPRD^{100D}$																			
G1.1	$ADF-ZSPRD^{100D}_{(3,2)}$	3	2	1	9358.39	548.03	18716.78	548.03	**18168.74**	181.69	16623.12	-548.03	0.66	10.48	66.67	6056.58	34.15	17.08	-548.03
G1.2	$ADF-ZSPRD^{100D}_{(3,1)}$	3	2	1	7956.29	1051.87	15912.58	1051.87	**14860.71**	148.61	12812.06	-1051.87	0.72	11.43	66.67	4953.87	15.13	7.56	-1051.87
G1.3	$ADF-ZSPRD^{100D}_{(3,0.5)}$	3	2	1	7516.24	1051.87	15032.47	1051.87	**13980.6**	139.81	12252.15	-1051.87	0.7	11.11	66.67	4660.49	14.29	7.15	-1051.87
G1.4	$ADF-ZSPRD^{100D}_{(2.7,2)}$	4	2	2	9358.39	2128.71	18716.78	4257.42	**14459.36**	144.59	16623.12	-3709.39	0.41	6.51	50	3614.84	4.4	4.4	-3709.39
G1.5	$ADF-ZSPRD^{100D}_{(2.7,1)}$	4	2	2	7956.29	2380.63	15912.58	4761.26	**11151.32**	111.51	12812.06	-3709.39	0.4	6.35	50	2787.83	3.34	3.34	-3709.39
G1.6	$ADF-ZSPRD^{100D}_{(2.7,0.5)}$	4	2	2	7516.24	6214.59	15032.47	12429.19	**2603.28**	26.03	12252.15	-11377.31	0.09	1.43	50	650.82	1.21	1.21	-11377.31
G2.1	$ADF-SPRD^{100D}-SMA_{(10,20)}$	16	8	8	3654.75	3595.33	29238.02	28762.65	**475.38**	4.75	11318.93	-16880.79	-0.02	-0.32	50	29.71	1.02	1.02	-26063.73
G2.2	$ADF-SPRD^{100D}-EMA_{(10,20)}$	26	16	10	2325.9	2814	37214.34	28139.96	**9074.38**	90.74	9075.09	-12812.06	0.04	0.63	61.54	349.09	1.32	0.83	-12812.06
G2.3	$ADF-SPRD^{100D}-MACD_{(12,26,9)}$	28	14	14	2007.56	2689.16	28105.87	37648.24	**-9542.37**	-95.42	8317.72	-17437.42	-0.09	-1.43	50	-340.8	0.75	0.75	-33014.43
G2.4	$ADF-SPRD^{100D}-RSI_{(14)}$	4	3	1	8538.67	377954.01	25616.01	377954.01	**-352338**	-3523.38	14476.98	-377954.01	-0.45	-7.14	75	-88084.5	0.07	0.02	-377954.01
G2.5	$ADF-SPRD^{100D}-BB_{(20)}$	18	7	11	5930.56	694.12	41513.95	7635.33	**33878.62**	338.79	13832.48	-1782.47	0.39	6.19	38.89	1882.22	5.44	8.54	-4189.2
G3	$ADF-SPRD^{100D}-DECTREE$	313	153	160	107.95	89.5	16516.96	14320.02	**2196.94**	21.97	918.24	-672.23	-0.96	-15.24	48.88	7.02	1.15	1.21	-2229.75
G4	$ADF-SPRD^{100D}-MLP$	235	115	120	125.12	104.94	14388.45	12592.31	**1796.14**	17.96	918.24	-626.71	-0.86	-13.65	48.94	7.65	1.14	1.19	-2206.41
Part VIII: Models derived using the spread obtained from $KALMAN-SPRD^{100D}$																			
H1.1	$KALMAN-ZSPRD^{100D}_{(3,2)}$	1	-	1	-	263.61	-	263.61	**-263.61**	-2.64	-	-263.61	-	-	-	-263.61	-	-	-263.61
H1.2	$KALMAN-ZSPRD^{100D}_{(3,1)}$	1	1	-	851	-	851	-	**851**	8.51	851	-	-	-	100	851	851	851	-
H1.3	$KALMAN-ZSPRD^{100D}_{(3,0.5)}$	1	1	-	2935.85	-	2935.85	-	**2935.85**	29.36	2935.85	-	-	-	100	2935.85	2935.85	2935.85	-
H1.4	$KALMAN-ZSPRD^{100D}_{(2.7,2)}$	1	-	1	-	643.85	-	643.85	**-643.85**	-6.44	-	-643.85	-	-	-	-643.85	-	-	-643.85
H1.5	$KALMAN-ZSPRD^{100D}_{(2.7,1)}$	1	1	-	498.81	-	498.81	-	**498.81**	4.99	498.81	-	-	-	100	498.81	498.81	498.81	-
H1.6	$KALMAN-ZSPRD^{100D}_{(2.7,0.5)}$	1	1	-	2621.39	-	2621.39	-	**2621.39**	26.21	2621.39	-	-	-	100	2621.39	2621.39	2621.39	-
H2.1	$KALMAN-SPRD^{100D}-SMA_{(10,20)}$	12	5	7	1095.42	961.53	5477.08	6730.72	**-1253.64**	-12.54	2517.6	-2680.28	-0.15	-2.38	41.67	-104.4	0.81	1.14	-4076.5
H2.2	$KALMAN-SPRD^{100D}-EMA_{(10,20)}$	19	8	11	2575.97	867.81	20607.74	9545.9	**11061.84**	110.62	11148.33	-3023.99	0.16	2.54	42.11	582.37	2.16	2.97	-3775.16
H2.3	$KALMAN-SPRD^{100D}-MACD_{(12,26,9)}$	34	11	23	1265.08	602.91	13915.86	13866.97	**48.89**	0.49	2913.71	-1571.95	-0.08	-1.27	32.35	1.38	1	2.1	-3739.35
H2.4	$KALMAN-SPRD^{100D}-RSI_{(14)}$	4	2	2	1153.22	6101.84	2306.44	12203.69	**-9897.24**	-98.97	1549.04	-9164.83	-0.53	-8.41	50	-2474.31	0.19	0.19	-10654.64
H2.5	$KALMAN-SPRD^{100D}-BB_{(20)}$	14	11	3	1047.43	1060.9	11521.75	3182.7	**8339.06**	83.39	2474.13	-1936.61	0.43	6.83	78.57	595.62	3.62	0.99	-2094.14
H3	$KALMAN-SPRD^{100D}-DECTREE$	317	165	152	108.53	98.42	17907.92	14959.68	**2948.24**	29.48	898.8	-918.24	-0.89	-14.13	52.05	9.3	1.2	1.1	-1613.44
H4	$KALMAN-SPRD^{100D}-MLP$	243	115	128	134.91	106.55	15515.18	13638.17	**1877.01**	18.77	1094.76	-787.41	-0.78	-12.38	47.33	7.74	1.14	1.27	-2945.26
Part IX: Models derived using the spread obtained from $RATIO-SPRD^{100D}$																			
I1.1	$RATIO-ZSPRD^{100D}_{(3,2)}$	2	-	2	-	489.76	-	979.53	**-979.53**	-9.8	-	-518.47	-15.81	-250.98	-	-489.76	-	-	-979.53
I1.2	$RATIO-ZSPRD^{100D}_{(3,1)}$	1	-	1	-	1592.18	-	1592.18	**-1592.18**	-15.92	-	-1592.18	-	-	-	-1592.18	-	-	-1592.18
I1.3	$RATIO-ZSPRD^{100D}_{(3,0.5)}$	1	-	1	-	1688.02	-	1688.02	**-1688.02**	-16.88	-	-1688.02	-	-	-	-1688.02	-	-	-1688.02
I1.4	$RATIO-ZSPRD^{100D}_{(2.7,2)}$	2	-	2	-	547.96	-	1095.91	**-1095.91**	-10.96	-	-568.66	-23.91	-379.56	-	-547.96	-	-	-1095.91
I1.5	$RATIO-ZSPRD^{100D}_{(2.7,1)}$	1	-	1	-	1674.13	-	1674.13	**-1674.13**	-16.74	-	-1674.13	-	-	-	-1674.13	-	-	-1674.13
I1.6	$RATIO-ZSPRD^{100D}_{(2.7,0.5)}$	1	-	1	-	1777.3	-	1777.3	**-1777.3**	-17.77	-	-1777.3	-	-	-	-1777.3	-	-	-1777.3
I2.1	$RATIO-SPRD^{100D}-SMA_{(10,20)}$	13	8	5	493.63	432.25	3949.02	2161.22	**1787.8**	17.88	1983.68	-670.84	-0.02	-0.32	61.54	137.54	1.83	1.14	-1519.65
I2.2	$RATIO-SPRD^{100D}-EMA_{(10,20)}$	15	7	8	980.1	312.73	6860.67	2501.81	**4358.86**	43.59	2524.4	-468.08	0.16	2.54	46.67	290.63	2.74	3.13	-965.51
I2.3	$RATIO-SPRD^{100D}-MACD_{(12,26,9)}$	31	14	17	542.67	225.01	7597.42	3825.11	**3772.31**	37.72	1366.95	-564.35	-0.06	-0.95	45.16	121.68	1.99	2.41	-1919.03
I2.4	$RATIO-SPRD^{100D}-RSI_{(14)}$	6	3	3	613.91	1658.74	1841.73	4976.21	**-3134.48**	-31.34	999.24	-4209.14	-0.36	-5.71	50	-522.41	0.37	0.37	-4245.74
I2.5	$RATIO-SPRD^{100D}-BB_{(20)}$	13	6	7	226.02	569.09	1356.12	3983.61	**-2627.49**	-26.27	428.2	-1889.83	-0.56	-8.89	46.15	-202.15	0.34	0.4	-2061.04
I3	$RATIO-SPRD^{100D}-DECTREE$	296	128	168	112.98	78.8	14461.45	13239.02	**1222.43**	12.22	734.68	-508.22	-1.07	-16.99	43.24	4.12	1.09	1.43	-2108.57
I4	$RATIO-SPRD^{100D}-MLP$	231	99	132	119.44	80.14	11824.73	10579.1	**1245.63**	12.46	734.68	-508.22	-1.03	-16.35	42.86	5.4	1.12	1.49	-1841.13
Part X: Models derived using the close price of QQQ.N																			
CLS-SYM-1.1	$CLOSE^{QQQ.N}-SMA_{(10,20)}$	13	6	7	194.37	151.12	1166.2	1057.82	**108.38**	1.08	605.78	-255.49	-0.28	-4.44	46.15	8.32	1.1	1.29	-788.38
CLS-SYM-1.2	$CLOSE^{QQQ.N}-EMA_{(10,20)}$	20	5	15	606.51	147.26	3032.57	2208.83	**823.74**	8.24	1524.27	-363.38	-0.08	-1.27	25	41.19	1.37	4.12	-712.96
CLS-SYM-1.3	$CLOSE^{QQQ.N}-MACD_{(12,26,9)}$	35	16	19	198.63	140.31	3178.11	2665.81	**512.3**	5.12	695.53	-296.02	-0.29	-4.6	45.71	14.62	1.19	1.42	-1251.08
CLS-SYM-1.4	$CLOSE^{QQQ.N}-RSI_{(14)}$	7	3	4	938.66	707.17	2815.99	2828.67	**-12.68**	-0.13	1724.49	-1923.52	-0.07	-1.11	42.86	-1.76	1	1.33	-1923.52
CLS-SYM-1.5	$CLOSE^{QQQ.N}-BB_{(20)}$	15	10	5	79.54	186.14	795.4	930.7	**-135.3**	-1.35	153.41	-575.2	-0.46	-7.3	66.67	-9.01	0.85	0.43	-600.51
Part XI: Models derived using the close price of XLE.N																			
CLS-SYM-2.1	$CLOSE^{XLE.N}-SMA_{(10,20)}$	19	9	10	492.93	337.96	4436.4	3379.63	**1056.77**	10.57	1969.29	-993.26	-0.03	-0.48	47.37	55.63	1.31	1.46	-2390.02
CLS-SYM-2.2	$CLOSE^{XLE.N}-EMA_{(10,20)}$	26	11	15	546.32	161.14	6009.56	2417.09	**3592.47**	35.92	2197.81	-326.2	0.12	1.9	42.31	138.19	2.49	3.39	-711.67
CLS-SYM-2.3	$CLOSE^{XLE.N}-MACD_{(12,26,9)}$	27	10	17	637.2	211.29	6372.04	3591.96	**2780.08**	27.8	1931.38	-613.01	0.05	0.79	37.04	102.99	1.77	3.02	-645.92
CLS-SYM-2.4	$CLOSE^{XLE.N}-RSI_{(14)}$	5	3	2	314.75	1213.82	944.26	2427.64	**-1483.38**	-14.83	365.04	-1229.73	-0.44	-6.98	60	-296.68	0.39	0.26	-2062.6
CLS-SYM-2.5	$CLOSE^{XLE.N}-BB_{(20)}$	20	17	3	198.62	500.07	3376.55	1500.22	**1876.33**	18.76	822.47	-1185.85	0.05	0.79	85	93.82	2.25	0.4	-1185.85

Table D.2.10: This table presents the back-test metrics for the pair $SCHB.N/SCHF$ based on a 30-day rolling window. The table is subdivided into eleven parts, and in each of these parts, we present the back-test metrics and the trading strategies which use the spread derived from various models. In Part I, the spread is derived from the $DIST^{V1.1}$ model, in Part II from the $DIST^{V1.2}$ model, in Part III from the $DIST^{V2}$ model, in Part IV from the $DIST^{V3}$ model, in Part V from the $DIST^{V4}$ model, in Part VI from the $JOHANSEN-SPRD$ model, in Part VIII from the $ADF-SPRD$ model, in from the $DIST^{V2}$ model, in Part VIII from the $KALMAN-SPRD$ model, and in Part IX from the $RATIO-SPRD$ model. In Part X and XI, we present the back-test metrics of the trading strategies which use the close price of SCHB.N, and SCHF.N, respectively. All $ numbers reported below are in USD.

(I) Trading Strategy Code	(II) Model Name	(III) Total Number of Trades	(IV) Number of Winning Trades	(V) Number of Loosing Trades	(VI) Average Profit per Trade ($)	(VII) Average Loss per Trade ($)	(VIII) Gross Profit ($)	(IX) Gross Loss ($)	(X) Net Profit ($)	(XI) ROI (%)	(XII) Max P&L ($)	(XIII) Min P&L ($)	(XIV) Daily Sharpe Ratio	(XV) Annualized Sharpe Ratio	(XVI) Hit Ratio	(XVII) Expectancy	(XVIII) Profit Factor	(XIX) Realized Risk Reward Ratio	(XX) Max Drawdown ($)
Part I: Models derived using the spread obtained from $DIST^{V1.1}-SPRD^{30D}$																			
A1	$DIST^{V1.1}-ZSPRD^{30D}_{(3,2)}$	2	-	2	-	138.52	-	277.05	-277.05	-2.77	-	-220.17	-2.52	-40	-	-138.52	-	-	-277.05
A1	$DIST^{V1.1}-ZSPRD^{30D}_{(3,1)}$	1	-	1	-	181.3	-	181.3	-181.3	-1.81	-	-181.3	-	-	-	-181.3	-	-	-181.3
A1	$DIST^{V1.1}-ZSPRD^{30D}_{(3,0.5)}$	1	-	1	-	153.49	-	153.49	-153.49	-1.53	-	-153.49	-	-	-	-153.49	-	-	-153.49
A1	$DIST^{V1.1}-ZSPRD^{30D}_{(2.7,2)}$	4	-	4	-	109.35	-	437.39	-437.39	-4.37	-	-220.17	-3.21	-50.96	-	-109.35	-	-	-437.39
A1	$DIST^{V1.1}-ZSPRD^{30D}_{(2.7,1)}$	2	1	1	16.14	181.3	16.14	181.3	-165.16	-1.65	16.14	-181.3	-1.68	-26.67	50	-82.58	0.09	0.09	-181.3
A1	$DIST^{V1.1}-ZSPRD^{30D}_{(2.7,0.5)}$	1	-	1	-	153.49	-	153.49	-153.49	-1.53	-	-153.49	-	-	-	-153.49	-	-	-153.49
A2	$DIST^{V1.1}-SPRD^{30D}-SMA_{(10,20)}$	10	3	7	39.45	189.45	118.36	1326.15	-1207.8	-12.08	61.13	-622.55	-1.35	-21.43	30	-120.78	0.09	0.21	-1207.8
A2	$DIST^{V1.1}-SPRD^{30D}-EMA_{(10,20)}$	23	13	10	93.51	123.69	1215.63	1236.91	-21.28	-0.21	237.02	-336.69	-1.06	-16.83	56.52	-0.93	0.98	0.76	-538.74
A2	$DIST^{V1.1}-SPRD^{30D}-MACD_{(12,26,9)}$	35	25	10	58.5	70.44	1462.6	704.41	758.18	7.58	180.99	-168.62	-1.75	-27.78	71.43	21.66	2.08	0.83	-143.04
A2	$DIST^{V1.1}-SPRD^{30D}-RSI_{(14)}$	4	3	1	399.94	166.87	1199.81	166.86	1032.94	10.33	658.17	-166.87	0.31	4.92	75	258.24	7.19	2.4	-166.87
A2	$DIST^{V1.1}-SPRD^{30D}-BB_{(20)}$	12	5	7	66.87	66.56	334.35	465.9	-131.54	-1.32	122.41	-123.14	-1.9	-30.16	41.67	-10.96	0.72	1	-331.26
A3	$DIST^{V1.1}-SPRD^{30D}-DECTREE$	358	155	203	22.36	23.87	3465.93	4846.15	-1380.22	-13.8	115	-192.07	-4.78	-75.88	43.3	-3.85	0.72	0.94	-1717.51
A4	$DIST^{V1.1}-SPRD^{30D}-MLP$	302	132	170	26.47	23.46	3493.67	3988.68	-495.01	-4.95	206.99	-208.41	-4.1	-65.09	43.71	-1.64	0.88	1.13	-894.37
Part II: Models derived using the spread obtained from $DIST^{V1.2}-SPRD^{30D}$																			
B1	$DIST^{V1.2}-ZSPRD^{30D}_{(3,2)}$	5	3	2	15.48	72.5	46.44	145	-98.56	-0.99	23.13	-111.04	-3.09	-49.05	60	-19.71	0.32	0.21	-134.94
B1	$DIST^{V1.2}-ZSPRD^{30D}_{(3,1)}$	5	1	4	18.06	55.6	18.06	222.42	-204.36	-2.04	18.06	-144.96	-3.01	-47.78	20	-40.87	0.08	0.32	-222.42
B1	$DIST^{V1.2}-ZSPRD^{30D}_{(3,0.5)}$	5	1	4	3.6	75.86	3.6	303.43	-299.83	-3	3.6	-197.61	-2.51	-39.85	20	-59.97	0.01	0.05	-303.43
B1	$DIST^{V1.2}-ZSPRD^{30D}_{(2.7,2)}$	11	8	3	47.91	50.05	383.28	150.16	233.12	2.33	110.73	-111.04	-2.1	-33.34	72.73	21.2	2.55	0.96	-111.04
B1	$DIST^{V1.2}-ZSPRD^{30D}_{(2.7,1)}$	10	5	5	128.15	73.91	640.76	369.57	271.19	2.71	221.28	-152.04	-0.98	-15.56	50	27.12	1.73	1.73	-152.04
B1	$DIST^{V1.2}-ZSPRD^{30D}_{(2.7,0.5)}$	10	5	5	105.97	90.09	529.87	450.44	79.43	0.79	161.55	-197.61	-1.16	-18.41	50	7.94	1.18	1.18	-197.61
B2	$DIST^{V1.2}-SPRD^{30D}-SMA_{(10,20)}$	17	5	12	120.26	133.15	601.31	1597.78	-996.46	-9.96	280.5	-207.19	-1.55	-24.61	29.41	-58.62	0.38	0.9	-1141.37
B2	$DIST^{V1.2}-SPRD^{30D}-EMA_{(10,20)}$	23	8	15	122.53	111.2	980.27	1668.04	-687.77	-6.88	307.61	-250.84	-1.26	-20	34.78	-29.91	0.59	1.1	-1311.34
B2	$DIST^{V1.2}-SPRD^{30D}-MACD_{(12,26,9)}$	28	10	18	86.45	61.12	864.45	1100.09	-235.64	-2.36	253.01	-189.14	-1.67	-26.51	35.71	-8.42	0.79	1.41	-725.93
B2	$DIST^{V1.2}-SPRD^{30D}-RSI_{(14)}$	8	1	7	7.73	153.9	7.73	1077.32	-1069.59	-10.7	7.73	-414.81	-2.04	-32.38	12.5	-133.7	0.01	0.05	-662.51
B2	$DIST^{V1.2}-SPRD^{30D}-BB_{(20)}$	15	6	9	84.45	74.95	506.69	674.56	-167.87	-1.68	191.06	-252.35	-1.48	-23.49	40	-11.19	0.75	1.13	-316.97
B3	$DIST^{V1.2}-SPRD^{30D}-DECTREE$	298	140	158	23.88	29.08	3342.61	4594.32	-1251.71	-12.52	152.1	-164.53	-4.26	-67.63	46.98	-4.2	0.73	0.82	-1598.22
B4	$DIST^{V1.2}-SPRD^{30D}-MLP$	219	107	112	24.84	33.5	2658.3	3752.02	-1093.73	-10.94	170.9	-171.77	-3.57	-56.67	48.86	-4.99	0.71	0.74	-1249.14
Part III: Models derived using the spread obtained from $DIST^{V2}-SPRD^{30D}$																			
C1	$DIST^{V2}-ZSPRD^{30D}_{(3,2)}$	2	2	-	138.52	-	277.05	-	277.05	2.77	220.17	-	-0.12	-1.9	100	138.52	277.05	138.52	-
C1	$DIST^{V2}-ZSPRD^{30D}_{(3,1)}$	1	1	-	181.3	-	181.3	-	181.3	1.81	181.3	-	-	-	100	181.3	181.3	181.3	-
C1	$DIST^{V2}-ZSPRD^{30D}_{(3,0.5)}$	1	1	-	153.49	-	153.49	-	153.49	1.53	153.49	-	-	-	100	153.49	153.49	153.49	-
C1	$DIST^{V2}-ZSPRD^{30D}_{(2.7,2)}$	4	4	-	109.35	-	437.39	-	437.39	4.37	220.17	-	-0.52	-8.25	100	109.35	437.39	109.35	-
C1	$DIST^{V2}-ZSPRD^{30D}_{(2.7,1)}$	2	1	1	181.3	16.14	181.3	16.14	165.16	1.65	181.3	-16.14	-0.5	-7.94	50	82.58	11.23	11.23	-16.14
C1	$DIST^{V2}-ZSPRD^{30D}_{(2.7,0.5)}$	1	1	-	153.49	-	153.49	-	153.49	1.53	153.49	-	-	-	100	153.49	153.49	153.49	-
C2	$DIST^{V2}-SPRD^{30D}-SMA_{(10,20)}$	10	7	3	189.45	39.45	1326.15	118.36	1207.8	12.08	622.55	-61.13	-0.15	-2.38	70	120.78	11.2	4.8	-87.93
C2	$DIST^{V2}-SPRD^{30D}-EMA_{(10,20)}$	23	10	13	123.69	93.51	1236.91	1215.63	21.28	0.21	336.69	-237.02	-1.05	-16.67	43.48	0.93	1.02	1.32	-410.71
C2	$DIST^{V2}-SPRD^{30D}-MACD_{(12,26,9)}$	35	10	25	70.44	58.5	704.41	1462.6	-758.18	-7.58	168.62	-180.99	-2.33	-36.99	28.57	-21.66	0.48	1.2	-1059.3
C2	$DIST^{V2}-SPRD^{30D}-RSI_{(14)}$	4	1	3	166.87	399.94	166.86	1199.81	-1032.94	-10.33	166.87	-658.17	-1.2	-19.05	25	-258.24	0.14	0.42	-840.4
C2	$DIST^{V2}-SPRD^{30D}-BB_{(20)}$	12	7	5	66.56	66.87	465.9	334.35	131.54	1.32	123.14	-122.41	-1.64	-26.03	58.33	10.96	1.39	1	-175.5
C3	$DIST^{V2}-SPRD^{30D}-DECTREE$	351	147	204	23.54	24.75	3460.9	5048.82	-1587.92	-15.88	115	-289.77	-4.36	-69.21	41.88	-4.52	0.69	0.95	-1910.26
C4	$DIST^{V2}-SPRD^{30D}-MLP$	330	137	193	26.98	26.61	3696.1	5135.19	-1439.08	-14.39	184.3	-289.77	-3.88	-61.59	41.52	-4.36	0.72	1.01	-1935.97
Part IV: Models derived using the spread obtained from $DIST^{V3}-SPRD^{30D}$																			
D1	$DIST^{V3}-ZSPRD^{30D}_{(3,2)}$	4	3	1	35.37	4.61	106.12	4.61	101.51	1.02	52.49	-4.61	-5.42	-86.04	75	25.38	23.01	7.67	-4.61
D1	$DIST^{V3}-ZSPRD^{30D}_{(3,1)}$	4	4	-	37.62	-	150.48	-	150.48	1.5	69.4	-	-4.36	-69.21	100	37.62	150.48	37.62	-
D1	$DIST^{V3}-ZSPRD^{30D}_{(3,0.5)}$	4	4	-	47.46	-	189.83	-	189.83	1.9	69.4	-	-3.81	-60.48	100	47.46	189.83	47.46	-
D1	$DIST^{V3}-ZSPRD^{30D}_{(2.7,2)}$	8	7	1	26.11	4.61	182.75	4.61	178.14	1.78	52.49	-4.61	-6.27	-99.53	87.5	22.27	39.62	5.66	-4.61
D1	$DIST^{V3}-ZSPRD^{30D}_{(2.7,1)}$	8	8	-	33.31	-	266.48	-	266.48	2.66	69.4	-	-5.22	-82.86	100	33.31	266.48	33.31	-
D1	$DIST^{V3}-ZSPRD^{30D}_{(2.7,0.5)}$	8	8	-	38.38	-	307.05	-	307.05	3.07	69.4	-	-4.62	-73.34	100	38.38	307.05	38.38	-
D2	$DIST^{V3}-SPRD^{30D}-SMA_{(10,20)}$	25	11	14	85.36	77.03	938.93	1078.38	-139.45	-1.39	171.06	-211.41	-1.6	-25.4	44	-5.58	0.87	1.11	-768.12
D2	$DIST^{V3}-SPRD^{30D}-EMA_{(10,20)}$	43	14	29	76.11	64.62	1065.52	1874.02	-808.5	-8.08	298.61	-184.93	-1.99	-31.59	32.56	-18.8	0.57	1.18	-936.91
D2	$DIST^{V3}-SPRD^{30D}-MACD_{(12,26,9)}$	44	17	27	59.73	59.76	1015.49	1613.46	-597.98	-5.98	207.03	-218.08	-2.05	-32.54	38.64	-13.59	0.63	1	-645.77
D2	$DIST^{V3}-SPRD^{30D}-RSI_{(14)}$	2	1	1	449.96	476.88	449.96	476.88	-26.91	-0.27	449.96	-476.88	-0.25	-3.97	50	-13.46	0.94	0.94	-476.88
D2	$DIST^{V3}-SPRD^{30D}-BB_{(20)}$	20	11	9	28.2	48.91	310.18	440.17	-129.99	-1.3	58.31	-132.53	-3.11	-49.37	55	-6.5	0.7	0.58	-194.39
D3	$DIST^{V3}-SPRD^{30D}-DECTREE$	320	144	176	27.72	23.96	3991.73	4217.52	-225.8	-2.26	352.34	-185.94	-3.75	-59.53	45	-0.71	0.95	1.16	-927.98
D4	$DIST^{V3}-SPRD^{30D}-MLP$	138	63	75	28.89	30.77	1820.24	2307.48	-487.24	-4.87	256.44	-281.43	-2.89	-45.88	45.65	-3.53	0.79	0.94	-865.9
Part V: Models derived using the spread obtained from $DIST^{V4}-SPRD^{30D}$																			
E1	$DIST^{V4}-ZSPRD^{30D}_{(3,2)}$	4	3	1	35.37	4.61	106.12	4.61	101.51	1.02	52.49	-4.61	-5.42	-86.04	75	25.38	23.01	7.67	-4.61
E1	$DIST^{V4}-ZSPRD^{30D}_{(3,1)}$	4	4	-	37.62	-	150.48	-	150.48	1.5	69.4	-	-4.36	-69.21	100	37.62	150.48	37.62	-
E1	$DIST^{V4}-ZSPRD^{30D}_{(3,0.5)}$	4	4	-	47.46	-	189.83	-	189.83	1.9	69.4	-	-3.81	-60.48	100	47.46	189.83	47.46	-
E1	$DIST^{V4}-ZSPRD^{30D}_{(2.7,2)}$	8	7	1	26.11	4.61	182.75	4.61	178.14	1.78	52.49	-4.61	-6.27	-99.53	87.5	22.27	39.62	5.66	-4.61
E1	$DIST^{V4}-ZSPRD^{30D}_{(2.7,1)}$	8	8	-	33.31	-	266.48	-	266.48	2.66	69.4	-	-5.22	-82.86	100	33.31	266.48	33.31	-
E1	$DIST^{V4}-ZSPRD^{30D}_{(2.7,0.5)}$	8	8	-	38.38	-	307.05	-	307.05	3.07	69.4	-	-4.62	-73.34	100	38.38	307.05	38.38	-
E2	$DIST^{V4}-SPRD^{30D}-SMA_{(10,20)}$	25	11	14	72.16	81.13	793.78	1135.86	-342.08	-3.42	153.71	-211.41	-1.79	-28.42	44	-13.68	0.7	0.89	-768.12
E2	$DIST^{V4}-SPRD^{30D}-EMA_{(10,20)}$	43	14	29	76.11	64.62	1065.52	1874.02	-808.5	-8.08	298.61	-184.93	-1.99	-31.59	32.56	-18.8	0.57	1.18	-936.91
E2	$DIST^{V4}-SPRD^{30D}-MACD_{(12,26,9)}$	44	17	27	59.73	59.76	1015.49	1613.46	-597.98	-5.98	207.03	-218.08	-2.05	-32.54	38.64	-13.59	0.63	1	-645.77
E2	$DIST^{V4}-SPRD^{30D}-RSI_{(14)}$	2	1	1	449.96	476.88	449.96	476.88	-26.91	-0.27	449.96	-476.88	-0.25	-3.97	50	-13.46	0.94	0.94	-476.88
E2	$DIST^{V4}-SPRD^{30D}-BB_{(20)}$	20	11	9	28.2	48.91	310.18	440.17	-129.99	-1.3	58.31	-132.53	-3.11	-49.37	55	-6.5	0.7	0.58	-194.39
E3	$DIST^{V4}-SPRD^{30D}-DECTREE$	307	142	165	24.86	26.89	3529.97	4437.53	-907.56	-9.08	189.97	-174.81	-4	-63.5	46.25	-2.96	0.8	0.92	-1278.93
E4	$DIST^{V4}-SPRD^{30D}-MLP$	151	69	82	25.28	27.32	1744.4	2240.16	-495.77	-4.96	98.79	-140.04	-3.97	-63.02	45.7	-3.28	0.78	0.93	-764.05
Part VI: Models derived using the spread obtained from $JOHANSEN-SPRD^{30D}$																			
F1	$JOHANSEN-ZSPRD^{30D}_{(3,2)}$	28	13	15	131.8	24.79	1713.37	371.82	1341.55	13.42	988.29	-184.39	-0.23	-3.65	46.43	47.91	4.61	5.32	-203.92
F1	$JOHANSEN-ZSPRD^{30D}_{(3,1)}$	25	12	13	145.52	27.35	1746.25	355.58	1390.68	13.91	988.29	-184.39	-0.22	-3.49	48	55.63	4.91	5.32	-198.02
F1	$JOHANSEN-ZSPRD^{30D}_{(3,0.5)}$	25	13	12	151.29	29.2	1966.79	350.46	1616.34	16.16	988.29	-184.39	-0.22	-3.49	52	64.65	5.61	5.18	-198.02
F1	$JOHANSEN-ZSPRD^{30D}_{(2.7,2)}$	29	13	16	132.22	24.96	1718.83	399.41	1319.42	13.19	988.29	-184.39	-0.23	-3.65	44.83	45.5	4.3	5.3	-235.18
F1	$JOHANSEN-ZSPRD^{30D}_{(2.7,1)}$	26	12	14	145.94	27.01	1751.22	378.12	1373.1	13.73	988.29	-184.39	-0.22	-3.49	46.15	52.8	4.63	5.4	-230.13
F1	$JOHANSEN-ZSPRD^{30D}_{(2.7,0.5)}$	26	14	12	147.3	29.01	2062.21	348.12	1714.09	17.14	988.29	-184.39	-0.21	-3.33	53.85	65.93	5.92	5.08	-198.02
F2	$JOHANSEN-SPRD^{30D}-SMA_{(10,20)}$	24	10	14	177.59	485.13	1775.86	6791.84	-5015.98	-50.16	861.74	-3480.35	0.11	1.75	41.67	-208.98	0.26	0.37	-5726.73
F2	$JOHANSEN-SPRD^{30D}-EMA_{(10,20)}$	41	18	23	207.06	470.88	3727.08	10830.13	-7103.05	-71.03	1043.76	-4020.71	0.02	0.32	43.9	-173.26	0.34	0.44	-8023.54
F2	$JOHANSEN-SPRD^{30D}-MACD_{(12,26,9)}$	43	14	29	349.66	150.68	4895.27	4369.85	525.42	5.25	2669	-988.29	-0.05	-0.79	32.56	12.23	1.12	2.32	-1849.54
F2	$JOHANSEN-SPRD^{30D}-RSI_{(14)}$	6	2	4	21.78	669.83	43.57	2679.32	-2635.75	-26.36	36.36	-1393.58	-0.67	-10.64	33.33	-439.32	0.02	0.03	-2635.75
F2	$JOHANSEN-SPRD^{30D}-BB_{(20)}$	24	13	11	242.94	202.66	3158.24	2229.24	929	9.29	957.95	-775.63	0.04	0.63	54.17	38.72	1.42	1.2	-834.38
F3	$JOHANSEN-SPRD^{30D}-DECTREE$	324	149	175	24.94	26.21	3716.48	4586.8	-870.32	-8.7	141.64	-195.28	-4.03	-63.97	45.99	-2.68	0.81	0.95	-1542.12
F4	$JOHANSEN-SPRD^{30D}-MLP$	204	98	106	26.07	34.98	2555.18	3708.26	-1153.07	-11.53	162.04	-189.27	-3.44	-54.61	48.04	-5.65	0.69	0.75	-1203.52
Part VII: Models derived using the spread obtained from $ADF-SPRD^{30D}$																			
G1	$ADF-ZSPRD^{30D}_{(3,2)}$	5	3	2	126.4	934.48	379.21	1868.97	-1489.76	-14.9	318.31	-976.02	-0.66	-10.48	60	-297.95	0.2	0.14	-1827.37
G1	$ADF-ZSPRD^{30D}_{(3,1)}$	5	3	2	283.98	821.7	851.94	1643.39	-791.45	-7.91	583.08	-1014.88	-0.4	-6.35	60	-158.29	0.52	0.35	-1403.67
G1	$ADF-ZSPRD^{30D}_{(3,0.5)}$	5	3	2	281.93	1641.15	845.8	3282.31	-2436.5	-24.37	583.08	-2060.34	-0.53	-8.41	60	-487.3	0.26	0.17	-3053.49
G1	$ADF-ZSPRD^{30D}_{(2.7,2)}$	10	6	4	140.86	581.45	845.16	2325.79	-1480.62	-14.81	318.31	-976.02	-0.54	-8.57	60	-148.06	0.36	0.24	-1828.62
G1	$ADF-ZSPRD^{30D}_{(2.7,1)}$	10	5	5	285.57	512.05	1427.82	2560.27	-1132.44	-11.32	583.08	-1014.88	-0.44	-6.98	50	-113.24	0.56	0.56	-1749.41
G1	$ADF-ZSPRD^{30D}_{(2.7,0.5)}$	10	3	7	336.84	637.73	1010.52	4464.11	-3453.6	-34.54	583.08	-2060.34	-0.58	-9.21	30	-345.36	0.23	0.53	-4029.01
G2	$ADF-SPRD^{30D}-SMA_{(10,20)}$	27	18	9	534.39	401.11	9618.96	3609.94	6009.01	60.09	1690.04	-1051.71	0.19	3.02	66.67	222.59	2.66	1.33	-1268.39
G2	$ADF-SPRD^{30D}-EMA_{(10,20)}$	41	26	15	436.93	484.11	11360.14	7261.6	4098.54	40.99	1672.08	-2223.46	0.03	0.48	63.41	99.92	1.56	0.9	-3157.05
G2	$ADF-SPRD^{30D}-MACD_{(12,26,9)}$	49	28	21	444.97	348.92	12459.17	7327.34	5131.83	51.32	3030.38	-1290.38	0.03	0.48	57.14	104.71	1.7	1.28	-3618.45
G2	$ADF-SPRD^{30D}-RSI_{(14)}$	-	-	-	-	-	-	-	-	-	-	-	-	-	-	-	-	-	-
G2	$ADF-SPRD^{30D}-BB_{(20)}$	21	9	12	234.74	385.97	2112.67	4631.6	-2518.93	-25.19	862.08	-1054.53	-0.5	-7.94	42.86	-119.93	0.46	0.61	-2642.32
G3	$ADF-SPRD^{30D}-DECTREE$	322	182	140	26.63	23.05	4846.61	3226.45	1620.15	16.2	289.77	-112.1	-3.73	-59.21	56.52	5.03	1.5	1.16	-334.18
G4	$ADF-SPRD^{30D}-MLP$	155	92	63	25.2	37.88	2318.72	2386.62	-67.9	-0.68	121.59	-252.21	-3.15	-50	59.35	-0.44	0.97	0.67	-797.34
Part VIII: Models derived using the spread obtained from $KALMAN-SPRD^{30D}$																			
H1	$KALMAN-ZSPRD^{30D}_{(3,2)}$	-	-	-	-	-	-	-	-	-	-	-	-	-	-	-	-	-	-
H1	$KALMAN-ZSPRD^{30D}_{(3,1)}$	-	-	-	-	-	-	-	-	-	-	-	-	-	-	-	-	-	-
H1	$KALMAN-ZSPRD^{30D}_{(3,0.5)}$	-	-	-	-	-	-	-	-	-	-	-	-	-	-	-	-	-	-
H1	$KALMAN-ZSPRD^{30D}_{(2.7,2)}$	5	4	1	138.6	225.56	554.41	225.56	328.85	3.29	270.58	-225.56	-0.23	-3.65	80	65.77	2.46	0.61	-225.56
H1	$KALMAN-ZSPRD^{30D}_{(2.7,1)}$	3	2	1	123.99	628.27	247.99	628.27	-380.28	-3.8	236.7	-628.27	-0.53	-8.41	66.67	-126.73	0.39	0.2	-628.27
H1	$KALMAN-ZSPRD^{30D}_{(2.7,0.5)}$	3	1	2	288.9	425.01	288.9	850.01	-561.11	-5.61	288.9	-501.43	-0.71	-11.27	33.33	-187.06	0.34	0.68	-850.01
H2	$KALMAN-SPRD^{30D}-SMA_{(10,20)}$	11	3	8	842.59	160.02	2527.76	1280.16	1247.59	12.48	2346.06	-437.31	0.01	0.16	27.27	113.39	1.97	5.27	-932.39
H2	$KALMAN-SPRD^{30D}-EMA_{(10,20)}$	17	8	9	512.91	167.68	4103.26	1509.09	2594.17	25.94	1797.97	-466.69	0.09	1.43	47.06	152.61	2.72	3.06	-938.82
H2	$KALMAN-SPRD^{30D}-MACD_{(12,26,9)}$	34	14	20	310	132.93	4340	2658.65	1681.34	16.81	1349.13	-333.75	-0.18	-2.86	41.18	49.47	1.63	2.33	-788.6
H2	$KALMAN-SPRD^{30D}-RSI_{(14)}$	4	1	3	1945.16	1155.98	1945.16	3467.94	-1522.78	-15.23	1945.16	-2942.77	-0.24	-3.81	25	-380.7	0.56	1.68	-2942.77
H2	$KALMAN-SPRD^{30D}-BB_{(20)}$	11	8	3	147.64	674.97	1181.16	2024.92	-843.76	-8.44	453.61	-1108.69	-0.42	-6.67	72.73	-76.68	0.58	0.22	-1479.58
H3	$KALMAN-SPRD^{30D}-DECTREE$	358	144	214	21.1	23.05	3038.23	4932.88	-1894.64	-18.95	167.06	-126.84	-4.86	-77.15	40.22	-5.29	0.62	0.92	-2047.57
H4	$KALMAN-SPRD^{30D}-MLP$	287	112	175	28.06	24.31	3142.89	4254.84	-1111.95	-11.12	250.01	-179.79	-4.12	-65.4	39.02	-3.88	0.74	1.15	-1385.6
Part IX: Models derived using the spread obtained from $RATIO-SPRD^{30D}$																			
I1	$RATIO-ZSPRD^{30D}_{(3,2)}$	4	3	1	118.79	109.38	356.38	109.38	247	2.47	289.77	-109.38	-0.54	-8.57	75	61.75	3.26	1.09	-109.38
I1	$RATIO-ZSPRD^{30D}_{(3,1)}$	4	3	1	164.13	152.03	492.38	152.03	340.35	3.4	414.81	-152.03	-0.28	-4.44	75	85.09	3.24	1.08	-152.03
I1	$RATIO-ZSPRD^{30D}_{(3,0.5)}$	4	3	1	180.26	120.28	540.79	120.28	420.51	4.21	414.81	-120.28	-0.21	-3.33	75	105.13	4.5	1.5	-120.28
I1	$RATIO-ZSPRD^{30D}_{(2.7,2)}$	6	4	2	98.8	55.39	395.19	110.78	284.41	2.84	289.77	-109.38	-0.8	-12.7	66.67	47.41	3.57	1.78	-110.78
I1	$RATIO-ZSPRD^{30D}_{(2.7,1)}$	6	5	1	119.53	152.03	597.66	152.03	445.64	4.46	414.81	-152.03	-0.42	-6.67	83.33	74.26	3.93	0.79	-152.03
I1	$RATIO-ZSPRD^{30D}_{(2.7,0.5)}$	6	5	1	139.73	120.28	698.67	120.28	578.39	5.78	414.81	-120.28	-0.32	-5.08	83.33	96.39	5.81	1.16	-120.28
I2	$RATIO-SPRD^{30D}-SMA_{(10,20)}$	17	7	10	146.21	81.29	1023.44	812.89	210.54	2.11	364.83	-182.68	-0.95	-15.08	41.18	12.39	1.26	1.8	-448.64
I2	$RATIO-SPRD^{30D}-EMA_{(10,20)}$	24	7	17	123.4	66.35	863.78	1128.01	-264.23	-2.64	248.67	-266.81	-1.46	-23.18	29.17	-11	0.77	1.86	-915.14
I2	$RATIO-SPRD^{30D}-MACD_{(12,26,9)}$	32	12	20	57.54	66.43	690.46	1328.57	-638.11	-6.38	156.26	-240.74	-1.97	-31.27	37.5	-19.94	0.52	0.87	-825.85
I2	$RATIO-SPRD^{30D}-RSI_{(14)}$	3	1	2	190.19	808.88	190.19	1617.76	-1427.57	-14.28	190.19	-1425.46	-0.74	-11.75	33.33	-475.89	0.12	0.24	-1425.46
I2	$RATIO-SPRD^{30D}-BB_{(20)}$	14	12	2	55.3	134.46	663.57	268.92	394.65	3.95	139	-237	-1.43	-22.7	85.71	28.18	2.47	0.41	-237
I3	$RATIO-SPRD^{30D}-DECTREE$	372	130	242	22.52	21.2	2927.27	5129.48	-2202.21	-22.02	112.86	-110.99	-5.31	-84.29	34.95	-5.92	0.57	1.06	-2411.62
I4	$RATIO-SPRD^{30D}-MLP$	357	123	234	23.4	21.48	2877.65	5025.72	-2148.07	-21.48	112.86	-110.99	-5.23	-83.02	34.45	-6.02	0.57	1.09	-2331.97
Part X: Models derived using the close price of SCHB.N																			
CLS-SYM-1	$CLOSE^{SCHB.N}-SMA_{(10,20)}$	14	8	6	275.75	104.83	2206.01	628.98	1577.04	15.77	789.43	-230.52	0.13	2.06	57.14	112.63	3.51	2.63	-324.24
CLS-SYM-1	$CLOSE^{SCHB.N}-EMA_{(10,20)}$	17	7	10	370.21	232.37	2591.45	2323.66	267.79	2.68	1083.32	-810.29	-0.15	-2.38	41.18	15.77	1.12	1.59	-630.81
CLS-SYM-1	$CLOSE^{SCHB.N}-MACD_{(12,26,9)}$	37	14	23	144.19	101.44	2018.6	2333.05	-314.45	-3.14	604.53	-326.15	-0.5	-7.94	37.84	-8.49	0.87	1.42	-1087.87
CLS-SYM-1	$CLOSE^{SCHB.N}-RSI_{(14)}$	5	2	3	313.96	850.97	627.91	2552.9	-1924.99	-19.25	584.15	-2050.03	-0.46	-7.3	40	-385	0.25	0.37	-2050.03
CLS-SYM-1	$CLOSE^{SCHB.N}-BB_{(20)}$	11	9	2	83.74	413.03	753.64	826.06	-72.41	-0.72	239.73	-780.29	-0.31	-4.92	81.82	-6.57	0.91	0.2	-780.29
Part XI: Models derived using the close price of SCHF.N																			
CLS-SYM-2	$CLOSE^{SCHF.N}-SMA_{(10,20)}$	20	7	13	314.26	125.66	2199.8	1633.59	566.2	5.66	1106.36	-575.54	-0.14	-2.22	35	28.31	1.35	2.5	-918.42
CLS-SYM-2	$CLOSE^{SCHF.N}-EMA_{(10,20)}$	23	8	15	331.11	93.37	2648.86	1400.61	1248.24	12.48	911.97	-332.73	-0.07	-1.11	34.78	54.26	1.89	3.55	-643.72
CLS-SYM-2	$CLOSE^{SCHF.N}-MACD_{(12,26,9)}$	30	10	20	221.35	120.16	2213.46	2403.27	-189.81	-1.9	1043.11	-326.35	-0.34	-5.4	33.33	-6.34	0.92	1.84	-1733.81
CLS-SYM-2	$CLOSE^{SCHF.N}-RSI_{(14)}$	5	2	3	617.93	304.16	1235.87	912.48	323.39	3.23	959.27	-697.61	-0.02	-0.32	40	64.68	1.35	2.03	-697.61
CLS-SYM-2	$CLOSE^{SCHF.N}-BB_{(20)}$	15	8	7	79.49	192.86	635.89	1349.99	-714.1	-7.14	252.09	-785.71	-0.51	-8.1	53.33	-47.62	0.47	0.41	-785.71

Table D.2.11: This table presents the back-test metrics for the pair $SCHB.N/SCHF$ based on a 50-day rolling window. The table is subdivided into eleven parts, and in each of these parts, we present the back-test metrics and the trading strategies which use the spread derived from various models. In Part I, the spread is derived from the $DIST^{V1.1}$ model, in Part II from the $DIST^{V1.2}$ model, in Part III from the $DIST^{V2}$ model, in Part IV from the $DIST^{V3}$ model, in Part V from the $DIST^{V4}$ model, in Part VI from the $JOHANSEN-SPRD$ model, in Part VIII from the $ADF-SPRD$ model, in from the $DIST^{V2}$ model, in Part VIII from the $KALMAN-SPRD$ model, and in Part IX from the $RATIO-SPRD$ model. In Part X and XI, we present the back-test metrics of the trading strategies which use the close price of SCHB.N, and SCHF.N, respectively. All $ numbers reported below are in USD.

(I) Trading Strategy Code	(II) Model Name	(III) Total Number of Trades	(IV) Number of Winning Trades	(V) Number of Loosing Trades	(VI) Average Profit per Trade ($)	(VII) Average Loss per Trade ($)	(VIII) Gross Profit ($)	(IX) Gross Loss ($)	(X) Net Profit ($)	(XI) ROI (%)	(XII) Max P&L ($)	(XIII) Min P&L ($)	(XIV) Daily Sharpe Ratio	(XV) Annualized Sharpe Ratio	(XVI) Hit Ratio	(XVII) Expectancy	(XVIII) Profit Factor	(XIX) Realized Risk Reward Ratio	(XX) Max Drawdown ($)
	Part I: Models derived using the spread obtained from $DIST^{V1.1}-SPRD^{50D}$																		
A1	$DIST^{V1.1}-ZSPRD^{50D}_{(3,2)}$	2	-	2	-	65.28	-	130.56	**-130.56**	-1.31	-	-98.65	-4.61	-73.18	-	-65.28	-	-	-130.56
A1	$DIST^{V1.1}-ZSPRD^{50D}_{(3,1)}$	1	-	1	-	66.31	-	66.31	**-66.31**	-0.66	-	-66.31	-	-	-	-66.31	-	-	-66.31
A1	$DIST^{V1.1}-ZSPRD^{50D}_{(3,0.5)}$	1	-	1	-	170.67	-	170.67	**-170.67**	-1.71	-	-170.67	-	-	-	-170.67	-	-	-170.67
A1	$DIST^{V1.1}-ZSPRD^{50D}_{(2.7,2)}$	3	1	2	59.66	38.57	59.66	77.13	**-17.47**	-0.17	59.66	-45.22	-2.76	-43.81	33.33	-5.83	0.77	1.55	-45.22
A1	$DIST^{V1.1}-ZSPRD^{50D}_{(2.7,1)}$	2	1	1	63.96	66.31	63.96	66.31	**-2.35**	-0.02	63.96	-66.31	-1.66	-26.35	50	-1.17	0.96	0.96	-66.31
A1	$DIST^{V1.1}-ZSPRD^{50D}_{(2.7,0.5)}$	2	1	1	63.3	170.67	63.3	170.67	**-107.37**	-1.07	63.3	-170.67	-1.24	-19.68	50	-53.68	0.37	0.37	-170.67
A2	$DIST^{V1.1}-SPRD^{50D}-SMA_{(10,20)}$	9	4	5	51.59	187.14	206.38	935.69	**-729.32**	-7.29	120.92	-622.55	-1.08	-17.14	44.44	-81.05	0.22	0.28	-830.62
A2	$DIST^{V1.1}-SPRD^{50D}-EMA_{(10,20)}$	22	13	9	90.34	133.55	1174.37	1201.94	**-27.58**	-0.28	237.02	-336.69	-1.06	-16.83	59.09	-1.26	0.98	0.68	-503.78
A2	$DIST^{V1.1}-SPRD^{50D}-MACD_{(12,26,9)}$	37	29	8	55.24	74.84	1602.02	598.68	**1003.34**	10.03	180.99	-171.06	-1.76	-27.94	78.38	27.12	2.68	0.74	-143.04
A2	$DIST^{V1.1}-SPRD^{50D}-RSI_{(14)}$	5	3	2	395.5	109.98	1186.49	219.95	**966.54**	9.67	658.17	-166.87	0.13	2.06	60	193.31	5.39	3.6	-166.87
A2	$DIST^{V1.1}-SPRD^{50D}-BB_{(20)}$	12	5	7	101.81	66.56	509.07	465.9	**43.18**	0.43	297.13	-123.14	-1.25	-19.84	41.67	3.6	1.09	1.53	-331.26
A3	$DIST^{V1.1}-SPRD^{50D}-DECTREE$	354	152	202	23.81	23.96	3618.57	4840.44	**-1221.87**	-12.22	162.66	-289.77	-4.32	-68.58	42.94	-3.45	0.75	0.99	-1753.28
A4	$DIST^{V1.1}-SPRD^{50D}-MLP$	296	127	169	26.18	23.99	3324.44	4054.27	**-729.82**	-7.3	289.77	-110.99	-4.13	-65.56	42.91	-2.46	0.82	1.09	-1188.26
	Part II: Models derived using the spread obtained from $DIST^{V1.2}-SPRD^{50D}$																		
B1	$DIST^{V1.2}-ZSPRD^{50D}_{(3,2)}$	7	4	3	59.67	34	238.69	102	**136.69**	1.37	102.64	-83.42	-2.02	-32.07	57.14	19.52	2.34	1.76	-83.42
B1	$DIST^{V1.2}-ZSPRD^{50D}_{(3,1)}$	7	2	5	149.15	157.87	298.3	789.36	**-491.07**	-4.91	197	-279.6	-1.24	-19.68	28.57	-70.16	0.38	0.94	-592.36
B1	$DIST^{V1.2}-ZSPRD^{50D}_{(3,0.5)}$	7	2	5	185.45	178.96	370.9	894.8	**-523.9**	-5.24	256.24	-320.86	-1.05	-16.67	28.57	-74.85	0.41	1.04	-638.56
B1	$DIST^{V1.2}-ZSPRD^{50D}_{(2.7,2)}$	11	6	5	30.84	48.88	185.07	244.39	**-59.32**	-0.59	101.3	-98.8	-2.88	-45.72	54.55	-5.39	0.76	0.63	-207.45
B1	$DIST^{V1.2}-ZSPRD^{50D}_{(2.7,1)}$	9	3	6	90.73	143.65	272.18	861.89	**-589.71**	-5.9	102.99	-279.6	-1.54	-24.45	33.33	-65.53	0.32	0.63	-691.01
B1	$DIST^{V1.2}-ZSPRD^{50D}_{(2.7,0.5)}$	9	3	6	136.04	161.33	408.12	967.97	**-559.85**	-5.6	149.86	-320.86	-1.2	-19.05	33.33	-62.22	0.42	0.84	-674.51
B2	$DIST^{V1.2}-SPRD^{50D}-SMA_{(10,20)}$	19	8	11	122.31	80.95	978.49	890.46	**88.02**	0.88	320.86	-221.02	-1.06	-16.83	42.11	4.64	1.1	1.51	-221.02
B2	$DIST^{V1.2}-SPRD^{50D}-EMA_{(10,20)}$	25	10	15	106.77	105.66	1067.68	1584.88	**-517.2**	-5.17	358.9	-339.95	-1.19	-18.89	40	-20.69	0.67	1.01	-817.51
B2	$DIST^{V1.2}-SPRD^{50D}-MACD_{(12,26,9)}$	24	8	16	78.56	69.03	628.51	1104.53	**-476.02**	-4.76	150.19	-278.15	-1.79	-28.42	33.33	-19.84	0.57	1.14	-769.03
B2	$DIST^{V1.2}-SPRD^{50D}-RSI_{(14)}$	8	1	7	23.99	170.13	23.99	1190.93	**-1166.94**	-11.67	23.99	-261.59	-2.73	-43.34	12.5	-145.87	0.02	0.14	-905.35
B2	$DIST^{V1.2}-SPRD^{50D}-BB_{(20)}$	10	6	4	40.59	34.63	243.53	138.52	**105.01**	1.05	74.61	-68.96	-3.05	-48.42	60	10.5	1.76	1.17	-103.44
B3	$DIST^{V1.2}-SPRD^{50D}-DECTREE$	290	138	152	21.47	23.94	2963.47	3638.5	**-675.03**	-6.75	168.44	-111.66	-4.78	-75.88	47.59	-2.33	0.81	0.9	-1155.02
B4	$DIST^{V1.2}-SPRD^{50D}-MLP$	273	138	135	23.11	23.37	3188.68	3154.73	**33.94**	0.34	162.96	-130.19	-4.51	-71.59	50.55	0.12	1.01	0.99	-556.4
	Part III: Models derived using the spread obtained from $DIST^{V2}-SPRD^{50D}$																		
C1	$DIST^{V2}-ZSPRD^{50D}_{(3,2)}$	2	2	-	65.28	-	130.56	-	**130.56**	1.31	98.65	-	-1.84	-29.21	100	65.28	130.56	65.28	-
C1	$DIST^{V2}-ZSPRD^{50D}_{(3,1)}$	1	1	-	66.31	-	66.31	-	**66.31**	0.66	66.31	-	-	-	100	66.31	66.31	66.31	-
C1	$DIST^{V2}-ZSPRD^{50D}_{(3,0.5)}$	1	1	-	170.67	-	170.67	-	**170.67**	1.71	170.67	-	-	-	100	170.67	170.67	170.67	-
C1	$DIST^{V2}-ZSPRD^{50D}_{(2.7,2)}$	3	2	1	38.57	59.66	77.13	59.66	**17.47**	0.17	45.22	-59.66	-2.56	-40.64	66.67	5.83	1.29	0.65	-59.66
C1	$DIST^{V2}-ZSPRD^{50D}_{(2.7,1)}$	2	1	1	66.31	63.96	66.31	63.96	**2.35**	0.02	66.31	-63.96	-1.64	-26.03	50	1.17	1.04	1.04	-63.96
C1	$DIST^{V2}-ZSPRD^{50D}_{(2.7,0.5)}$	2	1	1	170.67	63.3	170.67	63.3	**107.37**	1.07	170.67	-63.3	-0.59	-9.37	50	53.68	2.7	2.7	-63.3
C2	$DIST^{V2}-SPRD^{50D}-SMA_{(10,20)}$	9	5	4	187.14	51.59	935.69	206.38	**729.32**	7.29	622.55	-120.92	-0.33	-5.24	55.56	81.05	4.53	3.63	-120.92
C2	$DIST^{V2}-SPRD^{50D}-EMA_{(10,20)}$	22	9	13	133.55	90.34	1201.94	1174.37	**27.58**	0.28	336.69	-237.02	-1.05	-16.67	40.91	1.26	1.02	1.48	-410.71
C2	$DIST^{V2}-SPRD^{50D}-MACD_{(12,26,9)}$	37	8	29	74.84	55.24	598.68	1602.02	**-1003.34**	-10.03	171.06	-180.99	-2.53	-40.16	21.62	-27.12	0.37	1.35	-1174.39
C2	$DIST^{V2}-SPRD^{50D}-RSI_{(14)}$	5	2	3	109.98	395.5	219.95	1186.49	**-966.54**	-9.67	166.87	-658.17	-1.05	-16.67	40	-193.31	0.19	0.28	-840.4
C2	$DIST^{V2}-SPRD^{50D}-BB_{(20)}$	12	7	5	66.56	101.81	465.9	509.07	**-43.18**	-0.43	123.14	-297.13	-1.31	-20.8	58.33	-3.6	0.92	0.65	-175.5
C3	$DIST^{V2}-SPRD^{50D}-DECTREE$	353	151	202	23.03	24.15	3477.27	4878.81	**-1401.54**	-14.02	162.66	-289.77	-4.41	-70.01	42.78	-3.97	0.71	0.95	-1823.35
C4	$DIST^{V2}-SPRD^{50D}-MLP$	310	133	177	28.54	25.56	3796.15	4523.85	**-727.7**	-7.28	277.29	-179.79	-3.85	-61.12	42.9	-2.35	0.84	1.12	-1383.09
	Part IV: Models derived using the spread obtained from $DIST^{V3}-SPRD^{50D}$																		
D1	$DIST^{V3}-ZSPRD^{50D}_{(3,2)}$	8	5	3	37.38	92.86	186.9	278.59	**-91.69**	-0.92	73.23	-133.49	-2.14	-33.97	62.5	-11.46	0.67	0.4	-253.1
D1	$DIST^{V3}-ZSPRD^{50D}_{(3,1)}$	8	5	3	47.58	116.39	237.92	349.17	**-111.25**	-1.11	100.11	-173.38	-1.69	-26.83	62.5	-13.91	0.68	0.41	-322.1
D1	$DIST^{V3}-ZSPRD^{50D}_{(3,0.5)}$	8	5	3	56.31	78.36	281.55	235.07	**46.48**	0.46	100.11	-120.28	-1.89	-30	62.5	5.81	1.2	0.72	-209.19
D1	$DIST^{V3}-ZSPRD^{50D}_{(2.7,2)}$	13	9	4	28.63	71.32	257.7	285.29	**-27.58**	-0.28	73.23	-133.49	-2.56	-40.64	69.23	-2.12	0.9	0.4	-234.99
D1	$DIST^{V3}-ZSPRD^{50D}_{(2.7,1)}$	13	10	3	41.15	116.39	411.48	349.17	**62.31**	0.62	100.11	-173.38	-1.79	-28.42	76.92	4.79	1.18	0.35	-264.32
D1	$DIST^{V3}-ZSPRD^{50D}_{(2.7,0.5)}$	13	10	3	53.69	78.36	536.9	235.07	**301.83**	3.02	112.05	-120.28	-1.86	-29.53	76.92	23.21	2.28	0.69	-120.28
D2	$DIST^{V3}-SPRD^{50D}-SMA_{(10,20)}$	18	8	10	84.98	95.35	679.86	953.5	**-273.64**	-2.74	224.09	-216.74	-1.49	-23.65	44.44	-15.21	0.71	0.89	-805.27
D2	$DIST^{V3}-SPRD^{50D}-EMA_{(10,20)}$	33	12	21	124.96	70.25	1499.51	1475.32	**24.19**	0.24	300.9	-253.97	-1.28	-20.32	36.36	0.73	1.02	1.78	-717.26
D2	$DIST^{V3}-SPRD^{50D}-MACD_{(12,26,9)}$	39	21	18	84.13	79.14	1766.74	1424.5	**342.24**	3.42	265.78	-190.43	-1.25	-19.84	53.85	8.78	1.24	1.06	-389.42
D2	$DIST^{V3}-SPRD^{50D}-RSI_{(14)}$	6	3	3	202.69	213.81	608.07	641.43	**-33.36**	-0.33	423.07	-404.14	-0.56	-8.89	50	-5.56	0.95	0.95	-404.14
D2	$DIST^{V3}-SPRD^{50D}-BB_{(20)}$	19	13	6	55.85	70.31	726	421.84	**304.16**	3.04	194.53	-189.14	-1.63	-25.88	68.42	16.01	1.72	0.79	-207.2
D3	$DIST^{V3}-SPRD^{50D}-DECTREE$	307	138	169	24.69	25.23	3407.55	4263.27	**-855.71**	-8.56	189.97	-220.17	-4	-63.5	44.95	-2.79	0.8	0.98	-1108.88
D4	$DIST^{V3}-SPRD^{50D}-MLP$	189	82	107	31.41	26.68	2576	2854.92	**-278.92**	-2.79	147.49	-191.87	-3.61	-57.31	43.39	-1.47	0.9	1.18	-635.17
	Part V: Models derived using the spread obtained from $DIST^{V4}-SPRD^{50D}$																		
E1	$DIST^{V4}-ZSPRD^{50D}_{(3,2)}$	8	5	3	37.38	92.86	186.9	278.59	**-91.69**	-0.92	73.23	-133.49	-2.14	-33.97	62.5	-11.46	0.67	0.4	-253.1
E1	$DIST^{V4}-ZSPRD^{50D}_{(3,1)}$	8	5	3	47.58	116.39	237.92	349.17	**-111.25**	-1.11	100.11	-173.38	-1.69	-26.83	62.5	-13.91	0.68	0.41	-322.1
E1	$DIST^{V4}-ZSPRD^{50D}_{(3,0.5)}$	8	5	3	56.31	78.36	281.55	235.07	**46.48**	0.46	100.11	-120.28	-1.89	-30	62.5	5.81	1.2	0.72	-209.19
E1	$DIST^{V4}-ZSPRD^{50D}_{(2.7,2)}$	13	9	4	28.63	71.32	257.7	285.29	**-27.58**	-0.28	73.23	-133.49	-2.56	-40.64	69.23	-2.12	0.9	0.4	-234.99
E1	$DIST^{V4}-ZSPRD^{50D}_{(2.7,1)}$	13	10	3	41.15	116.39	411.48	349.17	**62.31**	0.62	100.11	-173.38	-1.79	-28.42	76.92	4.79	1.18	0.35	-264.32
E1	$DIST^{V4}-ZSPRD^{50D}_{(2.7,0.5)}$	13	10	3	53.69	78.36	536.9	235.07	**301.83**	3.02	112.05	-120.28	-1.86	-29.53	76.92	23.21	2.28	0.69	-120.28
E2	$DIST^{V4}-SPRD^{50D}-SMA_{(10,20)}$	18	6	12	74.7	97.85	448.18	1174.18	**-726**	-7.26	142.66	-216.74	-1.96	-31.11	33.33	-40.34	0.38	0.76	-805.27
E2	$DIST^{V4}-SPRD^{50D}-EMA_{(10,20)}$	33	12	21	124.96	70.25	1499.51	1475.32	**24.19**	0.24	300.9	-253.97	-1.28	-20.32	36.36	0.73	1.02	1.78	-717.26
E2	$DIST^{V4}-SPRD^{50D}-MACD_{(12,26,9)}$	39	21	18	84.13	79.14	1766.74	1424.5	**342.24**	3.42	265.78	-190.43	-1.25	-19.84	53.85	8.78	1.24	1.06	-389.42
E2	$DIST^{V4}-SPRD^{50D}-RSI_{(14)}$	6	3	3	202.69	213.81	608.07	641.43	**-33.36**	-0.33	423.07	-404.14	-0.56	-8.89	50	-5.56	0.95	0.95	-404.14
E2	$DIST^{V4}-SPRD^{50D}-BB_{(20)}$	19	13	6	55.85	70.31	726	421.84	**304.16**	3.04	194.53	-189.14	-1.63	-25.88	68.42	16.01	1.72	0.79	-207.2
E3	$DIST^{V4}-SPRD^{50D}-DECTREE$	303	132	171	25.33	25.81	3343.75	4414.24	**-1070.49**	-10.7	189.97	-220.17	-3.97	-63.02	43.56	-3.54	0.76	0.98	-1409.77
E4	$DIST^{V4}-SPRD^{50D}-MLP$	206	93	113	29.91	31.84	2781.32	3597.47	**-816.15**	-8.16	132.5	-265.94	-3.48	-55.24	45.15	-3.96	0.77	0.94	-1008.22
	Part VI: Models derived using the spread obtained from $JOHANSEN-SPRD^{50D}$																		
F1	$JOHANSEN-ZSPRD^{50D}_{(3,2)}$	21	8	13	27.98	46.26	223.85	601.36	**-377.51**	-3.78	67.73	-139.33	-2.68	-42.54	38.1	-17.97	0.37	0.6	-411.58
F1	$JOHANSEN-ZSPRD^{50D}_{(3,1)}$	19	6	13	69.55	71.1	417.31	924.27	**-506.96**	-5.07	216.55	-401.57	-1.27	-20.16	31.58	-26.68	0.45	0.98	-667.84
F1	$JOHANSEN-ZSPRD^{50D}_{(3,0.5)}$	18	5	13	75.52	85.37	377.58	1109.85	**-732.26**	-7.32	216.55	-401.57	-1.24	-19.68	27.78	-40.68	0.34	0.88	-777.97
F1	$JOHANSEN-ZSPRD^{50D}_{(2.7,2)}$	25	10	15	27.6	53.92	275.97	808.78	**-532.81**	-5.33	67.73	-183.45	-2.92	-46.35	40	-21.31	0.34	0.51	-566.88
F1	$JOHANSEN-ZSPRD^{50D}_{(2.7,1)}$	20	6	14	69.55	83.33	417.31	1166.67	**-749.36**	-7.49	216.55	-445	-0.91	-14.45	30	-37.47	0.36	0.83	-910.25
F1	$JOHANSEN-ZSPRD^{50D}_{(2.7,0.5)}$	19	5	14	75.52	96.59	377.58	1352.25	**-974.67**	-9.75	216.55	-445	-0.9	-14.29	26.32	-51.29	0.28	0.78	-1020.37
F2	$JOHANSEN-SPRD^{50D}-SMA_{(10,20)}$	26	17	9	232.39	131.81	3950.68	1186.31	**2764.37**	27.64	1231.47	-328.11	0.35	5.56	65.38	106.31	3.33	1.76	-459.75
F2	$JOHANSEN-SPRD^{50D}-EMA_{(10,20)}$	35	22	13	451.23	254.98	9927.13	3314.78	**6612.35**	66.12	4605.67	-1142.4	0.16	2.54	62.86	188.94	2.99	1.77	-1929.6
F2	$JOHANSEN-SPRD^{50D}-MACD_{(12,26,9)}$	35	19	16	236.72	153.02	4497.63	2448.39	**2049.24**	20.49	1092.74	-514.34	-0.18	-2.86	54.29	58.57	1.84	1.55	-1039.27
F2	$JOHANSEN-SPRD^{50D}-RSI_{(14)}$	7	3	4	451.38	704.7	1354.15	2818.8	**-1464.65**	-14.65	956.94	-1509.45	-0.72	-11.43	42.86	-209.2	0.48	0.64	-1855.78
F2	$JOHANSEN-SPRD^{50D}-BB_{(20)}$	19	5	14	81.23	292.24	406.14	4091.42	**-3685.28**	-36.85	191.46	-976.16	-0.41	-6.51	26.32	-193.95	0.1	0.28	-3638.76
F3	$JOHANSEN-SPRD^{50D}-DECTREE$	303	147	156	26.81	25.87	3941.62	4035.84	**-94.22**	-0.94	235.5	-289.77	-3.7	-58.74	48.51	-0.31	0.98	1.04	-924.74
F4	$JOHANSEN-SPRD^{50D}-MLP$	173	82	91	26.3	36.29	2156.36	3302.48	**-1146.13**	-11.46	147.49	-367.01	-3.04	-48.26	47.4	-6.62	0.65	0.72	-1340.17
	Part VII: Models derived using the spread obtained from $ADF-SPRD^{50D}$																		
G1	$ADF-ZSPRD^{50D}_{(3,2)}$	5	3	2	185.86	3624.57	557.58	7249.15	**-6691.57**	-66.92	374.94	-6771.48	-0.47	-7.46	60	-1338.31	0.08	0.05	-7079.79
G1	$ADF-ZSPRD^{50D}_{(3,1)}$	5	3	2	384.24	3343.2	1152.73	6686.4	**-5533.67**	-55.34	742.2	-5755.94	-0.45	-7.14	60	-1106.73	0.17	0.11	-5944.2
G1	$ADF-ZSPRD^{50D}_{(3,0.5)}$	5	2	3	412.97	1879.15	825.95	5637.44	**-4811.49**	-48.11	742.2	-5295.69	-0.43	-6.83	40	-962.3	0.15	0.22	-5637.44
G1	$ADF-ZSPRD^{50D}_{(2.7,2)}$	10	8	2	288.51	3624.57	2308.09	7249.15	**-4941.06**	-49.41	627.22	-6771.48	-0.27	-4.29	80	-494.11	0.32	0.08	-6771.48
G1	$ADF-ZSPRD^{50D}_{(2.7,1)}$	10	6	4	417.97	1792.11	2507.8	7168.46	**-4660.66**	-46.61	742.2	-5755.94	-0.3	-4.76	60	-466.07	0.35	0.23	-6166.1
G1	$ADF-ZSPRD^{50D}_{(2.7,0.5)}$	10	5	5	521.81	1246.92	2609.04	6234.6	**-3625.57**	-36.26	985.59	-5295.69	-0.26	-4.13	50	-362.56	0.42	0.42	-5295.69
G2	$ADF-SPRD^{50D}-SMA_{(10,20)}$	18	8	10	640.21	494.02	5121.71	4940.17	**181.54**	1.82	2919.67	-1095.9	-0.07	-1.11	44.44	10.04	1.04	1.3	-2360.9
G2	$ADF-SPRD^{50D}-EMA_{(10,20)}$	38	24	14	789.78	378.52	18954.65	5299.3	**13655.36**	136.55	11804.99	-957.88	0.13	2.06	63.16	359.38	3.58	2.09	-2103.24
G2	$ADF-SPRD^{50D}-MACD_{(12,26,9)}$	41	22	19	1297.72	397.92	28549.76	7560.39	**20989.38**	209.89	14862.78	-1383.86	0.17	2.7	53.66	511.96	3.78	3.26	-2788.56
G2	$ADF-SPRD^{50D}-RSI_{(14)}$	3	1	2	911.47	2652.7	911.47	5305.41	**-4393.94**	-43.94	911.47	-3214.69	-0.78	-12.38	33.33	-1464.76	0.17	0.34	-5305.41
G2	$ADF-SPRD^{50D}-BB_{(20)}$	19	10	9	323.67	394.66	3236.7	3551.96	**-315.26**	-3.15	967.5	-949.09	-0.23	-3.65	52.63	-16.6	0.91	0.82	-1906.69
G3	$ADF-SPRD^{50D}-DECTREE$	294	148	146	23.15	25.79	3425.66	3765.31	**-339.65**	-3.4	161.47	-133.15	-4.35	-69.05	50.34	-1.16	0.91	0.9	-1049.27
G4	$ADF-SPRD^{50D}-MLP$	129	46	83	35.81	47.28	1647.27	3924.4	**-2277.13**	-22.77	225.13	-316.07	-2.27	-36.04	35.66	-17.65	0.42	0.76	-2514.44
	Part VIII: Models derived using the spread obtained from $KALMAN-SPRD^{50D}$																		
H1	$KALMAN-ZSPRD^{50D}_{(3,2)}$	3	2	1	289.35	89.97	578.71	89.97	**488.74**	4.89	308.03	-89.97	0.27	4.29	66.67	162.93	6.43	3.22	-89.97
H1	$KALMAN-ZSPRD^{50D}_{(3,1)}$	1	-	1	-	166.36	-	166.36	**-166.36**	-1.66	-	-166.36	-	-	-	-166.36	-	-	-166.36
H1	$KALMAN-ZSPRD^{50D}_{(3,0.5)}$	1	1	-	203.04	-	203.04	-	**203.04**	2.03	203.04	-	-	-	100	203.04	203.04	203.04	-
H1	$KALMAN-ZSPRD^{50D}_{(2.7,2)}$	5	2	3	199.93	46.32	399.86	138.95	**260.91**	2.61	270.68	-89.97	-0.38	-6.03	40	52.18	2.88	4.32	-138.95
H1	$KALMAN-ZSPRD^{50D}_{(2.7,1)}$	2	1	1	162.86	501.67	162.86	501.67	**-338.81**	-3.39	162.86	-501.67	-0.58	-9.21	50	-169.41	0.32	0.32	-501.67
H1	$KALMAN-ZSPRD^{50D}_{(2.7,0.5)}$	2	-	2	-	110.68	-	221.35	**-221.35**	-2.21	-	-167.02	-2.8	-44.45	-	-110.68	-	-	-221.35
H2	$KALMAN-SPRD^{50D}-SMA_{(10,20)}$	14	5	9	451.13	218.95	2255.65	1970.56	**285.09**	2.85	856.39	-482.65	-0.22	-3.49	35.71	20.33	1.14	2.06	-734.96
H2	$KALMAN-SPRD^{50D}-EMA_{(10,20)}$	23	8	15	453.89	164.91	3631.11	2473.61	**1157.5**	11.57	1591.02	-331.16	-0.13	-2.06	34.78	50.31	1.47	2.75	-671.5
H2	$KALMAN-SPRD^{50D}-MACD_{(12,26,9)}$	37	8	29	366.08	115.16	2928.67	3339.62	**-410.95**	-4.11	1620.19	-324.25	-0.37	-5.87	21.62	-11.11	0.88	3.18	-1566.92
H2	$KALMAN-SPRD^{50D}-RSI_{(14)}$	4	2	2	1220.33	1766.41	2440.67	3532.82	**-1092.16**	-10.92	2169.84	-2942.44	-0.18	-2.86	50	-273.04	0.69	0.69	-2942.44
H2	$KALMAN-SPRD^{50D}-BB_{(20)}$	14	10	4	159.02	376.3	1590.25	1505.2	**85.05**	0.85	453.7	-1109.32	-0.27	-4.29	71.43	6.08	1.06	0.42	-1505.2
H3	$KALMAN-SPRD^{50D}-DECTREE$	345	150	195	23.11	25.33	3466.71	4938.94	**-1472.23**	-14.72	162.66	-289.77	-4.16	-66.04	43.48	-4.27	0.7	0.91	-1845
H4	$KALMAN-SPRD^{50D}-MLP$	288	119	169	23.68	26.31	2817.44	4446.06	**-1628.62**	-16.29	164.53	-289.77	-3.99	-63.34	41.32	-5.65	0.63	0.9	-1847.75
	Part IX: Models derived using the spread obtained from $RATIO-SPRD^{50D}$																		
I1	$RATIO-ZSPRD^{50D}_{(3,2)}$	3	3	-	118.79	-	356.38	-	**356.38**	3.56	289.77	-	-0.22	-3.49	100	118.79	356.38	118.79	-
I1	$RATIO-ZSPRD^{50D}_{(3,1)}$	3	3	-	180.26	-	540.79	-	**540.79**	5.41	414.81	-	0.14	2.22	100	180.26	540.79	180.26	-
I1	$RATIO-ZSPRD^{50D}_{(3,0.5)}$	3	3	-	170.33	-	511	-	**511**	5.11	414.81	-	0.09	1.43	100	170.33	511	170.33	-
I1	$RATIO-ZSPRD^{50D}_{(2.7,2)}$	5	4	1	97.18	22.05	388.74	22.05	**366.68**	3.67	289.77	-22.05	-0.64	-10.16	80	73.34	17.63	4.41	-22.05
I1	$RATIO-ZSPRD^{50D}_{(2.7,1)}$	5	4	1	154.32	50.07	617.3	50.07	**567.22**	5.67	414.81	-50.07	-0.22	-3.49	80	113.44	12.33	3.08	-50.07
I1	$RATIO-ZSPRD^{50D}_{(2.7,0.5)}$	5	4	1	149.98	50.07	599.91	50.07	**549.84**	5.5	414.81	-50.07	-0.24	-3.81	80	109.97	11.98	3	-50.07
I2	$RATIO-SPRD^{50D}-SMA_{(10,20)}$	15	6	9	167.26	115.67	1003.57	1040.99	**-37.42**	-0.37	364.83	-314.97	-0.87	-13.81	40	-2.49	0.96	1.45	-448.64
I2	$RATIO-SPRD^{50D}-EMA_{(10,20)}$	24	8	16	112.3	73.13	898.42	1170.03	**-271.61**	-2.72	248.67	-266.81	-1.44	-22.86	33.33	-11.32	0.77	1.54	-915.14
I2	$RATIO-SPRD^{50D}-MACD_{(12,26,9)}$	30	12	18	54.87	80.19	658.4	1443.45	**-785.05**	-7.85	156.26	-240.74	-1.93	-30.64	40	-26.17	0.46	0.68	-825.85
I2	$RATIO-SPRD^{50D}-RSI_{(14)}$	3	1	2	169.67	802.34	169.67	1604.68	**-1435.02**	-14.35	169.67	-1425.46	-0.75	-11.91	33.33	-478.37	0.11	0.21	-1425.46
I2	$RATIO-SPRD^{50D}-BB_{(20)}$	13	12	1	55.3	237	663.57	237	**426.57**	4.27	139	-237	-1.35	-21.43	92.31	32.82	2.8	0.23	-237
I3	$RATIO-SPRD^{50D}-DECTREE$	348	118	230	24.85	21.17	2931.95	4868.73	**-1936.78**	-19.37	123.14	-110.99	-5.13	-81.44	33.91	-5.56	0.6	1.17	-2209.93
I4	$RATIO-SPRD^{50D}-MLP$	308	110	198	27.73	22.34	3050.04	4423.22	**-1373.17**	-13.73	239.75	-124.63	-4.3	-68.26	35.71	-4.46	0.69	1.24	-1544.39
	Part X: Models derived using the close price of SCHB.N																		
CLS-SYM-1	$CLOSE^{SCHB.N}-SMA_{(10,20)}$	14	8	6	275.75	104.83	2206.01	628.98	**1577.04**	15.77	789.43	-230.52	0.13	2.06	57.14	112.63	3.51	2.63	-324.24
CLS-SYM-1	$CLOSE^{SCHB.N}-EMA_{(10,20)}$	17	7	10	370.21	232.37	2591.45	2323.66	**267.79**	2.68	1083.32	-810.29	-0.15	-2.38	41.18	15.77	1.12	1.59	-630.81
CLS-SYM-1	$CLOSE^{SCHB.N}-MACD_{(12,26,9)}$	37	14	23	144.19	101.44	2018.6	2333.05	**-314.45**	-3.14	604.53	-326.15	-0.5	-7.94	37.84	-8.49	0.87	1.42	-1087.87
CLS-SYM-1	$CLOSE^{SCHB.N}-RSI_{(14)}$	5	2	3	313.96	850.97	627.91	2552.9	**-1924.99**	-19.25	584.15	-2050.03	-0.46	-7.3	40	-385	0.25	0.37	-2050.03
CLS-SYM-1	$CLOSE^{SCHB.N}-BB_{(20)}$	11	9	2	83.74	413.03	753.64	826.06	**-72.41**	-0.72	239.73	-780.29	-0.31	-4.92	81.82	-6.57	0.91	0.2	-780.29
	Part XI: Models derived using the close price of SCHF.N																		
CLS-SYM-2	$CLOSE^{SCHF.N}-SMA_{(10,20)}$	20	7	13	314.26	125.66	2199.8	1633.59	**566.2**	5.66	1106.36	-575.54	-0.14	-2.22	35	28.31	1.35	2.5	-918.42
CLS-SYM-2	$CLOSE^{SCHF.N}-EMA_{(10,20)}$	23	8	15	331.11	93.37	2648.86	1400.61	**1248.24**	12.48	911.97	-332.73	-0.07	-1.11	34.78	54.26	1.89	3.55	-643.72
CLS-SYM-2	$CLOSE^{SCHF.N}-MACD_{(12,26,9)}$	30	10	20	221.35	120.16	2213.46	2403.27	**-189.81**	-1.9	1043.11	-326.35	-0.34	-5.4	33.33	-6.34	0.92	1.84	-1733.81
CLS-SYM-2	$CLOSE^{SCHF.N}-RSI_{(14)}$	5	2	3	617.93	304.16	1235.87	912.48	**323.39**	3.23	959.27	-697.61	-0.02	-0.32	40	64.68	1.35	2.03	-697.61
CLS-SYM-2	$CLOSE^{SCHF.N}-BB_{(20)}$	15	8	7	79.49	192.86	635.89	1349.99	**-714.1**	-7.14	252.09	-785.71	-0.51	-8.1	53.33	-47.62	0.47	0.41	-785.71

Table D.2.12: This table presents the back-test metrics for the pair $SCHB.N/SCHF$ based on a 100-day rolling window. The table is subdivided into eleven parts, and in each of these parts, we present the back-test metrics and the trading strategies which use the spread derived from various models. In Part I, the spread is derived from the $DIST^{V1.1}$ model, in Part II from the $DIST^{V1.2}$ model, in Part III from the $DIST^{V2}$ model, in Part IV from the $DIST^{V3}$ model, in Part V from the $DIST^{V4}$ model, in Part VI from the $JOHANSEN-SPRD$ model, in Part VIII from the $ADF-SPRD$ model, in from the $DIST^{V2}$ model, in Part VIII from the $KALMAN-SPRD$ model, and in Part IX from the $RATIO-SPRD$ model. In Part X and XI, we present the back-test metrics of the trading strategies which use the close price of SCHB.N, and SCHF.N, respectively. All $ numbers reported below are in USD.

(I) Trading Strategy Code	(II) Model Name	(III) Total Number of Trades	(IV) Number of Winning Trades	(V) Number of Loosing Trades	(VI) Average Profit per Trade ($)	(VII) Average Loss per Trade ($)	(VIII) Gross Profit ($)	(IX) Gross Loss ($)	(X) Net Profit ($)	(XI) ROI (%)	(XII) Max P&L ($)	(XIII) Min P&L ($)	(XIV) Daily Sharpe Ratio	(XV) Annualized Sharpe Ratio	(XVI) Hit Ratio	(XVII) Expectancy	(XVIII) Profit Factor	(XIX) Realized Risk Reward Ratio	(XX) Max Drawdown ($)
	Part I: Models derived using the spread obtained from $DIST^{V1.1}-SPRD^{100D}$																		
A1	$DIST^{V1.1}-ZSPRD^{100D}_{(3,2)}$	2	1	1	235.5	117.3	235.5	117.3	**118.2**	1.18	235.5	-117.3	-0.37	-5.87	50	59.1	2.01	2.01	-117.3
A1	$DIST^{V1.1}-ZSPRD^{100D}_{(3,1)}$	1	-	1	-	10.16	-	10.16	**-10.16**	-0.1	-	-10.16	-	-	-	-10.16	-	-	-10.16
A1	$DIST^{V1.1}-ZSPRD^{100D}_{(3,0.5)}$	1	-	1	-	42.88	-	42.88	**-42.88**	-0.43	-	-42.88	-	-	-	-42.88	-	-	-42.88
A1	$DIST^{V1.1}-ZSPRD^{100D}_{(2.7,2)}$	4	2	2	166.46	79.94	332.93	159.87	**173.06**	1.73	235.5	-117.3	-0.7	-11.11	50	43.26	2.08	2.08	-159.87
A1	$DIST^{V1.1}-ZSPRD^{100D}_{(2.7,1)}$	3	2	1	182.95	10.16	365.89	10.16	**355.74**	3.56	252.71	-10.16	-0.25	-3.97	66.67	118.59	36.02	18.01	-10.16
A1	$DIST^{V1.1}-ZSPRD^{100D}_{(2.7,0.5)}$	3	2	1	151.46	42.88	302.91	42.88	**260.03**	2.6	252.71	-42.88	-0.43	-6.83	66.67	86.68	7.06	3.53	-42.88
A2	$DIST^{V1.1}-SPRD^{100D}-SMA_{(10,20)}$	8	3	5	55.81	187.14	167.43	935.69	**-768.27**	-7.68	120.92	-622.55	-1.1	-17.46	37.5	-96.03	0.18	0.3	-830.62
A2	$DIST^{V1.1}-SPRD^{100D}-EMA_{(10,20)}$	22	14	8	92.73	147.79	1298.2	1182.33	**115.87**	1.16	237.02	-336.69	-0.99	-15.72	63.64	5.28	1.1	0.63	-484.16
A2	$DIST^{V1.1}-SPRD^{100D}-MACD_{(12,26,9)}$	34	26	8	61.29	85.87	1593.52	686.95	**906.57**	9.07	180.99	-259.32	-1.51	-23.97	76.47	26.66	2.32	0.71	-143.04
A2	$DIST^{V1.1}-SPRD^{100D}-RSI_{(14)}$	4	3	1	439.12	166.87	1317.36	166.86	**1150.5**	11.5	658.17	-166.87	0.38	6.03	75	287.62	7.89	2.63	-166.87
A2	$DIST^{V1.1}-SPRD^{100D}-BB_{(20)}$	11	4	7	159.61	66.56	638.44	465.9	**172.55**	1.73	434.52	-123.14	-0.86	-13.65	36.36	15.68	1.37	2.4	-331.26
A3	$DIST^{V1.1}-SPRD^{100D}-DECTREE$	314	131	183	23.48	24.41	3075.85	4467.68	**-1391.84**	-13.92	125.53	-117.3	-4.79	-76.04	41.72	-4.43	0.69	0.96	-1618.84
A4	$DIST^{V1.1}-SPRD^{100D}-MLP$	290	124	166	23.48	26.57	2911.81	4410.7	**-1498.89**	-14.99	152.4	-289.77	-4.07	-64.61	42.76	-5.17	0.66	0.88	-1750.18
	Part II: Models derived using the spread obtained from $DIST^{V1.2}-SPRD^{100D}$																		
B1	$DIST^{V1.2}-ZSPRD^{100D}_{(3,2)}$	5	3	2	26.49	136.86	79.47	273.73	**-194.26**	-1.94	62.62	-184.45	-1.95	-30.96	60	-38.85	0.29	0.19	-203.66
B1	$DIST^{V1.2}-ZSPRD^{100D}_{(3,1)}$	5	1	4	160.41	66.49	160.41	265.97	**-105.56**	-1.06	160.41	-156.04	-1.51	-23.97	20	-21.11	0.6	2.41	-203.37
B1	$DIST^{V1.2}-ZSPRD^{100D}_{(3,0.5)}$	5	2	3	34.41	120.06	68.83	360.19	**-291.36**	-2.91	53.68	-245.7	-1.82	-28.89	40	-58.27	0.19	0.29	-345.05
B1	$DIST^{V1.2}-ZSPRD^{100D}_{(2.7,2)}$	6	4	2	31.43	145.94	125.72	291.88	**-166.15**	-1.66	62.62	-230.41	-1.66	-26.35	66.67	-27.69	0.43	0.22	-230.41
B1	$DIST^{V1.2}-ZSPRD^{100D}_{(2.7,1)}$	6	2	4	103.33	69.84	206.67	279.34	**-72.68**	-0.73	160.41	-156.04	-1.5	-23.81	33.33	-12.12	0.74	1.48	-243.71
B1	$DIST^{V1.2}-ZSPRD^{100D}_{(2.7,0.5)}$	6	3	3	38.36	123.89	115.08	371.68	**-256.6**	-2.57	53.68	-216.85	-1.88	-29.84	50	-42.77	0.31	0.31	-310.28
B2	$DIST^{V1.2}-SPRD^{100D}-SMA_{(10,20)}$	9	5	4	40.94	126.81	204.68	507.24	**-302.56**	-3.03	151.19	-393.46	-1.26	-20	55.56	-33.61	0.4	0.32	-58.32
B2	$DIST^{V1.2}-SPRD^{100D}-EMA_{(10,20)}$	16	6	10	95.13	107.1	570.77	1071.03	**-500.25**	-5	177.22	-260.15	-1.46	-23.18	37.5	-31.27	0.53	0.89	-560.38
B2	$DIST^{V1.2}-SPRD^{100D}-MACD_{(12,26,9)}$	29	12	17	61.63	74.39	739.5	1264.65	**-525.15**	-5.25	280.18	-297.99	-1.6	-25.4	41.38	-18.11	0.58	0.83	-892.91
B2	$DIST^{V1.2}-SPRD^{100D}-RSI_{(14)}$	7	2	5	116.98	212.58	233.96	1062.92	**-828.96**	-8.29	122.05	-449.8	-1.25	-19.84	28.57	-118.43	0.22	0.55	-484.77
B2	$DIST^{V1.2}-SPRD^{100D}-BB_{(20)}$	9	6	3	55.09	148.01	330.56	444.04	**-113.48**	-1.13	133.21	-312.45	-1.27	-20.16	66.67	-12.6	0.74	0.37	-312.45
B3	$DIST^{V1.2}-SPRD^{100D}-DECTREE$	260	129	131	29.1	24.16	3754.41	3165.35	**589.06**	5.89	189.83	-164.53	-3.81	-60.48	49.62	2.27	1.19	1.2	-531.13
B4	$DIST^{V1.2}-SPRD^{100D}-MLP$	190	87	103	23.63	20.07	2056.13	2066.81	**-10.68**	-0.11	143.32	-108.91	-5	-79.37	45.79	-0.06	0.99	1.18	-442.69
	Part III: Models derived using the spread obtained from $DIST^{V2}-SPRD^{100D}$																		
C1	$DIST^{V2}-ZSPRD^{100D}_{(3,2)}$	2	1	1	117.3	235.5	117.3	235.5	**-118.2**	-1.18	117.3	-235.5	-0.85	-13.49	50	-59.1	0.5	0.5	-235.5
C1	$DIST^{V2}-ZSPRD^{100D}_{(3,1)}$	1	1	-	10.16	-	10.16	-	**10.16**	0.1	10.16	-	-	-	100	10.16	10.16	10.16	-
C1	$DIST^{V2}-ZSPRD^{100D}_{(3,0.5)}$	1	1	-	42.88	-	42.88	-	**42.88**	0.43	42.88	-	-	-	100	42.88	42.88	42.88	-
C1	$DIST^{V2}-ZSPRD^{100D}_{(2.7,2)}$	4	2	2	79.94	166.46	159.87	332.93	**-173.06**	-1.73	117.3	-235.5	-1.25	-19.84	50	-43.26	0.48	0.48	-332.93
C1	$DIST^{V2}-ZSPRD^{100D}_{(2.7,1)}$	3	1	2	10.16	182.95	10.16	365.89	**-355.74**	-3.56	10.16	-252.71	-2.06	-32.7	33.33	-118.59	0.03	0.06	-355.74
C1	$DIST^{V2}-ZSPRD^{100D}_{(2.7,0.5)}$	3	1	2	42.88	151.46	42.88	302.91	**-260.03**	-2.6	42.88	-252.71	-1.58	-25.08	33.33	-86.68	0.14	0.28	-260.03
C2	$DIST^{V2}-SPRD^{100D}-SMA_{(10,20)}$	9	6	3	256.91	39.45	1541.46	118.36	**1423.1**	14.23	622.55	-61.13	0.03	0.48	66.67	158.13	13.02	6.51	-87.93
C2	$DIST^{V2}-SPRD^{100D}-EMA_{(10,20)}$	22	8	14	147.79	92.73	1182.33	1298.2	**-115.87**	-1.16	336.69	-237.02	-1.06	-16.83	36.36	-5.28	0.91	1.59	-410.71
C2	$DIST^{V2}-SPRD^{100D}-MACD_{(12,26,9)}$	34	8	26	85.87	61.29	686.95	1593.52	**-906.57**	-9.07	259.32	-180.99	-2.15	-34.13	23.53	-26.66	0.43	1.4	-1165.89
C2	$DIST^{V2}-SPRD^{100D}-RSI_{(14)}$	4	1	3	166.87	439.12	166.86	1317.36	**-1150.5**	-11.5	166.87	-658.17	-1.23	-19.53	25	-287.62	0.13	0.38	-957.96
C2	$DIST^{V2}-SPRD^{100D}-BB_{(20)}$	11	7	4	66.56	159.61	465.9	638.44	**-172.55**	-1.73	123.14	-434.52	-1.05	-16.67	63.64	-15.68	0.73	0.42	-175.5
C3	$DIST^{V2}-SPRD^{100D}-DECTREE$	316	133	183	22.96	23.89	3053.2	4372.5	**-1319.3**	-13.19	126.1	-192.07	-4.62	-73.34	42.09	-4.17	0.7	0.96	-1512.15
C4	$DIST^{V2}-SPRD^{100D}-MLP$	246	97	149	24.74	26.77	2399.43	3988.45	**-1589.02**	-15.89	177.01	-179.79	-4.23	-67.15	39.43	-6.46	0.6	0.92	-1727.21
	Part IV: Models derived using the spread obtained from $DIST^{V3}-SPRD^{100D}$																		
D1	$DIST^{V3}-ZSPRD^{100D}_{(3,2)}$	9	6	3	65.14	14.27	390.84	42.81	**348.03**	3.48	141.54	-22.08	-2.16	-34.29	66.67	38.67	9.13	4.56	-22.08
D1	$DIST^{V3}-ZSPRD^{100D}_{(3,1)}$	8	6	2	79.28	16.66	475.65	33.33	**442.33**	4.42	112.05	-29.7	-1.97	-31.27	75	55.29	14.27	4.76	-29.7
D1	$DIST^{V3}-ZSPRD^{100D}_{(3,0.5)}$	8	6	2	77.02	8.22	462.13	16.45	**445.68**	4.46	174.81	-14.31	-1.59	-25.24	75	55.71	28.1	9.37	-14.31
D1	$DIST^{V3}-ZSPRD^{100D}_{(2.7,2)}$	11	7	4	64.63	12.27	452.44	49.08	**403.36**	4.03	141.54	-22.08	-2.33	-36.99	63.64	36.67	9.22	5.27	-22.08
D1	$DIST^{V3}-ZSPRD^{100D}_{(2.7,1)}$	10	7	3	77.05	14.93	539.35	44.8	**494.55**	4.95	112.05	-29.7	-2.11	-33.5	70	49.45	12.04	5.16	-41.18
D1	$DIST^{V3}-ZSPRD^{100D}_{(2.7,0.5)}$	10	7	3	75.23	8.22	526.58	24.65	**501.93**	5.02	177.13	-14.31	-1.76	-27.94	70	50.19	21.36	9.16	-22.51
D2	$DIST^{V3}-SPRD^{100D}-SMA_{(10,20)}$	19	7	12	138.3	53.2	968.12	638.34	**329.77**	3.3	343.54	-101.26	-1.12	-17.78	36.84	17.35	1.52	2.6	-522.68
D2	$DIST^{V3}-SPRD^{100D}-EMA_{(10,20)}$	34	11	23	131.43	60.27	1445.69	1386.26	**59.43**	0.59	343.62	-139.46	-1.41	-22.38	32.35	1.74	1.04	2.18	-827.97
D2	$DIST^{V3}-SPRD^{100D}-MACD_{(12,26,9)}$	34	12	22	61.52	64.03	738.19	1408.7	**-670.51**	-6.71	125.52	-213	-2.2	-34.92	35.29	-19.73	0.52	0.96	-694.25
D2	$DIST^{V3}-SPRD^{100D}-RSI_{(14)}$	5	2	3	496.09	186.43	992.18	559.28	**432.9**	4.33	656.75	-192.54	-0.17	-2.7	40	86.58	1.77	2.66	-186.74
D2	$DIST^{V3}-SPRD^{100D}-BB_{(20)}$	18	10	8	40.69	46.12	406.86	368.98	**37.89**	0.38	79.96	-153.08	-2.58	-40.96	55.56	2.11	1.1	0.88	-319.57
D3	$DIST^{V3}-SPRD^{100D}-DECTREE$	307	130	177	23.78	23.33	3091.6	4129.47	**-1037.87**	-10.38	246.56	-87.3	-4.51	-71.59	42.35	-3.38	0.75	1.02	-1847.68
D4	$DIST^{V3}-SPRD^{100D}-MLP$	93	39	54	27.56	36.37	1074.87	1963.8	**-888.93**	-8.89	245.86	-289.77	-2.87	-45.56	41.94	-9.56	0.55	0.76	-888.93
	Part V: Models derived using the spread obtained from $DIST^{V4}-SPRD^{100D}$																		
E1	$DIST^{V4}-ZSPRD^{100D}_{(3,2)}$	9	6	3	65.14	14.27	390.84	42.81	**348.03**	3.48	141.54	-22.08	-2.16	-34.29	66.67	38.67	9.13	4.56	-22.08
E1	$DIST^{V4}-ZSPRD^{100D}_{(3,1)}$	8	6	2	79.28	16.66	475.65	33.33	**442.33**	4.42	112.05	-29.7	-1.97	-31.27	75	55.29	14.27	4.76	-29.7
E1	$DIST^{V4}-ZSPRD^{100D}_{(3,0.5)}$	8	6	2	77.02	8.22	462.13	16.45	**445.68**	4.46	174.81	-14.31	-1.59	-25.24	75	55.71	28.1	9.37	-14.31
E1	$DIST^{V4}-ZSPRD^{100D}_{(2.7,2)}$	11	7	4	64.63	12.27	452.44	49.08	**403.36**	4.03	141.54	-22.08	-2.33	-36.99	63.64	36.67	9.22	5.27	-22.08
E1	$DIST^{V4}-ZSPRD^{100D}_{(2.7,1)}$	10	7	3	77.05	14.93	539.35	44.8	**494.55**	4.95	112.05	-29.7	-2.11	-33.5	70	49.45	12.04	5.16	-41.18
E1	$DIST^{V4}-ZSPRD^{100D}_{(2.7,0.5)}$	10	7	3	75.23	8.22	526.58	24.65	**501.93**	5.02	177.13	-14.31	-1.76	-27.94	70	50.19	21.36	9.16	-22.51
E2	$DIST^{V4}-SPRD^{100D}-SMA_{(10,20)}$	19	7	12	138.3	53.2	968.12	638.34	**329.77**	3.3	343.54	-101.26	-1.12	-17.78	36.84	17.35	1.52	2.6	-522.68
E2	$DIST^{V4}-SPRD^{100D}-EMA_{(10,20)}$	34	11	23	131.43	60.27	1445.69	1386.26	**59.43**	0.59	343.62	-139.46	-1.41	-22.38	32.35	1.74	1.04	2.18	-827.97
E2	$DIST^{V4}-SPRD^{100D}-MACD_{(12,26,9)}$	34	12	22	61.52	64.03	738.19	1408.7	**-670.51**	-6.71	125.52	-213	-2.2	-34.92	35.29	-19.73	0.52	0.96	-694.25
E2	$DIST^{V4}-SPRD^{100D}-RSI_{(14)}$	5	2	3	496.09	186.43	992.18	559.28	**432.9**	4.33	656.75	-192.54	-0.17	-2.7	40	86.58	1.77	2.66	-186.74
E2	$DIST^{V4}-SPRD^{100D}-BB_{(20)}$	18	10	8	40.69	46.12	406.86	368.98	**37.89**	0.38	79.96	-153.08	-2.58	-40.96	55.56	2.11	1.1	0.88	-319.57
E3	$DIST^{V4}-SPRD^{100D}-DECTREE$	306	128	178	24.25	23.96	3103.6	4265.22	**-1161.63**	-11.62	212.9	-105.68	-4.39	-69.69	41.83	-3.8	0.73	1.01	-1679.2
E4	$DIST^{V4}-SPRD^{100D}-MLP$	93	39	54	27.56	36.37	1074.87	1963.8	**-888.93**	-8.89	245.86	-289.77	-2.87	-45.56	41.94	-9.56	0.55	0.76	-888.93
	Part VI: Models derived using the spread obtained from $JOHANSEN-SPRD^{100D}$																		
F1	$JOHANSEN-ZSPRD^{100D}_{(3,2)}$	19	10	9	28.68	20.31	286.84	182.8	**104.04**	1.04	59.93	-65.4	-8.51	-135.09	52.63	5.47	1.57	1.41	-105.92
F1	$JOHANSEN-ZSPRD^{100D}_{(3,1)}$	18	10	8	30.48	28	304.82	224.02	**80.8**	0.81	59.93	-88.57	-8.27	-131.28	55.56	4.49	1.36	1.09	-184.59
F1	$JOHANSEN-ZSPRD^{100D}_{(3,0.5)}$	16	9	7	34.94	27.17	314.47	190.2	**124.27**	1.24	66.87	-65.4	-7.73	-122.71	56.25	7.77	1.65	1.29	-153.99
F1	$JOHANSEN-ZSPRD^{100D}_{(2.7,2)}$	20	10	10	28.01	18.66	280.14	186.57	**93.57**	0.94	59.93	-65.4	-8.32	-132.08	50	4.68	1.5	1.5	-90.76
F1	$JOHANSEN-ZSPRD^{100D}_{(2.7,1)}$	18	10	8	30.48	36.69	304.82	293.49	**11.34**	0.11	59.93	-93.46	-4.87	-77.31	55.56	0.63	1.04	0.83	-254.06
F1	$JOHANSEN-ZSPRD^{100D}_{(2.7,0.5)}$	16	9	7	34.94	37.09	314.47	259.66	**54.81**	0.55	66.87	-93.46	-4.56	-72.39	56.25	3.43	1.21	0.94	-223.45
F2	$JOHANSEN-SPRD^{100D}-SMA_{(10,20)}$	15	11	4	234.01	120.84	2574.11	483.36	**2090.74**	20.91	721.83	-225.08	0.01	0.16	73.33	139.37	5.33	1.94	-363.03
F2	$JOHANSEN-SPRD^{100D}-EMA_{(10,20)}$	26	15	11	386.2	266.45	5792.98	2930.95	**2862.03**	28.62	3439.35	-755.58	-0.18	-2.86	57.69	110.06	1.98	1.45	-901.55
F2	$JOHANSEN-SPRD^{100D}-MACD_{(12,26,9)}$	32	20	12	110.73	392.93	2214.61	4715.11	**-2500.5**	-25	727.94	-2607.33	-0.15	-2.38	62.5	-78.14	0.47	0.28	-3764.81
F2	$JOHANSEN-SPRD^{100D}-RSI_{(14)}$	8	5	3	348.23	4256.68	1741.17	12770.04	**-11028.88**	-110.29	602.99	-9443.97	-0.57	-9.05	62.5	-1378.61	0.14	0.08	-12026.58
F2	$JOHANSEN-SPRD^{100D}-BB_{(20)}$	22	12	10	144.33	340.5	1731.92	3404.95	**-1673.04**	-16.73	504.77	-1382.43	0.06	0.95	54.55	-76.03	0.51	0.42	-3060.77
F3	$JOHANSEN-SPRD^{100D}-DECTREE$	315	167	148	22.93	27.66	3829.84	4093.12	**-263.28**	-2.63	132.5	-123.14	-4.33	-68.74	53.02	-0.83	0.94	0.83	-569.55
F4	$JOHANSEN-SPRD^{100D}-MLP$	265	128	137	23.81	24.25	3047.9	3321.83	**-273.93**	-2.74	101.3	-245.15	-4.41	-70.01	48.3	-1.03	0.92	0.98	-913.14
	Part VII: Models derived using the spread obtained from $ADF-SPRD^{100D}$																		
G1	$ADF-ZSPRD^{100D}_{(3,2)}$	3	1	2	398.7	2255.55	398.7	4511.09	**-4112.39**	-41.12	398.7	-4017.88	-0.63	-10	33.33	-1370.89	0.09	0.18	-4511.09
G1	$ADF-ZSPRD^{100D}_{(3,1)}$	3	1	2	64.11	2177.21	64.11	4354.43	**-4290.32**	-42.9	64.11	-3821.09	-0.72	-11.43	33.33	-1430.18	0.01	0.03	-4354.43
G1	$ADF-ZSPRD^{100D}_{(3,0.5)}$	3	1	2	259.67	2764.49	259.67	5528.98	**-5269.31**	-52.69	259.67	-4822.41	-0.68	-10.79	33.33	-1756.54	0.05	0.09	-5528.98
G1	$ADF-ZSPRD^{100D}_{(2.7,2)}$	3	1	2	398.7	3454.28	398.7	6908.57	**-6509.87**	-65.1	398.7	-6264.14	-0.63	-10	33.33	-2170.08	0.06	0.12	-6908.57
G1	$ADF-ZSPRD^{100D}_{(2.7,1)}$	3	1	2	64.11	3386.94	64.11	6773.89	**-6709.78**	-67.1	64.11	-6089.93	-0.69	-10.95	33.33	-2236.71	0.01	0.02	-6773.89
G1	$ADF-ZSPRD^{100D}_{(2.7,0.5)}$	3	1	2	259.67	3919.65	259.67	7839.31	**-7579.64**	-75.8	259.67	-6973.52	-0.67	-10.64	33.33	-2526.69	0.03	0.07	-7839.31
G2	$ADF-SPRD^{100D}-SMA_{(10,20)}$	19	12	7	1205	1416.6	14460.01	9916.19	**4543.82**	45.44	7325.13	-6353.48	0.04	0.63	63.16	239.2	1.46	0.85	-6353.48
G2	$ADF-SPRD^{100D}-EMA_{(10,20)}$	31	18	13	844.14	839.51	15194.44	10913.63	**4280.81**	42.81	6998.58	-6815.23	0.01	0.16	58.06	138.01	1.39	1.01	-7038.36
G2	$ADF-SPRD^{100D}-MACD_{(12,26,9)}$	36	20	16	761.9	498.88	15238	7982.08	**7255.92**	72.56	6763.1	-3143.02	0.07	1.11	55.56	201.61	1.91	1.53	-3785.23
G2	$ADF-SPRD^{100D}-RSI_{(14)}$	5	1	4	571.45	1307.2	571.45	5228.78	**-4657.34**	-46.57	571.45	-3989.18	-0.56	-8.89	20	-931.47	0.11	0.44	-4807.9
G2	$ADF-SPRD^{100D}-BB_{(20)}$	16	6	10	339.98	304.43	2039.89	3044.3	**-1004.4**	-10.04	765.73	-961.54	-0.35	-5.56	37.5	-62.78	0.67	1.12	-2121.74
G3	$ADF-SPRD^{100D}-DECTREE$	299	124	175	27.67	24.7	3430.73	4322.02	**-891.29**	-8.91	289.77	-144.62	-4	-63.5	41.47	-2.98	0.79	1.12	-988.06
G4	$ADF-SPRD^{100D}-MLP$	181	72	109	24.78	24.98	1783.94	2723.11	**-939.18**	-9.39	121.37	-166.32	-4.53	-71.91	39.78	-5.19	0.66	0.99	-1118.02
	Part VIII: Models derived using the spread obtained from $KALMAN-SPRD^{100D}$																		
H1	$KALMAN-ZSPRD^{100D}_{(3,2)}$	2	2	-	360.34	-	720.68	-	**720.68**	7.21	692.86	-	0.54	8.57	100	360.34	720.68	360.34	-
H1	$KALMAN-ZSPRD^{100D}_{(3,1)}$	2	1	1	1254.22	236.5	1254.22	236.5	**1017.72**	10.18	1254.22	-236.5	0.38	6.03	50	508.86	5.3	5.3	-236.5
H1	$KALMAN-ZSPRD^{100D}_{(3,0.5)}$	2	2	-	795.03	-	1590.07	-	**1590.07**	15.9	1412.12	-	0.78	12.38	100	795.03	1590.07	795.03	-
H1	$KALMAN-ZSPRD^{100D}_{(2.7,2)}$	5	3	2	433.86	159.51	1301.58	319.01	**982.57**	9.83	1062.69	-258.47	0.18	2.86	60	196.51	4.08	2.72	-258.47
H1	$KALMAN-ZSPRD^{100D}_{(2.7,1)}$	4	2	2	1051.34	261.04	2102.68	522.08	**1580.6**	15.81	1657.91	-264.76	0.32	5.08	50	395.15	4.03	4.03	-264.76
H1	$KALMAN-ZSPRD^{100D}_{(2.7,0.5)}$	4	3	1	812.69	0.64	2438.08	0.64	**2437.45**	24.37	1825.89	-0.64	0.61	9.68	75	609.36	3833.46	1277.24	-0.64
H2	$KALMAN-SPRD^{100D}-SMA_{(10,20)}$	7	6	1	437.95	72.49	2627.68	72.49	**2555.19**	25.55	1027.87	-72.49	0.65	10.32	85.71	365	36.25	6.04	-72.49
H2	$KALMAN-SPRD^{100D}-EMA_{(10,20)}$	18	8	10	474.54	197.59	3796.34	1975.93	**1820.41**	18.2	1699.82	-462.65	-0.01	-0.16	44.44	101.1	1.92	2.4	-822.19
H2	$KALMAN-SPRD^{100D}-MACD_{(12,26,9)}$	31	12	19	270.95	226.16	3251.45	4297.08	**-1045.63**	-10.46	1620.44	-550.37	-0.37	-5.87	38.71	-33.73	0.76	1.2	-2497.19
H2	$KALMAN-SPRD^{100D}-RSI_{(14)}$	3	1	2	1190.23	1889.17	1190.23	3778.34	**-2588.12**	-25.88	1190.23	-2942.45	-0.47	-7.46	33.33	-862.81	0.32	0.63	-2942.45
H2	$KALMAN-SPRD^{100D}-BB_{(20)}$	11	8	3	171.62	442.6	1372.93	1327.79	**45.14**	0.45	453.66	-1109.72	-0.25	-3.97	72.73	4.12	1.03	0.39	-1327.79
H3	$KALMAN-SPRD^{100D}-DECTREE$	284	116	168	23.61	26.67	2738.9	4481.14	**-1742.24**	-17.42	117.95	-289.77	-4.1	-65.09	40.85	-6.13	0.61	0.89	-1849.53
H4	$KALMAN-SPRD^{100D}-MLP$	229	85	144	24	29.4	2040.4	4233.52	**-2193.12**	-21.93	116.93	-289.77	-3.99	-63.34	37.12	-9.58	0.48	0.82	-2279.07
	Part IX: Models derived using the spread obtained from $RATIO-SPRD^{100D}$																		
I1	$RATIO-ZSPRD^{100D}_{(3,2)}$	3	2	1	85.91	71.89	171.82	71.89	**99.92**	1	97.26	-71.89	-1.29	-20.48	66.67	33.31	2.39	1.19	-71.89
I1	$RATIO-ZSPRD^{100D}_{(3,1)}$	3	2	1	120.53	73.56	241.06	73.56	**167.5**	1.68	177.13	-73.56	-0.77	-12.22	66.67	55.84	3.28	1.64	-73.56
I1	$RATIO-ZSPRD^{100D}_{(3,0.5)}$	3	2	1	169.72	33.9	339.44	33.9	**305.54**	3.06	195.81	-33.9	-0.42	-6.67	66.67	101.85	10.01	5.01	-33.9
I1	$RATIO-ZSPRD^{100D}_{(2.7,2)}$	4	3	1	124.96	58.81	374.86	58.81	**316.06**	3.16	289.77	-58.81	-0.49	-7.78	75	79.01	6.37	2.12	-58.81
I1	$RATIO-ZSPRD^{100D}_{(2.7,1)}$	4	3	1	190.05	60.17	570.15	60.17	**509.98**	5.1	414.81	-60.17	-0.12	-1.9	75	127.5	9.48	3.16	-60.17
I1	$RATIO-ZSPRD^{100D}_{(2.7,0.5)}$	4	3	1	291.03	20.81	873.08	20.81	**852.27**	8.52	620	-20.81	0.22	3.49	75	213.07	41.96	13.99	-20.81
I2	$RATIO-SPRD^{100D}-SMA_{(10,20)}$	14	6	8	167.26	127.61	1003.57	1020.91	**-17.35**	-0.17	364.83	-374.87	-0.8	-12.7	42.86	-1.23	0.98	1.31	-448.64
I2	$RATIO-SPRD^{100D}-EMA_{(10,20)}$	22	7	15	136.82	71.9	957.72	1078.56	**-120.84**	-1.21	248.67	-266.81	-1.3	-20.64	31.82	-5.49	0.89	1.9	-915.14
I2	$RATIO-SPRD^{100D}-MACD_{(12,26,9)}$	29	13	16	48.45	78.05	629.88	1248.77	**-618.89**	-6.19	156.26	-240.74	-1.95	-30.96	44.83	-21.34	0.5	0.62	-825.85
I2	$RATIO-SPRD^{100D}-RSI_{(14)}$	2	-	2	-	810.8	-	1621.6	**-1621.6**	-16.22	-	-1429.06	-1.1	-17.46	-	-810.8	-	-	-1429.06
I2	$RATIO-SPRD^{100D}-BB_{(20)}$	12	11	1	55.86	237	614.46	237	**377.46**	3.77	139	-237	-1.31	-20.8	91.67	31.46	2.59	0.24	-237
I3	$RATIO-SPRD^{100D}-DECTREE$	329	112	217	22.53	20.66	2522.86	4483.32	**-1960.46**	-19.6	109.84	-92.19	-5.54	-87.94	34.04	-5.96	0.56	1.09	-2140.57
I4	$RATIO-SPRD^{100D}-MLP$	259	93	166	24.78	22.2	2304.81	3685.15	**-1380.34**	-13.8	116.36	-86.24	-5.08	-80.64	35.91	-5.33	0.63	1.12	-1420.62
	Part X: Models derived using the close price of SCHB.N																		
CLS-SYM-1	$CLOSE^{SCHB.N}-SMA_{(10,20)}$	14	8	6	275.75	104.83	2206.01	628.98	**1577.04**	15.77	789.43	-230.52	0.13	2.06	57.14	112.63	3.51	2.63	-324.24
CLS-SYM-1	$CLOSE^{SCHB.N}-EMA_{(10,20)}$	17	7	10	370.21	232.37	2591.45	2323.66	**267.79**	2.68	1083.32	-810.29	-0.15	-2.38	41.18	15.77	1.12	1.59	-630.81
CLS-SYM-1	$CLOSE^{SCHB.N}-MACD_{(12,26,9)}$	37	14	23	144.19	101.44	2018.6	2333.05	**-314.45**	-3.14	604.53	-326.15	-0.5	-7.94	37.84	-8.49	0.87	1.42	-1087.87
CLS-SYM-1	$CLOSE^{SCHB.N}-RSI_{(14)}$	5	2	3	313.96	850.97	627.91	2552.9	**-1924.99**	-19.25	584.15	-2050.03	-0.46	-7.3	40	-385	0.25	0.37	-2050.03
CLS-SYM-1	$CLOSE^{SCHB.N}-BB_{(20)}$	11	9	2	83.74	413.03	753.64	826.06	**-72.41**	-0.72	239.73	-780.29	-0.31	-4.92	81.82	-6.57	0.91	0.2	-780.29
	Part XI: Models derived using the close price of SCHF.N																		
CLS-SYM-2	$CLOSE^{SCHF.N}-SMA_{(10,20)}$	20	7	13	314.26	125.66	2199.8	1633.59	**566.2**	5.66	1106.36	-575.54	-0.14	-2.22	35	28.31	1.35	2.5	-918.42
CLS-SYM-2	$CLOSE^{SCHF.N}-EMA_{(10,20)}$	23	8	15	331.11	93.37	2648.86	1400.61	**1248.24**	12.48	911.97	-332.73	-0.07	-1.11	34.78	54.26	1.89	3.55	-643.72
CLS-SYM-2	$CLOSE^{SCHF.N}-MACD_{(12,26,9)}$	30	10	20	221.35	120.16	2213.46	2403.27	**-189.81**	-1.9	1043.11	-326.35	-0.34	-5.4	33.33	-6.34	0.92	1.84	-1733.81
CLS-SYM-2	$CLOSE^{SCHF.N}-RSI_{(14)}$	5	2	3	617.93	304.16	1235.87	912.48	**323.39**	3.23	959.27	-697.61	-0.02	-0.32	40	64.68	1.35	2.03	-697.61
CLS-SYM-2	$CLOSE^{SCHF.N}-BB_{(20)}$	15	8	7	79.49	192.86	635.89	1349.99	**-714.1**	-7.14	252.09	-785.71	-0.51	-8.1	53.33	-47.62	0.47	0.41	-785.71

Table D.2.13: This table presents the back-test metrics for the pair $SCHF.N/VO.N$ based on a 30-day rolling window. The table is subdivided into eleven parts, and in each of these parts, we present the back-test metrics and the trading strategies which use the spread derived from various models. In Part I, the spread is derived from the $DIST^{V1.1}$ model, in Part II from the $DIST^{V1.2}$ model, in Part III from the $DIST^{V2}$ model, in Part IV from the $DIST^{V3}$ model, in Part V from the $DIST^{V4}$ model, in Part VI from the $JOHANSEN-SPRD$ model, in Part VIII from the $ADF-SPRD$ model, in from the $DIST^{V2}$ model, in Part VIII from the $KALMAN-SPRD$ model, and in Part IX from the $RATIO-SPRD$ model. In Part X and XI, we present the back-test metrics of the trading strategies which use the close price of SCHF.N, and VO.N, respectively. All $ numbers reported below are in USD.

(I) Trading Strategy Code	(II) Model Name	(III) Total Number of Trades	(IV) Number of Winning Trades	(V) Number of Loosing Trades	(VI) Average Profit per Trade ($)	(VII) Average Loss per Trade ($)	(VIII) Gross Profit ($)	(IX) Gross Loss ($)	(X) Net Profit ($)	(XI) ROI (%)	(XII) Max P&L ($)	(XIII) Min P&L ($)	(XIV) Daily Sharpe Ratio	(XV) Annualized Sharpe Ratio	(XVI) Hit Ratio	(XVII) Expectancy	(XVIII) Profit Factor	(XIX) Realized Risk Reward Ratio	(XX) Max Drawdown ($)
Part I: Models derived using the spread obtained from $DIST^{V1.1}-SPRD^{30D}$																			
A1.1	$DIST^{V1.1}-ZSPRD^{30D}_{(3,2)}$	1	-	1	-	73.97	-	73.97	**-73.97**	-0.74	-	-73.97	-	-	-	-73.97	-	-	-73.97
A1.2	$DIST^{V1.1}-ZSPRD^{30D}_{(3,1)}$	1	1	-	188.04	-	188.04	-	**188.04**	1.88	188.04	-	-	-	100	188.04	188.04	188.04	-
A1.3	$DIST^{V1.1}-ZSPRD^{30D}_{(3,0.5)}$	1	1	-	180.63	-	180.63	-	**180.63**	1.81	180.63	-	-	-	100	180.63	180.63	180.63	-
A1.4	$DIST^{V1.1}-ZSPRD^{30D}_{(2.7,2)}$	7	2	5	32.24	38.47	64.47	192.33	**-127.85**	-1.28	49.45	-77.81	-4.2	-66.67	28.57	-18.27	0.34	0.84	-154.23
A1.5	$DIST^{V1.1}-ZSPRD^{30D}_{(2.7,1)}$	5	3	2	105.6	57.53	316.8	115.06	**201.73**	2.02	281.97	-86.46	-0.79	-12.54	60	40.35	2.75	1.84	-86.46
A1.6	$DIST^{V1.1}-ZSPRD^{30D}_{(2.7,0.5)}$	5	2	3	139.12	95.5	278.24	286.49	**-8.25**	-0.08	273.77	-141.08	-0.94	-14.92	40	-1.65	0.97	1.46	-200.03
A2.1	$DIST^{V1.1}-SPRD^{30D}-SMA_{(10,20)}$	14	3	11	54.94	90.2	164.81	992.22	**-827.42**	-8.27	86.55	-164.36	-2.76	-43.81	21.43	-59.1	0.17	0.61	-745.71
A2.2	$DIST^{V1.1}-SPRD^{30D}-EMA_{(10,20)}$	20	10	10	105.8	84.1	1057.97	841.02	**216.95**	2.17	349.25	-322.26	-1.03	-16.35	50	10.85	1.26	1.26	-376.04
A2.3	$DIST^{V1.1}-SPRD^{30D}-MACD_{(12,26,9)}$	30	19	11	55.94	93.15	1062.9	1024.65	**38.25**	0.38	121.82	-175.27	-1.79	-28.42	63.33	1.27	1.04	0.6	-487.28
A2.4	$DIST^{V1.1}-SPRD^{30D}-RSI_{(14)}$	4	3	1	490.36	183.78	1471.09	183.78	**1287.31**	12.87	723.94	-183.78	0.42	6.67	75	321.83	8	2.67	-183.78
A2.5	$DIST^{V1.1}-SPRD^{30D}-BB_{(20)}$	14	5	9	135.28	53.72	676.4	483.45	**192.95**	1.93	361.06	-143.98	-1.04	-16.51	35.71	13.77	1.4	2.52	-468.33
A3	$DIST^{V1.1}-SPRD^{30D}-DECTREE$	350	199	151	22.19	30.14	4416.75	4551.49	**-134.74**	-1.35	133.69	-151.34	-4.28	-67.94	56.86	-0.38	0.97	0.74	-1014.07
A4	$DIST^{V1.1}-SPRD^{30D}-MLP$	345	194	151	25.03	27	4855.9	4077.11	**778.78**	7.79	142.17	-125.32	-4.24	-67.31	56.23	2.26	1.19	0.93	-467.73
Part II: Models derived using the spread obtained from $DIST^{V1.2}-SPRD^{30D}$																			
B1.1	$DIST^{V1.2}-ZSPRD^{30D}_{(3,2)}$	11	3	8	15.93	44.82	47.8	358.55	**-310.74**	-3.11	29.94	-114.59	-4.54	-72.07	27.27	-28.25	0.13	0.36	-310.75
B1.2	$DIST^{V1.2}-ZSPRD^{30D}_{(3,1)}$	9	4	5	23.7	42.32	94.81	211.62	**-116.81**	-1.17	53.07	-83.83	-3.74	-59.37	44.44	-12.98	0.45	0.56	-169.88
B1.3	$DIST^{V1.2}-ZSPRD^{30D}_{(3,0.5)}$	9	3	6	43.56	75.79	130.68	454.74	**-324.06**	-3.24	68.29	-120.46	-2.82	-44.77	33.33	-36.01	0.29	0.57	-324.06
B1.4	$DIST^{V1.2}-ZSPRD^{30D}_{(2.7,2)}$	16	6	10	29.11	50	174.66	500	**-325.34**	-3.25	79.44	-114.59	-3.44	-54.61	37.5	-20.33	0.35	0.58	-325.34
B1.5	$DIST^{V1.2}-ZSPRD^{30D}_{(2.7,1)}$	12	8	4	42.32	42.25	338.58	169.01	**169.57**	1.7	101.97	-68.09	-2.57	-40.8	66.67	14.13	2	1	-101.3
B1.6	$DIST^{V1.2}-ZSPRD^{30D}_{(2.7,0.5)}$	12	8	4	62.57	96.32	500.59	385.27	**115.32**	1.15	100.91	-139.24	-1.66	-26.35	66.67	9.62	1.3	0.65	-157.02
B2.1	$DIST^{V1.2}-SPRD^{30D}-SMA_{(10,20)}$	16	7	9	126.63	73.81	886.41	664.32	**222.09**	2.22	437.55	-187.05	-0.94	-14.92	43.75	13.88	1.33	1.72	-521.74
B2.2	$DIST^{V1.2}-SPRD^{30D}-EMA_{(10,20)}$	26	10	16	58.37	102.95	583.69	1647.17	**-1063.48**	-10.63	202.7	-349.25	-1.69	-26.83	38.46	-40.91	0.35	0.57	-920.9
B2.3	$DIST^{V1.2}-SPRD^{30D}-MACD_{(12,26,9)}$	33	13	20	34.54	65.26	448.96	1305.11	**-856.15**	-8.56	107.49	-195.27	-2.66	-42.23	39.39	-25.95	0.34	0.53	-973.46
B2.4	$DIST^{V1.2}-SPRD^{30D}-RSI_{(14)}$	10	2	8	95.92	165.47	191.83	1323.78	**-1131.94**	-11.32	146.45	-342.19	-1.52	-24.13	20	-113.19	0.14	0.58	-955.33
B2.5	$DIST^{V1.2}-SPRD^{30D}-BB_{(20)}$	15	9	6	51.88	84.36	466.9	506.15	**-39.25**	-0.39	89.33	-306.51	-1.54	-24.45	60	-2.62	0.92	0.61	-118.11
B3	$DIST^{V1.2}-SPRD^{30D}-DECTREE$	302	155	147	24.73	30.53	3833.3	4487.67	**-654.38**	-6.54	142.1	-417.26	-3.35	-53.18	51.32	-2.17	0.85	0.81	-1117.55
B4	$DIST^{V1.2}-SPRD^{30D}-MLP$	276	131	145	26.76	28.28	3505.45	4100.56	**-595.11**	-5.95	190.88	-224.6	-3.76	-59.69	47.46	-2.16	0.85	0.95	-891.36
Part III: Models derived using the spread obtained from $DIST^{V2}-SPRD^{30D}$																			
C1.1	$DIST^{V2}-ZSPRD^{30D}_{(3,2)}$	1	1	-	73.97	-	73.97	-	**73.97**	0.74	73.97	-	-	-	100	73.97	73.97	73.97	-
C1.2	$DIST^{V2}-ZSPRD^{30D}_{(3,1)}$	1	-	1	-	188.04	-	188.04	**-188.04**	-1.88	-	-188.04	-	-	-	-188.04	-	-	-188.04
C1.3	$DIST^{V2}-ZSPRD^{30D}_{(3,0.5)}$	1	-	1	-	180.63	-	180.63	**-180.63**	-1.81	-	-180.63	-	-	-	-180.63	-	-	-180.63
C1.4	$DIST^{V2}-ZSPRD^{30D}_{(2.7,2)}$	7	5	2	38.47	32.24	192.33	64.47	**127.85**	1.28	77.81	-49.45	-3.3	-52.39	71.43	18.27	2.98	1.19	-49.45
C1.5	$DIST^{V2}-ZSPRD^{30D}_{(2.7,1)}$	5	2	3	57.53	105.6	115.06	316.8	**-201.73**	-2.02	86.46	-281.97	-1.36	-21.59	40	-40.35	0.36	0.54	-281.97
C1.6	$DIST^{V2}-ZSPRD^{30D}_{(2.7,0.5)}$	5	3	2	95.5	139.12	286.49	278.24	**8.25**	0.08	141.08	-273.77	-0.92	-14.6	60	1.65	1.03	0.69	-273.77
C2.1	$DIST^{V2}-SPRD^{30D}-SMA_{(10,20)}$	14	11	3	119.86	54.94	1318.46	164.81	**1153.66**	11.54	407.95	-86.55	-0.58	-9.21	78.57	82.4	8	2.18	-86.55
C2.2	$DIST^{V2}-SPRD^{30D}-EMA_{(10,20)}$	20	10	10	84.1	105.8	841.02	1057.97	**-216.95**	-2.17	322.26	-349.25	-1.19	-18.89	50	-10.85	0.79	0.79	-234.57
C2.3	$DIST^{V2}-SPRD^{30D}-MACD_{(12,26,9)}$	30	11	19	93.15	55.94	1024.65	1062.9	**-38.25**	-0.38	175.27	-121.82	-1.82	-28.89	36.67	-1.27	0.96	1.67	-403.72
C2.4	$DIST^{V2}-SPRD^{30D}-RSI_{(14)}$	4	1	3	183.78	490.36	183.78	1471.09	**-1287.31**	-12.87	183.78	-723.94	-1.17	-18.57	25	-321.83	0.12	0.37	-733.03
C2.5	$DIST^{V2}-SPRD^{30D}-BB_{(20)}$	14	9	5	53.72	135.28	483.45	676.4	**-192.95**	-1.93	143.98	-361.06	-1.25	-19.84	64.29	-13.77	0.71	0.4	-302.62
C3	$DIST^{V2}-SPRD^{30D}-DECTREE$	360	205	155	23.05	28.6	4726.14	4433.39	**292.75**	2.93	140.72	-153.49	-4.26	-67.63	56.94	0.81	1.07	0.81	-649.84
C4	$DIST^{V2}-SPRD^{30D}-MLP$	346	198	148	24.54	26.52	4859.52	3925.55	**933.97**	9.34	140.72	-121.04	-4.34	-68.9	57.23	2.7	1.24	0.93	-450.28
Part IV: Models derived using the spread obtained from $DIST^{V3}-SPRD^{30D}$																			
D1.1	$DIST^{V3}-ZSPRD^{30D}_{(3,2)}$	5	4	1	42.97	79.98	171.89	79.98	**91.91**	0.92	54.55	-79.98	-2.35	-37.31	80	18.38	2.15	0.54	-79.98
D1.2	$DIST^{V3}-ZSPRD^{30D}_{(3,1)}$	5	4	1	50.05	37.18	200.21	37.18	**163.03**	1.63	75.4	-37.18	-2.84	-45.08	80	32.61	5.39	1.35	-37.18
D1.3	$DIST^{V3}-ZSPRD^{30D}_{(3,0.5)}$	5	4	1	56.64	37.18	226.57	37.18	**189.39**	1.89	75.4	-37.18	-2.49	-39.53	80	37.88	6.09	1.52	-37.18
D1.4	$DIST^{V3}-ZSPRD^{30D}_{(2.7,2)}$	10	8	2	36.16	40.22	289.29	80.43	**208.86**	2.09	54.55	-79.98	-3.28	-52.07	80	20.89	3.6	0.9	-79.98
D1.5	$DIST^{V3}-ZSPRD^{30D}_{(2.7,1)}$	9	8	1	39.1	37.18	312.81	37.18	**275.63**	2.76	75.4	-37.18	-3.88	-61.59	88.89	30.63	8.41	1.05	-37.18
D1.6	$DIST^{V3}-ZSPRD^{30D}_{(2.7,0.5)}$	9	8	1	40.29	37.18	322.31	37.18	**285.13**	2.85	75.4	-37.18	-3.39	-53.81	88.89	31.68	8.67	1.08	-37.18
D2.1	$DIST^{V3}-SPRD^{30D}-SMA_{(10,20)}$	24	6	18	59.21	78.84	355.29	1419.2	**-1063.91**	-10.64	161.61	-316.54	-1.91	-30.32	25	-44.33	0.25	0.75	-1192.37
D2.2	$DIST^{V3}-SPRD^{30D}-EMA_{(10,20)}$	45	17	28	71.6	74.23	1217.24	2078.53	**-861.28**	-8.61	263.67	-223.25	-1.84	-29.21	37.78	-19.14	0.59	0.96	-1042.72
D2.3	$DIST^{V3}-SPRD^{30D}-MACD_{(12,26,9)}$	47	17	30	58.43	47.23	993.25	1416.88	**-423.63**	-4.24	156.73	-349.25	-2.07	-32.86	36.17	-9.01	0.7	1.24	-432.82
D2.4	$DIST^{V3}-SPRD^{30D}-RSI_{(14)}$	1	1	-	568.47	-	568.47	-	**568.47**	5.68	568.47	-	-	-	100	568.47	568.47	568.47	-
D2.5	$DIST^{V3}-SPRD^{30D}-BB_{(20)}$	21	12	9	37.69	45.21	452.28	406.94	**45.34**	0.45	105.37	-132.69	-2.66	-42.23	57.14	2.16	1.11	0.83	-183.3
D3	$DIST^{V3}-SPRD^{30D}-DECTREE$	319	167	152	25.13	29.8	4197.18	4530.12	**-332.94**	-3.33	129.62	-188.58	-3.96	-62.86	52.35	-1.04	0.93	0.84	-1429.15
D4	$DIST^{V3}-SPRD^{30D}-MLP$	285	151	134	26.95	26.82	4069.92	3593.45	**476.47**	4.76	173.36	-191.68	-3.8	-60.32	52.98	1.67	1.13	1.01	-784.94
Part V: Models derived using the spread obtained from $DIST^{V4}-SPRD^{30D}$																			
E1.1	$DIST^{V4}-ZSPRD^{30D}_{(3,2)}$	5	4	1	42.97	79.98	171.89	79.98	**91.91**	0.92	54.55	-79.98	-2.35	-37.31	80	18.38	2.15	0.54	-79.98
E1.2	$DIST^{V4}-ZSPRD^{30D}_{(3,1)}$	5	4	1	50.05	37.18	200.21	37.18	**163.03**	1.63	75.4	-37.18	-2.84	-45.08	80	32.61	5.39	1.35	-37.18
E1.3	$DIST^{V4}-ZSPRD^{30D}_{(3,0.5)}$	5	4	1	56.64	37.18	226.57	37.18	**189.39**	1.89	75.4	-37.18	-2.49	-39.53	80	37.88	6.09	1.52	-37.18
E1.4	$DIST^{V4}-ZSPRD^{30D}_{(2.7,2)}$	10	8	2	36.16	40.22	289.29	80.43	**208.86**	2.09	54.55	-79.98	-3.28	-52.07	80	20.89	3.6	0.9	-79.98
E1.5	$DIST^{V4}-ZSPRD^{30D}_{(2.7,1)}$	9	8	1	39.1	37.18	312.81	37.18	**275.63**	2.76	75.4	-37.18	-3.88	-61.59	88.89	30.63	8.41	1.05	-37.18
E1.6	$DIST^{V4}-ZSPRD^{30D}_{(2.7,0.5)}$	9	8	1	40.29	37.18	322.31	37.18	**285.13**	2.85	75.4	-37.18	-3.39	-53.81	88.89	31.68	8.67	1.08	-37.18
E2.1	$DIST^{V4}-SPRD^{30D}-SMA_{(10,20)}$	24	6	18	59.21	78.84	355.29	1419.2	**-1063.91**	-10.64	161.61	-316.54	-1.91	-30.32	25	-44.33	0.25	0.75	-1192.37
E2.2	$DIST^{V4}-SPRD^{30D}-EMA_{(10,20)}$	45	17	28	71.6	74.23	1217.24	2078.53	**-861.28**	-8.61	263.67	-223.25	-1.84	-29.21	37.78	-19.14	0.59	0.96	-1042.72
E2.3	$DIST^{V4}-SPRD^{30D}-MACD_{(12,26,9)}$	47	17	30	58.43	47.23	993.25	1416.88	**-423.63**	-4.24	156.73	-349.25	-2.07	-32.86	36.17	-9.01	0.7	1.24	-432.82
E2.4	$DIST^{V4}-SPRD^{30D}-RSI_{(14)}$	1	1	-	568.47	-	568.47	-	**568.47**	5.68	568.47	-	-	-	100	568.47	568.47	568.47	-
E2.5	$DIST^{V4}-SPRD^{30D}-BB_{(20)}$	21	12	9	37.69	45.21	452.28	406.94	**45.34**	0.45	105.37	-132.69	-2.66	-42.23	57.14	2.16	1.11	0.83	-183.3
E3	$DIST^{V4}-SPRD^{30D}-DECTREE$	313	158	155	26.6	29.93	4203.02	4639.24	**-436.22**	-4.36	155.74	-188.58	-3.84	-60.96	50.48	-1.39	0.91	0.89	-1276.53
E4	$DIST^{V4}-SPRD^{30D}-MLP$	285	151	134	26.95	26.82	4069.92	3593.45	**476.47**	4.76	173.36	-191.68	-3.8	-60.32	52.98	1.67	1.13	1.01	-784.94
Part VI: Models derived using the spread obtained from $JOHANSEN-SPRD^{30D}$																			
F1.1	$JOHANSEN-ZSPRD^{30D}_{(3,2)}$	23	13	10	67.28	44.53	874.63	445.29	**429.34**	4.29	417.42	-161.03	-0.41	-6.51	56.52	18.66	1.96	1.51	-242.96
F1.2	$JOHANSEN-ZSPRD^{30D}_{(3,1)}$	22	12	10	140.76	52.91	1689.09	529.06	**1160.03**	11.6	1055.34	-161.03	0.07	1.11	54.55	52.74	3.19	2.66	-326.73
F1.3	$JOHANSEN-ZSPRD^{30D}_{(3,0.5)}$	21	13	8	147.56	73.66	1918.22	589.31	**1328.91**	13.29	1055.34	-161.03	0.06	0.95	61.9	63.27	3.26	2	-321.07
F1.4	$JOHANSEN-ZSPRD^{30D}_{(2.7,2)}$	30	15	15	60.06	47.87	900.85	718.07	**182.78**	1.83	417.42	-161.03	-0.58	-9.21	50	6.09	1.25	1.25	-395.99
F1.5	$JOHANSEN-ZSPRD^{30D}_{(2.7,1)}$	28	14	14	124.91	53.02	1748.76	742.32	**1006.44**	10.06	1055.34	-161.03	-0.03	-0.48	50	35.94	2.36	2.36	-398.55
F1.6	$JOHANSEN-ZSPRD^{30D}_{(2.7,0.5)}$	26	15	11	131.25	78.65	1968.72	865.2	**1103.52**	11.04	1055.34	-161.03	-0.03	-0.48	57.69	42.44	2.28	1.67	-455.51
F2.1	$JOHANSEN-SPRD^{30D}-SMA_{(10,20)}$	18	7	11	314.97	791.21	2204.82	8703.34	**-6498.52**	-64.99	1413.1	-3531.8	-0.13	-2.06	38.89	-361.02	0.25	0.4	-7639.61
F2.2	$JOHANSEN-SPRD^{30D}-EMA_{(10,20)}$	31	21	10	325.6	449.24	6837.5	4492.44	**2345.06**	23.45	1655.04	-3008.14	-0.06	-0.95	67.74	75.63	1.52	0.72	-3086.35
F2.3	$JOHANSEN-SPRD^{30D}-MACD_{(12,26,9)}$	34	17	17	300.4	223.35	5106.79	3796.98	**1309.81**	13.1	1130.96	-1639.77	0.21	3.33	50	38.52	1.34	1.34	-2569.09
F2.4	$JOHANSEN-SPRD^{30D}-RSI_{(14)}$	9	5	4	494.62	678.38	2473.09	2713.54	**-240.44**	-2.4	866.3	-2462.32	-0.04	-0.63	55.56	-26.66	0.91	0.73	-2538.88
F2.5	$JOHANSEN-SPRD^{30D}-BB_{(20)}$	15	9	6	1626.39	122.86	14637.55	737.14	**13900.4**	139	9177.14	-256.47	0.37	5.87	60	926.69	19.86	13.24	-410.94
F3	$JOHANSEN-SPRD^{30D}-DECTREE$	315	152	163	30.17	27.44	4585.41	4473.35	**112.06**	1.12	271.41	-146.82	-3.58	-56.83	48.25	0.35	1.03	1.1	-1029.89
F4	$JOHANSEN-SPRD^{30D}-MLP$	229	120	109	27.8	31.36	3336.34	3417.78	**-81.43**	-0.81	173.27	-390.3	-3.09	-49.05	52.4	-0.36	0.98	0.89	-1110.36
Part VII: Models derived using the spread obtained from $ADF-SPRD^{30D}$																			
G1.1	$ADF-ZSPRD^{30D}_{(3,2)}$	2	2	-	85.42	-	170.85	-	**170.85**	1.71	152.51	-	-2.34	-37.15	100	85.42	170.85	85.42	-
G1.2	$ADF-ZSPRD^{30D}_{(3,1)}$	2	2	-	94.11	-	188.22	-	**188.22**	1.88	152.51	-	-2.44	-38.73	100	94.11	188.22	94.11	-
G1.3	$ADF-ZSPRD^{30D}_{(3,0.5)}$	2	2	-	473.54	-	947.08	-	**947.08**	9.47	903.02	-	0.23	3.65	100	473.54	947.08	473.54	-
G1.4	$ADF-ZSPRD^{30D}_{(2.7,2)}$	5	3	2	68.76	22.62	206.29	45.24	**161.06**	1.61	152.51	-42.2	-4	-63.5	60	32.21	4.56	3.04	-42.2
G1.5	$ADF-ZSPRD^{30D}_{(2.7,1)}$	5	3	2	80.03	100.36	240.09	200.72	**39.38**	0.39	152.51	-188.44	-2.8	-44.45	60	7.88	1.2	0.8	-188.44
G1.6	$ADF-ZSPRD^{30D}_{(2.7,0.5)}$	5	3	2	332.99	160.16	998.96	320.31	**678.65**	6.79	903.02	-188.44	-0.4	-6.35	60	135.73	3.12	2.08	-268.43
G2.1	$ADF-SPRD^{30D}-SMA_{(10,20)}$	20	8	12	253.27	210.24	2026.19	2522.9	**-496.71**	-4.97	559.4	-733.01	-1.03	-16.35	40	-24.84	0.8	1.2	-1308.67
G2.2	$ADF-SPRD^{30D}-EMA_{(10,20)}$	46	27	19	131.57	113.65	3552.36	2159.3	**1393.06**	13.93	957.7	-835.38	-1.48	-23.49	58.7	30.29	1.65	1.16	-835.38
G2.3	$ADF-SPRD^{30D}-MACD_{(12,26,9)}$	46	24	22	148.81	142.25	3571.36	3129.57	**441.79**	4.42	712.73	-612.61	-0.43	-6.83	52.17	9.59	1.14	1.05	-669.61
G2.4	$ADF-SPRD^{30D}-RSI_{(14)}$	3	1	2	1117.57	367.63	1117.57	735.26	**382.32**	3.82	1117.57	-371.22	-0.71	-11.27	33.33	127.39	1.52	3.04	-364.03
G2.5	$ADF-SPRD^{30D}-BB_{(20)}$	24	11	13	131.1	102.35	1442.09	1330.54	**111.55**	1.12	808.32	-276.24	-2.26	-35.88	45.83	4.64	1.08	1.28	-849.42
G3	$ADF-SPRD^{30D}-DECTREE$	347	167	180	29.9	23.83	4992.98	4288.95	**704.03**	7.04	185.67	-115.91	-3.78	-60.01	48.13	2.03	1.16	1.25	-483.08
G4	$ADF-SPRD^{30D}-MLP$	207	117	90	33.1	28.89	3872.98	2599.93	**1273.05**	12.73	215.83	-229.75	-3.04	-48.26	56.52	6.15	1.49	1.15	-479.07
Part VIII: Models derived using the spread obtained from $KALMAN-SPRD^{30D}$																			
H1.1	$KALMAN-ZSPRD^{30D}_{(3,2)}$	1	-	1	-	447.41	-	447.41	**-447.41**	-4.47	-	-447.41	-	-	-	-447.41	-	-	-447.41
H1.2	$KALMAN-ZSPRD^{30D}_{(3,1)}$	1	-	1	-	153.63	-	153.63	**-153.63**	-1.54	-	-153.63	-	-	-	-153.63	-	-	-153.63
H1.3	$KALMAN-ZSPRD^{30D}_{(3,0.5)}$	1	-	1	-	92	-	92	**-92**	-0.92	-	-92	-	-	-	-92	-	-	-92
H1.4	$KALMAN-ZSPRD^{30D}_{(2.7,2)}$	4	2	2	104.59	384.78	209.18	769.56	**-560.38**	-5.6	104.66	-716.73	-1.56	-24.76	50	-140.1	0.27	0.27	-716.73
H1.5	$KALMAN-ZSPRD^{30D}_{(2.7,1)}$	4	2	2	190.1	230.65	380.2	461.3	**-81.09**	-0.81	227.48	-444.9	-1.65	-26.19	50	-20.27	0.82	0.82	-444.9
H1.6	$KALMAN-ZSPRD^{30D}_{(2.7,0.5)}$	4	3	1	131.37	388.08	394.12	388.08	**6.03**	0.06	227.48	-388.08	-1.73	-27.46	75	1.51	1.02	0.34	-388.08
H2.1	$KALMAN-SPRD^{30D}-SMA_{(10,20)}$	16	11	5	197.02	76.46	2167.19	382.32	**1784.87**	17.85	651.49	-185.19	-1.68	-26.67	68.75	111.55	5.67	2.58	-197.14
H2.2	$KALMAN-SPRD^{30D}-EMA_{(10,20)}$	15	6	9	319.59	116.07	1917.53	1044.6	**872.93**	8.73	571.76	-253.51	-1.66	-26.35	40	58.2	1.84	2.75	-568.03
H2.3	$KALMAN-SPRD^{30D}-MACD_{(12,26,9)}$	36	14	22	143.55	99.05	2009.64	2179.17	**-169.53**	-1.7	817.01	-296.54	-2.6	-41.27	38.89	-4.71	0.92	1.45	-701.38
H2.4	$KALMAN-SPRD^{30D}-RSI_{(14)}$	4	2	2	334.15	635.75	668.29	1271.49	**-603.2**	-6.03	592.73	-1262.48	-0.79	-12.54	50	-150.8	0.53	0.53	-1262.48
H2.5	$KALMAN-SPRD^{30D}-BB_{(20)}$	6	5	1	99.91	448.04	499.54	448.04	**51.5**	0.51	141.38	-448.04	-2.08	-33.02	83.33	8.56	1.11	0.22	-448.04
H3	$KALMAN-SPRD^{30D}-DECTREE$	350	217	133	23.79	26.39	5163.33	3509.96	**1653.37**	16.53	130.13	-105.37	-4.45	-70.64	62	4.72	1.47	0.9	-263.6
H4	$KALMAN-SPRD^{30D}-MLP$	295	172	123	24.32	25.98	4183.42	3195.59	**987.84**	9.88	191.33	-134.45	-4.29	-68.1	58.31	3.35	1.31	0.94	-225.63
Part IX: Models derived using the spread obtained from $RATIO-SPRD^{30D}$																			
I1.1	$RATIO-ZSPRD^{30D}_{(3,2)}$	2	1	1	69.74	74.62	69.74	74.62	**-4.87**	-0.05	69.74	-74.62	-1.51	-23.97	50	-2.44	0.93	0.93	-74.62
I1.2	$RATIO-ZSPRD^{30D}_{(3,1)}$	2	1	1	111.79	31.73	111.79	31.73	**80.06**	0.8	111.79	-31.73	-1.1	-17.46	50	40.03	3.52	3.52	-31.73
I1.3	$RATIO-ZSPRD^{30D}_{(3,0.5)}$	2	2	-	89.59	-	179.19	-	**179.19**	1.79	172.2	-	-0.53	-8.41	100	89.59	179.19	89.59	-
I1.4	$RATIO-ZSPRD^{30D}_{(2.7,2)}$	6	4	2	39.22	42.8	156.88	85.61	**71.28**	0.71	69.74	-74.62	-2.77	-43.97	66.67	11.88	1.83	0.92	-85.61
I1.5	$RATIO-ZSPRD^{30D}_{(2.7,1)}$	5	4	1	100.42	120.42	401.69	120.42	**281.27**	2.81	157.26	-120.42	-0.86	-13.65	80	56.25	3.34	0.83	-120.42
I1.6	$RATIO-ZSPRD^{30D}_{(2.7,0.5)}$	5	4	1	127.12	81.2	508.47	81.2	**427.27**	4.27	172.2	-81.2	-0.65	-10.32	80	85.45	6.26	1.57	-81.2
I2.1	$RATIO-SPRD^{30D}-SMA_{(10,20)}$	17	10	7	60.01	87.49	600.06	612.41	**-12.35**	-0.12	175	-235.53	-1.51	-23.97	58.82	-0.73	0.98	0.69	-474.23
I2.2	$RATIO-SPRD^{30D}-EMA_{(10,20)}$	27	10	17	52.95	101.02	529.55	1717.36	**-1187.81**	-11.88	107.77	-420.82	-1.83	-29.05	37.04	-43.99	0.31	0.52	-1002.12
I2.3	$RATIO-SPRD^{30D}-MACD_{(12,26,9)}$	40	12	28	55.12	59.46	661.47	1664.93	**-1003.46**	-10.03	252.14	-171.24	-2.47	-39.21	30	-25.09	0.4	0.93	-1188.88
I2.4	$RATIO-SPRD^{30D}-RSI_{(14)}$	4	2	2	253.84	439.5	507.68	879	**-371.32**	-3.71	305.68	-553.68	-0.59	-9.37	50	-92.83	0.58	0.58	-553.68
I2.5	$RATIO-SPRD^{30D}-BB_{(20)}$	20	14	6	79.56	56.68	1113.82	340.09	**773.73**	7.74	374.24	-175.71	-1.08	-17.14	70	38.69	3.28	1.4	-221.23
I3	$RATIO-SPRD^{30D}-DECTREE$	402	151	251	25.04	20.92	3781.22	5250.85	**-1469.64**	-14.7	132.62	-142.17	-5.02	-79.69	37.56	-3.66	0.72	1.2	-1764.69
I4	$RATIO-SPRD^{30D}-MLP$	378	143	235	25.98	23.23	3714.78	5459.61	**-1744.84**	-17.45	186.25	-142.17	-4.5	-71.44	37.83	-4.62	0.68	1.12	-1969.72
Part X: Models derived using the close price of SCHF.N																			
CLS-SYM-1.1	$CLOSE^{SCHF.N}-SMA_{(10,20)}$	20	7	13	314.26	125.66	2199.8	1633.59	**566.2**	5.66	1106.36	-575.54	-0.14	-2.22	35	28.31	1.35	2.5	-918.42
CLS-SYM-1.2	$CLOSE^{SCHF.N}-EMA_{(10,20)}$	23	8	15	331.11	93.37	2648.86	1400.61	**1248.24**	12.48	911.97	-332.73	-0.07	-1.11	34.78	54.26	1.89	3.55	-643.72
CLS-SYM-1.3	$CLOSE^{SCHF.N}-MACD_{(12,26,9)}$	30	10	20	221.35	120.16	2213.46	2403.27	**-189.81**	-1.9	1043.11	-326.35	-0.34	-5.4	33.33	-6.34	0.92	1.84	-1733.81
CLS-SYM-1.4	$CLOSE^{SCHF.N}-RSI_{(14)}$	5	2	3	617.93	304.16	1235.87	912.48	**323.39**	3.23	959.27	-697.61	-0.02	-0.32	40	64.68	1.35	2.03	-697.61
CLS-SYM-1.5	$CLOSE^{SCHF.N}-BB_{(20)}$	15	8	7	79.49	192.86	635.89	1349.99	**-714.1**	-7.14	252.09	-785.71	-0.51	-8.1	53.33	-47.62	0.47	0.41	-785.71
Part XI: Models derived using the close price of VO.N																			
CLS-SYM-2.1	$CLOSE^{VO.N}-SMA_{(10,20)}$	15	5	10	407.5	131.94	2037.52	1319.42	**718.1**	7.18	1345.66	-357.26	-0.07	-1.11	33.33	47.86	1.54	3.09	-888.12
CLS-SYM-2.2	$CLOSE^{VO.N}-EMA_{(10,20)}$	20	6	14	305.56	123.3	1833.38	1726.2	**107.17**	1.07	700.63	-218.39	-0.27	-4.29	30	5.36	1.06	2.48	-812.37
CLS-SYM-2.3	$CLOSE^{VO.N}-MACD_{(12,26,9)}$	30	12	18	235.68	119.41	2828.19	2149.34	**678.86**	6.79	1213.06	-330.07	-0.19	-3.02	40	22.63	1.32	1.97	-845.26
CLS-SYM-2.4	$CLOSE^{VO.N}-RSI_{(14)}$	5	2	3	464.59	648.69	929.17	1946.08	**-1016.91**	-10.17	781.75	-1353.4	-0.35	-5.56	40	-203.38	0.48	0.72	-1353.4
CLS-SYM-2.5	$CLOSE^{VO.N}-BB_{(20)}$	15	13	2	85.35	600.28	1109.6	1200.56	**-90.96**	-0.91	190.76	-984.33	-0.29	-4.6	86.67	-6.04	0.92	0.14	-984.33

Table D.2.14: This table presents the back-test metrics for the pair $SCHF.N/VO.N$ based on a 50-day rolling window. The table is subdivided into eleven parts, and in each of these parts, we present the back-test metrics and the trading strategies which use the spread derived from various models. In Part I, the spread is derived from the $DIST^{V1.1}$ model, in Part II from the $DIST^{V1.2}$ model, in Part III from the $DIST^{V2}$ model, in Part IV from the $DIST^{V3}$ model, in Part V from the $DIST^{V4}$ model, in Part VI from the $JOHANSEN-SPRD$ model, in Part VIII from the $ADF-SPRD$ model, in from the $DIST^{V2}$ model, in Part VIII from the $KALMAN-SPRD$ model, and in Part IX from the $RATIO-SPRD$ model. In Part X and XI, we present the back-test metrics of the trading strategies which use the close price of SCHF.N, and VO.N, respectively. All $ numbers reported below are in USD.

(I) Trading Strategy Code	(II) Model Name	(III) Total Number of Trades	(IV) Number of Winning Trades	(V) Number of Loosing Trades	(VI) Average Profit per Trade ($)	(VII) Average Loss per Trade ($)	(VIII) Gross Profit ($)	(IX) Gross Loss ($)	(X) Net Profit ($)	(XI) ROI (%)	(XII) Max P&L ($)	(XIII) Min P&L ($)	(XIV) Daily Sharpe Ratio	(XV) Annualized Sharpe Ratio	(XVI) Hit Ratio	(XVII) Expectancy	(XVIII) Profit Factor	(XIX) Realized Risk Reward Ratio	(XX) Max Drawdown ($)
Part I: Models derived using the spread obtained from $DIST^{V1.1}-SPRD^{50D}$																			
A1.1	$DIST^{V1.1}-ZSPRD^{50D}_{(3,2)}$	2	1	1	94.44	135.45	94.44	135.45	**-41.01**	-0.41	94.44	-135.45	-1.06	-16.83	50	-20.51	0.7	0.7	-135.45
A1.2	$DIST^{V1.1}-ZSPRD^{50D}_{(3,1)}$	1	1	-	127.2	-	127.2	-	**127.2**	1.27	127.2	-	-	-	100	127.2	127.2	127.2	-
A1.3	$DIST^{V1.1}-ZSPRD^{50D}_{(3,0.5)}$	1	-	1	-	63.95	-	63.95	**-63.95**	-0.64	-	-63.95	-	-	-	-63.95	-	-	-63.95
A1.4	$DIST^{V1.1}-ZSPRD^{50D}_{(2.7,2)}$	3	2	1	65.1	135.45	130.2	135.45	**-5.25**	-0.05	94.44	-135.45	-1.29	-20.48	66.67	-1.74	0.96	0.48	-135.45
A1.5	$DIST^{V1.1}-ZSPRD^{50D}_{(2.7,1)}$	2	2	-	78.88	-	157.76	-	**157.76**	1.58	127.2	-	-1.07	-16.99	100	78.88	157.76	78.88	-
A1.6	$DIST^{V1.1}-ZSPRD^{50D}_{(2.7,0.5)}$	2	1	1	50.22	63.95	50.22	63.95	**-13.73**	-0.14	50.22	-63.95	-1.97	-31.27	50	-6.87	0.79	0.79	-63.95
A2.1	$DIST^{V1.1}-SPRD^{50D}-SMA_{(10,20)}$	13	3	10	54.94	89.59	164.81	895.94	**-731.14**	-7.31	86.55	-164.36	-2.61	-41.43	23.08	-56.24	0.18	0.61	-719.95
A2.2	$DIST^{V1.1}-SPRD^{50D}-EMA_{(10,20)}$	20	9	11	108.54	91.01	976.83	1001.14	**-24.31**	-0.24	266.07	-322.26	-1.15	-18.26	45	-1.22	0.98	1.19	-490.55
A2.3	$DIST^{V1.1}-SPRD^{50D}-MACD_{(12,26,9)}$	31	20	11	55.02	87.94	1100.47	967.29	**133.18**	1.33	121.82	-175.27	-1.8	-28.57	64.52	4.3	1.14	0.63	-476.57
A2.4	$DIST^{V1.1}-SPRD^{50D}-RSI_{(14)}$	4	3	1	490.36	183.78	1471.09	183.78	**1287.31**	12.87	723.94	-183.78	0.42	6.67	75	321.83	8	2.67	-183.78
A2.5	$DIST^{V1.1}-SPRD^{50D}-BB_{(20)}$	14	5	9	135.28	53.72	676.4	483.45	**192.95**	1.93	361.06	-143.98	-1.04	-16.51	35.71	13.77	1.4	2.52	-468.33
A3	$DIST^{V1.1}-SPRD^{50D}-DECTREE$	351	195	156	23.91	30.03	4662.13	4684.15	**-22.02**	-0.22	166.02	-200.44	-3.92	-62.23	55.56	-0.06	1	0.8	-695.94
A4	$DIST^{V1.1}-SPRD^{50D}-MLP$	330	181	149	23.9	27.75	4326.36	4134.19	**192.17**	1.92	142.17	-125.32	-4.32	-68.58	54.85	0.58	1.05	0.86	-624.79
Part II: Models derived using the spread obtained from $DIST^{V1.2}-SPRD^{50D}$																			
B1.1	$DIST^{V1.2}-ZSPRD^{50D}_{(3,2)}$	5	1	4	6.94	37.13	6.94	148.53	**-141.59**	-1.42	6.94	-52.01	-6.63	-105.25	20	-28.32	0.05	0.19	-148.53
B1.2	$DIST^{V1.2}-ZSPRD^{50D}_{(3,1)}$	5	-	5	-	48.15	-	240.74	**-240.74**	-2.41	-	-121.06	-4.44	-70.48	-	-48.15	-	-	-240.74
B1.3	$DIST^{V1.2}-ZSPRD^{50D}_{(3,0.5)}$	4	2	2	41.34	193.37	82.69	386.75	**-304.06**	-3.04	64.74	-291.39	-1.44	-22.86	50	-76.02	0.21	0.21	-322.01
B1.4	$DIST^{V1.2}-ZSPRD^{50D}_{(2.7,2)}$	9	4	5	27.8	38.49	111.2	192.44	**-81.24**	-0.81	43.25	-76.75	-3.92	-62.23	44.44	-9.03	0.58	0.72	-141.32
B1.5	$DIST^{V1.2}-ZSPRD^{50D}_{(2.7,1)}$	9	4	5	54.35	62.35	217.39	311.73	**-94.35**	-0.94	107.84	-121.06	-2.22	-35.24	44.44	-10.49	0.7	0.87	-265.74
B1.6	$DIST^{V1.2}-ZSPRD^{50D}_{(2.7,0.5)}$	7	3	4	82.47	172.56	247.42	690.26	**-442.83**	-4.43	155.72	-291.39	-1.37	-21.75	42.86	-63.25	0.36	0.48	-460.78
B2.1	$DIST^{V1.2}-SPRD^{50D}-SMA_{(10,20)}$	16	11	5	73.49	92.16	808.35	460.82	**347.53**	3.48	156.51	-173.36	-1.34	-21.27	68.75	21.72	1.75	0.8	-340.07
B2.2	$DIST^{V1.2}-SPRD^{50D}-EMA_{(10,20)}$	15	7	8	117.1	109.14	819.7	873.11	**-53.41**	-0.53	288.05	-266.07	-1.05	-16.67	46.67	-3.55	0.94	1.07	-447.11
B2.3	$DIST^{V1.2}-SPRD^{50D}-MACD_{(12,26,9)}$	29	12	17	75.62	62.1	907.48	1055.68	**-148.19**	-1.48	309.8	-141.13	-1.71	-27.15	41.38	-5.11	0.86	1.22	-707.74
B2.4	$DIST^{V1.2}-SPRD^{50D}-RSI_{(14)}$	10	1	9	127.91	197.53	127.91	1777.75	**-1649.84**	-16.5	127.91	-427.21	-1.96	-31.11	10	-164.98	0.07	0.65	-1350.54
B2.5	$DIST^{V1.2}-SPRD^{50D}-BB_{(20)}$	18	10	8	60.57	110.19	605.71	881.52	**-275.81**	-2.76	169.27	-291.38	-1.46	-23.18	55.56	-15.32	0.69	0.55	-224.45
B3	$DIST^{V1.2}-SPRD^{50D}-DECTREE$	272	147	125	25.55	28.25	3756.22	3530.66	**225.57**	2.26	146.01	-208.15	-3.85	-61.12	54.04	0.83	1.06	0.9	-1134.03
B4	$DIST^{V1.2}-SPRD^{50D}-MLP$	165	89	76	36.55	34.42	3252.68	2615.99	**636.69**	6.37	183.26	-182.17	-2.88	-45.72	53.94	3.86	1.24	1.06	-366.89
Part III: Models derived using the spread obtained from $DIST^{V2}-SPRD^{50D}$																			
C1.1	$DIST^{V2}-ZSPRD^{50D}_{(3,2)}$	2	1	1	135.45	94.44	135.45	94.44	**41.01**	0.41	135.45	-94.44	-0.81	-12.86	50	20.51	1.43	1.43	-94.44
C1.2	$DIST^{V2}-ZSPRD^{50D}_{(3,1)}$	1	-	1	-	127.2	-	127.2	**-127.2**	-1.27	-	-127.2	-	-	-	-127.2	-	-	-127.2
C1.3	$DIST^{V2}-ZSPRD^{50D}_{(3,0.5)}$	1	1	-	63.95	-	63.95	-	**63.95**	0.64	63.95	-	-	-	100	63.95	63.95	63.95	-
C1.4	$DIST^{V2}-ZSPRD^{50D}_{(2.7,2)}$	3	1	2	135.45	65.1	135.45	130.2	**5.25**	0.05	135.45	-94.44	-1.26	-20	33.33	1.74	1.04	2.08	-130.2
C1.5	$DIST^{V2}-ZSPRD^{50D}_{(2.7,1)}$	2	-	2	-	78.88	-	157.76	**-157.76**	-1.58	-	-127.2	-3.38	-53.66	-	-78.88	-	-	-157.76
C1.6	$DIST^{V2}-ZSPRD^{50D}_{(2.7,0.5)}$	2	1	1	63.95	50.22	63.95	50.22	**13.73**	0.14	63.95	-50.22	-1.8	-28.57	50	6.87	1.27	1.27	-50.22
C2.1	$DIST^{V2}-SPRD^{50D}-SMA_{(10,20)}$	13	10	3	89.59	54.94	895.94	164.81	**731.14**	7.31	164.36	-86.55	-1.2	-19.05	76.92	56.24	5.44	1.63	-86.55
C2.2	$DIST^{V2}-SPRD^{50D}-EMA_{(10,20)}$	20	11	9	91.01	108.54	1001.14	976.83	**24.31**	0.24	322.26	-266.07	-1.13	-17.94	55	1.22	1.02	0.84	-234.57
C2.3	$DIST^{V2}-SPRD^{50D}-MACD_{(12,26,9)}$	31	11	20	87.94	55.02	967.29	1100.47	**-133.18**	-1.33	175.27	-121.82	-1.91	-30.32	35.48	-4.3	0.88	1.6	-403.72
C2.4	$DIST^{V2}-SPRD^{50D}-RSI_{(14)}$	4	1	3	183.78	490.36	183.78	1471.09	**-1287.31**	-12.87	183.78	-723.94	-1.17	-18.57	25	-321.83	0.12	0.37	-733.03
C2.5	$DIST^{V2}-SPRD^{50D}-BB_{(20)}$	14	9	5	53.72	135.28	483.45	676.4	**-192.95**	-1.93	143.98	-361.06	-1.25	-19.84	64.29	-13.77	0.71	0.4	-302.62
C3	$DIST^{V2}-SPRD^{50D}-DECTREE$	355	201	154	22.46	28	4514.11	4311.36	**202.75**	2.03	140.72	-178.53	-4.34	-68.9	56.62	0.57	1.05	0.8	-502.03
C4	$DIST^{V2}-SPRD^{50D}-MLP$	306	171	135	27.43	28.51	4691.15	3849.34	**841.81**	8.42	166.02	-125.32	-3.88	-61.59	55.88	2.75	1.22	0.96	-437.6
Part IV: Models derived using the spread obtained from $DIST^{V3}-SPRD^{50D}$																			
D1.1	$DIST^{V3}-ZSPRD^{50D}_{(3,2)}$	6	2	4	53.64	82.66	107.27	330.63	**-223.36**	-2.23	60.35	-216.86	-1.86	-29.53	33.33	-37.23	0.32	0.65	-317.92
D1.2	$DIST^{V3}-ZSPRD^{50D}_{(3,1)}$	6	2	4	97.04	51.78	194.07	207.12	**-13.05**	-0.13	120.79	-130.77	-1.74	-27.62	33.33	-2.18	0.94	1.87	-199
D1.3	$DIST^{V3}-ZSPRD^{50D}_{(3,0.5)}$	6	5	1	43.49	136.12	217.45	136.12	**81.33**	0.81	120.79	-136.12	-1.59	-25.24	83.33	13.55	1.6	0.32	-136.12
D1.4	$DIST^{V3}-ZSPRD^{50D}_{(2.7,2)}$	13	8	5	41.3	70.33	330.44	351.64	**-21.2**	-0.21	64.36	-216.86	-1.99	-31.59	61.54	-1.63	0.94	0.59	-294.5
D1.5	$DIST^{V3}-ZSPRD^{50D}_{(2.7,1)}$	11	6	5	44.88	50.94	269.26	254.68	**14.59**	0.15	120.79	-130.77	-2.29	-36.35	54.55	1.33	1.06	0.88	-210.88
D1.6	$DIST^{V3}-ZSPRD^{50D}_{(2.7,0.5)}$	11	9	2	30.93	95.35	278.34	190.7	**87.64**	0.88	120.79	-136.12	-2.2	-34.92	81.82	7.97	1.46	0.32	-136.12
D2.1	$DIST^{V3}-SPRD^{50D}-SMA_{(10,20)}$	16	9	7	61.02	95.65	549.2	669.58	**-120.38**	-1.2	205	-149.34	-1.62	-25.72	56.25	-7.52	0.82	0.64	-342.28
D2.2	$DIST^{V3}-SPRD^{50D}-EMA_{(10,20)}$	33	14	19	88.76	91.89	1242.64	1745.86	**-503.22**	-5.03	224.13	-309.8	-1.48	-23.49	42.42	-15.26	0.71	0.97	-704.25
D2.3	$DIST^{V3}-SPRD^{50D}-MACD_{(12,26,9)}$	47	16	31	111.44	59.44	1782.98	1842.59	**-59.61**	-0.6	266.07	-200.76	-1.46	-23.18	34.04	-1.27	0.97	1.87	-752.04
D2.4	$DIST^{V3}-SPRD^{50D}-RSI_{(14)}$	2	-	2	-	782.2	-	1564.4	**-1564.4**	-15.64	-	-1257.89	-1.39	-22.07	-	-782.2	-	-	-1257.89
D2.5	$DIST^{V3}-SPRD^{50D}-BB_{(20)}$	21	14	7	47.83	39.6	669.63	277.21	**392.41**	3.92	110.89	-94.69	-2.54	-40.32	66.67	18.69	2.42	1.21	-94.69
D3	$DIST^{V3}-SPRD^{50D}-DECTREE$	303	161	142	22.15	29.51	3566.71	4189.96	**-623.25**	-6.23	114.85	-213.17	-4.17	-66.2	53.14	-2.05	0.85	0.75	-966.35
D4	$DIST^{V3}-SPRD^{50D}-MLP$	207	107	100	29.47	28.82	3153.41	2882.29	**271.12**	2.71	145.68	-186.25	-3.43	-54.45	51.69	1.31	1.09	1.02	-418.86
Part V: Models derived using the spread obtained from $DIST^{V4}-SPRD^{50D}$																			
E1.1	$DIST^{V4}-ZSPRD^{50D}_{(3,2)}$	6	2	4	53.64	82.66	107.27	330.63	**-223.36**	-2.23	60.35	-216.86	-1.86	-29.53	33.33	-37.23	0.32	0.65	-317.92
E1.2	$DIST^{V4}-ZSPRD^{50D}_{(3,1)}$	6	2	4	97.04	51.78	194.07	207.12	**-13.05**	-0.13	120.79	-130.77	-1.74	-27.62	33.33	-2.18	0.94	1.87	-199
E1.3	$DIST^{V4}-ZSPRD^{50D}_{(3,0.5)}$	6	5	1	43.49	136.12	217.45	136.12	**81.33**	0.81	120.79	-136.12	-1.59	-25.24	83.33	13.55	1.6	0.32	-136.12
E1.4	$DIST^{V4}-ZSPRD^{50D}_{(2.7,2)}$	13	8	5	41.3	70.33	330.44	351.64	**-21.2**	-0.21	64.36	-216.86	-1.99	-31.59	61.54	-1.63	0.94	0.59	-294.5
E1.5	$DIST^{V4}-ZSPRD^{50D}_{(2.7,1)}$	11	6	5	44.88	50.94	269.26	254.68	**14.59**	0.15	120.79	-130.77	-2.29	-36.35	54.55	1.33	1.06	0.88	-210.88
E1.6	$DIST^{V4}-ZSPRD^{50D}_{(2.7,0.5)}$	11	9	2	30.93	95.35	278.34	190.7	**87.64**	0.88	120.79	-136.12	-2.2	-34.92	81.82	7.97	1.46	0.32	-136.12
E2.1	$DIST^{V4}-SPRD^{50D}-SMA_{(10,20)}$	17	10	7	87.9	90.81	879.05	635.67	**243.38**	2.43	329.85	-149.34	-1.11	-17.62	58.82	14.31	1.38	0.97	-342.28
E2.2	$DIST^{V4}-SPRD^{50D}-EMA_{(10,20)}$	33	14	19	88.76	91.89	1242.64	1745.86	**-503.22**	-5.03	224.13	-309.8	-1.48	-23.49	42.42	-15.26	0.71	0.97	-704.25
E2.3	$DIST^{V4}-SPRD^{50D}-MACD_{(12,26,9)}$	47	16	31	111.44	59.44	1782.98	1842.59	**-59.61**	-0.6	266.07	-200.76	-1.46	-23.18	34.04	-1.27	0.97	1.87	-752.04
E2.4	$DIST^{V4}-SPRD^{50D}-RSI_{(14)}$	2	-	2	-	782.2	-	1564.4	**-1564.4**	-15.64	-	-1257.89	-1.39	-22.07	-	-782.2	-	-	-1257.89
E2.5	$DIST^{V4}-SPRD^{50D}-BB_{(20)}$	21	14	7	47.83	39.6	669.63	277.21	**392.41**	3.92	110.89	-94.69	-2.54	-40.32	66.67	18.69	2.42	1.21	-94.69
E3	$DIST^{V4}-SPRD^{50D}-DECTREE$	311	169	142	27.88	23.22	4711.04	3297.41	**1413.63**	14.14	190.88	-148.99	-3.85	-61.12	54.34	4.55	1.43	1.2	-358.85
E4	$DIST^{V4}-SPRD^{50D}-MLP$	210	112	98	33.48	32.29	3749.6	3164.3	**585.3**	5.85	326.54	-316.56	-2.76	-43.81	53.33	2.78	1.18	1.04	-784.89
Part VI: Models derived using the spread obtained from $JOHANSEN-SPRD^{50D}$																			
F1.1	$JOHANSEN-ZSPRD^{50D}_{(3,2)}$	17	6	11	43.62	60.78	261.74	668.61	**-406.87**	-4.07	206.36	-213	-0.63	-10	35.29	-23.94	0.39	0.72	-438.73
F1.2	$JOHANSEN-ZSPRD^{50D}_{(3,1)}$	17	6	11	46.25	69.97	277.49	769.72	**-492.23**	-4.92	196.99	-213	-0.61	-9.68	35.29	-28.96	0.36	0.66	-507.18
F1.3	$JOHANSEN-ZSPRD^{50D}_{(3,0.5)}$	17	6	11	17.29	123.64	103.71	1360.04	**-1256.33**	-12.56	37.49	-683.94	-0.39	-6.19	35.29	-73.91	0.08	0.14	-1271.28
F1.4	$JOHANSEN-ZSPRD^{50D}_{(2.7,2)}$	19	7	12	42.02	159.7	294.14	1916.39	**-1622.25**	-16.22	206.36	-1247.78	-0.14	-2.22	36.84	-85.39	0.15	0.26	-1686.51
F1.5	$JOHANSEN-ZSPRD^{50D}_{(2.7,1)}$	19	7	12	59.1	168.13	413.71	2017.5	**-1603.79**	-16.04	196.99	-1247.78	0.13	2.06	36.84	-84.41	0.21	0.35	-1754.97
F1.6	$JOHANSEN-ZSPRD^{50D}_{(2.7,0.5)}$	19	7	12	35.88	217.32	251.13	2607.83	**-2356.7**	-23.57	147.42	-1247.78	0.16	2.54	36.84	-124.04	0.1	0.17	-2519.07
F2.1	$JOHANSEN-SPRD^{50D}-SMA_{(10,20)}$	23	16	7	2026.47	184.28	32423.56	1289.96	**31133.6**	311.34	21375.57	-582.77	0.27	4.29	69.57	1353.74	25.14	11	-668.44
F2.2	$JOHANSEN-SPRD^{50D}-EMA_{(10,20)}$	29	15	14	387.62	763.15	5814.26	10684.09	**-4869.82**	-48.7	1734.37	-7142.58	0.17	2.7	51.72	-167.97	0.54	0.51	-8784.78
F2.3	$JOHANSEN-SPRD^{50D}-MACD_{(12,26,9)}$	35	17	18	203.4	262.23	3457.74	4720.08	**-1262.34**	-12.62	1639.04	-1398.5	-0.06	-0.95	48.57	-36.07	0.73	0.78	-2859.36
F2.4	$JOHANSEN-SPRD^{50D}-RSI_{(14)}$	7	6	1	1943.37	193.45	11660.24	193.45	**11466.79**	114.67	6863.33	-193.45	0.57	9.05	85.71	1638.02	60.28	10.05	-193.45
F2.5	$JOHANSEN-SPRD^{50D}-BB_{(20)}$	15	6	9	154.49	123.09	926.91	1107.85	**-180.94**	-1.81	502.64	-310.18	0.21	3.33	40	-12.06	0.84	1.26	-489.22
F3	$JOHANSEN-SPRD^{50D}-DECTREE$	330	159	171	28.29	26.85	4497.6	4591.68	**-94.08**	-0.94	150.47	-133.59	-3.92	-62.23	48.18	-0.29	0.98	1.05	-763.58
F4	$JOHANSEN-SPRD^{50D}-MLP$	216	112	104	32.41	24.78	3630.38	2577.18	**1053.2**	10.53	212.37	-114.66	-3.5	-55.56	51.85	4.87	1.41	1.31	-602.66
Part VII: Models derived using the spread obtained from $ADF-SPRD^{50D}$																			
G1.1	$ADF-ZSPRD^{50D}_{(3,2)}$	4	1	3	41.45	86.87	41.45	260.6	**-219.15**	-2.19	41.45	-244.21	-3.5	-55.56	25	-54.79	0.16	0.48	-260.6
G1.2	$ADF-ZSPRD^{50D}_{(3,1)}$	3	2	1	113.44	305.06	226.89	305.06	**-78.17**	-0.78	139.78	-305.06	-2.08	-33.02	66.67	-26.04	0.74	0.37	-305.06
G1.3	$ADF-ZSPRD^{50D}_{(3,0.5)}$	3	3	-	153.26	-	459.78	-	**459.78**	4.6	440.22	-	-0.89	-14.13	100	153.26	459.78	153.26	-
G1.4	$ADF-ZSPRD^{50D}_{(2.7,2)}$	7	2	5	156.95	53.35	313.89	266.73	**47.16**	0.47	272.44	-101.32	-3.09	-49.05	28.57	6.73	1.18	2.94	-225.28
G1.5	$ADF-ZSPRD^{50D}_{(2.7,1)}$	6	3	3	183.17	133.15	549.5	399.45	**150.05**	1.5	322.61	-198.03	-2.12	-33.65	50	25.01	1.38	1.38	-211.02
G1.6	$ADF-ZSPRD^{50D}_{(2.7,0.5)}$	5	3	2	190.31	181.89	570.92	363.79	**207.13**	2.07	551.35	-197.64	-0.89	-14.13	60	41.43	1.57	1.05	-197.64
G2.1	$ADF-SPRD^{50D}-SMA_{(10,20)}$	14	10	4	334.23	164.8	3342.28	659.18	**2683.1**	26.83	1290.27	-567.71	-0.78	-12.38	71.43	191.66	5.07	2.03	-570.9
G2.2	$ADF-SPRD^{50D}-EMA_{(10,20)}$	29	21	8	99.63	255.97	2092.27	2047.72	**44.55**	0.45	270.01	-546.88	-2.17	-34.45	72.41	1.52	1.02	0.39	-1300.34
G2.3	$ADF-SPRD^{50D}-MACD_{(12,26,9)}$	43	28	15	168.69	91.15	4723.37	1367.23	**3356.14**	33.56	608.5	-278.77	-0.51	-8.1	65.12	78.06	3.45	1.85	-363.98
G2.4	$ADF-SPRD^{50D}-RSI_{(14)}$	2	2	-	845.33	-	1690.65	-	**1690.65**	16.91	1412.65	-	0.38	6.03	100	845.33	1690.65	845.33	-
G2.5	$ADF-SPRD^{50D}-BB_{(20)}$	21	7	14	47.54	79.71	332.78	1115.89	**-783.11**	-7.83	125.8	-372.9	-4.71	-74.77	33.33	-37.3	0.3	0.6	-871.83
G3	$ADF-SPRD^{50D}-DECTREE$	348	208	140	24.3	27.41	5054.87	3837.39	**1217.48**	12.17	162.73	-293.77	-4	-63.5	59.77	3.5	1.32	0.89	-479.73
G4	$ADF-SPRD^{50D}-MLP$	284	159	125	23.15	23.53	3680.6	2941.51	**739.09**	7.39	114.84	-224.03	-4.37	-69.37	55.99	2.6	1.25	0.98	-445.74
Part VIII: Models derived using the spread obtained from $KALMAN-SPRD^{50D}$																			
H1.1	$KALMAN-ZSPRD^{50D}_{(3,2)}$	3	1	2	73	94.37	73	188.73	**-115.74**	-1.16	73	-128.63	-5.14	-81.59	33.33	-38.58	0.39	0.77	-128.63
H1.2	$KALMAN-ZSPRD^{50D}_{(3,1)}$	2	1	1	105.99	91.98	105.99	91.98	**14.01**	0.14	105.99	-91.98	-3.48	-55.24	50	7	1.15	1.15	-91.98
H1.3	$KALMAN-ZSPRD^{50D}_{(3,0.5)}$	2	2	-	163.64	-	327.28	-	**327.28**	3.27	194.3	-	-6.1	-96.83	100	163.64	327.28	163.64	-
H1.4	$KALMAN-ZSPRD^{50D}_{(2.7,2)}$	6	3	3	34.37	214.51	103.11	643.52	**-540.41**	-5.4	54.53	-421.69	-3.07	-48.73	50	-90.07	0.16	0.16	-540.41
H1.5	$KALMAN-ZSPRD^{50D}_{(2.7,1)}$	5	3	2	140.98	201.81	422.93	403.62	**19.31**	0.19	252.62	-388.15	-2.01	-31.91	60	3.86	1.05	0.7	-403.62
H1.6	$KALMAN-ZSPRD^{50D}_{(2.7,0.5)}$	5	3	2	82.83	150.9	248.5	301.8	**-53.29**	-0.53	114.64	-177.56	-3.87	-61.43	60	-10.66	0.82	0.55	-250.63
H2.1	$KALMAN-SPRD^{50D}-SMA_{(10,20)}$	12	7	5	266.55	143.66	1865.85	718.3	**1147.54**	11.48	952.83	-299.14	-1.14	-18.1	58.33	95.61	2.6	1.86	-363.07
H2.2	$KALMAN-SPRD^{50D}-EMA_{(10,20)}$	21	6	15	286.59	127.46	1719.57	1911.89	**-192.33**	-1.92	670.17	-287.31	-2.09	-33.18	28.57	-9.16	0.9	2.25	-1141.15
H2.3	$KALMAN-SPRD^{50D}-MACD_{(12,26,9)}$	34	12	22	156.65	117.97	1879.8	2595.42	**-715.62**	-7.16	487.89	-573.69	-2.66	-42.23	35.29	-21.06	0.72	1.33	-1068.97
H2.4	$KALMAN-SPRD^{50D}-RSI_{(14)}$	4	2	2	463.53	609.41	927.07	1218.82	**-291.75**	-2.92	850.64	-1209.81	-0.64	-10.16	50	-72.94	0.76	0.76	-1209.81
H2.5	$KALMAN-SPRD^{50D}-BB_{(20)}$	8	6	2	90.26	411.31	541.57	822.61	**-281.04**	-2.81	141.39	-774.65	-1.68	-26.67	75	-35.13	0.66	0.22	-774.65
H3	$KALMAN-SPRD^{50D}-DECTREE$	325	196	129	23.35	25.78	4577.28	3325.19	**1252.09**	12.52	142.17	-105.63	-4.35	-69.05	60.31	3.85	1.38	0.91	-404.86
H4	$KALMAN-SPRD^{50D}-MLP$	268	156	112	25.25	29.11	3939.65	3260.71	**678.94**	6.79	119.97	-191.93	-3.98	-63.18	58.21	2.53	1.21	0.87	-301.65
Part IX: Models derived using the spread obtained from $RATIO-SPRD^{50D}$																			
I1.1	$RATIO-ZSPRD^{50D}_{(3,2)}$	3	2	1	95.76	3	191.52	3	**188.52**	1.89	105.21	-3	-1.54	-24.45	66.67	62.84	63.82	31.91	-3
I1.2	$RATIO-ZSPRD^{50D}_{(3,1)}$	2	1	1	172.2	20.54	172.2	20.54	**151.66**	1.52	172.2	-20.54	-0.56	-8.89	50	75.83	8.38	8.38	-20.54
I1.3	$RATIO-ZSPRD^{50D}_{(3,0.5)}$	2	1	1	317.81	21.08	317.82	21.08	**296.74**	2.97	317.81	-21.08	-0.02	-0.32	50	148.37	15.08	15.08	-21.08
I1.4	$RATIO-ZSPRD^{50D}_{(2.7,2)}$	6	5	1	54.32	3	271.58	3	**268.58**	2.69	105.21	-3	-2.88	-45.72	83.33	44.76	90.5	18.1	-3
I1.5	$RATIO-ZSPRD^{50D}_{(2.7,1)}$	5	4	1	95.79	20.54	383.14	20.54	**362.6**	3.63	172.2	-20.54	-0.92	-14.6	80	72.52	18.65	4.66	-20.54
I1.6	$RATIO-ZSPRD^{50D}_{(2.7,0.5)}$	5	3	2	195.91	52.89	587.74	105.78	**481.96**	4.82	317.81	-84.71	-0.35	-5.56	60	96.39	5.56	3.7	-105.78
I2.1	$RATIO-SPRD^{50D}-SMA_{(10,20)}$	16	9	7	64.58	139.2	581.22	974.42	**-393.2**	-3.93	175	-428.34	-1.19	-18.89	56.25	-24.57	0.6	0.46	-474.23
I2.2	$RATIO-SPRD^{50D}-EMA_{(10,20)}$	25	9	16	55.36	105.02	498.23	1680.37	**-1182.14**	-11.82	107.77	-407.62	-1.83	-29.05	36	-47.29	0.3	0.53	-1002.12
I2.3	$RATIO-SPRD^{50D}-MACD_{(12,26,9)}$	38	10	28	72.2	57.55	722	1611.37	**-889.37**	-8.89	252.14	-171.24	-2.22	-35.24	26.32	-23.4	0.45	1.25	-1188.88
I2.4	$RATIO-SPRD^{50D}-RSI_{(14)}$	3	1	2	11.43	430.09	11.43	860.19	**-848.76**	-8.49	11.43	-553.68	-1.54	-24.45	33.33	-282.93	0.01	0.03	-553.68
I2.5	$RATIO-SPRD^{50D}-BB_{(20)}$	20	14	6	79.56	56.68	1113.82	340.09	**773.73**	7.74	374.24	-175.71	-1.08	-17.14	70	38.69	3.28	1.4	-221.23
I3	$RATIO-SPRD^{50D}-DECTREE$	377	144	233	26.93	20.95	3877.61	4881.76	**-1004.15**	-10.04	186.25	-112.67	-4.72	-74.93	38.2	-2.66	0.79	1.29	-1509.94
I4	$RATIO-SPRD^{50D}-MLP$	308	118	190	27.74	21.16	3273.76	4021	**-747.24**	-7.47	186.25	-98.09	-4.6	-73.02	38.31	-2.43	0.81	1.31	-1128.42
Part X: Models derived using the close price of SCHF.N																			
CLS-SYM-1.1	$CLOSE^{SCHF.N}-SMA_{(10,20)}$	20	7	13	314.26	125.66	2199.8	1633.59	**566.2**	5.66	1106.36	-575.54	-0.14	-2.22	35	28.31	1.35	2.5	-918.42
CLS-SYM-1.2	$CLOSE^{SCHF.N}-EMA_{(10,20)}$	23	8	15	331.11	93.37	2648.86	1400.61	**1248.24**	12.48	911.97	-332.73	-0.07	-1.11	34.78	54.26	1.89	3.55	-643.72
CLS-SYM-1.3	$CLOSE^{SCHF.N}-MACD_{(12,26,9)}$	30	10	20	221.35	120.16	2213.46	2403.27	**-189.81**	-1.9	1043.11	-326.35	-0.34	-5.4	33.33	-6.34	0.92	1.84	-1733.81
CLS-SYM-1.4	$CLOSE^{SCHF.N}-RSI_{(14)}$	5	2	3	617.93	304.16	1235.87	912.48	**323.39**	3.23	959.27	-697.61	-0.02	-0.32	40	64.68	1.35	2.03	-697.61
CLS-SYM-1.5	$CLOSE^{SCHF.N}-BB_{(20)}$	15	8	7	79.49	192.86	635.89	1349.99	**-714.1**	-7.14	252.09	-785.71	-0.51	-8.1	53.33	-47.62	0.47	0.41	-785.71
Part XI: Models derived using the close price of VO.N																			
CLS-SYM-2.1	$CLOSE^{VO.N}-SMA_{(10,20)}$	15	5	10	407.5	131.94	2037.52	1319.42	**718.1**	7.18	1345.66	-357.26	-0.07	-1.11	33.33	47.86	1.54	3.09	-888.12
CLS-SYM-2.2	$CLOSE^{VO.N}-EMA_{(10,20)}$	20	6	14	305.56	123.3	1833.38	1726.2	**107.17**	1.07	700.63	-218.39	-0.27	-4.29	30	5.36	1.06	2.48	-812.37
CLS-SYM-2.3	$CLOSE^{VO.N}-MACD_{(12,26,9)}$	30	12	18	235.68	119.41	2828.19	2149.34	**678.86**	6.79	1213.06	-330.07	-0.19	-3.02	40	22.63	1.32	1.97	-845.26
CLS-SYM-2.4	$CLOSE^{VO.N}-RSI_{(14)}$	5	2	3	464.59	648.69	929.17	1946.08	**-1016.91**	-10.17	781.75	-1353.4	-0.35	-5.56	40	-203.38	0.48	0.72	-1353.4
CLS-SYM-2.5	$CLOSE^{VO.N}-BB_{(20)}$	15	13	2	85.35	600.28	1109.6	1200.56	**-90.96**	-0.91	190.76	-984.33	-0.29	-4.6	86.67	-6.04	0.92	0.14	-984.33

Table D.2.15: This table presents the back-test metrics for the pair $SCHF.N/VO.N$ based on a 100-day rolling window. The table is subdivided into eleven parts, and in each of these parts, we present the back-test metrics and the trading strategies which use the spread derived from various models. In Part I, the spread is derived from the $DIST^{V1.1}$ model, in Part II from the $DIST^{V1.2}$ model, in Part III from the $DIST^{V2}$ model, in Part IV from the $DIST^{V3}$ model, in Part V from the $DIST^{V4}$ model, in Part VI from the $JOHANSEN-SPRD$ model, in Part VIII from the $ADF-SPRD$ model, in from the $DIST^{V2}$ model, in Part VIII from the $KALMAN-SPRD$ model, and in Part IX from the $RATIO-SPRD$ model. In Part X and XI, we present the back-test metrics of the trading strategies which use the close price of SCHF.N, and VO.N, respectively. All $ numbers reported below are in USD.

(I) Trading Strategy Code	(II) Model Name	(III) Total Number of Trades	(IV) Number of Winning Trades	(V) Number of Loosing Trades	(VI) Average Profit per Trade ($)	(VII) Average Loss per Trade ($)	(VIII) Gross Profit ($)	(IX) Gross Loss ($)	(X) Net Profit ($)	(XI) ROI (%)	(XII) Max P&L ($)	(XIII) Min P&L ($)	(XIV) Daily Sharpe Ratio	(XV) Annualized Sharpe Ratio	(XVI) Hit Ratio	(XVII) Expectancy	(XVIII) Profit Factor	(XIX) Realized Risk Reward Ratio	(XX) Max Drawdown ($)
Part I: Models derived using the spread obtained from $DIST^{V1.1}-SPRD^{100D}$																			
A1.1	$DIST^{V1.1}-ZSPRD^{100D}_{(3,2)}$	1	1	-	79.51	-	79.51	-	**79.51**	0.8	79.51	-	-	-	100	79.51	79.51	79.51	-
A1.2	$DIST^{V1.1}-ZSPRD^{100D}_{(3,1)}$	1	-	1	-	131.35	-	131.35	**-131.35**	-1.31	-	-131.35	-	-	-	-131.35	-	-	-131.35
A1.3	$DIST^{V1.1}-ZSPRD^{100D}_{(3,0.5)}$	1	-	1	-	231.06	-	231.06	**-231.06**	-2.31	-	-231.06	-	-	-	-231.06	-	-	-231.06
A1.4	$DIST^{V1.1}-ZSPRD^{100D}_{(2.7,2)}$	1	1	-	79.51	-	79.51	-	**79.51**	0.8	79.51	-	-	-	100	79.51	79.51	79.51	-
A1.5	$DIST^{V1.1}-ZSPRD^{100D}_{(2.7,1)}$	1	-	1	-	131.35	-	131.35	**-131.35**	-1.31	-	-131.35	-	-	-	-131.35	-	-	-131.35
A1.6	$DIST^{V1.1}-ZSPRD^{100D}_{(2.7,0.5)}$	1	-	1	-	231.06	-	231.06	**-231.06**	-2.31	-	-231.06	-	-	-	-231.06	-	-	-231.06
A2.1	$DIST^{V1.1}-SPRD^{100D}-SMA_{(10,20)}$	12	3	9	54.94	98.07	164.81	882.62	**-717.82**	-7.18	86.55	-164.36	-2.57	-40.8	25	-59.82	0.19	0.56	-719.95
A2.2	$DIST^{V1.1}-SPRD^{100D}-EMA_{(10,20)}$	20	10	10	109.46	92.42	1094.56	924.25	**170.32**	1.7	341.95	-322.26	-1.03	-16.35	50	8.52	1.18	1.18	-413.65
A2.3	$DIST^{V1.1}-SPRD^{100D}-MACD_{(12,26,9)}$	29	18	11	55.22	96.53	993.92	1061.86	**-67.94**	-0.68	121.82	-175.27	-1.79	-28.42	62.07	-2.34	0.94	0.57	-487.28
A2.4	$DIST^{V1.1}-SPRD^{100D}-RSI_{(14)}$	5	4	1	356.09	183.78	1424.37	183.78	**1240.6**	12.41	723.94	-183.78	0.29	4.6	80	248.12	7.75	1.94	-183.78
A2.5	$DIST^{V1.1}-SPRD^{100D}-BB_{(20)}$	13	5	8	186.01	60.13	930.07	481.05	**449.03**	4.49	614.73	-143.98	-0.6	-9.52	38.46	34.54	1.93	3.09	-468.33
A3	$DIST^{V1.1}-SPRD^{100D}-DECTREE$	315	174	141	23.74	29.44	4130.18	4150.66	**-20.48**	-0.2	142.17	-146.01	-4.13	-65.56	55.24	-0.06	1	0.81	-688.32
A4	$DIST^{V1.1}-SPRD^{100D}-MLP$	266	152	114	27.19	29.78	4132.28	3395.05	**737.23**	7.37	142.17	-200.44	-3.79	-60.16	57.14	2.77	1.22	0.91	-348.48
Part II: Models derived using the spread obtained from $DIST^{V1.2}-SPRD^{100D}$																			
B1.1	$DIST^{V1.2}-ZSPRD^{100D}_{(3,2)}$	5	1	4	16.01	130.43	16.01	521.72	**-505.71**	-5.06	16.01	-204.67	-2.72	-43.18	20	-101.14	0.03	0.12	-521.72
B1.2	$DIST^{V1.2}-ZSPRD^{100D}_{(3,1)}$	4	-	4	-	131.56	-	526.22	**-526.22**	-5.26	-	-206.08	-4.91	-77.94	-	-131.56	-	-	-526.23
B1.3	$DIST^{V1.2}-ZSPRD^{100D}_{(3,0.5)}$	4	-	4	-	76.59	-	306.35	**-306.35**	-3.06	-	-163.64	-3.52	-55.88	-	-76.59	-	-	-306.35
B1.4	$DIST^{V1.2}-ZSPRD^{100D}_{(2.7,2)}$	7	1	6	16.01	110.58	16.01	663.48	**-647.47**	-6.47	16.01	-204.67	-3.04	-48.26	14.29	-92.49	0.02	0.14	-663.48
B1.5	$DIST^{V1.2}-ZSPRD^{100D}_{(2.7,1)}$	6	-	6	-	105.2	-	631.19	**-631.19**	-6.31	-	-206.08	-4.23	-67.15	-	-105.2	-	-	-631.19
B1.6	$DIST^{V1.2}-ZSPRD^{100D}_{(2.7,0.5)}$	6	1	5	63.98	117.85	63.98	589.24	**-525.26**	-5.25	63.98	-282.89	-1.97	-31.27	16.67	-87.54	0.11	0.54	-525.26
B2.1	$DIST^{V1.2}-SPRD^{100D}-SMA_{(10,20)}$	10	5	5	109.47	82.28	547.36	411.41	**135.94**	1.36	238.66	-139.85	-1.09	-17.3	50	13.59	1.33	1.33	-262.24
B2.2	$DIST^{V1.2}-SPRD^{100D}-EMA_{(10,20)}$	20	10	10	93.09	91.16	930.89	911.56	**19.34**	0.19	194.74	-341.95	-1.23	-19.53	50	0.97	1.02	1.02	-236.24
B2.3	$DIST^{V1.2}-SPRD^{100D}-MACD_{(12,26,9)}$	28	12	16	109.97	59.54	1319.58	952.67	**366.91**	3.67	420.82	-210.22	-1.14	-18.1	42.86	13.11	1.39	1.85	-427.92
B2.4	$DIST^{V1.2}-SPRD^{100D}-RSI_{(14)}$	9	6	3	83.63	345.48	501.81	1036.45	**-534.64**	-5.35	178.64	-597.49	-0.81	-12.86	66.67	-59.39	0.48	0.24	-404.91
B2.5	$DIST^{V1.2}-SPRD^{100D}-BB_{(20)}$	8	2	6	20.6	152.27	41.2	913.64	**-872.44**	-8.72	28.34	-427.36	-1.53	-24.29	25	-109.05	0.05	0.14	-445.08
B3	$DIST^{V1.2}-SPRD^{100D}-DECTREE$	237	120	117	27.68	28.4	3322.19	3323.34	**-1.16**	-0.01	354.93	-261.77	-3.26	-51.75	50.63	-0.01	1	0.97	-781.09
B4	$DIST^{V1.2}-SPRD^{100D}-MLP$	153	88	65	24.57	32.38	2161.9	2104.82	**57.08**	0.57	110.62	-188.58	-3.95	-62.7	57.52	0.38	1.03	0.76	-468.53
Part III: Models derived using the spread obtained from $DIST^{V2}-SPRD^{100D}$																			
C1.1	$DIST^{V2}-ZSPRD^{100D}_{(3,2)}$	1	-	1	-	79.51	-	79.51	**-79.51**	-0.8	-	-79.51	-	-	-	-79.51	-	-	-79.51
C1.2	$DIST^{V2}-ZSPRD^{100D}_{(3,1)}$	1	1	-	131.35	-	131.35	-	**131.35**	1.31	131.35	-	-	-	100	131.35	131.35	131.35	-
C1.3	$DIST^{V2}-ZSPRD^{100D}_{(3,0.5)}$	1	1	-	231.06	-	231.06	-	**231.06**	2.31	231.06	-	-	-	100	231.06	231.06	231.06	-
C1.4	$DIST^{V2}-ZSPRD^{100D}_{(2.7,2)}$	1	-	1	-	79.51	-	79.51	**-79.51**	-0.8	-	-79.51	-	-	-	-79.51	-	-	-79.51
C1.5	$DIST^{V2}-ZSPRD^{100D}_{(2.7,1)}$	1	1	-	131.35	-	131.35	-	**131.35**	1.31	131.35	-	-	-	100	131.35	131.35	131.35	-
C1.6	$DIST^{V2}-ZSPRD^{100D}_{(2.7,0.5)}$	1	1	-	231.06	-	231.06	-	**231.06**	2.31	231.06	-	-	-	100	231.06	231.06	231.06	-
C2.1	$DIST^{V2}-SPRD^{100D}-SMA_{(10,20)}$	12	9	3	98.07	54.94	882.62	164.81	**717.82**	7.18	164.36	-86.55	-1.12	-17.78	75	59.82	5.36	1.79	-86.55
C2.2	$DIST^{V2}-SPRD^{100D}-EMA_{(10,20)}$	20	10	10	92.42	109.46	924.25	1094.56	**-170.32**	-1.7	322.26	-341.95	-1.16	-18.41	50	-8.52	0.84	0.84	-234.57
C2.3	$DIST^{V2}-SPRD^{100D}-MACD_{(12,26,9)}$	29	11	18	96.53	55.22	1061.86	993.92	**67.94**	0.68	175.27	-121.82	-1.74	-27.62	37.93	2.34	1.07	1.75	-403.72
C2.4	$DIST^{V2}-SPRD^{100D}-RSI_{(14)}$	5	1	4	183.78	356.09	183.78	1424.37	**-1240.6**	-12.41	183.78	-723.94	-1.21	-19.21	20	-248.12	0.13	0.52	-877.35
C2.5	$DIST^{V2}-SPRD^{100D}-BB_{(20)}$	13	8	5	60.13	186.01	481.05	930.07	**-449.03**	-4.49	143.98	-614.73	-0.95	-15.08	61.54	-34.54	0.52	0.32	-302.62
C3	$DIST^{V2}-SPRD^{100D}-DECTREE$	322	181	141	23.97	27.05	4337.99	3813.94	**524.05**	5.24	142.17	-121.04	-4.36	-69.21	56.21	1.63	1.14	0.89	-387.68
C4	$DIST^{V2}-SPRD^{100D}-MLP$	260	149	111	27.49	28.4	4095.31	3151.94	**943.38**	9.43	142.17	-121.04	-3.95	-62.7	57.31	3.63	1.3	0.97	-263.03
Part IV: Models derived using the spread obtained from $DIST^{V3}-SPRD^{100D}$																			
D1.1	$DIST^{V3}-ZSPRD^{100D}_{(3,2)}$	5	3	2	88.06	41.61	264.18	83.22	**180.96**	1.81	120.79	-79.17	-1.46	-23.18	60	36.19	3.17	2.12	-83.22
D1.2	$DIST^{V3}-ZSPRD^{100D}_{(3,1)}$	4	2	2	144.55	46.04	289.1	92.08	**197.01**	1.97	185.53	-61.27	-0.89	-14.13	50	49.25	3.14	3.14	-92.08
D1.3	$DIST^{V3}-ZSPRD^{100D}_{(3,0.5)}$	4	3	1	102.66	61.27	307.99	61.28	**246.72**	2.47	188.32	-61.27	-0.84	-13.33	75	61.68	5.03	1.68	-61.27
D1.4	$DIST^{V3}-ZSPRD^{100D}_{(2.7,2)}$	8	6	2	53.93	41.61	323.55	83.22	**240.33**	2.4	120.79	-79.17	-2.1	-33.34	75	30.04	3.89	1.3	-83.22
D1.5	$DIST^{V3}-ZSPRD^{100D}_{(2.7,1)}$	7	4	3	96.09	31.69	384.38	95.08	**289.29**	2.89	185.53	-61.27	-1.29	-20.48	57.14	41.32	4.04	3.03	-92.08
D1.6	$DIST^{V3}-ZSPRD^{100D}_{(2.7,0.5)}$	7	6	1	84.76	61.27	508.56	61.28	**447.28**	4.47	188.32	-61.27	-1.09	-17.3	85.71	63.89	8.3	1.38	-61.27
D2.1	$DIST^{V3}-SPRD^{100D}-SMA_{(10,20)}$	18	7	11	59.41	106.52	415.88	1171.73	**-755.86**	-7.56	162.32	-271.34	-1.83	-29.05	38.89	-41.99	0.35	0.56	-999.76
D2.2	$DIST^{V3}-SPRD^{100D}-EMA_{(10,20)}$	31	10	21	90.77	98.26	907.66	2063.5	**-1155.85**	-11.56	226.97	-341.95	-1.63	-25.88	32.26	-37.28	0.44	0.92	-1083.52
D2.3	$DIST^{V3}-SPRD^{100D}-MACD_{(12,26,9)}$	33	13	20	98.8	59.87	1284.42	1197.32	**87.09**	0.87	271.81	-200.29	-1.42	-22.54	39.39	2.63	1.07	1.65	-473.3
D2.4	$DIST^{V3}-SPRD^{100D}-RSI_{(14)}$	3	1	2	46.88	207.84	46.88	415.68	**-368.8**	-3.69	46.88	-261.13	-1.76	-27.94	33.33	-122.94	0.11	0.23	-154.54
D2.5	$DIST^{V3}-SPRD^{100D}-BB_{(20)}$	20	11	9	101.15	44.07	1112.64	396.63	**716**	7.16	429.56	-139.26	-0.99	-15.72	55	35.8	2.81	2.3	-192.23
D3	$DIST^{V3}-SPRD^{100D}-DECTREE$	302	170	132	27.53	28.17	4680.23	3718.26	**961.97**	9.62	148.85	-140.72	-3.87	-61.43	56.29	3.18	1.26	0.98	-505.03
D4	$DIST^{V3}-SPRD^{100D}-MLP$	218	118	100	26.3	28.33	3103.8	2832.68	**271.12**	2.71	182.25	-141.37	-3.91	-62.07	54.13	1.24	1.1	0.93	-857.11
Part V: Models derived using the spread obtained from $DIST^{V4}-SPRD^{100D}$																			
E1.1	$DIST^{V4}-ZSPRD^{100D}_{(3,2)}$	5	3	2	88.06	41.61	264.18	83.22	**180.96**	1.81	120.79	-79.17	-1.46	-23.18	60	36.19	3.17	2.12	-83.22
E1.2	$DIST^{V4}-ZSPRD^{100D}_{(3,1)}$	4	2	2	144.55	46.04	289.1	92.08	**197.01**	1.97	185.53	-61.27	-0.89	-14.13	50	49.25	3.14	3.14	-92.08
E1.3	$DIST^{V4}-ZSPRD^{100D}_{(3,0.5)}$	4	3	1	102.66	61.27	307.99	61.28	**246.72**	2.47	188.32	-61.27	-0.84	-13.33	75	61.68	5.03	1.68	-61.27
E1.4	$DIST^{V4}-ZSPRD^{100D}_{(2.7,2)}$	8	6	2	53.93	41.61	323.55	83.22	**240.33**	2.4	120.79	-79.17	-2.1	-33.34	75	30.04	3.89	1.3	-83.22
E1.5	$DIST^{V4}-ZSPRD^{100D}_{(2.7,1)}$	7	4	3	96.09	31.69	384.38	95.08	**289.29**	2.89	185.53	-61.27	-1.29	-20.48	57.14	41.32	4.04	3.03	-92.08
E1.6	$DIST^{V4}-ZSPRD^{100D}_{(2.7,0.5)}$	7	6	1	84.76	61.27	508.56	61.28	**447.28**	4.47	188.32	-61.27	-1.09	-17.3	85.71	63.89	8.3	1.38	-61.27
E2.1	$DIST^{V4}-SPRD^{100D}-SMA_{(10,20)}$	18	7	11	59.41	106.52	415.88	1171.73	**-755.86**	-7.56	162.32	-271.34	-1.83	-29.05	38.89	-41.99	0.35	0.56	-999.76
E2.2	$DIST^{V4}-SPRD^{100D}-EMA_{(10,20)}$	31	10	21	90.77	98.26	907.66	2063.5	**-1155.85**	-11.56	226.97	-341.95	-1.63	-25.88	32.26	-37.28	0.44	0.92	-1083.52
E2.3	$DIST^{V4}-SPRD^{100D}-MACD_{(12,26,9)}$	33	13	20	98.8	59.87	1284.42	1197.32	**87.09**	0.87	271.81	-200.29	-1.42	-22.54	39.39	2.63	1.07	1.65	-473.3
E2.4	$DIST^{V4}-SPRD^{100D}-RSI_{(14)}$	3	1	2	46.88	207.84	46.88	415.68	**-368.8**	-3.69	46.88	-261.13	-1.76	-27.94	33.33	-122.94	0.11	0.23	-154.54
E2.5	$DIST^{V4}-SPRD^{100D}-BB_{(20)}$	20	11	9	101.15	44.07	1112.64	396.63	**716**	7.16	429.56	-139.26	-0.99	-15.72	55	35.8	2.81	2.3	-192.23
E3	$DIST^{V4}-SPRD^{100D}-DECTREE$	300	161	139	29.02	27.44	4671.44	3814.52	**856.92**	8.57	230.66	-140.72	-3.66	-58.1	53.67	2.86	1.22	1.06	-505.42
E4	$DIST^{V4}-SPRD^{100D}-MLP$	218	118	100	26.3	28.33	3103.8	2832.68	**271.12**	2.71	182.25	-141.37	-3.91	-62.07	54.13	1.24	1.1	0.93	-857.11
Part VI: Models derived using the spread obtained from $JOHANSEN-SPRD^{100D}$																			
F1.1	$JOHANSEN-ZSPRD^{100D}_{(3,2)}$	13	6	7	277.35	42.64	1664.11	298.48	**1365.63**	13.66	1499.82	-111.65	0.09	1.43	46.15	105.04	5.58	6.5	-171.31
F1.2	$JOHANSEN-ZSPRD^{100D}_{(3,1)}$	12	5	7	348.91	60.46	1744.54	423.2	**1321.34**	13.21	1499.82	-111.65	0.11	1.75	41.67	110.13	4.12	5.77	-204.65
F1.3	$JOHANSEN-ZSPRD^{100D}_{(3,0.5)}$	11	5	6	340.83	59.07	1704.16	354.42	**1349.74**	13.5	1499.82	-111.65	0.12	1.9	45.45	122.69	4.81	5.77	-181.13
F1.4	$JOHANSEN-ZSPRD^{100D}_{(2.7,2)}$	13	7	6	255.25	46.22	1786.74	277.33	**1509.41**	15.09	1499.82	-111.65	0.04	0.63	53.85	116.12	6.44	5.52	-171.31
F1.5	$JOHANSEN-ZSPRD^{100D}_{(2.7,1)}$	13	6	7	311.19	50.76	1867.16	355.29	**1511.88**	15.12	1499.82	-111.65	0.05	0.79	46.15	116.28	5.26	6.13	-182.42
F1.6	$JOHANSEN-ZSPRD^{100D}_{(2.7,0.5)}$	12	6	6	304.46	48.57	1826.78	291.41	**1535.37**	15.35	1499.82	-111.65	0.06	0.95	50	127.95	6.27	6.27	-122.75
F2.1	$JOHANSEN-SPRD^{100D}-SMA_{(10,20)}$	18	10	8	3867.64	416.94	38676.38	3335.54	**35340.84**	353.41	34702.76	-946.2	0.28	4.44	55.56	1963.57	11.6	9.28	-1380.8
F2.2	$JOHANSEN-SPRD^{100D}-EMA_{(10,20)}$	26	12	14	870.75	864.33	10448.94	12100.66	**-1651.72**	-16.52	6409.74	-5279.43	0.09	1.43	46.15	-63.59	0.86	1.01	-7375.67
F2.3	$JOHANSEN-SPRD^{100D}-MACD_{(12,26,9)}$	26	10	16	2533.24	401.86	25332.45	6429.83	**18902.62**	189.03	21164.84	-1831.03	-0.14	-2.22	38.46	726.98	3.94	6.3	-3101.14
F2.4	$JOHANSEN-SPRD^{100D}-RSI_{(14)}$	4	1	3	2268.92	346.28	2268.92	1038.83	**1230.09**	12.3	2268.92	-866.25	-0.11	-1.75	25	307.52	2.18	6.55	-889.66
F2.5	$JOHANSEN-SPRD^{100D}-BB_{(20)}$	20	11	9	238.61	220.63	2624.7	1985.66	**639.04**	6.39	565.63	-487.43	0.08	1.27	55	31.95	1.32	1.08	-1335.53
F3	$JOHANSEN-SPRD^{100D}-DECTREE$	308	161	147	29.25	27.68	4708.48	4068.29	**640.19**	6.4	167.02	-172.1	-3.71	-58.89	52.27	2.08	1.16	1.06	-808.84
F4	$JOHANSEN-SPRD^{100D}-MLP$	195	91	104	29.62	28.57	2695.47	2970.77	**-275.3**	-2.75	130.13	-224.42	-3.57	-56.67	46.67	-1.41	0.91	1.04	-834.07
Part VII: Models derived using the spread obtained from $ADF-SPRD^{100D}$																			
G1.1	$ADF-ZSPRD^{100D}_{(3,2)}$	4	2	2	166.38	136.81	332.76	273.62	**59.14**	0.59	169.42	-204.71	-2.25	-35.72	50	14.78	1.22	1.22	-273.62
G1.2	$ADF-ZSPRD^{100D}_{(3,1)}$	2	1	1	53.19	379.81	53.19	379.81	**-326.62**	-3.27	53.19	-379.81	-2.47	-39.21	50	-163.31	0.14	0.14	-379.81
G1.3	$ADF-ZSPRD^{100D}_{(3,0.5)}$	2	1	1	102.3	435.65	102.3	435.65	**-333.35**	-3.33	102.3	-435.65	-2.01	-31.91	50	-166.67	0.23	0.23	-435.65
G1.4	$ADF-ZSPRD^{100D}_{(2.7,2)}$	7	2	5	202.12	221.15	404.24	1105.77	**-701.53**	-7.02	234.82	-632.42	-1.77	-28.1	28.57	-100.22	0.37	0.91	-1005.9
G1.5	$ADF-ZSPRD^{100D}_{(2.7,1)}$	5	1	4	53.19	337.62	53.19	1350.49	**-1297.3**	-12.97	53.19	-674.67	-2.59	-41.11	20	-259.46	0.04	0.16	-1297.3
G1.6	$ADF-ZSPRD^{100D}_{(2.7,0.5)}$	5	1	4	102.3	428.41	102.3	1713.63	**-1611.33**	-16.11	102.3	-849.2	-2.22	-35.24	20	-322.27	0.06	0.24	-1611.33
G2.1	$ADF-SPRD^{100D}-SMA_{(10,20)}$	18	15	3	157.51	76.71	2362.68	230.14	**2132.54**	21.33	421.28	-106.89	-2.69	-42.7	83.33	118.47	10.27	2.05	-156.31
G2.2	$ADF-SPRD^{100D}-EMA_{(10,20)}$	28	21	7	110.47	232.94	2319.96	1630.61	**689.35**	6.89	298.31	-703.22	-2.49	-39.53	75	24.62	1.42	0.47	-1001.18
G2.3	$ADF-SPRD^{100D}-MACD_{(12,26,9)}$	32	19	13	101.7	149.54	1932.35	1944.01	**-11.66**	-0.12	199.12	-664.73	-2.8	-44.45	59.38	-0.35	0.99	0.68	-1069.9
G2.4	$ADF-SPRD^{100D}-RSI_{(14)}$	2	1	1	355.04	51.85	355.04	51.85	**303.19**	3.03	355.04	-51.85	-0.74	-11.75	50	151.6	6.85	6.85	-51.85
G2.5	$ADF-SPRD^{100D}-BB_{(20)}$	18	7	11	59.15	93.93	414.07	1033.21	**-619.14**	-6.19	139.34	-204.58	-5.8	-92.07	38.89	-34.39	0.4	0.63	-509.69
G3	$ADF-SPRD^{100D}-DECTREE$	309	176	133	26.77	26.68	4712.29	3548.95	**1163.34**	11.63	266.87	-167.02	-3.7	-58.74	56.96	3.77	1.33	1	-448.46
G4	$ADF-SPRD^{100D}-MLP$	258	147	111	28.2	23.43	4145.38	2600.58	**1544.8**	15.45	439.49	-230.66	-3.23	-51.27	56.98	5.99	1.59	1.2	-274.46
Part VIII: Models derived using the spread obtained from $KALMAN-SPRD^{100D}$																			
H1.1	$KALMAN-ZSPRD^{100D}_{(3,2)}$	4	3	1	168.63	41.79	505.9	41.79	**464.12**	4.64	259.46	-41.79	-2.62	-41.59	75	116.03	12.11	4.04	-41.79
H1.2	$KALMAN-ZSPRD^{100D}_{(3,1)}$	4	2	2	408.68	223.08	817.37	446.16	**371.2**	3.71	658.28	-348.64	-0.87	-13.81	50	92.8	1.83	1.83	-446.16
H1.3	$KALMAN-ZSPRD^{100D}_{(3,0.5)}$	4	2	2	526.97	500.52	1053.95	1001.04	**52.91**	0.53	725.12	-800.22	-0.69	-10.95	50	13.23	1.05	1.05	-1001.04
H1.4	$KALMAN-ZSPRD^{100D}_{(2.7,2)}$	6	5	1	151.12	58.21	755.62	58.21	**697.42**	6.97	259.46	-58.21	-3.08	-48.89	83.33	116.23	12.98	2.6	-58.21
H1.5	$KALMAN-ZSPRD^{100D}_{(2.7,1)}$	5	3	2	203.21	227.07	609.63	454.13	**155.5**	1.56	272.05	-370.16	-1.82	-28.89	60	31.1	1.34	0.89	-454.13
H1.6	$KALMAN-ZSPRD^{100D}_{(2.7,0.5)}$	4	2	2	284.06	504.99	568.11	1009.99	**-441.88**	-4.42	313.48	-823.28	-1.12	-17.78	50	-110.47	0.56	0.56	-1009.99
H2.1	$KALMAN-SPRD^{100D}-SMA_{(10,20)}$	15	6	9	259.88	105.99	1559.25	953.88	**605.37**	6.05	591.62	-290.19	-1.91	-30.32	40	40.36	1.63	2.45	-486.54
H2.2	$KALMAN-SPRD^{100D}-EMA_{(10,20)}$	21	8	13	332.29	101.78	2658.31	1323.17	**1335.14**	13.35	750.42	-188.38	-1.65	-26.19	38.1	63.6	2.01	3.26	-554.36
H2.3	$KALMAN-SPRD^{100D}-MACD_{(12,26,9)}$	29	4	25	335.53	103.94	1342.12	2598.56	**-1256.44**	-12.56	990.52	-355.04	-2.32	-36.83	13.79	-43.34	0.52	3.23	-2033.56
H2.4	$KALMAN-SPRD^{100D}-RSI_{(14)}$	3	1	2	1510.46	719.8	1510.46	1439.59	**70.86**	0.71	1510.46	-1317.14	-0.31	-4.92	33.33	23.55	1.05	2.1	-1317.14
H2.5	$KALMAN-SPRD^{100D}-BB_{(20)}$	9	6	3	104.53	298.29	627.18	894.87	**-267.69**	-2.68	159.91	-774.69	-1.75	-27.78	66.67	-29.73	0.7	0.35	-836.69
H3	$KALMAN-SPRD^{100D}-DECTREE$	247	135	112	26.24	25.12	3542.43	2813.8	**728.64**	7.29	166.02	-120.79	-4.07	-64.61	54.66	2.95	1.26	1.04	-441.84
H4	$KALMAN-SPRD^{100D}-MLP$	181	103	78	24.15	26.54	2487.02	2069.98	**417.04**	4.17	166.02	-125.32	-3.93	-62.39	56.91	2.31	1.2	0.91	-326.05
Part IX: Models derived using the spread obtained from $RATIO-SPRD^{100D}$																			
I1.1	$RATIO-ZSPRD^{100D}_{(3,2)}$	1	1	-	57.91	-	57.92	-	**57.92**	0.58	57.91	-	-	-	100	57.91	57.92	57.91	-
I1.2	$RATIO-ZSPRD^{100D}_{(3,1)}$	1	1	-	112.67	-	112.66	-	**112.66**	1.13	112.67	-	-	-	100	112.67	112.66	112.67	-
I1.3	$RATIO-ZSPRD^{100D}_{(3,0.5)}$	1	1	-	165.41	-	165.41	-	**165.41**	1.65	165.41	-	-	-	100	165.41	165.41	165.41	-
I1.4	$RATIO-ZSPRD^{100D}_{(2.7,2)}$	3	3	-	30.51	-	91.54	-	**91.54**	0.92	60.35	-	-4.08	-64.77	100	30.51	91.54	30.51	-
I1.5	$RATIO-ZSPRD^{100D}_{(2.7,1)}$	3	3	-	82.83	-	248.5	-	**248.5**	2.48	173.36	-	-0.87	-13.81	100	82.83	248.5	82.83	-
I1.6	$RATIO-ZSPRD^{100D}_{(2.7,0.5)}$	3	3	-	130.07	-	390.21	-	**390.21**	3.9	178.43	-	-0.52	-8.25	100	130.07	390.21	130.07	-
I2.1	$RATIO-SPRD^{100D}-SMA_{(10,20)}$	16	9	7	64.1	147.83	576.92	1034.84	**-457.91**	-4.58	175	-488.76	-1.13	-17.94	56.25	-28.62	0.56	0.43	-474.23
I2.2	$RATIO-SPRD^{100D}-EMA_{(10,20)}$	23	9	14	55.64	112.58	500.75	1576.17	**-1075.42**	-10.75	107.77	-425.67	-1.72	-27.3	39.13	-46.76	0.32	0.49	-1002.12
I2.3	$RATIO-SPRD^{100D}-MACD_{(12,26,9)}$	38	10	28	64.25	62.13	642.45	1739.73	**-1097.28**	-10.97	252.14	-171.24	-2.44	-38.73	26.32	-28.87	0.37	1.03	-1188.88
I2.4	$RATIO-SPRD^{100D}-RSI_{(14)}$	3	1	2	59.6	458.46	59.6	916.92	**-857.32**	-8.57	59.6	-553.68	-1.39	-22.07	33.33	-285.79	0.07	0.13	-553.68
I2.5	$RATIO-SPRD^{100D}-BB_{(20)}$	18	12	6	92.72	56.68	1112.7	340.09	**772.61**	7.73	429.56	-175.71	-0.9	-14.29	66.67	42.93	3.27	1.64	-221.23
I3	$RATIO-SPRD^{100D}-DECTREE$	352	136	216	26.18	22.1	3560.32	4772.8	**-1212.48**	-12.12	190.88	-142.17	-4.55	-72.23	38.64	-3.44	0.75	1.18	-1380.97
I4	$RATIO-SPRD^{100D}-MLP$	314	121	193	26.81	23.14	3244.35	4465.91	**-1221.56**	-12.22	190.88	-112.67	-4.48	-71.12	38.54	-3.89	0.73	1.16	-1326.82
Part X: Models derived using the close price of SCHF.N																			
CLS-SYM-1.1	$CLOSE^{SCHF.N}-SMA_{(10,20)}$	20	7	13	314.26	125.66	2199.8	1633.59	**566.2**	5.66	1106.36	-575.54	-0.14	-2.22	35	28.31	1.35	2.5	-918.42
CLS-SYM-1.2	$CLOSE^{SCHF.N}-EMA_{(10,20)}$	23	8	15	331.11	93.37	2648.86	1400.61	**1248.24**	12.48	911.97	-332.73	-0.07	-1.11	34.78	54.26	1.89	3.55	-643.72
CLS-SYM-1.3	$CLOSE^{SCHF.N}-MACD_{(12,26,9)}$	30	10	20	221.35	120.16	2213.46	2403.27	**-189.81**	-1.9	1043.11	-326.35	-0.34	-5.4	33.33	-6.34	0.92	1.84	-1733.81
CLS-SYM-1.4	$CLOSE^{SCHF.N}-RSI_{(14)}$	5	2	3	617.93	304.16	1235.87	912.48	**323.39**	3.23	959.27	-697.61	-0.02	-0.32	40	64.68	1.35	2.03	-697.61
CLS-SYM-1.5	$CLOSE^{SCHF.N}-BB_{(20)}$	15	8	7	79.49	192.86	635.89	1349.99	**-714.1**	-7.14	252.09	-785.71	-0.51	-8.1	53.33	-47.62	0.47	0.41	-785.71
Part XI: Models derived using the close price of VO.N																			
CLS-SYM-2.1	$CLOSE^{VO.N}-SMA_{(10,20)}$	15	5	10	407.5	131.94	2037.52	1319.42	**718.1**	7.18	1345.66	-357.26	-0.07	-1.11	33.33	47.86	1.54	3.09	-888.12
CLS-SYM-2.2	$CLOSE^{VO.N}-EMA_{(10,20)}$	20	6	14	305.56	123.3	1833.38	1726.2	**107.17**	1.07	700.63	-218.39	-0.27	-4.29	30	5.36	1.06	2.48	-812.37
CLS-SYM-2.3	$CLOSE^{VO.N}-MACD_{(12,26,9)}$	30	12	18	235.68	119.41	2828.19	2149.34	**678.86**	6.79	1213.06	-330.07	-0.19	-3.02	40	22.63	1.32	1.97	-845.26
CLS-SYM-2.4	$CLOSE^{VO.N}-RSI_{(14)}$	5	2	3	464.59	648.69	929.17	1946.08	**-1016.91**	-10.17	781.75	-1353.4	-0.35	-5.56	40	-203.38	0.48	0.72	-1353.4
CLS-SYM-2.5	$CLOSE^{VO.N}-BB_{(20)}$	15	13	2	85.35	600.28	1109.6	1200.56	**-90.96**	-0.91	190.76	-984.33	-0.29	-4.6	86.67	-6.04	0.92	0.14	-984.33

Table D.2.16: This table presents the back-test metrics for the pair $USMV.N/XLE.N$ based on a 30-day rolling window. The table is subdivided into eleven parts, and in each of these parts, we present the back-test metrics and the trading strategies which use the spread derived from various models. In Part I, the spread is derived from the $DIST^{V1.1}$ model, in Part II from the $DIST^{V1.2}$ model, in Part III from the $DIST^{V2}$ model, in Part IV from the $DIST^{V3}$ model, in Part V from the $DIST^{V4}$ model, in Part VI from the $JOHANSEN-SPRD$ model, in Part VIII from the $ADF-SPRD$ model, in from the $DIST^{V2}$ model, in Part VIII from the $KALMAN-SPRD$ model, and in Part IX from the $RATIO-SPRD$ model. In Part X and XI, we present the back-test metrics of the trading strategies which use the close price of USMV.N, and XLE.N, respectively. All $ numbers reported below are in USD.

(I) Trading Strategy Code	(II) Model Name	(III) Total Number of Trades	(IV) Number of Winning Trades	(V) Number of Loosing Trades	(VI) Average Profit per Trade	(VII) Average Loss per Trade	(VIII) Gross Profit	(IX) Gross Loss	(X) Net Profit	(XI) ROI	(XII) Max P&L	(XIII) Min P&L	(XIV) Daily Sharpe Ratio	(XV) Annualized Sharpe Ratio	(XVI) Hit Ratio	(XVII) Expectancy	(XVIII) Profit Factor	(XIX) Realized Risk Reward Ratio	(XX) Max Drawdown
Part I: Models derived using the spread obtained from $DIST^{V1.1}-SPRD^{30D}$																			
A1.1	$DIST^{V1.1}-ZSPRD^{30D}_{(3,2)}$	5	2	3	246.57	120.57	493.13	361.72	**131.41**	1.31	349.1	-241.34	-0.55	-8.73	40	26.28	1.36	2.04	-241.34
A1.2	$DIST^{V1.1}-ZSPRD^{30D}_{(3,1)}$	5	3	2	207.92	248.2	623.75	496.4	**127.36**	1.27	394.23	-255.05	-0.45	-7.14	60	25.47	1.26	0.84	-281.55
A1.3	$DIST^{V1.1}-ZSPRD^{30D}_{(3,0.5)}$	5	3	2	241.66	366.72	724.96	733.44	**-8.48**	-0.08	285.65	-439.62	-0.45	-7.14	60	-1.7	0.99	0.66	-485.57
A1.4	$DIST^{V1.1}-ZSPRD^{30D}_{(2.7,2)}$	10	6	4	179.71	120.35	1078.23	481.39	**596.84**	5.97	349.1	-241.34	-0.47	-7.46	60	59.68	2.24	1.49	-332.49
A1.5	$DIST^{V1.1}-ZSPRD^{30D}_{(2.7,1)}$	10	7	3	180.95	212.34	1266.67	637.01	**629.66**	6.3	394.23	-255.05	-0.38	-6.03	70	62.97	1.99	0.85	-255.05
A1.6	$DIST^{V1.1}-ZSPRD^{30D}_{(2.7,0.5)}$	9	5	4	582.56	227.14	2912.78	908.56	**2004.21**	20.04	1305.62	-439.62	0.13	2.06	55.56	222.73	3.21	2.56	-439.62
A2.1	$DIST^{V1.1}-SPRD^{30D}-SMA_{(10,20)}$	14	9	5	295.99	709.59	2663.87	3547.93	**-884.06**	-8.84	1058.68	-1208.88	-0.35	-5.56	64.29	-63.1	0.75	0.42	-2628.02
A2.2	$DIST^{V1.1}-SPRD^{30D}-EMA_{(10,20)}$	22	12	10	207.38	593.66	2488.61	5936.64	**-3448.02**	-34.48	658.13	-1409.16	-0.59	-9.37	54.55	-156.69	0.42	0.35	-3990.95
A2.3	$DIST^{V1.1}-SPRD^{30D}-MACD_{(12,26,9)}$	29	19	10	217.72	418.39	4136.72	4183.92	**-47.2**	-0.47	483.62	-1406.3	-0.37	-5.87	65.52	-1.61	0.99	0.52	-1406.3
A2.4	$DIST^{V1.1}-SPRD^{30D}-RSI_{(14)}$	5	2	3	1358.85	383.3	2717.69	1149.9	**1567.79**	15.68	2588.89	-648.17	0.12	1.9	40	313.56	2.36	3.55	-1118.6
A2.5	$DIST^{V1.1}-SPRD^{30D}-BB_{(20)}$	17	6	11	661.03	158.99	3966.15	1748.88	**2217.27**	22.17	1220.04	-517.79	-0.05	-0.79	35.29	130.39	2.27	4.16	-1072.84
A3	$DIST^{V1.1}-SPRD^{30D}-DECTREE$	324	138	186	93.13	76.68	12852.03	14263.34	**-1411.3**	-14.11	640.08	-658.13	-1.24	-19.68	42.59	-4.36	0.9	1.21	-3655.43
A4	$DIST^{V1.1}-SPRD^{30D}-MLP$	292	110	182	124.91	72.84	13739.75	13257.46	**482.3**	4.82	1007.9	-625.8	-1.02	-16.19	37.67	1.65	1.04	1.71	-2929.98
Part II: Models derived using the spread obtained from $DIST^{V1.2}-SPRD^{30D}$																			
B1.1	$DIST^{V1.2}-ZSPRD^{30D}_{(3,2)}$	5	1	4	527.47	154.48	527.47	617.93	**-90.46**	-0.9	527.47	-297	-0.54	-8.57	20	-18.09	0.85	3.41	-357.26
B1.2	$DIST^{V1.2}-ZSPRD^{30D}_{(3,1)}$	5	2	3	600.22	206.48	1200.44	619.44	**581.01**	5.81	1118.36	-373.48	-0.06	-0.95	40	116.2	1.94	2.91	-373.48
B1.3	$DIST^{V1.2}-ZSPRD^{30D}_{(3,0.5)}$	5	2	3	644.73	292.71	1289.46	878.14	**411.32**	4.11	1118.36	-448.42	-0.11	-1.75	40	82.26	1.47	2.2	-691.53
B1.4	$DIST^{V1.2}-ZSPRD^{30D}_{(2.7,2)}$	12	7	5	139.03	147.86	973.24	739.29	**233.95**	2.34	527.47	-268.1	-0.65	-10.32	58.33	19.49	1.32	0.94	-292.1
B1.5	$DIST^{V1.2}-ZSPRD^{30D}_{(2.7,1)}$	12	5	7	573.48	266.16	2867.42	1863.12	**1004.3**	10.04	1118.36	-600.81	-0.13	-2.06	41.67	83.72	1.54	2.15	-807.37
B1.6	$DIST^{V1.2}-ZSPRD^{30D}_{(2.7,0.5)}$	12	7	5	538.24	533.07	3767.66	2665.34	**1102.32**	11.02	1118.36	-982.09	-0.09	-1.43	58.33	91.82	1.41	1.01	-1484.78
B2.1	$DIST^{V1.2}-SPRD^{30D}-SMA_{(10,20)}$	18	3	15	229.24	411.24	687.72	6168.65	**-5480.93**	-54.81	413.82	-1199.47	-1.05	-16.67	16.67	-304.47	0.11	0.56	-5624.96
B2.2	$DIST^{V1.2}-SPRD^{30D}-EMA_{(10,20)}$	25	11	14	322.66	392.43	3549.25	5494.01	**-1944.76**	-19.45	811.77	-2109.17	-0.39	-6.19	44	-77.79	0.65	0.82	-3541.09
B2.3	$DIST^{V1.2}-SPRD^{30D}-MACD_{(12,26,9)}$	27	20	7	300.38	335.65	6007.51	2349.57	**3657.95**	36.58	1139.5	-614.21	-0.04	-0.63	74.07	135.45	2.56	0.89	-1265.49
B2.4	$DIST^{V1.2}-SPRD^{30D}-RSI_{(14)}$	8	4	4	969.91	756.34	3879.64	3025.36	**854.28**	8.54	1540.74	-1220.72	-0.05	-0.79	50	106.79	1.28	1.28	-2593.03
B2.5	$DIST^{V1.2}-SPRD^{30D}-BB_{(20)}$	13	6	7	245.53	295.88	1473.19	2071.15	**-597.96**	-5.98	1006.62	-799.4	-0.45	-7.14	46.15	-46.02	0.71	0.83	-1828.63
B3	$DIST^{V1.2}-SPRD^{30D}-DECTREE$	281	127	154	90.68	85.33	11516.33	13140.7	**-1624.37**	-16.24	579.3	-526.75	-1.22	-19.37	45.2	-5.77	0.88	1.06	-3082.52
B4	$DIST^{V1.2}-SPRD^{30D}-MLP$	236	121	115	102.4	114.51	12390.42	13168.25	**-777.83**	-7.78	906.07	-625.8	-0.97	-15.4	51.27	-3.3	0.94	0.89	-3261.91
Part III: Models derived using the spread obtained from $DIST^{V2}-SPRD^{30D}$																			
C1.1	$DIST^{V2}-ZSPRD^{30D}_{(3,2)}$	5	3	2	120.57	246.57	361.72	493.13	**-131.41**	-1.31	241.34	-349.1	-0.78	-12.38	60	-26.28	0.73	0.49	-349.1
C1.2	$DIST^{V2}-ZSPRD^{30D}_{(3,1)}$	5	2	3	248.2	207.92	496.4	623.75	**-127.36**	-1.27	255.05	-394.23	-0.63	-10	40	-25.47	0.8	1.19	-408.91
C1.3	$DIST^{V2}-ZSPRD^{30D}_{(3,0.5)}$	5	2	3	366.72	241.66	733.44	724.96	**8.48**	0.08	439.62	-285.65	-0.44	-6.98	40	1.7	1.01	1.52	-477.09
C1.4	$DIST^{V2}-ZSPRD^{30D}_{(2.7,2)}$	10	4	6	120.35	179.71	481.39	1078.23	**-596.84**	-5.97	241.34	-349.1	-1.07	-16.99	40	-59.68	0.45	0.67	-745.74
C1.5	$DIST^{V2}-ZSPRD^{30D}_{(2.7,1)}$	10	3	7	212.34	180.95	637.01	1266.67	**-629.66**	-6.3	255.05	-394.23	-0.93	-14.76	30	-62.97	0.5	1.17	-1025.32
C1.6	$DIST^{V2}-ZSPRD^{30D}_{(2.7,0.5)}$	9	4	5	227.14	582.56	908.56	2912.78	**-2004.21**	-20.04	439.62	-1305.62	-0.69	-10.95	44.44	-222.73	0.31	0.39	-2438.65
C2.1	$DIST^{V2}-SPRD^{30D}-SMA_{(10,20)}$	14	5	9	709.59	295.99	3547.93	2663.87	**884.06**	8.84	1208.88	-1058.68	-0.14	-2.22	35.71	63.1	1.33	2.4	-1655.69
C2.2	$DIST^{V2}-SPRD^{30D}-EMA_{(10,20)}$	22	10	12	593.66	207.38	5936.64	2488.61	**3448.02**	34.48	1409.16	-658.13	0.01	0.16	45.45	156.69	2.39	2.86	-857.67
C2.3	$DIST^{V2}-SPRD^{30D}-MACD_{(12,26,9)}$	29	10	19	418.39	217.72	4183.92	4136.72	**47.2**	0.47	1406.3	-483.62	-0.36	-5.71	34.48	1.61	1.01	1.92	-1337.4
C2.4	$DIST^{V2}-SPRD^{30D}-RSI_{(14)}$	5	3	2	383.3	1358.85	1149.9	2717.69	**-1567.79**	-15.68	648.17	-2588.89	-0.36	-5.71	60	-313.56	0.42	0.28	-2717.69
C2.5	$DIST^{V2}-SPRD^{30D}-BB_{(20)}$	17	11	6	158.99	661.03	1748.88	3966.15	**-2217.27**	-22.17	517.79	-1220.04	-0.61	-9.68	64.71	-130.39	0.44	0.24	-2737.12
C3	$DIST^{V2}-SPRD^{30D}-DECTREE$	325	126	199	94.53	76.32	11911.21	15188.54	**-3277.43**	-32.77	614.64	-526.75	-1.4	-22.22	38.77	-10.08	0.78	1.24	-4843.37
C4	$DIST^{V2}-SPRD^{30D}-MLP$	251	101	150	117.84	82.38	11902.21	12356.41	**-454.21**	-4.54	1025.32	-527.47	-1	-15.87	40.24	-1.81	0.96	1.43	-3328.8
Part IV: Models derived using the spread obtained from $DIST^{V3}-SPRD^{30D}$																			
D1.1	$DIST^{V3}-ZSPRD^{30D}_{(3,2)}$	6	6	-	92.72	-	556.32	-	**556.32**	5.56	193.51	-	-0.86	-13.65	100	92.72	556.32	92.72	-
D1.2	$DIST^{V3}-ZSPRD^{30D}_{(3,1)}$	6	4	2	135.08	599.62	540.31	1199.23	**-658.93**	-6.59	304.63	-668.73	-0.66	-10.48	66.67	-109.8	0.45	0.23	-1199.23
D1.3	$DIST^{V3}-ZSPRD^{30D}_{(3,0.5)}$	6	4	2	226.06	707.7	904.25	1415.39	**-511.14**	-5.11	337.68	-870.42	-0.48	-7.62	66.67	-85.16	0.64	0.32	-1415.39
D1.4	$DIST^{V3}-ZSPRD^{30D}_{(2.7,2)}$	12	10	2	87.38	61.33	873.76	122.66	**751.1**	7.51	193.51	-68.08	-1.15	-18.26	83.33	62.59	7.12	1.42	-68.08
D1.5	$DIST^{V3}-ZSPRD^{30D}_{(2.7,1)}$	11	8	3	126.61	664.84	1012.9	1994.51	**-981.61**	-9.82	304.63	-795.28	-0.63	-10	72.73	-89.22	0.51	0.19	-1957.25
D1.6	$DIST^{V3}-ZSPRD^{30D}_{(2.7,0.5)}$	11	8	3	293.92	611.4	2351.33	1834.21	**517.12**	5.17	1032.17	-870.42	-0.21	-3.33	72.73	47.04	1.28	0.48	-1515.8
D2.1	$DIST^{V3}-SPRD^{30D}-SMA_{(10,20)}$	18	7	11	449.03	238.7	3143.21	2625.74	**517.47**	5.17	1120.69	-699.06	-0.29	-4.6	38.89	28.76	1.2	1.88	-1852.11
D2.2	$DIST^{V3}-SPRD^{30D}-EMA_{(10,20)}$	37	12	25	668.64	241.1	8023.66	6027.44	**1996.22**	19.96	1569.48	-1256.72	-0.18	-2.86	32.43	53.93	1.33	2.77	-2509.03
D2.3	$DIST^{V3}-SPRD^{30D}-MACD_{(12,26,9)}$	39	14	25	286.35	228.13	4008.86	5703.22	**-1694.36**	-16.94	746.2	-1304.02	-0.53	-8.41	35.9	-43.43	0.7	1.26	-3216.18
D2.4	$DIST^{V3}-SPRD^{30D}-RSI_{(14)}$	4	2	2	40.88	646.43	81.76	1292.86	**-1211.11**	-12.11	50.45	-679.31	-1.14	-18.1	50	-302.78	0.06	0.06	-1242.41
D2.5	$DIST^{V3}-SPRD^{30D}-BB_{(20)}$	22	13	9	183.28	347.39	2382.6	3126.48	**-743.87**	-7.44	1029.12	-653.35	-0.51	-8.1	59.09	-33.82	0.76	0.53	-2043.13
D3	$DIST^{V3}-SPRD^{30D}-DECTREE$	330	162	168	88.77	76.39	14381.19	12832.77	**1548.41**	15.48	415.22	-483.62	-1.3	-20.64	49.09	4.69	1.12	1.16	-1777.5
D4	$DIST^{V3}-SPRD^{30D}-MLP$	265	121	144	129.39	91.52	15655.91	13179.37	**2476.54**	24.77	989.86	-992.42	-0.82	-13.02	45.66	9.34	1.19	1.41	-1416.63
Part V: Models derived using the spread obtained from $DIST^{V4}-SPRD^{30D}$																			
E1.1	$DIST^{V4}-ZSPRD^{30D}_{(3,2)}$	6	6	-	92.72	-	556.32	-	**556.32**	5.56	193.51	-	-0.86	-13.65	100	92.72	556.32	92.72	-
E1.2	$DIST^{V4}-ZSPRD^{30D}_{(3,1)}$	6	4	2	135.08	599.62	540.31	1199.23	**-658.93**	-6.59	304.63	-668.73	-0.66	-10.48	66.67	-109.8	0.45	0.23	-1199.23
E1.3	$DIST^{V4}-ZSPRD^{30D}_{(3,0.5)}$	6	4	2	226.06	707.7	904.25	1415.39	**-511.14**	-5.11	337.68	-870.42	-0.48	-7.62	66.67	-85.16	0.64	0.32	-1415.39
E1.4	$DIST^{V4}-ZSPRD^{30D}_{(2.7,2)}$	12	10	2	87.38	61.33	873.76	122.66	**751.1**	7.51	193.51	-68.08	-1.15	-18.26	83.33	62.59	7.12	1.42	-68.08
E1.5	$DIST^{V4}-ZSPRD^{30D}_{(2.7,1)}$	11	8	3	126.61	664.84	1012.9	1994.51	**-981.61**	-9.82	304.63	-795.28	-0.63	-10	72.73	-89.22	0.51	0.19	-1957.25
E1.6	$DIST^{V4}-ZSPRD^{30D}_{(2.7,0.5)}$	11	8	3	293.92	611.4	2351.33	1834.21	**517.12**	5.17	1032.17	-870.42	-0.21	-3.33	72.73	47.04	1.28	0.48	-1515.8
E2.1	$DIST^{V4}-SPRD^{30D}-SMA_{(10,20)}$	18	7	11	449.03	238.7	3143.21	2625.74	**517.47**	5.17	1120.69	-699.06	-0.29	-4.6	38.89	28.76	1.2	1.88	-1852.11
E2.2	$DIST^{V4}-SPRD^{30D}-EMA_{(10,20)}$	37	12	25	668.64	241.1	8023.66	6027.44	**1996.22**	19.96	1569.48	-1256.72	-0.18	-2.86	32.43	53.93	1.33	2.77	-2509.03
E2.3	$DIST^{V4}-SPRD^{30D}-MACD_{(12,26,9)}$	39	14	25	286.35	228.13	4008.86	5703.22	**-1694.36**	-16.94	746.2	-1304.02	-0.53	-8.41	35.9	-43.43	0.7	1.26	-3216.18
E2.4	$DIST^{V4}-SPRD^{30D}-RSI_{(14)}$	4	2	2	40.88	646.43	81.76	1292.86	**-1211.11**	-12.11	50.45	-679.31	-1.14	-18.1	50	-302.78	0.06	0.06	-1242.41
E2.5	$DIST^{V4}-SPRD^{30D}-BB_{(20)}$	22	13	9	183.28	347.39	2382.6	3126.48	**-743.87**	-7.44	1029.12	-653.35	-0.51	-8.1	59.09	-33.82	0.76	0.53	-2043.13
E3	$DIST^{V4}-SPRD^{30D}-DECTREE$	351	165	186	82.32	72.93	13582.21	13565.71	**16.5**	0.16	390.72	-483.62	-1.44	-22.86	47.01	0.05	1	1.13	-1891.19
E4	$DIST^{V4}-SPRD^{30D}-MLP$	265	121	144	129.39	91.52	15655.91	13179.37	**2476.54**	24.77	989.86	-992.42	-0.82	-13.02	45.66	9.34	1.19	1.41	-1416.63
Part VI: Models derived using the spread obtained from $JOHANSEN-SPRD^{30D}$																			
F1.1	$JOHANSEN-ZSPRD^{30D}_{(3,2)}$	22	9	13	476.27	392.57	4286.43	5103.37	**-816.94**	-8.17	2526.74	-4420.61	-0.17	-2.7	40.91	-37.13	0.84	1.21	-4498.59
F1.2	$JOHANSEN-ZSPRD^{30D}_{(3,1)}$	20	9	11	563.03	659.16	5067.26	7250.71	**-2183.45**	-21.83	2791.99	-6821.44	-0.16	-2.54	45	-109.17	0.7	0.85	-6880.07
F1.3	$JOHANSEN-ZSPRD^{30D}_{(3,0.5)}$	19	9	10	307.97	718.89	2771.71	7188.91	**-4417.2**	-44.17	2173.26	-6821.44	-0.24	-3.81	47.37	-232.47	0.39	0.43	-6885.87
F1.4	$JOHANSEN-ZSPRD^{30D}_{(2.7,2)}$	26	10	16	296.6	393.44	2965.98	6295.06	**-3329.08**	-33.29	2526.74	-4420.61	-0.27	-4.29	38.46	-128.05	0.47	0.75	-5778.75
F1.5	$JOHANSEN-ZSPRD^{30D}_{(2.7,1)}$	22	10	12	374.27	831.61	3742.66	9979.37	**-6236.72**	-62.37	2791.99	-6821.44	-0.27	-4.29	45.45	-283.54	0.38	0.45	-9591.59
F1.6	$JOHANSEN-ZSPRD^{30D}_{(2.7,0.5)}$	20	10	10	157.52	986.69	1575.16	9866.88	**-8291.71**	-82.92	765.54	-6821.44	-0.36	-5.71	50	-414.59	0.16	0.16	-9597.4
F2.1	$JOHANSEN-SPRD^{30D}-SMA_{(10,20)}$	28	16	12	359.33	4167.54	5749.32	50010.44	**-44261.13**	-442.61	1167.58	-39853.74	-0.22	-3.49	57.14	-1580.88	0.11	0.09	-46695.7
F2.2	$JOHANSEN-SPRD^{30D}-EMA_{(10,20)}$	40	22	18	815.86	1029.42	17949.02	18529.63	**-580.61**	-5.81	6821.44	-11170.21	-0.11	-1.75	55	-14.52	0.97	0.79	-12016.52
F2.3	$JOHANSEN-SPRD^{30D}-MACD_{(12,26,9)}$	35	13	22	1462.69	1866.05	19015.03	41053.15	**-22038.13**	-220.38	7229.2	-15616.47	-0.16	-2.54	37.14	-629.76	0.46	0.78	-22290.78
F2.4	$JOHANSEN-SPRD^{30D}-RSI_{(14)}$	9	5	4	8801.09	2485.05	44005.47	9940.2	**34065.26**	340.65	42305.6	-9633.7	0.27	4.29	55.56	3785.53	4.43	3.54	-9799.53
F2.5	$JOHANSEN-SPRD^{30D}-BB_{(20)}$	21	12	9	556.23	8627.88	6674.78	77650.9	**-70976.12**	-709.76	2090.53	-68021.6	-0.24	-3.81	57.14	-3380.08	0.09	0.06	-73196.74
F3	$JOHANSEN-SPRD^{30D}-DECTREE$	318	162	156	91.14	95.52	14764.49	14900.7	**-136.2**	-1.36	432.22	-864.7	-1.14	-18.1	50.94	-0.43	0.99	0.95	-2864.83
F4	$JOHANSEN-SPRD^{30D}-MLP$	310	173	137	88.09	101.95	15239.72	13967.77	**1271.95**	12.72	468.47	-515.16	-1.13	-17.94	55.81	4.11	1.09	0.86	-2297.8
Part VII: Models derived using the spread obtained from $ADF-SPRD^{30D}$																			
G1.1	$ADF-ZSPRD^{30D}_{(3,2)}$	4	4	-	455.83	-	1823.33	-	**1823.33**	18.23	1042.98	-	0.57	9.05	100	455.83	1823.33	455.83	-
G1.2	$ADF-ZSPRD^{30D}_{(3,1)}$	4	2	2	1171.4	174.54	2342.79	349.09	**1993.71**	19.94	1555.85	-183.29	0.55	8.73	50	498.43	6.71	6.71	-183.29
G1.3	$ADF-ZSPRD^{30D}_{(3,0.5)}$	4	4	-	881.19	-	3524.78	-	**3524.78**	35.25	1735.81	-	0.75	11.91	100	881.19	3524.78	881.19	-
G1.4	$ADF-ZSPRD^{30D}_{(2.7,2)}$	11	6	5	535.45	85.58	3212.68	427.9	**2784.78**	27.85	1103.98	-105.73	0.37	5.87	54.55	253.19	7.51	6.26	-260.98
G1.5	$ADF-ZSPRD^{30D}_{(2.7,1)}$	11	5	6	609.87	134.84	3049.35	809.04	**2240.31**	22.4	1555.85	-261.83	0.34	5.4	45.45	203.63	3.77	4.52	-371.59
G1.6	$ADF-ZSPRD^{30D}_{(2.7,0.5)}$	11	7	4	708.25	251.38	4957.75	1005.53	**3952.21**	39.52	1735.81	-296.86	0.41	6.51	63.64	359.33	4.93	2.82	-558.69
G2.1	$ADF-SPRD^{30D}-SMA_{(10,20)}$	23	13	10	359.1	1043.04	4668.24	10430.42	**-5762.18**	-57.62	1080.56	-5384.55	-0.12	-1.9	56.52	-250.55	0.45	0.34	-6267.54
G2.2	$ADF-SPRD^{30D}-EMA_{(10,20)}$	39	22	17	278.76	1193.6	6132.81	20291.26	**-14158.45**	-141.58	910.58	-7094.5	-0.13	-2.06	56.41	-363.04	0.3	0.23	-14795.33
G2.3	$ADF-SPRD^{30D}-MACD_{(12,26,9)}$	35	20	15	277.81	511.34	5556.14	7670.13	**-2113.99**	-21.14	1077.25	-2841.05	0.08	1.27	57.14	-60.42	0.72	0.54	-3060.39
G2.4	$ADF-SPRD^{30D}-RSI_{(14)}$	3	-	3	-	839.08	-	2517.23	**-2517.23**	-25.17	-	-1245.38	0.14	2.22	-	-839.08	-	-	-2517.23
G2.5	$ADF-SPRD^{30D}-BB_{(20)}$	19	5	14	775.61	318.02	3878.04	4452.21	**-574.17**	-5.74	2963.39	-1592.1	-0.28	-4.44	26.32	-30.17	0.87	2.44	-3601.4
G3	$ADF-SPRD^{30D}-DECTREE$	307	163	144	91.98	106.16	14992.46	15287.41	**-294.95**	-2.95	658.13	-873.21	-1.06	-16.83	53.09	-0.97	0.98	0.87	-2354.92
G4	$ADF-SPRD^{30D}-MLP$	152	76	76	122.84	144.91	9335.51	11012.98	**-1677.46**	-16.77	640.28	-1037.64	-0.78	-12.38	50	-11.04	0.85	0.85	-3222.54
Part VIII: Models derived using the spread obtained from $KALMAN-SPRD^{30D}$																			
H1.1	$KALMAN-ZSPRD^{30D}_{(3,2)}$	6	4	2	220.96	129.13	883.83	258.27	**625.56**	6.26	384.67	-156.36	-0.08	-1.27	66.67	104.27	3.42	1.71	-258.27
H1.2	$KALMAN-ZSPRD^{30D}_{(3,1)}$	6	3	3	272.56	143.49	817.67	430.46	**387.21**	3.87	425.41	-283.13	-0.22	-3.49	50	64.54	1.9	1.9	-417.39
H1.3	$KALMAN-ZSPRD^{30D}_{(3,0.5)}$	6	3	3	280.16	105.66	840.48	316.97	**523.51**	5.24	389.74	-193.2	-0.14	-2.22	50	87.25	2.65	2.65	-193.2
H1.4	$KALMAN-ZSPRD^{30D}_{(2.7,2)}$	7	3	4	332.39	123.58	997.16	494.32	**502.84**	5.03	367.69	-212.47	-0.19	-3.02	42.86	71.85	2.02	2.69	-470.74
H1.5	$KALMAN-ZSPRD^{30D}_{(2.7,1)}$	7	4	3	237.23	153.51	948.93	460.52	**488.42**	4.88	411.17	-283.13	-0.19	-3.02	57.14	69.76	2.06	1.55	-417.39
H1.6	$KALMAN-ZSPRD^{30D}_{(2.7,0.5)}$	7	4	3	244.18	115.16	976.73	345.48	**631.25**	6.31	507.49	-221.71	-0.11	-1.75	57.14	90.17	2.83	2.12	-221.71
H2.1	$KALMAN-SPRD^{30D}-SMA_{(10,20)}$	15	5	10	510.79	329.61	2553.94	3296.12	**-742.17**	-7.42	718.17	-1799.21	-0.29	-4.6	33.33	-49.51	0.77	1.55	-2438.11
H2.2	$KALMAN-SPRD^{30D}-EMA_{(10,20)}$	16	8	8	525.96	214.11	4207.64	1712.88	**2494.76**	24.95	1544.33	-418.34	0.07	1.11	50	155.92	2.46	2.46	-899.91
H2.3	$KALMAN-SPRD^{30D}-MACD_{(12,26,9)}$	26	15	11	429.49	226.12	6442.34	2487.32	**3955.03**	39.55	1122.79	-536.9	0.05	0.79	57.69	152.1	2.59	1.9	-877.36
H2.4	$KALMAN-SPRD^{30D}-RSI_{(14)}$	4	1	3	540.3	747.13	540.3	2241.4	**-1701.1**	-17.01	540.3	-1806.43	-0.56	-8.89	25	-425.27	0.24	0.72	-2241.4
H2.5	$KALMAN-SPRD^{30D}-BB_{(20)}$	12	6	6	175.67	375.91	1054	2255.44	**-1201.45**	-12.01	460.61	-783.19	-0.58	-9.21	50	-100.12	0.47	0.47	-1753.11
H3	$KALMAN-SPRD^{30D}-DECTREE$	298	155	143	93	91.5	14414.7	13084.29	**1330.41**	13.3	1061.66	-451.43	-1.06	-16.83	52.01	4.46	1.1	1.02	-2412.37
H4	$KALMAN-SPRD^{30D}-MLP$	207	109	98	108.15	120.62	11788.62	11821.07	**-32.45**	-0.32	711.29	-1058.38	-0.84	-13.33	52.66	-0.15	1	0.9	-2039.54
Part IX: Models derived using the spread obtained from $RATIO-SPRD^{30D}$																			
I1.1	$RATIO-ZSPRD^{30D}_{(3,2)}$	5	3	2	141.52	392.1	424.57	784.2	**-359.62**	-3.6	255.05	-640.17	-0.64	-10.16	60	-71.92	0.54	0.36	-640.17
I1.2	$RATIO-ZSPRD^{30D}_{(3,1)}$	5	1	4	255.05	338.89	255.05	1355.56	**-1100.51**	-11.01	255.05	-873.11	-0.89	-14.13	20	-220.1	0.19	0.75	-1355.56
I1.3	$RATIO-ZSPRD^{30D}_{(3,0.5)}$	5	1	4	293.82	316.12	293.82	1264.49	**-970.67**	-9.71	293.82	-589.06	-1.09	-17.3	20	-194.13	0.23	0.93	-1264.49
I1.4	$RATIO-ZSPRD^{30D}_{(2.7,2)}$	11	5	6	179.02	186.87	895.1	1121.24	**-226.14**	-2.26	255.05	-606.32	-0.68	-10.79	45.45	-20.58	0.8	0.96	-868.08
I1.5	$RATIO-ZSPRD^{30D}_{(2.7,1)}$	10	4	6	267.68	315.12	1070.73	1890.73	**-820**	-8.2	439.62	-873.11	-0.62	-9.84	40	-82	0.57	0.85	-1236.27
I1.6	$RATIO-ZSPRD^{30D}_{(2.7,0.5)}$	9	4	5	267.8	504.15	1071.21	2520.75	**-1449.54**	-14.5	439.62	-1305.62	-0.58	-9.21	44.44	-161.09	0.42	0.53	-1883.97
I2.1	$RATIO-SPRD^{30D}-SMA_{(10,20)}$	13	6	7	482.54	344.76	2895.22	2413.34	**481.88**	4.82	927.14	-708.39	-0.22	-3.49	46.15	37.04	1.2	1.4	-1657.69
I2.2	$RATIO-SPRD^{30D}-EMA_{(10,20)}$	18	10	8	641.63	129.9	6416.26	1039.2	**5377.06**	53.77	1571.75	-331.28	0.3	4.76	55.56	298.76	6.17	4.94	-461.47
I2.3	$RATIO-SPRD^{30D}-MACD_{(12,26,9)}$	28	14	14	338.4	178.02	4737.63	2492.31	**2245.32**	22.45	939	-638.32	-0.2	-3.17	50	80.19	1.9	1.9	-802.7
I2.4	$RATIO-SPRD^{30D}-RSI_{(14)}$	5	3	2	265.57	970.55	796.72	1941.1	**-1144.38**	-11.44	703.34	-1812.29	-0.4	-6.35	60	-228.88	0.41	0.27	-1879.02
I2.5	$RATIO-SPRD^{30D}-BB_{(20)}$	15	12	3	159.71	583.47	1916.53	1750.4	**166.13**	1.66	372.67	-1050.16	-0.39	-6.19	80	11.08	1.09	0.27	-1182.56
I3	$RATIO-SPRD^{30D}-DECTREE$	325	111	214	104.46	66.62	11594.65	14256.86	**-2662.21**	-26.62	640.08	-436.22	-1.37	-21.75	34.15	-8.2	0.81	1.57	-3852.36
I4	$RATIO-SPRD^{30D}-MLP$	275	100	175	110.99	74.41	11099.34	13022.58	**-1923.24**	-19.23	640.08	-436.22	-1.24	-19.68	36.36	-7	0.85	1.49	-3456.52
Part X: Models derived using the close price of USMV.N																			
CLS-SYM-1.1	$CLOSE^{USMV.N}-SMA_{(10,20)}$	14	5	9	226.06	114.48	1130.28	1030.32	**99.95**	1	369.68	-432.1	-0.32	-5.08	35.71	7.13	1.1	1.97	-666.67
CLS-SYM-1.2	$CLOSE^{USMV.N}-EMA_{(10,20)}$	25	8	17	180.2	153.33	1441.59	2606.67	**-1165.09**	-11.65	590.3	-737.37	-0.52	-8.25	32	-46.6	0.55	1.18	-1124.97
CLS-SYM-1.3	$CLOSE^{USMV.N}-MACD_{(12,26,9)}$	46	11	35	163.48	61.53	1798.3	2153.62	**-355.32**	-3.55	534.16	-198.94	-0.63	-10	23.91	-7.73	0.84	2.66	-1531.05
CLS-SYM-1.4	$CLOSE^{USMV.N}-RSI_{(14)}$	4	1	3	1322.93	454.26	1322.93	1362.79	**-39.86**	-0.4	1322.93	-1093.72	-0.09	-1.43	25	-9.97	0.97	2.91	-1093.72
CLS-SYM-1.5	$CLOSE^{USMV.N}-BB_{(20)}$	17	13	4	57.26	233.76	744.34	935.05	**-190.71**	-1.91	240.17	-683.01	-0.45	-7.14	76.47	-11.22	0.8	0.24	-871.88
Part XI: Models derived using the close price of XLE.N																			
CLS-SYM-2.1	$CLOSE^{XLE.N}-SMA_{(10,20)}$	19	9	10	492.93	337.96	4436.4	3379.63	**1056.77**	10.57	1969.29	-993.26	-0.03	-0.48	47.37	55.63	1.31	1.46	-2390.02
CLS-SYM-2.2	$CLOSE^{XLE.N}-EMA_{(10,20)}$	26	11	15	546.32	161.14	6009.56	2417.09	**3592.47**	35.92	2197.81	-326.2	0.12	1.9	42.31	138.19	2.49	3.39	-711.67
CLS-SYM-2.3	$CLOSE^{XLE.N}-MACD_{(12,26,9)}$	27	10	17	637.2	211.29	6372.04	3591.96	**2780.08**	27.8	1931.38	-613.01	0.05	0.79	37.04	102.99	1.77	3.02	-645.92
CLS-SYM-2.4	$CLOSE^{XLE.N}-RSI_{(14)}$	5	3	2	314.75	1213.82	944.26	2427.64	**-1483.38**	-14.83	365.04	-1229.73	-0.44	-6.98	60	-296.68	0.39	0.26	-2062.6
CLS-SYM-2.5	$CLOSE^{XLE.N}-BB_{(20)}$	20	17	3	198.62	500.07	3376.55	1500.22	**1876.33**	18.76	822.47	-1185.85	0.05	0.79	85	93.82	2.25	0.4	-1185.85

Table D.2.17: This table presents the back-test metrics for the pair $USMV.N/XLE.N$ based on a 50-day rolling window. The table is subdivided into eleven parts, and in each of these parts, we present the back-test metrics and the trading strategies which use the spread derived from various models. In Part I, the spread is derived from the $DIST^{V1.1}$ model, in Part II from the $DIST^{V1.2}$ model, in Part III from the $DIST^{V2}$ model, in Part IV from the $DIST^{V3}$ model, in Part V from the $DIST^{V4}$ model, in Part VI from the $JOHANSEN-SPRD$ model, in Part VIII from the $ADF-SPRD$ model, in from the $DIST^{V2}$ model, in Part VIII from the $KALMAN-SPRD$ model, and in Part IX from the $RATIO-SPRD$ model. In Part X and XI, we present the back-test metrics of the trading strategies which use the close price of USMV.N, and XLE.N, respectively. All $ numbers reported below are in USD.

(I) Trading Strategy Code	(II) Model Name	(III) Total Number of Trades	(IV) Number of Winning Trades	(V) Number of Loosing Trades	(VI) Average Profit per Trade	(VII) Average Loss per Trade	(VIII) Gross Profit	(IX) Gross Loss	(X) Net Profit	(XI) ROI	(XII) Max P&L	(XIII) Min P&L	(XIV) Daily Sharpe Ratio	(XV) Annualized Sharpe Ratio	(XVI) Hit Ratio	(XVII) Expectancy	(XVIII) Profit Factor	(XIX) Realized Risk Reward Ratio	(XX) Max Drawdown
Part I: Models derived using the spread obtained from $DIST^{V1.1}-SPRD^{50D}$																			
A1.1	$DIST^{V1.1}-ZSPRD^{50D}_{(3,2)}$	6	3	3	230.19	200.22	690.56	600.67	**89.89**	0.9	299.08	-392.42	-0.5	-7.94	50	14.98	1.15	1.15	-585.66
A1.2	$DIST^{V1.1}-ZSPRD^{50D}_{(3,1)}$	6	3	3	613.05	77.16	1839.14	231.5	**1607.64**	16.08	1305.62	-137.34	0.22	3.49	50	267.94	7.94	7.94	-196.99
A1.3	$DIST^{V1.1}-ZSPRD^{50D}_{(3,0.5)}$	6	3	3	554.46	147.19	1663.38	441.58	**1221.8**	12.22	1282.1	-307.35	0.09	1.43	50	203.63	3.77	3.77	-407.07
A1.4	$DIST^{V1.1}-ZSPRD^{50D}_{(2.7,2)}$	8	6	2	213.42	315.09	1280.49	630.17	**650.32**	6.5	396.35	-363.66	-0.25	-3.97	75	81.29	2.03	0.68	-630.17
A1.5	$DIST^{V1.1}-ZSPRD^{50D}_{(2.7,1)}$	8	5	3	445.43	151.04	2227.15	453.12	**1774.03**	17.74	1366.91	-313.01	0.14	2.22	62.5	221.75	4.92	2.95	-418.62
A1.6	$DIST^{V1.1}-ZSPRD^{50D}_{(2.7,0.5)}$	8	5	3	578.94	136.22	2894.71	408.67	**2486.04**	24.86	1351.01	-277.43	0.29	4.6	62.5	310.76	7.08	4.25	-374.16
A2.1	$DIST^{V1.1}-SPRD^{50D}-SMA_{(10,20)}$	14	9	5	309.1	694.85	2781.91	3474.23	**-692.32**	-6.92	1058.68	-1208.88	-0.33	-5.24	64.29	-49.41	0.8	0.44	-2554.32
A2.2	$DIST^{V1.1}-SPRD^{50D}-EMA_{(10,20)}$	22	12	10	207.19	585.93	2486.22	5859.29	**-3373.07**	-33.73	658.13	-1409.16	-0.58	-9.21	54.55	-153.29	0.42	0.35	-3990.95
A2.3	$DIST^{V1.1}-SPRD^{50D}-MACD_{(12,26,9)}$	28	17	11	232.75	385.94	3956.73	4245.32	**-288.59**	-2.89	483.62	-1406.3	-0.38	-6.03	60.71	-10.33	0.93	0.6	-1406.3
A2.4	$DIST^{V1.1}-SPRD^{50D}-RSI_{(14)}$	5	3	2	921.31	559.3	2763.94	1118.6	**1645.34**	16.45	2588.89	-648.17	0.14	2.22	60	329.07	2.47	1.65	-1118.6
A2.5	$DIST^{V1.1}-SPRD^{50D}-BB_{(20)}$	17	6	11	661.03	151.74	3966.15	1669.11	**2297.04**	22.97	1220.04	-517.79	-0.04	-0.63	35.29	135.09	2.38	4.36	-1072.84
A3	$DIST^{V1.1}-SPRD^{50D}-DECTREE$	281	120	161	94.36	75.95	11323.09	12228.28	**-905.2**	-9.05	656.46	-436.22	-1.3	-20.64	42.7	-3.23	0.93	1.24	-3016.33
A4	$DIST^{V1.1}-SPRD^{50D}-MLP$	221	93	128	129.76	69.17	12067.49	8853.35	**3214.14**	32.14	864.7	-363.66	-0.93	-14.76	42.08	14.54	1.36	1.88	-1256.56
Part II: Models derived using the spread obtained from $DIST^{V1.2}-SPRD^{50D}$																			
B1.1	$DIST^{V1.2}-ZSPRD^{50D}_{(3,2)}$	5	3	2	487.15	316.6	1461.44	633.21	**828.23**	8.28	1091.45	-632.61	0.02	0.32	60	165.65	2.31	1.54	-633.21
B1.2	$DIST^{V1.2}-ZSPRD^{50D}_{(3,1)}$	4	2	2	670.36	254.71	1340.72	509.42	**831.31**	8.31	1091.45	-347.57	0.09	1.43	50	207.83	2.63	2.63	-509.42
B1.3	$DIST^{V1.2}-ZSPRD^{50D}_{(3,0.5)}$	4	2	2	677.6	297.19	1355.19	594.38	**760.81**	7.61	1091.45	-412.71	0.06	0.95	50	190.2	2.28	2.28	-412.71
B1.4	$DIST^{V1.2}-ZSPRD^{50D}_{(2.7,2)}$	7	4	3	420.02	268.31	1680.08	804.92	**875.16**	8.75	1118.36	-632.61	-0.05	-0.79	57.14	125	2.09	1.57	-633.21
B1.5	$DIST^{V1.2}-ZSPRD^{50D}_{(2.7,1)}$	5	3	2	487.78	254.71	1463.33	509.42	**953.91**	9.54	1118.36	-347.57	0.07	1.11	60	190.78	2.87	1.92	-509.42
B1.6	$DIST^{V1.2}-ZSPRD^{50D}_{(2.7,0.5)}$	5	2	3	691.05	369.54	1382.11	1108.61	**273.5**	2.74	1118.36	-514.23	-0.15	-2.38	40	54.7	1.25	1.87	-695.9
B2.1	$DIST^{V1.2}-SPRD^{50D}-SMA_{(10,20)}$	17	9	8	357.56	437.46	3218.07	3499.69	**-281.62**	-2.82	865.34	-1369.75	-0.3	-4.76	52.94	-16.58	0.92	0.82	-1621.59
B2.2	$DIST^{V1.2}-SPRD^{50D}-EMA_{(10,20)}$	21	11	10	309.67	396.05	3406.41	3960.48	**-554.07**	-5.54	948.4	-971.96	-0.37	-5.87	52.38	-26.39	0.86	0.78	-1305.75
B2.3	$DIST^{V1.2}-SPRD^{50D}-MACD_{(12,26,9)}$	31	19	12	255.32	336	4851.01	4031.94	**819.07**	8.19	1080.08	-1088.96	-0.28	-4.44	61.29	26.42	1.2	0.76	-1992.61
B2.4	$DIST^{V1.2}-SPRD^{50D}-RSI_{(14)}$	7	3	4	848.84	874.46	2546.52	3497.84	**-951.32**	-9.51	1578.52	-1852.66	-0.25	-3.97	42.86	-135.85	0.73	0.97	-3200.32
B2.5	$DIST^{V1.2}-SPRD^{50D}-BB_{(20)}$	12	4	8	225.46	236.09	901.82	1888.76	**-986.94**	-9.87	519.35	-650.95	-0.76	-12.06	33.33	-82.26	0.48	0.95	-1626.22
B3	$DIST^{V1.2}-SPRD^{50D}-DECTREE$	278	144	134	111.19	91.57	16011.67	12271	**3740.67**	37.41	912.91	-541.2	-0.89	-14.13	51.8	13.46	1.3	1.21	-1977.15
B4	$DIST^{V1.2}-SPRD^{50D}-MLP$	220	108	112	109.43	114.1	11818.59	12779.02	**-960.43**	-9.6	994.5	-790.05	-0.91	-14.45	49.09	-4.37	0.92	0.96	-2829.76
Part III: Models derived using the spread obtained from $DIST^{V2}-SPRD^{50D}$																			
C1.1	$DIST^{V2}-ZSPRD^{50D}_{(3,2)}$	6	3	3	200.22	230.19	600.67	690.56	**-89.89**	-0.9	392.42	-299.08	-0.61	-9.68	50	-14.98	0.87	0.87	-391.48
C1.2	$DIST^{V2}-ZSPRD^{50D}_{(3,1)}$	6	3	3	77.16	613.05	231.5	1839.14	**-1607.64**	-16.08	137.34	-1305.62	-0.78	-12.38	50	-267.94	0.13	0.13	-1607.64
C1.3	$DIST^{V2}-ZSPRD^{50D}_{(3,0.5)}$	6	3	3	147.19	554.46	441.58	1663.38	**-1221.8**	-12.22	307.35	-1282.1	-0.63	-10	50	-203.63	0.27	0.27	-1447.78
C1.4	$DIST^{V2}-ZSPRD^{50D}_{(2.7,2)}$	8	2	6	315.09	213.42	630.17	1280.49	**-650.32**	-6.5	363.66	-396.35	-0.84	-13.33	25	-81.29	0.49	1.48	-773.82
C1.5	$DIST^{V2}-ZSPRD^{50D}_{(2.7,1)}$	8	3	5	151.04	445.43	453.12	2227.15	**-1774.03**	-17.74	313.01	-1366.91	-0.73	-11.59	37.5	-221.75	0.2	0.34	-1774.03
C1.6	$DIST^{V2}-ZSPRD^{50D}_{(2.7,0.5)}$	8	3	5	136.22	578.94	408.67	2894.71	**-2486.04**	-24.86	277.43	-1351.01	-0.84	-13.33	37.5	-310.76	0.14	0.24	-2486.04
C2.1	$DIST^{V2}-SPRD^{50D}-SMA_{(10,20)}$	14	5	9	694.85	309.1	3474.23	2781.91	**692.32**	6.92	1208.88	-1058.68	-0.17	-2.7	35.71	49.41	1.25	2.25	-1655.69
C2.2	$DIST^{V2}-SPRD^{50D}-EMA_{(10,20)}$	22	10	12	585.93	207.19	5859.29	2486.22	**3373.07**	33.73	1409.16	-658.13	-	-	45.45	153.29	2.36	2.83	-857.67
C2.3	$DIST^{V2}-SPRD^{50D}-MACD_{(12,26,9)}$	28	11	17	385.94	232.75	4245.32	3956.73	**288.59**	2.89	1406.3	-483.62	-0.33	-5.24	39.29	10.33	1.07	1.66	-1337.4
C2.4	$DIST^{V2}-SPRD^{50D}-RSI_{(14)}$	5	2	3	559.3	921.31	1118.6	2763.94	**-1645.34**	-16.45	648.17	-2588.89	-0.37	-5.87	40	-329.07	0.4	0.61	-2717.69
C2.5	$DIST^{V2}-SPRD^{50D}-BB_{(20)}$	17	11	6	151.74	661.03	1669.11	3966.15	**-2297.04**	-22.97	517.79	-1220.04	-0.62	-9.84	64.71	-135.09	0.42	0.23	-2737.12
C3	$DIST^{V2}-SPRD^{50D}-DECTREE$	282	111	171	83.8	79.86	9302.26	13656.45	**-4354.19**	-43.54	583.4	-436.22	-1.48	-23.49	39.36	-15.44	0.68	1.05	-5316.83
C4	$DIST^{V2}-SPRD^{50D}-MLP$	207	81	126	108.89	99.51	8819.84	12538.7	**-3718.86**	-37.19	744.48	-1631.85	-0.94	-14.92	39.13	-17.97	0.7	1.09	-5729.93
Part IV: Models derived using the spread obtained from $DIST^{V3}-SPRD^{50D}$																			
D1.1	$DIST^{V3}-ZSPRD^{50D}_{(3,2)}$	6	1	5	116.08	208.17	116.08	1040.83	**-924.76**	-9.25	116.08	-586.92	-1.27	-20.16	16.67	-154.12	0.11	0.56	-1024.74
D1.2	$DIST^{V3}-ZSPRD^{50D}_{(3,1)}$	6	1	5	158.72	302.4	158.72	1512	**-1353.27**	-13.53	158.72	-752.63	-1.21	-19.21	16.67	-225.53	0.1	0.52	-1491.9
D1.3	$DIST^{V3}-ZSPRD^{50D}_{(3,0.5)}$	6	1	5	183.66	379.69	183.66	1898.45	**-1714.79**	-17.15	183.66	-793.74	-1.28	-20.32	16.67	-285.78	0.1	0.48	-1714.79
D1.4	$DIST^{V3}-ZSPRD^{50D}_{(2.7,2)}$	12	6	6	93.72	280.18	562.32	1681.1	**-1118.78**	-11.19	200.66	-668.73	-1.01	-16.03	50	-93.23	0.33	0.33	-1162.31
D1.5	$DIST^{V3}-ZSPRD^{50D}_{(2.7,1)}$	10	2	8	143.75	325.56	287.5	2604.51	**-2317.01**	-23.17	146.89	-837.82	-1.27	-20.16	20	-231.7	0.11	0.44	-2465.31
D1.6	$DIST^{V3}-ZSPRD^{50D}_{(2.7,0.5)}$	10	2	8	156.17	373.55	312.33	2988.37	**-2676.04**	-26.76	171.72	-880.24	-1.22	-19.37	20	-267.6	0.1	0.42	-2816.65
D2.1	$DIST^{V3}-SPRD^{50D}-SMA_{(10,20)}$	14	7	7	716.82	282.17	5017.72	1975.21	**3042.51**	30.43	2103	-909.88	0.09	1.43	50	217.32	2.54	2.54	-1523.51
D2.2	$DIST^{V3}-SPRD^{50D}-EMA_{(10,20)}$	32	15	17	417.28	340.44	6259.26	5787.54	**471.72**	4.72	1283.51	-1238.39	-0.27	-4.29	46.88	14.78	1.08	1.23	-3108.1
D2.3	$DIST^{V3}-SPRD^{50D}-MACD_{(12,26,9)}$	34	14	20	352.69	248.43	4937.61	4968.54	**-30.93**	-0.31	846.3	-925.84	-0.38	-6.03	41.18	-0.89	0.99	1.42	-3576.72
D2.4	$DIST^{V3}-SPRD^{50D}-RSI_{(14)}$	7	2	5	692.31	537	1384.62	2685.02	**-1300.4**	-13	1263.17	-921.83	-0.46	-7.3	28.57	-185.79	0.52	1.29	-2638.77
D2.5	$DIST^{V3}-SPRD^{50D}-BB_{(20)}$	18	10	8	283.94	196.6	2839.37	1572.83	**1266.54**	12.67	1029.12	-341.2	-0.24	-3.81	55.56	70.38	1.81	1.44	-860.61
D3	$DIST^{V3}-SPRD^{50D}-DECTREE$	297	132	165	104.55	90.95	13800.66	15006.68	**-1206.03**	-12.06	645.39	-864.7	-1.09	-17.3	44.44	-4.07	0.92	1.15	-3621.11
D4	$DIST^{V3}-SPRD^{50D}-MLP$	247	117	130	113.13	92.36	13236.77	12006.87	**1229.9**	12.3	884.66	-872.17	-0.95	-15.08	47.37	4.98	1.1	1.22	-1874.8
Part V: Models derived using the spread obtained from $DIST^{V4}-SPRD^{50D}$																			
E1.1	$DIST^{V4}-ZSPRD^{50D}_{(3,2)}$	6	1	5	116.08	208.17	116.08	1040.83	**-924.76**	-9.25	116.08	-586.92	-1.27	-20.16	16.67	-154.12	0.11	0.56	-1024.74
E1.2	$DIST^{V4}-ZSPRD^{50D}_{(3,1)}$	6	1	5	158.72	302.4	158.72	1512	**-1353.27**	-13.53	158.72	-752.63	-1.21	-19.21	16.67	-225.53	0.1	0.52	-1491.9
E1.3	$DIST^{V4}-ZSPRD^{50D}_{(3,0.5)}$	6	1	5	183.66	379.69	183.66	1898.45	**-1714.79**	-17.15	183.66	-793.74	-1.28	-20.32	16.67	-285.78	0.1	0.48	-1714.79
E1.4	$DIST^{V4}-ZSPRD^{50D}_{(2.7,2)}$	12	6	6	93.72	280.18	562.32	1681.1	**-1118.78**	-11.19	200.66	-668.73	-1.01	-16.03	50	-93.23	0.33	0.33	-1162.31
E1.5	$DIST^{V4}-ZSPRD^{50D}_{(2.7,1)}$	10	2	8	143.75	325.56	287.5	2604.51	**-2317.01**	-23.17	146.89	-837.82	-1.27	-20.16	20	-231.7	0.11	0.44	-2465.31
E1.6	$DIST^{V4}-ZSPRD^{50D}_{(2.7,0.5)}$	10	2	8	156.17	373.55	312.33	2988.37	**-2676.04**	-26.76	171.72	-880.24	-1.22	-19.37	20	-267.6	0.1	0.42	-2816.65
E2.1	$DIST^{V4}-SPRD^{50D}-SMA_{(10,20)}$	14	7	7	716.82	282.17	5017.72	1975.21	**3042.51**	30.43	2103	-909.88	0.09	1.43	50	217.32	2.54	2.54	-1523.51
E2.2	$DIST^{V4}-SPRD^{50D}-EMA_{(10,20)}$	32	15	17	417.28	340.44	6259.26	5787.54	**471.72**	4.72	1283.51	-1238.39	-0.27	-4.29	46.88	14.78	1.08	1.23	-3108.1
E2.3	$DIST^{V4}-SPRD^{50D}-MACD_{(12,26,9)}$	34	14	20	352.69	248.43	4937.61	4968.54	**-30.93**	-0.31	846.3	-925.84	-0.38	-6.03	41.18	-0.89	0.99	1.42	-3576.72
E2.4	$DIST^{V4}-SPRD^{50D}-RSI_{(14)}$	7	2	5	692.31	537	1384.62	2685.02	**-1300.4**	-13	1263.17	-921.83	-0.46	-7.3	28.57	-185.79	0.52	1.29	-2638.77
E2.5	$DIST^{V4}-SPRD^{50D}-BB_{(20)}$	18	10	8	283.94	196.6	2839.37	1572.83	**1266.54**	12.67	1029.12	-341.2	-0.24	-3.81	55.56	70.38	1.81	1.44	-860.61
E3	$DIST^{V4}-SPRD^{50D}-DECTREE$	297	127	170	102.64	90.34	13035.5	15357.19	**-2321.69**	-23.22	645.39	-864.7	-1.14	-18.1	42.76	-7.82	0.85	1.14	-4426.59
E4	$DIST^{V4}-SPRD^{50D}-MLP$	247	117	130	113.13	92.36	13236.77	12006.87	**1229.9**	12.3	884.66	-872.17	-0.95	-15.08	47.37	4.98	1.1	1.22	-1874.8
Part VI: Models derived using the spread obtained from $JOHANSEN-SPRD^{50D}$																			
F1.1	$JOHANSEN-ZSPRD^{50D}_{(3,2)}$	19	11	8	393.94	67.87	4333.29	543	**3790.29**	37.9	3108.41	-207.56	0.28	4.44	57.89	199.47	7.98	5.8	-272.39
F1.2	$JOHANSEN-ZSPRD^{50D}_{(3,1)}$	18	9	9	631.58	61.23	5684.25	551.05	**5133.2**	51.33	3108.41	-207.56	0.33	5.24	50	285.18	10.32	10.32	-289.1
F1.3	$JOHANSEN-ZSPRD^{50D}_{(3,0.5)}$	17	7	10	904.74	64.17	6333.18	641.66	**5691.52**	56.92	3108.41	-207.56	0.35	5.56	41.18	334.83	9.87	14.1	-432.47
F1.4	$JOHANSEN-ZSPRD^{50D}_{(2.7,2)}$	22	12	10	368.9	254.46	4426.84	2544.57	**1882.27**	18.82	3108.41	-1997.89	0.01	0.16	54.55	85.59	1.74	1.45	-1997.89
F1.5	$JOHANSEN-ZSPRD^{50D}_{(2.7,1)}$	20	9	11	631.55	245.02	5683.97	2695.25	**2988.72**	29.89	3108.41	-2140.51	0.08	1.27	45	149.44	2.11	2.58	-2148.57
F1.6	$JOHANSEN-ZSPRD^{50D}_{(2.7,0.5)}$	18	8	10	619.26	64.17	4954.08	641.66	**4312.42**	43.12	3108.41	-207.56	0.31	4.92	44.44	239.55	7.72	9.65	-432.47
F2.1	$JOHANSEN-SPRD^{50D}-SMA_{(10,20)}$	20	9	11	1949.28	2750.07	17543.52	30250.74	**-12707.22**	-127.07	5539.41	-13031.84	-0.11	-1.75	45	-635.36	0.58	0.71	-13092.25
F2.2	$JOHANSEN-SPRD^{50D}-EMA_{(10,20)}$	31	15	16	1418.05	1352.81	21270.82	21645.03	**-374.21**	-3.74	13416.11	-8649.62	-	-	48.39	-11.99	0.98	1.05	-15465.67
F2.3	$JOHANSEN-SPRD^{50D}-MACD_{(12,26,9)}$	29	17	12	6727.5	1117.83	114367.58	13413.99	**100953.59**	1009.54	87009.64	-5510.93	0.22	3.49	58.62	3481.1	8.53	6.02	-5768.87
F2.4	$JOHANSEN-SPRD^{50D}-RSI_{(14)}$	7	4	3	1961.95	309.04	7847.79	927.13	**6920.66**	69.21	4092.79	-731.37	0.32	5.08	57.14	988.6	8.46	6.35	-927.13
F2.5	$JOHANSEN-SPRD^{50D}-BB_{(20)}$	24	13	11	765.87	14441.9	9956.35	158860.89	**-148904.54**	-1489.05	4818.44	-149282.93	-0.2	-3.17	54.17	-6203.85	0.06	0.05	-151973.53
F3	$JOHANSEN-SPRD^{50D}-DECTREE$	299	142	157	83.89	97.04	11912.51	15235.13	**-3322.62**	-33.23	630.64	-880.56	-1.16	-18.41	47.49	-11.12	0.78	0.86	-4215.63
F4	$JOHANSEN-SPRD^{50D}-MLP$	287	143	144	83.04	95.99	11875.26	13822.68	**-1947.43**	-19.47	393.7	-704.09	-1.19	-18.89	49.83	-6.78	0.86	0.87	-2659.82
Part VII: Models derived using the spread obtained from $ADF-SPRD^{50D}$																			
G1.1	$ADF-ZSPRD^{50D}_{(3,2)}$	4	2	2	154.27	63.31	308.54	126.62	**181.92**	1.82	293.21	-72.68	-0.85	-13.49	50	45.48	2.44	2.44	-72.68
G1.2	$ADF-ZSPRD^{50D}_{(3,1)}$	4	2	2	962.94	67.55	1925.88	135.11	**1790.77**	17.91	1911.92	-128.51	-0.61	-9.68	50	447.69	14.25	14.25	-128.51
G1.3	$ADF-ZSPRD^{50D}_{(3,0.5)}$	4	2	2	1310.49	71.16	2620.99	142.32	**2478.66**	24.79	2581.79	-128.51	-0.57	-9.05	50	619.67	18.42	18.42	-128.51
G1.4	$ADF-ZSPRD^{50D}_{(2.7,2)}$	9	4	5	249.67	424.27	998.68	2121.33	**-1122.65**	-11.23	638.96	-1407.92	-0.25	-3.97	44.44	-124.77	0.47	0.59	-1688.92
G1.5	$ADF-ZSPRD^{50D}_{(2.7,1)}$	9	5	4	600.25	1356.66	3001.23	5426.66	**-2425.42**	-24.25	1911.92	-4676.35	-0.43	-6.83	55.56	-269.4	0.55	0.44	-5118.59
G1.6	$ADF-ZSPRD^{50D}_{(2.7,0.5)}$	9	4	5	854.57	1078.23	3418.29	5391.14	**-1972.85**	-19.73	2581.79	-4654.35	-0.46	-7.3	44.44	-219.29	0.63	0.79	-4927.77
G2.1	$ADF-SPRD^{50D}-SMA_{(10,20)}$	16	8	8	350.29	746.27	2802.31	5970.16	**-3167.85**	-31.68	1147.47	-2063.12	-0.12	-1.9	50	-197.99	0.47	0.47	-4323.13
G2.2	$ADF-SPRD^{50D}-EMA_{(10,20)}$	35	23	12	494.11	669.46	11364.57	8033.56	**3331.01**	33.31	4153.17	-2665.07	0.06	0.95	65.71	95.12	1.41	0.74	-3125.57
G2.3	$ADF-SPRD^{50D}-MACD_{(12,26,9)}$	34	16	18	175.96	649.89	2815.32	11698.08	**-8882.76**	-88.83	508.37	-2581.79	-0.2	-3.17	47.06	-261.25	0.24	0.27	-8985.9
G2.4	$ADF-SPRD^{50D}-RSI_{(14)}$	4	2	2	1815.78	1509.57	3631.55	3019.14	**612.41**	6.12	1986.93	-2546.77	0.36	5.71	50	153.1	1.2	1.2	-2546.77
G2.5	$ADF-SPRD^{50D}-BB_{(20)}$	19	8	11	685.48	146.98	5483.85	1616.8	**3867.05**	38.67	3195.93	-518.14	0.15	2.38	42.11	203.57	3.39	4.66	-518.14
G3	$ADF-SPRD^{50D}-DECTREE$	277	138	139	108.59	92.02	14985.67	12791.35	**2194.32**	21.94	835.7	-739.88	-0.94	-14.92	49.82	7.92	1.17	1.18	-3134.25
G4	$ADF-SPRD^{50D}-MLP$	196	99	97	118.88	122.87	11768.87	11918.82	**-149.95**	-1.5	923.66	-625.8	-0.81	-12.86	50.51	-0.77	0.99	0.97	-4352.14
Part VIII: Models derived using the spread obtained from $KALMAN-SPRD^{50D}$																			
H1.1	$KALMAN-ZSPRD^{50D}_{(3,2)}$	6	3	3	167.96	250.09	503.89	750.28	**-246.39**	-2.46	384.65	-393.34	-0.57	-9.05	50	-41.06	0.67	0.67	-496.33
H1.2	$KALMAN-ZSPRD^{50D}_{(3,1)}$	6	1	5	178.81	459.25	178.81	2296.25	**-2117.44**	-21.17	178.81	-1283.98	-0.98	-15.56	16.67	-352.89	0.08	0.39	-2123.98
H1.3	$KALMAN-ZSPRD^{50D}_{(3,0.5)}$	6	2	4	200.62	358.7	401.24	1434.82	**-1033.58**	-10.34	267.89	-947.67	-0.72	-11.43	33.33	-172.28	0.28	0.56	-1221.5
H1.4	$KALMAN-ZSPRD^{50D}_{(2.7,2)}$	10	4	6	203.43	161.12	813.73	966.75	**-153.02**	-1.53	384.65	-393.34	-0.57	-9.05	40	-15.3	0.84	1.26	-650.92
H1.5	$KALMAN-ZSPRD^{50D}_{(2.7,1)}$	9	3	6	208.2	515.23	624.6	3091.39	**-2466.79**	-24.67	313.44	-1283.98	-0.82	-13.02	33.33	-274.11	0.2	0.4	-2466.79
H1.6	$KALMAN-ZSPRD^{50D}_{(2.7,0.5)}$	9	3	6	204.17	311.03	612.5	1866.17	**-1253.66**	-12.54	313.44	-947.67	-0.7	-11.11	33.33	-139.31	0.33	0.66	-1253.66
H2.1	$KALMAN-SPRD^{50D}-SMA_{(10,20)}$	15	9	6	452.76	433.46	4074.83	2600.78	**1474.05**	14.74	1332.14	-683.9	-0.09	-1.43	60	98.27	1.57	1.04	-1340.13
H2.2	$KALMAN-SPRD^{50D}-EMA_{(10,20)}$	28	12	16	366.68	200.13	4400.17	3202.03	**1198.14**	11.98	922.8	-490.8	-0.22	-3.49	42.86	42.81	1.37	1.83	-1668.21
H2.3	$KALMAN-SPRD^{50D}-MACD_{(12,26,9)}$	25	15	10	467.5	213.77	7012.42	2137.74	**4874.69**	48.75	1202.81	-495.32	0.15	2.38	60	194.99	3.28	2.19	-495.32
H2.4	$KALMAN-SPRD^{50D}-RSI_{(14)}$	3	2	1	667.46	2728.2	1334.92	2728.2	**-1393.28**	-13.93	1136.38	-2728.2	-0.23	-3.65	66.67	-464.31	0.49	0.24	-2728.2
H2.5	$KALMAN-SPRD^{50D}-BB_{(20)}$	13	8	5	271.19	277.6	2169.52	1388	**781.52**	7.82	750.23	-724.32	-0.14	-2.22	61.54	60.13	1.56	0.98	-724.32
H3	$KALMAN-SPRD^{50D}-DECTREE$	260	125	135	90.03	86.42	11253.13	11666.89	**-413.76**	-4.14	636	-588.79	-1.16	-18.41	48.08	-1.59	0.96	1.04	-3444.12
H4	$KALMAN-SPRD^{50D}-MLP$	29	12	17	292.43	314	3509.16	5337.94	**-1828.77**	-18.29	660.97	-1641.03	-0.45	-7.14	41.38	-63.06	0.66	0.93	-2781.11
Part IX: Models derived using the spread obtained from $RATIO-SPRD^{50D}$																			
I1.1	$RATIO-ZSPRD^{50D}_{(3,2)}$	6	2	4	104.12	271.2	208.24	1084.79	**-876.55**	-8.77	193.24	-394.23	-1.33	-21.11	33.33	-146.1	0.19	0.38	-891.55
I1.2	$RATIO-ZSPRD^{50D}_{(3,1)}$	5	1	4	197.15	474.94	197.16	1899.74	**-1702.58**	-17.03	197.15	-1305.62	-0.86	-13.65	20	-340.52	0.1	0.42	-1702.59
I1.3	$RATIO-ZSPRD^{50D}_{(3,0.5)}$	5	2	3	67.12	536.17	134.23	1608.52	**-1474.29**	-14.74	99.72	-1275.49	-0.8	-12.7	40	-294.86	0.08	0.13	-1474.29
I1.4	$RATIO-ZSPRD^{50D}_{(2.7,2)}$	12	5	7	182.02	208.79	910.1	1461.53	**-551.43**	-5.51	363.66	-394.23	-0.84	-13.33	41.67	-45.94	0.62	0.87	-1038.45
I1.5	$RATIO-ZSPRD^{50D}_{(2.7,1)}$	9	3	6	282.91	432.72	848.72	2596.33	**-1747.61**	-17.48	408.11	-1305.62	-0.69	-10.95	33.33	-194.2	0.33	0.65	-1964.66
I1.6	$RATIO-ZSPRD^{50D}_{(2.7,0.5)}$	9	3	6	291.35	345.88	874.04	2075.3	**-1201.26**	-12.01	340.08	-1275.49	-0.59	-9.37	33.33	-133.49	0.42	0.84	-1613.92
I2.1	$RATIO-SPRD^{50D}-SMA_{(10,20)}$	13	6	7	469.65	344.76	2817.93	2413.34	**404.59**	4.05	927.14	-708.39	-0.24	-3.81	46.15	31.09	1.17	1.36	-1657.69
I2.2	$RATIO-SPRD^{50D}-EMA_{(10,20)}$	18	10	8	627.68	129.9	6276.78	1039.2	**5237.58**	52.38	1571.75	-331.28	0.28	4.44	55.56	291.01	6.04	4.83	-461.47
I2.3	$RATIO-SPRD^{50D}-MACD_{(12,26,9)}$	28	14	14	329.61	221.6	4614.57	3102.42	**1512.15**	15.12	939	-638.32	-0.26	-4.13	50	54.01	1.49	1.49	-824.92
I2.4	$RATIO-SPRD^{50D}-RSI_{(14)}$	5	2	3	382.71	653.49	765.42	1960.46	**-1195.04**	-11.95	703.34	-1785.41	-0.42	-6.67	40	-239.01	0.39	0.59	-1852.14
I2.5	$RATIO-SPRD^{50D}-BB_{(20)}$	15	12	3	159.71	583.47	1916.53	1750.4	**166.13**	1.66	372.67	-1050.16	-0.39	-6.19	80	11.08	1.09	0.27	-1182.56
I3	$RATIO-SPRD^{50D}-DECTREE$	294	105	189	97.12	68.23	10197.48	12895.94	**-2698.46**	-26.98	561.98	-359	-1.44	-22.86	35.71	-9.19	0.79	1.42	-3560.81
I4	$RATIO-SPRD^{50D}-MLP$	255	92	163	103.2	74.49	9494.07	12141.32	**-2647.25**	-26.47	536.77	-282.75	-1.39	-22.07	36.08	-10.38	0.78	1.39	-3265.45
Part X: Models derived using the close price of USMV.N																			
CLS-SYM-1.1	$CLOSE^{USMV.N}-SMA_{(10,20)}$	14	5	9	226.06	114.48	1130.28	1030.32	**99.95**	1	369.68	-432.1	-0.32	-5.08	35.71	7.13	1.1	1.97	-666.67
CLS-SYM-1.2	$CLOSE^{USMV.N}-EMA_{(10,20)}$	25	8	17	180.2	153.33	1441.59	2606.67	**-1165.09**	-11.65	590.3	-737.37	-0.52	-8.25	32	-46.6	0.55	1.18	-1124.97
CLS-SYM-1.3	$CLOSE^{USMV.N}-MACD_{(12,26,9)}$	46	11	35	163.48	61.53	1798.3	2153.62	**-355.32**	-3.55	534.16	-198.94	-0.63	-10	23.91	-7.73	0.84	2.66	-1531.05
CLS-SYM-1.4	$CLOSE^{USMV.N}-RSI_{(14)}$	4	1	3	1322.93	454.26	1322.93	1362.79	**-39.86**	-0.4	1322.93	-1093.72	-0.09	-1.43	25	-9.97	0.97	2.91	-1093.72
CLS-SYM-1.5	$CLOSE^{USMV.N}-BB_{(20)}$	17	13	4	57.26	233.76	744.34	935.05	**-190.71**	-1.91	240.17	-683.01	-0.45	-7.14	76.47	-11.22	0.8	0.24	-871.88
Part XI: Models derived using the close price of XLE.N																			
CLS-SYM-2.1	$CLOSE^{XLE.N}-SMA_{(10,20)}$	19	9	10	492.93	337.96	4436.4	3379.63	**1056.77**	10.57	1969.29	-993.26	-0.03	-0.48	47.37	55.63	1.31	1.46	-2390.02
CLS-SYM-2.2	$CLOSE^{XLE.N}-EMA_{(10,20)}$	26	11	15	546.32	161.14	6009.56	2417.09	**3592.47**	35.92	2197.81	-326.2	0.12	1.9	42.31	138.19	2.49	3.39	-711.67
CLS-SYM-2.3	$CLOSE^{XLE.N}-MACD_{(12,26,9)}$	27	10	17	637.2	211.29	6372.04	3591.96	**2780.08**	27.8	1931.38	-613.01	0.05	0.79	37.04	102.99	1.77	3.02	-645.92
CLS-SYM-2.4	$CLOSE^{XLE.N}-RSI_{(14)}$	5	3	2	314.75	1213.82	944.26	2427.64	**-1483.38**	-14.83	365.04	-1229.73	-0.44	-6.98	60	-296.68	0.39	0.26	-2062.6
CLS-SYM-2.5	$CLOSE^{XLE.N}-BB_{(20)}$	20	17	3	198.62	500.07	3376.55	1500.22	**1876.33**	18.76	822.47	-1185.85	0.05	0.79	85	93.82	2.25	0.4	-1185.85

Table D.2.18: This table presents the back-test metrics for the pair $USMV.N/XLE.N$ based on a 100-day rolling window. The table is subdivided into eleven parts, and in each of these parts, we present the back-test metrics and the trading strategies which use the spread derived from various models. In Part I, the spread is derived from the $DIST^{V1.1}$ model, in Part II from the $DIST^{V1.2}$ model, in Part III from the $DIST^{V2}$ model, in Part IV from the $DIST^{V3}$ model, in Part V from the $DIST^{V4}$ model, in Part VI from the $JOHANSEN-SPRD$ model, in Part VIII from the $ADF-SPRD$ model, in from the $DIST^{V2}$ model, in Part VIII from the $KALMAN-SPRD$ model, and in Part IX from the $RATIO-SPRD$ model. In Part X and XI, we present the back-test metrics of the trading strategies which use the close price of USMV.N, and XLE.N, respectively. All $ numbers reported below are in USD.

(I) Trading Strategy Code	(II) Model Name	(III) Total Number of Trades	(IV) Number of Winning Trades	(V) Number of Loosing Trades	(VI) Average Profit per Trade	(VII) Average Loss per Trade	(VIII) Gross Profit	(IX) Gross Loss	(X) Net Profit	(XI) ROI	(XII) Max P&L	(XIII) Min P&L	(XIV) Daily Sharpe Ratio	(XV) Annualized Sharpe Ratio	(XVI) Hit Ratio	(XVII) Expectancy	(XVIII) Profit Factor	(XIX) Realized Risk Reward Ratio	(XX) Max Drawdown
Part I: Models derived using the spread obtained from $DIST^{V1.1}-SPRD^{100D}$																			
A1.1	$DIST^{V1.1}-ZSPRD^{100D}_{(3,2)}$	3	3	-	385.13	-	1155.39	-	**1155.39**	11.55	580.91	-	1.16	18.41	100	385.13	1155.39	385.13	-
A1.2	$DIST^{V1.1}-ZSPRD^{100D}_{(3,1)}$	2	1	1	1244.75	34.51	1244.75	34.51	**1210.24**	12.1	1244.75	-34.51	0.5	7.94	50	605.12	36.07	36.07	-34.51
A1.3	$DIST^{V1.1}-ZSPRD^{100D}_{(3,0.5)}$	2	1	1	1038.07	145.18	1038.07	145.18	**892.88**	8.93	1038.07	-145.18	0.35	5.56	50	446.44	7.15	7.15	-145.18
A1.4	$DIST^{V1.1}-ZSPRD^{100D}_{(2.7,2)}$	4	3	1	385.13	208.25	1155.39	208.25	**947.14**	9.47	580.91	-208.25	0.25	3.97	75	236.78	5.55	1.85	-208.25
A1.5	$DIST^{V1.1}-ZSPRD^{100D}_{(2.7,1)}$	3	1	2	1244.75	70.93	1244.75	141.85	**1102.9**	11.03	1244.75	-107.34	0.28	4.44	33.33	367.59	8.78	17.55	-107.34
A1.6	$DIST^{V1.1}-ZSPRD^{100D}_{(2.7,0.5)}$	3	1	2	1038.07	218.61	1038.07	437.23	**600.84**	6.01	1038.07	-292.04	0.07	1.11	33.33	200.24	2.37	4.75	-292.04
A2.1	$DIST^{V1.1}-SPRD^{100D}-SMA_{(10,20)}$	12	7	5	373.56	575.51	2614.92	2877.53	**-262.62**	-2.63	1058.68	-1208.88	-0.27	-4.29	58.33	-21.92	0.91	0.65	-2421.93
A2.2	$DIST^{V1.1}-SPRD^{100D}-EMA_{(10,20)}$	24	15	9	214.66	610.35	3219.92	5493.12	**-2273.2**	-22.73	663.13	-1409.16	-0.47	-7.46	62.5	-94.72	0.59	0.35	-3990.95
A2.3	$DIST^{V1.1}-SPRD^{100D}-MACD_{(12,26,9)}$	27	17	10	230.41	419.17	3917	4191.71	**-274.71**	-2.75	483.62	-1406.3	-0.38	-6.03	62.96	-10.19	0.93	0.55	-1406.3
A2.4	$DIST^{V1.1}-SPRD^{100D}-RSI_{(14)}$	4	2	2	1644.95	559.3	3289.9	1118.6	**2171.3**	21.71	3161.09	-648.17	0.22	3.49	50	542.83	2.94	2.94	-1118.6
A2.5	$DIST^{V1.1}-SPRD^{100D}-BB_{(20)}$	15	7	8	663.74	181.37	4646.19	1450.97	**3195.22**	31.95	1220.04	-517.79	0.12	1.9	46.67	213.04	3.2	3.66	-1072.84
A3	$DIST^{V1.1}-SPRD^{100D}-DECTREE$	280	100	180	137.8	76.51	13779.61	13771.16	**8.45**	0.08	1058.38	-630.64	-0.97	-15.4	35.71	0.02	1	1.8	-2753.38
A4	$DIST^{V1.1}-SPRD^{100D}-MLP$	277	108	169	113.94	72.44	12305.07	12242.06	**63**	0.63	864.7	-499.66	-1.14	-18.1	38.99	0.23	1.01	1.57	-2299.17
Part II: Models derived using the spread obtained from $DIST^{V1.2}-SPRD^{100D}$																			
B1.1	$DIST^{V1.2}-ZSPRD^{100D}_{(3,2)}$	4	2	2	94.54	642.46	189.08	1284.93	**-1095.84**	-10.96	142	-684.87	-0.99	-15.72	50	-273.96	0.15	0.15	-1284.93
B1.2	$DIST^{V1.2}-ZSPRD^{100D}_{(3,1)}$	4	1	3	37.05	726.67	37.05	2180.01	**-2142.96**	-21.43	37.05	-1059.34	-1.19	-18.89	25	-535.74	0.02	0.05	-2180.01
B1.3	$DIST^{V1.2}-ZSPRD^{100D}_{(3,0.5)}$	4	3	1	698.55	1007.77	2095.64	1007.77	**1087.87**	10.88	1824.18	-1007.77	0.1	1.59	75	271.97	2.08	0.69	-1007.77
B1.4	$DIST^{V1.2}-ZSPRD^{100D}_{(2.7,2)}$	5	2	3	94.54	458.5	189.08	1375.49	**-1186.41**	-11.86	142	-717.26	-0.99	-15.72	40	-237.28	0.14	0.21	-1375.49
B1.5	$DIST^{V1.2}-ZSPRD^{100D}_{(2.7,1)}$	5	1	4	37.05	565.99	37.05	2263.94	**-2226.9**	-22.27	37.05	-1059.34	-1.08	-17.14	20	-445.38	0.02	0.07	-2263.94
B1.6	$DIST^{V1.2}-ZSPRD^{100D}_{(2.7,0.5)}$	5	3	2	698.55	700.59	2095.64	1401.18	**694.46**	6.94	1824.18	-1033.52	-0.01	-0.16	60	138.89	1.5	1	-1033.52
B2.1	$DIST^{V1.2}-SPRD^{100D}-SMA_{(10,20)}$	11	5	6	684.75	599.84	3423.76	3599.03	**-175.27**	-1.75	1142.81	-1606.42	-0.2	-3.17	45.45	-15.99	0.95	1.14	-2371.2
B2.2	$DIST^{V1.2}-SPRD^{100D}-EMA_{(10,20)}$	18	9	9	516.08	585	4644.68	5265.04	**-620.36**	-6.2	1449.11	-1442.49	-0.25	-3.97	50	-34.46	0.88	0.88	-3549.3
B2.3	$DIST^{V1.2}-SPRD^{100D}-MACD_{(12,26,9)}$	20	11	9	295.45	265.87	3249.94	2392.83	**857.11**	8.57	724.18	-931.6	-0.27	-4.29	55	42.86	1.36	1.11	-1380.02
B2.4	$DIST^{V1.2}-SPRD^{100D}-RSI_{(14)}$	7	4	3	844.65	1383.49	3378.58	4150.46	**-771.88**	-7.72	1712.94	-1884.75	-0.2	-3.17	57.14	-110.33	0.81	0.61	-3039.72
B2.5	$DIST^{V1.2}-SPRD^{100D}-BB_{(20)}$	15	5	10	567.79	407.57	2838.93	4075.69	**-1236.76**	-12.37	1006.62	-1148.22	-0.37	-5.87	33.33	-82.48	0.7	1.39	-1980.61
B3	$DIST^{V1.2}-SPRD^{100D}-DECTREE$	251	111	140	96.67	93.33	10730	13066.03	**-2336.04**	-23.36	506.25	-560.86	-1.27	-20.16	44.22	-9.31	0.82	1.04	-2968.49
B4	$DIST^{V1.2}-SPRD^{100D}-MLP$	172	88	84	88.23	85.96	7764.04	7220.55	**543.49**	5.43	459.81	-437.47	-1.18	-18.73	51.16	3.15	1.08	1.03	-1150.32
Part III: Models derived using the spread obtained from $DIST^{V2}-SPRD^{100D}$																			
C1.1	$DIST^{V2}-ZSPRD^{100D}_{(3,2)}$	3	-	3	-	385.13	-	1155.39	**-1155.39**	-11.55	-	-580.91	-2.68	-42.54	-	-385.13	-	-	-1155.39
C1.2	$DIST^{V2}-ZSPRD^{100D}_{(3,1)}$	2	1	1	34.51	1244.75	34.51	1244.75	**-1210.24**	-12.1	34.51	-1244.75	-0.84	-13.33	50	-605.12	0.03	0.03	-1244.75
C1.3	$DIST^{V2}-ZSPRD^{100D}_{(3,0.5)}$	2	1	1	145.18	1038.07	145.18	1038.07	**-892.88**	-8.93	145.18	-1038.07	-0.72	-11.43	50	-446.44	0.14	0.14	-1038.07
C1.4	$DIST^{V2}-ZSPRD^{100D}_{(2.7,2)}$	4	1	3	208.25	385.13	208.25	1155.39	**-947.14**	-9.47	208.25	-580.91	-1.15	-18.26	25	-236.78	0.18	0.54	-1155.39
C1.5	$DIST^{V2}-ZSPRD^{100D}_{(2.7,1)}$	3	2	1	70.93	1244.75	141.85	1244.75	**-1102.9**	-11.03	107.34	-1244.75	-0.68	-10.79	66.67	-367.59	0.11	0.06	-1244.75
C1.6	$DIST^{V2}-ZSPRD^{100D}_{(2.7,0.5)}$	3	2	1	218.61	1038.07	437.23	1038.07	**-600.84**	-6.01	292.04	-1038.07	-0.48	-7.62	66.67	-200.24	0.42	0.21	-1038.07
C2.1	$DIST^{V2}-SPRD^{100D}-SMA_{(10,20)}$	12	5	7	575.51	373.56	2877.53	2614.92	**262.62**	2.63	1208.88	-1058.68	-0.2	-3.17	41.67	21.92	1.1	1.54	-1655.69
C2.2	$DIST^{V2}-SPRD^{100D}-EMA_{(10,20)}$	24	9	15	610.35	214.66	5493.12	3219.92	**2273.2**	22.73	1409.16	-663.13	-0.11	-1.75	37.5	94.72	1.71	2.84	-970.37
C2.3	$DIST^{V2}-SPRD^{100D}-MACD_{(12,26,9)}$	27	10	17	419.17	230.41	4191.71	3917	**274.71**	2.75	1406.3	-483.62	-0.33	-5.24	37.04	10.19	1.07	1.82	-1337.4
C2.4	$DIST^{V2}-SPRD^{100D}-RSI_{(14)}$	4	2	2	559.3	1644.95	1118.6	3289.9	**-2171.3**	-21.71	648.17	-3161.09	-0.39	-6.19	50	-542.83	0.34	0.34	-128.81
C2.5	$DIST^{V2}-SPRD^{100D}-BB_{(20)}$	15	8	7	181.37	663.74	1450.97	4646.19	**-3195.22**	-31.95	517.79	-1220.04	-0.73	-11.59	53.33	-213.04	0.31	0.27	-2737.12
C3	$DIST^{V2}-SPRD^{100D}-DECTREE$	283	106	177	116.22	72.94	12319.46	12910.11	**-590.65**	-5.91	857.81	-499.66	-1.16	-18.41	37.46	-2.08	0.95	1.59	-2761.43
C4	$DIST^{V2}-SPRD^{100D}-MLP$	198	69	129	120.73	73.9	8330.37	9533.64	**-1203.27**	-12.03	818.31	-314.26	-1.2	-19.05	34.85	-6.07	0.87	1.63	-2356.3
Part IV: Models derived using the spread obtained from $DIST^{V3}-SPRD^{100D}$																			
D1.1	$DIST^{V3}-ZSPRD^{100D}_{(3,2)}$	4	2	2	167.93	294.93	335.86	589.87	**-254.01**	-2.54	188.97	-372.87	-0.78	-12.38	50	-63.5	0.57	0.57	-589.87
D1.2	$DIST^{V3}-ZSPRD^{100D}_{(3,1)}$	4	2	2	278.35	784.53	556.7	1569.06	**-1012.36**	-10.12	331.9	-839.62	-0.66	-10.48	50	-253.09	0.35	0.35	-1569.06
D1.3	$DIST^{V3}-ZSPRD^{100D}_{(3,0.5)}$	4	2	2	347.75	784.8	695.49	1569.6	**-874.11**	-8.74	470.69	-840.15	-0.56	-8.89	50	-218.53	0.44	0.44	-1569.6
D1.4	$DIST^{V3}-ZSPRD^{100D}_{(2.7,2)}$	4	2	2	105.81	353.28	211.62	706.56	**-494.94**	-4.95	146.89	-372.87	-1.03	-16.35	50	-123.74	0.3	0.3	-706.56
D1.5	$DIST^{V3}-ZSPRD^{100D}_{(2.7,1)}$	4	2	2	218.51	839.87	437.02	1679.74	**-1242.73**	-12.43	224.8	-950.3	-0.75	-11.91	50	-310.68	0.26	0.26	-1679.74
D1.6	$DIST^{V3}-ZSPRD^{100D}_{(2.7,0.5)}$	4	2	2	289.92	839.76	579.84	1679.52	**-1099.68**	-11	355.04	-950.07	-0.65	-10.32	50	-274.92	0.35	0.35	-1679.51
D2.1	$DIST^{V3}-SPRD^{100D}-SMA_{(10,20)}$	16	5	11	653.05	290.89	3265.27	3199.78	**65.49**	0.65	1182.8	-587.51	-0.28	-4.44	31.25	4.09	1.02	2.25	-1048.74
D2.2	$DIST^{V3}-SPRD^{100D}-EMA_{(10,20)}$	21	9	12	768.98	290.51	6920.8	3486.13	**3434.67**	34.35	1381.34	-711.29	0.02	0.32	42.86	163.59	1.99	2.65	-2117.66
D2.3	$DIST^{V3}-SPRD^{100D}-MACD_{(12,26,9)}$	28	11	17	410.99	267.6	4520.85	4549.16	**-28.31**	-0.28	1001.67	-1294.77	-0.33	-5.24	39.29	-0.98	0.99	1.54	-3193.01
D2.4	$DIST^{V3}-SPRD^{100D}-RSI_{(14)}$	7	4	3	686.18	1069.77	2744.72	3209.3	**-464.58**	-4.65	970.71	-1132.94	-0.23	-3.65	57.14	-66.42	0.86	0.64	-2152.88
D2.5	$DIST^{V3}-SPRD^{100D}-BB_{(20)}$	16	10	6	257.41	423.41	2574.1	2540.49	**33.62**	0.34	1004.06	-751.51	-0.33	-5.24	62.5	2.1	1.01	0.61	-751.51
D3	$DIST^{V3}-SPRD^{100D}-DECTREE$	291	137	154	111.48	94.29	15273.08	14520.98	**752.1**	7.52	645.39	-835.7	-0.96	-15.24	47.08	2.59	1.05	1.18	-2296.29
D4	$DIST^{V3}-SPRD^{100D}-MLP$	250	114	136	117.06	86.79	13345.38	11802.97	**1542.41**	15.42	890.6	-387.91	-1.01	-16.03	45.6	6.17	1.13	1.35	-3970.92
Part V: Models derived using the spread obtained from $DIST^{V4}-SPRD^{100D}$																			
E1.1	$DIST^{V4}-ZSPRD^{100D}_{(3,2)}$	4	2	2	167.93	294.93	335.86	589.87	**-254.01**	-2.54	188.97	-372.87	-0.78	-12.38	50	-63.5	0.57	0.57	-589.87
E1.2	$DIST^{V4}-ZSPRD^{100D}_{(3,1)}$	4	2	2	278.35	784.53	556.7	1569.06	**-1012.36**	-10.12	331.9	-839.62	-0.66	-10.48	50	-253.09	0.35	0.35	-1569.06
E1.3	$DIST^{V4}-ZSPRD^{100D}_{(3,0.5)}$	4	2	2	347.75	784.8	695.49	1569.6	**-874.11**	-8.74	470.69	-840.15	-0.56	-8.89	50	-218.53	0.44	0.44	-1569.6
E1.4	$DIST^{V4}-ZSPRD^{100D}_{(2.7,2)}$	4	2	2	105.81	353.28	211.62	706.56	**-494.94**	-4.95	146.89	-372.87	-1.03	-16.35	50	-123.74	0.3	0.3	-706.56
E1.5	$DIST^{V4}-ZSPRD^{100D}_{(2.7,1)}$	4	2	2	218.51	839.87	437.02	1679.74	**-1242.73**	-12.43	224.8	-950.3	-0.75	-11.91	50	-310.68	0.26	0.26	-1679.74
E1.6	$DIST^{V4}-ZSPRD^{100D}_{(2.7,0.5)}$	4	2	2	289.92	839.76	579.84	1679.52	**-1099.68**	-11	355.04	-950.07	-0.65	-10.32	50	-274.92	0.35	0.35	-1679.51
E2.1	$DIST^{V4}-SPRD^{100D}-SMA_{(10,20)}$	16	5	11	653.05	290.89	3265.27	3199.78	**65.49**	0.65	1182.8	-587.51	-0.28	-4.44	31.25	4.09	1.02	2.25	-1048.74
E2.2	$DIST^{V4}-SPRD^{100D}-EMA_{(10,20)}$	21	9	12	768.98	290.51	6920.8	3486.13	**3434.67**	34.35	1381.34	-711.29	0.02	0.32	42.86	163.59	1.99	2.65	-2117.66
E2.3	$DIST^{V4}-SPRD^{100D}-MACD_{(12,26,9)}$	28	11	17	410.99	267.6	4520.85	4549.16	**-28.31**	-0.28	1001.67	-1294.77	-0.33	-5.24	39.29	-0.98	0.99	1.54	-3193.01
E2.4	$DIST^{V4}-SPRD^{100D}-RSI_{(14)}$	7	4	3	686.18	1069.77	2744.72	3209.3	**-464.58**	-4.65	970.71	-1132.94	-0.23	-3.65	57.14	-66.42	0.86	0.64	-2152.88
E2.5	$DIST^{V4}-SPRD^{100D}-BB_{(20)}$	16	10	6	257.41	423.41	2574.1	2540.49	**33.62**	0.34	1004.06	-751.51	-0.33	-5.24	62.5	2.1	1.01	0.61	-751.51
E3	$DIST^{V4}-SPRD^{100D}-DECTREE$	288	134	154	116.53	92.53	15614.48	14249.68	**1364.8**	13.65	645.39	-842.6	-0.94	-14.92	46.53	4.74	1.1	1.26	-2251.45
E4	$DIST^{V4}-SPRD^{100D}-MLP$	250	114	136	117.06	86.79	13345.38	11802.97	**1542.41**	15.42	890.6	-387.91	-1.01	-16.03	45.6	6.17	1.13	1.35	-3970.92
Part VI: Models derived using the spread obtained from $JOHANSEN-SPRD^{100D}$																			
F1.1	$JOHANSEN-ZSPRD^{100D}_{(3,2)}$	14	10	4	103.51	428.78	1035.15	1715.14	**-679.99**	-6.8	546.84	-1022.46	-0.5	-7.94	71.43	-48.56	0.6	0.24	-1217
F1.2	$JOHANSEN-ZSPRD^{100D}_{(3,1)}$	13	9	4	159.42	311.77	1434.82	1247.1	**187.72**	1.88	546.84	-1022.46	-0.5	-7.94	69.23	14.44	1.15	0.51	-1156.94
F1.3	$JOHANSEN-ZSPRD^{100D}_{(3,0.5)}$	10	5	5	289.34	250.51	1446.72	1252.55	**194.17**	1.94	546.84	-1022.46	-0.43	-6.83	50	19.42	1.16	1.16	-1249.25
F1.4	$JOHANSEN-ZSPRD^{100D}_{(2.7,2)}$	15	10	5	103.51	348.33	1035.15	1741.64	**-706.5**	-7.06	546.84	-1022.46	-0.5	-7.94	66.67	-47.08	0.59	0.3	-1243.51
F1.5	$JOHANSEN-ZSPRD^{100D}_{(2.7,1)}$	13	9	4	159.42	311.77	1434.82	1247.1	**187.72**	1.88	546.84	-1022.46	-0.5	-7.94	69.23	14.44	1.15	0.51	-1156.94
F1.6	$JOHANSEN-ZSPRD^{100D}_{(2.7,0.5)}$	10	5	5	289.34	250.51	1446.72	1252.55	**194.17**	1.94	546.84	-1022.46	-0.43	-6.83	50	19.42	1.16	1.16	-1249.25
F2.1	$JOHANSEN-SPRD^{100D}-SMA_{(10,20)}$	16	12	4	1268.56	3113.74	15222.78	12454.97	**2767.81**	27.68	10906.72	-7067.41	-0.01	-0.16	75	172.99	1.22	0.41	-12349.33
F2.2	$JOHANSEN-SPRD^{100D}-EMA_{(10,20)}$	21	7	14	449.64	1201.95	3147.45	16827.36	**-13679.92**	-136.8	1555.53	-7614.1	-0.18	-2.86	33.33	-651.48	0.19	0.37	-14537.55
F2.3	$JOHANSEN-SPRD^{100D}-MACD_{(12,26,9)}$	31	11	20	740.76	1426.84	8148.38	28536.84	**-20388.46**	-203.88	2985.85	-18578.48	-0.19	-3.02	35.48	-657.78	0.29	0.52	-20426.23
F2.4	$JOHANSEN-SPRD^{100D}-RSI_{(14)}$	8	3	5	5453.69	586.38	16361.06	2931.88	**13429.19**	134.29	10420.23	-2087.99	0.49	7.78	37.5	1678.65	5.58	9.3	-2484.81
F2.5	$JOHANSEN-SPRD^{100D}-BB_{(20)}$	17	8	9	44193.22	1675.1	353545.75	15075.92	**338469.84**	3384.7	344648.17	-12541.14	0.24	3.81	47.06	19910.53	23.45	26.38	-12935.69
F3	$JOHANSEN-SPRD^{100D}-DECTREE$	292	156	136	88.99	89.32	13882.03	12147.23	**1734.79**	17.35	550.19	-499.66	-1.14	-18.1	53.42	5.93	1.14	1	-2486.4
F4	$JOHANSEN-SPRD^{100D}-MLP$	249	122	127	93.81	93.38	11444.66	11859.78	**-415.12**	-4.15	579.3	-1251.83	-1.04	-16.51	49	-1.66	0.96	1	-2556.19
Part VII: Models derived using the spread obtained from $ADF-SPRD^{100D}$																			
G1.1	$ADF-ZSPRD^{100D}_{(3,2)}$	3	2	1	1959.31	96.13	3918.62	96.13	**3822.49**	38.22	3610.92	-96.13	0.62	9.84	66.67	1274.23	40.76	20.38	-96.13
G1.2	$ADF-ZSPRD^{100D}_{(3,1)}$	3	2	1	2332.99	47.59	4665.98	47.59	**4618.39**	46.18	3876.55	-47.59	0.69	10.95	66.67	1539.54	98.05	49.02	-47.59
G1.3	$ADF-ZSPRD^{100D}_{(3,0.5)}$	3	2	1	2205.09	189.77	4410.18	189.76	**4220.41**	42.2	3876.55	-189.77	0.65	10.32	66.67	1406.88	23.24	11.62	-189.77
G1.4	$ADF-ZSPRD^{100D}_{(2.7,2)}$	6	3	3	1377.94	456.1	4133.83	1368.3	**2765.53**	27.66	3610.92	-760.08	0.26	4.13	50	460.92	3.02	3.02	-1272.17
G1.5	$ADF-ZSPRD^{100D}_{(2.7,1)}$	6	3	3	1642.9	688.07	4928.7	2064.21	**2864.49**	28.64	3876.55	-1444.03	0.27	4.29	50	477.42	2.39	2.39	-2016.62
G1.6	$ADF-ZSPRD^{100D}_{(2.7,0.5)}$	6	2	4	2311.95	617.46	4623.9	2469.85	**2154.06**	21.54	3876.55	-1444.03	0.24	3.81	33.33	358.91	1.87	3.74	-2091.63
G2.1	$ADF-SPRD^{100D}-SMA_{(10,20)}$	17	12	5	414.76	484.94	4977.11	2424.7	**2552.41**	25.52	1473.02	-789.43	0.1	1.59	70.59	150.16	2.05	0.86	-789.43
G2.2	$ADF-SPRD^{100D}-EMA_{(10,20)}$	31	18	13	534.36	695.29	9618.47	9038.77	**579.7**	5.8	2094.41	-3785.18	0.03	0.48	58.06	18.64	1.06	0.77	-4224.75
G2.3	$ADF-SPRD^{100D}-MACD_{(12,26,9)}$	27	12	15	262.5	619.06	3150.03	9285.96	**-6135.93**	-61.36	809.17	-3610.92	-0.23	-3.65	44.44	-227.3	0.34	0.42	-6729.51
G2.4	$ADF-SPRD^{100D}-RSI_{(14)}$	5	2	3	2417.19	611.24	4834.39	1833.73	**3000.66**	30.01	2514.26	-1315.34	0.45	7.14	40	600.13	2.64	3.95	-1794.8
G2.5	$ADF-SPRD^{100D}-BB_{(20)}$	13	5	8	1062.15	209.46	5310.78	1675.64	**3635.13**	36.35	3784.45	-391.94	0.18	2.86	38.46	279.61	3.17	5.07	-745.98
G3	$ADF-SPRD^{100D}-DECTREE$	316	139	177	93.01	89.97	12928.06	15924	**-2995.94**	-29.96	881.67	-422.9	-1.23	-19.53	43.99	-9.48	0.81	1.03	-3957.17
G4	$ADF-SPRD^{100D}-MLP$	244	95	149	121.25	86.29	11519.09	12857.88	**-1338.79**	-13.39	835.7	-372.68	-1.05	-16.67	38.93	-5.5	0.9	1.41	-3639.48
Part VIII: Models derived using the spread obtained from $KALMAN-SPRD^{100D}$																			
H1.1	$KALMAN-ZSPRD^{100D}_{(3,2)}$	2	-	2	-	638.27	-	1276.53	**-1276.53**	-12.77	-	-1082.55	-1.22	-19.37	-	-638.27	-	-	-1276.53
H1.2	$KALMAN-ZSPRD^{100D}_{(3,1)}$	2	1	1	18.9	948.37	18.9	948.37	**-929.47**	-9.29	18.9	-948.37	-0.89	-14.13	50	-464.74	0.02	0.02	-948.37
H1.3	$KALMAN-ZSPRD^{100D}_{(3,0.5)}$	2	1	1	133.03	928.4	133.03	928.4	**-795.37**	-7.95	133.03	-928.4	-0.72	-11.43	50	-397.69	0.14	0.14	-928.4
H1.4	$KALMAN-ZSPRD^{100D}_{(2.7,2)}$	4	2	2	166.82	750.94	333.65	1501.87	**-1168.23**	-11.68	254.33	-1173.39	-0.64	-10.16	50	-292.06	0.22	0.22	-1501.87
H1.5	$KALMAN-ZSPRD^{100D}_{(2.7,1)}$	4	1	3	335.38	719.17	335.38	2157.52	**-1822.13**	-18.22	335.38	-1041.64	-0.86	-13.65	25	-455.53	0.16	0.47	-2157.52
H1.6	$KALMAN-ZSPRD^{100D}_{(2.7,0.5)}$	4	1	3	492.6	526.37	492.6	1579.1	**-1086.49**	-10.86	492.6	-1021.96	-0.63	-10	25	-271.62	0.31	0.94	-1579.1
H2.1	$KALMAN-SPRD^{100D}-SMA_{(10,20)}$	12	5	7	780.07	111.56	3900.34	780.89	**3119.45**	31.19	1652.8	-336.76	0.25	3.97	41.67	259.98	4.99	6.99	-362.92
H2.2	$KALMAN-SPRD^{100D}-EMA_{(10,20)}$	22	10	12	547.6	213.59	5475.98	2563.08	**2912.89**	29.13	1634.45	-519.36	-	-	45.45	132.37	2.14	2.56	-711.52
H2.3	$KALMAN-SPRD^{100D}-MACD_{(12,26,9)}$	23	9	14	414.84	162.52	3733.6	2275.22	**1458.38**	14.58	774.07	-439.14	-0.18	-2.86	39.13	63.41	1.64	2.55	-787.2
H2.4	$KALMAN-SPRD^{100D}-RSI_{(14)}$	5	2	3	572.08	620.54	1144.16	1861.62	**-717.46**	-7.17	1043.7	-1027.32	-0.3	-4.76	40	-143.49	0.61	0.92	-1861.62
H2.5	$KALMAN-SPRD^{100D}-BB_{(20)}$	12	9	3	128.5	407.68	1156.47	1223.05	**-66.58**	-0.67	269.33	-849.2	-0.42	-6.67	75	-5.55	0.95	0.32	-849.2
H3	$KALMAN-SPRD^{100D}-DECTREE$	271	125	146	91.54	89.15	11442.36	13015.7	**-1573.34**	-15.73	568.31	-464.51	-1.24	-19.68	46.13	-5.8	0.88	1.03	-3907.41
H4	$KALMAN-SPRD^{100D}-MLP$	189	74	115	114.35	100.14	8461.79	11515.66	**-3053.87**	-30.54	646.58	-350.19	-1.19	-18.89	39.15	-16.17	0.73	1.14	-3993.73
Part IX: Models derived using the spread obtained from $RATIO-SPRD^{100D}$																			
I1.1	$RATIO-ZSPRD^{100D}_{(3,2)}$	2	-	2	-	821.13	-	1642.25	**-1642.25**	-16.42	-	-1462	-1.07	-16.99	-	-821.13	-	-	-1642.25
I1.2	$RATIO-ZSPRD^{100D}_{(3,1)}$	2	1	1	34.51	1282.1	34.51	1282.1	**-1247.6**	-12.48	34.51	-1282.1	-0.83	-13.18	50	-623.8	0.03	0.03	-1282.1
I1.3	$RATIO-ZSPRD^{100D}_{(3,0.5)}$	2	1	1	145.18	1055.62	145.18	1055.62	**-910.44**	-9.1	145.18	-1055.62	-0.72	-11.43	50	-455.22	0.14	0.14	-1055.62
I1.4	$RATIO-ZSPRD^{100D}_{(2.7,2)}$	4	2	2	292.81	889.01	585.62	1778.01	**-1192.39**	-11.92	377.37	-1462	-0.54	-8.57	50	-298.1	0.33	0.33	-1778.01
I1.5	$RATIO-ZSPRD^{100D}_{(2.7,1)}$	4	2	2	367.05	694.38	734.1	1388.76	**-654.66**	-6.55	626.76	-1282.1	-0.39	-6.19	50	-163.66	0.53	0.53	-1388.76
I1.6	$RATIO-ZSPRD^{100D}_{(2.7,0.5)}$	4	3	1	353.23	1055.62	1059.7	1055.62	**4.08**	0.04	764.87	-1055.62	-0.2	-3.17	75	1.02	1	0.33	-1055.62
I2.1	$RATIO-SPRD^{100D}-SMA_{(10,20)}$	12	6	6	353.98	405.29	2123.88	2431.72	**-307.84**	-3.08	927.14	-708.39	-0.36	-5.71	50	-25.65	0.87	0.87	-1657.69
I2.2	$RATIO-SPRD^{100D}-EMA_{(10,20)}$	18	9	9	647.69	124.55	5829.21	1120.98	**4708.23**	47.08	1571.75	-331.28	0.22	3.49	50	261.57	5.2	5.2	-461.47
I2.3	$RATIO-SPRD^{100D}-MACD_{(12,26,9)}$	25	13	12	391.52	208.83	5089.78	2505.9	**2583.88**	25.84	939	-638.32	-0.13	-2.06	52	103.36	2.03	1.87	-802.7
I2.4	$RATIO-SPRD^{100D}-RSI_{(14)}$	4	2	2	382.71	1215.43	765.42	2430.85	**-1665.43**	-16.65	703.34	-2302.04	-0.44	-6.98	50	-416.36	0.31	0.31	-128.81
I2.5	$RATIO-SPRD^{100D}-BB_{(20)}$	14	11	3	165.19	583.47	1817.06	1750.4	**66.66**	0.67	372.67	-1050.16	-0.4	-6.35	78.57	4.75	1.04	0.28	-1182.56
I3	$RATIO-SPRD^{100D}-DECTREE$	296	102	194	110.18	69.3	11238.15	13445.17	**-2207.01**	-22.07	640.08	-282.75	-1.35	-21.43	34.46	-7.46	0.84	1.59	-3028.34
I4	$RATIO-SPRD^{100D}-MLP$	216	84	132	117.71	76.27	9887.33	10067.61	**-180.28**	-1.8	640.08	-603.9	-1.16	-18.41	38.89	-0.83	0.98	1.54	-1831.53
Part X: Models derived using the close price of USMV.N																			
CLS-SYM-1.1	$CLOSE^{USMV.N}-SMA_{(10,20)}$	14	5	9	226.06	114.48	1130.28	1030.32	**99.95**	1	369.68	-432.1	-0.32	-5.08	35.71	7.13	1.1	1.97	-666.67
CLS-SYM-1.2	$CLOSE^{USMV.N}-EMA_{(10,20)}$	25	8	17	180.2	153.33	1441.59	2606.67	**-1165.09**	-11.65	590.3	-737.37	-0.52	-8.25	32	-46.6	0.55	1.18	-1124.97
CLS-SYM-1.3	$CLOSE^{USMV.N}-MACD_{(12,26,9)}$	46	11	35	163.48	61.53	1798.3	2153.62	**-355.32**	-3.55	534.16	-198.94	-0.63	-10	23.91	-7.73	0.84	2.66	-1531.05
CLS-SYM-1.4	$CLOSE^{USMV.N}-RSI_{(14)}$	4	1	3	1322.93	454.26	1322.93	1362.79	**-39.86**	-0.4	1322.93	-1093.72	-0.09	-1.43	25	-9.97	0.97	2.91	-1093.72
CLS-SYM-1.5	$CLOSE^{USMV.N}-BB_{(20)}$	17	13	4	57.26	233.76	744.34	935.05	**-190.71**	-1.91	240.17	-683.01	-0.45	-7.14	76.47	-11.22	0.8	0.24	-871.88
Part XI: Models derived using the close price of XLE.N																			
CLS-SYM-2.1	$CLOSE^{XLE.N}-SMA_{(10,20)}$	19	9	10	492.93	337.96	4436.4	3379.63	**1056.77**	10.57	1969.29	-993.26	-0.03	-0.48	47.37	55.63	1.31	1.46	-2390.02
CLS-SYM-2.2	$CLOSE^{XLE.N}-EMA_{(10,20)}$	26	11	15	546.32	161.14	6009.56	2417.09	**3592.47**	35.92	2197.81	-326.2	0.12	1.9	42.31	138.19	2.49	3.39	-711.67
CLS-SYM-2.3	$CLOSE^{XLE.N}-MACD_{(12,26,9)}$	27	10	17	637.2	211.29	6372.04	3591.96	**2780.08**	27.8	1931.38	-613.01	0.05	0.79	37.04	102.99	1.77	3.02	-645.92
CLS-SYM-2.4	$CLOSE^{XLE.N}-RSI_{(14)}$	5	3	2	314.75	1213.82	944.26	2427.64	**-1483.38**	-14.83	365.04	-1229.73	-0.44	-6.98	60	-296.68	0.39	0.26	-2062.6
CLS-SYM-2.5	$CLOSE^{XLE.N}-BB_{(20)}$	20	17	3	198.62	500.07	3376.55	1500.22	**1876.33**	18.76	822.47	-1185.85	0.05	0.79	85	93.82	2.25	0.4	-1185.85

Table D.2.19: This table presents the back-test metrics for the pair $VO.N/VXUS.N$ based on a 30-day rolling window. The table is subdivided into eleven parts, and in each of these parts, we present the back-test metrics and the trading strategies which use the spread derived from various models. In Part I, the spread is derived from the $DIST^{V1.1}$ model, in Part II from the $DIST^{V1.2}$ model, in Part III from the $DIST^{V2}$ model, in Part IV from the $DIST^{V3}$ model, in Part V from the $DIST^{V4}$ model, in Part VI from the $JOHANSEN-SPRD$ model, in Part VIII from the $ADF-SPRD$ model, in from the $DIST^{V2}$ model, in Part VIII from the $KALMAN-SPRD$ model, and in Part IX from the $RATIO-SPRD$ model. In Part X and XI, we present the back-test metrics of the trading strategies which use the close price of VO.N, and VXUS.N, respectively. All $ numbers reported below are in USD.

(I) Trading Strategy Code	(II) Model Name	(III) Total Number of Trades	(IV) Number of Winning Trades	(V) Number of Loosing Trades	(VI) Average Profit per Trade ($)	(VII) Average Loss per Trade ($)	(VIII) Gross Profit ($)	(IX) Gross Loss ($)	(X) Net Profit ($)	(XI) ROI (%)	(XII) Max P&L ($)	(XIII) Min P&L ($)	(XIV) Daily Sharpe Ratio	(XV) Annualized Sharpe Ratio	(XVI) Hit Ratio	(XVII) Expectancy	(XVIII) Profit Factor	(XIX) Realized Risk Reward Ratio	(XX) Max Drawdown ($)
Part I: Models derived using the spread obtained from $DIST^{V1.1}-SPRD^{30D}$																			
A1.1	$DIST^{V1.1}-ZSPRD^{30D}_{(3,2)}$	1	-	1	-	109.23	-	109.23	**-109.23**	-1.09	-	-109.23	-	-	-	-109.23	-	-	-109.23
A1.2	$DIST^{V1.1}-ZSPRD^{30D}_{(3,1)}$	1	1	-	117.28	-	117.28	-	**117.28**	1.17	117.28	-	-	-	100	117.28	117.28	117.28	-
A1.3	$DIST^{V1.1}-ZSPRD^{30D}_{(3,0.5)}$	1	1	-	110.89	-	110.89	-	**110.89**	1.11	110.89	-	-	-	100	110.89	110.89	110.89	-
A1.4	$DIST^{V1.1}-ZSPRD^{30D}_{(2.7,2)}$	4	-	4	-	60.45	-	241.8	**-241.8**	-2.42	-	-90.39	-8.92	-141.6	-	-60.45	-	-	-241.8
A1.5	$DIST^{V1.1}-ZSPRD^{30D}_{(2.7,1)}$	2	1	1	145.11	33.51	145.11	33.51	**111.6**	1.12	145.11	-33.51	-0.76	-12.06	50	55.8	4.33	4.33	-33.51
A1.6	$DIST^{V1.1}-ZSPRD^{30D}_{(2.7,0.5)}$	2	1	1	138.65	67.69	138.65	67.69	**70.96**	0.71	138.65	-67.69	-0.8	-12.7	50	35.48	2.05	2.05	-67.69
A2.1	$DIST^{V1.1}-SPRD^{30D}-SMA_{(10,20)}$	17	7	10	91.49	88.61	640.45	886.11	**-245.66**	-2.46	216.07	-168.73	-1.47	-23.34	41.18	-14.44	0.72	1.03	-466.55
A2.2	$DIST^{V1.1}-SPRD^{30D}-EMA_{(10,20)}$	20	11	9	56.99	92.23	626.86	830.1	**-203.24**	-2.03	159.89	-171.1	-1.75	-27.78	55	-10.16	0.76	0.62	-382.48
A2.3	$DIST^{V1.1}-SPRD^{30D}-MACD_{(12,26,9)}$	31	20	11	57.94	88.12	1158.85	969.31	**189.54**	1.9	108.8	-244.03	-1.74	-27.62	64.52	6.12	1.2	0.66	-649.89
A2.4	$DIST^{V1.1}-SPRD^{30D}-RSI_{(14)}$	3	2	1	713.67	236.17	1427.34	236.17	**1191.17**	11.91	736.97	-236.17	0.45	7.14	66.67	397.09	6.04	3.02	-236.17
A2.5	$DIST^{V1.1}-SPRD^{30D}-BB_{(20)}$	17	9	8	91.57	26.85	824.09	214.81	**609.28**	6.09	222.43	-78.92	-1.45	-23.02	52.94	35.84	3.84	3.41	-145.98
A3	$DIST^{V1.1}-SPRD^{30D}-DECTREE$	385	181	204	27.08	22.44	4900.71	4578.23	**322.48**	3.22	163.09	-133.03	-4.31	-68.42	47.01	0.84	1.07	1.21	-778.42
A4	$DIST^{V1.1}-SPRD^{30D}-MLP$	335	144	191	30.56	25.56	4400.02	4882.35	**-482.33**	-4.82	120.53	-183.49	-3.99	-63.34	42.99	-1.44	0.9	1.2	-1164.63
Part II: Models derived using the spread obtained from $DIST^{V1.2}-SPRD^{30D}$																			
B1.1	$DIST^{V1.2}-ZSPRD^{30D}_{(3,2)}$	8	5	3	27.08	19.48	135.38	58.44	**76.95**	0.77	61.44	-44.65	-4.43	-70.32	62.5	9.62	2.32	1.39	-45.09
B1.2	$DIST^{V1.2}-ZSPRD^{30D}_{(3,1)}$	8	6	2	49.22	46.55	295.33	93.1	**202.23**	2.02	92.18	-47.93	-2.4	-38.1	75	25.28	3.17	1.06	-60.74
B1.3	$DIST^{V1.2}-ZSPRD^{30D}_{(3,0.5)}$	8	4	4	53.08	40.19	212.34	160.77	**51.57**	0.52	87.26	-91.84	-2.39	-37.94	50	6.45	1.32	1.32	-91.84
B1.4	$DIST^{V1.2}-ZSPRD^{30D}_{(2.7,2)}$	10	5	5	27.08	55.82	135.38	279.09	**-143.71**	-1.44	61.44	-146.58	-2.87	-45.56	50	-14.37	0.49	0.49	-191.23
B1.5	$DIST^{V1.2}-ZSPRD^{30D}_{(2.7,1)}$	10	7	3	47.28	90.69	330.97	272.08	**58.88**	0.59	92.18	-187.96	-1.79	-28.42	70	5.89	1.22	0.52	-239.73
B1.6	$DIST^{V1.2}-ZSPRD^{30D}_{(2.7,0.5)}$	10	3	7	70.22	47.44	210.65	332.1	**-121.45**	-1.21	87.26	-127.07	-2.39	-37.94	30	-12.14	0.63	1.48	-210.45
B2.1	$DIST^{V1.2}-SPRD^{30D}-SMA_{(10,20)}$	14	2	12	153.73	87.96	307.46	1055.51	**-748.05**	-7.48	221.71	-195.41	-1.95	-30.96	14.29	-53.42	0.29	1.75	-710.07
B2.2	$DIST^{V1.2}-SPRD^{30D}-EMA_{(10,20)}$	20	7	13	110.09	147.57	770.62	1918.42	**-1147.8**	-11.48	337.9	-304.77	-1.33	-21.11	35	-57.39	0.4	0.75	-1535.42
B2.3	$DIST^{V1.2}-SPRD^{30D}-MACD_{(12,26,9)}$	25	11	14	87.74	83.66	965.15	1171.21	**-206.06**	-2.06	307.15	-201.72	-1.43	-22.7	44	-8.24	0.82	1.05	-665.5
B2.4	$DIST^{V1.2}-SPRD^{30D}-RSI_{(14)}$	11	3	8	212.85	142.65	638.55	1141.22	**-502.67**	-5.03	333.05	-374.2	-0.98	-15.56	27.27	-45.71	0.56	1.49	-1059.54
B2.5	$DIST^{V1.2}-SPRD^{30D}-BB_{(20)}$	14	10	4	88.64	45.64	886.4	182.57	**703.82**	7.04	168.06	-87.14	-1.31	-20.8	71.43	50.28	4.86	1.94	-87.14
B3	$DIST^{V1.2}-SPRD^{30D}-DECTREE$	319	171	148	28.81	22.51	4925.66	3331.04	**1594.62**	15.95	163.09	-122.88	-4.07	-64.61	53.61	5	1.48	1.28	-381.47
B4	$DIST^{V1.2}-SPRD^{30D}-MLP$	300	161	139	30.01	28.29	4831.02	3932.1	**898.92**	8.99	251.22	-174.86	-3.57	-56.67	53.67	3	1.23	1.06	-366.33
Part III: Models derived using the spread obtained from $DIST^{V2}-SPRD^{30D}$																			
C1.1	$DIST^{V2}-ZSPRD^{30D}_{(3,2)}$	1	1	-	109.23	-	109.23	-	**109.23**	1.09	109.23	-	-	-	100	109.23	109.23	109.23	-
C1.2	$DIST^{V2}-ZSPRD^{30D}_{(3,1)}$	1	-	1	-	117.28	-	117.28	**-117.28**	-1.17	-	-117.28	-	-	-	-117.28	-	-	-117.28
C1.3	$DIST^{V2}-ZSPRD^{30D}_{(3,0.5)}$	1	-	1	-	110.89	-	110.89	**-110.89**	-1.11	-	-110.89	-	-	-	-110.89	-	-	-110.89
C1.4	$DIST^{V2}-ZSPRD^{30D}_{(2.7,2)}$	4	4	-	60.45	-	241.8	-	**241.8**	2.42	90.39	-	-3.84	-60.96	100	60.45	241.8	60.45	-
C1.5	$DIST^{V2}-ZSPRD^{30D}_{(2.7,1)}$	2	1	1	33.51	145.11	33.51	145.11	**-111.6**	-1.12	33.51	-145.11	-1.65	-26.19	50	-55.8	0.23	0.23	-145.11
C1.6	$DIST^{V2}-ZSPRD^{30D}_{(2.7,0.5)}$	2	1	1	67.69	138.65	67.69	138.65	**-70.96**	-0.71	67.69	-138.65	-1.28	-20.32	50	-35.48	0.49	0.49	-138.65
C2.1	$DIST^{V2}-SPRD^{30D}-SMA_{(10,20)}$	17	10	7	88.61	91.49	886.11	640.45	**245.66**	2.46	168.73	-216.07	-1.22	-19.37	58.82	14.44	1.38	0.97	-343.07
C2.2	$DIST^{V2}-SPRD^{30D}-EMA_{(10,20)}$	20	9	11	92.23	56.99	830.1	626.86	**203.24**	2.03	171.1	-159.89	-1.53	-24.29	45	10.16	1.32	1.62	-268.45
C2.3	$DIST^{V2}-SPRD^{30D}-MACD_{(12,26,9)}$	31	11	20	88.12	57.94	969.31	1158.85	**-189.54**	-1.9	244.03	-108.8	-1.89	-30	35.48	-6.12	0.84	1.52	-728.55
C2.4	$DIST^{V2}-SPRD^{30D}-RSI_{(14)}$	3	1	2	236.17	713.67	236.17	1427.34	**-1191.17**	-11.91	236.17	-736.97	-1	-15.87	33.33	-397.09	0.17	0.33	-690.36
C2.5	$DIST^{V2}-SPRD^{30D}-BB_{(20)}$	17	8	9	26.85	91.57	214.81	824.09	**-609.28**	-6.09	78.92	-222.43	-2.34	-37.15	47.06	-35.84	0.26	0.29	-532.84
C3	$DIST^{V2}-SPRD^{30D}-DECTREE$	384	174	210	26.6	23.51	4628.68	4937.6	**-308.92**	-3.09	133.78	-133.03	-4.38	-69.53	45.31	-0.81	0.94	1.13	-972.86
C4	$DIST^{V2}-SPRD^{30D}-MLP$	353	152	201	30.58	24.56	4648.24	4936.44	**-288.19**	-2.88	240.22	-95.42	-4.06	-64.45	43.06	-0.82	0.94	1.25	-1062.18
Part IV: Models derived using the spread obtained from $DIST^{V3}-SPRD^{30D}$																			
D1.1	$DIST^{V3}-ZSPRD^{30D}_{(3,2)}$	8	6	2	36.3	61.09	217.79	122.19	**95.6**	0.96	84.26	-69.6	-2.77	-43.97	75	11.95	1.78	0.59	-69.6
D1.2	$DIST^{V3}-ZSPRD^{30D}_{(3,1)}$	8	5	3	72.38	73.85	361.92	221.55	**140.37**	1.4	97.67	-165.49	-1.51	-23.97	62.5	17.55	1.63	0.98	-165.49
D1.3	$DIST^{V3}-ZSPRD^{30D}_{(3,0.5)}$	8	5	3	79.78	75.82	398.92	227.45	**171.46**	1.71	97.67	-165.49	-1.42	-22.54	62.5	21.43	1.75	1.05	-165.49
D1.4	$DIST^{V3}-ZSPRD^{30D}_{(2.7,2)}$	13	10	3	35.07	40.78	350.74	122.33	**228.41**	2.28	84.26	-69.6	-3.25	-51.59	76.92	17.57	2.87	0.86	-69.6
D1.5	$DIST^{V3}-ZSPRD^{30D}_{(2.7,1)}$	13	9	4	67.44	59.1	607	236.42	**370.59**	3.71	107.94	-165.49	-1.64	-26.03	69.23	28.51	2.57	1.14	-165.49
D1.6	$DIST^{V3}-ZSPRD^{30D}_{(2.7,0.5)}$	12	7	5	76.48	60.59	535.35	302.98	**232.38**	2.32	107.94	-165.49	-1.63	-25.88	58.33	19.36	1.77	1.26	-165.6
D2.1	$DIST^{V3}-SPRD^{30D}-SMA_{(10,20)}$	24	9	15	77.08	80	693.74	1200.07	**-506.33**	-5.06	189.54	-225.92	-1.85	-29.37	37.5	-21.1	0.58	0.96	-768.43
D2.2	$DIST^{V3}-SPRD^{30D}-EMA_{(10,20)}$	47	17	30	95.39	56.21	1621.71	1686.41	**-64.7**	-0.65	240.87	-167.33	-1.69	-26.83	36.17	-1.38	0.96	1.7	-738.52
D2.3	$DIST^{V3}-SPRD^{30D}-MACD_{(12,26,9)}$	41	14	27	76.4	66.21	1069.64	1787.71	**-718.07**	-7.18	333.05	-201.72	-1.8	-28.57	34.15	-17.51	0.6	1.15	-1325.8
D2.4	$DIST^{V3}-SPRD^{30D}-RSI_{(14)}$	4	2	2	358.82	177.42	717.64	354.85	**362.8**	3.63	647.23	-343.8	-0.15	-2.38	50	90.7	2.02	2.02	-354.85
D2.5	$DIST^{V3}-SPRD^{30D}-BB_{(20)}$	21	15	6	64.89	79.67	973.32	478.04	**495.28**	4.95	357.65	-131.57	-1.28	-20.32	71.43	23.59	2.04	0.81	-300.67
D3	$DIST^{V3}-SPRD^{30D}-DECTREE$	344	158	186	26.14	26.68	4129.68	4961.76	**-832.07**	-8.32	135.86	-254.08	-4.11	-65.24	45.93	-2.42	0.83	0.98	-1375.83
D4	$DIST^{V3}-SPRD^{30D}-MLP$	218	91	127	31.18	28.99	2837.82	3681.78	**-843.96**	-8.44	212.18	-140.79	-3.62	-57.47	41.74	-3.87	0.77	1.08	-1168.93
Part V: Models derived using the spread obtained from $DIST^{V4}-SPRD^{30D}$																			
E1.1	$DIST^{V4}-ZSPRD^{30D}_{(3,2)}$	8	6	2	36.3	61.09	217.79	122.19	**95.6**	0.96	84.26	-69.6	-2.77	-43.97	75	11.95	1.78	0.59	-69.6
E1.2	$DIST^{V4}-ZSPRD^{30D}_{(3,1)}$	8	5	3	72.38	73.85	361.92	221.55	**140.37**	1.4	97.67	-165.49	-1.51	-23.97	62.5	17.55	1.63	0.98	-165.49
E1.3	$DIST^{V4}-ZSPRD^{30D}_{(3,0.5)}$	8	5	3	79.78	75.82	398.92	227.45	**171.46**	1.71	97.67	-165.49	-1.42	-22.54	62.5	21.43	1.75	1.05	-165.49
E1.4	$DIST^{V4}-ZSPRD^{30D}_{(2.7,2)}$	13	10	3	35.07	40.78	350.74	122.33	**228.41**	2.28	84.26	-69.6	-3.25	-51.59	76.92	17.57	2.87	0.86	-69.6
E1.5	$DIST^{V4}-ZSPRD^{30D}_{(2.7,1)}$	13	9	4	67.44	59.1	607	236.42	**370.59**	3.71	107.94	-165.49	-1.64	-26.03	69.23	28.51	2.57	1.14	-165.49
E1.6	$DIST^{V4}-ZSPRD^{30D}_{(2.7,0.5)}$	12	7	5	76.48	60.59	535.35	302.98	**232.38**	2.32	107.94	-165.49	-1.63	-25.88	58.33	19.36	1.77	1.26	-165.6
E2.1	$DIST^{V4}-SPRD^{30D}-SMA_{(10,20)}$	24	9	15	77.08	80	693.74	1200.07	**-506.33**	-5.06	189.54	-225.92	-1.85	-29.37	37.5	-21.1	0.58	0.96	-768.43
E2.2	$DIST^{V4}-SPRD^{30D}-EMA_{(10,20)}$	47	17	30	95.39	56.21	1621.71	1686.41	**-64.7**	-0.65	240.87	-167.33	-1.69	-26.83	36.17	-1.38	0.96	1.7	-738.52
E2.3	$DIST^{V4}-SPRD^{30D}-MACD_{(12,26,9)}$	41	14	27	76.4	66.21	1069.64	1787.71	**-718.07**	-7.18	333.05	-201.72	-1.8	-28.57	34.15	-17.51	0.6	1.15	-1325.8
E2.4	$DIST^{V4}-SPRD^{30D}-RSI_{(14)}$	4	2	2	358.82	177.42	717.64	354.85	**362.8**	3.63	647.23	-343.8	-0.15	-2.38	50	90.7	2.02	2.02	-354.85
E2.5	$DIST^{V4}-SPRD^{30D}-BB_{(20)}$	21	15	6	64.89	79.67	973.32	478.04	**495.28**	4.95	357.65	-131.57	-1.28	-20.32	71.43	23.59	2.04	0.81	-300.67
E3	$DIST^{V4}-SPRD^{30D}-DECTREE$	328	153	175	29.45	26.93	4506.05	4712.14	**-206.09**	-2.06	145.6	-254.08	-3.84	-60.96	46.65	-0.63	0.96	1.09	-1244.25
E4	$DIST^{V4}-SPRD^{30D}-MLP$	218	91	127	31.18	28.99	2837.82	3681.78	**-843.96**	-8.44	212.18	-140.79	-3.62	-57.47	41.74	-3.87	0.77	1.08	-1168.93
Part VI: Models derived using the spread obtained from $JOHANSEN-SPRD^{30D}$																			
F1.1	$JOHANSEN-ZSPRD^{30D}_{(3,2)}$	21	9	12	74	20.92	666.04	251.04	**415**	4.15	421.03	-119.75	-0.32	-5.08	42.86	19.76	2.65	3.54	-136.81
F1.2	$JOHANSEN-ZSPRD^{30D}_{(3,1)}$	21	9	12	81.91	24.75	737.2	296.97	**440.23**	4.4	421.03	-119.75	-0.32	-5.08	42.86	20.97	2.48	3.31	-182.59
F1.3	$JOHANSEN-ZSPRD^{30D}_{(3,0.5)}$	21	9	12	87.75	27.21	789.73	326.53	**463.2**	4.63	421.03	-119.75	-0.32	-5.08	42.86	22.06	2.42	3.22	-189.15
F1.4	$JOHANSEN-ZSPRD^{30D}_{(2.7,2)}$	25	11	14	93.56	28.96	1029.2	405.44	**623.76**	6.24	421.03	-130.04	-0.26	-4.13	44	24.95	2.54	3.23	-266.86
F1.5	$JOHANSEN-ZSPRD^{30D}_{(2.7,1)}$	24	11	13	220.16	29.93	2421.81	389.12	**2032.69**	20.33	1621.5	-130.04	0.04	0.63	45.83	84.69	6.22	7.36	-250.39
F1.6	$JOHANSEN-ZSPRD^{30D}_{(2.7,0.5)}$	23	11	12	270.36	32.31	2973.92	387.77	**2586.15**	25.86	2040.55	-130.04	0.08	1.27	47.83	112.45	7.67	8.37	-250.39
F2.1	$JOHANSEN-SPRD^{30D}-SMA_{(10,20)}$	26	15	11	226.66	142.5	3399.89	1567.46	**1832.43**	18.32	772.66	-436.6	-0.27	-4.29	57.69	70.47	2.17	1.59	-436.6
F2.2	$JOHANSEN-SPRD^{30D}-EMA_{(10,20)}$	29	16	13	295.76	227.58	4732.2	2958.55	**1773.65**	17.74	918.25	-800.52	0.18	2.86	55.17	61.15	1.6	1.3	-1365.5
F2.3	$JOHANSEN-SPRD^{30D}-MACD_{(12,26,9)}$	40	25	15	202.35	239.21	5058.68	3588.21	**1470.47**	14.7	2099.09	-652.27	-0.34	-5.4	62.5	36.76	1.41	0.85	-1130.56
F2.4	$JOHANSEN-SPRD^{30D}-RSI_{(14)}$	8	5	3	1319.72	662.16	6598.6	1986.49	**4612.11**	46.12	5338.3	-1622.95	0.26	4.13	62.5	576.51	3.32	1.99	-1622.95
F2.5	$JOHANSEN-SPRD^{30D}-BB_{(20)}$	21	13	8	240.79	538.51	3130.32	4308.11	**-1177.79**	-11.78	1223.09	-2065.71	-0.11	-1.75	61.9	-56.12	0.73	0.45	-3424.52
F3	$JOHANSEN-SPRD^{30D}-DECTREE$	338	160	178	25.5	27.79	4080.33	4946.92	**-866.58**	-8.67	174.23	-144.36	-4.15	-65.88	47.34	-2.56	0.82	0.92	-1154.62
F4	$JOHANSEN-SPRD^{30D}-MLP$	266	117	149	28.33	29.59	3314.44	4409.49	**-1095.05**	-10.95	145.74	-165.24	-3.7	-58.74	43.98	-4.12	0.75	0.96	-1659.48
Part VII: Models derived using the spread obtained from $ADF-SPRD^{30D}$																			
G1.1	$ADF-ZSPRD^{30D}_{(3,2)}$	3	1	2	100.01	1281.34	100.01	2562.67	**-2462.66**	-24.63	100.01	-1394.95	-1.13	-17.94	33.33	-820.93	0.04	0.08	-2462.66
G1.2	$ADF-ZSPRD^{30D}_{(3,1)}$	3	1	2	276.45	1929.92	276.45	3859.83	**-3583.39**	-35.83	276.45	-2267.13	-0.99	-15.72	33.33	-1194.54	0.07	0.14	-3583.39
G1.3	$ADF-ZSPRD^{30D}_{(3,0.5)}$	3	1	2	321.35	1929.92	321.35	3859.83	**-3538.49**	-35.38	321.35	-2267.13	-0.97	-15.4	33.33	-1179.57	0.08	0.17	-3538.49
G1.4	$ADF-ZSPRD^{30D}_{(2.7,2)}$	8	3	5	99.7	603.32	299.11	3016.62	**-2717.51**	-27.18	147.99	-1394.95	-0.71	-11.27	37.5	-339.69	0.1	0.17	-2768.62
G1.5	$ADF-ZSPRD^{30D}_{(2.7,1)}$	8	3	5	387.38	1098.49	1162.13	5492.45	**-4330.32**	-43.3	669.71	-2267.13	-0.65	-10.32	37.5	-541.29	0.21	0.35	-4546.29
G1.6	$ADF-ZSPRD^{30D}_{(2.7,0.5)}$	8	3	5	279.8	1294.11	839.4	6470.55	**-5631.15**	-56.31	433.74	-2267.13	-0.83	-13.18	37.5	-703.89	0.13	0.22	-5715.47
G2.1	$ADF-SPRD^{30D}-SMA_{(10,20)}$	25	14	11	881.96	1948.26	12347.38	21430.9	**-9083.51**	-90.84	3775.11	-14377.72	-0.15	-2.38	56	-363.34	0.58	0.45	-14377.72
G2.2	$ADF-SPRD^{30D}-EMA_{(10,20)}$	45	26	19	874.31	634.04	22732.18	12046.85	**10685.33**	106.85	6900.25	-2385.22	0.1	1.59	57.78	237.49	1.89	1.38	-6199.66
G2.3	$ADF-SPRD^{30D}-MACD_{(12,26,9)}$	41	24	17	588.59	761.33	14126.22	12942.61	**1183.61**	11.84	2764.77	-2544.89	-0.05	-0.79	58.54	28.91	1.09	0.77	-4376.09
G2.4	$ADF-SPRD^{30D}-RSI_{(14)}$	1	1	-	145.76	-	145.76	-	**145.76**	1.46	145.76	-	-	-	100	145.76	145.76	145.76	-
G2.5	$ADF-SPRD^{30D}-BB_{(20)}$	22	8	14	828.18	558.65	6625.45	7821.04	**-1195.59**	-11.96	2572.44	-1442.81	-0.15	-2.38	36.36	-54.4	0.85	1.48	-3552.45
G3	$ADF-SPRD^{30D}-DECTREE$	319	149	170	25.58	30.64	3811.66	5208.52	**-1396.87**	-13.97	131.85	-344.11	-3.62	-57.47	46.71	-4.38	0.73	0.83	-1976.13
G4	$ADF-SPRD^{30D}-MLP$	243	117	126	28.88	30.28	3379.42	3815.32	**-435.9**	-4.36	234.61	-214.61	-3.53	-56.04	48.15	-1.79	0.89	0.95	-1170.23
Part VIII: Models derived using the spread obtained from $KALMAN-SPRD^{30D}$																			
H1.1	$KALMAN-ZSPRD^{30D}_{(3,2)}$	3	2	1	533.21	2007.16	1066.43	2007.16	**-940.73**	-9.41	737.81	-2007.16	-0.28	-4.44	66.67	-313.49	0.53	0.27	-2007.16
H1.2	$KALMAN-ZSPRD^{30D}_{(3,1)}$	3	2	1	674.69	1159.49	1349.37	1159.49	**189.88**	1.9	931.66	-1159.49	-0.03	-0.48	66.67	63.35	1.16	0.58	-1159.49
H1.3	$KALMAN-ZSPRD^{30D}_{(3,0.5)}$	2	1	1	417.71	1896.92	417.71	1896.92	**-1479.22**	-14.79	417.71	-1896.92	-0.51	-8.1	50	-739.61	0.22	0.22	-1896.92
H1.4	$KALMAN-ZSPRD^{30D}_{(2.7,2)}$	7	4	3	327.86	733.8	1311.46	2201.39	**-889.93**	-8.9	737.81	-2007.16	-0.26	-4.13	57.14	-127.16	0.6	0.45	-2007.16
H1.5	$KALMAN-ZSPRD^{30D}_{(2.7,1)}$	6	4	2	398.6	615.49	1594.4	1230.99	**363.41**	3.63	931.66	-1159.49	-0.05	-0.79	66.67	60.6	1.3	0.65	-1159.49
H1.6	$KALMAN-ZSPRD^{30D}_{(2.7,0.5)}$	4	2	2	364.56	1116.88	729.11	2233.76	**-1504.65**	-15.05	417.71	-1896.92	-0.44	-6.98	50	-376.16	0.33	0.33	-1922.36
H2.1	$KALMAN-SPRD^{30D}-SMA_{(10,20)}$	15	5	10	773.43	349.08	3867.14	3490.79	**376.35**	3.76	1046.49	-1505.59	-0.11	-1.75	33.33	25.05	1.11	2.22	-2789.5
H2.2	$KALMAN-SPRD^{30D}-EMA_{(10,20)}$	24	8	16	708.82	316.59	5670.56	5065.45	**605.12**	6.05	1411.63	-543.9	-0.13	-2.06	33.33	25.18	1.12	2.24	-2450.34
H2.3	$KALMAN-SPRD^{30D}-MACD_{(12,26,9)}$	32	13	19	425.81	309.63	5535.55	5882.9	**-347.35**	-3.47	3176.12	-773.01	-0.17	-2.7	40.62	-10.89	0.94	1.38	-4809.62
H2.4	$KALMAN-SPRD^{30D}-RSI_{(14)}$	2	1	1	1671.43	5545.02	1671.43	5545.02	**-3873.59**	-38.74	1671.43	-5545.02	-0.4	-6.35	50	-1936.79	0.3	0.3	-5545.02
H2.5	$KALMAN-SPRD^{30D}-BB_{(20)}$	14	10	4	345.34	1109.81	3453.42	4439.25	**-985.83**	-9.86	600.06	-2443.16	-0.19	-3.02	71.43	-70.4	0.78	0.31	-3596.06
H3	$KALMAN-SPRD^{30D}-DECTREE$	366	168	198	26.29	23.15	4416.54	4584.63	**-168.09**	-1.68	240.86	-85.25	-4.3	-68.26	45.9	-0.46	0.96	1.14	-839.84
H4	$KALMAN-SPRD^{30D}-MLP$	307	130	177	29.59	22.95	3847.29	4062.29	**-215**	-2.15	240.86	-93.25	-4.06	-64.45	42.35	-0.7	0.95	1.29	-942.1
Part IX: Models derived using the spread obtained from $RATIO-SPRD^{30D}$																			
I1.1	$RATIO-ZSPRD^{30D}_{(3,2)}$	2	1	1	56.54	19.76	56.54	19.76	**36.78**	0.37	56.54	-19.76	-2.48	-39.37	50	18.39	2.86	2.86	-19.76
I1.2	$RATIO-ZSPRD^{30D}_{(3,1)}$	2	1	1	107.94	41.53	107.94	41.53	**66.4**	0.66	107.94	-41.53	-1.12	-17.78	50	33.2	2.6	2.6	-41.53
I1.3	$RATIO-ZSPRD^{30D}_{(3,0.5)}$	2	1	1	107.94	1.49	107.94	1.49	**106.44**	1.06	107.94	-1.49	-1.28	-20.32	50	53.22	72.29	72.29	-1.49
I1.4	$RATIO-ZSPRD^{30D}_{(2.7,2)}$	3	2	1	69.75	16.59	139.5	16.59	**122.91**	1.23	82.96	-16.59	-2.15	-34.13	66.67	40.97	8.41	4.2	-16.59
I1.5	$RATIO-ZSPRD^{30D}_{(2.7,1)}$	3	2	1	132.86	38.51	265.72	38.51	**227.21**	2.27	157.78	-38.51	-0.75	-11.91	66.67	75.74	6.9	3.45	-38.51
I1.6	$RATIO-ZSPRD^{30D}_{(2.7,0.5)}$	3	3	-	102.38	-	307.15	-	**307.15**	3.07	197.47	-	-0.51	-8.1	100	102.38	307.15	102.38	-
I2.1	$RATIO-SPRD^{30D}-SMA_{(10,20)}$	16	6	10	58.78	83.41	352.65	834.05	**-481.4**	-4.81	133.25	-207.84	-2	-31.75	37.5	-30.09	0.42	0.7	-799.95
I2.2	$RATIO-SPRD^{30D}-EMA_{(10,20)}$	26	5	21	98.66	74.86	493.3	1572.07	**-1078.77**	-10.79	204.53	-352.24	-1.89	-30	19.23	-41.49	0.31	1.32	-937.75
I2.3	$RATIO-SPRD^{30D}-MACD_{(12,26,9)}$	40	16	24	71.76	73.47	1148.18	1763.18	**-615**	-6.15	268.59	-204.97	-1.7	-26.99	40	-15.37	0.65	0.98	-659.29
I2.4	$RATIO-SPRD^{30D}-RSI_{(14)}$	3	1	2	311.76	581.02	311.76	1162.04	**-850.28**	-8.5	311.76	-828.99	-0.76	-12.06	33.33	-283.46	0.27	0.54	-828.99
I2.5	$RATIO-SPRD^{30D}-BB_{(20)}$	19	12	7	44.95	51.94	539.43	363.55	**175.87**	1.76	83.48	-70.04	-2.62	-41.59	63.16	9.26	1.48	0.87	-146.53
I3	$RATIO-SPRD^{30D}-DECTREE$	388	138	250	28.6	19.67	3947.48	4917.65	**-970.18**	-9.7	214.61	-93.46	-4.54	-72.07	35.57	-2.5	0.8	1.45	-1515.42
I4	$RATIO-SPRD^{30D}-MLP$	360	125	235	29.75	20.57	3719.05	4834.56	**-1115.51**	-11.16	214.61	-93.46	-4.56	-72.39	34.72	-3.1	0.77	1.45	-1489.52
Part X: Models derived using the close price of VO.N																			
CLS-SYM-1.1	$CLOSE^{VO.N}-SMA_{(10,20)}$	15	5	10	407.5	131.94	2037.52	1319.42	**718.1**	7.18	1345.66	-357.26	-0.07	-1.11	33.33	47.86	1.54	3.09	-888.12
CLS-SYM-1.2	$CLOSE^{VO.N}-EMA_{(10,20)}$	20	6	14	305.56	123.3	1833.38	1726.2	**107.17**	1.07	700.63	-218.39	-0.27	-4.29	30	5.36	1.06	2.48	-812.37
CLS-SYM-1.3	$CLOSE^{VO.N}-MACD_{(12,26,9)}$	30	12	18	235.68	119.41	2828.19	2149.34	**678.86**	6.79	1213.06	-330.07	-0.19	-3.02	40	22.63	1.32	1.97	-845.26
CLS-SYM-1.4	$CLOSE^{VO.N}-RSI_{(14)}$	5	2	3	464.59	648.69	929.17	1946.08	**-1016.91**	-10.17	781.75	-1353.4	-0.35	-5.56	40	-203.38	0.48	0.72	-1353.4
CLS-SYM-1.5	$CLOSE^{VO.N}-BB_{(20)}$	15	13	2	85.35	600.28	1109.6	1200.56	**-90.96**	-0.91	190.76	-984.33	-0.29	-4.6	86.67	-6.04	0.92	0.14	-984.33
Part XI: Models derived using the close price of VXUS.N																			
CLS-SYM-2.1	$CLOSE^{VXUS.N}-SMA_{(10,20)}$	15	6	9	314.7	147.73	1888.19	1329.58	**558.62**	5.59	928.16	-483.97	-0.12	-1.9	40	37.24	1.42	2.13	-710.8
CLS-SYM-2.2	$CLOSE^{VXUS.N}-EMA_{(10,20)}$	23	6	17	500.43	151.67	3002.58	2578.36	**424.22**	4.24	1067.79	-550.04	-0.15	-2.38	26.09	18.46	1.16	3.3	-1087.54
CLS-SYM-2.3	$CLOSE^{VXUS.N}-MACD_{(12,26,9)}$	32	11	21	188.51	103.43	2073.65	2171.98	**-98.33**	-0.98	939.15	-336.67	-0.37	-5.87	34.38	-3.06	0.95	1.82	-1391.6
CLS-SYM-2.4	$CLOSE^{VXUS.N}-RSI_{(14)}$	6	3	3	309.07	270.45	927.22	811.36	**115.86**	1.16	384.77	-577.08	-0.16	-2.54	50	19.31	1.14	1.14	-577.08
CLS-SYM-2.5	$CLOSE^{VXUS.N}-BB_{(20)}$	19	12	7	67.21	145.66	806.56	1019.65	**-213.09**	-2.13	191.4	-832.35	-0.42	-6.67	63.16	-11.21	0.79	0.46	-832.35

Table D.2.20: This table presents the back-test metrics for the pair $VO.N/VXUS.N$ based on a 50-day rolling window. The table is subdivided into eleven parts, and in each of these parts, we present the back-test metrics and the trading strategies which use the spread derived from various models. In Part I, the spread is derived from the $DIST^{V1.1}$ model, in Part II from the $DIST^{V1.2}$ model, in Part III from the $DIST^{V2}$ model, in Part IV from the $DIST^{V3}$ model, in Part V from the $DIST^{V4}$ model, in Part VI from the $JOHANSEN-SPRD$ model, in Part VIII from the $ADF-SPRD$ model, in from the $DIST^{V2}$ model, in Part VIII from the $KALMAN-SPRD$ model, and in Part IX from the $RATIO-SPRD$ model. In Part X and XI, we present the back-test metrics of the trading strategies which use the close price of VO.N, and VXUS.N, respectively. All \$ numbers reported below are in USD.

(I) Trading Strategy Code	(II) Model Name	(III) Total Number of Trades	(IV) Number of Winning Trades	(V) Number of Loosing Trades	(VI) Average Profit per Trade (\$)	(VII) Average Loss per Trade (\$)	(VIII) Gross Profit (\$)	(IX) Gross Loss (\$)	(X) Net Profit (\$)	(XI) ROI (%)	(XII) Max P&L (\$)	(XIII) Min P&L (\$)	(XIV) Daily Sharpe Ratio	(XV) Annualized Sharpe Ratio	(XVI) Hit Ratio	(XVII) Expectancy	(XVIII) Profit Factor	(XIX) Realized Risk Reward Ratio	(XX) Max Drawdown (\$)
Part I: Models derived using the spread obtained from $DIST^{V1.1}-SPRD^{50D}$																			
A1.1	$DIST^{V1.1}-ZSPRD^{50D}_{(3,2)}$	3	1	2	49.37	99.81	49.37	199.62	**-150.26**	-1.5	49.37	-109.23	-2.33	-36.99	33.33	-50.09	0.25	0.49	-150.26
A1.2	$DIST^{V1.1}-ZSPRD^{50D}_{(3,1)}$	1	1	-	110.89	-	110.89	-	**110.89**	1.11	110.89	-	-	-	100	110.89	110.89	110.89	-
A1.3	$DIST^{V1.1}-ZSPRD^{50D}_{(3,0.5)}$	1	-	1	-	92.22	-	92.22	**-92.22**	-0.92	-	-92.22	-	-	-	-92.22	-	-	-92.22
A1.4	$DIST^{V1.1}-ZSPRD^{50D}_{(2.7,2)}$	4	2	2	27.19	80.69	54.39	161.38	**-107**	-1.07	49.37	-109.23	-2.59	-41.11	50	-26.75	0.34	0.34	-109.23
A1.5	$DIST^{V1.1}-ZSPRD^{50D}_{(2.7,1)}$	2	2	-	59.5	-	119.01	-	**119.01**	1.19	110.89	-	-1.27	-20.16	100	59.5	119.01	59.5	-
A1.6	$DIST^{V1.1}-ZSPRD^{50D}_{(2.7,0.5)}$	2	1	1	17.98	92.22	17.98	92.22	**-74.24**	-0.74	17.98	-92.22	-2.43	-38.58	50	-37.12	0.19	0.19	-92.22
A2.1	$DIST^{V1.1}-SPRD^{50D}-SMA_{(10,20)}$	17	7	10	91.49	74.16	640.45	741.58	**-101.13**	-1.01	216.07	-168.73	-1.47	-23.34	41.18	-5.94	0.86	1.23	-432.58
A2.2	$DIST^{V1.1}-SPRD^{50D}-EMA_{(10,20)}$	21	12	9	55.76	120.29	669.06	1082.65	**-413.59**	-4.14	159.89	-201.45	-1.65	-26.19	57.14	-19.7	0.62	0.46	-474.04
A2.3	$DIST^{V1.1}-SPRD^{50D}-MACD_{(12,26,9)}$	33	21	12	60.41	87.92	1268.63	1055.02	**213.61**	2.14	110.59	-244.03	-1.71	-27.15	63.64	6.48	1.2	0.69	-738.52
A2.4	$DIST^{V1.1}-SPRD^{50D}-RSI_{(14)}$	4	3	1	460.16	236.17	1380.47	236.17	**1144.3**	11.44	690.36	-236.17	0.35	5.56	75	286.07	5.85	1.95	-236.17
A2.5	$DIST^{V1.1}-SPRD^{50D}-BB_{(20)}$	16	8	8	115.86	26.85	926.9	214.81	**712.09**	7.12	438.49	-78.92	-0.88	-13.97	50	44.51	4.31	4.32	-145.98
A3	$DIST^{V1.1}-SPRD^{50D}-DECTREE$	354	152	202	30.12	21.25	4578.67	4292.67	**286**	2.86	144.03	-133.03	-4.23	-67.15	42.94	0.81	1.07	1.42	-1010.39
A4	$DIST^{V1.1}-SPRD^{50D}-MLP$	320	144	176	30.75	23.44	4427.39	4125.79	**301.6**	3.02	133.78	-133.03	-4.07	-64.61	45	0.94	1.07	1.31	-847.72
Part II: Models derived using the spread obtained from $DIST^{V1.2}-SPRD^{50D}$																			
B1.1	$DIST^{V1.2}-ZSPRD^{50D}_{(3,2)}$	7	2	5	14.36	45.06	28.73	225.3	**-196.57**	-1.97	20.97	-59.82	-5.77	-91.6	28.57	-28.08	0.13	0.32	-204.33
B1.2	$DIST^{V1.2}-ZSPRD^{50D}_{(3,1)}$	7	3	4	32.94	68.24	98.83	272.95	**-174.12**	-1.74	78.06	-91.18	-2.92	-46.35	42.86	-24.87	0.36	0.48	-272.95
B1.3	$DIST^{V1.2}-ZSPRD^{50D}_{(3,0.5)}$	7	3	4	50.42	141.97	151.27	567.88	**-416.62**	-4.17	84.92	-266.33	-1.74	-27.62	42.86	-59.51	0.27	0.36	-432.65
B1.4	$DIST^{V1.2}-ZSPRD^{50D}_{(2.7,2)}$	10	4	6	28.51	50.15	114.03	300.9	**-186.86**	-1.87	76.08	-76.54	-3.66	-58.1	40	-18.69	0.38	0.57	-277.16
B1.5	$DIST^{V1.2}-ZSPRD^{50D}_{(2.7,1)}$	10	5	5	44.08	103.68	220.39	518.38	**-297.99**	-2.98	84.19	-226.55	-1.91	-30.32	50	-29.8	0.43	0.43	-518.38
B1.6	$DIST^{V1.2}-ZSPRD^{50D}_{(2.7,0.5)}$	9	4	5	58.96	139.83	235.83	699.15	**-463.32**	-4.63	84.92	-266.33	-1.72	-27.3	44.44	-51.49	0.34	0.42	-547.51
B2.1	$DIST^{V1.2}-SPRD^{50D}-SMA_{(10,20)}$	15	7	8	147.1	127.91	1029.71	1023.24	**6.47**	0.06	426.94	-522.38	-0.75	-11.91	46.67	0.44	1.01	1.15	-556.24
B2.2	$DIST^{V1.2}-SPRD^{50D}-EMA_{(10,20)}$	19	12	7	72.28	97.75	867.33	684.27	**183.06**	1.83	227.3	-233.22	-1.3	-20.64	63.16	9.64	1.27	0.74	-458.56
B2.3	$DIST^{V1.2}-SPRD^{50D}-MACD_{(12,26,9)}$	22	10	12	75.97	99.51	759.72	1194.11	**-434.39**	-4.34	337.9	-287.03	-1.36	-21.59	45.45	-19.75	0.64	0.76	-863.02
B2.4	$DIST^{V1.2}-SPRD^{50D}-RSI_{(14)}$	10	3	7	101	170.5	303	1193.48	**-890.49**	-8.9	153.41	-440.87	-1.36	-21.59	30	-89.05	0.25	0.59	-752.61
B2.5	$DIST^{V1.2}-SPRD^{50D}-BB_{(20)}$	17	12	5	55.85	88.73	670.22	443.64	**226.57**	2.27	159.73	-307.24	-1.39	-22.07	70.59	13.33	1.51	0.63	-105.59
B3	$DIST^{V1.2}-SPRD^{50D}-DECTREE$	266	134	132	27.95	28.25	3745.13	3729.13	**16**	0.16	131.29	-212.18	-3.8	-60.32	50.38	0.06	1	0.99	-676.45
B4	$DIST^{V1.2}-SPRD^{50D}-MLP$	253	135	118	31.92	31.74	4309.78	3745.35	**564.44**	5.64	227.97	-226.41	-3.12	-49.53	53.36	2.23	1.15	1.01	-630.93
Part III: Models derived using the spread obtained from $DIST^{V2}-SPRD^{50D}$																			
C1.1	$DIST^{V2}-ZSPRD^{50D}_{(3,2)}$	3	2	1	99.81	49.37	199.62	49.37	**150.26**	1.5	109.23	-49.37	-1.18	-18.73	66.67	50.09	4.04	2.02	-49.37
C1.2	$DIST^{V2}-ZSPRD^{50D}_{(3,1)}$	1	-	1	-	110.89	-	110.89	**-110.89**	-1.11	-	-110.89	-	-	-	-110.89	-	-	-110.89
C1.3	$DIST^{V2}-ZSPRD^{50D}_{(3,0.5)}$	1	1	-	92.22	-	92.22	-	**92.22**	0.92	92.22	-	-	-	100	92.22	92.22	92.22	-
C1.4	$DIST^{V2}-ZSPRD^{50D}_{(2.7,2)}$	4	2	2	80.69	27.19	161.38	54.39	**107**	1.07	109.23	-49.37	-1.82	-28.89	50	26.75	2.97	2.97	-54.39
C1.5	$DIST^{V2}-ZSPRD^{50D}_{(2.7,1)}$	2	-	2	-	59.5	-	119.01	**-119.01**	-1.19	-	-110.89	-2.91	-46.19	-	-59.5	-	-	-119.01
C1.6	$DIST^{V2}-ZSPRD^{50D}_{(2.7,0.5)}$	2	1	1	92.22	17.98	92.22	17.98	**74.24**	0.74	92.22	-17.98	-1.47	-23.34	50	37.12	5.13	5.13	-17.98
C2.1	$DIST^{V2}-SPRD^{50D}-SMA_{(10,20)}$	17	10	7	74.16	91.49	741.58	640.45	**101.13**	1.01	168.73	-216.07	-1.36	-21.59	58.82	5.94	1.16	0.81	-343.07
C2.2	$DIST^{V2}-SPRD^{50D}-EMA_{(10,20)}$	21	9	12	120.29	55.76	1082.65	669.06	**413.59**	4.14	201.45	-159.89	-1.27	-20.16	42.86	19.7	1.62	2.16	-268.45
C2.3	$DIST^{V2}-SPRD^{50D}-MACD_{(12,26,9)}$	33	12	21	87.92	60.41	1055.02	1268.63	**-213.61**	-2.14	244.03	-110.59	-1.86	-29.53	36.36	-6.48	0.83	1.46	-728.55
C2.4	$DIST^{V2}-SPRD^{50D}-RSI_{(14)}$	4	1	3	236.17	460.16	236.17	1380.47	**-1144.3**	-11.44	236.17	-690.36	-1.14	-18.1	25	-286.07	0.17	0.51	-833.74
C2.5	$DIST^{V2}-SPRD^{50D}-BB_{(20)}$	16	8	8	26.85	115.86	214.81	926.9	**-712.09**	-7.12	78.92	-438.49	-1.61	-25.56	50	-44.51	0.23	0.23	-421.92
C3	$DIST^{V2}-SPRD^{50D}-DECTREE$	361	161	200	28.44	24.27	4578.82	4853.3	**-274.47**	-2.74	133.78	-133.03	-4.22	-66.99	44.6	-0.76	0.94	1.17	-941.17
C4	$DIST^{V2}-SPRD^{50D}-MLP$	316	136	180	30.05	25.57	4086.3	4603.49	**-517.19**	-5.17	165.81	-130.21	-4.04	-64.13	43.04	-1.64	0.89	1.17	-1068.82
Part IV: Models derived using the spread obtained from $DIST^{V3}-SPRD^{50D}$																			
D1.1	$DIST^{V3}-ZSPRD^{50D}_{(3,2)}$	6	5	1	41.09	192.93	205.43	192.93	**12.5**	0.12	58.41	-192.93	-1.54	-24.45	83.33	2.08	1.06	0.21	-192.93
D1.2	$DIST^{V3}-ZSPRD^{50D}_{(3,1)}$	6	3	3	59.97	49.55	179.91	148.66	**31.25**	0.31	98.6	-101.59	-2.1	-33.34	50	5.21	1.21	1.21	-101.59
D1.3	$DIST^{V3}-ZSPRD^{50D}_{(3,0.5)}$	6	3	3	88.28	45.6	264.83	136.8	**128.03**	1.28	103.23	-105.73	-1.6	-25.4	50	21.34	1.94	1.94	-105.73
D1.4	$DIST^{V3}-ZSPRD^{50D}_{(2.7,2)}$	11	6	5	40.88	74.3	245.29	371.48	**-126.19**	-1.26	58.41	-257.74	-1.76	-27.94	54.55	-11.47	0.66	0.55	-317.65
D1.5	$DIST^{V3}-ZSPRD^{50D}_{(2.7,1)}$	9	3	6	73.89	56.56	221.66	339.36	**-117.7**	-1.18	98.6	-167.16	-2.05	-32.54	33.33	-13.08	0.65	1.31	-167.16
D1.6	$DIST^{V3}-ZSPRD^{50D}_{(2.7,0.5)}$	9	4	5	72.69	41.83	290.74	209.16	**81.58**	0.82	103.23	-170.37	-1.72	-27.3	44.44	9.06	1.39	1.74	-170.37
D2.1	$DIST^{V3}-SPRD^{50D}-SMA_{(10,20)}$	20	11	9	68.7	32.46	755.73	292.12	**463.62**	4.64	187.75	-62.39	-1.96	-31.11	55	23.18	2.59	2.12	-88.35
D2.2	$DIST^{V3}-SPRD^{50D}-EMA_{(10,20)}$	37	13	24	92.41	75.77	1201.36	1818.53	**-617.17**	-6.17	391.35	-317.45	-1.46	-23.18	35.14	-16.67	0.66	1.22	-553.42
D2.3	$DIST^{V3}-SPRD^{50D}-MACD_{(12,26,9)}$	45	11	34	91.52	58.8	1006.67	1999.33	**-992.66**	-9.93	271.58	-136.81	-2.05	-32.54	24.44	-22.07	0.5	1.56	-1291.05
D2.4	$DIST^{V3}-SPRD^{50D}-RSI_{(14)}$	3	-	3	-	313.64	-	940.92	**-940.92**	-9.41	-	-569.05	-1.83	-29.05	-	-313.64	-	-	-630.36
D2.5	$DIST^{V3}-SPRD^{50D}-BB_{(20)}$	20	13	7	79.48	73.46	1033.22	514.2	**519.02**	5.19	389.4	-182.97	-1.09	-17.3	65	25.95	2.01	1.08	-259.81
D3	$DIST^{V3}-SPRD^{50D}-DECTREE$	291	126	165	29.17	25.58	3675.48	4220.5	**-545.02**	-5.45	313.53	-145.17	-3.8	-60.32	43.3	-1.87	0.87	1.14	-1202.19
D4	$DIST^{V3}-SPRD^{50D}-MLP$	275	130	145	31.78	26.41	4131.89	3830.11	**301.78**	3.02	212.18	-168.31	-3.47	-55.08	47.27	1.1	1.08	1.2	-926.44
Part V: Models derived using the spread obtained from $DIST^{V4}-SPRD^{50D}$																			
E1.1	$DIST^{V4}-ZSPRD^{50D}_{(3,2)}$	6	5	1	41.09	192.93	205.43	192.93	**12.5**	0.12	58.41	-192.93	-1.54	-24.45	83.33	2.08	1.06	0.21	-192.93
E1.2	$DIST^{V4}-ZSPRD^{50D}_{(3,1)}$	6	3	3	59.97	49.55	179.91	148.66	**31.25**	0.31	98.6	-101.59	-2.1	-33.34	50	5.21	1.21	1.21	-101.59
E1.3	$DIST^{V4}-ZSPRD^{50D}_{(3,0.5)}$	6	3	3	88.28	45.6	264.83	136.8	**128.03**	1.28	103.23	-105.73	-1.6	-25.4	50	21.34	1.94	1.94	-105.73
E1.4	$DIST^{V4}-ZSPRD^{50D}_{(2.7,2)}$	11	6	5	40.88	74.3	245.29	371.48	**-126.19**	-1.26	58.41	-257.74	-1.76	-27.94	54.55	-11.47	0.66	0.55	-317.65
E1.5	$DIST^{V4}-ZSPRD^{50D}_{(2.7,1)}$	9	3	6	73.89	56.56	221.66	339.36	**-117.7**	-1.18	98.6	-167.16	-2.05	-32.54	33.33	-13.08	0.65	1.31	-167.16
E1.6	$DIST^{V4}-ZSPRD^{50D}_{(2.7,0.5)}$	9	4	5	72.69	41.83	290.74	209.16	**81.58**	0.82	103.23	-170.37	-1.72	-27.3	44.44	9.06	1.39	1.74	-170.37
E2.1	$DIST^{V4}-SPRD^{50D}-SMA_{(10,20)}$	20	11	9	68.7	32.46	755.73	292.12	**463.62**	4.64	187.75	-62.39	-1.96	-31.11	55	23.18	2.59	2.12	-88.35
E2.2	$DIST^{V4}-SPRD^{50D}-EMA_{(10,20)}$	37	13	24	92.41	75.77	1201.36	1818.53	**-617.17**	-6.17	391.35	-317.45	-1.46	-23.18	35.14	-16.67	0.66	1.22	-553.42
E2.3	$DIST^{V4}-SPRD^{50D}-MACD_{(12,26,9)}$	45	11	34	91.52	58.8	1006.67	1999.33	**-992.66**	-9.93	271.58	-136.81	-2.05	-32.54	24.44	-22.07	0.5	1.56	-1291.05
E2.4	$DIST^{V4}-SPRD^{50D}-RSI_{(14)}$	3	-	3	-	313.64	-	940.92	**-940.92**	-9.41	-	-569.05	-1.83	-29.05	-	-313.64	-	-	-630.36
E2.5	$DIST^{V4}-SPRD^{50D}-BB_{(20)}$	20	13	7	79.48	73.46	1033.22	514.2	**519.02**	5.19	389.4	-182.97	-1.09	-17.3	65	25.95	2.01	1.08	-259.81
E3	$DIST^{V4}-SPRD^{50D}-DECTREE$	309	131	178	31.02	24.44	4064.19	4350.96	**-286.78**	-2.87	313.53	-145.17	-3.77	-59.85	42.39	-0.93	0.93	1.27	-1228.63
E4	$DIST^{V4}-SPRD^{50D}-MLP$	275	130	145	31.78	26.41	4131.89	3830.11	**301.78**	3.02	212.18	-168.31	-3.47	-55.08	47.27	1.1	1.08	1.2	-926.44
Part VI: Models derived using the spread obtained from $JOHANSEN-SPRD^{50D}$																			
F1.1	$JOHANSEN-ZSPRD^{50D}_{(3,2)}$	13	8	5	99.96	76.55	799.66	382.74	**416.92**	4.17	282.26	-297.82	-0.65	-10.32	61.54	32.07	2.09	1.31	-315.69
F1.2	$JOHANSEN-ZSPRD^{50D}_{(3,1)}$	11	6	5	113.38	76.55	680.29	382.74	**297.55**	2.98	329.23	-297.82	-0.56	-8.89	54.55	27.06	1.78	1.48	-315.69
F1.3	$JOHANSEN-ZSPRD^{50D}_{(3,0.5)}$	11	6	5	130.33	76.55	781.98	382.74	**399.24**	3.99	407.69	-297.82	-0.51	-8.1	54.55	36.3	2.04	1.7	-315.69
F1.4	$JOHANSEN-ZSPRD^{50D}_{(2.7,2)}$	15	6	9	75.07	89.99	450.42	809.9	**-359.48**	-3.59	161.14	-297.82	-1.07	-16.99	40	-23.97	0.56	0.83	-609.86
F1.5	$JOHANSEN-ZSPRD^{50D}_{(2.7,1)}$	13	4	9	66.69	85.87	266.78	772.8	**-506.03**	-5.06	102.05	-297.82	-1	-15.87	30.77	-38.92	0.35	0.78	-670.75
F1.6	$JOHANSEN-ZSPRD^{50D}_{(2.7,0.5)}$	13	5	8	93.98	100.34	469.9	802.72	**-332.82**	-3.33	182.67	-297.82	-0.84	-13.33	38.46	-25.6	0.59	0.94	-497.55
F2.1	$JOHANSEN-SPRD^{50D}-SMA_{(10,20)}$	17	10	7	363.66	426.33	3636.65	2984.32	**652.33**	6.52	1499.37	-1281.4	-0.09	-1.43	58.82	38.34	1.22	0.85	-1302.64
F2.2	$JOHANSEN-SPRD^{50D}-EMA_{(10,20)}$	30	17	13	352.1	302.91	5985.71	3937.86	**2047.86**	20.48	1362.29	-873.98	-0.2	-3.17	56.67	68.28	1.52	1.16	-1338.52
F2.3	$JOHANSEN-SPRD^{50D}-MACD_{(12,26,9)}$	32	15	17	192.06	290.84	2880.9	4944.33	**-2063.43**	-20.63	1085.34	-1924.07	0.02	0.32	46.88	-64.46	0.58	0.66	-2969.84
F2.4	$JOHANSEN-SPRD^{50D}-RSI_{(14)}$	7	2	5	347.97	173.7	695.94	868.51	**-172.57**	-1.73	685.71	-305.6	0.21	3.33	28.57	-24.66	0.8	2	-374.77
F2.5	$JOHANSEN-SPRD^{50D}-BB_{(20)}$	20	10	10	1089.2	139.63	10891.98	1396.31	**9495.67**	94.96	9709.63	-405.36	0.15	2.38	50	474.78	7.8	7.8	-526.45
F3	$JOHANSEN-SPRD^{50D}-DECTREE$	336	155	181	25.47	26.32	3948.56	4764.15	**-815.59**	-8.16	132.9	-226.41	-4.19	-66.51	46.13	-2.43	0.83	0.97	-1088.57
F4	$JOHANSEN-SPRD^{50D}-MLP$	260	118	142	27.61	26.48	3258.47	3759.63	**-501.16**	-5.01	132.49	-170.65	-4.09	-64.93	45.38	-1.93	0.87	1.04	-694.34
Part VII: Models derived using the spread obtained from $ADF-SPRD^{50D}$																			
G1.1	$ADF-ZSPRD^{50D}_{(3,2)}$	5	3	2	599.25	9103.61	1797.76	18207.22	**-16409.46**	-164.09	1515.53	-16687.35	-0.45	-7.14	60	-3281.89	0.1	0.07	-18162.94
G1.2	$ADF-ZSPRD^{50D}_{(3,1)}$	5	2	3	698.97	5724.25	1397.94	17172.76	**-15774.82**	-157.75	1305.55	-16053.35	-0.45	-7.14	40	-3154.96	0.08	0.12	-17080.38
G1.3	$ADF-ZSPRD^{50D}_{(3,0.5)}$	5	1	4	1305.55	4293.04	1305.55	17172.17	**-15866.62**	-158.67	1305.55	-16053.35	-0.45	-7.14	20	-3173.32	0.08	0.3	-17172.17
G1.4	$ADF-ZSPRD^{50D}_{(2.7,2)}$	7	3	4	472.48	4664.79	1417.45	18659.15	**-17241.71**	-172.42	1135.21	-16687.35	-0.4	-6.35	42.86	-2462.95	0.08	0.1	-18614.87
G1.5	$ADF-ZSPRD^{50D}_{(2.7,1)}$	7	4	3	791.73	5724.25	3166.91	17172.76	**-14005.85**	-140.06	1656.16	-16053.35	-0.34	-5.4	57.14	-2001.02	0.18	0.14	-16243.16
G1.6	$ADF-ZSPRD^{50D}_{(2.7,0.5)}$	7	2	5	1479.3	3535.77	2958.6	17678.84	**-14720.23**	-147.2	2031.71	-16053.35	-0.35	-5.56	28.57	-2102.96	0.17	0.42	-16221.9
G2.1	$ADF-SPRD^{50D}-SMA_{(10,20)}$	25	14	11	1488.98	490.06	20845.71	5390.71	**15455**	154.55	9918.92	-1565.55	0.24	3.81	56	618.2	3.87	3.04	-1565.55
G2.2	$ADF-SPRD^{50D}-EMA_{(10,20)}$	37	20	17	919.15	1137.85	18382.92	19343.54	**-960.62**	-9.61	8180.68	-8615.1	-0.04	-0.63	54.05	-26.05	0.95	0.81	-13413.75
G2.3	$ADF-SPRD^{50D}-MACD_{(12,26,9)}$	43	25	18	1172.57	645.23	29314.35	11614.17	**17700.18**	177	16053.35	-1924.29	0.13	2.06	58.14	411.64	2.52	1.82	-2875.27
G2.4	$ADF-SPRD^{50D}-RSI_{(14)}$	2	2	-	2558.15	-	5116.29	-	**5116.29**	51.16	4275.86	-	0.98	15.56	100	2558.15	5116.29	2558.15	-
G2.5	$ADF-SPRD^{50D}-BB_{(20)}$	16	7	9	481.62	572.4	3371.37	5151.59	**-1780.22**	-17.8	972.21	-2455.1	-0.26	-4.13	43.75	-111.26	0.65	0.84	-3947.7
G3	$ADF-SPRD^{50D}-DECTREE$	296	146	150	27.76	28.62	4053.17	4292.79	**-239.62**	-2.4	183.92	-254.08	-3.59	-56.99	49.32	-0.81	0.94	0.97	-1026.28
G4	$ADF-SPRD^{50D}-MLP$	235	106	129	27.12	35.93	2874.39	4635.2	**-1760.81**	-17.61	182.12	-182.06	-3.59	-56.99	45.11	-7.49	0.62	0.75	-2073.33
Part VIII: Models derived using the spread obtained from $KALMAN-SPRD^{50D}$																			
H1.1	$KALMAN-ZSPRD^{50D}_{(3,2)}$	2	-	2	-	1078.25	-	2156.49	**-2156.49**	-21.56	-	-2007.52	-0.9	-14.29	-	-1078.25	-	-	-2156.49
H1.2	$KALMAN-ZSPRD^{50D}_{(3,1)}$	1	-	1	-	1253.2	-	1253.2	**-1253.2**	-12.53	-	-1253.2	-	-	-	-1253.2	-	-	-1253.2
H1.3	$KALMAN-ZSPRD^{50D}_{(3,0.5)}$	1	-	1	-	621.01	-	621.01	**-621.01**	-6.21	-	-621.01	-	-	-	-621.01	-	-	-621.01
H1.4	$KALMAN-ZSPRD^{50D}_{(2.7,2)}$	5	3	2	347.71	1325.39	1043.14	2650.78	**-1607.64**	-16.08	737.89	-2007.52	-0.4	-6.35	60	-321.53	0.39	0.26	-2345.54
H1.5	$KALMAN-ZSPRD^{50D}_{(2.7,1)}$	3	1	2	284.44	1136.07	284.44	2272.15	**-1987.71**	-19.88	284.44	-1897.16	-0.68	-10.79	33.33	-662.62	0.13	0.25	-1987.71
H1.6	$KALMAN-ZSPRD^{50D}_{(2.7,0.5)}$	3	2	1	356.29	1297.66	712.57	1297.66	**-585.08**	-5.85	585.61	-1297.66	-0.29	-4.6	66.67	-194.97	0.55	0.27	-1297.66
H2.1	$KALMAN-SPRD^{50D}-SMA_{(10,20)}$	19	8	11	612.81	369.1	4902.51	4060.13	**842.38**	8.42	1546.79	-909.53	-0.09	-1.43	42.11	44.38	1.21	1.66	-1954.46
H2.2	$KALMAN-SPRD^{50D}-EMA_{(10,20)}$	22	8	14	831.32	295.33	6650.59	4134.65	**2515.94**	25.16	1530.75	-658.69	0.02	0.32	36.36	114.32	1.61	2.81	-1382.57
H2.3	$KALMAN-SPRD^{50D}-MACD_{(12,26,9)}$	31	9	22	744.76	291.12	6702.88	6404.64	**298.23**	2.98	3493.93	-819.68	-0.12	-1.9	29.03	9.6	1.05	2.56	-2190.9
H2.4	$KALMAN-SPRD^{50D}-RSI_{(14)}$	3	1	2	2025.15	2699.04	2025.15	5398.08	**-3372.93**	-33.73	2025.15	-4364.57	-0.38	-6.03	33.33	-1124.47	0.38	0.75	-4364.57
H2.5	$KALMAN-SPRD^{50D}-BB_{(20)}$	13	10	3	159.01	831.68	1590.12	2495.05	**-904.93**	-9.05	367.33	-2443.69	-0.23	-3.65	76.92	-69.64	0.64	0.19	-2443.69
H3	$KALMAN-SPRD^{50D}-DECTREE$	354	156	198	26.61	24	4151.38	4752.83	**-601.45**	-6.01	144.03	-120.96	-4.39	-69.69	44.07	-1.7	0.87	1.11	-1022.55
H4	$KALMAN-SPRD^{50D}-MLP$	291	111	180	30.93	27.63	3433.78	4972.63	**-1538.85**	-15.39	144.03	-212.18	-3.93	-62.39	38.14	-5.29	0.69	1.12	-1789.56
Part IX: Models derived using the spread obtained from $RATIO-SPRD^{50D}$																			
I1.1	$RATIO-ZSPRD^{50D}_{(3,2)}$	3	3	-	67.76	-	203.27	-	**203.27**	2.03	97.33	-	-2.14	-33.97	100	67.76	203.27	67.76	-
I1.2	$RATIO-ZSPRD^{50D}_{(3,1)}$	2	2	-	147.59	-	295.18	-	**295.18**	2.95	197.51	-	-0.06	-0.95	100	147.59	295.18	147.59	-
I1.3	$RATIO-ZSPRD^{50D}_{(3,0.5)}$	2	2	-	213.16	-	426.33	-	**426.33**	4.26	328.66	-	0.37	5.87	100	213.16	426.33	213.16	-
I1.4	$RATIO-ZSPRD^{50D}_{(2.7,2)}$	6	5	1	41.05	65.06	205.25	65.06	**140.19**	1.4	82.96	-65.06	-2.53	-40.16	83.33	23.36	3.15	0.63	-65.06
I1.5	$RATIO-ZSPRD^{50D}_{(2.7,1)}$	5	4	1	122.24	46.86	488.94	46.86	**442.08**	4.42	197.51	-46.86	-0.73	-11.59	80	88.42	10.43	2.61	-46.86
I1.6	$RATIO-ZSPRD^{50D}_{(2.7,0.5)}$	5	5	-	130.92	-	654.6	-	**654.6**	6.55	328.66	-	-0.18	-2.86	100	130.92	654.6	130.92	-
I2.1	$RATIO-SPRD^{50D}-SMA_{(10,20)}$	16	5	11	67.27	79.36	336.36	872.93	**-536.57**	-5.37	133.25	-207.84	-2.06	-32.7	31.25	-33.54	0.39	0.85	-799.95
I2.2	$RATIO-SPRD^{50D}-EMA_{(10,20)}$	26	6	20	100.98	70.78	605.88	1415.61	**-809.73**	-8.1	204.53	-271.58	-1.9	-30.16	23.08	-31.14	0.43	1.43	-770.53
I2.3	$RATIO-SPRD^{50D}-MACD_{(12,26,9)}$	39	14	25	85.75	75.11	1200.52	1877.83	**-677.31**	-6.77	268.59	-204.97	-1.65	-26.19	35.9	-17.36	0.64	1.14	-784.22
I2.4	$RATIO-SPRD^{50D}-RSI_{(14)}$	3	-	3	-	426.66	-	1279.97	**-1279.97**	-12.8	-	-863.31	-1.48	-23.49	-	-426.66	-	-	-969.41
I2.5	$RATIO-SPRD^{50D}-BB_{(20)}$	18	11	7	42.53	51.94	467.87	363.55	**104.32**	1.04	83.48	-70.04	-2.71	-43.02	61.11	5.79	1.29	0.82	-146.53
I3	$RATIO-SPRD^{50D}-DECTREE$	370	127	243	27.27	19.57	3463.09	4755.42	**-1292.33**	-12.92	214.61	-84.26	-4.81	-76.36	34.32	-3.49	0.73	1.39	-1629.69
I4	$RATIO-SPRD^{50D}-MLP$	334	115	219	30.28	20.79	3482.04	4553.28	**-1071.24**	-10.71	214.61	-93.46	-4.47	-70.96	34.43	-3.21	0.76	1.46	-1372.7
Part X: Models derived using the close price of VO.N																			
CLS-SYM-1.1	$CLOSE^{VO.N}-SMA_{(10,20)}$	15	5	10	407.5	131.94	2037.52	1319.42	**718.1**	7.18	1345.66	-357.26	-0.07	-1.11	33.33	47.86	1.54	3.09	-888.12
CLS-SYM-1.2	$CLOSE^{VO.N}-EMA_{(10,20)}$	20	6	14	305.56	123.3	1833.38	1726.2	**107.17**	1.07	700.63	-218.39	-0.27	-4.29	30	5.36	1.06	2.48	-812.37
CLS-SYM-1.3	$CLOSE^{VO.N}-MACD_{(12,26,9)}$	30	12	18	235.68	119.41	2828.19	2149.34	**678.86**	6.79	1213.06	-330.07	-0.19	-3.02	40	22.63	1.32	1.97	-845.26
CLS-SYM-1.4	$CLOSE^{VO.N}-RSI_{(14)}$	5	2	3	464.59	648.69	929.17	1946.08	**-1016.91**	-10.17	781.75	-1353.4	-0.35	-5.56	40	-203.38	0.48	0.72	-1353.4
CLS-SYM-1.5	$CLOSE^{VO.N}-BB_{(20)}$	15	13	2	85.35	600.28	1109.6	1200.56	**-90.96**	-0.91	190.76	-984.33	-0.29	-4.6	86.67	-6.04	0.92	0.14	-984.33
Part XI: Models derived using the close price of VXUS.N																			
CLS-SYM-2.1	$CLOSE^{VXUS.N}-SMA_{(10,20)}$	15	6	9	314.7	147.73	1888.19	1329.58	**558.62**	5.59	928.16	-483.97	-0.12	-1.9	40	37.24	1.42	2.13	-710.8
CLS-SYM-2.2	$CLOSE^{VXUS.N}-EMA_{(10,20)}$	23	6	17	500.43	151.67	3002.58	2578.36	**424.22**	4.24	1067.79	-550.04	-0.15	-2.38	26.09	18.46	1.16	3.3	-1087.54
CLS-SYM-2.3	$CLOSE^{VXUS.N}-MACD_{(12,26,9)}$	32	11	21	188.51	103.43	2073.65	2171.98	**-98.33**	-0.98	939.15	-336.67	-0.37	-5.87	34.38	-3.06	0.95	1.82	-1391.6
CLS-SYM-2.4	$CLOSE^{VXUS.N}-RSI_{(14)}$	6	3	3	309.07	270.45	927.22	811.36	**115.86**	1.16	384.77	-577.08	-0.16	-2.54	50	19.31	1.14	1.14	-577.08
CLS-SYM-2.5	$CLOSE^{VXUS.N}-BB_{(20)}$	19	12	7	67.21	145.66	806.56	1019.65	**-213.09**	-2.13	191.4	-832.35	-0.42	-6.67	63.16	-11.21	0.79	0.46	-832.35

Table D.2.21: This table presents the back-test metrics for the pair $VO.N/VXUS.N$ based on a 100-day rolling window. The table is subdivided into eleven parts, and in each of these parts, we present the back-test metrics and the trading strategies which use the spread derived from various models. In Part I, the spread is derived from the $DIST^{V1.1}$ model, in Part II from the $DIST^{V1.2}$ model, in Part III from the $DIST^{V2}$ model, in Part IV from the $DIST^{V3}$ model, in Part V from the $DIST^{V4}$ model, in Part VI from the $JOHANSEN-SPRD$ model, in Part VIII from the $ADF-SPRD$ model, in from the $DIST^{V2}$ model, in Part VIII from the $KALMAN-SPRD$ model, and in Part IX from the $RATIO-SPRD$ model. In Part X and XI, we present the back-test metrics of the trading strategies which use the close price of VO.N, and VXUS.N, respectively. All $ numbers reported below are in USD.

(I) Trading Strategy Code	(II) Model Name	(III) Total Number of Trades	(IV) Number of Winning Trades	(V) Number of Loosing Trades	(VI) Average Profit per Trade ($)	(VII) Average Loss per Trade ($)	(VIII) Gross Profit ($)	(IX) Gross Loss ($)	(X) Net Profit ($)	(XI) ROI (%)	(XII) Max P&L ($)	(XIII) Min P&L ($)	(XIV) Daily Sharpe Ratio	(XV) Annualized Sharpe Ratio	(XVI) Hit Ratio	(XVII) Expectancy	(XVIII) Profit Factor	(XIX) Realized Risk Reward Ratio	(XX) Max Drawdown ($)
Part I: Models derived using the spread obtained from $DIST^{V1.1}-SPRD^{100D}$																			
A1.1	$DIST^{V1.1}-ZSPRD^{100D}_{(3,2)}$	1	1	-	20.7	-	20.7	-	**20.7**	0.21	20.7	-	-	-	100	20.7	20.7	20.7	-
A1.2	$DIST^{V1.1}-ZSPRD^{100D}_{(3,1)}$	1	-	1	-	202.77	-	202.78	**-202.78**	-2.03	-	-202.77	-	-	-	-202.77	-	-	-202.77
A1.3	$DIST^{V1.1}-ZSPRD^{100D}_{(3,0.5)}$	1	-	1	-	257.42	-	257.42	**-257.42**	-2.57	-	-257.42	-	-	-	-257.42	-	-	-257.42
A1.4	$DIST^{V1.1}-ZSPRD^{100D}_{(2.7,2)}$	1	1	-	20.7	-	20.7	-	**20.7**	0.21	20.7	-	-	-	100	20.7	20.7	20.7	-
A1.5	$DIST^{V1.1}-ZSPRD^{100D}_{(2.7,1)}$	1	-	1	-	202.77	-	202.78	**-202.78**	-2.03	-	-202.77	-	-	-	-202.77	-	-	-202.77
A1.6	$DIST^{V1.1}-ZSPRD^{100D}_{(2.7,0.5)}$	1	-	1	-	257.42	-	257.42	**-257.42**	-2.57	-	-257.42	-	-	-	-257.42	-	-	-257.42
A2.1	$DIST^{V1.1}-SPRD^{100D}-SMA_{(10,20)}$	15	7	8	91.49	76.43	640.45	611.44	**29**	0.29	216.07	-168.73	-1.34	-21.27	46.67	1.94	1.05	1.2	-428.41
A2.2	$DIST^{V1.1}-SPRD^{100D}-EMA_{(10,20)}$	21	13	8	56.15	104.33	729.9	834.68	**-104.78**	-1.05	159.89	-171.1	-1.67	-26.51	61.9	-5	0.87	0.54	-382.48
A2.3	$DIST^{V1.1}-SPRD^{100D}-MACD_{(12,26,9)}$	31	19	12	57.51	91.64	1092.76	1099.68	**-6.92**	-0.07	108.8	-244.03	-1.77	-28.1	61.29	-0.22	0.99	0.63	-738.52
A2.4	$DIST^{V1.1}-SPRD^{100D}-RSI_{(14)}$	4	3	1	449.54	236.17	1348.61	236.17	**1112.44**	11.12	690.36	-236.17	0.32	5.08	75	278.11	5.71	1.9	-236.17
A2.5	$DIST^{V1.1}-SPRD^{100D}-BB_{(20)}$	15	8	7	141.95	30.35	1135.63	212.46	**923.17**	9.23	647.23	-78.92	-0.52	-8.25	53.33	61.54	5.35	4.68	-145.98
A3	$DIST^{V1.1}-SPRD^{100D}-DECTREE$	324	141	183	29.27	21.57	4127.11	3946.58	**180.53**	1.81	133.78	-133.03	-4.4	-69.85	43.52	0.56	1.05	1.36	-751.57
A4	$DIST^{V1.1}-SPRD^{100D}-MLP$	298	129	169	29.15	25.78	3760.28	4357.01	**-596.73**	-5.97	189.24	-133.03	-4.12	-65.4	43.29	-2	0.86	1.13	-798.13
Part II: Models derived using the spread obtained from $DIST^{V1.2}-SPRD^{100D}$																			
B1.1	$DIST^{V1.2}-ZSPRD^{100D}_{(3,2)}$	2	-	2	-	115.78	-	231.56	**-231.56**	-2.32	-	-195.82	-2.37	-37.62	-	-115.78	-	-	-231.56
B1.2	$DIST^{V1.2}-ZSPRD^{100D}_{(3,1)}$	2	-	2	-	33.74	-	67.48	**-67.48**	-0.67	-	-49.6	-8.28	-131.44	-	-33.74	-	-	-67.48
B1.3	$DIST^{V1.2}-ZSPRD^{100D}_{(3,0.5)}$	2	-	2	-	72.08	-	144.16	**-144.16**	-1.44	-	-94.56	-7.05	-111.92	-	-72.08	-	-	-144.16
B1.4	$DIST^{V1.2}-ZSPRD^{100D}_{(2.7,2)}$	4	-	4	-	89.32	-	357.3	**-357.3**	-3.57	-	-195.82	-2.68	-42.54	-	-89.32	-	-	-357.3
B1.5	$DIST^{V1.2}-ZSPRD^{100D}_{(2.7,1)}$	4	-	4	-	36.21	-	144.82	**-144.82**	-1.45	-	-72.38	-6.97	-110.65	-	-36.21	-	-	-144.82
B1.6	$DIST^{V1.2}-ZSPRD^{100D}_{(2.7,0.5)}$	4	1	3	50.74	75.66	50.74	227	**-176.25**	-1.76	50.74	-94.56	-2.89	-45.88	25	-44.06	0.22	0.67	-226.99
B2.1	$DIST^{V1.2}-SPRD^{100D}-SMA_{(10,20)}$	14	9	5	93.93	149.44	845.41	747.18	**98.23**	0.98	212.48	-481.93	-0.87	-13.81	64.29	7.03	1.13	0.63	-481.93
B2.2	$DIST^{V1.2}-SPRD^{100D}-EMA_{(10,20)}$	21	16	5	73.93	87.29	1182.86	436.43	**746.42**	7.46	190.94	-151.78	-1.3	-20.64	76.19	35.54	2.71	0.85	-151.78
B2.3	$DIST^{V1.2}-SPRD^{100D}-MACD_{(12,26,9)}$	27	18	9	90.77	100.02	1633.87	900.2	**733.67**	7.34	413.21	-267.4	-0.94	-14.92	66.67	27.18	1.82	0.91	-457.38
B2.4	$DIST^{V1.2}-SPRD^{100D}-RSI_{(14)}$	9	4	5	133.1	197.75	532.41	988.77	**-456.37**	-4.56	282.72	-485.69	-0.88	-13.97	44.44	-50.72	0.54	0.67	-248.72
B2.5	$DIST^{V1.2}-SPRD^{100D}-BB_{(20)}$	11	3	8	41.33	32.49	124	259.91	**-135.91**	-1.36	48.65	-81.74	-4.1	-65.09	27.27	-12.36	0.48	1.27	-239.02
B3	$DIST^{V1.2}-SPRD^{100D}-DECTREE$	294	137	157	30.37	29.83	4160.98	4683.54	**-522.56**	-5.23	170.39	-300.74	-3.31	-52.54	46.6	-1.78	0.89	1.02	-938.15
B4	$DIST^{V1.2}-SPRD^{100D}-MLP$	91	45	46	40.52	45.51	1823.2	2093.29	**-270.09**	-2.7	288.94	-192.26	-2.29	-36.35	49.45	-2.97	0.87	0.89	-679.99
Part III: Models derived using the spread obtained from $DIST^{V2}-SPRD^{100D}$																			
C1.1	$DIST^{V2}-ZSPRD^{100D}_{(3,2)}$	1	-	1	-	20.7	-	20.7	**-20.7**	-0.21	-	-20.7	-	-	-	-20.7	-	-	-20.7
C1.2	$DIST^{V2}-ZSPRD^{100D}_{(3,1)}$	1	1	-	202.77	-	202.78	-	**202.78**	2.03	202.77	-	-	-	100	202.77	202.78	202.77	-
C1.3	$DIST^{V2}-ZSPRD^{100D}_{(3,0.5)}$	1	1	-	257.42	-	257.42	-	**257.42**	2.57	257.42	-	-	-	100	257.42	257.42	257.42	-
C1.4	$DIST^{V2}-ZSPRD^{100D}_{(2.7,2)}$	1	-	1	-	20.7	-	20.7	**-20.7**	-0.21	-	-20.7	-	-	-	-20.7	-	-	-20.7
C1.5	$DIST^{V2}-ZSPRD^{100D}_{(2.7,1)}$	1	1	-	202.77	-	202.78	-	**202.78**	2.03	202.77	-	-	-	100	202.77	202.78	202.77	-
C1.6	$DIST^{V2}-ZSPRD^{100D}_{(2.7,0.5)}$	1	1	-	257.42	-	257.42	-	**257.42**	2.57	257.42	-	-	-	100	257.42	257.42	257.42	-
C2.1	$DIST^{V2}-SPRD^{100D}-SMA_{(10,20)}$	16	9	7	137.4	91.49	1236.6	640.45	**596.16**	5.96	607.23	-216.07	-0.62	-9.84	56.25	37.26	1.93	1.5	-343.07
C2.2	$DIST^{V2}-SPRD^{100D}-EMA_{(10,20)}$	21	8	13	104.33	56.15	834.68	729.9	**104.78**	1.05	171.1	-159.89	-1.56	-24.76	38.1	5	1.14	1.86	-268.45
C2.3	$DIST^{V2}-SPRD^{100D}-MACD_{(12,26,9)}$	31	12	19	91.64	57.51	1099.68	1092.76	**6.92**	0.07	244.03	-108.8	-1.77	-28.1	38.71	0.22	1.01	1.59	-728.55
C2.4	$DIST^{V2}-SPRD^{100D}-RSI_{(14)}$	4	1	3	236.17	449.54	236.17	1348.61	**-1112.44**	-11.12	236.17	-690.36	-1.11	-17.62	25	-278.11	0.18	0.53	-699.23
C2.5	$DIST^{V2}-SPRD^{100D}-BB_{(20)}$	15	7	8	30.35	141.95	212.46	1135.63	**-923.17**	-9.23	78.92	-647.23	-1.23	-19.53	46.67	-61.54	0.19	0.21	-421.92
C3	$DIST^{V2}-SPRD^{100D}-DECTREE$	326	136	190	28.38	24.6	3859.51	4674.8	**-815.29**	-8.15	133.78	-120.01	-4.34	-68.9	41.72	-2.5	0.83	1.15	-1073.42
C4	$DIST^{V2}-SPRD^{100D}-MLP$	306	132	174	30.51	25.63	4027.32	4458.93	**-431.61**	-4.32	175.8	-84.91	-4.01	-63.66	43.14	-1.41	0.9	1.19	-1134.66
Part IV: Models derived using the spread obtained from $DIST^{V3}-SPRD^{100D}$																			
D1.1	$DIST^{V3}-ZSPRD^{100D}_{(3,2)}$	4	2	2	42.34	84.37	84.69	168.75	**-84.06**	-0.84	58.31	-151.27	-1.88	-29.84	50	-21.02	0.5	0.5	-151.27
D1.2	$DIST^{V3}-ZSPRD^{100D}_{(3,1)}$	3	2	1	109.64	18.8	219.28	18.8	**200.48**	2	180.36	-18.8	-0.83	-13.18	66.67	66.83	11.67	5.83	-18.8
D1.3	$DIST^{V3}-ZSPRD^{100D}_{(3,0.5)}$	3	2	1	137.18	18.8	274.35	18.8	**255.56**	2.56	211.72	-18.8	-0.57	-9.05	66.67	85.19	14.6	7.3	-18.8
D1.4	$DIST^{V3}-ZSPRD^{100D}_{(2.7,2)}$	10	8	2	30.18	84.37	241.46	168.75	**72.71**	0.73	58.31	-151.27	-2.42	-38.42	80	7.27	1.43	0.36	-151.27
D1.5	$DIST^{V3}-ZSPRD^{100D}_{(2.7,1)}$	7	5	2	67.05	32.29	335.25	64.58	**270.68**	2.71	180.36	-45.78	-1.5	-23.81	71.43	38.67	5.19	2.08	-45.78
D1.6	$DIST^{V3}-ZSPRD^{100D}_{(2.7,0.5)}$	7	5	2	89.84	25.14	449.19	50.29	**398.9**	3.99	211.72	-31.49	-1.14	-18.1	71.43	56.99	8.93	3.57	-31.49
D2.1	$DIST^{V3}-SPRD^{100D}-SMA_{(10,20)}$	21	11	10	51.28	67.9	564.03	679.02	**-114.99**	-1.15	125.01	-188.27	-1.94	-30.8	52.38	-5.48	0.83	0.76	-485.26
D2.2	$DIST^{V3}-SPRD^{100D}-EMA_{(10,20)}$	34	9	25	103.6	85.98	932.42	2149.54	**-1217.12**	-12.17	199.43	-418.01	-1.67	-26.51	26.47	-35.8	0.43	1.2	-829.44
D2.3	$DIST^{V3}-SPRD^{100D}-MACD_{(12,26,9)}$	35	8	27	79.74	69.24	637.93	1869.5	**-1231.57**	-12.32	173.72	-215.13	-2.32	-36.83	22.86	-35.18	0.34	1.15	-1202.18
D2.4	$DIST^{V3}-SPRD^{100D}-RSI_{(14)}$	4	1	3	119.99	224.35	120	673.05	**-553.05**	-5.53	119.99	-413.21	-1.32	-20.95	25	-138.26	0.18	0.53	-167.05
D2.5	$DIST^{V3}-SPRD^{100D}-BB_{(20)}$	23	14	9	94.07	40.01	1317.01	360.05	**956.97**	9.57	496.85	-112.92	-0.94	-14.92	60.87	41.61	3.66	2.35	-133.55
D3	$DIST^{V3}-SPRD^{100D}-DECTREE$	288	130	158	30.59	23.79	3976.46	3759.02	**217.44**	2.17	277.59	-145.17	-3.61	-57.31	45.14	0.76	1.06	1.29	-506.15
D4	$DIST^{V3}-SPRD^{100D}-MLP$	268	119	149	28.48	24.47	3389.62	3646.22	**-256.6**	-2.57	139.29	-180.36	-4.02	-63.82	44.4	-0.96	0.93	1.16	-680.24
Part V: Models derived using the spread obtained from $DIST^{V4}-SPRD^{100D}$																			
E1.1	$DIST^{V4}-ZSPRD^{100D}_{(3,2)}$	4	2	2	42.34	84.37	84.69	168.75	**-84.06**	-0.84	58.31	-151.27	-1.88	-29.84	50	-21.02	0.5	0.5	-151.27
E1.2	$DIST^{V4}-ZSPRD^{100D}_{(3,1)}$	3	2	1	109.64	18.8	219.28	18.8	**200.48**	2	180.36	-18.8	-0.83	-13.18	66.67	66.83	11.67	5.83	-18.8
E1.3	$DIST^{V4}-ZSPRD^{100D}_{(3,0.5)}$	3	2	1	137.18	18.8	274.35	18.8	**255.56**	2.56	211.72	-18.8	-0.57	-9.05	66.67	85.19	14.6	7.3	-18.8
E1.4	$DIST^{V4}-ZSPRD^{100D}_{(2.7,2)}$	10	8	2	30.18	84.37	241.46	168.75	**72.71**	0.73	58.31	-151.27	-2.42	-38.42	80	7.27	1.43	0.36	-151.27
E1.5	$DIST^{V4}-ZSPRD^{100D}_{(2.7,1)}$	7	5	2	67.05	32.29	335.25	64.58	**270.68**	2.71	180.36	-45.78	-1.5	-23.81	71.43	38.67	5.19	2.08	-45.78
E1.6	$DIST^{V4}-ZSPRD^{100D}_{(2.7,0.5)}$	7	5	2	89.84	25.14	449.19	50.29	**398.9**	3.99	211.72	-31.49	-1.14	-18.1	71.43	56.99	8.93	3.57	-31.49
E2.1	$DIST^{V4}-SPRD^{100D}-SMA_{(10,20)}$	21	11	10	51.28	67.9	564.03	679.02	**-114.99**	-1.15	125.01	-188.27	-1.94	-30.8	52.38	-5.48	0.83	0.76	-485.26
E2.2	$DIST^{V4}-SPRD^{100D}-EMA_{(10,20)}$	34	9	25	103.6	85.98	932.42	2149.54	**-1217.12**	-12.17	199.43	-418.01	-1.67	-26.51	26.47	-35.8	0.43	1.2	-829.44
E2.3	$DIST^{V4}-SPRD^{100D}-MACD_{(12,26,9)}$	35	8	27	79.74	69.24	637.93	1869.5	**-1231.57**	-12.32	173.72	-215.13	-2.32	-36.83	22.86	-35.18	0.34	1.15	-1202.18
E2.4	$DIST^{V4}-SPRD^{100D}-RSI_{(14)}$	4	1	3	119.99	224.35	120	673.05	**-553.05**	-5.53	119.99	-413.21	-1.32	-20.95	25	-138.26	0.18	0.53	-167.05
E2.5	$DIST^{V4}-SPRD^{100D}-BB_{(20)}$	23	14	9	94.07	40.01	1317.01	360.05	**956.97**	9.57	496.85	-112.92	-0.94	-14.92	60.87	41.61	3.66	2.35	-133.55
E3	$DIST^{V4}-SPRD^{100D}-DECTREE$	298	132	166	32.29	23.6	4262.17	3917.62	**344.55**	3.45	277.59	-120.96	-3.62	-57.47	44.3	1.16	1.09	1.37	-624.2
E4	$DIST^{V4}-SPRD^{100D}-MLP$	268	119	149	28.48	24.47	3389.62	3646.22	**-256.6**	-2.57	139.29	-180.36	-4.02	-63.82	44.4	-0.96	0.93	1.16	-680.24
Part VI: Models derived using the spread obtained from $JOHANSEN-SPRD^{100D}$																			
F1.1	$JOHANSEN-ZSPRD^{100D}_{(3,2)}$	6	2	4	84.54	38.13	169.08	152.51	**16.57**	0.17	163.9	-121.97	-4.79	-76.04	33.33	2.76	1.11	2.22	-142.2
F1.2	$JOHANSEN-ZSPRD^{100D}_{(3,1)}$	6	2	4	84.54	38.13	169.08	152.51	**16.57**	0.17	163.9	-121.97	-4.79	-76.04	33.33	2.76	1.11	2.22	-142.2
F1.3	$JOHANSEN-ZSPRD^{100D}_{(3,0.5)}$	6	2	4	84.54	38.13	169.08	152.51	**16.57**	0.17	163.9	-121.97	-4.79	-76.04	33.33	2.76	1.11	2.22	-142.2
F1.4	$JOHANSEN-ZSPRD^{100D}_{(2.7,2)}$	8	4	4	45.64	49.72	182.57	198.88	**-16.31**	-0.16	163.9	-121.97	-5.17	-82.07	50	-2.04	0.92	0.92	-184.9
F1.5	$JOHANSEN-ZSPRD^{100D}_{(2.7,1)}$	8	4	4	47.57	49.72	190.3	198.88	**-8.58**	-0.09	163.9	-121.97	-5.12	-81.28	50	-1.07	0.96	0.96	-184.9
F1.6	$JOHANSEN-ZSPRD^{100D}_{(2.7,0.5)}$	7	4	3	49.08	61.14	196.32	183.42	**12.9**	0.13	163.9	-121.97	-4.85	-76.99	57.14	1.84	1.07	0.8	-173.1
F2.1	$JOHANSEN-SPRD^{100D}-SMA_{(10,20)}$	16	8	8	492.33	191.65	3938.67	1533.22	**2405.44**	24.05	2454.54	-747.4	-0.34	-5.4	50	150.34	2.57	2.57	-932.18
F2.2	$JOHANSEN-SPRD^{100D}-EMA_{(10,20)}$	27	13	14	287.2	7113.15	3733.57	99584.05	**-95850.48**	-958.5	1242.9	-94749.63	-0.08	-1.27	48.15	-3549.88	0.04	0.04	-97620.43
F2.3	$JOHANSEN-SPRD^{100D}-MACD_{(12,26,9)}$	33	15	18	299.69	163.7	4495.42	2946.64	**1548.78**	15.49	1335.08	-497.17	-0.17	-2.7	45.45	46.91	1.53	1.83	-995.51
F2.4	$JOHANSEN-SPRD^{100D}-RSI_{(14)}$	3	1	2	263.11	716.91	263.12	1433.82	**-1170.7**	-11.71	263.11	-1379.63	-0.13	-2.06	33.33	-390.27	0.18	0.37	-1433.82
F2.5	$JOHANSEN-SPRD^{100D}-BB_{(20)}$	13	5	8	176.32	207.65	881.59	1661.17	**-779.58**	-7.8	426.36	-822.31	0.38	6.03	38.46	-59.97	0.53	0.85	-1200.6
F3	$JOHANSEN-SPRD^{100D}-DECTREE$	311	153	158	27.66	26.6	4231.32	4202.49	**28.84**	0.29	163.09	-153.85	-3.93	-62.39	49.2	0.09	1.01	1.04	-768.97
F4	$JOHANSEN-SPRD^{100D}-MLP$	265	111	154	26.82	28.44	2976.69	4379.05	**-1402.36**	-14.02	153.96	-200.22	-3.99	-63.34	41.89	-5.29	0.68	0.94	-1618.65
Part VII: Models derived using the spread obtained from $ADF-SPRD^{100D}$																			
G1.1	$ADF-ZSPRD^{100D}_{(3,2)}$	1	1	-	654.55	-	654.55	-	**654.55**	6.55	654.55	-	-	-	100	654.55	654.55	654.55	-
G1.2	$ADF-ZSPRD^{100D}_{(3,1)}$	1	-	1	-	222.44	-	222.44	**-222.44**	-2.22	-	-222.44	-	-	-	-222.44	-	-	-222.44
G1.3	$ADF-ZSPRD^{100D}_{(3,0.5)}$	1	-	1	-	71.31	-	71.31	**-71.31**	-0.71	-	-71.31	-	-	-	-71.31	-	-	-71.31
G1.4	$ADF-ZSPRD^{100D}_{(2.7,2)}$	2	1	1	452.11	960.24	452.1	960.24	**-508.14**	-5.08	452.11	-960.24	-0.33	-5.24	50	-254.07	0.47	0.47	-960.24
G1.5	$ADF-ZSPRD^{100D}_{(2.7,1)}$	2	-	2	-	2431.5	-	4863	**-4863**	-48.63	-	-4404.15	-0.92	-14.6	-	-2431.5	-	-	-4863
G1.6	$ADF-ZSPRD^{100D}_{(2.7,0.5)}$	2	-	2	-	3503.36	-	7006.72	**-7006.72**	-70.07	-	-6705.69	-0.8	-12.7	-	-3503.36	-	-	-7006.72
G2.1	$ADF-SPRD^{100D}-SMA_{(10,20)}$	16	6	10	1297.73	1428.24	7786.38	14282.42	**-6496.04**	-64.96	2226.21	-9400.64	-0.21	-3.33	37.5	-406	0.55	0.91	-13547.92
G2.2	$ADF-SPRD^{100D}-EMA_{(10,20)}$	29	15	14	847.72	2205.43	12715.77	30876.03	**-18160.26**	-181.6	2490.71	-12059.13	-0.27	-4.29	51.72	-626.34	0.41	0.38	-27322.54
G2.3	$ADF-SPRD^{100D}-MACD_{(12,26,9)}$	33	19	14	518.14	1140.42	9844.67	15965.81	**-6121.14**	-61.21	2198.97	-6259.82	-0.2	-3.17	57.58	-185.42	0.62	0.45	-9824.56
G2.4	$ADF-SPRD^{100D}-RSI_{(14)}$	3	2	1	365.29	5488.24	730.59	5488.24	**-4757.65**	-47.58	719.86	-5488.24	-0.5	-7.94	66.67	-1585.69	0.13	0.07	-5488.24
G2.5	$ADF-SPRD^{100D}-BB_{(20)}$	18	5	13	779.27	748.26	3896.32	9727.38	**-5831.05**	-58.31	2724.97	-2924.97	-0.33	-5.24	27.78	-323.91	0.4	1.04	-9161.85
G3	$ADF-SPRD^{100D}-DECTREE$	317	141	176	28.11	27.01	3964.02	4754.1	**-790.08**	-7.9	201.25	-170.39	-3.85	-61.12	44.48	-2.49	0.83	1.04	-1021
G4	$ADF-SPRD^{100D}-MLP$	251	114	137	31.05	23.88	3539.4	3271.75	**267.65**	2.68	201.25	-178.13	-3.64	-57.78	45.42	1.07	1.08	1.3	-451.12
Part VIII: Models derived using the spread obtained from $KALMAN-SPRD^{100D}$																			
H1.1	$KALMAN-ZSPRD^{100D}_{(3,2)}$	2	1	1	258.34	1159.73	258.34	1159.73	**-901.39**	-9.01	258.34	-1159.73	-0.55	-8.73	50	-450.7	0.22	0.22	-1159.73
H1.2	$KALMAN-ZSPRD^{100D}_{(3,1)}$	2	1	1	10.25	216.19	10.25	216.2	**-205.94**	-2.06	10.25	-216.19	-1.26	-20	50	-102.97	0.05	0.05	-216.19
H1.3	$KALMAN-ZSPRD^{100D}_{(3,0.5)}$	2	2	-	99.46	-	198.92	-	**198.92**	1.99	188.67	-	-	-	100	99.46	198.92	99.46	-
H1.4	$KALMAN-ZSPRD^{100D}_{(2.7,2)}$	2	1	1	217.97	1159.73	217.96	1159.73	**-941.77**	-9.42	217.97	-1159.73	-0.59	-9.37	50	-470.88	0.19	0.19	-1159.73
H1.5	$KALMAN-ZSPRD^{100D}_{(2.7,1)}$	2	-	2	-	122.66	-	245.33	**-245.33**	-2.45	-	-216.19	-1.68	-26.67	-	-122.66	-	-	-245.33
H1.6	$KALMAN-ZSPRD^{100D}_{(2.7,0.5)}$	2	1	1	188.67	29.13	188.67	29.14	**159.54**	1.6	188.67	-29.13	-0.13	-2.06	50	79.77	6.48	6.48	-29.13
H2.1	$KALMAN-SPRD^{100D}-SMA_{(10,20)}$	13	6	7	564.26	220.36	3385.58	1542.5	**1843.08**	18.43	1276.43	-356.95	0.09	1.43	46.15	141.74	2.19	2.56	-737.86
H2.2	$KALMAN-SPRD^{100D}-EMA_{(10,20)}$	22	11	11	618.51	283.38	6803.56	3117.18	**3686.37**	36.86	1531.34	-493.31	0.11	1.75	50	167.56	2.18	2.18	-1754.85
H2.3	$KALMAN-SPRD^{100D}-MACD_{(12,26,9)}$	31	8	23	744.17	313.52	5953.32	7211	**-1257.68**	-12.58	3175.98	-1054.37	-0.2	-3.17	25.81	-40.53	0.83	2.37	-5001.15
H2.4	$KALMAN-SPRD^{100D}-RSI_{(14)}$	3	1	2	2025.2	2201.2	2025.2	4402.41	**-2377.2**	-23.77	2025.2	-3915.1	-0.3	-4.76	33.33	-792.54	0.46	0.92	-3915.1
H2.5	$KALMAN-SPRD^{100D}-BB_{(20)}$	11	9	2	257.07	1276.52	2313.61	2553.04	**-239.43**	-2.39	447.12	-2443.19	-0.14	-2.22	81.82	-21.74	0.91	0.2	-2553.04
H3	$KALMAN-SPRD^{100D}-DECTREE$	298	139	159	26.2	24.83	3641.12	3947.36	**-306.23**	-3.06	200.51	-123.2	-4.25	-67.47	46.64	-1.03	0.92	1.06	-996.14
H4	$KALMAN-SPRD^{100D}-MLP$	259	113	146	24.99	24.63	2823.56	3595.62	**-772.07**	-7.72	128.79	-183.49	-4.44	-70.48	43.63	-2.98	0.79	1.01	-875.39
Part IX: Models derived using the spread obtained from $RATIO-SPRD^{100D}$																			
I1.1	$RATIO-ZSPRD^{100D}_{(3,2)}$	3	2	1	46.61	55.84	93.22	55.84	**37.38**	0.37	62.08	-55.84	-2.28	-36.19	66.67	12.46	1.67	0.83	-55.84
I1.2	$RATIO-ZSPRD^{100D}_{(3,1)}$	3	3	-	61.11	-	183.32	-	**183.32**	1.83	109.73	-	-1.74	-27.62	100	61.11	183.32	61.11	-
I1.3	$RATIO-ZSPRD^{100D}_{(3,0.5)}$	3	2	1	109.95	235.91	219.91	235.91	**-16.01**	-0.16	152.22	-235.91	-0.77	-12.22	66.67	-5.32	0.93	0.47	-235.91
I1.4	$RATIO-ZSPRD^{100D}_{(2.7,2)}$	7	5	2	66.77	34.49	333.87	68.98	**264.89**	2.65	183.49	-66.53	-1.49	-23.65	71.43	37.84	4.84	1.94	-66.53
I1.5	$RATIO-ZSPRD^{100D}_{(2.7,1)}$	7	6	1	105.04	28.58	630.22	28.58	**601.64**	6.02	260.13	-28.58	-0.75	-11.91	85.71	85.94	22.05	3.67	-28.58
I1.6	$RATIO-ZSPRD^{100D}_{(2.7,0.5)}$	6	5	1	163.85	326.93	819.24	326.93	**492.31**	4.92	430.66	-326.93	-0.29	-4.6	83.33	82.04	2.51	0.5	-326.93
I2.1	$RATIO-SPRD^{100D}-SMA_{(10,20)}$	15	5	10	70.14	83.41	350.7	834.05	**-483.35**	-4.83	133.25	-207.84	-1.95	-30.96	33.33	-32.23	0.42	0.84	-799.95
I2.2	$RATIO-SPRD^{100D}-EMA_{(10,20)}$	26	6	20	100.98	78.1	605.88	1562.04	**-956.15**	-9.56	204.53	-418.01	-1.66	-26.35	23.08	-36.77	0.39	1.29	-770.53
I2.3	$RATIO-SPRD^{100D}-MACD_{(12,26,9)}$	39	16	23	80.72	84.2	1291.49	1936.62	**-645.13**	-6.45	268.59	-204.97	-1.58	-25.08	41.03	-16.53	0.67	0.96	-777.07
I2.4	$RATIO-SPRD^{100D}-RSI_{(14)}$	3	1	2	156.02	621.1	156.02	1242.2	**-1086.19**	-10.86	156.02	-828.99	-1.04	-16.51	33.33	-362.09	0.13	0.25	-828.99
I2.5	$RATIO-SPRD^{100D}-BB_{(20)}$	16	10	6	40.9	55.74	409.01	334.44	**74.57**	0.75	83.48	-70.04	-2.68	-42.54	62.5	4.66	1.22	0.73	-146.53
I3	$RATIO-SPRD^{100D}-DECTREE$	287	103	184	29.03	19.99	2990.36	3678.99	**-688.63**	-6.89	313.53	-82.96	-4.19	-66.51	35.89	-2.4	0.81	1.45	-828.99
I4	$RATIO-SPRD^{100D}-MLP$	261	89	172	32.75	21.63	2914.56	3719.69	**-805.13**	-8.05	214.61	-183.49	-3.97	-63.02	34.1	-3.08	0.78	1.51	-1023.74
Part X: Models derived using the close price of VO.N																			
CLS-SYM-1.1	$CLOSE^{VO.N}-SMA_{(10,20)}$	15	5	10	407.5	131.94	2037.52	1319.42	**718.1**	7.18	1345.66	-357.26	-0.07	-1.11	33.33	47.86	1.54	3.09	-888.12
CLS-SYM-1.2	$CLOSE^{VO.N}-EMA_{(10,20)}$	20	6	14	305.56	123.3	1833.38	1726.2	**107.17**	1.07	700.63	-218.39	-0.27	-4.29	30	5.36	1.06	2.48	-812.37
CLS-SYM-1.3	$CLOSE^{VO.N}-MACD_{(12,26,9)}$	30	12	18	235.68	119.41	2828.19	2149.34	**678.86**	6.79	1213.06	-330.07	-0.19	-3.02	40	22.63	1.32	1.97	-845.26
CLS-SYM-1.4	$CLOSE^{VO.N}-RSI_{(14)}$	5	2	3	464.59	648.69	929.17	1946.08	**-1016.91**	-10.17	781.75	-1353.4	-0.35	-5.56	40	-203.38	0.48	0.72	-1353.4
CLS-SYM-1.5	$CLOSE^{VO.N}-BB_{(20)}$	15	13	2	85.35	600.28	1109.6	1200.56	**-90.96**	-0.91	190.76	-984.33	-0.29	-4.6	86.67	-6.04	0.92	0.14	-984.33
Part XI: Models derived using the close price of VXUS.N																			
CLS-SYM-2.1	$CLOSE^{VXUS.N}-SMA_{(10,20)}$	15	6	9	314.7	147.73	1888.19	1329.58	**558.62**	5.59	928.16	-483.97	-0.12	-1.9	40	37.24	1.42	2.13	-710.8
CLS-SYM-2.2	$CLOSE^{VXUS.N}-EMA_{(10,20)}$	23	6	17	500.43	151.67	3002.58	2578.36	**424.22**	4.24	1067.79	-550.04	-0.15	-2.38	26.09	18.46	1.16	3.3	-1087.54
CLS-SYM-2.3	$CLOSE^{VXUS.N}-MACD_{(12,26,9)}$	32	11	21	188.51	103.43	2073.65	2171.98	**-98.33**	-0.98	939.15	-336.67	-0.37	-5.87	34.38	-3.06	0.95	1.82	-1391.6
CLS-SYM-2.4	$CLOSE^{VXUS.N}-RSI_{(14)}$	6	3	3	309.07	270.45	927.22	811.36	**115.86**	1.16	384.77	-577.08	-0.16	-2.54	50	19.31	1.14	1.14	-577.08
CLS-SYM-2.5	$CLOSE^{VXUS.N}-BB_{(20)}$	19	12	7	67.21	145.66	806.56	1019.65	**-213.09**	-2.13	191.4	-832.35	-0.42	-6.67	63.16	-11.21	0.79	0.46	-832.35

Table D.2.22: This table presents the back-test metrics for the pair $VWO.N/XLE.N$ based on a 30-day rolling window. The table is subdivided into eleven parts, and in each of these parts, we present the back-test metrics and the trading strategies which use the spread derived from various models. In Part I, the spread is derived from the $DIST^{V1.1}$ model, in Part II from the $DIST^{V1.2}$ model, in Part III from the $DIST^{V2}$ model, in Part IV from the $DIST^{V3}$ model, in Part V from the $DIST^{V4}$ model, in Part VI from the $JOHANSEN-SPRD$ model, in Part VIII from the $ADF-SPRD$ model, in from the $DIST^{V2}$ model, in Part VIII from the $KALMAN-SPRD$ model, and in Part IX from the $RATIO-SPRD$ model. In Part X and XI, we present the back-test metrics of the trading strategies which use the close price of VWO.N, and XLE.N, respectively. All $ numbers reported below are in USD.

(I) Trading Strategy Code	(II) Model Name	(III) Total Number of Trades	(IV) Number of Winning Trades	(V) Number of Loosing Trades	(VI) Average Profit per Trade ($)	(VII) Average Loss per Trade ($)	(VIII) Gross Profit ($)	(IX) Gross Loss ($)	(X) Net Profit ($)	(XI) ROI (%)	(XII) Max P&L ($)	(XIII) Min P&L ($)	(XIV) Daily Sharpe Ratio	(XV) Annualized Sharpe Ratio	(XVI) Hit Ratio	(XVII) Expectancy	(XVIII) Profit Factor	(XIX) Realized Risk Reward Ratio	(XX) Max Drawdown ($)
Part I: Models derived using the spread obtained from $DIST^{V1.1}-SPRD^{30D}$																			
A1.1	$DIST^{V1.1}-ZSPRD^{30D}_{(3,2)}$	7	3	4	150.52	124.14	451.57	496.56	**-44.99**	-0.45	243.09	-338.73	-0.85	-13.49	42.86	-6.42	0.91	1.21	-481.62
A1.2	$DIST^{V1.1}-ZSPRD^{30D}_{(3,1)}$	5	3	2	472.71	247.17	1418.13	494.35	**923.78**	9.24	971.96	-338.73	0.07	1.11	60	184.76	2.87	1.91	-338.73
A1.3	$DIST^{V1.1}-ZSPRD^{30D}_{(3,0.5)}$	5	3	2	392.16	278.29	1176.49	556.59	**619.9**	6.2	817.16	-338.73	-0.06	-0.95	60	123.98	2.11	1.41	-338.73
A1.4	$DIST^{V1.1}-ZSPRD^{30D}_{(2.7,2)}$	14	5	9	127.78	128.59	638.92	1157.35	**-518.42**	-5.18	243.09	-428.48	-1.13	-17.94	35.71	-37.04	0.55	0.99	-715.99
A1.5	$DIST^{V1.1}-ZSPRD^{30D}_{(2.7,1)}$	12	4	8	438.77	226.88	1755.09	1815.01	**-59.91**	-0.6	971.96	-435.14	-0.39	-6.19	33.33	-5.02	0.97	1.93	-863.61
A1.6	$DIST^{V1.1}-ZSPRD^{30D}_{(2.7,0.5)}$	12	5	7	350.62	224.06	1753.11	1568.4	**184.71**	1.85	817.16	-428.48	-0.39	-6.19	41.67	15.41	1.12	1.56	-657.59
A2.1	$DIST^{V1.1}-SPRD^{30D}-SMA_{(10,20)}$	20	15	5	194.38	426.32	2915.68	2131.62	**784.06**	7.84	411.98	-1255.4	-0.3	-4.76	75	39.2	1.37	0.46	-1538.4
A2.2	$DIST^{V1.1}-SPRD^{30D}-EMA_{(10,20)}$	27	20	7	145.04	471.82	2900.74	3302.71	**-401.98**	-4.02	414.96	-1146.37	-0.47	-7.46	74.07	-14.91	0.88	0.31	-2257
A2.3	$DIST^{V1.1}-SPRD^{30D}-MACD_{(12,26,9)}$	37	29	8	156.42	488.72	4536.06	3909.79	**626.27**	6.26	474.78	-993.95	-0.41	-6.51	78.38	16.94	1.16	0.32	-993.95
A2.4	$DIST^{V1.1}-SPRD^{30D}-RSI_{(14)}$	4	1	3	1213.31	649.77	1213.31	1949.31	**-736**	-7.36	1213.31	-1267.67	-0.32	-5.08	25	-184	0.62	1.87	-1801.61
A2.5	$DIST^{V1.1}-SPRD^{30D}-BB_{(20)}$	14	4	10	225.16	291.64	900.64	2916.39	**-2015.75**	-20.16	572.77	-650.1	-0.89	-14.13	28.57	-143.99	0.31	0.77	-2296.48
A3	$DIST^{V1.1}-SPRD^{30D}-DECTREE$	312	165	147	71.3	93.17	11764.34	13695.76	**-1931.41**	-19.31	495.14	-1065.21	-1.22	-19.37	52.88	-6.2	0.86	0.77	-2221.92
A4	$DIST^{V1.1}-SPRD^{30D}-MLP$	275	159	116	76.48	103.38	12160.32	11992.48	**167.83**	1.68	830.64	-565.95	-1.16	-18.41	57.82	0.61	1.01	0.74	-1930.33
Part II: Models derived using the spread obtained from $DIST^{V1.2}-SPRD^{30D}$																			
B1.1	$DIST^{V1.2}-ZSPRD^{30D}_{(3,2)}$	7	2	5	76.96	64.1	153.92	320.48	**-166.57**	-1.67	138.83	-98.24	-2.12	-33.65	28.57	-23.8	0.48	1.2	-320.48
B1.2	$DIST^{V1.2}-ZSPRD^{30D}_{(3,1)}$	7	3	4	54.73	114.05	164.2	456.19	**-291.98**	-2.92	81.48	-207.19	-1.62	-25.72	42.86	-41.71	0.36	0.48	-385.41
B1.3	$DIST^{V1.2}-ZSPRD^{30D}_{(3,0.5)}$	7	3	4	54.73	144.52	164.2	578.09	**-413.89**	-4.14	81.48	-233.1	-1.72	-27.3	42.86	-59.12	0.28	0.38	-507.31
B1.4	$DIST^{V1.2}-ZSPRD^{30D}_{(2.7,2)}$	15	6	9	117.21	94.72	703.24	852.5	**-149.26**	-1.49	218.82	-226.93	-1.25	-19.84	40	-9.95	0.82	1.24	-546.09
B1.5	$DIST^{V1.2}-ZSPRD^{30D}_{(2.7,1)}$	14	8	6	155.68	95.49	1245.41	572.94	**672.47**	6.72	694.28	-280.45	-0.47	-7.46	57.14	48.03	2.17	1.63	-494.68
B1.6	$DIST^{V1.2}-ZSPRD^{30D}_{(2.7,0.5)}$	14	7	7	224.76	135.94	1573.32	951.58	**621.74**	6.22	848.49	-411.12	-0.36	-5.71	50	44.41	1.65	1.65	-806.1
B2.1	$DIST^{V1.2}-SPRD^{30D}-SMA_{(10,20)}$	21	12	9	285.3	236.68	3423.63	2130.12	**1293.51**	12.94	963.01	-992.39	-0.23	-3.65	57.14	61.58	1.61	1.21	-1199.69
B2.2	$DIST^{V1.2}-SPRD^{30D}-EMA_{(10,20)}$	25	13	12	241.36	261.61	3137.65	3139.28	**-1.63**	-0.02	1150.76	-778.62	-0.36	-5.71	52	-0.07	1	0.92	-1273.76
B2.3	$DIST^{V1.2}-SPRD^{30D}-MACD_{(12,26,9)}$	32	17	15	191.84	231.9	3261.24	3478.56	**-217.32**	-2.17	1350.54	-488.88	-0.48	-7.62	53.12	-6.81	0.94	0.83	-1749.33
B2.4	$DIST^{V1.2}-SPRD^{30D}-RSI_{(14)}$	5	3	2	432.76	538.52	1298.28	1077.04	**221.25**	2.21	1210.36	-781.09	-0.15	-2.38	60	44.25	1.21	0.8	-781.09
B2.5	$DIST^{V1.2}-SPRD^{30D}-BB_{(20)}$	14	10	4	173.07	113.77	1730.66	455.08	**1275.59**	12.76	590.13	-186.92	-0.27	-4.29	71.43	91.12	3.8	1.52	-222.96
B3	$DIST^{V1.2}-SPRD^{30D}-DECTREE$	314	162	152	101.4	78.5	16426.87	11931.72	**4495.14**	44.95	797.43	-429.98	-1	-15.87	51.59	14.31	1.38	1.29	-1900.95
B4	$DIST^{V1.2}-SPRD^{30D}-MLP$	220	121	99	123.43	101.49	14935.54	10047.55	**4887.99**	48.88	983.88	-602.64	-0.77	-12.22	55	22.22	1.49	1.22	-1254.59
Part III: Models derived using the spread obtained from $DIST^{V2}-SPRD^{30D}$																			
C1.1	$DIST^{V2}-ZSPRD^{30D}_{(3,2)}$	7	4	3	124.14	150.52	496.56	451.57	**44.99**	0.45	338.73	-243.09	-0.78	-12.38	57.14	6.42	1.1	0.82	-299.1
C1.2	$DIST^{V2}-ZSPRD^{30D}_{(3,1)}$	5	2	3	247.17	472.71	494.35	1418.13	**-923.78**	-9.24	338.73	-971.96	-0.67	-10.64	40	-184.76	0.35	0.52	-1079.4
C1.3	$DIST^{V2}-ZSPRD^{30D}_{(3,0.5)}$	5	2	3	278.29	392.16	556.59	1176.49	**-619.9**	-6.2	338.73	-817.16	-0.59	-9.37	40	-123.98	0.47	0.71	-837.75
C1.4	$DIST^{V2}-ZSPRD^{30D}_{(2.7,2)}$	14	9	5	128.59	127.78	1157.35	638.92	**518.42**	5.18	428.48	-243.09	-0.69	-10.95	64.29	37.04	1.81	1.01	-299.1
C1.5	$DIST^{V2}-ZSPRD^{30D}_{(2.7,1)}$	12	8	4	226.88	438.77	1815.01	1755.09	**59.91**	0.6	435.14	-971.96	-0.37	-5.87	66.67	5.02	1.03	0.52	-971.96
C1.6	$DIST^{V2}-ZSPRD^{30D}_{(2.7,0.5)}$	12	7	5	224.06	350.62	1568.4	1753.11	**-184.71**	-1.85	428.48	-817.16	-0.48	-7.62	58.33	-15.41	0.89	0.64	-1095.47
C2.1	$DIST^{V2}-SPRD^{30D}-SMA_{(10,20)}$	20	5	15	426.32	194.38	2131.62	2915.68	**-784.06**	-7.84	1255.4	-411.98	-0.51	-8.1	25	-39.2	0.73	2.19	-1305
C2.2	$DIST^{V2}-SPRD^{30D}-EMA_{(10,20)}$	27	7	20	471.82	145.04	3302.71	2900.74	**401.98**	4.02	1146.37	-414.96	-0.39	-6.19	25.93	14.91	1.14	3.25	-1323.02
C2.3	$DIST^{V2}-SPRD^{30D}-MACD_{(12,26,9)}$	37	8	29	488.72	156.42	3909.79	4536.06	**-626.27**	-6.26	993.95	-474.78	-0.52	-8.25	21.62	-16.94	0.86	3.12	-1233.83
C2.4	$DIST^{V2}-SPRD^{30D}-RSI_{(14)}$	4	3	1	649.77	1213.31	1949.31	1213.31	**736**	7.36	1267.67	-1213.31	0.03	0.48	75	184	1.61	0.54	-1213.31
C2.5	$DIST^{V2}-SPRD^{30D}-BB_{(20)}$	14	10	4	291.64	225.16	2916.39	900.64	**2015.75**	20.16	650.1	-572.77	-0.02	-0.32	71.43	143.99	3.24	1.3	-572.77
C3	$DIST^{V2}-SPRD^{30D}-DECTREE$	332	161	171	70.2	89.56	11302.58	15315.06	**-4012.48**	-40.12	495.14	-776.54	-1.39	-22.07	48.49	-12.09	0.74	0.78	-4712.82
C4	$DIST^{V2}-SPRD^{30D}-MLP$	223	129	94	78.43	101.27	10117.36	9519.68	**597.68**	5.98	409.19	-666.35	-1.11	-17.62	57.85	2.68	1.06	0.77	-2254.25
Part IV: Models derived using the spread obtained from $DIST^{V3}-SPRD^{30D}$																			
D1.1	$DIST^{V3}-ZSPRD^{30D}_{(3,2)}$	6	4	2	141.54	83.73	566.16	167.46	**398.7**	3.99	274.83	-138.93	-0.61	-9.68	66.67	66.46	3.38	1.69	-138.93
D1.2	$DIST^{V3}-ZSPRD^{30D}_{(3,1)}$	6	3	3	136.47	228.23	409.42	684.68	**-275.27**	-2.75	150.02	-569.46	-0.72	-11.43	50	-45.88	0.6	0.6	-606
D1.3	$DIST^{V3}-ZSPRD^{30D}_{(3,0.5)}$	6	3	3	253.82	259.44	761.47	778.33	**-16.86**	-0.17	417.7	-569.46	-0.45	-7.14	50	-2.81	0.98	0.98	-699.65
D1.4	$DIST^{V3}-ZSPRD^{30D}_{(2.7,2)}$	11	8	3	118.91	98.74	951.25	296.21	**655.04**	6.55	316.1	-138.93	-0.73	-11.59	72.73	59.55	3.21	1.2	-138.93
D1.5	$DIST^{V3}-ZSPRD^{30D}_{(2.7,1)}$	11	8	3	164.56	290.82	1316.48	872.46	**444.02**	4.44	316.1	-569.46	-0.45	-7.14	72.73	40.38	1.51	0.57	-569.46
D1.6	$DIST^{V3}-ZSPRD^{30D}_{(2.7,0.5)}$	11	8	3	218.3	323.7	1746.41	971.1	**775.32**	7.75	417.7	-569.46	-0.28	-4.44	72.73	70.5	1.8	0.67	-576.31
D2.1	$DIST^{V3}-SPRD^{30D}-SMA_{(10,20)}$	22	5	17	577.6	248.45	2887.99	4223.61	**-1335.61**	-13.36	1740.81	-1276.21	-0.39	-6.19	22.73	-60.69	0.68	2.32	-2773.62
D2.2	$DIST^{V3}-SPRD^{30D}-EMA_{(10,20)}$	43	9	34	452.85	195.53	4075.69	6647.91	**-2572.22**	-25.72	836.21	-1320.2	-0.58	-9.21	20.93	-59.82	0.61	2.32	-3061.49
D2.3	$DIST^{V3}-SPRD^{30D}-MACD_{(12,26,9)}$	48	12	36	211.2	169.21	2534.41	6091.69	**-3557.28**	-35.57	702.55	-730.55	-0.93	-14.76	25	-74.11	0.42	1.25	-4173.66
D2.4	$DIST^{V3}-SPRD^{30D}-RSI_{(14)}$	2	1	1	227.48	2319	227.48	2319	**-2091.51**	-20.92	227.48	-2319	-0.67	-10.64	50	-1045.76	0.1	0.1	-2319
D2.5	$DIST^{V3}-SPRD^{30D}-BB_{(20)}$	24	17	7	96.26	184.93	1636.46	1294.53	**341.94**	3.42	202.93	-494.63	-0.82	-13.02	70.83	14.24	1.26	0.52	-618.57
D3	$DIST^{V3}-SPRD^{30D}-DECTREE$	338	164	174	83.74	82.89	13733.32	14422.58	**-689.26**	-6.89	981.37	-429.05	-1.26	-20	48.52	-2.04	0.95	1.01	-3743.39
D4	$DIST^{V3}-SPRD^{30D}-MLP$	298	127	171	93.18	72.69	11833.54	12430.59	**-597.05**	-5.97	1062.21	-526.04	-1.09	-17.3	42.62	-2	0.95	1.28	-2730.59
Part V: Models derived using the spread obtained from $DIST^{V4}-SPRD^{30D}$																			
E1.1	$DIST^{V4}-ZSPRD^{30D}_{(3,2)}$	6	4	2	141.54	83.73	566.16	167.46	**398.7**	3.99	274.83	-138.93	-0.61	-9.68	66.67	66.46	3.38	1.69	-138.93
E1.2	$DIST^{V4}-ZSPRD^{30D}_{(3,1)}$	6	3	3	136.47	228.23	409.42	684.68	**-275.27**	-2.75	150.02	-569.46	-0.72	-11.43	50	-45.88	0.6	0.6	-606
E1.3	$DIST^{V4}-ZSPRD^{30D}_{(3,0.5)}$	6	3	3	253.82	259.44	761.47	778.33	**-16.86**	-0.17	417.7	-569.46	-0.45	-7.14	50	-2.81	0.98	0.98	-699.65
E1.4	$DIST^{V4}-ZSPRD^{30D}_{(2.7,2)}$	11	8	3	118.91	98.74	951.25	296.21	**655.04**	6.55	316.1	-138.93	-0.73	-11.59	72.73	59.55	3.21	1.2	-138.93
E1.5	$DIST^{V4}-ZSPRD^{30D}_{(2.7,1)}$	11	8	3	164.56	290.82	1316.48	872.46	**444.02**	4.44	316.1	-569.46	-0.45	-7.14	72.73	40.38	1.51	0.57	-569.46
E1.6	$DIST^{V4}-ZSPRD^{30D}_{(2.7,0.5)}$	11	8	3	218.3	323.7	1746.41	971.1	**775.32**	7.75	417.7	-569.46	-0.28	-4.44	72.73	70.5	1.8	0.67	-576.31
E2.1	$DIST^{V4}-SPRD^{30D}-SMA_{(10,20)}$	22	4	18	708.68	247.89	2834.71	4462.03	**-1627.32**	-16.27	1740.81	-1276.21	-0.42	-6.67	18.18	-73.99	0.64	2.86	-3066.25
E2.2	$DIST^{V4}-SPRD^{30D}-EMA_{(10,20)}$	43	9	34	452.85	195.53	4075.69	6647.91	**-2572.22**	-25.72	836.21	-1320.2	-0.58	-9.21	20.93	-59.82	0.61	2.32	-3061.49
E2.3	$DIST^{V4}-SPRD^{30D}-MACD_{(12,26,9)}$	48	12	36	211.2	169.21	2534.41	6091.69	**-3557.28**	-35.57	702.55	-730.55	-0.93	-14.76	25	-74.11	0.42	1.25	-4173.66
E2.4	$DIST^{V4}-SPRD^{30D}-RSI_{(14)}$	2	1	1	227.48	2319	227.48	2319	**-2091.51**	-20.92	227.48	-2319	-0.67	-10.64	50	-1045.76	0.1	0.1	-2319
E2.5	$DIST^{V4}-SPRD^{30D}-BB_{(20)}$	24	17	7	96.26	184.93	1636.46	1294.53	**341.94**	3.42	202.93	-494.63	-0.82	-13.02	70.83	14.24	1.26	0.52	-618.57
E3	$DIST^{V4}-SPRD^{30D}-DECTREE$	316	146	170	88.52	76.29	12923.65	12970	**-46.35**	-0.46	595.44	-338.73	-1.32	-20.95	46.2	-0.15	1	1.16	-3004.46
E4	$DIST^{V4}-SPRD^{30D}-MLP$	265	115	150	114.08	81.18	13119.6	12177.64	**941.96**	9.42	1247.92	-726.55	-0.85	-13.49	43.4	3.56	1.08	1.41	-2899.25
Part VI: Models derived using the spread obtained from $JOHANSEN-SPRD^{30D}$																			
F1.1	$JOHANSEN-ZSPRD^{30D}_{(3,2)}$	24	10	14	44	497.56	440	6965.79	**-6525.79**	-65.26	90.78	-5456.16	-0.27	-4.29	41.67	-271.89	0.06	0.09	-6729.23
F1.2	$JOHANSEN-ZSPRD^{30D}_{(3,1)}$	21	9	12	58.16	289.79	523.41	3477.48	**-2954.08**	-29.54	112.36	-2411.92	-0.35	-5.56	42.86	-140.66	0.15	0.2	-3257.39
F1.3	$JOHANSEN-ZSPRD^{30D}_{(3,0.5)}$	20	9	11	58.16	284.13	523.41	3125.45	**-2602.04**	-26.02	112.36	-2048.27	-0.36	-5.71	45	-130.1	0.17	0.2	-2905.35
F1.4	$JOHANSEN-ZSPRD^{30D}_{(2.7,2)}$	27	12	15	41.74	689.38	500.89	10340.72	**-9839.83**	-98.4	90.78	-5456.16	-0.32	-5.08	44.44	-364.47	0.05	0.06	-10042.51
F1.5	$JOHANSEN-ZSPRD^{30D}_{(2.7,1)}$	23	11	12	54.48	569.17	599.23	6830.06	**-6230.83**	-62.31	112.36	-3486.36	-0.4	-6.35	47.83	-270.88	0.09	0.1	-6570.66
F1.6	$JOHANSEN-ZSPRD^{30D}_{(2.7,0.5)}$	22	11	11	54.48	588.91	599.23	6478.02	**-5878.8**	-58.79	112.36	-3486.36	-0.41	-6.51	50	-267.22	0.09	0.09	-6218.63
F2.1	$JOHANSEN-SPRD^{30D}-SMA_{(10,20)}$	33	19	14	703.85	901.65	13373.09	12623.16	**749.92**	7.5	6869.33	-6944.93	-0.19	-3.02	57.58	22.79	1.06	0.78	-8287.38
F2.2	$JOHANSEN-SPRD^{30D}-EMA_{(10,20)}$	36	18	18	830.24	354.08	14944.32	6373.39	**8570.93**	85.71	7389.51	-1273.58	-0.12	-1.9	50	238.08	2.34	2.34	-2864.52
F2.3	$JOHANSEN-SPRD^{30D}-MACD_{(12,26,9)}$	40	24	16	510.21	12193.98	12244.95	195103.6	**-182858.65**	-1828.59	3486.36	-191555.27	-0.16	-2.54	60	-4571.47	0.06	0.04	-192178.79
F2.4	$JOHANSEN-SPRD^{30D}-RSI_{(14)}$	6	2	4	391.52	681.22	783.04	2724.88	**-1941.84**	-19.42	513.94	-1083.69	-0.6	-9.52	33.33	-323.68	0.29	0.57	-2062.31
F2.5	$JOHANSEN-SPRD^{30D}-BB_{(20)}$	23	6	17	227.87	702.37	1367.22	11940.29	**-10573.08**	-105.73	493.4	-4300.55	-0.34	-5.4	26.09	-459.67	0.11	0.32	-11208.86
F3	$JOHANSEN-SPRD^{30D}-DECTREE$	325	148	177	96.37	84.83	14262.17	15014.86	**-752.7**	-7.53	776.54	-350.69	-1.19	-18.89	45.54	-2.31	0.95	1.14	-2275.77
F4	$JOHANSEN-SPRD^{30D}-MLP$	236	126	110	96.88	100.04	12206.54	11004.38	**1202.17**	12.02	649.12	-795.12	-0.97	-15.4	53.39	5.09	1.11	0.97	-2395.9
Part VII: Models derived using the spread obtained from $ADF-SPRD^{30D}$																			
G1.1	$ADF-ZSPRD^{30D}_{(3,2)}$	8	4	4	98.31	81.85	393.23	327.39	**65.84**	0.66	197.68	-109.55	-1.28	-20.32	50	8.23	1.2	1.2	-182.37
G1.2	$ADF-ZSPRD^{30D}_{(3,1)}$	7	3	4	277.44	214.38	832.31	857.53	**-25.22**	-0.25	394.19	-497.67	-0.32	-5.08	42.86	-3.59	0.97	1.29	-857.53
G1.3	$ADF-ZSPRD^{30D}_{(3,0.5)}$	7	3	4	196.2	226.93	588.6	907.72	**-319.12**	-3.19	344.19	-372.31	-0.78	-12.38	42.86	-45.58	0.65	0.86	-907.72
G1.4	$ADF-ZSPRD^{30D}_{(2.7,2)}$	11	7	4	93.12	92.25	651.86	369	**282.86**	2.83	197.68	-131.39	-0.99	-15.72	63.64	25.72	1.77	1.01	-131.39
G1.5	$ADF-ZSPRD^{30D}_{(2.7,1)}$	10	3	7	364.24	191.72	1092.73	1342.07	**-249.34**	-2.49	558.04	-497.67	-0.48	-7.62	30	-24.93	0.81	1.9	-1176.46
G1.6	$ADF-ZSPRD^{30D}_{(2.7,0.5)}$	10	4	6	439.09	191.78	1756.34	1150.66	**605.68**	6.06	908.71	-372.31	0.16	2.54	40	60.57	1.53	2.29	-956.34
G2.1	$ADF-SPRD^{30D}-SMA_{(10,20)}$	23	14	9	330.27	486.78	4623.75	4381.04	**242.71**	2.43	759.86	-1176.23	-0.13	-2.06	60.87	10.56	1.06	0.68	-1917
G2.2	$ADF-SPRD^{30D}-EMA_{(10,20)}$	39	27	12	183.03	447.09	4941.68	5365.12	**-423.44**	-4.23	1399.57	-1148.31	-0.21	-3.33	69.23	-10.86	0.92	0.41	-2428.93
G2.3	$ADF-SPRD^{30D}-MACD_{(12,26,9)}$	42	29	13	167.15	458.24	4847.27	5957.07	**-1109.8**	-11.1	682.74	-1372.14	-0.43	-6.83	69.05	-26.41	0.81	0.36	-2955.67
G2.4	$ADF-SPRD^{30D}-RSI_{(14)}$	3	2	1	1554.13	567.26	3108.27	567.26	**2541**	25.41	2817.41	-567.26	0.32	5.08	66.67	847.07	5.48	2.74	-567.26
G2.5	$ADF-SPRD^{30D}-BB_{(20)}$	17	5	12	357.27	1003.08	1786.36	12036.92	**-10250.56**	-102.51	755.58	-10627.21	0.23	3.65	29.41	-603	0.15	0.36	-11040.62
G3	$ADF-SPRD^{30D}-DECTREE$	326	157	169	85.06	86.14	13354.76	14557.35	**-1202.59**	-12.03	787.62	-429.98	-1.26	-20	48.16	-3.69	0.92	0.99	-3152.5
G4	$ADF-SPRD^{30D}-MLP$	251	126	125	123.96	76.89	15618.61	9611.77	**6006.84**	60.07	660.34	-429.98	-0.86	-13.65	50.2	23.93	1.62	1.61	-1266.05
Part VIII: Models derived using the spread obtained from $KALMAN-SPRD^{30D}$																			
H1.1	$KALMAN-ZSPRD^{30D}_{(3,2)}$	7	3	4	97.36	278.65	292.07	1114.61	**-822.54**	-8.23	150.63	-919.22	-0.75	-11.91	42.86	-117.5	0.26	0.35	-988.09
H1.2	$KALMAN-ZSPRD^{30D}_{(3,1)}$	6	2	4	237.78	405.15	475.56	1620.61	**-1145.05**	-11.45	385.22	-1017.29	-0.7	-11.11	33.33	-190.86	0.29	0.59	-1620.61
H1.3	$KALMAN-ZSPRD^{30D}_{(3,0.5)}$	5	3	2	232.54	768.44	697.63	1536.89	**-839.26**	-8.39	452.85	-1492.87	-0.41	-6.51	60	-167.85	0.45	0.3	-1536.89
H1.4	$KALMAN-ZSPRD^{30D}_{(2.7,2)}$	11	5	6	183.38	250.03	916.91	1500.2	**-583.29**	-5.83	331.9	-991.26	-0.6	-9.52	45.45	-53.05	0.61	0.73	-994.57
H1.5	$KALMAN-ZSPRD^{30D}_{(2.7,1)}$	10	5	5	302.9	435.71	1514.5	2178.55	**-664.05**	-6.64	548.37	-1081.65	-0.43	-6.83	50	-66.4	0.7	0.7	-1473.15
H1.6	$KALMAN-ZSPRD^{30D}_{(2.7,0.5)}$	9	6	3	274.42	616.06	1646.49	1848.18	**-201.68**	-2.02	535.79	-1492.87	-0.29	-4.6	66.67	-22.38	0.89	0.45	-1492.87
H2.1	$KALMAN-SPRD^{30D}-SMA_{(10,20)}$	15	7	8	625.58	80.27	4379.03	642.16	**3736.87**	37.37	1458.92	-306.21	0.2	3.17	46.67	249.15	6.82	7.79	-323.6
H2.2	$KALMAN-SPRD^{30D}-EMA_{(10,20)}$	16	5	11	764.87	217.94	3824.37	2397.38	**1426.99**	14.27	1334.19	-404.4	-0.12	-1.9	31.25	89.19	1.6	3.51	-876.92
H2.3	$KALMAN-SPRD^{30D}-MACD_{(12,26,9)}$	32	13	19	336.06	157.8	4368.74	2998.15	**1370.59**	13.71	1063.65	-541.68	-0.31	-4.92	40.62	42.81	1.46	2.13	-1194.27
H2.4	$KALMAN-SPRD^{30D}-RSI_{(14)}$	4	1	3	997.09	967.41	997.08	2902.24	**-1905.15**	-19.05	997.09	-1478.92	-0.58	-9.21	25	-476.29	0.34	1.03	-2902.24
H2.5	$KALMAN-SPRD^{30D}-BB_{(20)}$	12	7	5	127.02	385.44	889.11	1927.18	**-1038.07**	-10.38	219.66	-1135.39	-0.7	-11.11	58.33	-86.52	0.46	0.33	-1697.06
H3	$KALMAN-SPRD^{30D}-DECTREE$	318	197	121	73.48	98.86	14476.07	11961.66	**2514.42**	25.14	429.98	-1291	-1.04	-16.51	61.95	7.91	1.21	0.74	-1450.86
H4	$KALMAN-SPRD^{30D}-MLP$	228	135	93	76.16	117.78	10282.13	10953.28	**-671.15**	-6.71	1080.93	-1248.76	-0.95	-15.08	59.21	-2.94	0.94	0.65	-2881.89
Part IX: Models derived using the spread obtained from $RATIO-SPRD^{30D}$																			
I1.1	$RATIO-ZSPRD^{30D}_{(3,2)}$	5	3	2	132.33	571.98	396.99	1143.96	**-746.96**	-7.47	197.18	-1024.58	-0.6	-9.52	60	-149.39	0.35	0.23	-1024.58
I1.2	$RATIO-ZSPRD^{30D}_{(3,1)}$	4	3	1	274.37	971.96	823.11	971.96	**-148.85**	-1.49	409.19	-971.96	-0.3	-4.76	75	-37.21	0.85	0.28	-971.96
I1.3	$RATIO-ZSPRD^{30D}_{(3,0.5)}$	4	3	1	300.6	817.16	901.8	817.16	**84.64**	0.85	409.19	-817.16	-0.23	-3.65	75	21.16	1.1	0.37	-817.16
I1.4	$RATIO-ZSPRD^{30D}_{(2.7,2)}$	10	7	3	76.2	390.67	533.38	1172.01	**-638.63**	-6.39	118.63	-1024.58	-0.63	-10	70	-63.86	0.46	0.2	-1024.58
I1.5	$RATIO-ZSPRD^{30D}_{(2.7,1)}$	9	5	4	207.86	439.84	1039.3	1759.34	**-720.04**	-7.2	338.73	-971.96	-0.56	-8.89	55.56	-79.98	0.59	0.47	-1313.17
I1.6	$RATIO-ZSPRD^{30D}_{(2.7,0.5)}$	9	5	4	223.6	363.7	1117.99	1454.8	**-336.81**	-3.37	338.73	-817.16	-0.51	-8.1	55.56	-37.4	0.77	0.61	-1095.47
I2.1	$RATIO-SPRD^{30D}-SMA_{(10,20)}$	20	7	13	236.66	215.45	1656.59	2800.88	**-1144.28**	-11.44	543.12	-436.01	-0.75	-11.91	35	-57.21	0.59	1.1	-1328.45
I2.2	$RATIO-SPRD^{30D}-EMA_{(10,20)}$	21	8	13	495.73	167.89	3965.85	2182.55	**1783.31**	17.83	1242	-374.54	-0.16	-2.54	38.1	84.95	1.82	2.95	-975.81
I2.3	$RATIO-SPRD^{30D}-MACD_{(12,26,9)}$	37	7	30	406.01	184.43	2842.08	5532.84	**-2690.76**	-26.91	971.96	-529.01	-0.73	-11.59	18.92	-72.72	0.51	2.2	-2978.05
I2.4	$RATIO-SPRD^{30D}-RSI_{(14)}$	3	2	1	399.54	2389.11	799.08	2389.11	**-1590.04**	-15.9	571.59	-2389.11	-0.42	-6.67	66.67	-529.92	0.33	0.17	-2389.11
I2.5	$RATIO-SPRD^{30D}-BB_{(20)}$	14	11	3	201.04	403.41	2211.45	1210.23	**1001.22**	10.01	644.1	-814.22	-0.23	-3.65	78.57	71.51	1.83	0.5	-814.22
I3	$RATIO-SPRD^{30D}-DECTREE$	332	138	194	90.91	62.82	12546.02	12186.49	**359.53**	3.6	565.95	-371.56	-1.32	-20.95	41.57	1.09	1.03	1.45	-2793.18
I4	$RATIO-SPRD^{30D}-MLP$	283	118	165	103.16	71.94	12173.33	11869.41	**303.92**	3.04	565.95	-410.93	-1.17	-18.57	41.7	1.08	1.03	1.43	-3457.3
Part X: Models derived using the close price of VWO.N																			
CLS-SYM-1.1	$CLOSE^{VWO.N}-SMA_{(10,20)}$	15	6	9	230.99	239.78	1385.96	2158.06	**-772.1**	-7.72	679.96	-536.93	-0.43	-6.83	40	-51.47	0.64	0.96	-853.38
CLS-SYM-1.2	$CLOSE^{VWO.N}-EMA_{(10,20)}$	26	6	20	586.9	150.62	3521.39	3012.49	**508.9**	5.09	1242.77	-650.86	-0.14	-2.22	23.08	19.6	1.17	3.9	-1491.05
CLS-SYM-1.3	$CLOSE^{VWO.N}-MACD_{(12,26,9)}$	29	11	18	238.08	143.51	2618.9	2583.23	**35.67**	0.36	884.37	-347.88	-0.3	-4.76	37.93	1.23	1.01	1.66	-1298.22
CLS-SYM-1.4	$CLOSE^{VWO.N}-RSI_{(14)}$	6	3	3	205.52	522.84	616.55	1568.52	**-951.97**	-9.52	310.49	-1337.12	-0.39	-6.19	50	-158.66	0.39	0.39	-1337.12
CLS-SYM-1.5	$CLOSE^{VWO.N}-BB_{(20)}$	17	11	6	70.92	230.58	780.12	1383.47	**-603.35**	-6.03	100.93	-491.85	-0.63	-10	64.71	-35.48	0.56	0.31	-689.89
Part XI: Models derived using the close price of XLE.N																			
CLS-SYM-2.1	$CLOSE^{XLE.N}-SMA_{(10,20)}$	19	9	10	492.93	337.96	4436.4	3379.63	**1056.77**	10.57	1969.29	-993.26	-0.03	-0.48	47.37	55.63	1.31	1.46	-2390.02
CLS-SYM-2.2	$CLOSE^{XLE.N}-EMA_{(10,20)}$	26	11	15	546.32	161.14	6009.56	2417.09	**3592.47**	35.92	2197.81	-326.2	0.12	1.9	42.31	138.19	2.49	3.39	-711.67
CLS-SYM-2.3	$CLOSE^{XLE.N}-MACD_{(12,26,9)}$	27	10	17	637.2	211.29	6372.04	3591.96	**2780.08**	27.8	1931.38	-613.01	0.05	0.79	37.04	102.99	1.77	3.02	-645.92
CLS-SYM-2.4	$CLOSE^{XLE.N}-RSI_{(14)}$	5	3	2	314.75	1213.82	944.26	2427.64	**-1483.38**	-14.83	365.04	-1229.73	-0.44	-6.98	60	-296.68	0.39	0.26	-2062.6
CLS-SYM-2.5	$CLOSE^{XLE.N}-BB_{(20)}$	20	17	3	198.62	500.07	3376.55	1500.22	**1876.33**	18.76	822.47	-1185.85	0.05	0.79	85	93.82	2.25	0.4	-1185.85

Table D.2.23: This table presents the back-test metrics for the pair $VWO.N/XLE.N$ based on a 50-day rolling window. The table is subdivided into eleven parts, and in each of these parts, we present the back-test metrics and the trading strategies which use the spread derived from various models. In Part I, the spread is derived from the $DIST^{V1.1}$ model, in Part II from the $DIST^{V1.2}$ model, in Part III from the $DIST^{V2}$ model, in Part IV from the $DIST^{V3}$ model, in Part V from the $DIST^{V4}$ model, in Part VI from the $JOHANSEN-SPRD$ model, in Part VIII from the $ADF-SPRD$ model, in from the $DIST^{V2}$ model, in Part VIII from the $KALMAN-SPRD$ model, and in Part IX from the $RATIO-SPRD$ model. In Part X and XI, we present the back-test metrics of the trading strategies which use the close price of VWO.N, and XLE.N, respectively. All $ numbers reported below are in USD.

(I) Trading Strategy Code	(II) Model Name	(III) Total Number of Trades	(IV) Number of Winning Trades	(V) Number of Loosing Trades	(VI) Average Profit per Trade ($)	(VII) Average Loss per Trade ($)	(VIII) Gross Profit ($)	(IX) Gross Loss ($)	(X) Net Profit ($)	(XI) ROI (%)	(XII) Max P&L ($)	(XIII) Min P&L ($)	(XIV) Daily Sharpe Ratio	(XV) Annualized Sharpe Ratio	(XVI) Hit Ratio	(XVII) Expectancy	(XVIII) Profit Factor	(XIX) Realized Risk Reward Ratio	(XX) Max Drawdown ($)
Part I: Models derived using the spread obtained from $DIST^{V1.1}-SPRD^{50D}$																			
A1.1	$DIST^{V1.1}-ZSPRD^{50D}_{(3,2)}$	9	4	5	317.46	160.54	1269.86	802.71	**467.15**	4.67	494.81	-369.05	-0.36	-5.71	44.44	51.88	1.58	1.98	-369.05
A1.2	$DIST^{V1.1}-ZSPRD^{50D}_{(3,1)}$	8	4	4	132.72	297.4	530.87	1189.61	**-658.74**	-6.59	331.49	-409.19	-0.89	-14.13	50	-82.34	0.45	0.45	-990.22
A1.3	$DIST^{V1.1}-ZSPRD^{50D}_{(3,0.5)}$	8	1	7	247	214.79	247	1503.55	**-1256.54**	-12.57	247	-559.07	-1.24	-19.68	12.5	-157.07	0.16	1.15	-1503.55
A1.4	$DIST^{V1.1}-ZSPRD^{50D}_{(2.7,2)}$	10	7	3	320.38	57.9	2242.67	173.71	**2068.96**	20.69	999.81	-96.64	0.16	2.54	70	206.9	12.91	5.53	-173.71
A1.5	$DIST^{V1.1}-ZSPRD^{50D}_{(2.7,1)}$	9	6	3	266.51	160.99	1599.08	482.96	**1116.12**	11.16	747.63	-170.75	-0.09	-1.43	66.67	124.03	3.31	1.66	-326.37
A1.6	$DIST^{V1.1}-ZSPRD^{50D}_{(2.7,0.5)}$	8	3	5	497.41	125.57	1492.23	627.83	**864.4**	8.64	1058.74	-217.86	-0.11	-1.75	37.5	108.05	2.38	3.96	-408.86
A2.1	$DIST^{V1.1}-SPRD^{50D}-SMA_{(10,20)}$	18	13	5	209.13	426.32	2718.68	2131.62	**587.06**	5.87	411.98	-1255.4	-0.3	-4.76	72.22	32.6	1.28	0.49	-1538.4
A2.2	$DIST^{V1.1}-SPRD^{50D}-EMA_{(10,20)}$	27	21	6	136.87	545.53	2874.21	3273.16	**-398.95**	-3.99	414.96	-1146.37	-0.47	-7.46	77.78	-14.76	0.88	0.25	-2257
A2.3	$DIST^{V1.1}-SPRD^{50D}-MACD_{(12,26,9)}$	37	28	9	156.02	448.02	4368.47	4032.14	**336.33**	3.36	474.78	-993.95	-0.44	-6.98	75.68	9.12	1.08	0.35	-993.95
A2.4	$DIST^{V1.1}-SPRD^{50D}-RSI_{(14)}$	5	2	3	611.82	669.01	1223.63	2007.02	**-783.39**	-7.83	1209.91	-1267.67	-0.34	-5.4	40	-156.68	0.61	0.91	-1801.61
A2.5	$DIST^{V1.1}-SPRD^{50D}-BB_{(20)}$	14	4	10	225.16	291.64	900.64	2916.39	**-2015.75**	-20.16	572.77	-650.1	-0.89	-14.13	28.57	-143.99	0.31	0.77	-2296.48
A3	$DIST^{V1.1}-SPRD^{50D}-DECTREE$	291	154	137	74.22	74.96	11429.87	10269.34	**1160.54**	11.61	420.74	-381.88	-1.37	-21.75	52.92	3.99	1.11	0.99	-1457.67
A4	$DIST^{V1.1}-SPRD^{50D}-MLP$	261	159	102	79.66	108.15	12666.51	11030.94	**1635.57**	16.36	525.48	-756.98	-1.09	-17.3	60.92	6.27	1.15	0.74	-2847.02
Part II: Models derived using the spread obtained from $DIST^{V1.2}-SPRD^{50D}$																			
B1.1	$DIST^{V1.2}-ZSPRD^{50D}_{(3,2)}$	8	3	5	396.97	93.93	1190.91	469.67	**721.24**	7.21	591.99	-132.92	-0.22	-3.49	37.5	90.16	2.54	4.23	-246.18
B1.2	$DIST^{V1.2}-ZSPRD^{50D}_{(3,1)}$	8	6	2	271.72	1064.55	1630.32	2129.1	**-498.78**	-4.99	448.04	-1179	-0.33	-5.24	75	-62.35	0.77	0.26	-1234.61
B1.3	$DIST^{V1.2}-ZSPRD^{50D}_{(3,0.5)}$	8	6	2	301.32	1094.58	1807.92	2189.16	**-381.24**	-3.81	644.1	-1206.14	-0.29	-4.6	75	-47.66	0.83	0.28	-1206.14
B1.4	$DIST^{V1.2}-ZSPRD^{50D}_{(2.7,2)}$	12	6	6	201.48	78.72	1208.89	472.35	**736.54**	7.37	591.99	-132.92	-0.41	-6.51	50	61.38	2.56	2.56	-246.18
B1.5	$DIST^{V1.2}-ZSPRD^{50D}_{(2.7,1)}$	11	8	3	211.54	722.88	1692.31	2168.65	**-476.34**	-4.76	448.04	-1179	-0.37	-5.87	72.73	-43.28	0.78	0.29	-1326.09
B1.6	$DIST^{V1.2}-ZSPRD^{50D}_{(2.7,0.5)}$	11	9	2	207.46	1094.58	1867.12	2189.16	**-322.04**	-3.22	644.1	-1206.14	-0.32	-5.08	81.82	-29.25	0.85	0.19	-1206.14
B2.1	$DIST^{V1.2}-SPRD^{50D}-SMA_{(10,20)}$	22	14	8	341.78	299.56	4784.88	2396.5	**2388.38**	23.88	1121.35	-734.3	-0.1	-1.59	63.64	108.59	2	1.14	-1205.24
B2.2	$DIST^{V1.2}-SPRD^{50D}-EMA_{(10,20)}$	28	16	12	312.29	222.54	4996.68	2670.54	**2326.14**	23.26	1698.66	-821.18	-0.14	-2.22	57.14	83.06	1.87	1.4	-962.76
B2.3	$DIST^{V1.2}-SPRD^{50D}-MACD_{(12,26,9)}$	29	13	16	280.97	215.55	3652.63	3448.87	**203.76**	2.04	1945.91	-510.19	-0.33	-5.24	44.83	7.04	1.06	1.3	-1726.42
B2.4	$DIST^{V1.2}-SPRD^{50D}-RSI_{(14)}$	6	3	3	741.82	869.48	2225.46	2608.45	**-382.99**	-3.83	1220.09	-1734.88	-0.2	-3.17	50	-63.83	0.85	0.85	-1734.88
B2.5	$DIST^{V1.2}-SPRD^{50D}-BB_{(20)}$	14	7	7	319.26	67.74	2234.83	474.2	**1760.62**	17.61	1257.81	-188.02	-0.07	-1.11	50	125.76	4.71	4.71	-262.7
B3	$DIST^{V1.2}-SPRD^{50D}-DECTREE$	288	146	142	103.84	74.31	15160.22	10552.14	**4608.08**	46.08	756.98	-435.05	-0.99	-15.72	50.69	15.99	1.44	1.4	-1636.5
B4	$DIST^{V1.2}-SPRD^{50D}-MLP$	222	126	96	95.38	94.46	12018.23	9068.1	**2950.13**	29.5	444.59	-777.03	-0.94	-14.92	56.76	13.3	1.33	1.01	-1345.55
Part III: Models derived using the spread obtained from $DIST^{V2}-SPRD^{50D}$																			
C1.1	$DIST^{V2}-ZSPRD^{50D}_{(3,2)}$	9	5	4	160.54	317.46	802.71	1269.86	**-467.15**	-4.67	369.05	-494.81	-0.73	-11.59	55.56	-51.88	0.63	0.51	-703.63
C1.2	$DIST^{V2}-ZSPRD^{50D}_{(3,1)}$	8	4	4	297.4	132.72	1189.61	530.87	**658.74**	6.59	409.19	-331.49	-0.27	-4.29	50	82.34	2.24	2.24	-331.49
C1.3	$DIST^{V2}-ZSPRD^{50D}_{(3,0.5)}$	8	7	1	214.79	247	1503.55	247	**1256.54**	12.57	559.07	-247	0.02	0.32	87.5	157.07	6.09	0.87	-247
C1.4	$DIST^{V2}-ZSPRD^{50D}_{(2.7,2)}$	10	3	7	57.9	320.38	173.71	2242.67	**-2068.96**	-20.69	96.64	-999.81	-1.06	-16.83	30	-206.9	0.08	0.18	-2242.67
C1.5	$DIST^{V2}-ZSPRD^{50D}_{(2.7,1)}$	9	3	6	160.99	266.51	482.96	1599.08	**-1116.12**	-11.16	170.75	-747.63	-0.93	-14.76	33.33	-124.03	0.3	0.6	-1442.49
C1.6	$DIST^{V2}-ZSPRD^{50D}_{(2.7,0.5)}$	8	5	3	125.57	497.41	627.83	1492.23	**-864.4**	-8.64	217.86	-1058.74	-0.62	-9.84	62.5	-108.05	0.42	0.25	-1273.26
C2.1	$DIST^{V2}-SPRD^{50D}-SMA_{(10,20)}$	19	5	14	426.32	199.96	2131.62	2799.42	**-667.8**	-6.68	1255.4	-411.98	-0.48	-7.62	26.32	-35.12	0.76	2.13	-1305
C2.2	$DIST^{V2}-SPRD^{50D}-EMA_{(10,20)}$	27	6	21	545.53	136.87	3273.16	2874.21	**398.95**	3.99	1146.37	-414.96	-0.39	-6.19	22.22	14.76	1.14	3.99	-1326.04
C2.3	$DIST^{V2}-SPRD^{50D}-MACD_{(12,26,9)}$	37	9	28	448.02	156.02	4032.14	4368.47	**-336.33**	-3.36	993.95	-474.78	-0.49	-7.78	24.32	-9.12	0.92	2.87	-1233.83
C2.4	$DIST^{V2}-SPRD^{50D}-RSI_{(14)}$	5	3	2	669.01	611.82	2007.02	1223.63	**783.39**	7.83	1267.67	-1209.91	0.01	0.16	60	156.68	1.64	1.09	-1209.91
C2.5	$DIST^{V2}-SPRD^{50D}-BB_{(20)}$	14	10	4	291.64	225.16	2916.39	900.64	**2015.75**	20.16	650.1	-572.77	-0.02	-0.32	71.43	143.99	3.24	1.3	-572.77
C3	$DIST^{V2}-SPRD^{50D}-DECTREE$	305	150	155	90.02	93.34	13503.73	14467.65	**-963.92**	-9.64	535.17	-776.54	-1.14	-18.1	49.18	-3.16	0.93	0.96	-3078.24
C4	$DIST^{V2}-SPRD^{50D}-MLP$	210	120	90	91.15	98.08	10938.17	8827.16	**2111.01**	21.11	535.17	-604.47	-1.02	-16.19	57.14	10.05	1.24	0.93	-1433.83
Part IV: Models derived using the spread obtained from $DIST^{V3}-SPRD^{50D}$																			
D1.1	$DIST^{V3}-ZSPRD^{50D}_{(3,2)}$	5	2	3	249.44	287.92	498.89	863.76	**-364.87**	-3.65	417.7	-555.01	-0.63	-10	40	-72.97	0.58	0.87	-863.76
D1.2	$DIST^{V3}-ZSPRD^{50D}_{(3,1)}$	5	3	2	272.96	328.13	818.89	656.27	**162.62**	1.63	635.07	-427.57	-0.3	-4.76	60	32.52	1.25	0.83	-656.27
D1.3	$DIST^{V3}-ZSPRD^{50D}_{(3,0.5)}$	5	3	2	272.58	263.76	817.74	527.51	**290.23**	2.9	635.07	-274.03	-0.25	-3.97	60	58.05	1.55	1.03	-527.51
D1.4	$DIST^{V3}-ZSPRD^{50D}_{(2.7,2)}$	10	5	5	154.42	227.2	772.09	1136	**-363.91**	-3.64	417.7	-555.01	-0.71	-11.27	50	-36.39	0.68	0.68	-1056.64
D1.5	$DIST^{V3}-ZSPRD^{50D}_{(2.7,1)}$	9	4	5	267.21	219.89	1068.84	1099.43	**-30.59**	-0.31	635.07	-427.57	-0.48	-7.62	44.44	-3.42	0.97	1.22	-1034.27
D1.6	$DIST^{V3}-ZSPRD^{50D}_{(2.7,0.5)}$	9	4	5	285.76	217.91	1143.04	1089.54	**53.5**	0.53	635.07	-364.43	-0.46	-7.3	44.44	5.92	1.05	1.31	-1024.38
D2.1	$DIST^{V3}-SPRD^{50D}-SMA_{(10,20)}$	22	4	18	827.67	282.65	3310.67	5087.67	**-1777**	-17.77	1970.85	-1043.1	-0.4	-6.35	18.18	-80.79	0.65	2.93	-2145.44
D2.2	$DIST^{V3}-SPRD^{50D}-EMA_{(10,20)}$	45	10	35	370.91	204.3	3709.08	7150.66	**-3441.58**	-34.42	924.93	-1217.39	-0.68	-10.79	22.22	-76.49	0.52	1.82	-3983.94
D2.3	$DIST^{V3}-SPRD^{50D}-MACD_{(12,26,9)}$	38	8	30	113.32	178.47	906.52	5354.07	**-4447.55**	-44.48	280.9	-659.47	-1.46	-23.18	21.05	-117.05	0.17	0.63	-4369.96
D2.4	$DIST^{V3}-SPRD^{50D}-RSI_{(14)}$	5	2	3	221.16	676.03	442.32	2028.08	**-1585.76**	-15.86	435.16	-1012.49	-0.72	-11.43	40	-317.15	0.22	0.33	-2014.35
D2.5	$DIST^{V3}-SPRD^{50D}-BB_{(20)}$	19	16	3	252.64	485.29	4042.32	1455.88	**2586.44**	25.86	1073.22	-1083.96	-0.04	-0.63	84.21	136.12	2.78	0.52	-1083.96
D3	$DIST^{V3}-SPRD^{50D}-DECTREE$	325	154	171	66.68	77.56	10268.09	13262	**-2993.9**	-29.94	414.08	-436.03	-1.58	-25.08	47.38	-9.22	0.77	0.86	-5235.91
D4	$DIST^{V3}-SPRD^{50D}-MLP$	252	106	146	120.91	85.75	12816.53	12519.73	**296.8**	2.97	827.73	-756.98	-0.91	-14.45	42.06	1.17	1.02	1.41	-2999.97
Part V: Models derived using the spread obtained from $DIST^{V4}-SPRD^{50D}$																			
E1.1	$DIST^{V4}-ZSPRD^{50D}_{(3,2)}$	5	2	3	249.44	287.92	498.89	863.76	**-364.87**	-3.65	417.7	-555.01	-0.63	-10	40	-72.97	0.58	0.87	-863.76
E1.2	$DIST^{V4}-ZSPRD^{50D}_{(3,1)}$	5	3	2	272.96	328.13	818.89	656.27	**162.62**	1.63	635.07	-427.57	-0.3	-4.76	60	32.52	1.25	0.83	-656.27
E1.3	$DIST^{V4}-ZSPRD^{50D}_{(3,0.5)}$	5	3	2	272.58	263.76	817.74	527.51	**290.23**	2.9	635.07	-274.03	-0.25	-3.97	60	58.05	1.55	1.03	-527.51
E1.4	$DIST^{V4}-ZSPRD^{50D}_{(2.7,2)}$	10	5	5	154.42	227.2	772.09	1136	**-363.91**	-3.64	417.7	-555.01	-0.71	-11.27	50	-36.39	0.68	0.68	-1056.64
E1.5	$DIST^{V4}-ZSPRD^{50D}_{(2.7,1)}$	9	4	5	267.21	219.89	1068.84	1099.43	**-30.59**	-0.31	635.07	-427.57	-0.48	-7.62	44.44	-3.42	0.97	1.22	-1034.27
E1.6	$DIST^{V4}-ZSPRD^{50D}_{(2.7,0.5)}$	9	4	5	285.76	217.91	1143.04	1089.54	**53.5**	0.53	635.07	-364.43	-0.46	-7.3	44.44	5.92	1.05	1.31	-1024.38
E2.1	$DIST^{V4}-SPRD^{50D}-SMA_{(10,20)}$	21	4	17	827.67	294.52	3310.67	5006.82	**-1696.14**	-16.96	1970.85	-1043.1	-0.39	-6.19	19.05	-80.74	0.66	2.81	-2154.47
E2.2	$DIST^{V4}-SPRD^{50D}-EMA_{(10,20)}$	45	10	35	370.91	204.3	3709.08	7150.66	**-3441.58**	-34.42	924.93	-1217.39	-0.68	-10.79	22.22	-76.49	0.52	1.82	-3983.94
E2.3	$DIST^{V4}-SPRD^{50D}-MACD_{(12,26,9)}$	38	8	30	113.32	178.47	906.52	5354.07	**-4447.55**	-44.48	280.9	-659.47	-1.46	-23.18	21.05	-117.05	0.17	0.63	-4369.96
E2.4	$DIST^{V4}-SPRD^{50D}-RSI_{(14)}$	5	2	3	221.16	676.03	442.32	2028.08	**-1585.76**	-15.86	435.16	-1012.49	-0.72	-11.43	40	-317.15	0.22	0.33	-2014.35
E2.5	$DIST^{V4}-SPRD^{50D}-BB_{(20)}$	19	16	3	252.64	485.29	4042.32	1455.88	**2586.44**	25.86	1073.22	-1083.96	-0.04	-0.63	84.21	136.12	2.78	0.52	-1083.96
E3	$DIST^{V4}-SPRD^{50D}-DECTREE$	319	139	180	75.45	87.45	10487.26	15740.83	**-5253.57**	-52.54	471.16	-565.95	-1.41	-22.38	43.57	-16.47	0.67	0.86	-7216.1
E4	$DIST^{V4}-SPRD^{50D}-MLP$	229	98	131	122.6	93.7	12014.35	12274.56	**-260.21**	-2.6	827.09	-745.34	-0.86	-13.65	42.79	-1.15	0.98	1.31	-2878.36
Part VI: Models derived using the spread obtained from $JOHANSEN-SPRD^{50D}$																			
F1.1	$JOHANSEN-ZSPRD^{50D}_{(3,2)}$	17	8	9	42.01	179.34	336.08	1614.03	**-1277.95**	-12.78	120.07	-749.65	-0.25	-3.97	47.06	-75.17	0.21	0.23	-1430.91
F1.2	$JOHANSEN-ZSPRD^{50D}_{(3,1)}$	15	6	9	177.87	197.98	1067.2	1781.78	**-714.58**	-7.15	686.56	-749.65	0.22	3.49	40	-47.64	0.6	0.9	-1279.15
F1.3	$JOHANSEN-ZSPRD^{50D}_{(3,0.5)}$	15	7	8	186.83	243.56	1307.82	1948.5	**-640.68**	-6.41	778.04	-749.65	0.23	3.65	46.67	-42.7	0.67	0.77	-1279.15
F1.4	$JOHANSEN-ZSPRD^{50D}_{(2.7,2)}$	17	8	9	43.52	178.68	348.18	1608.13	**-1259.95**	-12.6	120.07	-749.65	-0.44	-6.98	47.06	-74.11	0.22	0.24	-1412.91
F1.5	$JOHANSEN-ZSPRD^{50D}_{(2.7,1)}$	15	6	9	190.9	197.32	1145.39	1775.88	**-630.48**	-6.3	764.75	-749.65	0.08	1.27	40	-42.03	0.64	0.97	-1273.25
F1.6	$JOHANSEN-ZSPRD^{50D}_{(2.7,0.5)}$	15	7	8	199.79	242.82	1398.56	1942.6	**-544.03**	-5.44	868.78	-749.65	0.11	1.75	46.67	-36.25	0.72	0.82	-1273.25
F2.1	$JOHANSEN-SPRD^{50D}-SMA_{(10,20)}$	20	9	11	2737.83	512.08	24640.45	5632.83	**19007.62**	190.08	14057	-1926.9	0.26	4.13	45	950.38	4.37	5.35	-3657.62
F2.2	$JOHANSEN-SPRD^{50D}-EMA_{(10,20)}$	33	16	17	2882.5	603.03	46119.96	10251.45	**35868.51**	358.69	38418.19	-2264.55	0.06	0.95	48.48	1086.76	4.5	4.78	-4513.69
F2.3	$JOHANSEN-SPRD^{50D}-MACD_{(12,26,9)}$	33	17	16	1546.28	530.05	26286.75	8480.81	**17805.94**	178.06	12641.89	-2215.91	0.1	1.59	51.52	539.67	3.1	2.92	-3902.46
F2.4	$JOHANSEN-SPRD^{50D}-RSI_{(14)}$	8	3	5	346.81	1735.64	1040.44	8678.19	**-7637.75**	-76.38	608.83	-5946.02	-0.28	-4.44	37.5	-954.72	0.12	0.2	-8010.5
F2.5	$JOHANSEN-SPRD^{50D}-BB_{(20)}$	15	8	7	738.64	16100.04	5909.16	112700.3	**-106791.14**	-1067.91	3350.16	-105357.19	-0.2	-3.17	53.33	-7119.97	0.05	0.05	-111537.46
F3	$JOHANSEN-SPRD^{50D}-DECTREE$	316	176	140	71.42	105.86	12569.2	14820.84	**-2251.64**	-22.52	362.12	-839.77	-1.2	-19.05	55.7	-7.12	0.85	0.67	-3230.06
F4	$JOHANSEN-SPRD^{50D}-MLP$	265	136	129	99.19	97.9	13489.73	12628.5	**861.24**	8.61	675.91	-525.98	-1.06	-16.83	51.32	3.25	1.07	1.01	-1551.5
Part VII: Models derived using the spread obtained from $ADF-SPRD^{50D}$																			
G1.1	$ADF-ZSPRD^{50D}_{(3,2)}$	9	4	5	177.2	307.98	708.81	1539.91	**-831.1**	-8.31	325.94	-1108.22	-0.44	-6.98	44.44	-92.37	0.46	0.58	-1214.79
G1.2	$ADF-ZSPRD^{50D}_{(3,1)}$	8	2	6	248.26	531.65	496.52	3189.91	**-2693.39**	-26.93	420.41	-2016.56	-0.48	-7.62	25	-336.67	0.16	0.47	-2693.39
G1.3	$ADF-ZSPRD^{50D}_{(3,0.5)}$	8	2	6	144.72	609.89	289.44	3659.35	**-3369.92**	-33.7	213.32	-2439.01	-0.5	-7.94	25	-421.24	0.08	0.24	-3369.92
G1.4	$ADF-ZSPRD^{50D}_{(2.7,2)}$	10	3	7	221.43	339.53	664.3	2376.7	**-1712.4**	-17.12	574.58	-1108.22	-0.64	-10.16	30	-171.24	0.28	0.65	-2311.79
G1.5	$ADF-ZSPRD^{50D}_{(2.7,1)}$	9	1	8	324.79	1082.17	324.79	8657.34	**-8332.55**	-83.33	324.79	-5394.77	-0.5	-7.94	11.11	-925.85	0.04	0.3	-8469.97
G1.6	$ADF-ZSPRD^{50D}_{(2.7,0.5)}$	9	1	8	324.79	1219.78	324.79	9758.2	**-9433.41**	-94.33	324.79	-5806.04	-0.52	-8.25	11.11	-1048.17	0.03	0.27	-9570.83
G2.1	$ADF-SPRD^{50D}-SMA_{(10,20)}$	16	11	5	1270.28	368.98	13973.12	1844.88	**12128.23**	121.28	11196.9	-803.26	0.23	3.65	68.75	758.01	7.57	3.44	-1119.66
G2.2	$ADF-SPRD^{50D}-EMA_{(10,20)}$	29	20	9	306.95	787.29	6138.91	7085.64	**-946.73**	-9.47	1633.56	-3124.56	-0.25	-3.97	68.97	-32.6	0.87	0.39	-5662.6
G2.3	$ADF-SPRD^{50D}-MACD_{(12,26,9)}$	29	17	12	190.41	493.1	3236.9	5917.25	**-2680.35**	-26.8	1212.03	-1465.43	-0.54	-8.57	58.62	-92.43	0.55	0.39	-5222.71
G2.4	$ADF-SPRD^{50D}-RSI_{(14)}$	3	3	-	1872.89	-	5618.68	-	**5618.68**	56.19	3084.41	-	1.92	30.48	100	1872.89	5618.68	1872.89	-
G2.5	$ADF-SPRD^{50D}-BB_{(20)}$	16	4	12	615.74	240.58	2462.98	2886.93	**-423.95**	-4.24	1180.75	-1443.16	-0.29	-4.6	25	-26.5	0.85	2.56	-1957.39
G3	$ADF-SPRD^{50D}-DECTREE$	331	160	171	83.38	81.78	13341.18	13984.43	**-643.26**	-6.43	571.13	-387.7	-1.33	-21.11	48.34	-1.94	0.95	1.02	-2792.54
G4	$ADF-SPRD^{50D}-MLP$	246	104	142	124.03	84.75	12898.8	12034.56	**864.24**	8.64	748.82	-429.16	-0.93	-14.76	42.28	3.52	1.07	1.46	-1948.39
Part VIII: Models derived using the spread obtained from $KALMAN-SPRD^{50D}$																			
H1.1	$KALMAN-ZSPRD^{50D}_{(3,2)}$	8	4	4	102.38	344.04	409.51	1376.15	**-966.64**	-9.67	130.46	-575.45	-1.04	-16.51	50	-120.83	0.3	0.3	-1376.15
H1.2	$KALMAN-ZSPRD^{50D}_{(3,1)}$	6	3	3	175.88	665.79	527.64	1997.38	**-1469.74**	-14.7	224.48	-1463.16	-0.69	-10.95	50	-244.96	0.26	0.26	-1997.38
H1.3	$KALMAN-ZSPRD^{50D}_{(3,0.5)}$	6	3	3	212.8	595.93	638.41	1787.79	**-1149.38**	-11.49	272.29	-1314.83	-0.65	-10.32	50	-191.56	0.36	0.36	-1787.79
H1.4	$KALMAN-ZSPRD^{50D}_{(2.7,2)}$	12	6	6	121.03	268.54	726.21	1611.27	**-885.06**	-8.85	216.7	-575.45	-0.92	-14.6	50	-73.75	0.45	0.45	-1243.9
H1.5	$KALMAN-ZSPRD^{50D}_{(2.7,1)}$	9	5	4	236.5	519.44	1182.52	2077.76	**-895.23**	-8.95	385.18	-1463.16	-0.48	-7.62	55.56	-99.44	0.57	0.46	-1755.39
H1.6	$KALMAN-ZSPRD^{50D}_{(2.7,0.5)}$	9	5	4	256.62	466.82	1283.1	1867.28	**-584.18**	-5.84	385.18	-1314.83	-0.45	-7.14	55.56	-64.88	0.69	0.55	-1628.18
H2.1	$KALMAN-SPRD^{50D}-SMA_{(10,20)}$	17	5	12	978.25	160.5	4891.24	1926	**2965.24**	29.65	1467.68	-396.68	0.05	0.79	29.41	174.41	2.54	6.1	-1051.7
H2.2	$KALMAN-SPRD^{50D}-EMA_{(10,20)}$	26	7	19	633.6	160.92	4435.19	3057.49	**1377.7**	13.78	1455.66	-404.81	-0.23	-3.65	26.92	52.96	1.45	3.94	-1169.06
H2.3	$KALMAN-SPRD^{50D}-MACD_{(12,26,9)}$	29	7	22	413.32	245.48	2893.24	5400.55	**-2507.32**	-25.07	1140.47	-789.49	-0.55	-8.73	24.14	-86.45	0.54	1.68	-3062.34
H2.4	$KALMAN-SPRD^{50D}-RSI_{(14)}$	1	-	1	-	2457.54	-	2457.54	**-2457.54**	-24.58	-	-2457.54	-	-	-	-2457.54	-	-	-2457.54
H2.5	$KALMAN-SPRD^{50D}-BB_{(20)}$	10	5	5	165.09	732.44	825.43	3662.2	**-2836.77**	-28.37	424.51	-1535.4	-0.72	-11.43	50	-283.68	0.23	0.23	-3182.44
H3	$KALMAN-SPRD^{50D}-DECTREE$	291	166	125	71.51	89.69	11870.06	11211.82	**658.23**	6.58	429.98	-769.57	-1.24	-19.68	57.04	2.25	1.06	0.8	-1784.19
H4	$KALMAN-SPRD^{50D}-MLP$	223	122	101	76.03	87.27	9276.11	8814.21	**461.89**	4.62	459.76	-583.16	-1.19	-18.89	54.71	2.07	1.05	0.87	-1974.36
Part IX: Models derived using the spread obtained from $RATIO-SPRD^{50D}$																			
I1.1	$RATIO-ZSPRD^{50D}_{(3,2)}$	10	5	5	132.86	368.16	664.29	1840.81	**-1176.52**	-11.77	197.18	-986.4	-0.76	-12.06	50	-117.65	0.36	0.36	-1472.23
I1.2	$RATIO-ZSPRD^{50D}_{(3,1)}$	8	4	4	234.79	356.23	939.17	1424.92	**-485.75**	-4.86	409.19	-787.27	-0.55	-8.73	50	-60.72	0.66	0.66	-1065.59
I1.3	$RATIO-ZSPRD^{50D}_{(3,0.5)}$	7	5	2	249.22	648.87	1246.11	1297.73	**-51.63**	-0.52	409.19	-1050.73	-0.31	-4.92	71.43	-7.36	0.96	0.38	-1050.73
I1.4	$RATIO-ZSPRD^{50D}_{(2.7,2)}$	13	6	7	101.81	322.83	610.85	2259.8	**-1648.95**	-16.49	187.97	-1002.74	-0.84	-13.33	46.15	-126.86	0.27	0.32	-2071.83
I1.5	$RATIO-ZSPRD^{50D}_{(2.7,1)}$	10	4	6	148.53	366.85	594.11	2201.1	**-1606.99**	-16.07	197.65	-817.16	-0.96	-15.24	40	-160.7	0.27	0.4	-2044.51
I1.6	$RATIO-ZSPRD^{50D}_{(2.7,0.5)}$	9	5	4	153.46	430.87	767.31	1723.47	**-956.16**	-9.56	232.84	-1050.73	-0.64	-10.16	55.56	-106.21	0.45	0.36	-1507.56
I2.1	$RATIO-SPRD^{50D}-SMA_{(10,20)}$	19	7	12	236.66	229.06	1656.59	2748.67	**-1092.08**	-10.92	543.12	-436.01	-0.73	-11.59	36.84	-57.49	0.6	1.03	-1276.25
I2.2	$RATIO-SPRD^{50D}-EMA_{(10,20)}$	21	7	14	548.31	173.87	3838.14	2434.16	**1403.98**	14.04	1242	-374.54	-0.2	-3.17	33.33	66.83	1.58	3.15	-1227.42
I2.3	$RATIO-SPRD^{50D}-MACD_{(12,26,9)}$	37	7	30	406.01	196.36	2842.08	5890.94	**-3048.86**	-30.49	971.96	-529.01	-0.75	-11.91	18.92	-82.4	0.48	2.07	-3303.46
I2.4	$RATIO-SPRD^{50D}-RSI_{(14)}$	4	2	2	365.81	1088.32	731.61	2176.64	**-1445.04**	-14.45	571.59	-2162.92	-0.42	-6.67	50	-361.26	0.34	0.34	-2162.92
I2.5	$RATIO-SPRD^{50D}-BB_{(20)}$	14	11	3	196.85	403.41	2165.39	1210.23	**955.17**	9.55	644.1	-814.22	-0.24	-3.81	78.57	68.22	1.79	0.49	-814.22
I3	$RATIO-SPRD^{50D}-DECTREE$	293	125	168	85.68	63.93	10709.95	10740.37	**-30.42**	-0.3	514.22	-315.15	-1.45	-23.02	42.66	-0.11	1	1.34	-2389.53
I4	$RATIO-SPRD^{50D}-MLP$	277	111	166	102.05	64.88	11328.05	10769.82	**558.22**	5.58	514.22	-315.15	-1.3	-20.64	40.07	2.01	1.05	1.57	-2333.61
Part X: Models derived using the close price of VWO.N																			
CLS-SYM-1.1	$CLOSE^{VWO.N}-SMA_{(10,20)}$	15	6	9	230.99	239.78	1385.96	2158.06	**-772.1**	-7.72	679.96	-536.93	-0.43	-6.83	40	-51.47	0.64	0.96	-853.38
CLS-SYM-1.2	$CLOSE^{VWO.N}-EMA_{(10,20)}$	26	6	20	586.9	150.62	3521.39	3012.49	**508.9**	5.09	1242.77	-650.86	-0.14	-2.22	23.08	19.6	1.17	3.9	-1491.05
CLS-SYM-1.3	$CLOSE^{VWO.N}-MACD_{(12,26,9)}$	29	11	18	238.08	143.51	2618.9	2583.23	**35.67**	0.36	884.37	-347.88	-0.3	-4.76	37.93	1.23	1.01	1.66	-1298.22
CLS-SYM-1.4	$CLOSE^{VWO.N}-RSI_{(14)}$	6	3	3	205.52	522.84	616.55	1568.52	**-951.97**	-9.52	310.49	-1337.12	-0.39	-6.19	50	-158.66	0.39	0.39	-1337.12
CLS-SYM-1.5	$CLOSE^{VWO.N}-BB_{(20)}$	17	11	6	70.92	230.58	780.12	1383.47	**-603.35**	-6.03	100.93	-491.85	-0.63	-10	64.71	-35.48	0.56	0.31	-689.89
Part XI: Models derived using the close price of XLE.N																			
CLS-SYM-2.1	$CLOSE^{XLE.N}-SMA_{(10,20)}$	19	9	10	492.93	337.96	4436.4	3379.63	**1056.77**	10.57	1969.29	-993.26	-0.03	-0.48	47.37	55.63	1.31	1.46	-2390.02
CLS-SYM-2.2	$CLOSE^{XLE.N}-EMA_{(10,20)}$	26	11	15	546.32	161.14	6009.56	2417.09	**3592.47**	35.92	2197.81	-326.2	0.12	1.9	42.31	138.19	2.49	3.39	-711.67
CLS-SYM-2.3	$CLOSE^{XLE.N}-MACD_{(12,26,9)}$	27	10	17	637.2	211.29	6372.04	3591.96	**2780.08**	27.8	1931.38	-613.01	0.05	0.79	37.04	102.99	1.77	3.02	-645.92
CLS-SYM-2.4	$CLOSE^{XLE.N}-RSI_{(14)}$	5	3	2	314.75	1213.82	944.26	2427.64	**-1483.38**	-14.83	365.04	-1229.73	-0.44	-6.98	60	-296.68	0.39	0.26	-2062.6
CLS-SYM-2.5	$CLOSE^{XLE.N}-BB_{(20)}$	20	17	3	198.62	500.07	3376.55	1500.22	**1876.33**	18.76	822.47	-1185.85	0.05	0.79	85	93.82	2.25	0.4	-1185.85

Table D.2.24: This table presents the back-test metrics for the pair $VWO.N/XLE.N$ based on a 100-day rolling window. The table is subdivided into eleven parts, and in each of these parts, we present the back-test metrics and the trading strategies which use the spread derived from various models. In Part I, the spread is derived from the $DIST^{V1.1}$ model, in Part II from the $DIST^{V1.2}$ model, in Part III from the $DIST^{V2}$ model, in Part IV from the $DIST^{V3}$ model, in Part V from the $DIST^{V4}$ model, in Part VI from the $JOHANSEN-SPRD$ model, in Part VIII from the $ADF-SPRD$ model, in from the $DIST^{V2}$ model, in Part VIII from the $KALMAN-SPRD$ model, and in Part IX from the $RATIO-SPRD$ model. In Part X and XI, we present the back-test metrics of the trading strategies which use the close price of VWO.N, and XLE.N, respectively. All $ numbers reported below are in USD.

(I) Trading Strategy Code	(II) Model Name	(III) Total Number of Trades	(IV) Number of Winning Trades	(V) Number of Loosing Trades	(VI) Average Profit per Trade ($)	(VII) Average Loss per Trade ($)	(VIII) Gross Profit ($)	(IX) Gross Loss ($)	(X) Net Profit ($)	(XI) ROI (%)	(XII) Max P&L ($)	(XIII) Min P&L ($)	(XIV) Daily Sharpe Ratio	(XV) Annualized Sharpe Ratio	(XVI) Hit Ratio	(XVII) Expectancy	(XVIII) Profit Factor	(XIX) Realized Risk Reward Ratio	(XX) Max Drawdown ($)
	Part I: Models derived using the spread obtained from $DIST^{V1.1}-SPRD^{100D}$																		
A1.1	$DIST^{V1.1}-ZSPRD^{100D}_{(3,2)}$	4	2	2	579.2	114.02	1158.41	228.05	**930.36**	9.3	965.26	-120.27	0.16	2.54	50	232.59	5.08	5.08	-228.05
A1.2	$DIST^{V1.1}-ZSPRD^{100D}_{(3,1)}$	3	1	2	783.36	78.24	783.36	156.48	**626.89**	6.27	783.36	-98.54	0.11	1.75	33.33	208.93	5.01	10.01	-98.54
A1.3	$DIST^{V1.1}-ZSPRD^{100D}_{(3,0.5)}$	3	1	2	539.59	145.51	539.59	291.01	**248.58**	2.49	539.59	-192.47	-0.17	-2.7	33.33	82.84	1.85	3.71	-192.47
A1.4	$DIST^{V1.1}-ZSPRD^{100D}_{(2.7,2)}$	6	4	2	353.57	72.11	1414.29	144.22	**1270.07**	12.7	1077.67	-96.64	0.14	2.22	66.67	211.69	9.81	4.9	-96.64
A1.5	$DIST^{V1.1}-ZSPRD^{100D}_{(2.7,1)}$	4	1	3	934.6	113.68	934.6	341.04	**593.56**	5.94	934.6	-209.18	-0.01	-0.16	25	148.39	2.74	8.22	-267.12
A1.6	$DIST^{V1.1}-ZSPRD^{100D}_{(2.7,0.5)}$	3	1	2	711.73	133.2	711.73	266.4	**445.33**	4.45	711.73	-192.47	-0.01	-0.16	33.33	148.42	2.67	5.34	-192.47
A2.1	$DIST^{V1.1}-SPRD^{100D}-SMA_{(10,20)}$	16	10	6	203.58	370.07	2035.85	2220.42	**-184.57**	-1.85	411.98	-1255.4	-0.4	-6.35	62.5	-11.54	0.92	0.55	-1593.91
A2.2	$DIST^{V1.1}-SPRD^{100D}-EMA_{(10,20)}$	25	19	6	120.63	545.53	2291.89	3273.16	**-981.27**	-9.81	414.96	-1146.37	-0.54	-8.57	76	-39.25	0.7	0.22	-2257
A2.3	$DIST^{V1.1}-SPRD^{100D}-MACD_{(12,26,9)}$	35	27	8	164.11	484.48	4430.91	3875.85	**555.06**	5.55	474.78	-993.95	-0.41	-6.51	77.14	15.84	1.14	0.34	-993.95
A2.4	$DIST^{V1.1}-SPRD^{100D}-RSI_{(14)}$	3	1	2	1456.32	900.8	1456.32	1801.61	**-345.29**	-3.45	1456.32	-1267.67	-0.19	-3.02	33.33	-115.18	0.81	1.62	-1801.61
A2.5	$DIST^{V1.1}-SPRD^{100D}-BB_{(20)}$	13	4	9	225.16	318.81	900.64	2869.25	**-1968.61**	-19.69	572.77	-650.1	-0.88	-13.97	30.77	-151.43	0.31	0.71	-2296.48
A3	$DIST^{V1.1}-SPRD^{100D}-DECTREE$	287	161	126	78.32	88.23	12610.18	11117.18	**1493**	14.93	390.54	-540.62	-1.28	-20.32	56.1	5.21	1.13	0.89	-1524.94
A4	$DIST^{V1.1}-SPRD^{100D}-MLP$	171	106	65	83.08	90.97	8806.06	5913.02	**2893.04**	28.93	1253.73	-489.57	-0.93	-14.76	61.99	16.92	1.49	0.91	-1185.24
	Part II: Models derived using the spread obtained from $DIST^{V1.2}-SPRD^{100D}$																		
B1.1	$DIST^{V1.2}-ZSPRD^{100D}_{(3,2)}$	4	1	3	44.63	201.68	44.63	605.05	**-560.43**	-5.6	44.63	-321.95	-1.71	-27.15	25	-140.11	0.07	0.22	-605.05
B1.2	$DIST^{V1.2}-ZSPRD^{100D}_{(3,1)}$	3	-	3	-	698.58	-	2095.74	**-2095.74**	-20.96	-	-1274.15	-1.65	-26.19	-	-698.58	-	-	-2095.74
B1.3	$DIST^{V1.2}-ZSPRD^{100D}_{(3,0.5)}$	2	-	2	-	506.72	-	1013.44	**-1013.44**	-10.13	-	-556.31	-9.39	-149.06	-	-506.72	-	-	-1013.44
B1.4	$DIST^{V1.2}-ZSPRD^{100D}_{(2.7,2)}$	5	-	5	-	208	-	1040.01	**-1040.01**	-10.4	-	-412.12	-2.09	-33.18	-	-208	-	-	-1040.01
B1.5	$DIST^{V1.2}-ZSPRD^{100D}_{(2.7,1)}$	4	-	4	-	641.1	-	2564.41	**-2564.41**	-25.64	-	-1274.15	-1.8	-28.57	-	-641.1	-	-	-2564.41
B1.6	$DIST^{V1.2}-ZSPRD^{100D}_{(2.7,0.5)}$	3	1	2	107.25	532.22	107.25	1064.43	**-957.18**	-9.57	107.25	-607.3	-1.25	-19.84	33.33	-319.08	0.1	0.2	-1064.43
B2.1	$DIST^{V1.2}-SPRD^{100D}-SMA_{(10,20)}$	14	9	5	545.4	488.48	4908.63	2442.38	**2466.26**	24.66	1000.15	-933.46	0.04	0.63	64.29	176.21	2.01	1.12	-1831.95
B2.2	$DIST^{V1.2}-SPRD^{100D}-EMA_{(10,20)}$	14	7	7	630.72	156.89	4415.04	1098.26	**3316.78**	33.17	1400.71	-647.64	0.15	2.38	50	236.91	4.02	4.02	-647.64
B2.3	$DIST^{V1.2}-SPRD^{100D}-MACD_{(12,26,9)}$	37	12	25	237.82	161.79	2853.89	4044.73	**-1190.84**	-11.91	1526.89	-726.38	-0.55	-8.73	32.43	-32.19	0.71	1.47	-2259.98
B2.4	$DIST^{V1.2}-SPRD^{100D}-RSI_{(14)}$	4	2	2	716.65	754.55	1433.3	1509.11	**-75.81**	-0.76	1147.19	-964.11	-0.18	-2.86	50	-18.95	0.95	0.95	-545
B2.5	$DIST^{V1.2}-SPRD^{100D}-BB_{(20)}$	10	4	6	81.67	374.5	326.67	2247.03	**-1920.35**	-19.2	194.51	-1039.71	-0.9	-14.29	40	-192.04	0.15	0.22	-2165.17
B3	$DIST^{V1.2}-SPRD^{100D}-DECTREE$	233	127	106	91.61	74.39	11633.96	7884.92	**3749.05**	37.49	797.43	-444.57	-0.99	-15.72	54.51	16.1	1.48	1.23	-1838.27
B4	$DIST^{V1.2}-SPRD^{100D}-MLP$	46	25	21	68.17	41.74	1704.2	876.45	**827.74**	8.28	326.7	-94.97	-1.71	-27.15	54.35	18	1.94	1.63	-216.55
	Part III: Models derived using the spread obtained from $DIST^{V2}-SPRD^{100D}$																		
C1.1	$DIST^{V2}-ZSPRD^{100D}_{(3,2)}$	4	2	2	114.02	579.2	228.05	1158.41	**-930.36**	-9.3	120.27	-965.26	-0.75	-11.91	50	-232.59	0.2	0.2	-1158.41
C1.2	$DIST^{V2}-ZSPRD^{100D}_{(3,1)}$	3	2	1	78.24	783.36	156.48	783.36	**-626.89**	-6.27	98.54	-783.36	-0.73	-11.59	66.67	-208.93	0.2	0.1	-783.36
C1.3	$DIST^{V2}-ZSPRD^{100D}_{(3,0.5)}$	3	2	1	145.51	539.59	291.01	539.59	**-248.58**	-2.49	192.47	-539.59	-0.59	-9.37	66.67	-82.84	0.54	0.27	-539.59
C1.4	$DIST^{V2}-ZSPRD^{100D}_{(2.7,2)}$	6	2	4	72.11	353.57	144.22	1414.29	**-1270.07**	-12.7	96.64	-1077.67	-0.83	-13.18	33.33	-211.69	0.1	0.2	-1414.29
C1.5	$DIST^{V2}-ZSPRD^{100D}_{(2.7,1)}$	4	3	1	113.68	934.6	341.04	934.6	**-593.56**	-5.94	209.18	-934.6	-0.57	-9.05	75	-148.39	0.36	0.12	-934.6
C1.6	$DIST^{V2}-ZSPRD^{100D}_{(2.7,0.5)}$	3	2	1	133.2	711.73	266.4	711.73	**-445.33**	-4.45	192.47	-711.73	-0.61	-9.68	66.67	-148.42	0.37	0.19	-711.73
C2.1	$DIST^{V2}-SPRD^{100D}-SMA_{(10,20)}$	16	6	10	389.38	196.33	2336.27	1963.28	**373**	3.73	1255.4	-411.98	-0.31	-4.92	37.5	23.31	1.19	1.98	-1305
C2.2	$DIST^{V2}-SPRD^{100D}-EMA_{(10,20)}$	25	6	19	545.53	120.63	3273.16	2291.89	**981.27**	9.81	1146.37	-414.96	-0.32	-5.08	24	39.25	1.43	4.52	-961.28
C2.3	$DIST^{V2}-SPRD^{100D}-MACD_{(12,26,9)}$	35	8	27	484.48	164.11	3875.85	4430.91	**-555.06**	-5.55	993.95	-474.78	-0.5	-7.94	22.86	-15.84	0.87	2.95	-1233.83
C2.4	$DIST^{V2}-SPRD^{100D}-RSI_{(14)}$	3	2	1	900.8	1456.32	1801.61	1456.32	**345.29**	3.45	1267.67	-1456.32	-0.03	-0.48	66.67	115.18	1.24	0.62	-
C2.5	$DIST^{V2}-SPRD^{100D}-BB_{(20)}$	13	9	4	318.81	225.16	2869.25	900.64	**1968.61**	19.69	650.1	-572.77	-	-	69.23	151.43	3.19	1.42	-572.77
C3	$DIST^{V2}-SPRD^{100D}-DECTREE$	282	142	140	81.03	88.74	11506.39	12423.12	**-916.72**	-9.17	547.93	-787.62	-1.21	-19.21	50.35	-3.26	0.93	0.91	-2035.88
C4	$DIST^{V2}-SPRD^{100D}-MLP$	182	96	86	100.89	96.76	9685.17	8321.64	**1363.53**	13.64	619.57	-436.58	-1	-15.87	52.75	7.5	1.16	1.04	-1505.19
	Part IV: Models derived using the spread obtained from $DIST^{V3}-SPRD^{100D}$																		
D1.1	$DIST^{V3}-ZSPRD^{100D}_{(3,2)}$	3	3	-	142.14	-	426.42	-	**426.42**	4.26	220.07	-	-0.09	-1.43	100	142.14	426.42	142.14	-
D1.2	$DIST^{V3}-ZSPRD^{100D}_{(3,1)}$	3	1	2	409.19	66.31	409.19	132.63	**276.57**	2.77	409.19	-78.87	-0.22	-3.49	33.33	92.17	3.09	6.17	-132.63
D1.3	$DIST^{V3}-ZSPRD^{100D}_{(3,0.5)}$	3	1	2	409.19	892.38	409.19	1784.75	**-1375.56**	-13.76	409.19	-1271.98	-0.73	-11.59	33.33	-458.56	0.23	0.46	-1784.75
D1.4	$DIST^{V3}-ZSPRD^{100D}_{(2.7,2)}$	8	5	3	124.63	82.45	623.15	247.36	**375.78**	3.76	220.07	-128.75	-0.84	-13.33	62.5	46.97	2.52	1.51	-128.75
D1.5	$DIST^{V3}-ZSPRD^{100D}_{(2.7,1)}$	6	3	3	165.41	67.28	496.22	201.83	**294.39**	2.94	273.41	-160.11	-0.68	-10.79	50	49.07	2.46	2.46	-169.99
D1.6	$DIST^{V3}-ZSPRD^{100D}_{(2.7,0.5)}$	6	4	2	168	826.82	671.99	1653.64	**-981.66**	-9.82	273.41	-1077.2	-0.58	-9.21	66.67	-163.58	0.41	0.2	-1653.65
D2.1	$DIST^{V3}-SPRD^{100D}-SMA_{(10,20)}$	24	9	15	401.46	226.92	3613.15	3403.87	**209.28**	2.09	816.15	-872.25	-0.37	-5.87	37.5	8.72	1.06	1.77	-1801.07
D2.2	$DIST^{V3}-SPRD^{100D}-EMA_{(10,20)}$	39	11	28	421.64	166.6	4638.06	4664.84	**-26.78**	-0.27	1091.18	-813.16	-0.42	-6.67	28.21	-0.66	0.99	2.53	-1983.16
D2.3	$DIST^{V3}-SPRD^{100D}-MACD_{(12,26,9)}$	30	8	22	395.69	241.47	3165.53	5312.35	**-2146.82**	-21.47	1198.67	-1216.71	-0.54	-8.57	26.67	-71.54	0.6	1.64	-3489.9
D2.4	$DIST^{V3}-SPRD^{100D}-RSI_{(14)}$	3	1	2	325.89	1354.39	325.89	2708.78	**-2382.89**	-23.83	325.89	-1960.81	-0.83	-13.18	33.33	-794.35	0.12	0.24	-747.97
D2.5	$DIST^{V3}-SPRD^{100D}-BB_{(20)}$	19	16	3	145.58	230.86	2329.36	692.57	**1636.79**	16.37	345.12	-454.62	-0.36	-5.71	84.21	86.14	3.36	0.63	-454.62
D3	$DIST^{V3}-SPRD^{100D}-DECTREE$	295	132	163	83.1	77.71	10969.8	12666.7	**-1696.89**	-16.97	455.57	-394.77	-1.36	-21.59	44.75	-5.75	0.87	1.07	-2314.33
D4	$DIST^{V3}-SPRD^{100D}-MLP$	158	74	84	121.74	81.74	9008.65	6866.07	**2142.57**	21.43	1472.38	-378.48	-0.77	-12.22	46.84	13.57	1.31	1.49	-897.21
	Part V: Models derived using the spread obtained from $DIST^{V4}-SPRD^{100D}$																		
E1.1	$DIST^{V4}-ZSPRD^{100D}_{(3,2)}$	3	3	-	142.14	-	426.42	-	**426.42**	4.26	220.07	-	-0.09	-1.43	100	142.14	426.42	142.14	-
E1.2	$DIST^{V4}-ZSPRD^{100D}_{(3,1)}$	3	1	2	409.19	66.31	409.19	132.63	**276.57**	2.77	409.19	-78.87	-0.22	-3.49	33.33	92.17	3.09	6.17	-132.63
E1.3	$DIST^{V4}-ZSPRD^{100D}_{(3,0.5)}$	3	1	2	409.19	892.38	409.19	1784.75	**-1375.56**	-13.76	409.19	-1271.98	-0.73	-11.59	33.33	-458.56	0.23	0.46	-1784.75
E1.4	$DIST^{V4}-ZSPRD^{100D}_{(2.7,2)}$	8	5	3	124.63	82.45	623.15	247.36	**375.78**	3.76	220.07	-128.75	-0.84	-13.33	62.5	46.97	2.52	1.51	-128.75
E1.5	$DIST^{V4}-ZSPRD^{100D}_{(2.7,1)}$	6	3	3	165.41	67.28	496.22	201.83	**294.39**	2.94	273.41	-160.11	-0.68	-10.79	50	49.07	2.46	2.46	-169.99
E1.6	$DIST^{V4}-ZSPRD^{100D}_{(2.7,0.5)}$	6	4	2	168	826.82	671.99	1653.64	**-981.66**	-9.82	273.41	-1077.2	-0.58	-9.21	66.67	-163.58	0.41	0.2	-1653.65
E2.1	$DIST^{V4}-SPRD^{100D}-SMA_{(10,20)}$	24	9	15	401.46	226.92	3613.15	3403.87	**209.28**	2.09	816.15	-872.25	-0.37	-5.87	37.5	8.72	1.06	1.77	-1801.07
E2.2	$DIST^{V4}-SPRD^{100D}-EMA_{(10,20)}$	39	11	28	421.64	166.6	4638.06	4664.84	**-26.78**	-0.27	1091.18	-813.16	-0.42	-6.67	28.21	-0.66	0.99	2.53	-1983.16
E2.3	$DIST^{V4}-SPRD^{100D}-MACD_{(12,26,9)}$	30	8	22	395.69	241.47	3165.53	5312.35	**-2146.82**	-21.47	1198.67	-1216.71	-0.54	-8.57	26.67	-71.54	0.6	1.64	-3489.9
E2.4	$DIST^{V4}-SPRD^{100D}-RSI_{(14)}$	3	1	2	325.89	1354.39	325.89	2708.78	**-2382.89**	-23.83	325.89	-1960.81	-0.83	-13.18	33.33	-794.35	0.12	0.24	-747.97
E2.5	$DIST^{V4}-SPRD^{100D}-BB_{(20)}$	19	16	3	145.58	230.86	2329.36	692.57	**1636.79**	16.37	345.12	-454.62	-0.36	-5.71	84.21	86.14	3.36	0.63	-454.62
E3	$DIST^{V4}-SPRD^{100D}-DECTREE$	292	133	159	82.66	81.08	10994.12	12891.9	**-1897.78**	-18.98	455.57	-486.57	-1.31	-20.8	45.55	-6.5	0.85	1.02	-2192.78
E4	$DIST^{V4}-SPRD^{100D}-MLP$	158	74	84	121.74	81.74	9008.65	6866.07	**2142.57**	21.43	1472.38	-378.48	-0.77	-12.22	46.84	13.57	1.31	1.49	-897.21
	Part VI: Models derived using the spread obtained from $JOHANSEN-SPRD^{100D}$																		
F1.1	$JOHANSEN-ZSPRD^{100D}_{(3,2)}$	10	7	3	166.52	85.57	1165.63	256.7	**908.93**	9.09	486.23	-232.12	-0.29	-4.6	70	90.89	4.54	1.95	-232.12
F1.2	$JOHANSEN-ZSPRD^{100D}_{(3,1)}$	9	6	3	124.54	12.48	747.25	37.43	**709.82**	7.1	486.23	-16.35	0.29	4.6	66.67	78.87	19.96	9.98	-16.35
F1.3	$JOHANSEN-ZSPRD^{100D}_{(3,0.5)}$	9	6	3	137.9	12.48	827.41	37.43	**789.98**	7.9	486.23	-16.35	0.29	4.6	66.67	87.78	22.11	11.05	-16.35
F1.4	$JOHANSEN-ZSPRD^{100D}_{(2.7,2)}$	11	7	4	166.04	77.9	1162.26	311.61	**850.65**	8.51	486.23	-232.12	-0.3	-4.76	63.64	77.34	3.73	2.13	-232.12
F1.5	$JOHANSEN-ZSPRD^{100D}_{(2.7,1)}$	10	7	3	125.65	17.83	879.57	53.5	**826.07**	8.26	486.23	-28.92	0.36	5.71	70	82.61	16.44	7.05	-28.92
F1.6	$JOHANSEN-ZSPRD^{100D}_{(2.7,0.5)}$	10	7	3	137.1	17.83	959.73	53.5	**906.23**	9.06	486.23	-28.92	0.36	5.71	70	90.62	17.94	7.69	-28.92
F2.1	$JOHANSEN-SPRD^{100D}-SMA_{(10,20)}$	19	6	13	2153.07	1871.56	12918.43	24330.22	**-11411.79**	-114.12	7670.16	-11811.22	-0.23	-3.65	31.58	-600.58	0.53	1.15	-21060.55
F2.2	$JOHANSEN-SPRD^{100D}-EMA_{(10,20)}$	22	11	11	2691.8	159.17	29609.77	1750.84	**27858.94**	278.59	12079.79	-849.68	0.52	8.25	50	1266.32	16.91	16.91	-849.68
F2.3	$JOHANSEN-SPRD^{100D}-MACD_{(12,26,9)}$	32	16	16	8221.39	8094.48	131542.29	129511.7	**2030.59**	20.31	123504.36	-116005.92	-	-	50	63.46	1.02	1.02	-116258.75
F2.4	$JOHANSEN-SPRD^{100D}-RSI_{(14)}$	4	2	2	1031.04	990.64	2062.07	1981.29	**80.79**	0.81	1833.09	-1953.43	-0.5	-7.94	50	20.2	1.04	1.04	-1953.43
F2.5	$JOHANSEN-SPRD^{100D}-BB_{(20)}$	21	12	9	722.8	704.33	8673.61	6338.93	**2334.68**	23.35	3109.57	-2889.43	0.26	4.13	57.14	111.13	1.37	1.03	-4722.46
F3	$JOHANSEN-SPRD^{100D}-DECTREE$	295	160	135	92.18	101.74	14749.19	13735.28	**1013.91**	10.14	591.06	-871.18	-1.03	-16.35	54.24	3.44	1.07	0.91	-2896.08
F4	$JOHANSEN-SPRD^{100D}-MLP$	150	76	74	106.83	88.71	8119.04	6564.42	**1554.62**	15.55	704.94	-526.04	-0.94	-14.92	50.67	10.37	1.24	1.2	-2042.14
	Part VII: Models derived using the spread obtained from $ADF-SPRD^{100D}$																		
G1.1	$ADF-ZSPRD^{100D}_{(3,2)}$	5	2	3	430.09	178.82	860.18	536.47	**323.71**	3.24	536.12	-351.15	-	-	40	64.74	1.6	2.41	-388.44
G1.2	$ADF-ZSPRD^{100D}_{(3,1)}$	5	2	3	177.05	342.81	354.09	1028.43	**-674.34**	-6.74	280.37	-375.71	-0.68	-10.79	40	-134.87	0.34	0.52	-724.59
G1.3	$ADF-ZSPRD^{100D}_{(3,0.5)}$	4	-	4	-	399.32	-	1597.3	**-1597.3**	-15.97	-	-730.94	-1.37	-21.75	-	-399.32	-	-	-1597.3
G1.4	$ADF-ZSPRD^{100D}_{(2.7,2)}$	7	3	4	306.4	149.22	919.21	596.86	**322.35**	3.22	536.12	-201.54	0.47	7.46	42.86	46.06	1.54	2.05	-268.8
G1.5	$ADF-ZSPRD^{100D}_{(2.7,1)}$	6	3	3	495.82	297.98	1487.46	893.95	**593.5**	5.94	1249.09	-433.48	-0.43	-6.83	50	98.92	1.66	1.66	-590.11
G1.6	$ADF-ZSPRD^{100D}_{(2.7,0.5)}$	5	2	3	441.86	452.72	883.72	1358.16	**-474.44**	-4.74	866.02	-592.14	-0.5	-7.94	40	-94.89	0.65	0.98	-895.98
G2.1	$ADF-SPRD^{100D}-SMA_{(10,20)}$	18	12	6	521.84	610.35	6262.07	3662.13	**2599.94**	26	1513.79	-1107.52	0.22	3.49	66.67	144.48	1.71	0.85	-1703.34
G2.2	$ADF-SPRD^{100D}-EMA_{(10,20)}$	26	18	8	362.41	7879.96	6523.39	63039.7	**-56516.31**	-565.16	2323.99	-57423.85	-0.14	-2.22	69.23	-2173.77	0.1	0.05	-59374.86
G2.3	$ADF-SPRD^{100D}-MACD_{(12,26,9)}$	28	17	11	145.61	572.57	2475.4	6298.25	**-3822.86**	-38.23	574.8	-1339.23	-0.47	-7.46	60.71	-136.56	0.39	0.25	-5430.75
G2.4	$ADF-SPRD^{100D}-RSI_{(14)}$	1	1	-	2979.79	-	2979.79	-	**2979.79**	29.8	2979.79	-	-	-	100	2979.79	2979.79	2979.79	-
G2.5	$ADF-SPRD^{100D}-BB_{(20)}$	14	6	8	701.45	433.25	4208.71	3466.02	**742.69**	7.43	1359.62	-1945.89	0.22	3.49	42.86	53.08	1.21	1.62	-2531.64
G3	$ADF-SPRD^{100D}-DECTREE$	304	140	164	95.55	81.35	13376.81	13341.89	**34.91**	0.35	779.49	-439.03	-1.14	-18.1	46.05	0.11	1	1.17	-1649.61
G4	$ADF-SPRD^{100D}-MLP$	203	97	106	105.84	98.75	10266.78	10467.04	**-200.26**	-2	597.49	-526.04	-1.06	-16.83	47.78	-0.99	0.98	1.07	-3023.62
	Part VIII: Models derived using the spread obtained from $KALMAN-SPRD^{100D}$																		
H1.1	$KALMAN-ZSPRD^{100D}_{(3,2)}$	4	2	2	61.52	677.31	123.04	1354.63	**-1231.59**	-12.32	89.08	-1009.9	-0.93	-14.76	50	-307.9	0.09	0.09	-1265.55
H1.2	$KALMAN-ZSPRD^{100D}_{(3,1)}$	4	2	2	293.08	317.64	586.17	635.28	**-49.12**	-0.49	344.11	-554.87	-0.43	-6.83	50	-12.28	0.92	0.92	-554.87
H1.3	$KALMAN-ZSPRD^{100D}_{(3,0.5)}$	3	2	1	227.71	380.71	455.41	380.71	**74.7**	0.75	242.06	-380.71	-0.4	-6.35	66.67	24.92	1.2	0.6	-380.71
H1.4	$KALMAN-ZSPRD^{100D}_{(2.7,2)}$	6	2	4	82.57	474.89	165.15	1899.57	**-1734.42**	-17.34	158.44	-1073.33	-1.08	-17.14	33.33	-289.09	0.09	0.17	-1899.57
H1.5	$KALMAN-ZSPRD^{100D}_{(2.7,1)}$	5	3	2	154.39	633.2	463.18	1266.4	**-803.22**	-8.03	232.57	-1185.99	-0.58	-9.21	60	-160.64	0.37	0.24	-1249.3
H1.6	$KALMAN-ZSPRD^{100D}_{(2.7,0.5)}$	3	1	2	213.5	696.28	213.5	1392.56	**-1179.06**	-11.79	213.5	-1272.63	-0.75	-11.91	33.33	-393.05	0.15	0.31	-1392.56
H2.1	$KALMAN-SPRD^{100D}-SMA_{(10,20)}$	15	9	6	471.98	190.23	4247.86	1141.38	**3106.48**	31.06	1652.81	-464.35	0.06	0.95	60	207.1	3.72	2.48	-852.8
H2.2	$KALMAN-SPRD^{100D}-EMA_{(10,20)}$	24	8	16	553.94	160.16	4431.55	2562.54	**1869.01**	18.69	1573.1	-386.01	-0.17	-2.7	33.33	77.85	1.73	3.46	-981.11
H2.3	$KALMAN-SPRD^{100D}-MACD_{(12,26,9)}$	28	7	21	574.02	219.22	4018.14	4603.68	**-585.53**	-5.86	1202.57	-753.63	-0.37	-5.87	25	-20.91	0.87	2.62	-2635.7
H2.4	$KALMAN-SPRD^{100D}-RSI_{(14)}$	1	-	1	-	14.89	-	14.89	**-14.89**	-0.15	-	-14.89	-	-	-	-14.89	-	-	-14.89
H2.5	$KALMAN-SPRD^{100D}-BB_{(20)}$	7	5	2	154.29	405.06	771.46	810.13	**-38.66**	-0.39	246.28	-424.03	-0.52	-8.25	71.43	-5.52	0.95	0.38	-810.13
H3	$KALMAN-SPRD^{100D}-DECTREE$	258	151	107	75.87	107.48	11456.88	11500.49	**-43.61**	-0.44	477.36	-769.57	-1.12	-17.78	58.53	-0.16	1	0.71	-2612.48
H4	$KALMAN-SPRD^{100D}-MLP$	150	87	63	88.96	94.74	7739.91	5968.33	**1771.58**	17.72	500.06	-713.81	-1.02	-16.19	58	11.81	1.3	0.94	-2155.25
	Part IX: Models derived using the spread obtained from $RATIO-SPRD^{100D}$																		
I1.1	$RATIO-ZSPRD^{100D}_{(3,2)}$	2	1	1	122.53	965.26	122.53	965.26	**-842.72**	-8.43	122.53	-965.26	-0.75	-11.91	50	-421.36	0.13	0.13	-965.26
I1.2	$RATIO-ZSPRD^{100D}_{(3,1)}$	1	-	1	-	775.74	-	775.74	**-775.74**	-7.76	-	-775.74	-	-	-	-775.74	-	-	-775.74
I1.3	$RATIO-ZSPRD^{100D}_{(3,0.5)}$	1	-	1	-	562.48	-	562.48	**-562.48**	-5.62	-	-562.48	-	-	-	-562.48	-	-	-562.48
I1.4	$RATIO-ZSPRD^{100D}_{(2.7,2)}$	6	4	2	76.06	515.21	304.26	1030.41	**-726.15**	-7.26	123.37	-965.26	-0.65	-10.32	66.67	-121.01	0.3	0.15	-965.26
I1.5	$RATIO-ZSPRD^{100D}_{(2.7,1)}$	4	3	1	167.37	950.67	502.1	950.67	**-448.58**	-4.49	209.18	-950.67	-0.47	-7.46	75	-112.14	0.53	0.18	-950.67
I1.6	$RATIO-ZSPRD^{100D}_{(2.7,0.5)}$	2	1	1	173.83	1031.32	173.83	1031.32	**-857.49**	-8.57	173.83	-1031.32	-0.68	-10.79	50	-428.74	0.17	0.17	-1031.32
I2.1	$RATIO-SPRD^{100D}-SMA_{(10,20)}$	17	7	10	236.66	217.22	1656.59	2172.16	**-515.56**	-5.16	543.12	-326.39	-0.64	-10.16	41.18	-30.31	0.76	1.09	-1107.21
I2.2	$RATIO-SPRD^{100D}-EMA_{(10,20)}$	19	8	11	481.19	159.68	3849.53	1756.49	**2093.04**	20.93	1242	-374.54	-0.1	-1.59	42.11	110.19	2.19	3.01	-903.25
I2.3	$RATIO-SPRD^{100D}-MACD_{(12,26,9)}$	35	8	27	374.2	193.3	2993.6	5219.08	**-2225.48**	-22.25	971.96	-529.01	-0.68	-10.79	22.86	-63.57	0.57	1.94	-2762.73
I2.4	$RATIO-SPRD^{100D}-RSI_{(14)}$	2	1	1	571.59	2506.6	571.6	2506.6	**-1935.01**	-19.35	571.59	-2506.6	-0.51	-8.1	50	-967.5	0.23	0.23	-
I2.5	$RATIO-SPRD^{100D}-BB_{(20)}$	12	8	4	233.46	347.49	1867.65	1389.97	**477.68**	4.78	644.1	-814.22	-0.3	-4.76	66.67	39.83	1.34	0.67	-814.22
I3	$RATIO-SPRD^{100D}-DECTREE$	282	114	168	93.16	64.41	10620.67	10821.48	**-200.82**	-2.01	525.98	-315.15	-1.35	-21.43	40.43	-0.71	0.98	1.45	-2149.88
I4	$RATIO-SPRD^{100D}-MLP$	202	82	120	108.16	75.88	8868.72	9105.72	**-237.01**	-2.37	732.39	-315.15	-1.17	-18.57	40.59	-1.18	0.97	1.43	-1986.86
	Part X: Models derived using the close price of VWO.N																		
CLS-SYM-1.1	$CLOSE^{VWO.N}-SMA_{(10,20)}$	15	6	9	230.99	239.78	1385.96	2158.06	**-772.1**	-7.72	679.96	-536.93	-0.43	-6.83	40	-51.47	0.64	0.96	-853.38
CLS-SYM-1.2	$CLOSE^{VWO.N}-EMA_{(10,20)}$	26	6	20	586.9	150.62	3521.39	3012.49	**508.9**	5.09	1242.77	-650.86	-0.14	-2.22	23.08	19.6	1.17	3.9	-1491.05
CLS-SYM-1.3	$CLOSE^{VWO.N}-MACD_{(12,26,9)}$	29	11	18	238.08	143.51	2618.9	2583.23	**35.67**	0.36	884.37	-347.88	-0.3	-4.76	37.93	1.23	1.01	1.66	-1298.22
CLS-SYM-1.4	$CLOSE^{VWO.N}-RSI_{(14)}$	6	3	3	205.52	522.84	616.55	1568.52	**-951.97**	-9.52	310.49	-1337.12	-0.39	-6.19	50	-158.66	0.39	0.39	-1337.12
CLS-SYM-1.5	$CLOSE^{VWO.N}-BB_{(20)}$	17	11	6	70.92	230.58	780.12	1383.47	**-603.35**	-6.03	100.93	-491.85	-0.63	-10	64.71	-35.48	0.56	0.31	-689.89
	Part XI: Models derived using the close price of XLE.N																		
CLS-SYM-2.1	$CLOSE^{XLE.N}-SMA_{(10,20)}$	19	9	10	492.93	337.96	4436.4	3379.63	**1056.77**	10.57	1969.29	-993.26	-0.03	-0.48	47.37	55.63	1.31	1.46	-2390.02
CLS-SYM-2.2	$CLOSE^{XLE.N}-EMA_{(10,20)}$	26	11	15	546.32	161.14	6009.56	2417.09	**3592.47**	35.92	2197.81	-326.2	0.12	1.9	42.31	138.19	2.49	3.39	-711.67
CLS-SYM-2.3	$CLOSE^{XLE.N}-MACD_{(12,26,9)}$	27	10	17	637.2	211.29	6372.04	3591.96	**2780.08**	27.8	1931.38	-613.01	0.05	0.79	37.04	102.99	1.77	3.02	-645.92
CLS-SYM-2.4	$CLOSE^{XLE.N}-RSI_{(14)}$	5	3	2	314.75	1213.82	944.26	2427.64	**-1483.38**	-14.83	365.04	-1229.73	-0.44	-6.98	60	-296.68	0.39	0.26	-2062.6
CLS-SYM-2.5	$CLOSE^{XLE.N}-BB_{(20)}$	20	17	3	198.62	500.07	3376.55	1500.22	**1876.33**	18.76	822.47	-1185.85	0.05	0.79	85	93.82	2.25	0.4	-1185.85

References

Abhishek, K., Singh, M., Ghosh, S., Anand, A., 2012. Weather forecasting model using artificial neural network. Procedia Technology 4, 311–318.

Ahmed, S., Nielsen, I.E., Tripathi, A., Siddiqui, S., Rasool, G., Ramachandran, R.P., 2022. Transformers in time-series analysis: A tutorial. arXiv preprint arXiv:2205.01138 .

Akita, R., Yoshihara, A., Matsubara, T., Uehara, K., 2016. Deep learning for stock prediction using numerical and textual information, in: 2016 IEEE/ACIS 15th International Conference on Computer and Information Science (ICIS), IEEE Computer Society. pp. 1–6.

Alex, G., 2014. Generating sequences with recurrent neural networks. Working paper, University of Toronto.

Alex, G., Jurgen, S., 2008.

Alexander, C., Dimitriu, A., 2002. The cointegration alpha: Enhanced index tracking and long-short equity market neutral strategies .

Amilon, H., 2003. A neural network versus Black-Scholes: a comparison of pricing and hedging performances. Journal of Forecasting 22, 317–335.

Anders, U., Korn, O., Schmitt, C., 1998. Improving the pricing of options: a neural network approach. Journal of Forecasting 17, 369–388.

Andersen, T., Benzoni, L., Lund, J., 2002. An empirical investigation of continuous-time equity return models. Journal of Finance 57, 1239–1284.

Andreevna, L.M., 2022. Increasing the accuracy of financial accounting by applying machine-learning for options pricing .

Andreou, P.C., Charalambous, C., H., M.S., 2002. Critical assessment of option pricing methods using artificial neural networks, in: Proceedings of the 2002 International Conference on Artificial Neural Networks;, pp. 1131–1136.

Andreou, P.C., Charalambous, C., H., M.S., 2004. Option pricing and trading with artificial neural networks and advanced parametric models with implied parameters, in: Proceedings of the 2004 International Joint Conference on Neural Networks vol. 4., IEEE. pp. 2741–2746.

Andreou, P.C., Charalambous, C., Martzoukos, S., 2006. Robust artificial neural networks for pricing of european options. Computational Economics 27, 329–351.

Andreou, P.C., Charalambous, C., Martzoukos, S.H., 2008. Pricing and trading european options by combining artificial neural networks and parametric models with implied parameters. European Journal of Operational Research 185, 1415–1433.

Andreou, P.C., Charalambous, C., Martzoukos, S.H., 2010. Generalized parameter functions for option pricing. Journal of Banking and Finance 34, 633–646.

Appel, G., . The major trend power index. Scientific Investment Systems, Inc 62.

Avellaneda, M., Lee, J.H., 2010. Statistical arbitrage in the us equities market. Quantitative Finance 10, 761–782.

Bai, M., Liu, X., Yang, K., Li, Y., 2019. Stock investment strategy based on decision tree, in: 2019 IEEE 7th International Conference on Computer Science and Network Technology (ICCSNT), IEEE. pp. 151–155.

Bakshi, C., Cao, C., Chen, Z., 1997a. Empirical performance of alternative option pricing models. Journal of Finance 52, 2003–2049.

Bakshi, G., Cao, C., Chen, Z., 1997b. Pricing and hedging long-term options. Working paper, University of Maryland, Pennsylvania State University, and The Ohio State University.

Bakshi, G., Madan, D., 2000. Spanning and derivative-security valuation. Journal of financial economics 55, 205–238.

Bao, W., Yue, J., Rao, Y., 2017. A deep learning framework for financial time series using stacked autoencoders and long-short term memory.

Bates, D., 1996. Jumps and stochastic volatility: exchange rate processes implicit in Deutschemark options. Review of Financial Studies 9, 69–107.

Bates, D.S., 2006. Maximum Likelihood Estimation of Latent Affine Processes. Review of Financial Studies 19, 909–965.

Baughman, D., Liu, Y., 1995. Fundamental and Practical Aspects of Neural Computing. Neural Networks in Bioprocessing and Chemical Engineering , 21–109.

Baur, D.G., 2003. What is co-movement? .

Beale, M.H., Hagan, M.T., Demuth, H.B., 2010. Neural network toolbox. User's Guide, MathWorks 2, 77–81.

Becker, S., Cheridito, P., Jentzen, A., 2019. Deep optimal stopping. Journal of Machine Learning Research 20, 74.

Bennell, J., Sutcliffe, C.M.S., 2004. Black-Scholes versus artificial neural networks in pricing FTSE 100 options. Intelligent Systems in Accounting, Finance and Management 12, 243–260.

Black, F., Scholes, M., 1973. The pricing of options and corporate liabilities. Journal of Political Economy 81, 637–659.

Black, F., Scholes, M., 1975. Fact and fantasy in the use of options. Financial Analysts Journal 31, 36–41, 61–72.

Bloch, D.A., 2019. Neural networks based dynamic implied volatility surface. Available at SSRN 3492662 .

Bogomolov, T., 2011. Pairs trading in the land down under, in: Finance and Corporate Governance Conference.

Bollinger, J., 1992. Using bollinger bands. Stocks & Commodities 10, 47–51.

Bowen, D., Hutchinson, M.C., O'Sullivan, N., 2010. High-frequency equity pairs trading: transaction costs, speed of execution, and patterns in returns. The Journal of Trading 5, 31–38.

Boyle, P.P., Vorst, T., 1992. Option replication in discrete time with transaction costs. The Journal of Finance 47, 271–293.

Breiman, L., 1996. Bagging predictors. Machine learning 24, 123–140.

Broussard, J.P., Vaihekoski, M., 2012. Profitability of pairs trading strategy in an illiquid market with multiple share classes. Journal of International Financial Markets, Institutions and Money 22, 1188–1201.

Bucci, A., 2020. Cholesky–ann models for predicting multivariate realized volatility. Journal of Forecasting 39, 865–876.

Buehler, H., Gonon, L., Teichmann, J., Wood, B., 2019. Deep hedging. Quantitative Finance 19, 1271–1291.

Caldeira, J., Moura, G.V., 2013. Selection of a portfolio of pairs based on cointegration: A statistical arbitrage strategy. Available at SSRN 2196391 .

Cao, J., Chen, J., Hull, J., 2020. A neural network approach to understanding implied volatility movements. Quantitative Finance 20, 1405–1413.

Cao, J., Chen, J., Hull, J., Poulos, Z., 2021. Deep hedging of derivatives using reinforcement learning. The Journal of Financial Data Science 3, 10–27.

Cao, L., Luo, D., Zhang, C., 2006. Fuzzy genetic algorithms for pairs mining, in: Pacific Rim International Conference on Artificial Intelligence, Springer. pp. 711–720.

Carbonneau, A., Godin, F., 2021. Deep equal risk pricing of financial derivatives with multiple hedging instruments. arXiv preprint arXiv:2102.12694 .

Carr, P.P., Wu, L., 2003. The Finite Moment Log Stable Process and Option Pricing. Journal of Finance 58, 753–777.

Carverhill, A., Cheuk, T.H.F., 2003. Alternative neural network approach for option pricing and hedging. Working paper, School of Business, University of Hong Kong.

Chan, E., 2013. Algorithmic trading: winning strategies and their rationale. volume 625. John Wiley & Sons.

Chang, E., 2022. Cnn-lstm vs ann: Option pricing theory .

Chaudhuri, T., Singh, P., 2015. Execution of pairs trading strategy: Some propositions. Available at SSRN 2630947 .

Chaudhuri, T.D., Ghosh, I., Singh, P., 2017. Application of machine learning tools in predictive modeling of pairs trade in indian stock market. IUP Journal of Applied Finance 23.

Chen, F., Sutcliffe, C., 2012. Pricing and hedging short sterling options Using neural networks. Intelligent Systems in Accounting, Finance and Management 19, 128–149.

Chen, H., Chen, S., Chen, Z., Li, F., 2019. Empirical investigation of an equity pairs trading strategy. Management Science 65, 370–389.

Chen, K., Zhou, Y., Dai, F., 2015. A lstm-based method for stock returns prediction: A case study of china stock market, IEEE Computer Society. p. 2823–2824.

Corrado, C., Su, T., 1997. lmplied volatility skews and stock index skewness and kurtosis implied by s&p 500 index option prices. Journal of Derivatives , 8–19.

De Ryck, T., Lanthaler, S., Mishra, S., 2021. On the approximation of functions by tanh neural networks. Neural Networks 143, 732–750.

Dickey, D.A., Fuller, W.A., 1979. Distribution of the estimators for autoregressive time series with a unit root. Journal of the American statistical association 74, 427–431.

Diebold, F., Mariano, R., 1995. Comparing predictive accuracy. Journal of Business and Economic Statistics 13, 253–263.

Do, B., Faff, R., 2010. Does simple pairs trading still work? Financial Analysts Journal 66, 83–95.

Do, B., Faff, R., 2012. Are pairs trading profits robust to trading costs? Journal of Financial Research 35, 261–287.

Do, B., Faff, R., Hamza, K., 2006. A new approach to modeling and estimation for pairs trading, in: Proceedings of 2006 financial management association European conference, Citeseer. pp. 87–99.

Donaldson, R.G., Kamstra, M., 1997. An artificial neural network-garch model for international stock return volatility. Journal of Empirical Finance 4, 17–46.

Douglas E., J.S., 2002. A First Look at Music Composition using LSTM Recurrent Neural Networks. Istituto Dalle Molle Di Studi Sull Intelligenza Artificiale .

Drakos, S., 2016. Statistical arbitrage in s&p500. Journal of Mathematical Finance 6, 166–177.

Dugas, C., Bengio, Y., Bélisle, F., Nadeau, C., Garcia, R., 2001. Incorporating second-order functional knowledge for better option pricing, in: Leen, T.K., Dietterich, T.G., Tresp, V. (Eds.), Advances in Neural Information Processing Systems 13. MIT Press, Cambridge, MA, pp. 451–457.

Dumas, B., Fleming, F., Whaley, R., 1996. Implied volatility functions: empirical tests. Journal of Finance 53, 2059–2106.

Dunis, C.L., Giorgioni, G., Laws, J., Rudy, J., 2010. Statistical arbitrage and high-frequency data with an application to eurostoxx 50 equities. Liverpool Business School, Working paper .

Dunis, C.L., Laws, J., Evans, B., 2006. Modelling and trading the gasoline crack spread: A non-linear story. Derivatives Use, Trading & Regulation 12, 126–145.

Dunis, C.L., Laws, J., Evans, B., 2009. Modelling and trading the soybean-oil crush spread with recurrent and higher order networks: A comparative analysis, in: Artificial Higher Order Neural Networks for Economics and Business. IGI Global, pp. 348–366.

Dunis, C.L., Laws, J., Middleton, P.W., Karathanasopoulos, A., 2015. Trading and hedging the corn/ethanol crush spread using time-varying leverage and nonlinear models. The European Journal of Finance 21, 352–375.

Eberlein, E., Raible, S., 1999. Term structure models driven by general lévy processes. Mathematical Finance 9, 31–53.

Engelberg, J., Gao, P., Jagannathan, R., 2009. An anatomy of pairs trading: the role of idiosyncratic news, common information and liquidity, in: Third Singapore International Conference on Finance.

Engle, R.F., Granger, C.W., 1987. Co-integration and error correction: representation, estimation, and testing. Econometrica: journal of the Econometric Society , 251–276.

Fallahpour, S., Hakimian, H., Taheri, K., Ramezanifar, E., 2016. Pairs trading strategy optimization using the reinforcement learning method: a cointegration approach. Soft Computing 20, 5051–5066.

Fécamp, S., Mikael, J., Warin, X., 2019. Risk management with machine-learning-based algorithms. arXiv preprint arXiv:1902.05287 .

Ferguson, R., Green, A., 2018. Deeply learning derivatives. arXiv preprint arXiv:1809.02233 .

Figueiredo, M., Saporito, Y., 2022. Forecasting the term structure of commodities future prices using machine learning. Digital Finance , 1–34doi:10.1007/s42521-022-00069-3.

Forsee F.D., .H.M., 1997. Gauss-Newton approximation to Bayesian learning, pp. 415–447.

Franses, P.H., Van Dijk, D., et al., 2000. Non-linear time series models in empirical finance. Cambridge university press.

Garcia, R., Gençay, R., 1998. Option pricing with neural networks and a homogeneity hint, in: Refenes, A.P.N., Burgess, A.N., Moody, J.E. (Eds.), Decision Technologies for Computational Finance: Proceedings of the Fifth International Conference Computational Finance, Springer. pp. 195–205. Advances in Computational Management Science, vol. 2.

Garcia, R., Gençay, R., 2000. Pricing and hedging derivatives securities with neural networks and a homogeneity hint. Journal of Econometrics 94, 93–115.

Gatev, E., Goetzmann, W.N., Rouwenhorst, K.G., 2006. Pairs trading: Performance of a relative-value arbitrage rule. The Review of Financial Studies 19, 797–827.

Gatev, Goetzmann, W., Rouwenhorst, K.G., et al., 1999. Pairs trading: Performance of a relative value arbitrage rule. Technical Report. Yale School of Management.

Gautam, A., Singh, V., 2020. Parametric versus non-parametric time series forecasting methods: A review. Journal of Engineering Science & Technology Review 13.

Gençay, R., Gibson, R., 2007. Model risk for European style stock index options. IEEE Transactions on Neural Networks 18, 193–202.

Gençay, R., Qi, M., 2001. Pricing and hedging derivative securities with neural networks: Bayesian regularization, early stopping and bagging. IEEE Transactions on Neural Networks 12, 726–734.

Gençay, R., Salih, A., 2003. Degree of mispricing with the Black-Scholes model and non parametric cures. Annals of Economics and Finance 4, 73–101.

Gers, F.A., Schmidhuber, E., 2001. Lstm recurrent networks learn simple context-free and context-sensitive languages. IEEE Transactions on Neural Networks 12, 1333–1340.

Ghaziri, H., Elfakhani, S., Assi, J., 2000. Neural networks approach to pricing options. Neural Network World 10, 271–277.

Ghosn, J., Bengio, Y., 2002. Multi-task learning for option pricing. Working paper 2002s-53, CIRANO, Montreal.

Gil-Pelaez, J., 1951. Note on the inversion theorem. Biometrika 38, 481–482.

Gradojevic, N., Gençay, R., Kukolj, D., 2009. Option pricing with modular neural networks. IEEE Transactions on Neural Networks 20, 626–637.

Gradojevic, N., Kukolj, D., 2011. Parametric option pricing: a divide-and-conquer approach. Physica D: Nonlinear Phenomena 240, 1528–1535.

Gu, B., Zhang, T., Meng, H., Zhang, J., 2021. Short-term forecasting and uncertainty analysis of wind power based on long short-term memory, cloud model and non-parametric kernel density estimation. Renewable Energy 164, 687–708.

Guo, Y., Zhang, Z., Jiang, J., Wu, W., Zhang, C., Cui, B., Li, J., 2021. Model averaging in distributed machine learning: a case study with Apache Spark. The VLDB Journal 30, 693—-712. doi:https://doi.org/10.1007/s00778-021-00664-7.

Gupta, P., Malsa, N., Saxena, N., Agarwal, S., Singh, S.P., 2020. Short-term load forecasting using parametric and non-parametric approaches, in: Soft Computing: Theories and Applications: Proceedings of SoCTA 2018, Springer. pp. 747–755.

Gybenko, G., et al., 1989. Approximation by superposition of sigmoidal functions. Mathematics of Control, Signals and Systems 2, 303–314.

Hahn, J.T., 2013. Option pricing using artificial neural networks: an Australian perspective. Citeseer.

Hajizadeh, E., 2020. Developing an optimized artificial intelligence model for s&p 500 option pricing: A hybrid garch model. International Journal of Financial Engineering 7, 2050025.

Hamid, S.A., Habib, A., 2005. Can neural networks learn the black-scholes model? a simplified approach .

Hamid, S.A., Iqbal, Z., 2004. Using neural networks for forecasting volatility of s&p 500 index futures prices. Journal of Business Research 57, 1116–1125.

Van der Have, R., van Dijk, D., Kole, H., Eisma, I.H., Diepen, G., 2017. Pairs trading using machine learning: An empirical study. Erasmus University Rotterdam .

Heaton, J., 2008. Introduction to Neural Networks for Java. Heaton Research Inc.

Herrmann, R., Narr, A., 1997. Risk neutrality. Risk 10 (Technology Supplement) 23, 26–29.

Heston, S., 1993. A closed-form solution for options with stochastic volatility with applications to bond and currency options. Review of Financial Studies 6, 327–343.

Hihi, S., Bengio, Y., 1995. Hierarchical recurrent neural networks for long-term dependencies. Advances in neural information processing systems 8.

Hogan, S., Jarrow, R., Teo, M., Warachka, M., 2004. Testing market efficiency using statistical arbitrage with applications to momentum and value strategies. Journal of Financial economics 73, 525–565.

Hornik, K., Stinchcombe, M., White, H., 1989. Multilayer feedforward networks are universal approximators. Neural networks 2, 359–366.

Hornik, K., Stinchcombe, M., White, H., 1990. Universal approximation of an unknown mapping and its derivatives using multilayer feedforward networks. Neural Networks 3, 551–560.

Horvath, B., Teichmann, J., Žurič, Ž., 2021. Deep hedging under rough volatility. Risks 9, 138.

Hou, Y., Edara, P., 2018. Network scale travel time prediction using deep learning. Transportation Research Record 2672, 115–123.

Huck, N., 2009. Pairs selection and outranking: An application to the s&p 100 index. European Journal of Operational Research 196, 819–825.

Huck, N., 2010. Pairs trading and outranking: The multi-step-ahead forecasting case. European Journal of Operational Research 207, 1702–1716.

Huck, N., 2013. The high sensitivity of pairs trading returns. Applied Economics Letters 20, 1301–1304.

Huck, N., 2015. Pairs trading: does volatility timing matter? Applied Economics 47, 6239–6256.

Huck, N., Afawubo, K., 2015. Pairs trading and selection methods: is cointegration superior? Applied Economics 47, 599–613.

Hutchinson, J.M., Lo, A.W., Poggio, T., 1994. A non parametric approach to pricing and hedging derivative securities via learning networks. Journal of Finance 49, 851–889.

Ince, H., 2006. Non-parametric regression methods. Computational Management Science 3, 161–174.

Ivașcu, C.F., 2021. Option pricing using machine learning. Expert Systems with Applications 163, 113799.

Jacobs, H., Weber, M., 2015. On the determinants of pairs trading profitability. Journal of Financial Markets 23, 75–97.

Jang, H., Lee, J., 2019. Generative bayesian neural network model for risk-neutral pricing of american index options. Quantitative Finance 19, 587–603.

Jiahong, L., Hui, B., Junjie, W., 2017. Sentiment-aware stock market prediction: A deep learning method, in: 2017 International Conference on Service Systems and Service Management, pp. 1–6.

Johansen, S., 1988. Statistical analysis of cointegration vectors. Journal of economic dynamics and control 12, 231–254.

Johansen, S., 1991. Estimation and hypothesis testing of cointegration vectors in gaussian vector autoregressive models. Econometrica: journal of the Econometric Society , 1551–1580.

Jonsson, E., Deumic, A., 2022. Machine learning for financial time series prediction: A comparative study on stock market data .

Karakoyun, E.S., Cibikdiken, A., 2018. Comparison of arima time series model and lstm deep learning algorithm for bitcoin price forecasting, in: The 13th multidisciplinary academic conference in Prague, pp. 171–180.

Kavinnilaa, J., Hemalatha, E., Jacob, M.S., Dhanalakshmi, R., 2021. Stock price prediction based on lstm deep learning model, in: 2021 International Conference on System, Computation, Automation and Networking (ICSCAN), IEEE. pp. 1–4.

Ke, A., Yang, A., 2019. Option pricing with deep learning. Department of Computer Science, Standford University, In CS230: Deep learning 8, 1–8.

Khaldi, R., El Afia, A., Chiheb, R., 2019. Forecasting of btc volatility: comparative study between parametric and nonparametric models. Progress in Artificial Intelligence 8, 511–523.

Kim, B.H., Lee, D., Lee, J., 2006. Local volatility function approximation using reconstructed radial basis function networks, in: International Symposium on Neural Networks, Springer. pp. 524–530.

Kim, K., 2011. Performance analysis of pairs trading strategy utilizing high frequency data with an application to kospi 100 equities. Available at SSRN 1913707 .

Kim, T., Oh, K., Kim, C., Do, J., 2004. Artificial neural networks for non-stationary time.

Kingma, D.P., Ba, J.L., 2005. pp. 1–13.

Klimasauskas, C., 1991. Neural nets tell why. Dr. Dobb's Journal 4, 16.

Ko, P.C., 2009. Option valuation based on the neural regression model. Expert Systems with Applications 26, 464–471.

Kohler, M., Krzyżak, A., Todorovic, N., 2010. Pricing of high-dimensional american options by neural networks. Mathematical Finance: An International Journal of Mathematics, Statistics and Financial Economics 20, 383–410.

Krauss, C., 2017. Statistical arbitrage pairs trading strategies: Review and outlook. Journal of Economic Surveys 31, 513–545.

Kumar, H., Patil, S.B., 2015. Estimation & forecasting of volatility using arima, arfima and neural network based techniques, in: 2015 IEEE International Advance Computing Conference (IACC), IEEE. pp. 992–997.

Kyoung-Sook, M., Hongjoong, K., 2019. Performance of deep learning in prediction of stock market volatility. Economic Computation & Economic Cybernetics Studies & Research 53.

Lajbcygier, P., Connor, J.T., 1997. Improved option pricing using artificial neural networks and bootstrap methods. International Journal of Neural Systems 8, 457–471.

Lajbcygier, P., Flitman, A., 1996. A comparison of non-parametric regression techniques for the pricing of options using an implied volatility, in: Refenes, A.P.N., Abu-Mostafa, Y., Moody, J., Weigend, A. (Eds.), Decision Technologies for Financial Engineering: Proceedings of the Fourth International Conference on Neural Networks in Capital Markets. World Scientific, New York, pp. 201–213.

Lajbcygier, P., Flitman, A., Swan, A., Hyndman, R., 1997. The pricing and trading of options using a hybrid neural network model with historical volatility. NeuroVe$t Journal 5, 27–41.

Lam, M., 2004. Neural network techniques for financial performance prediction: integrating fundamental and technical analysis. Decision support systems 37, 567–581.

Lee, J., Bahri, Y., Novak, R., Schoenholz, S.S., Pennington, J., Sohl-Dickstein, J., 2017. Deep neural networks as gaussian processes. arXiv preprint arXiv:1711.00165 .

Leland, H.E., 1985. Option pricing and replication with transactions costs. The journal of finance 40, 1283–1301.

Li, Y., Lv, S., Liu, X., Zhang, Q., 2022. Incorporating transformers and attention networks for stock movement prediction. Complexity 2022.

Liang, L., Cai, X., 2022. Time-sequencing european options and pricing with deep learning–analyzing based on interpretable ale method. Expert Systems with Applications 187, 115951.

Liang, X., Zhang, H., Li, X., 2009a. A simple method of forecasting option prices based on neural networks, in: Next-Generation Applied Intelligence: 22nd International Conference on Industrial, Engineering and Other Applications of Applied Intelligent Systems, IEA/AIE 2009, Tainan, Taiwan, June 24-27, 2009. Proceedings 22, Springer. pp. 586–593.

Liang, X., Zhang, H., Xiao, J., Chen, Y., 2009b. Improving option price forecasts with neural networks and support vector regressions. Neurocomputing 72, 3055–3065.

Liang, X., Zhang, H., Yang, J., 2006. Pricing options in hong kong market based on neural networks, in: Neural Information Processing: 13th International Conference, ICONIP 2006, Hong Kong, China, October 3-6, 2006. Proceedings, Part III 13, Springer. pp. 410–419.

Lim, B., Zohren, S., 2021. Time-series forecasting with deep learning: A survey. Philosophical Transactions of the Royal Society A: Mathematical, Physical and Engineering Sciences 379, 20200209. doi:https://doi.org/10.1098/rsta.2020.0209.

Lin, F.H.T., 2018. Dynamic asset allocation for pairs trading.

Lin, Y.X., McCRAE, M., Gulati, C., 2006. Loss protection in pairs trading through minimum profit bounds: A cointegration approach. Advances in Decision Sciences 2006.

Liu, B., Chang, L.B., Geman, H., 2017. Intraday pairs trading strategies on high frequency data: The case of oil companies. Quantitative Finance 17, 87–100.

Liu, Y., 2019. Novel volatility forecasting using deep learning–long short term memory recurrent neural networks. Expert Systems with Applications 132, 99–109.

Liu, Y., Zhang, X., 2023. Option pricing using lstm: A perspective of realized skewness. Mathematics 11, 314.

Mackay, D.J.C., 1992. Bayesian interpolation. Neural Computation 4, 415–447.

Mantri, J.K., Gahan, P., Nayak, B.B., 2014. Artificial neural networks–an application to stock market volatility. Soft-Computing in Capital Market: Research and Methods of Computational Finance for Measuring Risk of Financial Instruments 179.

Martel, C.G., Artiles, M.D.G., Rodriguez, F.F., 2009. A financial option pricing model based on learning algorithms, in: Proceedings of the World Multiconference on Applied Economics, Business and Development, AEBD'09, pp. 153–157.

Martin, S., 2006. Option Pricing Formulae using Fourier Transform: Theory and Application.

Masini, R.P., Medeiros, M.C., Mendes, E.F., 2021. Machine learning advances for time series forecasting. Journal of Economic Surveys doi:https://doi.org/10.1111/joes.12429.

Meire, F., Charles, B., Oriol, V., 2017. Bayesian recurrent neural networks. CoRR abs/1704.02798.

de Melo Mendes, B.V., Leal, R.P.C., 2005. Robust multivariate modeling in finance. International Journal of Managerial Finance .

Merton, R., 1973. Theory of rational option pricing. Bell Journal of Economics 4, 141–183.

Merton, R., 1976. Option pricing when the underlying stock returns are discontinuous. Journal of Financial Economics 4, 125–144.

Miao, G.J., 2014. High frequency and dynamic pairs trading based on statistical arbitrage using a two-stage correlation and cointegration approach. International Journal of Economics and Finance 6, 96–110.

Mikkelsen, A., Kjærland, F., 2018. High-frequency pairs trading on a small stock exchange .

Mostafa, F., Dillon, T., 2008. A neural network approach to option pricing, in: Constantino, M., Larran, M., Brebbia, C.A. (Eds.), Computational Finance and its Applications III. WIT Press, Southampton, pp. 71–86.

Muslumov, A., Yuksel, A., Yuksel, S.A., 2009. The profitability of pairs trading in an emerging market setting: evidence from the istanbul stock exchange. Empirical Economics Letters 8, 1–6.

Nath, P., 2003. High frequency pairs trading with us treasury securities: Risks and rewards for hedge funds. Available at SSRN 565441 .

Nelson, D., Pereira, A., de Oliveira, R., 2017. Stock market's price movement prediction with lstm neural networks, pp. 1419–1426.

Nguyen, T.N., Tran, M.N., Kohn, R., 2022. Recurrent conditional heteroskedasticity. Journal of Applied Econometrics 37, 1031–1054.

Nino, S., 2020. Transformers and time series forecasting .

Opitz, M., Possegger, H., Bischof, H., 2017. Efficient model averaging for deep neural networks, in: Lai, S.H., Lepetit, V., Nishino, K., Sato, Y. (Eds.), Computer Vision – ACCV 2016, Springer International Publishing, Cham. pp. 205–220.

Ormoneit, D., 1999. A regularization approach to continuous learning with an application to financial derivatives pricing. Neural Networks 12, 1405–1412.

Ouyang, K., Shokri, R., Rosenblum, D.S., Yang, W., 2018. A non-parametric generative model for human trajectories., in: IJCAI, pp. 3812–3817.

Papadakis, G., Wysocki, P., 2007. Pairs trading and accounting information. Boston university and mit working paper .

Paredes, M.S., Kadry, S., 2022. Pricing european options with deep learning models, in: 2022 Fifth International Conference of Women in Data Science at Prince Sultan University (WiDS PSU), IEEE. pp. 106–111.

Pathan, R.K., Biswas, M., Khandaker, M.U., 2020. Time series prediction of covid-19 by mutation rate analysis using recurrent neural network-based lstm model. Chaos, Solitons & Fractals 138, 110018.

Pires, M., Marwala, T., 2004. American option pricing using multi-layer perceptron and support vector machine, pp. 1279 – 1285 vol.2. doi:10.1109/ICSMC.2004.1399801.

Pires, M., Marwala, T., 2005. American option pricing using bayesian multi-layer perceptrons and bayesian support vector machines, pp. 219 – 224. doi:10.1109/ICCCYB.2005.1511576.

PTF Pro, . Pair trade finder pro. URL: https://pairtradefinder.com.

Puspaningrum, H., Lin, Y.X., Gulati, C.M., 2010. Finding the optimal pre-set boundaries for pairs trading strategy based on cointegration technique. Journal of Statistical Theory and Practice 4, 391–419.

Qi, M., Maddala, G.S., 1996. Option pricing using artificial neural networks: the case of S&P 500 index call options, in: Refenes, A.P.N., Abu-Mostafa, Y., Moody, J., Weigend, A. (Eds.), Neural Networks in Financial Engineering: Proceedings of the Third International Conference on Neural Networks in the Capital Markets, World Scientific, New York. pp. 78–91.

Rad, H., Low, R.K.Y., Faff, R., 2016. The profitability of pairs trading strategies: distance, cointegration and copula methods. Quantitative Finance 16, 1541–1558.

Ramos-Pérez, E., Alonso-González, P.J., Núñez-Velázquez, J.J., 2019. Forecasting volatility with a stacked model based on a hybridized artificial neural network. Expert Systems with Applications 129, 1–9.

Ramos-Requena, J.P., Trinidad-Segovia, J., Sánchez-Granero, M., 2017. Introducing hurst exponent in pair trading. Physica A: statistical mechanics and its applications 488, 39–45.

Ramos-Requena, J.P., Trinidad-Segovia, J.E., Sánchez-Granero, M.Á., 2020. Some notes on the formation of a pair in pairs trading. Mathematics 8, 348.

Ravazzolo, F., van Dijk, D., Verbeek, M., 2007b. Predictive Gains from Forecast Combination Using Time-varying Model Weight. Econometric Institute Report 2007 26.

Ravazzolo, F., Paap, R., van Dijk, D., Franses, P.H., 2007a. Bayesian model averaging in the presence of structural breaks, in: Wohar, M., Rapach, D. (Eds.), Forecasting in the Presence of Structural Breaks and Model Uncertainty. Elsevier, pp. 813–817.

Rouah, F., 2013. The Heston Model and Its Extensions in Matlab and C#. John Wiley & Sons, Hoboken, NJ.

Rubinstein, M., 1985. Nonparametric tests of alternative option pricing models using all reported trades and quotes on the 30 most active CBOE option classes from August 23, 1976 through August 31, 1978. Journal of Finance 40, 455–480.

Ruf, J., Wang, W., 2020. Neural networks for option pricing and hedging: a literature review. Journal of Computational Finance, Forthcoming .

Ruf, J., Wang, W., 2021. Hedging with linear regressions and neural networks. Journal of Business & Economic Statistics , 1–13.

Sarmento, S.M., Horta, N., 2020. A Machine Learning Based Pairs Trading Investment Strategy. Springer.

Schittenkopf, C., Dorffner, G., 2001. Risk neutral density extraction from option prices: improved pricing with mixture density networks. IEEE Transactions on Neural Networks 12, 716–725.

Schmidt, A.D., 2009. Pairs trading: a cointegration approach .

Scikit, . Decision trees. URL: https://scikit-learn.org/stable/modules/tree.html#tree-algorithms-id3-c4-5-c5-0-and-cart.

Seni, G., Elder, J.F., 2010. Ensemble methods in data mining: improving accuracy through combining predictions. Synthesis lectures on data mining and knowledge discovery 2, 1–126.

Sepp, H., Jurgen, S., 1997. Long Short-Term Memory. Neural Computation 9, 1735–1780.

Sharpe, W.F., 1994. The sharpe ratio. Journal of portfolio management 21, 49–58.

Shin, H.J., Ryu, J., 2012. A dynamic hedging strategy for option transaction using artificial neural networks. International Journal of Software Engineering and its Applications 6, 111–116.

So, D., Le, Q., Liang, C., 2019. The evolved transformer, in: International Conference on Machine Learning, PMLR. pp. 5877–5886.

Stock Charts, . Macd (moving average convergence/divergence oscillator). URL: https://school.stockcharts.com/doku.php?id=technical_indicators:moving_average_convergence_divergence_macd.

Stübinger, J., Bredthauer, J., 2017. Statistical arbitrage pairs trading with high-frequency data. International Journal of Economics and Financial Issues 7, 650–662.

Stübinger, J., Endres, S., 2018. Pairs trading with a mean-reverting jump–diffusion model on high-frequency data. Quantitative Finance 18, 1735–1751.

Thomaidis, N.S., Kondakis, N., Dounias, G.D., 2006a. An intelligent statistical arbitrage trading system, in: Hellenic Conference on Artificial Intelligence, Springer. pp. 596–599.

Thomaidis, N.S., Tzastoudis, V.S., Dounias, G.D., 2006b. Improving neural network based option price forecasting, in: 2006, S., Heraklion, C., Greece, M., 2006, P., Antoniou, G., Potamias, G., Spyropoulos, C., Plexousakis, D. (Eds.), Advances in Artificial Intelligence: 4th Hellenic Conference on AI, SETN 2006, Heraklion, Crete, Greece, May 18-20, 2006, Proceedings. Springer, Berlin, pp. 378–388. Lecture Notes in Computer Science, vol. 3955.

Umeorah, N., Mashele, P., Agbaeze, O., Mba, J.C., 2023. Barrier options and greeks: Modeling with neural networks. Axioms 12, 384.

Vejendla, A., Enke, D., 2013. Evaluation of garch, rnn and fnn models for forecasting volatility in the financial markets. IUP Journal of Financial Risk management 10.

Vidyamurthy, G., 2004. Pairs Trading: quantitative methods and analysis. volume 217. John Wiley & Sons.

Vidyamurthy, G., 2011. Pairs Trading: Quantitative Methods and Analysis. Wiley Finance, Wiley. URL: https://books.google.com.au/books?id=SQLU014X7JwC.

Wang, C., Chen, Y., Zhang, S., Zhang, Q., 2022. Stock market index prediction using deep transformer model. Expert Systems with Applications 208, 118128.

Wang, C.P., Lin, S.H., Huang, H.H., Wu, P.C., 2012. Using neural network for forecasting txo price under different volatility models. Expert Systems with Applications 39, 5025–5032.

Wen, Q., Zhou, T., Zhang, C., Chen, W., Ma, Z., Yan, J., Sun, L., 2022. Transformers in time series: A survey. arXiv preprint arXiv:2202.07125 .

Wilder, J.W., 1978. New concepts in technical trading systems. Trend Research.

Wilmott, P., Hoggard, T., Whalley, A.E., 1994. Hedging option portfolios in the presence of transaction costs. Advances in Futures and Options Research 7.

Woo, G., Liu, C., Sahoo, D., Kumar, A., Hoi, S., 2022. Etsformer: Exponential smoothing transformers for time-series forecasting. arXiv preprint arXiv:2202.01381 .

Xavier, G., Antoine, B., Yoshua, B., 2011. Deep sparse rectifier neural networks. Working paper, Universit´e de Montr´eal.

Yang, Y., Goncu, A., Pantelous, A., 2017. Pairs trading with commodity futures: evidence from the chinese market. China Finance Review International .

Yao, J., Li, Y., Tan, L., 2000. Option price forecasting using neural networks. Omega 28, 455–466.

Ye, T., Zhang, L., 2019. Derivatives pricing via machine learning. Boston University Questrom School of Business Research Paper .

Zakamulin, V., 2017. Market timing with moving averages: The anatomy and performance of trading rules. Springer.

Zeng, A., Chen, M., Zhang, L., Xu, Q., 2022. Are transformers effective for time series forecasting? arXiv preprint arXiv:2205.13504 .

Zeng, Y., Klabjan, D., 2019. Online adaptive machine learning based algorithm for implied volatility surface modeling. Knowledge-Based Systems 163, 376–391.

Zhang, J., Huang, W., 2021. Option hedging using lstm-rnn: an empirical analysis. Quantitative Finance 21, 1753–1772.

Zhang, Q., Qin, C., Zhang, Y., Bao, F., Zhang, C., Liu, P., 2022. Transformer-based attention network for stock movement prediction. Expert Systems with Applications 202, 117239.

Zhang, W., Liu, H., Wu, X., Xiao, L., Qian, Y., Fang, Z., 2019. Lane marking detection and classification with combined deep neural network for driver assistance. Proceedings of the Institution of Mechanical Engineers, Part D: Journal of Automobile Engineering 233, 1259–1268.

Zhao, K., Zhang, J., Liu, Q., 2022. Dual-hybrid modeling for option pricing of csi 300etf. Information 13, 36.